ASM HANDBOOK®

Volume

3

Alloy Phase Diagrams

ASM INTERNATIONAL
The Materials Information Society

Contents

Section 1
Introduction to Alloy Phase Diagrams ..... 1•1
Common Terms ..... 1•1
Phases ..... 1•1
Equilibrium ..... 1•1
Polymorphism ..... 1•1
Metastable Phases ..... 1•1
Systems ..... 1•1
Phase Diagrams ..... 1•2
System Components ..... 1•2
Phase Rule ..... 1•2
Unary Diagrams ..... 1•2
Invariant Equilibrium ..... 1•2
Univariant Equilibrium ..... 1•2
Bivariant Equilibrium ..... 1•2
Binary Diagrams ..... 1•2
Miscible Solids ..... 1•2
Eutectic Reactions ..... 1•3
Three-Phase Equilibrium ..... 1•3
Intermediate Phases ..... 1•3
Metastable Equilibrium ..... 1•4
Ternary Diagrams ..... 1•4
Vertical Sections ..... 1•4
Isothermal Sections ..... 1•5
Projected Views ..... 1•5
Thermodynamic Principles ..... 1•5
Internal Energy ..... 1•5
Closed System ..... 1•5
First Law ..... 1•5
Enthalpy ..... 1•6
Heat Capacity ..... 1•6
Second Law ..... 1•6
Entropy ..... 1•6
Third Law ..... 1•7
Gibbs Energy ..... 1•7
Features of Phase Diagrams ..... 1•7
Phase-Field Rule ..... 1•7
Theorem of LeChâtelier ..... 1•7
Clausius-Clapeyron Equation ..... 1•7
Solutions ..... 1•8
Mixtures ..... 1•8
Curves and Intersections ..... 1•8
Congruent Transformations ..... 1•10
Common Construction Errors ..... 1•10
High-Order Transitions ..... 1•10
Crystal Structure ..... 1•10
Crystal Systems ..... 1•10
Lattice Dimensions ..... 1•10
Lattice Points ..... 1•10
Crystal Structure Nomenclature ..... 1•15
Solid-Solution Mechanisms ..... 1•16
Determination of Phase Diagrams ..... 1•16
Chemical Analysis ..... 1•16
Cooling Curves ..... 1•16
Crystal Properties ..... 1•17
Physical Properties ..... 1•17
Metallographic Methods ..... 1•17
Thermodynamic Modeling ..... 1•17
Reading Phase Diagrams ..... 1•17
Composition Scales ..... 1•17
Lines and Labels ..... 1•18
Lever Rule ..... 1•18
Phase-Fraction Lines ..... 1•18
Solidification ..... 1•18
Coring ..... 1•18
Liquation ..... 1•19
Eutectic Microstructures ..... 1•19
Eutectoid Microstructures ..... 1•19
Microstructures of Other Invariant Reactions ..... 1•20
Solid-State Precipitation ..... 1•20
Examples of Phase Diagrams ..... 1•20
The Copper-Zinc System ..... 1•20
The Aluminum-Copper System ..... 1•21
The Titanium-Aluminum, Titanium-Chromium and Titanium-Vanadium Systems ..... 1•21
The Iron-Carbon System ..... 1•22
The Iron-Cementite System ..... 1•22
The Iron-Chromium-Nickel System ..... 1•24
Practical Applications of Phase Diagrams ..... 1•24
Alloy Design ..... 1•24
Age-Hardening Alloys ..... 1•24
Austenitic Stainless Steel ..... 1•24
Permanent Magnets ..... 1•25
Processing ..... 1•25
Hacksaw Blades ..... 1•25
Hardfacing ..... 1•26
Performance ..... 1•26
Heating Elements ..... 1•26
Electric Motor Housings ..... 1•26
Carbide Cutting Tools ..... 1•26
Solid State Electronics ..... 1•27
Bibliography ..... 1•27
Other References ..... 1•29
Index of Terms ..... 1•30

Section 2
Binary Phase Diagrams ..... 2•1
Introduction ..... 2•3
Binary General References ..... 2•4
Key to Titles ..... 2•4
Binary Alloy Phase Diagrams Index ..... 2•5
References Cited in Index ..... 2•22
Binary Phase Diagrams and Crystal Structure Data ..... 2•25

Section 3
Ternary Phase Diagrams ..... 3•1
Introduction ..... 3•3

(continued)

Ternary Alloy Phase Diagrams ..... 3•5
Ternary References ..... 3•59

Section 4
Appendix ..... 4•1
Symbols for the Chemical Elements ..... 4•3
Standard Atomic Weights of the Elements (periodic chart) ..... 4•4
Melting and Boiling Points of the Elements at Atmospheric Pressure ..... 4•5
Allotropic Transformations of the Elements at Atmospheric Pressure ..... 4•7
Magnetic-Phase-Transition Temperatures of the Elements ..... 4•9
Crystal Structures and Lattice Parameters of Allotropes of the Metallic Elements ..... 4•10
Crystal Structure Nomenclature Arranged Alphabetically by Pearson Symbol Designation ..... 4•13
Temperature Conversions (tables) ..... 4•17
Abbreviations ..... 4•19
Greek Alphabet ..... 4•19

Section 1
Introduction to Alloy Phase Diagrams

Hugh Baker, Editor

ALLOY PHASE DIAGRAMS are useful to metallurgists, materials engineers, and materials scientists in four major areas: (1) development of new alloys for specific applications, (2) fabrication of these alloys into useful configurations, (3) design and control of heat treatment procedures for specific alloys that will produce the required mechanical, physical, and chemical properties, and (4) solving problems that arise with specific alloys in their performance in commercial applications, thus improving product predictability. In all these areas, the use of phase diagrams allows research, development, and production to be done more efficiently and cost effectively.

In the area of alloy development, phase diagrams have proved invaluable for tailoring existing alloys to avoid overdesign in current applications, designing improved alloys for existing and new applications, designing special alloys for special applications, and developing alternative alloys or alloys with substitute alloying elements to replace those containing scarce, expensive, hazardous, or "critical" alloying elements. Application of alloy phase diagrams in processing includes their use to select proper parameters for working ingots, blooms, and billets, finding causes and cures for microporosity and cracks in castings and welds, controlling solution heat treating to prevent damage caused by incipient melting, and developing new processing technology.

In the area of performance, phase diagrams give an indication of which phases are thermodynamically stable in an alloy and can be expected to be present over a long time when the part is subjected to a particular temperature (e.g., in an automotive exhaust system). Phase diagrams also are consulted when attacking service problems such as pitting and intergranular corrosion, hydrogen damage, and hot corrosion.

In a majority of the more widely used commercial alloys, the allowable composition range encompasses only a small portion of the relevant phase diagram. The nonequilibrium conditions that are usually encountered in practice, however, necessitate the knowledge of a much greater portion of the diagram. Therefore, a thorough understanding of alloy phase diagrams in general and their practical use will prove to be of great help to a metallurgist expected to solve problems in any of the areas mentioned above.

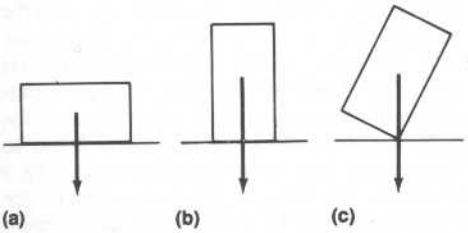

Fig. 1 Mechanical equilibria: (a) Stable. (b) Metastable. (c) Unstable

Common Terms

Before the subject of alloy phase diagrams is discussed in detail, several of the commonly used terms will be discussed.

Phases. All materials exist in gaseous, liquid, or solid form (usually referred to as a *phase*), depending on the conditions of state. *State variables* include composition, temperature, pressure, magnetic field, electrostatic field, gravitational field, and so on. The term "phase" refers to that region of space occupied by a physically homogeneous material. However, there are two uses of the term: the strict sense normally used by physical scientists and the somewhat looser sense normally used by materials engineers.

In the strictest sense, homogeneous means that the physical properties throughout the region of space occupied by the phase are absolutely identical, and any change in condition of state, no matter how small, will result in a different phase. For example, a sample of solid metal with an apparently homogeneous appearance is not truly a single-phase material, because the pressure condition varies in the sample due to its own weight in the gravitational field.

In a phase diagram, however, each single-phase field (phase fields are discussed in a following section) is usually given a single label, and engineers often find it convenient to use this label to refer to all the materials lying within the field, regardless of how much the physical properties of the materials continuously change from one part of the field to another. This means that in engineering practice, the distinction between the terms "phase" and "phase field" is seldom made, and all materials having the same phase name are referred to as the same phase.

Equilibrium. There are three types of equilibria: stable, metastable, and unstable. These three conditions are illustrated in a mechanical sense in Fig. 1. Stable equilibrium exists when the object is in its lowest energy condition; metastable equilibrium exists when additional energy must be introduced before the object can reach true stability; unstable equilibrium exists when no additional energy is needed before reaching metastability or stability. Although true stable equilibrium conditions seldom exist in metal objects, the study of equilibrium systems is extremely valuable, because it constitutes a limiting condition from which actual conditions can be estimated.

Polymorphism. The structure of solid elements and compounds under stable equilibrium conditions is crystalline, and the crystal structure of each is unique. Some elements and compounds, however, are *polymorphic* (multishaped); that is, their structure transforms from one crystal structure to another with changes in temperature and pressure, each unique structure constituting a distinctively separate phase. The term *allotropy* (existing in another form) is usually used to describe polymorphic changes in chemical elements. Crystal structure of metals and alloys is discussed in a later section of this Introduction; the allotropic transformations of the elements are listed in the Appendix to this Volume.

Metastable Phases. Under some conditions, metastable crystal structures can form instead of stable structures. Rapid freezing is a common method of producing metastable structures, but some (such as Fe_3C, or "cementite") are produced at moderately slow cooling rates. With extremely rapid freezing, even thermodynamically unstable structures (such as amorphous metal "glasses") can be produced.

Systems. A physical *system* consists of a substance (or a group of substances) that is isolated from its surroundings, a concept used to facilitate study of the effects of conditions of state. "Isolated" means that there is no interchange of mass between the substance and its surroundings. The substances in alloy systems, for example, might be two metals, such as copper and zinc; a metal and a nonmetal, such as iron and carbon; a metal and an intermetallic compound, such as iron and cementite; or several metals, such as aluminum,

magnesium, and manganese. These substances constitute the *components* comprising the system and should not be confused with the various phases found within the system. A system, however, also can consist of a single component, such as an element or compound.

Phase Diagrams. In order to record and visualize the results of studying the effects of state variables on a system, diagrams were devised to show the relationships between the various phases that appear within the system under equilibrium conditions. As such, the diagrams are variously called *constitutional diagrams*, *equilibrium diagrams*, or *phase diagrams*. A single-component phase diagram can be simply a one- or two-dimensional plot showing the phase changes in the substance as temperature and/or pressure change. Most diagrams, however, are two- or three-dimensional plots describing the phase relationships in systems made up of two or more components, and these usually contain fields (areas) consisting of mixed-phase fields, as well as single-phase fields. The plotting schemes in common use are described in greater detail in subsequent sections of this Introduction.

System Components. Phase diagrams and the systems they describe are often classified and named for the number (in Latin) of components in the system:

Number of components	Name of system or diagram
One	Unary
Two	Binary
Three	Ternary
Four	Quaternary
Five	Quinary
Six	Sexinary
Seven	Septenary
Eight	Octanary
Nine	Nonary
Ten	Decinary

Phase Rule. The *phase rule*, first announced by J. Willard Gibbs in 1876, relates the physical state of a mixture to the number of constituents in the system and to its conditions. It was also Gibbs who first called each homogeneous region in a system by the term "phase." When pressure and temperature are the state variables, the rule can be written as follows:

$$f = c - p + 2$$

where f is the number of independent variables (called *degrees of freedom*), c is the number of components, and p is the number of stable phases in the system.

Unary Diagrams

Invariant Equilibrium. According to the phase rule, three phases can exist in stable equilibrium only at a single point on a unary diagram ($f = 1 - 3 + 2 = 0$). This limitation is illustrated as point O in the hypothetical unary pressure-temperature (PT) diagram shown in Fig. 2. In this diagram, the three states (or phases)—solid, liquid, and gas—are represented by the three correspondingly labeled fields. Stable equilibrium between any two phases occurs along their mutual boundary, and *invariant equilibrium* among all three phases occurs at the so-called *triple point*, O, where the three boundaries intersect. This point also is called an *invariant point* because, at that location on the diagram, all externally controllable factors are fixed (no degrees of freedom). At this point, all three states (phases) are in equilibrium, but any changes in pressure and/or temperature will cause one or two of the states (phases) to disappear.

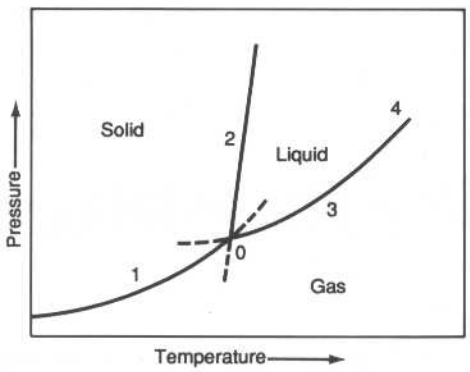

Fig. 2 Schematic pressure-temperature phase diagram

Univariant Equilibrium. The phase rule says that stable equilibrium between two phases in a unary system allows one degree of freedom ($f = 1 - 2 + 2$). This condition, called *univariant equilibrium* or *monovariant equilibrium*, is illustrated as lines 1, 2, and 3 separating the single-phase fields in Fig. 2. Either pressure or temperature may be freely selected, but not both. Once a pressure is selected, there is only one temperature that will satisfy equilibrium conditions, and conversely. The three curves that issue from the triple point are called *triple curves*: line 1, representing the reaction between the solid and the gas phases, is the *sublimation curve*; line 2 is the *melting curve*; and line 3 is the *vaporization curve*. The vaporization curve ends at point 4, called a *critical point*, where the physical distinction between the liquid and gas phases disappears.

Bivariant Equilibrium. If both the pressure and temperature in a unary system are freely and arbitrarily selected, the situation corresponds to having two degrees of freedom, and the phase rule says that only one phase can exit in stable equilibrium ($p = 1 - 2 + 2$). This situation is called *bivariant equilibrium*.

Binary Diagrams

If the system being considered comprises two components, a composition axis must be added to the PT plot, requiring construction of a three-dimensional graph. Most metallurgical problems, however, are concerned only with a fixed pressure of one atmosphere, and the graph reduces to a two-dimensional plot of temperature and composition (TX diagram).

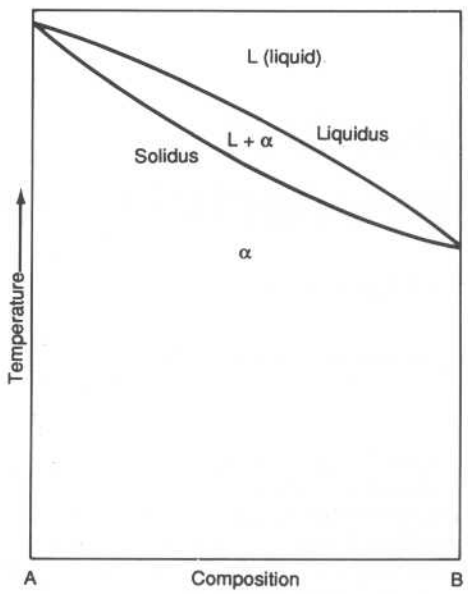

Fig. 3 Schematic binary phase diagram showing miscibility in both the liquid and solid states

The Gibbs phase rule applies to all states of matter (solid, liquid, and gaseous), but when the effect of pressure is constant, the rule reduces to:

$$f = c - p + 1$$

The stable equilibria for binary systems are summarized as follows:

Number of components	Number of phases	Degrees of freedom	Equilibrium
2	3	0	Invariant
2	2	1	Univariant
2	1	2	Bivariant

Miscible Solids. Many systems are comprised of components having the same crystal structure, and the components of some of these systems are completely miscible (completely soluble in each other) in the solid form, thus forming a *continuous solid solution*. When this occurs in a binary system, the phase diagram usually has the general appearance of that shown in Fig. 3. The diagram consists of two single-phase fields separated by a two-phase field. The boundary between the liquid field and the two-phase field in Fig. 3 is called the *liquidus*; that between the two-phase field and the solid field is the *solidus*. In general, a liquidus is the locus of points in a phase diagram representing the temperatures at which alloys of the various compositions of the system begin to freeze on cooling or finish melting on heating; a solidus is the locus of points representing the temperatures at which the various alloys finish freezing on cooling or begin melting on heating. The phases in equilibrium across the two-phase field in Fig. 3 (the liquid and solid solutions) are called *conjugate phases*.

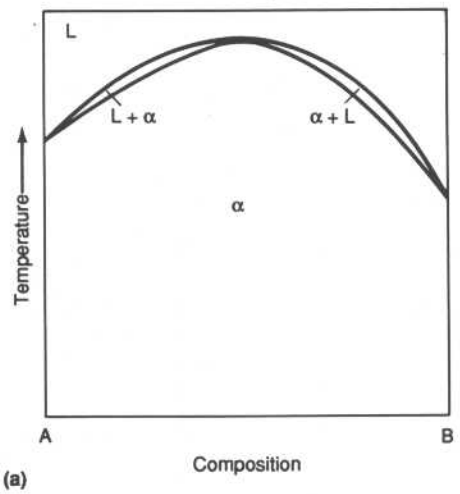

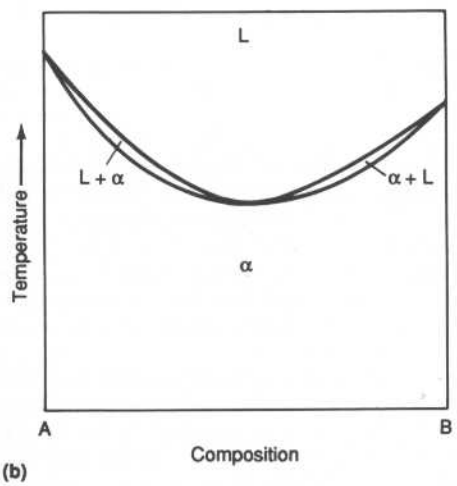

Fig. 4 Schematic binary phase diagrams with solid-state miscibility where the liquidus shows a maximum (a) and a minimum (b)

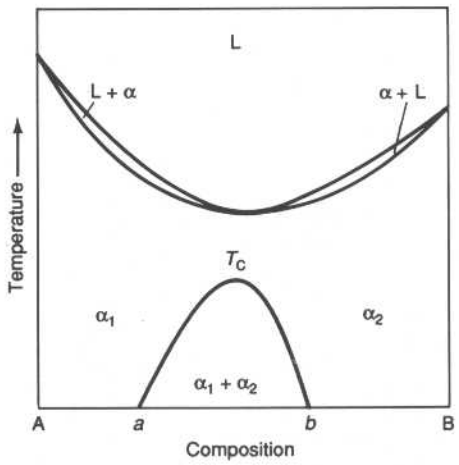

Fig. 5 Schematic binary phase diagram with a minimum in the liquidus and a miscibility gap in the solid state

If the solidus and liquidus meet tangentially at some point, a maximum or minimum is produced in the two-phase field, splitting it into two portions as shown in Fig. 4. It also is possible to have a gap in miscibility in a single-phase field; this is shown in Fig. 5. Point T_c, above which phases α_1 and α_2 become indistinguishable, is a critical point similar to point 4 in Fig. 2. Lines a-T_c and b-T_c, called *solvus* lines, indicate the limits of solubility of component B in A and A in B, respectively. The configurations of these and all other phase diagrams depend on the thermodynamics of the system, as discussed later in this Introduction.

Eutectic Reactions. If the two-phase field in the solid region of Fig. 5 is expanded so that it touches the solidus at some point, as shown in Fig. 6(a), complete miscibility of the components is lost. Instead of a single solid phase, the diagram now shows two separate solid *terminal phases*, which are in three-phase equilibrium with the liquid at point P, an invariant point that occurred by coincidence. (Three-phase equilibrium is discussed in the following section.) Then, if this two-phase field in the solid region is even further widened so that the solvus lines no longer touch at the invariant point, the diagram passes through a series of configurations, finally taking on the more familiar shape shown in Fig. 6(b). The three-phase reaction that takes place at the invariant point E, where a liquid phase freezes into a mixture of two solid phases, is called a *eutectic* reaction (from the Greek word for "easily melted"). The alloy that corresponds to the eutectic composition is called a *eutectic alloy*. An alloy having a composition to the left of the eutectic point is called a *hypoeutectic alloy* (from the Greek word for "less than"); an alloy to the right is a *hypereutectic alloy* (meaning "greater than").

In the eutectic system described above, the two components of the system have the same crystal structure. This, and other factors, allows complete miscibility between them. Eutectic systems, however, also can be formed by two components having different crystal structures. When this occurs, the liquidus and solidus curves (and their extensions into the two-phase field) for each of the terminal phases (see Fig. 6c) resemble those for the situation of complete miscibility between system components shown in Fig. 3.

Three-Phase Equilibrium. Reactions involving three conjugate phases are not limited to the eutectic reaction. For example, upon cooling, a single solid phase can change into a mixture of two new solid phases or, conversely, two solid phases can react to form a single new phase. These and the other various types of invariant reactions observed in binary systems are listed in Table 1 and illustrated in Fig. 7 and 8.

Intermediate Phases. In addition to the three solid terminal-phase fields, α, β, and ε, the diagram in Fig. 7 displays five other solid-phase fields, γ, δ, δ′, η, and σ, at intermediate compositions. Such phases are called *intermediate phases*. Many intermediate phases, such as those

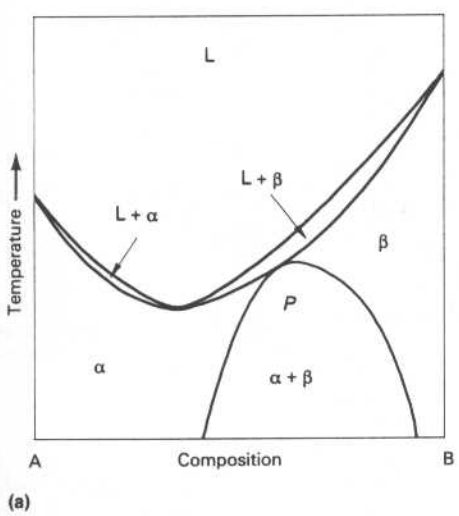

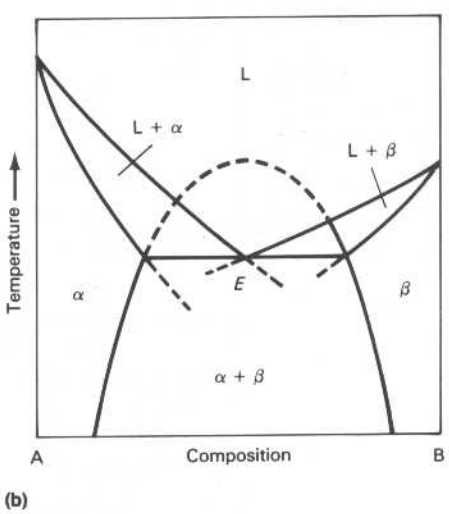

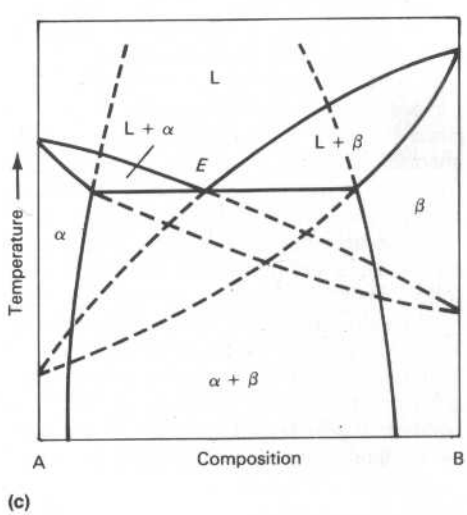

Fig. 6 Schematic binary phase diagrams with invariant points. (a) Hypothetical diagram of the type shown in Fig. 5, except that the miscibility gap in the solid touches the solidus curve at invariant point P; an actual diagram of this type probably does not exist. (b) and (c) Typical eutectic diagrams for components having the same crystal structure (b) and components having different crystal structures (c); the eutectic (invariant) points are labeled E. The dashed lines in (b) and (c) are metastable extensions of the stable-equilibria lines.

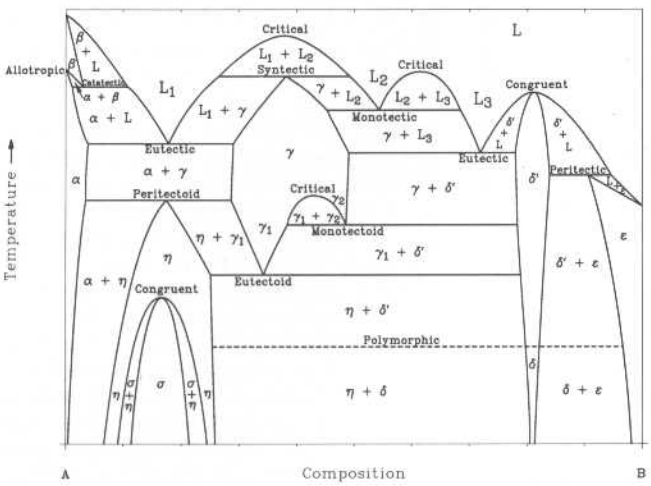

Fig. 7 Hypothetical binary phase diagram showing intermediate phases formed by various invariant reactions and a polymorphic transformation

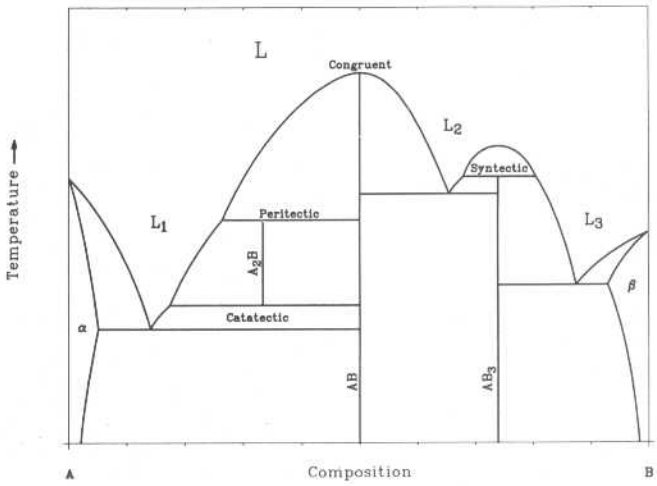

Fig. 8 Hypothetical binary phase diagram showing three intermetallic line compounds and four melting reactions

illustrated in Fig. 7, have fairly wide ranges of homogeneity. However, many others have very limited or no significant homogeneity range.

When an intermediate phase of limited (or no) homogeneity range is located at or near a specific ratio of component elements that reflects the normal positioning of the component atoms in the crystal structure of the phase, it is often called a compound (or *line compound*). When the components of the system are metallic, such an intermediate phase is often called an *intermetallic compound.* (Intermetallic compounds should not be confused with chemical compounds, where the type of bonding is different from that in crystals and where the ratio has chemical significance.) Three intermetallic compounds (with four types of melting reactions) are shown in Fig. 8.

In the hypothetical diagram shown in Fig. 8, an alloy of composition AB will freeze and melt isothermally, without the liquid or solid phases undergoing changes in composition; such a phase change is alled *congruent.* All other reactions are *incongruent*; that is, two phases are formed from one phase on melting. Congruent and incongruent phase changes, however, are not limited to line compounds: the terminal component B (pure phase ε) and the highest-melting composition of intermediate phase δ′ in Fig. 7, for example, freeze and melt congruently, while δ′ and ε freeze and melt incongruently at other compositions.

Metastable Equilibrium. In Fig. 6(c), dashed lines indicate the portions of the liquidus and solidus lines that disappear into the two-phase solid region. These dashed lines represent valuable information, as they indicate conditions that would exist under metastable equilibrium, such as might theoretically occur during extremely rapid cooling. Metastable extensions of some stable-equilibria lines also appear in Fig. 2 and 6(b).

Ternary Diagrams

When a third component is added to a binary system, illustrating equilibrium conditions in two dimensions becomes more complicated. One option is to add a third composition dimension to the base, forming a solid diagram having binary diagrams as its vertical sides. This can be represented as a modified isometric projection, such as shown in Fig. 9. Here, boundaries of single-phase fields (liquidus, solidus, and solvus lines in the binary diagrams) become surfaces; single- and two-phase areas become volumes; three-phase lines become volumes; and four-phase points, while not shown in Fig. 9, can exist as an invariant plane. The composition of a binary eutectic liquid, which is a point in a two-component system, becomes a line in a ternary diagram, as shown in Fig. 9.

Although three-dimensional projections can be helpful in understanding the relationships in a diagram, reading values from them is difficult. Therefore, ternary systems are often represented by views of the binary diagrams that comprise the faces and two-dimensional projections of the liquidus and solidus surfaces, along with a series of two-dimensional horizontal sections (*isotherms*) and vertical sections (*isopleths*) through the solid diagram.

Vertical sections are often taken through one corner (one component) and a congruently melting binary compound that appears on the opposite face; when such a plot can be read like any other true binary diagram, it is called a *quasibinary* section. One possibility is illustrated by line 1-2 in the isothermal section shown in Fig. 10. A vertical section between a congruently melting binary compound on one face and one on a dif-

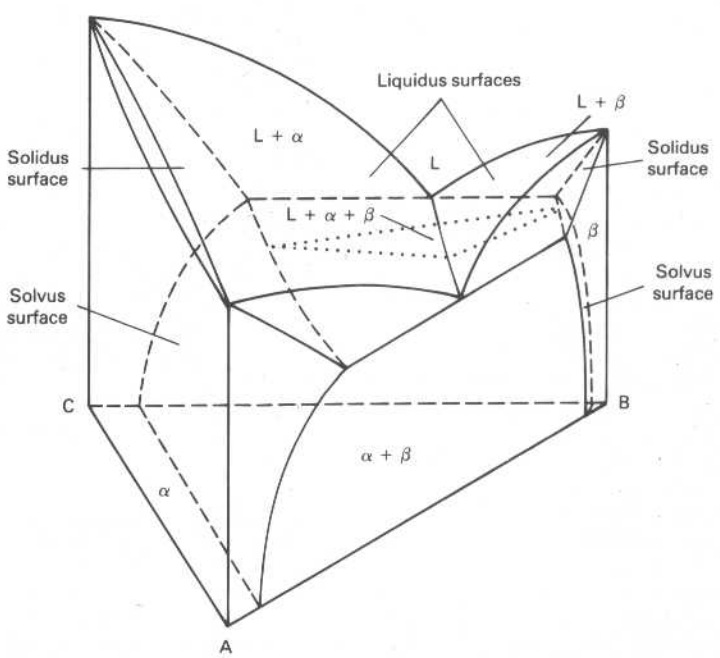

Fig. 9 Ternary phase diagram showing three-phase equilibrium. Source: 56Rhi

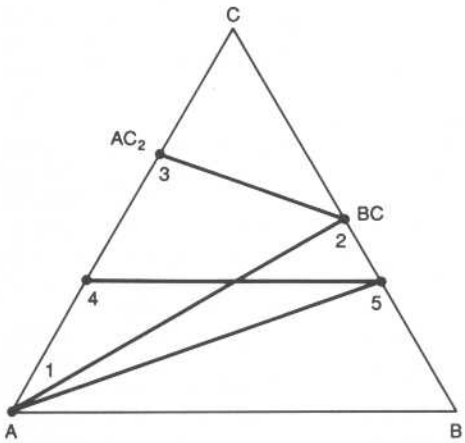

Fig. 10 Isothermal section of a ternary diagram with phase boundaries deleted for simplification

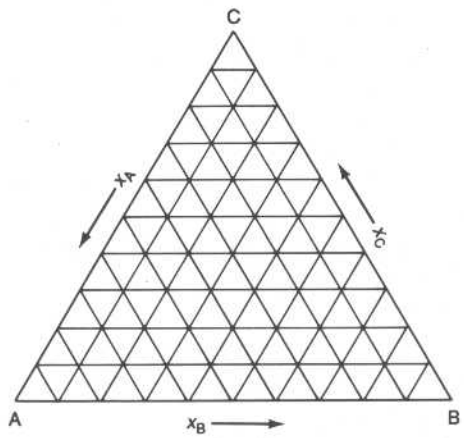

Fig. 11 Triangular composition grid for isothermal sections; x is the composition of each constituent in mole fraction or percent

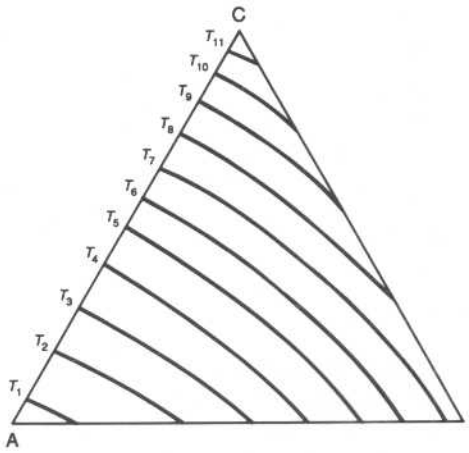

Fig. 12 Liquidus projection of a ternary phase diagram showing isothermal contour lines. Source: Adapted from 56Rhi

ferent face might also form a quasibinary section (see line 2-3).

All other vertical sections are not true binary diagrams, and the term *pseudobinary* is applied to them. A common pseudobinary section is one where the percentage of one of the components is held constant (the section is parallel to one of the faces), as shown by line 4-5 in Fig. 10. Another is one where the ratio of two constituents is held constant and the amount of the third is varied from 0 to 100% (line 1-5).

Isothermal Sections. Composition values in the triangular isothermal sections are read from a triangular grid consisting of three sets of lines parallel to the faces and placed at regular composition intervals (see Fig. 11). Normally, the point of the triangle is placed at the top of the illustration, component A is placed at the bottom left, B at the bottom right, and C at the top. The amount of component A is normally indicated from point C to point A, the amount of component B from point A to point B, and the amount of component C from point B to point C. This scale arrangement is often modified when only a corner area of the diagram is shown.

Projected Views. Liquidus, solidus, and solvus surfaces by their nature are not isothermal. Therefore, equal-temperature (isothermal) contour lines are often added to the projected views of these surfaces to indicate their shape (see Fig. 12). In addition to (or instead of) contour lines, views often show lines indicating the temperature troughs (also called "valleys" or "grooves") formed at the intersections of two surfaces. Arrowheads are often added to these lines to indicate the direction of decreasing temperature in the trough.

Table 1 Invariant reactions

Type	Reaction	
Eutectic (involves liquid and solid)	$L_1 \rightarrow L_2 + S$	Monotectic
	$L \rightarrow S_1 + S_2$	Eutectic
	$S_1 \rightarrow L + S_2$	Catatectic (Metatectic)
Eutectoid (involves solid only)	$S_1 \rightarrow S_1 + S_2$	Monotectoid
	$S_1 \rightarrow S_2 + S_3$	Eutectoid
Peritectic (involves liquid and solid)	$L_1 + S \rightarrow L_2$	Syntectic
	$L + S_2 \rightarrow S_1$	Peritectic
Peritectoid (involves solid only)	$S_1 + S_3 \rightarrow S_2$	Peritectoid

Thermodynamic Principles

The reactions between components, the phases formed in a system, and the shape of the resulting phase diagram can be explained and understood through knowledge of the principles, laws, and terms of thermodynamics, and how they apply to the system.

Internal Energy. The sum of the kinetic energy (energy of motion) and potential energy (stored energy) of a system is called its *internal energy*, E. Internal energy is characterized solely by the state of the system.

Closed System. A thermodynamic system that undergoes no interchange of mass (material) with its surroundings is called a *closed system*. A closed system, however, can interchange energy with its surroundings.

First Law. The *First Law of Thermodynamics*, as stated by Julius von Mayer, James Joule, and Hermann von Helmholtz in the 1840s, states that *energy can be neither created nor destroyed.* Therefore, it is called the *Law of Conservation of Energy*. This law means that the total energy of an isolated system remains constant throughout any operations that are carried out on it; that is, for any quantity of energy in one form that disappears from the system, an equal quantity of another form (or other forms) will appear.

For example, consider a closed gaseous system to which a quantity of heat energy, δQ, is added and a quantity of work, δW, is extracted. The First Law describes the change in internal energy, dE, of the system as follows:

$$dE = \delta Q - \delta W$$

In the vast majority of industrial processes and material applications, the only work done by or on a system is limited to pressure/volume terms.

Any energy contributions from electric, magnetic, or gravitational fields are neglected, except for electrowinning and electrorefining processes such as those used in the production of copper, aluminum, magnesium, the alkaline metals, and the alkaline earths. With the neglect of field effects, the work done by a system can be measured by summing the changes in volume, dV, times each pressure causing a change. Therefore, when field effects are neglected, the First Law can be written:

$$dE = \delta Q - P dV$$

Enthalpy. Thermal energy changes under constant pressure (again neglecting any field effects) are most conveniently expressed in terms of the *enthalpy*, H, of a system. Enthalpy, also called *heat content*, is defined by:

$$H = E + PV$$

Enthalpy, like internal energy, is a function of the state of the system, as is the product PV.

Heat Capacity. The *heat capacity*, C, of a substance is the amount of heat required to raise its temperature one degree; that is:

$$C = \frac{\delta Q}{\delta T}$$

However, if the substance is kept at constant volume ($dV = 0$):

$$\delta Q = dE$$

and

$$C_v = \left(\frac{\delta Q}{\delta T}\right)_v = \left(\frac{dE}{dT}\right)_v$$

If, instead, the substance is kept at constant pressure (as in many metallurgical systems),

$$C_p = \left(\frac{dE}{dT} + \frac{P dV}{dT}\right)_p$$

$$C_p = \left[\frac{d\,(E + PV)}{dT}\right]_p$$

and

$$C_p = \left(\frac{dH}{dT}\right)_p$$

Second Law. While the First Law establishes the relationship between the heat absorbed and the work performed by a system, it places no restriction on the source of the heat or its flow direction. This restriction, however, is set by the *Second Law of Thermodynamics*, which was advanced by Rudolf Clausius and William Thomson (Lord Kelvin). The Second Law states that *the spontaneous flow of heat always is from the higher temperature body to the lower temperature body*. In other words, *all naturally occurring processes tend to take place spontaneously in the direction that will lead to equilibrium.*

Entropy. The Second Law is most conveniently stated in terms of *entropy*, S, another property of state possessed by all systems. Entropy represents the energy (per degree of absolute temperature, T) in a system that is not available for work. In terms of entropy, the Second Law states that *all natural processes tend to occur only with an increase in entropy, and the direction of the process always is such as to lead to an increase in entropy*. For processes taking place in a system in equilibrium with its surroundings, the change in entropy is defined as follows:

$$dS \equiv \frac{\delta Q}{T} \equiv \frac{dE + P dV}{T}$$

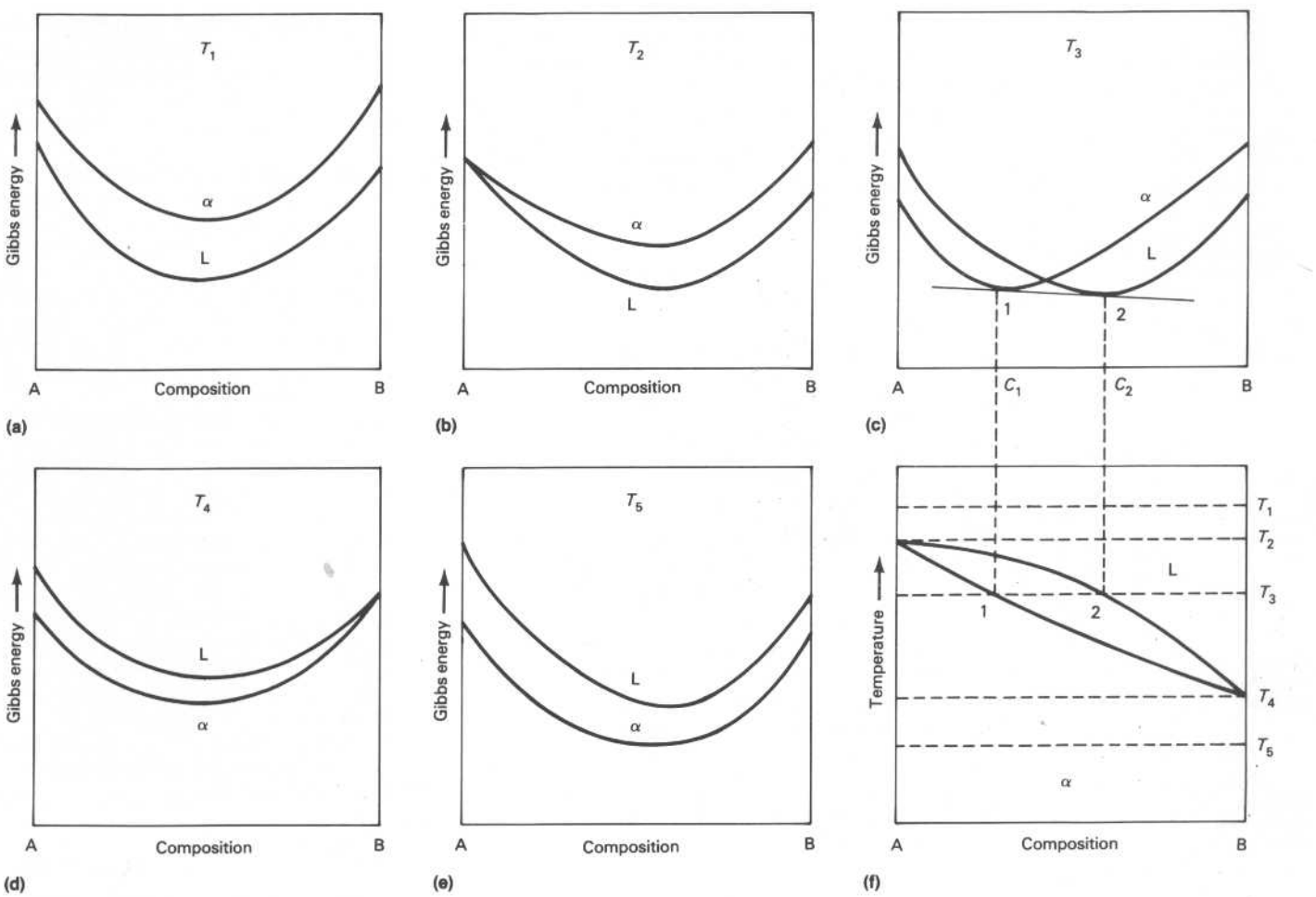

Fig. 13 Use of Gibbs energy curves to construct a binary phase diagram that shows miscibility in both the liquid and solid states. Source: Adapted from 66Pri

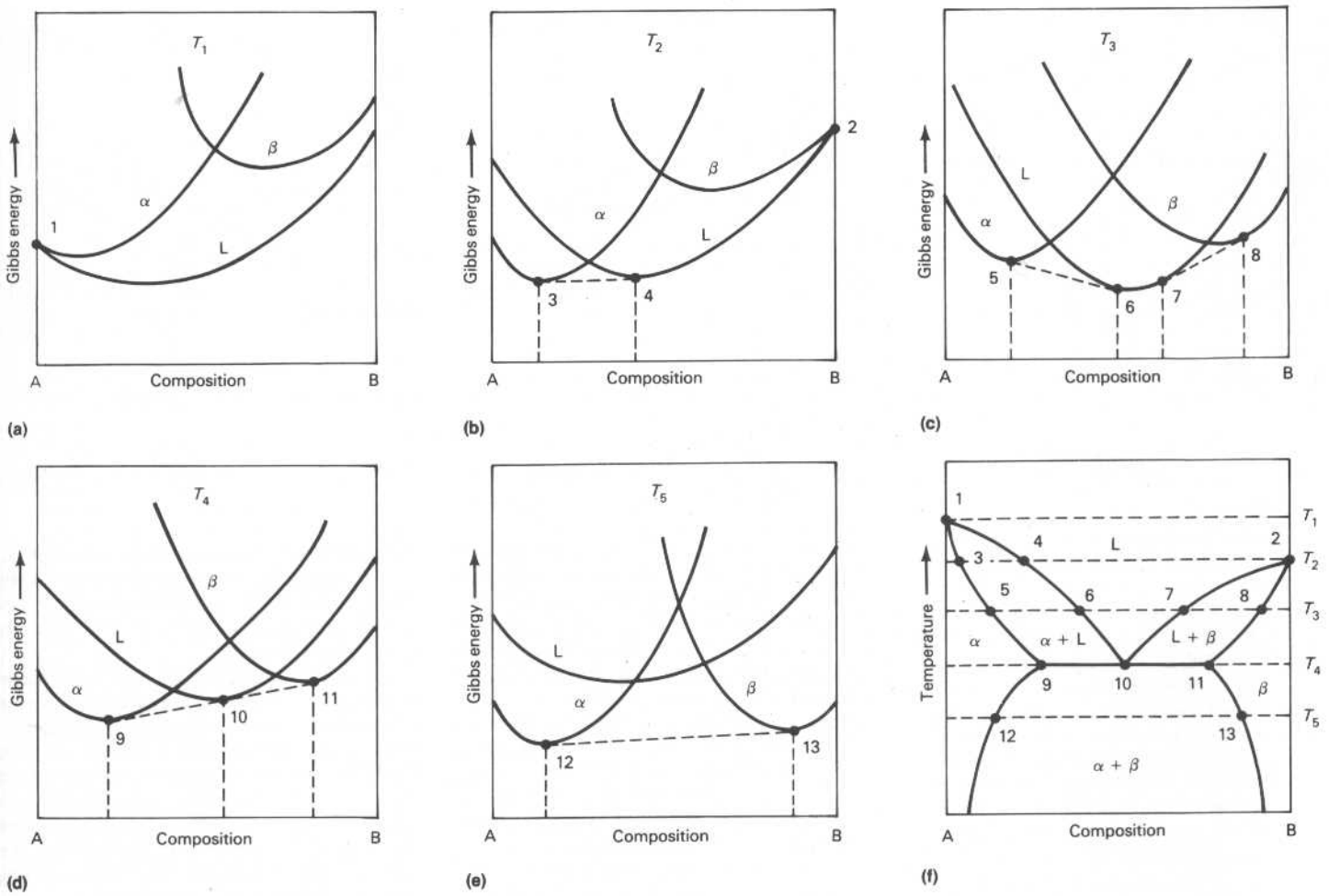

Fig. 14 Use of Gibbs energy curves to construct a binary phase diagram of the eutectic type. Source: Adapted from 68Gor

Third Law. A principle advanced by Theodore Richards, Walter Nernst, Max Planck, and others, often called the *Third Law of Thermodynamics*, states that *the entropy of all chemically homogeneous materials can be taken as zero at absolute zero temperature (0 K)*. This principle allows calculation of the absolute values of entropy of pure substances solely from heat capacity.

Gibbs Energy. Because both S and V are difficult to control experimentally, an additional term, *Gibbs energy*, G, is introduced, whereby:

$$G \equiv E + PV - TS \equiv H - TS$$

and

$$dG = dE + PdV + VdP - TdS - SdT$$

However,

$$dE = TdS - PdV$$

Therefore,

$$dG = VdP - SdT$$

Here, the change in Gibbs energy of a system undergoing a process is expressed in terms of two independent variables, pressure and absolute temperature, which are readily controlled experimentally. If the process is carried out under conditions of constant pressure and temperature, the change in Gibbs energy of a system at equilibrium with its surroundings (a reversible process) is zero. For a spontaneous (irreversible) process, the change in Gibbs energy is less than zero (negative); that is, the Gibbs energy decreases during the process, and it reaches a minimum at equilibrium.

Features of Phase Diagrams

The areas (fields) in a phase diagram, and the position and shapes of the points, lines, surfaces, and intersections in it, are controlled by thermodynamic principles and the thermodynamic properties of all of the phases that constitute the system.

Phase-field Rule. The *phase-field rule* specifies that at constant temperature and pressure, the number of phases in adjacent fields in a multicomponent diagram must differ by one.

Theorem of Le Châtelier. The *theorem of Henri Le Châtelier*, which is based on thermodynamic principles, states that *if a system in equilibrium is subjected to a constraint by which the equilibrium is altered, a reaction occurs that opposes the constraint, i.e., a reaction that partially nullifies the alteration.* The effect of this theorem on lines in a phase diagram can be seen in Fig. 2. The slopes of the sublimation line (1) and the vaporization line (3) show that the system reacts to increasing pressure by making the denser phases (solid and liquid) more stable at higher pressure. The slope of the melting line (2) indicates that this hypothetical substance contracts on freezing. (Note that the boundary between liquid water and ordinary ice, which expands on freezing, slopes toward the pressure axis.)

Clausius-Clapeyron Equation. The theorem of Le Châtelier was quantified by Benoit Clapeyron and Rudolf Clausius to give the following equation:

$$\frac{dP}{dT} = \frac{\Delta H}{T\Delta V}$$

where dP/dT is the slope of the univariant lines in a PT diagram such as those shown in Fig. 2, ΔV is the difference in molar volume of the two phases in the reaction, and ΔH is the difference in molar enthalpy of the two phases (the heat of the reaction).

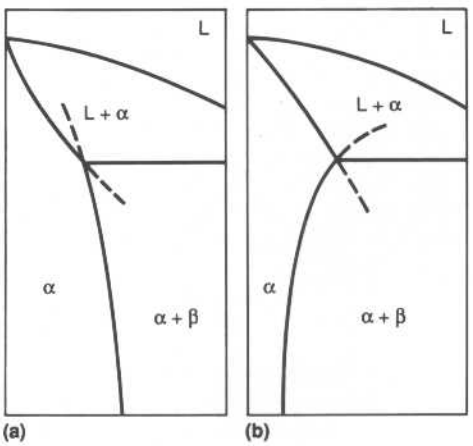

Fig. 15 Examples of acceptable intersection angles for boundaries of two-phase fields. Source: 56Rhi

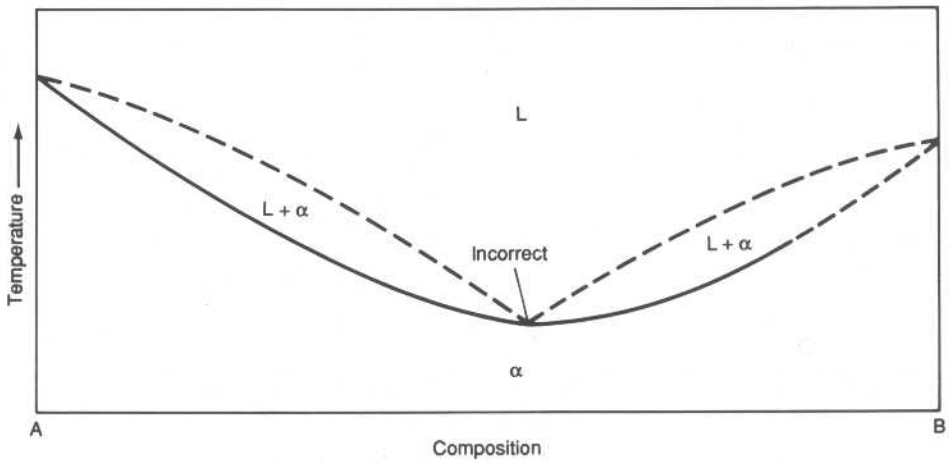

Fig. 16 An example of a binary phase diagram with a minimum in the liquidus that violates the Gibbs-Konovalov Rule. Source: 81Goo

Solutions. The shapes of liquidus, solidus, and solvus curves (or surfaces) in a phase diagram are determined by the Gibbs energies of the relevant phases. In this instance, the Gibbs energy must include not only the energy of the constituent components, but also the energy of mixing of these components in the phase.

Consider, for example, the situation of complete miscibility shown in Fig. 3. The two phases, liquid and solid α, are in stable equilibrium in the two-phase field between the liquidus and solidus lines. The Gibbs energies at various temperatures are calculated as a function of composition for ideal liquid solutions and for ideal solid solutions of the two components, A and B. The result is a series of plots similar to those shown in Fig. 13(a) to (e).

At temperature T_1, the liquid solution has the lower Gibbs energy and, therefore, is the more stable phase. At T_2, the melting temperature of A, the liquid and solid are equally stable only at a composition of pure A. At temperature T_3, between the melting temperatures of A and B, the Gibbs energy curves cross. Temperature T_4 is the melting temperature of B, while T_5 is below it.

Construction of the two-phase liquid-plus-solid field of the phase diagram in Fig. 13(f) is as follows. According to thermodynamic principles, the compositions of the two phases in equilibrium with each other at temperature T_3 can be determined by constructing a straight line that is tangential to both curves in Fig. 13(c). The points of tangency, 1 and 2, are then transferred to the phase diagram as points on the solidus and liquidus, respectively. This is repeated at sufficient temperatures to determine the curves accurately.

If, at some temperature, the Gibbs energy curves for the liquid and the solid tangentially touch at some point, the resulting phase diagram will be similar to those shown in Fig. 4(a) and (b), where a maximum or minimum appears in the liquidus and solidus curves.

Mixtures. The two-phase field in Fig. 13(f) consists of a mixture of liquid and solid phases. As stated above, the compositions of the two phases in equilibrium at temperature T_3 are C_1 and C_2. The horizontal isothermal line connecting points 1 and 2, where these compositions intersect temperature T_3, is called a *tie line*. Similar tie lines connect the coexisting phases throughout all two-phase fields (areas) in binary and (volumes) in ternary systems, while *tie triangles* connect the coexisting phases throughout all three-phase regions (volumes) in ternary systems.

Eutectic phase diagrams, a feature of which is a field where there is a mixture of two solid phases, also can be constructed from Gibbs energy curves. Consider the temperatures indicated on the phase diagram in Fig. 14(f) and the Gibbs energy curves for these temperatures (Fig. 14a-e). When the points of tangency on the energy curves are transferred to the diagram, the typical shape of a eutectic system results. The mixture of solid α and ß that forms upon cooling through the eutectic point k has a special microstructure, as discussed later.

Binary phase diagrams that have three-phase reactions other than the eutectic reaction, as well as diagrams with multiple three-phase reactions, also can be constructed from appropriate Gibbs energy curves. Likewise, Gibbs energy surfaces and tangential planes can be used to construct ternary phase diagrams.

Curves and Intersections. Thermodynamic principles also limit the shape of the various boundary curves (or surfaces) and their intersections. For example, see the *PT* diagram shown in Fig. 2. The Clausius-Clapeyron equation requires that at the intersection of the triple curves in such a diagram, the angle between adjacent curves should never exceed 180° or, alternatively, the extension of each triple curve between two phases must lie within the field of third phase.

The angle at which the boundaries of two-phase fields meet also is limited by thermodynamics. That is, the angle must be such that the extension of each beyond the point of intersection projects into a two-phase field, rather than a one-phase field. An example of correct intersections can be

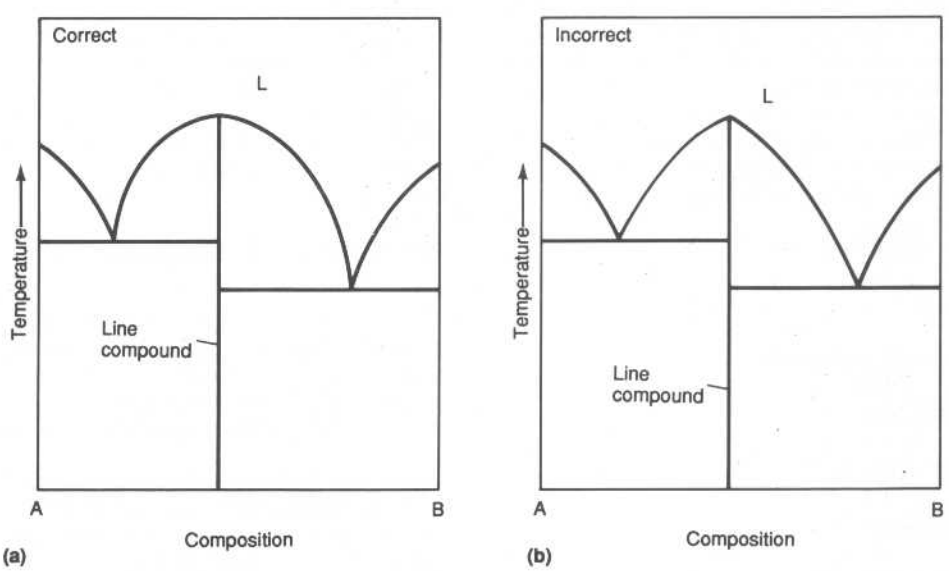

Fig. 17 Schematic diagrams of binary systems containing congruent-melting compounds but having no association of the component atoms in the melt common. The diagram in (a) is consistent with the Gibbs-Konovalov Rule, whereas that in (b) violates the rule. Source: 81Goo

Typical Phase-Rule Violations

(See Fig. 18)

1. A two-phase field cannot be extended to become part of a pure-element side of a phase diagram at zero solute. In example 1, the liquidus and the solidus must meet at the melting point of the pure element.
2. Two liquidus curves must meet at one composition at a eutectic temperature.
3. A tie line must terminate at a phase boundary.
4. Two solvus boundaries (or two liquidus, or two solidus, or a solidus and a solvus) of the same phase must meet (i.e., intersect) at one composition at an invariant temperature. (There should not be two solubility values for a phase boundary at one temperature.)
5. A phase boundary must extrapolate into a two-phase field after crossing an invariant point. The validity of this feature, and similar features related to invariant temperatures, is easily demonstrated by constructing hypothetical free-energy diagrams slightly below and slightly above the invariant temperature and by observing the relative positions of the relevant tangent points to the free energy curves. After intersection, such boundaries can also be extrapolated into metastable regions of the phase diagram. Such extrapolations are sometimes indicated by dashed or dotted lines.
6. Two single-phase fields (α and β) should not be in contact along a horizontal line. (An invariant-temperature line separates two-phase fields in contact.)
7. A single-phase field (α in this instance) should not be apportioned into subdivisions by a single line. Having created a horizontal (invariant) line at 6 (which is an error), there may be a temptation to extend this line into a single-phase field, α, creating an additional error.
8. In a binary system, an invariant-temperature line should involve equilibrium among three phases.
9. There should be a two-phase field between two single-phase fields (Two single phases cannot touch except at a point. However, second-order and higher-order transformations may be exceptions to this rule.)
10. When two phase boundaries touch at a point, they should touch at an extremity of temperature.
11. A touching liquidus and solidus (or any two touching boundaries) must have a horizontal common tangent at the congruent point. In this instance, the solidus at the melting point is too "sharp" and appears to be discontinuous.
12. A local minimum point in the lower part of a single-phase field (in this instance, the liquid) cannot be drawn without an additional boundary in contact with it. (In this instance, a horizontal monotectic line is most likely missing.)
13. A local maximum point in the lower part of a single-phase field cannot be drawn without a monotectic, monotectoid, syntectic, and sintectoid reaction occurring below it at a lower temperature. Alternatively, a solidus curve must be drawn to touch the liquidus at point 13.
14. A local maximum point in the upper part of a single-phase field cannot be drawn without the phase boundary touching a reversed monotectic, or a monotectoid, horizontal reaction line coinciding with the temperature of the maximum. When a 14 type of error is introduced, a minimum may be created on either side (or on one side) of 14. This introduces an additional error, which is the opposite of 13, but equivalent to 13 in kind.
15. A phase boundary cannot terminate within a phase field. (Termination due to lack of data is, of course, often shown in phase diagrams, but this is recognized to be artificial.)
16. The temperature of an invariant reaction in a binary system must be constant. (The reaction line must be horizontal.)
17. The liquidus should not have a discontinuous sharp peak at the melting point of a compound. (This rule is not applicable if the liquid retains the molecular state of the compound, i.e., in the situation of an ideal association.)
18. The compositions of all three phases at an invariant reaction must be different.
19. A four-phase equilibrium is not allowed in a binary system.
20. Two separate phase boundaries that create a two-phase field between two phases in equilibrium should not cross each other.

Problems Connected With Phase-Boundary Curvatures

Although phase rules are not violated, three additional unusual situations (21, 22, and 23) have also been included in Fig. 18. In each instance, a more subtle thermodynamic problem may exist related to these situations. Examples are discussed below where several thermodynamically unlikely diagrams are considered. The problems with each of these situations involve an indicated rapid change of slope of a phase boundary. If such situations are to be associated with realistic thermodynamics, the temperature (or the composition) dependence of the thermodynamic functions of the phase (or phases) involved would be expected to show corresponding abrupt and unrealistic variations in the phase diagram regions where such abrupt phase boundary changes are proposed, without any clear reason for them. Even the onset of ferromagnetism in a phase does not normally cause an abrupt change of slope of the related phase boundaries. The unusual changes of slope considered here are:

21. Two inflection points are located too closely to each other.
22. An abrupt reversal of the boundary direction (more abrupt than a typical smooth "retrograde"). This particular change can occur only if there is an accompanying abrupt change in the temperature dependence of the thermodynamic properties of either of the two phases involved (in this instance, δ or λ in relation to the boundary). The boundary turn at 22 is very unlikely to be explained by any realistic change in the composition dependence of the Gibbs energy functions.
23. An abrupt change in the slope of a single-phase boundary. This particular change can occur only by an abrupt change in the composition dependence of the thermodynamic properties of the single phase involved (in this instance, the δ phase). It cannot be explained by any possible abrupt change in the temperature dependence of the Gibbs energy function of the phase. (If the temperature dependence were involved, there would also be a change in the boundary of the ε phase.)

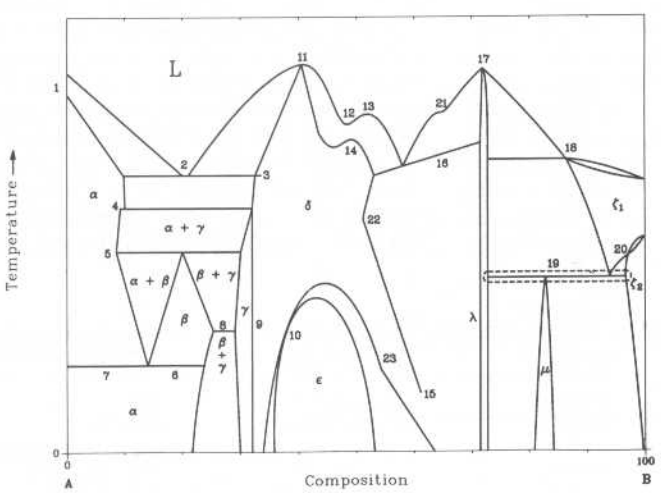

Fig. 18 Hypothetical binary phase diagram showing many typical errors of construction. See the accompanying text for discussion of the errors at points 1 to 23. Source: 91Oka1

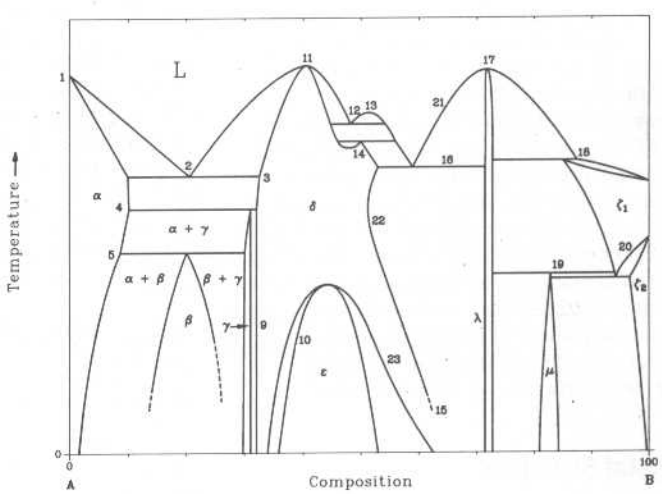

Fig. 19 Error-free version of the phase diagram shown in Fig. 18. Source: 91Oka1

seen in Fig. 6(b), where both the solidus and solvus lines are concave. However, the curvature of both boundaries need not be concave; Fig. 15 shows two equally acceptable (but unlikely) intersections where convex and concave lines are mixed.

Congruent Transformations. The *congruent point* on a phase diagram is where different phases of same composition are in equilibrium. The *Gibbs-Konovalov Rule* for congruent points, which was developed by Dmitry Konovalov from a thermodynamic expression given by J. Willard Gibbs, states that the slope of phase boundaries at congruent transformations must be zero (horizontal). Examples of correct slope at the maximum and minimum points on liquidus and solidus curves can be seen in Fig. 4. Often, the inner curve on a diagram such as that shown in Fig. 4 is erroneously drawn with a sharp inflection (see Fig. 16).

A similar common construction error is found in the diagrams of systems containing congruently melting compounds (such as the line compounds shown in Fig. 17) but having little or no association of the component atoms in the melt (as with most metallic systems). This type of error is especially common in partial diagrams, where one or more system components is a compound instead of an element. (The slope of liquidus and solidus curves, however, must *not* be zero when they terminate at an element, or at a compound having complete association in the melt.)

Common Construction Errors. Hiroaki Okamoto and Thaddeus Massalski have prepared the hypothetical binary phase shown in Fig. 18, which exhibits many typical errors of construction (marked as points 1 to 23). The explanation for each error is given in the accompanying text; one possible error-free version of the same diagram is shown in Fig. 19.

Higher-Order Transitions. The transitions considered in this Introduction up to this point have been limited to the common thermodynamic types called *first-order transitions*—that is, changes involving distinct phases having different lattice parameters, enthalpies, entropies, densities, and so on. Transitions not involving discontinuities in composition, enthalpy, entropy, or molar volume are called *higher-order transitions* and occur less frequently. The change in the magnetic quality of iron from ferromagnetic to paramagnetic as the temperature is raised above 771 °C (1420 °F) is an example of a second-order transition: no phase change is involved and the Gibbs phase rule does not come into play in the transition. Another example of a higher-order transition is the continuous change from a random arrangement of the various kinds of atoms in a multicomponent crystal structure (a *disordered structure*) to an arrangement where there is some degree of *crystal ordering* of the atoms (an *ordered structure*, or *superlattice*), or the reverse reaction.

Crystal Structure

A *crystal* is a solid consisting of atoms or molecules arranged in a pattern that is repetitive in three dimensions. The arrangement of the atoms or molecules in the interior of a crystal is called its *crystal structure*. The *unit cell* of a crystal is the smallest pattern of arrangement that can be contained in a parallelepiped, the edges of which form the *a*, *b*, and *c* axes of the crystal. The three-dimensional aggregation of unit cells in the crystal forms a *space lattice*, or *Bravais lattice* (see Fig. 20).

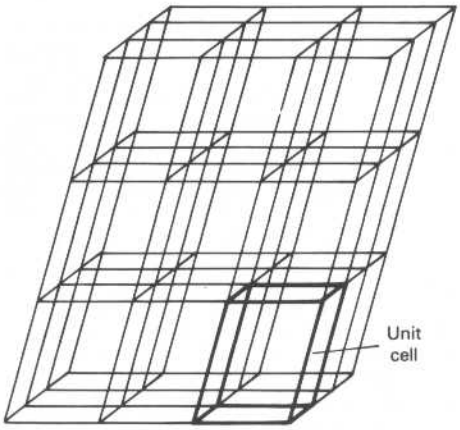

Fig. 20 A space lattice

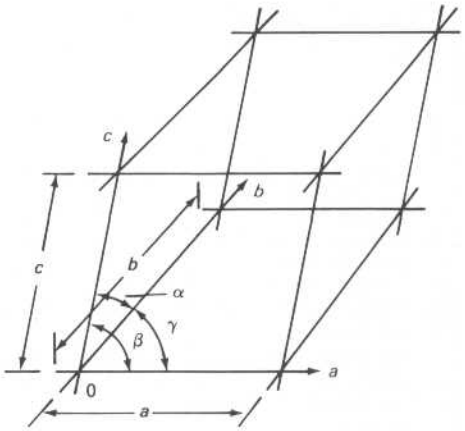

Fig. 21 Crystal axes and unit-cell edge lengths. Unit-cell faces are shown, but to avoid confusion they are not labeled.

Crystal Systems. Seven different *crystal systems* are recognized in crystallography, each having a different set of axes, unit-cell edge lengths, and interaxial angles (see Table 2). Unit-cell *edge lengths* *a*, *b*, and *c* are measured along the corresponding *a*, *b*, and *c* axes (see Fig. 21). Unit-cell faces are identified by capital letters: face *A* contains axes *b* and *c*, face *B* contains *c* and *a*, and face *C* contains *a* and *b*. (Faces are not labeled in Fig. 21.) *Interaxial angle* α occurs in face *A*, angle β in face *B*, and angle γ in face *C* (see Fig. 21).

Lattice Dimensions. It should be noted that the unit-cell edge lengths and interaxial angles are unique for each crystalline substance. The unique edge lengths are called *lattice parameters*. The term *lattice constant* also has been used for the length of an edge, but the values of edge length are not constant, varying with composition within a phase field and also with temperature due to thermal expansion and contraction. (Reported lattice parameter values are assumed to be room-temperature values unless otherwise specified.) Interaxial angles other than 90° or 120° also can change slightly with changes in composition. When the edges of the unit cell are not equal in all three directions, all unequal lengths must be stated to completely define the crystal. The same is true if all interaxial angles are not equal. When defining the unit-cell size of an alloy phase, the possibility of crystal ordering occurring over several unit cells should be considered. For example, in the copper-gold system, a superlattice forms that is made up of 10 cells of the disordered lattice, creating what is called *long-period ordering*.

Lattice Points. As shown in Fig. 20, a space lattice can be viewed as a three-dimensional network of straight lines. The intersections of the lines (called *lattice points*) represent locations in space for the same kind of atom or group of atoms of identical composition, arrangement, and orientation. There are five basic arrangements for lattice points within a unit cell. The first four are: primitive (simple), having lattice points solely at cell corners; base-face centered (end-centered), having lattice points centered on the *C* faces, or ends of the cell; all-face centered, having lattice points centered on all faces; and innercentered (body-centered), having lattice points at the center of the volume of the unit cell. The fifth arrangement, the primitive rhombohedral unit cell, is considered a separate basic arrangement, as shown in the following section on crystal structure nomenclature. These five basic arrangements are identified by capital letters as follows: *P* for the primitive cubic, *C* for the cubic cell with lattice points on the two *C* faces, *F* for all-face-centered cubic, *I* for innercentered (body-centered) cubic, and *R* for primitive rhombohedral.

Table 2 Relationships of edge lengths and of interaxial angles for the seven crystal systems

Crystal system	Edge lengths	Interaxial angles	Examples
Triclinic (anorthic)	$a \neq b \neq c$	$\alpha \neq \beta \neq \gamma \neq 90°$	HgK
Monoclinic	$a \neq b \neq c$	$\alpha = \gamma = 90° \neq \beta$	β-S; $CoSb_2$
Orthorhombic	$a \neq b \neq c$	$\alpha = \beta = \gamma = 90°$	α-S; Ga; Fe_3C (cementite)
Tetragonal	$a = b \neq c$	$\alpha = \beta = \gamma = 90°$	β-Sn (white); TiO_2
Hexagonal	$a = b \neq c$	$\alpha = \beta = 90°$; $\gamma = 120°$	Zn; Cd; NiAs
Rhombohedral(a)	$a = b = c$	$\alpha = \beta = \gamma \neq 90°$	As; Sb; Bi; calcite
Cubic	$a = b = c$	$\alpha = \beta = \gamma = 90°$	Cu; Ag; Au; Fe; NaCl

(a) Rhombohedral crystals (sometimes called trigonal) also can be described by using hexagonal axes (rhombohedral-hexagonal).

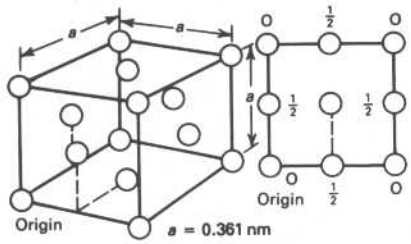

Face-centered cubic: Fm$\bar{3}$m, Cu

cF4

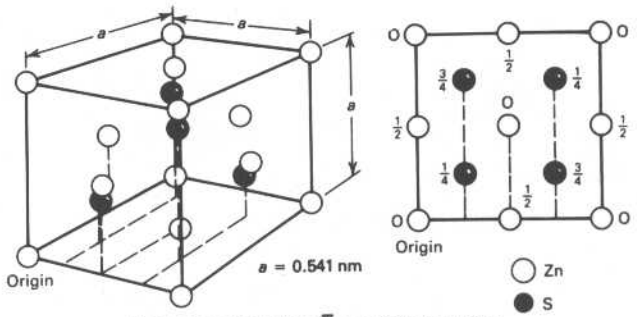

Face-centered cubic: F$\bar{4}$3*m*, ZnS (sphalerite)

cF8

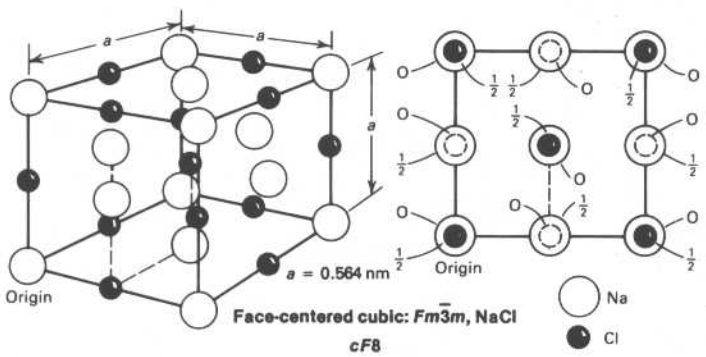

Face-centered cubic: *Fm*$\bar{3}$*m*, NaCl

cF8

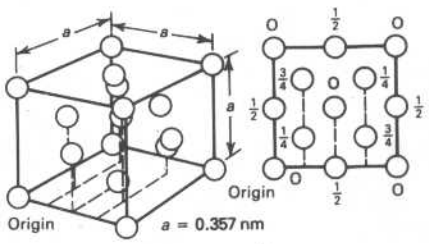

Face-centered cubic: *Fd*$\bar{3}$*m*, C (diamond)

cF8

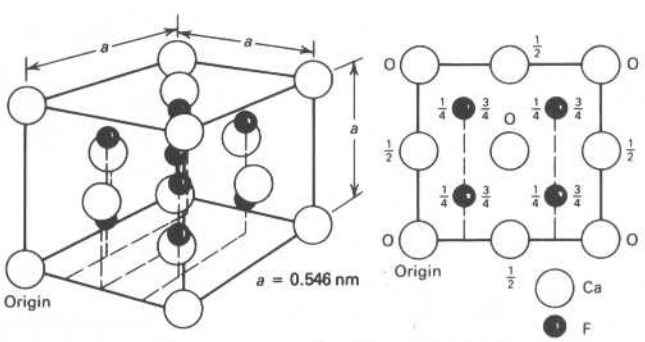

Face-centered cubic: *Fm*$\bar{3}$*m*, CaF_2 (fluorite)

cF12

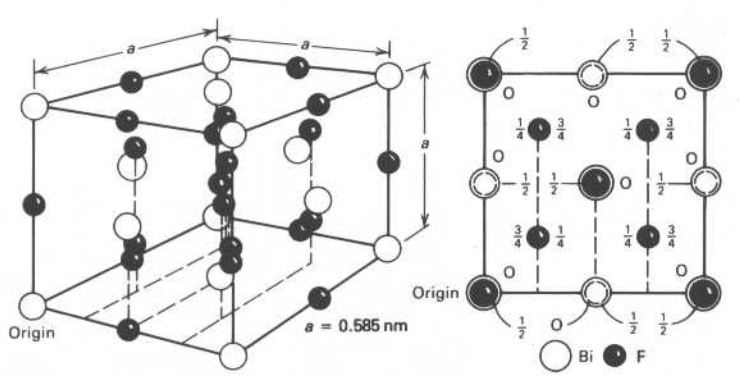

Face-centered cubic: superlattice: *Fm*$\bar{3}$*m*, BiF_3

cF16

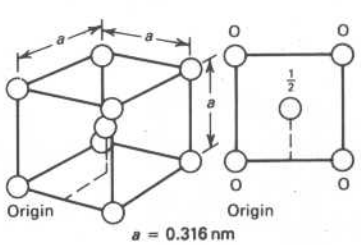

Body-centered cubic: *Im*$\bar{3}$*m*, W

cI2

Fig. 22 Schematic drawings of the unit cells and ion positions for some simple metal crystals, arranged alphabetically according to Pearson symbol. Also listed are the space lattice and crystal system, space-group notation, and prototype for each crystal. Reported lattice parameters are for the prototype crystal. **(continued)**

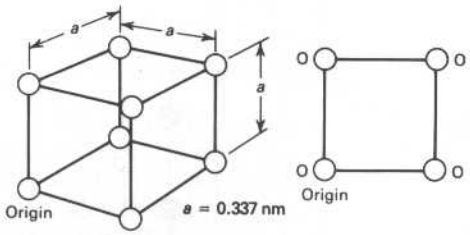

Primitive cubic: $Pm\bar{3}m$, αPo
cP1

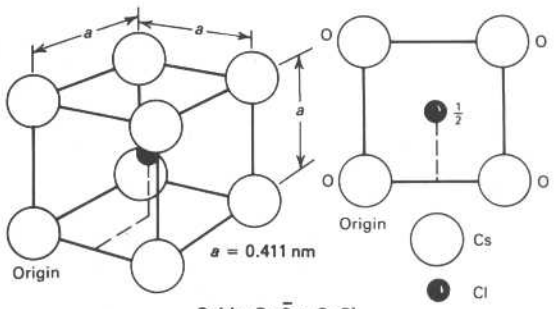

Cubic: $Pm\bar{3}m$, CsCl
cP2

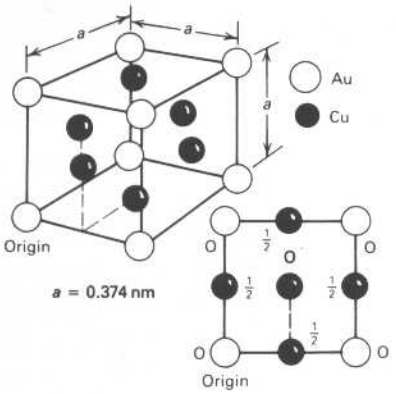

Cubic superlattice: $Pm\bar{3}m$, $AuCu_3$
cP4

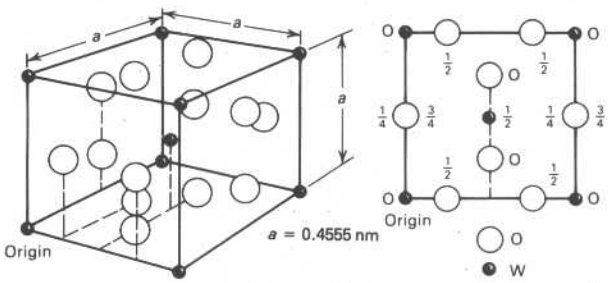

Cubic: $Pm\bar{3}n$, Cr_3Si
cP8

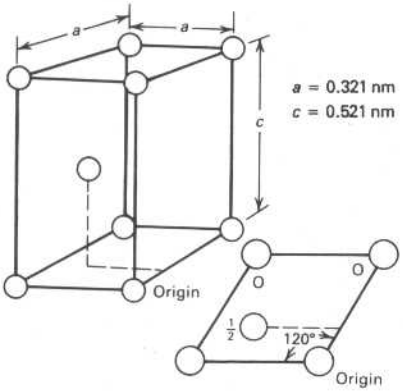

Close-packed hexagonal: $P6_3/mmc$, Mg
hP2

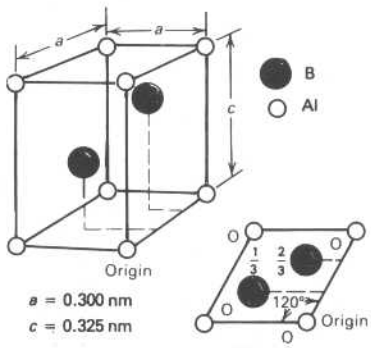

Hexagonal: $P6/mmm$, AlB_2
hP3

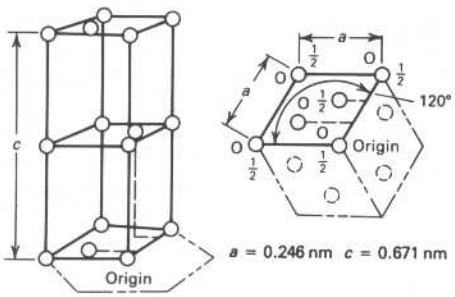

Hexagonal: $P6_3/mmc$, C (graphite)
hP4

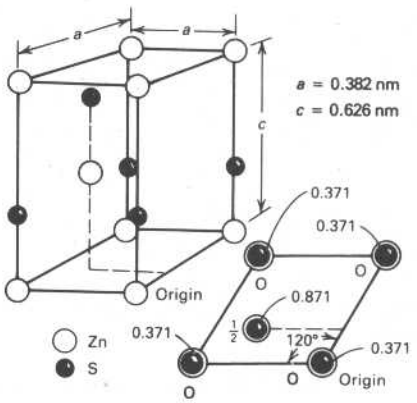

Hexagonal: $P6_3mc$, ZnS (wurtzite)
hP4

Fig. 22 Schematic drawings of the unit cells and ion positions for some simple metal crystals, arranged alphabetically according to Pearson symbol. Also listed are the space lattice and crystal system, space-group notation, and prototype for each crystal. Reported lattice parameters are for the prototype crystal. **(continued)**

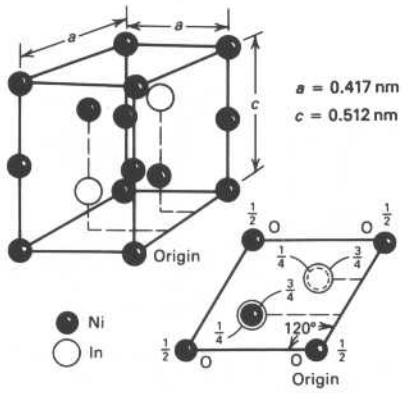

Hexagonal: $P6_3/mmc$, $InNi_2$
hP6

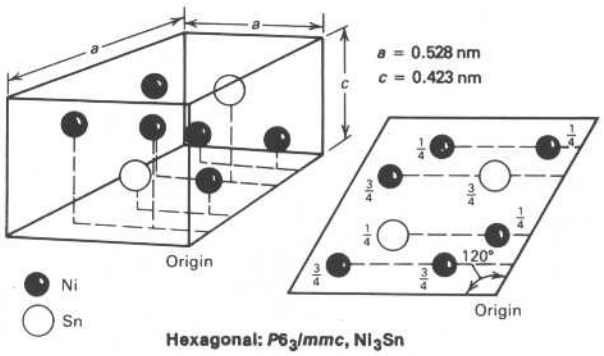

Hexagonal: $P6_3/mmc$, Ni_3Sn
hP8

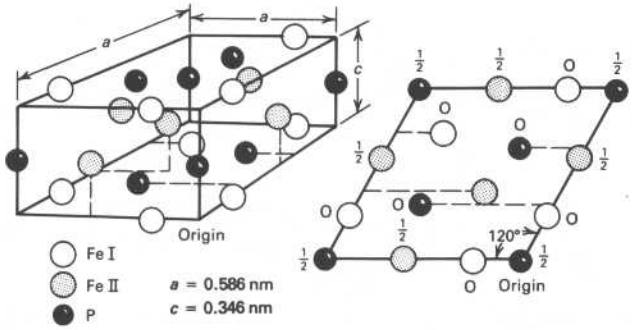

Hexagonal: $P\bar{6}2m$, Fe_2P
hP9

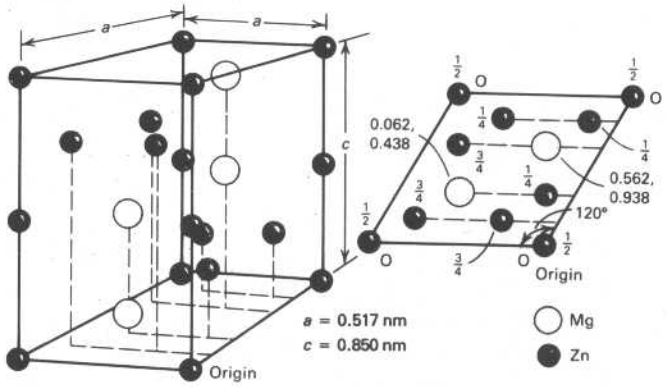

Hexagonal: $P6_3/mmc$, $MgZn_2$
hP12

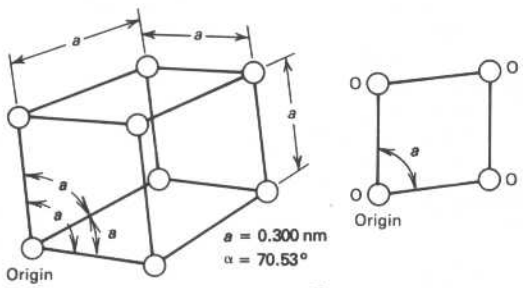

Rhombohedral: $R\bar{3}m$, α Hg
hR1

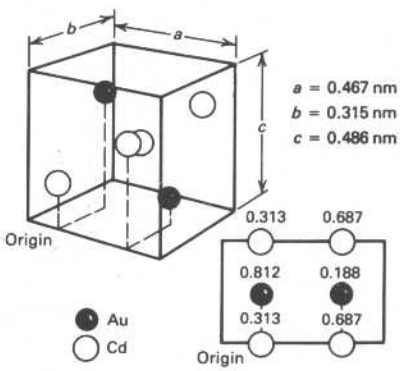

Orthorhombic: *Pmma*, AuCd
oP4

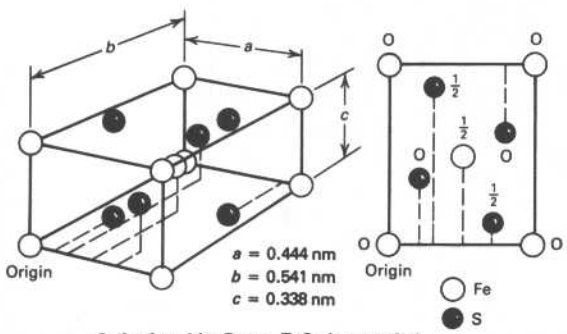

Orthorhombic: *Pnnm*, FeS_2 (marcasite)
oP6

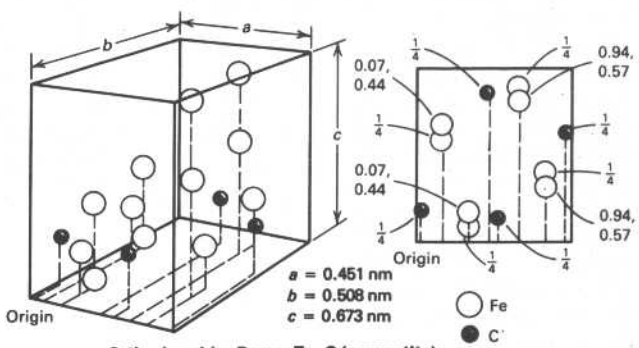

Orthorhombic: *Pnma*, Fe_3C (cementite)
oP16

Fig. 22 Schematic drawings of the unit cells and ion positions for some simple metal crystals, arranged alphabetically according to Pearson symbol. Also listed are the space lattice and crystal system, space-group notation, and prototype for each crystal. Reported lattice parameters are for the prototype crystal. **(continued)**

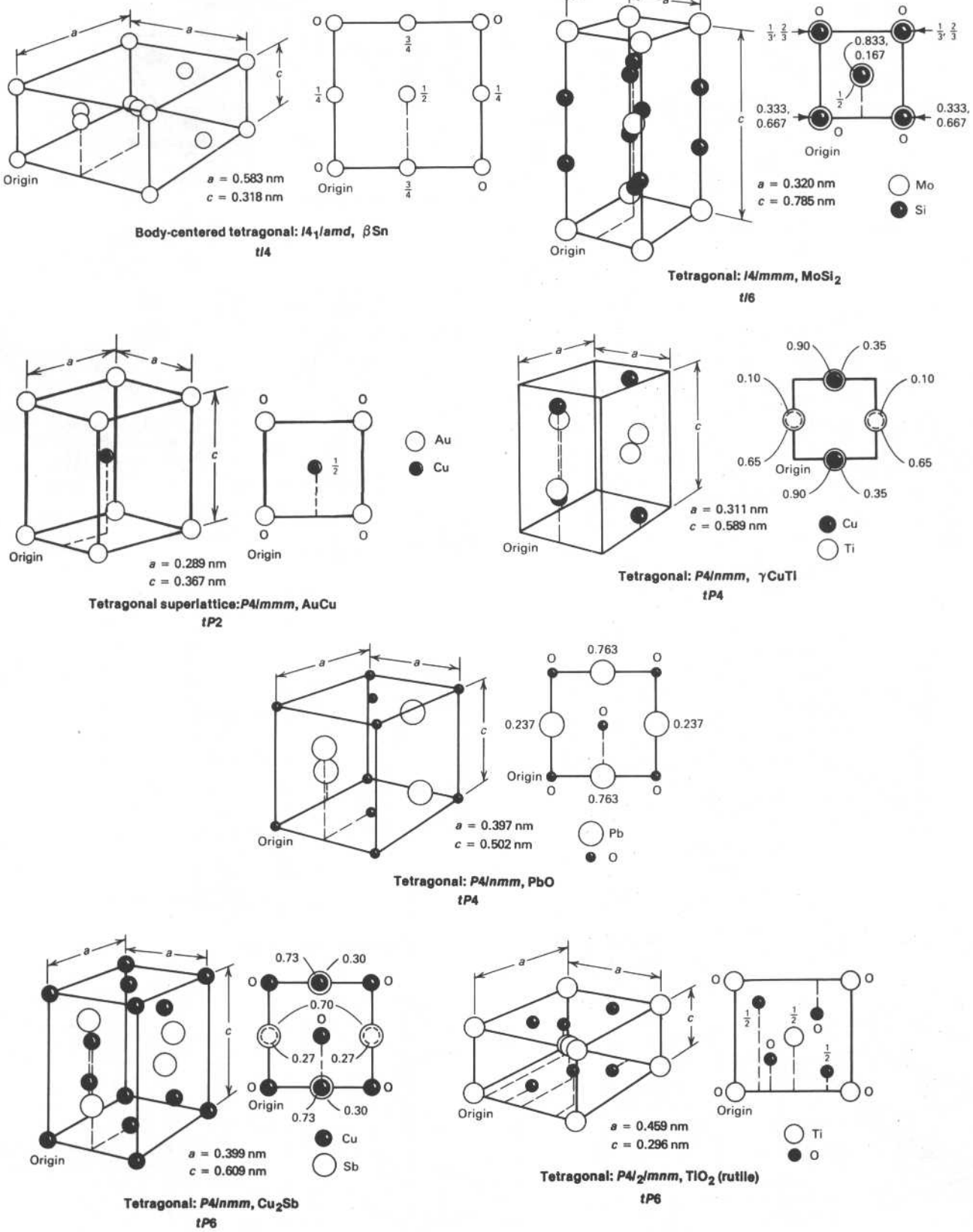

Fig. 22 Schematic drawings of the unit cells and ion positions for some simple metal crystals, arranged alphabetically according to Pearson symbol. Also listed are the space lattice and crystal system, space-group notation, and prototype for each crystal. Reported lattice parameters are for the prototype crystal.

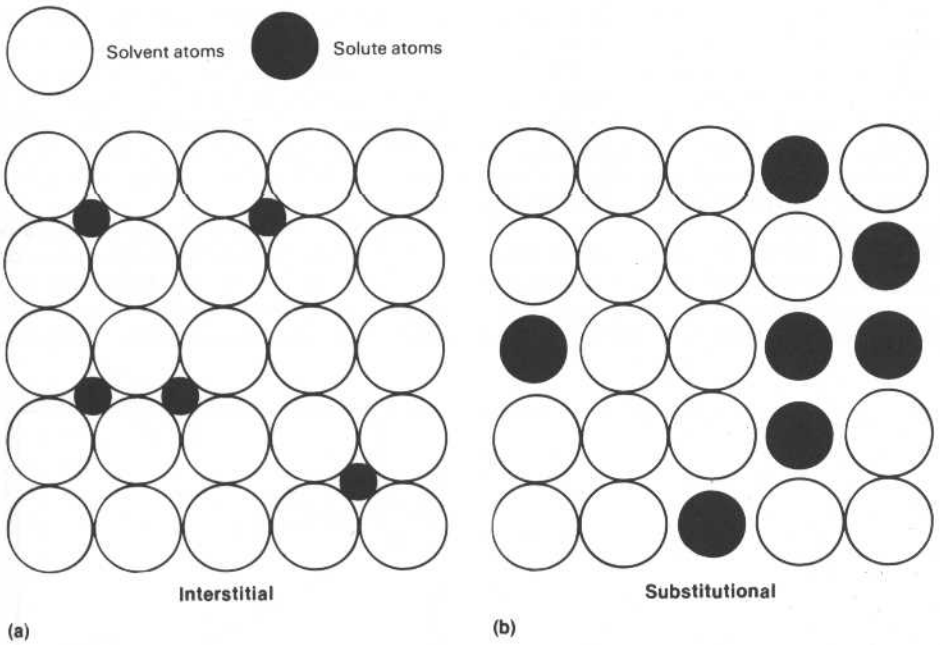

Fig. 23 Solid-solution mechanisms. (a) Interstitial. (b) Substitutional

Table 3 The 14 space (Bravais) lattices and their Pearson symbols

Crystal system	Space lattice	Pearson symbol
Triclinic (anorthic)	Primitive	*aP*
Monoclinic	Primitive	*mP*
	Base-centered(a)	*mC*
Orthorhombic	Primitive	*oP*
	Base-centered(a)	*oC*
	Face-centered	*oF*
	Body-centered	*oI*
Tetragonal	Primitive	*tP*
	Body-centered	*tI*
Hexagonal	Primitive	*hP*
Rhombohedral	Primitive	*hR*
Cubic	Primitive	*cP*
	Face-centered	*cF*
	Body-centered	*cI*

(a) The face that has a lattice point at its center may be chosen as the *c* face (the *xy* plane), denoted by the symbol *C*, or as the *a* or *b* face, denoted by *A* or *B*, because the choice of axes is arbitrary and does not alter the actual translations of the lattice.

Crystal Structure Nomenclature. When the seven crystal systems are considered together with the five space lattices, the combinations listed in Table 3 are obtained. These 14 combinations form the basis of the system of *Pearson symbols* developed by William B. Pearson, which are widely used to identify crystal types. As can be seen in Table 3, the Pearson symbol uses a small letter to identify the crystal system and a capital letter to identify the space lattice. To these is added a number equal to the number of atoms in the unit cell conventionally selected for the particular crystal type. When determining the number of atoms in the unit cell, it should be remembered that each atom that is shared with an adjacent cell (or cells) must be counted as only a fraction of an atom. The Pearson symbols for some simple metal crystals are shown in Fig. 22, along with schematic drawings illustrating the atom arrangements in the unit cell. It should be noted that in these schematic representations, the different kinds of atoms in the prototype crystal illustrated are drawn to represent their relative sizes, but in order to show the arrangements more clearly, all the atoms are shown much smaller than their true effective size in real crystals.

Several of the many possible crystal structures are so commonly found in metallic systems that they are often identified by three-letter abbreviations that combine the space lattice with the crystal system. For example, bcc is used for body-centered cubic (two atoms per unit cell), fcc for face-centered cubic (four atoms per unit cell), and cph for close-packed hexagonal (two atoms per unit cell).

Space-group notation is a symbolic description of the space lattice and symmetry of a crystal. It consists of the symbol for the space lattice followed by letters and numbers that designate the symmetry of the crystal. The space-group notation for each unit cell illustrated in Fig. 22 is identified next to it. For a more complete list of Pearson symbols and space-group notations, consult the Appendix.

To assist in classification and identification, each crystal structure type is assigned a representative substance (element or phase) having that structure. The substance selected is called the *structure prototype*. Generally accepted prototypes for some metal crystals are listed in Fig. 22.

An important source of information on crystal structures for many years was *Structure Reports* (*Strukturbericht* in German). In this publication, crystal structures were classified by a designation consisting of a capital letter (*A* for elements, *B* for AB-type phases, *C* for AB_2-type phases, *D* for other binary phases, *E* for ternary phases, and *L* for superlattices), followed by a number consecutively assigned (within each group) at the time the type was reported. To further distinguish among crystal types, inferior letters and numbers, as well as prime marks, were added to some designations. Because the Strukturbericht designation cannot be conveniently and systematically expanded to

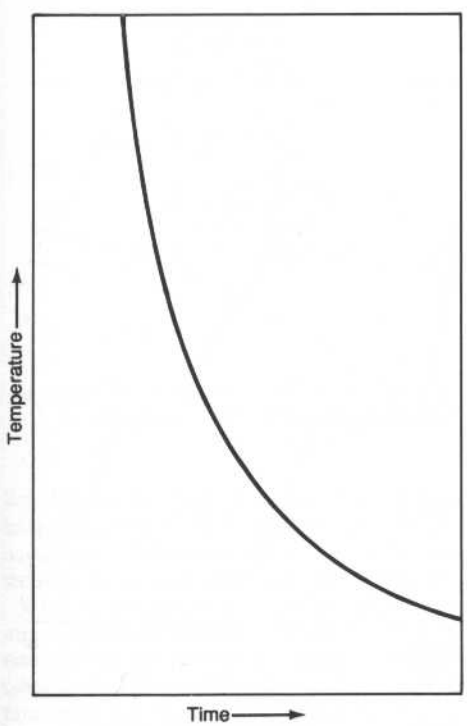

Fig. 24 Ideal cooling curve with no phase change

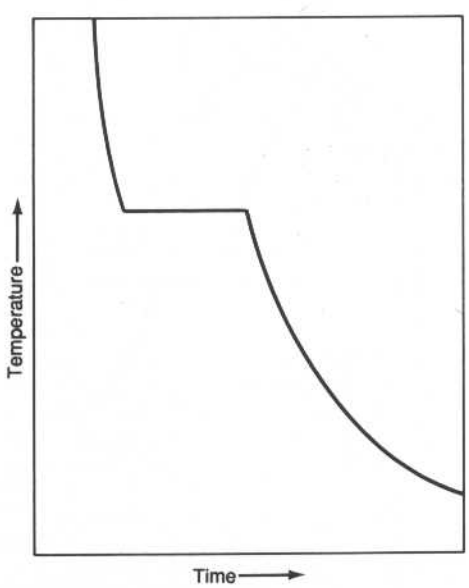

Fig. 25 Ideal freezing curve of a pure metal

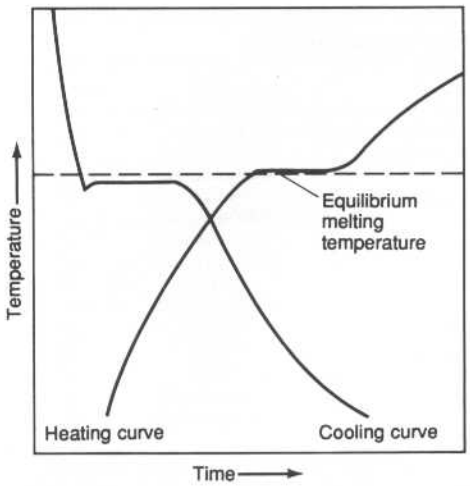

Fig. 26 Natural freezing and melting curves of a pure metal. Source: 56Rhi

cover the large variety of crystal structures currently being encountered, the system is falling into disuse.

The relations among common Pearson symbols, space groups, structure prototypes, and Strukturbericht designations for crystal systems are given in various tables in the Appendix. Crystallographic information for the metallic elements can be found in the table of allotropes in the Appendix; data for intermetallic phases of the systems included in this Volume are listed with the phase diagrams. Crystallographic data for an exhaustive list of intermediate phases are presented in 91Vil (see the Bibliography at the end of this Introduction).

Solid-Solution Mechanisms. There are only two mechanisms by which a crystal can dissolve atoms of a different element. If the atoms of the solute element are sufficiently smaller than the atoms comprising the solvent crystal, the solute atoms can fit into the spaces between the larger atoms to form an *interstitial solid solution* (see Fig. 23a). The only solute atoms small enough to fit into the interstices of metal crystals, however, are hydrogen, nitrogen, carbon, and boron. (The other small-diameter atoms, such as oxygen, tend to form compounds with metals rather than dissolve in them.) The rest of the elements dissolve in solid metals by replacing a solvent atom at a lattice point to form a *substitutional solid solution* (see Fig. 23b). When both small and large solute atoms are present, the solid solution can be both interstitial and substitutional. The addition of foreign atoms by either mechanism results in distortion of the crystal lattice and an increase in its internal energy. This distortion energy causes some hardening and strengthening of the alloy, called *solution hardening*. The solvent phase becomes saturated with the solute atoms and reaches its limit of homogeneity when the distortion energy reaches a critical value determined by the thermodynamics of the system.

Determination of Phase Diagrams

The data used to construct phase diagrams are obtained from a wide variety of measurements, many of which are conducted for reasons other than the determination of phase diagrams. No one research method will yield all of the information needed to construct an accurate diagram, and no diagram can be considered fully reliable without corroborating results obtained from the use of at least one other method.

Knowledge of the chemical composition of the sample and the individual phases is important in the construction of accurate phase diagrams. For example, the samples used should be prepared from high-purity constituents and accurately analyzed.

Chemical analysis is used in the determination of phase-field boundaries by measuring compositions of phases in a sample equilibrated at a fixed temperature by means of such methods as the diffusion-couple technique. The composition of individual phases can be measured by wet chemical methods, electron probe microanalysis, and so on.

Cooling Curves. One of the most widely used methods for the determination of phase boundaries is thermal analysis. The temperature of a sample is monitored while allowed to cool naturally from an elevated temperature (usually in the

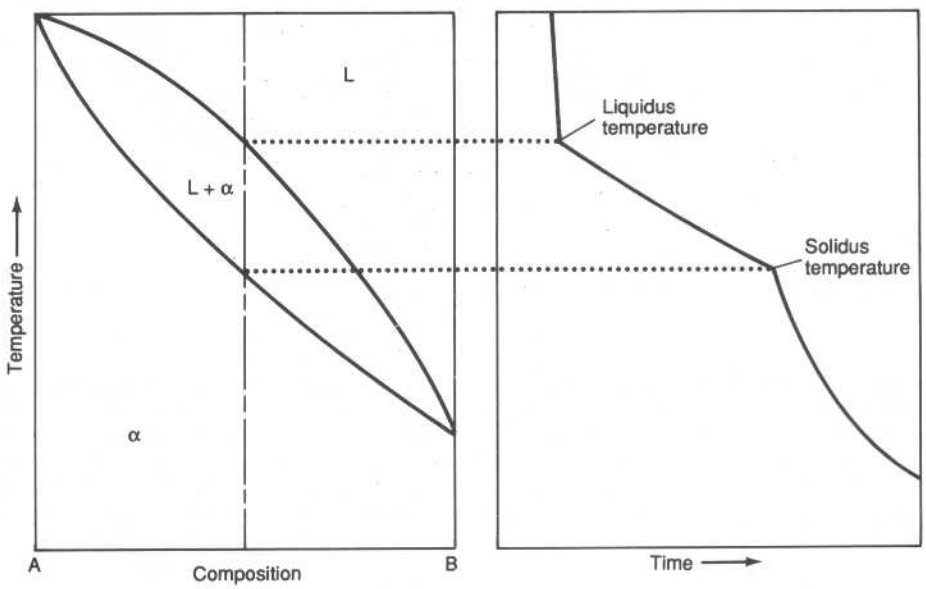

Fig. 27 Ideal freezing curve of a solid-solution alloy

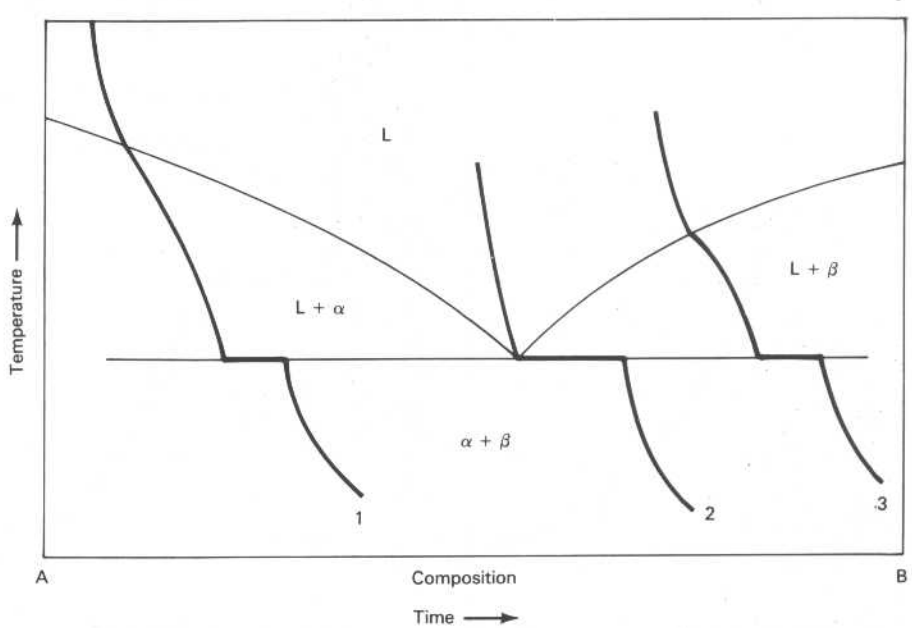

Fig. 28 Ideal freezing curves of (1) a hypoeutectic alloy, (2) a eutectic alloy, and (3) a hypereutectic alloy superimposed on a portion of a eutectic phase diagram. Source: Adapted from 66Pri

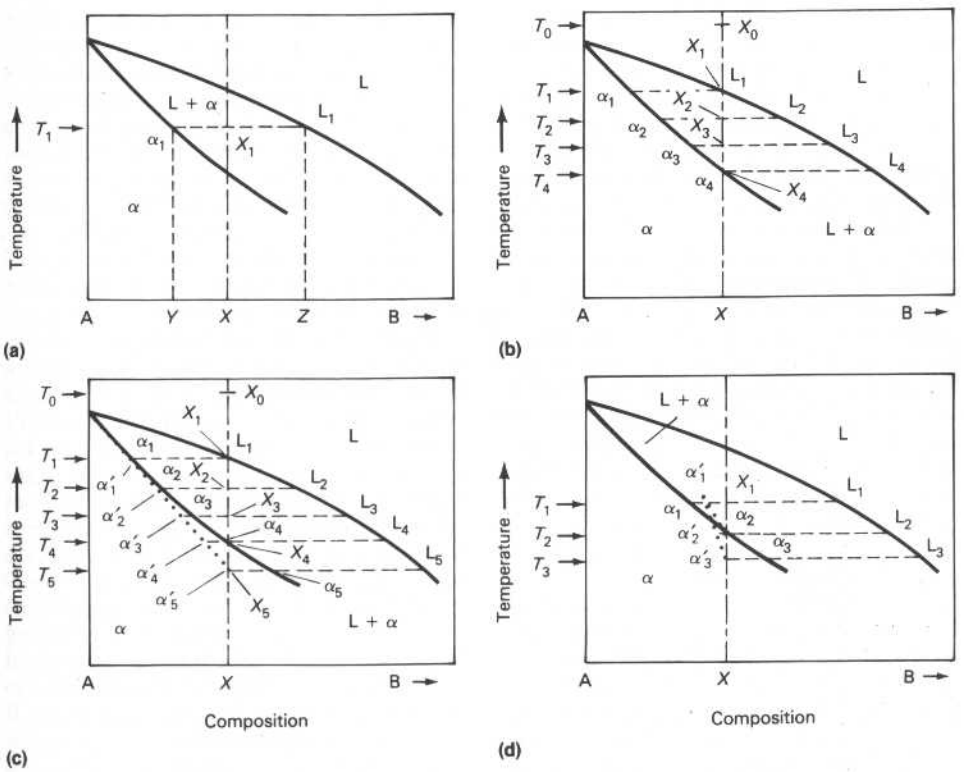

Fig. 29 Portion of a binary phase diagram containing a two-phase liquid-plus-solid field illustrating (a) the lever rule and its application to (b) equilibrium freezing, (c) nonequilibrium freezing and (d) heating of a homogenized sample. Source: 56Rhi

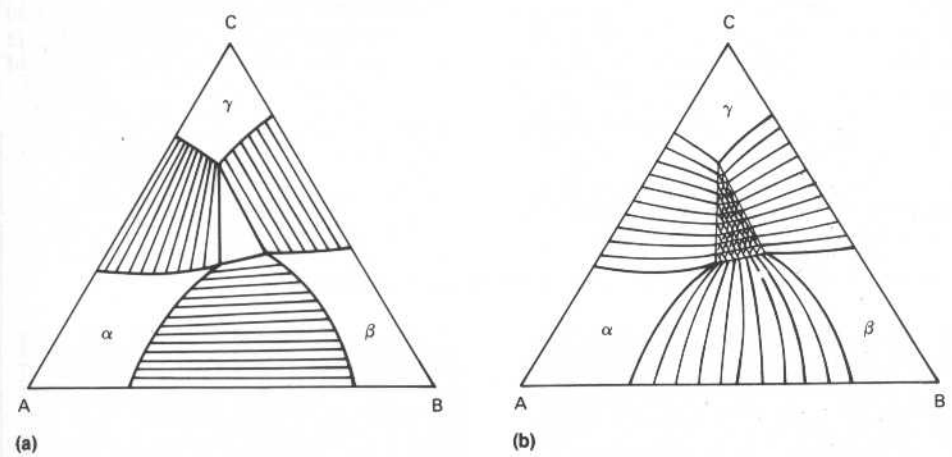

Fig. 30 Alternative systems for showing phase relationships in multiphase regions of ternary diagram isothermal sections. (a) Tie lines. (b) Phase-fraction lines. Source: 84Mor

liquid field). The shape of the resulting curves of temperature versus time are then analyzed for deviations from the smooth curve found for materials undergoing no phase changes (see Fig. 24).

When a pure element is cooled through its freezing temperature, its temperature is maintained near that temperature until freezing is complete (see Fig. 25). The true freezing/melting temperature, however, is difficult to determine from a cooling curve because of the nonequilibrium conditions inherent in such a dynamic test. This is illustrated in the cooling and heating curves shown in Fig. 26, where the effects of both supercooling and superheating can be seen. The dip in the cooling curve often found at the start of freezing is caused by a delay in the start of crystallization.

The continual freezing that occurs during cooling through a two-phase liquid-plus-solid field results in a reduced slope to the curve between the liquidus and solidus temperatures (see Fig. 27). By preparing several samples having compositions across the diagram, the shape of the liquidus curves and the eutectic temperature of eutectic system can be determined (see Fig. 28). Cooling curves can be similarly used to investigate all other types of phase boundaries.

Differential thermal analysis is a technique used to increase test sensitivity by measuring the difference between the temperature of the sample and a reference material that does not undergo phase transformation in the temperature range being investigated.

Crystal Properties. X-ray diffraction methods are used to determine both crystal structure and lattice parameters of solid phases present in a system at various temperatures (phase identification). Lattice parameter scans across a phase field are useful in determining the limits of homogeneity of the phase; the parameters change with changing composition within the single-phase field, but they remain constant once the boundary is crossed into a two-phase field.

Physical Properties. Phase transformations within a sample are usually accompanied by changes in its physical properties (linear dimensions and specific volume, electrical properties, magnetic properties, hardness, etc.). Plots of these changes versus temperature or composition can be used in a manner similar to cooling curves to locate phase boundaries.

Metallographic Methods. Metallography can be used in many ways to aid in phase diagram determination. The most important problem with metallographic methods is that they usually rely on rapid quenching to preserve (or indicate) elevated-temperature microstructures for room-temperature observation. Hot-stage metallography, however, is an alternative. The application of metallographic techniques is discussed in the section on reading phase diagrams.

Thermodynamic Modeling. Because a phase diagram is a representation of the thermodynamic relationships between competing phases, it is theoretically possible to determine a diagram by considering the behavior of relevant Gibbs energy functions for each phase present in the system and physical models for the reactions in the system. How this can be accomplished is demonstrated for the simple problem of complete solid miscibility shown in Fig. 13. The models required to calculate the possible boundaries in the more complicated diagrams usually encountered are, of course, also more complicated, and involve the use of the equations governing solutions and solution interaction originally developed for physical chemistry. Although modeling alone cannot produce a reliable phase diagram, it is a powerful technique for validating those portions of a phase diagram already derived from experimental data. In addition, modeling can be used to estimate the relations in areas of diagrams where no experimental data exist, allowing much more efficient design of subsequent experiments.

Reading Phase Diagrams

Composition Scales. Phase diagrams to be used by scientists are usually plotted in atomic percentage (or mole fraction), while those to be used by

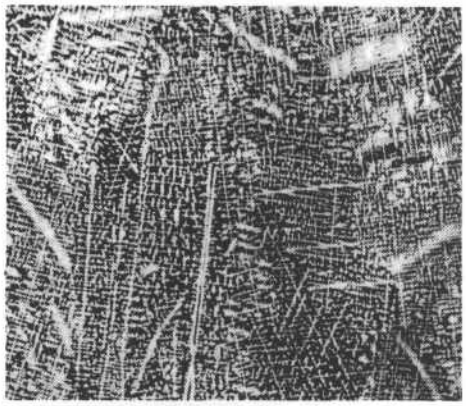

Fig. 31 Copper alloy C71500 (copper nickel, 30%) ingot. Dendritic structure shows coring: light areas are nickel rich; dark areas are low in nickel. 20×. Source: 85ASM

engineers are usually plotted in weight percentage. Conversions between weight and atomic composition also can be made using the equations given in the box below and standard atomic weights listed in the Appendix.

Lines and Labels. Magnetic transitions (Curie temperature and Néel temperature) and uncertain or speculative boundaries are usually shown in phase diagrams as nonsolid lines of various types. The components of metallic systems, which usually are pure elements, are identified in phase diagrams by their symbols. (The symbols used for chemical elements are listed in the Appendix.) Allotropes of polymorphic elements are distinguished by small (lower-case) Greek letter prefixes. (The Greek alphabet appears in the Appendix.)

Terminal solid phases are normally designated by the symbol (in parentheses) for the allotrope of the component element, such as (Cr) or (αTi). Continuous solid solutions are designated by the names of both elements, such as (Cu,Pd) or (βTi,βY).

Intermediate phases in phase diagrams are normally labeled with small (lower-case) Greek letters. However, certain Greek letters are conventionally used for certain phases, particularly disordered solutions: for example, β for disordered bcc, ζ or ε for disordered cph, γ for the γ-brass-type structure, and σ for the σCrFe-type structure.

For line compounds, a stoichiometric phase name is used in preference to a Greek letter (for example, A_2B_3 rather than δ). Greek letter prefixes are used to indicate high- and low-temperature forms of the compound (for example, αA_2B_3 for the low-temperature form and βA_2B_3 for the high-temperature form).

Lever Rule. As explained in the section on the features of phase diagrams, a tie line is an imaginary horizontal line drawn in a two-phase field connecting two points that represent two coexisting phases in equilibrium at the temperature indicated by the line. Tie lines can be used to determine the fractional amounts of the phases in equilibrium by employing the *lever rule*. The lever rule is a mathematical expression derived by the principle of conservation of matter in which the phase amounts can be calculated from the bulk composition of the alloy and compositions of the conjugate phases, as shown in Fig. 29(a).

At the left end of the line between α_1 and L_1, the bulk composition is *Y*% component B and 100 – *Y*% component A, and consists of 100% α solid solution. As the percentage of component B in the bulk composition moves to the right, some liquid appears along with the solid. With further increases in the amount of B in the alloy, more of the mixture consists of liquid, until the material becomes entirely liquid at the right end of the tie line. At bulk composition *X*, which is less than halfway to point L_1, there is more solid present than liquid. According to the lever rule, the percentages of the two phases present can be calculated as follows:

$$\%\ \text{liquid} = \frac{\text{length of line } \alpha_1 X_1}{\text{length of line } \alpha_1 L_1} \times 100$$

$$\%\ \text{solid } \alpha = \frac{\text{length of line } X_1 L_1}{\text{length of line } \alpha_1 L_1} \times 100$$

It should be remembered that the calculated amounts of the phases present are either in weight or atomic percentages and, as shown in the box on page 29, do not directly indicate the area or volume percentages of the phases observed in microstructures.

Phase-Fraction Lines. Reading the phase relationships in many ternary diagram sections (and other types of sections) often can be difficult because of the great many lines and areas present. *Phase-fraction lines* are used by some to simplify this task. In this approach, the sets of often nonparallel tie lines in the two-phase fields of isothermal sections (see Fig. 30a) are replaced with sets of curving lines of equal phase fraction (Fig. 30b). Note that the phase-fraction lines extend through the three-phase region, where they appear as a triangular network. As with tie lines, the number of phase-fraction lines used is up to the individual using the diagram. Although this approach to reading diagrams may not seem helpful for such a simple diagram, it can be a useful aid in more complicated systems. For more information on this topic, see 84Mor and 91Mor.

Solidification. Tie lines and the lever rule can be used to understand the freezing of a solid-solution alloy. Consider the series of tie lines at different temperatures shown in Fig. 29(b), all of which intersect the bulk composition X. The first crystals to freeze have the composition α_1. As the temperature is reduced to T_2 and the solid crystals grow, more A atoms are removed from the liquid than B atoms, thus shifting the composition of the remaining liquid to L_2. Therefore, during freezing, the compositions of both the layer of solid freezing out on the crystals and the remaining liquid continuously shift to higher B contents and become leaner in A. Therefore, for equilibrium to be maintained, the solid crystals must absorb B atoms from the liquid and B atoms must migrate (diffuse) from the previously frozen material into subsequently deposited layers. When this happens, the average composition of the solid material follows the solidus line to temperature T_4, where it equals the bulk composition of the alloy.

Coring. If cooling takes place too rapidly for maintenance of equilibrium, the successive layers deposited on the crystals will have a range of local compositions from their centers to their edges (a condition known as *coring*). The development of

Composition Conversions

The following equations can be used to make conversions in binary systems:

$$\text{wt\% A} = \frac{\text{at.\% A} \times \text{at. wt of A}}{(\text{at.\% A} \times \text{at. wt of A}) + (\text{at.\% B} \times \text{at. wt of B})} \times 100$$

$$\text{at.\% A} = \frac{\text{wt\% A} / \text{at. wt of A}}{(\text{at.\% A} / \text{at. wt of A}) + (\text{wt\% B} / \text{at. wt of B})} \times 100$$

The equation for converting from atomic percentages to weight percentages in higher-order systems is similar to that for binary systems, except that an additional term is added to the denominator for each additional component. For ternary systems, for example:

$$\text{wt\% A} = \frac{\text{at.\% A} \times \text{at. wt of A}}{(\text{at.\% A} \times \text{at. wt of A}) + (\text{at.\% B} \times \text{at. wt of B}) + (\text{at.\% C} \times \text{at. wt of C})} \times 100$$

$$\text{at.\% A} = \frac{\text{wt\% A} / \text{at. wt of A}}{(\text{wt\% A} / \text{at. wt of A}) + (\text{wt\% B} / \text{at. wt of B}) + (\text{wt\% C} / \text{at. wt of C})} \times 100$$

The conversion from weight to atomic percentages for higher-order systems is easy to accomplish on a computer with a spreadsheet program.

this condition is illustrated in Fig. 29(c). Without diffusion of B atoms from the material that solidified at temperature T_1 into the material freezing at T_2, the average composition of the solid formed up to that point will not follow the solidus line. Instead it will remain to the left of the solidus, following compositions α'_1 through α'_5. Note that final freezing does not occur until temperature T_5, which means that nonequilibrium solidification takes place over a greater temperature range than equilibrium freezing. Because most metals freeze by the formation and growth of "treelike" crystals, called *dendrites*, coring is sometimes called *dendritic segregation*. An example of cored dendrites is shown in Fig. 31.

Liquation. Because the lowest freezing material in a cored microstructure is segregated to the edges of the solidifying crystals (the grain boundaries), this material can remelt when the alloy sample is heated to temperatures below the equilibrium solidus line. If grain-boundary melting (called *liquation*, or "burning") occurs while the sample also is under stress, such as during hot forming, the liquefied grain boundaries will rupture and the sample will lose its ductility and be characterized as *hot short*.

Liquation also can have a deleterious effect on the mechanical properties (and microstructure) of the sample after it returns to room temperature. This is illustrated in Fig. 29(d) for a homogenized sample. If homogenized alloy X is heated into the liquid-plus-solid region for some reason (inadvertently or during welding, etc.), it will begin to melt when it reaches temperature T_2; the first liquid to appear will have the composition L_2. When the sample is heated at normal rates to temperature T_1, the liquid formed so far will have a composition L_1, but the solid will not have time to reach the equilibrium composition α_1. The average composition will instead lie at some intermediate value, such as α'_1. According to the lever rule, this means that less than the equilibrium amount of liquid will form at this temperature. If the sample is then rapidly cooled from temperature T_1, solidification will occur in the normal manner, with a layer of material having composition α_1 deposited on existing solid grains. This is followed by layers of increasing B content up to composition α_3 at temperature T_3, where all of the liquid is converted to solid. This produces coring in the previously melted regions along the grain boundaries, and sometimes even voids that decrease the strength of the sample. Homogenization heat treatment will eliminate the coring, but not the voids.

Eutectic Microstructures. When an alloy of eutectic composition (such as alloy 2 in Fig. 28) is cooled from the liquid state, the eutectic reaction occurs at the eutectic temperature, where the two distinct liquidus curves meet. At this temperature, both α and β solid phases must deposit on the grain nuclei until all of the liquid is converted to solid. This simultaneous deposition results in microstructures made up of distinctively shaped particles of one phase in a matrix of the other phase, or alternate layers of the two phases. Examples of characteristic eutectic microstructures include spheroidal, nodular, or globular; acicular (needles) or rod; and lamellar (platelets, Chinese script or dendritic, or filigreed). Each eutectic alloy has its own characteristic microstructure when slowly cooled (see Fig. 32). More rapid cooling, however, can affect the microstructure obtained (see Fig. 33). Care must be taken in characterizing eutectic structures, because elongated particles can appear nodular and flat platelets can appear elongated or needlelike when viewed in cross section.

If the alloy has a composition different from the eutectic composition (such as alloy 1 or 3 in Fig. 28), the alloy will begin to solidify before the eutectic temperature is reached. If the alloy is hypoeutectic (such as alloy 1), some dendrites of α will form in the liquid before the remaining liquid solidifies at the eutectic temperature. If the alloy is hypereutectic (such as alloy 3), the first (primary) material to solidify will be dendrites of β. The microstructure produced by slow cooling of a hypoeutectic and hypereutectic alloy will consist of relatively large particles of *primary constituent*, consisting of the phase that begins to freeze first surrounded by relatively fine eutectic structure. In many instances, the shape of the particles will show a relationship to their dendritic origin (see Fig. 34a). In other instances, the initial dendrites will have filled out somewhat into *idiomorphic particles* (particles having their own characteristic shape) that reflect the crystal structure of the phase (see Fig. 34b).

As stated earlier, cooling at a rate that does not allow sufficient time to reach equilibrium conditions will affect the resulting microstructure. For example, it is possible for an alloy in a eutectic system to obtain some eutectic structure in an alloy outside the normal composition range for such a structure. This is illustrated in Fig. 35. With relatively rapid cooling of alloy X, the composition of the solid material that forms will follow line α_1-α_4 rather than the solidus line to α_4. As a result, the last liquid to solidify will have the eutectic composition L_4, rather than L_3, and will form some eutectic structure in the microstructure. The question of what takes place when the temperature reaches T_5 is discussed later.

Eutectoid Microstructures. Because the diffusion rates of atoms are so much lower in solids than in liquids, nonequilibrium transformation is even more important in solid/solid reactions (such as the eutectoid reaction) than in liquid/solid reactions (such as the eutectic reaction). With slow cooling through the eutectoid tempera-

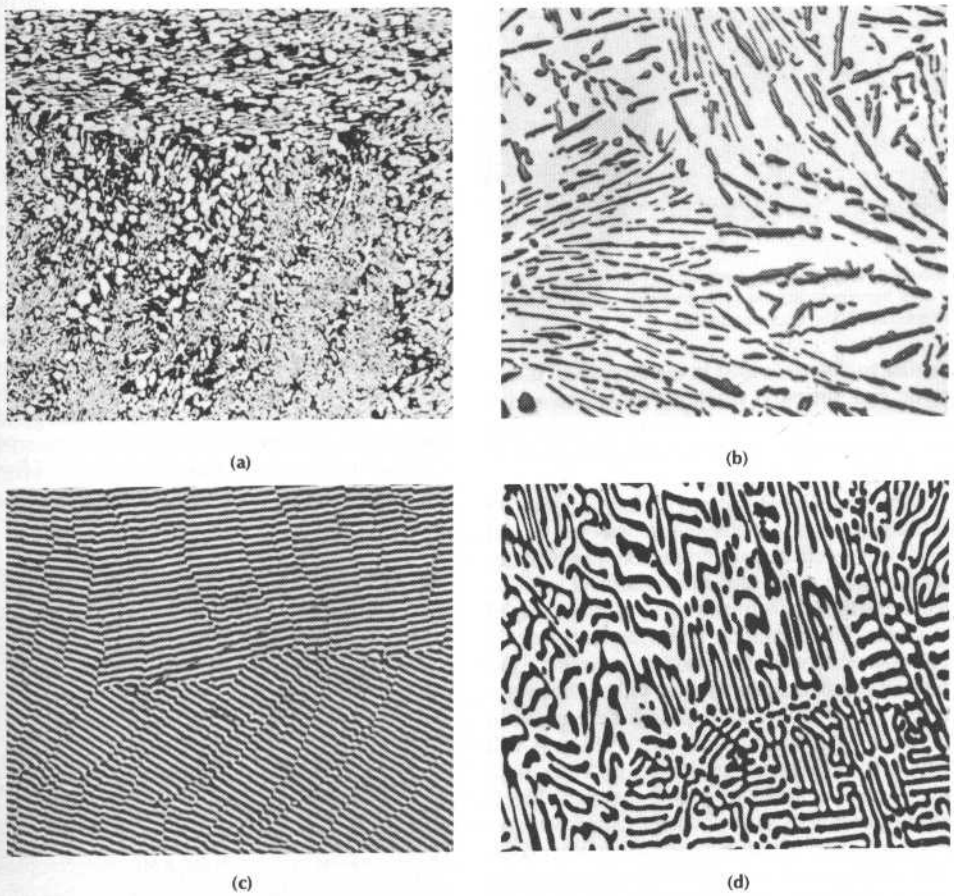

Fig. 32 Examples of characteristic eutectic microstructures in slowly cooled alloys. (a) 50Sn-50In alloy showing globules of tin-rich intermetallic phase (light) in a matrix of dark indium-rich intermetallic phase. 150×. (b) Al-13Si alloy showing an acicular structure consisting of short, angular particles of silicon (dark) in a matrix of aluminum. 200×. (c) Al-33Cu alloy showing a lamellar structure consisting of dark platelets of $CuAl_2$ and light platelets of aluminum solid solution. 180×. (d) Mg-37Sn alloy showing a lamellar structure consisting of Mg_2Sn "Chinese script" (dark) in a matrix of magnesium solid solution. 250×. Source: 85ASM

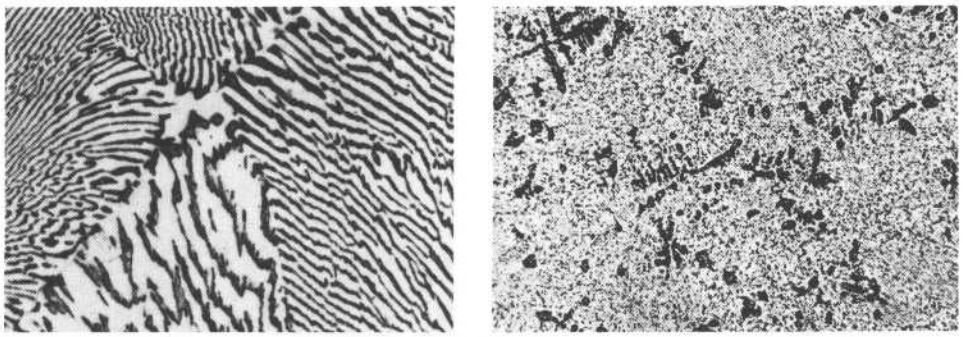

(a) (b)

Fig. 33 Effect of cooling rate on the microstructure of Sn-37Pb alloy (eutectic soft solder). (a) Slowly cooled sample shows a lamellar structure consisting of dark platelets of lead-rich solid solution and light platelets of tin. 375×. (b) More rapidly cooled sample shows globules of lead-rich solid solution, some of which exhibit a slightly dendritic structure, in a matrix of tin. 375×. Source: 85ASM

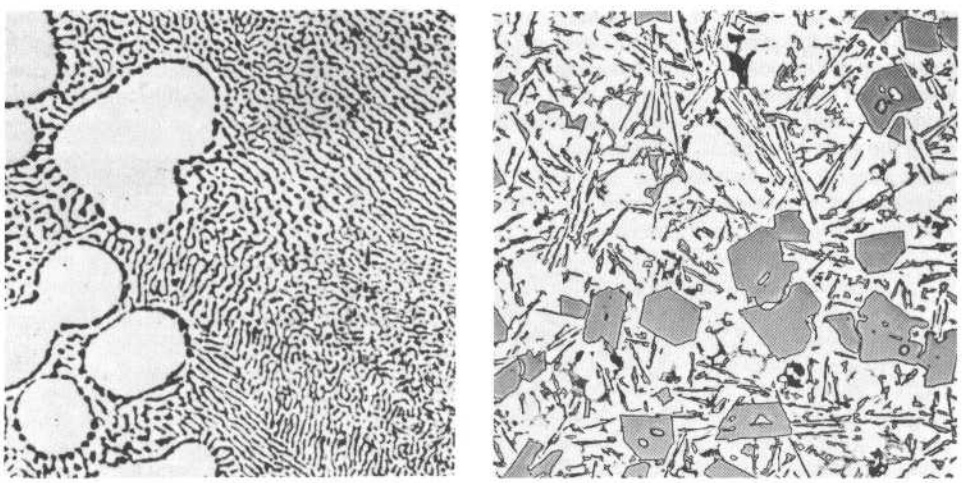

(a) (b)

Fig. 34 Examples of primary particle shape. (a) Sn-30Pb hypoeutectic alloy showing dendritic particles of tin-rich solid solution in a matrix of tin-lead eutectic. 500×. (b) Al-19Si hypereutectic alloy, phosphorus-modified, showing idiomorphic particles of silicon in a matrix of aluminum-silicon eutectic. 100×. Source: 85ASM

ture, most alloys of eutectoid composition, such as alloy 2 in Fig. 36, transform from a single-phase microstructure to a lamellar structure consisting of alternate platelets of α and β arranged in groups (or "colonies"). The appearance of this structure is very similar to lamellar eutectic structure (see Fig. 37). When found in cast irons and steels, this structure is called "pearlite" because of its shiny mother-of-pearl appearance under the microscope (especially under oblique illumination); when similar eutectoid structure is found in nonferrous alloys, it often is called "pearlite-like" or "pearlitic."

The terms *hypoeutectoid* and *hypereutectoid* have the same relationship to the eutectoid composition as hypoeutectic and hypereutectic do in a eutectic system; alloy 1 in Fig. 36 is a hypoeutectoid alloy, whereas alloy 3 is hypereutectoid. The solid-state transformation of such alloys takes place in two steps, much like the freezing of hypoeutectic and hypereutectic alloys, except that the microconstituents that form before the eutectoid temperature is reached are referred to as *proeutectoid constituents* rather than "primary."

Microstructures of Other Invariant Reactions. Phase diagrams can be used in a manner similar to that described in the discussion of eutectic and eutectoid reactions to determine the microstructures expected to result from cooling an alloy through any of the other six types of reactions listed in Table 1.

Solid-State Precipitation. If alloy X in Fig. 35 is homogenized at a temperature between T_3 and T_5, it will reach an equilibrium condition; that is, the β portion of the eutectic constituent will dissolve and the microstructure will consist solely of α grains. Upon cooling below temperature T_5, this microstructure will no longer represent equilibrium conditions, but instead will be supersaturated with B atoms. In order for the sample to return to equilibrium, some of the B atoms will tend to congregate in various regions of the sample to form colonies of new β material. The B atoms in some of these colonies, called *Guinier-Preston zones*, will drift apart, while other colonies will grow large enough to form incipient, but not distinct, particles. The difference in crystal structures and lattice parameters between the α and β phases causes lattice strain at the boundary between the two materials, thereby raising the total energy level of the sample and hardening and strengthening it. At this stage, the incipient particles are difficult to distinguish in the microstructure. Instead, there usually is only a general darkening of the structure. If sufficient time is allowed, the β regions will break away from their host grains of α and precipitate as distinct particles, thereby relieving the lattice strain and returning the hardness and strength to the former levels. This process is illustrated for a simple eutectic system, but it can occur wherever similar conditions exist in a phase diagram; that is, there is a range of alloy compositions in the system for which there is a transition on cooling from a single-solid region to a region that also contains a second solid phase, and where the boundary between the regions slopes away from the composition line as cooling continues. Several examples of such systems are shown schematically in Fig. 38.

Although this entire process is called *precipitation hardening*, the term normally refers only to the portion before much actual precipitation takes place. Because the process takes some time, the term *age hardening* is often used instead. The rate at which aging occurs depends on the level of supersaturation (how far from equilibrium), the amount of lattice strain originally developed (amount of lattice mismatch), the fraction left to be relieved (how far along the process has progressed), and the aging temperature (the mobility of the atoms to migrate). The β precipitate usually takes the form of small idiomorphic particles situated along the grain boundaries and within the grains of α phase. In most instances, the particles are more or less uniform in size and oriented in a systematic fashion. Examples of precipitation microstructures are shown in Fig. 39.

Examples of Phase Diagrams

The general principles of reading alloy phase diagrams are discussed in the preceding section. The application of these principles to actual diagrams for typical alloy systems is illustrated below.

The Copper-Zinc System. The metallurgy of brass alloys has long been of great commercial importance. The copper and zinc contents of five of the most common wrought brasses are:

UNS No.	Common name	Zinc content, wt% Nominal	Range
C23000	Red brass, 85%	15	14.0-16.0
C24000	Low brass, 80%	20	18.5-21.5
C26000	Cartridge brass, 70%	30	28.5-31.5
C27000	Yellow brass, 65%	35	32.5-37.0
C28000	Muntz metal, 60%	40	37.0-41.0

As can be seen in Fig. 40, these alloys encompass a wide range of the copper-zinc phase diagram. The alloys on the high-copper end (red brass, low brass, and cartridge brass) lie within the copper solid-solution phase field and are called alpha brasses after the old designation for this field. As expected, the microstructure of these brasses consists solely of grains of copper solid solution (see

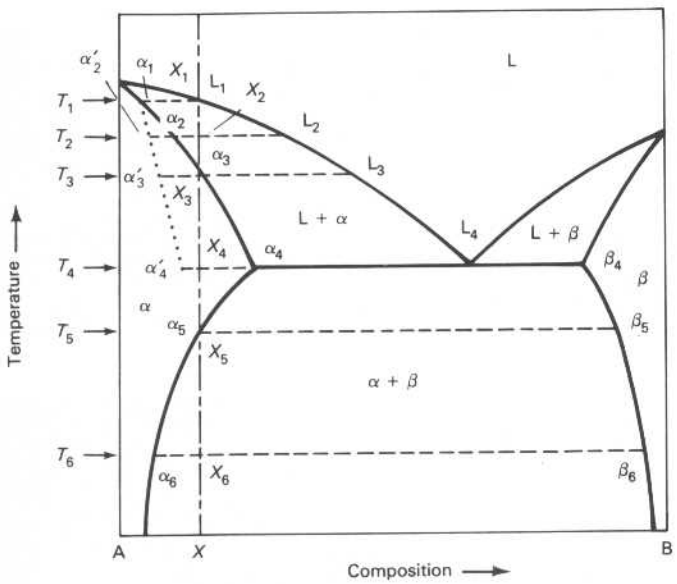

Fig. 35 Schematic binary phase diagram, illustrating the effect of cooling rate on an alloy lying outside the equilibrium eutectic transformation line. Rapid solidification into a terminal phase field can result in some eutectic structure being formed; homogenization at temperatures in the single-phase field will eliminate the eutectic structure; β phase will precipitate out of solution upon slow cooling into the α-plus-β field. Source: Adapted from 56Rhi

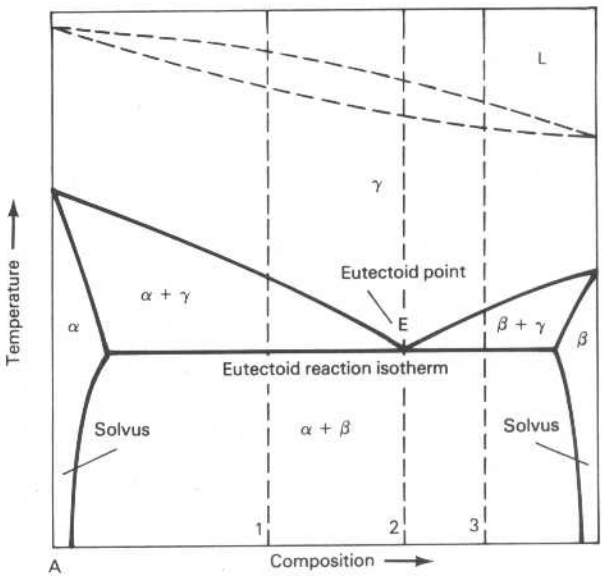

Fig. 36 Schematic binary phase diagram of a eutectoid system. Source: Adapted from 56Rhi

Fig. 41a). The strain on the copper crystals caused by the presence of the zinc atoms, however, produces solution hardening in the alloys. As a result, the strength of the brasses, in both the work-hardened and the annealed conditions, increases with increasing zinc content.

The composition range for those brasses containing higher amounts of zinc (yellow brass and Muntz metal), however, overlaps into the two-phase (Cu)-plus-β field. Therefore, the microstructure of these so-called alpha-beta alloys shows various amounts of β phase (see Fig. 41b and c), and their strengths are further increased over those of the alpha brasses.

The Aluminum-Copper System. Another alloy system of great commercial importance is aluminum-copper. Although the phase diagram of this system is fairly complicated (see Fig. 42), the alloys of concern in this discussion are limited to the region at the aluminum side of the diagram where a simple eutectic is formed between the aluminum solid solution and the θ (Al_2Cu) phase. This family of alloys (designated the 2*xxx* series) has nominal copper contents ranging from 2.3 to 6.3 wt%, making them hypoeutectic alloys.

A critical feature of this region of the diagram is the shape of the aluminum solvus line. At the eutectic temperature (548.2 °C, or 1018.8 °F), 5.65 wt% Cu will dissolve in aluminum. At lower temperatures, however, the amount of copper that can remain in the aluminum solid solution under equilibrium conditions drastically decreases, reaching less than 1% at room temperature. This is the typical shape of the solvus line for precipitation hardening; if any of these alloys are homogenized at temperatures in or near the solid-solution phase field, they can be strengthened by aging at a substantially lower temperature.

The Titanium-Aluminum, Titanium-Chromium, and Titanium-Vanadium Systems. The phase diagrams of titanium systems are domi-

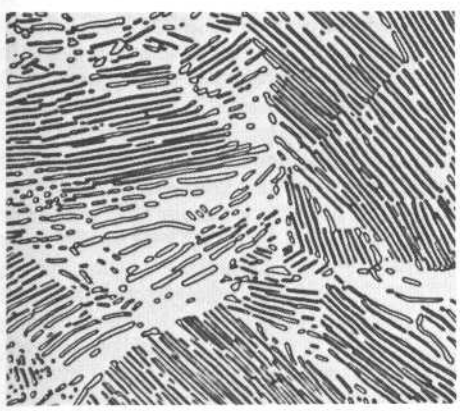

Fig. 37 Fe-0.8C alloy showing a typical pearlite eutectoid structure of alternate layers of light ferrite and dark cementite. 500×. Source: 85ASM

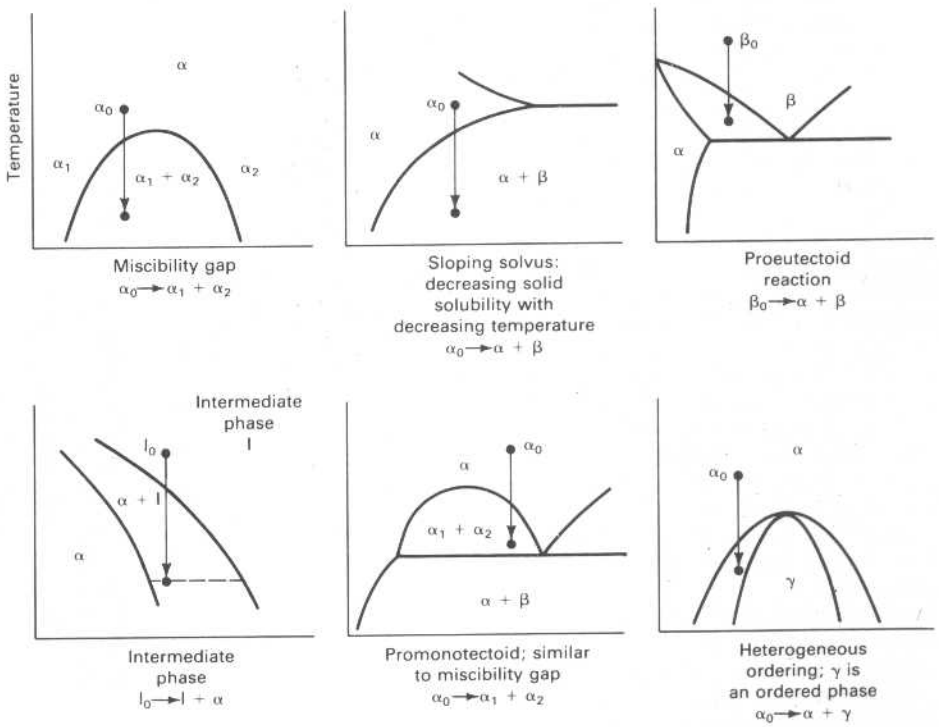

Fig. 38 Examples of binary phase diagrams that give rise to precipitation reactions. Source: 85ASM

nated by the fact that there are two allotropic forms of solid titanium: cph αTi is stable at room temperature and up to 882 °C (1620 °F); bcc βTi is stable from 882 °C (1620 °F) to the melting temperature. Most alloying elements used in commercial titanium alloys can be classified as alpha stabilizers (such as aluminum) or beta stabilizers (such as vanadium and chromium), depending on whether the allotropic transformation temperature is raised or lowered by the alloying addition (see Fig. 43). Beta stabilizers are further classified as those that are completely miscible with βTi (such as vanadium, molybdenum, tantalum, and niobium) and those that form eutectoid systems with titanium (such as chromium and iron). Tin and zirconium also are often alloyed in titanium, but instead of stabilizing either phase, they have extensive solubilities in both αTi and βTi. The microstructures of commercial titanium alloys are complicated, because most contain more than one of these four types of alloying elements.

The Iron-Carbon System. The iron-carbon diagram maps out the stable equilibrium conditions between iron and the graphitic form of carbon (see Fig. 44). Note that there are three allotropic forms of solid iron: the low-temperature phase, α; the medium-temperature phase, γ; and the high-temperature phase, δ. In addition, ferritic iron undergoes a magnetic phase transition at 771 °C (1420 °F) between the low-temperature ferromagnetic state and the higher-temperature paramagnetic state. The common name for bcc α-iron is "ferrite" (from *ferrum*, Latin for "iron"); the fcc γ phase is called "austenite" after William Roberts-Austen; bcc δ-iron is also commonly called ferrite, because (except for its temperature range) it is the same as α-iron. The main feature of the iron-carbon diagram is the presence of both a eutectic and a eutectoid reaction, along with the great difference between the solid solubilities of carbon in ferrite and austenite. It is these features that allow such a wide variety of microstructures and mechanical properties to be developed in iron-carbon alloys through proper heat treatment.

The Iron-Cementite System. In the solidification of steels, stable equilibrium conditions do not exist. Instead, any carbon not dissolved in the iron is tied up in the form of the metastable intermetallic compound, Fe_3C (also called cementite because of its hardness), rather than remaining as free graphite (see Fig. 45). It is, therefore, the iron-cementite phase diagram, rather than the iron-carbon diagram, that is important to industrial metallurgy. It should be remembered, however, that although cementite is an extremely enduring phase, given sufficient time, or the presence of a catalyzing substance, it will break down to iron and carbon. In cast irons, silicon is the catalyzing agent that allows free carbon (flakes, nodules, etc.) to appear in the microstructure (see Fig. 46).

The boundary lines on the iron-carbon and iron-cementite diagrams that are important to the heat treatment of steel and cast iron have been assigned special designations, which have been found useful in describing the treatments. These lines, where thermal arrest takes place during heating or cooling due to a solid-state reaction,

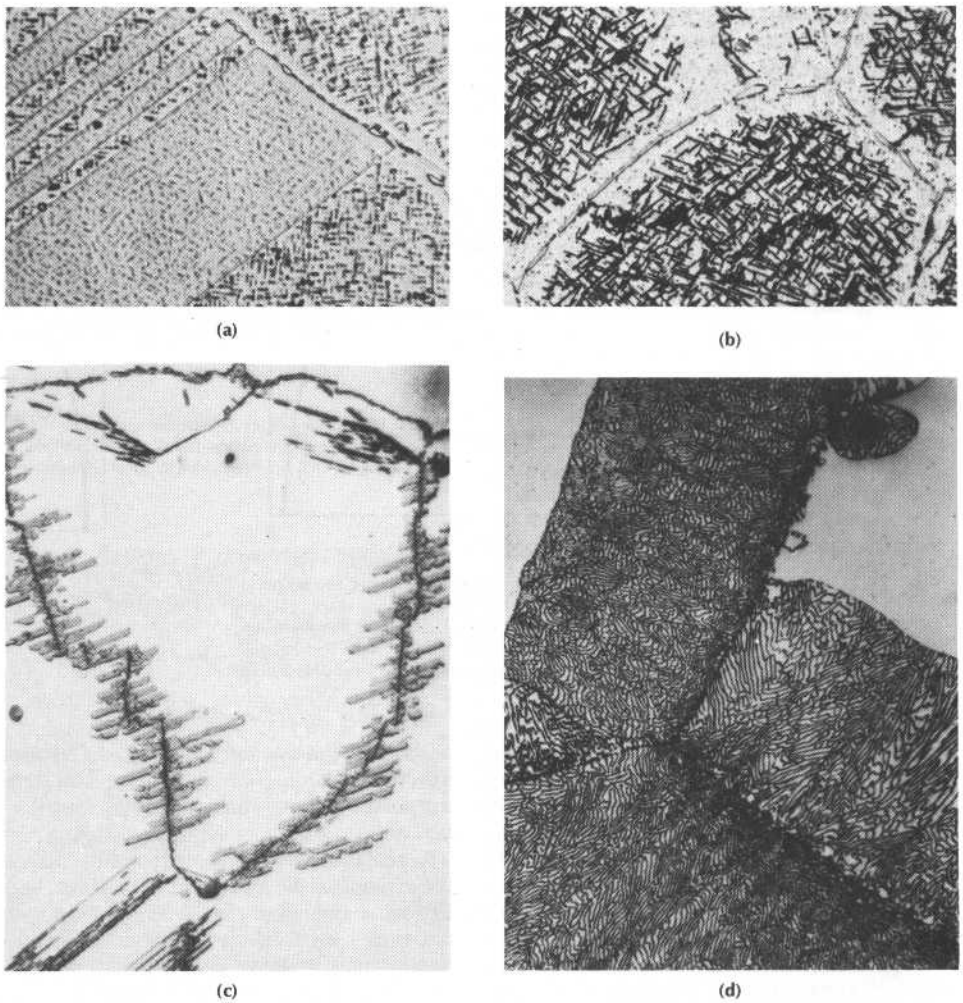

Fig. 39 Examples of characteristic precipitation microstructures. (a) General and grain-boundary precipitation of Co_3Ti (γ′ phase) in a Co-12Fe-6Ti alloy aged 3×10^3 min at 800 °C (1470 °F). 1260×. (b) General precipitation (intragranular Widmanstätten) and localized grain-boundary precipitation in an Al-18Ag alloy aged 90 h at 375 °C (710 °F), with a distinct precipitation-free zone near the grain boundaries. 500×. (c) Preferential, or localized, precipitation along grain boundaries in a Ni-20Cr-1Al alloy. 500×. (d) Cellular, or discontinuous, precipitation growing out uniformly from the grain boundaries in an Fe-24.8Zn alloy aged 6 min at 600 °C (1110 °F). 1000×. Source: 85ASM

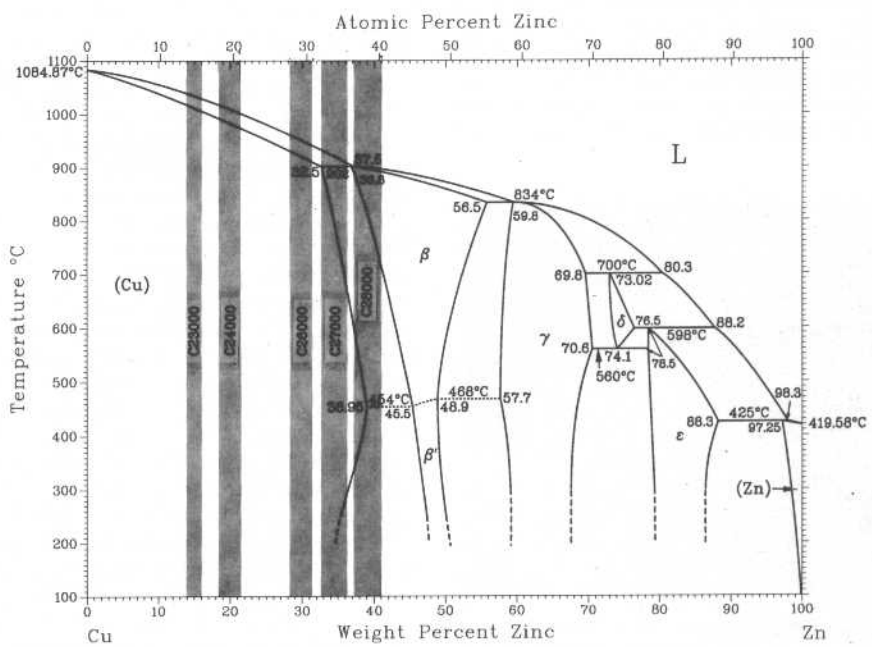

Fig. 40 The copper-zinc phase diagram, showing the composition range for five common brasses. Source: Adapted from 90Mas

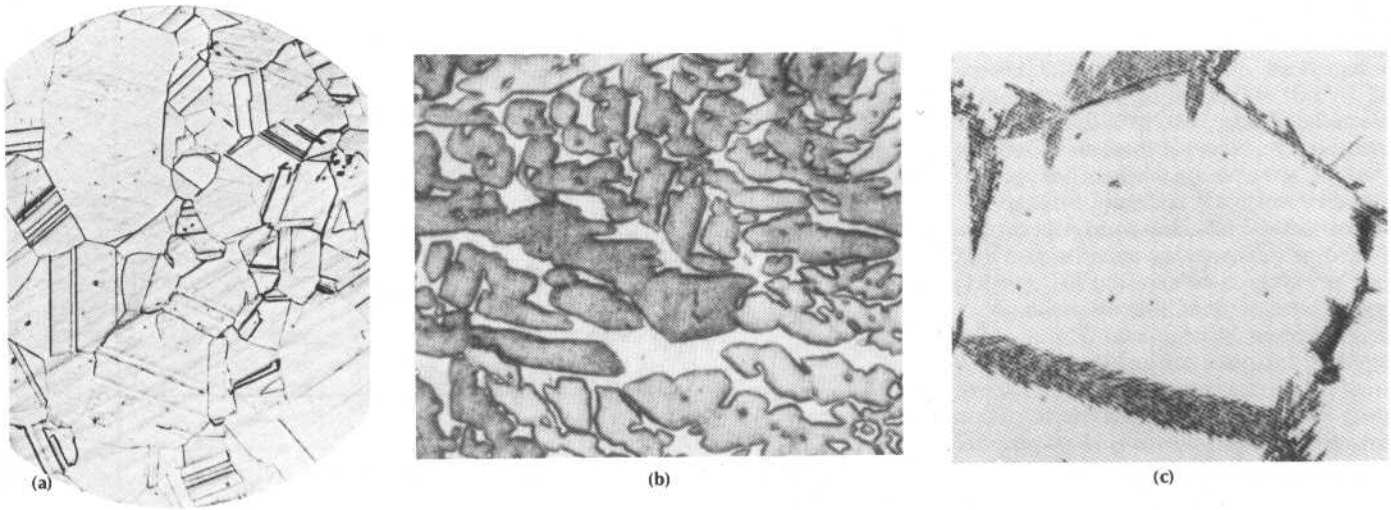

Fig. 41 The microstructures of two common brasses. (a) C26000 (cartridge brass, 70%), hot rolled, annealed, cold rolled 70%, and annealed at 638 °C (1180 °F), showing equiaxed grains of copper solid solution. Some grains are twinned. 75×. (b) C28000 (Muntz metal, 60%) ingot, showing dendrites of copper solid solution in a matrix of β. 200×. (c) C28000 (Muntz metal, 60%), showing feathers of copper solid solution that formed at β grain boundaries during quenching of the all-β structure. 100×. Source: 85ASM

are assigned the letter "A" for *arrêt* (French for "arrest"). These designations are shown in Fig. 45. To further differentiate the lines, an "e" is added to identify those indicating the changes occurring at equilibrium (to give Ae_1, Ae_3, Ae_4, and Ae_{cm}). Also, because the temperatures at which changes actually occur on heating or cooling are displaced somewhat from the equilibrium values, the "e" is replaced with "c" (for *chauffage*, French for "heating") when identifying the slightly higher temperatures associated with changes that occur on heating. Likewise, "e" is replaced with "r" (for *refroidissement*, French for "cooling") when identifying those slightly lower temperatures associated with changes occurring on cooling. These designations are convenient terms because they are used not only for binary alloys of iron and carbon, but also for commercial steels and cast irons, regardless of the other elements present in them. Alloying elements such as manganese, chromium, nickel, and molybdenum, however, do affect these temperatures (mainly A_3). For example, nickel lowers A_3, whereas chromium raises it.

The microstructures obtained in steels by slowly cooling are as follows. At carbon contents from 0.007 to 0.022%, the microstructure consists of ferrite grains with cementite precipitated in from ferrite, usually in too fine a form to be visible by light microscopy. (Because certain other metal atoms that may be present can substitute for some of the iron atoms in Fe_3C, the more general term, "carbide," is often used instead of "cementite" when describing microstructures.) In the hypoeutectoid range (from 0.022 to 0.76% C), ferrite and pearlite grains constitute the microstructure. In the hypereutectoid range (from 0.76 to 2.14% C), pearlite grains plus carbide precipitated from austenite are visible.

Slowly cooled hypoeutectic cast irons (from 2.14 to 4.3% C) have a microstructure consisting of dendritic pearlite grains (transformed from hypoeutectic primary austenite) and grains of iron-cementite eutectic (called "ledeburite") consisting of carbide and transformed austenite, plus carbide precipitated from austenite and particles of free carbon. For slowly cooled hypereutectic cast iron (between 4.3 and 6.67% C), the microstructure shows primary particles of carbide and free carbon, plus grains of transformed austenite.

Cast irons and steels, of course, are not used in their slowly cooled as-cast condition. Instead, they are more rapidly cooled from the melt, then subjected to some type of heat treatment and, for wrought steels, some type of hot and/or cold work. The great variety of microconstituents and microstructures that result from these treatments is beyond the scope of a discussion of stable and metastable equilibrium phase diagrams. Phase diagrams are invaluable, however, when designing heat treatments. For example, normalizing is usually accomplished by air cooling from about 55 °C (100 °F) above the upper transformation temperature (A_3 for hypoeutectoid alloys and A_{cm} for hypereutectoid alloys). Full annealing is done by controlled cooling from about 28 to 42 °C (50 to 75 °F) above A_3 for both hypoeutectoid and hypereutectoid alloys. All tempering and process

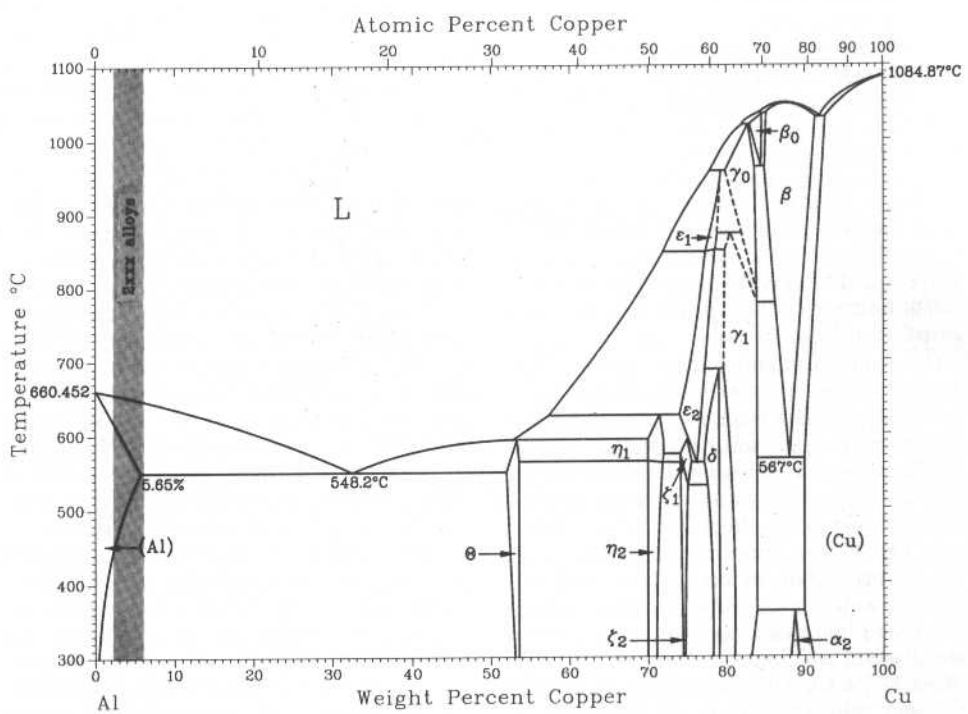

Fig. 42 The aluminum-copper phase diagram, showing the composition range for the 2xxx series of precipitation-hardenable aluminum alloys. Source: 90Mas

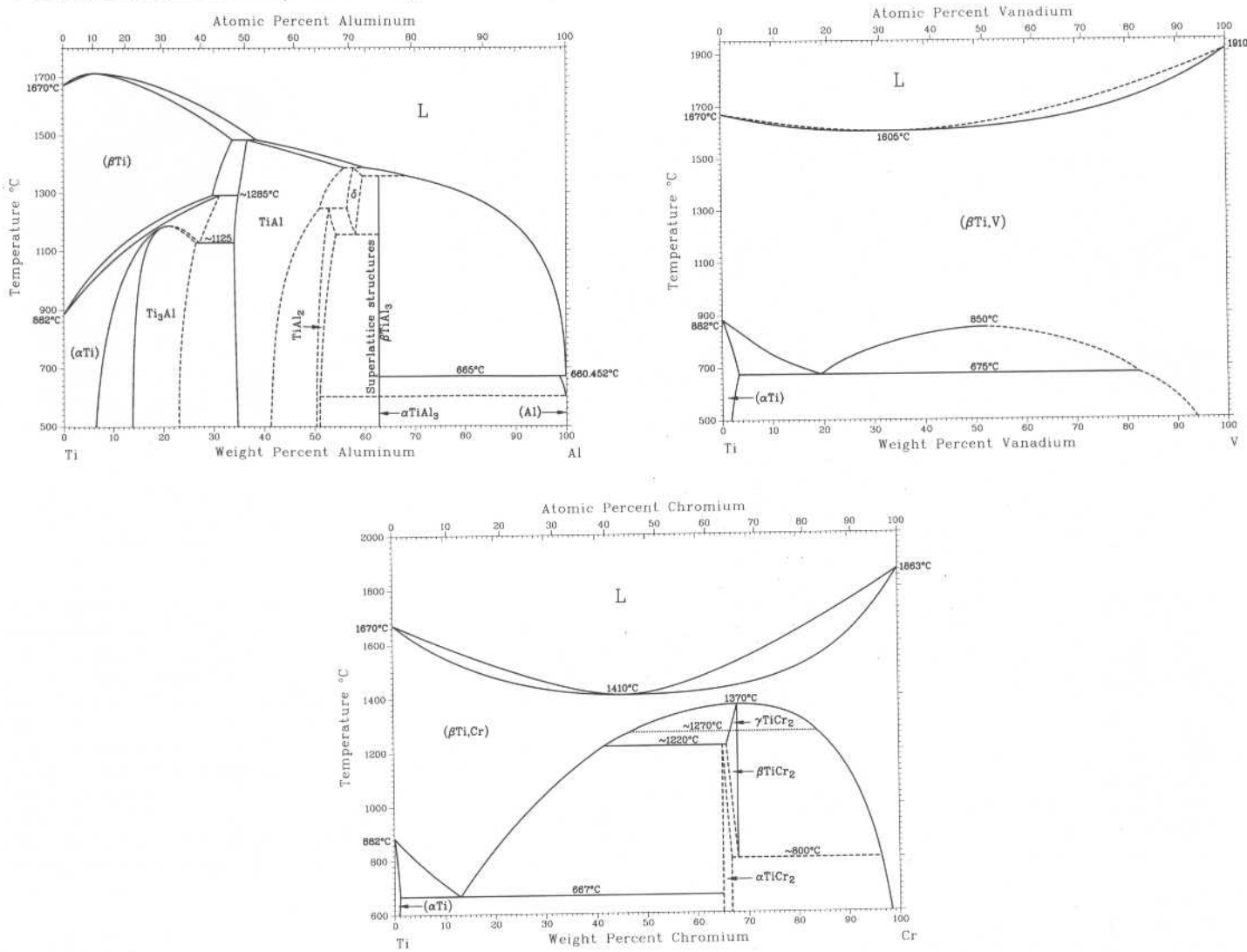

Fig. 43 Three representative binary titanium phase diagrams, showing alpha stabilization (Ti-Al), beta stabilization with complete miscibility (Ti-V), and beta stabilization with a eutectoid reaction (Ti-Cr). Source: 90Mas

annealing operations are done at temperatures below the lower transformation temperature (A_1). Austenitizing is done at a temperature sufficiently above A_3 and A_{cm} to ensure complete transformation to austenite, but low enough to prevent grain growth from being too rapid.

The Iron-Chromium-Nickel System. Many commercial cast irons and steels contain ferrite-stabilizing elements (such as silicon, chromium, molybdenum, and vanadium) and/or austenite stabilizers (such as manganese and nickel). The diagram for the binary iron-chromium system is representative of the effect of a ferrite stabilizer (see Fig. 47). At temperatures just below the solidus, bcc chromium forms a continuous solid solution with bcc (δ) ferrite. At lower temperatures, the γ-iron phase appears on the iron side of the diagram and forms a "loop" extending to about 11.2% Cr. Alloys containing up to 11.2% Cr, and sufficient carbon, are hardenable by quenching from temperatures within the loop.

At still lower temperatures, the bcc solid solution is again continuous bcc ferrite, but this time with αFe. This continuous bcc phase field confirms that δ-ferrite is the same as α-ferrite. The nonexistence of γ-iron in Fe-Cr alloys having more than about 13% Cr, in the absence of carbon, is an important factor in both the hardenable and nonhardenable grades of iron-chromium stainless steels. At these lower temperatures, a material known as sigma phase also appears in different amounts from about 14 to 90% Cr. Sigma is a hard, brittle phase and usually should be avoided in commercial stainless steels. Formation of sigma, however, is time dependent; long periods at elevated temperatures are usually required.

The diagram for the binary iron-nickel system is representative of the effect of an austenite stabilizer (see Fig. 47). The fcc nickel forms a continuous solid solution with fcc (γ) austenite that dominates the diagram, although the α-ferrite phase field extends to about 6% Ni. The diagram for the ternary iron-chromium-nickel system shows how the addition of ferrite-stabilizing chromium affects the iron-nickel system (see Fig. 48). As can be seen, the popular 18-8 stainless steel, which contains about 8% Ni, is an all-austenite alloy at 900 °C (1652 °F), even though it also contains about 18% Cr.

Practical Applications of Phase Diagrams

The following are but a few of the many instances where phase diagrams and phase relationships have proved invaluable in the efficient solving of practical metallurgical problems.

Alloy Design

Age Hardening Alloys. One of the earliest uses of phase diagrams in alloy development was in the suggestion in 1919 by the U.S. Bureau of Standards that precipitation of a second phase from solid solution would harden an alloy. The age hardening of certain aluminum-copper alloys (then called "Duralumin" alloys) had been accidentally discovered in 1904, but this process was

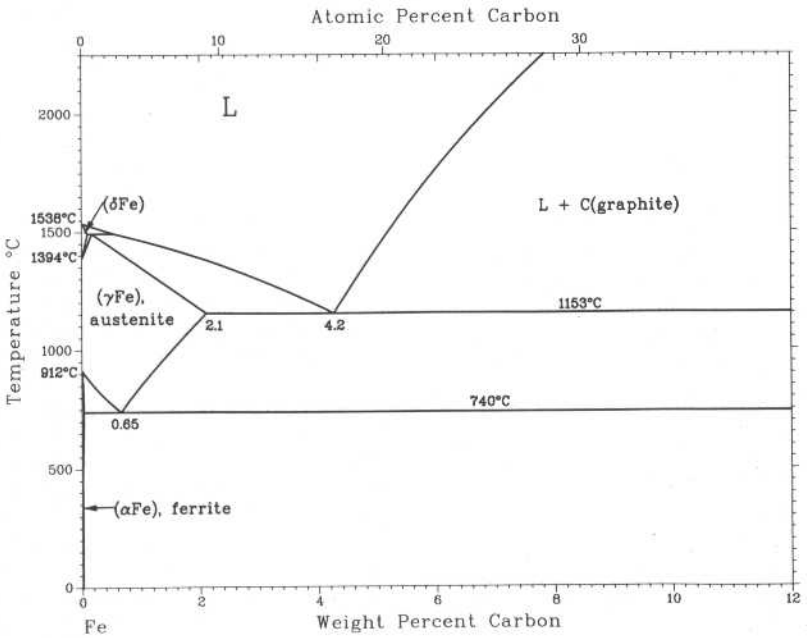

Fig. 44 The iron-carbon phase diagram. Source: Adapted from 90Mas

thought to be a unique and curious phenomenon. The work at the Bureau, however, showed the scientific basis of this process (which was discussed in previous sections of this Introduction). This work has now led to the development of several families of commercial "age hardening" alloys covering different base metals.

Austenitic Stainless Steel. In connection with a research project aimed at the conservation of always expensive, sometimes scarce, materials, the question arose: Can manganese and aluminum be substituted for nickel and chromium in stainless steels? (In other words, can standard chromium-nickel stainless steels be replaced with an austenitic alloy system?) The answer came in two stages—in both instances with the help of phase diagrams. It was first determined that manganese should be capable of replacing nickel because it stabilizes the γ-iron phase (austenite), and aluminum may substitute for chromium because it stabilizes the α-iron phase (ferrite), leaving only a small γ loop (see Fig. 47 and 49). Aluminum is known to impart good high-temperature oxidation resistance to iron. Next, the literature on phase diagrams of the aluminum-iron-manganese system was reviewed, which suggested that a range of compositions exists where the alloy would be austenitic at room temperature. A nonmagnetic alloy with austenitic structure containing 44% Fe, 45% Mn, and 11% Al was prepared. However, it proved to be very brittle, presumably because of the precipitation of a phase based on β-Mn. By examining the phase diagram for carbon-iron-manganese (Fig. 50), as well as the diagram for aluminum-carbon-iron, the researcher determined that the problem could be solved through the addition of carbon to the aluminum-iron-manganese system, which would move the composition away from the βMn phase field. The carbon addition also would further stabilize the austenite phase, permitting reduced manganese content. With this information, the composition of the alloy was modified to 7 to 10% Al, 30 to 35% Mn, and 0.75 to 1% C, with the balance iron. It had good mechanical properties, oxidation resistance, and moderate stainlessness.

Permanent Magnets. A problem with permanent magnets based on Fe-Nd-B is that they show high magnetization and coercivity at room temperature, but unfavorable properties at higher temperatures. Because hard magnetic properties are limited by nucleation of severed magnetic domains, the surface and interfaces of grains in the sintered and heat-treated material are the controlling factor. Therefore, the effects of alloying additives on the phase diagrams and microstructural development of the Fe-Nd-B alloy system plus additives were studied. These studies showed that the phase relationships and domain-nucleation difficulties were very unfavorable for the production of a magnet with good magnetic properties at elevated temperatures by the sintering method. However, such a magnet might be produced from Fe-Nd-C material by some other process, such as melt spinning or bonding (see 91Hay).

Processing

Hacksaw Blades. In the production of hacksaw blades, a strip of high-speed steel for the cutting edges is joined to a backing strip of low-alloy steel by laser or electron beam welding. As a result, a very hard martensitic structure forms in the weld area that must be softened by heat treatment before the composite strip can be further rolled or set. To avoid the cost of the heat treatment, an alternative technique was investigated. This technique involved alloy additions during welding to create a microstructure that would not require subsequent heat treatment. Instead of expensive experiments, several mathematical simulations were made based on additions of various steels or pure metals. In these simulations, the hardness of

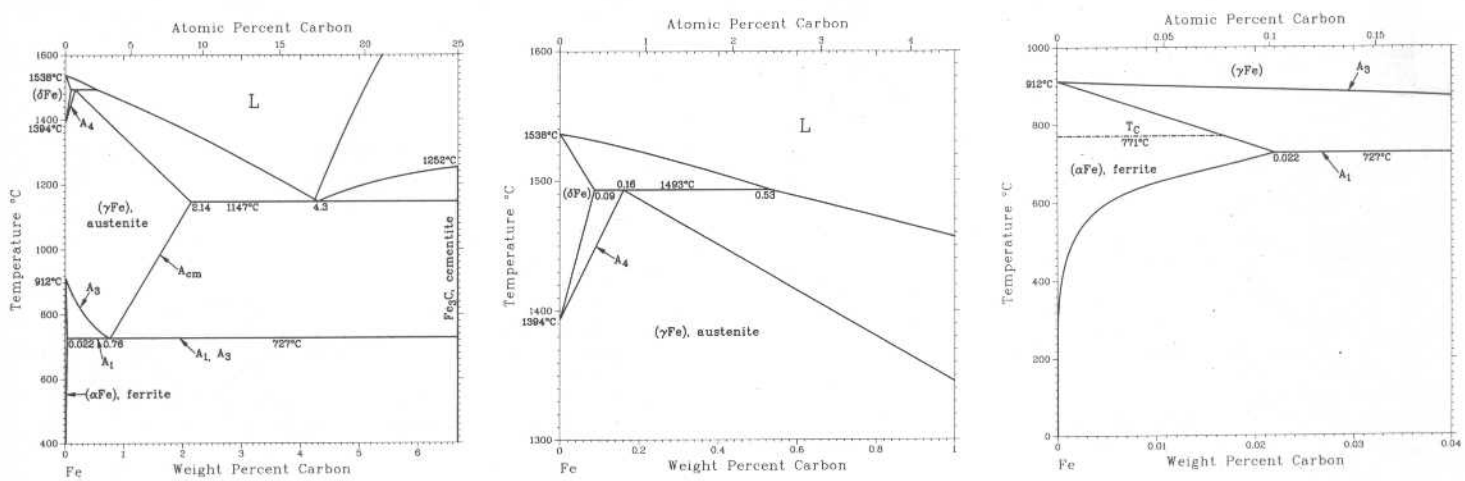

Fig. 45 The iron-cementite phase diagram and details of the (δFe) and (αFe) phase fields. Source: Adapted from 90Mas

the weld was determined by combining calculations of the equilibrium phase diagrams and available information to calculate (assuming the average composition of the weld) the martensite transformation temperatures and amounts of retained austenite, untransformed ferrite, and carbides formed in the postweld microstructure. Of those alloy additions considered, chromium was found to be the most efficient (see 91Hay).

Hardfacing. A phase diagram was used to design a nickel-base hardfacing alloy for corrosion and wear resistance. For corrosion resistance, a matrix of at least 15% Cr was desired; for abrasion resistance, a minimum amount of primary chromium-boride particles was desired. After consulting the B-Cr-Ni phase diagram, a series of samples having acceptable amounts of total chromium borides and chromium matrix were made and tested. Subsequent fine tuning of the composition to ensure fabricability of welding rods, weldability, and the desired combination of corrosion, abrasion, and impact resistance led to a patented alloy.

Performance

Heating elements made of Nichrome (a nickel-chromium-iron alloy registered by Driver-Harris Company, Inc., Harrison, NJ) in a heat treating furnace were failing prematurely. Reference to nickel-base phase diagrams suggested that low-melting eutectics can be produced by very small quantities of the chalcogens (sulfur, selenium, or tellurium), and it was thought that one of these eutectics could be causing the problem. Investigation of the furnace system resulted in the discovery that the tubes conveying protective atmosphere to the furnace were made of sulfur-cured rubber, which could result in liquid metal being formed at temperatures as low as 637 °C (1179 °F) (see Fig. 51). Armed with this information, a metallurgist solved the problem by substituting neoprene for the rubber.

Electric Motor Housings. At moderately high service temperatures, cracks developed in electric motor housings that had been extruded from aluminum produced from a combination of recycled and virgin metal. Extensive studies revealed that the cracking was caused by small amounts of lead and bismuth in the recycled metal reacting to form bismuth-lead eutectic at the grain boundaries at 327 and ~270 °C (621 and ~518 °F), respectively, much below the melting point of pure aluminum (660.45 °C, or 1220.81 °F) (see Fig. 52). The question became: How much lead and bismuth can be tolerated in this instance? The phase diagrams showed that aluminum alloys containing either lead or bismuth in amounts exceeding their respective solubility limits (<0.05% and ~0.2%) can lead to hot cracking of the aluminum.

Carbide Cutting Tools. A manufacturer of carbide cutting tools once experienced serious trouble with brittleness of the sintered carbide. No impurities were found. The range of compositions for cobalt-bonded sintered carbides is shown in the shaded area of Fig. 53, along the dashed line connecting pure tungsten carbide (marked "WC") on the right and pure cobalt at the lower left. At 1400 °C (2552 °F), materials with these compositions consist of particles of tungsten carbide suspended in liquid metal. However, when there is a deficiency of carbon, compositions drop into the region labeled WC + η + liquid, or the region labeled WC + η where tungsten carbide particles are surrounded by a matrix of η phase. The η

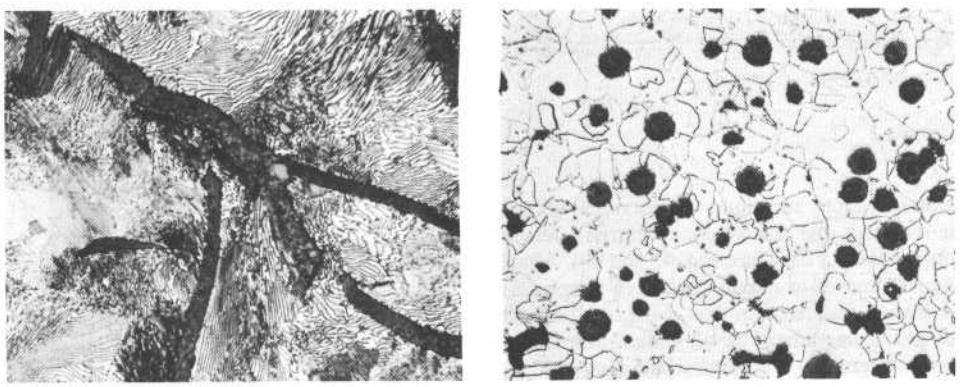

(a) (b)

Fig. 46 The microstructures of two types of cast irons. (a) As-cast class 30 gray iron, showing type A graphite flakes in a matrix of pearlite. 500×. (b) As-cast grade 60-45-12 ductile iron, showing graphite nodules (produced by the addition of a calcium-silicon compound during pouring) in a ferrite matrix. 100×. Source: 85ASM

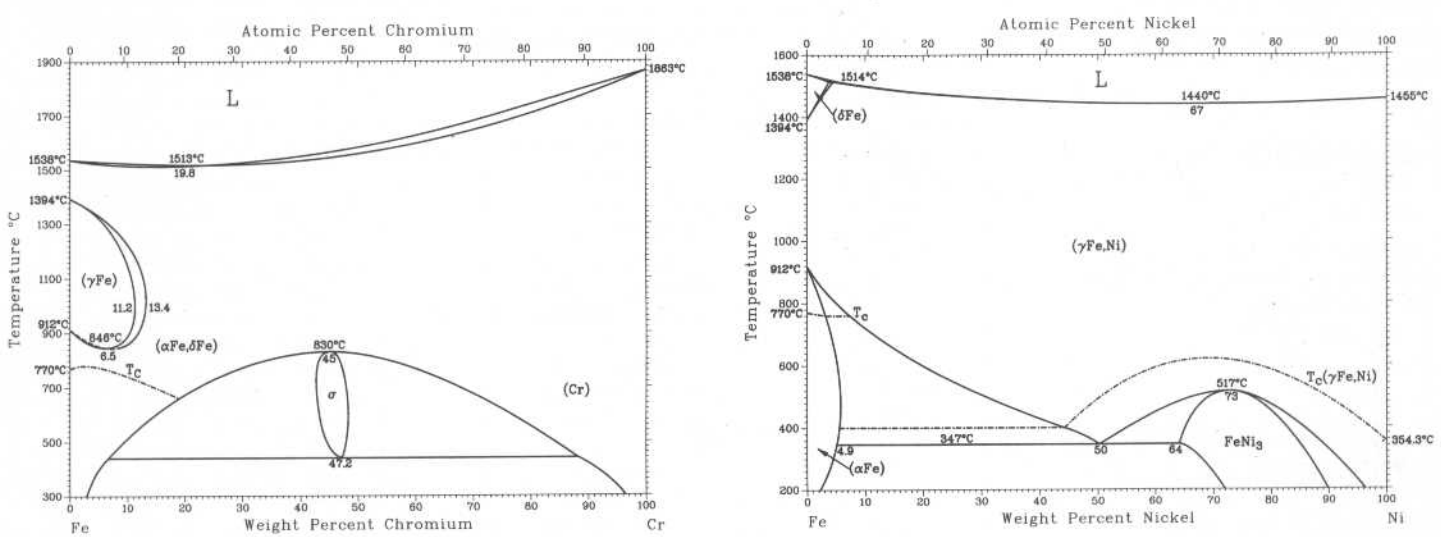

Fig. 47 Two representative binary iron phase diagrams, showing ferrite stabilization (Fe-Cr) and austenite stabilization (Fe-Ni). Source: 90Mas

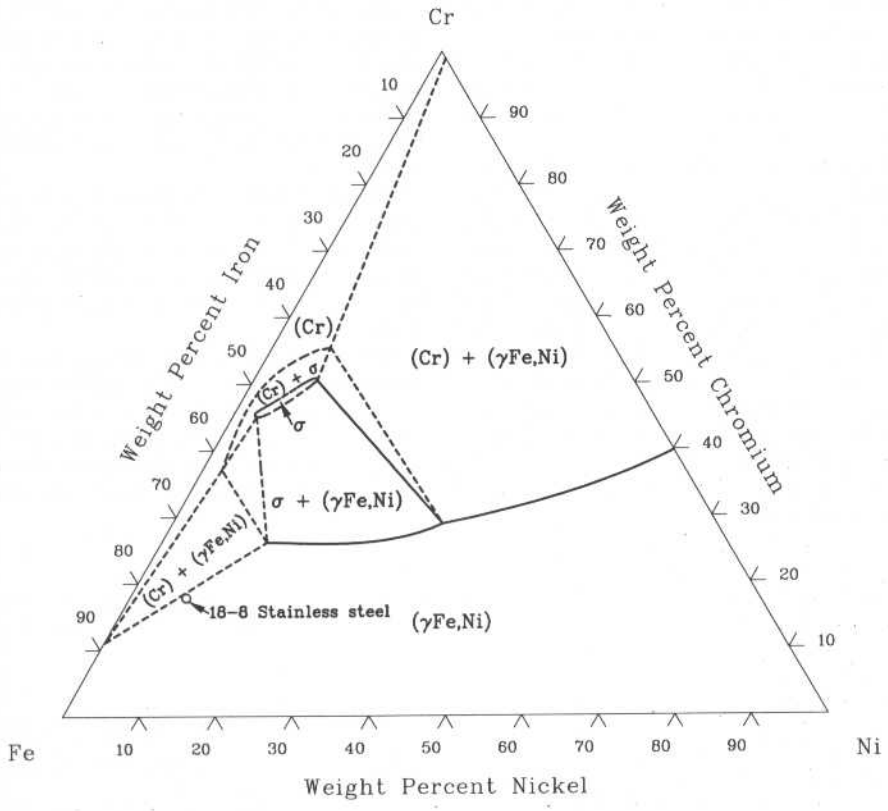

Fig. 48 The isothermal section at 900 °C (1652 °F) of the iron-chromium-nickel ternary phase diagram, showing the nominal composition of 18-8 stainless steel. Source: Adapted from Ref 1

phase is known to be brittle. The upward adjustment of the carbon content by only a few hundredths of a weight percent eliminated this problem.

Solid-State Electronics. In the early stages of the solid-state industry, a phenomenon known as the "purple plague" nearly destroyed the fledgling industry. Components were failing where the gold lead wires were fused to aluminized transistor and integrated circuits. A purple residue was formed, which was thought to be a product of corrosion. Actually, what was happening was the formation of an intermetallic compound, an aluminum-gold precipitate (Al_2Au) that is purple in color and very brittle. Millions of actual and opportunity dollars were lost in identifying the problem and its solution, which could have been avoided had the proper phase diagram been examined (see Fig. 54).

A question concerning purple plague problems, however, has remained unresolved: whether or not the presence of silicon near the gold-aluminum interface has an influence on the stability and rate of formation of the damaging intermetallic phase. An examination of the phase relationships in the Al-Al_2Au-Si subternary system showed no stable ternary Al-Au-Si phases (see 91Hay). It was suggested instead that the reported effect of silicon may be due to a reaction between silicon and alumina (Al_2O_3) at the aluminum-gold interface that becomes thermodynamically feasible in the presence of gold.

BIBLIOGRAPHY

35Mar: J.S. Marsh, *Principles of Phase Diagrams*, McGraw-Hill, 1935. *This out-of-print book is an early thorough presentation of the principles of heterogeneous equilibrium in organic, inorganic salt, and metallic systems.*

44Mas: G. Masing (B.A. Rogers, transl.), *Ternary Alloys: Introduction to the Theory of Three Component Systems*, Reinhold, 1944; available from U·M·I, 300 North Zeeb Rd., Ann Arbor, MI 48106. *This out-of-print book, originally published in German in 1932, is one of the first to thoroughly discuss the theory underlying ternary alloy systems and their application to industrial alloys.*

56Rhi: F.N. Rhines, *Phase Diagrams in Metallurgy: Their Development and Application*, McGraw-Hill, 1956. *This out-of-print book is a basic text designed for undergraduate students in metallurgy.*

66Pri: A. Prince, *Alloy Phase Equilibria*, Elsevier, 1966. *This out-of-print book covers the thermodynamic approach to binary, ternary, and quaternary phase diagrams.*

68Gor: P. Gordon, *Principles of Phase Diagrams in Materials Systems*, McGraw-Hill, 1968;

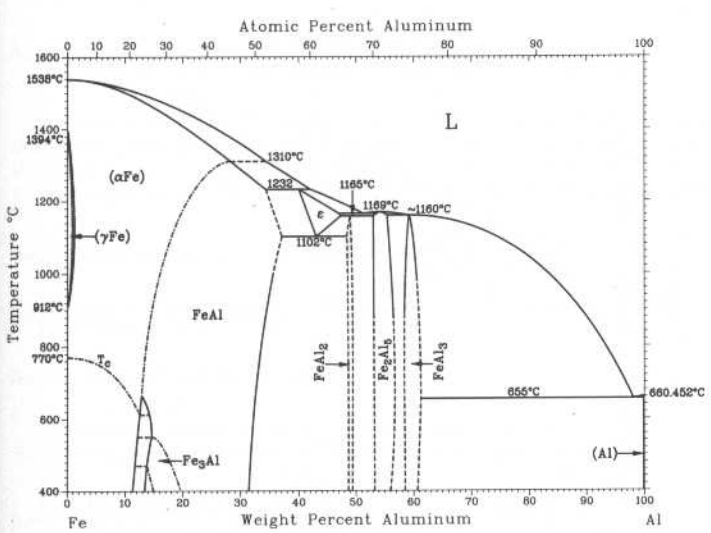

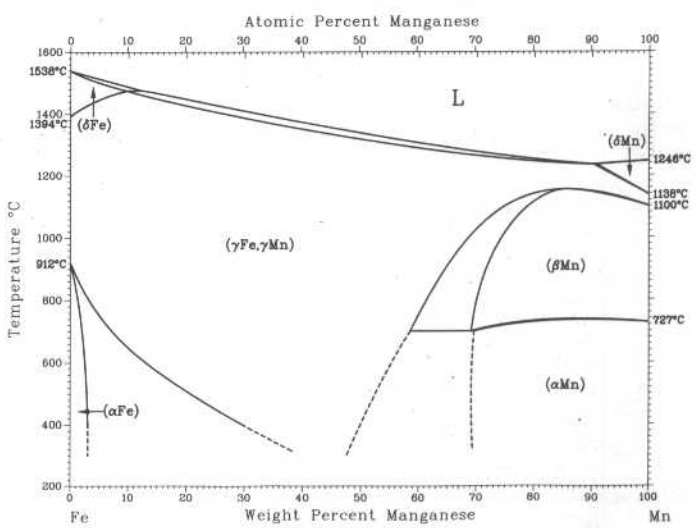

Fig. 49 The aluminum-iron and iron-manganese phase diagrams. Source: Ref 2

reprinted by Robert E. Krieger Publishing, 1983. *Covers the thermodynamic basis of phase diagrams; the presentation is aimed at materials engineers and scientists.*

70Kau: L. Kaufman and H. Bernstein, *Computer Calculations of Phase Diagrams*, Academic Press, 1970. *A comprehensive presentation of thermodynamic modeling with the aid of computers.*

75Gok: N.A. Gokcen, *Thermodynamics*, Techscience, 1975. *Chapter XV discusses the role of thermodynamics in phase diagrams and Gibbs energy diagrams.*

77Luk: H.L. Lukas, E.T. Henig, and B. Zimmerman, Optimization of Phase Diagrams by a Least Squares Method Using Simultaneously Different Types of Data, *Calphad*, Vol 1 (No. 3), 1977, p 225-236. *Presents the use of a computer-aided program for determining phase boundary lines that best fit scattered data points.*

81Goo: D.A. Goodman, J.W. Cahn, and L.H. Bennett, The Centennial of the Gibbs-Konovalov Rule for Congruent Points, *Bull. Alloy Phase Diagrams*, Vol 2 (No. 1), 1981, p 29-34. *Presents the theoretical basis for the rule and its application to phase diagram evaluation.*

81Hil: M. Hillert, A Discussion of Methods of Calculating Phase Diagrams, *Bull. Alloy Phase Diagrams*, Vol 2 (No. 3), 1981, p 265-268. *Presents a brief description of the various methods for thermodynamic modeling of phase diagrams.*

82Pel: A.D. Pelton, W.T. Thompson, and C.W. Bale, *F*A*C*T* (Facility for the Analysisof Chemical Thermodynamics)*, McGill University, 1982. *Describes a thermodynamic database and computer program for modeling phase diagrams.*

84Mor: J.E. Morral, Two-Dimensional Phase Fraction Charts, *Scr. Metall.*, Vol 18 (No. 4), 1984, p 407-410. *Gives a general description of phase-fraction charts.*

85ASM: *Metals Handbook*, 9th ed., Vol 9, *Metallography and Microstructures*, American Society for Metals, 1985. *A comprehensive reference covering terms and definitions, metallographic techniques, microstructures of industrial metals and alloys, and principles of microstructures and crystal structures.*

89Mas: T.B. Massalski, Phase Diagrams in Materials Science, *ASM News*, Vol 20 (No. 7), July 1989, p 8-9. *A concise presentation of the role of phase diagrams in materials science, and the worldwide efforts to make reliable diagrams readily available.*

90Mas: T.B. Massalski, Ed., *Binary Alloy Phase Diagrams*, 2nd ed., ASM International, 1990. *The most comprehensive collection of binary phase diagrams published to date: diagrams for 2965 systems, presented in both atomic and weight percent, with crystal data and discussion.*

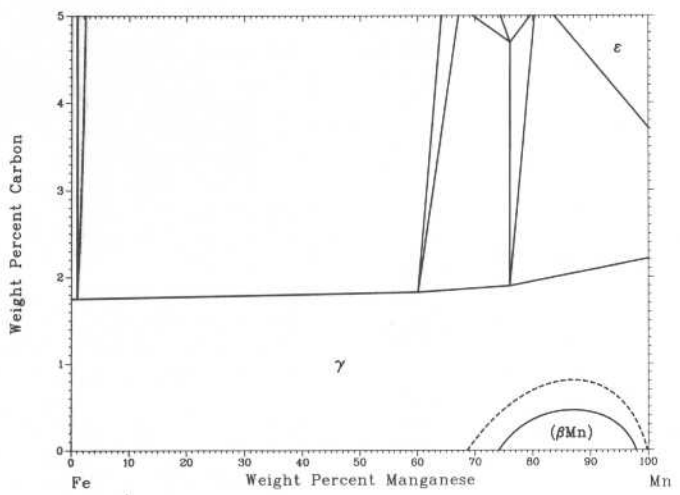

Fig. 50 The isothermal section at 1100 °C (2012 °F) of the iron-manganese-carbon phase diagram. Source: Adapted from Ref 3

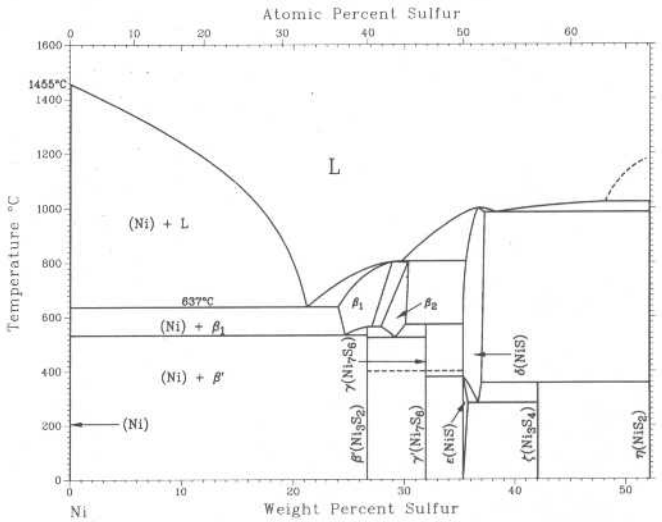

Fig. 51 The nickel-sulfur phase diagram. Source: Adapted from 90Mas

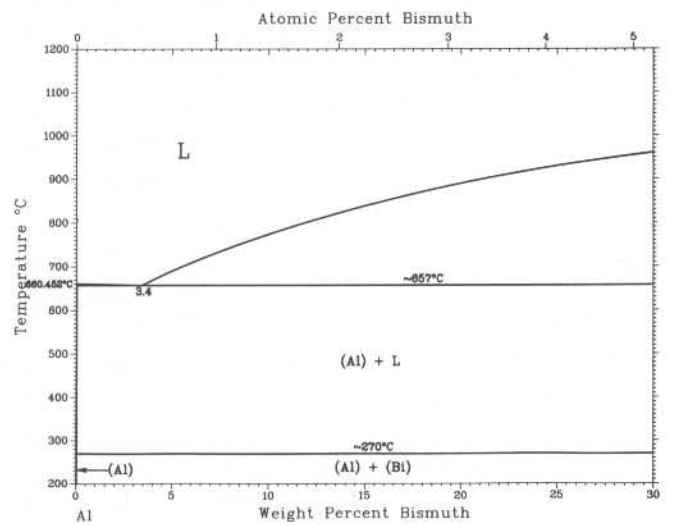

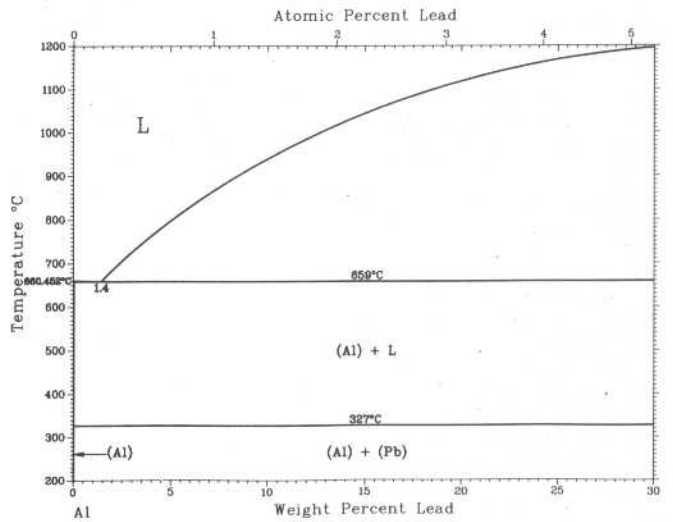

Fig. 52 The aluminum-bismuth and aluminum-lead phase diagrams. Source: Adapted from 90Mas

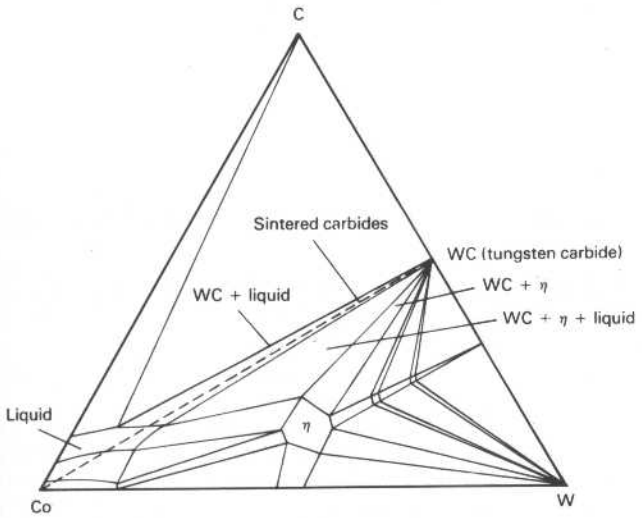

Fig. 53 The isothermal section at 1400 °C (2552 °F) of the cobalt-tungsten-carbon phase diagram. Source: Adapted from Ref 4

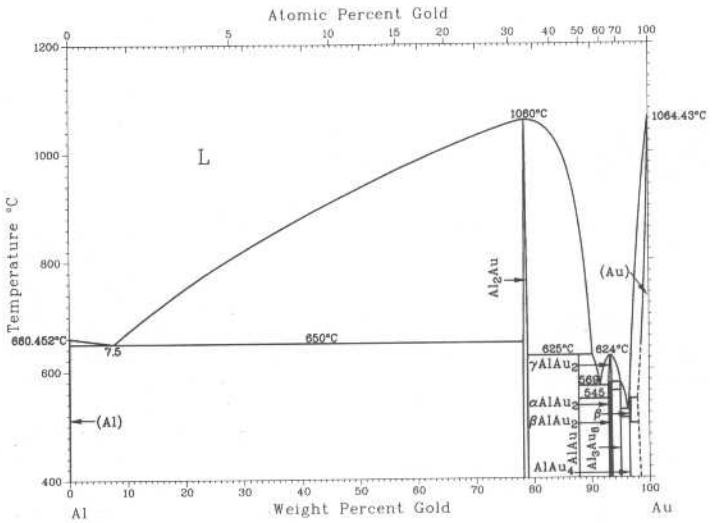

Fig. 54 The aluminum-gold phase diagram. Source: Ref 5

Volume Fraction

In order to relate the weight fraction of a phase present in an alloy specimen as determined from a phase diagramto its two-dimensional appearance as observed in a micrograph, it is necessary to be able to convert between weight-fraction values and areal-fraction values, both in decimal fractions. This conversion can be developed as follows:

The weight fraction of the phase is determined from the phase diagram, using the lever rule.

$$\text{Volume portion of the phase} = \frac{\text{weight fraction of the phase}}{\text{phase density}}$$

Total volume of all phases present = sum of the volume portions of each phase.

$$\text{Volume fraction of the phase} = \frac{\text{weight fraction of the phase}}{\text{phase density} \times \text{total volume}}$$

It has been shown by stereology and quantitative metallography that areal fraction is equal to volume fraction [85ASM]. (Areal fraction of a phase is the sum of areas of the phase intercepted by a microscopic traverse of the observed region of the specimen divided by the total area of the observed region.) Therefore:

$$\text{Areal fraction of the phase} = \frac{\text{weight fraction of the phase}}{\text{phase density} \times \text{total volume}}$$

The phase density value for the preceding equation can be obtained by measurement or calculation. The densities of chemical elements, and some line compounds, can be found in the literature. Alternatively, the density of a unit cell of a phase comprising one or more elements can be calculated from information about its crystal structure and the atomic weights of the elements comprising it as follows:

$$\text{Weight of each element} = \text{number of atoms} \times \frac{\text{atomic weight}}{\text{Avogadro's number}}$$

Total cell weight = sum of weights of each element

Density = total cell weight / cell volume

For example, the calculated density of pure copper, which has a fcc structure and a lattice parameter of 0.36146 nm, is:

$$\rho = \frac{4 \text{ atoms/cell} \times 63.546 \text{ g/mol}}{6.0227 \times 10^{23} \text{ atoms/mol} \times (0.36146 \times 10^{-9} \text{ m})^3} = 8.937 \text{Mg/m}^3$$

This compares favorably with the published value of 8.93.

91Hay: F.H. Hayes, Ed., *User Aspects of Phase Diagrams*, The Institute of Metals, London, 1991. *A collection of 35 papers and posters presented at a conference held June 1990 in Petten, The Netherlands.*

91Mor: J.E. Morral and H. Gupta, Phase Boundary, ZPF, and Topological Lines on Phase Diagrams, *Scr. Metall.*, Vol 25 (No. 6), 1991, p 1393-1396. *Reviews three different ways of considering the lines on a phase diagram.*

91Oka1: H. Okamoto and T.B. Massalski, Thermodynamically Improbable Phase Diagrams, *J. Phase Equilibria*, Vol 12 (No. 2), 1991, p 148-168. *Presents examples of phase-rule violations and problems with phase-boundary curvatures; also discusses unusual diagrams.*

91Oka2: H. Okamoto, Reevaluation of Thermodynamic Models for Phase Diagram Evaluation, *J. Phase Equilibria*, Vol 12 (No. 6), 1991, p 623-643. *Reviews the basic principles of thermodynamic calculation of phase diagrams, simplification of thermodynamic models, and reliability of thermodynamic data and parameters; also presents examples of unlikely calculated phase diagrams.*

91Vil: P. Villars and L.D. Calvert, *Pearson's Handbook of Crystallographic Data for Intermediate Phases*, ASM International, 1991. *This third edition of Pearson's comprehensive compilation includes data from all the international literature from 1913 to 1989.*

OTHER REFERENCES

1. G.V. Raynor and V.G. Rivlin, *Phase Equilibria in Iron Ternary Alloys*, Vol 4, The Institute of Metals, London, 1988
2. H. Okamoto, *Phase Diagrams of Binary Iron Alloys*, ASM International, 1992
3. R. Benz, J.F. Elliott, and J. Chipman, *Metall. Trans.*, Vol 4, 1973, p 1449
4. P. Rautala and J.T. Norton, *Trans. AIME*, Vol 194, 1952, p 1047
5. H. Okamoto, Ed., Binary Alloy Phase Diagrams Updating Service, ASM International, 1992

Index of Terms

Age hardening ..... 1•22
Allotropy ..... 1•1
Binary ..... 1•2
Bivariant equilibrium ..... 1•2
Bravais lattice ..... 1•10
Catatectic ..... 1•5
Clausius-Clapeyron equation ..... 1•8
Closed system ..... 1•5
Component ..... 1•2
Congruent phase change ..... 1•4
Congruent point ..... 1•10
Conjugate phases ..... 1•3
Constitutional diagram ..... 1•2
Continuous solid solution ..... 1•2
Coring ..... 1•19
Critical point ..... 1•2
Crystal ..... 1•10
Crystal structure ..... 1•10
Crystal system ..... 1•10
Decinary ..... 1•2
Degrees of freedom ..... 1•2
Dendrite ..... 1•19
Dendritic segregation ..... 1•19
Disorder ..... 1•10
Edge length ..... 1•10
Enthalpy ..... 1•6
Entropy ..... 1•7
Equilibrium diagram ..... 1•2
Eutectic ..... 1•3
Eutectoid ..... 1•5
First Law of Thermodynamics ..... 1•6
First-order transition ..... 1•10
Gibbs energy ..... 1•7
Gibbs-Konovalov Rule ..... 1•8
Guinier-Preston zones ..... 1•21
Heat capacity ..... 1•6
Heat content ..... 1•6
Higher-order transition ..... 1•10
Hot short ..... 1•19
Hypereutectic ..... 1•3
Hypereutectoid ..... 1•21
Hypoeutectic ..... 1•3
Hypoeutectoid ..... 1•21
Idiomorphic particles ..... 1•20
Incongruent phase change ..... 1•4
Interaxial angle ..... 1•10
Intermediate phase ..... 1•4
Intermetallic compound ..... 1•4
Internal energy ..... 1•5
Interstitional solid solution ..... 1•16
Invariant equilibrium ..... 1•2
Invariant point ..... 1•2
Isopleth ..... 1•5
Isotherm ..... 1•5
Lattice constant ..... 1•10
Lattice parameter ..... 1•10
Lattice points ..... 1•15
Law of Conservation of Energy ..... 1•6
Lever rule ..... 1•18
Line compound ..... 1•4
Liquation ..... 1•19
Liquidus ..... 1•2
Long-period ordering ..... 1•15
Melting curve ..... 1•2
Metatectic ..... 1•5
Monotectic ..... 1•5
Monotectoid ..... 1•5
Monovariant equilibrium ..... 1•2
Nonary ..... 1•2
Octanary ..... 1•2
Ordered structure ..... 1•10
Pearson symbol ..... 1•15
Peritectic ..... 1•5
Peritectoid ..... 1•5
Phase ..... 1•1
Phase diagram ..... 1•2
Phase-field rule ..... 1•7
Phase-fraction line ..... 1•19
Phase rule ..... 1•2
Polymorphic ..... 1•1
Precipitation hardening ..... 1•22
Primary constituent ..... 1•20
Proeutectoid constituent ..... 1•21
Prototype ..... 1•16
Pseudobinary ..... 1•5
Quasibinary ..... 1•5
Quaternary ..... 1•2
Quinary ..... 1•2
Second Law of Thermodynamics ..... 1•7
Septenary ..... 1•2
Sexinary ..... 1•2
Solidus ..... 1•2
Solution hardening ..... 1•17
Solvus ..... 1•3
Space-group notation ..... 1•16
Space lattice ..... 1•10
State variable ..... 1•1
Structure prototype ..... 1•16
Sublimation curve ..... 1•2
Substitutional solid solution ..... 1•17
Superlattice ..... 1•10
Syntectic ..... 1•5
System ..... 1•1
Terminal phase ..... 1•3
Ternary ..... 1•2
Theorem of Le Châtelier ..... 1•7
Third Law of Thermodynamics ..... 1•7
Tie line ..... 1•8
Tie triangle ..... 1•8
Triple curve ..... 1•2
Triple point ..... 1•2
Unary ..... 1•2
Unit cell ..... 1•10
Univariant equilibrium ..... 1•2
Vaporization curve ..... 1•2

Section 2
Binary Alloy Phase Diagrams

Introduction ..... 2•3
Binary General References ..... 2•4
Key to Titles ..... 2•4
Binary Alloy Phase Diagrams Index ..... 2•5
References Cited in Binary Alloy Phase Diagrams Index ..... 2•22
Binary Phase Diagrams and Crystal Structure Data ..... 2•25
List of Binary Systems Included:

Ag-Al ..... 2•25
Ag-As ..... 2•25
Ag-Au ..... 2•25
Ag-Be ..... 2•26
Ag-Bi ..... 2•26
Ag-Ca ..... 2•26
Ag-Cd ..... 2•27
Ag-Ce ..... 2•27
Ag-Co ..... 2•27
Ag-Cu ..... 2•28
Ag-Dy ..... 2•28
Ag-Er ..... 2•28
Ag-Eu ..... 2•29
Ag-Fe ..... 2•29
Ag-Ga ..... 2•29
Ag-Gd ..... 2•30
Ag-Ge ..... 2•30
Ag-Hg ..... 2•30
Ag-Ho ..... 2•31
Ag-In ..... 2•31
Ag-La ..... 2•31
Ag-Li ..... 2•32
Ag-Mg ..... 2•32
Ag-Mo ..... 2•32
Ag-Na ..... 2•33
Ag-Nd ..... 2•33
Ag-Ni ..... 2•33
Ag-P ..... 2•34
Ag-Pb ..... 2•34
Ag-Pd ..... 2•34
Ag-Pr ..... 2•35
Ag-Pt ..... 2•35
Ag-S ..... 2•35
Ag-Sb ..... 2•35
Ag-Sc ..... 2•36
Ag-Se ..... 2•36
Ag-Si ..... 2•37
Ag-Sm ..... 2•37
Ag-Sn ..... 2•37
Ag-Sr ..... 2•38
Ag-Te ..... 2•38
Ag-Ti ..... 2•38
Ag-Tl ..... 2•39
Ag-Y ..... 2•39
Ag-Yb ..... 2•39
Ag-Zn ..... 2•40
Ag-Zr ..... 2•40
Al-As ..... 2•40
Al-Au ..... 2•41
Al-Ba ..... 2•41
Al-Be ..... 2•41
Al-Bi ..... 2•42
Al-Ca ..... 2•42
Al-Cd ..... 2•42
Al-Ce ..... 2•43
Al-Co ..... 2•43
Al-Cr ..... 2•43
Al-Cu ..... 2•44
Al-Er ..... 2•44
Al-Fe ..... 2•44
Al-Ga ..... 2•45
Al-Gd ..... 2•45
Al-Ge ..... 2•45
Al-H ..... 2•46
Al-Hg ..... 2•46
Al-Ho ..... 2•46
Al-In ..... 2•47
Al-La ..... 2•47
Al-Li ..... 2•47
Al-Mg ..... 2•48
Al-Mn ..... 2•48
Al-Nb ..... 2•48
Al-Nd ..... 2•49
Al-Ni ..... 2•49
Al-Pb ..... 2•49
Al-Pd ..... 2•50
Al-Pr ..... 2•50
Al-Pt ..... 2•50
Al-S ..... 2•51
Al-Sb ..... 2•51
Al-Se ..... 2•51
Al-Si ..... 2•52
Al-Sn ..... 2•52
Al-Sr ..... 2•52
Al-Ta ..... 2•53
Al-Te ..... 2•53
Al-Th ..... 2•53
Al-Ti ..... 2•54
Al-U ..... 2•54
Al-V ..... 2•54
Al-W ..... 2•55
Al-Y ..... 2•55
Al-Yb ..... 2•55
Al-Zn ..... 2•56
Al-Zr ..... 2•56
As-Au ..... 2•56
As-Bi ..... 2•57
As-Cd ..... 2•57
As-Co ..... 2•58
As-Cu ..... 2•58
As-Fe ..... 2•58
As-Ga ..... 2•59
As-Ge ..... 2•59
As-In ..... 2•59
As-K ..... 2•60
As-Mn ..... 2•60
As-Nd ..... 2•60
As-Ni ..... 2•61
As-P ..... 2•61
As-Pb ..... 2•61
As-Pd ..... 2•62
As-S ..... 2•62
As-Sb ..... 2•62
As-Se ..... 2•63
As-Si ..... 2•63
As-Sn ..... 2•63
As-Te ..... 2•64
As-Tl ..... 2•64
As-Yb ..... 2•64
As-Zn ..... 2•65
Au-Be ..... 2•65
Au-Bi ..... 2•65
Au-Ca ..... 2•66
Au-Cd ..... 2•66
Au-Ce ..... 2•67
Au-Co ..... 2•67
Au-Cr ..... 2•67
Au-Cu ..... 2•68
Au-Dy ..... 2•68
Au-Eu ..... 2•68
Au-Fe ..... 2•69
Au-Ga ..... 2•69
Au-Ge ..... 2•69
Au-Hg ..... 2•70
Au-In ..... 2•70
Au-K ..... 2•70
Au-La ..... 2•71
Au-Li ..... 2•71
Au-Mg ..... 2•71
Au-Mn ..... 2•72
Au-Na ..... 2•72
Au-Nb ..... 2•73
Au-Ni ..... 2•73
Au-Pb ..... 2•73
Au-Pd ..... 2•74
Au-Pr ..... 2•74
Au-Pt ..... 2•74
Au-Pu ..... 2•75
Au-Rb ..... 2•75
Au-Sb ..... 2•75
Au-Se ..... 2•76
Au-Si ..... 2•76
Au-Sn ..... 2•76
Au-Sr ..... 2•77
Au-Te ..... 2•77
Au-Th ..... 2•77
Au-Ti ..... 2•78
Au-Tl ..... 2•78
Au-U ..... 2•78
Au-V ..... 2•79
Au-Yb ..... 2•79
Au-Zn ..... 2•79
Au-Zr ..... 2•80
B-C ..... 2•80
B-Co ..... 2•80
B-Cr ..... 2•81
B-Cu ..... 2•81
B-Fe ..... 2•81
B-Mn ..... 2•82
B-Mo ..... 2•82
B-Nb ..... 2•82
B-Ni ..... 2•83
B-Pd ..... 2•83
B-Pt ..... 2•83
B-Re ..... 2•84
B-Ru ..... 2•84
B-Sc ..... 2•84
B-Si ..... 2•85
B-Ta ..... 2•85
B-Ti ..... 2•85
B-V ..... 2•86
B-W ..... 2•86
B-Y ..... 2•86
B-Zr ..... 2•87
Ba-Ca ..... 2•87
Ba-Cd ..... 2•87
Ba-Cu ..... 2•88
Ba-Ga ..... 2•88
Ba-Ge ..... 2•88
Ba-H ..... 2•89
Ba-Hg ..... 2•89
Ba-In ..... 2•89
Ba-Li ..... 2•90
Ba-Mg ..... 2•90
Ba-Na ..... 2•90
Ba-P ..... 2•91
Ba-Pb ..... 2•91
Ba-Se ..... 2•91
Ba-Si ..... 2•92
Ba-Te ..... 2•92
Ba-Tl ..... 2•92
Ba-Zn ..... 2•93
Be-Co ..... 2•93
Be-Cr ..... 2•93
Be-Cu ..... 2•94
Be-Fe ..... 2•94
Be-Hf ..... 2•95
Be-Nb ..... 2•95
Be-Ni ..... 2•95
Be-Pd ..... 2•96
Be-Si ..... 2•96
Be-Th ..... 2•96
Be-Ti ..... 2•97
Be-W ..... 2•97
Be-Zr ..... 2•97
Bi-Ca ..... 2•98
Bi-Cd ..... 2•98
Bi-Cs ..... 2•98
Bi-Cu ..... 2•99
Bi-Ga ..... 2•99
Bi-Ge ..... 2•99
Bi-Hg ..... 2•100
Bi-In ..... 2•100
Bi-K ..... 2•100
Bi-La ..... 2•101
Bi-Li ..... 2•101
Bi-Mg ..... 2•101
Bi-Mn ..... 2•102
Bi-Na ..... 2•102
Bi-Nd ..... 2•102
Bi-Ni ..... 2•103
Bi-Pb ..... 2•103
Bi-Pd ..... 2•103
Bi-Pt ..... 2•104
Bi-Rb ..... 2•104
Bi-S ..... 2•104
Bi-Sb ..... 2•105
Bi-Se ..... 2•105
Bi-Sm ..... 2•106
Bi-Sn ..... 2•106
Bi-Sr ..... 2•106
Bi-Te ..... 2•107
Bi-Tl ..... 2•107
Bi-U ..... 2•107
Bi-Y ..... 2•108
Bi-Yb ..... 2•108
Bi-Zn ..... 2•108
Bi-Zr ..... 2•109
C-Co ..... 2•109
C-Cr ..... 2•109
C-Cu ..... 2•110
C-Fe ..... 2•110
C-Hf ..... 2•111
C-La ..... 2•111
C-Mn ..... 2•111
C-Mo ..... 2•112
C-Ni ..... 2•112
C-Pr ..... 2•112
C-Sc ..... 2•113
C-Si ..... 2•113
C-Ta ..... 2•113
C-Th ..... 2•114
C-Ti ..... 2•114
C-U ..... 2•114
C-V ..... 2•115
C-W ..... 2•115
C-Y ..... 2•115
C-Zr ..... 2•116
Ca-Cd ..... 2•116
Ca-Cu ..... 2•116
Ca-Ga ..... 2•117
Ca-Ge ..... 2•117
Ca-Hg ..... 2•117
Ca-In ..... 2•118
Ca-Li ..... 2•118
Ca-Mg ..... 2•118
Ca-Na ..... 2•119
Ca-Nd ..... 2•119
Ca-Ni ..... 2•119
Ca-O ..... 2•120
Ca-Pb ..... 2•120
Ca-Pd ..... 2•120
Ca-Pt ..... 2•121
Ca-Sb ..... 2•121
Ca-Si ..... 2•121
Ca-Sr ..... 2•122
Ca-Tl ..... 2•122
Ca-Yb ..... 2•122
Ca-Zn ..... 2•123
Cd-Cu ..... 2•123
Cd-Eu ..... 2•123
Cd-Ga ..... 2•124
Cd-Gd ..... 2•124
Cd-Ge ..... 2•124
Cd-Hg ..... 2•125
Cd-In ..... 2•125
Cd-La ..... 2•125
Cd-Li ..... 2•126
Cd-Mg ..... 2•126
Cd-Na ..... 2•126
Cd-Ni ..... 2•127
Cd-P ..... 2•127
Cd-Pb ..... 2•127
Cd-Sb ..... 2•128
Cd-Se ..... 2•128
Cd-Sm ..... 2•128
Cd-Sn ..... 2•129
Cd-Sr ..... 2•129
Cd-Te ..... 2•129
Cd-Th ..... 2•130
Cd-Tl ..... 2•130
Cd-Y ..... 2•130
Cd-Yb ..... 2•131
Cd-Zn ..... 2•131
Ce-Co ..... 2•131
Ce-Cu ..... 2•132
Ce-Fe ..... 2•132
Ce-Ga ..... 2•133
Ce-Ge ..... 2•133
Ce-In ..... 2•133
Ce-Ir ..... 2•134
Ce-Mg ..... 2•134
Ce-Mn ..... 2•134
Ce-Ni ..... 2•135
Ce-O ..... 2•135
Ce-Pd ..... 2•135
Ce-Pu ..... 2•136
Ce-S ..... 2•136
Ce-Si ..... 2•136
Ce-Sn ..... 2•137
Ce-Te ..... 2•137
Ce-Ti ..... 2•137
Ce-Tl ..... 2•138
Ce-Zn ..... 2•138
Cl-Cs ..... 2•138
Cl-Ga ..... 2•139
Cl-Hg ..... 2•139
Cl-In ..... 2•139
Cl-Na ..... 2•140
Co-Cr ..... 2•140
Co-Cu ..... 2•140
Co-Dy ..... 2•141
Co-Er ..... 2•141
Co-Fe ..... 2•141
Co-Ga ..... 2•142
Co-Gd ..... 2•142
Co-Ge ..... 2•142
Co-Hf ..... 2•143
Co-Ho ..... 2•143
Co-Mn ..... 2•143
Co-Mo ..... 2•144
Co-Nb ..... 2•144
Co-Nd ..... 2•144
Co-Ni ..... 2•145
Co-P ..... 2•145
Co-Pd ..... 2•145
Co-Pr ..... 2•146
Co-Pt ..... 2•146
Co-Pu ..... 2•146
Co-Re ..... 2•147
Co-S ..... 2•147
Co-Sb ..... 2•147
Co-Se ..... 2•148
Co-Si ..... 2•148
Co-Sm ..... 2•148
Co-Sn ..... 2•149
Co-Ta ..... 2•149
Co-Tb ..... 2•149
Co-Te ..... 2•150
Co-Th ..... 2•150
Co-Ti ..... 2•150
Co-V ..... 2•151
Co-W ..... 2•151
Co-Y ..... 2•151
Co-Zn ..... 2•152
Cr-Cu ..... 2•152
Cr-Fe ..... 2•152
Cr-Ga ..... 2•153
Cr-Ge ..... 2•153
Cr-Hf ..... 2•153
Cr-Ir ..... 2•154
Cr-Lu ..... 2•154
Cr-Mn ..... 2•154
Cr-Mo ..... 2•155
Cr-Nb ..... 2•155
Cr-Ni ..... 2•155
Cr-O ..... 2•156
Cr-Os ..... 2•156
Cr-Pd ..... 2•156
Cr-Pt ..... 2•157
Cr-Re ..... 2•157
Cr-Rh ..... 2•157
Cr-Ru ..... 2•158
Cr-S ..... 2•158
Cr-Sb ..... 2•158
Cr-Sc ..... 2•159
Cr-Se ..... 2•159
Cr-Si ..... 2•160
Cr-Sn ..... 2•160

(continued)

Cr-Ta .... 2•160
Cr-Te .... 2•161
Cr-Ti .... 2•161
Cr-U ..... 2•161
Cr-V ..... 2•162
Cr-W .... 2•162
Cr-Zr .... 2•162
Cs-Ge ... 2•163
Cs-Hg ... 2•163
Cs-In .... 2•163
Cs-K ..... 2•164
Cs-Na ... 2•164
Cs-O ..... 2•164
Cs-Rb ... 2•165
Cs-S ..... 2•165
Cs-Sb ... 2•165
Cs-Se ... 2•166
Cs-Sn ... 2•166
Cs-Te ... 2•166
Cs-Tl .... 2•167
Cu-Dy .. 2•167
Cu-Er ... 2•167
Cu-Eu ... 2•168
Cu-Fe ... 2•168
Cu-Ga .. 2•168
Cu-Gd .. 2•169
Cu-Ge .. 2•169
Cu-H .... 2•169
Cu-Hf ... 2•170
Cu-Hg .. 2•170
Cu-In .... 2•170
Cu-Ir ..... 2•171
Cu-La ... 2•171
Cu-Li .... 2•171
Cu-Mg .. 2•172
Cu-Mn .. 2•172
Cu-Nb .. 2•172
Cu-Nd .. 2•173
Cu-Ni ... 2•173
Cu-O .... 2•174
Cu-P ..... 2•174
Cu-Pb ... 2•175
Cu-Pd ... 2•175
Cu-Pt .... 2•175
Cu-Pu ... 2•176
Cu-Rh .. 2•176
Cu-S ..... 2•176
Cu-Sb ... 2•177
Cu-Se ... 2•178
Cu-Si .... 2•178
Cu-Sn ... 2•178
Cu-Sr .... 2•179
Cu-Te ... 2•179
Cu-Th ... 2•180
Cu-Ti .... 2•180
Cu-Tl .... 2•181
Cu-V .... 2•181
Cu-Yb .. 2•181
Cu-Zn ... 2•182
Cu-Zr ... 2•182
Dy-Fe ... 2•182
Dy-Ga .. 2•183
Dy-Ge .. 2•183
Dy-In .... 2•183
Dy-Mn . 2•184
Dy-Ni ... 2•184
Dy-Pb ... 2•184
Dy-Pd ... 2•185
Dy-S ..... 2•185
Dy-Sb ... 2•185
Dy-Sn ... 2•186
Dy-Te ... 2•186
Dy-Tl ... 2•186
Dy-Zr ... 2•187
Er-Fe .... 2•187
Er-Ga ... 2•187
Er-Ge ... 2•188
Er-In ..... 2•188
Er-Mn ... 2•188
Er-Ni .... 2•189
Er-Pd .... 2•189
Er-Pt ..... 2•189
Er-Ru .... 2•190
Er-Se .... 2•190
Er-Te .... 2•190
Er-Ti ..... 2•191
Er-Tl ..... 2•191
Eu-Ga ... 2•191
Eu-Ge ... 2•192
Eu-In .... 2•192
Eu-Mg .. 2•192
Eu-Pb ... 2•193
Eu-Pd ... 2•193
Eu-Pt .... 2•193
Eu-Te .... 2•194
Fe-Ga ... 2•194
Fe-Gd ... 2•194
Fe-Ge ... 2•195
Fe-H ..... 2•195
Fe-Hf .... 2•195
Fe-Ho ... 2•196
Fe-Ir ..... 2•196
Fe-La .... 2•196
Fe-Lu .... 2•197
Fe-Mn .. 2•197
Fe-Mo .. 2•197
Fe-N ..... 2•198
Fe-Nb ... 2•198
Fe-Nd ... 2•198
Fe-Ni .... 2•199
Fe-O ..... 2•199
Fe-P ..... 2•200
Fe-Pd .... 2•200
Fe-Pu .... 2•200
Fe-Rh ... 2•201
Fe-S ..... 2•201
Fe-Sb .... 2•202
Fe-Sc .... 2•202
Fe-Se .... 2•202
Fe-Si ..... 2•203
Fe-Sm ... 2•203
Fe-Sn .... 2•203
Fe-Tb .... 2•204
Fe-Te .... 2•204
Fe-Th .... 2•204
Fe-Ti ..... 2•205
Fe-Tm .. 2•205
Fe-U ..... 2•205
Fe-V ..... 2•206
Fe-W .... 2•206
Fe-Zn .... 2•206
Fe-Zr .... 2•207
Ga-Gd .. 2•207
Ga-Ho .. 2•207
Ga-In .... 2•208
Ga-La .... 2•208
Ga-Li .... 2•208
Ga-Lu .... 2•209
Ga-Mg .. 2•209
Ga-Mn .. 2•209
Ga-Mo .. 2•210
Ga-Na .... 2•210
Ga-Nb .. 2•210
Ga-Nd .. 2•211
Ga-Ni .... 2•211
Ga-Pb .... 2•211
Ga-Pd .... 2•212
Ga-Pr .... 2•212
Ga-Pt .... 2•212
Ga-Pu .... 2•213
Ga-S ..... 2•213
Ga-Sb .... 2•214
Ga-Sc .... 2•214
Ga-Se .... 2•214
Ga-Sm .. 2•215
Ga-Sn .... 2•215
Ga-Sr .... 2•215
Ga-Tb .... 2•216
Ga-Te .... 2•216
Ga-Tl .... 2•216
Ga-Tm .. 2•217
Ga-U .... 2•217
Ga-V ..... 2•217
Ga-Y ..... 2•218
Ga-Yb ... 2•218
Ga-Zn ... 2•218
Ga-Zr .... 2•219
Gd-Ge ... 2•219
Gd-In .... 2•219
Gd-Mg .. 2•220
Gd-Mn .. 2•220
Gd-Ni ... 2•220
Gd-Pb ... 2•221
Gd-Pd ... 2•221
Gd-Rh ... 2•221
Gd-Sb ... 2•222
Gd-Se .... 2•222
Gd-Sn ... 2•222
Gd-Te .... 2•223
Gd-Ti .... 2•223
Gd-Tl .... 2•223
Ge-Ho ... 2•224
Ge-In .... 2•224
Ge-K ..... 2•224
Ge-La .... 2•225
Ge-Li .... 2•225
Ge-Lu .... 2•225
Ge-Mg .. 2•226
Ge-Mn .. 2•226
Ge-Mo .. 2•227
Ge-Na .... 2•227
Ge-Nb .. 2•227
Ge-Nd .. 2•228
Ge-Ni .... 2•228
Ge-P ..... 2•228
Ge-Pb .... 2•229
Ge-Pd .... 2•229
Ge-Pr .... 2•229
Ge-Pt .... 2•230
Ge-S ..... 2•230
Ge-Sb .... 2•230
Ge-Sc .... 2•231
Ge-Se .... 2•231
Ge-Si .... 2•231
Ge-Sm .. 2•232
Ge-Sn .... 2•232
Ge-Sr .... 2•232
Ge-Tb .... 2•233
Ge-Te .... 2•233
Ge-Ti .... 2•233
Ge-Tl .... 2•234
Ge-Tm .. 2•234
Ge-U ..... 2•234
Ge-Y ..... 2•235
Ge-Yb .... 2•235
Ge-Zn .... 2•235
H-La ..... 2•236
H-Nb .... 2•236
H-Nd .... 2•237
H-Ni ..... 2•237
H-Pd ..... 2•237
H-Sr ..... 2•238
H-Ta ..... 2•238
H-Ti ..... 2•238
H-U ..... 2•239
H-V ..... 2•239
H-Zr ..... 2•239
Hf-Ir ..... 2•240
Hf-Mn .. 2•240
Hf-Mo .. 2•240
Hf-N ..... 2•241
Hf-Nb .... 2•241
Hf-Ni .... 2•241
Hf-O ..... 2•242
Hf-Os .... 2•242
Hf-Rh .... 2•242
Hf-Si ..... 2•243
Hf-Ta .... 2•243
Hf-U ..... 2•243
Hf-V ..... 2•244
Hf-W .... 2•244
Hf-Zr .... 2•244
Hg-In .... 2•245
Hg-K .... 2•245
Hg-La ... 2•245
Hg-Li .... 2•246
Hg-Mg .. 2•246
Hg-Na ... 2•246
Hg-Pb ... 2•247
Hg-Rb ... 2•247
Hg-S ..... 2•247
Hg-Se ... 2•248
Hg-Sn ... 2•248
Hg-Sr .... 2•248
Hg-Te ... 2•249
Hg-Tl .... 2•249
Hg-Zn ... 2•249
Ho-In .... 2•250
Ho-Mn .. 2•250
Ho-Pd ... 2•250
Ho-Sb ... 2•251
Ho-Te ... 2•251
Ho-Tl .... 2•251
In-K ..... 2•252
In-La ..... 2•252
In-Li ..... 2•252
In-Lu .... 2•253
In-Mg ... 2•253
In-Mn ... 2•253
In-Na .... 2•254
In-Nb .... 2•254
In-Nd .... 2•254
In-Ni ..... 2•255
In-P ..... 2•255
In-Pb ..... 2•255
In-Pd ..... 2•256
In-Pr ..... 2•256
In-Pt ..... 2•256
In-Pu ..... 2•257
In-Rb .... 2•257
In-S ..... 2•257
In-Sb ..... 2•258
In-Sc ..... 2•258
In-Se ..... 2•259
In-Si ..... 2•259
In-Sm ... 2•260
In-Sn ..... 2•260
In-Sr ..... 2•260
In-Tb .... 2•261
In-Te .... 2•261
In-Th .... 2•261
In-Ti ..... 2•262
In-Tl ..... 2•262
In-Tm ... 2•262
In-V ..... 2•263
In-Y ..... 2•263
In-Yb .... 2•263
In-Zn .... 2•264
Ir-La ..... 2•264
Ir-Mo .... 2•264
Ir-Nb ..... 2•265
Ir-Ni ..... 2•265
Ir-Pd ..... 2•265
Ir-Pt ..... 2•266
Ir-Rh ..... 2•266
Ir-Ru ..... 2•266
Ir-Ta ..... 2•267
Ir-Th ..... 2•267
Ir-Ti ..... 2•267
Ir-U ..... 2•268
Ir-V ..... 2•268
Ir-W ..... 2•268
Ir-Zr ..... 2•269
K-Na ..... 2•269
K-Pb ..... 2•269
K-Rb ..... 2•270
K-S ..... 2•270
K-Sb ..... 2•270
K-Se ..... 2•271
K-Sn ..... 2•271
K-Te ..... 2•271
K-Tl ..... 2•272
La-Mg .. 2•272
La-Mn .. 2•272
La-Ni .... 2•273
La-Pb .... 2•273
La-S ..... 2•273
La-Sb .... 2•274
La-Sc .... 2•274
La-Se .... 2•274
La-Sn .... 2•275
La-Tl ..... 2•275
La-Zn .... 2•275
Li-Mg ... 2•276
Li-Na .... 2•276
Li-Pb ..... 2•276
Li-Pd ..... 2•277
Li-S ..... 2•277
Li-Se ..... 2•277
Li-Si ..... 2•278
Li-Sn ..... 2•278
Li-Sr ..... 2•278
Li-Te ..... 2•279
Li-Tl ..... 2•279
Li-Zn .... 2•279
Lu-Pb .... 2•280
Lu-Tl .... 2•280
Mg-Mn .2•280
Mg-Ni ...2•281
Mg-Pb ...2•281
Mg-Sb ...2•281
Mg-Sc ...2•282
Mg-Si ...2•282
Mg-Sm .2•282
Mg-Sn ...2•283
Mg-Sr ...2•283
Mg-Th ..2•283
Mg-Tl ...2•284
Mg-Y ....2•284
Mg-Yb ..2•284
Mg-Zn ..2•285
Mg-Zr ...2•285
Mn-Mo .2•285
Mn-N ....2•286
Mn-Nd ..2•286
Mn-Ni ...2•286
Mn-O ....2•287
Mn-P ....2•287
Mn-Pd ...2•287
Mn-Pr ...2•288
Mn-Pu ...2•288
Mn-Sb ...2•288
Mn-Si ...2•289
Mn-Sm .2•289
Mn-Sn ...2•289
Mn-Ti ...2•290
Mn-U ....2•290
Mn-V ....2•290
Mn-Y ....2•291
Mn-Zn ..2•291
Mn-Zr ...2•291
Mo-N ....2•292
Mo-Nb ..2•292
Mo-Ni ...2•292
Mo-O ....2•293
Mo-Os ..2•293
Mo-P ....2•293
Mo-Pd ...2•294
Mo-Pt ...2•294
Mo-Pu ...2•294
Mo-Rh ..2•295
Mo-Ru ..2•295
Mo-S ....2•295
Mo-Si ...2•296
Mo-Ta ...2•296
Mo-Ti ...2•296
Mo-U ....2•297
Mo-V ....2•297
Mo-W ...2•297
Mo-Zr ...2•298
N-Nb ....2•298
N-Ni ....2•298
N-Ta ....2•299
N-Th ....2•299
N-Ti .....2•299
N-U ..... 2•300
N-Zr ..... 2•300
Na-O .... 2•300
Na-Pb ... 2•301
Na-Rb .. 2•301
Na-S ..... 2•301
Na-Sb ... 2•302
Na-Se ... 2•302
Na-Sn ... 2•302
Na-Sr ... 2•303
Na-Te ... 2•303
Na-Tl ... 2•303
Nb-Ni ... 2•304
Nb-Os .. 2•304
Nb-Pd .. 2•304
Nb-Pt ... 2•305
Nb-Rh .. 2•305
Nb-Ru .. 2•305
Nb-Si ... 2•306
Nb-Ta ... 2•306
Nb-Th .. 2•306
Nb-Ti ... 2•307
Nb-U .... 2•307
Nb-V .... 2•307
Nb-W ... 2•308
Nb-Zr ... 2•308
Nd-Ni ... 2•308
Nd-Pt ... 2•309
Nd-Rh .. 2•309
Nd-Sb .. 2•309
Nd-Si ... 2•310
Nd-Sn .. 2•310
Nd-Te ... 2•310
Nd-Ti ....2•311
Nd-Tl ....2•311
Nd-Zn ...2•311
Ni-O ..... 2•312
Ni-Os ... 2•312
Ni-P ..... 2•313
Ni-Pb ... 2•313
Ni-Pd ... 2•314
Ni-Pr .... 2•314
Ni-Pt .... 2•314
Ni-Pu ... 2•315
Ni-Re ... 2•315
Ni-Rh ... 2•316
Ni-Ru ... 2•316
Ni-S ..... 2•316
Ni-Sb ... 2•317
Ni-Sc .... 2•317
Ni-Se .... 2•317
Ni-Si .... 2•318
Ni-Sm .. 2•318
Ni-Sn ... 2•318
Ni-Ta .... 2•319
Ni-Te .... 2•319
Ni-Ti .... 2•319
Ni-U ..... 2•320
Ni-V ..... 2•320
Ni-W .... 2•320
Ni-Y ..... 2•321
Ni-Yb ... 2•321
Ni-Zn ... 2•321
Ni-Zr .... 2•322
Np-Pu .. 2•322
Np-U .... 2•322
O-Pb .... 2•323
O-Pr ..... 2•323
O-Pu .... 2•323
O-Sn .... 2•324
O-Ti ..... 2•324
O-V ..... 2•325
O-W ..... 2•325
O-Y ..... 2•326
O-Zr ..... 2•326
Os-Pt ... 2•326
Os-Pu ... 2•327
Os-Re ... 2•327
Os-Rh .. 2•327
Os-Ru .. 2•328
Os-Si .... 2•328
Os-Ti .... 2•328
Os-U .... 2•329
Os-V .... 2•329
Os-W ... 2•329
Os-Zr ... 2•330
P-Pd ..... 2•330
P-Pr ..... 2•330
P-Ru ..... 2•331
P-Sn ..... 2•331
P-Ti ..... 2•331
P-Zn ..... 2•332
Pb-Pd ... 2•332
Pb-Pr .... 2•332
Pb-Pt .... 2•333
Pb-Pu ... 2•333
Pb-Rb ... 2•333
Pb-Rh ... 2•334
Pb-S ..... 2•334
Pb-Sb .... 2•334
Pb-Se .... 2•335
Pb-Sn .... 2•335
Pb-Sr .... 2•335
Pb-Te .... 2•336
Pb-Tl .... 2•336
Pb-Y ..... 2•336
Pb-Yb ... 2•337
Pb-Zn .... 2•337
Pd-Pt .... 2•337
Pd-Pu .... 2•338
Pd-Rh .... 2•338
Pd-Ru .... 2•338
Pd-S ..... 2•339
Pd-Sb .... 2•339
Pd-Se .... 2•339
Pd-Si ..... 2•340
Pd-Sm .. 2•340
Pd-Sn .... 2•340
Pd-Te .... 2•341
Pd-Ti ..... 2•341
Pd-Tl ..... 2•342
Pd-U ..... 2•342
Pd-V ..... 2•342
Pd-W .... 2•343
Pd-Y ..... 2•343
Pd-Yb ... 2•343
Pd-Zn .... 2•344
Pr-Sb .... 2•344
Pr-Se .... 2•344
Pr-Si ..... 2•345
Pr-Sn .... 2•345
Pr-Te .... 2•345
Pr-Tl ..... 2•346
Pr-Zn .... 2•346
Pt-Rh .... 2•346
Pt-Si ..... 2•347
Pt-Sn .... 2•347
Pt-Te .... 2•347
Pt-Ti ..... 2•348
Pt-Tl ..... 2•348
Pt-U ..... 2•348
Pt-V ..... 2•349
Pt-Zr ..... 2•349
Pu-Sc .... 2•349
Pu-U ..... 2•350
Pu-Zn .... 2•350
Pu-Zr .... 2•350
Rb-Sb .... 2•351
Rb-Se .... 2•351
Rb-Tl .... 2•351
Re-Ru .... 2•352
Re-Si .... 2•352
Re-Te .... 2•352
Re-U .... 2•353
Re-V .... 2•353
Rh-Se .... 2•353
Rh-Ta .... 2•354
Rh-Ti .... 2•354
Rh-U .... 2•354
Rh-V .... 2•355
Ru-Si .... 2•355
Ru-Ta .... 2•355
Ru-Ti .... 2•356
Ru-U .... 2•356
Ru-V .... 2•356
S-Se ..... 2•357
S-Sn ..... 2•357
S-Te ..... 2•358
S-Ti ..... 2•358
Sb-Se .... 2•358
Sb-Si .... 2•359
Sb-Sm .. 2•359
Sb-Sn .... 2•359
Sb-Sr .... 2•360
Sb-Tb .... 2•360
Sb-Te .... 2•360
Sb-Tl .... 2•361
Sb-U ..... 2•361
Sb-Y ..... 2•361
Sb-Zn .... 2•362
Sc-Ti .... 2•362
Sc-Y ..... 2•362
Sc-Zr .... 2•363
Se-Sn .... 2•363
Se-Sr .... 2•363
Se-Te .... 2•364
Se-Tl .... 2•364
Se-Tm .. 2•364
Se-U ..... 2•365
Si-Sn .... 2•365
Si-Sr ..... 2•365
Si-Ta ..... 2•366
Si-Te ..... 2•366
Si-Th .... 2•366
Si-Ti ..... 2•367
Si-U ..... 2•367
Si-V ..... 2•367
Si-Zn .... 2•368
Si-Zr ..... 2•368
Sm-Sn .. 2•368
Sm-Tl .... 2•369
Sm-Zn .. 2•369
Sn-Zr .... 2•369
Sn-Te .... 2•370
Sn-Ti .... 2•370
Sn-Tl .... 2•370
Sn-U ..... 2•371
Sn-Y ..... 2•371
Sn-Yb ... 2•371
Sn-Zn .... 2•372
Sn-Zr .... 2•372
Sr-Te .... 2•372
Sr-Tl ..... 2•373
Sr-Zn .... 2•373
Ta-Th .... 2•373
Ta-Ti .... 2•374
Ta-U .... 2•374
Ta-V .... 2•374
Ta-W .... 2•375
Ta-Zr .... 2•375
Tb-Tl .... 2•375
Te-Tl .... 2•376
Te-U .... 2•376
Te-Yb ... 2•376
Te-Zn .... 2•377
Th-Ti .... 2•377
Th-Tl .... 2•377
Th-Zn .... 2•378
Th-Zr .... 2•378
Ti-U ..... 2•378
Ti-V ..... 2•379
Ti-W .... 2•379
Ti-Y ..... 2•379
Ti-Zr ..... 2•380
Tl-Yb .... 2•380
Tl-Zn .... 2•380
U-Zr ..... 2•381
V-W ..... 2•381
V-Zr ..... 2•381
W-Zr .... 2•382
Y-Zn ..... 2•382
Y-Zr ..... 2•382
Yb-Zn .. 2•383

Introduction to Binary Alloy Phase Diagrams

THE 1046 BINARY SYSTEMS presented in this Section have been selected for their commercial importance from the almost 3000 systems covered in *Binary Alloy Phase Diagrams*, Second Edition. The diagrams used were reproduced from that compilation, from more recent evaluations, or, in some instances, updated evaluations based on the most recent literature. The source is indicated with each phase diagram. "Unpublished" indicates the source is a complete evaluation that has not yet been published in the *Journal of Phase Equilibria* or in a monograph. The crystal structure data shown with the diagrams have been updated in some instances with information from *Pearson's Handbook of Crystallographic Data for Intermetallic Phases*, Second Edition.

Except when the information for a system is from one of the General References listed in the following pages, the specific author of the information is listed as the source, along with the year the investigation was completed. To locate the author's complete investigation of a system, consult the Binary Alloy Phase Diagrams Index in this Section, which lists source information for all 2965 binary alloy systems for which data exist.

Because this Handbook is designed to be used mainly by engineers to solve industrial problems, the primary composition scale is plotted in weight percent. Atomic percentages are shown as a secondary scale at the top of the diagrams. Conversions between weight and atomic composition also can be made using the standard atomic weights listed in the Appendix. For the sake of clarity, grid lines are not superimposed on the phase diagrams. However, tick marks are provided along the composition scale as well as the temperature scale, which is shown in degrees Celsius. Celsius temperatures can be easily converted to degrees Fahrenheit using the table in the Appendix. Magnetic transitions (Curie temperature and Néel temperature) are shown as dot-dashed lines. Dashed lines are used to denote uncertain or speculative boundaries.

All diagrams presented in this Section of the Handbook are for stable equilibrium conditions, except where metastable conditions are indicated.

Binary Alloy Phase Diagrams Index

This index gives source information for all 2965 binary alloy systems. Column 2 designates all binary abstracts published in *Binary Alloy Phase Diagrams*, Second Edition (called "M2") and indicates if information for the system has been updated in the *Binary Alloy Phase Diagrams Updating Service* by listing the update year. Abstracts are a shortened version of the full evaluation giving concise descriptions of key features of the system, crystal structure data, primary references, and the equilibrium diagram, if any. Column 3 gives the source of the original abstract or the most recent full evaluation. Full evaluations include expanded information on the phase diagram, and any lattice parameter, thermodynamic, magnetism, and pressure information and ancillary figures available. A key to abbreviated titles of Alloy Phase Diagram Program source publications and General References used in column 3 precede the index. Systems marked "unpublished" have been submitted to the Alloy Phase Diagram Program, but have not yet been published. References to sources that are non-Alloy Phase Diagram publications follow the index. Column 4 indicates whether the evaluation includes a phase diagram (D) or is text only (T). Diagrams for systems marked by an asterisk are published in this handbook.

Binary General References

The following list of references has provided the foundation of much of the phase diagram data that is currently cited in the literature. To conserve space, these references will be cited by their general reference symbol in the index.

[Brandes]: E.A. Brandes and R.F. Flint, Ed., *Manganese Phase Diagrams,* The Manganese Centre, 17 Avenue Hoche, 75008 Paris, France (1980).

[Chiotti]: P. Chiotti, V.V. Akhachinskij, and I. Ansara, *The Chemical Thermodynamics of Actinide Elements and Compounds,* Part 5: The Actinide Binary Alloys, V. Medvedev, M.H. Rand, E.F. Westrum, Jr., and F.L. Oetting, Ed., International Atomic Energy Agency, Vienna (1981).

[Elliott]: R.P. Elliott, *Constitution of Binary Alloys, First Supplement,* McGraw-Hill, New York or General Electric Co., Business Growth Services, Schenectady, New York (1965).

[Hafnium]: P.J. Spencer, O. von Goldbeck, R. Ferro, R. Marazza, K. Girgis, and O. Kubaschewski, *Hafnium: Physico-Chemical Properties of Its Compounds and Alloys,* K.L. Komerek, Ed., Atomic Energy Review Special Issue No. 8, International Atomic Energy Agency, Vienna (1981).

[Hansen]: M. Hansen and K. Anderko, *Constitution of Binary Alloys*, McGraw-Hill, New York or General Electric Co., Business Growth Services, Schenectady, New York (1958).

[Hultgren, B]: R. Hultgren, P.D. Desai, D.T. Hawkins, M. Gleiser, and K.K. Kelley, *Selected Values of the Thermodynamic Properties of Binary Alloys*, American Society for Metals, Metals Park, Ohio (1973).

[Ivanov]: O.S. Ivanov, T.A. Badaeva, R.M. Sofronova, V.B. Kishenevskii, and N.P. Kushnir, *Phase Diagrams of Uranium Alloys,* Nauka, Moscow (1972).

[Kubaschewski]: O. Kubaschewski, *Iron--Binary Phase Diagrams,* Springer-Verlag, New York (1982).

[Metals]: *Metals Handbook*, Metallography, Structures and Phase Diagrams, Vol. 8, 8th ed., American Society for Metals, Metals Park, OH (1973).

[Moffatt]: W.G. Moffatt, Ed., *Handbook of Binary Phase Diagrams,* Business Growth Services, General Electric Co., Schenectady, NY (1976).

[Molybdenum]: L. Brewer, *Molybdenum: Physico-Chemical Properties of Its Compounds and Alloys,* O. Kubaschewski, Ed., Atomic Energy Review Special Issue No. 7, International Atomic Energy Agency, Vienna (1980).

[Pearson3]: P. Villars and L.D. Calvert, *Pearson's Handbook of Crystallographic Data for Intermetallic Phases,* Vol. 1, 2, and 3, American Society for Metals, Metals Park, OH (1985).

[Pearson4]: P. Villars and L.D. Calvert, *Pearson's Handbook of Crystallographic Data for Intermetallic Phases*, 2nd ed., Vol. 1, 2, 3, and 4, ASM International, Materials Park, OH (1991).

[Plutonium]: M.H. Rand, D.T. Livey, P. Feschotte, H. Nowotny, K. Seifert, and R. Ferro, *Plutonium: Physico-Chemical Properties of Its Compounds and Alloys,* O. Kubaschewski, Ed., Atomic Energy Review Special Issues No. 1, International Atomic Energy Agency, Vienna (1966).

[Shunk]: F.A. Shunk, *Constitution of Binary Alloys, Second Supplement,* McGraw-Hill, New York or General Electric Co., Business Growth Services, Schenectady, New York (1969).

[Smith]: J.F. Smith, O.N. Carlson, D.T. Peterson, and T.E. Scott, *Thorium: Preparation and Properties,* Iowa State University Press, Ames, IA (1975).

[Smithells]: C.J. Smithells and E.A. Brandes, *Metals Reference Book,* 5th ed., Butterworths, Woburn, MA (1976).

[Thorium]: M.H. Rand, O. von Goldbeck, R. Ferro, K. Girgis, and A.L. Dragoo, *Thorium: Physico-Chemical Properties of Its Compounds and Alloys,* O. Kubaschewski, Ed., Atomic Energy Review Special Issue No. 5, International Atomic Energy Agency, Vienna (1975).

[Zirconium]: C.B. Alcock, K.T. Jacob, S. Zador, O. von Goldbeck, H. Nowotny, K. Seifert, and O. Kubaschewski, *Zirconium: Physico-Chemical Properties of Its Compounds and Alloys,* O. Kubaschewski, Ed., Atomic Energy Review Special Issue No. 6, International Atomic Energy Agency, Vienna (1976).

Key to Titles

Key to titles of Alloy Phase Diagram Publications abbreviated under "Published" and "Data Source":

BAPD
Bulletin of Alloy Phase Diagrams
ASM International

Binary Beryllium
Phase Diagrams of Binary Beryllium Alloys
ASM International, 1987

Binary Gold
Phase Diagrams of Binary Gold Alloys
ASM International, 1988

Binary Iron
Phase Diagrams of Binary Iron Alloys
ASM International, 1993

Binary Magnesium
Phase Diagrams of Binary Magnesium Alloys
ASM International, 1988

Binary Nickel
Phase Diagrams of Binary Nickel Alloys
ASM International, 1991

Binary Titanium
Phase Diagrams of Binary Titanium Alloys
ASM International, 1987

Binary Tungsten
Phase Diagrams of Binary Tungsten Alloys
The Indian Institute of Metals, 1991

Binary Vanadium
Phase Diagrams of Binary Vanadium Alloys
ASM International, 1989

Indium
Phase Diagrams of Indium Alloys and Their Engineering Applications
ASM International, 1992

JAPD
Journal of Alloy Phase Diagrams
The Indian Institute of Metals

JPE
Journal of Phase Equilibria
ASM International

M2
Binary Alloy Phase Diagrams, 2nd edition
ASM International, 1990

91
Binary Alloy Phase Diagrams Updating Service
ASM International, Dec. 1991

92
Binary Alloy Phase Diagrams Updating Service
ASM International, July and Dec. 1992

Binary Alloys Index

System	Published	Data source	Data type
Ac-Ag	M2	Unpublished	T
Ac-Au	M2	Binary Gold	T
Ac-B	M2	M2	D
Ac-Cr	M2	BAPD 6(5)	D
Ac-Cu	M2	M2	T
Ac-H	M2	M2	T
Ac-Mg	M2	Unpublished	T
Ac-Mo	M2	M2	D
Ac-O	M2	M2	T
Ac-Pt	M2	BAPD 10(4a)	D
Ac-S	M2	M2	T
Ac-W		Binary Tungsten	T
*Ag-Al	M2	BAPD 8(6)	D
Ag-Am	No Data		
Ag-Ar	M2	Unpublished	T
*Ag-As	M2	BAPD 11(2)	D
Ag-At	M2	Unpublished	T
*Ag-Au	M2	Binary Gold	D
Ag-B	M2,92	BAPD 11(6)	T
Ag-Ba	M2,92	Unpublished	D
*Ag-Be	M2	Binary Beryllium	D
*Ag-Bi	M2	BAPD 1(2)	D
Ag-Br	M2	M2	T
Ag-C	M2	BAPD 9(3)	D
*Ag-Ca	M2	BAPD 9(3)	D
*Ag-Cd	M2	[Hansen]	D
*Ag-Ce	M2	BAPD 6(5)	D
Ag-Cl	M2	M2	T
*Ag-Co	M2	BAPD 7(3)	D
Ag-Cr	M2	BAPD 11(3)	D
Ag-Cs	M2	BAPD 7(3)	T
*Ag-Cu	M2	Unpublished	D
*Ag-Dy	M2	BAPD 6(1)	D
*Ag-Er	M2	BAPD 6(1)	D
*Ag-Eu	M2	BAPD 6(1)	D
Ag-F	M2	M2	T
*Ag-Fe	M2	Binary Iron	D
Ag-Fr	M2	Unpublished	T
*Ag-Ga	M2,92	JPE 13(3)	D
*Ag-Gd	M2	BAPD 6(2)	D
*Ag-Ge	M2	BAPD 9(1)	D
Ag-H	M2,92	JPE 12(6)	T
Ag-He	M2	Unpublished	T
Ag-Hf	M2	BAPD 10(2)	T
*Ag-Hg	M2	Unpublished	D
*Ag-Ho	M2	BAPD 6(2)	D
Ag-I	M2	M2	T
*Ag-In	M2	Indium	D
Ag-Ir	M2	BAPD 7(4)	D
Ag-K	M2	BAPD 7(3)	T
Ag-Kr	M2	Unpublished	T
*Ag-La	M2	BAPD 4(4)	D
*Ag-Li	M2	BAPD 7(3)	D
Ag-Lu	M2	BAPD 4(4)	D
*Ag-Mg	M2	Binary Magnesium	D
Ag-Mn	M2	BAPD 11(5)	D
*Ag-Mo	M2	BAPD 11(6)	D
Ag-N	M2	BAPD 11(5)	T
*Ag-Na	M2	BAPD 7(2)	D
Ag-Nb	M2	BAPD 10(6)	T
*Ag-Nd	M2	BAPD 6(1)	D
Ag-Ne	M2	Unpublished	T
*Ag-Ni	M2	Binary Nickel	D
Ag-Np	M2	M2	T
Ag-O	M2	JPE 13(2)	D
Ag-Os	M2	BAPD 7(4)	D
*Ag-P	M2	BAPD 9(3)	D
Ag-Pa	M2	M2	T
*Ag-Pb	M2	BAPD 8(4)	D
*Ag-Pd	M2	BAPD 9(3)	D
Ag-Pm	M2,91	M2	T
Ag-Po	M2	M2	T
*Ag-Pr	M2	BAPD 6(1)	D
*Ag-Pt	M2	BAPD 8(4)	D
Ag-Pu	M2	[70Woo]	D
Ag-Ra	M2	Unpublished	T
Ag-Rb	M2	BAPD 7(1)	T
Ag-Re	M2	BAPD 9(3)	D
Ag-Rh	M2	BAPD 7(4)	D
Ag-Rn	M2	Unpublished	T
Ag-Ru	M2	BAPD 7(4)	D
*Ag-S	M2	BAPD 7(3)	D
*Ag-Sb	M2	[Hansen]	D
*Ag-Sc	M2	BAPD 4(4)	D
*Ag-Se	M2	BAPD 11(3)	D
*Ag-Si	M2	BAPD 10(6)	D
*Ag-Sm	M2,91	BAPD 6(2)	D
*Ag-Sn	M2	BAPD 8(4)	D
*Ag-Sr	M2	BAPD 11(2)	D
Ag-Ta	M2	BAPD 9(3)	T
Ag-Tb	M2	BAPD 6(2)	D
Ag-Tc	M2	Unpublished	T
*Ag-Te	M2	JPE 12(1)	D
Ag-Th	M2,92	JPE 12(3)	D
*Ag-Ti	M2	Binary Titanium	D
*Ag-Tl	M2	BAPD 10(6)	D
Ag-Tm	M2	M2	D
Ag-U	M2	BAPD 10(6)	D
Ag-V	M2	Binary Vanadium	D
Ag-W	M2,92	Binary Tungsten	D
Ag-Xe	M2	Unpublished	T
*Ag-Y	M2	BAPD 4(4)	D
*Ag-Yb	M2	BAPD 6(2)	D
*Ag-Zn	M2	[40And]	D
*Ag-Zr	M2	JPE 13(2)	D
Al-Am	M2	BAPD 10(3)	T
*Al-As	M2	BAPD 5(6)	D
*Al-Au	M2,91	BAPD 8(2)	D
Al-B	M2	BAPD 11(6)	D
*Al-Ba	M2,92	BAPD 2(3)	D
*Al-Be	M2	Binary Beryllium	D
*Al-Bi	M2	BAPD 5(3)	D
Al-Br	No Data		
Al-C	M2,91,92	M2	D
*Al-Ca	M2	BAPD 9(6)	D
*Al-Cd	M2	BAPD 3(2)	D
*Al-Ce	M2	BAPD 9(6)	D
Al-Cl	No Data		
Al-Cm	No Data		
*Al-Co	M2	BAPD 10(6)	D
*Al-Cr	M2	Unpublished	D
Al-Cs	M2	Unpublished	T
*Al-Cu	M2	[85Mur]	D
Al-Dy	M2	M2	D
*Al-Er	M2	BAPD 9(6)	D
Al-Eu	M2,91	M2	D
Al-F	No Data		
*Al-Fe	M2	Binary Iron	D
*Al-Ga	M2	BAPD 4(2)	D
*Al-Gd	M2	BAPD 9(6)	D
*Al-Ge	M2	BAPD 5(4)	D
*Al-H	M2	JPE 13(1)	D
Al-Hf	M2	Unpublished	D
*Al-Hg	M2	BAPD 6(3)	D
*Al-Ho	M2	BAPD 9(6)	D
Al-I	No Data		
*Al-In	M2	Indium	D
Al-Ir	M2	M2	D
Al-K	M2	Unpublished	T
*Al-La	M2	BAPD 9(6)	D
*Al-Li	M2,91	BAPD 3(2)	D
Al-Lu	M2	M2	D
*Al-Mg	M2	Binary Magnesium	D
*Al-Mn	M2	BAPD 8(5)	D
Al-Mo	M2,91	Unpublished	D
Al-N	M2	BAPD 7(4)	D
Al-Na	M2	BAPD 4(4)	D
*Al-Nb	M2	Unpublished	D
*Al-Nd	M2,91	BAPD 10(1)	D
*Al-Ni	M2	Binary Nickel	D
Al-Np	M2	BAPD 10(2)	T
Al-O	M2	BAPD 6(6)	D
Al-Os	M2	Unpublished	T
Al-P	M2	BAPD 6(3)	D
*Al-Pb	M2	BAPD 5(1)	D
*Al-Pd	M2	BAPD 7(4)	D
Al-Pm	M2	M2	D
*Al-Pr	M2	BAPD 10(1)	D
*Al-Pt	M2	BAPD 7(1)	D
Al-Pu	M2	BAPD 10(4a)	D
Al-Rb	M2	Unpublished	T
Al-Re	M2	Unpublished	T
Al-Rh	M2	M2	D
Al-Ru	M2	M2	D
*Al-S	M2,91	BAPD 8(2)	D
*Al-Sb	M2	BAPD 5(5)	D
Al-Sc	M2,91	BAPD 10(1)	D
*Al-Se	M2	BAPD 10(6)	D
*Al-Si	M2	BAPD 5(1)	D

(continued)

System	Published	Data source	Data type
Al-Sm	M2	BAPD 10(1)	D
*Al-Sn	M2	BAPD 4(4)	D
*Al-Sr	M2	BAPD 10(6)	D
*Al-Ta	M2	Unpublished	D
Al-Tb	M2	M2	D
Al-Tc	M2	M2	T
*Al-Te	M2	BAPD 11(2)	D
*Al-Th	M2	BAPD 10(4a)	D
*Al-Ti	M2	Binary Titanium	D
Al-Tl	M2,92	BAPD 10(2)	D
Al-Tm	M2	M2	D
*Al-U	M2,91	BAPD 11(1)	D
*Al-V	M2	Binary Vanadium	D
*Al-W	M2	Binary Tungsten	D
*Al-Y	M2	BAPD 10(1)	D
*Al-Yb	M2	BAPD 10(1)	D
*Al-Zn	M2	BAPD 4(1)	D
*Al-Zr	M2,92	JPE 13(3)	D
Am-As	M2	M2	T
Am-B	M2	M2	D
Am-Be	M2	Binary Beryllium	T
Am-Bi	M2	M2	T
Am-C	M2	M2	T
Am-Co	M2	M2	T
Am-Cr	M2	BAPD 6(5)	D
Am-Cu	M2	M2	T
Am-Fe	M2	M2	T
Am-H	M2	M2	T
Am-Ir	M2	M2	T
Am-Mo	M2	[Molybdenum]	D
Am-N	M2	M2	T
Am-Ni	M2	Binary Nickel	T
Am-O	M2,91	[Elliott]	T
Am-Os	M2	M2	T
Am-P	M2	M2	T
Am-Pd	M2	M2	T
Am-Pt	M2	BAPD 10(2)	D
Am-Pu	M2	[66Ell]	D
Am-Rh	M2	M2	T
Am-Ru	M2	M2	T
Am-S	M2	M2	T
Am-Sb	M2	M2	T
Am-Se	M2	M2	T
Am-Si	M2	M2	D
Am-Te	M2	M2	T
Am-W		Binary Tungsten	T
Ar-Au	M2	Binary Gold	T
Ar-Be	M2	Binary Beryllium	T
Ar-Cu	M2	Unpublished	T
Ar-Mg	M2	Binary Magnesium	T
Ar-Mo	M2	[Molybdenum]	D
Ar-W		Binary Tungsten	T
*As-Au	M2	Binary Gold	D
As-B	M2	M2	D
As-Ba	M2	M2	T
As-Be	M2	Binary Beryllium	T
*As-Bi	M2	[53Gea]	D
As-Bk	M2	M2	T
As-Br	No Data		
As-C	M2	M2	T
As-Ca	M2	M2	T
*As-Cd	M2	JPE 13(2)	D
As-Ce	M2	BAPD 7(3)	T
As-Cf	M2	M2	T
As-Cl	No Data		
As-Cm	M2	M2	T
*As-Co	M2	BAPD 11(6)	D
As-Cr	M2	BAPD 11(5)	D
As-Cs	M2	M2	T
*As-Cu	M2	BAPD 9(5)	D
As-Dy	M2	M2	D
As-Er	M2	M2	D
As-Eu	M2	BAPD 7(3)	D
As-F	No Data		
*As-Fe	M2	Binary Iron	D
*As-Ga	M2	M2	D
As-Gd	M2	BAPD 7(4)	T
*As-Ge	M2,91	BAPD 6(3)	D
As-H	M2	M2	T
As-Hf	M2	M2	T
As-Hg	M2	M2	T
As-Ho	M2	M2	D
As-I	No Data		
*As-In	M2	Indium	D
As-Ir	M2	M2	T
*As-K	M2	[61Dor1]	D
As-La	M2	BAPD 7(4)	T
As-Li	M2	M2	T
As-Lu	M2	M2	D
As-Mg	M2	Binary Magnesium	D
*As-Mn	M2	BAPD 10(5)	D
As-Mo	M2,91	[Molybdenum]	D
As-N	M2	M2	T
As-Na	M2	M2	T
As-Nb	M2	M2	T
*As-Nd	M2	BAPD 7(4)	D
*As-Ni	M2	Binary Nickel	D
As-Np	M2	M2	T
As-O	M2	M2	T
As-Os	M2	M2	D
*As-P	M2	JPE 12(3)	D
As-Pa	M2	M2	T
*As-Pb	M2	BAPD 11(2)	D
*As-Pd	M2,91,92	BAPD 11(5)	D
As-Pm	No Data		
As-Pr	M2	BAPD 7(4)	T
As-Pt	M2	BAPD 11(5)	D
As-Pu	M2	M2	T
As-Rb	M2	M2	T
As-Re	M2	M2	T
As-Rh	M2	M2	T
As-Ru	M2	M2	T
*As-S	M2	M2	D
*As-Sb	M2	M2	D
As-Sc	M2	BAPD 7(4)	T
*As-Se	M2	M2	D
*As-Si	M2	BAPD 6(3)	D
As-Sm	M2	M2	D
*As-Sn	M2,91	BAPD 11(3)	D
As-Sr	M2	M2	T
As-Ta	M2	M2	T
As-Tb	M2	M2	D
As-Tc	M2	M2	T
*As-Te	M2	M2	D
As-Th	M2	[Smith]	D
As-Ti	M2	Binary Titanium	D
*As-Tl	M2	Unpublished	D
As-Tm	M2	M2	D
As-U	M2	M2	D
As-V	M2	JPE 12(4)	T
As-W	M2	Binary Tungsten	T
As-Y	M2	BAPD 7(4)	T
*As-Yb	M2	M2	D
*As-Zn	M2	JPE 13(2)	D
As-Zr	M2,91	BAPD 11(6)	T
At-Au	M2	Binary Gold	T
At-Mo	M2	M2	D
At-W		Binary Tungsten	T
Au-B	M2	Binary Gold	D
Au-Ba	M2	Binary Gold	T
*Au-Be	M2	Binary Beryllium	D
*Au-Bi	M2	M2	D
Au-Br	M2	Binary Gold	T
Au-C	M2	Binary Gold	D
*Au-Ca	M2	Binary Gold	D
*Au-Cd	M2	Binary Gold	D
*Au-Ce	M2	Binary Gold	D
Au-Cl	M2	Binary Gold	D
Au-Cm	No Data		
*Au-Co	M2	Binary Gold	D
*Au-Cr	M2	Binary Gold	D
Au-Cs	M2	Binary Gold	D
*Au-Cu	M2	Binary Gold	D
*Au-Dy	M2	Binary Gold	D
Au-Er	M2	Binary Gold	D
*Au-Eu	M2	M2	D
Au-F	M2	Binary Gold	T
*Au-Fe	M2	Binary Iron	D
Au-Fr	M2	[68Gul1]	T
*Au-Ga	M2	Binary Gold	D
Au-Gd	M2	Binary Gold	D
*Au-Ge	M2	Binary Gold	D
Au-H	M2	Binary Gold	T
Au-He	M2	Binary Gold	T
Au-Hf	M2	Binary Gold	D
*Au-Hg	M2	BAPD 10(1)	D
Au-Ho	M2	Binary Gold	D
Au-I	M2	Binary Gold	T
*Au-In	M2	Indium	D
Au-Ir	M2	Binary Gold	T
*Au-K	M2	Binary Gold	D
Au-Kr	M2	Binary Gold	T
*Au-La	M2	Binary Gold	D
*Au-Li	M2	Binary Gold	D
Au-Lu	M2	Binary Gold	D
*Au-Mg	M2	Binary Magnesium	D
*Au-Mn	M2	Binary Gold	D
Au-Mo	M2	Binary Gold	D
Au-N	M2	Binary Gold	T
*Au-Na	M2	Binary Gold	D
*Au-Nb	M2	Binary Gold	D
Au-Nd	M2	Binary Gold	D
Au-Ne	M2	Binary Gold	T
*Au-Ni	M2	Binary Gold	D
Au-Np	M2	Binary Gold	T
Au-O	M2	Binary Gold	T
Au-Os	M2	Binary Gold	T
Au-P	M2	Binary Gold	D
Au-Pa	M2	Binary Gold	T
*Au-Pb	M2	Binary Gold	D
*Au-Pd	M2	Binary Gold	D
Au-Pm	M2	Binary Gold	D
Au-Po	M2	Binary Gold	T
*Au-Pr	M2	Binary Gold	D
*Au-Pt	M2	Binary Gold	D
*Au-Pu	M2	Binary Gold	D
Au-Ra	M2	Binary Gold	T
*Au-Rb	M2	Binary Gold	D
Au-Re	M2	Binary Gold	T
Au-Rh	M2	Binary Gold	D
Au-Rn	M2	Binary Gold	T
Au-Ru	M2	Binary Gold	D
Au-S	M2	Binary Gold	D
*Au-Sb	M2	Binary Gold	D

(continued)

System	Published	Data source	Data type
Au-Sc	M2	Binary Gold	D
*Au-Se	M2	Binary Gold	D
*Au-Si	M2	Binary Gold	D
Au-Sm	M2	Binary Gold	D
*Au-Sn	M2	Binary Gold	D
*Au-Sr	M2	Binary Gold	D
Au-Ta	M2	Binary Gold	D
Au-Tb	M2	Binary Gold	D
Au-Tc	M2	Binary Gold	T
*Au-Te	M2	Binary Gold	D
*Au-Th	M2,91	Binary Gold	D
*Au-Ti	M2	Binary Gold	D
*Au-Tl	M2	Binary Gold	D
Au-Tm	M2	Binary Gold	D
*Au-U	M2	M2	D
*Au-V	M2	Binary Vanadium	D
Au-W	M2	Binary Tungsten	D
Au-Xe	M2	Binary Gold	T
Au-Y	M2	Binary Gold	T
*Au-Yb	M2	Binary Gold	D
*Au-Zn	M2	BAPD 10(1)	D
*Au-Zr	M2	Binary Gold	D
B-Ba	M2	M2	D
B-Be	M2	Binary Beryllium	D
B-Bi	M2,91	M2	D
*B-C	M2,92	M2	D
B-Ca	M2	M2	D
B-Cd	M2	Unpublished	D
B-Ce	M2	Unpublished	D
B-Cm	No Data		
*B-Co	M2	BAPD 9(4)	D
*B-Cr	M2	BAPD 7(3)	D
B-Cs	No Data		
*B-Cu	M2	BAPD 3(1)	D
B-Dy	M2	Unpublished	D
B-Er	M2	Unpublished	D
B-Eu	M2	Unpublished	D
*B-Fe	M2	Binary Iron	D
B-Ga	M2,91	M2	D
B-Gd	M2	Unpublished	D
B-Ge	M2	BAPD 5(5)	D
B-H	M2	M2	T
B-Hf	M2	M2	D
B-Hg	M2	Unpublished	D
B-Ho	M2	Unpublished	D
B-In	M2	Indium	D
B-Ir	M2	M2	T
B-K	M2	M2	T
B-La	M2,91	Unpublished	D
B-Li	M2	BAPD 10(3)	T
B-Lu	M2	Unpublished	D
B-Mg	M2	Binary Magnesium	D
*B-Mn	M2,91	BAPD 7(6)	D
*B-Mo	M2,91	BAPD 9(4)	D
B-N	M2	M2	D
B-Na	M2	M2	T
*B-Nb	M2	M2	D
B-Nd	M2	Unpublished	D
*B-Ni	M2	Binary Nickel	D
B-Np	M2	M2	D
B-O	M2	M2	D
B-Os	M2	M2	D
B-P	M2	M2	T
B-Pa	M2	M2	D
B-Pb	M2	M2	D
*B-Pd	M2	Unpublished	D
B-Pm	M2	Unpublished	D
B-Pr	M2	Unpublished	D
*B-Pt	M2	M2	D
B-Pu	M2	Unpublished	D
B-Rb	No Data		
*B-Re	M2	[72Por]	D
B-Rh	M2	[Moffatt]	D
*B-Ru	M2	[63Obr]	D
B-S	M2	[Moffatt]	D
B-Sb	M2,91	M2	D
*B-Sc	M2	BAPD 11(4)	D
B-Se	M2	[69Bor]	D
*B-Si	M2	BAPD 5(5)	D
B-Sm	M2	Unpublished	D
B-Sn	M2	M2	D
B-Sr	M2	M2	D
*B-Ta	M2	M2	D
B-Tb	M2	BAPD 11(4)	D
B-Tc	M2	M2	D
B-Te	No Data		
B-Th	M2	[Moffatt]	D
*B-Ti	M2	Binary Titanium	D
B-Tl	M2,91	M2	D
B-Tm	M2	Unpublished	D
B-U	M2	M2	D
*B-V	M2,91	Binary Vanadium	D
*B-W	M2,92	Binary Tungsten	D
*B-Y	M2	Unpublished	D
B-Yb	M2	Unpublished	D
B-Zn	M2,91	M2	D
*B-Zr	M2	[Zirconium]	D
Ba-Be	M2,91	Binary Beryllium	D
Ba-Bi	M2	[38Gru]	D
Ba-Br	M2	M2	D
Ba-C	M2	M2	T
*Ba-Ca	M2	BAPD 7(4)	D
*Ba-Cd	M2	M2	D
Ba-Ce	M2	M2	T
Ba-Cl	M2	M2	D
Ba-Cm	No Data		
Ba-Co	M2	Unpublished	T
Ba-Cr	M2	BAPD 6(3)	T
Ba-Cs	M2	BAPD 5(5)	T
*Ba-Cu	M2	BAPD 5(6)	D
Ba-Dy	M2	M2	T
Ba-Er	M2	M2	T
Ba-Eu	M2,91	BAPD 9(3)	D
Ba-F	M2	M2	D
Ba-Fe	M2	M2	D
*Ba-Ga	M2	JPE 12(5)	D
Ba-Gd	M2	M2	T
*Ba-Ge	M2	M2	D
*Ba-H	M2	[60Pet1]	D
Ba-Hf	No Data		
*Ba-Hg	M2	M2	D
Ba-Ho	M2	M2	T
Ba-I	M2	M2	D
*Ba-In	M2	Indium	D
Ba-Ir	No Data		
Ba-K	M2	BAPD 5(5)	T
Ba-La	M2	M2	D
*Ba-Li	M2	BAPD 5(5)	D
Ba-Lu	M2	M2	T
*Ba-Mg	M2	Binary Magnesium	D
Ba-Mn	M2	[64Obi1]	D
Ba-Mo	M2	M2	D
Ba-N	M2	M2	T
*Ba-Na	M2	BAPD 6(1)	D
Ba-Nb	No Data		
Ba-Nd	M2	BAPD 9(3)	D
Ba-Ni	M2	Binary Nickel	D
Ba-Np	No Data		
Ba-O	M2	M2	D
Ba-Os	No Data		
*Ba-P	M2	M2	D
*Ba-Pb	M2	[Hansen]	D
Ba-Pd	M2,91	JPE 12(4)	D
Ba-Pm	M2	M2	D
Ba-Po	M2	M2	T
Ba-Pr	M2	BAPD 9(3)	D
Ba-Pt	M2,91	JPE 12(4)	D
Ba-Pu	M2	M2	T
Ba-Rb	M2	BAPD 5(5)	T
Ba-Re	No Data		
Ba-Rh	M2	M2	T
Ba-Ru	No Data		
Ba-S	M2	M2	D
Ba-Sb	M2	M2	T
Ba-Sc	M2	M2	D
*Ba-Se	M2	JPE 12(4)	D
*Ba-Si	M2	[64Obi2]	D
Ba-Sm	M2	BAPD 9(3)	D
Ba-Sn	M2,91	M2	D
Ba-Sr	M2,91	BAPD 8(6)	D
Ba-Ta	No Data		
Ba-Tb	M2	M2	T
Ba-Tc	No Data		
*Ba-Te	M2	Unpublished	D
Ba-Th	No Data		
Ba-Ti	M2	Binary Titanium	D
*Ba-Tl	M2	[66Bru]	D
Ba-Tm	M2	M2	T
Ba-U	No Data		
Ba-V	M2	Binary Vanadium	D
Ba-W	M2	Binary Tungsten	T
Ba-Y	M2	M2	D
Ba-Yb	M2,91	BAPD 9(3)	D
*Ba-Zn	M2	JPE 12(4)	D
Ba-Zr	No Data		
Be-Bi	M2	Binary Beryllium	D
Be-Br	M2	Binary Beryllium	T
Be-C	M2	Binary Beryllium	T
Be-Ca	M2,91	Binary Beryllium	D
Be-Cd	M2	Binary Beryllium	T
Be-Ce	M2	Binary Beryllium	D
Be-Cl	M2	Binary Beryllium	D
Be-Cm	M2	Binary Beryllium	T
*Be-Co	M2	BAPD 9(5)	D
*Be-Cr	M2	Binary Beryllium	D
Be-Cs	M2	Binary Beryllium	T
*Be-Cu	M2,92	BAPD 8(3)	D
Be-Dy	M2	Binary Beryllium	T
Be-Er	M2	Binary Beryllium	T
Be-Eu	M2	Binary Beryllium	T
Be-F	M2	Binary Beryllium	T
*Be-Fe	M2	Binary Iron	D

(continued)

System	Published	Data source	Data type
Be-Ga	M2	Binary Beryllium	D
Be-Gd	M2	Binary Beryllium	T
Be-Ge	M2	Binary Beryllium	D
Be-H	M2,91	Binary Beryllium	D
*Be-Hf	M2	Binary Beryllium	D
Be-Hg	M2	Binary Beryllium	T
Be-Ho	M2	Binary Beryllium	T
Be-I	M2	Binary Beryllium	T
Be-In	M2	Indium	D
Be-Ir	M2	Binary Beryllium	T
Be-K	M2	Binary Beryllium	T
Be-La	M2	Binary Beryllium	T
Be-Li	M2	Binary Beryllium	D
Be-Lu	M2	Binary Beryllium	T
Be-Mg	M2	Binary Magnesium	D
Be-Mn	M2	Binary Beryllium	T
Be-Mo	M2	Binary Beryllium	D
Be-N	M2	Binary Beryllium	T
Be-Na	M2	Binary Beryllium	D
*Be-Nb	M2,91	Binary Beryllium	D
Be-Nd	M2	Binary Beryllium	T
*Be-Ni	M2	Binary Nickel	D
Be-Np	M2	Binary Beryllium	T
Be-O	M2,91	Binary Beryllium	D
Be-Os	M2	Binary Beryllium	T
Be-P	M2	Binary Beryllium	T
Be-Pa	M2	Binary Beryllium	T
Be-Pb	M2	Binary Beryllium	T
*Be-Pd	M2	Binary Beryllium	D
Be-Pm	M2	M2	T
Be-Po	M2	Binary Beryllium	T
Be-Pr	M2	Binary Beryllium	T
Be-Pt	M2	Binary Beryllium	D
Be-Pu	M2	Binary Beryllium	D
Be-Rb	M2	Binary Beryllium	T
Be-Re	M2	Binary Beryllium	D
Be-Rh	M2	Binary Beryllium	T
Be-Ru	M2	Binary Beryllium	D
Be-S	M2	Binary Beryllium	T
Be-Sb	M2	Binary Beryllium	D
Be-Sc	M2	Binary Beryllium	T
Be-Se	M2	Binary Beryllium	T
*Be-Si	M2	Binary Beryllium	D
Be-Sm	M2	Binary Beryllium	T
Be-Sn	M2	Binary Beryllium	D
Be-Sr	M2	Binary Beryllium	D
Be-Ta	M2	Binary Beryllium	D
Be-Tb	M2	Binary Beryllium	T
Be-Tc	M2	Binary Beryllium	T
Be-Te	M2	Binary Beryllium	T
*Be-Th	M2	Binary Beryllium	D
*Be-Ti	M2	Binary Beryllium	D
Be-Tl	No Data		
Be-Tm	M2	Binary Beryllium	T
Be-U	M2	Binary Beryllium	D
Be-V	M2	Binary Vanadium	D
*Be-W	M2	Binary Tungsten	D
Be-Y	M2	Binary Beryllium	D
Be-Yb	M2	Binary Beryllium	D
Be-Zn	M2	Binary Beryllium	D
*Be-Zr	M2	Binary Beryllium	D
Bi-Br	M2	M2	D
Bi-C	M2	Unpublished	T
*Bi-Ca	M2,91	M2	D
*Bi-Cd	M2	BAPD 9(4)	D
Bi-Ce	M2	BAPD 9(4)	D
Bi-Cl	M2	M2	D
Bi-Cm	M2	M2	T
Bi-Co	M2	JPE 12(3)	D
Bi-Cr	M2	BAPD 9(3)	D
*Bi-Cs	M2	JPE 12(4)	D
*Bi-Cu	M2	BAPD 5(2)	D
Bi-Dy	M2	BAPD 10(4a)	D
Bi-Er	M2	M2	D
Bi-Eu	M2	BAPD 10(4a)	T
Bi-Fe	M2	Binary Iron	D
*Bi-Ga	M2	M2	D
Bi-Gd	M2	BAPD 10(4a)	D
*Bi-Ge	M2	BAPD 7(6)	D
Bi-H	M2	M2	T
Bi-Hf	M2	M2	D
*Bi-Hg	M2	Unpublished	D
Bi-Ho	M2	M2	D
Bi-I	M2	M2	D
*Bi-In	M2	Indium	D
Bi-Ir	M2	M2	D
*Bi-K	M2	JPE 12 (1)	D
*Bi-La	M2	BAPD 10(4a)	D
*Bi-Li	M2	JPE 12(4)	D
Bi-Lu	M2	M2	D
*Bi-Mg	M2	Binary Magnesium	D
*Bi-Mn	M2	M2	D
Bi-Mo	M2	M2	D
Bi-N	M2	M2	T
*Bi-Na	M2	JPE 12(4)	D
Bi-Nb	M2	[Moffatt]	D
*Bi-Nd	M2	BAPD 10(4a)	D
*Bi-Ni	M2	Binary Nickel	D
Bi-Np	M2	M2	T
Bi-O	M2	M2	T
Bi-Os	M2	Unpublished	D
Bi-P	M2	M2	T
Bi-Pa	M2	BAPD 2(4)	T
*Bi-Pb	M2,92	JPE 13(1)	D
*Bi-Pd	M2	Unpublished	D
Bi-Pm	No Data		
Bi-Po	M2	M2	T
Bi-Pr	M2	M2	D
*Bi-Pt	M2	JPE 12(2)	D
Bi-Pu	M2	[Chiotti]	D
*Bi-Rb	M2	Unpublished	D
Bi-Re	M2	M2	D
Bi-Rh	M2	[Elliott]	D
Bi-Ru	M2	[Moffatt]	D
*Bi-S	M2	Unpublished	D
*Bi-Sb	M2	Unpublished	D
Bi-Sc	M2	BAPD 10(4a)	T
*Bi-Se	M2	Unpublished	D
Bi-Si	M2	BAPD 6(4)	D
*Bi-Sm	M2	M2	D
*Bi-Sn	M2	M2	D
*Bi-Sr	M2	[Elliott]	D
Bi-Ta	M2,92	JPE 13(3)	T
Bi-Tb	M2	M2	D
Bi-Tc	No Data		
*Bi-Te	M2	Unpublished	D
Bi-Th	M2	M2	D
Bi-Ti	M2	Binary Titanium	D
*Bi-Tl	M2	Unpublished	D
Bi-Tm	M2	M2	D
*Bi-U	M2	[Chiotti]	D
Bi-V	M2	Binary Vanadium	D
Bi-W	M2	Binary Tungsten	T
Bi-Xe	M2	[Elliott]	T
*Bi-Y	M2	BAPD 10(4a)	D
*Bi-Yb	M2	M2	D
*Bi-Zn	M2,91	M2	D
*Bi-Zr	M2,91	BAPD 11(3)	D
Bk-Mo	M2	[Molybdenum]	D
Bk-N	M2	M2	T
Bk-O	M2	M2	T
Bk-P	M2	M2	T
Bk-S	M2	M2	T
Bk-Sb	M2	M2	T
Bk-W		Binary Tungsten	T
Br-Cu	M2	Unpublished	D
Br-In	M2	Indium	D
Br-K	M2	M2	D
Br-Mg	M2	Binary Magnesium	T
Br-Mo	M2	M2	D
Br-Na	M2	M2	D
Br-Ni	M2	Binary Nickel	T
Br-Rb	M2	M2	D
Br-Sc	M2	M2	D
Br-Sr	M2	M2	D
Br-Te	M2	M2	D

(continued)

System	Published	Data source	Data type
Br-W	M2	Binary Tungsten	T
C-Ca	M2	M2	T
C-Cd	M2	M2	T
C-Ce	M2	M2	D
*C-Co	M2	JPE 12(4)	D
*C-Cr	M2	BAPD 11(2)	D
C-Cs	M2	[87Gor]	T
*C-Cu	M2	Unpublished	D
C-Dy	M2	BAPD 7(5)	T
C-Er	M2	BAPD 7(5)	T
C-Eu	M2	BAPD 7(5)	T
*C-Fe	M2	Binary Iron	D
C-Ga	No Data		
C-Gd	M2	BAPD 7(5)	T
C-Ge	M2	BAPD 5(5)	D
*C-Hf	M2	BAPD 11(4)	D
C-Hg	M2	M2	T
C-Ho	M2	BAPD 7(5)	T
C-In	M2	Indium	T
C-Ir	M2	M2	D
C-K	M2	M2	T
*C-La	M2	BAPD 7(5)	D
C-Li	M2	BAPD 10(1)	D
C-Lu	M2	BAPD 7(6)	T
C-Mg	M2	Binary Magnesium	T
*C-Mn	M2	M2	D
*C-Mo	M2	M2	D
C-Na	M2	M2	T
C-Nb	M2	Unpublished	D
C-Nd	M2	BAPD 7(6)	T
*C-Ni	M2	Binary Nickel	D
C-Np	M2	M2	T
C-Os	M2	[Moffatt]	D
C-Pa	M2	M2	T
C-Pb	M2	M2	T
C-Pd	M2	M2	D
C-Po	M2	M2	T
*C-Pr	M2	M2	D
C-Pt	M2	M2	D
C-Pu	M2	M2	D
C-Rb	M2	M2	T
C-Re	M2	M2	D
C-Rh	M2	M2	D
C-Ru	M2	M2	D
C-Sb	M2	M2	T
*C-Sc	M2	M2	D
C-Se	M2	M2	T
*C-Si	M2	BAPD 5(5)	D
C-Sm	M2	BAPD 7(6)	T
C-Sn	M2	M2	T
C-Sr	M2	M2	T
*C-Ta	M2	[86Bar1]	D
C-Tb	M2	BAPD 7(6)	T
C-Tc	M2,91	M2	D
C-Te	No Data		
*C-Th	M2	[69Ben1]	D
*C-Ti	M2	Binary Titanium	D
C-Tl	M2	M2	T
C-Tm	M2	BAPD 7(6)	T
*C-U	M2	[67Sto,69Ben2]	D
*C-V	M2,91	Binary Vanadium	D
*C-W	M2,91	Binary Tungsten	D
*C-Y	M2	BAPD 7(6)	D
C-Yb	M2	BAPD 7(6)	T
C-Zn	M2	M2	T
*C-Zr	M2	M2	D
*Ca-Cd	M2	M2	D
Ca-Ce	M2	BAPD 8(6)	D
Ca-Cl	M2	M2	D
Ca-Cm	No Data		
Ca-Co	M2	M2	D
Ca-Cr	M2	BAPD 6(3)	T
Ca-Cs	M2	BAPD 6(2)	T
*Ca-Cu	M2	BAPD 5(6)	D
Ca-Dy	M2	BAPD 8(6)	T
Ca-Er	M2	BAPD 8(6)	T
Ca-Eu	M2	BAPD 8(6)	D
Ca-F	M2	M2	D
Ca-Fe	M2	Binary Iron	D
*Ca-Ga	M2,92	JPE 13(3)	D
Ca-Gd	M2	BAPD 8(6)	T
*Ca-Ge	M2	M2	D
Ca-H	M2	M2	D
*Ca-Hg	M2	M2	D
Ca-Ho	M2	M2	T
*Ca-In	M2	Indium	D
Ca-Ir	M2	Unpublished	T
Ca-K	M2	BAPD 6(1)	T
Ca-La	M2	BAPD 8(6)	D
*Ca-Li	M2	BAPD 8(2)	D
Ca-Lu	M2	M2	D
*Ca-Mg	M2	Binary Magnesium	D
Ca-Mn	M2	[Shunk]	D
Ca-Mo	M2	M2	D
Ca-N	M2	BAPD 11(5)	D
*Ca-Na	M2	BAPD 6(1)	D
Ca-Nb	M2	M2	T
*Ca-Nd	M2	BAPD 8(6)	D
*Ca-Ni	M2,91	Binary Nickel	D
Ca-Np	No Data		
*Ca-O	M2	BAPD 6(4)	D
Ca-Os	No Data		
Ca-P	M2	M2	T
*Ca-Pb	M2	JPE 13(2)	D
*Ca-Pd	M2,92	M2	D
Ca-Pm	M2	M2	D
Ca-Po	M2	M2	T
Ca-Pr	M2	BAPD 8(6)	T
*Ca-Pt	M2	M2	D
Ca-Pu	M2	BAPD 10(4a)	D
Ca-Rb	M2	BAPD 6(1)	T
Ca-Re	No Data		
Ca-Rh	M2	M2	T
Ca-Ru	No Data		
Ca-S	M2	M2	T
*Ca-Sb	M2	M2	D
Ca-Sc	M2	M2	D
Ca-Se	M2	M2	T
*Ca-Si	M2	M2	D
Ca-Sm	M2	BAPD 8(6)	T
Ca-Sn	M2,91	M2	D
*Ca-Sr	M2	BAPD 7(5)	D
Ca-Ta	No Data		
Ca-Tb	M2	M2	D
Ca-Te	M2	M2	T
Ca-Th	No Data		
Ca-Ti	M2	Binary Titanium	D
*Ca-Tl	M2	M2	D
Ca-Tm	M2	M2	D
Ca-U	M2	M2	T
Ca-V	M2	Binary Vanadium	D
Ca-W	M2	Binary Tungsten	T
Ca-Y	M2	BAPD 8(6)	D
*Ca-Yb	M2	BAPD 8(6)	D
*Ca-Zn	M2	BAPD 11(4)	D
Ca-Zr	No Data		
Cd-Ce	M2	BAPD 9(1)	D
Cd-Co	M2	M2	T
Cd-Cr	M2	JPE 13(2)	D
Cd-Cs	M2	BAPD 8(6)	D
*Cd-Cu	M2	BAPD 11(2)	D
Cd-Dy	M2	BAPD 9(1)	T
Cd-Er	M2	BAPD 9(1)	T
*Cd-Eu	M2	BAPD 9(1)	D
Cd-Fe	M2	Binary Iron	D
*Cd-Ga	M2	Unpublished	D
*Cd-Gd	M2	BAPD 9(1)	D
*Cd-Ge	M2	BAPD 7(2)	D
Cd-H	M2	M2	T
Cd-Hf	M2	M2	T
*Cd-Hg	M2	JPE 13(4)	D
Cd-Ho	M2	BAPD 9(1)	T
*Cd-In	M2	JPE 13(3)	D
Cd-Ir	No Data		
Cd-K	M2	BAPD 8(6)	D
Cd-Kr	M2	M2	T
*Cd-La	M2	BAPD 9(1)	D
*Cd-Li	M2	BAPD 9(1)	D
Cd-Lu	M2	BAPD 9(1)	T
*Cd-Mg	M2	BAPD 5(1)	D
Cd-Mn	M2	Unpublished	D
Cd-Mo	M2	M2	D
Cd-N	M2	BAPD 9(3)	T
*Cd-Na	M2	BAPD 9(1)	D
Cd-Nb	M2	M2	T
Cd-Nd	M2	BAPD 9(2)	D
*Cd-Ni	M2	Binary Nickel	D
Cd-Np	M2	BAPD 2(4)	D
Cd-O	M2	BAPD 8(2)	D
Cd-Os	M2	M2	T
*Cd-P	M2	M2	D
*Cd-Pb	M2	BAPD 9(6)	D
Cd-Pd	M2	M2	D
Cd-Pm	M2	M2	D
Cd-Po	M2	M2	T
Cd-Pr	M2	BAPD 9(2)	D
Cd-Pt	M2	[52Now]	D
Cd-Pu	M2	[64Wit]	D
Cd-Rb	M2	BAPD 8(6)	D
Cd-Re	M2	M2	T
Cd-Rh	M2	M2	T
Cd-Ru	No Data		
Cd-S	M2	Unpublished	D
*Cd-Sb	M2	M2	D
Cd-Sc	M2	BAPD 9(2)	T
*Cd-Se	M2	Unpublished	D
Cd-Si	M2	BAPD 6(6)	D
*Cd-Sm	M2	BAPD 9(2)	D
*Cd-Sn	M2	BAPD 10(3)	D
*Cd-Sr	M2	M2	D
Cd-Ta	No Data		
Cd-Tb	M2	BAPD 9(2)	T
Cd-Tc	M2	M2	T
*Cd-Te	M2	BAPD 10(4)	D
*Cd-Th	M2	Unpublished	D
Cd-Ti	M2	Binary Titanium	D
*Cd-Tl	M2	M2	D
Cd-Tm	M2	BAPD 9(2)	T
Cd-U	M2	BAPD 1(2)	D
Cd-V	M2	Binary Vanadium	D
Cd-W	M2	Binary Tungsten	T
*Cd-Y	M2	BAPD 9(2)	D
*Cd-Yb	M2	BAPD 9(2)	D
*Cd-Zn	M2	BAPD 5(1)	D
Cd-Zr	M2	[Zirconium]	D
Ce-Cl	M2	M2	D

(continued)

System	Published	Data source	Data type
Ce-Cm	No Data		
*Ce-Co	M2	[74Gsc1]	D
Ce-Cr	M2	BAPD 11(5)	D
Ce-Cs	No Data		
*Ce-Cu	M2	BAPD 9(3a)	D
Ce-Dy	M2	BAPD 3(1)	T
Ce-Er	M2	M2	D
Ce-Eu	M2	BAPD 3(2)	D
*Ce-Fe	M2	Binary Iron	D
*Ce-Ga	M2	M2	D
Ce-Gd	M2	BAPD 3(2)	D
*Ce-Ge	M2	BAPD 10(2)	D
Ce-H	M2	M2	D
Ce-Hf	M2	M2	D
Ce-Hg	M2	Unpublished	D
Ce-Ho	M2	M2	D
*Ce-In	M2	Indium	D
*Ce-Ir	M2	JPE 12(5)	D
Ce-La	M2	BAPD 2(4)	D
Ce-Li	No Data		
Ce-Lu	M2	M2	D
*Ce-Mg	M2	Binary Magnesium	D
*Ce-Mn	M2	Unpublished	D
Ce-Mo	M2	Unpublished	D
Ce-N	M2	[74Gsc2]	D
Ce-Na	No Data		
Ce-Nb	M2	M2	D
Ce-Nd	M2	M2	D
*Ce-Ni	M2	Binary Nickel	D
Ce-Np	No Data		
*Ce-O	M2	M2	D
Ce-Os	M2	M2	T
Ce-P	M2	M2	T
Ce-Pb	M2	M2	D
*Ce-Pd	M2,91	M2	D
Ce-Pm	M2	M2	D
Ce-Po	M2	[Shunk]	T
Ce-Pr	M2	BAPD 3(2)	D
Ce-Pt	M2	M2	D
*Ce-Pu	M2	[Plutonium]	D
Ce-Rb	No Data		
Ce-Re	M2	M2	T
Ce-Rh	M2	M2	D
Ce-Ru	M2,92	M2	D
*Ce-S	M2	[74Gsc1]	D
Ce-Sb	M2	M2	D
Ce-Sc	M2	BAPD 3(2)	D
Ce-Se	M2	M2	D
*Ce-Si	M2	BAPD 10(1)	D
Ce-Sm	M2	BAPD 3(2)	D
*Ce-Sn	M2	M2	D
Ce-Sr	No Data		
Ce-Ta	M2	[66Den1]	D
Ce-Tb	M2	M2	D
Ce-Tc	M2	M2	T
*Ce-Te	M2	M2	D
Ce-Th	M2	M2	D
*Ce-Ti	M2	Binary Titanium	D
*Ce-Tl	M2	Unpublished	D
Ce-Tm	M2	M2	D
Ce-U	M2	[Elliott]	D
Ce-V	M2	Binary Vanadium	D
Ce-W	M2	Binary Tungsten	D
Ce-Y	M2	BAPD 3(2)	D
Ce-Yb	M2	BAPD 3(1)	T
*Ce-Zn	M2	M2	D
Ce-Zr	M2,91	JPE 12(1)	D
Cf-Mo	M2	[Molybdenum]	D
Cf-O	M2	M2	T
Cf-Pt	M2	M2	T
Cf-S	M2	M2	T
Cf-Sb	M2	M2	T
Cf-W		Binary Tungsten	T
*Cl-Cs	M2	M2	D
Cl-Cu	M2	Unpublished	D
Cl-Dy	M2	M2	D
Cl-Er	M2	M2	D
*Cl-Ga	M2	M2	D
Cl-Gd	M2	M2	D
*Cl-Hg	M2	M2	D
*Cl-In	M2	Indium	D
Cl-K	M2	M2	D
Cl-La	M2	M2	D
Cl-Mg	M2	Binary Magnesium	T
Cl-Mo	M2	M2	D
*Cl-Na	M2	M2	D
Cl-Ni	M2	Binary Nickel	D
Cl-Pd	M2	M2	D
Cl-Rb	M2	M2	D
Cl-Sc	M2	M2	D
Cl-Sn	M2	M2	D
Cl-Sr	M2	M2	D
Cl-Te	M2	M2	D
Cl-Th	M2	M2	D
Cl-Tl	M2	M2	D
Cl-Tm	M2	M2	D
Cl-W	M2	Binary Tungsten	T
Cl-Y	M2	M2	D
Cl-Yb	M2	M2	D
Cm-Cr	M2	BAPD 6(5)	D
Cm-Cu	M2	M2	T
Cm-Ir	M2	M2	T
Cm-Mo	M2	[Molybdenum]	D
Cm-N	M2	M2	T
Cm-O	M2	M2	T
Cm-P	M2	M2	T
Cm-Pd	M2	M2	T
Cm-Pt	M2	BAPD 10(2)	D
Cm-Rh	M2	M2	T
Cm-S	M2	M2	T
Cm-Sb	M2	M2	T
Cm-Se	M2	M2	T
Cm-Si	M2	M2	T
Cm-Te	M2	M2	T
Cm-W	M2	Binary Tungsten	T
*Co-Cr	M2	BAPD 11(4)	D
Co-Cs	No Data		
*Co-Cu	M2	BAPD 5(2)	D
*Co-Dy	M2	M2	D
*Co-Er	M2	M2	D
Co-Eu	No Data		
*Co-Fe	M2	Binary Iron	D
*Co-Ga	M2	M2	D
*Co-Gd	M2	M2	D
*Co-Ge	M2	JPE 12(1)	D
Co-H	M2	M2	D
*Co-Hf	M2	JPE 12(4)	D
Co-Hg	M2	M2	T
*Co-Ho	M2	M2	D
Co-In	M2	Indium	D
Co-Ir	M2	[52Kos]	D
Co-K	M2	Unpublished	T
Co-La	M2	[74Ray1]	D
Co-Li	M2	BAPD 11(5)	T
Co-Lu	M2	M2	D
Co-Mg	M2	Binary Magnesium	D
*Co-Mn	M2	BAPD 11(2)	D
*Co-Mo	M2	[Molybdenum]	D
Co-N	M2	Unpublished	T
Co-Na	M2	BAPD 11(5)	T
*Co-Nb	M2	[67Par]	D
*Co-Nd	M2	[74Ray2]	D
*Co-Ni	M2	Binary Nickel	D
Co-Np	M2	M2	T
Co-O	M2	M2	D
Co-Os	M2	[52Kos]	D
*Co-P	M2	BAPD 11(6)	D
Co-Pb	M2	M2	D
*Co-Pd	M2,91	JPE 12(1)	D
Co-Pm	No Data		
*Co-Pr	M2	[74Ray1]	D
*Co-Pt	M2	M2	D
*Co-Pu	M2	[61Poo]	D
Co-Rb	M2	Unpublished	T
*Co-Re	M2	M2	D
Co-Rh	M2	[52Kos]	D
Co-Ru	M2	[52Kos]	D
*Co-S	M2	[08Fri]	D
*Co-Sb	M2,91	BAPD 11(3)	D
Co-Sc	M2	[Moffatt]	D
*Co-Se	M2	M2	D
*Co-Si	M2	JPE 12(5)	D
*Co-Sm	M2	[Moffatt]	D
*Co-Sn	M2	JPE 12(1)	D
Co-Sr	M2	JPE 13(3)	T
*Co-Ta	M2,91	[86Bar2]	D
*Co-Tb	M2	M2	D
Co-Tc	M2	M2	T
*Co-Te	M2	Unpublished	D
*Co-Th	M2	Unpublished	D
Co-Ti	M2	Binary Titanium	D
*Co-Tl	M2	M2	T
Co-Tm	M2	M2	T
Co-U	M2	Unpublished	D
*Co-V	M2	JPE 12(3)	D
*Co-W	M2	Binary Tungsten	D
*Co-Y	M2,92	JPE 12(5)	D
Co-Yb	M2	[76Ian]	D
*Co-Zn	M2	M2	D
Co-Zr	M2	[64Pec]	D
Cr-Cs	M2	BAPD 5(4)	D
*Cr-Cu	M2	BAPD 5(4)	D
Cr-Dy	M2	M2	D
Cr-Er	M2	M2	D
Cr-Eu	M2	M2	D
*Cr-Fe	M2	Binary Iron	D
*Cr-Ga	M2	[72Bor]	D
Cr-Gd	M2	[Elliott]	D
*Cr-Ge	M2	BAPD 7(5)	D
Cr-H	M2	JPE 12(6)	D
*Cr-Hf	M2	BAPD 7(6)	D
Cr-Hg	M2	BAPD 10(2)	D
Cr-Ho	M2	[75Sve]	D
Cr-In	M2	Indium	D
*Cr-Ir	M2	BAPD 11(1)	D
Cr-K	M2	BAPD 5(4)	D
Cr-La	M2	M2	D
Cr-Li	M2	BAPD 5(4)	D
*Cr-Lu	M2,92	[Moffatt]	D
Cr-Mg	M2	Binary Magnesium	T
*Cr-Mn	M2	BAPD 7(5)	D
*Cr-Mo	M2	BAPD 8(3)	D
Cr-N	M2	Unpublished	D
Cr-Na	M2	BAPD 5(4)	D
*Cr-Nb	M2	BAPD 7(5)	D
Cr-Nd	M2	[Moffatt]	D
*Cr-Ni	M2	Binary Nickel	D

(continued)

System	Published	Data source	Data type
Cr-Np	M2	BAPD 6(5)	D
*Cr-O	M2	[80Ban]	D
*Cr-Os	M2	BAPD 11(1)	D
Cr-P	M2	BAPD 11(5)	D
Cr-Pb	M2	BAPD 9(2)	D
*Cr-Pd	M2	BAPD 11(1)	D
Cr-Pm	No Data		
Cr-Po	M2	BAPD 9(2)	T
Cr-Pr	M2	M2	D
*Cr-Pt	M2	BAPD 11(1)	D
Cr-Pu	M2	BAPD 6(5)	D
Cr-Ra	M2	BAPD 6(4)	T
Cr-Rb	M2	BAPD 5(4)	D
*Cr-Re	M2	BAPD 8(2)	D
*Cr-Rh	M2	BAPD 8(2)	D
*Cr-Ru	M2	BAPD 8(2)	D
*Cr-S	M2,91	Unpublished	D
*Cr-Sb	M2,92	BAPD 11(5)	D
*Cr-Sc	M2	BAPD 6(5)	D
*Cr-Se	M2	Unpublished	D
*Cr-Si	M2	BAPD 8(5)	D
Cr-Sm	M2	[73Sve]	D
*Cr-Sn	M2	BAPD 9(2)	D
Cr-Sr	M2	BAPD 6(4)	T
*Cr-Ta	M2	BAPD 8(2)	D
Cr-Tb	M2	[71Sve]	D
Cr-Tc	M2	BAPD 7(6)	D
*Cr-Te	M2	Unpublished	D
Cr-Th	M2	BAPD 6(5)	D
*Cr-Ti	M2	Binary Titanium	D
Cr-Tl	No Data		
Cr-Tm	M2	M2	D
*Cr-U	M2	BAPD 6(5)	D
*Cr-V	M2	Binary Vanadium	D
*Cr-W	M2	Binary Tungsten	D
Cr-Y	M2,92	BAPD 6(5)	D
Cr-Yb	M2	M2	D
Cr-Zn	M2	JPE 13(2)	D
*Cr-Zr	M2	BAPD 7(3)	D
Cs-Cu	M2	BAPD 8(1)	T
Cs-F	M2	M2	D
Cs-Fe	M2	Binary Iron	T
Cs-Ga	M2	BAPD 11(4)	D
*Cs-Ge	M2	M2	D
Cs-H	M2	M2	T
Cs-Hf	M2	BAPD 8(1)	D
*Cs-Hg	M2	[Hansen]	D
Cs-Ho	No Data		
Cs-I	M2	M2	D
*Cs-In	M2	Indium	D
Cs-Ir	M2	M2	T
*Cs-K	M2	BAPD 4(4)	D
Cs-La	No Data		
Cs-Li	M2	BAPD 10(3)	D
Cs-Lu	No Data		
Cs-Mg	M2	Binary Magnesium	D
Cs-Mo	M2,91	M2	D
Cs-N	M2	M2	T
*Cs-Na	M2	BAPD 3(3)	D
Cs-Nb	M2	BAPD 9(1)	D
Cs-Nd	No Data		
Cs-Ni	No Data		
Cs-Np	No Data		
*Cs-O	M2	M2	D
Cs-Os	M2	[81Loe]	T
Cs-P	M2	M2	T
Cs-Pb	M2	M2	T
Cs-Pd	M2	[81Loe]	T
Cs-Pr	M2	M2	D
Cs-Pt	M2	[81Loe]	T
Cs-Pu	No Data		
*Cs-Rb	M2	BAPD 4(4)	D
Cs-Re	No Data		
Cs-Rh	M2	[81Loe]	T
Cs-Ru	M2	[81Loe]	T
*Cs-S	M2	[Smithells]	D
*Cs-Sb	M2	[61Dor2]	D
Cs-Sc	No Data		
*Cs-Se	M2	M2	D
Cs-Si	M2	M2	T
Cs-Sm	No Data		
*Cs-Sn	M2	[87Mel]	D
Cs-Sr	M2	BAPD 6(1)	T
Cs-Ta	M2,91	JAPD 6(2)	D
*Cs-Te	M2	Unpublished	D
Cs-Th	No Data		
Cs-Ti	M2	BAPD 10(2)	D
*Cs-Tl	M2	[81Bus]	D
Cs-Tm	No Data		
Cs-U	No Data		
Cs-V	M2	Binary Vanadium	D
Cs-W	M2	Binary Tungsten	T
Cs-Y	No Data		
Cs-Yb	No Data		
Cs-Zn	M2	BAPD 8(5)	T
Cs-Zr	M2	BAPD 8(1)	D
*Cu-Dy	M2	BAPD 9(3a)	D
*Cu-Er	M2	BAPD 9(3a)	D
*Cu-Eu	M2	BAPD 9(3a)	D
Cu-F	M2	Unpublished	T
*Cu-Fe	M2	Binary Iron	D
Cu-Fr	M2	M2	T
*Cu-Ga	M2	Unpublished	D
*Cu-Gd	M2	BAPD 9(3a)	D
*Cu-Ge	M2	BAPD 7(1)	D
*Cu-H	M2	[86Bar3]	D
Cu-He	M2	Unpublished	T
*Cu-Hf	M2	BAPD 9(1)	D
*Cu-Hg	M2	BAPD 6(6)	D
Cu-Ho	M2	BAPD 9(3a)	D
Cu-I	M2	M2	T
*Cu-In	M2,91	Indium	D
*Cu-Ir	M2	BAPD 8(2)	D
Cu-K	M2	BAPD 7(3)	T
Cu-Kr	M2	Unpublished	T
*Cu-La	M2,91	BAPD 2(3)	D
*Cu-Li	M2	BAPD 7(2)	D
Cu-Lu	M2	BAPD 9(3a)	D
*Cu-Mg	M2,92	Binary Magnesium	D
*Cu-Mn	M2	Unpublished	D
Cu-Mo	M2	BAPD 11(2)	D
Cu-N	M2	M2	T
Cu-Na	M2	BAPD 7(2)	D
*Cu-Nb	M2,91	BAPD 2(4)	D
*Cu-Nd	M2	BAPD 9(3a)	D
Cu-Ne	M2	Unpublished	T
*Cu-Ni	M2	Binary Nickel	D
Cu-Np	M2	M2	T
*Cu-O	M2,91	BAPD 5(2)	D
Cu-Os	M2	Unpublished	D
*Cu-P	M2	M2	D
Cu-Pa	M2	M2	T
*Cu-Pb	M2	BAPD 5(5)	D
*Cu-Pd	M2	JPE 12(2)	D
Cu-Pm	M2	BAPD 9(3a)	D
Cu-Po	M2	Unpublished	T
Cu-Pr	M2	BAPD 9(3a)	D
*Cu-Pt	M2	Unpublished	D
*Cu-Pu	M2	[67Kut1]	D
Cu-Ra	M2	[68Gul1]	T
Cu-Rb	M2	BAPD 7(1)	T
Cu-Re	M2	Unpublished	D
*Cu-Rh	M2	BAPD 2(4)	D
Cu-Rn	M2	Unpublished	T
Cu-Ru	M2,92	Unpublished	D
*Cu-S	M2	BAPD 4(3)	D
*Cu-Sb	M2	M2	D
Cu-Sc	M2	BAPD 9(3a)	D
*Cu-Se	M2	BAPD 2(3)	D
*Cu-Si	M2	BAPD 7(2)	D
Cu-Sm	M2	BAPD 9(3a)	D
*Cu-Sn	M2	BAPD 11(3)	D
*Cu-Sr	M2	BAPD 5(4)	D
Cu-Ta	M2	BAPD 10(6)	D
Cu-Tb	M2	BAPD 9(3a)	D
Cu-Tc	M2	Unpublished	D
*Cu-Te	M2	Unpublished	D
*Cu-Th	M2	BAPD 7(1)	D
*Cu-Ti	M2	Binary Titanium	D
*Cu-Tl	M2	BAPD 5(2)	D
Cu-Tm	M2	BAPD 9(3a)	D
Cu-U	M2	[Metals]	D
*Cu-V	M2	Binary Vanadium	D
Cu-W	M2	Binary Tungsten	D
Cu-Xe	M2	Unpublished	T
Cu-Y	M2,92	BAPD 2(3)	D
*Cu-Yb	M2	BAPD 9(3a)	D
*Cu-Zn	M2	Unpublished	D
*Cu-Zr	M2	BAPD 11(5)	D
D-Fe		Binary Iron	D
D-Nb	M2	BAPD 4(1)	T
D-Ta	92	[90Con]	D
D-V	M2	Binary Vanadium	D
Dy-Er	M2	BAPD 4(3)	D
*Dy-Fe	M2	Binary Iron	D
*Dy-Ga	M2	[Moffatt]	D
Dy-Gd	M2	BAPD 4(3)	D
*Dy-Ge	M2,91	[77Ere]	D
Dy-H	M2	[58Mul]	D
Dy-Hf	No Data		
Dy-Hg	M2	Unpublished	D
Dy-Ho	M2	BAPD 4(3)	D
Dy-I	M2	M2	D
*Dy-In	M2	Indium	D
Dy-Ir	M2	JPE 13(2)	D
Dy-K	No Data		
Dy-La	M2	M2	D
Dy-Lu	M2	M2	D
Dy-Mg	M2,92	Binary Magnesium	D
*Dy-Mn	M2	[67Kir1]	D
Dy-Mo	M2	M2	D
Dy-N	M2	M2	T
Dy-Na	No Data		
Dy-Nb	No Data		
Dy-Nd	M2	BAPD 3(3)	D
*Dy-Ni	M2	Binary Nickel	D
Dy-Np	No Data		
Dy-O	M2	M2	T
Dy-Os	M2	[80Pal,59Boz]	T
Dy-P	M2	M2	T
*Dy-Pb	M2	[68Mcm]	D
*Dy-Pd	M2	M2	D
Dy-Pm	M2	M2	D
Dy-Po	M2	M2	T
Dy-Pr	M2	M2	D
Dy-Pt	M2	M2	D
Dy-Pu	M2,92	M2	D

(continued)

System	Published	Data source	Data type
Dy-Re	M2	[65Ell]	T
Dy-Rh	M2	M2	D
Dy-Ru	M2	M2	D
*Dy-S	M2	M2	D
*Dy-Sb	M2	M2	D
Dy-Sc	No Data		
Dy-Se	M2	M2	T
Dy-Si	M2	M2	T
Dy-Sm	M2	M2	D
*Dy-Sn	M2	M2	D
Dy-Sr	No Data		
Dy-Ta	M2	[66Den1]	D
Dy-Tb	M2	M2	D
Dy-Tc	M2	M2	T
*Dy-Te	M2	M2	D
Dy-Th	M2	[69Bad]	D
Dy-Ti	M2	M2	D
*Dy-Tl	M2	Unpublished	D
Dy-Tm	M2	M2	D
Dy-U	M2	M2	T
Dy-V	M2	Binary Vanadium	D
Dy-W	M2	Binary Tungsten	D
Dy-Y	M2	BAPD 4(1)	D
Dy-Yb	M2	M2	D
Dy-Zn	M2	M2	D
*Dy-Zr	M2	[60Cro]	D
*Er-Fe	M2	Binary Iron	D
*Er-Ga	M2	M2	D
Er-Gd	M2	BAPD 4(3)	D
*Er-Ge	M2	M2	D
Er-H	M2	[58Mul]	D
Er-Hf	M2	[Hafnium]	D
Er-Hg	M2	Unpublished	D
Er-Ho	M2	BAPD 4(3)	D
Er-I	M2	M2	D
*Er-In	M2	Indium	D
Er-Ir	M2	JPE 13(2)	D
Er-K	No Data		
Er-La	M2	M2	D
Er-Li	No Data		
Er-Lu	M2	M2	D
Er-Mg	M2	Binary Magnesium	D
*Er-Mn	M2	[67Kir2]	D
Er-Mo	M2	M2	D
Er-N	M2	M2	T
Er-Na	No Data		
Er-Nb	M2	[61Lov]	T
Er-Nd	M2	BAPD 3(3)	D
*Er-Ni	M2	Binary Nickel	D
Er-Np	No Data		
Er-O	M2	[61Lov]	D
Er-Os	M2	M2	T
Er-P	M2	M2	T
Er-Pb	M2	M2	T
*Er-Pd	M2,91	[73Loe]	D
Er-Pm	M2	M2	D
Er-Po	M2	[Shunk]	T
Er-Pr	M2	M2	D
*Er-Pt	M2	M2	D
Er-Pu	M2	M2	D
Er-Re	M2	M2	D
Er-Rh	M2	[73Gha]	D
*Er-Ru	M2	M2	D
Er-S	M2	M2	T
Er-Sb	M2	M2	T
Er-Sc	M2	BAPD 4(1)	D
*Er-Se	M2	M2	D
Er-Si	M2	M2	D
Er-Sm	M2	M2	D
Er-Sn	M2	M2	D
Er-Ta	M2	[66Den1]	D
Er-Tb	M2	BAPD 4(3)	D
Er-Tc	M2	M2	T
*Er-Te	M2	M2	D
Er-Th	M2	M2	D
*Er-Ti	M2	Binary Titanium	D
*Er-Tl	M2	Unpublished	D
Er-Tm	M2	M2	D
Er-U	M2	M2	T
Er-V	M2	Binary Vanadium	D
Er-W	M2	Binary Tungsten	D
Er-Y	M2	BAPD 4(1)	D
Er-Yb	M2	M2	D
Er-Zn	M2	M2	D
Er-Zr	M2	[Zirconium]	D
Es-Mo	M2	[Molybdenum]	D
Es-O	M2	M2	T
Es-W		Binary Tungsten	T
Eu-Fe	M2	Binary Iron	D
*Eu-Ga	M2	[78Yat]	D
*Eu-Ge	M2	JPE 12(4)	D
Eu-H	M2	M2	T
Eu-Hf	M2	M2	D
Eu-Hg	M2	Unpublished	T
Eu-Ho	M2	BAPD 4(2)	T
*Eu-In	M2	Indium	D
Eu-Ir	M2	Unpublished	T
Eu-K	No Data		
Eu-La	M2,91	M2	D
*Eu-Mg	M2,92	Binary Magnesium	D
Eu-Mn	M2	M2	D
Eu-Mo	M2	M2	D
Eu-N	M2	M2	T
Eu-Na	No Data		
Eu-Nb	M2	M2	D
Eu-Ni	M2,92	Binary Nickel	D
Eu-Np	No Data		
Eu-O	M2	M2	D
Eu-Os	No Data		
Eu-P	M2	M2	T
*Eu-Pb	M2	[67Mcm]	D
*Eu-Pd	M2	M2	D
Eu-Po	M2	M2	T
Eu-Pr	No Data		
*Eu-Pt	M2	[81Ian]	D
Eu-Pu	M2	M2	D
Eu-Re	M2	M2	T
Eu-Rh	No Data		
Eu-Ru	No Data		
Eu-S	M2	M2	D
Eu-Sb	M2	M2	T
Eu-Sc	M2	M2	D
Eu-Se	M2	M2	T
Eu-Si	M2	M2	T
Eu-Sm	M2	M2	T
Eu-Sn	M2	M2	T
Eu-Sr	No Data		
Eu-Ta	M2	M2	D
Eu-Tb	No Data		
*Eu-Te	M2	[70Sad]	D
Eu-Th	M2	M2	D
Eu-Ti	M2	Binary Titanium	T
Eu-Tl	M2	M2	T
Eu-U	M2	M2	D
Eu-V	M2	Binary Vanadium	D
Eu-W	M2	Binary Tungsten	D
Eu-Y	M2	M2	D
Eu-Yb	M2	M2	D
Eu-Zn	M2	M2	D
Eu-Zr	M2	M2	D
F-In	M2	Indium	T
F-K	M2	M2	D
F-Mg	M2	Binary Magnesium	T
F-Mo	M2	M2	D
F-Na	M2	M2	D
F-Ni	M2	Binary Nickel	T
F-Rb	M2	M2	D
F-Sm	M2	M2	D
F-Sn	M2	M2	D
F-W	92	Binary Tungsten	T
F-Yb	M2	M2	D
*Fe-Ga	M2,91	Binary Iron	D
*Fe-Gd	M2	Binary Iron	D
*Fe-Ge	M2	Binary Iron	D
*Fe-H	M2	Binary Iron	D
*Fe-Hf	M2	Binary Iron	D
Fe-Hg	M2	Binary Iron	D
*Fe-Ho	M2,91	Binary Iron	D
Fe-In	M2	Binary Iron	D
*Fe-Ir	M2	Binary Iron	D
Fe-K	M2	Binary Iron	D
*Fe-La	M2	Binary Iron	D
Fe-Li	M2	Binary Iron	D
*Fe-Lu	M2	Binary Iron	D
Fe-Mg	M2	Binary Iron	D
*Fe-Mn	M2	Binary Iron	D
*Fe-Mo	M2	Binary Iron	D
*Fe-N	M2	Binary Iron	D
Fe-Na	M2	Binary Iron	D
*Fe-Nb	M2	Binary Iron	D
*Fe-Nd	M2	Binary Iron	D
*Fe-Ni	M2	Binary Iron	D
Fe-Np	M2	Binary Iron	T
*Fe-O	M2	Binary Iron	D
Fe-Os	M2	Binary Iron	D
*Fe-P	M2	Binary Iron	D
Fe-Pb	M2	Binary Iron	D
*Fe-Pd	M2	Binary Iron	D
Fe-Pm	M2	Binary Iron	D
Fe-Pr	M2	Binary Iron	D
Fe-Pt	M2	Binary Iron	D
*Fe-Pu	M2	Binary Iron	D
Fe-Rb	M2	Binary Iron	T
Fe-Re		Binary Iron	D
*Fe-Rh	M2	Binary Iron	D
Fe-Ru	M2	Binary Iron	D
*Fe-S	M2	Binary Iron	D
*Fe-Sb	M2	Binary Iron	D
*Fe-Sc	M2	Binary Iron	D
*Fe-Se	M2,91	Binary Iron	D
*Fe-Si	M2	Binary Iron	D
*Fe-Sm	M2	Binary Iron	D
*Fe-Sn	M2,92	Binary Iron	D
Fe-Sr	M2	Binary Iron	D
Fe-Ta	M2	Binary Iron	D
*Fe-Tb	M2	Binary Iron	D
Fe-Tc	M2	Binary Iron	D
*Fe-Te	M2	Binary Iron	D
*Fe-Th	M2,91	Binary Iron	D
*Fe-Ti	M2	Binary Iron	D
Fe-Tl	M2	Binary Iron	T
*Fe-Tm	M2	Binary Iron	D
*Fe-U	M2	Binary Iron	D
*Fe-V	M2	Binary Iron	D
*Fe-W	M2	Binary Iron	D

(continued)

System	Published	Data source	Data type
Fe-Y	M2	Binary Iron	D
Fe-Yb	M2	Binary Iron	D
*Fe-Zn	M2	Binary Iron	D
*Fe-Zr	M2	Binary Iron	D
Fm-Mo	M2	[Molybdenum]	D
Fr-Mg	M2	[68Gul2]	T
Fr-Mo	M2	[Molybdenum]	D
Fr-W		Binary Tungsten	T
*Ga-Gd	M2	BAPD 11(1)	D
Ga-Ge	M2	BAPD 6(3)	D
Ga-H	No Data		
Ga-Hf	M2	M2	D
Ga-Hg	M2	[60Pre]	D
*Ga-Ho	M2	M2	D
Ga-I	M2	M2	D
*Ga-In	M2	Indium	D
Ga-Ir	M2	M2	T
Ga-K	M2	BAPD 11(4)	D
*Ga-La	M2	BAPD 11(1)	D
*Ga-Li	M2	JPE 12(1)	D
*Ga-Lu	M2	[79Yat]	D
*Ga-Mg	M2,91	Binary Magnesium	D
*Ga-Mn	M2	[80Lu]	D
*Ga-Mo	M2	[Molybdenum]	D
Ga-N	M2	M2	T
*Ga-Na	M2	BAPD 11(4)	D
*Ga-Nb	M2	M2	D
*Ga-Nd	M2	[Moffatt]	D
*Ga-Ni	M2	Binary Nickel	D
Ga-Np	M2	M2	T
Ga-O	M2	M2	T
Ga-Os	M2	M2	T
Ga-P	M2	[Shunk]	D
*Ga-Pb	M2	JPE 12(1)	D
*Ga-Pd	M2	M2	D
Ga-Pm	M2,92	M2	D
*Ga-Pr	M2	M2	D
*Ga-Pt	M2	M2	D
*Ga-Pu	M2	BAPD 9(3)	D
Ga-Rb	M2,92	BAPD 11(4)	D
Ga-Re	M2	M2	D
Ga-Rh	M2	M2	T
Ga-Ru	M2	M2	T
*Ga-S	M2	[67Rus]	D
*Ga-Sb	M2	BAPD 9(5)	D
*Ga-Sc	M2	[79Yat]	D
*Ga-Se	M2	[Moffatt]	D
Ga-Si	M2	BAPD 6(4)	D
*Ga-Sm	M2	[Moffatt]	D
*Ga-Sn	M2	JPE 13(2)	D
*Ga-Sr	M2	JPE 13(2)	D
Ga-Ta	M2	M2	D
*Ga-Tb	M2	[Moffatt]	D
*Ga-Te	M2	Unpublished	D
Ga-Th	M2	M2	T
Ga-Ti	M2	Binary Titanium	D
*Ga-Tl	M2	JPE 12(6)	D
*Ga-Tm	M2	[Moffatt]	D
*Ga-U	M2	[73Bus]	D
*Ga-V	M2	Binary Vanadium	D
Ga-W	M2	Binary Tungsten	T
*Ga-Y	M2	[77Yat]	D
*Ga-Yb	M2,92	JPE 13(1)	D
*Ga-Zn	M2	BAPD 11(1)	D
*Ga-Zr	M2	[Shunk]	D
*Gd-Ge	M2	BAPD 10(2)	D
Gd-H	M2	[60Bec]	D
Gd-Hg	M2	Unpublished	D
Gd-Ho	M2	BAPD 4(3)	D
Gd-I	M2	M2	D
*Gd-In	M2	Indium	D
Gd-Ir	M2	Unpublished	D
Gd-K	No Data		
Gd-La	M2	BAPD 2(4)	D
Gd-Li	No Data		
Gd-Lu	M2	M2	D
*Gd-Mg	M2	Binary Magnesium	D
Gd-Mn	M2	M2	D
Gd-Mo	M2	BAPD 1(2)	D
Gd-N	M2	M2	T
Gd-Na	No Data		
Gd-Nb	M2	M2	T
Gd-Nd	M2	BAPD 3(3)	D
*Gd-Ni	M2	Binary Nickel	D
Gd-Np	No Data		
Gd-O	M2	M2	T
Gd-Os	M2	[80Pal]	T
Gd-P	M2	M2	T
*Gd-Pb	M2	JPE 12(6)	D
*Gd-Pd	M2	M2	D
Gd-Pm	M2	M2	D
Gd-Po	M2	M2	T
Gd-Pr	M2	M2	D
Gd-Pt	M2	M2	D
Gd-Pu	M2	M2	D
Gd-Re	M2	M2	D
*Gd-Rh	M2	M2	D
Gd-Ru	M2	[Moffatt]	D
Gd-S	M2	M2	D
*Gd-Sb	M2	M2	D
Gd-Sc	M2	BAPD 4(2)	D
*Gd-Se	M2	[82Pri]	D
Gd-Si	M2	BAPD 9(5)	D
Gd-Sm	M2	BAPD 4(2)	D
*Gd-Sn	M2	JPE 12(6)	D
Gd-Sr	No Data		
Gd-Ta	M2	[66Den1]	D
Gd-Tb	M2	BAPD 4(3)	D
Gd-Tc	M2	M2	T
*Gd-Te	M2	M2	D
Gd-Th	M2	[69Bad]	D
*Gd-Ti	M2	Binary Titanium	D
*Gd-Tl	M2	Unpublished	D
Gd-Tm	M2	M2	D
Gd-U	M2	[Elliott]	T
Gd-V	M2	Binary Vanadium	D
Gd-W	M2	Binary Tungsten	D
Gd-Y	M2	BAPD 4(2)	D
Gd-Yb	M2	BAPD 4(3)	D
Gd-Zn	M2	M2	D
Gd-Zr	M2	M2	D
Ge-H	M2	[Elliott]	T
Ge-Hf	M2	BAPD 11(3)	D
Ge-Hg	M2	Unpublished	T
*Ge-Ho	M2	[80Ere]	D
Ge-I	M2	M2	D
*Ge-In	M2	Indium	D
Ge-Ir	M2	M2	T
*Ge-K	M2	M2	D
*Ge-La	M2	BAPD 10(4)	D
*Ge-Li	M2	M2	D
*Ge-Lu	M2	M2	D
*Ge-Mg	M2	Binary Magnesium	D
*Ge-Mn	M2	BAPD 11(5)	D
*Ge-Mo	M2	BAPD 8(1)	D
Ge-N	M2	BAPD 11(6)	T
*Ge-Na	M2	M2	D
*Ge-Nb	M2	[Moffatt]	D
*Ge-Nd	M2	BAPD 10(2)	D
*Ge-Ni	M2	Binary Nickel	D
Ge-Np	No Data		
Ge-O	M2	[56Tru]	D
Ge-Os	M2	M2	T
*Ge-P	M2,91	BAPD 6(3)	D
*Ge-Pb	M2	BAPD 5(4)	D
*Ge-Pd	M2	JPE 13(4)	D
Ge-Pm	No Data		
*Ge-Pr	M2,91	BAPD 10(3)	D
*Ge-Pt	M2	JPE 13(4)	D
Ge-Pu	M2	M2	T
Ge-Rb	M2	M2	D
Ge-Re	M2	[Moffatt]	D
Ge-Rh	M2	M2	D
Ge-Ru	M2	M2	D
*Ge-S	M2	[63Liu]	D
*Ge-Sb	M2	BAPD 7(3)	D
*Ge-Sc	M2	BAPD 7(6)	D
*Ge-Se	M2	BAPD 11(3)	D
*Ge-Si	M2	BAPD 5(2)	D
*Ge-Sm	M2	BDPD 9(5)	D
*Ge-Sn	M2	BAPD 5(3)	D
*Ge-Sr	M2	M2	D
Ge-Ta	M2,92	JPE 12(6)	T
*Ge-Tb	M2	M2	D
*Ge-Te	M2	M2	D
Ge-Th	M2	[Thorium]	D
*Ge-Ti	M2	Binary Titanium	D
*Ge-Tl	M2	BAPD 6(2)	D
*Ge-Tm	M2	M2	D
*Ge-U	M2	[60Lya]	D
Ge-V	M2	Binary Vanadium	D
Ge-W	M2	Binary Tungsten	D
*Ge-Y	M2	BAPD 9(1)	D
*Ge-Yb	M2	[83Ere]	D
*Ge-Zn	M2	BAPD 6(6)	D
Ge-Zr	M2	BAPD 7(1)	D
H-Hf	M2,91	M2	D
H-Hg	M2	M2	T
H-Ho	M2	M2	T
H-In	M2	Indium	T
H-Ir	M2,91	Unpublished	T
H-K	M2	M2	T
*H-La	M2	BAPD 11(1)	D
H-Li	M2	M2	D
H-Lu	M2	[82Sub]	D
H-Mg	M2	BAPD 8(5)	D
H-Mn	M2	Unpublished	D
H-Mo	M2	[Molybdenum]	D
H-Na	M2	BAPD 11(3)	D
*H-Nb	M2	BAPD 4(1)	D
*H-Nd	M2	M2	D
*H-Ni	M2	Binary Nickel	D
H-Np	M2	M2	T
H-Os	M2	Unpublished	T
H-Pa	M2	M2	T
H-Pb	M2	M2	T
*H-Pd	M2	Unpublished	D
H-Po	M2	[Shunk]	T
H-Pr	M2	M2	D
H-Pt	M2,91	Unpublished	T
H-Pu	M2	[56Mul]	D
H-Rb	M2	M2	T
H-Re	M2	Unpublished	T
H-Rh	M2,91	Unpublished	T
H-Ru	M2,91	Unpublished	T
H-Sb	M2	M2	T

(continued)

System	Published	Data source	Data type
H-Sc	M2	M2	D
H-Se	M2	M2	T
H-Si	M2	Unpublished	D
H-Sm	M2	M2	D
H-Sn	M2	M2	T
*H-Sr	M2	[64Pet]	D
*H-Ta	M2	JPE 12(3)	D
H-Tb	M2	M2	T
H-Te	No Data		
H-Th	M2	[Smith]	D
*H-Ti	M2,92	Binary Titanium	D
H-Tl	M2	M2	T
H-Tm	M2	M2	D
*H-U	M2	Unpublished	D
*H-V	M2	Binary Vanadium	D
H-W	M2	Binary Tungsten	T
H-Y	M2	BAPD 9(3)	D
H-Yb	M2	M2	D
H-Zn	M2	BAPD 10(6)	D
*H-Zr	M2	BAPD 11(4)	D
He-Mo	M2	[Molybdenum]	D
He-W		Binary Tungsten	T
Hf-Hg	M2	M2	D
Hf-In	M2	Indium	T
*Hf-Ir	M2	M2	D
Hf-K	M2	BAPD 8(1)	D
Hf-La	No Data		
Hf-Li	M2	BAPD 10(3)	D
Hf-Lu	No Data		
Hf-Mg	M2	Binary Magnesium	D
*Hf-Mn	M2	Unpublished	D
*Hf-Mo	M2	[Molybdenum]	D
*Hf-N	M2	BAPD 11(2)	D
Hf-Na	M2	BAPD 8(1)	D
*Hf-Nb	M2,91	JPE 12(2)	D
*Hf-Ni	M2,91	Binary Nickel	D
Hf-Np	No Data		
*Hf-O	M2	[Hafnium]	D
*Hf-Os	M2	M2	D
Hf-P	M2	M2	T
Hf-Pd	M2	[72Shu]	D
Hf-Po	M2	M2	T
Hf-Pr	M2	[71Gri]	D
Hf-Pt	M2	M2	T
Hf-Pu	M2	M2	D
Hf-Rb	M2	BAPD 8(1)	D
Hf-Re	M2	[63Tay]	D
*Hf-Rh	M2	M2	D
Hf-Ru	M2	M2	D
Hf-Si	M2	M2	T
Hf-Sb	M2	M2	T
Hf-Sc	M2	M2	D
Hf-Se	M2	M2	T
*Hf-Si	M2	BAPD 10(4)	D
Hf-Sm	No Data		
Hf-Sn	M2	JPE 12(4)	D
Hf-Sr	No Data		
*Hf-Ta	M2	JAPD 5(2)	D
Hf-Tb	No Data		
Hf-Tc	M2	M2	T
Hf-Te	M2	M2	D
Hf-Th	M2	[58Gib]	D
Hf-Ti	M2	Binary Titanium	D
Hf-Tl	No Data		
Hf-Tm	No Data		
*Hf-U	M2	[60Pet2]	D
*Hf-V	M2	Binary Vanadium	D
*Hf-W	M2,92	Binary Tungsten	D
Hf-Y	M2	[62Lun]	D
Hf-Yb	M2	[Moffatt]	D
Hf-Zn	M2	M2	T
*Hf-Zr	M2	BAPD 3(1)	D
Hg-Ho	M2	Unpublished	D
*Hg-In	M2	Indium	D
Hg-Ir	M2	M2	D
*Hg-K	M2	[79Vol]	D
*Hg-La	M2	Unpublished	D
*Hg-Li	M2	[Hansen]	D
Hg-Lu	M2	Unpublished	T
*Hg-Mg	M2	Binary Magnesium	D
Hg-Mn	M2	M2	D
Hg-Mo	M2	M2	D
Hg-N	M2	M2	T
*Hg-Na	M2	M2	D
Hg-Nb	M2	Unpublished	D
Hg-Nd	M2	Unpublished	D
Hg-Ni	M2,91	Binary Nickel	D
Hg-Np	No Data		
Hg-O	M2	M2	T
Hg-Os	M2	M2	D
Hg-P	No Data		
*Hg-Pb	M2	[Hansen]	D
Hg-Pd	M2	BAPD 11(1)	D
Hg-Po	M2	M2	T
Hg-Pr	M2	Unpublished	D
Hg-Pt	M2	BAPD 11(1)	D
Hg-Pu	M2	[59Sch]	D
*Hg-Rb	M2	[Hansen]	D
Hg-Re	M2	M2	D
Hg-Rh	M2	[67Jan]	D
Hg-Ru	M2	M2	D
*Hg-S	M2	JPE 13(5)	D
Hg-Sb	M2	BAPD 11(4)	D
Hg-Sc	M2	Unpublished	T
*Hg-Se	M2	JPE 13(5)	D
Hg-Si	M2	Unpublished	T
Hg-Sm	M2	Unpublished	D
*Hg-Sn	M2	M2	D
*Hg-Sr	M2	M2	D
Hg-Ta	M2	[05Bol]	T
Hg-Tb	M2	Unpublished	D
*Hg-Te	M2	Unpublished	D
Hg-Th	M2	[58Dom]	D
Hg-Ti	M2	Binary Titanium	D
*Hg-Tl	M2	Unpublished	D
Hg-Tm	M2	Unpublished	T
Hg-U	M2	M2	D
Hg-V	M2	Binary Vanadium	D
Hg-W	M2	Binary Tungsten	T
Hg-Y	M2	Unpublished	D
Hg-Yb	M2	Unpublished	D
*Hg-Zn	M2	Unpublished	D
Hg-Zr	M2	M2	D
Ho-I	M2	M2	D
*Ho-In	M2	Indium	D
Ho-Ir	M2	Unpublished	D
Ho-K	No Data		
Ho-La	M2	M2	D
Ho-Li	No Data		
Ho-Lu	M2	M2	D
Ho-Mg	M2	Binary Magnesium	D
*Ho-Mn	M2	[67Kir2]	D
Ho-Mo	M2	M2	D
Ho-N	M2	M2	T
Ho-Na	No Data		
Ho-Nb	No Data		
Ho-Nd	M2	M2	D
Ho-Ni	M2,92	Binary Nickel	D
Ho-Np	No Data		
Ho-O	M2	M2	T
Ho-Os	M2	M2	T
Ho-P	M2	M2	T
Ho-Pb	M2	M2	T
*Ho-Pd	M2,91	M2	D
Ho-Pm	M2	M2	D
Ho-Po	M2	M2	T
Ho-Pr	M2	M2	D
Ho-Pt	M2	M2	D
Ho-Pu	M2,91	M2	D
Ho-Rb	No Data		
Ho-Re	M2	M2	T
Ho-Rh	M2	M2	D
Ho-Ru	M2	M2	D
Ho-S	M2	M2	T
*Ho-Sb	M2	M2	D
Ho-Sc	M2	M2	D
Ho-Se	M2,91	M2	T
Ho-Si	M2	[Pearson3]	T
Ho-Sm	M2	M2	D
Ho-Sn	M2	M2	T
Ho-Sr	No Data		
Ho-Ta	M2	[Moffatt]	D
Ho-Tb	M2	BAPD 4(3)	D
Ho-Tc	M2	M2	T
*Ho-Te	M2	[74Yar]	D
Ho-Th	M2	M2	D
Ho-Ti	No Data		
*Ho-Tl	M2	Unpublished	D
Ho-Tm	M2	M2	D
Ho-U	M2	M2	T
Ho-V	M2	Binary Vanadium	D
Ho-W	M2	Binary Tungsten	D
Ho-Y	M2	BAPD 4(1)	D
Ho-Yb	M2	M2	D
Ho-Zn	M2	M2	D
Ho-Zr	M2	M2	D
I-In	M2	Indium	D
I-K	M2	M2	D
I-Mg	M2	Binary Magnesium	T
I-Mo	M2	M2	D
I-Na	M2	M2	D
I-Ni	M2	Binary Nickel	T
I-Rb	M2,91	M2	D
I-Se	M2	M2	D
I-Sr	M2	M2	D
I-Tb	M2	M2	D
I-Te	M2	M2	D
I-Th	M2	[Smith]	D
I-Tl	M2	M2	D
I-W	M2	Binary Tungsten	T
I-Y	M2	M2	D
In-Ir	M2	Indium	T
*In-K	M2,92	Indium	D
In-Kr	M2	M2	T
*In-La	M2	Indium	D
*In-Li	M2	Indium	D
*In-Lu	M2	Indium	D
*In-Mg	M2	Indium	D
*In-Mn	M2,92	Indium	D
In-Mo	M2	Indium	D
In-N	M2	Indium	T

(continued)

System	Published	Data source	Data type
*In-Na	M2	Indium	D
*In-Nb	M2	Indium	D
*In-Nd	M2,91	Indium	D
*In-Ni	M2	Indium	D
In-Np	No Data		
In-O	M2,91	Indium	D
In-Os	M2	Indium	T
*In-P	M2	Indium	D
*In-Pb	M2	Indium	D
*In-Pd	M2	Indium	D
In-Pm	M2	Indium	D
*In-Pr	M2	Indium	D
*In-Pt	M2,91	Indium	D
*In-Pu	M2	Indium	D
*In-Rb	M2	Indium	D
In-Re	M2	Indium	T
In-Rh	M2	Indium	T
In-Ru	M2	Indium	T
*In-S	M2	Indium	D
*In-Sb	M2	Indium	D
*In-Sc	M2	Indium	D
*In-Se	M2,91	Indium	D
*In-Si	M2	Indium	D
*In-Sm	M2	Indium	D
*In-Sn	M2,91	Indium	D
*In-Sr	M2	Indium	D
In-Ta	M2	Indium	D
*In-Tb	M2	Indium	D
*In-Te	M2,91	Indium	D
*In-Th	M2	Indium	D
*In-Ti	M2	Indium	D
*In-Tl	M2	Indium	D
*In-Tm	M2	Indium	D
In-U	M2	Indium	D
*In-V	M2	Indium	D
In-W	M2	Binary Tungsten	T
*In-Y	M2	Indium	D
*In-Yb	M2	Indium	D
*In-Zn	M2	Indium	D
In-Zr	M2	Indium	D
Ir-K	M2	[64Rhy]	T
*Ir-La	M2	JPE 12(5)	D
Ir-Li	M2	JPE 13(1)	D
Ir-Lu	M2	Unpublished	D
Ir-Mg	M2	Binary Magnesium	D
Ir-Mn	M2	Unpublished	D
*Ir-Mo	M2	[Molybdenum]	D
Ir-N	M2	[05Emi]	T
Ir-Na	M2	[64Rhy]	T
*Ir-Nb	M2	Unpublished	D
Ir-Nd	M2	Unpublished	D
*Ir-Ni	M2	Binary Nickel	D
Ir-Np	M2	M2	T
Ir-O	M2	M2	T
Ir-Os	M2	Unpublished	D
Ir-P	M2	BAPD 11(4)	D
Ir-Pa	M2	M2	T
Ir-Pb	M2	M2	T
*Ir-Pd	M2,91	JPE 12(5)	D
Ir-Pm	M2	Unpublished	D
Ir-Pr	M2	Unpublished	D
*Ir-Pt	M2	[30Mul, 56Rau]	D
Ir-Pu	M2	M2	T
Ir-Rb	M2	[76Vol]	T
Ir-Re	M2	Unpublished	D
*Ir-Rh	M2,91	JPE 12(5)	D
*Ir-Ru	M2	JPE 13(5)	D
Ir-S	M2	M2	T
Ir-Sb	M2	Unpublished	D
Ir-Sc	M2	Unpublished	T
Ir-Se	M2	M2	T
Ir-Si	M2	M2	T
Ir-Sm	M2	Unpublished	D
Ir-Sn	M2	M2	T
Ir-Sr	M2	M2	T
*Ir-Ta	M2	[Metals]	D
Ir-Tb	M2	Unpublished	D
Ir-Tc	M2	M2	D
Ir-Te	M2	M2	D
*Ir-Th	M2	JPE 12(5)	D
*Ir-Ti	M2,92	Binary Titanium	D
Ir-Tl	No Data		
Ir-Tm	M2	Unpublished	D
*Ir-U	M2	JPE 13(5)	D
*Ir-V	M2	Binary Vanadium	D
*Ir-W	M2,92	Binary Tungsten	D
Ir-Y	M2	Unpublished	D
Ir-Yb	M2	JPE 13(2)	D
Ir-Zn	M2	[64Rhy]	T
*Ir-Zr	M2	JPE 13(5)	D
K-La	No Data		
K-Li	M2	BAPD 10(3)	D
K-Mg	M2	Binary Magnesium	D
K-Mo	M2	M2	D
K-N	M2	M2	T
*K-Na	M2	BAPD 3(3)	D
K-Nb	M2	BAPD 9(4)	D
K-Nd	No Data		
K-Ni	M2	[65Swi]	T
K-Np	No Data		
K-O	M2	M2	T
K-Os	M2	M2	T
K-P	M2	M2	T
*K-Pb	M2	M2	D
K-Pd	M2	M2	T
K-Pr	No Data		
K-Pu	M2	[59Sch]	T
*K-Rb	M2	BAPD 4(4)	D
K-Re	No Data		
K-Rh	M2	M2	T
K-Ru	M2	M2	T
*K-S	M2	M2	D
*K-Sb	M2	[61Dor2]	D
*K-Se	M2	M2	D
K-Si	M2	M2	T
K-Sm	No Data		
*K-Sn	M2	M2	D
K-Sr	M2	BAPD 6(2)	T
K-Ta	M2	JAPD 6(1)	D
K-Tb	No Data		
*K-Te	M2	BAPD 11(5)	D
K-Th	M2	M2	T
K-Ti	M2	BAPD 10(2)	D
*K-Tl	M2	M2	T
K-Tm	No Data		
K-U	M2	M2	T
K-V	M2	Binary Vanadium	D
K-W	M2	Binary Tungsten	T
K-Y	No Data		
K-Yb	No Data		
K-Zn	M2	BAPD 8(6)	D
K-Zr	M2	BAPD 10(3)	D
Kr-Mo	M2	[Molybdenum]	D
Kr-W		Binary Tungsten	T
La-Li	No Data		
La-Lu	M2	M2	D
*La-Mg	M2	Binary Magnesium	D
*La-Mn	M2	BAPD 11(5)	D
La-Mo	M2	M2	D
La-N	M2	M2	T
La-Na	No Data		
La-Nb	M2	Unpublished	D
La-Nd	M2	BAPD 2(4)	D
*La-Ni	M2,91	Binary Nickel	D
La-Np	No Data		
La-O	M2	M2	T
La-Os	M2	M2	T
La-P	M2	M2	T
*La-Pb	M2,92	JPE 13(1)	D
La-Pd	M2	M2	T
La-Pm	M2	M2	D
La-Pr	M2	M2	D
La-Pt	M2	M2	D
La-Pu	M2	M2	D
La-Rb	No Data		
La-Re	M2	M2	D
La-Rh	M2	M2	D
La-Ru	M2,91	M2	D
*La-S	M2	Unpublished	D
*La-Sb	M2	[54Vog]	D
*La-Sc	M2	BAPD 3(1)	D
*La-Se	M2	M2	D
La-Si	M2	M2	T
La-Sm	M2	M2	D
*La-Sn	M2,92	JPE 13(1)	D
La-Sr	No Data		
La-Ta	M2	[Moffatt]	D
La-Tb	M2	M2	D
La-Te	M2	[65Haa]	D
La-Th	M2	[69Bad]	D
La-Ti	M2	Binary Titanium	D
*La-Tl	M2	Unpublished	D
La-Tm	M2	M2	D
La-U	M2	M2	T
La-V	M2	Binary Vanadium	D
La-W	M2	Binary Tungsten	D
La-Y	M2	BAPD 3(1)	D
La-Yb	M2	M2	D
*La-Zn	M2	[41Rol]	D
La-Zr	M2	M2	T
*Li-Mg	M2	Binary Magnesium	D
Li-Mn	M2	[64Obi1]	D
Li-Mo	M2	M2	D
Li-N	M2,92	JPE 13(3)	D
*Li-Na	M2	BAPD 10(3)	D
Li-Nb	M2	BAPD 9(4)	D
Li-Ni	M2	Binary Nickel	D
Li-Np	No Data		
Li-O	M2,92	JPE 13(3)	T
Li-Os	M2	JPE 13(1)	T
Li-P	M2	Unpublished	T
*Li-Pb	M2	[Hansen]	D
*Li-Pd	M2	JPE 13(1)	D
Li-Pt	M2	JPE 12(6)	D
Li-Pu	M2	M2	D
Li-Rb	M2	BAPD 10(3)	D
Li-Re	M2	JPE 12(6)	T
Li-Rh	M2	JPE 12(6)	D
Li-Ru	M2	JPE 12(6)	T
*Li-S	M2	Unpublished	D
Li-Sb	M2	M2	D
*Li-Se	M2	[71Cun]	D
*Li-Si	M2	BAPD 11(3)	D
*Li-Sn	M2	[Moffatt]	D

(continued)

System	Published	Data source	Data type
*Li-Sr	M2	BAPD 10(3)	D
Li-Ta	M2	JAPD 6(1)	D
Li-Tb	No Data		
Li-Tc	M2	Unpublished	T
*Li-Te	M2	JPE 13(3)	D
Li-Th	No Data		
Li-Ti	M2	BAPD 10(2)	D
*Li-Tl	M2	[34Gru]	D
Li-Tm	No Data		
Li-U	M2	M2	T
Li-V	M2	Binary Vanadium	D
Li-W	M2	Binary Tungsten	T
Li-Y	No Data		
Li-Yb	No Data		
*Li-Zn	M2	JPE 12(1)	D
Li-Zr	M2	BAPD 8(1)	D
Lr-Mo	M2	[Molybdenum]	D
Lu-Mg	M2	Binary Magnesium	D
Lu-Mn	M2	M2	D
Lu-Mo	M2	[Molybdenum]	D
Lu-N	M2	M2	T
Lu-Na	No Data		
Lu-Nb	No Data		
Lu-Nd	M2	M2	D
Lu-Ni	M2	Binary Nickel	T
Lu-Np	No Data		
Lu-O	M2	M2	T
Lu-Os	M2	M2	T
Lu-P	M2	M2	T
*Lu-Pb	M2	[69Mcm]	D
Lu-Pd	M2	M2	T
Lu-Pm	M2	M2	D
Lu-Po	M2	M2	T
Lu-Pr	M2	M2	D
Lu-Pt	M2	M2	D
Lu-Pu	M2,91	M2	D
Lu-Rb	No Data		
Lu-Re	M2	M2	T
Lu-Rh	M2	M2	D
Lu-Ru	M2	M2	D
Lu-S	M2	M2	T
Lu-Sb	M2,91	M2	T
Lu-Sc	No Data		
Lu-Se	M2	M2	T
Lu-Si	M2	M2	D
Lu-Sm	M2	M2	D
Lu-Sn	M2	M2	D
Lu-Sr	No Data		
Lu-Ta	M2	[66Den1]	D
Lu-Tb	M2	M2	D
Lu-Tc	M2	M2	T
Lu-Te	M2	M2	T
Lu-Th	M2	M2	D
Lu-Ti	M2	M2	D
*Lu-Tl	M2	M2	D
Lu-Tm	M2	M2	D
Lu-U	M2	M2	T
Lu-V	M2	Binary Vanadium	D
Lu-W	M2	Binary Tungsten	D
Lu-Y	M2	M2	D
Lu-Yb	M2,91	BAPD 4(3	D
Lu-Zn	M2	M2	D
Lu-Zr	M2	M2	D
Md-Mo	M2	[Molybdenum]	D
*Mg-Mn	M2	Binary Magnesium	D
Mg-Mo	M2	Binary Magnesium	D
Mg-N	M2	Binary Magnesium	D
Mg-Na	M2	Binary Magnesium	D
Mg-Nb	M2	Binary Magnesium	D
Mg-Nd	M2,91	Binary Magnesium	D
*Mg-Ni	M2	Binary Nickel	D
Mg-Np	M2	[68Gul1]	T
Mg-O	M2	Binary Magnesium	D
Mg-Os	M2	[68Gul2]	T
Mg-P	M2	Binary Magnesium	T
Mg-Pa	M2	[68Gul1]	T
*Mg-Pb	M2	Binary Magnesium	D
Mg-Pd	M2	Binary Magnesium	D
Mg-Pm	M2	[68Gul2]	T
Mg-Po	M2	Binary Magnesium	T
Mg-Pr	M2	BAPD 10(1)	D
Mg-Pt	M2	Binary Magnesium	T
Mg-Pu	M2	M2	D
Mg-Ra	M2	[68Gul2]	T
Mg-Rb	M2	Binary Magnesium	D
Mg-Re	M2	[68Gul2]	T
Mg-Rh	M2	Binary Magnesium	T
Mg-Ru	M2	Binary Magnesium	T
Mg-S	M2	Binary Magnesium	D
*Mg-Sb	M2	Binary Magnesium	D
*Mg-Sc	M2	Binary Magnesium	D
Mg-Se	M2	Binary Magnesium	T
*Mg-Si	M2	Binary Magnesium	D
*Mg-Sm	M2	M2	D
*Mg-Sn	M2	Binary Magnesium	D
*Mg-Sr	M2	Binary Magnesium	D
Mg-Ta	M2	[68Gul2]	T
Mg-Tb	M2	Binary Magnesium	D
Mg-Tc	M2	[68Gul2]	T
Mg-Te	M2	Binary Magnesium	T
*Mg-Th	M2	Binary Magnesium	D
Mg-Ti	M2	Binary Magnesium	D
*Mg-Tl	M2	Binary Magnesium	D
Mg-Tm	M2	Binary Magnesium	D
Mg-U	M2	Binary Magnesium	D
Mg-V	M2	Binary Magnesium	D
Mg-W	M2	Binary Tungsten	T
*Mg-Y	M2,92	Binary Magnesium	D
*Mg-Yb	M2	Binary Magnesium	D
*Mg-Zn	M2	Binary Magnesium	D
*Mg-Zr	M2	Binary Magnesium	D
*Mn-Mo	M2	[Molybdenum]	D
*Mn-N	M2	BAPD 11(1)	D
Mn-Na	No Data		
Mn-Nb	M2	M2	D
*Mn-Nd	M2,92	[70Kir]	D
*Mn-Ni	M2	JPE 12(3)	D
Mn-Np	M2	M2	T
*Mn-O	M2	M2	D
*Mn-P	M2	[50Ber]	D
Mn-Pb	M2	[56Pel]	D
*Mn-Pd	M2	[Hansen]	D
Mn-Pm	91	[90Sac]	D
*Mn-Pr	M2	M2	D
Mn-Pt	M2	[55Rau]	D
*Mn-Pu	M2	[55Kon]	D
Mn-Rb	No Data		
Mn-Re	M2	[61Sav]	D
Mn-Rh	M2	[55Rau,59Hel]	D
Mn-Ru	M2	M2	D
Mn-S	M2	Unpublished	D
*Mn-Sb	M2	M2	D
Mn-Sc	M2	M2	D
Mn-Se	M2	Unpublished	D
*Mn-Si	M2,91	BAPD 11(5)	D
*Mn-Sm	M2	[70Kir]	D
*Mn-Sn	M2	M2	D
Mn-Sr	M2	M2	D
Mn-Ta	M2	[60Sav]	D
Mn-Tb	M2	[70Kir]	D
Mn-Tc	M2	M2	T
Mn-Te	M2	Unpublished	D
Mn-Th	M2	[Brandes]	D
*Mn-Ti	M2	Binary Titanium	D
Mn-Tl	M2	M2	D
Mn-Tm	M2	M2	D
*Mn-U	M2	[Hansen]	D
*Mn-V	M2,92	Binary Vanadium	D
Mn-W	M2	Binary Tungsten	T
*Mn-Y	M2,91	JPE 12(4)	D
Mn-Yb	M2	M2	D
*Mn-Zn	M2	BAPD 11(4)	D
*Mn-Zr	M2	Unpublished	D
*Mo-N	M2	M2	D
Mo-Na	M2	M2	D
*Mo-Nb	M2,91	[Molybdenum]	D
Mo-Nd	M2	M2	D
Mo-Ne	M2	[Molybdenum]	D
*Mo-Ni	M2,91	Binary Nickel	D
Mo-No	M2	[Molybdenum]	D
Mo-Np	M2	[Molybdenum]	D
*Mo-O	M2	BAPD 1(2)	D
*Mo-Os	M2	[Molybdenum]	D
*Mo-P	M2	[Molybdenum]	D
Mo-Pa	M2	[Molybdenum]	D
Mo-Pb	M2	M2	D
*Mo-Pd	M2,92	M2	D
Mo-Pm	M2	M2	D
Mo-Po	M2	[Molybdenum]	T
Mo-Pr	M2	M2	D
*Mo-Pt	M2	BAPD 1(2)	D
*Mo-Pu	M2	[Molybdenum]	D
Mo-Ra	M2	[Molybdenum]	D
Mo-Rb	M2	M2	D
Mo-Re	M2	M2	D

(continued)

System	Published	Data source	Data type
*Mo-Rh	M2	[Molybdenum]	D
Mo-Rn	M2	[Molybdenum]	D
*Mo-Ru	M2	M2	D
*Mo-S	M2	BAPD 1(2)	D
Mo-Sb	M2	[Molybdenum]	D
Mo-Sc	M2	[Molybdenum]	D
Mo-Se	M2	[Molybdenum]	D
*Mo-Si	M2	JPE 12(4)	D
Mo-Sm	M2	M2	D
Mo-Sn	M2	BAPD 1(2)	D
Mo-Sr	M2	M2	D
*Mo-Ta	M2	JAPD 2(3)	D
Mo-Tb	M2	M2	D
Mo-Tc	M2	[Molybdenum]	D
Mo-Te	M2	[Molybdenum]	D
Mo-Th	M2	[Molybdenum]	D
*Mo-Ti	M2	Binary Titanium	D
Mo-Tl	M2	M2	D
Mo-Tm	M2	M2	D
*Mo-U	M2	M2	D
*Mo-V	M2	JPE 13(1)	D
*Mo-W	M2	Binary Tungsten	D
Mo-Xe	M2	[Molybdenum]	D
Mo-Y	M2	[Molybdenum]	D
Mo-Yb	M2	M2	D
Mo-Zn	M2	[Molybdenum]	D
*Mo-Zr	M2	[Zirconium]	D
N-Na	M2	M2	T
*N-Nb	M2	[74Lev]	D
N-Nd	M2	M2	T
*N-Ni	M2	Binary Nickel	D
N-Np	M2	M2	T
N-Os	M2	M2	T
N-Pa	M2	M2	T
N-Pb	M2	M2	T
N-Pd	M2	[10Sie]	T
N-Pr	M2	M2	T
N-Pt	No Data		
N-Pu	M2	BAPD 10(5)	D
N-Rb	M2	M2	T
N-Re	M2	M2	T
N-Rh	No Data		
N-Ru	No Data		
N-Sb	No Data		
N-Sc	M2	M2	T
N-Se	M2	M2	T
N-Si	M2	BAPD 11(6)	D
N-Sm	M2	M2	T
N-Sn	M2	[08Fis,10Sie]	T
N-Sr	M2	M2	T
*N-Ta	M2	[75Gat]	D
N-Tb	M2	M2	T
N-Tc	M2	M2	T
N-Te	M2	M2	T
*N-Th	M2	M2	D
*N-Ti	M2	Binary Titanium	D
N-Tl	M2	M2	T
N-Tm	M2	M2	T
*N-U	M2	[Metals]	D
N-V	M2	Binary Vanadium	D
N-W	M2	Binary Tungsten	D
N-Y	M2	M2	D
N-Yb	M2	M2	T
N-Zn	M2	BAPD 9(3)	T
*N-Zr	M2	[Zirconium]	D
Na-Nb	M2	BAPD 9(4)	D
Na-Nd	No Data		
Na-Ni	M2	Binary Nickel	T
Na-Np	No Data		
*Na-O	M2	BAPD 8(3)	D
Na-Os	M2	[81Loe]	T
Na-P	No Data		
*Na-Pb	M2	[Metals]	D
Na-Pd	M2	M2	D
Na-Po	M2	M2	T
Na-Pr	No Data		
Na-Pt	M2	M2	D
Na-Pu	M2	M2	T
*Na-Rb	M2	BAPD 3(3)	D
Na-Re	No Data		
Na-Rh	M2	[81Loe]	T
Na-Ru	M2	[81Loe]	T
*Na-S	M2	M2	D
*Na-Sb	M2	[06Mat]	D
Na-Sc	No Data		
*Na-Se	M2	M2	D
Na-Si	M2	JPE 13(1)	T
Na-Sm	No Data		
*Na-Sn	M2	M2	D
*Na-Sr	M2	BAPD 6(1)	D
Na-Ta	M2,91	JAPD 6(1)	D
Na-Tb	No Data		
*Na-Te	M2	BAPD 11(5)	D
Na-Th	M2	[42Gru]	D
Na-Ti	M2	BAPD 10(2)	D
*Na-Tl	M2	[36Gru]	D
Na-Tm	No Data		
Na-U	M2	M2	T
Na-V	M2	Binary Vanadium	D
Na-W	M2	Binary Tungsten	T
Na-Y	No Data		
Na-Yb	No Data		
Na-Zn	M2	BAPD 8(6)	D
Na-Zr	M2	BAPD 8(1)	D
Nb-Nd	M2	M2	T
*Nb-Ni	M2	Binary Nickel	D
Nb-Np	No Data		
Nb-O	M2	[59Ell,Shunk]	D
*Nb-Os	M2	[77Wat]	D
Nb-P	M2	M2	T
Nb-Pb	M2	M2	T
*Nb-Pd	M2	BAPD 9(4)	D
Nb-Pr	No Data		
*Nb-Pt	M2	M2	D
Nb-Pu	M2	M2	D
Nb-Rb	M2	BAPD 11(3)	D
Nb-Re	M2	[60Gra]	D
*Nb-Rh	M2	[64Rit]	D
*Nb-Ru	M2	M2	D
Nb-S	M2	M2	D
Nb-Sb	M2	M2	D
Nb-Sc	M2	M2	D
Nb-Se	M2	M2	D
*Nb-Si	M2	Unpublished	D
Nb-Sm	M2,92	[Moffatt]	D
Nb-Sn	M2	[Shunk]	D
Nb-Sr	No Data		
*Nb-Ta	M2	JAPD 3(1)	D
Nb-Tb	No Data		
Nb-Tc	M2	M2	T
Nb-Te	M2	M2	D
*Nb-Th	M2	[56Car]	D
*Nb-Ti	M2	Binary Titanium	D
Nb-Tl	M2	M2	D
Nb-Tm	No Data		
*Nb-U	M2	M2	D
*Nb-V	M2	Binary Vanadium	D
*Nb-W	M2	Binary Tungsten	D
Nb-Y	M2	JPE 12(2)	D
Nb-Yb	M2	M2	D
Nb-Zn	M2	JPE 13(4)	D
*Nb-Zr	M2,92	BAPD 3(1)	D
*Nd-Ni	M2,92	Binary Nickel	D
Nd-Np	No Data		
Nd-O	M2	M2	D
Nd-Os	M2	M2	T
Nd-P	M2	M2	T
Nd-Pb	M2	M2	T
Nd-Pd	M2,92	M2	D
Nd-Pm	M2	M2	D
Nd-Pr	M2	BAPD 3(2)	D
*Nd-Pt	M2	M2	D
Nd-Pu	M2	M2	D
Nd-Rb	No Data		
Nd-Re	M2	M2	T
*Nd-Rh	M2	M2	D
Nd-Ru	M2,91	M2	D
Nd-S	M2	M2	T
*Nd-Sb	M2	M2	D
Nd-Sc	M2	BAPD 3(3)	D
Nd-Se	M2	M2	T
*Nd-Si	M2	BAPD 10(3)	D
Nd-Sm	M2	BAPD 3(2)	D
*Nd-Sn	M2	M2	D
Nd-Sr	M2	[78Esh]	D
Nd-Ta	M2	[Moffatt]	D
Nd-Tb	M2	M2	D
*Nd-Te	M2	M2	D
Nd-Th	M2	[67Bad1]	D
*Nd-Ti	M2	Binary Titanium	D
*Nd-Tl	M2	Unpublished	D
Nd-Tm	M2	M2	D
Nd-U	M2	M2	D
Nd-V	M2	Binary Vanadium	D
Nd-W	M2	Binary Tungsten	D
Nd-Y	M2	BAPD 3(2)	D
Nd-Yb	M2	BAPD 3(2)	D
*Nd-Zn	M2	[72Mas]	D
Nd-Zr	M2	[Shunk,Elliott]	T
Ne-W		Binary Tungsten	T
Ni-Np	M2	Binary Nickel	T
*Ni-O	M2	Binary Nickel	D
*Ni-Os	M2	Binary Nickel	D
*Ni-P	M2	Binary Nickel	D
*Ni-Pb	M2	Binary Nickel	D
*Ni-Pd	M2	Binary Nickel	D
Ni-Pm	M2	Binary Nickel	T
Ni-Po	M2	[Moffatt]	D
*Ni-Pr	M2	Binary Nickel	D
*Ni-Pt	M2	Binary Nickel	D
*Ni-Pu	M2	Binary Nickel	D
Ni-Rb	No Data		
*Ni-Re	M2,92	Binary Nickel	D
*Ni-Rh	M2	Binary Nickel	D
*Ni-Ru	M2	Binary Nickel	D
*Ni-S	M2	Binary Nickel	D
*Ni-Sb	M2	Binary Nickel	D
*Ni-Sc	M2	Binary Nickel	D
*Ni-Se	M2	Binary Nickel	D
*Ni-Si	M2	Binary Nickel	D
*Ni-Sm	M2	Binary Nickel	D
*Ni-Sn	M2	Binary Nickel	D
Ni-Sr	M2	Binary Nickel	D
*Ni-Ta	M2	Binary Nickel	D
Ni-Tb	M2	Binary Nickel	T

(continued)

System	Published	Data source	Data type
Ni-Tc	M2	Binary Nickel	D
*Ni-Te	M2	Binary Nickel	D
Ni-Th	M2,91	Binary Nickel	D
*Ni-Ti	M2	Binary Nickel	D
Ni-Tl	M2	[08Vos]	D
Ni-Tm	M2	Binary Nickel	T
*Ni-U	M2	Binary Nickel	D
*Ni-V	M2	Binary Nickel	D
*Ni-W	M2,91	Binary Tungsten	D
*Ni-Y	M2	Binary Nickel	D
*Ni-Yb	M2	Binary Nickel	D
*Ni-Zn	M2	Binary Nickel	D
*Ni-Zr	M2	Binary Nickel	D
Np-O	M2	M2	D
Np-Os	M2	M2	T
Np-P	M2	M2	T
Np-Pb	No Data		
Np-Pd	M2	M2	T
Np-Pr	No Data		
Np-Pt	M2	BAPD 10(2)	T
*Np-Pu	M2	BAPD 6(3)	D
Np-Rb	No Data		
Np-Re	M2	M2	T
Np-Rh	M2	M2	T
Np-Ru	M2	M2	T
Np-S	M2	M2	T
Np-Sb	M2	M2	T
Np-Sc	No Data		
Np-Se	M2	M2	T
Np-Si	M2	M2	T
Np-Sm	No Data		
Np-Sn	M2	M2	T
Np-Sr	No Data		
Np-Ta	No Data		
Np-Tb	No Data		
Np-Te	M2	M2	T
Np-Th	No Data		
Np-Ti	No Data		
Np-Tl	M2	M2	T
Np-Tm	No Data		
*Np-U	M2	BAPD 6(3)	D
Np-V	No Data		
Np-W	M2	Binary Tungsten	T
Np-Y	No Data		
Np-Yb	No Data		
Np-Zn	No Data		
Np-Zr	No Data		
O-Os	M2	M2	T
O-Pa	M2	M2	T
*O-Pb	M2	BAPD 9(2)	D
O-Pd	M2	[Pearson3]	T
O-Pm	M2	M2	T
O-Po	M2	M2	T
*O-Pr	M2	M2	D
O-Pt	M2	[Pearson3]	T
*O-Pu	M2	BAPD 11(2)	D
O-Rb	M2	M2	D
O-Re	M2	[Pearson3]	T
O-Rh	M2	M2	T
O-Ru	M2	M2	T
O-Sb	M2	M2	D
O-Sc	M2	M2	D
O-Se	M2	M2	T
O-Si	M2	BAPD 11(1)	D
O-Sm	M2	M2	T
*O-Sn	M2	[Hansen]	
O-Sr	M2	[56Swa, 63Sch]	T
O-Ta	M2	[72Jeh]	D
O-Tb	M2	M2	D
O-Tc	M2	M2	T
O-Te	M2	M2	D
O-Th	M2	[Smith]	D
*O-Ti	M2	Binary Titanium	D
O-Tl	M2	M2	T
O-Tm	M2	M2	T
O-U	M2	[Elliott]	D
*O-V	M2	Binary Vanadium	D
*O-W	M2	Binary Tungsten	D
*O-Y	M2	BAPD 11(1)	D
O-Yb	M2	M2	T
O-Zn	M2	BAPD 8(2)	D
*O-Zr	M2	BAPD 7(2)	D
Os-P	M2	M2	D
Os-Pb	No Data		
Os-Pd	M2	[63Tyl]	D
Os-Pr	M2	M2	D
*Os-Pt	M2	M2	D
*Os-Pu	M2	[55Kon]	D
Os-Rb	M2	[81Loe]	T
*Os-Re	M2	[62Tyl1]	D
*Os-Rh	M2	M2	D
*Os-Ru	M2	[62Tyl2]	D
Os-S	M2	M2	D
Os-Sb	M2	M2	T
Os-Sc	M2	M2	T
Os-Se	M2	M2	D
*Os-Si	M2	M2	D
Os-Sm	M2	[59Com,80Pal]	T
Os-Sn	M2	M2	T
Os-Sr	No Data		
Os-Ta	M2	[60Kau]	D
Os-Tb	M2	[59Boz,80Pal]	T
Os-Tc	M2	M2	T
Os-Te	M2	M2	D
Os-Th	M2	M2	D
*Os-Ti	M2	Binary Nickel	D
Os-Tl	No Data		
Os-Tm	M2	M2	T
*Os-U	M2	[Shunk]	D
*Os-V	M2	Binary Vanadium	D
*Os-W	M2,92	Binary Tungsten	D
Os-Y	M2	[73Sav]	D
Os-Yb	M2	M2	D
Os-Zn	M2	M2	T
*Os-Zr	M2	M2	D
P-Pa	M2	M2	T
P-Pb	M2	[1898Gra, 22Bru]	T
*P-Pd	M2	Unpublished	D
*P-Pr	M2	[Moffatt]	D
P-Pt	M2	BAPD 11(5)	D
P-Pu	M2	M2	T
P-Rb	M2	M2	T
P-Re	M2	M2	T
P-Rh	M2	BAPD 11(4)	D
*P-Ru	M2	M2	D
P-S	91	[79Bla]	D
P-Sb	M2,91	JPE 12(2)	D
P-Sc	M2	M2	T
P-Se	M2	Unpublished	D
P-Si	M2	BAPD 6(2)	D
P-Sm	M2	M2	T
*P-Sn	M2	[20Viv]	D
P-Sr	M2	M2	T
P-Ta	M2	[Pearson3]	T
P-Tb	M2	M2	T
P-Tc	M2	M2	T
P-Te	M2	[42Mon]	T
P-Th	M2	M2	D
*P-Ti	M2	Binary Titanium	D
P-Tl	M2	Unpublished	D
P-Tm	M2	M2	T
P-U	M2	M2	T
P-V	M2	JPE 12(4)	T
P-W	M2	Binary Tungsten	T
P-Y	M2	M2	T
P-Yb	M2	M2	T
*P-Zn	M2	JPE 12(4)	D
P-Zr	M2	M2	T
Pa-Pt	M2	BAPD 10(2)	T
Pa-Rh	M2	M2	T
Pa-Sb	M2	M2	T
Pa-Th	M2	M2	T
Pa-W	M2	Binary Tungsten	T
*Pb-Pd	M2	M2	D
Pb-Pm	M2	[63Wil]	T
Pb-Po	M2	M2	T
*Pb-Pr	M2	M2	D
*Pb-Pt	M2	[Hansen]	D
*Pb-Pu	M2	BAPD 9(3)	D
*Pb-Rb	M2	[77Kuz, 64Hew]	D
Pb-Re	No Data		
*Pb-Rh	M2	M2	D
Pb-Ru	M2	M2	T
*Pb-S	M2	BAPD 7(4)	D
*Pb-Sb	M2	BAPD 2(1)	D
Pb-Sc	No Data		
*Pb-Se	M2	Unpublished	D
Pb-Si	M2	BAPD 5(3)	D
Pb-Sm	M2	[Moffatt]	D
*Pb-Sn	M2	BAPD 9(2)	D
*Pb-Sr	M2	[81Bru]	D
Pb-Ta	No Data		
Pb-Tb	M2	M2	T
*Pb-Te	M2	BAPD 10(4)	D
Pb-Th	M2	M2	D
Pb-Ti	M2	Binary Titanium	D
*Pb-Tl	M2	[Hultgren,B]	D
Pb-Tm	M2	M2	T
Pb-U	M2	BAPD 8(6)	D
Pb-V	M2	Binary Vanadium	T
Pb-W	M2	Binary Tungsten	T
*Pb-Y	M2	[67Car]	D
*Pb-Yb	M2	JPE 12(4)	D
*Pb-Zn	M2	[Hansen]	D
Pb-Zr	M2	M2	D
Pd-Pr	M2	JAPD 6(2)	D
*Pd-Pt	M2,91	M2	D
*Pd-Pu	M2	[67Kut1]	D
Pd-Rb	M2	[81Loe]	T
Pd-Re	M2	M2	D
*Pd-Rh	M2	M2	D
*Pd-Ru	M2	M2	D
*Pd-S	M2,92	[76Mat]	D
*Pd-Sb	M2,92	M2	D
Pd-Sc	M2	M2	D
*Pd-Se	M2,91	JPE 13(1)	D
*Pd-Si	M2,91	JPE 12(3)	D
*Pd-Sm	M2	M2	D
*Pd-Sn	M2	M2	D
Pd-Sr	M2	M2	T
Pd-Ta	M2	JAPD 6(2)	D
Pd-Tb	M2,91	M2	T
Pd-Tc	M2	M2	D

(continued)

System	Published	Data source	Data type
*Pd-Te	M2	JPE 13(1)	D
Pd-Th	M2	M2	D
*Pd-Ti	M2	Binary Titanium	D
*Pd-Tl	M2	M2	D
Pd-Tm	M2	M2	T
*Pd-U	M2,92	[56Cat, 63Pel]	D
*Pd-V	M2	Binary Vanadium	D
*Pd-W	M2,91,92	Binary Tungsten	D
*Pd-Y	M2,91	M2	D
*Pd-Yb	M2	[73Ian]	D
*Pd-Zn	M2	M2	D
Pd-Zr	M2,92	JAPD 6(1)	D
Pm-Po	M2	M2	T
Pm-Pr	M2	M2	D
Pm-Pu	M2,92	M2	D
Pm-Rh	M2	M2	D
Pm-Ru	M2	M2	D
Pm-Sm	M2	M2	D
Pm-Tb	M2	M2	D
Pm-Th	M2	M2	D
Pm-Tl	M2	[88Sac]	D
Pm-Tm	M2	M2	D
Pm-V	M2	Binary Vanadium	D
Pm-W	M2	Binary Tungsten	T
Pm-Y	M2	M2	D
Po-Pr	M2	[63Ker,Shunk]	T
Po-Pt	M2	M2	T
Po-S	M2	[Hansen]	T
Po-Sc	M2	M2	T
Po-Sm	M2	M2	T
Po-Sr	M2	M2	T
Po-Ta	M2	[60Wit]	T
Po-Tb	M2	M2	T
Po-Ti	M2	M2	T
Po-Tm	M2	M2	T
Po-W	M2	Binary Tungsten	T
Po-Y	M2	M2	T
Po-Yb	M2	M2	T
Po-Zn	M2	M2	T
Po-Zr	M2	M2	T
Pr-Pt	M2	M2	D
Pr-Pu	M2	M2	D
Pr-Rb	No Data		
Pr-Re	M2	[64Ell]	D
Pr-Rh	M2	M2	D
Pr-Ru	M2	M2	D
Pr-S	M2,91	M2	T
*Pr-Sb	M2	M2	D
Pr-Sc	No Data		
*Pr-Se	M2	[70Yar]	D
*Pr-Si	M2	M2	D
Pr-Sm	M2	M2	D
*Pr-Sn	M2	M2	D
Pr-Sr	No Data		
Pr-Ta	M2	[Moffatt]	D
Pr-Tb	M2	M2	D
Pr-Tc	M2	[64Dar]	T
*Pr-Te	M2	[70Yar]	D
Pr-Th	M2	[67Bad1]	D
Pr-Ti	M2	M2	D
*Pr-Tl	M2	Unpublished	D
Pr-Tm	M2	M2	D
Pr-U	M2	M2	D
Pr-V	M2	Binary Vanadium	D
Pr-W	M2	Binary Tungsten	D
Pr-Y	M2	M2	D
Pr-Yb	No Data		
*Pr-Zn	M2	[70Mas]	D
Pt-Pu	M2	BAPD 10(4a)	D
Pt-Rb	M2	[81Loe]	T
Pt-Re	M2	M2	D
*Pt-Rh	M2,92	[Moffatt]	D
Pt-Ru	M2	[72Hut]	D
Pt-S	M2	Unpublished	D
Pt-Sb	M2,92	M2	D
Pt-Sc	M2	M2	D
Pt-Se	M2	M2	T
*Pt-Si	M2	JPE 12(5)	D
Pt-Sm	M2	M2	D
*Pt-Sn	M2	[Hansen]	D
Pt-Sr	M2	M2	D
Pt-Ta	M2	[81Wat]	D
Pt-Tb	M2	M2	D
Pt-Tc	M2	M2	D
*Pt-Te	M2	M2	D
Pt-Th	M2	BAPD 11(3)	D
*Pt-Ti	M2	Binary Titanium	D
*Pt-Tl	M2	M2	D
Pt-Tm	M2	M2	D
*Pt-U	M2	BAPD 11(3)	D
*Pt-V	M2	Binary Vanadium	D
Pt-W	M2,91	Binary Tungsten	D
Pt-Y	M2	BAPD 11(5)	D
Pt-Yb	M2	M2	D
Pt-Zn	M2	JPE 12(4)	D
*Pt-Zr	M2	M2	D
Pu-Rb	No Data		
Pu-Re	M2	[67Bow]	D
Pu-Rh	M2	[78Lan]	D
Pu-Ru	M2	[67Kut2]	D
Pu-S	M2	M2	T
Pu-Sb	M2	M2	T
*Pu-Sc	M2	M2	D
Pu-Se	M2	M2	T
Pu-Si	M2	[Shunk]	D
Pu-Sm	M2	M2	D
Pu-Sn	M2	BAPD 9(2)	D
Pu-Sr	M2	M2	T
Pu-Ta	M2	JPE 12(5)	D
Pu-Tb	M2	M2	D
Pu-Te	M2	M2	T
Pu-Th	M2	BAPD 6(3)	D
Pu-Ti	M2	Binary Titanium	D
Pu-Tl	M2	[58Boc]	T
Pu-Tm	M2	M2	D
*Pu-U	M2,92	BAPD 10(2)	D
Pu-V	M2,91	JPE 12(5)	D
Pu-W	M2	Binary Tungsten	D
Pu-Y	M2	M2	D
Pu-Yb	M2	M2	D
*Pu-Zn	M2	[Chiotti]	D
*Pu-Zr	M2	[Elliott]	D
Ra-S	M2	M2	T
Ra-Se	M2	M2	T
Ra-W	M2	Binary Tungsten	T
Rb-Re	No Data		
Rb-Rh	M2	[81Loe]	T
Rb-Ru	M2	[81Loe]	T
Rb-S	M2	M2	D
*Rb-Sb	M2	[61Dor2]	D
Rb-Sc	No Data		
*Rb-Se	M2	M2	D
Rb-Si	M2	M2	T
Rb-Sm	No Data		
Rb-Sn	M2	M2	T
Rb-Sr	M2	BAPD 6(1)	T
Rb-Ta	M2,91	JAPD 6(3)	D
Rb-Tb	No Data		
Rb-Te	M2	Unpublished	D
Rb-Th	No Data		
Rb-Ti	M2	BAPD 10(2)	D
*Rb-Tl	M2	[70Thu]	D
Rb-Tm	No Data		
Rb-U	No Data		
Rb-V	M2	Binary Vanadium	D
Rb-W	M2	Binary Tungsten	T
Rb-Y	No Data		
Rb-Yb	No Data		
Rb-Zn	M2	BAPD 8(5)	D
Rb-Zr	M2	BAPD 8(1)	D
Re-Rh	M2	[62Tyl3]	D
*Re-Ru	M2	[62Rud]	D
Re-S	M2	M2	T
Re-Sb	M2	M2	D
Re-Sc	M2	[66Sav]	D
Re-Se	M2	M2	T
*Re-Si	M2	Unpublished	D
Re-Sm	M2	M2	T
Re-Sn	M2	M2	D
Re-Sr	No Data		
Re-Ta	M2	[60Bro]	D
Re-Tb	M2	[68Sav]	D
Re-Tc	M2	M2	D
*Re-Te	M2	[77Kur]	D
Re-Th	M2	[77Gar]	D
Re-Ti	M2	Binary Titanium	D
Re-Tl	No Data		
Re-Tm	M2	M2	T
*Re-U	M2	M2	D
*Re-V	M2	Binary Vanadium	D
Re-W	M2,92	Binary Tungsten	D
Re-Y	M2	[61Lun]	D
Re-Yb	M2	M2	T
Re-Zn	M2	M2	T
Re-Zr	M2	M2	D
Rh-Ru	M2	[84Pas]	D
Rh-S	M2,92	[Moffatt]	D
Rh-Sb	M2	[Shunk]	D
Rh-Sc	M2	[58Com, 61Dwi]	T
*Rh-Se	M2	M2	D
Rh-Si	M2,92	JPE 13(1)	D
Rh-Sm	M2	M2	D
Rh-Sn	M2	[Hansen]	D
Rh-Sr	M2	M2	T
*Rh-Ta	M2	[64Gie]	D
Rh-Tb	M2	M2	D
Rh-Tc	M2	M2	D
Rh-Te	M2,91	M2	D
Rh-Th	M2	[63Tho]	D
*Rh-Ti	M2	Binary Titanium	D
Rh-Tl	No Data		
Rh-Tm	M2	M2	T
*Rh-U	M2	[Ivanov]	D
*Rh-V	M2	Binary Vanadium	D

(continued)

System	Published	Data source	Data type
Rh-W	M2	Binary Tungsten	D
Rh-Y	M2	M2	D
Rh-Yb	M2	[76Ian]	D
Rh-Zn	M2	M2	D
Rh-Zr	M2	Unpublished	D
Rn-W		Binary Tungsten	T
Ru-S	M2,91	M2	D
Ru-Sb	M2	M2	T
Ru-Sc	M2	[Moffatt]	D
Ru-Se	M2	M2	D
*Ru-Si	M2,92	M2	D
Ru-Sm	M2,91	M2	D
Ru-Sn	M2	M2	D
Ru-Sr	No Data		
*Ru-Ta	M2,91	M2	D
Ru-Tb	M2	M2	D
Ru-Tc	M2	M2	T
Ru-Te	M2	M2	D
Ru-Th	M2	[63Tho]	D
*Ru-Ti	M2	Binary Titanium	D
Ru-Tl	No Data	D	
Ru-Tm	M2	M2	D
*Ru-U	M2	BAPD 2(4)	D
*Ru-V	M2	Binary Vanadium	D
Ru-W	M2,92	Binary Tungsten	D
Ru-Y	M2	M2	D
Ru-Yb	M2	[76Ian]	D
Ru-Zn	M2	M2	D
Ru-Zr	M2	Unpublished	D
S-Sb	M2	M2	D
S-Sc	M2	M2	T
*S-Se	M2	Unpublished	D
S-Si	M2	M2	D
S-Sm	M2	M2	D
*S-Sn	M2	BAPD 7(3)	D
S-Sr	M2	M2	T
S-Ta	No Data		
S-Tb	M2	M2	T
S-Tc	M2	M2	T
*S-Te	M2	BAPD 10(4)	D
S-Th	M2	M2	T
*S-Ti	M2	Binary Titanium	D
S-Tl	M2	M2	D
S-Tm	M2	M2	T
S-U	M2	M2	D
S-V	M2	Binary Vanadium	D
S-W	M2	Binary Tungsten	D
S-Y	M2	M2	T
S-Yb	M2	[78Eli]	D
S-Zn	M2	Unpublished	D
S-Zr	M2	M2	D
*Sb-Se	M2	M2	D
*Sb-Si	M2	BAPD 6(5)	D
*Sb-Sm	M2	M2	D
*Sb-Sn	M2	[71Pre]	D
*Sb-Sr	M2	[75Vak]	D
Sb-Ta	No Data		
*Sb-Tb	M2	M2	D
*Sb-Te	M2	M2	D
Sb-Th	M2	M2	T
Sb-Ti	M2	Binary Titanium	D
*Sb-Tl	M2	Unpublished	D
Sb-Tm	M2	M2	T
*Sb-U	M2	BAPD 1(2)	D
Sb-V	M2	Binary Vanadium	T
Sb-W	M2,92	Binary Tungsten	T
*Sb-Y	M2	[70Sch]	D
Sb-Yb	M2	M2	D
*Sb-Zn	M2	[27Tak,66Vui]	D
Sb-Zr	M2	Unpublished	D
Sc-Se	M2	M2	T
Sc-Si	M2	BAPD 7(4)	D
Sc-Sm	No Data		
Sc-Sn	M2	M2	T
Sc-Sr	M2	M2	D
Sc-Ta	M2	[66Den1]	D
Sc-Tb	M2	M2	D
Sc-Tc	M2	M2	T
Sc-Te	M2	M2	D
Sc-Th	M2,91	[69Bad]	D
*Sc-Ti	M2	Binary Titanium	D
Sc-Tl	No Data		
Sc-Tm	No Data		
Sc-U	M2	M2	D
Sc-V	M2	Binary Vanadium	D
Sc-W	M2	Binary Tungsten	D
*Sc-Y	M2	BAPD 4(2)	D
Sc-Yb	M2	M2	D
Sc-Zn	M2	[Pearson3]	T
*Sc-Zr	M2	JPE 12(1)	D
Se-Si	M2	M2	T
Se-Sm	M2	M2	T
*Se-Sn	M2	BAPD 7(1)	D
*Se-Sr	M2	[75Lys]	D
Se-Ta	M2	[Pearson3]	T
Se-Tb	M2	M2	T
*Se-Te	M2	Unpublished	D
Se-Th	M2	[Hansen]	D
Se-Ti	M2	Binary Titanium	T
*Se-Tl	M2	[81Mor]	D
*Se-Tm	M2	M2	D
*Se-U	M2	[75Ell]	D
Se-V	M2	Binary Vanadium	D
Se-W	M2	Binary Tungsten	T
Se-Y	M2	M2	T
Se-Yb	M2	M2	D
Se-Zn	M2	Unpublished	D
Se-Zr	M2	M2	T
Si-Sm	M2	BAPD 9(5)	D
*Si-Sn	M2	BAPD 5(3)	D
*Si-Sr	M2	BAPD 10(6)	D
*Si-Ta	M2	Unpublished	D
Si-Tb	M2	M2	T
Si-Tc	M2	M2	T
*Si-Te	M2	[80Dav]	D
*Si-Th	M2	[Thorium]	D
*Si-Ti	M2	Binary Titanium	D
Si-Tl	M2	BAPD 6(6)	D
Si-Tm	M2	M2	D
*Si-U	M2	M2	D
*Si-V	M2	Binary Vanadium	D
Si-W	M2	Binary Tungsten	D
Si-Y	M2,91	BAPD 7(5)	D
Si-Yb	M2	M2	D
*Si-Zn	M2	BAPD 6(6)	D
*Si-Zr	M2	BAPD 11(5)	D
*Sm-Sn	M2	[82Bor]	D
Sm-Sr	No Data		
Sm-Ta	M2	[66Den2]	D
Sm-Tb	M2	M2	D
Sm-Te	M2	M2	T
Sm-Th	M2	M2	D
Sm-Ti	No Data		
*Sm-Tl	M2	Unpublished	D
Sm-Tm	M2	M2	D
Sm-U	M2	M2	D
Sm-V	M2	Binary Vanadium	D
Sm-W	M2	Binary Tungsten	D
Sm-Y	M2	BAPD 4(2)	D
Sm-Yb	No Data		
*Sm-Zn	M2	[Moffatt]	D
Sm-Zr	M2	[Elliott]	T
Sn-Sr	M2	M2	D
Sn-Ta	M2	M2	T
Sn-Tb	No Data		
Sn-Tc	M2	M2	T
*Sn-Te	M2	BAPD 7(1)	D
Sn-Th	M2	BAPD 10(4a)	D
*Sn-Ti	M2	Binary Titanium	D
*Sn-Tl	M2	M2	D
Sn-Tm	M2	M2	T
*Sn-U	M2	BAPD 8(4)	D
Sn-V	M2	Binary Vanadium	D
Sn-W	M2	Binary Tungsten	T
*Sn-Y	M2	M2	D
*Sn-Yb	M2	JPE 12(4)	D
*Sn-Zn	M2	BAPD 6(4)	D
*Sn-Zr	M2	BAPD 4(2)	D
Sr-Ta	No Data		
Sr-Tb	No Data		
*Sr-Te	M2	[75Lys]	D
Sr-Th	No Data		
Sr-Ti	M2	Binary Titanium	D
*Sr-Tl	M2	M2	D
Sr-Tm	No Data		
Sr-U	M2	M2	T
Sr-V	M2	Binary Vanadium	D
Sr-W	M2	Binary Tungsten	T
Sr-Y	M2	M2	D
Sr-Yb	No Data		
*Sr-Zn	M2	M2	D
Sr-Zr	No Data		
T-Ta	92	[90Con]	D
Ta-Tb	M2	[66Den1]	D
Ta-Tc	M2	M2	T
Ta-Te	M2,92	JPE 13(3)	T
*Ta-Th	M2	JAPD 5(1)	D
*Ta-Ti	M2	Binary Titanium	D
Ta-Tl	M2	M2	D
Ta-Tm	M2	[66Den1]	D
*Ta-U	M2	JAPD 4(3)	D
*Ta-V	M2	Binary Vanadium	D
*Ta-W	M2	Binary Tungsten	D
Ta-Y	M2	M2	D
Ta-Yb	M2	M2	D
Ta-Zn	M2	[Pearson3]	T
*Ta-Zr	M2	JAPD 5(2)	D
Tb-Tc	M2	M2	T

(continued)

System	Published	Data source	Data type
Tb-Te	M2	M2	T
Tb-Th	M2	[67Bad2]	D
Tb-Ti	M2	[83Kub]	D
*Tb-Tl	M2	Unpublished	D
Tb-Tm	M2	M2	D
Tb-U	M2	[Elliott]	T
Tb-V	M2	Binary Vanadium	D
Tb-W	M2	Binary Tungsten	D
Tb-Y	M2	BAPD 4(2)	D
Tb-Yb	M2	M2	D
Tb-Zn	M2	M2	D
Tb-Zr	M2	[Moffatt]	D
Tc-Te	M2	M2	D
Tc-Th	M2	[65Dar]	T
Tc-Ti	M2	Binary Titanium	D
Tc-U	M2	[65Dar]	T
Tc-V	M2	Binary Vanadium	D
Tc-W	M2	Binary Tungsten	D
Tc-Y	M2	M2	T
Tc-Zn	M2	[64Cha]	D
Tc-Zr	M2	M2	T
Te-Th	M2	M2	T
Te-Ti	M2	Binary Titanium	T
*Te-Tl	M2,91	M2	D
Te-Tm	M2	M2	D
*Te-U	M2	[Moffatt]	D
Te-V	M2	Binary Vanadium	D
Te-W	M2	Binary Tungsten	D
Te-Y	M2	M2	D
*Te-Yb	M2	M2	D
*Te-Zn	M2	BAPD 8(1)	D
Te-Zr	M2	M2	D
*Th-Ti	M2	Binary Titanium	D
*Th-Tl	M2	M2	D
Th-Tm	M2	[Moffatt]	D
Th-U	M2	BAPD 6(5)	D
Th-V	M2	Binary Vanadium	D
Th-W	M2	Binary Tungsten	D
Th-Y	M2	[60Eas]	D
Th-Yb	M2	M2, D	
*Th-Zn	M2	[61Chi]	D
*Th-Zr	M2	[58Gib,61Joh]	D
Ti-Tm	M2	M2	D
*Ti-U	M2	Binary Titanium	D
*Ti-V	M2	Binary Vanadium	D
*Ti-W	M2	Binary Tungsten	D
*Ti-Y	M2	Binary Titanium	D
Ti-Yb	M2	M2	D
Ti-Zn	M2	Binary Titanium	D
*Ti-Zr	M2	Binary Titanium	D
Tl-Tm	M2	M2	D
Tl-U	M2	[52Ian,63Joh]	T
Tl-V	M2	Binary Vanadium	D
Tl-W	M2	Binary Tungsten	T
Tl-Y	M2,91	M2	T
*Tl-Yb	M2	Unpublished	D
*Tl-Zn	M2	[07Veg,52Sei]	D
Tl-Zr	M2	M2	T
Tm-U	M2	M2	T
Tm-V	M2	Binary Vanadium	D
Tm-W	M2	Binary Tungsten	D
Tm-Y	M2	M2	D
Tm-Yb	M2	M2	D
Tm-Zn	M2	M2	D
Tm-Zr	M2	[Shunk]	T
U-V	M2	Binary Vanadium	D
U-W	M2	Binary Tungsten	D
U-Y	M2	M2	D
U-Yb	M2	M2	D
U-Zn	M2	BAPD 1(2)	D
*U-Zr	M2,92	BAPD 10(2)	D
*V-W	M2	Binary Tungsten	D
V-Y	M2	Binary Vanadium	D
V-Yb	M2	Binary Vanadium	D
V-Zn	M2	Binary Vanadium	D
*V-Zr	M2	Binary Vanadium	D
W-Xe		Binary Tungsten	T
W-Y	M2	Binary Tungsten	D
W-Yb	M2	Binary Tungsten	D
W-Zn	M2	Binary Tungsten	T
*W-Zr	M2,92	Binary Tungsten	D
Y-Yb	M2	M2	D
*Y-Zn	M2	M2	D
*Y-Zr	M2	JPE 12(4)	D
*Yb-Zn	M2	[68Mas]	D
Yb-Zr	M2	M2	D
Zn-Zr	M2	JPE 13(4)	D

References Cited in Binary Alloys Index

The references listed below represent the best available sources for the diagrams and data developed from them. They do not, however, represent *evaluations* conducted under the International Alloy Phase Diagram Programme.

1898Gra: A. Granger, *Ann. Chim. Phys., 14,* 5-90 (1898).

05Bol: W. v.Bolton, *Z. Elektrochem., 11,* 51 (1905).

05Emi: F. Emich, *Monatsh. Chem., 26,* 1013 (1905).

06Mat: C.H. Mathewson, *Z. Anorg. Allg. Chem., 50,* 192-195 (1906).

07Veg: A.V. Vegesack, *Z. Anorg. Allg. Chem., 52,* 30-34 (1907).

08Fis: F. Fisher and G. Iliovich, *Ber. Dtsch. Chem Ges., 41,* 3802, 4449 (1908); *42,* 527 (1909); quoted in [Elliott].

08Fri: K. Friedrich, *Metallurgie, 5,* 212-215 (1908).

08Vos: G. Voss, *Z. Anorg. Allg. Chem., 57,* 49-52 (1908).

10Sie: A. Sieverts and W. Krumbhaar, *Ber. Dtsch. Chem. Ges.,43,* 894 (1910) in German.

20Viv: A.C. Vivian, *J. Inst. Met. 23,* 325-366 (1920).

22Bru: A. Brukel, *Z. Anorg. Allg. Chem., 125,* 255-256 (1922).

27Tak: T. Takei, *Sci. Rep. Tohoku Univ., 16,* 1031-1056 (1927).

30Mul: L. Muller, *Ann. Phys., 7,* 9-47 (1930) in German.

34Gru: G. Grube and G. Schaufler, *Z. Elektrochem., 40,* 593-600 (1934).

36Gru: G. Grube and A. Schmidt, *Z. Elektrochem., 42,* 201-209 (1936).

38Gru: G. Grube and A. Dietrich, *Z. Elektrochem., 44,* 755-758 (1938).

40And: K.W. Andrews, H.E. Davies, W. Hume-Rothery, and C.R. Oswin, *Proc. Roy. Soc. (London), A177,* 149-167 (1940-1941).

41Rol: L. Rolla and A. Iandelli, *Ric. Sci., 20,* 1216-1226 (1941).

42Gru: G. Grube and L. Botzenhardt, *Z. Elektrochem., 48,* 418-425 (1942).

42Mon: E. Montignie, *Bull. Soc. Chim. Fr., 9,* 658-661 (1942).

50Ber: J. Berak and T. Heumann, *Z. Metallkd., 41,* 19-23 (1950).

52Ian: A. Iandelli and R. Ferro, *Ann. Chim. (Rome), 42,* 598-606 (1952).

52Now: H. Nowotny, E. Bauer, A. Stampfl, and H. Bittner, *Monatsh. Chem., 83,* 221-236 (1952).

52Kos: W. Koster and E. Horn, *Z. Metallkd., 43,* 444-449 (1952).

52Sei: W. Seith, H. Johnson, and J. Wagner, *Z. Metallkd., 46,* 773-779 (1952).

53Gea: G.A. Geach and R.A. Jettery, *J. Met., 5,* 1084 (1953).

54Vog: R. Vogel and H. Klose, *Z. Metallkd., 45,* 633-638 (1954).

55Kon: S.T. Konobeevsky, Conf. Acad. Sci. USSR. Peaceful Uses Atomic Energy, Div. Chem. Sci., 1 (1955).

55Rau: E. Raub and W. Mahler, *Z. Metallkd., 46,* 282-290 (1955).

56Car: O.N. Carlson, J.M. Dickenson, H.E. Lunt, and H.A. Wilhelm, *Trans. AIME, 206,* 132-136 (1956).

56Cat: J.A. Catterall, J.D. Grogan, and R.J. Pleasance, *J. Inst.Met., 85,* 63-67 (1956).

56Mul: R.N.P. Mulford and G.E. Sturdy, *J. Am. Chem. Soc., 78,* 3897-3901 (1956).

56Pel: E. Pelzel, *Metall, 10,* 717-718 (1956).

56Rau: E. Raub and W. Plate, *Z. Metallkd., 47,* 688-693 (1956) in German.

56Swa: H.E. Swanson, N.T. Gilfrich, and G.M. Ugrinic, NBS Circ. 539 (1956).

56Tru: F.A. Trumbore, C.D. Thurmond, and M. Kowalchik, *J. Chem. Phys., 24,* 1112 (1956).

58Boc: A.A. Bochvar *et al.,* Proc. U.N. Int Conf. Peaceful Uses At. Energy, 2nd, Geneva, Vol. 6, 184-193 (1958); quoted from [Shunk].

58Com: V.B. Compton, *Acta Crystallogr., 11,* 446 (1958).

58Dom: R.F. Domagala, R.P. Elliott, and W. Rostoker, *Trans. AIME, 212,* 393-395 (1958)

58Gib: E.D. Gibson, B.A. Loomis, and O.N. Carlson, *Trans. ASM, 50,* 348-369 (1958).

58Mul: R.N.R. Mulford, USAEC, AECU-3813 (1958).

59Boz: R.M. Bozworth, B.T. Matthias, H. Suhl, E. Corenzwit, and D.D. Davis, *Phys. Rev., 115,* 1595-1596 (1959).

59Com: V.B. Compton and B.T. Matthias, *Acta Crystallogr., 12,* 651-654 (1959).

59Ell: R.P. Elliott, *Trans. ASM, 52,* 990-1014 (1959).

59Hel: A. Hellawell, *J. Less-Common Met., 1,* 343-347 (1959).

59Sch: F.W. Schonfeld, E.M. Cramer, W.N. Miner, F.H. Elinger, and A.S. Coffinberry, *Progress in Nuclear Energy,* Ser. V, Vol. 2, Pergamon Press, New York, 579-599, (1959).

60Bec: R.L. Beck, USAEC, LAR-10, 93 p (1960).

60Bro: J.H. Brophy, P. Schwarzkopt, and J. Wulff, *Trans. AIME, 218,* 910-914 (1960).

60Cro: J. Croni, C.E. Armantrout, and H. Kato, U.S. Bur. Mines, Rep. Invest. 5688, 12 p (1960).

60Eas: D.T. Eash and O.N. Carlson, *Trans, ASM, 52,* 1097-1114 (1960).

60Gra: N.J. Grant and B.C. Giessen, WADD Tech. Rept., 60-132, 90-112 (1960); *J. Met., 13,* 87 (1961); as quoted in [Elliott].

60Kau: A.R. Kaufmann, E.J. Rapperport, and M.F. Smith, WADD Tech. Rep. 60-132, 33-39 (1960).

60Lya: V.S. Lyashenko and V. Bykov, *At.Energy (USSR), 8,* 146-148 (1960) in Russian; TR: *Sov. J. At. Energy, 8,* 132-134 (1960).

60Pet1: D.T. Peterson and M. Indig, *J. Am. Chem. Soc., 80,* 5645-5646 (1960).

60Pet2: D.T. Peterson and D.J. Beerntsen, *Trans. ASM, 52,* 763-777 (1960).

60Pre: B. Predel, *Z. Phys. Chem., 24,* 206-216 (1960).

60Sav: E.M. Savitskii and C.V. Kopetskii, *Zh. Neorg. Khim., 5,* 2638-2640 (1960) in Russian; TR: *Russ J. Inorg. Chem., 5,* 1274-1275 (1960).

60Wit: W.G. Witteman, A.L. Giorgi, and D.T. Vier, *J. Phys. Chem.,64,* 434-440 (1960).

61Chi: P. Chiotti and K.J. Gill, *Trans. AIME, 221,* 573-580 (1961).

61Dor1: F.W. Dorn, W. Klemm, and S. Lohmeyer, *Z. Anorg. Allg. Chem., 209,* 204-209 (1961).

61Dor2: F.W. Dorn and W. Klemm, *Z. Anorg. Allg. Chem., 309,* 189-203 (1961).

61Dwi: A.E. Dwight, J.W. Downey, and R.A. Conner, Jr., *Acta Crystallogr., 14,* 75-76 (1961).

61Joh: R.H. Johnson and R.W.K. Honeycombe, *J. Nucl. Mater, 4,* 66-69 (1961).

61Lun: C.E. Lundin, in *The Rare Earths,* F.H. Spedding and A.H. Daane, Ed., John Wiley & Sons, New York, 263-264 (1961).

61Lov: B. Love, WADD Tech. Rep., 61-123, 179p (1961); quoted in [Elliott].

61Poo: D.M. Poole, M.G. Bale, P.G. Mardon, J.A.C. Marples, and J.L. Nichols, *Plutonium 1960,* Cleaver-Humes Press, London, 267-280 (1961).

61Sav: E.M. Savitskii, M.A. Tylkina, R.V. Kirilenko, and C.V. Kopetskii, *Zh. Neorg. Khim., 6,* 1474-1476 (1961) in Russian; TR: *Russ. J. Inorg. Chem., 6,* 755-756 (1961).

62Lun: C.E. Lundin and D.T. Klodt, *Trans. AIME, 224,* 367-372 (1962).

62Rap: E.J. Rapperport and M.F. Smith, Tech. Rep., WADD-TR-60-132, Pt. II, 8-27 (1962).

62Rud: E. Rudy, B. Kietter, and H. Froelich, *Z. Metallkd., 53,* 90-92 (1962).

62Tyl1: M.A. Tylkina, V.P. Polyakova, and E.M. Savitskii, *Zh. Neorg. Khim., 7,* 1469-1470 (1962) in Russian; TR: *Russ. J. Inorg. Chem., 7,* 755-756 (1962).

62Tyl2: M.A. Tylkina, V.P. Polyakova, and E.M. Savitskii, *Zh. Neorg. Khim., 7,* 1467-1468 (1962) in Russian; TR: *Russ. J. Inorg. Chem., 7,* 755-756 (1962).

62Tyl3: M.A. Tylkina, V.P. Polyakova, and E.M. Savitskii, *Zh. Neorg. Khim., 7,* 1919-1927 (1962) in Russian; TR: *Russ. J. Inorg. Chem., 7,* 990-996 (1962).

63Joh: I. Johnson and M.G. Chasanov, *Trans. ASM, 56,* 272-277 (1963).

63Ker: C.J. Kershner and R.H. Steinmeyer, USAEC, MLM-1163, F1-F6 (1963).

63Liu: C.H. Liu, A.S. Pashinkin, and A.V. Novoselova, *Dokl. Akad. Nauk SSSR, 151,* 1335-1338 (1963) in Russian; TR: *Dokl. Chem., 151,* 662-664 (1963).

63Obr: W. Obrowski, *Metall, 17,* 108-112 (1963).

63Pel: G.P. Pells, *J. Inst. Met., 92,* 416-418 (1963-1964).

63Sch: S.J. Schneider, NBS Monograph 68, 31 pp (1963).

63Tay: A. Taylor, B.J. Kagle, and N.J. Doyle, *J. Less-Common Met., 5,* 26-40 (1963).

63Tho: J.R. Thompson, *J. Less-Common Met., 5,* 437-442 (1963).

63Tyl: M.A. Tylkina, V.P. Polyakova, and O.Kh. Khamidov, *Zh. Neorg. Khim., 8,* 776-778 (1963) in Russian; TR: *Russ. J. Inorg. Chem., 8,* 395-397 (1963).

63Wil: G.P. Williams and L. Slifkin, *Acta Metall., 11,* 319-322 (1963).

64Cha: M.G. Chasanov, I. Johnson, and R.V. Schablaske, *J. Less-Common Met., 7,* 127-132 (1964).

64Dar: J.B. Darby, Jr., L.J. Norton, and J.W. Downey, *J. Less-Common Met., 6,* 165-167 (1964).

64Ell: R.P. Elliott, in *Rare Earth Research III,* Proc. 4th Conf. Rare Earth Res., L. Eyring, Ed., Gordon and Breach, New York, 215-245 (1964).

64Gie: B.C. Giessen, H. Ibach, and N.J. Grant, *Trans. AIME, 230,* 113-122 (1964).

64Hew: I.F. Hewaidy, E. Busmann, and W. Klemm, *Z. Anorg. Allg. Chem., 328,* 283-293 (1964).

64Obi1: I. Obinata, Y. Takeuchi, K. Kurihara, and M. Watanabe, *Nippon Kinzoku Gakkaishi, 28,* 562-568 (1964).

64Obi2: I. Obinata, Y. Takeuchi, K. Kurihara, and M. Watanabe, *Nippon Kinzoku Gakkaishi, 28,* 568-576 (1964).

64Pec: W.H. Pechin, D.E. Williams, and W.L. Larsen, *Trans. ASM, 57,* 464-473 (1964).

64Pet: D.T. Peterson and R.P. Colburn, USAEC Comm. IS-613, 13 p (1964); quoted from [Shunk].

64Rhy: D.W. Rhys and E.G. Price, *Met. Ind., 105,* 243-247 (1964).

64Rit: D.L. Ritter, B.C. Giessen, and N.J. Grant, *Trans. AIME, 230,* 1250-1267 (1964).

64Wit: L.J. Wittenburg and G.R. Grove, USAEC, MLM-1208, 8-11 (1964); USAEC, MLM-1244 , p 56 (1964); quoted in [Shunk].

65Dar: J.B. Darby, Jr., A.F. Berndt, and J.W. Downey, *J. Less-Common Met., 9,* 466-468 (1965).

65Ell: R.P. Elliott, in *Rare Earth Research III,* L. Eyring, Ed., Gordon and Breach, Science Publishers, New York, 215-245 (1965).

65Haa: D.J. Haase, H. Steinfink, and E.J. Weiss, in *Rare Earth Research 111,* Gordon and Breach, Science Publishers, New York, 535-544 (1965).

65Swi: J.H. Swisher, NASA Tech. Note, NASA-TN-D-2734, 18 p (1965); quoted in [Shunk].

66Bru: G. Bruzzone, *Ann. Chim. (Rome), 56,* 1306-1319 (1966).

66Den1: D.H. Dennison, M.J. Tschetter, and K.A. Gschneidner, Jr., *J. Less-Common Met.,10* (2), 108-115 (1966).

66Den2: D.H. Dennison, M.J. Tschetter, and K.A. Gschneidner, Jr., *J. Less-Common Met.,11,* 423-435 (1966).

66Ell: F.H. Ellinger, K.A. Johnson, and V.O. Struebing, *J. Nucl. Mat., 20,* 83-86 (1966).

66Sav: E.M. Savitskiy, M.A. Tylkina, and O.Kh. Khamidov, *Russ. Metall., 4,* 52-56 (1966).

66Vui: G. Vuillard and J.P. Piton, *Compt. Rend. C, 263,* 1018-1021 (1966).

67Bad1: T.A. Badayeva and R.I. Juznetsova, *Russ. Metall.,* (1), 89-92 (1967).

67Bad2: T.A. Badayeva and R.I. Juznetsova, *Russ. Metall., 6,* 99-100 (1967).

67Bow: D.F. Bowersox and J.A. Leary, *J. Nucl. Mater., 21,* 219-224 (1967).

67Car: O.N. Carlson, F.A. Schmidt, and D.E. Diesburg, *Trans. ASM, 60*(2), 119-124 (1967).

67Jan: G. Jangg, H.R. Kirchmayr, and W. Lugscheider, *Z. Metallkd., 58,* 724-726 (1967) in German.

67Kir1: H.R. Kirchmayr and W. Lugscheider, *Z. Metallkd., 58*(3), 185-188 (1967).

67Kir2: H.R. Kirchmayr and W. Lugscheider, *Z. Metallkd., 58,* 185-193 (1967) in German.

67Kut1: V.I. Kutaitsev, N.T. Chebortarev, I.G. Lebedev, M.A. Andrianov, V.N. Konev, and T.S. Menshikova, *Plutonium 1965,* Chapman & Hall, London, 420-449 (1967).

67Kut2: V.I. Kutaitsev, N.T. Chebortarev, I.G. Lebedev, M.A. Andrianov, V.N. Konev, and T.S. Menshikova, *Plutonium 1965,* Chapman & Hall, London, 420-447 (1967).

67Mcm: O.D. McMasters and K.A. Gschneidner, Jr., *J. Less-Common Met., 13,* 193-199 (1967).

67Par: J.K. Pargeter and W. Hume-Rothery, *J. Less-Common Met., 12,* 366-374 (1967).

67Rus: P.G. Rustamov, B.N. Mardakhaev, and M.G. Safarov, *Inorg. Mater.,3*(3), 429-433 (1967).

67Sto: E.K. Storms, *The Refractory Carbides,* Academic Press, New York (1967).

68Gul1: B.B. Gulyaev and G.F. Dvorshkaya, in *Phase Diagrams of Metallic Systems,* E.M. Savitskii, Ed., Akad. Nauk SSSR, 267-273 (1968) in Russian.

68Gul2: B.B. Gulyaev, in *Phase Diagrams of Metallic Systems,* E.M. Savitskii, Ed., Nauka, Moscow, 257-267 (1986) in Russian.

68Mas: J.T. Mason and P. Chiotti, *Trans. AIME, 242,* 1167-1171 (1968).

68Mcm: O.D. McMasters, T.J. O'Keefe, and K.A. Gschneidner, Jr., *Trans. Metall. Soc. AIME, 242*(5), 936-939 (1968).

68Sav: E.M. Savitskii and O.Kh. Khamidov, *Russ. Metall.,* (6), 108-111 (1968).

69Bad: T.A. Badayera and R.I. Kuznetsova, *Izv. Akad. Nauk SSSR, Met.,* (15), 156-193 (1969) in Russian; TR: *Russ. Metall.,* (5), 101-106 (1969).

69Ben1: R. Benz and P. L. Stone, *High Temp. Sci., 1,* 114-127 (1969).

69Ben2: R. Benz, C.G. Hoffman, and G.N. Rupert, *High. Temp. Sci., 1,* 342-359 (1969).

69Bor: V.A. Boryaleova, Ya Kh. Grinberg, E.G. Shukov, V.A. Koryazhkin, and Z.S. Medvedeva, *Inorg. Mater. J,* 397-399 (1969).

69Mcm: O.D. McMasters and K.A. Gschneidner, Jr., *J. Less-Common Met., 19,* 337-344 (1969).

70Kir: H.R. Kirchmayr and W. Lugscheider, *Z. Metallkd, 61,* 22-23 (1970).

70Mas: J.T. Mason and P. Chiotti, *Metall. Trans., 1,* 2119-2123 (1970).

70Sad: O.A. Sadovskaya and E.I. Yarembash, *Russ. Inorg. Mater., 6*(7), 1097-1101 (1970).

70Sch: F.A. Schmidt and O.D. McMasters, *J. Less-Common Met., 21,* 415-425 (1970).

70Thu: R. Thummel and W. Klemm, *Z. Anorg. Allg. Chem., 376,* 44-63 (1970) in German.

70Woo: D.H. Wood, E.M. Cramer, and P.L. Wallace, *Nucl. Metall., 17,* 707-719 (1970).

70Yar: E.I. Yarembach, *Colloq. Intern. CNRS (Paris), 1,* 472-481 (1970).

71Cun: P.T. Cunningham, S.A. Johnson, and E.J. Cairns, *J. Electrochem. Soc., 118,* 1941-1944 (1971).

71Gri: R.B. Griffin and K.A. Gschneidner, Jr., *Metall. Trans., 2*(9), 2517-2524 (1971).

71Pre: B. Predel and W. Schwermann, *J. Inst. Met., 99,* 169-173 (1971).

71Sve: V.N. Svechnikov, G.F. Kobzenko, and V.G. Ivanchenko, *Metallofizika,* (33), 93-95 (1971).

72Bor: J.D. Bornand and P. Feschotte, *J Less-Common Met., 29,* 81-91 (1972) in French.

72Hut: J.M. Hutchinson, Jr., *Platinum Met. Rev., 16,* 88-90 (1972).

72Jeh: H. Jehn and E. Olzi, *J. Less-Common Met., 27,* 297-309 (1972).

72Mas: J.T. Mason and P. Chiotti, *Metall. Trans., 3,* 2851-2855 (1972).

72Por: K.I. Portnoi and V.M. Romashov, *Sov. Powder Metall. Met. Ceram., 11,* 378-384 (1972).

72Shu: A.K. Shurin and V.V. Pet'kov, *Russ. Metall., (2),* 122-144 (1972).

73Bus: K.H.J. Buschow, *J. Less-Common Met., 31,* 165-168 (1973).

73Gha: H. Ghassem and A. Raman, *Metall. Trans.,4,* 745-748 (1973).

73Ian: A. Iandelli and A. Palenzona, *Rev. Chim. Miner.,* 303-308 (1973).

73Loe: O. Loebich, Jr. and E. Raub, *J. Less-Common Met., 30,* 47-62 (1973).

73Sav: E. Savitskii, V. Polyakova, and E. Tsyganova, *Redkozemel. Met., Splavy Soedineniya,* Izd. Nauk, Moscow, 182-184 (1973).

73Sve: V.N. Svechnikov, G.F. Kobzenko, and V.G. Ivanchenko, *Dokl. Akad. Nauk SSSR, 213,* 1062-1064 (1973).

74Gsc1: K.A. Gschneidner, Jr. and M.E. Verkade, Document IS-RIC-7, Rare Earth Information Center, Iowa State Univ., Ames, IA, 40-41 (1974).

74Gsc2: K.A. Gschneidner, Jr. and M.E. Verkade, IS-RIC-7, Rare Earth Information Center, Iowa State Univ., Ames, IA, 30-31 (1974).

74Lev: Yu.V. Levinskiy, *Russ. Metall.,* (1), 34-37 (1974).

74Ray1: A.E. Ray, *Cobalt,* (1), 13-20 (1974).

74Ray2: A.E. Ray, *Cobalt,* (1), 3-20 (1974).

74Yar: E.I. Yarambash, E.S. Vigileva, A.A. Eliseev, A.V. Zachatskaya, T.G. Aminov, and M.A. Chernitsyna, *Inorg. Mater., 10*(8), 1212-1215 (1974).

75Ell: G.V. Ellert, V.G. Sevast'yanov, and V.K. Slovyanskikh, *Russ. J. Inorg. Chem., 20*(1), 120-124 (1975).

75Gat: J. Gatterer, D. Dufek, P. Ettmayer, and R. Kieffer, *Monatsh. Chem., 106,* 1137-1147 (1975).

75Lys: Yu.B. Lyskova and A.V. Vakhobov, *Inorg. Mater., 11,* 361-362 (1975).

75Sve: V.N. Svechnikov, G.F. Kobzenko, and V.G. Ivanchenko, *Metallofizika,* (59), 77-83 (1975).

75Vak: A.V. Vakhobov, Z.U. Niyazova, and B.N. Polev, *Inorg. Mater., 11,* 306-307 (1975).

76Ian: A. Iandelli and A. Palenzona, *Rev. Chim. Minerale, 13,* 55-61 (1976).

76Mat: P. Matkovic, M. El-Boragy, and K. Schubert, *J. Less-Common Met., 50,* 165-176 (1976).

76Vol: A.E. Vol and I.K Kagan, *Handbook of Binary Metallic Systems,* Nauka, Moscow (1976) in Russian; TR: NBS/NSF, 760-761 (1985).

77Ere: V.N. Eremenko, V.G. Batalin, Yu.I. Buyanov, and I.M. Obushenko, *Dop. Akad. Nauk Ukr. RSR, B,* (6) 516-521 (1977) in Russian.

77Gar: S.P. Garg and R.J. Ackermann, *J. Nucl. Mater., 64,* 265-274 (1977).

77Kur: T.Kh. Kurbanov, R.A. Dovlyatshina, I.A. Dzhavodova, and F.A. Akhmenov, *Russ J. Inorg. Chem., 22,* 622-624 (1977).

77Kuz: A.N. Kuznetsov, K.A. Chuntonov, and S.P. Yatsenko, *Russ. Metall.,* (5), 178-180 (1977).

77Wat: R.M. Waterstrat and R.C. Manuszewski, *J. Less Common Met.,* 51, 55-67 (1977).

77Yat: S.P. Yatsenko, *J. Chim. Phys., 74,* 836-843 (1977).

78Eli: A.A. Eliseev, G.M. Kuz'micheva, and V.I. Yushrov, *Zh. Neorg. Khim.,23,*(2), 492-296 (1978) in Russian; TR: *Russ J. Inorg. Chem., 23*(2), 273-276 (1978).

78Esh: K.K. Eshnov, M.A. Zukhuritdinov, A.V. Vakhobov, and T.D. Zhurayev, *Russ. Metall.,* (1), 171-173 (1978).

78Lan: C.C. Land, D.E. Peterson, and R.B. Root, *J. Nucl. Mat., 75,* 262-273 (1978).

78Yat: S.P. Yatsenko, B.G. Semenov, and K.A. Chuntonov, *Izv. Akad. Nauk SSSR, Met.,* (5) 222-224 (1978) in Russian; TR: *Russ. Metall.,* (51), 173-174 (1978).

79Bla: R. Blachnik and A. Hoppe, *Z. Anorg. Allg. Chem, 457,* 91-104 (1979) in German.

79Vol: A.E. Vol and I.K. Kagan, *Handbook of Binary Metallic Systems,* Vol. 4, Nauka, Moscow (1979) in Russian; translated by NBS and NSF, 588-605 (1986).

79Yat: S.P. Yatsenko, A.A. Semyannikov, B.G. Semenov, and K.A. Chuntonov, *J. Less-Common Met., 64,* 185-199 (1979).

80Ban: G. Banik, T. Schmitt, P. Ettmayer, and B. Lux, *Z. Metallkd.,71*(10), 644-645 (1980) in German.

80Dav: T.G. Davey and E.H. Baker, *J. Mater. Sci. Lett., 15,* 1601-1602 (1980).

80Ere: V.N. Eremenko, I.M. Obushenko, and Yu.I. Buyanov, *Dop. Akad. Nauk Ukr. RSRA,* (7), 87-91 (1980).

80Lu: X.S. Lu, J.K. Liang, and M.G. Zhou, *Acta Phys. Sin. (China),29,* 469-484 (1980).

80Pal: A. Palenzona, *J. Less-Common Met., 72*(1), P21-P24 (1980).

81Bru: G. Bruzzone, E. Franceschi, and F. Merlo, *J. Less-Common Met., 81,* 155-160 (1981).

81Bus: V.D. Busmanov and S.P. Yatsenko, *Russ. Metall.,* (5), 157-160 (1981).

81Ian: A. Iandelli and A. Palenzona, *J. Less-Common Met.,80,* P71-P82 (1981).

81Loe: O. Loebich, Jr. and C.J. Raub, *Platinum Met. Rev., 25*(3), 113-120 (1981).

81Mor: G. Morgaut, B. Legendre, S. Mareglier-Lacordaire, and C. Souleau, *Ann. Chim. Fr., 6,* 315-326 (1981).

81Wat: R.M. Waterstrat, *J. Less-Common Met., 80,* P31-P36 (1981).

82Bor: G. Borzone, A. Borsese, and R. Ferro, *J. Less-Common Met., 85,* 195-203 (1982).

82Pri: N.Yu. Pribyl'skii, I.G. Vasileva, and R.S. Gamidov, *Mater. Res. Bull., 17,* 1147-1153 (1982).

82Sub: P.R. Subramanian and J.F. Smith, *J. Less-Common Met., 87,* 205-213 (1982).

83Ere: V.N. Eremenko, K.A. Meleshevich, and Yu.I. Buyanov, *Dop. Akad. Nauk Ukr. RSRA,* (3), 83-88 (1983).

83Kub: O. Kubaschewski-Von Goldbeck, *Titanium: Physicochemical Properties of Its Compounds and Alloys,* Atomic Energy Review; Spec. Issue No. 9, O. Kubaschewski, Ed., IAEA, Vienna, 156 (1983).

84Pas: J.D.A. Paschoal, H. Kleykamp, and F. Thummler, *J. Less-Common Met., 98,* 279-284 (1984).

85Mur: J.L. Murray, *Int. Met. Rev., 30*(5), 211-233, 1985.

86Bar1: O.M. Barabash and Yu.N. Koval, *Crystal Structure of Metals and Alloys,* Naukova Dumka, Kiev, 211-212 (1986).

86Bar2: O.M. Barabash and Yu. N. Koval, *Crystal Structure of Metals and Alloys,* Naukova Dumka, Kiev, 247-248 (1986).

86Bar3: O.M. Barabash and Yu.N. Koval, *Crystal Structure of Metals and Alloys,* Naukova Dumka, Kiev, 296-297 (1986) in Russian.

87Gor: O.V. Gordiichuk, Author's Abstract of Candidate's Thesis, Chemical Sciences, Kiev (1987).

87Mel: L.Z. Melenkov, S.P. Yatsenko, K.A. Chuntonov, and Yu. N. Grin, *Izv. Akad. Nauk SSSR, Met.,* (2), 201-203 (1987) in Russian; TR: *Russ. Metall.,* (2), 2 08-211 (1987).

88Sac: A. Saccone, S. Delfino, and R. Ferro, *J. Less-Common Met., 143,* 1-23 (1988).

90Con: J.B. Condon, T. Schober, and R. Lasser, *J. Nucl. Mater., 170,* 24-30 (1990).

90Sac: A. Saccone, S. Delfino, and R. Ferro, *Calphad, 14*(2), 161 (1990).

Ag-Al

A.J. McAlister, 1987

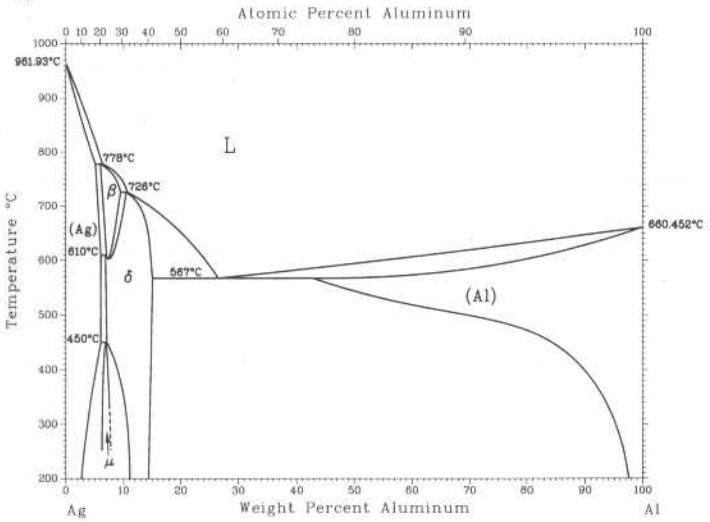

Phase	Composition, wt% Al	Pearson symbol	Space group
(Ag)	0.0	*cF*4	$Fm\bar{3}m$
β	6.1 to 7.4	*cI*2	$Im\bar{3}m$
δ	6.9 to 15.3	*hP*2	$P6_3/mmc$
μ	~6.2 to 7.3	*cP*20	$P4_132$
			$P2_13$(a)
(Al)	100	*cF*4	$Fm\bar{3}m$

(a) ~300 °C

Ag-As

M.R. Baren, 1990

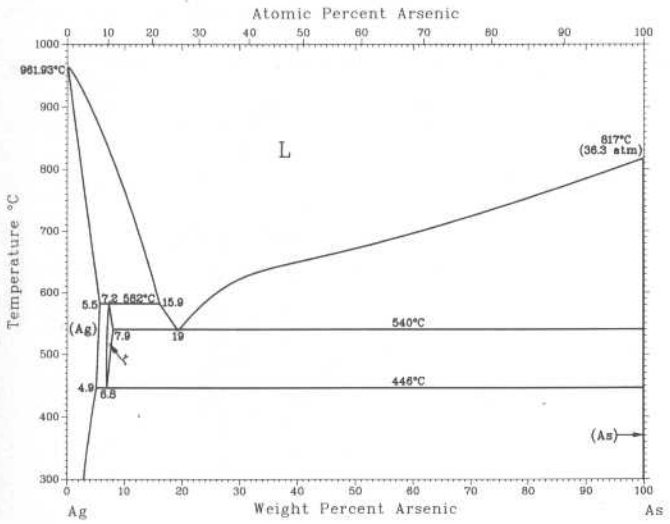

Phase	Composition, wt% As	Pearson symbol	Space group
(Ag)	0 to 5.5	*cF*4	$Fm\bar{3}m$
ζ	6.8 to 7.9	*hP*2	$P6_3/mmc$
(As)	100	*hR*2	$R\bar{3}m$

Ag-Au

H. Okamoto and T.B. Massalski, 1987

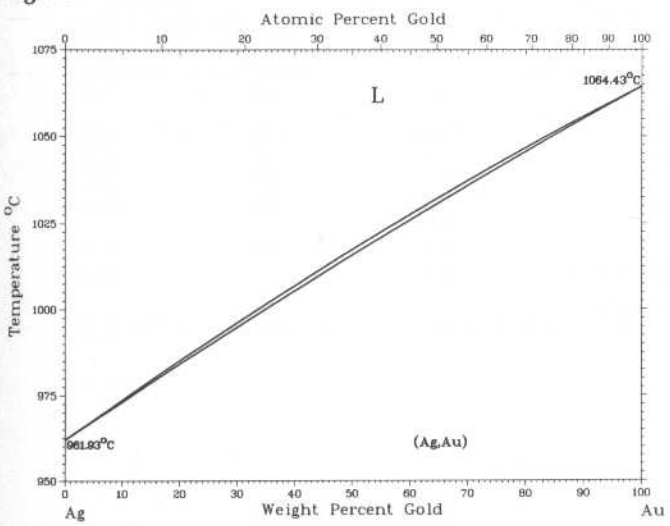

Phase	Composition, wt% Au	Pearson symbol	Space group
(Ag,Au)	0 to 100	*cF*4	$Fm\bar{3}m$

Ag-Be

H. Okamoto and L.E. Tanner, 1987

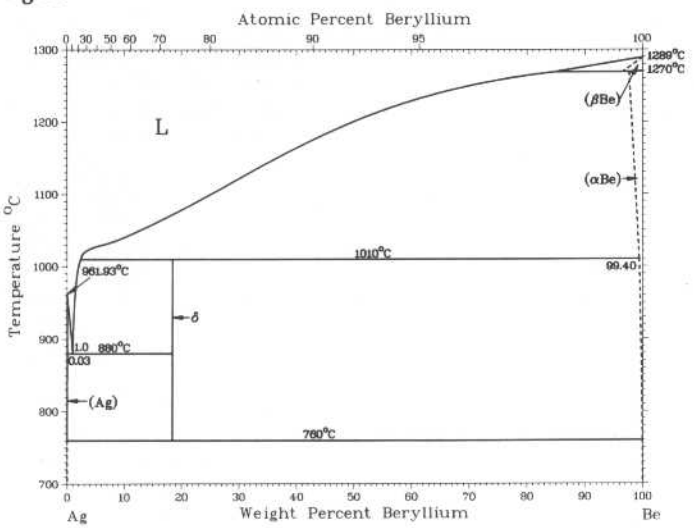

Phase	Composition, wt% Be	Pearson symbol	Space group
(Ag)	0 to 0.03	*cF*4	$Fm\bar{3}m$
δ or $AgBe_2$	~18?	*cF*24	$Fd\bar{3}m$
(αBe)	99.40 to 100	*hP*2	$P6_3/mmc$
(βBe)	100	*cI*2	$Im\bar{3}m$
Questionable phases (stable? metastable?)			
γ	~12	?	?
$AgBe_{12}$	50	*tI*26	*I*4/*mmm*

Ag-Bi

R.P. Elliott and F.A. Shunk, 1980

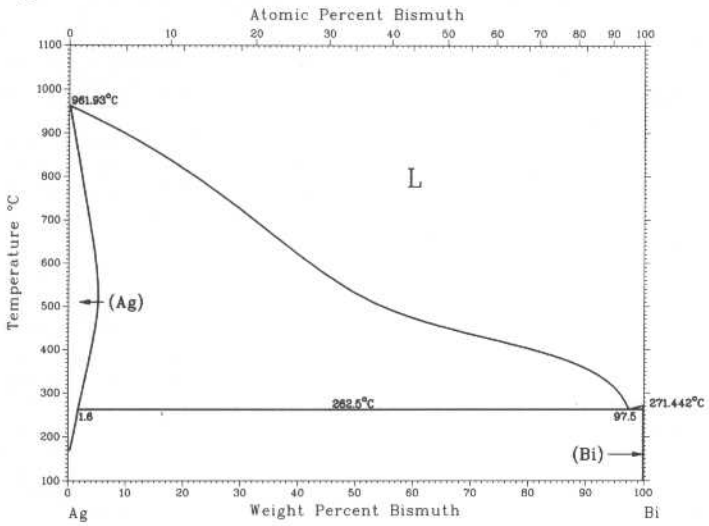

Phase	Composition, wt% Bi	Pearson symbol	Space group
(Ag)	0 to 4.945	*cF*4	$Fm\bar{3}m$
(Bi)	~100	*hR*2	$R\bar{3}m$

Ag-Ca

M.R. Baren, 1988

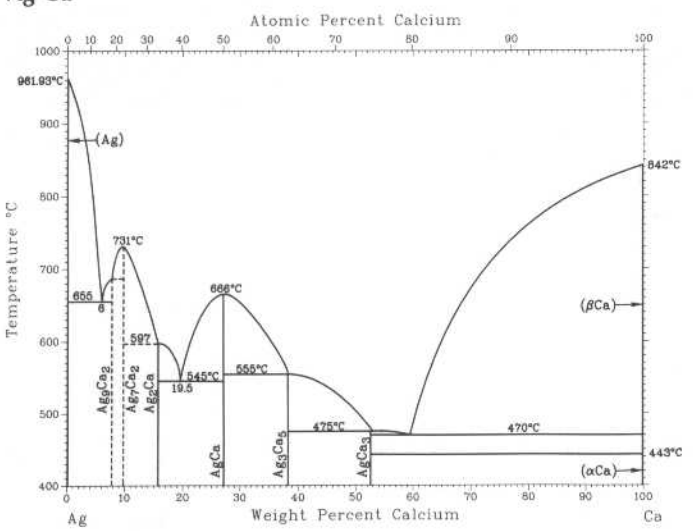

Phase	Composition, wt% Ca	Pearson symbol	Space group
(Ag)	0	*cF*4	$Fm\bar{3}m$
Ag_9Ca_2	7.7	...	...
Ag_7Ca_2	9.6	*hP*18	$P6_322$
Ag_2Ca	15.6	*oI*12	*Imma*
AgCa	27.1	*oC*8	*Cmcm*
Ag_3Ca_5	38.2	*tI*32	*I*4/*mcm*
$AgCa_3$	52.7	...	...
(αCa)	100	*cF*4	$Fm\bar{3}m$
(βCa)(a)	100	*cI*2	$Im\bar{3}m$

(a) Above 443 °C

Ag-Cd

From [Hansen]

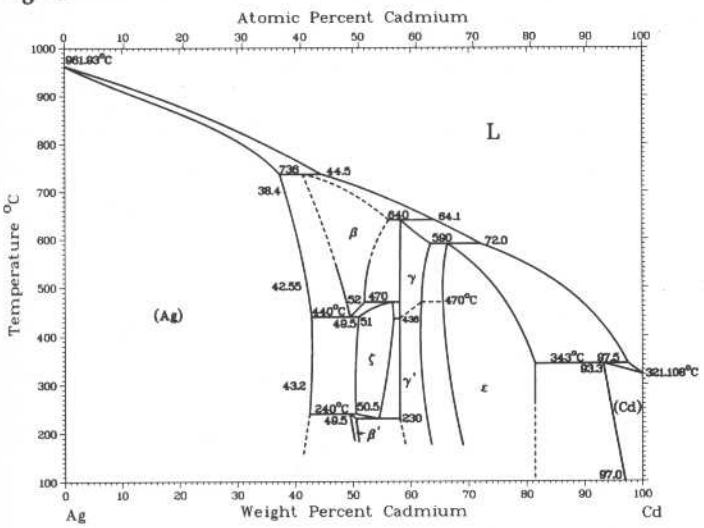

Phase	Composition, wt% Cd	Pearson symbol	Space group
(Ag)	0 to 43.2	*cF*4	$Fm\bar{3}m$
β	41 to 56	*cI*2	$Im\bar{3}m$
β′	49.5 to 51.0	(a)	...
ζ	50.5 to 57	(b)	...
γ′	58 to 63.5	...	...
γ	58 to 63.5	*cI*52	$I\bar{4}3m$
ε	65.4 to 82	*hP*2	$P6_3/mmc$
(Cd)	93.3 to 100	*hP*2	$P6_3/mmc$

(a) Ordered bcc. (b) cph

Ag-Ce

K.A. Gschneidner, Jr. and F.W. Calderwood, 1985

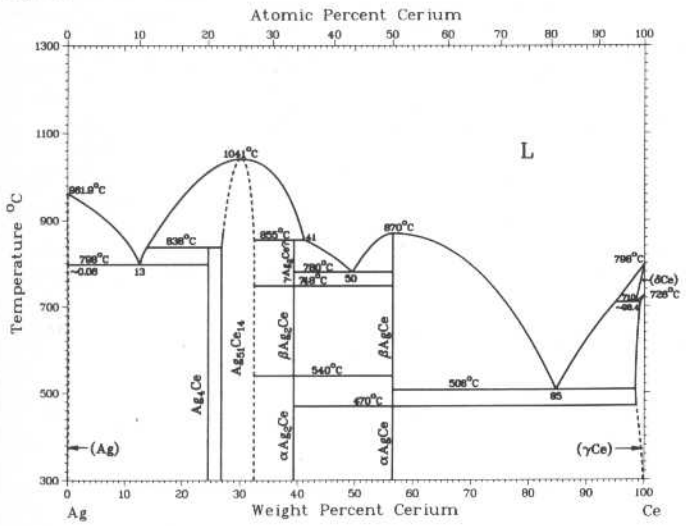

Phase	Composition, wt% Ce	Pearson symbol	Space group
(Ag)	0 to ~0.06	*cF*4	$Fm\bar{3}m$
$Ag_{51}Ce_{14}$	26.2 to ~30	*hP*65	*P*6/*m*
αAg_2Ce	39.3	*oI*12	*Imma*
AgCe	56.5	*cP*2	$Pm\bar{3}m$
(δCe)	~98 to 100	*cI*2	$Im\bar{3}m$
(γCe)	~98 to 100	*cF*4	$Fm\bar{3}m$
(βCe)	100	*hP*4	$P6_3/mmc$
(αCe)	100	*cF*4	$Fm\bar{3}m$

Ag-Co

I. Karakaya and W.T. Thompson, 1986

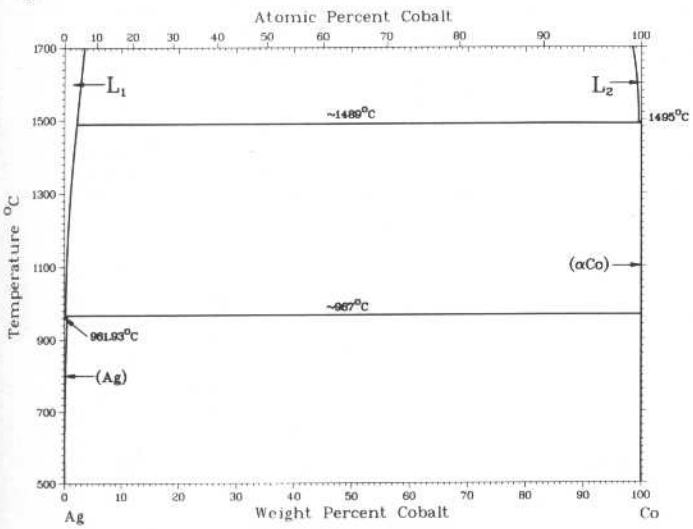

Phase	Composition, wt% Co	Pearson symbol	Space group
(Ag)	0 to 0.44	*cF*4	$Fm\bar{3}m$
(εCo)(a)	100	*hP*2	$P6_3/mmc$
(αCo)	~100	*cF*4	$Fm\bar{3}m$

(a) Below 422 °C

Ag-Cu

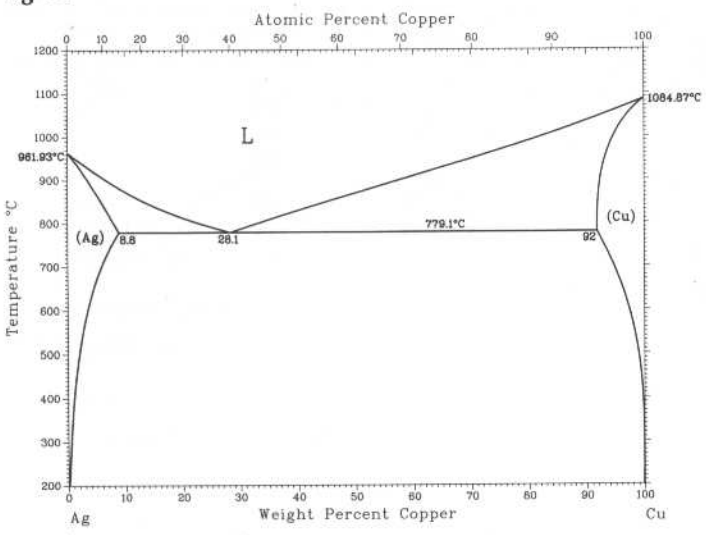

P.R. Subramanian and J.H. Perepezko, unpublished

Phase	Composition, wt% Cu	Pearson symbol	Space group
(Ag)	0 to 8.8	*cF*4	$Fm\bar{3}m$
(Cu)	92.0 to 100	*cF*4	$Fm\bar{3}m$

Ag-Dy

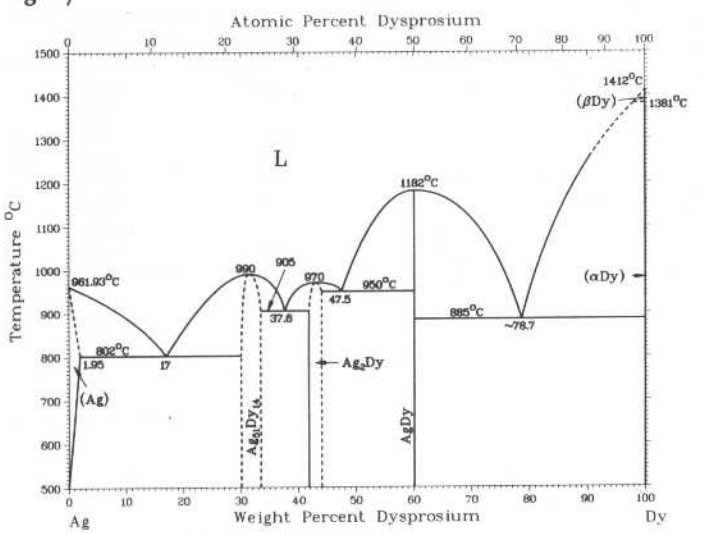

K.A. Gschneidner, Jr. and F.W. Calderwood, 1985

Phase	Composition, wt% Dy	Pearson symbol	Space group
(Ag)	0 to 1.95	*cF*4	$Fm\bar{3}m$
$Ag_{51}Dy_{14}$	29.2 to 34.0	*hP*65	...
Ag_2Dy	41.8 to 44.0	*tI*6	*I*4/*mmm*
AgDy	60.1	*cP*2	$Pm\bar{3}m$
(βDy)	100	*cI*2	$Im\bar{3}m$
(αDy)	100	*hP*2	$P6_3/mmc$
(α′Dy)(a)	100	...	...

(a) Below −187 °C

Ag-Er

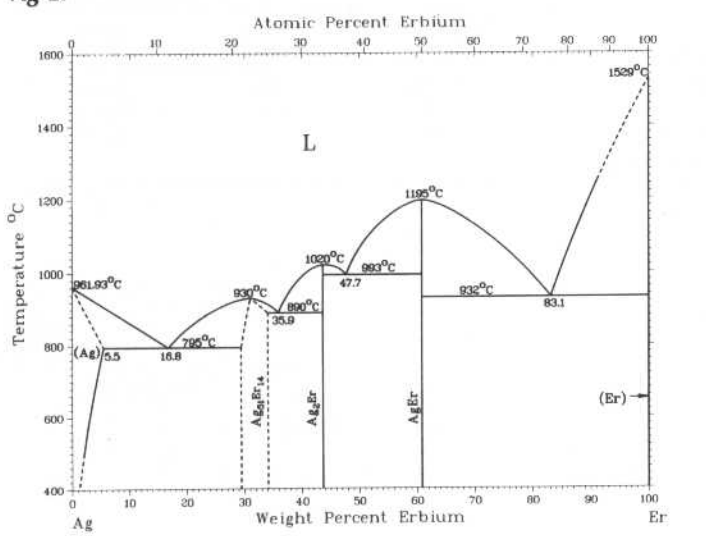

K.A. Gschneidner, Jr. and F.W. Calderwood, 1985

Phase	Composition, wt% Er	Pearson symbol	Space group
(Ag)	0 to 5.5	*cF*4	$Fm\bar{3}m$
$Ag_{51}Er_{14}$	29.8 to 34.7	*hP*65	...
Ag_2Er	43.6	*tI*6	*I*4/*mmm*
AgEr	60.8	*cP*2	$Pm\bar{3}m$
(Er)	100	*hP*2	$P6_3/mmc$

Ag-Eu

K.A. Gschneidner, Jr. and F.W. Calderwood, 1985

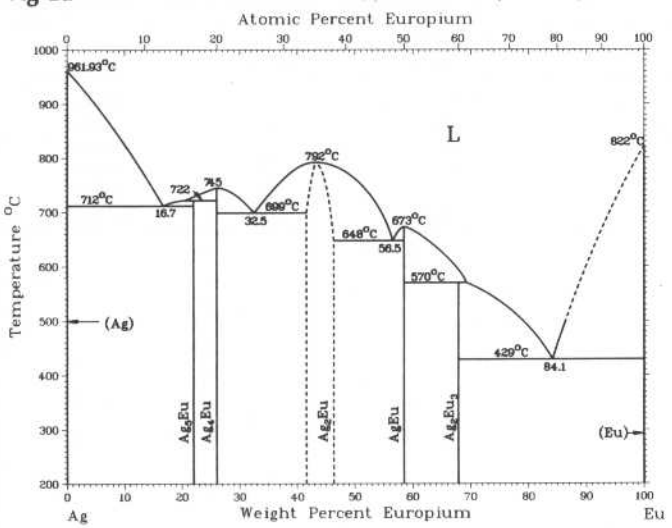

Phase	Composition, wt% Eu	Pearson symbol	Space group
(Ag)	0	*cF*4	$Fm\bar{3}m$
Ag_5Eu	22.0	*hP*6	*P*6/*mmm*
Ag_4Eu	26	*tI*10	*I*4/*m*
Ag_2Eu	41.3	*oI*12	*Imma*
AgEu	58.5	*oP*8	*Pnma*
Ag_2Eu_3	67.9	*tP*10	*P*4/*mbm*
(Eu)	100	*cI*2	$Im\bar{3}m$

Ag-Fe

L.J. Swartzendruber, 1984

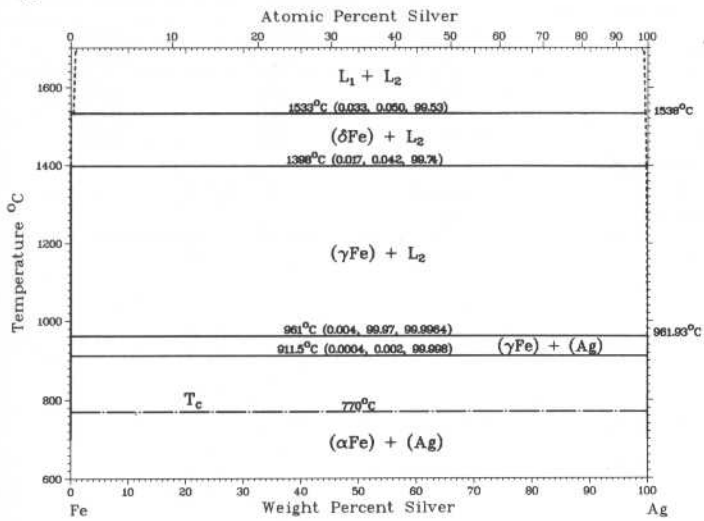

Phase	Composition, wt% Ag	Pearson symbol	Space group
δ or (δFe)	0 to 0.033	*cI*2	$Im\bar{3}m$
γ or (γFe)	0 to 0.042	*cF*4	$Fm\bar{3}m$
α or (αFe)	0 to 0.0004	*cI*2	$Im\bar{3}m$
(Ag)	99.99663 to 100	*cF*4	$Fm\bar{3}m$

Ag-Ga

H. Okamoto, 1992

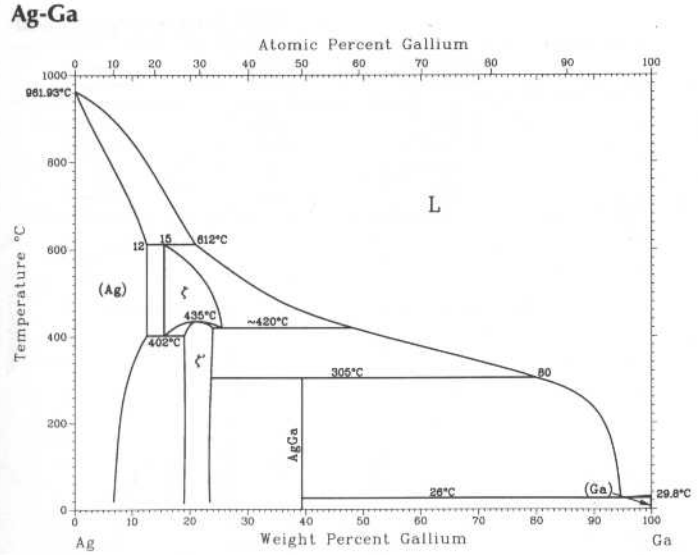

Phase	Composition, wt% Ga	Pearson symbol	Space group
(Ag)	0 to 12	*cF*4	$Fm\bar{3}m$
ζ	15 to 25	*hP*2	$P6_3/mmc$
ζ′	18 to 24	*hP*9	$P\bar{3}$
AgGa	39.2	*cI*2	$Im\bar{3}m$
(Ga)	100	*oC*8	*Cmca*

Ag-Gd

K.A. Gschneidner, Jr. and F.W. Calderwood, 1985

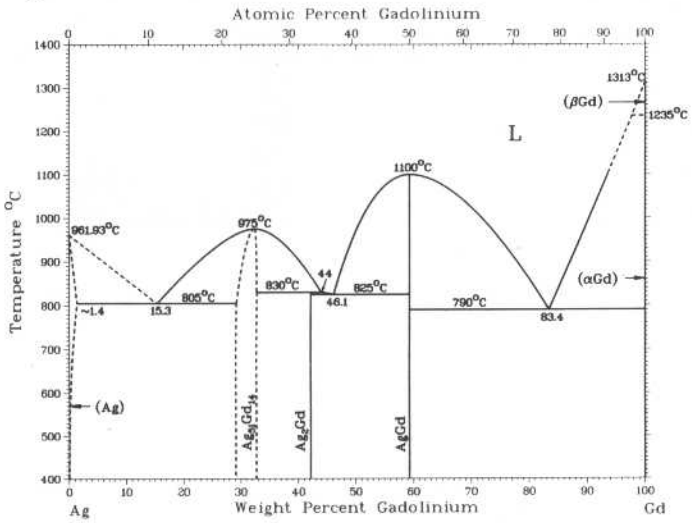

Phase	Composition, wt% Gd	Pearson symbol	Space group
(Ag)	0 to ~1.4	*cF*4	$Fm\bar{3}m$
$Ag_{51}Gd_{14}$	28.5	*tP*65	*P*6/*m*
Ag_2Gd	42.1	*tI*6	*I*4/*mmm*
AgGd	59.3	*cP*2	$Pm\bar{3}m$
(βGd)	100	*cI*2	$Im\bar{3}m$
(αGd)	100	*hP*2	$P6_3/mmc$

Ag-Ge

R.W. Olesinski and G.J. Abbaschian, 1988

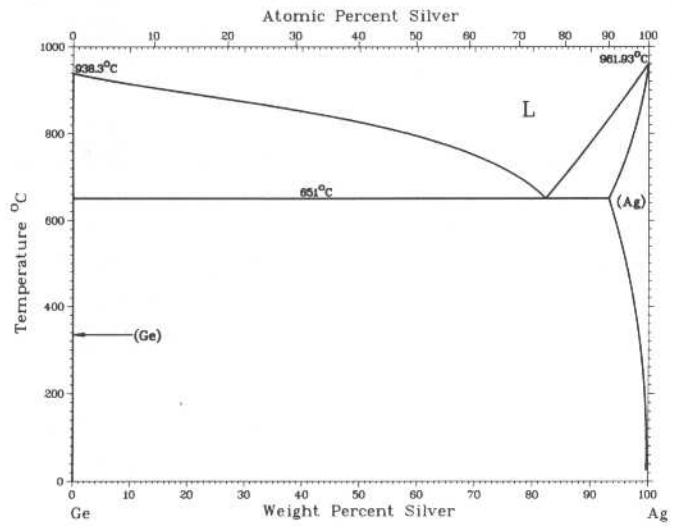

Phase	Composition, wt% Ag	Pearson symbol	Space group
(Ge)	~0	*cF*8	$Fd\bar{3}m$
GeII (HP)	0	*tI*4	$I4_1/amd$
(Ag)	93.3 to 100	*cF*4	$Fm\bar{3}m$
Metastable phases			
β (cph)	83 to 86	*hP**	...
Tetragonal	85	*t***	...

Ag-Hg

M.R. Baren, unpublished

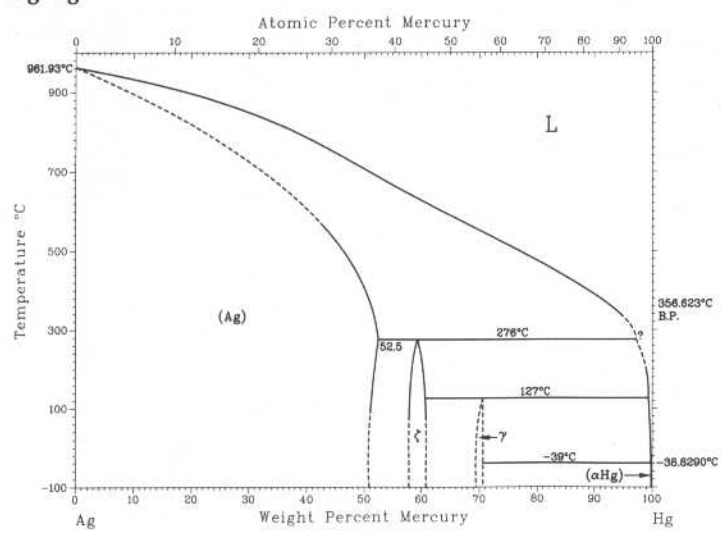

Phase	Composition, wt% Hg	Pearson symbol	Space group
(Ag)	0 to 52.5	*cF*4	$Fm\bar{3}m$
ζ	58.9 to 61.3	*hP*2	$P6_3/mmc$
γ	70.0 to 71.0	*cI**	*I*23
(αHg)	100	*hR*1	$R\bar{3}m$

Ag-Ho

K.A. Gschneidner, Jr. and F.W. Calderwood, 1985

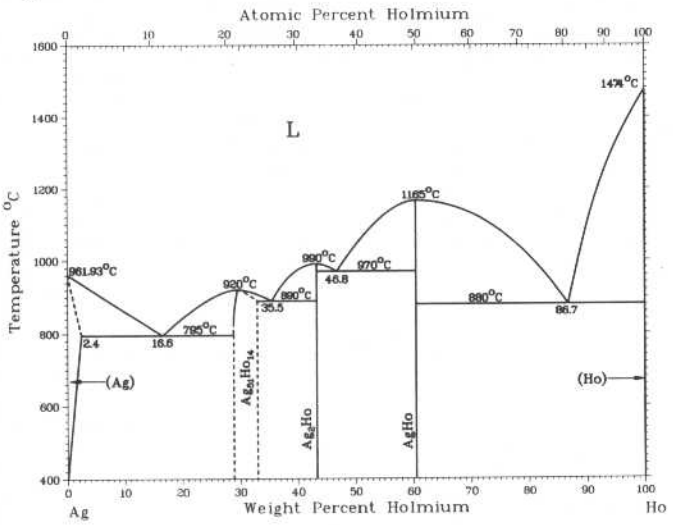

Phase	Composition, wt% Ho	Pearson symbol	Space group
(Ag)	0 to 2.4	*cF*4	$Fm\bar{3}m$
$Ag_{51}Ho_{14}$	29.5	*hP*65	*P*6/*m*
Ag_2Ho	43.3	*tI*6	*I*4/*mmm*
AgHo	60.5	*cP*2	$Pm\bar{3}m$
(Ho)	100	*hP*2	$P6_3/mmc$

Ag-In

M.R. Baren, 1992

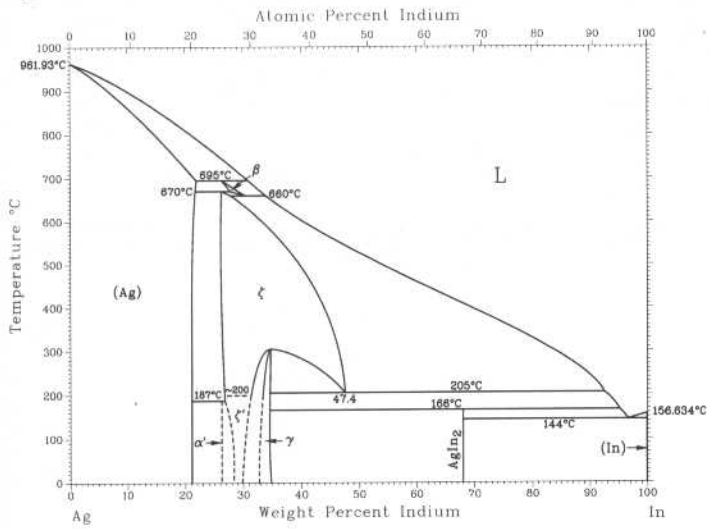

Phase	Composition, wt% In	Pearson symbol	Space group
α(Ag)	0 to 22.1	*cF*4	$Fm\bar{3}m$
β	26.2 to 31.3	*cI*2	$Im\bar{3}m$
α′(Ag_3In)	26	*cP*4?	$Pm\bar{3}m$?
ζ	26.2 to 47.6	*hP**	...
ζ′	?	*hP*8	$P6_3/mmc$
γ(Ag_2In)	32.5 to 35.0	*cP*52	$P\bar{4}3m$
φ($AgIn_2$)	68.1	*tI*12	*I*4/*mcm*
(In)	100	*tI*2	*I*4/*mmm*
Metastable phases			
...	19.4	*hP*2	$P6_3/mmc$
...	71 to 81	*cF*4	$Fm\bar{3}m$

Ag-La

K.A. Gschneidner, Jr. and F.W. Calderwood, 1983

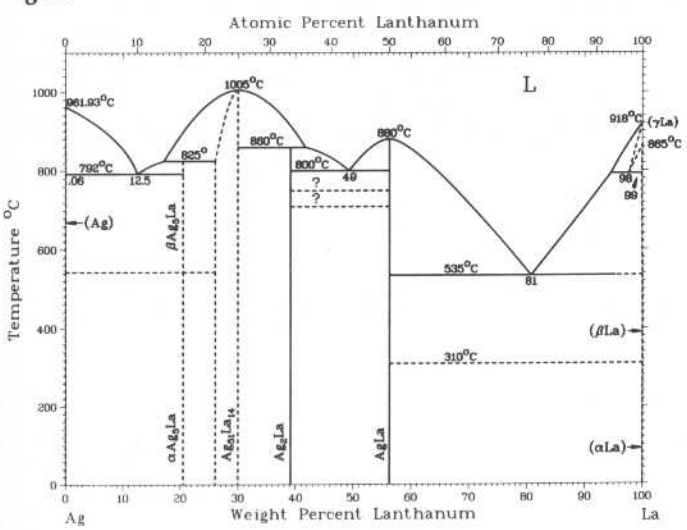

Phase	Composition, wt% La	Pearson symbol	Space group
(Ag)	0	*cF*4	$Fm\bar{3}m$
Ag_5La	20.5	*hP*?	...
$Ag_{51}La_{14}$	26.1	*hP*65	...
Ag_2La	39.1	*oI*12	*Imma*
AgLa	56.3	*cP*2	$Pm\bar{3}m$
(γLa)	100	*cI*2	$Im\bar{3}m$
(βLa)	100	*cF*4	$Fm\bar{3}m$
(αLa)	100	*hP*4	$P6_3/mmc$

Ag-Li

A.D. Pelton, 1986

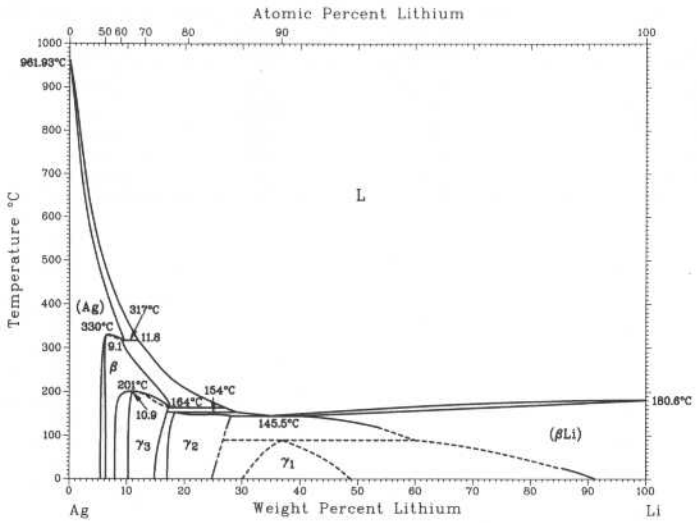

Phase	Composition, wt% Li	Pearson symbol	Space group
(Ag)	0 to 9.1	*cF*4	$Fm\bar{3}m$
β	6.1 to 18	*cP*2	$Pm\bar{3}m$
γ_3	10.9 to 17	Cubic (*cP*52?)	$P\bar{4}3m$?
γ_2	17 to 28	Cubic (*cI*52?)	$I\bar{4}3m$?
γ_1	32 to 43	Cubic	...
(βLi)	39 to 100	*cI*2	$Im\bar{3}m$
(αLi)	100	*hP*2	$P6_3/mmc$

Ag-Mg

A.A. Nayeb-Hashemi and J.B. Clark, 1988, with modifications

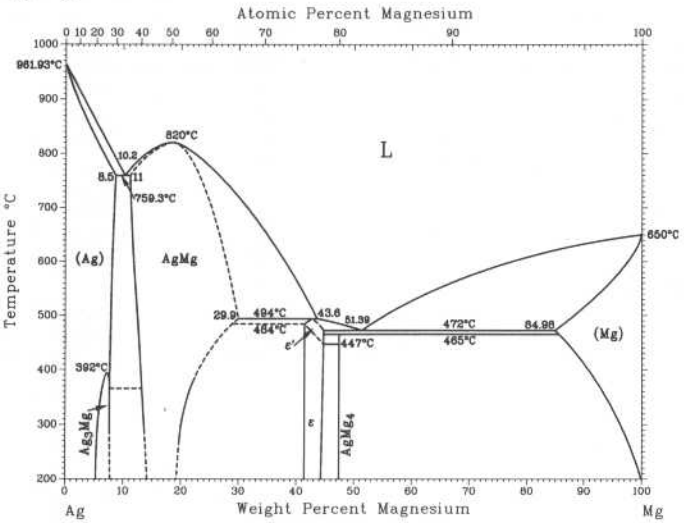

Phase	Composition, wt% Mg	Pearson symbol	Space group
(Ag) or α	0 to 8.5	*cF*4	$Fm\bar{3}m$
Ag_3Mg ord or α′	7	*cP*4	$Pm\bar{3}m$
AgMg or β′	11 to 29.9	*cP*2	$Pm\bar{3}m$
ε′	41.4 to 44.7	*tI**	...
ε	41.4 to 44.7	*cF**	...
$AgMg_4$	47	*hP**	...
(Mg) or δ	84.98 to 100	*hP*2	$P6_3/mmc$

The two-phase region between (Ag) and Ag_3Mg (ordered) is not shown here.

Ag-Mo

M.R. Baren, 1990

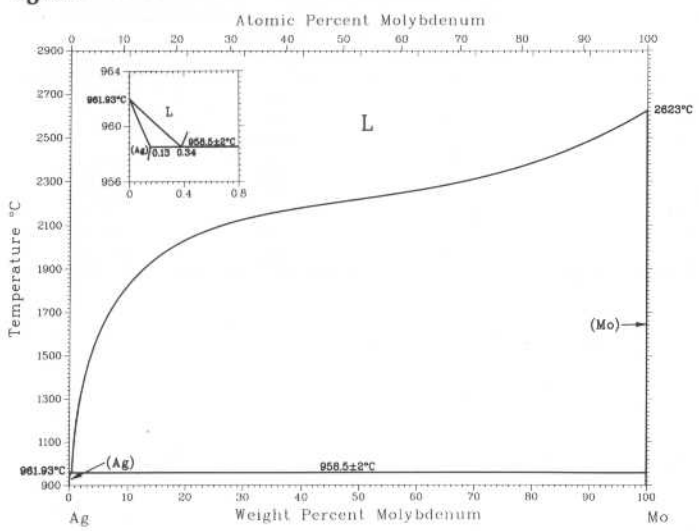

Phase	Composition, wt% Mo	Pearson symbol	Space group
(Ag)	0 to 0.13	*cF*4	$Fm\bar{3}m$
(Mo)	100	*cI*2	$Im\bar{3}m$

Ag-Na

A.D. Pelton, 1986

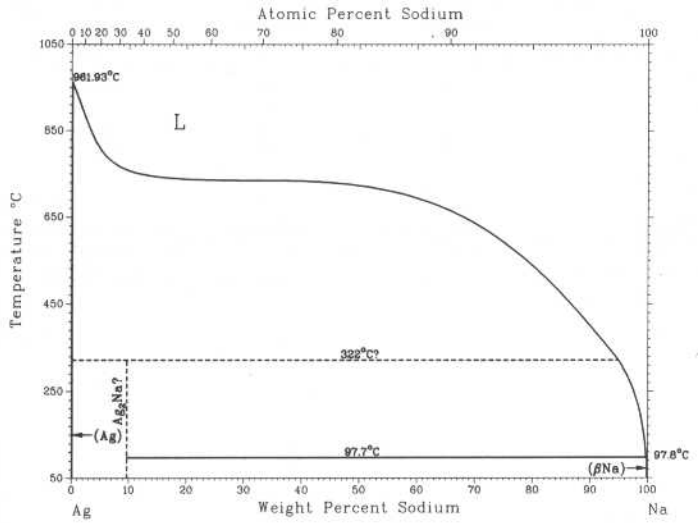

Phase	Composition, wt % Na	Pearson symbol	Space group
(Ag)	0	*cF*4	$Fm\bar{3}m$
Ag_2Na	9.6	*cF*24	$Fd\bar{3}m$
(βNa)	100	*cI*2	$Im\bar{3}m$

Ag-Nd

K.A. Gschneidner , Jr. and F.W. Calderwood, 1985

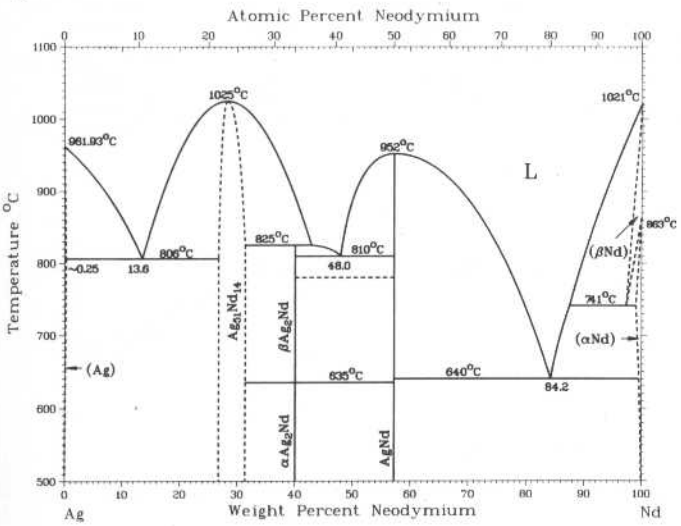

Phase	Composition, wt % Nd	Pearson symbol	Space group
(Ag)	0 to ~5	*cF*4	$Fm\bar{3}m$
$Ag_{51}Nd_{14}$	26.8 to 31.4	*hP*65	...
βAg_2Nd	40.0	*hP*?	...
αAg_2Nd	40.0	*oI*12	*Imma*
AgNd	57.2	*cP*2	$Pm\bar{3}m$
(βNd)	97.4 to 100	*cI*2	$Im\bar{3}m$
(αNd)	99.0 to 100	*hP*4	$P6_3/mmc$

Ag-Ni

M. Singleton and P. Nash, 1991

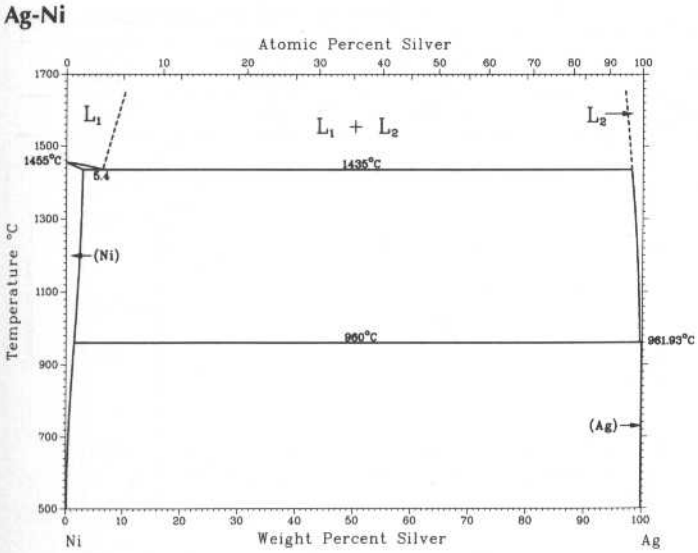

Phase	Composition, wt % Ag	Pearson symbol	Space group
(Ni)	0 to 1.8	*cF*4	$Fm\bar{3}m$
(Ag)	99.3 to 100	*cF*4	$Fm\bar{3}m$

Ag-P

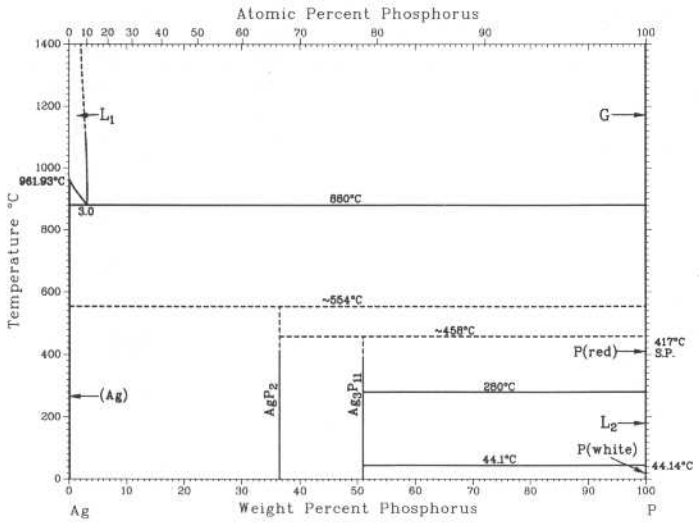

I. Karakaya and W.T. Thompson, 1988

Phase	Composition, wt% P	Pearson symbol	Space group
(Ag)	0	*cF*4	$Fm\bar{3}m$
AgP_2	36.5	(a)	...
Ag_3P_{11}	51.0	(b)	*Cm*
P(black)	100	*oC*8(c)	*Cmca*
P(white)	100	(d)	...
P(red)	100	(e)	...

(a) Monoclinic structure with β = 113.48°. (b) Monoclinic structure with β = 118.84°. (c) At high pressures black P transforms to a rhombohedral structure. (d) Cubic below –35 °C. (e) Cubic with 66 atoms per unit cell

Ag-Pb

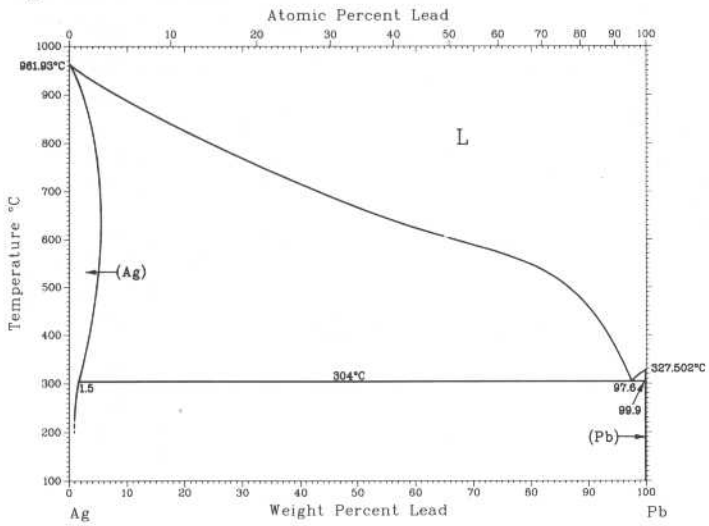

I. Karakaya and W.T. Thompson, 1987

Phase	Composition, wt% Pb	Pearson symbol	Space group
(Ag)	0 to 5.2	*cF*4	$Fm\bar{3}m$
(Pb)	99.9 to 100	*cF*4	$Fm\bar{3}m$

Ag-Pd

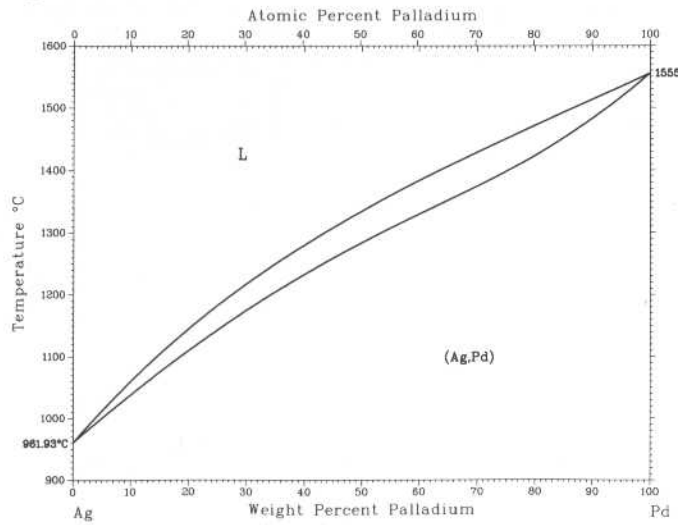

I. Karakaya and W.T. Thompson, 1988

Phase	Composition, wt% Pd	Pearson symbol	Space group
(Ag,Pd)	0 to 100	*cF*4	$Fm\bar{3}m$

Ag-Pr

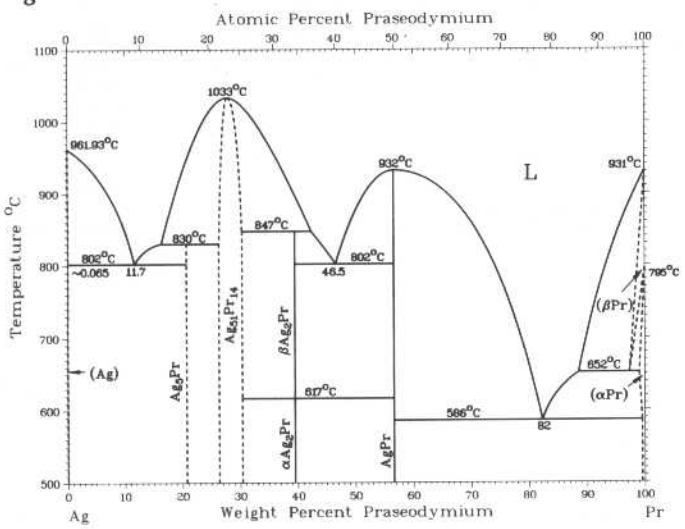

K.A. Gschneidner, Jr. and F.W. Calderwood, 1985

Phase	Composition, wt% Pr	Pearson symbol	Space group
(Ag)	0 to ~0.065	*cF*4	$Fm\bar{3}m$
Ag_5Pr	20.8	...	...
$Ag_{51}Pr_{14}$	26.4 to 30.3	*hP*65	...
βAg_2Pr	39.5	*hP*?	...
αAg_2Pr	39.5	*oI*12	*Imma*
AgPr	56.6	*cP*2	$Pm\bar{3}m$
(βPr)	97.3 to 100	*cI*2	$Im\bar{3}m$
(αPr)	99.0 to 100	*hP*4	$P6_3/mmc$

Ag-Pt

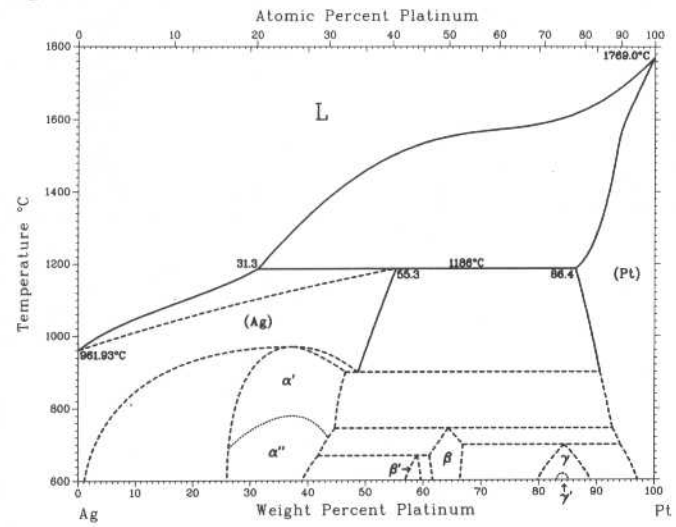

I. Karakaya and W.T. Thompson, 1987

Phase	Composition(a), wt% Pt	Pearson symbol	Space group
(Ag)	0 to 55.3	*cF*4	$Fm\bar{3}m$
(Pt)	86.4 to 100	*cF*4	$Fm\bar{3}m$
α′	26 to 47	*cF*4	$Fm\bar{3}m$
α″	26 to 43	*cP*4	$Pm\bar{3}m$
β(b)	61 to 67	...	...
β′(b)	57 to 60	...	...
γ	80 to 89	*cP*4	$Pm\bar{3}m$
γ′	83 to 85	*cF**	...

Note: α′, α″, β, β′, γ, and γ′ phases are questionable. (a) Rough composition from phase diagram. (b) Rhombohedrally distorted cubic structure

Ag-S

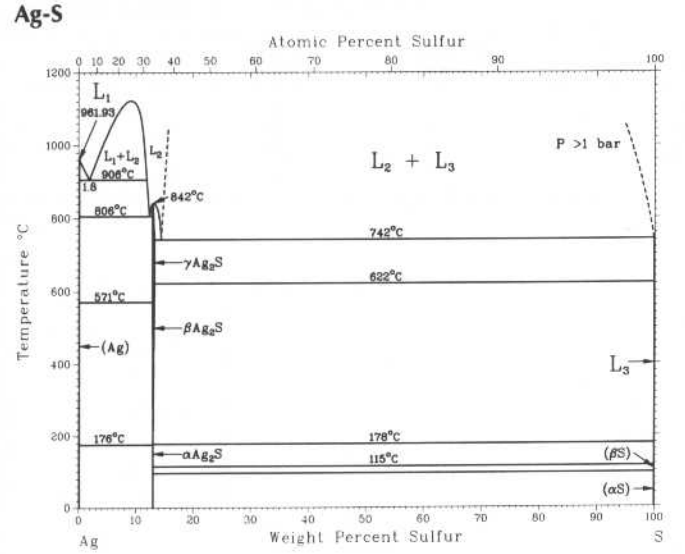

R.C. Sharma and Y.A. Chang, 1986

Phase	Composition, wt% S	Pearson symbol	Space group
(Ag)	0.04	*cF*4	$Fm\bar{3}m$
αAg_2S	12.9	*mP*24	$P2_1/c$
αAg_2S (acanthite)	12.9	*mP*12	$P2_1/n$
$\beta Ag_{2+\delta}S$	12.9	*cI*6	...
$\gamma Ag_{2+\delta}S$	12.9	*cF*12	...
δAg_2S(a)	12.9	*t***	...
(αS)	~100	*oF*128	*Fddd*
(βS)	~100	*mP**	$P2_1/c$

(a) High-pressure phase

Ag-Sb

From [Hansen]

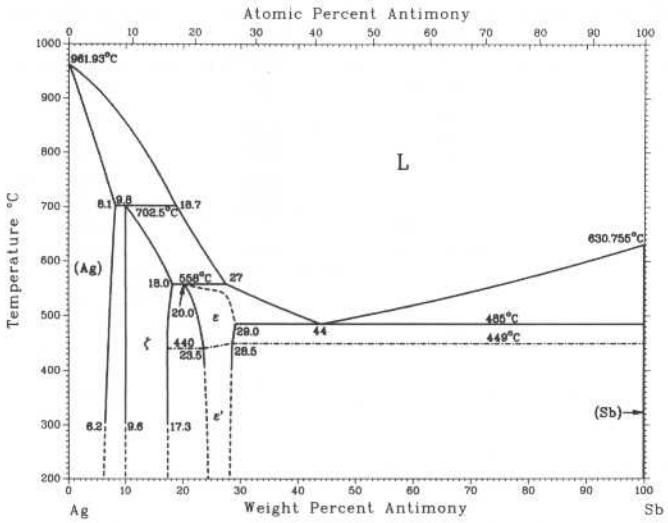

Phase	Composition, wt% Sb	Pearson symbol	Space group
(Ag)	0 to 8.1	*cF*4	$Fm\bar{3}m$
ζ	9.6 to 18.0	*hP*2	$P6_3/mmc$
ε	20.0 to 29.0	*tP*4	*P*4/*mmm*
ε′	23.5 to 28.5	(a)	...
(Sb)	100	*hR*2	$R\bar{3}m$

(a) Ordered orthorhombic, $L6_0$ related

Ag-Sc

K.A. Gschneidner, Jr. and F.W. Calderwood, 1983

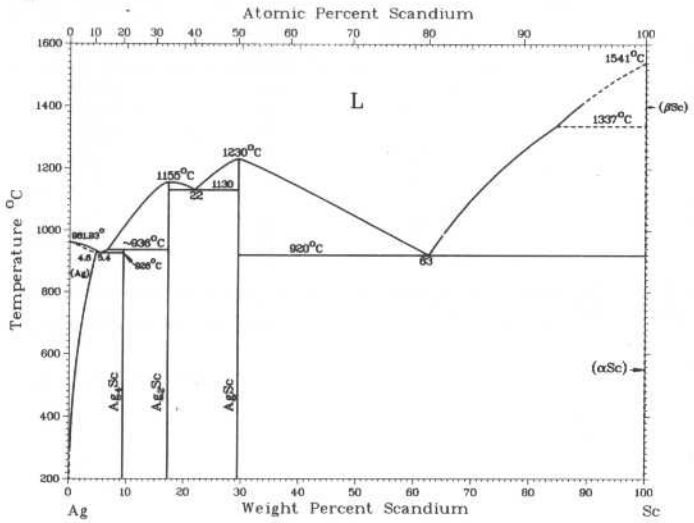

Phase	Composition, wt% Sc	Pearson symbol	Space group
(Ag)	0 to 4.6	*cF*4	$Fm\bar{3}m$
Ag_4Sc	9	*tI*10	*I*4/*m*
Ag_2Sc	17.2	*tI*6	*I*4/*mmm*
AgSc	29.4	*cP*2	$Pm\bar{3}m$
(βSc)	100	*cI*2	$Im\bar{3}m$
(αSc)	100	*hP*2	$P6_3/mmc$

Ag-Se

I. Karakaya and W.T. Thompson, 1990

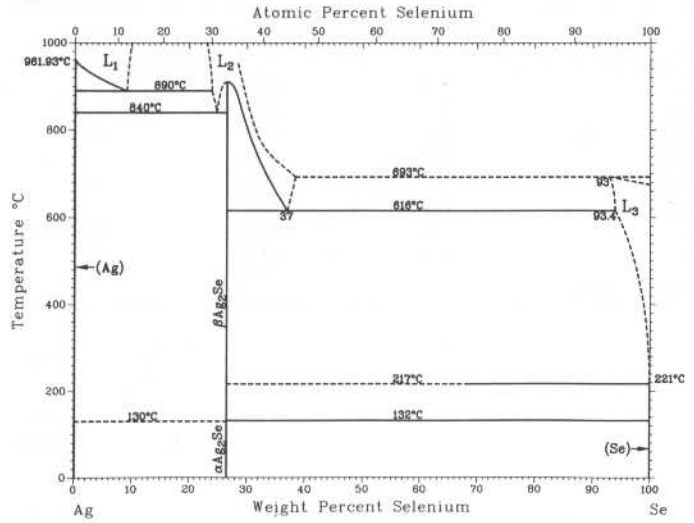

Phase	Composition, wt% Se	Pearson symbol	Space group
(Ag)	0	*cF*4	$Fm\bar{3}m$
βAg_2Se	26.8	*cI**	...
αAg_2Se	26.8	*o***	...
(Se)	100	*hP*3	$P3_121$

Ag-Si

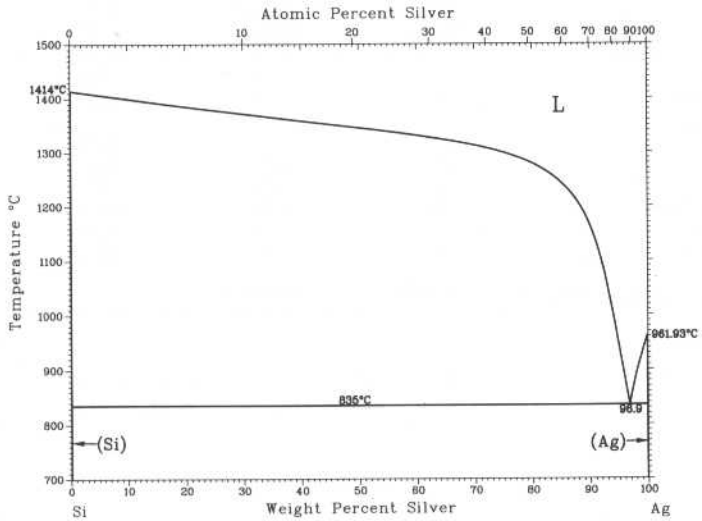

R.W. Olesinski and G.J. Abbaschian, 1989

Phase	Composition, wt% Ag	Pearson symbol	Space group
(Si)	0	*cF*8	$Fd\bar{3}m$
SiII(HP)	0	*tI*4	$I4_1/amd$
(Ag)	100	*cF*4	$Fm\bar{3}m$
Metastable phases			
$SiAg_2$	~90	(a)	...
β	92 to 99	(b)	...

(a) Orthorhombic. (b) cph

Ag-Sm

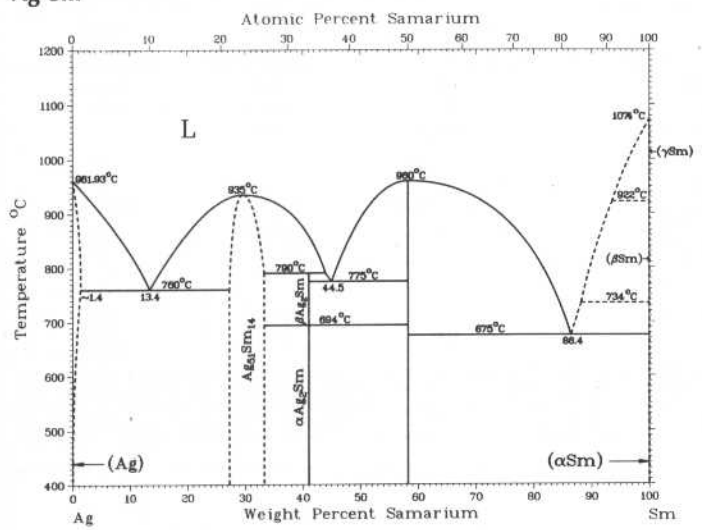

K.A. Gschneidner, Jr. and F.W. Calderwood, 1985

Phase	Composition, wt% Sm	Pearson symbol	Space group
(Ag)	0 to ~1.4	*cF*4	$Fm\bar{3}m$
$Ag_{51}Sm_{14}$	~27.6 to 32.3	*hP*65	*P*6/*m*
βAg_2Sm	41.0	*hP*?	$P6_3(?)$
αAg_2Sm	41.0	...	...
AgSm	58.2	*cP*2	$Pm\bar{3}m$
(γSm)	100	...	...
(βSm)	100	*hP*2	$P6_3/mmc$
(αSm)	100	*hR*3	$R\bar{3}m$

Ag-Sn

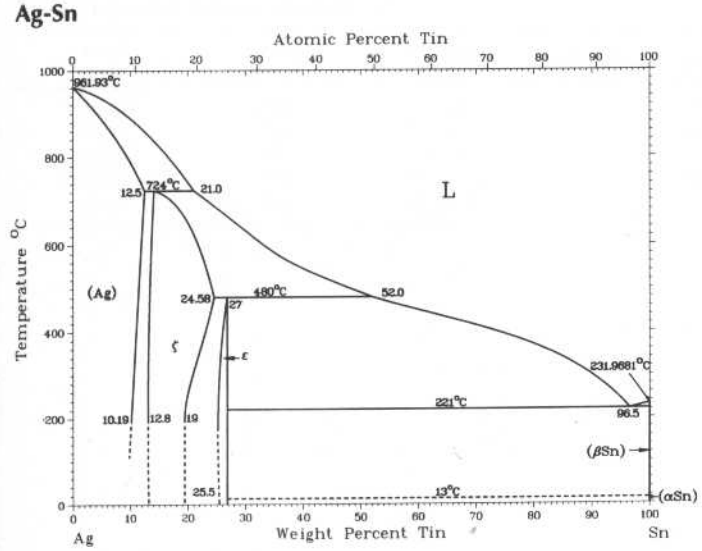

I. Karakaya and W.T. Thompson, 1987

Phase	Composition, wt% Sn	Pearson symbol	Space group
(Ag)	0 to 12.5	*cF*4	$Fm\bar{3}m$
ζ	12.8 to 24.58	*hP*2	$P6_3/mmc$
ε	25.5 to 27	*oP*8	*Pmmn*
(βSn)	99.92 to 100	*tI*4	$I4_1/amd$
(αSn)	100	*cF*8	$Fd\bar{3}m$

Ag-Sr

M.R. Baren, 1990

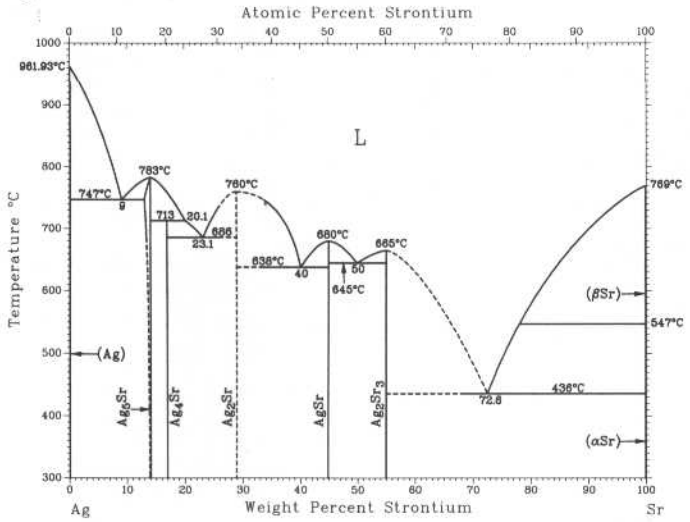

Phase	Composition, wt% Sr	Pearson symbol	Space group
(Ag)	0	*cF*4	$Fm\bar{3}m$
Ag_5Sr	12.9 to 14.1	*hP*6	*P6/mmm*
Ag_4Sr	17	...	...
Ag_2Sr	28.9	...	*Imma*
AgSr	44.8	*oP*8	*Pnma*
Ag_2Sr_3	55	*hR*45	$R\bar{3}$
Ag_3Sr_7(a)	65	*hP*20	$P6_3mc$
(αSr)	100	*cF*4	$Fm\bar{3}m$
(βSr)(b)	100	*cI*2	$Im\bar{3}m$

(a) Not shown on diagram; probably a peritectic reaction. (b) Above 547 °C

Ag-Te

I. Karakaya and W.T. Thompson, 1991

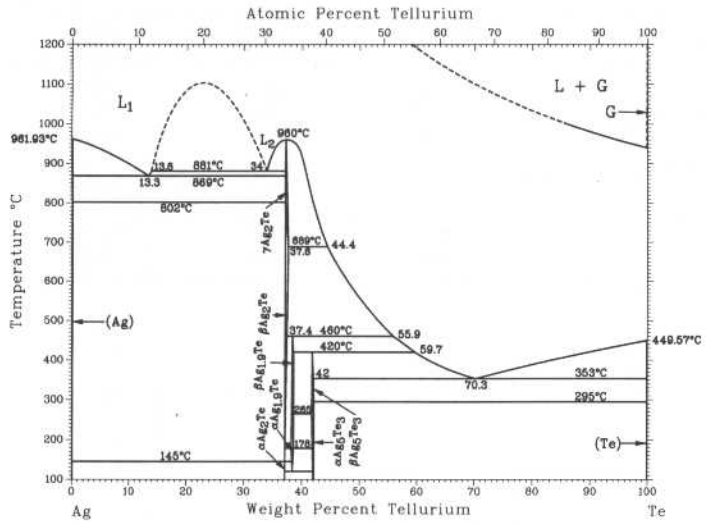

Phase	Composition(a), wt% Te	Pearson symbol	Space group
(Ag)	0	*cF*4	$Fm\bar{3}m$
αAg_2Te	37.1	*mP*12	*P21/c*
βAg_2Te(b)	37.1 to 37.6	*cF*12	...
γAg_2Te(c)	37.1 to 37.6	...	...
$\alpha Ag_{1.9}Te$	38.23 to 38.6	...	...
αAg_5Te_3(d)	41.67 to 42.06	*hP*55	*P6/mmm*
AgTe(e)	...	*oP*32	...
Ag_2TeII(f)	...	...	...
Ag_2TeIII(g)	...	...	...
$AgTe_4$-$AgTe_{2.33}$(h)	...	...	...
$AgTe_3$(j)	...	*hR*12	$R\bar{3}m$
(Te)	100	*hP*3	$P3_121$

(a) Compositions are taken from the assessed diagram. (b) fcc structure. (c) bcc structure. (d) Referred to as Ag_7Te_4 by [Pearson2]. (e) Mineral empressite (regarded as metastable). (f) Tetragonal structure stable at pressures 2200 to 2500 kPa. Lattice parameters were measured at 2400 kPa pressure. (g) Tetragonal structure stable at pressures over 2500 kPa. Lattice parameters were measured at 4000 kPa pressure. (h) Simple cubic structure (metastable). (j) Stable at temperatures higher than 358 °C and pressures over 4.0 GPa

Ag-Ti

J.L. Murray and K.J. Bhansali, 1987

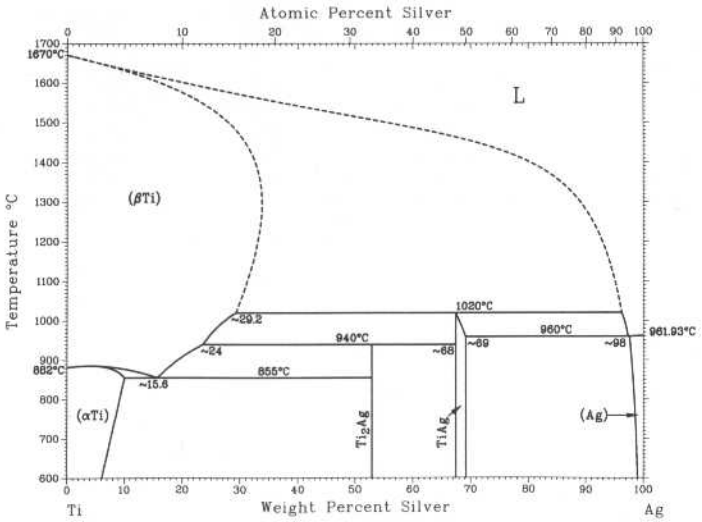

Phase	Composition, wt% Ag	Pearson symbol	Space group
(αTi)	0 to ~1.0	*hP*2	$P6_3/mmc$
(βTi)	0 to 29.2	*cI*2	$Im\bar{3}m$
Ti_2Ag	52.9	*tI*6	*I4/mmm*
TiAg	~68 to ~69	*tP*4	*P4/nmn*
(Ag)	~98 to 100	*cF*4	$Fm\bar{3}m$

Ag-Tl

M.R. Baren, 1989

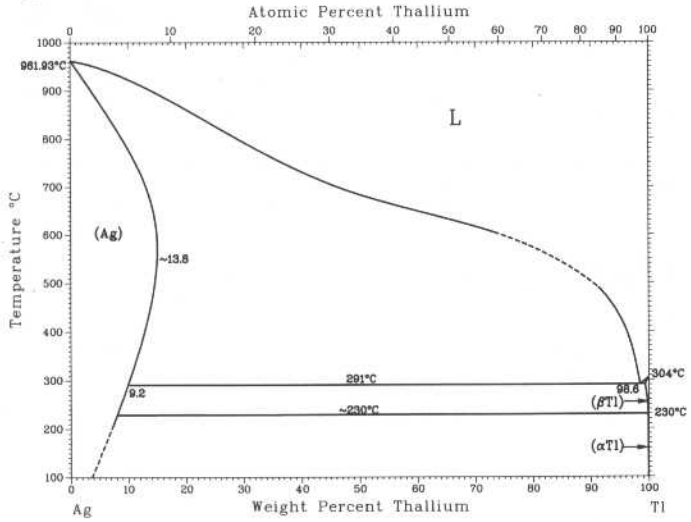

Phase	Composition, wt% Tl	Pearson symbol	Space group
(Ag)	0 to ~13.8	*cF*4	$Fm\bar{3}m$
(αTl)	100	*hP*2	$P6_3/mmc$
(βTl)(a)	? to 100	*cI*2	$Im\bar{3}m$

(a) Above 230 °C

Ag-Y

K.A. Gschneidner, Jr. and F.W. Calderwood, 1983

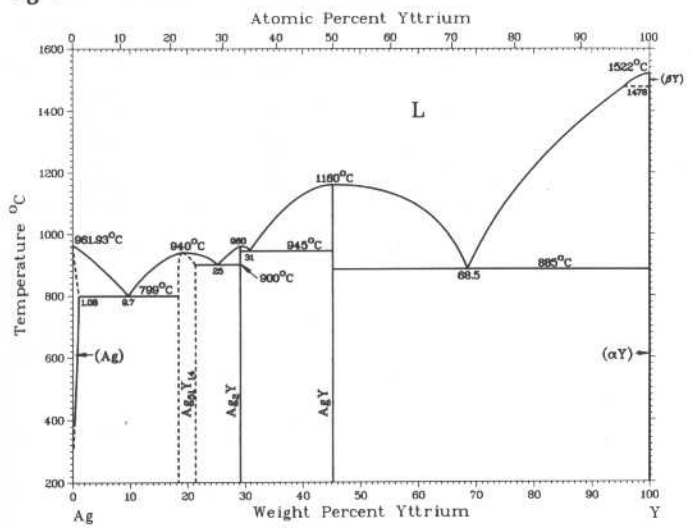

Phase	Composition, wt% Y	Pearson symbol	Space group
(Ag)	0 to 1.08	*cF*4	$Fm\bar{3}m$
$Ag_{51}Y_{14}$	18.4	*hP*65	...
Ag_2Y	29.2	*tI*6	*I*4/*mmm*
AgY	45.1	*cP*2	$Pm\bar{3}m$
(βY)	100	*cI*2	$Im\bar{3}m$
(αY)	100	*hP*2	$P6_3/mmc$

Ag-Yb

K.A. Gschneidner, Jr. and F.W. Calderwood, 1985

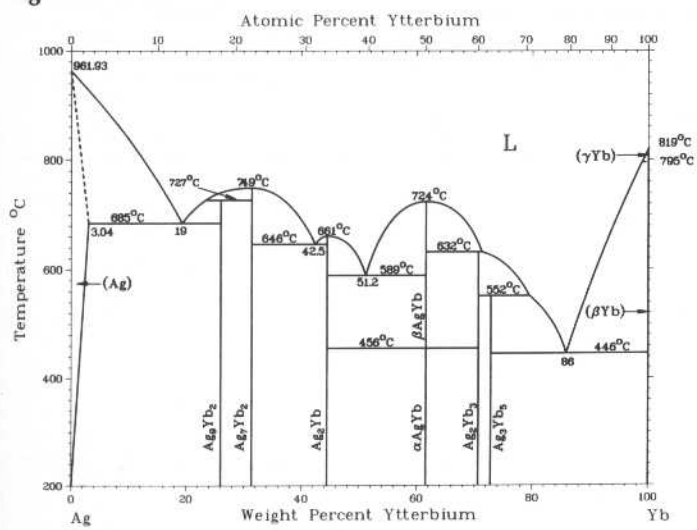

Phase	Composition, wt% Yb	Pearson symbol	Space group
(Ag)	0 to 3.04	*cF*4	$Fm\bar{3}m$
Ag_9Yb_2	...	...	...
Ag_7Yb_2	31.4	*hP*18	...
Ag_2Yb	44.5	*oI*2	*Imma*
βAgYb	61.6	*cP*2	$Pm\bar{3}m$
αAgYb	61.6	*oP*8	*Pnma*
Ag_2Yb_3	70.6	*tP*10	*P*4/*mbm*
Ag_3Yb_5	72.8	*tI*32	*I*4/*mcm*
(γYb)	100	*cI*2	$Im\bar{3}m$
(βYb)	100	*cF*4	$Fm\bar{3}m$
(αYb)	100	*hP*2	$P6_3/mmc$

Ag-Zn

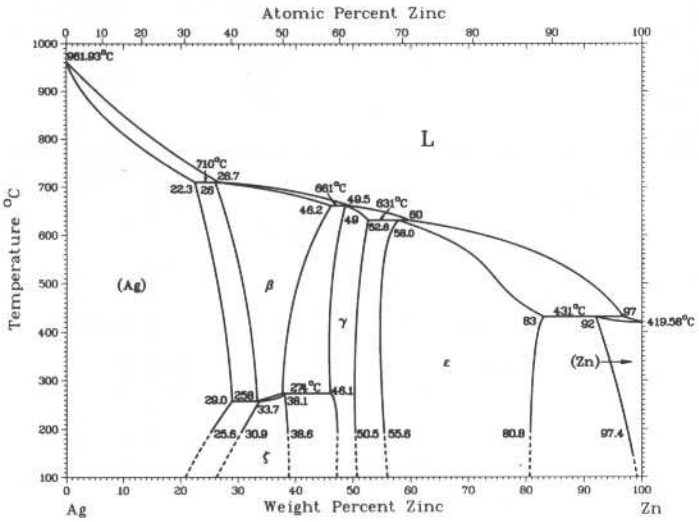

K.W. Andrews, H.E. Davies, W. Hume-Rothery, and C.R. Oswin, 1940

Phase	Composition, wt% Zn	Pearson symbol	Space group
(Ag)	0 to 29.0	*cF*4	$Fm\bar{3}m$
ζ(AgZn)	26 to ~38.8	(a)	...
β(AgZn)	26 to 46.2	*cI*2	$Im\bar{3}m$
γ(Ag_5Zn_8)	46.1 to 52.6	*cI*52	$I\bar{3}m$
ε	~54.3 to 83	*hP*2	$P6_3/mmc$
(Zn)	92 to 100	*hP*2	$P6_3/mmc$

(a) Ordered hexagonal

Ag-Zr

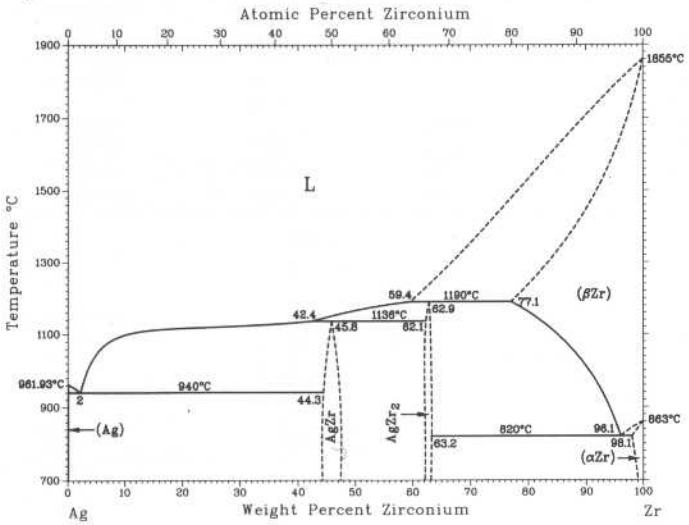

I. Karakaya and W.T. Thompson, 1992

Phase	Composition, wt% Zr	Pearson symbol	Space group
(Ag)	0 to 0.08	*cF*4	$Fm\bar{3}m$
AgZr	~45.8	*tP*4	*P*4/*nmm*
$AgZr_2$	~62.9	*tI*6	*I*4/*mmm*
(αZr)	98.1 to 100	*hP*2	$P6_3/mmc$
(βZr)	100	*cI*2	$Im\bar{3}m$

Al-As

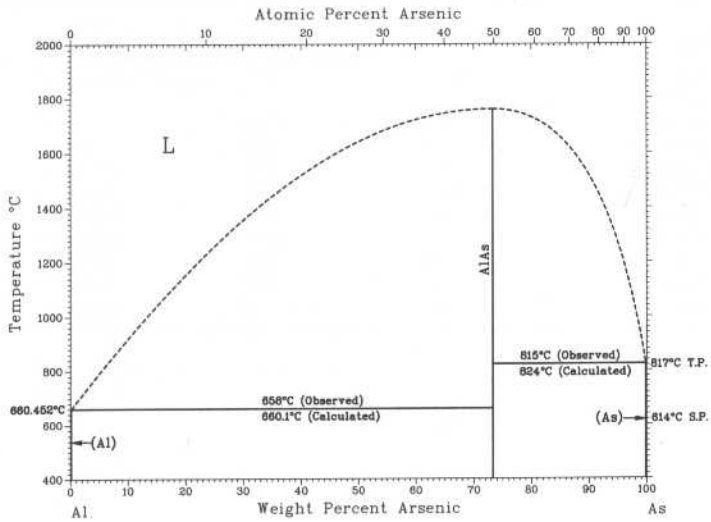

A.J. McAlister, 1984

Phase	Composition, wt% As	Pearson symbol	Space group
(Al)	0	*cF*4	$Fm\bar{3}m$
AlAs	73.5	*cF*8	$F\bar{4}3m$
(As)	100	*hR*2	$R\bar{3}m$

Al-Au

H. Okamoto, 1991

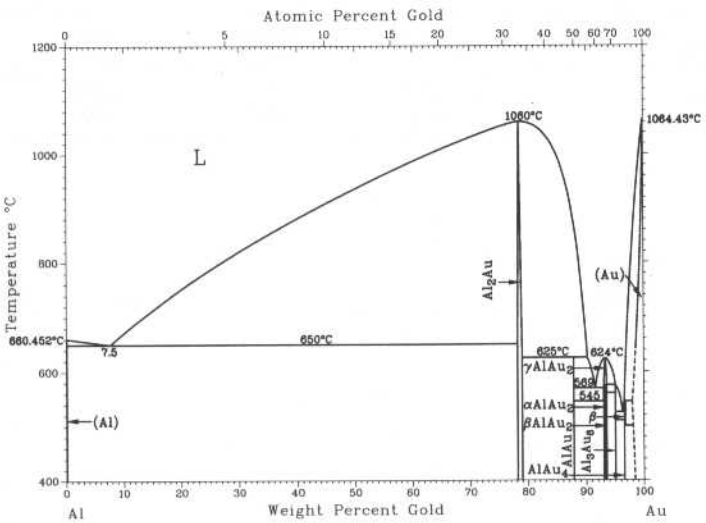

Phase	Composition, wt% Au	Pearson symbol	Space group
(Al)	0 to 0.44	*cF*4	$Fm\bar{3}m$
Al_2Au	78 to 79	*cF*12	$Fm\bar{3}m$
AlAu	88	*mP*28	$P2_1/m$
$\gamma AlAu_2$	93 to 93.6	*tI*6	*I*4/*mmm*
$\beta AlAu_2$	93.2 to 93.4	*oP*32	*Pnmn*
$\alpha AlAu_2$	93.5 to 93.6	*oP*12	*Pnma*
Al_3Au_8	95.1	*hR*132	$R\bar{3}c$
β	96.7 to 96.9	*cI*2	$Im\bar{3}m$
$AlAu_4$	96.7	*cP*20	$P2_13$
(Au)	98 to 100	*cF*4	$Fm\bar{3}m$

Al-Ba

H. Okamoto, 1992

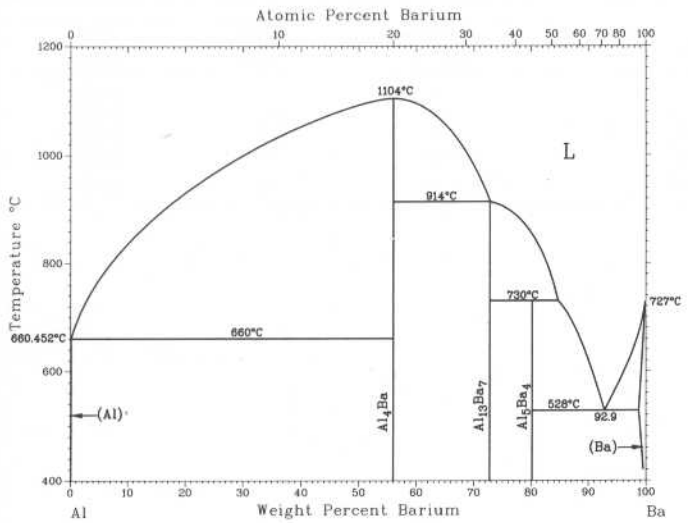

Phase	Composition, wt% Ba	Pearson symbol	Space group
(Al)	0	*cF*4	$Fm\bar{3}m$
Al_4Ba	56	*tI*10	*I*4/*mmm*
$Al_{13}Ba_7$	73	*hP*20	$P\bar{3}m1$
Al_5Ba_4	80.3	*hP*18	$P6_3/mmc$
(Ba)	100	*cI*2	$Im\bar{3}m$
Other phases			
Al_5Ba_3	75.3	*hP*16	$P6_3/mmc$

Al-Be (calculated)

J.L. Murray and D.J. Kahan, 1988

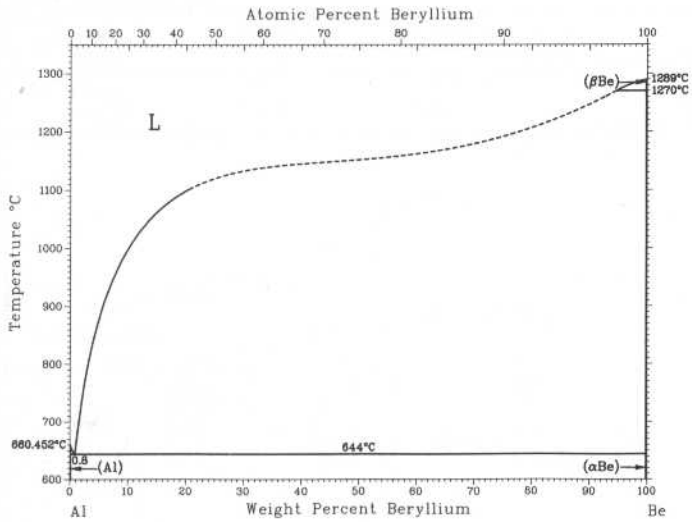

Phase	Composition, wt% Be	Pearson symbol	Space group
(Al)	0 to 0.10	*cF*4	$Fm\bar{3}m$
(βBe)	99.979 to 100	*cI*2	$Im\bar{3}m$
(αBe)	99.979 to 100	*hP*2	$P6_3/mmc$

Al-Bi

A.J. McAllister, 1984

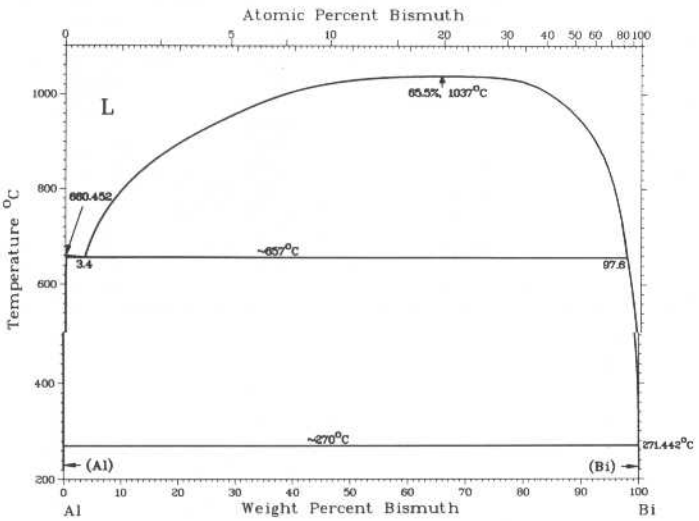

Phase	Composition, wt% Bi	Pearson symbol	Space group
(Al)	0 to ~0.23	*cF*4	$Fm\bar{3}m$
(Bi)	100	*hR*2	$R\bar{3}m$

Al-Ca

V.P. Itkin, C.B. Alcock, P.J. van Ekeren, and H.A.J. Oonk, 1988

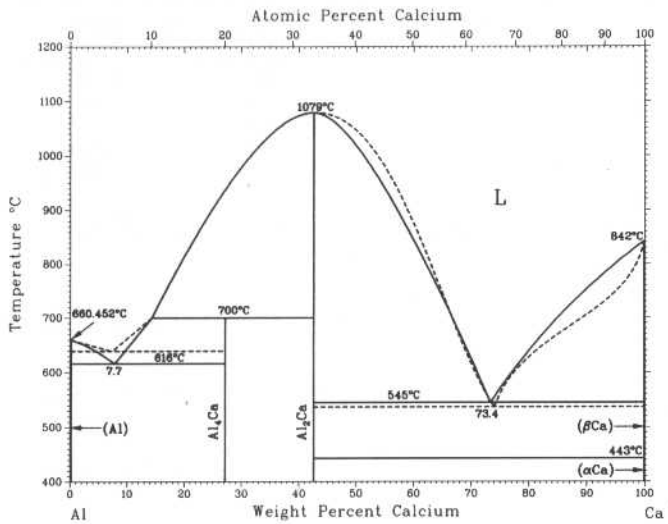

Phase	Composition, wt% Ca	Pearson symbol	Space group
(Al)	0	*cF*4	$Fm\bar{3}m$
Al_4Ca	27	*tI*10	*I*4/*mmm*
Al_2Ca	42.6	*cF*24	$Fd\bar{3}m$
(αCa)	100	*cF*4	$Fm\bar{3}m$
(βCa)	100	*cI*2	$Im\bar{3}m$

Dashed lines = calculated.

Al-Cd

A.J. McAlister, 1982

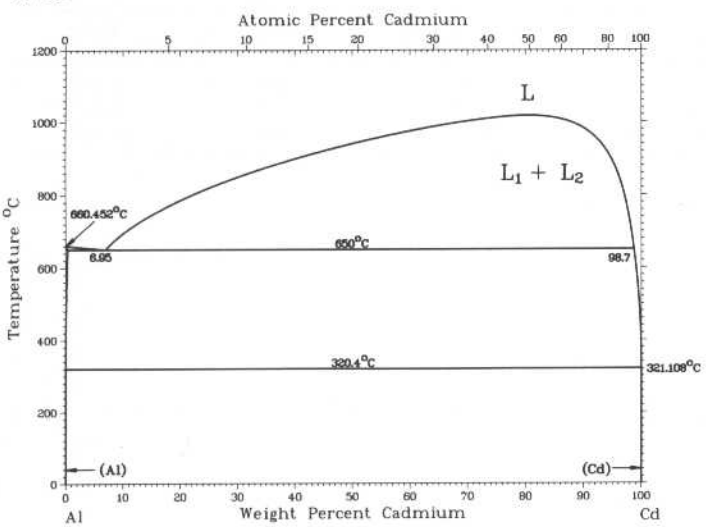

Phase	Composition, wt% Cd	Pearson symbol	Space group
(Al)	0	*cF*4	$Fm\bar{3}m$
(Cd)	100	*hP*2	$P6_3/mmc$

Al-Ce

K.A. Gschneidner, Jr. and F.W. Calderwood, 1988

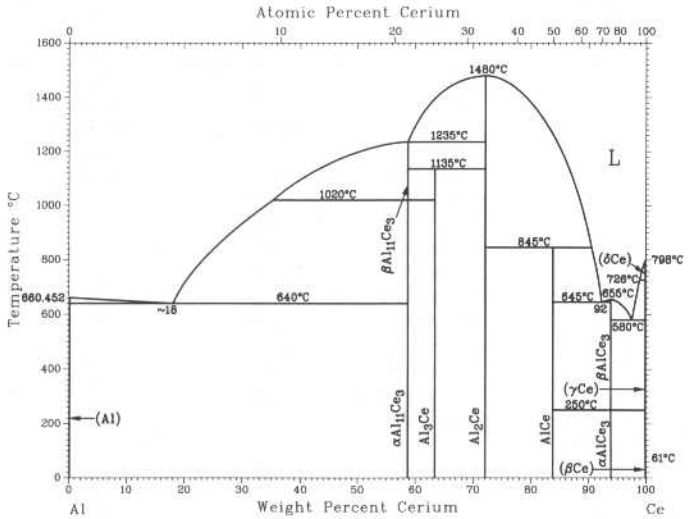

Phase	Composition, wt% Ce	Pearson symbol	Space group
(Al)	0	*cF*4	$Fm\bar{3}m$
$\alpha Al_{11}Ce_3$	58.6	*oI*28	*Immm*
$\beta Al_{11}Ce_3$	58.6	*tI*10	$I4/mmm$
Al_3Ce	63	*hP*8	$P6_3/mmc$
Al_2Ce	72.2	*cF*24	$Fd\bar{3}m$
AlCe	83.9	*oC*16	*Cmc*2 or *Cmcm*
$\alpha AlCe_3$	94	*hP*8	$P6_3/mmc$
$\beta AlCe_3$	94	*cP*4	$Pm\bar{3}m$
(αCe)	100	*cF*4	$Fm\bar{3}m$
(βCe)	100	*hP*4	$P6_3/mmc$
(γCe)	100	*cF*4	$Fm\bar{3}m$
(δCe)	100	*cI*2	$Im\bar{3}m$

Al-Co

A.J. McAlister, 1989

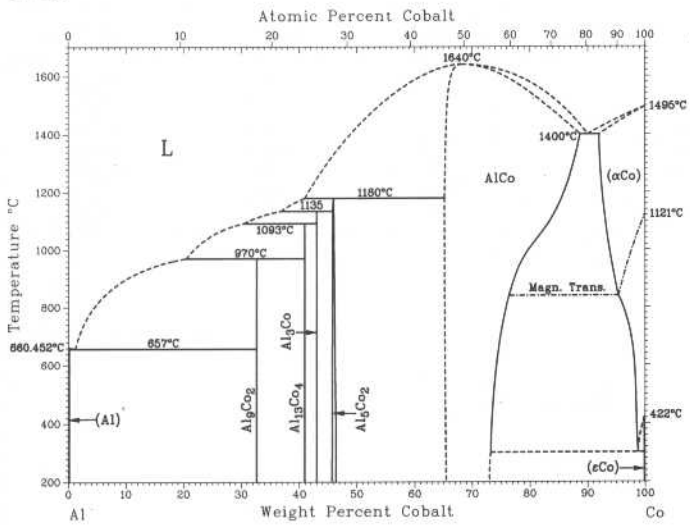

Phase	Composition, wt% Co	Pearson symbol	Space group
(Al)	~0	*cF*4	$Fm\bar{3}m$
Al_9Co_2	32.6	*mP*22	$P2_1/a$
$Al_{13}Co_4$	40.2	*mC*93	*Cm*
Al_3Co	42.9	...	(a)
Al_5Co_2	46.7	*hP*28	$P6_3/mmc$
AlCo	~67 to 88.9	*cP*2	$Pm\bar{3}m$
(εCo)	92 to 100	*hP*2	$P6_3/mmc$
(αCo)	~97 to 100	*cF*4	$Fm\bar{3}m$
Metastable phases			
I	95 to 98	...	(b)
α_{II}	93 to 94	...	(b)
α_{III}	92 to 93	...	(b)
α_{IV}	93 to 94	...	(b)
α			

(a) Unknown. (b) Hexagonal

Al-Cr

J.L. Murray, unpublished

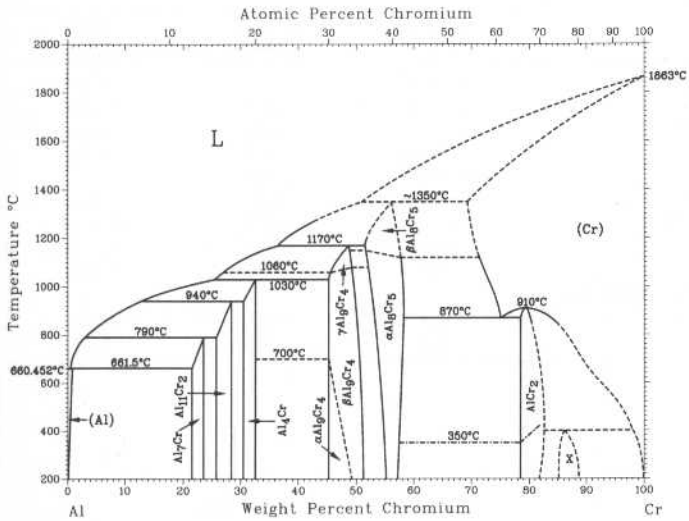

Phase	Composition, wt% Cr	Pearson symbol	Space group
(Al)	0 to 0.71	*cF*4	$Fm\bar{3}m$
Al_7Cr ($Al_{13}Cr_2$)	~21.4 to ~23.4	*mC*104	*C*2/*m*
$Al_{11}Cr_2$ (Al_5Cr)	~25.7 to ~28	*mP*48	*P*2
Al_4Cr	~30.4 to ~33	*mP*180	*P*2/*m*
αAl_9Cr_4	~45 to ~49.3	*cI*52	$I\bar{4}3m$
αAl_8Cr_5	~51.5 to ~58	*hR*26	$R\bar{3}m$
$AlCr_2$	~78.5 to ~82.8	*tI*6	*I*4/*mmm*
X(a)	~85	...	...
(Cr)	69 to 100	*cI*2	$Im\bar{3}m$

(a) It has been proposed that the structure is analogous to the ω phase seen in, for example, Zr at high pressure, but based on ordered bcc $AlCr_2$ rather than on the disordered bcc structure.

Al-Cu

J.L. Murray, 1985

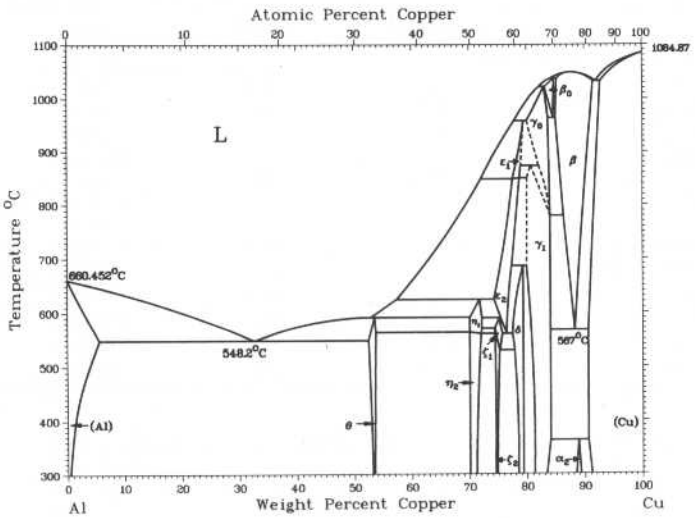

Phase	Composition, wt% Cu	Pearson symbol	Space group
(Al)	0 to 5.65	*cF*4	$Fm\bar{3}m$
θ	52.5 to 53.7	*tI*12	*I*4/*mcm*
η_1	70.0 to 72.2	*oP*16 or *oC*16	*Pban* or *Cmmm*
η_2	70.0 to 72.1	*mC*20	*C*2/*m*
ζ_1	74.4 to 77.8	*hP*42	*P*6/*mmm*
ζ_2	74.4 to 75.2	(a)	...
ε_1	77.5 to 79.4	(b)	...
ε_2	72.2 to 78.7	*hP*4	$P6_3/mmc$
δ	77.4 to 78.3	(c)	$R\bar{3}m$
γ_0	77.8 to 84	(d)	...
γ_1	79.7 to 84	*cP*52	$P\bar{4}3m$
β_0	83.1 to 84.7	(d)	...
β	85.0 to 91.5	*cI*2	$Im\bar{3}m$
α_2	88.5 to 89	(e)	...
(Cu)	90.6 to 100	*cF*4	$Fm\bar{3}m$
Metastable phases			
θ′	...	*tP*6	...
β′	...	*cF*16	$Fm\bar{3}m$
Al_3Cu_2	61 to 70	*hP*5	$P\bar{3}m1$

(a) Monoclinic? (b) Cubic? (c) Rhombohedral. (d) Unknown. (e) DO_{22}-type long-period superlattice

Al-Er

K.A. Gschneidner, Jr. and F.W. Calderwood, 1988

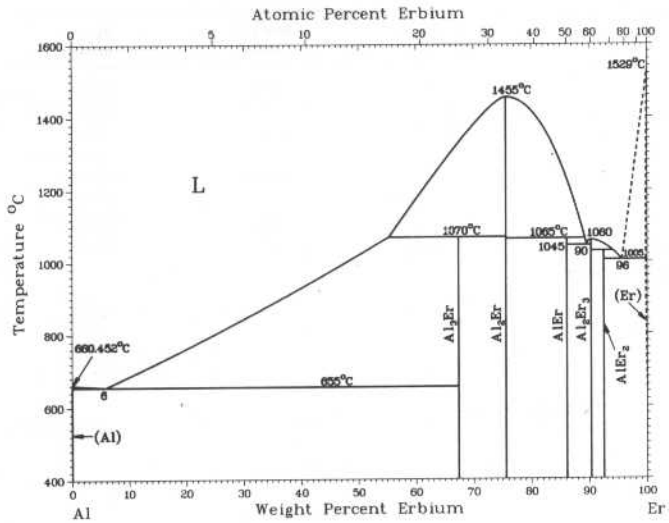

Phase	Composition, wt% Er	Pearson symbol	Space group
(Al)	0	*cF*4	$Fm\bar{3}m$
Al_3Er	67	*cP*4	$Pm\bar{3}m$
Al_2Er	75.6	*cF*24	$Fd\bar{3}m$
AlEr	86.1	*oP*16	*Pmma*
Al_2Er_3	90	*tP*20	$P4_2/mnm$
$AlEr_2$	92.6	*oP*12	*Pnma*
(Er)	100	*hP*2	$P6_3/mmc$

Al-Fe

U.R. Kattner and B.P. Burton, 1992

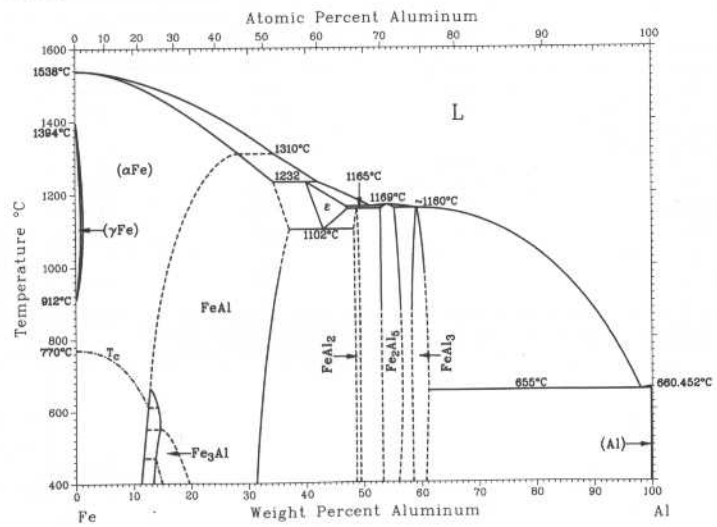

Phase	Composition, wt% Al	Pearson symbol	Space group
(αFe)	0 to ~28	*cI*2	$Im\bar{3}m$
(γFe)	0 to 0.6	*cF*4	$Fm\bar{3}m$
FeAl	12.8 to ~37	*cP*8	$Pm\bar{3}m$
Fe_3Al	~13 to ~20	*cF*16	$Fm\bar{3}m$
ε	~40 to ~47	*cI*16?	...
$FeAl_2$	48 to 49.4	*aP*18	*P*1
Fe_2Al_5	53 to 57	*oC*?	*Cmcm*
$FeAl_3$	58.5 to 61.3	*mC*102	*C*2/*m*
(Al)	100	*cF*4	$Fm\bar{3}m$
Metastable phases			
Fe_2Al_9	68.5	*mP*22	$P2_1/c$
$FeAl_6$	74.3	*oC*28	$Cmc2_1$

Al-Ga

J.L. Murray, 1983

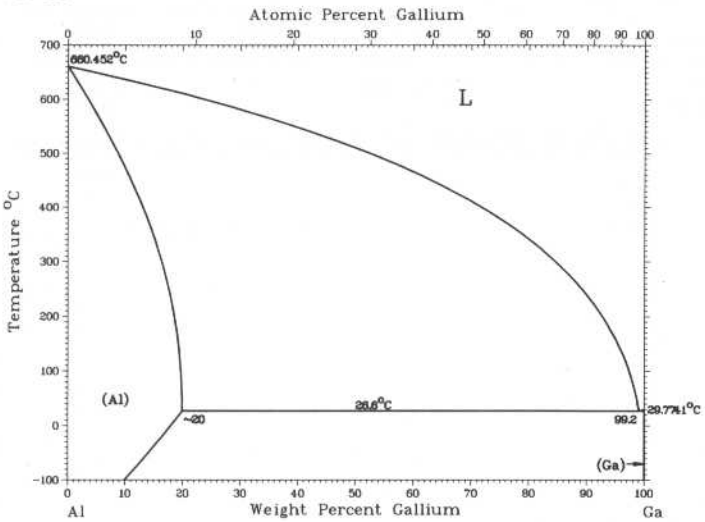

Phase	Composition, wt% Ga	Pearson symbol	Space group
(Al)	0 to ~20(a)	*cF*4	$Fm\bar{3}m$
(Ga)	100	*oC*8	*Cmca*
Metastable phases			
α′	83 to 92.4	*tI*2	*I*4/*mmm*
ϕ	94 to 95	(b)	(b)

(a) Can be extended to 83 wt% Ga by splat quenching. (b) Undetermined, low symmetry

Al-Gd

K.A. Gschneidner, Jr. and F.W. Calderwood, 1988

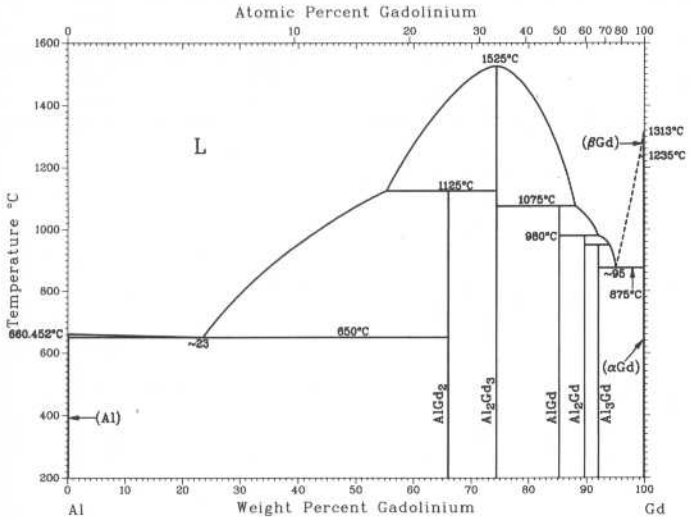

Phase	Composition, wt% Gd	Pearson symbol	Space group
(Al)	0	*cF*4	$Fm\bar{3}m$
Al_3Gd	66	*hP*8	$P6_3/mmc$
Al_2Gd	74.4	*cF*24	$Fd\bar{3}m$
AlGd	85.4	*oP*16	*Pmma*
Al_2Gd_3	90	*tP*20	$P4_2/mnm$
$AlGd_2$	92.1	*oP*12	*Pnma*
(βGd)	100	*cI*2	$Im\bar{3}m$
(αGd)	100	*hP*2	$P6_3/mmc$

Al-Ge

A.J. McAlister and J.L. Murray, 1984

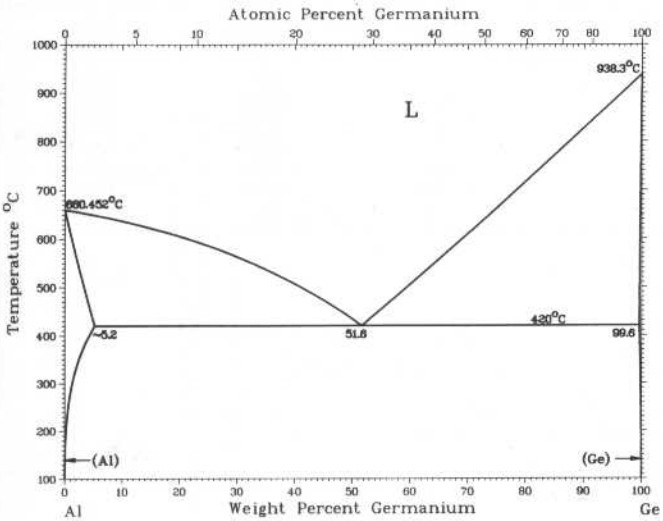

Phase	Composition, wt% Ge	Pearson symbol	Space group
(Al)	0 to ~5.2	*cF*4	$Fm\bar{3}m$
(Ge)	99.6 to 100	*cF*8	$Fd\bar{3}m$
Metastable phases			
γ_1	...	*hR**	...
		*t***	...
γ_2	...	*cP**	...
		*mC**	...
		*t***	...
γ_3	...	*cP**	...
		*hP**	...

Al-H

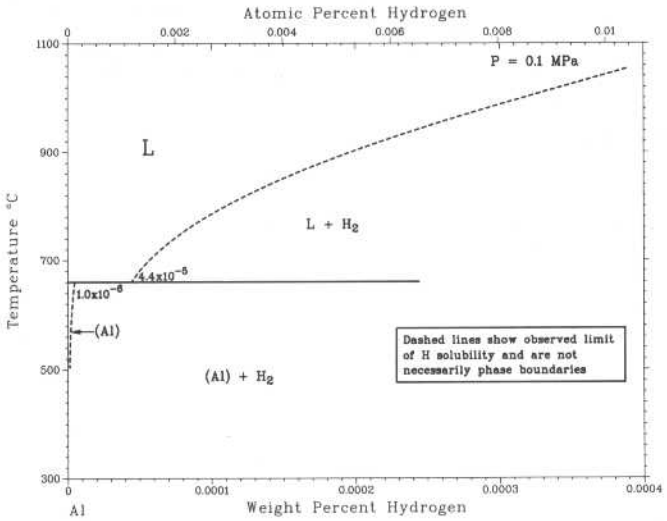

A. San-Martin and F.D. Manchester, 1992

Phase	Composition, wt% H	Pearson symbol	Space group
(Al)	0 to 4.48×10^{-6}(a)	*cF*4	$Fm\bar{3}m$
AlH_3(b)	10.1	...	$R\bar{3}c$

(a) At 660 °C and 0.1 MPa. (b) Produced by chemical reaction of organic solvents at atmospheric pressure

Al-Hg

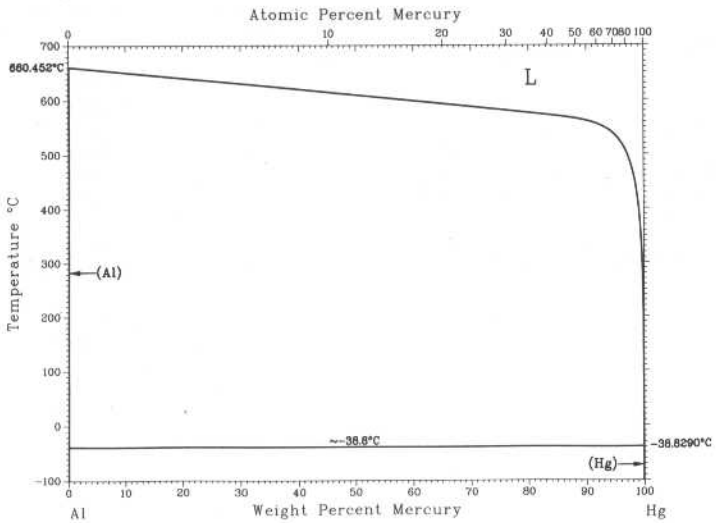

A.J. McAlister, 1985

Phase	Composition, wt% Hg	Pearson symbol	Space group
(Al)	0	*cF*4	$Fm\bar{3}m$
(Hg)	100	*hR*1	$R\bar{3}m$

Al-Ho

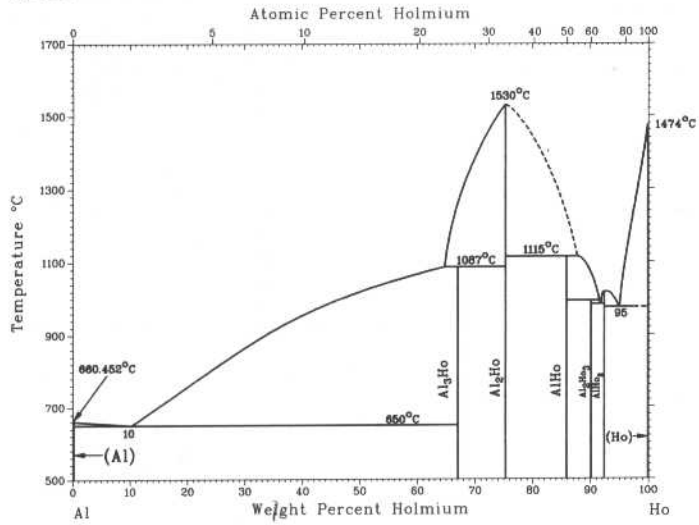

K.A. Gschneidner, Jr. and F.W. Calderwood, 1988

Phase	Composition, wt% Ho	Pearson symbol	Space group
(Al)	0	*cF*4	$Fm\bar{3}m$
Al_3Ho	67	*hR*20	$R\bar{3}m$
Al_2Ho	75.3	*cF*24	$Fd\bar{3}m$
AlHo	85.9	*oP*16	*Pmma*
Al_2Ho_3	90	*tP*20	$P4_2/mnm$
$AlHo_2$	92.5	*oP*12	*Pnma*
(Ho)	100	*hP*2	$P6_3/mmc$

Al-In

J.L. Murray, 1983

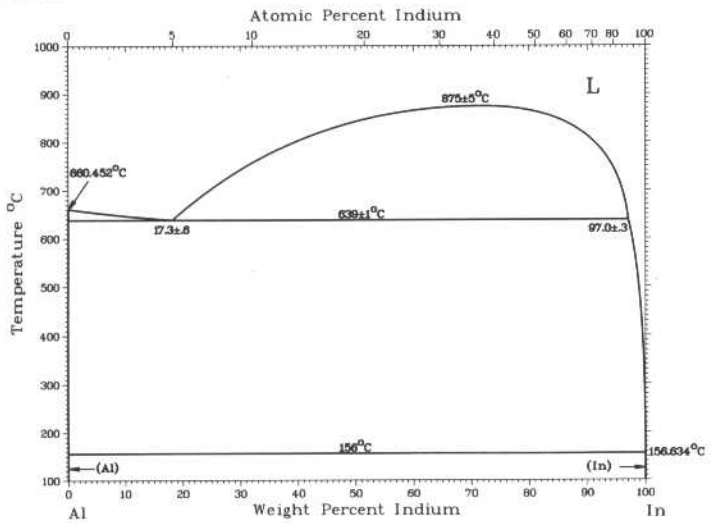

Phase	Composition, wt% In	Pearson symbol	Space group
(Al)	0 to 0.19	*cF*4	$Fm\bar{3}m$
(In)	~100	*tI*2	*I*4/*mmm*
Metastable phases			
(In′)	...	*cF*4	$Fm\bar{3}m$

Al-La

K.A. Gschneidner, Jr. and F.W. Calderwood, 1988

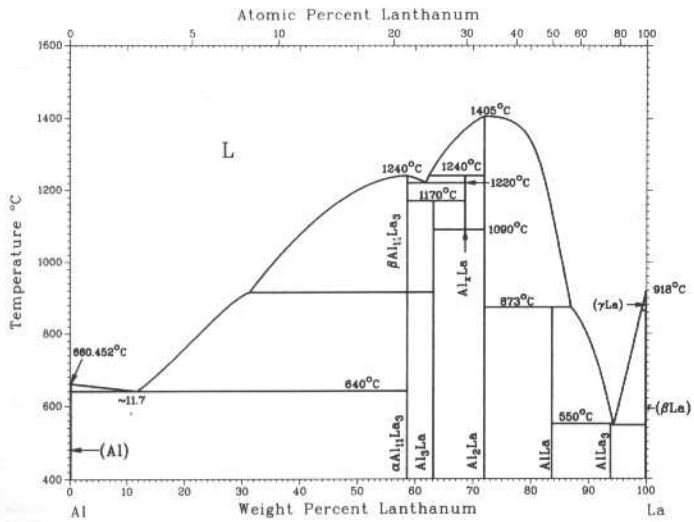

Phase	Composition, wt% La	Pearson symbol	Space group
(Al)	0 to ~0.05	*cF*4	$Fm\bar{3}m$
$\alpha Al_{11}La_3$	58.4	*oI*28	*Immm*
$\beta Al_{11}La_3$	58.4	*tI*10	*I*4/*mmm*
Al_3La	63	*hP*8	$P6_3/mmc$
Al_4La	68.1	*hP*3	$P6_3/mmm$
Al_2La	72.0	*cF*24	$Fd\bar{3}m$
AlLa	83.7	*oC*16	*Cmc*2 or *Cmcm*
$AlLa_3$	94	*hP*8	$P6_3/mmc$
(αLa)	100	*hP*4	$P6_3/mmc$
(βLa)	100	*cF*4	$Fm\bar{3}m$
(γLa)	100	*cI*2	$Im\bar{3}m$

Al-Li

A.J. McAlister, 1991

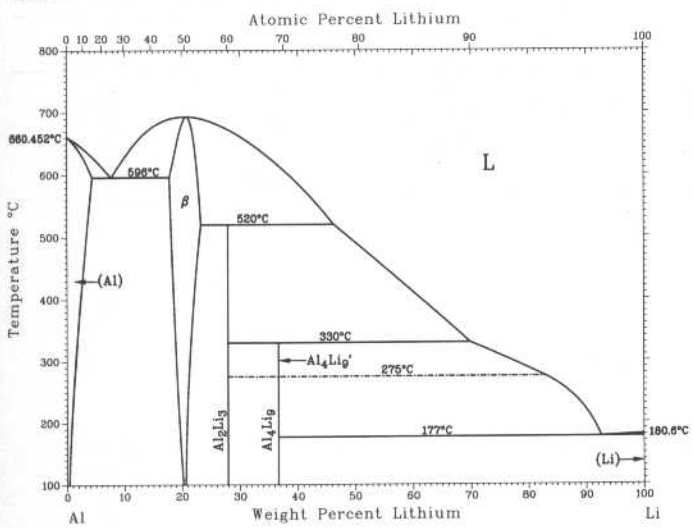

Phase	Composition, wt% Li	Pearson symbol	Space group
(Al)	0 to 4	*cF*4	$Fm\bar{3}m$
β	17 to 24	*cF*16	$Fd\bar{3}m$
Al_2Li_3	28 to 29	*hR*15	$R\bar{3}m$
Al_4Li_9	36.6	*mC*26	*C*2/*m*
Al_4Li_9'	36.6	...	...
(βLi)	100	*cI*2	$Im\bar{3}m$
(αLi)	100	*hP*2	$P6_3/mmc$
Metastable phases			
Al_3Li	...	*cP*4	$Pm\bar{3}m$

Al-Mg

J.L. Murray, 1988

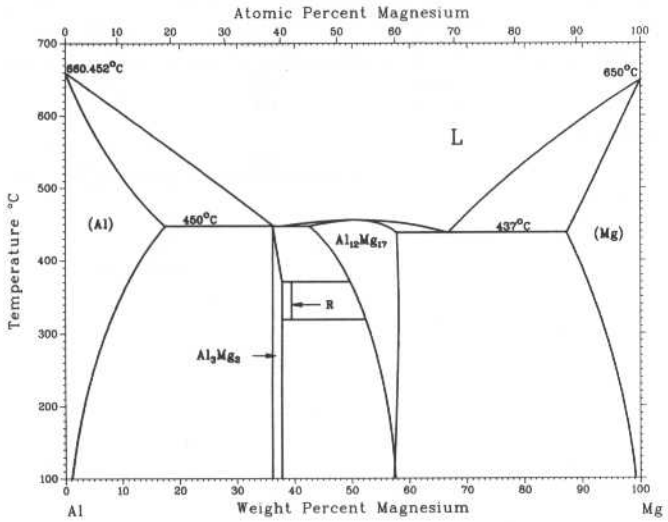

Phase	Composition, wt% Mg	Pearson symbol	Space group
(Al)	0 to 17.1	*cF*4	$Fm\bar{3}m$
$\beta(Al_3Mg_2)$	36.1 to 37.8	*cF*1168	$Fd\bar{3}m$
R	39	*hR*53	$R\bar{3}$
$\gamma(Al_{12}Mg_{17})$	42 to 58.0	*cI*58	$I\bar{4}3m$
(Mg)	87.1 to 100	*hP*2	$P6_3/mmc$
Metastable phases			
Al_2Mg	31.0	*tI*24	$I4_1/amd$
γ'	38 to 56.2	(a)	...

(a) Tetragonal

Al-Mn

A.J. McAlister and J.L. Murray, 1987

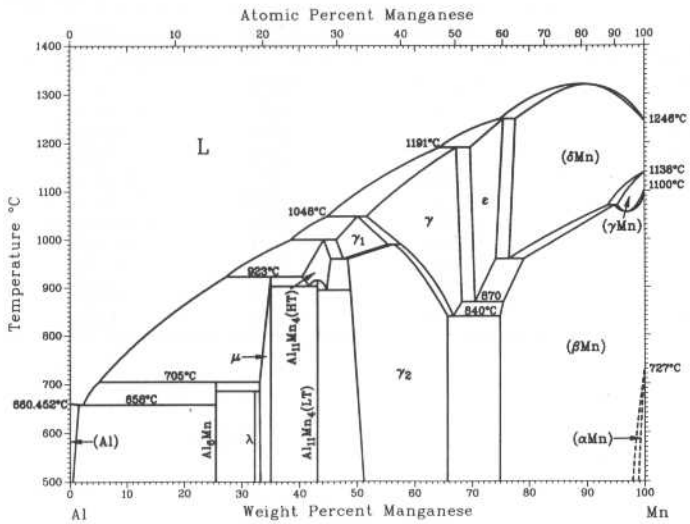

Phase	Composition, wt% Mn	Pearson symbol	Space group
(Al)	0 to 1.25	*cF*4	$Fm\bar{3}m$
G(a)	(b)	*cI*26	$Im\bar{3}m$
Al_6Mn	25.2	*oC*28	*Cmcm*
λ("Al_4Mn")(c)	~29.4 to ~32	(d)	...
μ	~32 to 34.8	(d)	...
$Al_{10}Mn_3(\phi)$	(b)	*hP*28	$P6_3/mmc$
$Al_{11}Mn_4$(LT)(e)	43	*aP*30	$P\bar{1}$
$Al_{11}Mn_4$(HT)(e)	40 to 45.0	oP160	*Pnma*
γ_1	47 to 55.7	(f)	...
$\gamma_{2(g)}$	48.2 to 64	*hR*26	$R\bar{3}m$
γ	51.8 to 68.2	(f)	...
ε	69.8 to 75	*hP*2	$P6_3/mmc$
τ	(b)	*tP*2	*P4/mmm*
(δMn)	76.5 to 100	*cI*2	$Im\bar{3}m$
(γMn)	95.3 to 100	*cF*4	$Fm\bar{3}m$
(βMn)	75.0 to 100	*cP*20	$P4_132$
(αMn)	~99 to 100	*cI*58	$I\bar{4}3m$

(a) Several other structures have been ascribed to the G phase or variants of the G phase (G′, G″). (b) Metastable phase. (c) A simple orthorhombic structure was reported in an alloy described as "Al_4Mn." (d) Hexagonal. (e) Variants of this structure are described as complex stacking sequences along the *b* axis. (f) Unknown. (g) The structure has been described as distorted γ-brass type, cubic (bcc or fcc), and rhombohedral.

Al-Nb

U.R. Kattner, unpublished

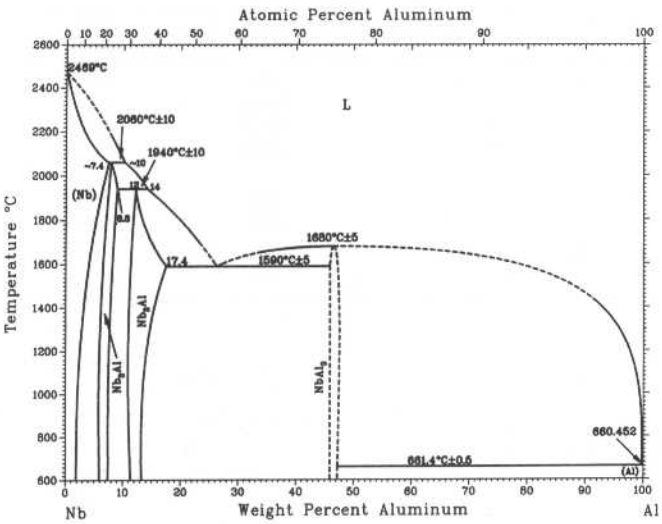

Phase	Composition, wt% Al	Pearson symbol	Space group
(Nb)	0 to ~7.4	*cI*2	$Im\bar{3}m$
Nb_3Al	18.6 to 8.8	*cP*8	$Pm\bar{3}n$
Nb_2Al	11 to 17.4	*tP*30	$P4_2/mnm$
$NbAl_3$	47	*tI*8	*I4/mmm*
(Al)	100	*cF*4	$Fm\bar{3}m$

Al-Nd

H. Okamoto, 1991

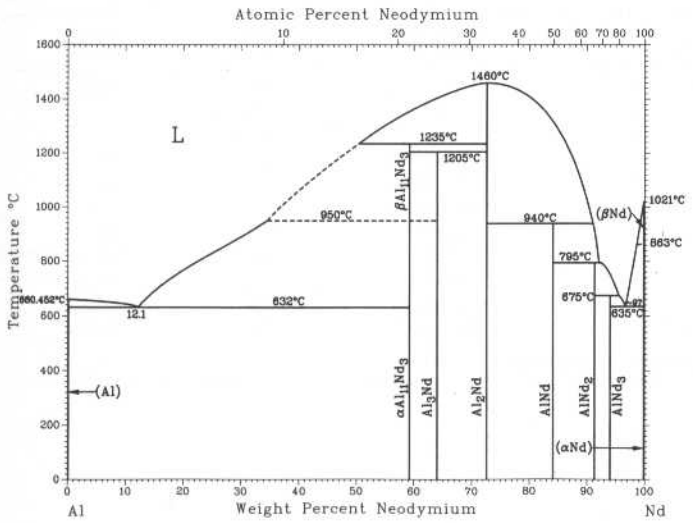

Phase	Composition, wt% Nd	Pearson symbol	Space group
(Al)	0 to 0.05	*cF*4	$Fm\bar{3}m$
$\alpha Al_{11}Nd_3$	59.3	*oI*28	*Immm*
$\beta Al_{11}Nd_3$	59.3	*tI*10	*I*4/*mmm*
Al_3Nd	64	*hP*8	$P6_3/mmc$
Al_2Nd	72.7	*cF*24	$Fd\bar{3}m$
AlNd	84.2	*oP*16	*Pmma*
$AlNd_2$	91.5	*oP*12	*Pnma*
$AlNd_3$	94	*hP*8	$P6_3/mmc$
(αNd)	100	*hP*4	$P6_3/mmc$
(βNd)	100	*cI*2	$Im\bar{3}m$

Al-Ni

P. Nash, M.F. Singleton, and J.L. Murray, 1991

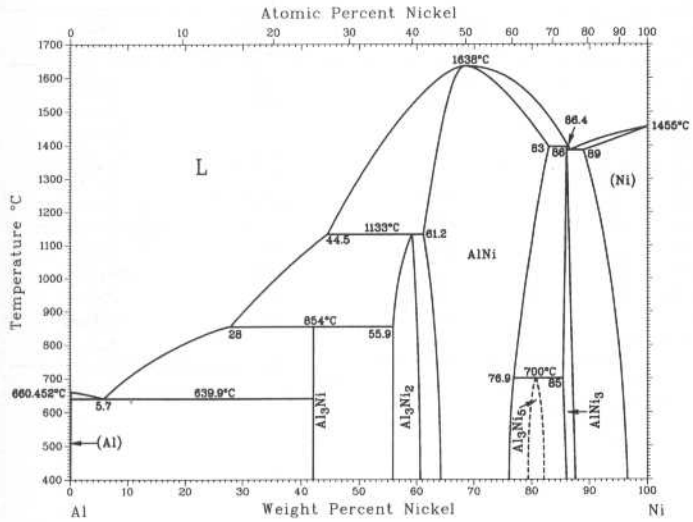

Phase	Composition, wt% Ni	Pearson symbol	Space group
(Al)	0 to 0.24	*cF*4	$Fm\bar{3}m$
Al_3Ni	42	*oP*16	*Pnma*
Al_3Ni_2	55.9 to 60.7	*hP*5	$P\bar{3}m1$
AlNi	61 to 83.0	*cP*2	$Pm\bar{3}m$
Al_3Ni_5	79 to ~82	...	*Cmmm*
$AlNi_3$	85 to 87	*cP*4	$Pm\bar{3}m$
(Ni)	89.0 to 100	*cF*4	$Fm\bar{3}m$

Al-Pb

A.J. McAlister, 1984

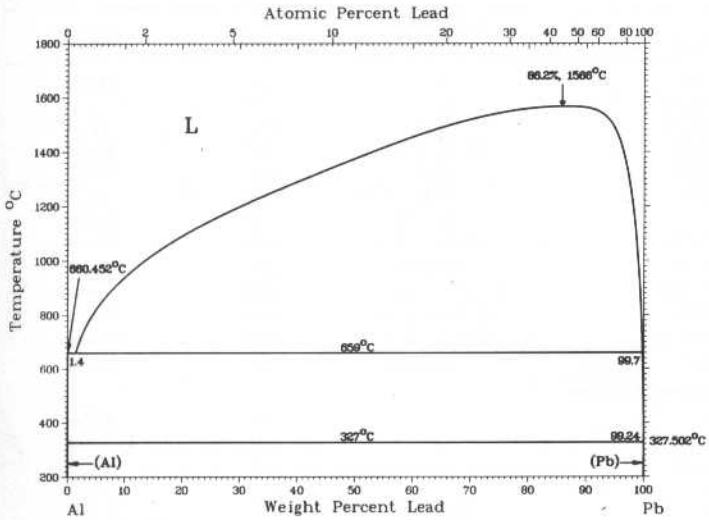

Phase	Composition, wt% Pb	Pearson symbol	Space group
(Al)	0	*cF*4	$Fm\bar{3}m$
(Pb)	99.7 to 100	*cF*4	$Fm\bar{3}m$

Al-Pd

A.J. McAlister, 1986

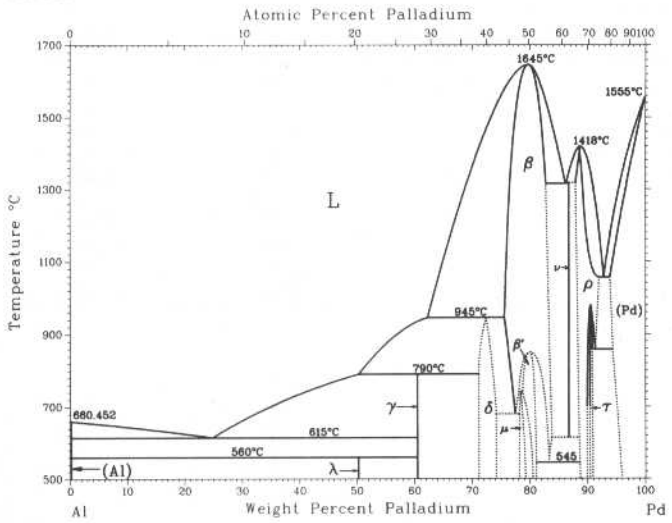

Phase	Composition, wt% Pd	Pearson symbol	Space group
(Al)	0	*cF*4	$Fm\bar{3}m$
λ	~50	(a)	...
γ	~60.1	(b)	...
δ	71 to 73.7	*hP*5	$P\bar{3}m1$
β	76 to 83	*cP*8	$Pm\bar{3}m$
β′	78.8 to 81.5	*hR*78	$R\bar{3}$
μ	78 to 79	*cP*8	$P2_13$
ν	86.8	*oP*16	*Pbam*
ρ	88 to 91	*oP*12	*Pnma*
τ	90.5 to 90.9	*oP*28	*Pbmn*
(Pd)	94 to 100	*cF*4	$Fm\bar{3}m$

(a) Hexagonal. (b) Orthorhombic

Al-Pr

K.A. Gschneidner, Jr. and F.W. Calderwood, 1989

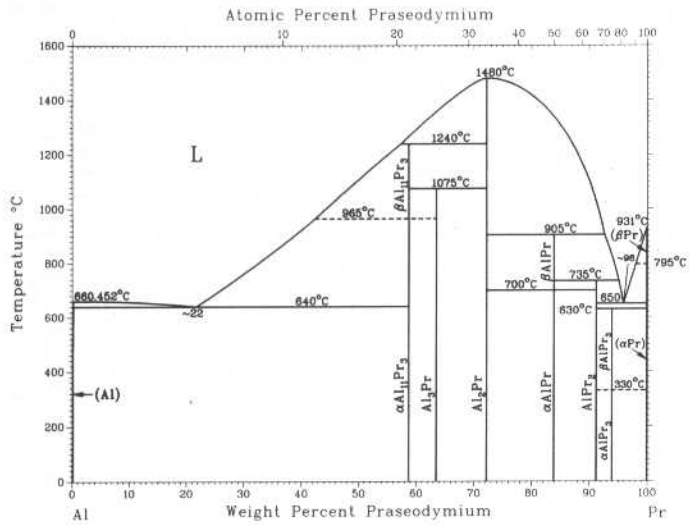

Phase	Composition, wt% Pr	Pearson symbol	Space group
(Al)	0 to ~0.5	*cF*4	$Fm\bar{3}m$
$\alpha Al_{11}Pr_3$	58.7	*oI*28	*Immm*
$\beta Al_{11}Pr_3$	58.7	*tI*10	*I4/mmm*
Al_3Pr	64	*hP*8	$P6_3/mmc$
Al_2Pr	72.3	*cF*24	$Fd\bar{3}m$
αAlPr	83.9	*oP*16	*Pnma*
βAlPr	83.9	*oC*16	*Cmc*2 or *Cmcm*
$AlPr_2$	91.3	*oP*12	*Pnma*
$\alpha AlPr_3$	94	*hP*8	$P6_3/mmc$
$\beta AlPr_3$	94	*cP*4	$Pm\bar{3}m$
(αPr)	100	*hP*4	$P6_3/mmc$
(βPr)	100	*cI*2	$Im\bar{3}m$

Al-Pt

A.J. McAlister and D.J. Kahan, 1986

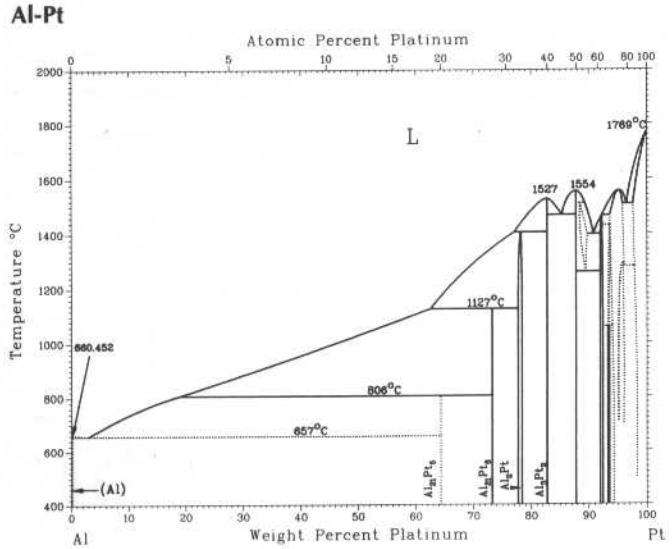

Phase	Composition, wt% Pt	Pearson symbol	Space group
(Al)	0	*cF*4	$Fm\bar{3}m$
$Al_{21}Pt_5$	63.2	*c***	...
$Al_{21}Pt_8$	72.8	*tI*116	$I4_1a$
Al_2Pt	76.9 to 78.5	*cF*12	$Fm\bar{3}m$
Al_3Pt_2	82.8	*hP*5	*P*3*m*1
AlPt	87.9	*cP*8	$P2_13$
β	~89 to ~90	*cP*2	$Pm\bar{3}m$
Al_3Pt_5	~92.0 to ~92.5	*oP*16	*Pbam*
$AlPt_2$	~93 to ~94	*oP*12	*Pnma*
$AlPt_2$(LT)	~93 to ~94	*oP*24	*Pnma*
$AlPt_3$	~93.7 to ~96.18	*cP*4	$Pm\bar{3}m$
$AlPt_3$(LT)	~95.3 to ~96.25	*tP*16	*P*4/*mbm*
(Pt)	~97.4 to 100	*cF*4	$Fm\bar{3}m$
Metastable phases			
α′	...	*cF*4	$Fm\bar{3}m$
Al_4Pt	~64	*hP**	...
Al_6Pt	~54	*o***	...
ε′	...	*c***	...
λ′	45 to 71	...	...

Al-S

R.C. Sharma and Y.A. Chang, 1991

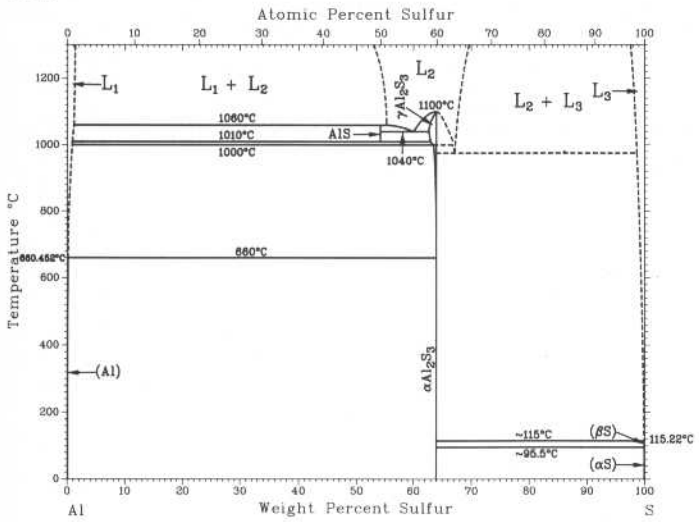

Phase	Composition, wt% S	Pearson symbol	Space group
(Al)	0	*cF*4	$Fm\bar{3}m$
αAl_2S_3	64	*hP*30	...
βAl_2S_3(a)	64	(b)	$P6_3mc$
γAl_2S_3	63 to 64	*hR*10	*R*3*c*
Al_2S_3(c)	64	(d)	$I4_1/amd$
Al_2S_3(e)	64	(f)	$Fd\bar{3}m$
(αS)	100	*oF*128	*Fddd*
(βS)	100	*mP**	$P2_1/c$

(a) Stable in the presence of Al_4C_3 between 1000 and 1100 °C. (b) Hexagonal. (c) High pressure, formed at 2 to 65 kbar and 1000 to 1200 °C. (d) Tetragonal. (e) High pressure, formed at 40 kbar and 400 °C. (f) Cubic

Al-Sb

A.J. McAlister, 1984

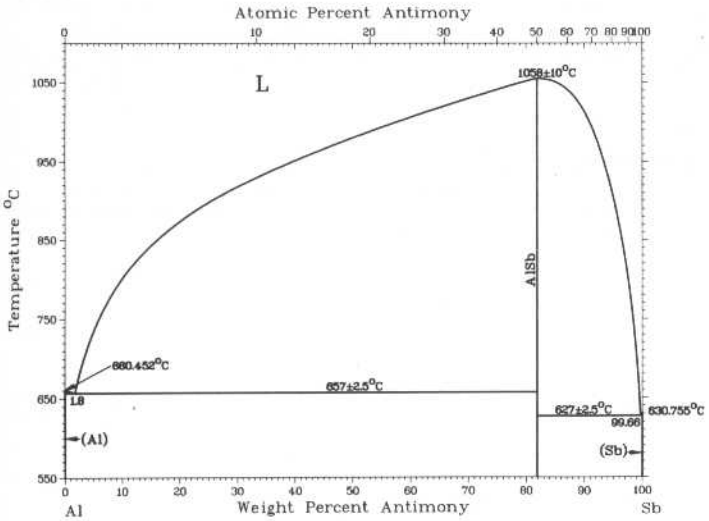

Phase	Composition, wt% Sb	Pearson symbol	Space group
(Al)	0	*cF*4	$Fm\bar{3}m$
AlSb	81.9	*cF*8	$F\bar{4}3m$
(Sb)	100	*hR*2	$R\bar{3}m$
High-pressure phase			
AlSb(a)	81.9	*tI*4	$I4_1/amd$

(a) At 120 kbar

Al-Se

J.M. Howe, 1989

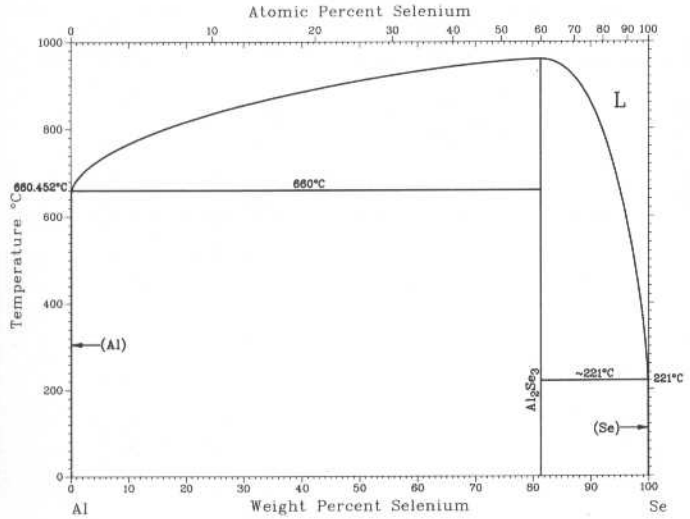

Phase	Composition, wt% Se	Pearson symbol	Space group
(Al)	<0.009	*cF*4	$Fm\bar{3}m$
Al_2Se_3	81	*mC*20	C_c
(Se)	100	*hP*3	$P3_121$

Al-Si

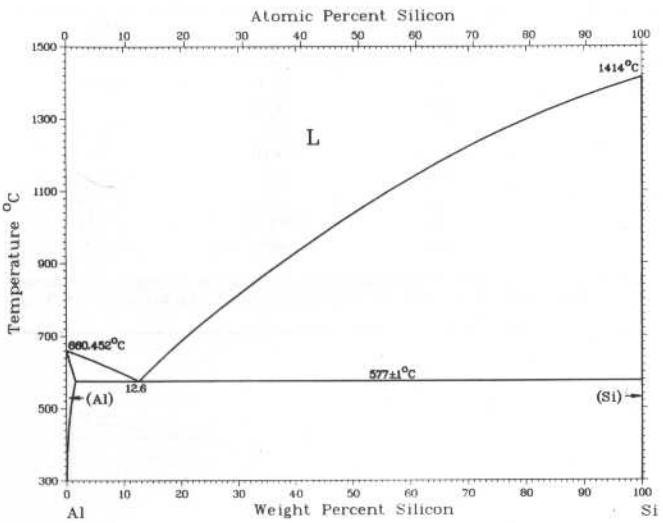

J.L. Murray and A.J. McAlister, 1984

Phase	Composition, wt% Si	Pearson symbol	Space group
(Al)	0 to 1.6	*cF*4	$Fm\bar{3}m$
(Si)	99.985 to 100	*cF*8	$Fd\bar{3}m$

Al-Sn

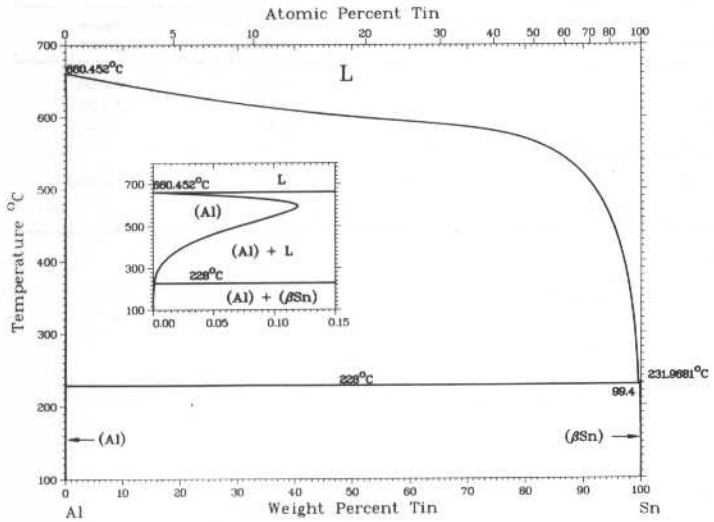

A.J. McAlister and D.J. Kahan, 1983

Phase	Composition, wt% Sn	Pearson symbol	Space group
(Al)	0	*cF*4	$Fm\bar{3}m$
(βSn)	100	*tI*4	$I4_1/amd$
(αSn)	100	*cF*8	$Fd\bar{3}m$
Metastable phase			
Γ	>81.5	*hP*1	*P*6/*mmm*

Al-Sr

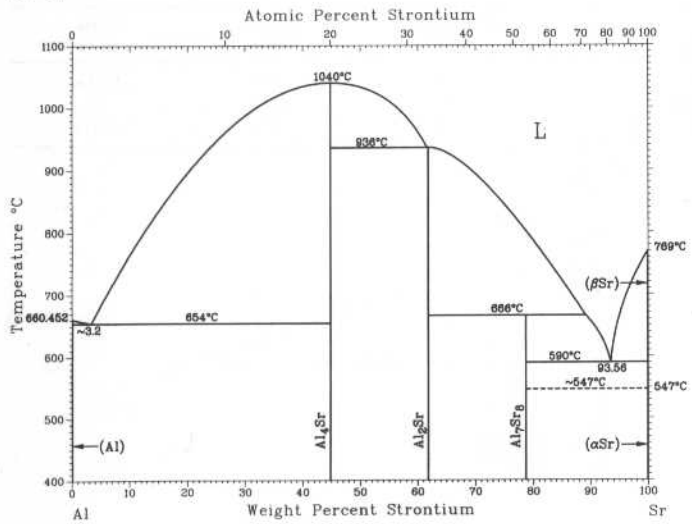

C.B. Alcock and V.P. Itkin, 1989

Phase	Composition, wt% Sr	Pearson symbol	Space group
(Al)	0	*cF*4	$Fm\bar{3}m$
Al_4Sr	45	*tI*10	*I*4/*mmm*
Al_2Sr	61.9	*oI*12	*Imma*
Al_7Sr_8	78.8	*cP*60	$P2_13$
(βSr)	100	*cI*2	$Im\bar{3}m$
(αSr)	100	*cF*4	$Fm\bar{3}m$

Al-Ta

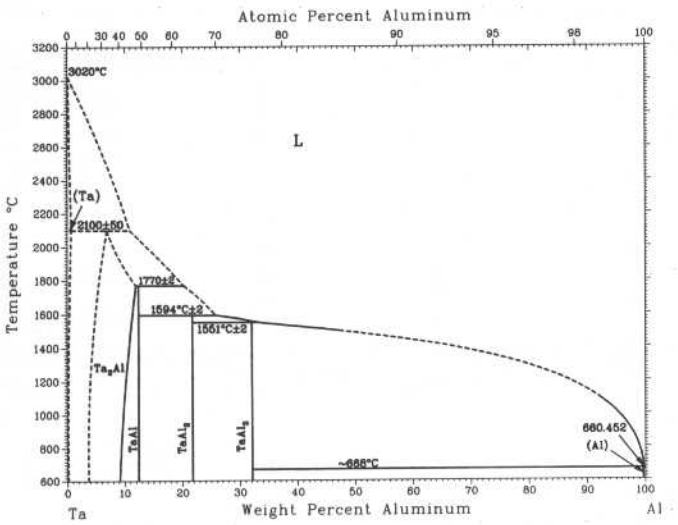

U.R. Kattner, unpublished

Phase	Composition, wt% Al	Pearson symbol	Space group
(Ta)	0 to 0.6	*cI*2	$Im\bar{3}m$
Ta_2Al	4 to 9	*tP*30	$P4_2/mnm$
TaAl	12.3	...	...
$TaAl_2$	22	*c*, *h*, or *o*	...
$TaAl_3$	32	*tI*8	*I*4/*mmm*
(Al)	100	*cF*4	$Fm\bar{3}m$

Note: Different unit cells are proposed for $TaAl_2$.

Al-Te

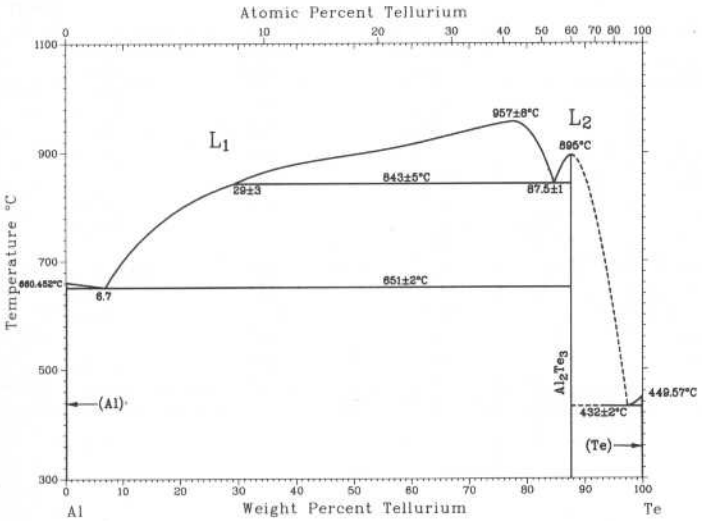

N. Prabhu and J.M. Howe, 1990

Phase	Composition, wt% Te	Pearson symbol	Space group
(Al)	0	*cF*4	$Fm\bar{3}m$
Al_2Te_3	88	*hP*4	$P6_3/mc$
(Te)	100	*hP*3	$P3_121$

Al-Th

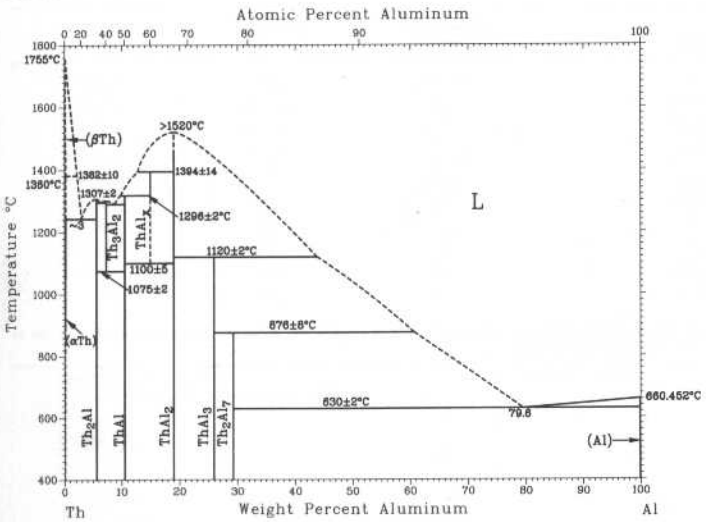

M.E. Kassner and D.E. Peterson, 1989

Phase	Composition, wt% Al	Pearson symbol	Space group
(αTh)	0 to 0.10	*cF*4	$Fm\bar{3}m$
(βTh)	0	*cI*2	$Im\bar{3}m$
Th_2Al	5.5	*tI*12	*I*4/*mcm*
Th_3Al_2	7	*tP*10	*P*4/*mbm*
ThAl	10.4	*oC*8	*Cmcm*
$ThAl_x$	15.6 to 16.2	(a)	...
Th_2Al_3(b)	15	(a)	...
Th_4Al_7(b)	16.9	(a)	...
$ThAl_2$	18.9	*hP*3	*P*6/*mmm*
$ThAl_3$	26	*hP*8	$P6_3/mmc$
Th_2Al_7	29.0	*oP*18	*Pbam*
(Al)	100	*cF*4	$Fm\bar{3}m$

(a) Tetragonal. (b) Considered same as $ThAl_x$

Al-Ti

J.L. Murray, 1987

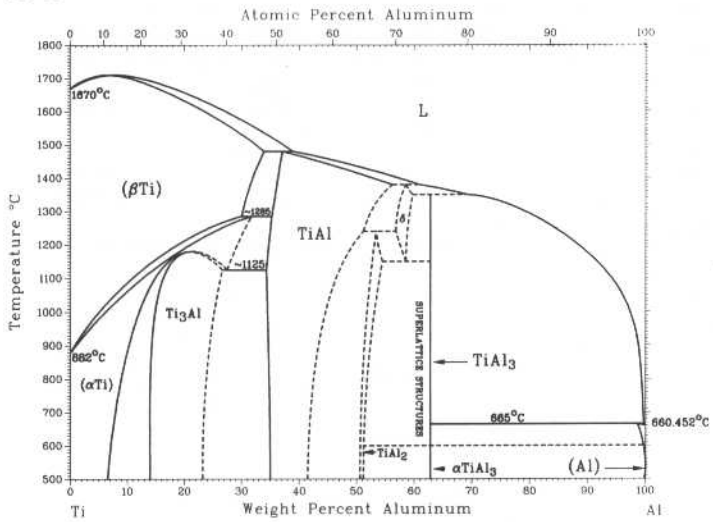

Phase	Composition, wt% Al	Pearson symbol	Space group
(βTi)	0 to 33.8	*cI*2	$Im\bar{3}m$
(αTi)	0 to 32	*hP*2	$P6_3/mmc$
Ti_3Al	14 to 26	*hP*8	$P6_3/mmc$
TiAl	34 to 56.2	*tP*4	*P*4/*mmm*
Ti_3Al_5(a)	44 to 49	*tP*32	*I*4/*mbm*
$TiAl_2$	51 to 54	*tI*24	$I4_1/amd$
αTiAl$_2$(b)	...	*oC*12	*Cmmm*
δ	57 to 59.8	(c)	...
$TiAl_3$	63	*tI*8	*I*4/*mmm*
αTiAl$_2$	63	(d)	...
(Al)	98.8 to 100	*cF*4	$Fm\bar{3}m$

(a) Not an equilibrium phase. (b) Not shown on the assessed diagram. (c) Long-period superlattice structures. (d) Tetragonal; a superstructure of the $D0_{22}$ lattice

Al-U

M.E. Kassner, M.G. Adamson, P.H. Adler, and D.E. Peterson, 1990

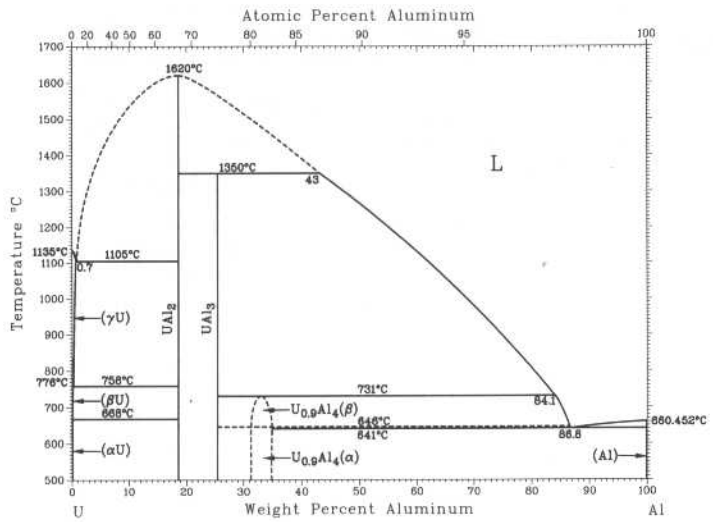

Phase	Composition, wt% Al	Pearson symbol	Space group
(γU)	0 to 0.6	*cI*2	$Im\bar{3}m$
(βU)	0 to 0.06	*tP*30	$P\bar{4}n2$
(αU)	0	*oC*4	*Cmcm*
UAl_2	18.5	(a)	...
	18.5	*cF*24	$Fd\bar{3}m$
UAl_3	25	*cP*4	$Pm\bar{3}m$
	25	(a)	...
UAl_4(b)	31	*oI*20	*I*2*ma* or *Imma*
$U_{0.9}Al_4(\alpha)$	33.5	*oI*20	*Imma*
$U_{0.9}Al_4(\beta)$	33.5	*oI*20	*Imma*
UAl_5	...	(c)	...
(Al)	100	*cF*4	$Fm\bar{3}m$

(a) Cubic. (b) Considered same as $U_{0.9}Al_4(\alpha)$. (c) Unknown

Al-V

J.L. Murray, 1989

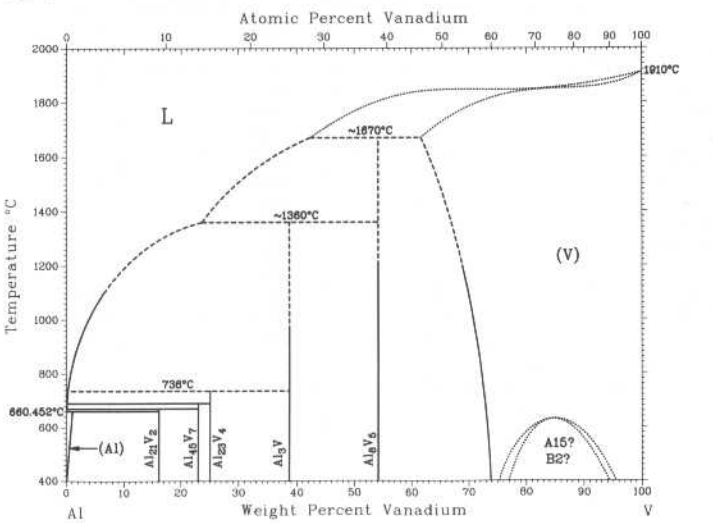

Phase	Composition, wt% V	Pearson symbol	Space group
(Al)	0 to 0.6	*cF*4	$Fm\bar{3}m$
$Al_{21}V_2$	~15.3 to 15.9	*cF*176	$Fd\bar{3}m$
$Al_{45}V_7$	~23.1	*mC*104	*C*2/*m*
$Al_{23}V_4$	~24.7	*hP*54	$P6_3/mmc$
Al_3V	~39	*tI*8	*I*4/*mmm*
Al_8V_5	54.2	*cI*52	$I4\bar{3}m$
(V)	~65 to 100	*cI*2	$Im\bar{3}m$
AlV_3	(a)	*cP*8	$Pm\bar{3}m$
βAlV_3	(a)	*h***	...
αAlV_3	(a)	*t***	...

Note: The structure of $Al_{23}V_4$ is related to that of Co_2Al_5 (ϕ). It contains nearly regular icosahedra as structural elements. (a) Unknown

Al-W

From [Metals]

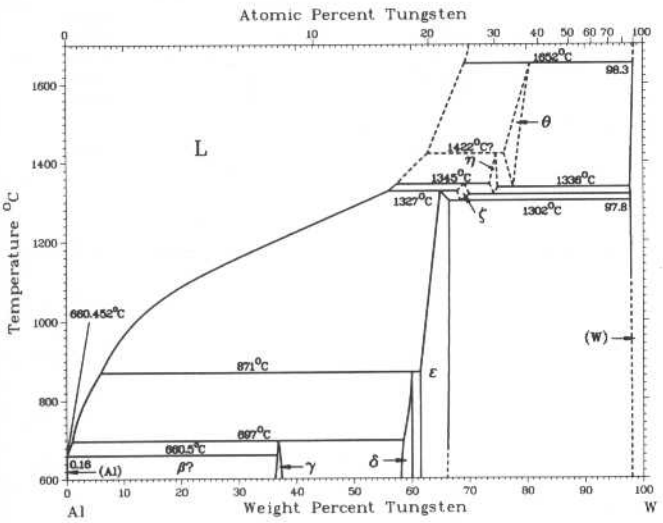

Phase	Composition, wt% W	Pearson symbol	Space group
(Al)	0	*cF*4	$Fm\bar{3}m$
γ	~37	*cI*26	$Im\bar{3}$
δ	~58 to 60	*hP*12	$P6_3$
ε	~62 to 66	*mC*30	*Cm*
(W)	100	*cI*2	$Im\bar{3}m$

Al-Y

K.A. Gschneidner, Jr. and F.W. Calderwood, 1989

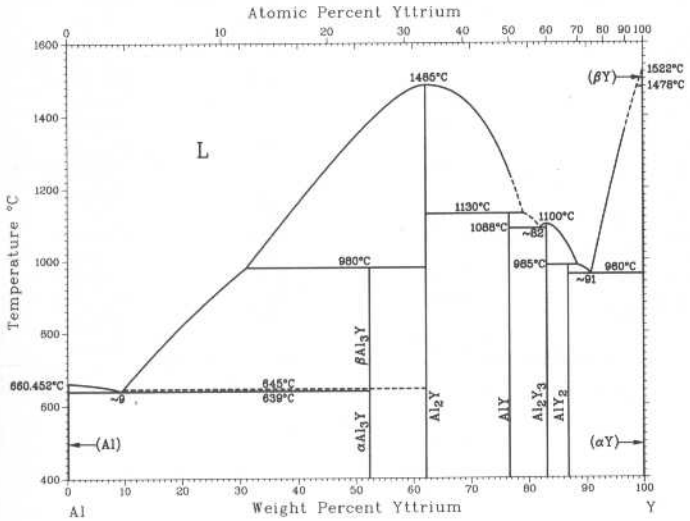

Phase	Composition, wt% Y	Pearson symbol	Space group
(Al)	0 to ~0.17	*cF*4	$Fm\bar{3}m$
αAl_3Y	52	*hP*8	$P6_3/mmc$
βAl_3Y	52	*hR*12	$R\bar{3}m$
Al_2Y	62.2	*cF*24	$Fd\bar{3}m$
AlY	76.7	*oC*8	*Cmcm*
Al_2Y_3	83	*tP*20	$P4_2/mnm$
AlY_2	86.8	*oP*12	*Pnma*
AlY_3(a)	91	*cP*4	$Pm\bar{3}m$
(αY)	100	*hP*2	$P6_3/mmc$
(βY)	100	*cI*2	$Im\bar{3}m$

(a) Metastable

Al-Yb

K.A. Gschneidner, Jr. and F.W. Calderwood, 1989

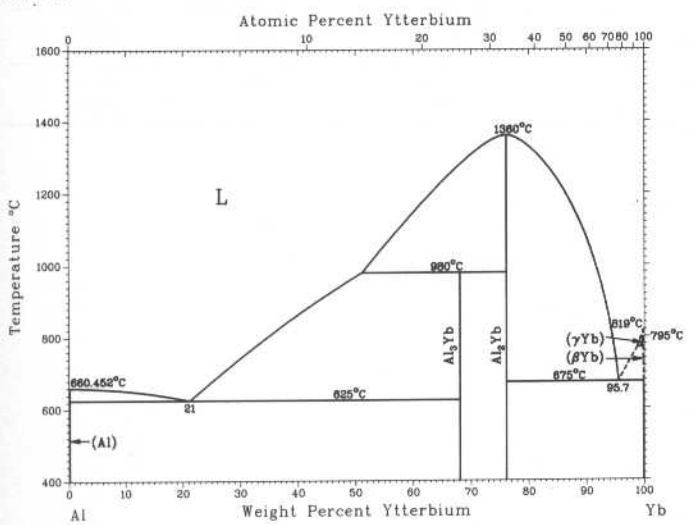

Phase	Composition, wt% Yb	Pearson symbol	Space group
(Al)	0	*cF*4	$Fm\bar{3}m$
Al_3Yb	68	*cP*4	$Pm\bar{3}m$
Al_2Yb	76.2	*cF*24	$Fd\bar{3}m$
(γYb)	99.6 to 100	*cI*2	$Im\bar{3}m$
(βYb)	99.9 to 100	*cF*4	$Fm\bar{3}m$

Al-Zn

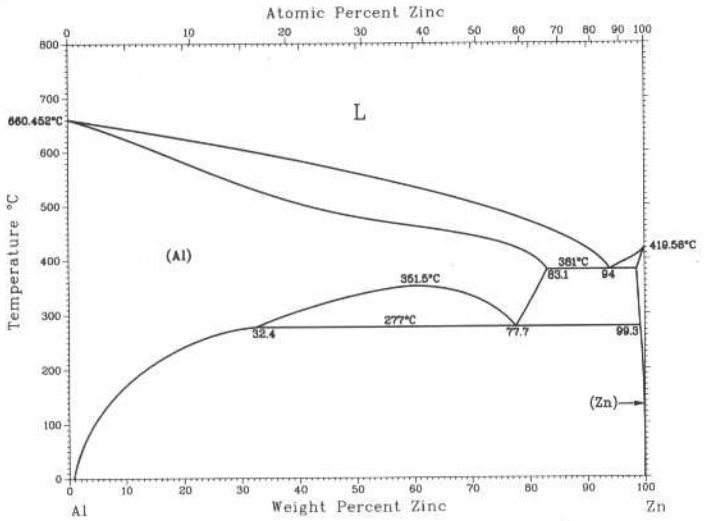

J.L. Murray, 1983

Phase	Composition, wt% Zn	Pearson symbol	Space group
(Al)	0 to 83.1	*cF*4	$Fm\bar{3}m$
(Zn)	98.8 to 100	*hP*2	$P6_3/mmc$
Metastable phases			
$(\alpha'Al)_R$	78 to ~85	...	$R\bar{3}m$
"*R*"	(a)	...	...
Y	...	...	...

(a) Coherent precipitate

Al-Zr

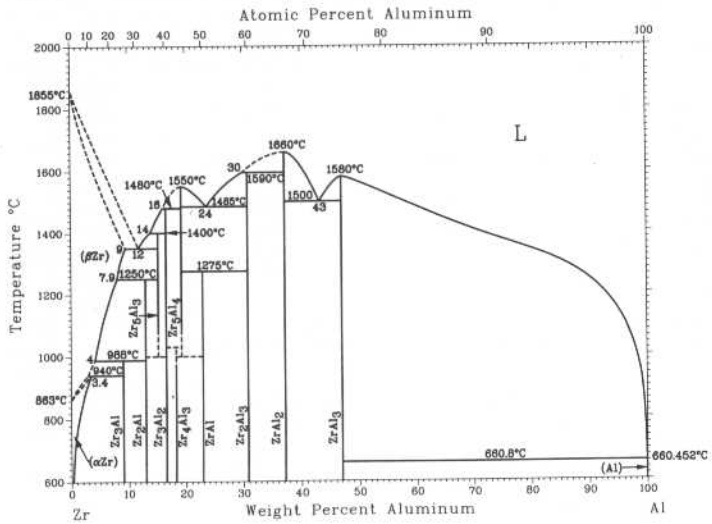

J. Murray, A. Peruzzi, and J.P. Abriata, 1992

Phase	Composition, wt% Al	Pearson symbol	Space group
(αZr)	0 to 3.4	*hP*2	$P6_3/mmc$
(βZr)	0 to 9.4	*cI*2	$Im\bar{3}m$
Zr_3Al	9.0	*cP*4	$Pm\bar{3}m$
Zr_2Al	12.9	*hP*6	$P6_3/mmc$
Zr_5Al_3	15.1	*tI*32	$I4/mcm$
Zr_3Al_2	16	*tP*20	$P4_2/mmm$
Zr_4Al_3	18.2	*hP*7	$P\bar{6}$
Zr_5Al_4	19.1	*hP*18	$P6_3/mcm$
ZrAl	22.8	*oC*8	*Cmcm*
Zr_2Al_3	31	*oF*40	*Fdd*2
$ZrAl_2$	37.2	*hP*12	$P6_3/mmc$
$ZrAl_3$	47	*tI*16	*I*4/*mmm*
(Al)	99.86 to 100	*cF*4	$Fm\bar{3}m$

As-Au

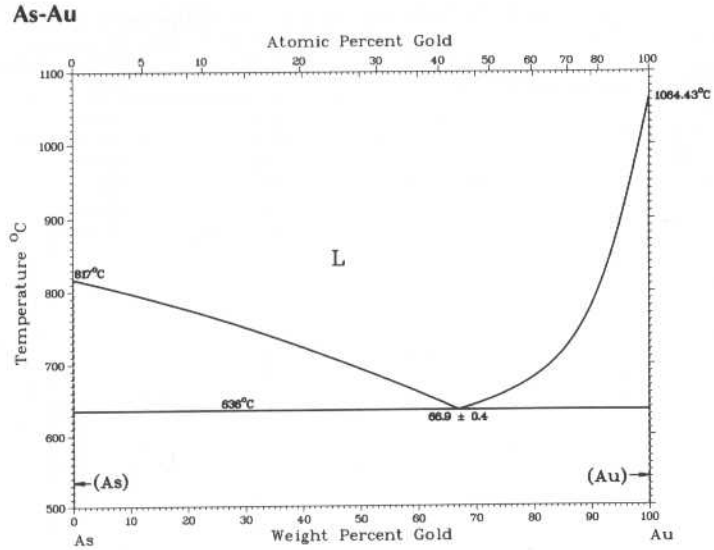

H. Okamoto and T.B. Massalski, 1987

Phase	Composition, wt% Au	Pearson symbol	Space group
(As)	0	*hR*2	$R\bar{3}m$
(Au)	100	*cF*4	$Fm\bar{3}m$

As-Bi

G.A. Geach and R.A. Jettery, 1953

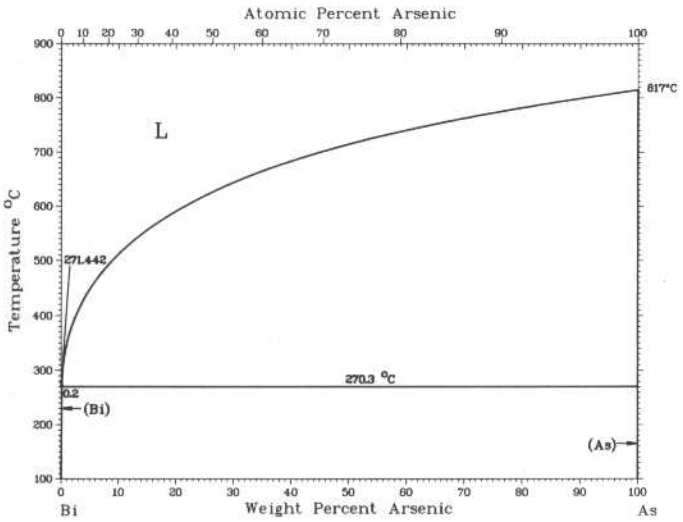

Phase	Composition, wt% As	Pearson symbol	Space group
(Bi)	0 to ~0.2	*hR*2	$R\bar{3}m$
(As)	~100	*hR*2	$R\bar{3}m$

As-Cd

H. Okamoto, 1992

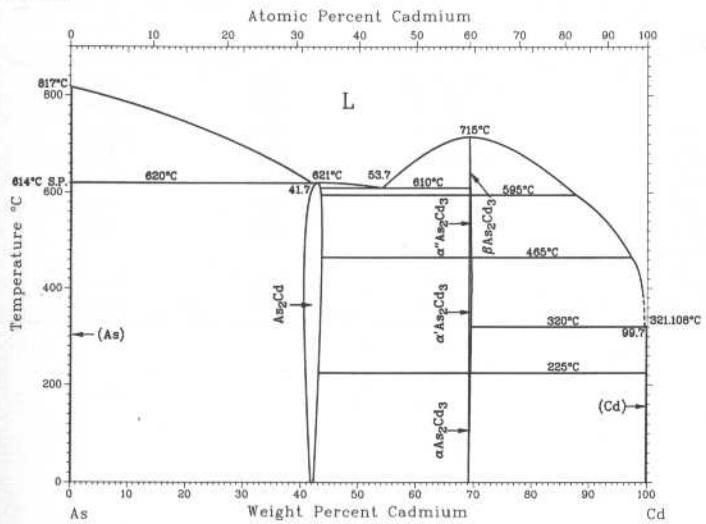

Phase	Composition, wt% Cd	Pearson symbol	Space group
(As)	0	*hR*2	$R\bar{3}m$
As_2Cd	42.8	*tI*12	$I4_122$
βAs_2Cd_3	69	*cF*12	$Fm\bar{3}m$
$\alpha''As_2Cd_3$	69	*tP*40	$P4_2/nmc$
$\alpha'As_2Cd_3$	69	*tP*160	$P4_2/nbc$
αAs_2Cd_3	69	*tI*160	$I4_1cd$
(Cd)	100	*hP*2	$P6_3/mmc$
High-pressure phases			
As_2CdII	42.8	...	...
AS_2CdIII(a)	42.8	...	...
AsCd	60	*oP*16	*Pbca*
As_2Cd_3(b)	69	*hP*30	...
As_2Cd_3II(c)	69	*hP*5	$P\bar{3}m1$
		*oP**	*Pmmn*
As_2Cd_3II'	69	...	...
As_2Cd_3III	69	...	...
As_2Cd_3III'	69	...	...
Metastable phase			
As_4Cd	27	*t**20	...
Other phases			
As_2Cd_3(d)	69	*tI*160	$I4_1/acd$
As_2Cd_3(e)	69	*tI*160	$I4_1\alpha$
As_2Cd_3(f)	69	*tI*160	*Iacd*

(a) >46 kbar. (b) 55 kbar. (c) 30 kbar. (d) Also might be βAs_2Cd_3. (e) Vapor deposition. (f) Synthesis at 675 °C

As-Co

K. Ishida and T. Nishizawa, 1990

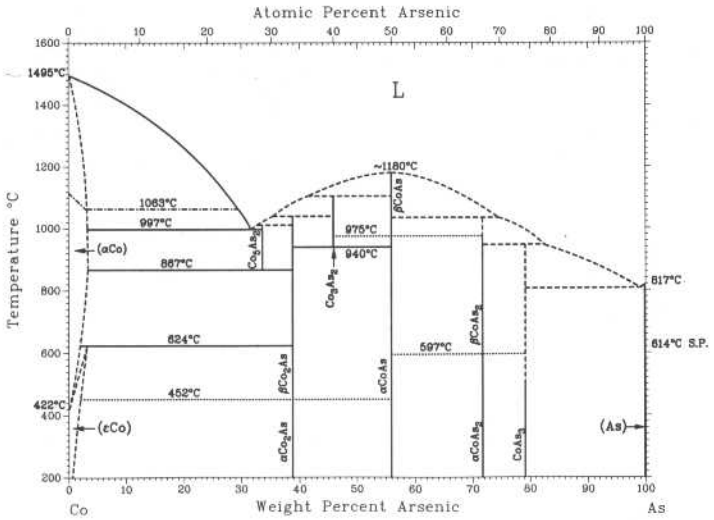

Phase	Composition, wt % As	Pearson symbol	Space group
(αCo)	0 to ~3.2	*cF*4	$Fm\bar{3}m$
(εCo)	0 to ~3	*hP*2	$P6_3/mmc$
Co_5As_2	33.7	*hP*42	$P6_3cm$
βCo_2As(a)	38.8 to 39.2	*hP*9	$P\bar{6}2m$
αCo_2As(a)	38.8	...	...
Co_3As_2	46	?	?
βCoAs	55.9	*hP*4	$P6_3/mmc$
αCoAs	55.9	*oP*8	$Pna2_1$
$\beta CoAs_2$	71.8	*oP*6	*Pnnm*
$\alpha CoAs_2$	71.8	*mP*12	$P2_1/c$
$CoAs_3$	79 to 79.2	*cI*32	$Im\bar{3}$
(As)	~100	*hR*2	$R\bar{3}m$

(a) αCo_2As (low-temperature form) transforms into βCo_2As (high-temperature form) at 452 °C

As-Cu

P.R. Subramanian and D.E. Laughlin, 1988

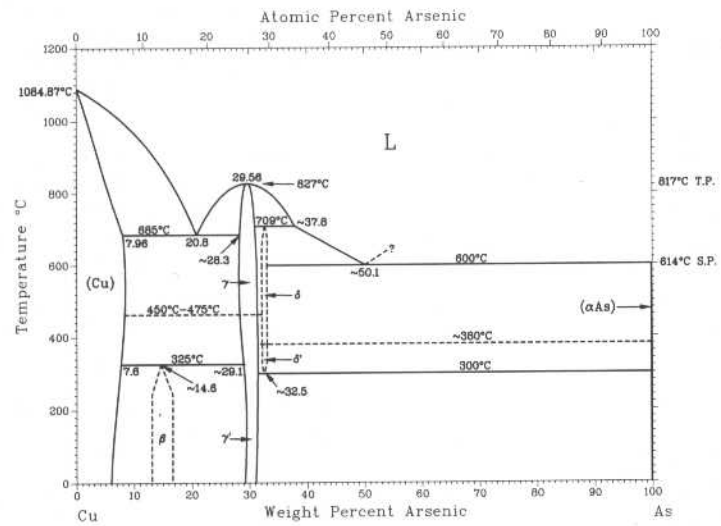

Phase	Composition, wt % As	Pearson symbol	Space group
(Cu)	0 to ~7.96	*cF*4	$Fm\bar{3}m$
β	12.8 to 16.4	*hP*2	$P6_3/mmc$
γ(HT)	28.2 to 31.2	*hP*8	$P6_3/mmc$
γ′(LT)	28.8 to 31.2	*hP*24	$P\bar{3}c1$
δ(HT)	32.1 to 33.1	*cF*16	$Fm\bar{3}m$
δ′(LT)	32.1 to 33.1	*oI*28	*Ibam*
(As)	100	*hR*2	$R\bar{3}m$
Metastable phases			
Cu_2As	~37.1	*tP*6	*P*4/*nmm*
Cu_3As_4	~61.12	*oI*28	*Immm*

As-Fe

H. Okamoto, 1992

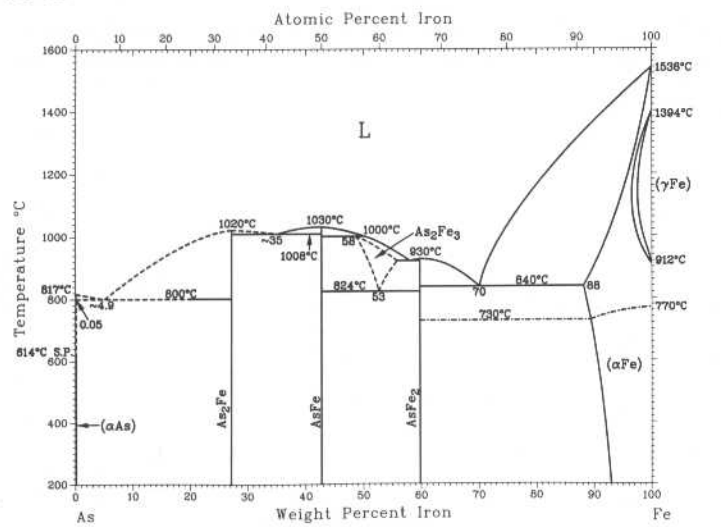

Phase	Composition, wt % Fe	Pearson symbol	Space group
(αAs)	0 to 0.05	*hR*2	$R\bar{3}m$
As_2Fe	27.1	*oP*6	*Pnnm*
AsFe	42.7	*oP*8	*Pnma*
As_2Fe_3	50 to 55	...	...
$AsFe_2$	59.9	*tP*6	*P*4/*nmm*
(αFe)	88 to 100	*cI*2	$Im\bar{3}m$
(γFe)	98.7 to 100	*cF*4	$Fm\bar{3}m$
High-pressure phase			
As_5Fe_{12}	64.2	*hR*17	*R*3

As-Ga

H. Okamoto, 1990

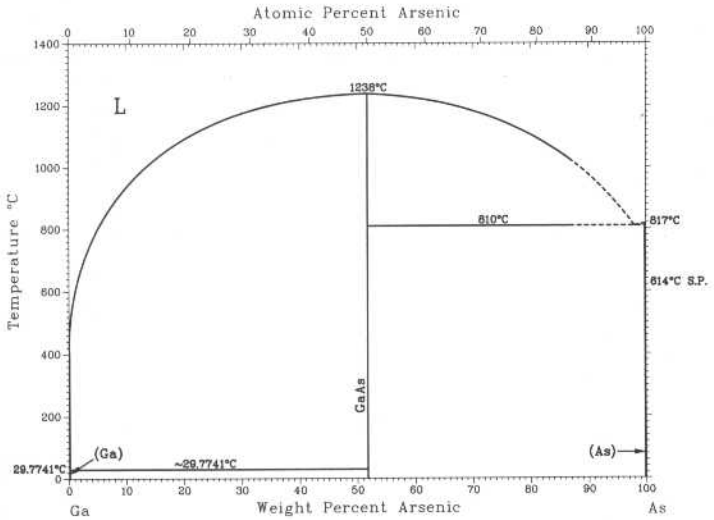

Phase	Composition, wt% As	Pearson symbol	Space group
(Ga)	0	*oC*8	*Cmca*
GaAs	51.8	*cF*8	$F\bar{4}3m$
(As)	100	*hR*2	$R\bar{3}m$

As-Ge

H. Okamoto, 1991

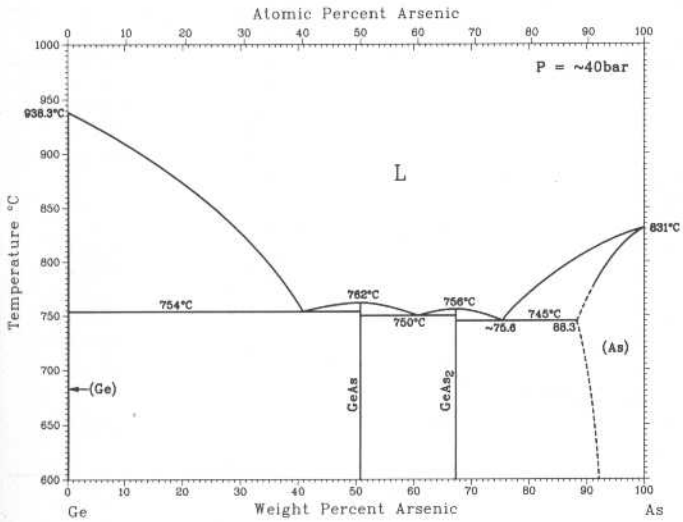

Phase	Composition, wt% As	Pearson symbol	Space group
(Ge)	0 to 0.19	*cF*8	$Fm\bar{3}m$
GeAs	50.8	*mC*24	*C*2/*m*
GeAs(a)	50.8	*tI*4	*I*4*mm*
$GeAs_2$	67.4	*oP*24	*Pbam*
(As)	88 to 100	*hR*2	$R\bar{3}m$

(a) High-pressure phase

As-In

H. Okamoto, 1992

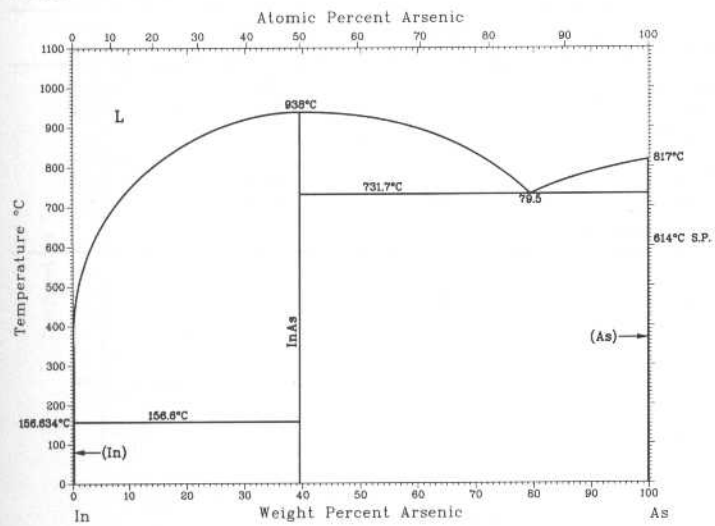

Phase	Composition, wt% As	Pearson symbol	Space group
Stable phases			
(In)	0	*tI*2	*I*4/*mmm*
InAs	39.5	*cF*8	$F\bar{4}3m$
(As)	100	*hR*2	$R\bar{3}m$
High-pressure phases			
InAs II(a)	39.5	*cF*8	$Fm\bar{3}m$
InAs III(b)	39.5	*tI*4	*I*4/*amd*

(a) Between 7 and 15 GPa. (b) Above 17 GPa (hysteresis between 15 and 17 GPa)

As-K

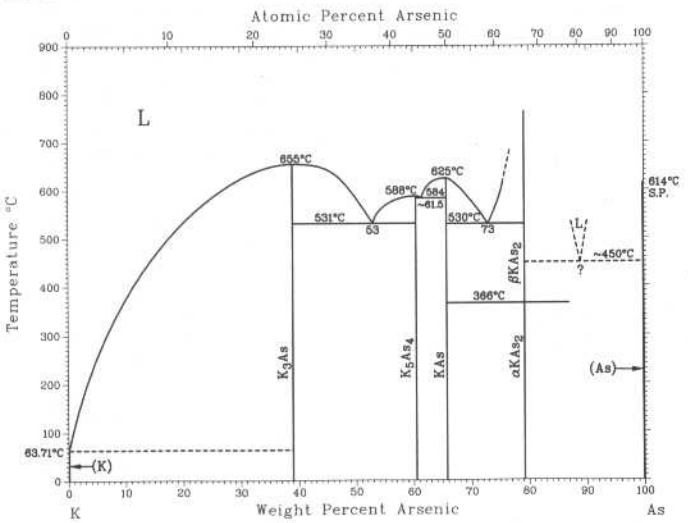

F.W. Dorn, W. Klemm, and S. Lohmeyer, 1961

Phase	Composition, wt% As	Pearson symbol	Space group
(K)	~0	*cI*2	$Im\bar{3}m$
K_3As	39	*hP*8	$P6_3/mmc$
K_5As_4	60.5	...	...
KAs	65.7	*oP*16	$P2_12_12_1$
βKAs_2	79.3	...	...
αKAs_2	79.3	...	...
(As)	~100	*hR*8	$R\bar{3}m$

As-Mn

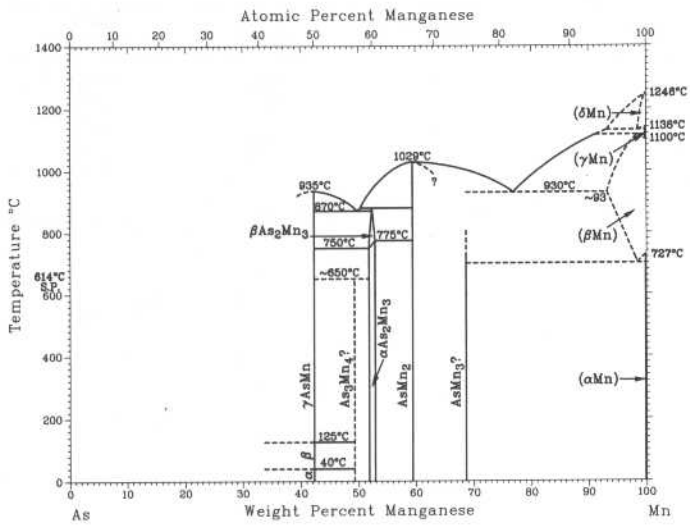

H. Okamoto, 1989

Phase	Composition, wt% Mn	Pearson symbol	Space group
(As)	0	*hR*2	$R\bar{3}m$
γAsMn	42.3	*hP*4	$P6_3/mmc$
βAsMn	42.3	*oP*8	*Pnma*
αAsMn	42.3	*hP*4	$P6_3/mmc$
As_3Mn_4	49.4	*tI**	...
βAs_2Mn_3	52	...	...
αAs_2Mn_3	52	(a)	...
$AsMn_2$	59.5	*tP*6	*P4/nmm*
$AsMn_3$	69	*oP*16	*Pmmn*
(δMn)	100	*cI*2	$Im\bar{3}m$
(γMn)	100	*cF*4	$Fm\bar{3}m$
(βMn)	~ 93 to 100	*cP*20	$P4_132$
(αMn)	100	*cI*58	$I4\bar{3}m$
High-pressure phase			
$AsMn_2$	59.5	*hP*9	$P\bar{6}2m$

(a) Distorted cubic

As-Nd

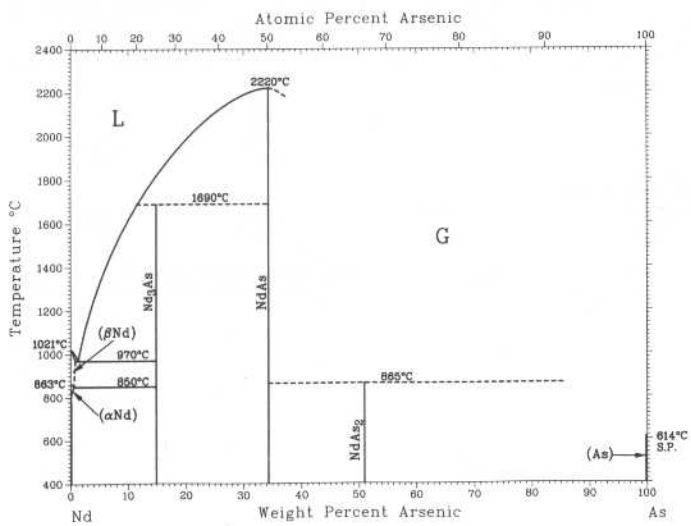

K.A. Gschneidner, Jr. and F.W. Calderwood, 1986

Phase	Composition, wt% As	Pearson symbol	Space group
(αNd)	0	*hP*4	$P6_3/mmc$
(βNd)	0	*cI*2	$Im\bar{3}m$
Nd_3As	15	(a)	...
NdAs	34.2	*cF*8	$Fm\bar{3}m$
$NdAs_2$	51.0	*mP*12	$P2_1/c$
(As)	100	*hR*2	$R\bar{3}m$

(a) Structure not known

As-Ni

M. Singleton and P. Nash, 1991

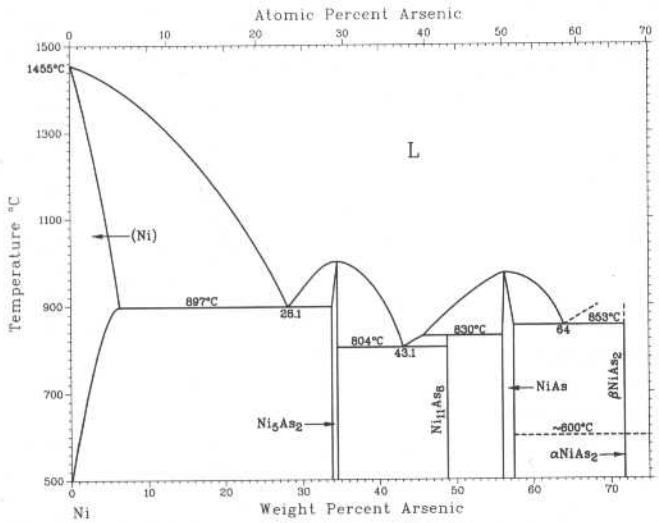

Phase	Composition, wt% As	Pearson symbol	Space group
(Ni)	0 to 6.30	*cF*4	$Fm\bar{3}m$
Ni_5As_2	33.27 to 33.99	*hP*42	Pb_3cm
$Ni_{11}As_8$	48.1	*tP*76	$P4_12_12$
NiAs	56.1 to 57.4	*hP*4	$P6_3/mmc$
$\alpha NiAs_2$	71.86(a)	*oP*24	*Pbca*
$\beta NiAs_2$	71.86	*oP*6	*Pnnm*

(a) Up to 600 °C

As-P

I. Karakaya and W.T. Thompson, 1991

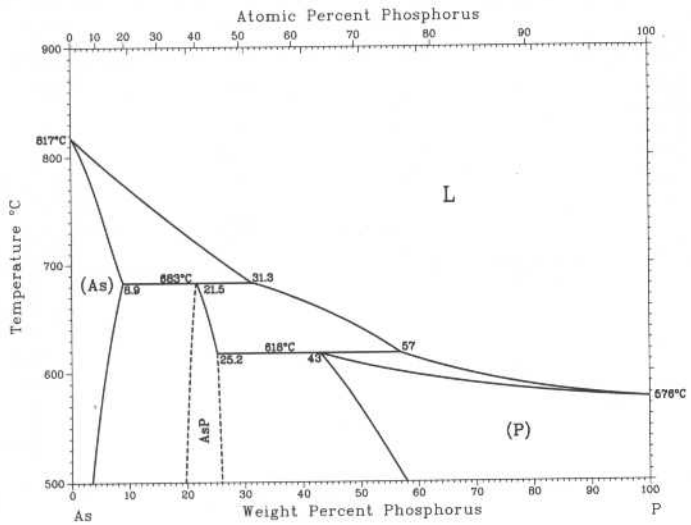

Phase	Composition, wt% P	Pearson symbol	Space group
(As)	0 to 8.9	*hR*2	$R\bar{3}m$
AsP	~21.5	...	...
P (black)	100	*oC*8(a)	*Cmca*
P (white)	43 to 100	(b)	...
P (red)	100	(c)	...

(a) At high pressures, transforms to a rhombohedral structure. (b) Cubic at 35 °C. (c) Cubic with 66 atoms per unit cell

As-Pb

N.A. Gokcen, 1990

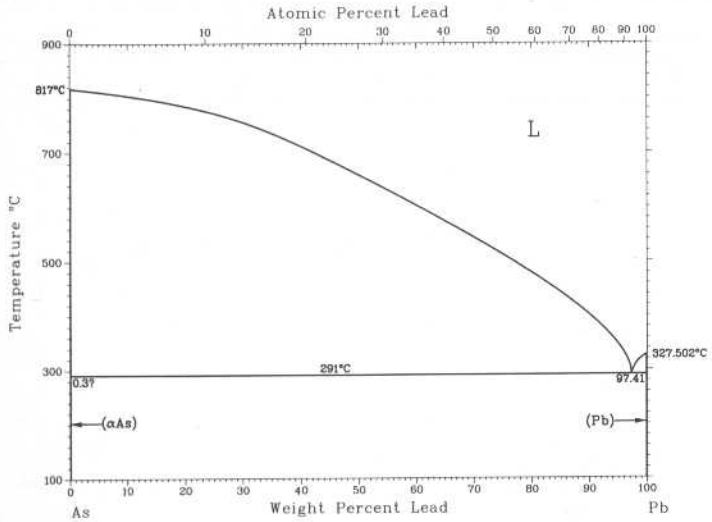

Phase	Composition, wt% Pb	Pearson symbol	Space group
(As)	0	*hR*2	$R\bar{3}m$
(Pb)	100	*cF*4	$Fm\bar{3}m$

As-Pd

H. Okamoto, 1992

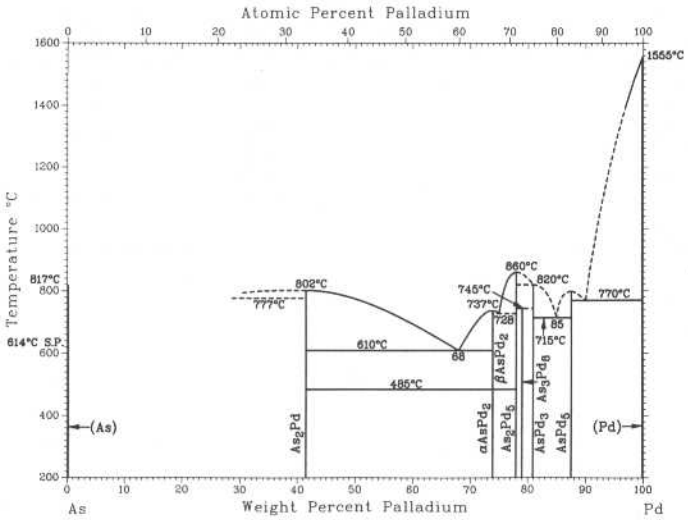

Phase	Composition, wt% Pb	Pearson symbol	Space group
(As)	0	*hR*2	$R\bar{3}m$
As_2Pd	41.5	*cP*12	$Pa\bar{3}$
$\beta AsPd_2$	74.0	*hP*9	$P\bar{6}2m$
$\alpha AsPd_2$	74.0	*mP*54	*P*2/*m*
As_2Pd_5	78.0	*hP**	...
As_2Pd_5	78.0	*hP*84	$P\bar{3}m1$
As_2Pd_5	78.0	*hP**	$P6_322$
As_2Pd_5	78.0	*hP**	$P\bar{3}m1$
As_3Pd_8	79.1	*hP*33	*P*3
$AsPd_3$	81	*tI*32	$I\bar{4}$
$AsPd_5$	87.6	*mC*24	*C*2
(Pd)	100	*cF*4	$Fm\bar{3}m$
Metastable phase			
$AsPd_5$	87.6	*cI*2	$Im\bar{3}m$
Questionable phases			
$\alpha AsPd_2$	74.0	*oC*24	$Cmc2_1$
$\alpha AsPd_2$	74.0	*hP**	...
As_2Pd_5	78.0	*o***	...
$AsPd_7$	90.9	...	...

As-S

H. Okamoto, 1990

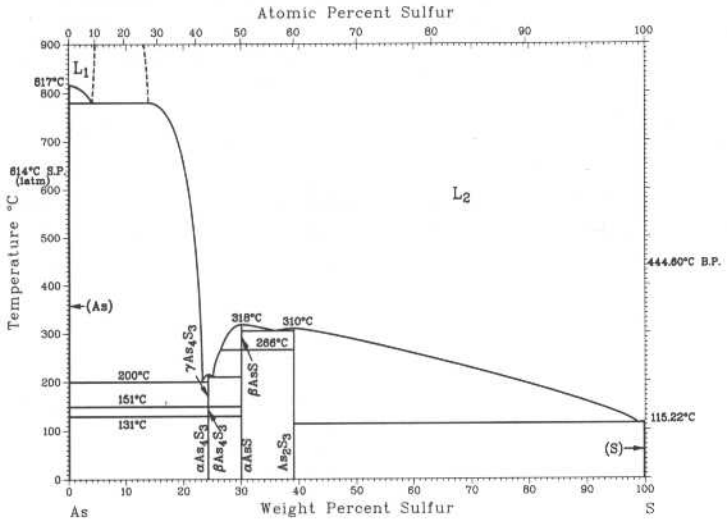

Phase	Composition, wt% S	Pearson symbol	Space group
(αAs)	0	*hR*2	$R\bar{3}m$
γAs_4S_3	24.3	...	...
βAs_4S_3	24.3	*t***	...
αAs_4S_3	24.3	*oP*28	*Pnma*
βAsS	30.0	*mP*32	$P2_1/n$
αAsS	30.0	*mP*32	$P2_1/c$
As_2S_3	39	*mP*20	$P2_1/c$
(S)	100	*oF*128	*Fddd*

As-Sb

H. Okamoto, 1990

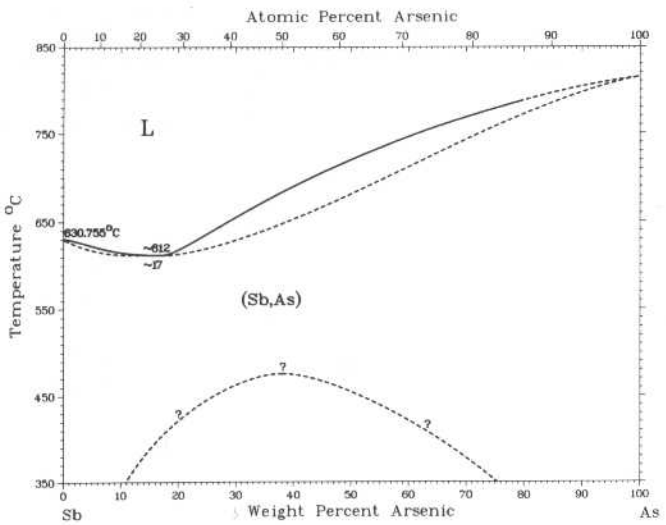

Phase	Composition, wt% As	Pearson symbol	Space group
(Sb,As)	0 to 100	*hR*2	$R\bar{3}m$

As-Se

H. Okamoto, 1990

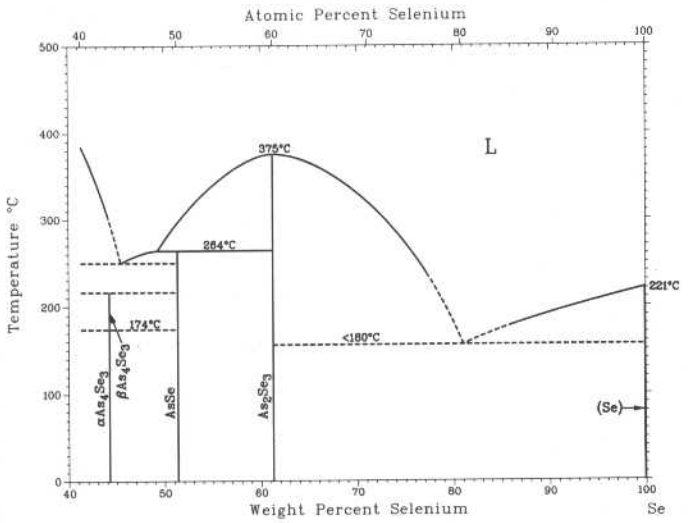

Phase	Composition, wt% Se	Pearson symbol	Space group
(As)	0	*hR*2	$R\bar{3}m$
βAs_4Se_3	44.2	*mC*112	*C*2/*c*
αAs_4Se_3	44.2	*oP*28	*Pnma*
AsSe	51.3	*mP*32	$P2_1/c$
As_2Se_3	61	*mP*20	$P2_1/c$
(γSe)	100	*hP*3	$P3_121$

As-Si

R. W. Olesinski and G.J. Abbaschian, 1985

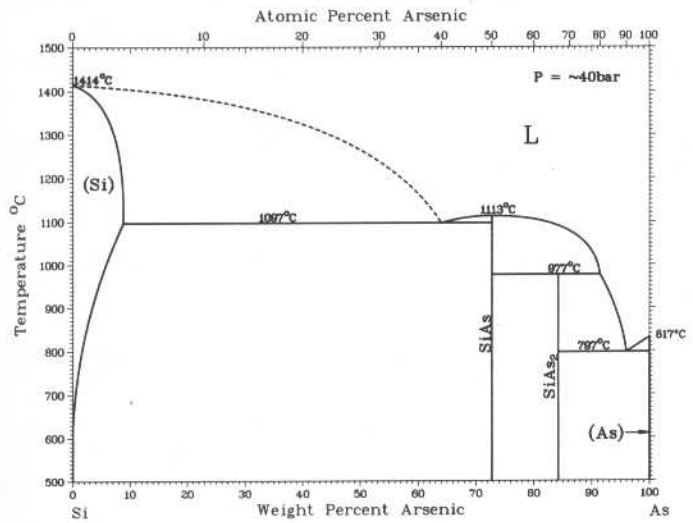

Phase	Composition, wt% As	Pearson symbol	Space group
(Si)	0 to 8.8	*cF*8	$Fd\bar{3}m$
SiAs	72.7	*o***	...
$SiAs_2$	84.2	*oP**	*Pbam*
$SiAs_2$(a)	84.2	*cP*12	$Pa\bar{3}$
(As)	~100	*hR*2	$R\bar{3}m$

(a) High-pressure phase

As-Sn

N.A. Gokcen, 1990

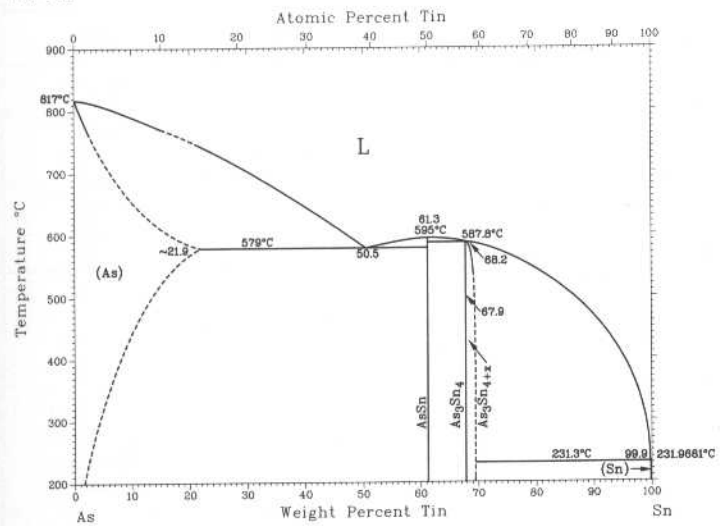

Phase	Composition, wt% Sn	Pearson symbol	Space group
(As)	0 to ~21.9	*hR*2	$R\bar{3}m$
AsSn	61.3	*cF*8	$Fm\bar{3}m$
As_3Sn_4	67.87 to 70?	*hR*7	$R\bar{3}m$
(βSn)(a)	99.9 to 100	*tI*4	$I4_1/amd$
(αSn)(b)	100	*cF*8	$Fm\bar{3}m$

(a) White tin, stable above 13 °C. (b) Grey tin, stable below 13 °C

As-Te

H. Okamoto, 1990

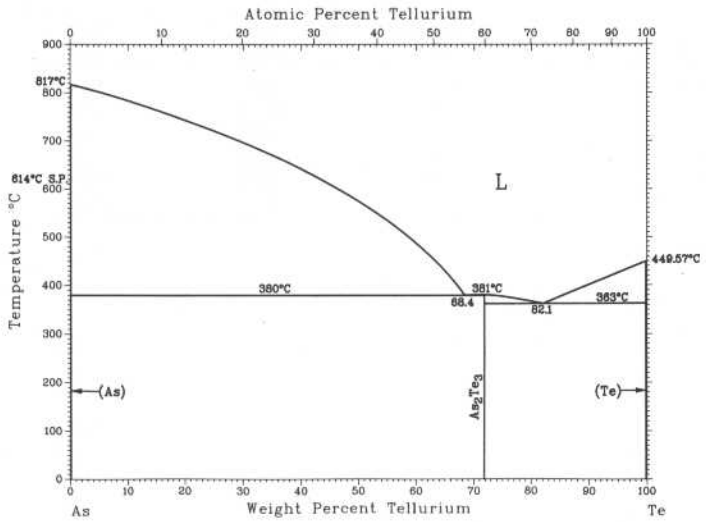

Phase	Composition, wt % Te	Pearson symbol	Space group
(As)	0	*hR*2	$R\bar{3}m$
As_2Te_3	72	*mC*20	*Cm*/2
(Te)	100	*hP*3	$P3_121$

As-Tl

R.C. Sharma and Y.A. Chang, unpublished

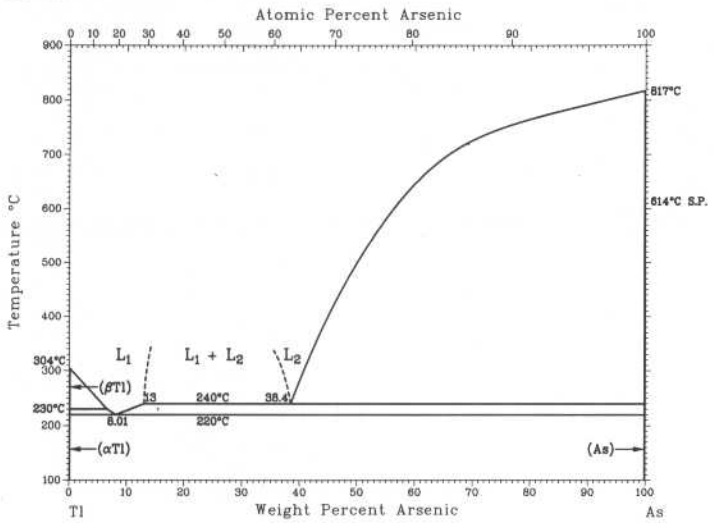

Phase	Composition, wt % As	Pearson symbol	Space group
(αTl)	0	*hP*2	$P6_3/mmc$
(βTl)	0	*cI*2	$Im\bar{3}m$
(As)	100	*hR*2	$R\bar{3}m$

As-Yb

H. Okamoto, 1990

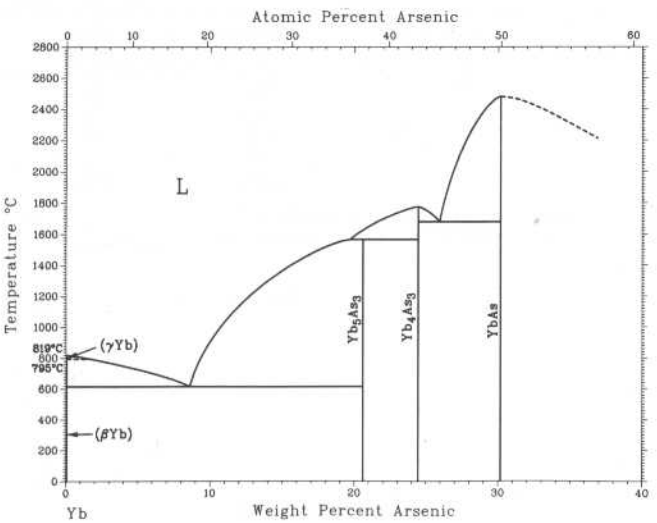

Phase	Composition, wt % As	Pearson symbol	Space group
(αYb)	0	*hP*2	$P6_3/mmc$
(βYb)	0	*cF*4	$Fm\bar{3}m$
(γYb)	0	*cI*2	$Im\bar{3}m$
Yb_5As_3	20.6	*hP*16	$P6_3/mcm$
αYb_4As_3	24.5	*hR*28	*R*3
βYb_4As_3	24.5	*cI*28	$I\bar{4}3d$
YbAs	30.2	*cF*8	$Fm\bar{3}m$
(As)	100	*hR*2	$R\bar{3}m$

As-Zn

H. Okamoto, 1992

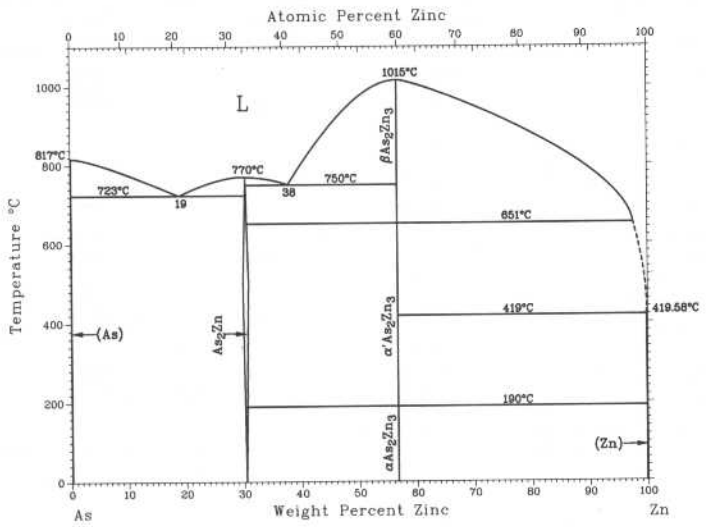

Phase	Composition, wt% Zn	Pearson symbol	Space group
(αAs)	0	*hR*2	$R\bar{3}m$
As_2Zn	30.3	*mP*24	$P2_1/c$
βAs_2Zn_3	56.7	*cF*12	$Fm\bar{3}m$
$\alpha' As_2Zn_3$	56.7	*tP*160	$P4_2/nbc$
αAs_2Zn_3	56.7	*tI*160	$I4_1cd$
(Zn)	100	*hP*2	$P6_3/mmc$
High-pressure phases			
AsZn	46.6	*oP*16	*Pbca*
As_2Zn_3II(a)	56.7	*cF**	...
As_2Zn_3II′	56.7	*oP**	*Pmmn*
As_2Zn_3III	56.7	...	...
As_2Zn_3(b)	56.7	*hP*30	...
Other phases			
As_2Zn	30.39	*o**32	...
As_2Zn_3	56.7	*cI*80	*Ia*3
	56.7	*tP*40	$P4_2/mmc$

(a) At 55 kbar. (b) At 70 kbar

Au-Be

H. Okamoto and T.B. Massalski, 1987

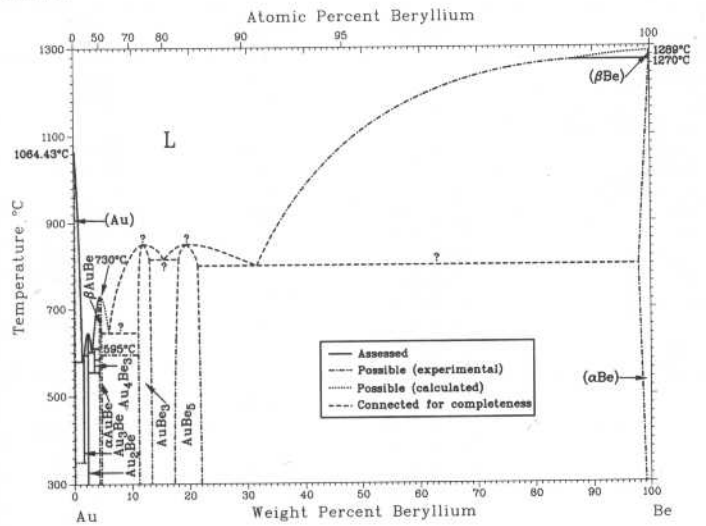

Phase	Composition, wt% Be	Pearson symbol	Space group
(Au)	0 to 0.009	*cF*4	$Fm\bar{3}m$
Au_3Be	2	*o***	...
Au_2Be	2.2	*tI*6	*I*4/*mmm*
Au_4Be_3	3.3	...	...
βAuBe	4.2 to 4.6	...	...
αAuBe	4.2 to 4.6	*cP*8	$P2_13$
$AuBe_3$	11 to 13	*cF*16	$Fd\bar{3}m$
$AuBe_5$	17 to 22	*cF*24	$F\bar{4}3m$
(βBe)	? to 100	*cI*2	$Im\bar{3}m$
(αBe)	94.81 to 100	*hP*2	$P6_3/mmc$

Au-Bi

H. Okamoto, 1990

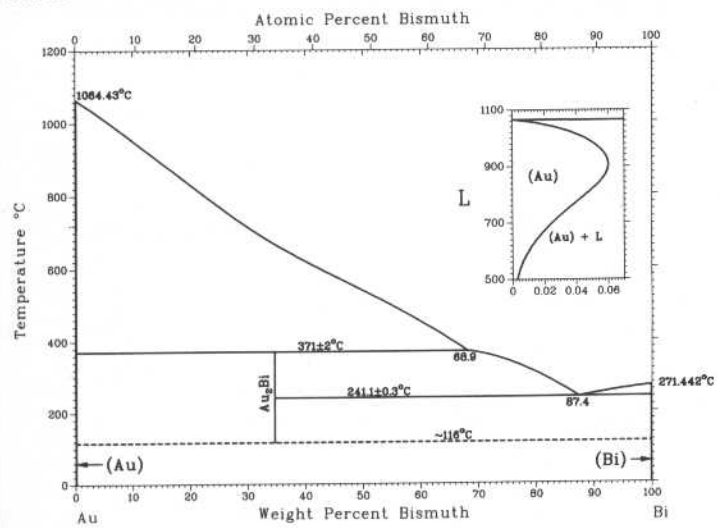

Phase	Composition, wt% Bi	Pearson symbol	Space group
(Au)	0	*cF*4	$Fm\bar{3}m$
Au_2Bi	34.6	*cF*24	$Fd\bar{3}m$
(Bi)	100	*hR*2	$R\bar{3}m$
Metastable phases			
π	76 to 81	*cP*1	$Pm\bar{3}m$
π'	61	*hR*1	$R\bar{3}m$
Microcrystalline	46 to 71	~200 π'-like unit cells	...
(AuBi)?	56	Complex	...

Au-Ca

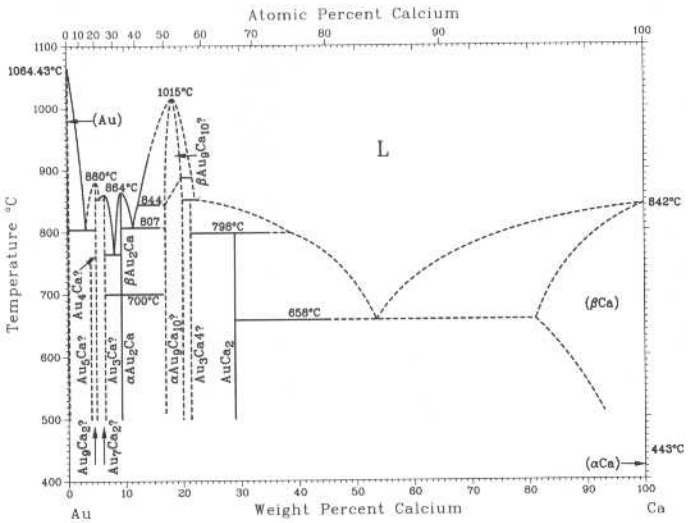

H. Okamoto, T.B. Massalski, C.B. Alcock, and V.P. Itkin, 1987

Phase	Composition, wt% Ca	Pearson symbol	Space group
(Au)	0 to <4.3	*cF*4	$Fm\bar{3}m$
Au_5Ca	3.9	*cF*24	$F\bar{4}3m$
Au_9Ca_2	4.3	?	...
Au_4Ca	5	?	...
Au_7Ca_2	5.5	(a)	...
Au_3Ca	6	(b)	...
βAu_2Ca	9.2	?	...
αAu_2Ca	9.2	?	...
AuCa	17	*oC*8	*Cmcm*
βAu_9Ca_{10}	17 to 20	(c)	...
αAu_9Ca_{10}	16 to 20.2	?	...
Au_3Ca_4	21.3	?	...
$AuCa_2$	29.0	?	...
(βCa)	81.2 to 100	*cI*2	$Im\bar{3}m$
(αCa)	? to 100	*cF*4	$Fm\bar{3}m$

(a) Same as Au_3Ca? (b) Not cubic. (c) Same as AuCa?

Au-Cd

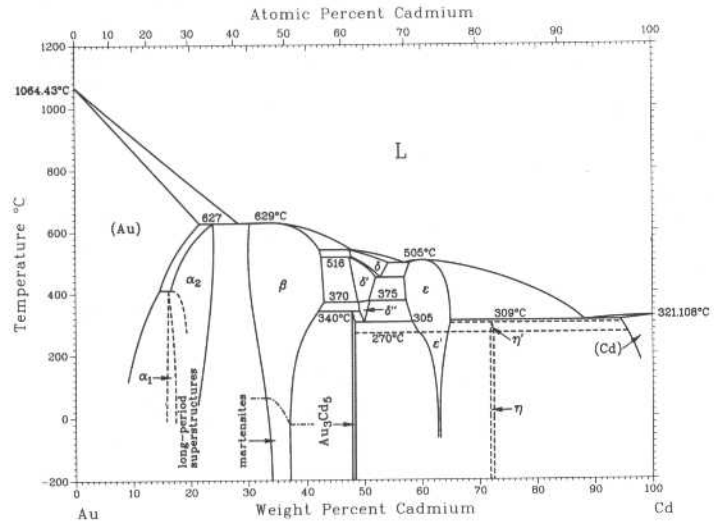

H. Okamoto and T.B. Massalski, 1987

Phase	Composition, wt% Cd	Pearson symbol	Space group
(Au)	0 to 21.6	*cF*4	$Fm\bar{3}m$
α_1	~16	...	$Pm\bar{3}m$
Long-period superstructures			
Au_3Cd	15	*tI*16	*I*4/*mmm*
4*H* (1*d*)	~16	*hP*4	$P6_3/mmc$
$9a_0$-4*H* (2*d*)	15 to 17	(a)	...
6*H*	16 to 17	*hR*3	$R\bar{3}m$
9*R*	16.7 to 19.7	(b)	...
$7a_0$ - 2*H*	19 to 23	(a)	$P6_3/mmc$
$9a_0$ - 2*H*	19 to 23	(a)	$P6_3/mcm$
α_2	16.3 to 24.0	*hP**	...
β	30 to 43	*cP*2	$Pm\bar{3}m$
β′ (c)	34.1	*oP*4	*Pmma*
β″ (c)	36	(a)	...
δ	47.3 to 54.3	*cI*52	$I\bar{4}3m$
δ′	47.3 to 52.0	*cI*52	$I\bar{4}3m$
δ″	48.9 to 50.9	...	...
Au_3Cd_5	47.8 to 48.3	*tI*32	*I*4/*mcm*
ε	57.0 to 65.0	(d)	...
ε′	59 to 64	(d)	...
η	72	...	...
η′	72	...	...
(Cd)	94.0 to 100	*hP*2	$P6_3/mmc$

Note: *d* = dimensional. (a) Hexagonal. (b) Rhombohedral. (c) Not shown in the assessed diagram. (d) bct

Au-Ce

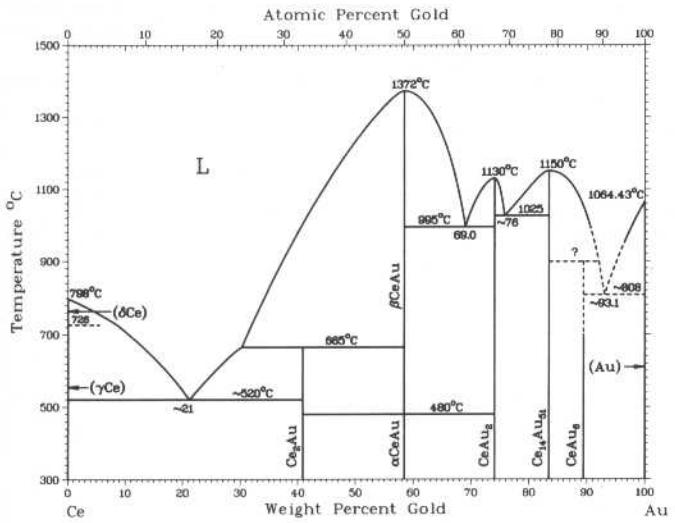

K.A. Gschneidner, Jr., F.W. Calderwood, H. Okamoto, and T.B. Massalski, 1987

Phase	Composition, wt% Au	Pearson symbol	Space group
(αCe)	0	*cF*4	$Fm\bar{3}m$
(βCe)	0	*hP*4	$P6_3/mmc$
(γCe)	0	*cF*4	$Fm\bar{3}m$
(δCe)	0	*cI*2	$Im\bar{3}m$
Ce_2Au	41.2	*oP*12	*Pnma*
αCeAu	58	*oP*8	*Pnma*
βCeAu	58	*oC*8	*Cmcm*
$CeAu_2$	73.8	*oI*12	*Imma*
$Ce_{14}Au_{51}$	81 to 83.7	*hP*65	*P6/m*
$CeAu_6$	89.4	*mC*28	*C/2c*
(Au)	100	*cF*4	$Fm\bar{3}m$

Au-Co

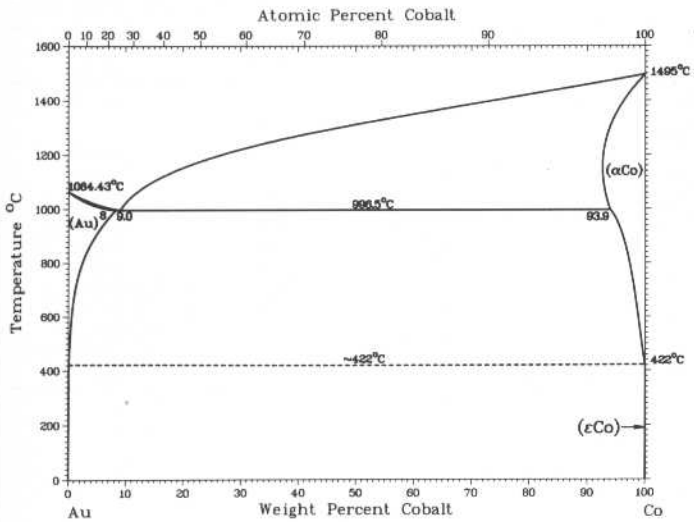

H. Okamoto, T.B. Massalski, M. Hasebe, and T. Nishizawa, 1987

Phase	Composition, wt% Co	Pearson symbol	Space group
(Au)	0 to 8	*cF*4	$Fm\bar{3}m$
(αCo)	92.1 to 100	*cF*4	$Fm\bar{3}m$
(εCo)	? to 100	*hP*2	$P6_3/mmc$

Au-Cr

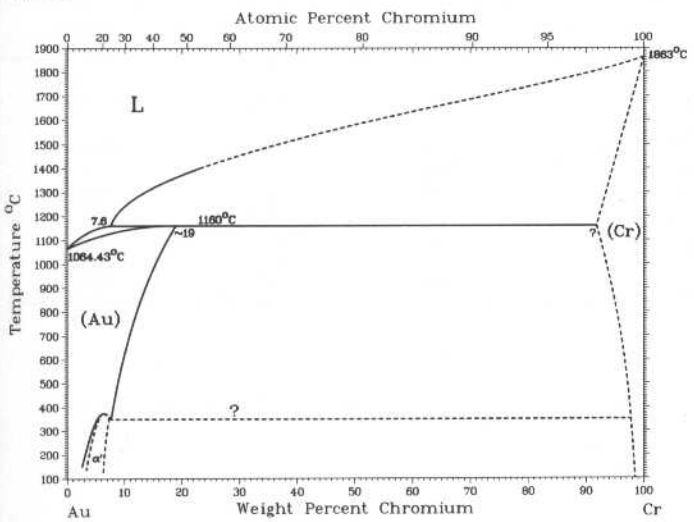

H. Okamoto and T.B. Massalski, 1987

Phase	Composition, wt% Cr	Pearson symbol	Space group
(Au)	0 to ~19	*cF*4	$Fm\bar{3}m$
α′	2 to 8	*tI*10	*I4/m*
(Cr)	~90 to 100	*cI*2	$Im\bar{3}m$

Au-Cu

H. Okamoto, D.J. Chakrabarti, D.E. Laughlin, and T.B. Massalski, 1987

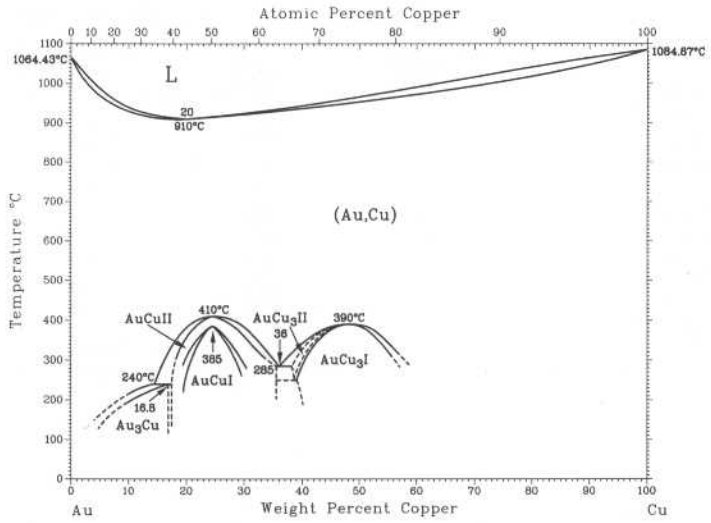

Phase	Composition, wt% Cu	Pearson symbol	Space group
(Au,Cu)	0 to 100	*cF*4	$Fm\bar{3}m$
Au_3Cu	3 to 16.8	*cP*4	$Pm\bar{3}m$
AuCu(I)	19 to 30	*tP*4	*P*4/*mmm*
AuCu(II)	16.8 to 35	*oI*40	*Imma*
$AuCu_3$(I)	40 to 58	*cP*4	$Pm\bar{3}m$
$AuCu_3$(II)	39 to ?	*tP*28	$P\bar{4}mm$

Au-Dy

K.A. Gschneidner, Jr., F.W. Calderwood, H. Okamoto, and T.B. Massalski, 1987

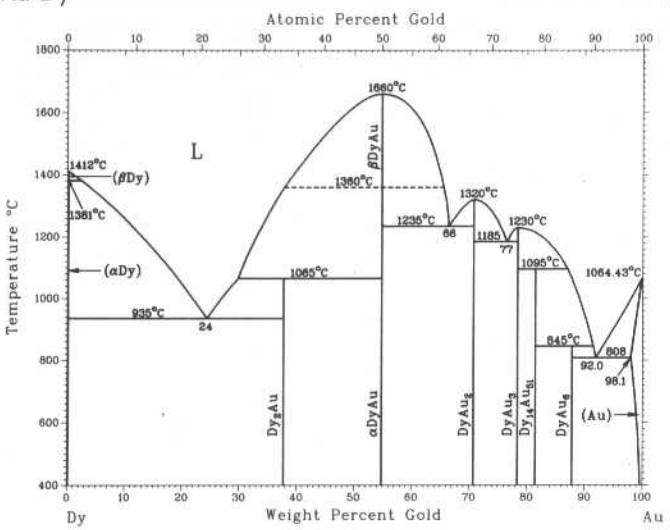

Phase	Composition, wt% Au	Pearson symbol	Space group
(αDy)	0	*hP*2	$P6_3/mmc$
(α′Dy)	0	(a)	...
(βDy)	0	*cI*2	$Im\bar{3}m$
Dy_2Au	37.7	*oP*12	*Pnma*
αDyAu	55	*oC*8	*Cmcm*
βDyAu	56	*cP*2	$Pm\bar{3}m$
$DyAu_2$	70.8	*tI*6	*I*4/*mmm*
$DyAu_3$	78	*oP*8	*Pmmn*
$Dy_{14}Au_{51}$	~81.6	*hP*65	*P*6/*m*
$DyAu_6$	87.9	*tP*56	$P4_2/ncm$
(Au)	98.1 to 100	*cF*4	$Fm\bar{3}m$

(a) Orthorhombic distortion, $T \leq 86$ K

Au-Eu

H. Okamoto, 1990

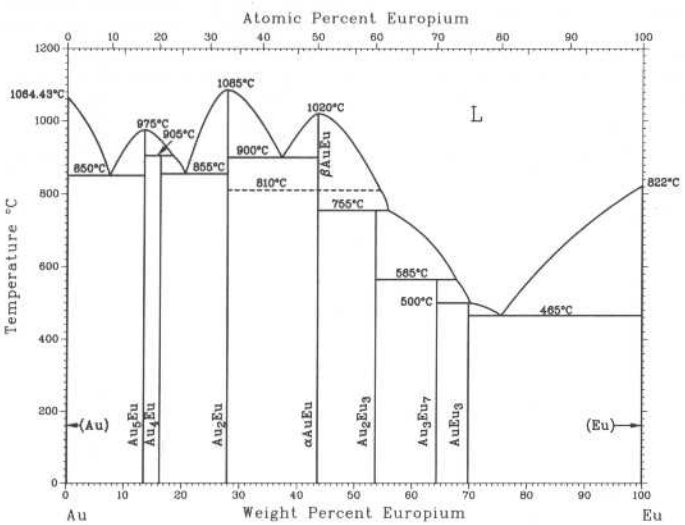

Phase	Composition, wt% Eu	Pearson symbol	Space group
(Au)	0	*cF*4	$Fm\bar{3}m$
Au_5Eu	13.4	*hP*6	*P*6/*mmm*
Au_4Eu	16	...	...
Au_2Eu	27.8	*oI*12	*Imma*
βAuEu	43.6	...	...
αAuEu	43.6	*oP*8	*Pnma*
Au_2Eu_3	54	*hR*45	$R\bar{3}$
Au_3Eu_7	64	*hP*20	$P6_3/mc$
$AuEu_3$	70	*oP*16	*Pnma*
(Eu)	100	*cI*2	$Im\bar{3}m$

Au-Fe

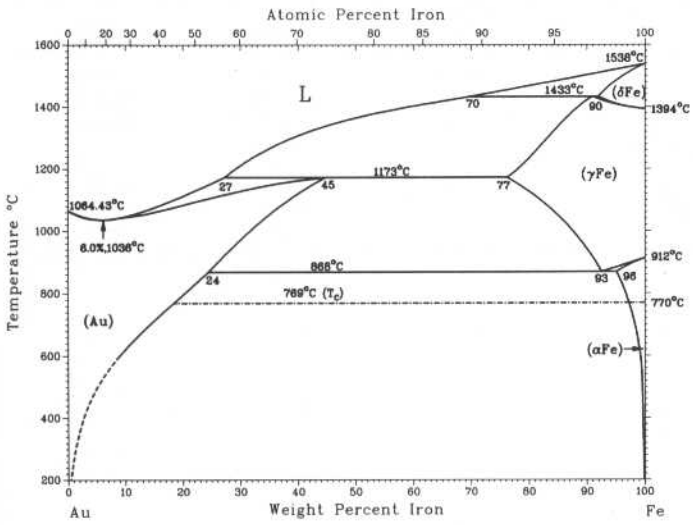

H. Okamoto, T.B. Massalski, L.J. Swartzendruber, and P.A. Beck, 1987

Phase	Composition, wt% Fe	Pearson symbol	Space group
(Au)	0 to 45	*cF*4	$Fm\bar{3}m$
(γFe)	77 to 100	*cF*4	$Fm\bar{3}m$
(αFe)	96 to 100	*cI*2	$Im\bar{3}m$
(δFe)	93 to 100	*cI*2	$Im\bar{3}m$
Metastable phases			
Amorphous(a)	19 to 72	...	...
fcc(b)	30 to 32	...	...
bcc(b)	32 to 53	...	...

(a) Found in thin films deposited at liquid nitrogen temperature or below. (b) Formed by crystallization on heating amorphous phase

Au-Ga

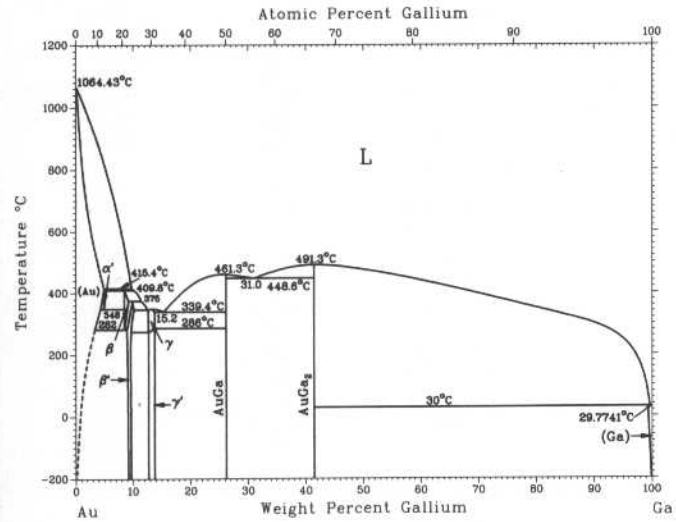

T.B. Massalski and H. Okamoto, 1987

Phase	Composition, wt% Ga	Pearson symbol	Space group
(Au)	0 to 4.8	*cF*4	$Fm\bar{3}m$
α′	4.9 to 5.5	*hP*16	$P6_3/mmc$
β	8.3 to 9.1	(a)	...
β′	8.7 to 10.5	(b)	...
γ	13.1 to 14	(b)	...
γ′	13.1 to 14	(b)	...
AuGa	26.1	*oP*8	*Pnma*
$AuGa_2$	41.5	*cF*12	$Fm\bar{3}m$
(Ga)	100	*oC*8	*Cmca*

(a) Hexagonal. (b) Orthorhombic

Au-Ge

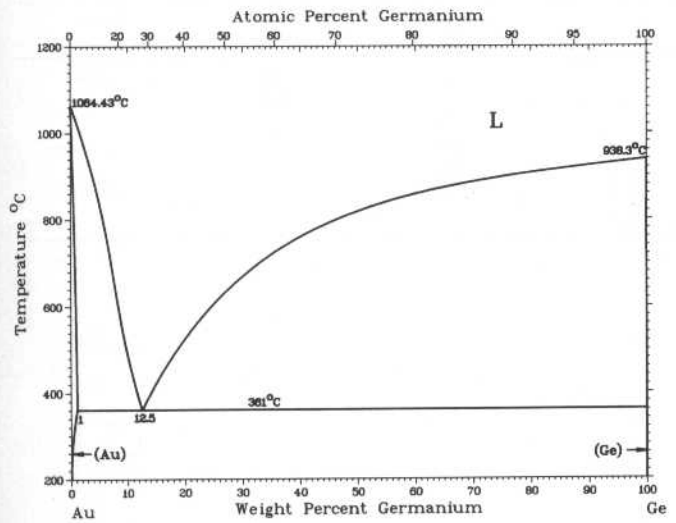

H. Okamoto and T.B. Massalski, 1987

Phase	Composition, wt% Ge	Pearson symbol	Space group
(Au)	0 to 1(a)	*cF*4	$Fm\bar{3}m$
(Ge)	100(a)	*cF*8	$Fd\bar{3}m$
Metastable phases			
β	7 to 11(a)	*hP*2	$P6_3/mmc$
γ	11 to 29(a)	*tI**	...

(a) Approximate composition from the phase diagram

Au-Hg

H. Okamoto and T.B. Massalski, 1989

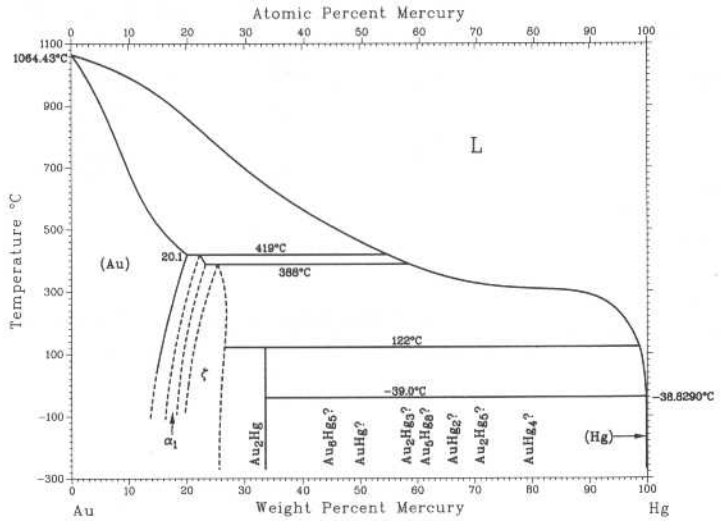

Phase	Composition, wt% Hg	Pearson symbol	Space group
(Au)	0 to 20.1	*cF*4	$Fm\bar{3}m$
α_1	16.2 to 23	*hP*36	$P6_3/mmc$
ζ	21 to 26	*hP*2	$P6_3/mmc$
Au_2Hg	33.7	*hP*~150	...
		*hP*22	$P6_3/mcm$
Au_6Hg_5	46.0	*hP*22	$P6_3/mcm$
Au_5Hg_8	62.0	*cI*52	$I\bar{4}3m$
(Hg)	100	*hR*1	$R\bar{3}m$

Au-In

H. Okamoto and T.B. Massalski, 1992

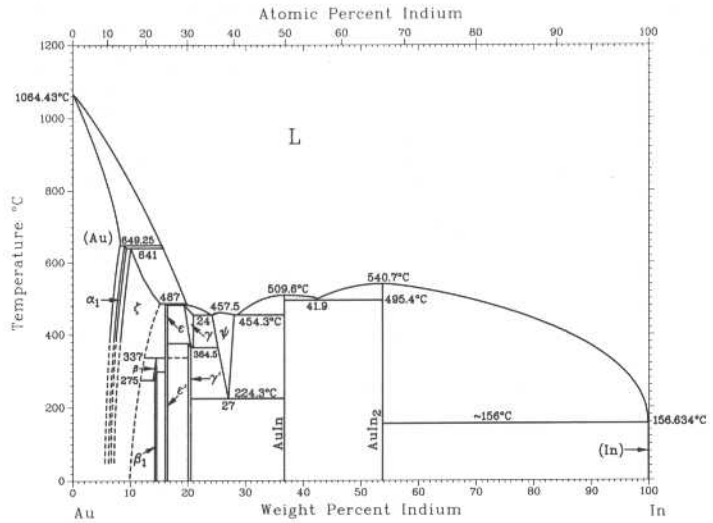

Phase	Composition, wt% In	Pearson symbol	Space group
(Au)	0 to 7.8	*cF*4	$Fm\bar{3}/m$
α_1	7.4 to 8.9	*hP*16	$P6_3/mmc$
		*hP*4	$P6_3/mmc$
ζ	8 to 14.8	*hP*2	$P6_3/mmc$
β	13.8 to 14.3	(a)	...
		(b)	...
β_1	13.9 to 14.5	*hP*26	*P*3
		(a)	...
ε	15.9 to 16.3	(b)	...
ε'	15.9 to 16.3	*oP*8	*Pmmn*
γ	19.1 to 21.1	*cP*52	$P\bar{4}3m$
		*cP*76	$P\bar{4}3m$
γ'	19.8 to 20.5	*hP*60	*P*3
ψ	24.1 to 27.6	*hP*5	$P\bar{3}m1$
AuIn	37 to 36.9	(c)	...
$AuIn_2$	53.9	*cF*12	$Fm\bar{3}m$
(In)	100	*tI*2	*I*4/*mmm*

(a) Hexagonal. (b) Orthorhombic. (c) Triclinic

Au-K

A.D. Pelton, 1987

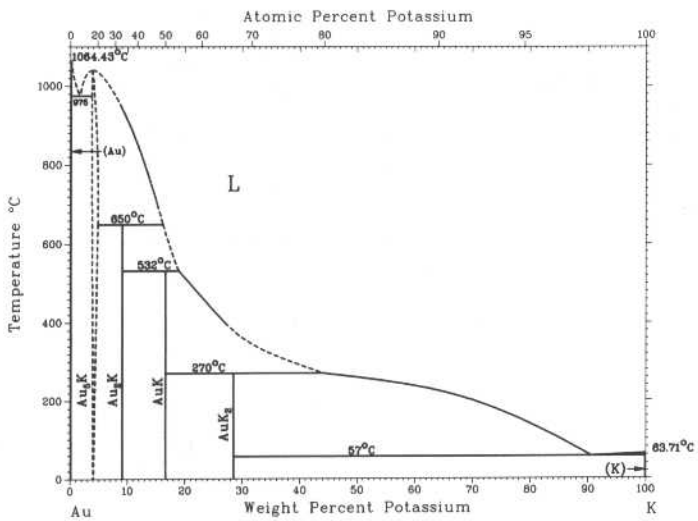

Phase	Composition, wt% K	Pearson symbol	Space group
(Au)	0	*cF*4	$Fm\bar{3}m$
Au_5K	3.8	*hP*6	*P*6/*mmm*
Au_2K	9.0	...	...
AuK	16.6	...	...
AuK_2	28.5	...	...
(K)	100	*cI*2	$Im\bar{3}m$

Note: At 25 °C

Au-La

K.A. Gschneidner, Jr., F.W. Calderwood, H. Okamoto, and T.B. Massalski, 1987

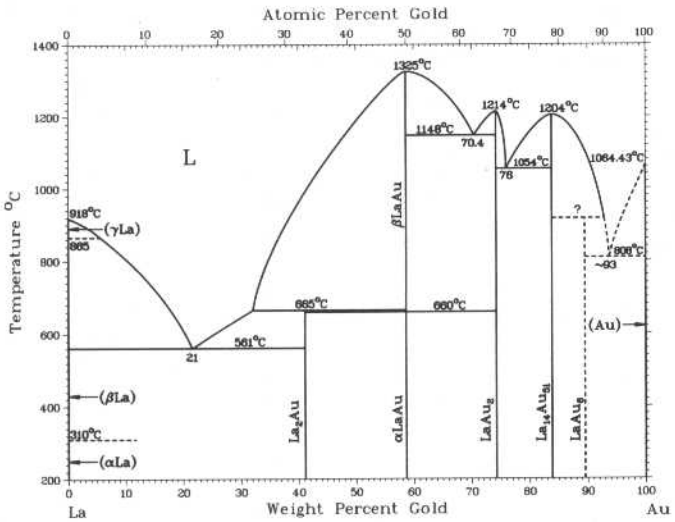

Phase	Composition, wt% Au	Pearson symbol	Space group
(αLa)	0	*hP4*	$P6_3/mmc$
(βLa)	0	*cF4*	$Fm\bar{3}m$
(γLa)	0	*cI2*	$Im\bar{3}m$
La_2Au	41.5	*oP12*	*Pnma*
αLaAu	59	*oP8*	*Pnma*
βLaAu	59	*oC8*	*Cmcm*
$LaAu_2$	74.0	*oI12*	*Imma*
$La_{14}Au_{51}$	~81 to ~83.8	*hP65*	*P6/m*
$LaAu_6$	89.5	*mC28*	*C2/c*
(Au)	100	*cF4*	$Fm\bar{3}m$

Au-Li

A.D. Pelton, 1987

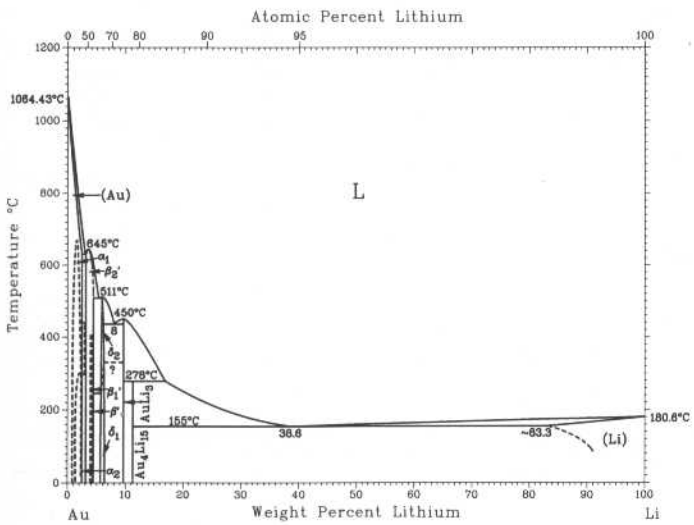

Phase	Composition, wt% Li	Pearson symbol	Space group
(αAu)	0 to 0.7	*cF4*	$Fm\bar{3}m$
(α_1Au)	0.7 to 1	*cP4*	$Pm\bar{3}m$
(α_2Au)	2 to 2.3	(b)	...
Au_5Li_4	2.7	(c)	...
β'_2	3 to 4	*oP2*	...
β'_1	4 to 4.1	*tP2*?(b)	...
β′	4.1 to 4.3	*cP2*	$Pm\bar{3}m$
$\delta_{2(HT)}$	5.6 to 6.3	*hP9*	...
$\delta_{1(LT)}$	5.6 to 6.3	(d)	...
$AuLi_3$	10	*cF16*	$Fm\bar{3}m$
Au_4Li_{15}	12	*cI76*	$I\bar{4}3d$
(βLi)(a)	100	*cI2*	$Im\bar{3}m$
(αLi)(e)	100	*hP2*	$P6_3/mmc$

(a) At 25 °C. (b) Complex. (c) Hexagonal. (d) Similar to δ_2. (e) *T* less than –201 °C

Au-Mg

A.A. Nayeb-Hashemi and J.B. Clark, 1988

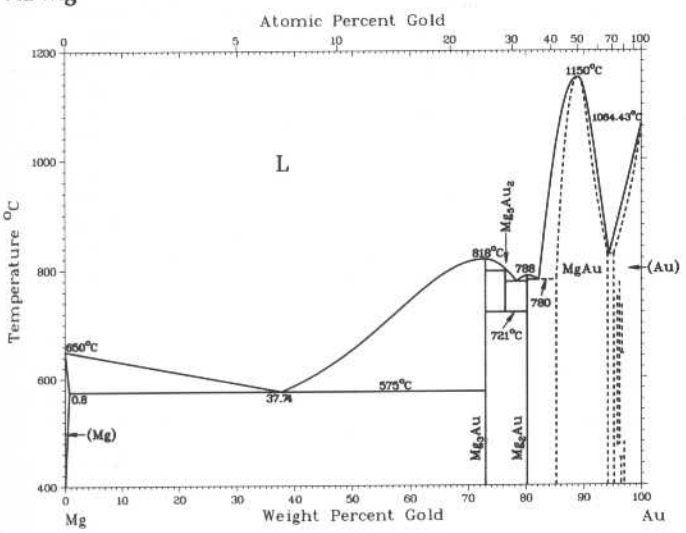

Phase	Composition, wt% Au	Pearson symbol	Space group
(Mg)	0 to 0.8	*hP2*	$P6_3/mmc$
Mg_3Au	73	*hP8*	$P6_3/mmc$ or $P\bar{3}c1$
Mg_5Au_2	76.42	...	...
Mg_2Au	80.20	...	*Pnam* or $Pna2_1$
(MgAu)	89.5	*cP2*	$Pm\bar{3}m$
$Mg_{26}Au_{74}$	96	*oC160*	*Cm2m*
$Mg_{24}Au_{76}$	96.3	*oC64*	*Cmcm*
$Mg_{23}Au_{77}$	96.6	*hP108*	$P6_3/mcm$
$Mg_{22}Au_{78}$	96.64	*tI16*	*I4/mmm*
Mg_4Au_{15}	96.81	*mP38*	*B2/m*
$MgAu_4$	97	(a)	...
(Au)	100	*cF4*	$Fm\bar{3}m$

(a) Structure reportedly is related to that of the "*X*-phase," Mg_4Au_{15}.

Au-Mn

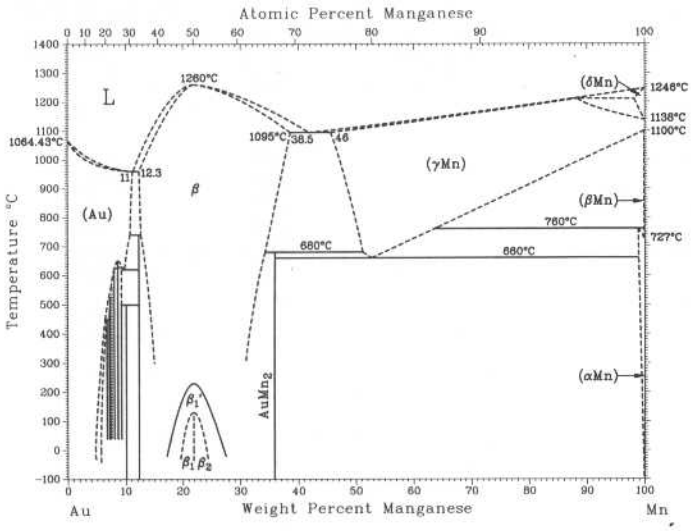

T.B. Massalski and H. Okamoto, 1987

Phase	Composition, wt% Mn	Pearson symbol	Space group
(Au)	0 to 11	*cF*4	$Fm\bar{3}m$
Au_4Mn	5 to 6	*tI*10	*I*4/*m*
$Au_{33}Mn_9$	7.07	(a)	$P2_1/b$
$Au_{22}Mn_6$	7.07	(a)	...
α″	7.0 to 7.2	(b)	*Pnnm*
$Au_{31}Mn_9$	7.49	(c)	...
2*d*-APS(I)	...	(d)	...
$Au_{31}Mn_9$	7.49	(b)	...
$Au_{72}Mn_{21}$	5.52	(a)	...
$Au_{41}Mn_{12}$	7.55	(a)	...
$Au_{167}Mn_{49}$	7.57	(b)	...
$Au_{95}Mn_{28}$	7.59	(a)	...
$Au_{27}Mn_8$	7.63	(b)	...
$Au_{13}Mn_4$ (η)	7.50	(b)	...
2*d*-Au_3Mn(e)	~8	*oP*32	*Pnnm*
Au_3Mn	7.2 to 10	...	...
5*H*	...	(b)	...
3*R*	...	(b)	...
M = 1	...	*tI*8	*I*4/*mmm*
$6H_1$	...	(b)	...
$6H_2$	...	(b)	...
Au_3Mn(I)(f)	9	(b)	...
X ($Au_{11}Mn_4$)	9.21	(a)	...
(f)	~9.2	(b)	...
$Au_{11}Mn_4$I(f)	~9.2	(a)	...
$Au_{11}Mn_4$II(f)	~9.2	(a)	...
$Au_{11}Mn_4$III(e,f)	~9.2	(a)	...
AABB(f)	~9.2	(g)	...
Au_5Mn_2	10.04	(a)	*C*2/*m*
Au_2Mn	12.24	*tI*6	*I*4/*mmm*
β	12.3 to 38.5	*cP*2	$Pm\bar{3}m$
β′$_1$	16 to 29	(g)	...
β_1	19 to 22	(g)	...
β_2	22 to 25	(g)	...
	23	(b)	...
$AuMn_2$	36	*tI*6	*I*4/*mmm*
(δMn)	100	*cI*2	$Im\bar{3}m$
(γMn)	46 to 100	*cF*4	$Fm\bar{3}m$
(βMn)	100	*cP*20	$P4_132$
(αMn)	100	*cI*58	$I\bar{4}3m$
(γMn1)(f)	67 to 100	(g)	...
(γMn2)(f)	60.5 to 75.3	(g)	...
(f)	73.4	(b)	...

Note: 2*d* = two dimensional. APS = antiphase structure. (a) Monoclinic. (b) Orthorhombic. (c) Square island. (d) Lozenge island. (e) Thin film. (f) Metastable. (g) Tetragonal

Au-rich region of the Au-Mn phase diagram

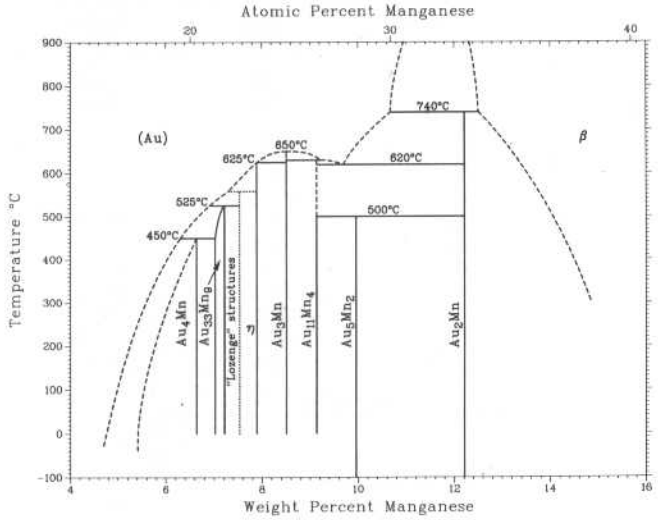

Au-Na

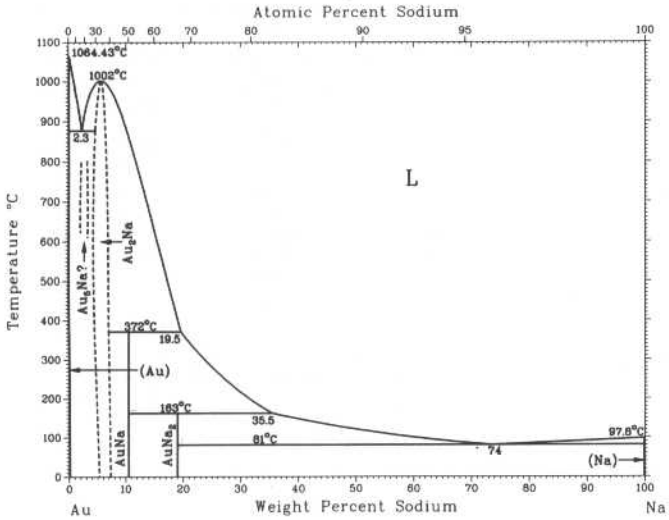

A.D. Pelton, 1987

Phase	Composition, wt% Na	Pearson symbol	Space group
(Au)	0	*cF*4	$Fm\bar{3}m$
Au_5Na(a)	2 to 3	...	...
Au_2Na	5 to 7	*cF*24	$Fd\bar{3}m$
AuNa	10	(b)	...
$AuNa_2$	18.9 to 21	*tI*12	*I*4/*mcm*
(Na)	100	*cI*2	$Im\bar{3}m$
(Na)(c)	100	*hP*2	$P6_3/mmc$

(a) Existence requires verification; *T* = 775 °C. (b) Complex structure. (c) *T* is less than −237 °C.

Au-Nb

H. Okamoto and T.B. Massalski, 1987

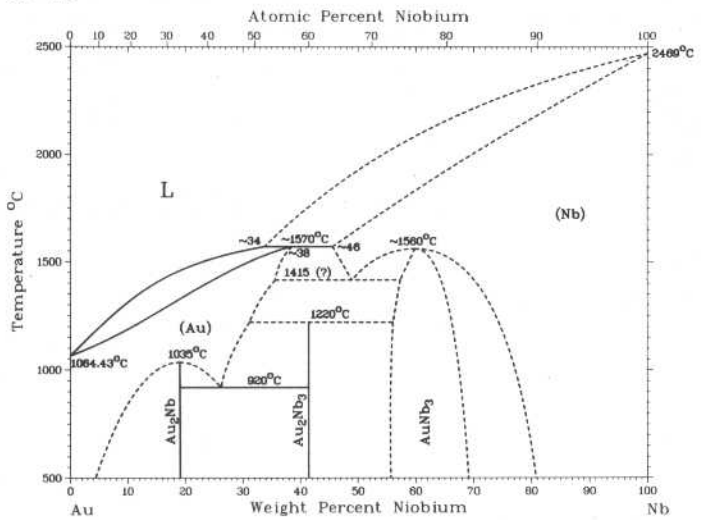

Phase	Composition, wt% Nb	Pearson symbol	Space group
(Au)	0 to ~38	*cF*4	$Fm\bar{3}m$
Au_2Nb	19.1	*hP*3	*P*6/*mmm*
Au_2Nb_3	41	*tI*10	*I*4/*mmm*
$AuNb_3$	56 to 70	*cP*8	$Pm\bar{3}n$
(Nb)	~46 to 100	*cI*2	$Im\bar{3}m$

Au-Ni

H. Okamoto and T.B. Massalski, 1991

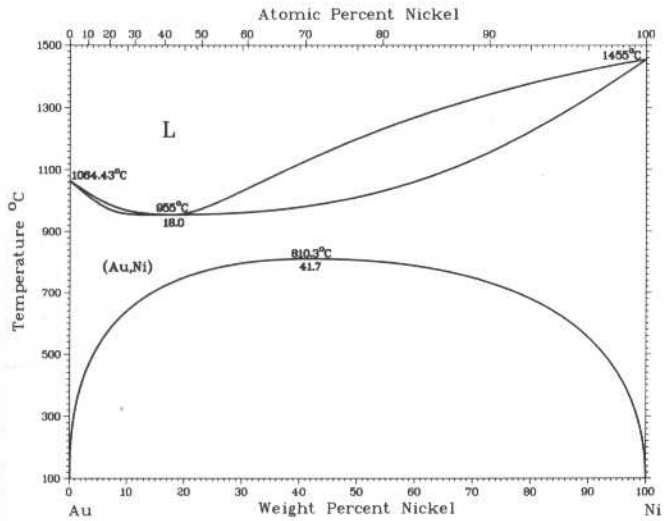

Phase	Composition, wt% Ni	Pearson symbol	Space group
(Au,Ni)	0 to 100	*cF*4	$Fm\bar{3}m$

Au-Pb

H. Okamoto and T.B. Massalski, 1987

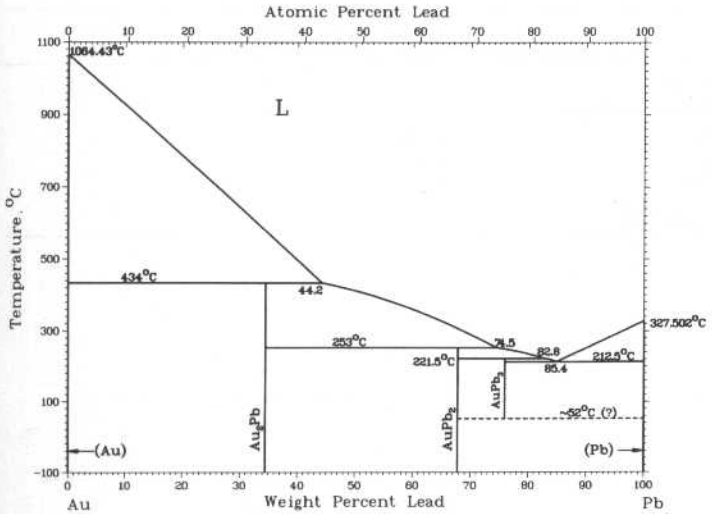

Phase	Composition, wt% Pb	Pearson symbol	Space group
(Au)	0 to 0.12	*cF*4	$Fm\bar{3}m$
Au_2Pb	34.4	*cF*24	$Fd\bar{3}m$
$AuPb_2$	67.8	*tI*12	*I*4/*mcm*
$AuPb_3$	75.9	*tI*32	$I\bar{4}2m$
(Pb)	99.81 to 100	*cF*4	$Fm\bar{3}m$

Au-Pd

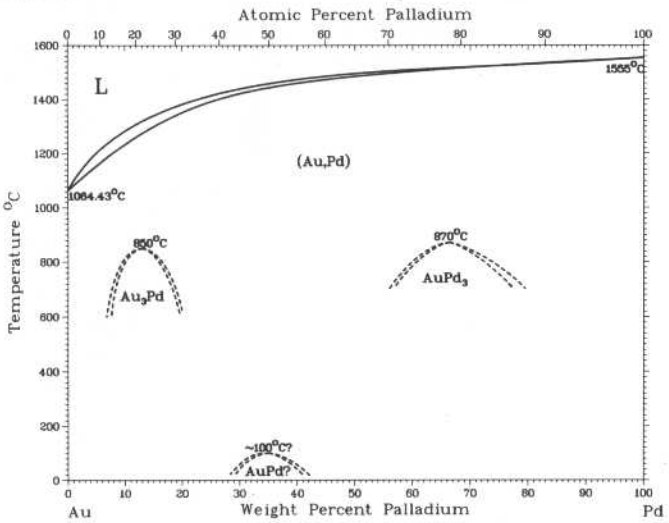

H. Okamoto and T.B. Massalski, 1987

Phase	Composition, wt% Pd	Pearson symbol	Space group
(Au,Pd)	0 to 100	*cF*4	$Fm\bar{3}m$
Au_3Pd	7 to 20	*cP*4	$Pm\bar{3}m$
AuPd	?	(a)	...
$AuPd_3$	53 to 83	*cP*4(?)	$Pm\bar{3}m$

(a) Long period?

Au-Pr

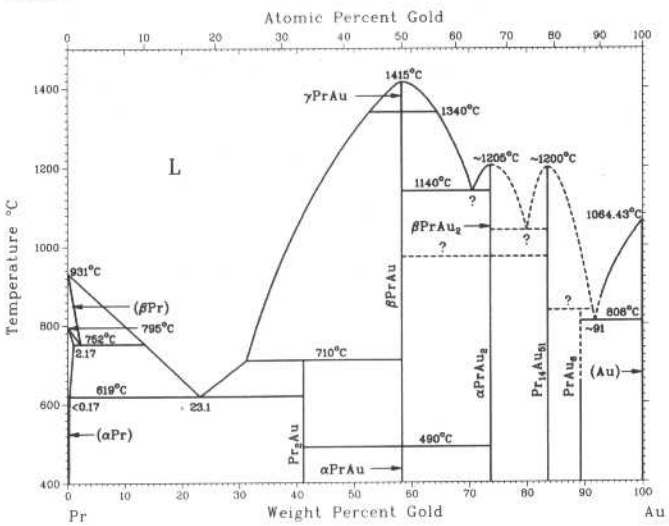

K.A. Gschneidner, Jr., F.W. Calderwood, H. Okamoto, and T.B. Massalski, 1987

Phase	Composition, wt% Au	Pearson symbol	Space group
(αPr)	0 to <0.17	*hP*4	$P6_3/mmc$
(βPr)	0 to 2.17	*cI*2	$Im\bar{3}m$
Pr_2Au	41.1	*oP*12	*Pnma*
αPrAu	58	*oP*8	*Pnma*
βPrAu	58	*oC*8	*Cmcm*
γPrAu	58	*cP*2	$Pm\bar{3}m$
$\alpha PrAu_2$	73.7	*oI*12	*Imma*
$\beta PrAu_2$	73.7	*tP*108	$P4/nmm$
$Pr_{14}Au_{51}$	~81 to ~83.6	*hP*65	$P6/m$
$PrAu_6$	89.3	*mC*28	$C2/c$
(Au)	~99.93 to 100	*cF*4	$Fm\bar{3}m$

Au-Pt

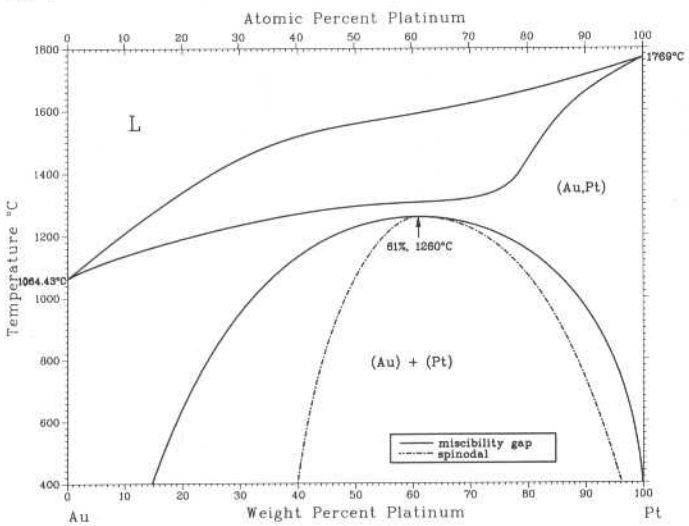

H. Okamoto and T.B. Massalski, 1987

Phase	Composition, wt% Pt	Pearson symbol	Space group
(Au,Pt)	0 to 100	*cF*4	$Fm\bar{3}m$
Metastable phases			
Au_3Pt	4.9 to 39.8	...	...
AuPt	49.8	(a)	...
$AuPt_3$	74.8	...	...

(a) Tetragonal

Au-Pu

H. Okamoto, T.B. Massalski, and D.E. Peterson, 1987

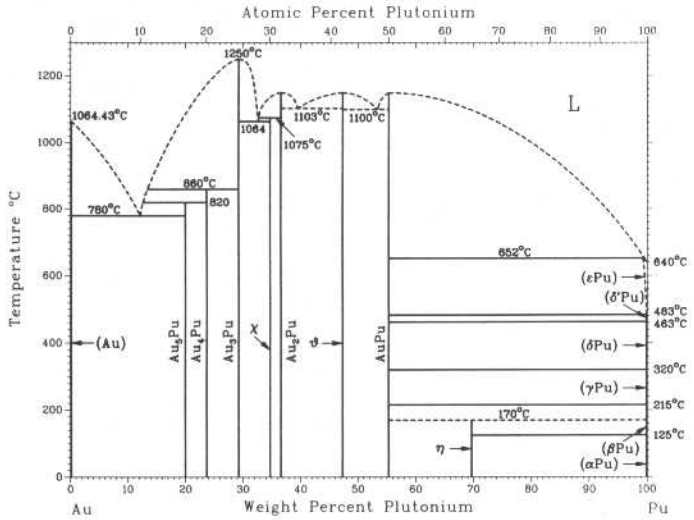

Phase	Composition, wt% Pu	Pearson symbol	Space group
(Au)	0	*cF*4	$Fm\bar{3}m$
Au_5Pu (ν)	19.9	Unknown	...
Au_4Pu (μ)	23.7	Unknown	...
Au_3Pu (λ)	29.2	(a)	...
χ	35	Unknown	...
Au_2Pu(ι)	38.2	Unknown	...
θ	47	Unknown	...?
AuPu(ζ)	55.3	Unknown	...
η	70	Unknown	...
(εPu)	99.2 to 100	*cI*2	$Im\bar{3}m$
(δ'Pu)	100	*tI*2	*I*4/*mmm*
(δPu)	100	*cF*4	$Fm\bar{3}m$
(γPu)	100	*oF*8	*Fddd*
(βPu)	100	*mC*34	*C*2/*m*
(αPu)	100	*mP*16	$P2_1/m$

(a) Hexagonal

Au-Rb

A.D. Pelton, 1987

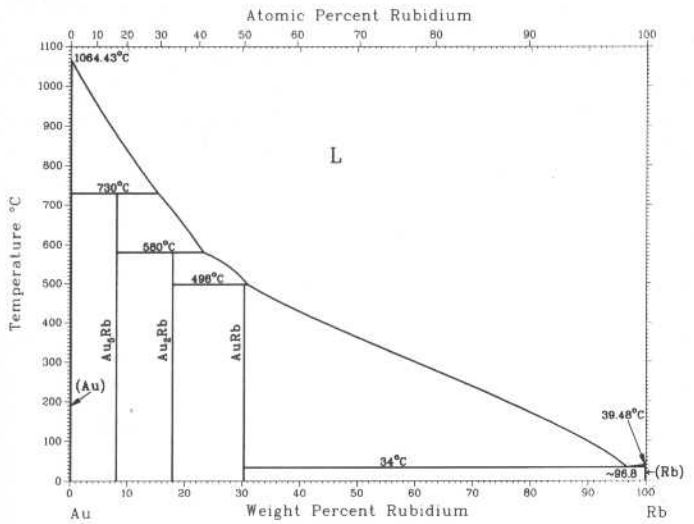

Phase	Composition, wt% Rb	Pearson symbol	Space group
(Au)	0	*cF*4	$Fm\bar{3}m$
Au_5Rb	8.0	*hP*6	*P*6/*mmm*
Au_2Rb	17.8	...	...
AuRb	30.3	*cP*2	$Pm\bar{3}m$
(Rb)	100	*cI*2	$Im\bar{3}m$

Au-Sb

H. Okamoto and T.B. Massalski, 1987

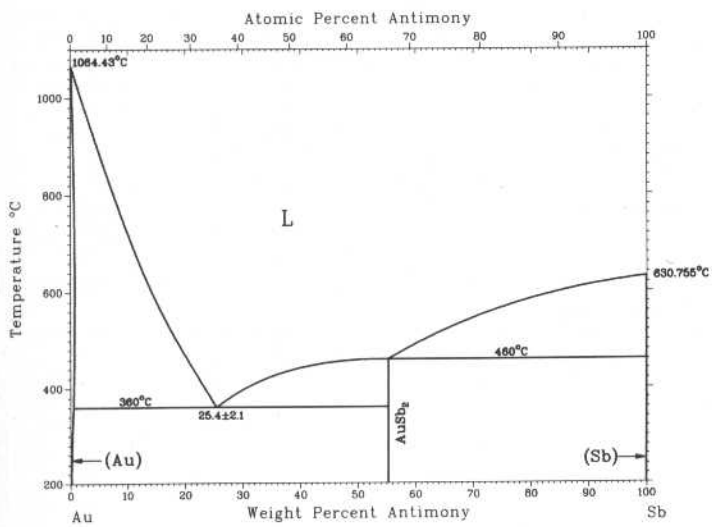

Phase	Composition, wt% Sb	Pearson symbol	Space group
(Au)	0 to 0.75	*cF*4	$Fm\bar{3}m$
$AuSb_2$	55.3	*cP*12	*Pa*3
(Sb)	100	*hR*2	$R\bar{3}m$
Metastable phases			
...	8 to 10	*hP*2	$P6_3/mmc$
...	61 to 76	*cP*1	$Pm\bar{3}m$

Au-Se

H. Okamoto and T.B. Massalski, 1987

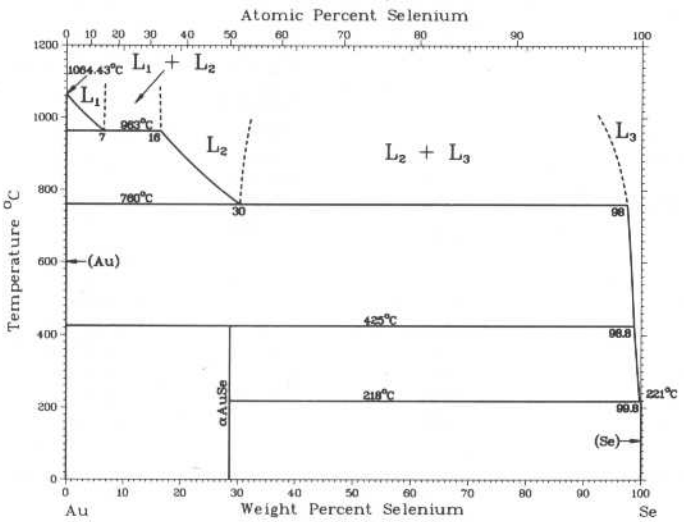

Phase	Composition, wt% Se	Pearson symbol	Space group
(Au)	0	*cF*4	$Fm\bar{3}m$
αAuSe	29	*mC*24	*C*2/*m*
βAuSe(a)	29	*mC*12	*C*2/*m*
(γSe)	100	*hP*3	$P3_121$

(a) Metastable

Au-Si

H. Okamoto and T.B. Massalski, 1987

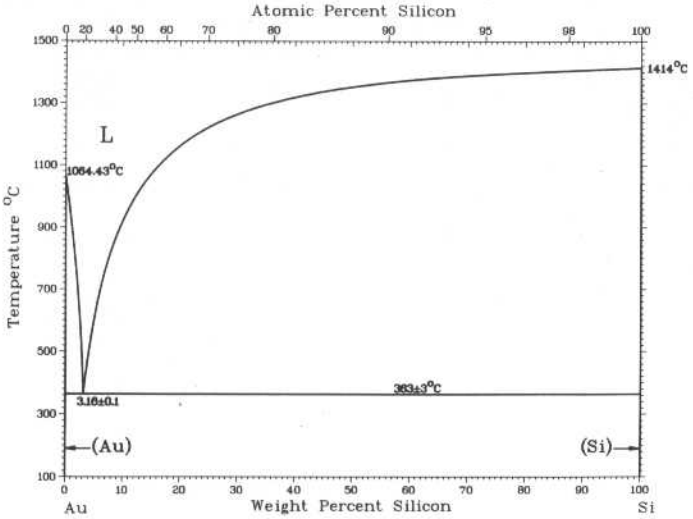

Phase	Composition, wt% Si	Pearson symbol	Space group
(Au)	0	*cF*4	$Fm\bar{3}m$
(Si)	100	*cF*8	$Fd\bar{3}m$

Au-Sn

H. Okamoto and T.B. Massalski, 1987

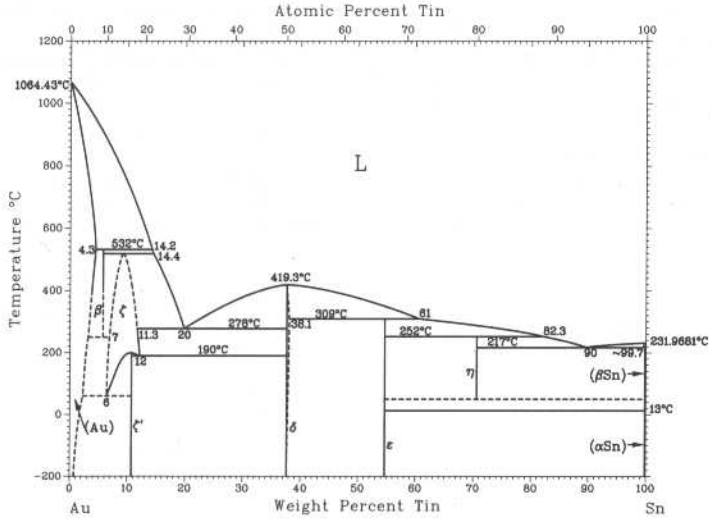

Phase	Composition, wt% Sn	Pearson symbol	Space group
(Au)	0 to 4.3	*cF*4	$Fm\bar{3}m$
β or $Au_{10}Sn$	5.7	*hP*16	$P6_3/mmc$
ζ	7 to 12	*hP*2	$P6_3/mmc$
ζ′ or Au_5Sn	10.8	(a)	$R\bar{3}$
δ or AuSn	38 to 38.08	*hP*4	$P6_3/mmc$
ε or $AuSn_2$	54.7	(b)	*Pbca*
η or $AuSn_4$	71	*oC*20	*Aba*2
(βSn)	99.7 to 100	*tI*4	$I4_1/amd$
(αSn)	99.990 to 100	*cF*8	$Fm\bar{3}m$

(a) Hexagonal. (b) Orthorhombic

Au-Sr

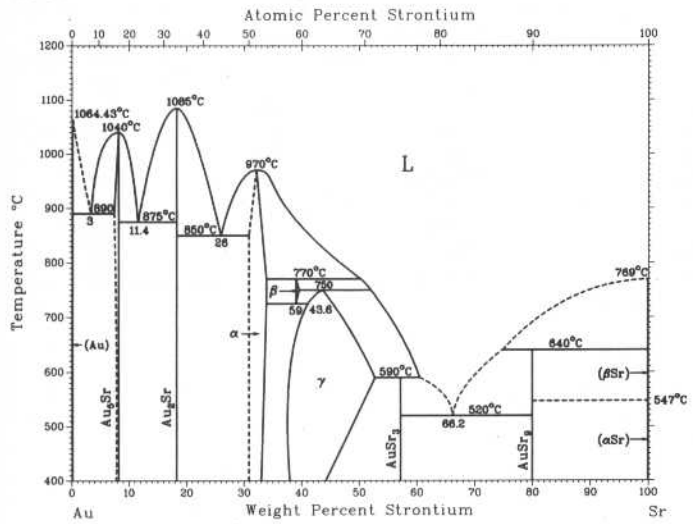

C.B. Alcock, V.P. Itkin, H. Okamoto, and T.B. Massalski, 1987

Phase	Composition, wt% Sr	Pearson symbol	Space group
(Au)	0	*cF*4	$Fm\bar{3}m$
Au_5Sr	7.7 to 8.2	*hP*6	*P*6/*mmm*
Au_2Sr	18.2	*oI*12	*Imma*
α	32.1 to 34	?	...
β	39 to 40	?	...
γ	38.5 to 52.7	?	...
$AuSr_3$	57	?(a)	...
$AuSr_9$	80	?(b)	...
(βSr)	100	*cI*2	$Im\bar{3}m$
(αSr)	100	*cF*4	$Fm\bar{3}m$

(a) Complex. (b) Hexagonal

Au-Te

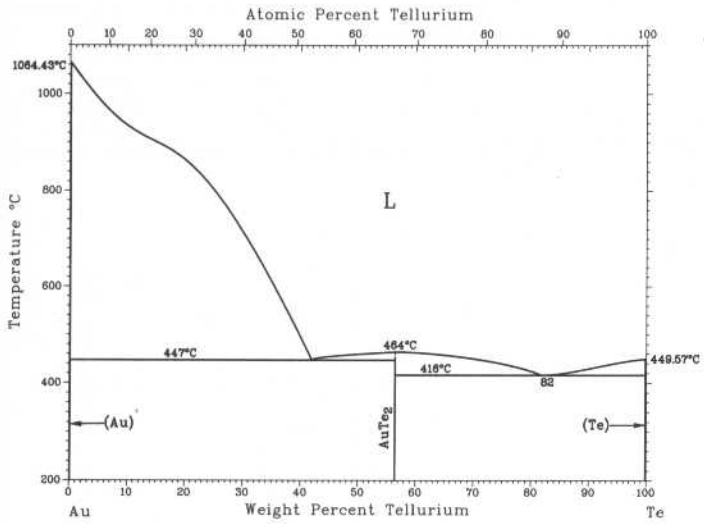

H. Okamoto and T.B. Massalski, 1987

Phase	Composition, wt% Te	Pearson symbol	Space group
(Au)	0 to 0.10	*cF*4	$Fm\bar{3}m$
$AuTe_2$ (calaverite)	56.5	*mC*6	*C*2/*m*
(Te)	100	*hP*3	$P3_121$
Metastable phases and other phases			
Petzite (a)	24.4	...	...
Montbrayite(a)	49	*aP*60	*P*1
Krennerite(a)	56.5	*oP*24	*Pma*2
(b)	48.9 to 79	*cP*1	$Pm\bar{3}m$
(c)	91.8	(d)	...
(e)	60 to 100	(f)	...

(a) Natural ore. May be stable only with additional impurities. (b) Splat cooled at room temperature. Complete decomposition in 10 min at 165 °C (>69.6 at.% Te), 8 min at 260 °C or 10 h at 175 °C (62.5 at.% Te). (c) Splat cooled at room temperature. (d) Unidentified structure. (e) Vapor deposition of Te on Au at room temperature. (f) Amorphous

Au-Th

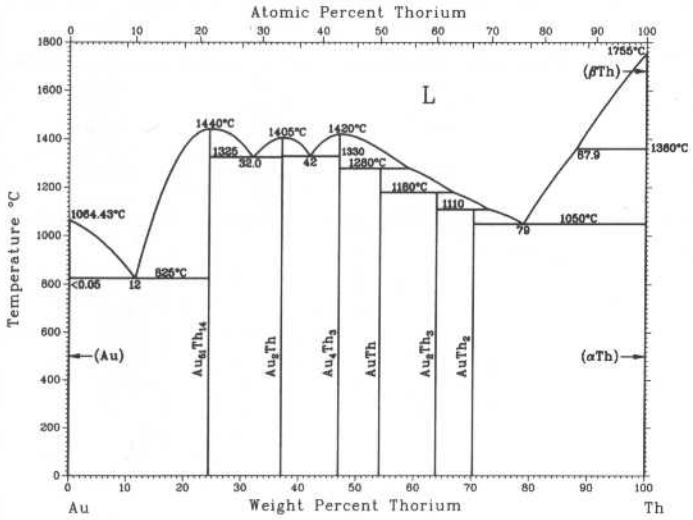

H. Okamoto, T.B. Massalski, and D.E. Peterson, 1991

Phase	Composition, wt% Th	Pearson symbol	Space group
(Au)	~0	*cF*4	$Fm\bar{3}m$
$Au_{51}Th_{14}$	24.44	*hP*65	*P*6/*m*
Au_2Th	37.08	*hP*3	*P*6/*mmm*
Au_4Th_3	46.91	*hR*42	*R*3
AuTh	54	*oC*8	*Cmcm*
Au_2Th_3	64	(a)	...
$AuTh_2$	70.21	*tI*12	*I*4/*mcm*
(βTh)	100	*cI*2	$Im\bar{3}m$
(αTh)	~100	*cF*4	$Fm\bar{3}m$

(a) Cubic?

Au-Ti

J.L. Murray, 1987

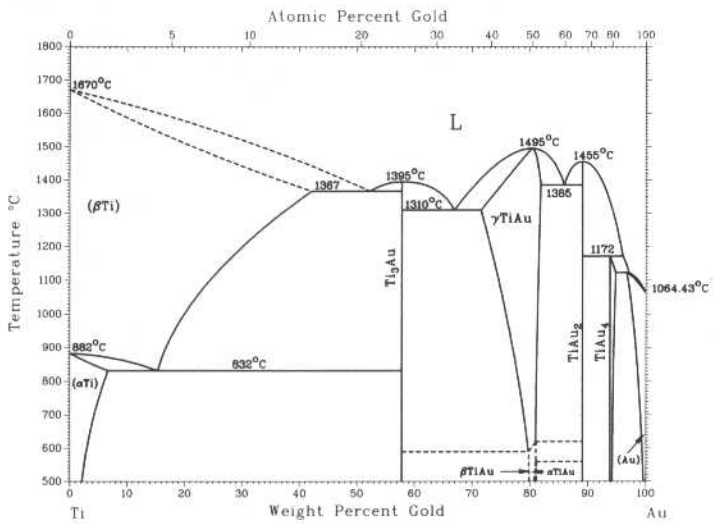

Phase	Composition, wt% Au	Pearson symbol	Space group
(αTi)	0 to 6.6	*hP*2	$P6_3/mmc$
(βTi)	0 to 42	*cI*2	$Im\bar{3}m$
Ti_3Au	58	*cP*8	$Pm\bar{3}n$
γTiAu	72 to 82	*cP*2	$Pm\bar{3}m$
βTiAu	80 to 80.4	*oP*4	*Pmma*
αTiAu	80.4	*tP*4	*P4/nmm*
$TiAu_2$	89.2	*tI*6	*I4/mmm*
$TiAu_4$	94 to 95	*tI*10	*I4/m*
(Au)	97 to 100	*cF*4	$Fm\bar{3}m$

Au-Tl

H. Okamoto and T.B. Massalski, 1987

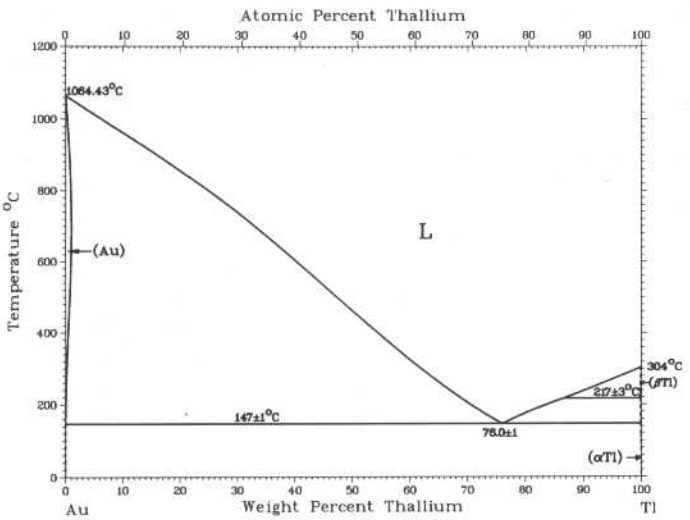

Phase	Composition, wt% Tl	Pearson symbol	Space group
(Au)	0 to 1.04	*cF*4	$Fm\bar{3}m$
(αTl)	100	*hP*2	$P6_3/mmc$
(βTl)	100	*cI*2	$Im\bar{3}m$

Au-U

H. Okamoto, 1990

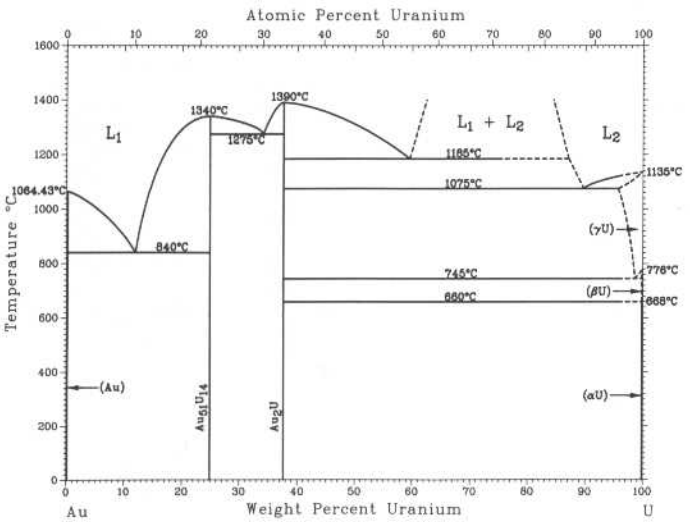

Phase	Composition, wt% U	Pearson symbol	Space group
(Au)	0	*cF*4	$Fm\bar{3}m$
$Au_{51}U_{14}$	24.9	*hP*65	*P6/m*
Au_2U	37.6	*hP*3	*P6/mmm*
(γU)	100	*cI*2	$Im\bar{3}m$
(βU)	100	*tP*30	$P4_2/mnm$
(αU)	100	*oC*4	*Cmcm*

Au-V

J.F. Smith, 1989

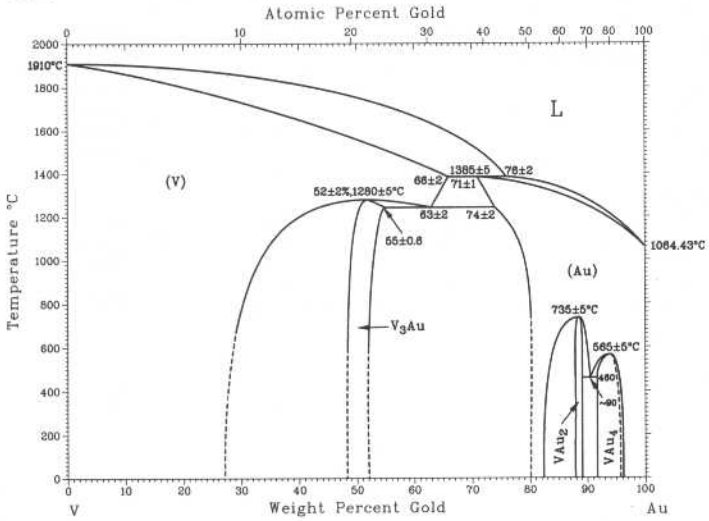

Phase	Composition, wt % Au	Pearson symbol	Space group
(V)	0 to ~66	*cI*2	$Im\bar{3}m$
V_3Au(a)	48 to 55	*cP*8	$Pm\bar{3}n$
VAu_2	88 to 89	*oC*12	(b)
VAu_4	92 to 96	*tI*10	*I*4/*m*
(Au)	~71 to 100	*cF*4	$Fm\bar{3}m$

(a) In the presence of small amounts of O or N, a second phase with the Cu_3Au-type structure may co-exist with the Cr_3Si-type structure. (b) Crystal structure related to the $MoSi_2$-type structure, but with a unit cell of twice the size.

Au-Yb

K.A. Gschneidner, Jr., F.W. Calderwood, H. Okamoto, and T.B. Massalski, 1987

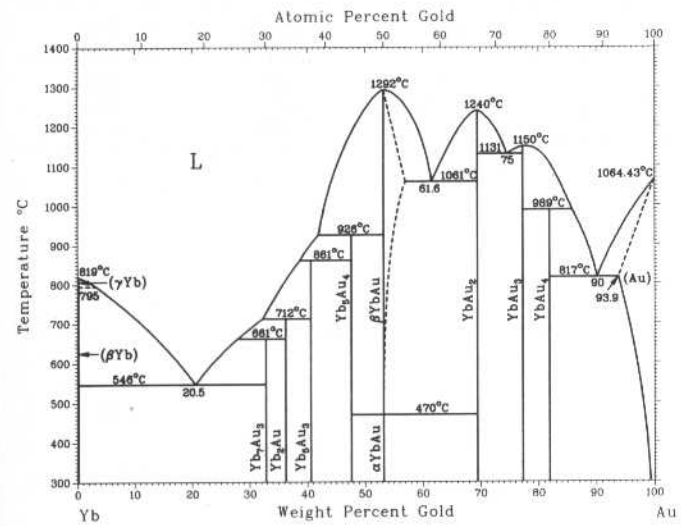

Phase	Composition, wt % Au	Pearson symbol	Space group
(βYb)	0	*cF*4	$Fm\bar{3}m$
(γYb)	0	*cI*2	$Im\bar{3}m$
Yb_7Au_3	33	*hP*20	$P6_3/mc$
Yb_2Au	36.2	*oP*12	*Pnma*
Yb_5Au_3	40.6	*tI*32	*I*4/*mcm*
Tb_5Au_4	47.6	*oP*36	*Pnma*
αYbAu	53	*oP*8	*Pnma*
βYbAu	53	*cP*2	$Pm\bar{3}m$
$YbAu_2$	69.5	*tI*6	*I*4/*mmm*
$YbAu_2$	77	*oP*8	*Pmmn*
$YbAu_4$	82	*tI*10	*I*4/*m*
(Au)	93.9 to 100	*cF*4	$Fm\bar{3}m$

Au-Zn

H. Okamoto and T.B. Massalski, 1990

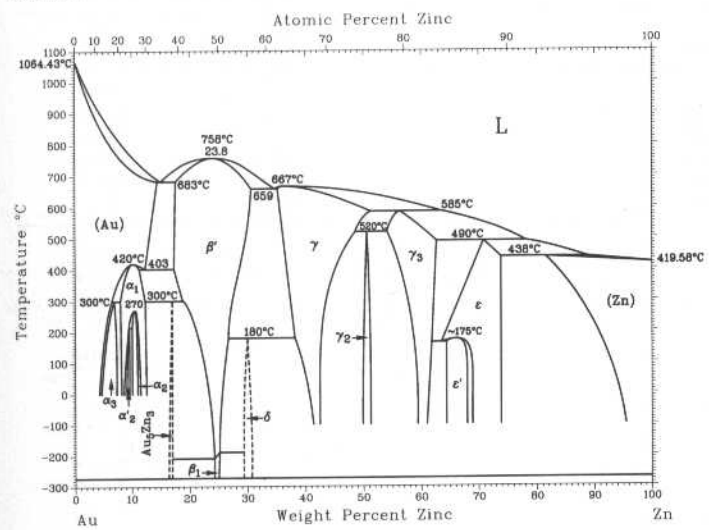

Phase	Composition, wt % Zn	Pearson symbol	Space group
(Au)	0 to 14	*cF*4	$Fm\bar{3}m$
α_3	~4 to 7.4	(a)	$Pn\bar{2}n$ or *Pnmn*
α_1	~7.9 to 11.7	(b)	...
α'_2	9.0 to 9.5	(b)	$I4_1/acd$
α_2	~9.7 to 10.2	(a)	*Abam* (*Cmca*)
Au_5Zn_3	16.6	(a)	...
β′	17 to 31	*cP*2	$Pm\bar{3}m$
β_1	24 to 26	?	...
δ	30	?	...
γ	38 to 51	*cI*52	...
γ_2	50 to 51	*cP*32	$Pm\bar{3}m$
γ_3	54 to 62.7	*hP**	*P6*/*mmm*
ε	64 to 73	*hP*2	$P6_3/mmc$
ε′	64 to 67	(c)	...
(Zn)	80.4 to 100	*hP*2	$P6_3/mmc$

(a) Orthorhombic, antiphase domain. (b) Tetragonal, antiphase domain. (c) Orthorhombic, pseudocell

Au-Zr

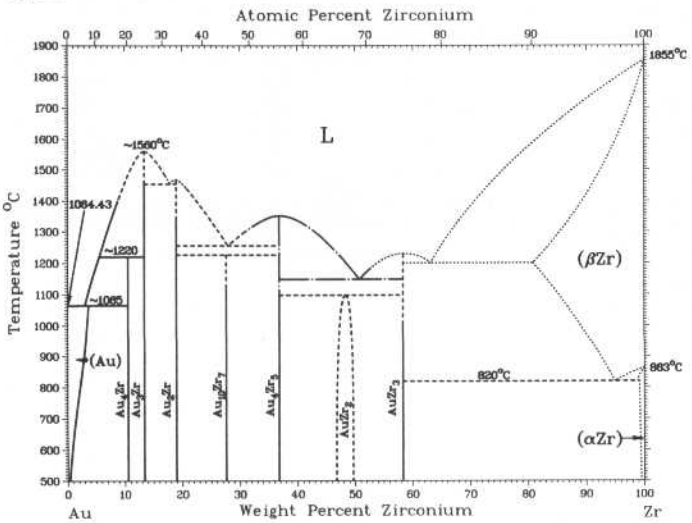

T.B. Massalski, H. Okamoto, and J.P. Abriata, 1987

Phase	Composition, wt% Zr	Pearson symbol	Space group
(Au)	0	*cF*4	$Fm\bar{3}m$
Au_4Zr	10	*oP*20	*Pnma*
Au_3Zr	13	*oP*8	*Pmmn*
Au_2Zr	18.8	*tI*6	*I*4/*mmm*
$Au_{10}Zr_7$	27	*tI*34	?
Au_4Zr_5	36.7	...	...
$AuZr_2$	48.1	*tI*6	*I*4/*mmm*
$AuZr_3$	58	*cP*8	$Pm\bar{3}n$
(βZr)	100	*cI*2	$Im\bar{3}m$
(αZr)	100	*hP*2	$P6_3/mmc$

B-C

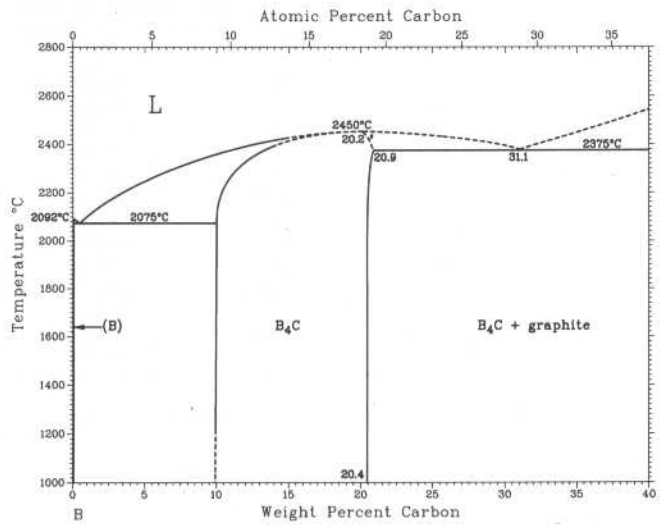

H. Okamoto, 1992

Phase	Composition, wt% C	Pearson symbol	Space group
(βB)	0	*hR*108	$R\bar{3}m$
"B_4C"	10 to 20.9	*hR*15	$R\bar{3}m$
(C)	100	*hP*4	$P6_3/mmc$

B-Co

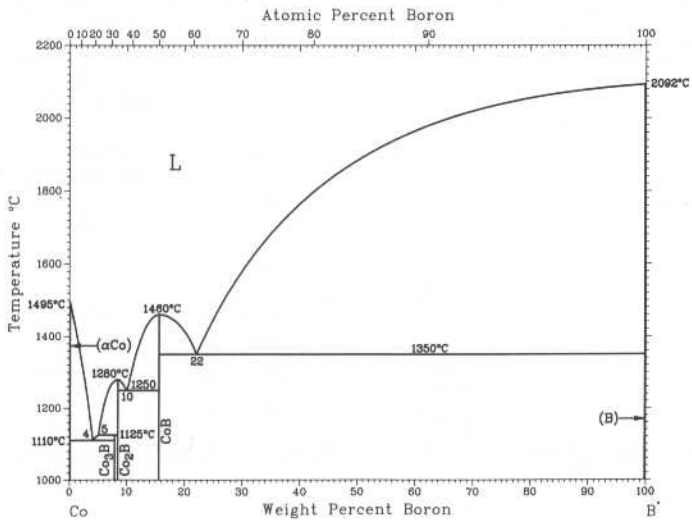

P.K. Liao and K.E. Spear, 1988

Phase	Composition, wt% B	Pearson symbol	Space group
(αCo)	~0	*cF*4	$Fm\bar{3}m$
(εCo)	~0	*hP*2	$P6_3/mmc$
Co_3B	7.8	...	*Pbnm*
Co_2B	8.4	*tI*12	*I*4/*mcm*
CoB	15.5	*oP*8	*Pnma*
(βB)	100	*hR*108	$R\bar{3}m$

B-Cr

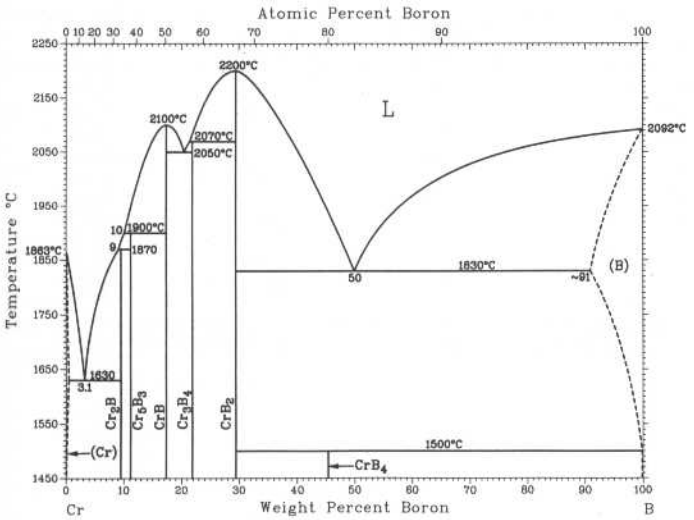

P.K. Liao and K.E. Spear, 1986

Phase	Composition, wt% B	Pearson symbol	Space group
(αCr)	0 to ~ 0.2	*cI*2	$Im\bar{3}m$
Cr_4B(a)	5	*oF*40	*Fddd*
Cr_2B	9.4	*oF*40	*Fddd*
Cr_2B(a)	9.4	(b)	*Abmm*
Cr_2B(a)	9.4	*tI*12	*I*4/*mcm*
Cr_5B_3	11.1	*tI*32	*I*4/*mcm*
CrB	17.2	*oC*8	*Cmcm*
Cr_3B_4	21.7	*oI*14	*Immm*
CrB_2	29.4	*hP*3	*P*6/*mmm*
CrB_4	45	(b)	...
CrB_6(a)	55.5	(c)	...
(βB)	~91 to 100	*hR*108	$R\bar{3}m$

(a) Unstable or stability is uncertain. (b) Orthorhombic. (c) Tetragonal

B-Cu

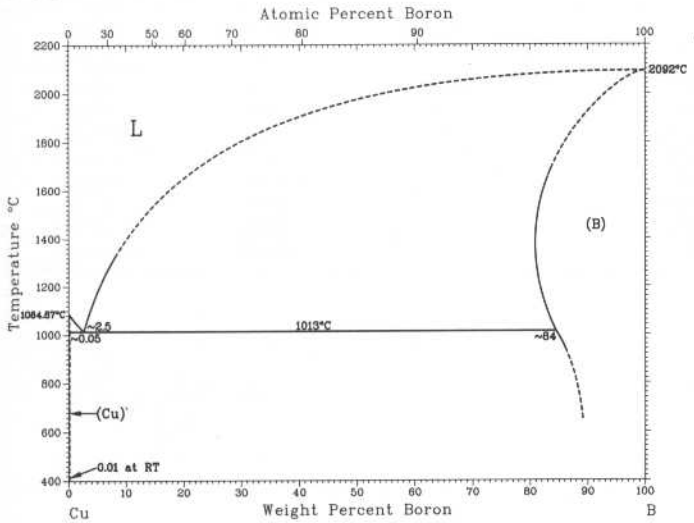

D.J. Chakrabarti and D.E. Laughlin, 1982

Phase	Composition, wt% B	Pearson symbol	Space group
(Cu)	0 to ~0.05	*cF*4	$Fm\bar{3}m$
(B)	>80	*tP*192	$P4_12_12$ or $P4_32_12$(?)
(B)	>80	*hR*105	$R\bar{3}m$
(βB)	100	*hR*108	$R\bar{3}m$
(αB)	100	*hR*12	$R\bar{3}m$
		*tP*192	$P4_12_12$ or $P4_32_12$(?)

B-Fe

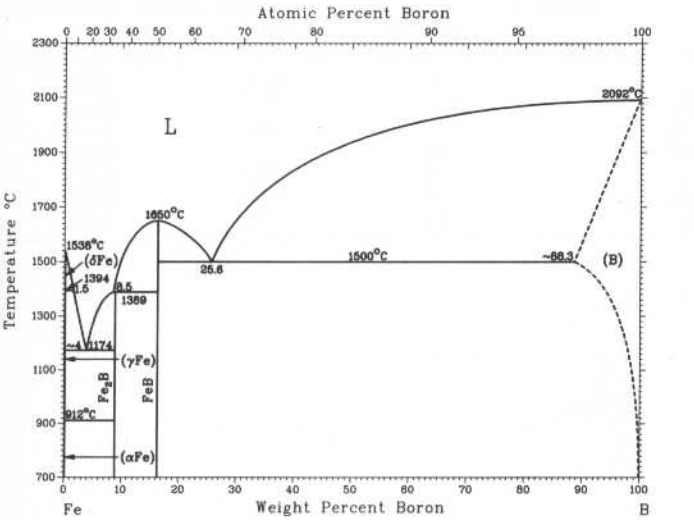

P.K. Liao and K.E. Spear, unpublished

Phase	Composition, wt% Fe	Pearson symbol	Space group
(αFe)	0	*cI*2	$Im\bar{3}m$
Fe_3B	8.8	*tI*12	*I*4/*mcm*
FeB	16.0 to 16.2	*oP*8	*Pbmn*
(βB)	100	*hR*108	$R\bar{3}m$
Metastable phases			
Fe_3B	~6	*oP*16	*Pnma*
Fe_3B(HT)	~6	(a)	...
Fe_3B(LT)	~6	(b)	...

(a) bct. (b) Tetragonal

B-Mn

P.K. Liao and K.E. Spear, 1986

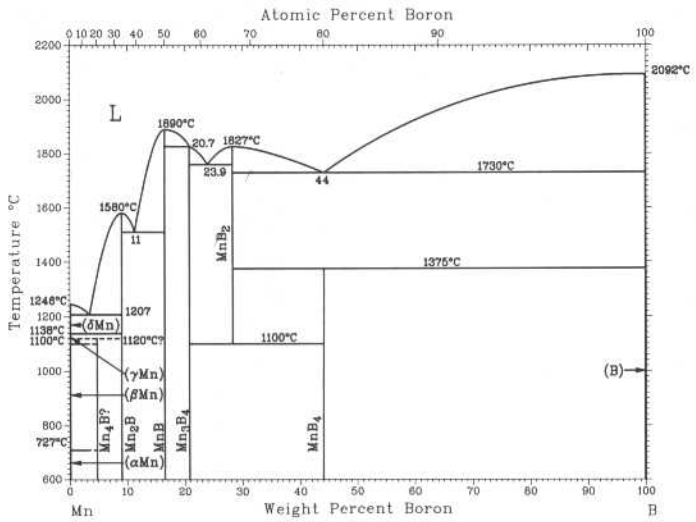

Phase	Composition, wt% B	Pearson symbol	Space group
(δMn)	0	*cI*2	$Im\bar{3}m$
Mn_4B(a)	5	*oF*40	*Fddd*
Mn_2B(a)	9.0	(b)	*Fddd*
	9.0	*tI*12	*I*4/*mcm*
MnB	16	*oP*	*Pnma*
Mn_3B_4	20.8	*oI*14	*Immm*
MnB_2	28.3	*hP*3	*P*6/*mmm*
MnB_4	44	(c)	*C*2/*m*
$MnB_{\sim 23}$(d)	...	*hR*108	$R\bar{3}m$
(βB)	100	*hR*108	$R\bar{3}m$

(a) Probably not thermodynamically stable. Also, orthorhombic Mn_4B and Mn_2B may refer to the same phase. (b) Orthorhombic. (c) Monoclinic. (d) Probably the Mn-rich boundary or rhombohedral B

B-Mo

K.E. Spear and P.K. Liao, 1988

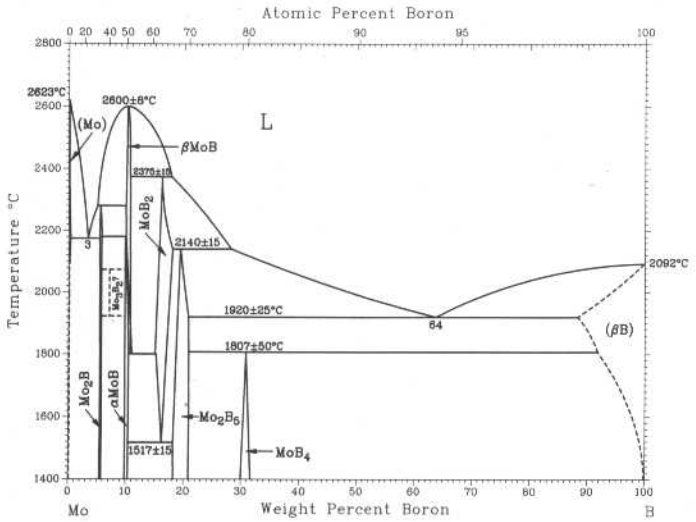

Phase	Composition, wt% B	Pearson symbol	Space group
(Mo)	0 to <0.1	*cI*2	$Im\bar{3}m$
Mo_2B	~5	*tI*12	*I*4/*mcm*
αMoB	9 to 10	$tI16$	$I4_1/amd$
βMoB	9 to 10.4	*oC*8	*Cmcm*
MoB_2	16 to 18	*hP*3	*P*6/*mmm*
Mo_2B_5	18.6 to 20	*hR*21	$R\bar{3}m$
MoB_4	~30	*hP*20	$P6_3/mmc$
(βB)	>92 to 100	*hR*108	$R\bar{3}m$

B-Nb

H. Okamoto, 1990

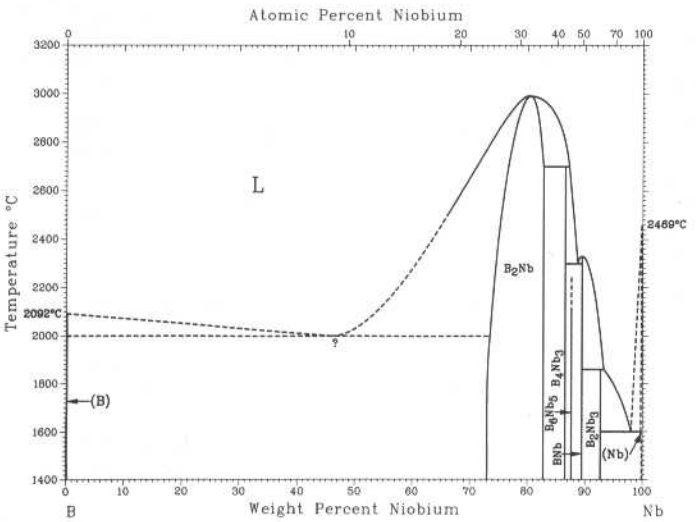

Phase	Composition, wt% Nb	Pearson symbol	Space group
(βB)	0	*hR*108	$R\bar{3}m$
B_2Nb	73 to 83	*hP*3	*P*6/*mmm*
B_4Nb_3	86.6	*oI*14	*Immm*
B_6Nb_5	87.8	*oC**	Cmmm
BNb	90	*oC*8	*Cmcm*
B_2Nb_3	93	*tP*10	*P*4/*mbm*
(Nb)	100	*cI*2	$Im\bar{3}m$

B-Ni

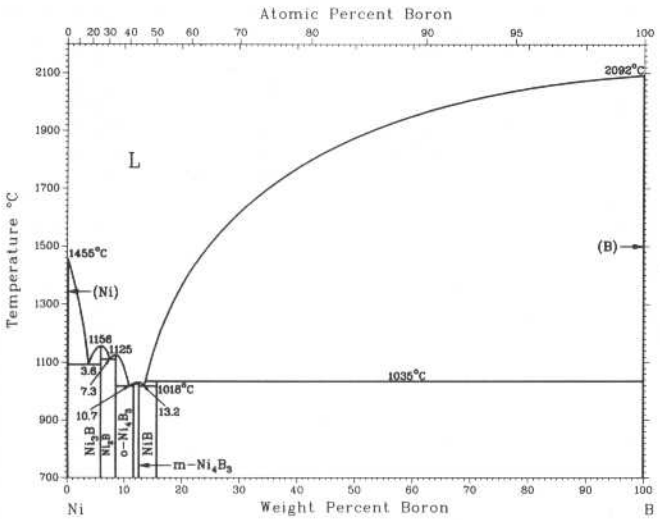

P.K. Liao and K.E. Spear, 1991

Phase	Composition, wt% B	Pearson symbol	Space group
(Ni)	0	*cF*4	$Fm\bar{3}m$
Ni_3B	6	*oP*6	*Pnma*
Ni_2B	8.4	*tI*12	*I4/mcm*
Ni_4B_3	11.5	(a)	*Pnma*
Ni_4B_3	12.5	(b)	*C2/c*
NiB	16	*oC*8	*Cmcm*
NiB_2(c)	26.9	(d)	...
NiB_{12}(c)	68.8	(d)	...
(βB)	100	*hR*108	$R\bar{3}m$

(a) Orthorhombic. (b) Monoclinic. (c) Existence of these compounds has been reported, but is highly unlikely. (d) Cubic

B-Pd

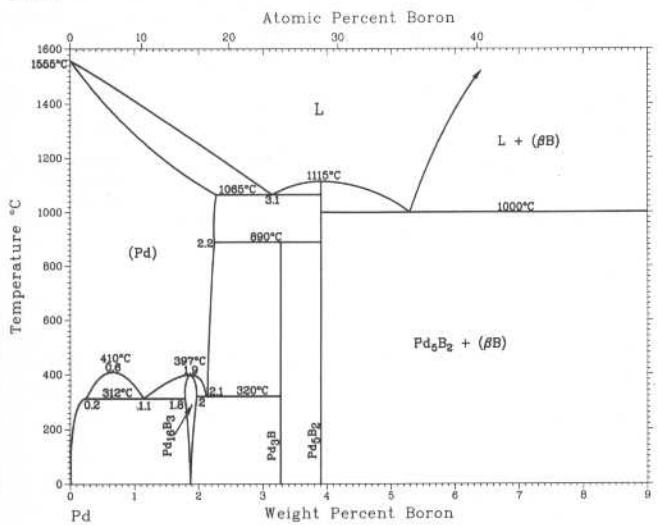

P.K. Liao and K.E. Spear, unpublished

Phase	Composition, wt% B	Pearson symbol	Space group
(Pd)	0.00 to 2.2	*cF*4	$Fm\bar{3}m$
$Pd_{16}B_3$	1.9	...	...
Pd_3B	3.4	*oP*16	*Pnma*
Pd_5B_2	3.9	*mC*28	*C2/c*
(βB)	100	*hR*105	$FR\bar{3}m$

B-Pt

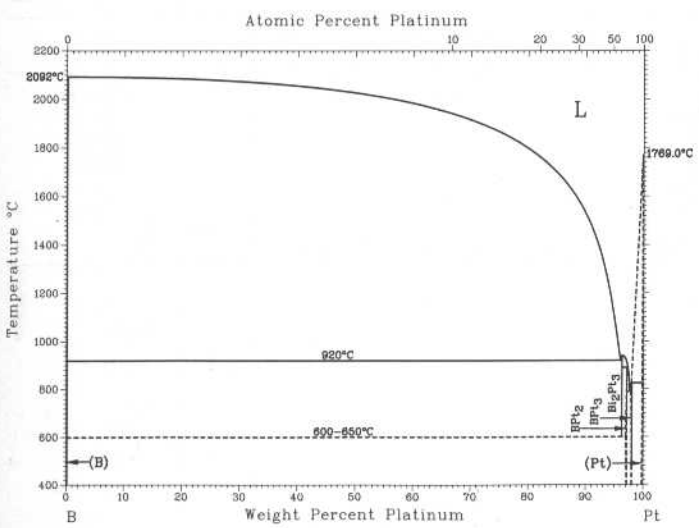

H. Okamoto, 1990

Phase	Composition, wt% Pt	Pearson symbol	Space group
(βB)	0	*hR*108	$R\bar{3}m$
B_2Pt_3	96	...	...
BPt_2	97.3	*hP*6	$P6_3/mmc$
BPt_3	98	*t***	...
(Pt)	100	*cF*4	$Fm\bar{3}m$

B-Re

K.I. Portnoi and V.M. Romashov, 1972

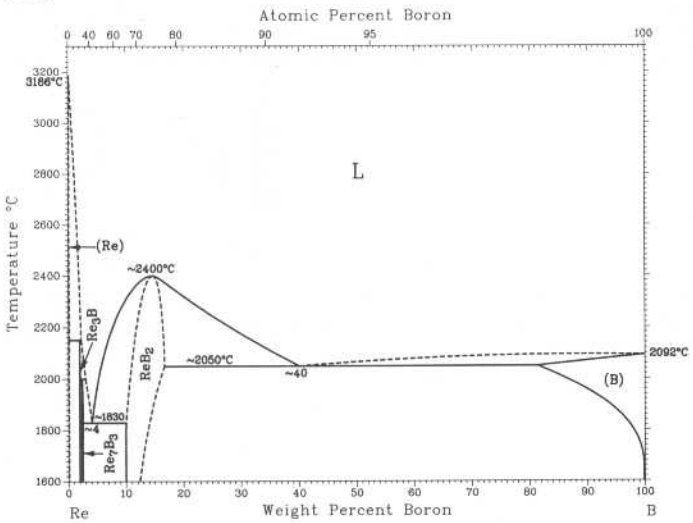

Phase	Composition, wt % B	Pearson symbol	Space group
(Re)	0 to ~0.06	*hP2*	$P6_3/mmc$
Re_3B	~2	*oC16*	*Cmcm*
Re_7B_3	~2.4	*hP20*	$P6_3/mc$
ReB_2	~10 to ~17	*hP6*	$P6_3/mmc$
(B)	~85 to 100	*hR105*	$R\bar{3}m$

B-Ru

W. Obrowski, 1963

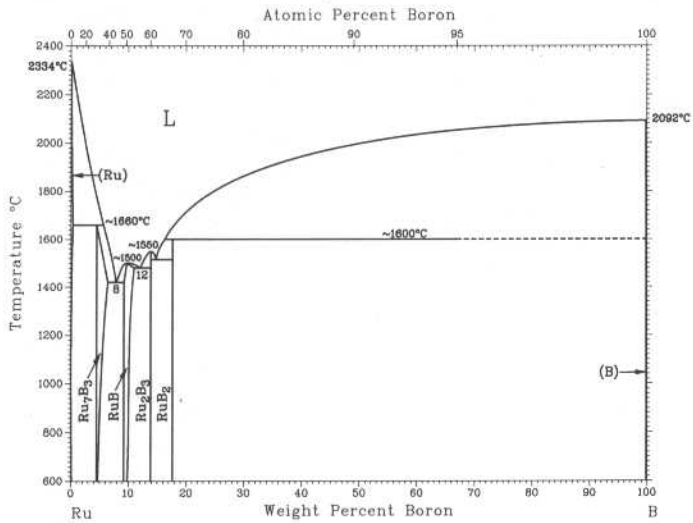

Phase	Composition, wt % B	Pearson symbol	Space group
(Ru)	0 to ~0.2	*hP2*	$P6_3/mmc$
Ru_7B_3	~4 to 6	*hP20*	$P6_3/mc$
RuB	~9 to 11	*hP2*	$P\bar{6}m2$
Ru_2B_3	14	*hP12*	$P6_3/mmc$
RuB_2	17.6	*oP6*	*Pmmn*
(B)	~100	*hR105*	$R\bar{3}m$

B-Sc

K.E. Spear and P.K. Liao, 1990

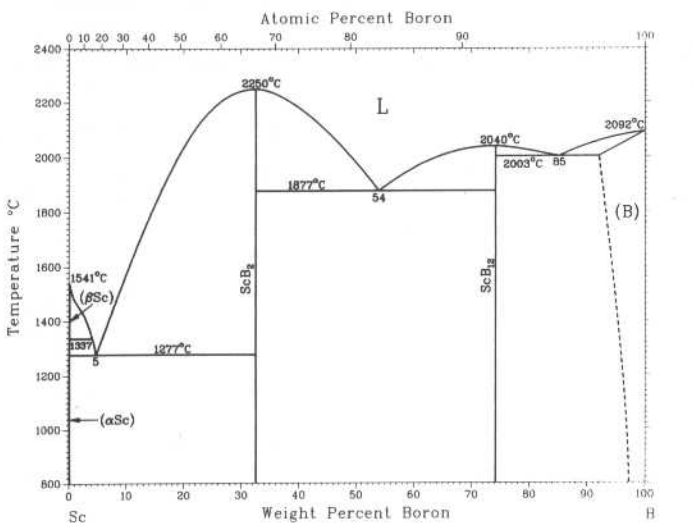

Phase	Composition, wt % B	Pearson symbol	Space group
(αSc)	0	*hP2*	$P6_3/mmc$
(βSc)	0	*cI2*	$Im\bar{3}m$
ScB_2	33	*hP3*	*P6/mmm*
ScB_{12}	73	*tI26*	*I4/mmm*
ScB_{20}	(a)	...	...
(βB)	100	hR108	$R\bar{3}m$

(a) Metastable, rhombohedral (βB)

B-Si

R.W. Olesinski and G.J. Abbaschian, 1984

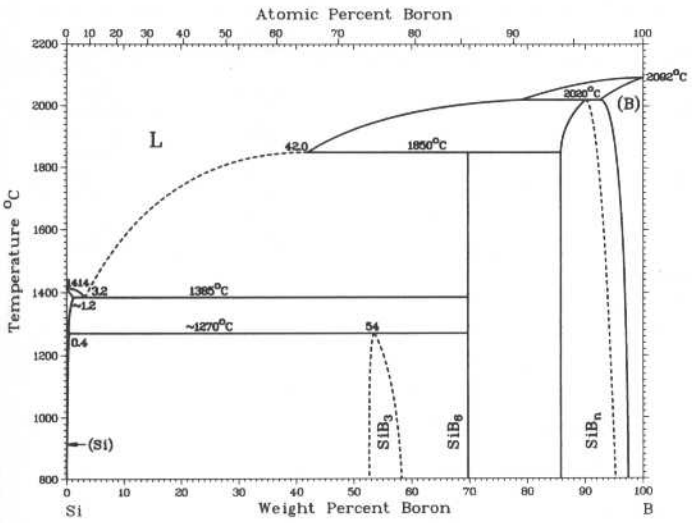

Phase	Composition, wt% B	Pearson symbol	Space group
(αSi)	0 to ~1.2	*cF*8	$Fd\bar{3}m$
(βSi) (HP)	0	*tI*4	$I4_1/amd$
SiB_3	52.7 to 58.4	*hR*15	$R\bar{3}m$
SiB_6	69.8	*oP*280	*Pnnm*
SiB_n	84.3 to ~93	*hR*12	$R\bar{3}m$
(B)	~93 to ~100	*hR*12	$R\bar{3}m$
(βB)(a)	100	*hR*105	$R\bar{3}m$

(a) Assumed to be the only stable phase of pure B

B-Ta

H. Okamoto, 1990

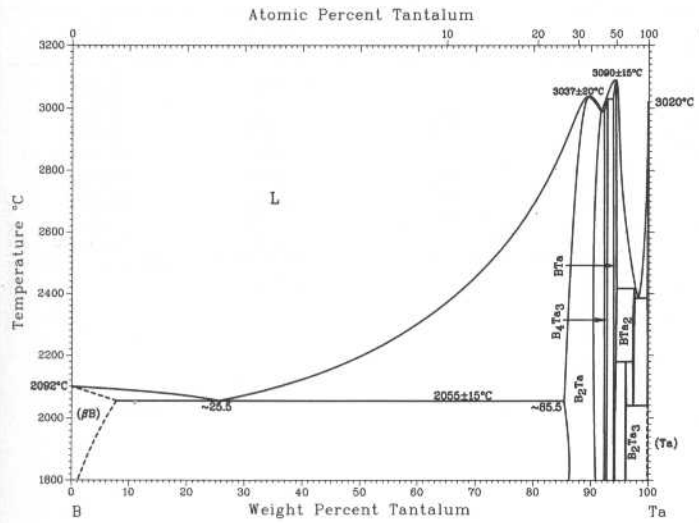

Phase	Composition, wt% Ta	Pearson symbol	Space group
(βB)	0 to ~2	*hR*108	$R\bar{3}m$
B_2Ta	~85.5 to 91	*hP*3	*P6/mmm*
B_4Ta_3	92.4 to 92.9	*oI*14	*Immm*
BTa	94 to 95	*oC*8	*Cmcm*
B_2Ta_3	96.0 to 96.3	*tP*10	*P4/mbm*
BTa_2	97.4 to 97.7	*tI*12	*I4/mcm*
(Ta)	100	*cI*2	$Im\bar{3}m$

B-Ti

J.L. Murray, P.K Liao, and K.E. Spear, 1987

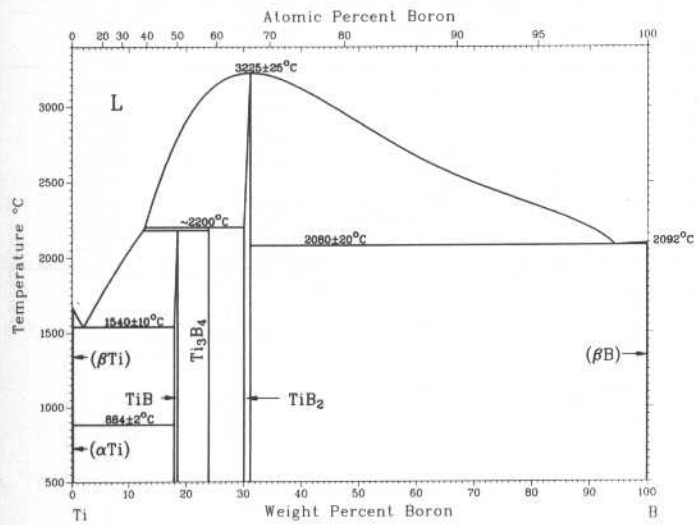

Phase	Composition, wt% B	Pearson symbol	Space group
(αTi)	0 to <0.05	*hP*2	$P6_3/mmc$
(βTi)	0 to <0.05	*cI*2	$Im\bar{3}m$
TiB	18 to 18.4	*oP*8	*Pnma*
Ti_3B_4	22.4	*oI*14	*Immm*
TiB_2	30.1 to 31.1	*hP*3	*P6/mmm*
(βB)	~100	*hR*108	$R\bar{3}m$

B-V

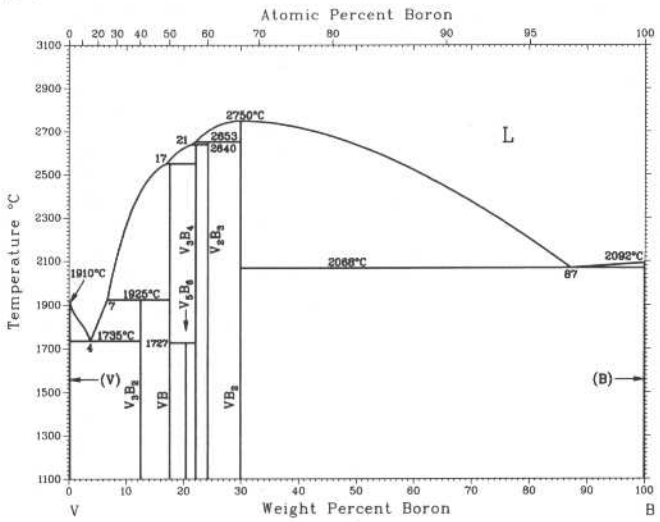

K.E. Spear, P.K. Liao, and J.F. Smith, 1991

Phase	Composition, wt% B	Pearson symbol	Space group
(V)	0	*cI*2	$Im\bar{3}m$
V_3B_2	12	*tP*10	*P4/mbm*
VB	18	*oC*8	*Cmcm*
V_5B_6	20.3	(a)	*Ammm*
V_3B_4	22	*oI*14	*Immm*
V_2B_3	24	(a)	*Cmcm*
VB_2	30	*hP*3	*P6/mmm*
(βB)	100	*hR*108	$R\bar{3}m$

(a) Orthorhombic

B-W

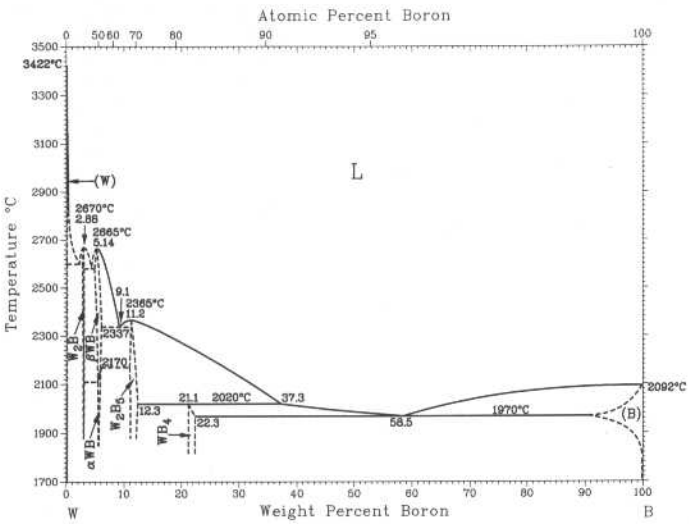

S.V. Nagender Naidu and P. Rama Rao, 1991

Phase	Composition, wt% B	Pearson symbol	Space group
(W)	0	*cI*2	$Im\bar{3}m$
W_2B	2.9	*tI*12	*I4/mcm*
βWB	5.2	*oC*8	*Cmcm*
αWB	5.4	*tI*16	$I4_1/amd$
W_2B_5	11.1	*hP*14	$P6_3/mmc$
WB_4	21.1	*hP*20	$P6_3/mmc$
(B)	100	*hR*12	$R\bar{3}m$
		*tP*50	$P4_2/nnm$

B-Y

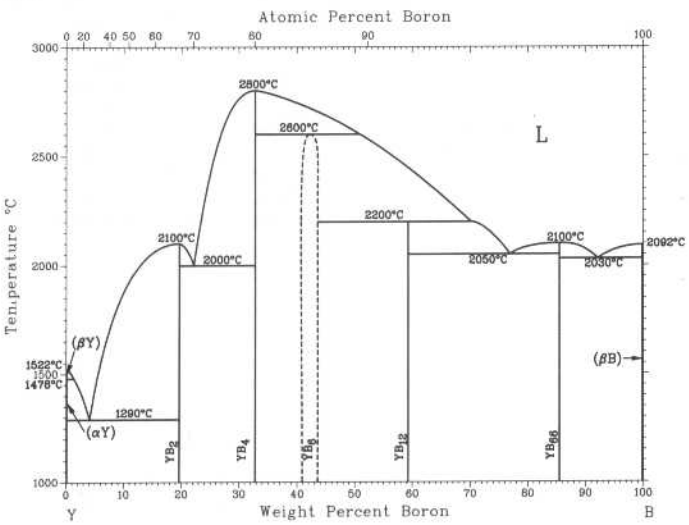

P.K. Liao and K.E. Spear, unpublished

Phase	Composition, wt% B	Pearson symbol	Space group
(βY)	0	*cI*2	$Im\bar{3}m$
(α)Y	0	*hP*2	$P6_3/mmc$
YB_2	19.6	*hP*3	*P6/mmm*
YB_4	32.7	*tP*20	*P4/mbm*
YB_6	42.2	*cP*7	$Pm\bar{3}m$
YB_{12}	59.3	*cF*52	$Fm\bar{3}m$
YB_{66}	85.6	...	$Fm\bar{3}c$
(βB)	100	*hR*108	$R\bar{3}m$

B-Zr

From [Zirconium]

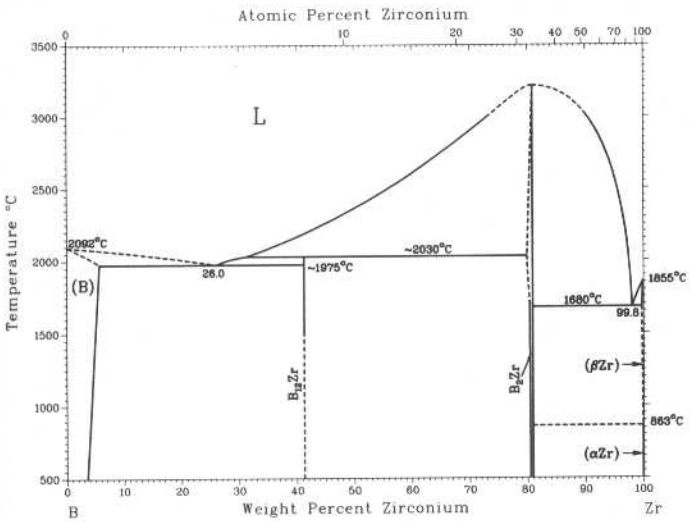

Phase	Composition, wt% Zr	Pearson symbol	Space group
(B)	~0	*hR*105	$R\bar{3}m$
$B_{12}Zr$	40.9	*cF*52	$Fm\bar{3}m$
B_2Zr	80 to 83.8	*hP*3	*P6/mmm*
(βZr)	99.8 to 100	*cI*2	$Im\bar{3}m$
(αZr)	~100	*hP*2	$P6_3/mmc$

Ba-Ca

C.B. Alcock and V.P. Itkin, 1986

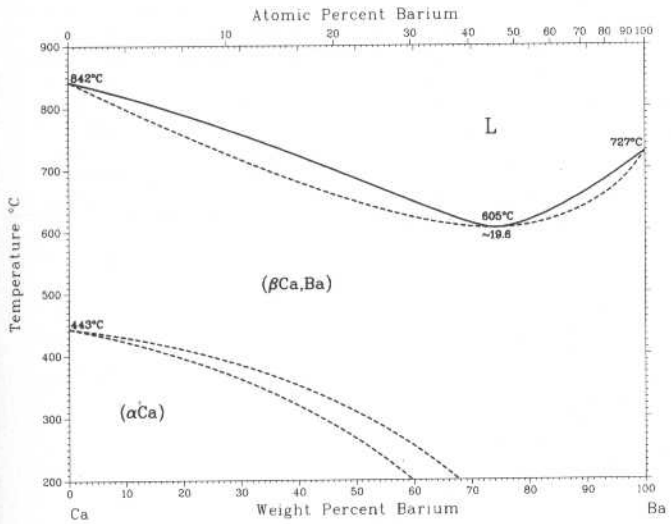

Phase	Composition, wt% Ba	Pearson symbol	Space group
(αCa)	0 to 60	*cF*4	$Fm\bar{3}m$
(βCa,Ba)	0 to 100	*cI*2	$Im\bar{3}m$

Ba-Cd

H. Okamoto, 1990

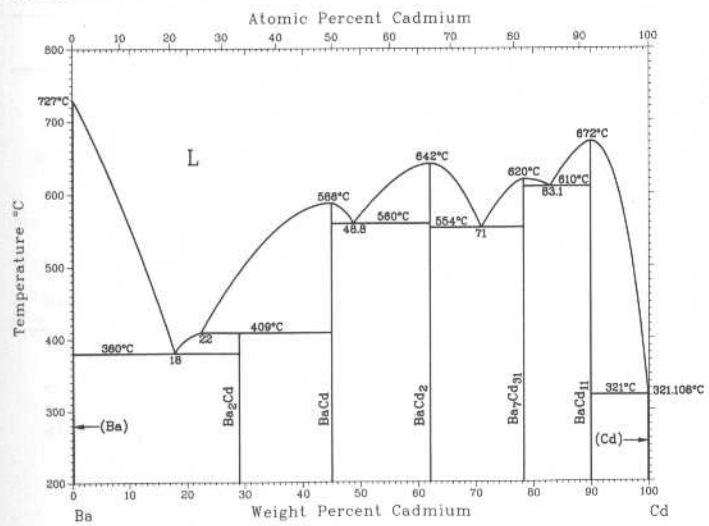

Phase	Composition, wt% Cd	Pearson symbol	Space group
(Ba)	0	*cI*2	$Im\bar{3}m$
Ba_2Cd	29.0	*tI*6	*I4/mmm*
BaCd	45	*cP*2	$Pm\bar{3}m$
$BaCd_2$	62.1	*oI*12	*Imma*
Ba_7Cd_{31}	78.4	*hP*41	*P6/mmm*
$BaCd_{11}$	90.0	*tI*48	$I4_1/amd$
(Cd)	100	*hP*2	$P6_3/mmc$

Ba-Cu

D.J. Chakrabarti and D.E. Laughlin, 1984

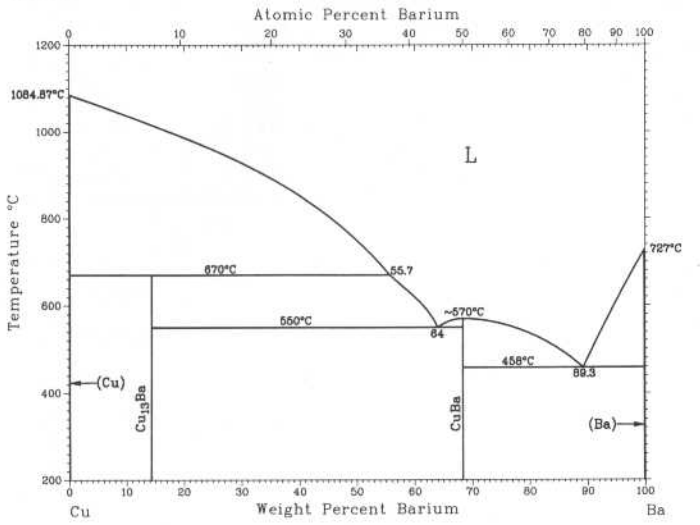

Phase	Composition, wt% Ba	Pearson symbol	Space group
(Cu)	0	*cF*4	$Fm\bar{3}m$
$Cu_{13}Ba$	14.25	*cF*112	$Fm\bar{3}c$
CuBa	68.3	*hP*8	$P6_3/mmc$
(Ba)	100	*cI*2	$Im\bar{3}m$
Pressure-stabilized phase			
Ba	100	*hP*2	$P6_3/mmc$

Ba-Ga

V.P. Itkin and C.B. Alcock, 1991

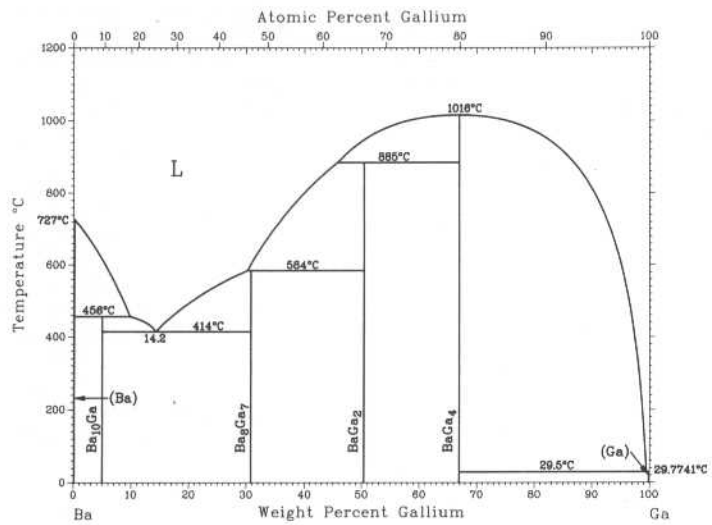

Phase	Composition, wt% Ga	Pearson symbol	Space group
(Ba)	0	*cI*2	$Im\bar{3}m$
$Ba_{10}Ga$	4.8	*cF*176	$Fd\bar{3}m$
Ba_8Ga_7	30.8	*cP*60	$P2_13$
$BaGa_2$	50.4	*hP*3	*P*6/*mmm*
$BaGa_4$	67	*tI*10	*I*4/*mmm*
(Ga)	100	*hP*2	$P6_3/mmc$

Ba-Ge

P.R. Subramanian, 1990

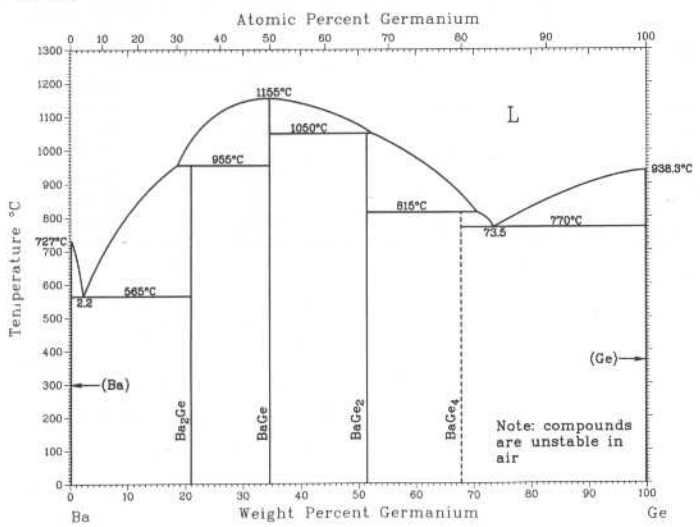

Phase	Composition, wt% Ge	Pearson symbol	Space group
(Ba)	0	*cI*2	$Im\bar{3}m$
Ba_2Ge	20.9	*oP*12	*Pnma*
BaGe	35	*oC*8	*Cmcm*
$BaGe_2$	51.4	*cP*84	$P4_132$
		*oP*24	*Pmna*
$BaGe_4$	68	...	...
(Ge)	100	*cF*8	$Fd\bar{3}m$
High-pressure phase			
$BaGe_2$(a)	51.4	*tI*12	$I4_1/amd$

(a) Prepared at 1000 °C, 40 kbar pressure

Ba-H

D.T. Peterson and M. Indig, 1960

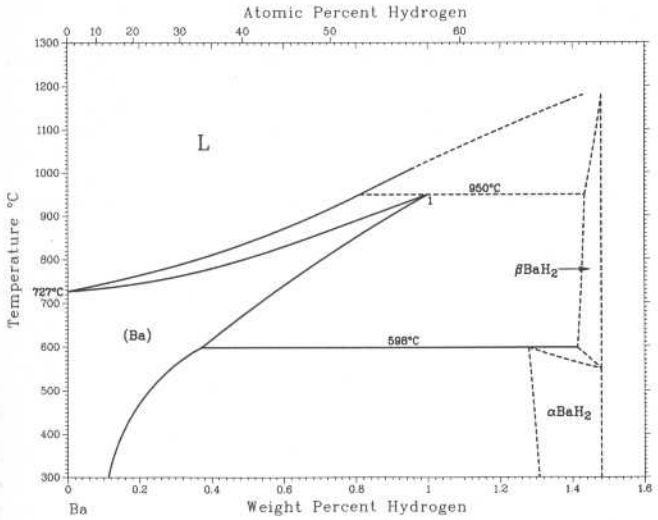

Phase	Composition, wt% H	Pearson symbol	Space group
(Ba)	0 to 1	*cI*2	$Im\bar{3}m$
αBaH_2	~1.3 to 1.5	*oP*12	*Pnma*
βBaH_2	~1.4 to 1.5	*cI**	...

Ba-Hg

P.R. Subramanian, 1990

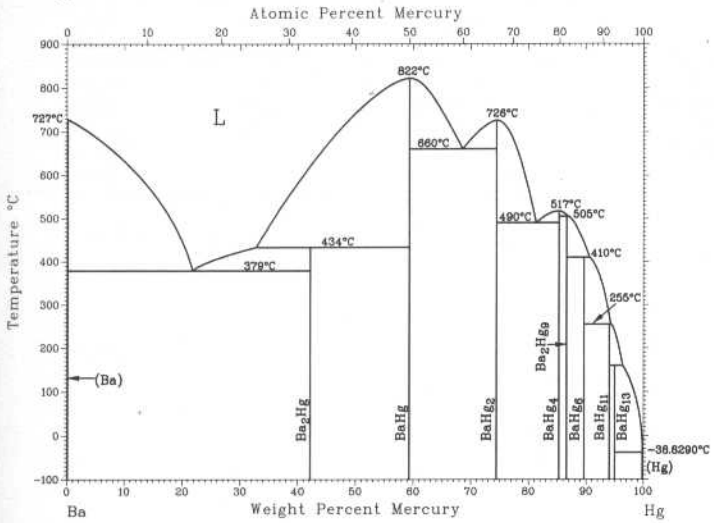

Phase	Composition, wt% Hg	Pearson symbol	Space group
(Ba)	0	*cI*2	$Im\bar{3}m$
Ba_2Hg	42.2	*tI*6	*I4/mmm*
BaHg	59	*cP*2	$Pm\bar{3}m$
$BaHg_2$	74.5	*oI*12	*Imma*
$BaHg_4$	85	...	...
Ba_2Hg_9	~86.7	*hP*38	*P6/mmm*
$BaHg_6$	~89.8	...	...
$BaHg_{11}$	~94.1	*cP*36	$Pm\bar{3}m$
$BaHg_{13}$	~95	...	...
(Hg)	~100	*hR*1	$R\bar{3}m$

Ba-In

H. Okamoto, 1992

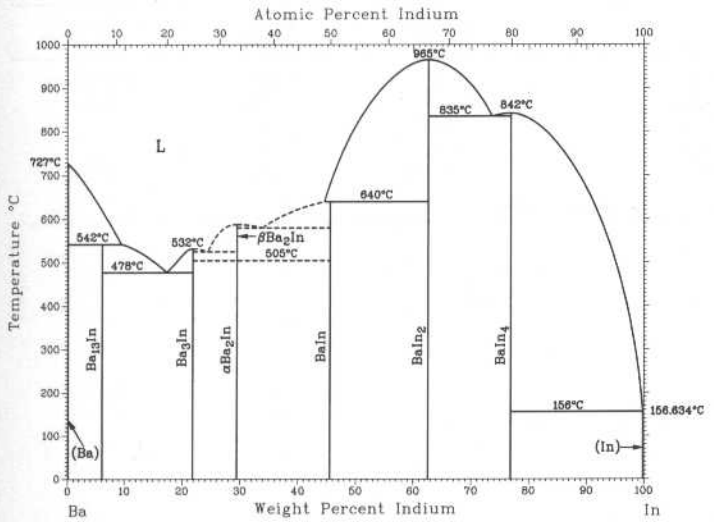

Phase	Composition, wt% In	Pearson symbol	Space group
(Ba)	0	*cI*2	$Im\bar{3}m$
$Ba_{13}In$	6.0	...	...
Ba_3In	22	...	...
βBa_2In	29.5	...	...
αBa_2In	29.5	...	...
BaIn	46	(a)	...
$BaIn_2$	62.6	*oI*12	*Imma*
$BaIn_4$	77	*tI*10	*I4/mmm*
(In)	100	*tI*2	*I4/mmm*

Ba-Li

A.D. Pelton, 1984

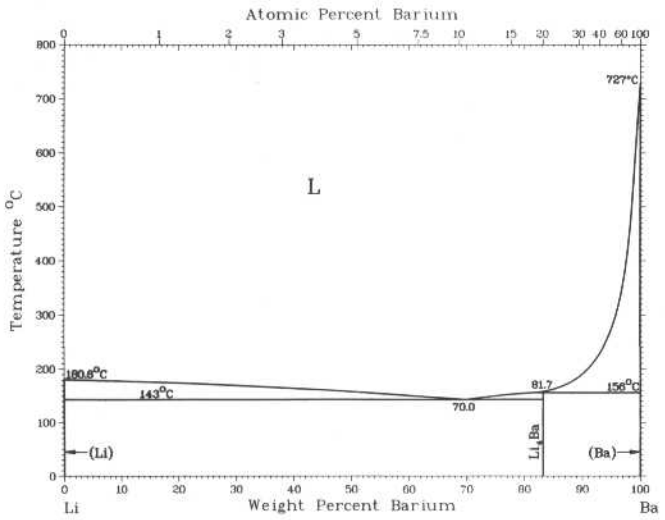

Phase	Composition, wt% Ba	Pearson symbol	Space group
(βLi)	0	*cI*2	$Im\bar{3}m$
(αLi)(a)	0	*hP*2	$P6_3/mmc$
Li_4Ba	83	*hP*30	$P6_3/mmc$
(Ba)	100	*cI*2	$Im\bar{3}m$

(a) Exists below –201 °C

Ba-Mg

A.A. Nayeb-Hashemi and J.B. Clark, 1988

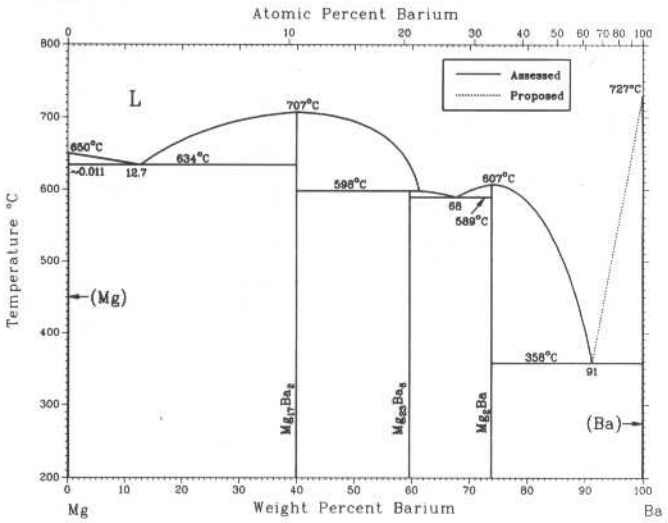

Phase	Composition, wt% Ba	Pearson symbol	Space group
(Mg)	0.0 to ~0.011	*hP*2	$P6_3/mmc$
$Mg_{17}Ba_2$	39.94	*hR*19	$R\bar{3}m$
$Mg_{23}Ba_6$	59.58	*cF*116	$Fm\bar{3}m$
Mg_2Ba	73.85	*hP*12	$P6_3/mmc$
(αBa)	100	*cI*2	$Im\bar{3}m$

Ba-Na

A.D. Pelton, 1985

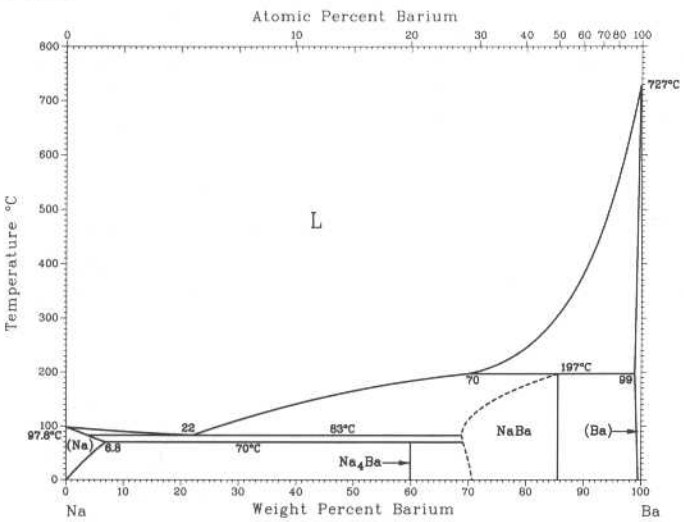

Phase	Composition, wt% Ba	Pearson symbol	Space group
(αNa)	0	*hP*2	$P6_3/mmc$
(βNa)	0 to 6.8	*cI*2	$Im\bar{3}m$
Na_4Ba	60	(a)	...
NaBa	69 to 86	(b)	...
(Ba)	99 to 100	*cI*2	$Im\bar{3}m$

(a) Tetragonal. (b) Orthorhombic

Ba-P

P.R. Subramanian, 1990

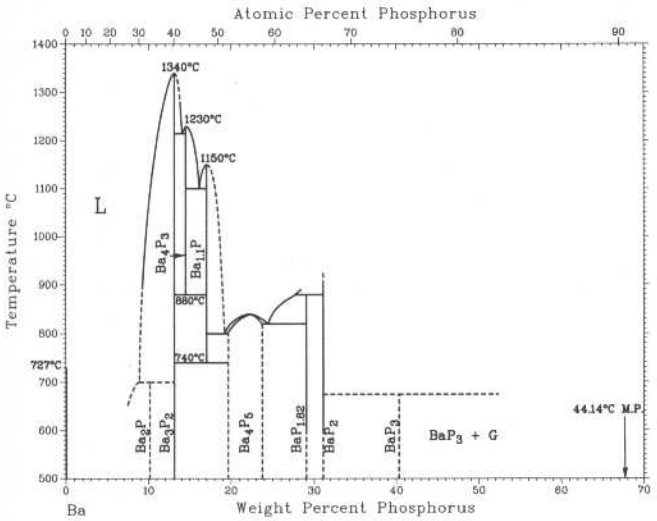

Phase	Composition, wt% P	Pearson symbol	Space group
(Ba)	0	*cI*2	$Im\bar{3}m$
Ba_2P	10.1	...	...
Ba_3P_2	13	*cI*28	$I\bar{4}3d$
Ba_4P_3	~14.5	...	...
$Ba_{1.1}P$	~17.0	...	...
Ba_4P_5	~22.0	...	...
$BaP_{1.82}$	~29.0	...	...
BaP_2	31.1	...	...
BaP_3	40	*mC*16	*C*2/*m*
Ba_3P_{14}	~51.3	*mP*34	*P*21/*a*
BaP_{10}	~69.3	*oC*44	$Cmc2_1$

Ba-Pb

From [Hansen]

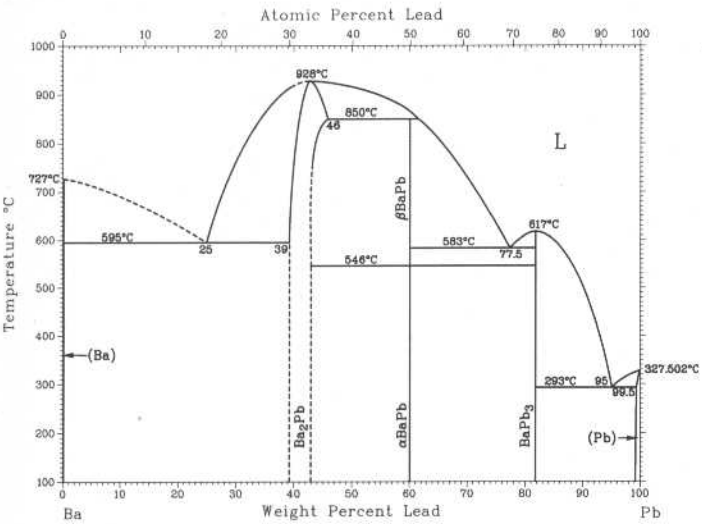

Phase	Composition, wt% Pb	Pearson symbol	Space group
(Ba)	0	*cI*2	$Im\bar{3}m$
Ba_2Pb	~39 to 43.0	*oP*12	*Pnma*
βBaPb	60	...	...
αBaPb	60	*oC*8	*Cmcm*
$BaPb_3$	82	*hR*12	$R\bar{3}m$
(Pb)	99.5 to 100	*cF*4	$Fm\bar{3}m$

Ba-Se

H. Okamoto, 1991

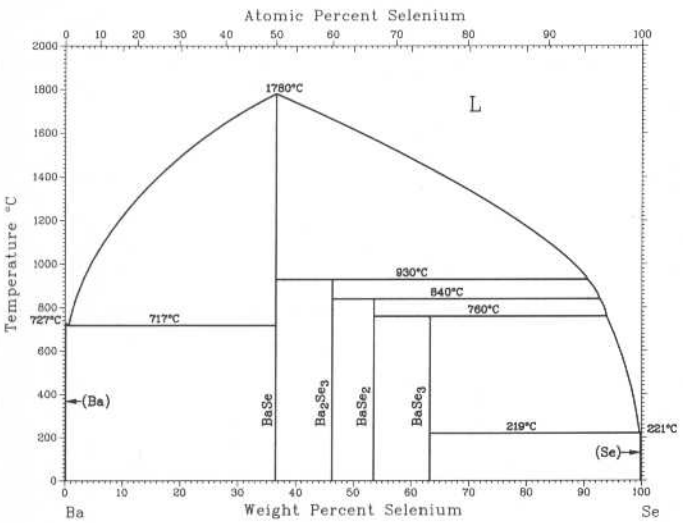

Phase	Composition, wt% Se	Pearson symbol	Space group
(Ba)	0	*cI*2	$Im\bar{3}m$
BaSe	37	*cF*8	$Fm\bar{3}m$
Ba_2Se_3	46	...	...
$BaSe_2$	53.5	*mC*12	*C*2/*c*
$BaSe_3$	63	*tP*8	$P\bar{4}2_1m$
(γSe)	100	*hP*3	$P3_121$

Ba-Si

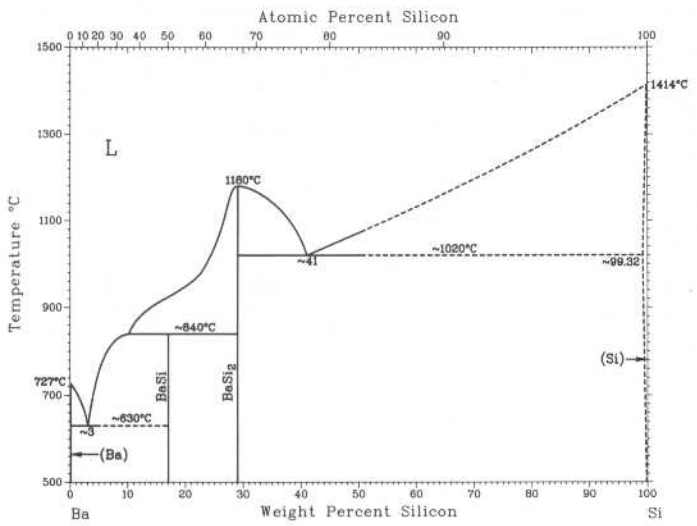

I. Obinata, Y. Takeuchi, K. Kurihara, and M. Watanabe, 1964

Phase	Composition, wt% Si	Pearson symbol	Space group
(Ba)	~0	*cI*2	$Im\bar{3}m$
Ba_2Si(a)	9.3	*oP*12	*Pnma*
Ba_5Si_3(a)	10.9	*tP*32	*P4/ncc*
BaSi	17	*oC*8	*Cmcm*
Ba_3Si_4	21.4	*tP*28	$P4_2/mnm$
$BaSi_2$	29.1	*oP*24	*Pnma*
		*hP*3	*P6/mmm*
(Si)	~100	*cF*8	$Fd\bar{3}m$

(a) Found after the diagram was constructed

Ba-Te

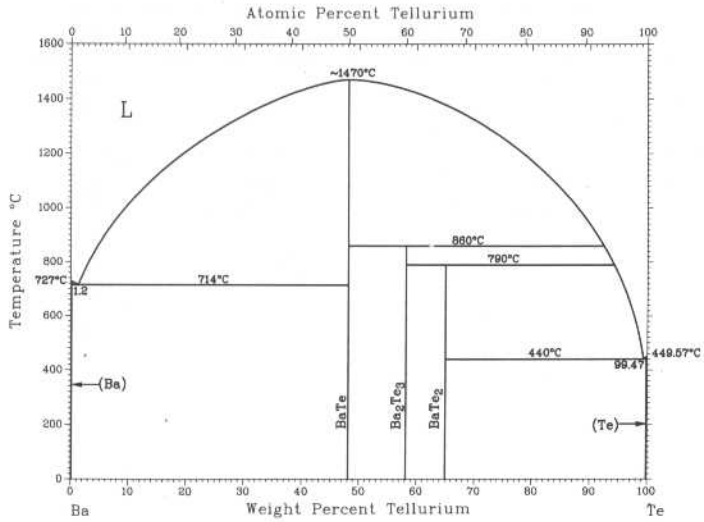

H. Okamoto, unpublished

Phase	Composition, wt% Te	Pearson symbol	Space group
(Ba)	0	*cI*2	$Im\bar{3}m$
BaTe	48	*cF*8	$Fm\bar{3}m$
Ba_2Te_3	58	...	...
$BaTe_2$	65.1	...	...
(Te)	100	*hP*3	$P3_121$

Ba-Tl

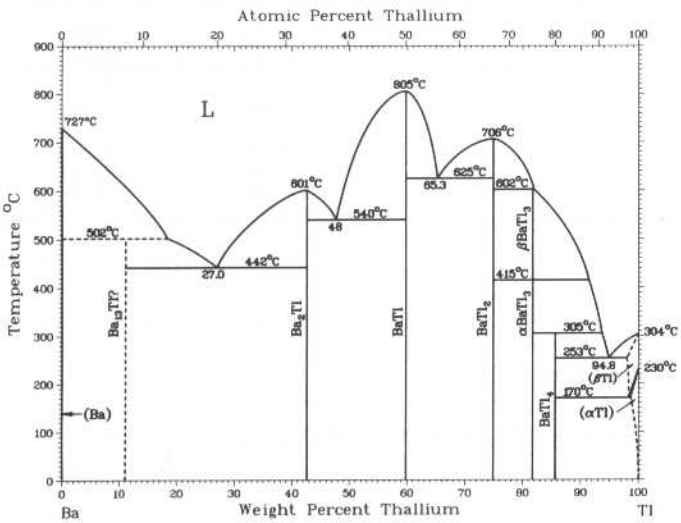

G. Bruzzone, 1966

Phase	Composition, wt% Tl	Pearson symbol	Space group
(Ba)	~0	*cI*2	$Im\bar{3}m$
$Ba_{13}Tl$	~10	...	...
Ba_2Tl	42.6	...	...
BaTl	60	...	...
$BaTl_2$	74.9	*hP*6	$P6_3/mmc$
$\alpha BaTl_3$	79	...	...
$\beta BaTl_3$	79	...	...
$BaTl_4$	86	...	...
(βTl)	~98 to 100	*hP*2	$P6_3/mmc$
(αTl)	~98.7 to 100	*cI*2	$Im\bar{3}m$

Ba-Zn

H. Okamoto, 1991

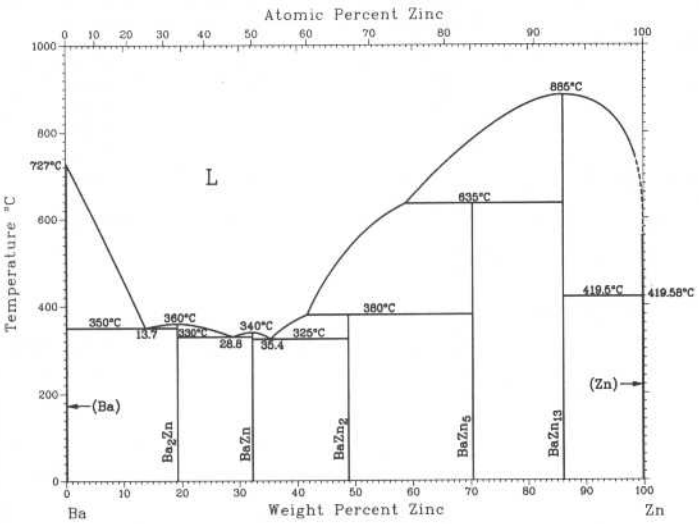

Phase	Composition, wt% Zn	Pearson symbol	Space group
(Ba)	0	*cI*2	$Im\bar{3}m$
Ba_2Zn	19.2	*tI*6	*I*4/*mmm*
BaZn	32	*cP*2	$Pm\bar{3}m$
$BaZn_2$	48.8	*oI*12	*Imma*
$BaZn_5$	70.4	*oC*25	*Cmcm*
$BaZn_{13}$	86.2	*cF*112	$Fm\bar{3}c$
(Zn)	100	*hP*2	$P6_3/mmc$

Be-Co

H. Okamoto, L.E. Tanner, and T. Nishizawa, 1988

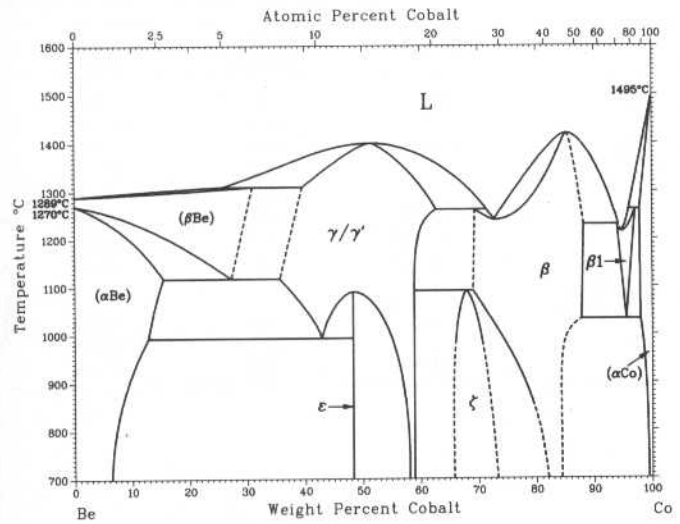

Phase	Composition, wt% Co	Pearson symbol	Space group
(βBe)	0 to 29	*cI*2	$Im\bar{3}m$
(αBe)	0 to 15.61	*hP*2	$P6_3/mmc$
$Be_{12}Co$	(a)	*tI*26	*I*4/*mmm*
γ	34.7 to ?	*cI*52	$Im\bar{3}m$
γ′	? to 62	*cF*416	$Fm\bar{3}m$
ε	~47	*hP*19	*P*6*m*2
		*hP*48	$P6_3/mcm$
δ	(a)	*cF*24	$F4\bar{3}m$
β′	(a)	*cI*2	$Im\bar{3}m$
ζ′	(a)	(b)	?
ζ	66 to 70	*hP*96	$P6_3/mcm$
β	70 to 88	*cP*2	$Pm\bar{3}m$
β1	94 to 97	*cI*2?	$Im\bar{3}m$
(αCo)	98 to 100	*cF*4	$Fm\bar{3}m$
(εCo)	99.9 to 100(a)	*hP*2	$P6_3/mmc$
Metastable phases			
...	~86.7	(c)	?
...	91 to 97	(d)	?

(a) Not shown in the assessed diagram. (b) Orthorhombic. (c) bct. (d) Tetragonal

Be-Cr

M. Venkatraman and J.P. Neumann, 1987

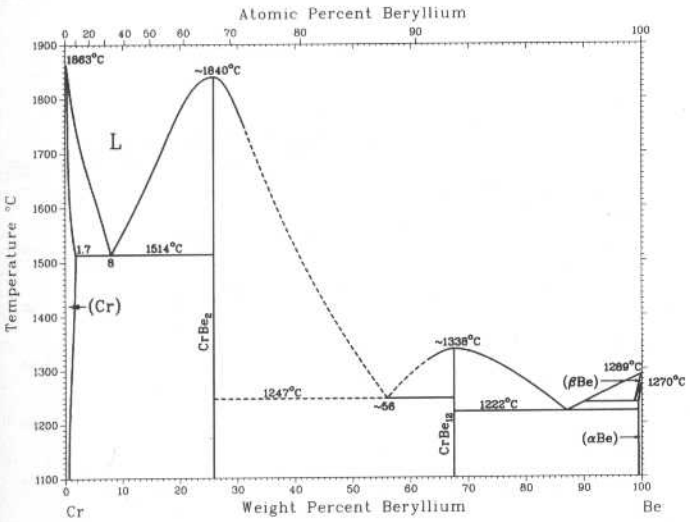

Phase	Composition, wt% Be	Pearson symbol	Space group
(Cr)	0 to 1.7	*cI*2	$Im\bar{3}m$
$CrBe_2$	25.8 to ~26	*hP*12	$P6_3/mmc$
$CrBe_{12}$	67.5	*tI*26	*I*4/*mmm*
(βBe)	~98.9 to 100	*cI*2	$Im\bar{3}m$
(αBe)	~99.54 to 100	*hP*2	$P6_3/mmc$

Be-Cu

H. Okamoto, 1992

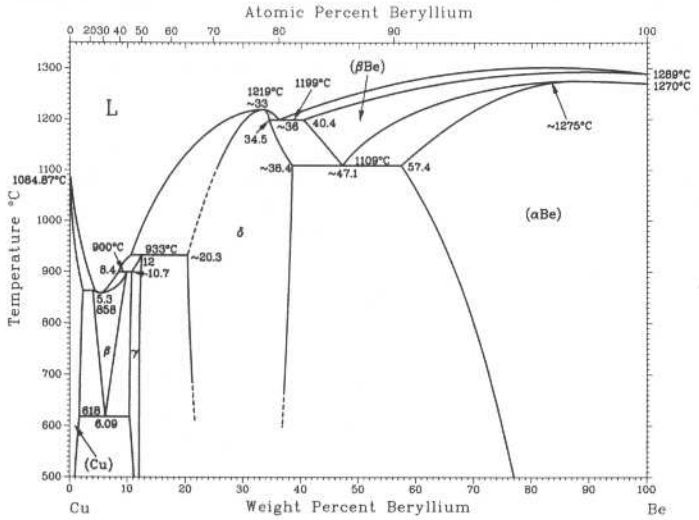

Phase	Composition, wt% Be	Pearson symbol	Space group
(Cu)	0 to 2.2	*cF*4	$Fm\bar{3}m$
β	4.3 to 9.8	*cI*2	$Im\bar{3}m$
γ	10.3 to 12.4	*cP*2	$Pm\bar{3}m$
δ	~20.4 to ~38.5	*cF*24	$Fd\bar{3}m$
(βBe)	40.4 to 100	*cI*2	$Im\bar{3}m$
(αBe)	57.5 to 100	*hP*2	$P6_3/mmc$

Be-Fe

H. Okamoto and L.E. Tanner, 1992

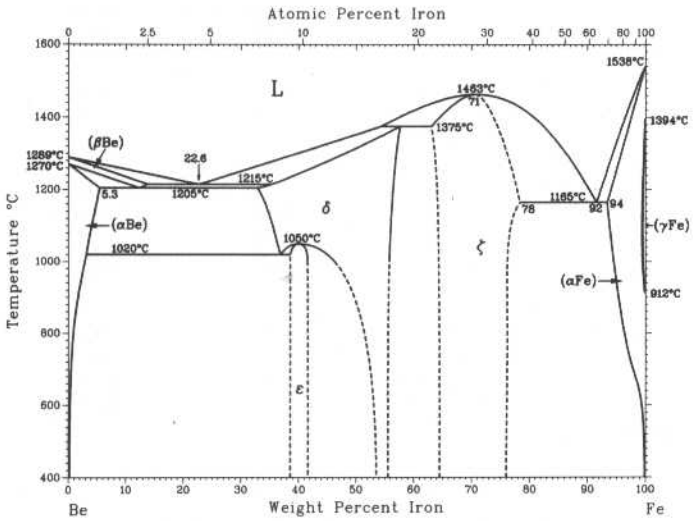

Phase	Composition, wt% Fe	Pearson symbol	Space group
(βBe)	0 to 11	*cI*2	$Im\bar{3}m$
(αBe)	0 to 5.3	*hP*2	$P6_3/mmc$
ε	~35 to 41	*hP*19	$P\bar{6}m2$
		*hP*48	$P6_3/mcm$
δ	32 to 58	*cF*24	$Fd\bar{3}m$
ζ	62 to 78	*hP*12	$P6_3/mmc$
(γFe)	99.7 to 100	*cF*4	$Fm\bar{3}m$
(αFe)	94 to 100	*cI*2	$Im\bar{3}m$
Metastable phases			
...	~86	*cF*16	$Fd\bar{3}m$
β	?	*cP*2	$Pm\bar{3}m$
BeF_3	~95	*cF*16	$Fm\bar{3}m$

Be-rich portion of the Be-Fe phase diagram

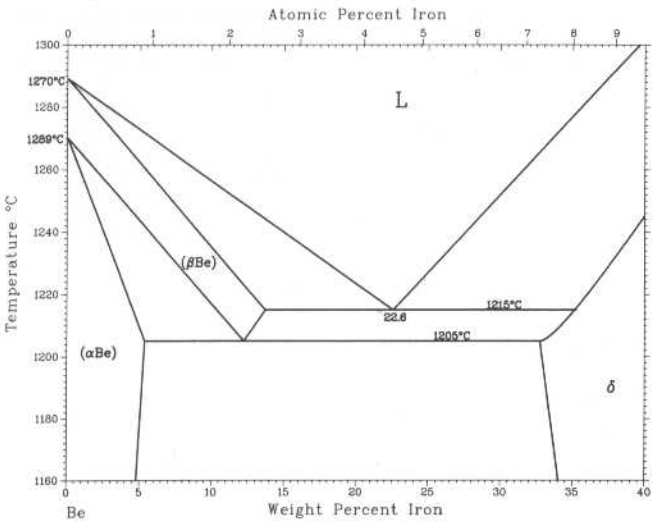

Be-Hf

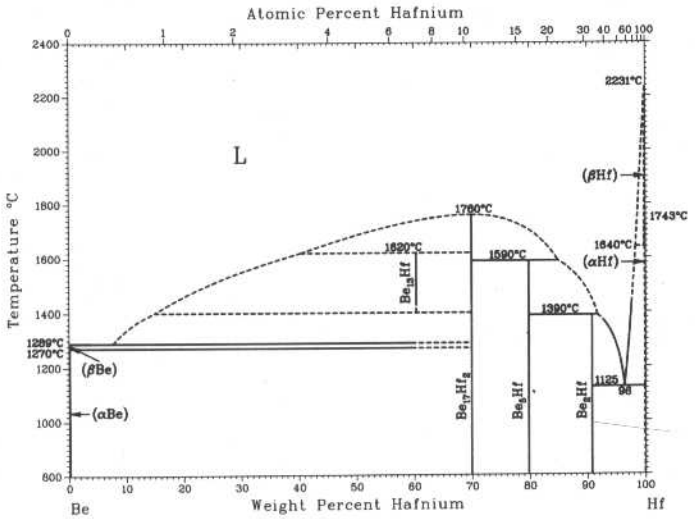

H. Okamoto and L.E. Tanner, 1987

Phase	Composition, wt% Hf	Pearson symbol	Space group
(βBe)	0	*cI*2	$Im\bar{3}m$
(αBe)	0	*hP*2	$P6_3/mmc$
$Be_{13}Hf$	60.2	*cF*112	$Fm\bar{3}c$
$Be_{17}Hf$	69.9	*hP**	$P\bar{6}m2$
($\alpha Be_{17}Hf_2$)	(a)	*hR*19	$R\bar{3}m$
($\beta Be_{17}Hf_2$)	(b)	*hP*38	$P6_3/mmc$
Be_5Hf	79.9	*hP*6	*P*6/*mmm*
Be_2Hf	90.8	*hP*3	*P*6/*mmm*
(βHf)	100	*cI*2	$Im\bar{3}m$
(αHf)	100	*hP*2	$P6_3/mmc$
Metastable phases			
BeHf	95	*oC*8	*Cmcm*
α′	99.7 to 100(c)	...	...

(a) Be-poor side. (b) Be-rich side. (c) Acicular martensite

Be-Nb

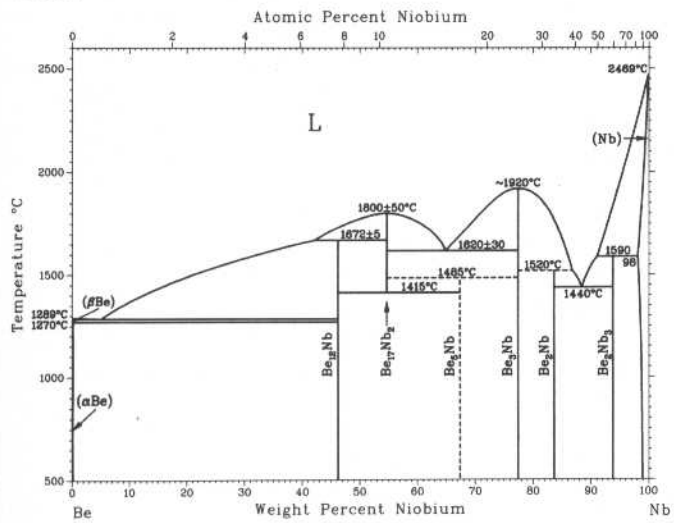

H. Okamoto and L.E. Tanner, 1987

Phase	Composition, wt% Nb	Pearson symbol	Space group
(βB)	0	*cI*2	$Im\bar{3}m$
(αBe)	0	*hP*2	$P6_3/mmc$
$Be_{12}Nb$	46.2	*tI*26	*I*4/*mmm*
$Be_{17}Nb_2$	54.7	*hR*19	$R\bar{3}m$
(a)	56.3	*hP**	...
Be_5Nb	67.4	*hP*6	*P*6/*mmm*
Be_3Nb	77	*hR*12	$R\bar{3}m$
(b)	83.7	*hP**	...
Be_2Nb	83.7	*cF*24	$Fd\bar{3}m$
	83.7	...	...
	83.73	...	...
Be_2Nb_3	94	*tP*10	*P*4/*mbm*
(Nb)	98.6 to 100	*cI*2	$Im\bar{3}m$

(a) Proposed as Be_8Nb. (b) Reported as Be_2Nb

Be-Ni

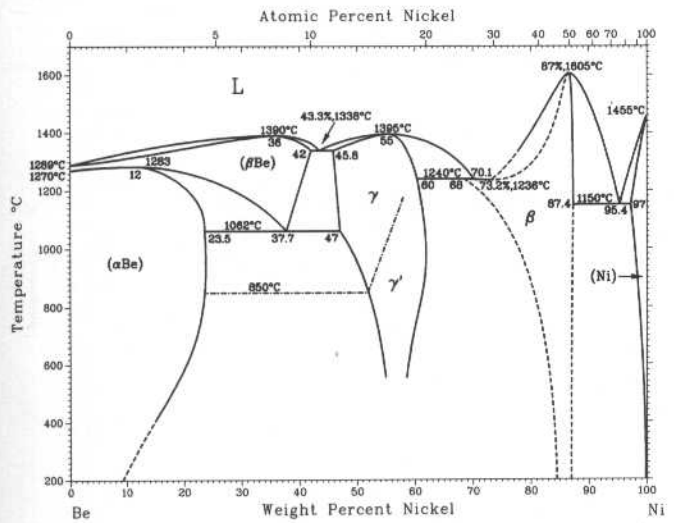

H. Okamoto and L.E. Tanner, 1991

Phase	Composition, wt% Ni	Pearson symbol	Space group
(βBe)	0 to 23.5	*cI*2	$Im\bar{3}m$
(αBe)	0 to 42	*hP*2	$P6_3/mmc$
γ	45.8 to >51	*cI*52	$I\bar{4}3m$
γ′	51 to 62	*cF*416	*F*23
β	68 to 87.4	*cP*2	$Pm\bar{3}m$
(Ni)	95.4 to 100	*cF*4	$Fm\bar{3}m$
Metastable phases			
?	92.2 to 93.4	*o***	?
β′	>87 to <95	*tI**	?
γ′$BeNi_3$	95	?	?

Be-Pd

H. Okamoto and L.E. Tanner, 1987

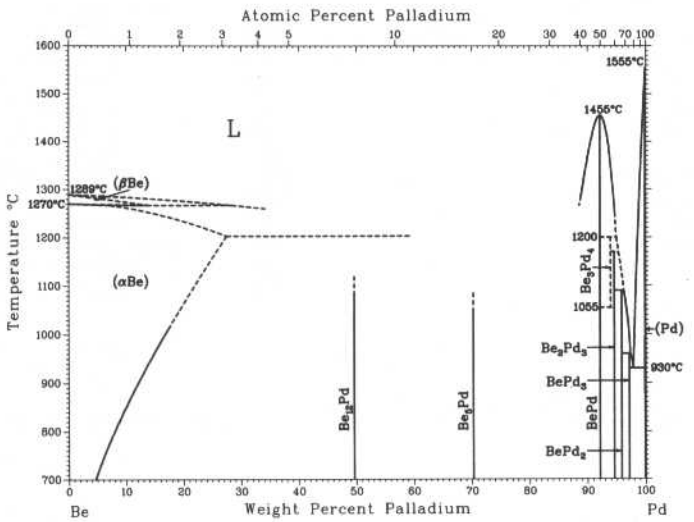

Phase	Composition, wt% Pd	Pearson symbol	Space group
(βBe)	0	*cI*2	$Im\bar{3}m$
(αBe)	0 to 38	*hP*2	$P6_3/mmc$
$Be_{12}Pd$	49.6	*tI*26	$I4/mmm$
Be_5Pd	70.3	*cF*24	$F\bar{4}3m$
BePd	92	*cP*2	$Pm\bar{3}m$
Be_3Pd_4	94.0	?	?
Be_2Pd_3	95	?	?
$BePd_2$	95.9	?	?
$BePd_3$	97	(a)	?
(Pd)	99.9 to 100	*cF*4	$Fm\bar{3}m$

(a) Orthorhombic

Be-Si

H. Okamoto and L.E. Tanner, 1987

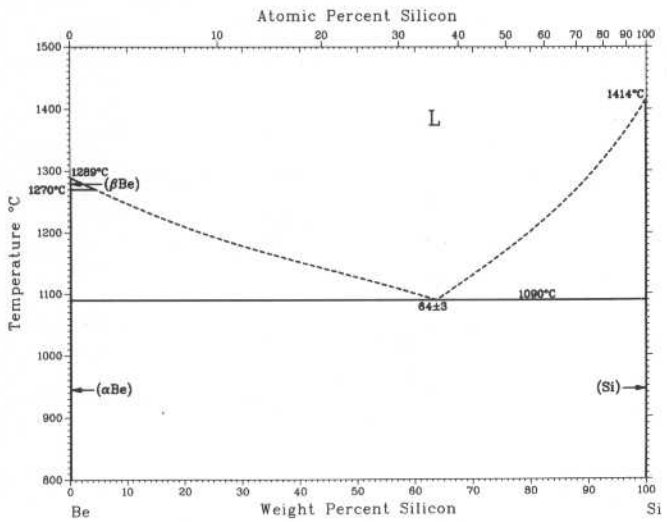

Phase	Composition, wt% Si	Pearson symbol	Space group
(βBe)	0	*cI*2	$Im\bar{3}m$
(αBe)	0	*hP*2	$P6_3/mmc$
(Si)	100	*cF*8	$Fd\bar{3}m$

Be-Th

H. Okamoto, L.E. Tanner, and D.E. Peterson, 1987

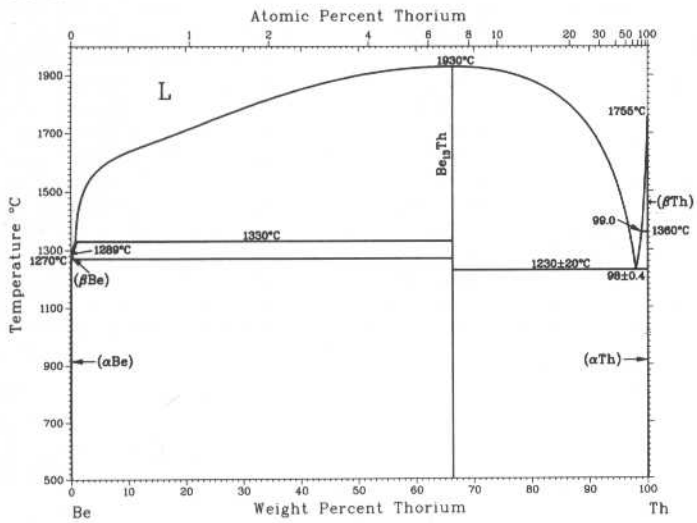

Phase	Composition, wt% Th	Pearson symbol	Space group
(βBe)	0	*cI*2	$Im\bar{3}m$
(αBe)	0	*hP*2	$P6_3/mmc$
$Be_{13}Th$	66.44	*cF*112	$Fm\bar{3}c$
(βTh)	100	*cI*2	$Im\bar{3}m$
(αTh)	100	*cF*4	$Fm\bar{3}m$

Be-Ti

J.L. Murray, 1987

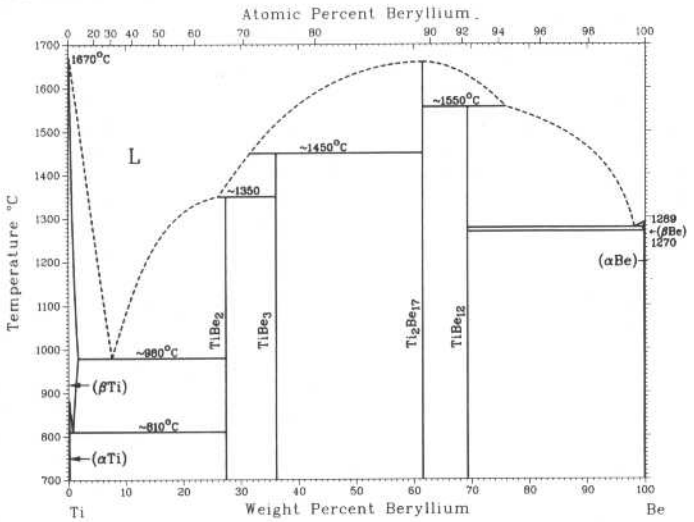

Phase	Composition, wt% Be	Pearson symbol	Space group
(βTi)	0 to ~1.5	*cI*2	$Im\bar{3}m$
(αTi)	~0	*hP*2	$P6_3/mmc$
$TiBe_2$	27.4	*cF*24	$Fd\bar{3}m$
$TiBe_3$	36	*hR*12	$R\bar{3}m$
αTi_2Be_{17}	61.6	*hR*19	$R\bar{3}m$
βTi_2Be_{17}	61.6	*hP*38	$P6_3/mmc$
$TiBe_{12}$	69.3	*tI*26	$I4/mmm$
TiBe(a)	~16	*cP*2	$Pm\bar{3}m$
(βBe)	~100	*cI*2	$Im\bar{3}m$
(αBe)	~100	*hP*2	$P6_3/mmc$

(a) Metastable

Be-W

H. Okamoto and L.E. Tanner, 1987

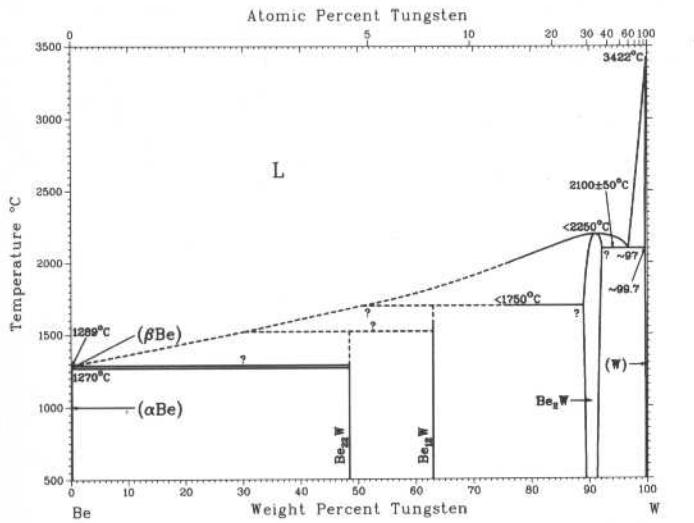

Phase	Composition, wt% W	Pearson symbol	Space group
(βBe)	0	*cI*2	$Im\bar{3}m$
(αBe)	0	*hP*2	$P6_3/mmc$
$Be_{24}W$?(a)	46	(b)	...
$Be_{22}W$	47.8	*cF*184	$Fd\bar{3}m$
$Be_{12}W$	63.0	*tI*26	$I4/mmm$
Be_2W	~89 to ~92	*hP*12	$P6_3/mmc$
(W)	~99.7 to 100	*cI*2	$Im\bar{3}m$

(a) Not accepted in the assessed phase diagram. (b) Tetragonal

Be-Zr

H. Okamoto, L.E. Tanner, and J.P. Abriata, 1987

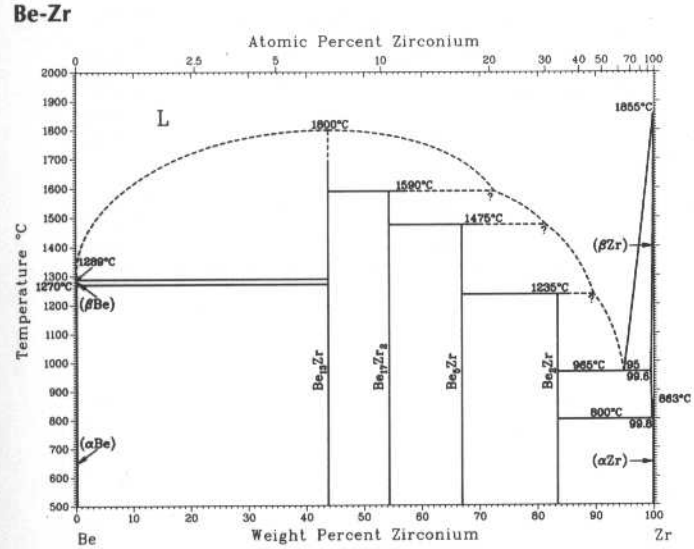

Phase	Composition, wt% Zr	Pearson symbol	Space group
(βBe)	0	*cI*2	$Im\bar{3}m$
(αBe)	0	*hP*2	$P6_3/mmc$
$Be_{13}Zr$	43.6	*cF*112	$Fm\bar{3}c$
$Be_{12}Zr$(a)	43.6	*tI**	...
$Be_{17}Zr_2$	54.3	*hR*19	$R\bar{3}m$
Be_5Zr	67.0	*hP*6	$P6/mmm$
Be_2Zr	83.5	*hP*3	$P6/mmm$
(βZr)	100	*cI*2	$Im\bar{3}m$
(αZr)	100	*hP*2	$P6_3/mmc$
Metastable phases			
BeZr	91	*oC*8	*Cmcm*
α′	99 to 100	(b)	...

(a) Not accepted in the assessed diagram. (b) Acicular martensite

Bi-Ca

H. Okamoto, 1991

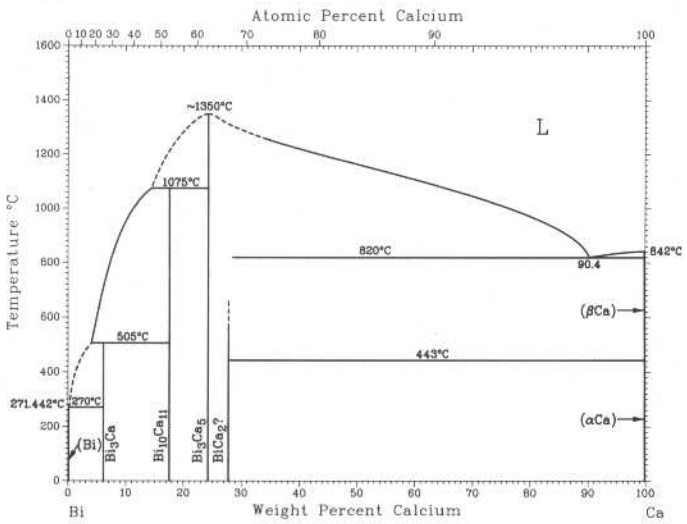

Phase	Composition, wt% Ca	Pearson symbol	Space group
(Bi)	0	*hR*2	$R\bar{3}m$
Bi_3Ca	6	...	...
$Bi_{10}Ca_{11}$	17.4	*tI*84	*I*4/*mmm*
Bi_3Ca_5	24.2	*oP*32	*Pnma*
$BiCa_2$	27.8	*tI*12	*I*4/*mmm*
(αCa)	100	*cF*4	$Fm\bar{3}m$
(βCa)	100	*cI*2	$Im\bar{3}m$

Bi-Cd

Z. Moser, J. Dutkiewicz, L. Zabdyr, and J. Salawa, 1988

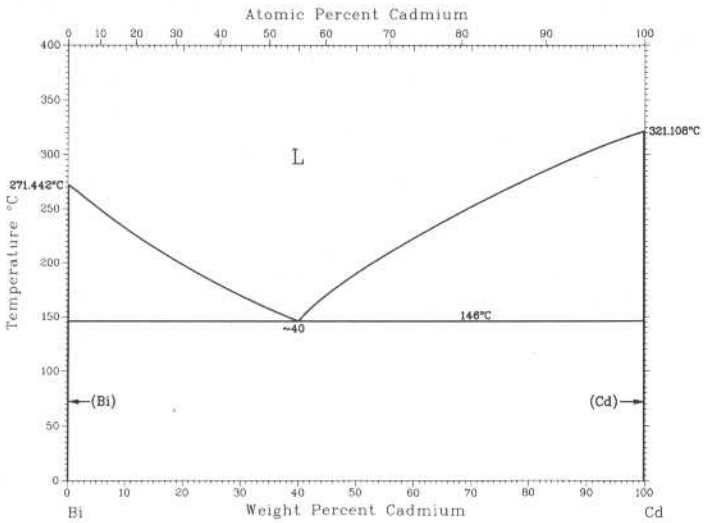

Phase	Composition, wt% Cd	Pearson symbol	Space group
(Bi)	0	*hR*2	$R\bar{3}m$
(Cd)	100	*hP*2	$P6_3/mmc$

Bi-Cs

J. Sangster and A.D. Pelton, 1991

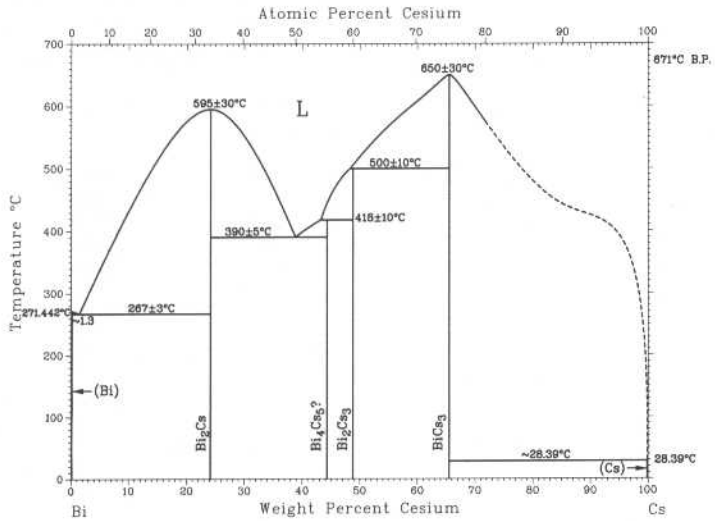

Phase	Composition, wt% Cs	Pearson symbol	Space group
(αBi)	0	*hR*2	$R\bar{3}m$
Bi_2Cs	24.1	*cF*24	$Fd\bar{3}m$
Bi_4Cs_5(?)	44.3	...	...
Bi_2Cs_3	49	...	...
$BiCs_3$	66	*cF*16	$Fd\bar{3}m$
	66	*cF*16	$Fm\bar{3}m$
(Cs)	100	*cI*2	$Im\bar{3}m$

Bi-Cu

D.J. Chakrabarti and D.E. Laughlin, 1984

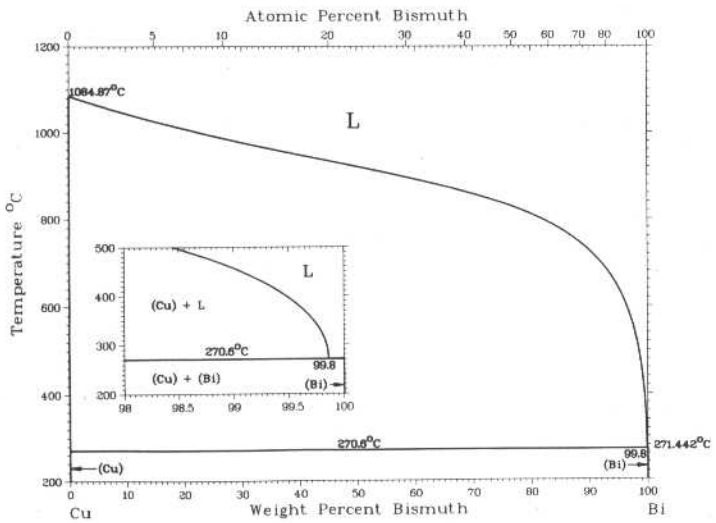

Phase	Composition, wt% Bi	Pearson symbol	Space group
(Cu)	0 to 0.010	*cF*4	$Fm\bar{3}m$
(Bi)	100	*hR*2	$R\bar{3}m$
Metastable phase			
Cu_5Bi_2	57	...	...

Bi-Ga

H. Okamoto, 1990

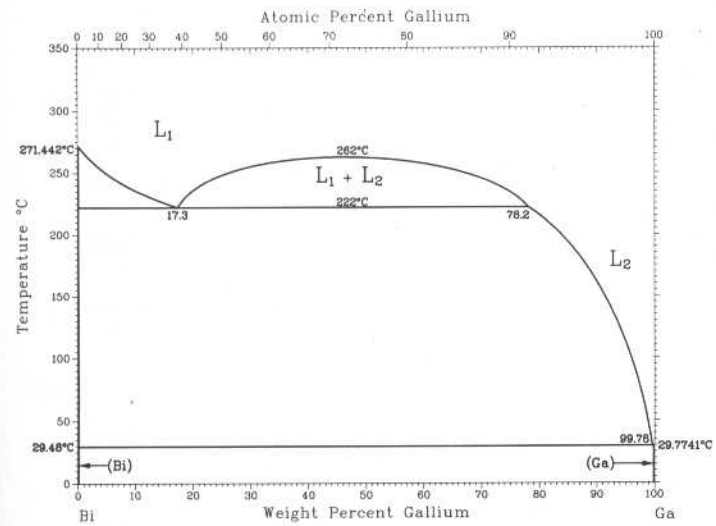

Phase	Composition, wt% Ga	Pearson symbol	Space group
(Bi)	~0	*hR*2	$R\bar{3}m$
(Ga)	~100	*oC*8	*Cmca*

Bi-Ge

R.W. Olesinski and G.J. Abbaschian, 1986

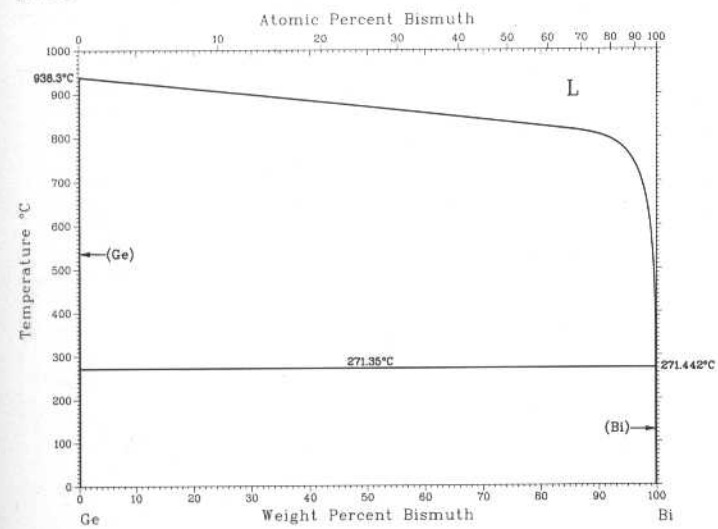

Phase	Composition, wt% Bi	Pearson symbol	Space group
(Ge)	0	*cF*8	$Fd\bar{3}m$
(GeII)(HP)	0	*tI*4	$I4_1/amd$
(Bi)	100	*hR*2	$R\bar{3}m$

Bi-Hg

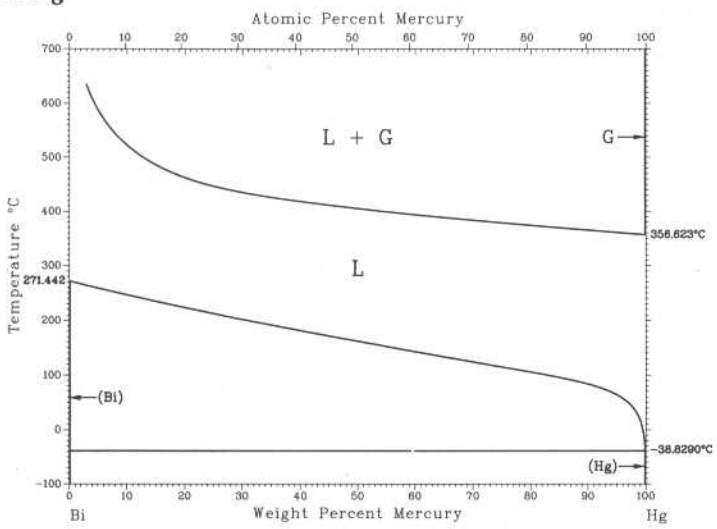

L. Zabdyr and C. Guminski, unpublished

Phase	Composition, wt% Hg	Pearson symbol	Space group
(Bi)	0	*hR*2	$R\bar{3}m$
(Hg)	100	*hR*1	$R\bar{3}m$

Bi-In

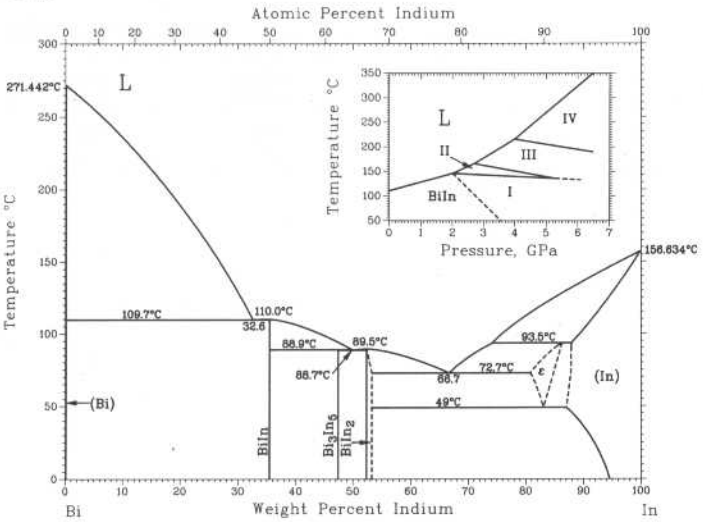

H. Okamoto, 1992

Phase	Composition, wt% In	Pearson symbol	Space group
Stable phases			
(αBi)	0 to 0.005	*hR*2	$R\bar{3}m$
BiIn	35.4	*tP*4	*P*4/*nmm*
Bi_3In_5	47.5 to 47.97	*tI*32	*I*4/*mcm*
$BiIn_2$	52.5 to 53.5	*hP*6	$P6_3/mmc$
ε	80 to 86	*tI*2	...
(In)	~86 to 100	*tI*2	*I*4/*mmm*
High-pressure/metastable phases			
(γBi)	0	*mP*4	$P2_1/m$
(βBi)	0	*mC*4	*C*2/*m*
Bi_4In	12	*tI*4	$I4_1/amd$
Bi_3In	~15	*oI**	*Immb*
γ	12 to 42	*hP*1	*P*6/*mmm*
γ_1	21 to 35.4	*oI**	...
γ_2	21 to 35.4	*oI**	...
X	21 to 35.4	*oI**	...
BiIn′	35.4	*tP*4	*P*4/*nmm*
α_2	45 to 51	*cI*2	$Im\bar{3}m$
Bi_2In_3(a)	45	*hP**	...
$BiIn_3$	62	*t***	...
α_1	~59 to 76	*tI*2	*I*4/*mmm*

(a) Thin film. Probably Bi_3In_5

Bi-K

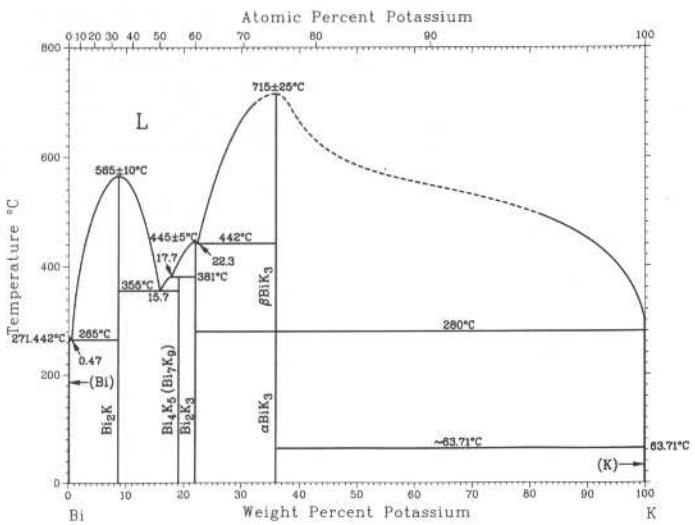

A. Petric and A.D. Pelton, 1991

Phase	Composition, wt% K	Pearson symbol	Space group
(Bi)	0	*hR*2	$R\bar{3}m$
Bi_2K	8.5	*cF*24	$Fd\bar{3}m$
BiK_5(a)	19.0	...	...
Bi_2K_3	22	...	...
αBiK_3(b)	36	*hP*8	$P6_3/mmc$
βBiK_3(c)	36	*cF*16	$Fm\bar{3}m$
(K)	100	*cI*2	$Im\bar{3}m$

(a) Might be Bi_7K_9. (b) Stable below 280 °C. (c) Stable above 280 °C

Bi-La

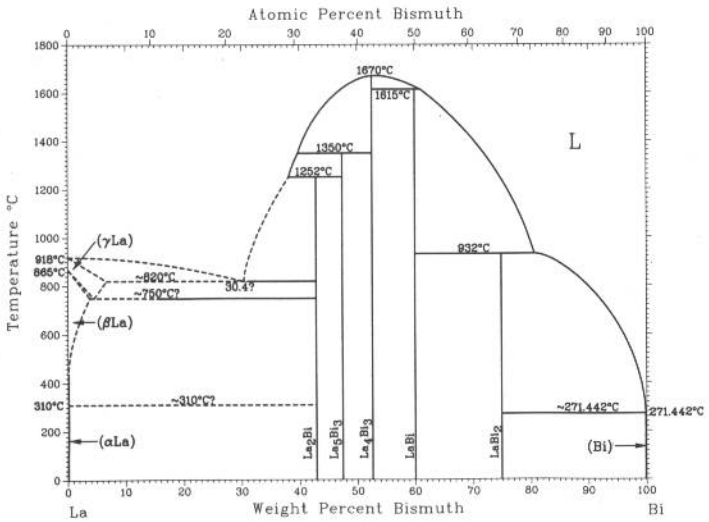

K.A. Gschneidner, Jr. and F.W. Calderwood, 1989

Phase	Composition, wt% Bi	Pearson symbol	Space group
(γLa)	0 to ?	*cI*2	$Im\bar{3}m$
(βLa)	0 to ?	*cF*4	$Fm\bar{3}m$
(αLa)	0	*hP*4	$P6_3/mmc$
La_5Bi	42.9	*tI*12	$I4/mmm$
La_5Bi_3	47.4	*hP*16	$P6_3/mcm$
La_4Bi_3	53.1	*cI*28	$I\bar{4}3d$
LaBi	60.1	*cF*8	$Fm\bar{3}m$
$LaBi_2$(a)	75.1	*o*?12	...
$LaBi_2$(a)	75.1	*aP*27(?)	$P1$ or $P\bar{1}$
(αBi)	100	*hR*2	$R\bar{3}m$

(a) Conflicting reports regarding $LaBi_2$ structure

Bi-Li

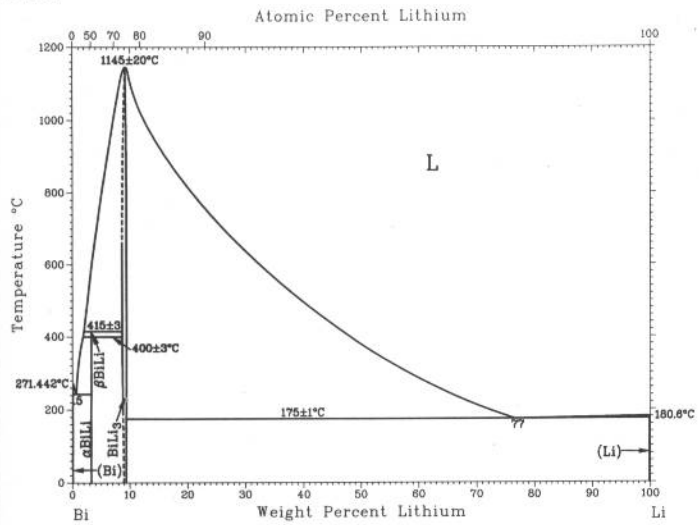

J. Sangster and A.D. Pelton, 1991

Phase	Composition, wt% Li	Pearson symbol	Space group
(αLi)	0	*hR*2	$R\bar{3}m$
αBiLi(a)	3.2	*tP*4	$P4/mmm$
βBiLi	3.2	...	...
$BiLi_3$	8.6 to 9.2(b)	*cF*16	$Fm\bar{3}m$
(αLi)(c)	100	*hP*2	$P6_3/mmc$
(βLi)	100	*cI*2	$Im\bar{3}m$

(a) Below 415 °C. (b) At 380 °C. (c) Below –201 °C

Bi-Mg

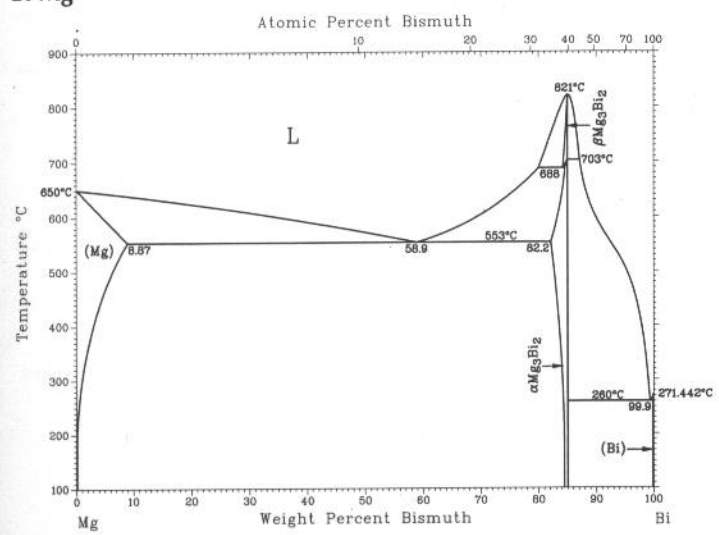

A.A. Nayeb-Hashemi and J.B. Clark, 1988

Phase	Composition, wt% Bi	Pearson symbol	Space group
(Mg)	0 to 8.87	*hP*2	$P6_3/mmc$
Mg_3Bi_2(LT) or αMg_3Bi_2	82.2 to 85	*hP*5	$P\bar{3}m1$
Mg_3Bi_2(HT) or βMg_3Bi_2	85	(a)	...
(Bi)	100	*hR*2	$R\bar{3}m$

(a) The structure of the high-temperature Mg_3Bi_2 is unknown.

Bi-Mn

H. Okamoto, 1990

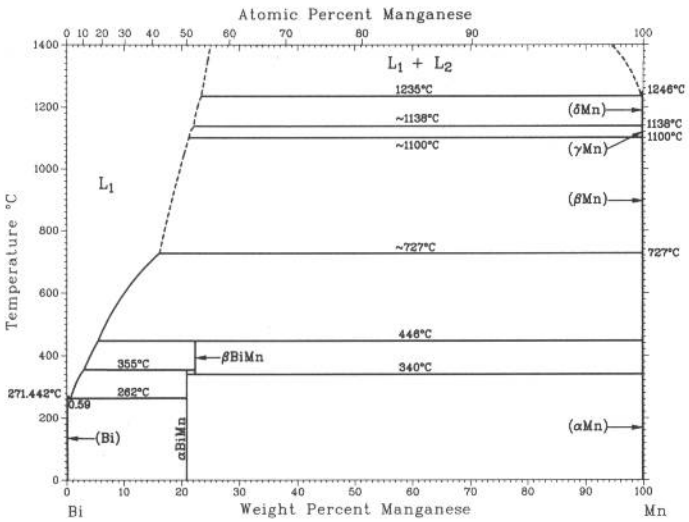

Phase	Composition, wt% Mn	Pearson symbol	Space group
(Bi)	0	*hR*2	$R\bar{3}m$
βBiMn	22.1	*o**32	...
αBiMn	20.8	*hP*4	$P6_3/mmc$
(δMn)	100	*cI*2	$Im\bar{3}m$
(γMn)	100	*cF*4	$Fm\bar{3}m$
(βMn)	100	*cP*20	$P4_132$
(αMn)	100	*cI*58	$I43m$

Bi-Na

J. Sangster and A.D. Pelton, 1991

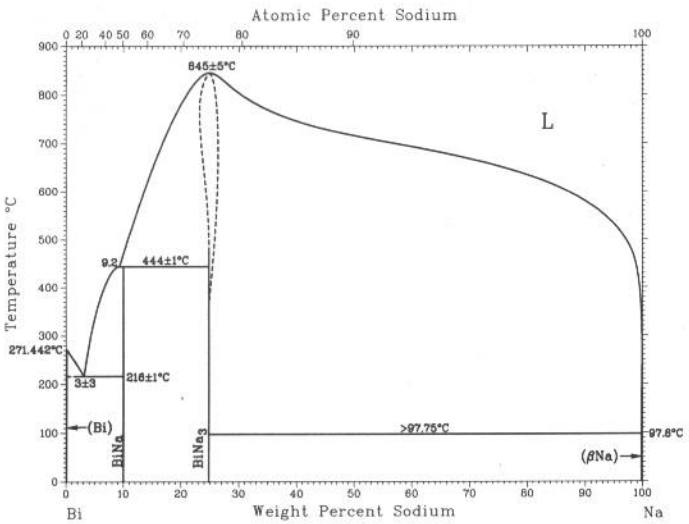

Phase	Composition, wt% Na	Pearson symbol	Space group
(αBi)	0	*hR*2	$R\bar{3}m$
BiNa	10.1	*tP*4	$P4/mmm$
$BiNa_3$(a)	23.4 to 27.5(b)	*hP*8	$P6_3/mmc$
(αNa)(c)	100	*hP*2	$P6_3/mmc$
(βNa)	100	*cI*2	$Im\bar{3}m$

(a) Might be *hP*24, Cu_3As prototype. (b) At 800 °C. (c) Below –237 °C

Bi-Nd

K.A. Gschneidner, Jr. and F.W. Calderwood, 1989

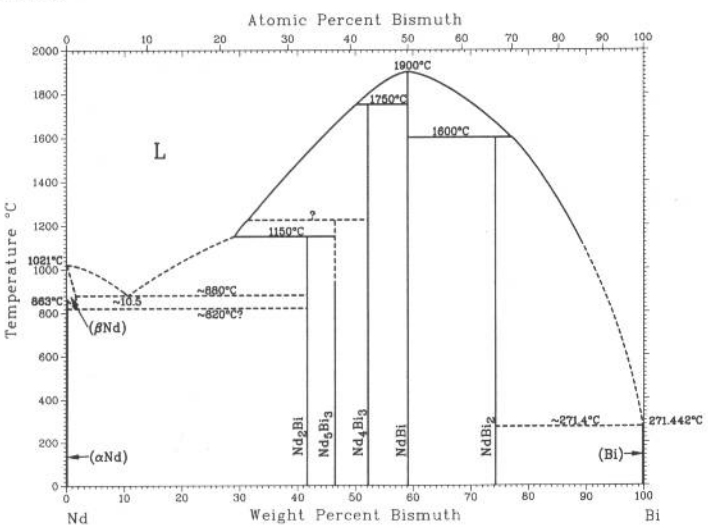

Phase	Composition, wt% Bi	Pearson symbol	Space group
(αNd)	0	*hP*4	$P6_3/mmc$
Nd_2Bi	42.0	*tI*12	$I4/mmm$
Nd_5Bi_3	46.5	*hP*16	$P6_3/mcm$
Nd_4Bi_3	52.1	*cI*28	$I\bar{4}3d$
NdBi	59.1	*cF*8	$Fm\bar{3}m$
$NdBi_2$	74.4	*aP*27(?)	$P1$ or $P\bar{1}$
(αBi)	100	*hR*2	$R\bar{3}m$

Bi-Ni

P. Nash, 1991

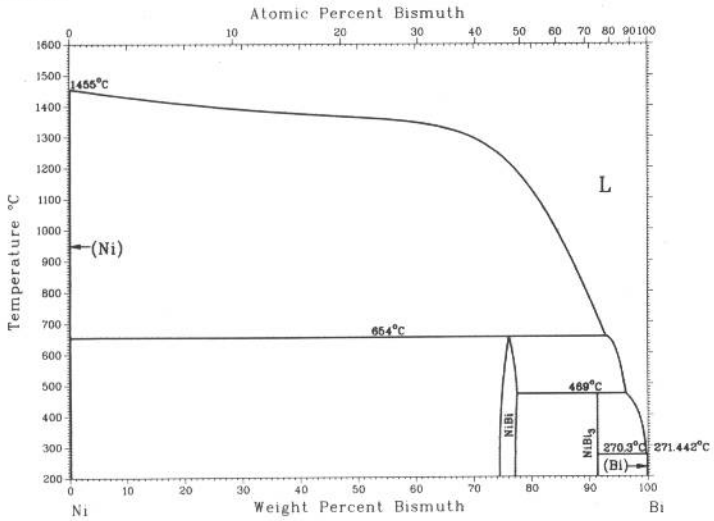

Phase	Composition, wt% Bi	Pearson symbol	Space group
(Ni)	0	*cF*4	$Fm\bar{3}m$
NiBi	74 to 77	*hP*4	$P6_3/mmc$
$NiBi_3$	91	...	...
(Bi)	100	*hR*2	$R\bar{3}m$

Bi-Pb

N.A. Gokcen, 1992

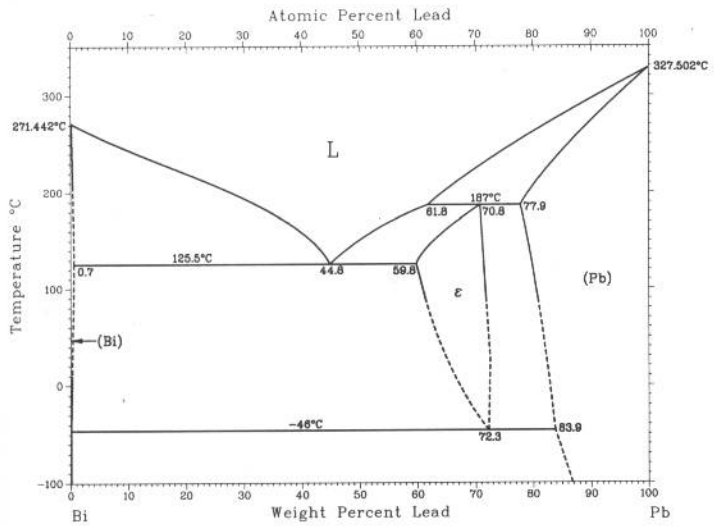

Phase	Composition, wt% Pb	Pearson symbol	Space group
(Bi)	0 to 0.7	*hR*2	$R\bar{3}m$
ε	59.8 to 73	*hP*2	$P6_3/mmc$
(Pb)	77.9 to 100	*cF*4	$Fm\bar{3}m$

Bi-Pd

H. Okamoto, unpublished

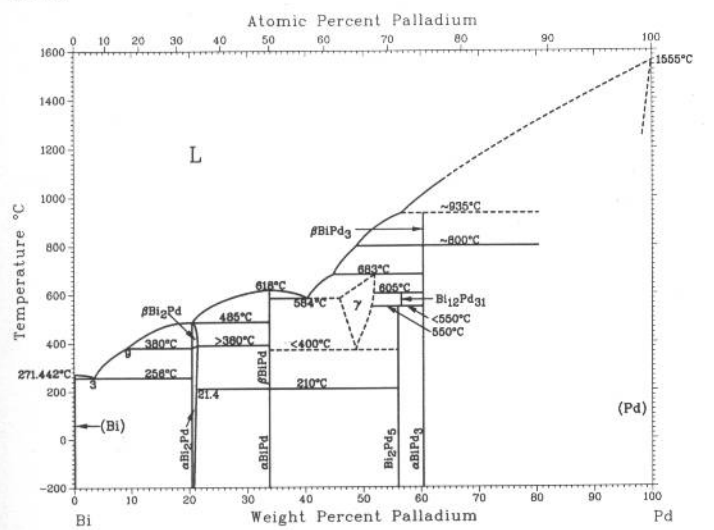

Phase	Composition, wt% Pd	Pearson symbol	Space group
(αBi)	0	*hR*2	$R\bar{3}m$
βBi_2Pd	20.3	*tI*6	*I*4/*mmm*
αBi_2Pd	20.3	*mC*12	*C*2/*m*
βBiPd	33.7	*oC*32	$Cmc2_1$
αBiPd	33.7	*mP*32	$P2_1$
γ(a)	45.9	*hP*16	...
Bi_2Pd_5	56.0	*mC*28	*C*2/*m*
$Bi_{12}Pd_{31}$	56.8	*hR*44	*R*3
$\beta BiPd_3$	60	...	...
$\alpha BiPd_3$	60	*oP*16	*Pmma*
(Pd)	100	*cF*4	$Fm\bar{3}m$

(a) Superlattice of NiAs type

Bi-Pt

H. Okamoto, 1991

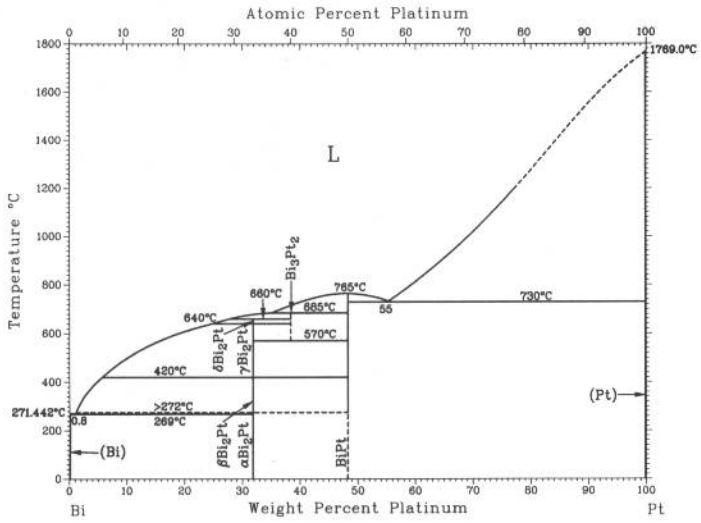

Phase	Composition, wt% Pt	Pearson symbol	Space group
(αBi)	0	*hR*2	$R\bar{3}m$
δBi_2Pt	31.8	*oP*6	*Pnnm*
γBi_2Pt	31.8	*hP*9	$P\bar{3}$
βBi_2Pt	31.8	*cP*12	*Pa*3
αBi_2Pt	31.8	*oP*24	*Pbca*
Bi_3Pt_2	38	*o***	...
		*hP*4	$P6_3/mmc$
BiPt	48.2	*hP*4	$P6_3/mmc$
(Pt)	100	*cF*4	$Fm\bar{3}m$

Bi-Rb

A.D. Pelton and A. Petric, unpublished

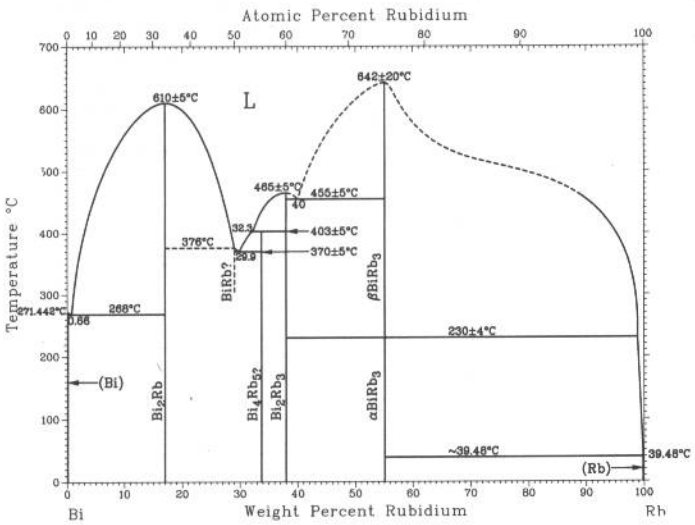

Phase	Composition, wt% Rb	Pearson symbol	Space group
(Bi)	0	*hR*2	$R\bar{3}m$
Bi_2Rb	17.0	*cF*24	$Fd\bar{3}m$
BiRb(?)	29.0	...	...
Bi_4Rb_5	33.9	...	...
Bi_2Rb_3	38	...	...
$\alpha BiRb_3$(a)	55	*hP*8	$P6_3/mmc$
$\beta BiRb_3$(b)	55	*cF*16	$Fm\bar{3}m$
(Rb)	100	*cI*2	$Im\bar{3}m$

(a) Stable below 230 °C. (b) Stable above 230 °C

Bi-S

J.-C. Lin, R.C. Sharma, and Y.A. Chang, unpublished

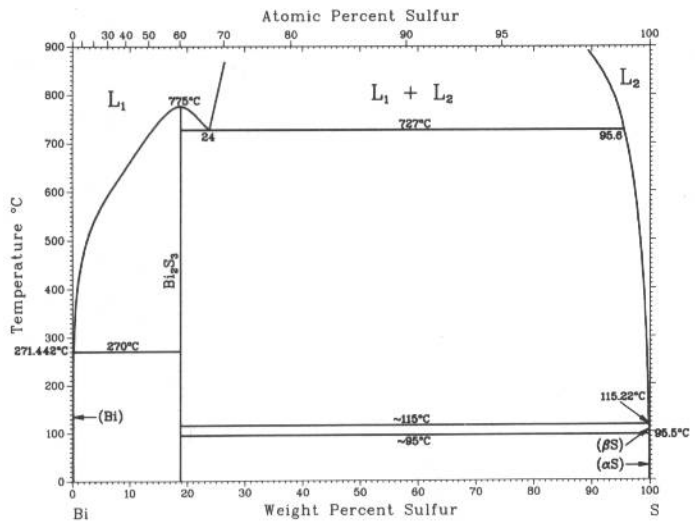

Phase	Composition, wt% S	Pearson symbol	Space group
(αBi)	0	*hR*2	$R\bar{3}m$
Bi_2S_3	19	*oP*20	*Pnma*
(αS)	100	*oF*128	*Fddd*
(βS)	100	*mP**	$P2_1/c$

Bi-Sb

H. Okamoto, unpublished

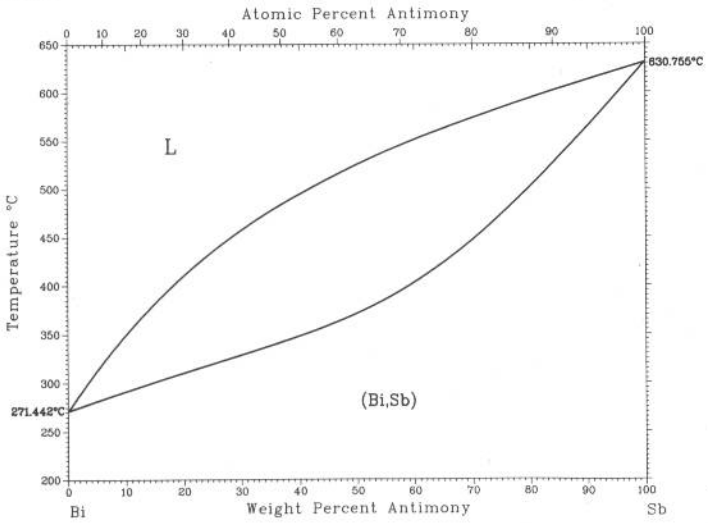

Phase	Composition, wt% Sb	Pearson symbol	Space group
(Bi,Sb)	0 to 100	*hR*2	$R\bar{3}m$
High-pressure phases			
(BiII)	0 to 2.1	*mC*4	*C*2/*m*
(Bi,SbIII)	0 to 100	*mP*4	$P2_1/m$
(BiIII′)	0 to ?	...	...
(BiIV)	0 to ?	*m**8	...
(BiV)	0 to ?	*cI*2	$Im\bar{3}m$
(SbII)	70 to 100	*cP*1	$Pm\bar{3}m$
(SbIII)	? to 100	*hP*2	$P6_3/mmc$

(a) At room temperature. (b) High-temperature, high-pressure phase

Bi-Se

H. Okamoto, unpublished

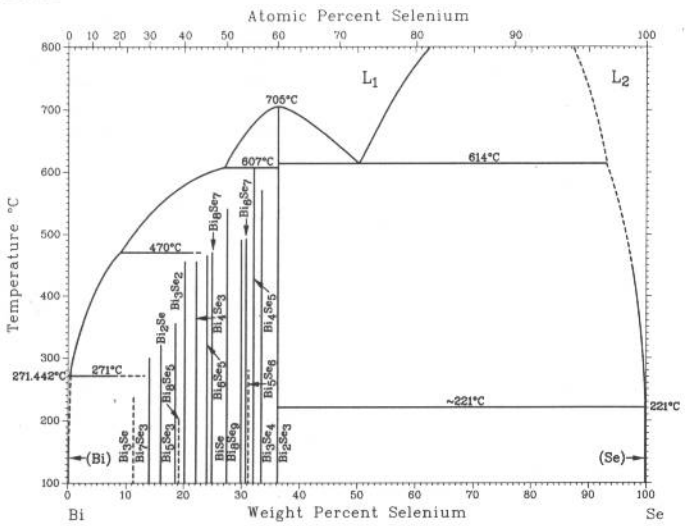

Phase	Composition, wt% Se	Pearson symbol	Space group
(αBi)	0	*hR*2	$R\bar{3}m$
Bi_7Se_3	14	*hR*20	$R\bar{3}m$
Bi_2Se	15.9	*hP*9	$P\bar{3}m1$
Bi_5Se_3(a)	18.5	*hP*48	$P\bar{3}m1$
Bi_3Se_2	20	*hP*30	$P\bar{3}m1$
Bi_4Se_3	22.1	*hR*7	$R\bar{3}m$
Bi_6Se_5	24.0	*hP*33	$P\bar{3}m1$
Bi_8Se_7	24.8	*hP*45	$P\bar{3}m1$
BiSe	27.4	*hP*12	$P\bar{3}m1$
Bi_8Se_9	29.8	*hP*17	$R\bar{3}m$
Bi_6Se_7	30.6	*hP*39	$P\bar{3}m1$
Bi_4Se_5	32.1	*hP*27	$P\bar{3}m1$
Bi_3Se_4	33.5	*hP*42	$P\bar{3}m1$
Bi_2Se_3	36	*hR*5	$R\bar{3}m$
(Se)	100	*hP*3	$P3_121$
Metastable phases			
BiSe(b)	27.4	*cF*8	$Fm\bar{3}m$
Bi_2Se_3IIIa	36	*c***	...
High-pressure phases			
Bi_2Se_3II(c)	36	*oP*20	*Pnma*
Bi_2Se_3III	36	*tP*40	$P4_2/nmc$
$BiSe_2$	43.1	...	...

(a) Laitakarite. (b) Thin film. (c) Bismuthite

Bi-Sm

H. Okamoto, 1990

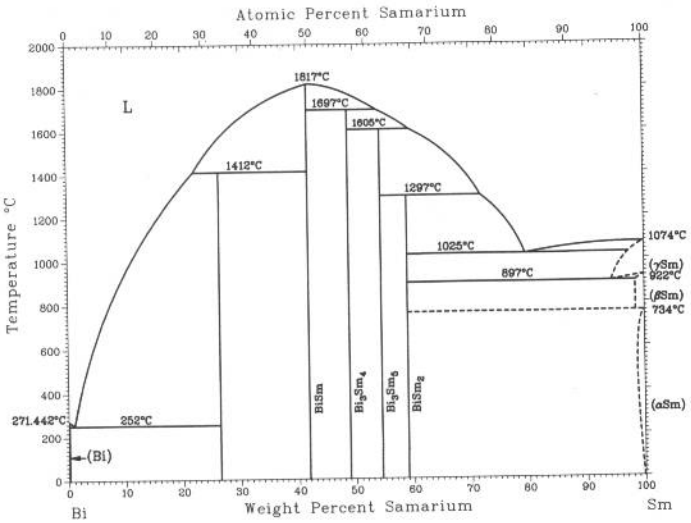

Phase	Composition, wt% Sm	Pearson symbol	Space group
(αBi)	0	*hR*2	$R\bar{3}m$
Bi_2Sm	26.5	*oP*12	*Pmmm*
BiSm	42.8	*cF*8	$Fm\bar{3}m$
Bi_3Sm_4	48.9	*cI*28	$I\bar{4}3d$
Bi_3Sm_5	54.5	*hP*16	$P6_3/mcm$
$BiSm_2$	59.0	*tI*6	*I4/mmm*
(γSm)	100	*cI*2	$Im\bar{3}m$
(βSm)	100	*hP*2	$P6_3/mmc$
(αSm)	100	*hR*3	$Rm\bar{3}m$

Bi-Sn

H. Okamoto, 1990

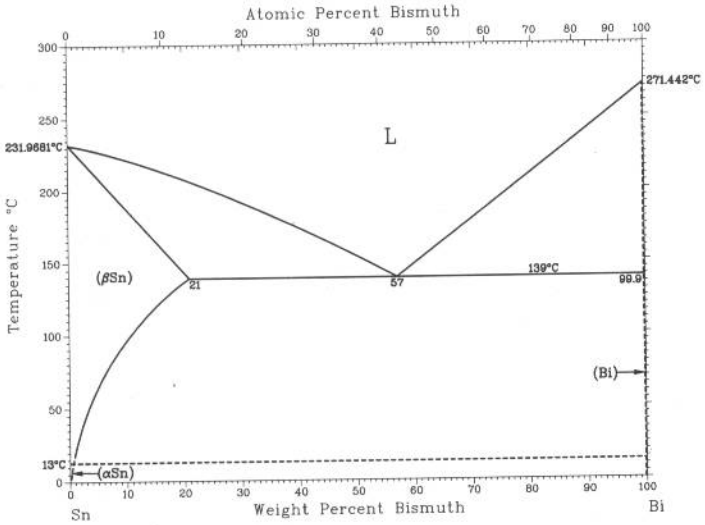

Phase	Composition, wt% Bi	Pearson symbol	Space group
(βSn)	0 to 21	*tI*4	$I4_1/amd$
(αSn)	0 to ?	*cF*8	$Fd\bar{3}m$
(Bi)	99.9 to 100	*hR*2	$R\bar{3}m$

Bi-Sr

From [Elliott]

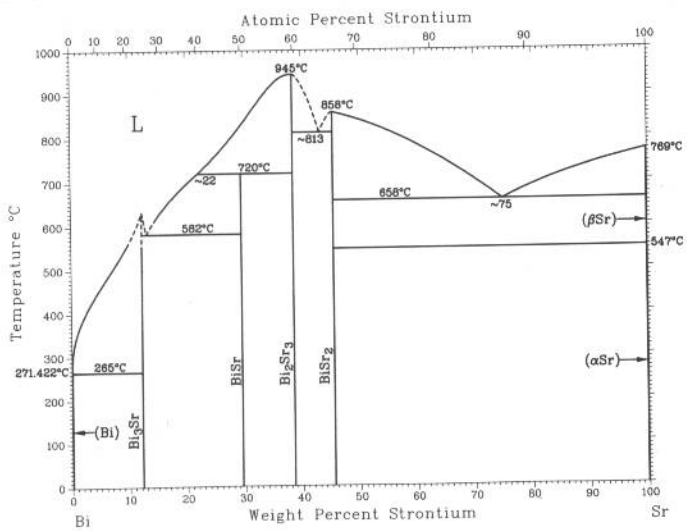

Phase	Composition, wt% Sr	Pearson symbol	Space group
(Bi)	0	*hR*2	$R\bar{3}m$
Bi_3Sr	12	*cP*4	$Pm\bar{3}m$
BiSr	29.5	...	...
Bi_2Sr_3	39	...	...
$BiSr_2$	45.7	*tI*12	*I4/mmm*
(βSr)	100	*cI*2	$Im\bar{3}m$
(αSr)	100	cF	$Fm\bar{3}m$

Bi-Te

H. Okamoto and L.E. Tanner, unpublished

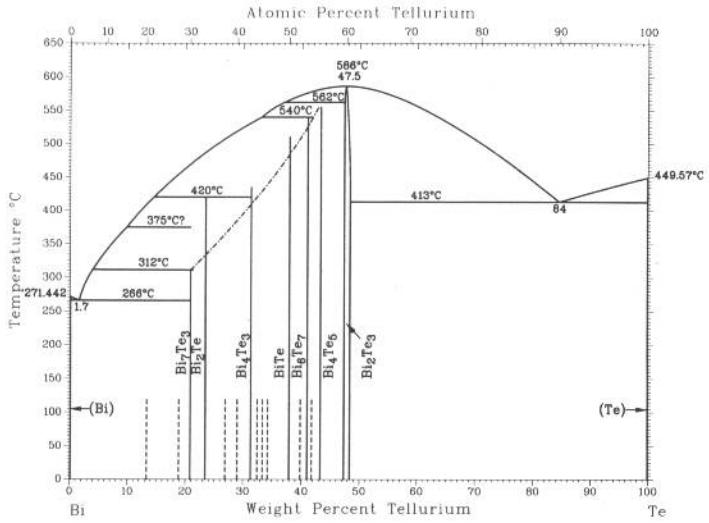

Phase	Composition, wt% Te	Pearson symbol	Space group
(αBi)	0 to ?	*hR*2	$R\bar{3}m$
Bi_2Te_3	47.5 to 48.0	*hR*5	$R\bar{3}m$
(αTe)	99.992 to 100	*hP*3	$P3_121$
Stacking variants			
Bi_7Te_3	21	*hR*20	$R\bar{3}m$
Bi_2Te	23.4	...	$P\bar{3}m1$
Bi_4Te_3	31.5	*hR*7	$R\bar{3}m$
BiTe	37.9	*hP*12	$P\bar{3}m1$
Bi_6Te_7	41.6	*hP*39	$P\bar{3}m1$
Bi_4Te_5	43.3	*hP*27	$P\bar{3}m1$
Metastable phases			
BiTe(a)	37.9	*cF*8	$Fm\bar{3}m$
Bi_2Te_5	60.4	...	...
High-pressure phase			
Bi_2Te_3II	48	*hR*5	$R\bar{3}m$

(a) Thin film

Bi-Tl

H. Okamoto, unpublished

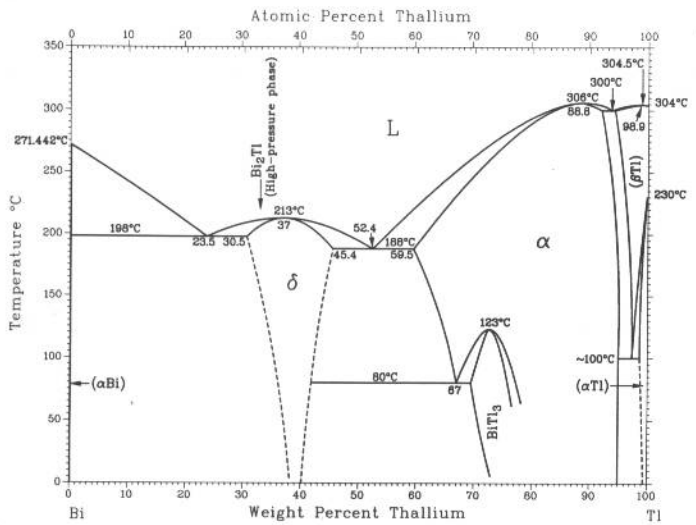

Phase	Composition, wt% Tl	Pearson symbol	Space group
(γBi)(a)	0	*mP*4	$P2_1/m$
(βBi)(a)	0	*mC*4	$C2/m$
(αBi)	0	*hR*2	$R\bar{3}m$
Bi_2Tl(a)	33.8	...	...
δ	30.5 to 45.4	*hP*3	$P6/mmm$
BiTl(b)	...	*cP*2	$Pm\bar{3}m$
α	59.5 to 94.9	*cF*4	$Fm\bar{3}m$
$BiTl_3$	69.5 to 76.6	*hP*2	$P6_3/mmc$
		*hP*8	$P6_3/mmc$
$BiTl_3$I(c)	~74.6	*cP*4	$Pm\bar{3}m$
$BiTl_7$(a)	87.3	...	...
(γTl)(a)	100	*cF*4	$Fm\bar{3}m$
(βTl)	94.9 to 100	*cI*2	$Im\bar{3}m$
(αTl)	98.98 to 100	*hP*2	$P6_3/mmc$

Note: Not all high-pressure phases of Bi are listed. (a) High-pressure phase. (b) Not accepted in the assessed diagram. (c) Metastable?

Bi-U

From [Chiotti]

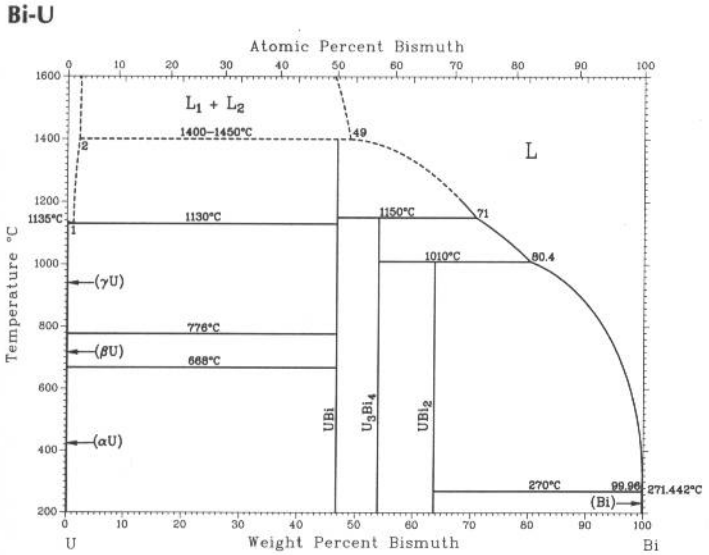

Phase	Composition, wt% Bi	Pearson symbol	Space group
(γU)	0	*cI*2	$Im\bar{3}m$
(βU)	0	*tP*30	$P4_2/mnm$
(αU)	0	*oC*4	*Cmcm*
UBi	46.7	*cF*8	$Fm\bar{3}m$
U_3Bi_4	53.9	*cI*28	$I\bar{4}3d$
UBi_2	63.8	*tP*6	*P*4/*nmm*
(Bi)	100	*hR*2	$R\bar{3}m$

Bi-Y

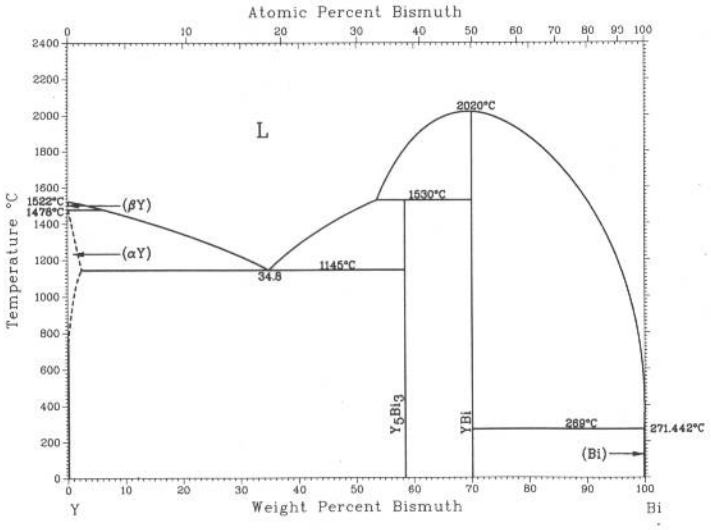

K.A. Gschneidner, Jr. and F.W. Calderwood, 1989

Phase	Composition, wt% Bi	Pearson symbol	Space group
(αY)	0	*hP*2	$P6_3/mmc$
Y_5Bi_3	58.5	*oP*32	*Pnma*
YBi	70.1	*cF*8	$Fm\bar{3}m$
(αBi)	100	*hR*2	$R\bar{3}m$

Bi-Yb

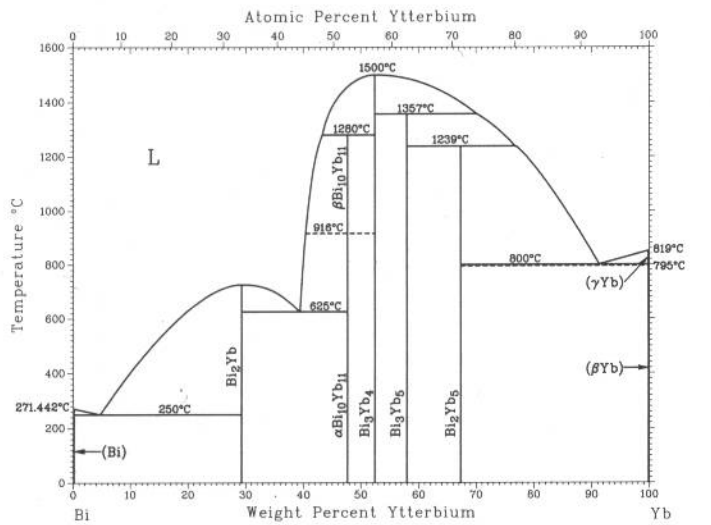

H. Okamoto, 1990

Phase	Composition, wt% Yb	Pearson symbol	Space group
(αBi)	0	*hR*2	$R\bar{3}m$
Bi_2Yb	29.3	*oC*12	*Cmcm*
$\beta Bi_{10}Yb_{11}$	47.7	*tI*84	*I4/mmm*
$\alpha Bi_{10}Yb_{11}$	47.7	...	...
Bi_3Yb_4	52.4	*cI*28	$I\bar{4}3d$
Bi_3Yb_5	58	*oP*32	*Pnma*
Bi_2Yb_5	67.4	*oP**	$Pn2_1a$
(γYb)	100	*cI*2	$Im\bar{3}m$
(βYb)	100	*cF*4	$Fm\bar{3}m$
(αYb)	100	*hP*2	$P6_3/mmc$

Bi-Zn

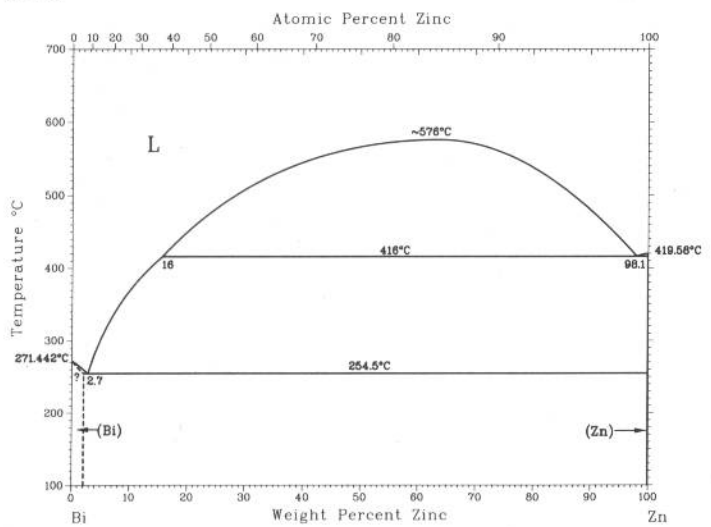

H. Okamoto, 1990

Phase	Composition, wt% Zn	Pearson symbol	Space group
(Bi)	0 to ?	*hR*2	$R\bar{3}m$
(Zn)	~100	*hP*2	$P6_3/mmc$

Bi-Zr

H. Okamoto, 1990

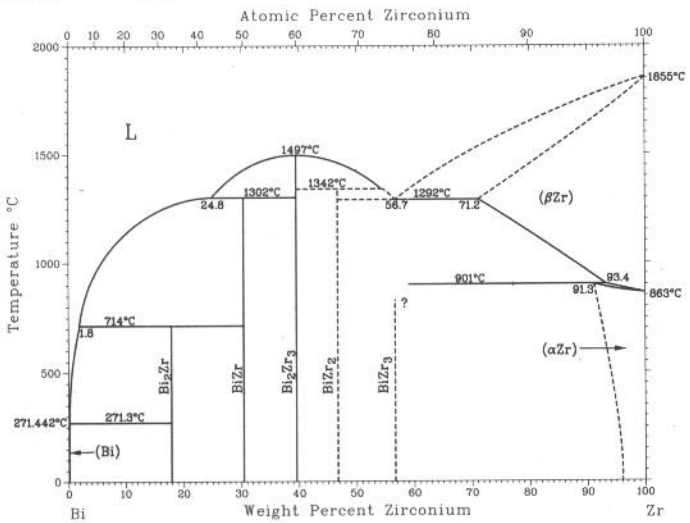

Phase	Composition, wt% Zr	Pearson symbol	Space group
(αBi)	0	*hR*2	$R\bar{3}m$
Bi_2Zr	17.9	*oP*24	*Pnnm*
BiZr	30.4	...	...
Bi_2Zr_3	39.6	...	...
$BiZr_2$	46.7	...	...
$BiZr_3$	56.7	*tI*32	$I\bar{4}$
(βZr)	71.2 to 100	*cI*2	$Im\bar{3}m$
(αZr)	91.3 to 100	*hP*2	$P6_3/mmc$

C-Co

K. Ishida and T. Nishizawa, 1991

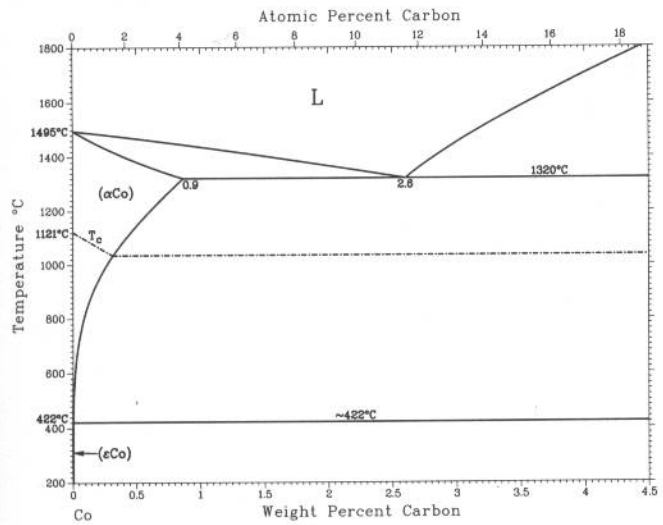

Phase	Composition, wt% C	Pearson symbol	Space group
(αCo)	0 to 0.9	*cF*4	$Fm\bar{3}m$
(εCo)	~0	*hP*2	$P6_3/mmc$
C	~100	*hP*4	$P6_3/mmc$
Metastable phases			
(ε′Co)	~0.3 to ~0.4	(a)	...
Co_3C	6	*oP*6	*Pnma*
Co_2C	9	*oP*6	*Pnnm*

(a) Hexagonal

C-Cr

M. Venkatraman and J.P. Neumann, 1990

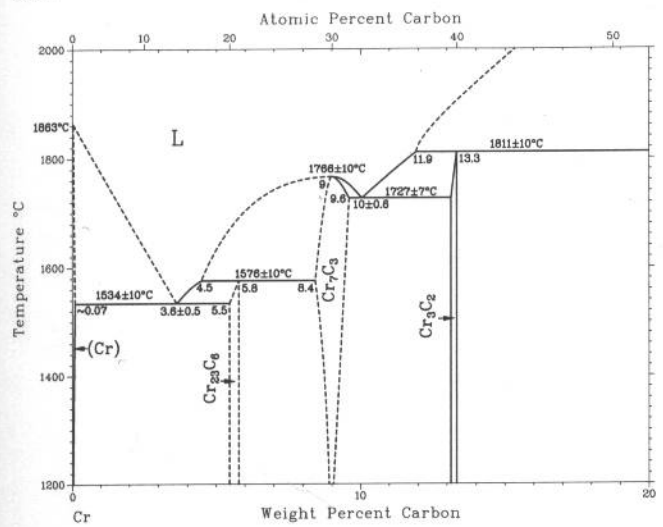

Phase	Composition, wt% C	Pearson symbol	Space group
(Cr)	0 to ~0.07	*cI*2	$Im\bar{3}m$
$Cr_{23}C_6$	5.5 to 5.8	*cF*116	$Fm\bar{3}m$
Cr_3C(a)	~7	*oP*16	*Pnma*
Cr_7C_3	~9	*oP*40	*Pnma*
Cr_3C_2	~13	*oP*20	*Pnma*
CrC(?)	~19	...	...
(C)	~100	*hP*4	$P6_3/mmc$

(a) Metastable

C-Cu

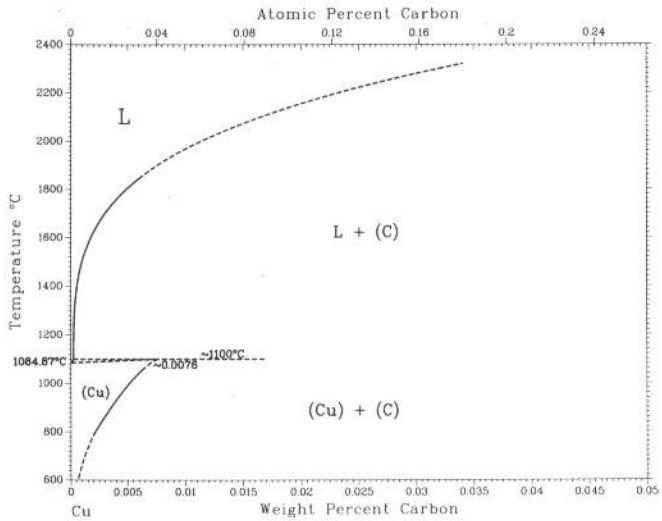

P.R. Subramanian and D.E. Laughlin, unpublished

Phase	Composition, wt% C	Pearson symbol	Space group
(Cu)	0 to 0.01	*cF*4	$Fm\bar{3}m$
(C)	100	*hP*4	$P6_3/mmc$

H. Okamoto, 1992

Phase	Composition, wt% C	Pearson symbol	Space group
(δFe)	0 to 0.09	*cI*2	$Im\bar{3}m$
(γFe)	0 to 2.1	*cF*4	$Fm\bar{3}m$
(αFe)	0 to 0.021	*cI*2	$Im\bar{3}m$
(C)	100	*hP*4	$P6_3/mmc$
Metastable/high-pressure phases			
(εFe)	0	*hP*2	$P6_3/mmc$
Martensite	<2.1	*tI*4	*I*4/*mmm*
Fe_4C	5.1	*cP*5	$P\bar{4}3m$
Fe_3C (θ)	6.7	*oP*16	*Pnma*
Fe_5C_2 (χ)	7.9	*mC*28	*C*2/*c*
Fe_7C_3	8.4	*hP*20	$P6_3mc$
Fe_7C_3	8.4	*oP*40	*Pnma*
Fe_2C (η)	9.7	*oP*6	*Pnnm*
Fe_2C (ε)	9.7	*hP**	$P6_322$
Fe_2C	9.7	*hP**	$P\bar{3}m1$
(C)	100	*cF*8	$Fd\bar{3}m$

C-Fe

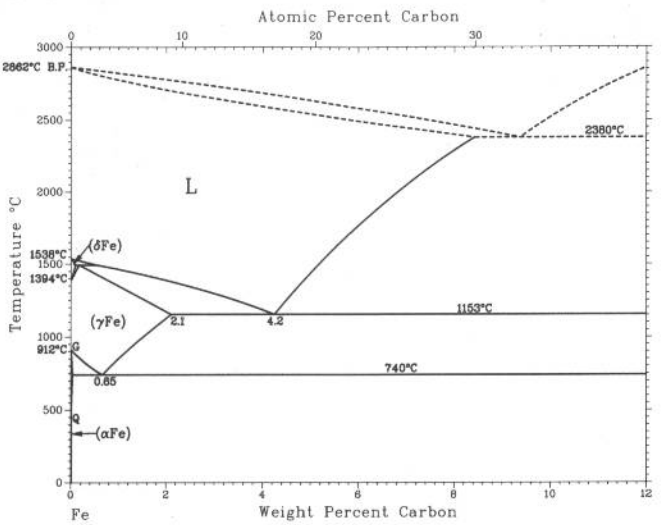

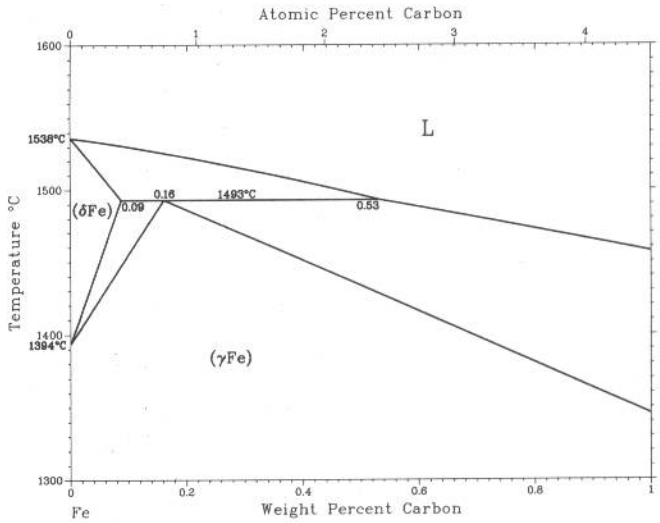

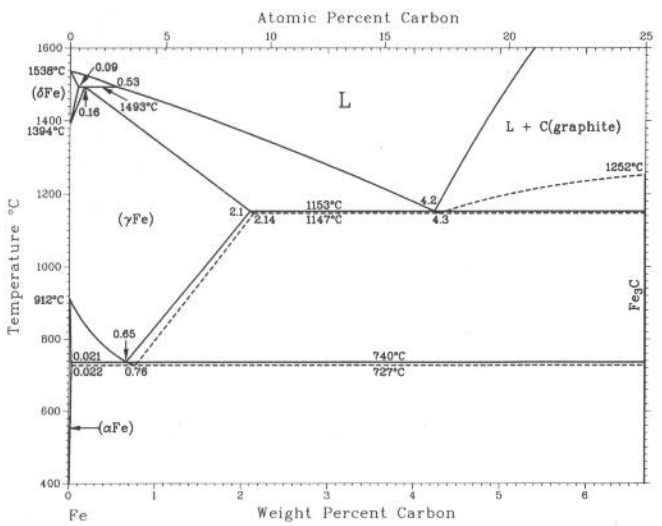

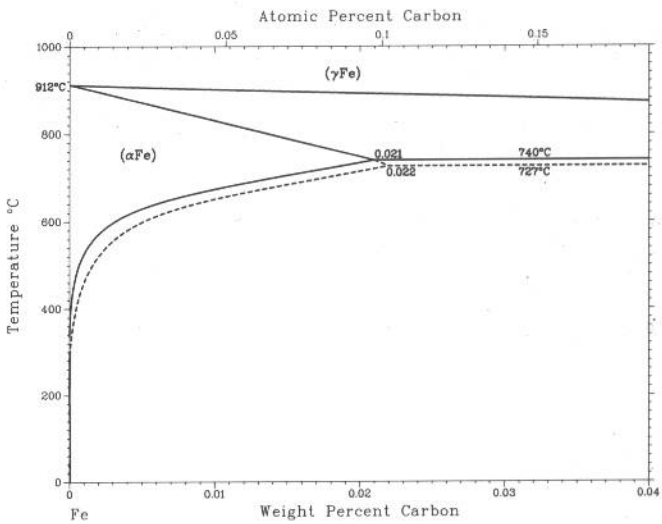

C-Hf

H. Okamoto, 1990

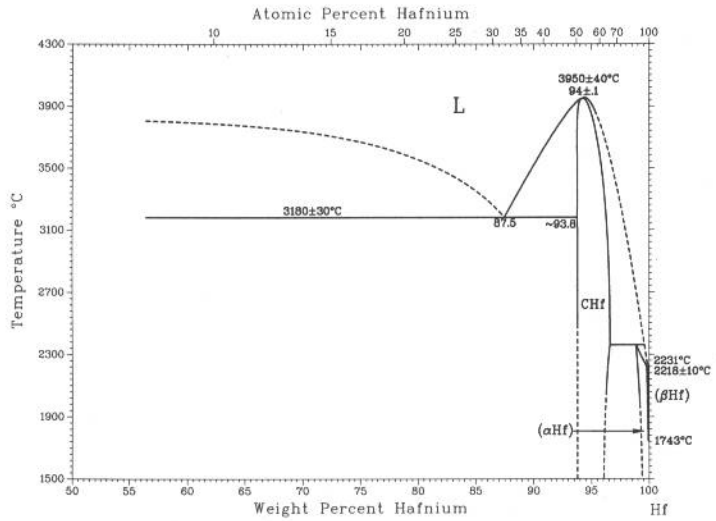

Phase	Composition, wt% Hf	Pearson symbol	Space group
(C)	0	*hP*4	$P6_3/mmc$
CHf	~93.8 to 96.6	*cF*8	$Fm\bar{3}m$
(βHf)	99.9 to 100	*cI*2	$Im\bar{3}m$
(αHf)	98.9 to 100	*hP*2	$P6_3/mmc$

C-La

K.A. Gschneidner, Jr. and F.W. Calderwood, 1986

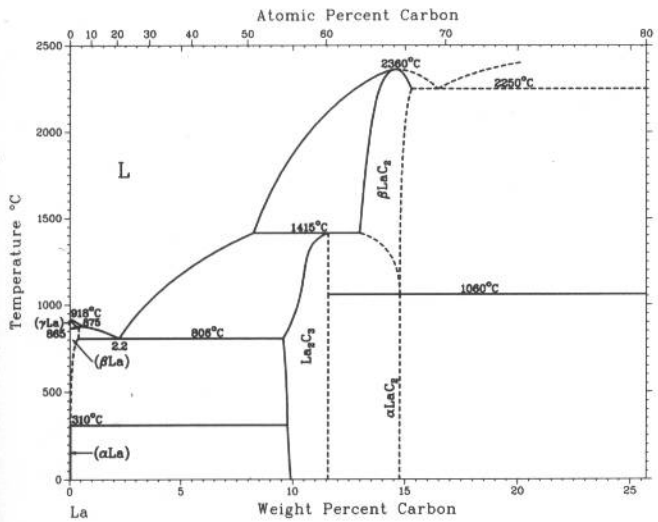

Phase	Composition, wt% C	Pearson symbol	Space group
(αLa)	0	*hP*4	$P6_3/mmc$
(βLa)	0 to ~0.3	*cF*4	$Fm\bar{3}m$
(γLa)	0 to ~0.2	*cI*2	$Im\bar{3}m$
La_2C_3	~9 to ~11	*cI*40	$I\bar{4}3d$
αLaC_2	~15	*tI*6	$I4/mmm$
βLaC_2	~13 to ~15	*cF*12	$Fm\bar{3}m$
(C)	100	*hP*4	$P6_3/mmc$

C-Mn

H. Okamoto, 1990

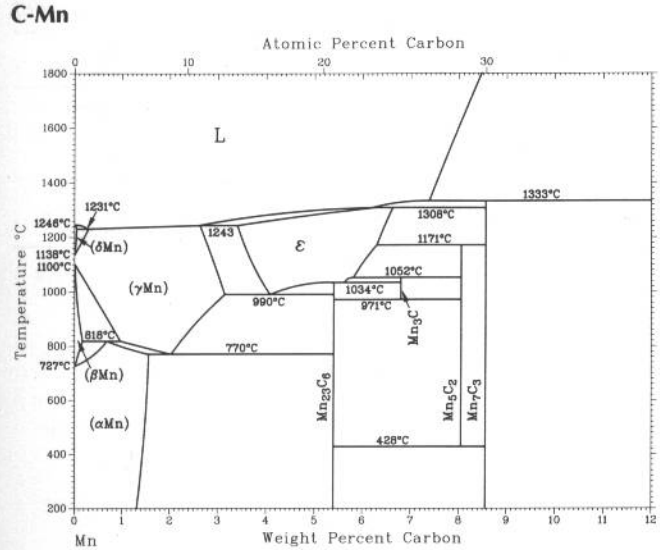

Phase	Composition, wt% C	Pearson symbol	Space group
(δMn)	0 to 0.02	*cI*2	$Im\bar{3}m$
(γMn)	0 to 3	*cF*4	$Fm\bar{3}m$
(βMn)	0 to 0.1	*cP*20	$P4_132$
(αMn)	0 to 1.5	*cI*58	$I\bar{4}3m$
ε	3.3 to 6.6	...	...
$Mn_{23}C_6$	5.4	*cF*116	$Fm\bar{3}m$
Mn_3C	6.8	*oP*16	*Pnma*
Mn_5C_2	8.1	*mC*28	*C*2/*c*
Mn_7C_3	8.6	*oP*40	*Pnma*
(C)	100	*hP*4	$P6_3/mmc$

C-Mo

H. Okamoto, 1990

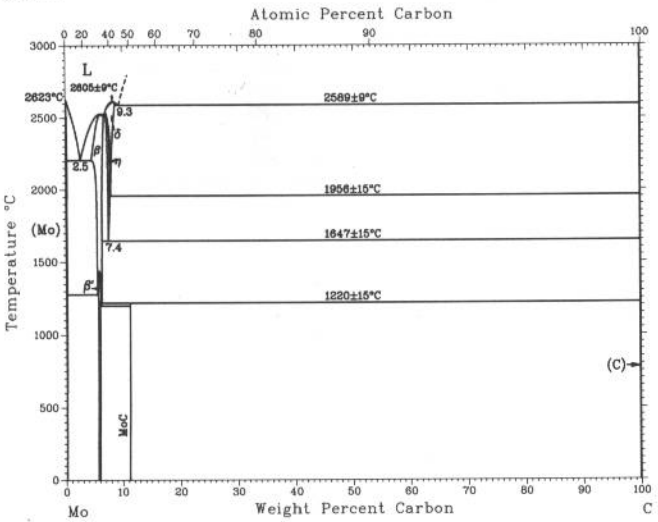

Phase	Composition, wt% C	Pearson symbol	Space group
(Mo)	0 to 0.14	*cI*2	$Im\bar{3}m$
β	4.4 to 6.6	*hP*3	$P6_3/mmc$
β′	~5.7	*oP*12	*Pbcn*
β″	~5.9	...	...
η	6.8 to 7.7	*hP*8	$P6_3/mmc$
δ	6.8 to 8.6	*oF*8	$Fm\bar{3}m$
MoC	11	*hP*2	$P\bar{6}m2$
(C)	100	*hP*4	$P6_3/mmc$

C-Ni

M.F. Singleton and P. Nash, 1991

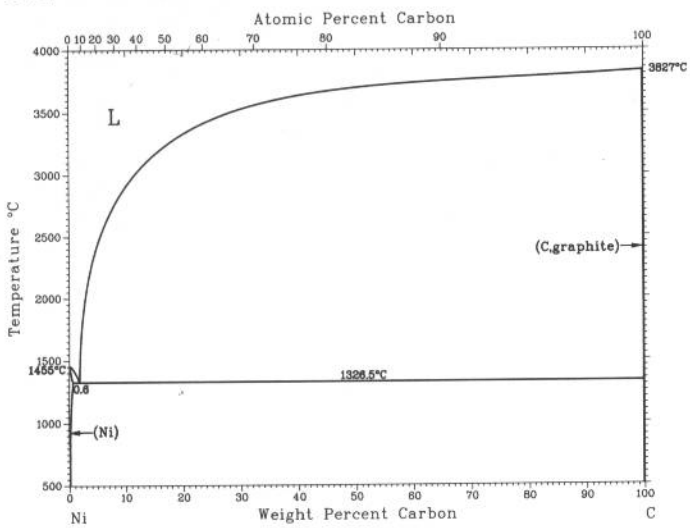

Phase	Composition, wt% C	Pearson symbol	Space group
(Ni)	0 to 0.6(a)	*cF*4	$Fm\bar{3}m$
(C, graphite)	~100	*hP*4	$P6_3/mmc$
Metastable phase			
Ni_3C	...	*oP*16	*Pnma*

(a) Can be extended to 1.6 wt% C at 1314 °C

C-Pr

H. Okamoto, 1990

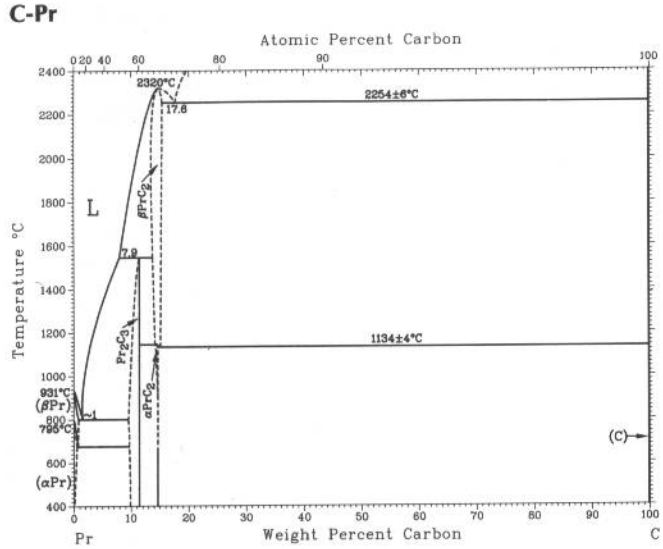

Phase	Composition, wt% C	Pearson symbol	Space group
(αPr)	0 to ?	*hP*4	$P6_3/mmc$
(βPr)	0 to ?	*cI*2	$Im\bar{3}m$
Pr_2C_3	~9 to ~11	*cI*40	$I\bar{4}3d$
αPrC_2	~14.6	*tI*6	*I*4/*mmm*
βPrC_2	...	*c***	...
(C)	100	*hP*4	$P6_3/mmc$

C-Sc

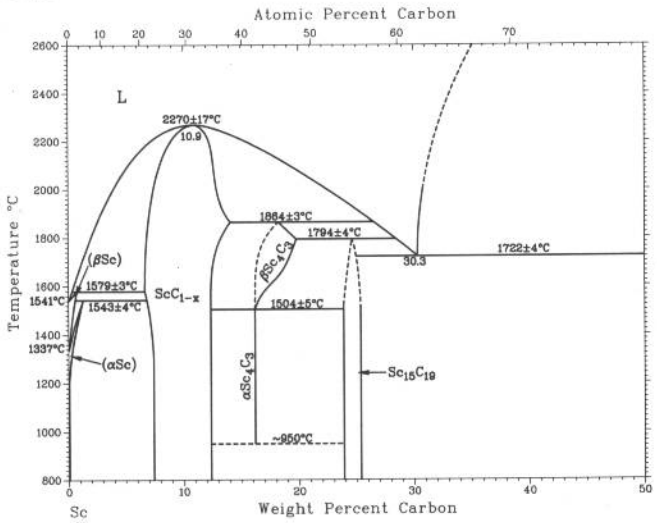

O.V. Gordiichuk, 1987

Phase	Composition, wt% C	Pearson symbol	Space group
(αSc)	0	*hP*2	$P6_3/mmc$
(βSc)	0	*cI*2	$Im\bar{3}m$
Sc_2C	~12	*hR*3	$R\bar{3}m$
Sc_4C_3	16.7	*cI*28	$I\bar{4}3d$
$Sc_{13}C_{10}$	17.1	*c***	...
$Sc_{15}C_{19}$	25.3	*tP*68	$P\bar{4}2_1c$
(C)	100	*hP*4	$P6_3/mmc$

C-Si

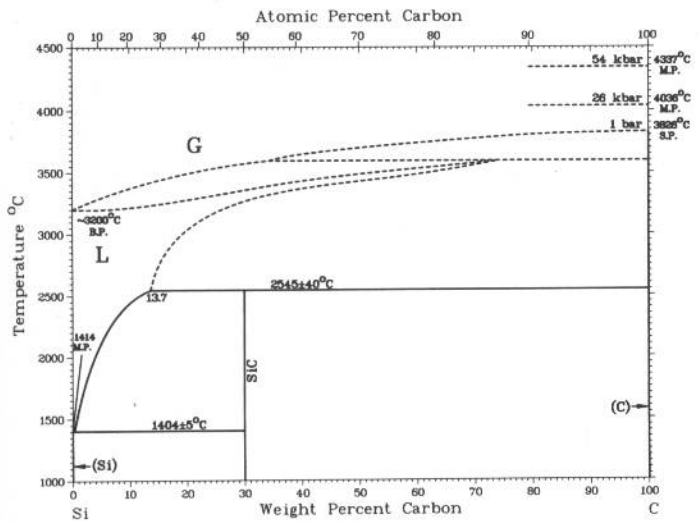

R.W. Olesinski and G.J. Abbaschian, 1984

Phase	Composition, wt% C	Pearson symbol	Space group
(Si)	0	*cF*8	$Fd\bar{3}m$
SiC or βSiC	30	*cF*8	$F\bar{4}3m$
(C)	100	*hP*4	$P6_3/mmc$
Metastable			
αSiC(a)	30	(b)	...
Amorphous	22 to 40	...	...
High pressure			
SiC II	...	*tI*4	$I4_1/amd$

(a) Other SiC polytypes have been reported. (b) Hexagonal

C-Ta

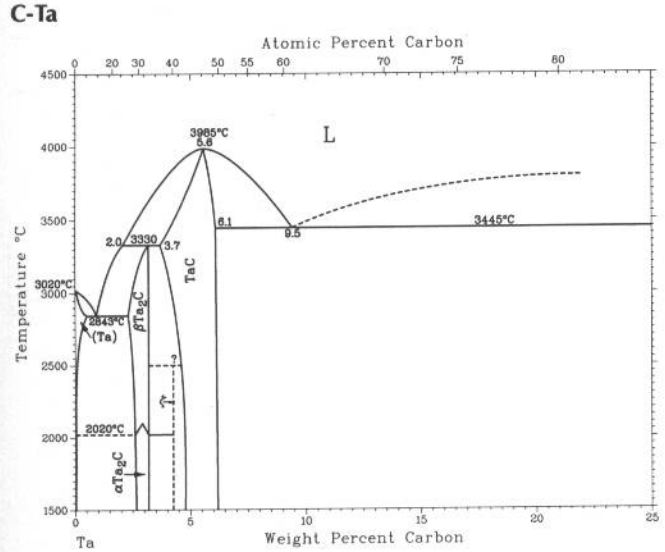

O.M. Barabash and Yu. N. Koval, 1986

Phase	Composition, wt% C	Pearson symbol	Space group
(Ta)	0 to 0.5	*cI*2	$Im\bar{3}m$
αTa_2C	2.6 to 3.2	*hP*3	$P\bar{3}m1$
βTa_2C	2.3 to 3.2	*hP*3	$P6_3/mmc$
ζ	~4.2	*hR*20	$R\bar{3}m$
TaC	3.7 to 6.1	*cF*8	$Fm\bar{3}m$
(C)	100	*hP*4	$P6_3/mmc$

C-Th

R. Benz and P.L. Stone, 1969

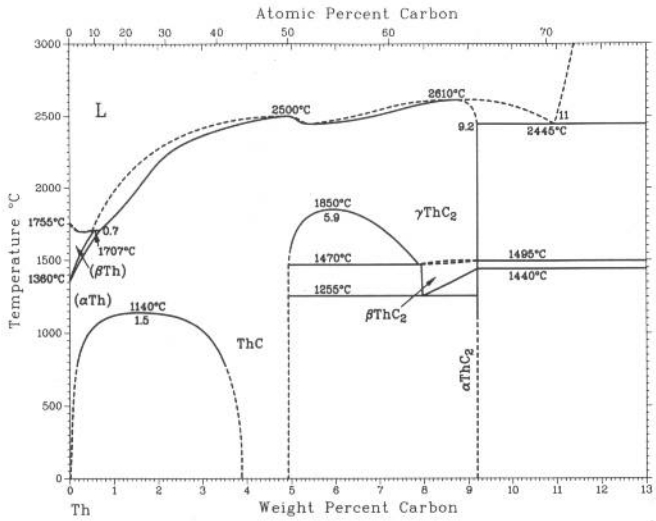

Phase	Composition, wt% C	Pearson symbol	Space group
(βTh)	0 to 0.3	*cI*2	$Im\bar{3}m$
(αTh)	0 to ?	*cF*4	$Fm\bar{3}m$
ThC	?	*cF*8	$Fm\bar{3}m$
γThC_2	? to 9.2	*cP*12	$Pa\bar{3}$
βThC_2	~8.1 to 9.1	*tP*6	$P4_2/mmc$
αThC_2	~9.1	*mC*12	*C*2/*c*

C-Ti

J.L. Murray, 1987

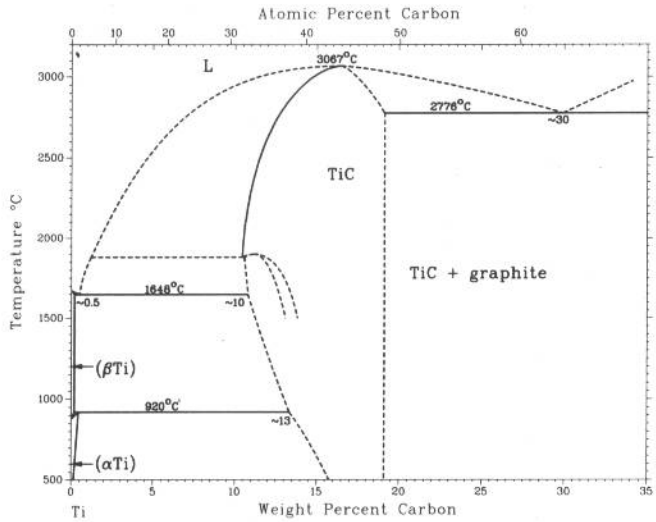

Phase	Composition, wt% C	Pearson symbol	Space group
(βTi)	0 to 0.2	*cI*2	$Im\bar{3}m$
(αTi)	0 to 0.4	*hP*2	$P6_3/mmc$
TiC	~10 to 19.3	*cF*8	$Fm\bar{3}m$
Ti_2C	~10 to 12.4	*cF*48	$Fd\bar{3}m$
(C)	100	*hP*4	$P6_3/mmc$

C-U

E.K. Storms, 1967; and R. Benz, 1969

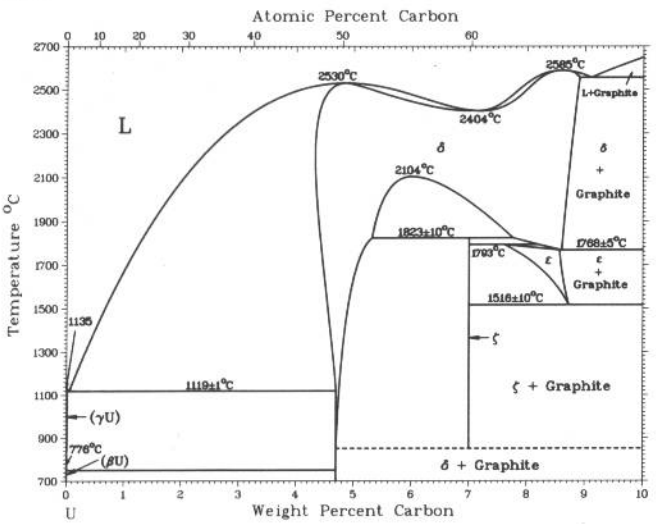

Phase	Composition, wt% C	Pearson symbol	Space group
(γU)	0	*cI*2	$Im\bar{3}m$
(βU)	0	*tP*30	$P4_2/mnm$
δ	~4.3 to 8.9	*cF*8	$Fm\bar{3}m$
ε	~7.6 to 8.7	*tI*6	*I*4/*mmm*
ζ	7.0	*cI*40	$I\bar{4}3d$

C-V

H. Okamoto, 1991

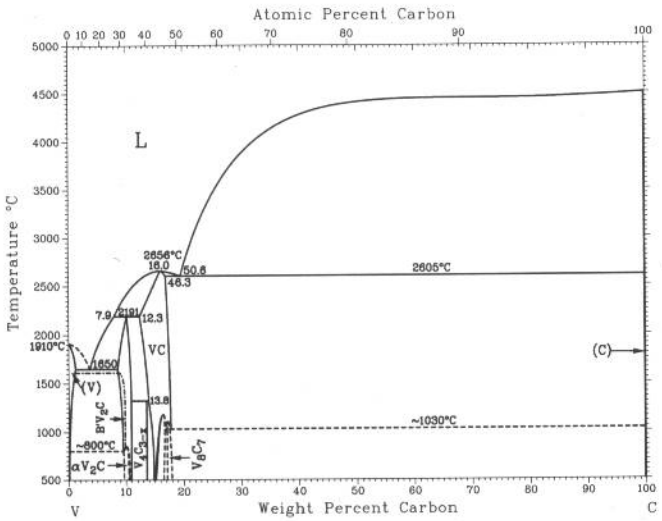

Phase	Composition, wt% C	Pearson symbol	Space group
(V)	0 to 1.0	*cI*2	$Im\bar{3}m$
αV_2C	9.6 to 10.4	*oP*12	*Pbcn*
βV_2C	8.5 to 10.8	*hP*3	$P6_3/mmc$(b)
$\beta' V_2C$(a)	~8.6 to 9.9	*hP*9	$P\bar{3}1m$(b)
V_4C_{3-x}	~13.6	*hR*20	$R\bar{3}m$
VC(b)	12.3 to 17.9	*cF*8	$Fm\bar{3}m$
V_6C_5(c)	15.1 to 16.7	*C*44	*B*2
V_8C_7	16.7 to 17.9	*cP*60	$P4_132$ $P4_332$
(C)	100	*hP*4	$P6_3/mmc$

(a) High-temperature form. (b) Either one or the other of these two space groups is in error, or the postulated transition in the diagram is in error, with the transition being first order, requiring a two-phase region between the ordered and disordered structures. (c) Enantiomorphic and twinned forms have been described with other lattice parameters and/or space groups.

C-W

R.V. Sara, 1965; and E. Rudy and J.R. Hoffman, 1967

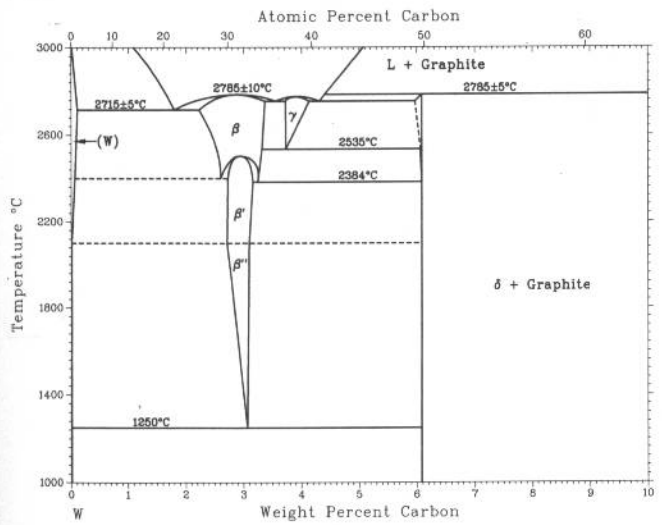

Phase	Composition, wt% C	Pearson symbol	Space group
(W)	0	*cI*2	$Im\bar{3}m$
β	~2.2 to 3.3	...	...
β′	~2.7 to 3.1	*hP*3	$P6_3/mmc$
β″	~2.7 to 3.05	*hP*3	$P\bar{3}m1$
γ	~3.7 to 4.1	*cF*8	$Fm\bar{3}m$
δ	6.1	*hP*2	$P\bar{6}m2$

C-Y

K.A. Gschneidner, Jr. and F.W. Calderwood, 1986

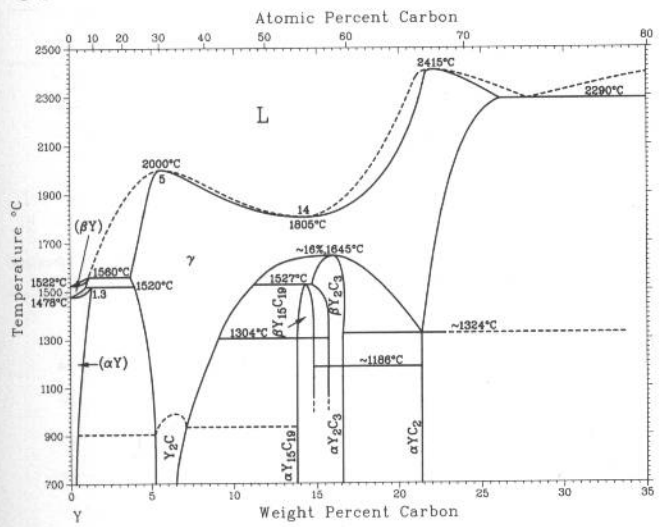

Phase	Composition, wt% C	Pearson symbol	Space group
(αY)	0 to 1.3	*hP*2	$P6_3/mmc$
(βY)	0 to 1.0	*cI*2	$Im\bar{3}m$
Y_2C	~6.2	*hR*3	$R\bar{3}m$
γ	~3.7 to 25.8	*cF*5	$Fm\bar{3}m$
$\alpha Y_{15}C_{19}$	14.6	*tP*68	$P\bar{4}2_1c$
Y_2C_3(a)	~17	*cI*40	$I\bar{4}3d$
αYC_2	~21.3	*tI*6	*I*4/*mmm*
"βYC_2"	~21.3	*cF*12	$Fm\bar{3}m$
(C)	100	*hP*4	$P6_3/mmc$

(a) Metastable form produced under pressure at high temperature

C-Zr

H. Okamoto, 1990

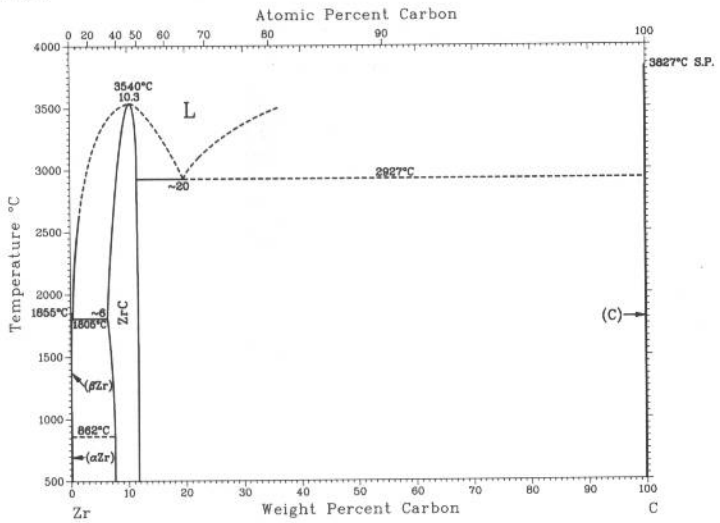

Phase	Composition, wt% C	Pearson symbol	Space group
(βZr)	0	*cI*2	$Im\bar{3}m$
(αZr)	0	*hP*2	$P6_3/mmc$
ZrC	~6 to 12	*cF*8	$Fm\bar{3}m$
(C)	0	*hP*4	$P6_3/mmc$

Ca-Cd

P.R. Subramanian, 1990

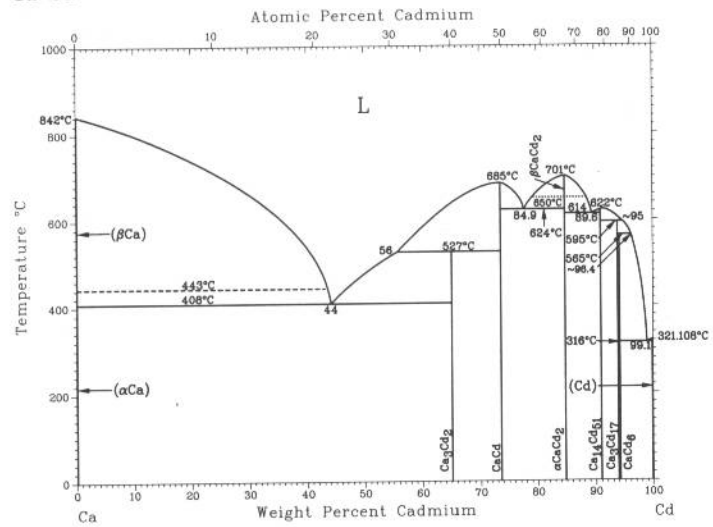

Phase	Composition, wt% Cd	Pearson symbol	Space group
(αCa)(a)	0	*cF*4	$Fm\bar{3}m$
(βCa)(b)	0	*cI*2	$Im\bar{3}m$
Ca_3Cd_2	65	*tP*20	$P4_2nm$
CaCd	73.7	*cP*2	$Pm\bar{3}m$
$\alpha CaCd_2$(c)	84.9	*hP*12	$P6_3/mmc$
$\beta CaCd_2$	84.9	*oI*12	*Imma*
$Ca_{14}Cd_{51}$	91.1	*hP*68	*P6/m*
Ca_3Cd_{17}	94	...	...
$CaCd_6$	94.4	*cI*184	$Im\bar{3}$
(Cd)	100	*hP*2	$P6_3/mmc$

(a) Below 443 °C. (b) From 443 to 842 °C. (c) From 0 to 650 °C. (d) From 650 to 701 °C

Ca-Cu

D.J. Chakrabarti and D.E. Laughlin, 1984

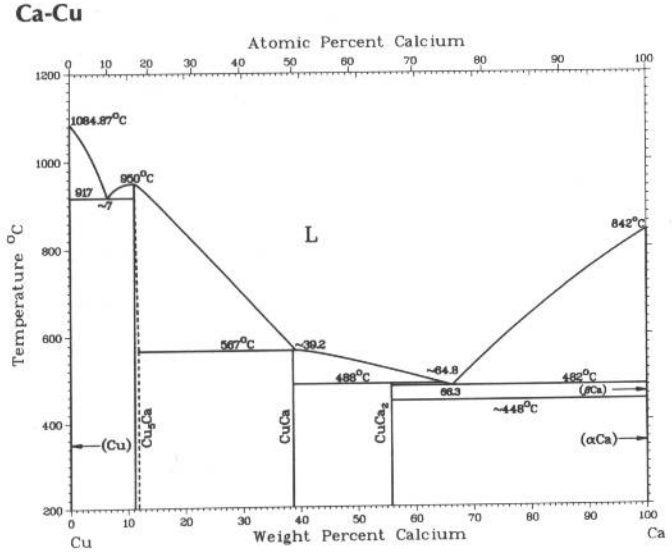

Phase	Composition, wt% Ca	Pearson symbol	Space group
(Cu)	0	*cF*4	$Fm\bar{3}m$
Cu_5Ca	10.7 to 11.4	*hP*6	*P6/mmm*
αCuCa(b)	38.7	*mP*20	$P2_1/c$
βCuCa(c)	38.7	*oP*40	*Pnma*
$CuCa_2$	55.8	*oP*12	*Pnma*
(αCa)	100	*cF*4	$Fm\bar{3}m$
(βCa)	100	*cI*2	$Im\bar{3}m$

(a) A much wider homogeneity range (approximately 14.1 to 20 at.% Ca) indicated. (b) High temperature; 94.3° interaxial angle. (c) Low temperature

Ca-Ga

V.P. Itkin and C.B. Alcock, 1992

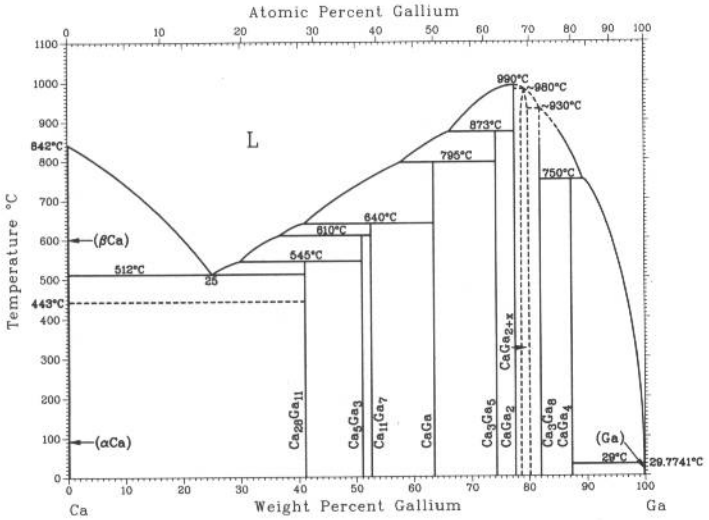

Phase	Composition, wt% Ga	Pearson symbol	Space group
(αCa)(a)	0	*cF*4	$Fm\bar{3}m$
(βCa)(b)	0	*cI*2	$Im\bar{3}m$
$Ca_{28}Ga_{11}$	40.6	*oI*78	*Imm*2
Ca_5Ga_3	51.1	*tI*32	*I*4/*mcm*
$Ca_{11}Ga_7$	52.6	*cF*144	$Fm\bar{3}m$
CaGa	63.5	*oC*8	*Cmcm*
Ca_3Ga_5	72.4	*oC*32	*Cmcm*
$CaGa_2$	77.7	*hP*6	$P6_3/mmc$
$CaGa_{2+x}$	78.5 to 80.7	*hP*3	*P*6/*mmc*
Ca_3Ga_8	82.2	*oI*22	*Immm*
$CaGa_4$	87	*mC*10	*C*2/*m*
(Ga)	100	*oC*8	*Cmca*

(a) <443 °C. (b) From 443 to 842 °C

Ca-Ge

H. Okamoto, 1990

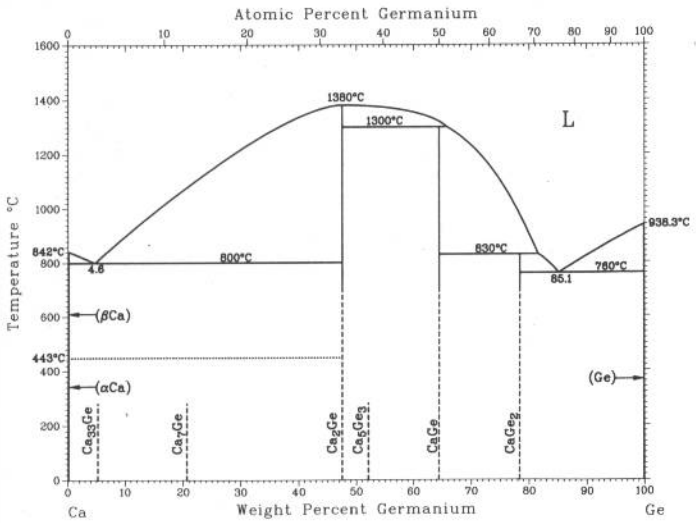

Phase	Composition, wt% Ge	Pearson symbol	Space group
(βCa)	0	*cI*2	$Im\bar{3}m$
(αCa)	0	*cF*4	$Fm\bar{3}m$
$Ca_{33}Ge$	5.1	*cF*48	$Fd\bar{3}m$
Ca_7Ge	20.6	*cF*32	$Fm\bar{3}m$
Ca_2Ge	47.5	*oP*12	*Pnma*
Ca_5Ge_3	52.1	*tI*32	*I*4/*mcm*
CaGe	64.4	*oC*8	*Cmcm*
$CaGe_2$	78.4	*hR*6	$R\bar{3}m$
(Ge)	100	*cF*8	$Fm\bar{3}m$

Ca-Hg

P.R. Subramanian, 1990

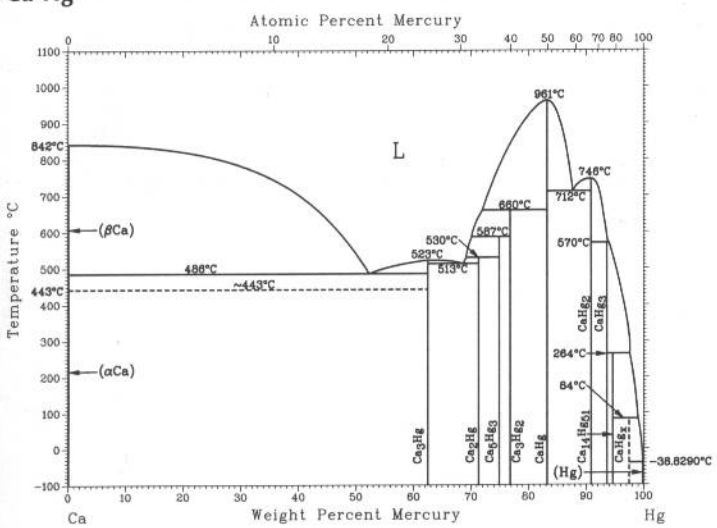

Phase	Composition, wt% Hg	Pearson symbol	Space group
(αCa)(a)	0	*cF*4	$Fm\bar{3}m$
(βCa)(b)	0	*cI*2	$Im\bar{3}m$
Ca_3Hg	63	*oP*16	*Pnma*
		*cI*32	$I\bar{4}3m$
Ca_2Hg	71.4	*oP*12	*Pnma*
Ca_5Hg_3	75.0	*tI*32	*I*4/*mcm*
Ca_3Hg_2	77	*tP*10	*P*4/*mbm*
CaHg	83.3	*cP*2	$Pm\bar{3}m$
$CaHg_2$	90.9	*hP*3	$P\bar{3}m1$
		*hP*3	*P*6/*mmm*
$CaHg_3$	94	*hP*8	$P6_3/mmc$
$Ca_{14}Hg_{51}$	94.8	*hP*68	*P*6/*m*
$CaHg_x$	~98	...	...
(Hg)	100	*hR*1	$R\bar{3}m$

(a) Below 443 °C. (b) From 443 to 842 °C

Ca-In

H. Okamoto, V.P. Itkin, and C.B. Alcock, 1992

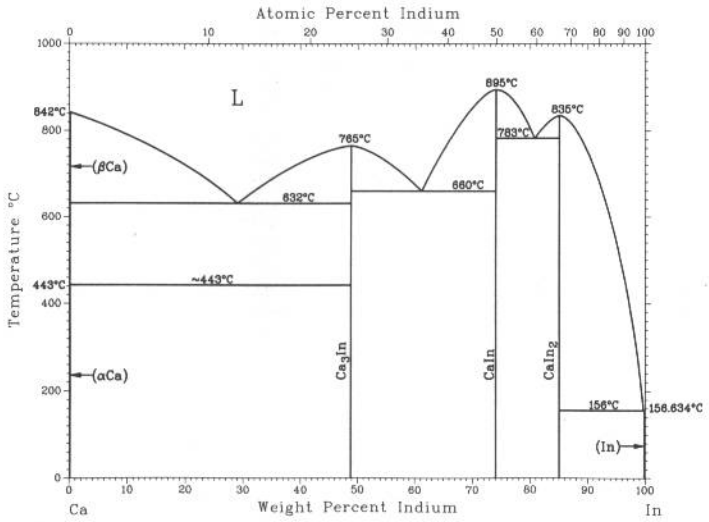

Phase	Composition, wt% In	Pearson symbol	Space group
(βCa)	0	*cI*2	$Im\bar{3}m$
(αCa)	0	*cF*4	$Fm\bar{3}m$
Ca_3In	49	*cF*16	$Fm\bar{3}m$
CaIn	74.1	*cP*2	$Pm\bar{3}m$
$CaIn_2$	85.2	*hP*6	$P6_3/mmc$
(In)	100	*tI*2	$I4/mmm$

Ca-Li

C.W. Bale and A.D. Pelton, 1987

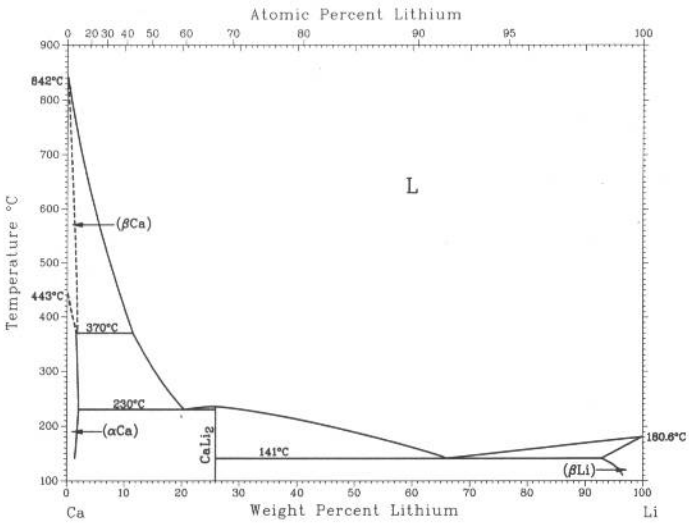

Phase	Composition, wt% Li	Pearson symbol	Space group
(αCa)	0	*cF*4	$Fm\bar{3}m$
(βCa)	0	*cI*2	$Im\bar{3}m$
$CaLi_2$	87.4	*hP*12	$P6_3/mmc$
(αLi)	100	*hP*2	$P6_3/mmc$
(βLi)	100	*cI*2	$Im\bar{3}m$

Ca-Mg

A.A. Nayeb-Hashemi and J.B. Clark, 1988

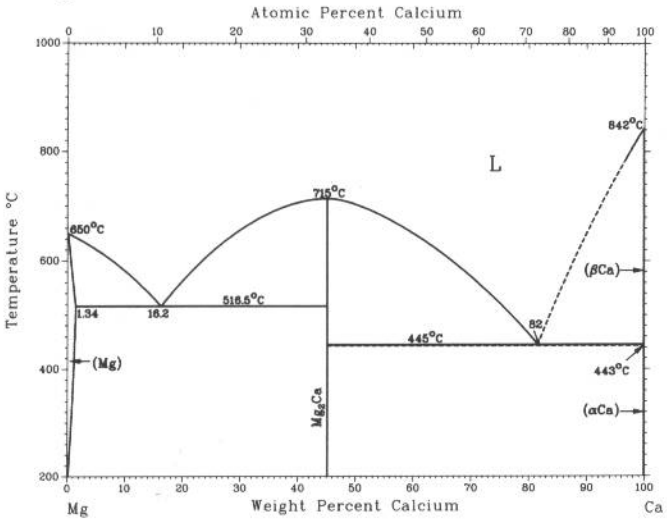

Phase	Composition, wt% Ca	Pearson symbol	Space group
(Mg)	0	*hP*2	$P6_3/mmc$
Mg_2Ca	45.2	*hP*12	$P6_3/mmc$
(βCa)	100	*cI*2	$Im\bar{3}m$
(αCa)	100	*cF*4	$Fm\bar{3}m$

Ca-Na

A.D. Pelton, 1985

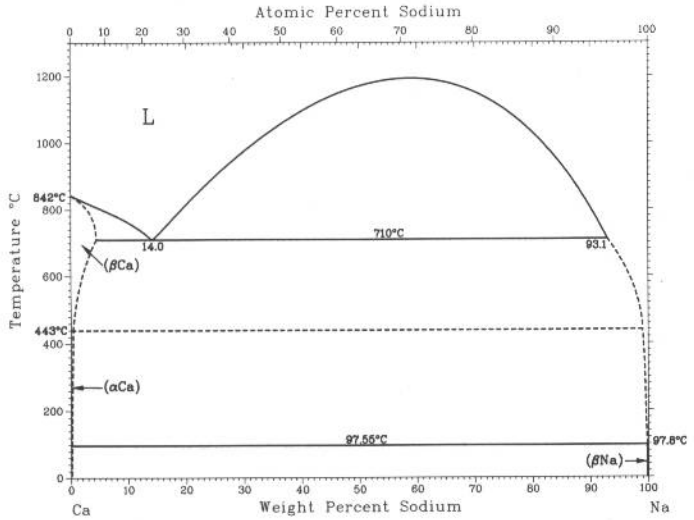

Phase	Composition, wt% Na	Pearson symbol	Space group
(αCa)	0	*cF*4	$Fm\bar{3}m$
(βCa)	0 to ~4.4	*cI*2	$Im\bar{3}m$
(βNa)	100	*cI*2	$Im\bar{3}m$
(αNa)	100	*hP*2	$P6_3/mmc$

Ca-Nd

K.A. Gschneidner, Jr. and F.W. Calderwood, 1987

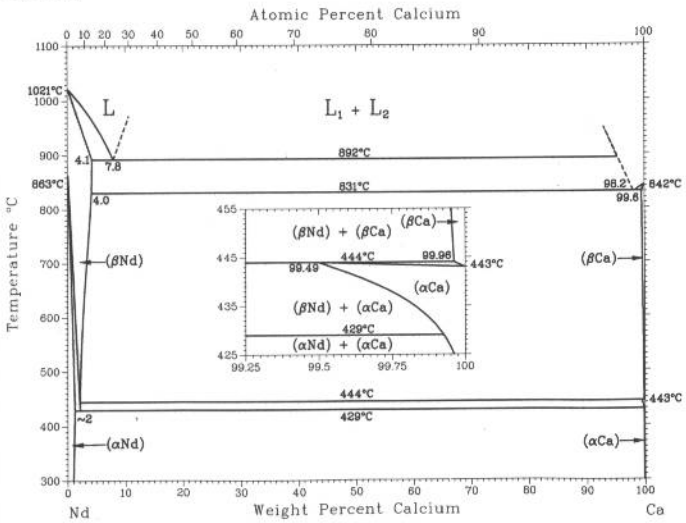

Phase	Composition, wt% Ca	Pearson symbol	Space group
(αNd)	0	*hP*4	$P6_3/mmc$
(βNd)	0	*cI*2	$Im\bar{3}m$
(αCa)	99.5 to 100	*cF*4	$Fm\bar{3}m$
(βCa)	99.6 to 100	*cI*2	$Im\bar{3}m$

Ca-Ni

H. Okamoto, 1991

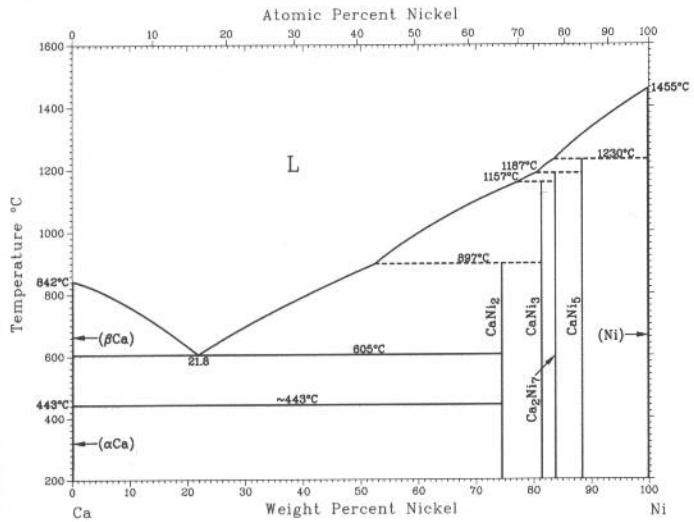

Phase	Composition, wt% Ni	Pearson symbol	Space group
(βCa)	0	*cI*2	$Im\bar{3}m$
(αCa)	0	*cF*4	$Fm\bar{3}m$
$CaNi_2$	74.6	*cF*24	$Fd\bar{3}m$
Ca_2Ni_5(a)	78.5	*hP**	?
$CaNi_3$	82	*hR*12	$R\bar{3}m$
Ca_2Ni_7	83.7	*hR*18	$R\bar{3}m$
$CaNi_5$	88.0	*hP*6	*P6/mmm*
(Ni)	100	*cF*4	$Fm\bar{3}m$

(a) Not shown on diagram

Ca-O (condensed system)

H.A. Wriedt, 1985

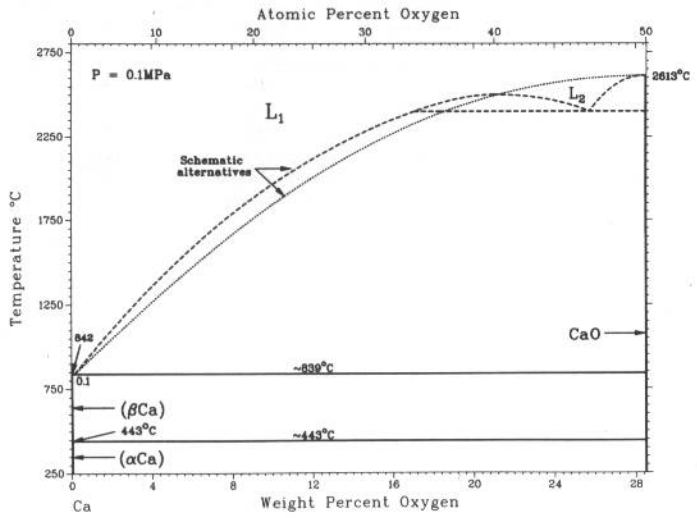

Phase	Composition, wt% O	Pearson symbol	Space group
(αCa)	0	*cF*4	$Fm\bar{3}m$
(βCa)	0	*cI*2	$Im\bar{3}m$
CaO	28.5	*cF*8	$Fm\bar{3}m$
CaO_2	44.4	*tI*6	*I*4/*mmm*
CaO_4	62	...	...
CaO_6	66.6	...	...

Ca-Pb

V.P. Itkin and C.B. Alcock, 1992

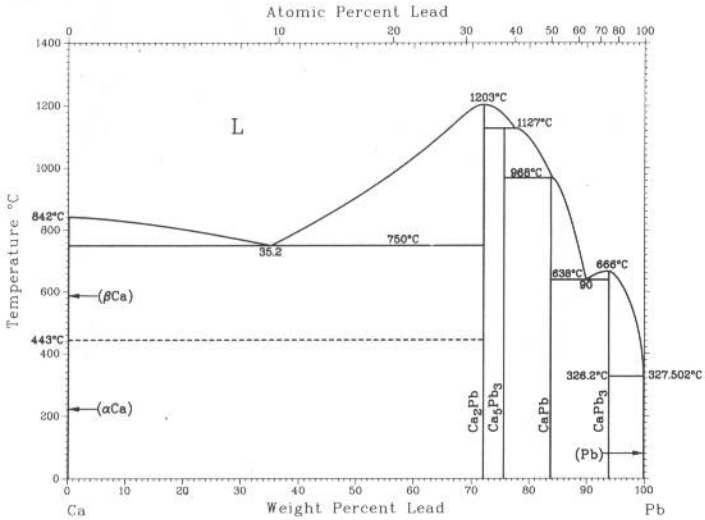

Phase	Composition, wt% Pb	Pearson symbol	Space group
(αCa)	0	*cF*4	$Fm\bar{3}m$
(βCa)	0	*cI*2	$Im\bar{3}m$
Ca_2Pb	72.1	*oP*12	*Pnma*
Ca_5Pb_3	75.6	*hP*48	$P6_3/mc$
CaPb	83.8	*tP*4	*P*4/*mmm*
$CaPb_3$	94	*cP*4	$Pm\bar{3}m$
(Pb)	99.9 to 100	*cF*4	$Fm\bar{3}m$

Ca-Pd

H. Okamoto, 1992

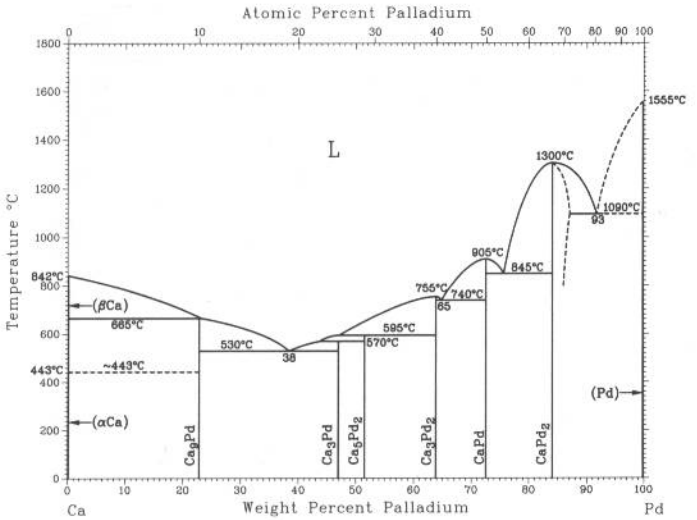

Phase	Composition, wt% Pd	Pearson symbol	Space group
(βCa)	0	*cI*2	$Im\bar{3}m$
(αCa)	0	*cF*4	$Fm\bar{3}m$
Ca_9Pd	~23	...	...
Ca_3Pd	47	*oP*16	*Pnma*
Ca_5Pd_2	51.5	*mC*28	*C*2/*c*
Ca_3Pd_2	64	*hR*45	$R\bar{3}$
CaPd	72.6	*cP*2	$Pm\bar{3}m$
$CaPd_2$	84.2	*cF*24	$Fd\bar{3}m$
$CaPd_5$	93.2	*hP*6	*P*6/*mmm*
(Pd)	100	*cF*4	$Fm\bar{3}m$

Ca-Pt

P.R. Subramanian, 1990

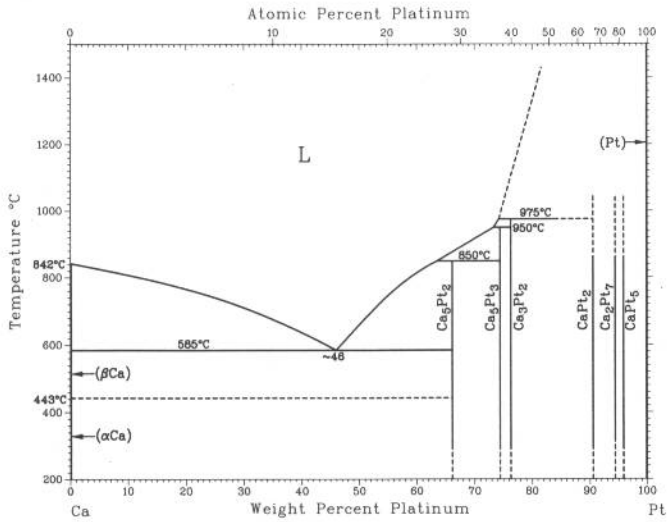

Phase	Composition, wt% Pt	Pearson symbol	Space group
(αCa)	0	*cF*4	$Fm\bar{3}m$
(βCa)	0	*cI*2	$Im\bar{3}m$
Ca_5Pt_2	66.1	*mC*28	*C*2/*c*
Ca_5Pt_3	74.5	*tI*32	*I*4/*mcm*
Ca_3Pt_2	76	*hR*45	$R\bar{3}$
$CaPt_2$	~90.7	*cF*24	$Fd\bar{3}m$
Ca_2Pt_7	~94.5	*hP*36	$P6_3/mmc$
$CaPt_5$	96.0	*hP*6	*P*6/*mmm*
(Pt)	100	*cF*4	$Fm\bar{3}m$

Ca-Sb

P.R. Subramanian, 1990

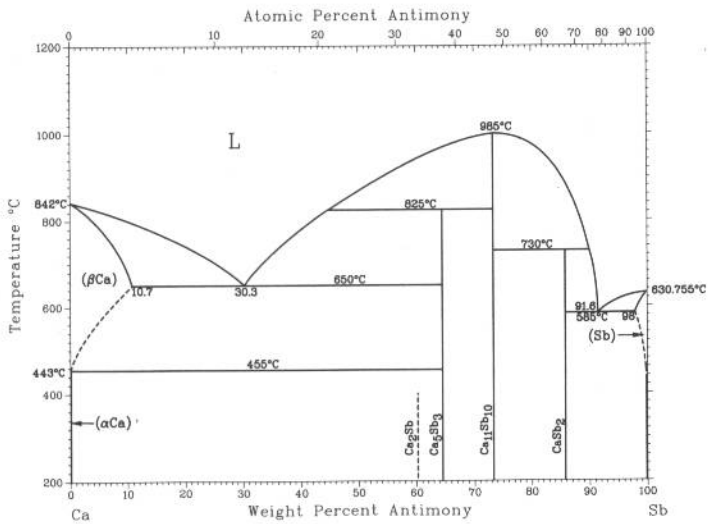

Phase	Composition, wt% Sb	Pearson symbol	Space group
(αCa)	0	*cF*4	$Fm\bar{3}m$
(βCa)	0 to 10.7	*cI*2	$Im\bar{3}m$
Ca_2Sb	~60.3	*tI*12	*I*4/*mmm*
		*tI*14(b)	*I*4/*mmm*
αCa_5Sb_3(a)	~64.6	*oP*32	*Pnma*
βCa_5Sb_3(b)	~64.6	*hP*16	$P6_3/mcm$
$Ca_{11}Sb_{10}$	~73.4	*tI*84	*I*4/*mmm*
CaSb(c)	75	*cF*8	$F\bar{4}3m$
$CaSb_2$	~85.9	*mP*6	$P2_1/m$
(Sb)	98.0 to 100	*hR*2	$R\bar{3}m$

(a) Room temperature modification. (b) High-temperature modification; allotropic transformation temperature unknown. (c) Not shown on diagram

Ca-Si

P.R. Subramanian, 1990

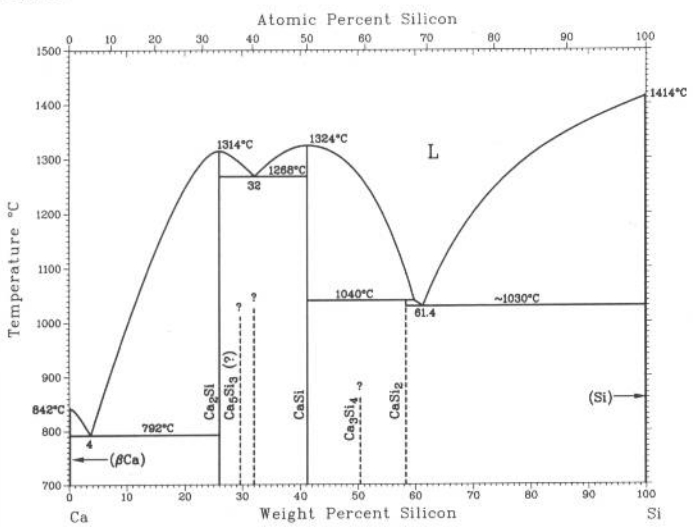

Phase	Composition, wt% Si	Pearson symbol	Space group
(αCa)	0	*cF*4	$Fm\bar{3}m$
(βCa)	0	*cI*2	$Im\bar{3}m$
Ca_2Si	25.9	*oP*12	*Pnma*
Ca_5Si_3	29.6	*tI*32	*I*4/*mcm*
CaSi	41.2	*oC*8	*Cmcm*
Ca_3Si_4	~48.3	...	...
$CaSi_2$	58.4	*hR*6	$R\bar{3}m$
(Si)	100	*cF*8	$Fd\bar{3}m$
High-pressure phase			
$CaSi_2$(a)	58.4	*tI*12	$I4_1/amd$

(a) Prepared by high-temperature/high-pressure treatment of rhombohedral $CaSi_2$ at 1000 to 1500 °C and 40 kbar, followed by quenching to ambient conditions

Ca-Sr

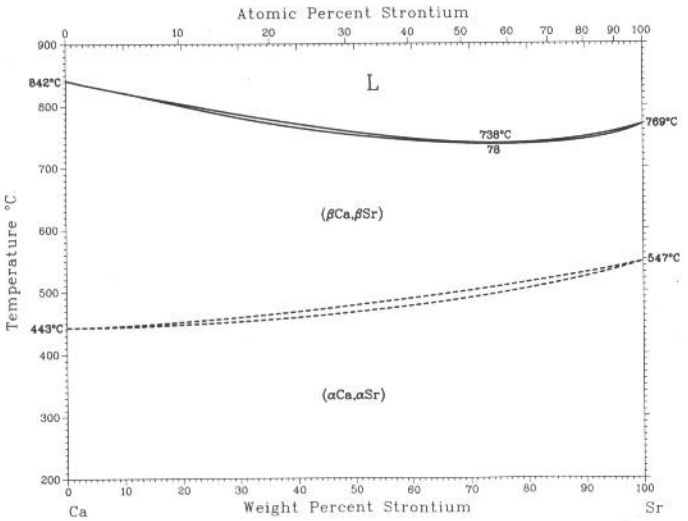

C.B. Alcock and V.P. Itkin, 1986

Phase	Composition, wt% Sr	Pearson symbol	Space group
(αCa, αSr)	0 to 100	*cF*4	$Fm\bar{3}m$
(βCa, βSr)	0 to 100	*cI*2	$Im\bar{3}m$

Ca-Tl

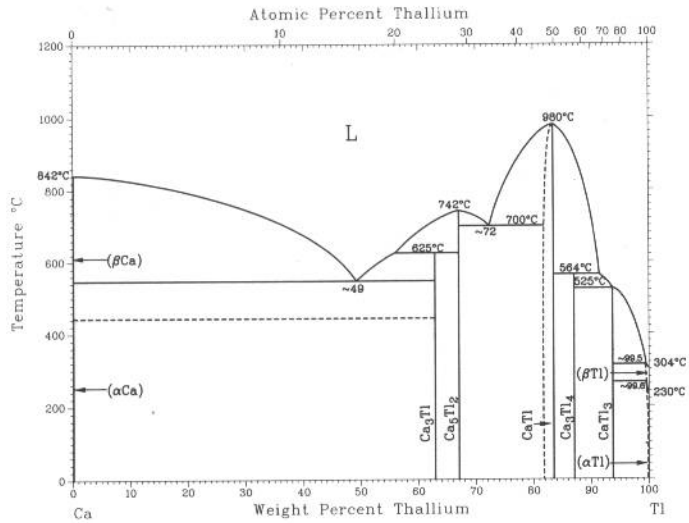

P.R. Subramanian, 1990

Phase	Composition, wt% Tl	Pearson symbol	Space group
(αCa)	0	*cF*4	$Fm\bar{3}m$
(βCa)	0	*cI*2	$Im\bar{3}m$
Ca_3Tl	63	*cF*16	$Fm\bar{3}m$
Ca_5Tl_2	~67.1	...	...
CaTl	83.6	*cP*2	$Pm\bar{3}m$
Ca_3Tl_4	~87.2	...	...
$CaTl_3$	94	*cP*4	$Pm\bar{3}m$
(αTl)	~99.6	*hP*2	$P6_3/mmc$
(βTl)	~99.5	*cI*2	$Im\bar{3}m$

Ca-Yb

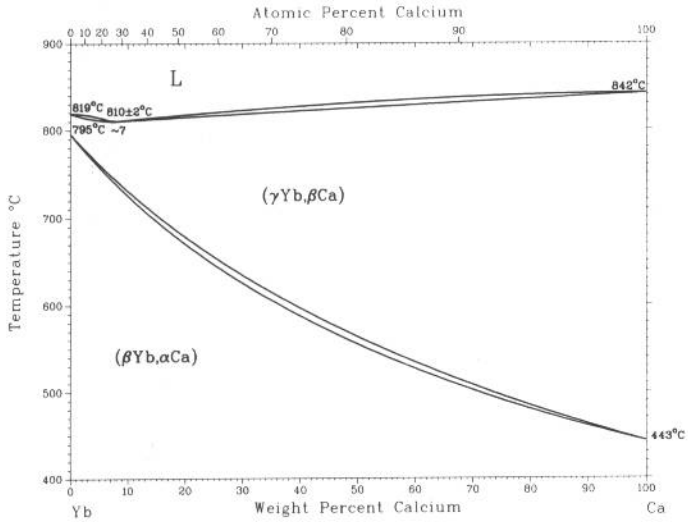

K.A. Gschneidner, Jr. and F.W. Calderwood, 1987

Phase	Composition, wt% Ca	Pearson symbol	Space group
(αYb)	0	*hP*2	$P6_3/mmc$
(βYb)	0	*cF*4	$Fm\bar{3}m$
(γYb)	0	*cI*2	$Im\bar{3}m$
(αCa)	100	*cF*4	$Fm\bar{3}m$
(βCa)	100	*cI*2	$Im\bar{3}m$

Ca-Zn

V.P. Itkin and C.B. Alcock, 1990

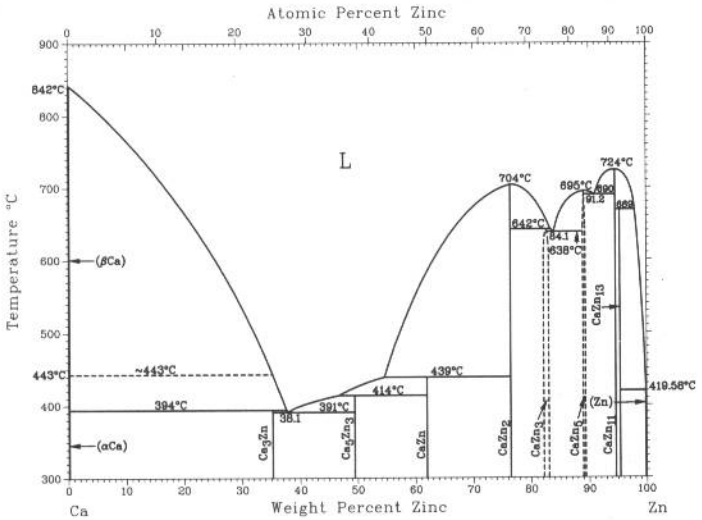

Phase	Composition, wt% Zn	Pearson symbol	Space group
(βCa)	0	*cI*2	$Im\bar{3}m$
(αCa)	0	*cF*4	$Fm\bar{3}m$
Ca_3Zn	35	*oC*16	*Cmcm*
Ca_5Zn_3	46.5	*tI*32	*I*4/*mcm*
CaZn	62.0	*oC*8	*Cmcm*
$CaZn_2$	76.6	*oI*12	*Imma*
$CaZn_3$	82 to 83	*hP*32	$P6_3/mmc$
$CaZn_5$	81.7 to 89.5	*hP*6	*P*6/*mmm*
$CaZn_{11}$	94.7	*tI*48	$I4_1/amd$
$CaZn_{13}$	95.5	*cF*112	$Fm\bar{3}c$
(Zn)	100	*hP*2	$P6_3/mmc$

Cd-Cu

P.R. Subramanian and D.E. Laughlin, 1990

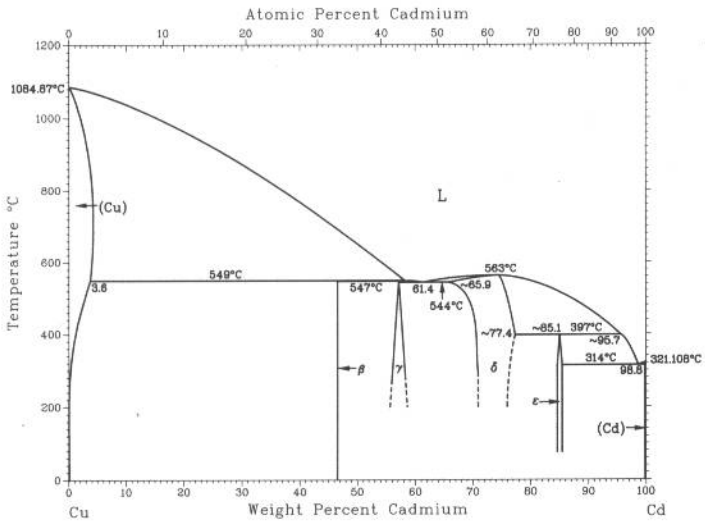

Phase	Composition, wt% Cd	Pearson symbol	Space group
(Cu)	0 to 3.6	*cF*4	$Fm\bar{3}m$
β	46.9	*hP*24	$P6_3/mmc$
γ	56.0 to 58.3(a)	*cF*1124	$F\bar{4}3m$
δ	65.9 to 77	*cI*52	...
ε	84.6 to 85.9	*hP*28	$P6_3/mmc$
(Cd)	~99.9 to 100	*hP*2	$P6_3/mmc$

(a) At 300 °C

Cd-Eu

K.A. Gschneidner, Jr. and F.W. Calderwood, 1988

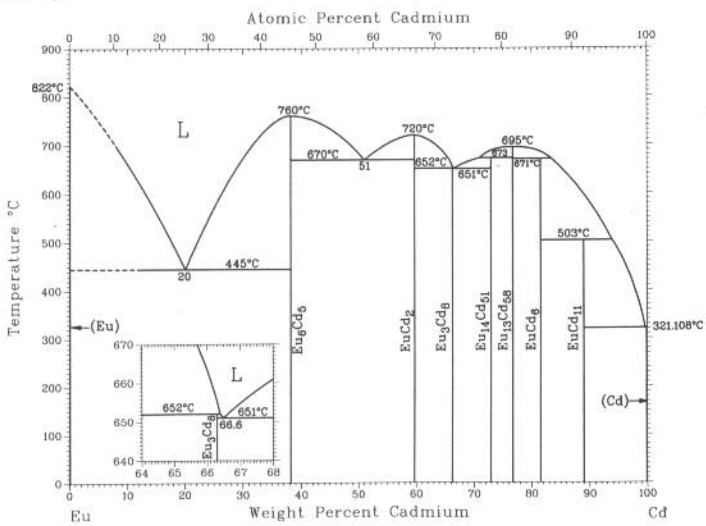

Phase	Composition, wt% Cd	Pearson symbol	Space group
(Eu)	0	*cI*2	$Im\bar{3}m$
EuCd(a)	38.2	*cP*2	$Pm\bar{3}m$
$EuCd_2$	59.7	*oI*12	*Imma*
Eu_3Cd_8	66.3	(b)	...
$Eu_{14}Cd_{51}$	73.0	*hP*65	*P*6/*m*
$Eu_{13}Cd_{58}$	76.8	*hP*142	$P6_3/mmc$
$EuCd_6$	81.6	*cI*168	$Im\bar{3}$
$EuCd_{11}$	88.8 to 89.1	*tI*48	*I*4/*amd*
(Cd)	100	*hP*2	$P6_3/mmc$

(a) Defect structure reported as Eu_6Cd_5. (b) Structure not known

Cd-Ga

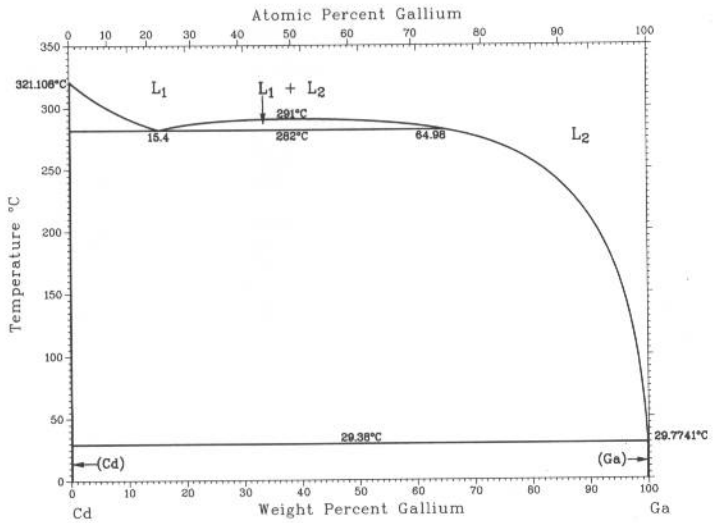

Z. Moser, J. Dutkiewicz, W. Gasior, and J. Salawa, unpublished

Phase	Composition, wt% Ga	Pearson symbol	Space group
(Cd)	0	*hP*2	$P6_3/mmc$
(Ga)	100	*oC*8	*Cmca*

Cd-Gd

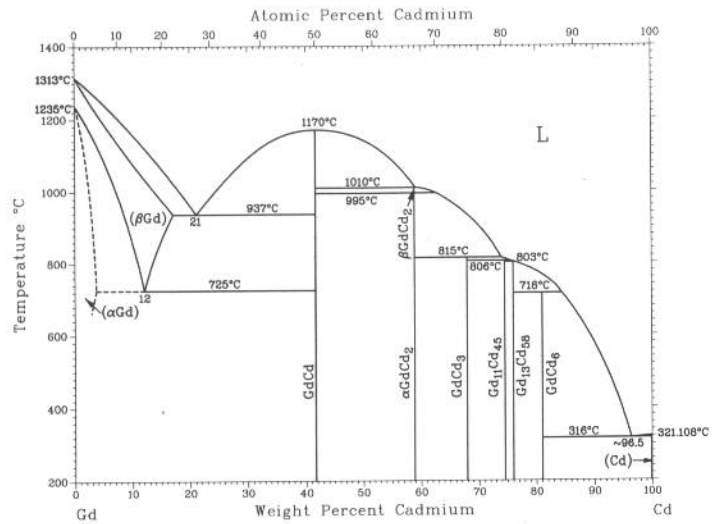

K.A. Gschneidner, Jr. and F.W. Calderwood, 1988

Phase	Composition, wt% Cd	Pearson symbol	Space group
(αGd)	0 to ~3.6	*hP*2	$P6_3/mmc$
(βGd)	0 to ~17	*cI*2	$Im\bar{3}m$
GdCd	41.7	*cP*2	$Pm\bar{3}m$
$GdCd_2$	58.9	*hP*3	$P\bar{3}m1$
$GdCd_3$	68	*hP*8	$P6_3/mmc$
$Gd_{11}Cd_{45}$	74.6	*cF*448	$F\bar{4}3m$
$Gd_{13}Cd_{58}$	76.1	*hP*142	$P6_3/mmc$
$GdCd_6$	81.1	*cI*168	$Im\bar{3}$
(Cd)	100	*hP*2	$P6_3/mmc$

Cd-Ge

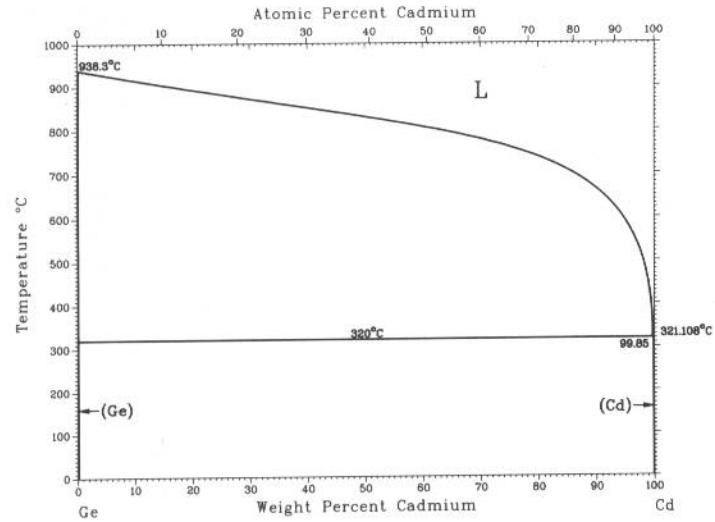

R.W. Olesinski and G.J. Abbaschian, 1986

Phase	Composition, wt% Cd	Pearson symbol	Space group
(Ge)	0.0	*cF*8	$Fd\bar{3}m$
GeII(HP)	0.0	*tI*4	$I4_1/amd$
(Cd)	100	*hP*2	$P6_3/mmc$

Cd-Hg

C. Guminski and L.A. Zabdyr, 1992

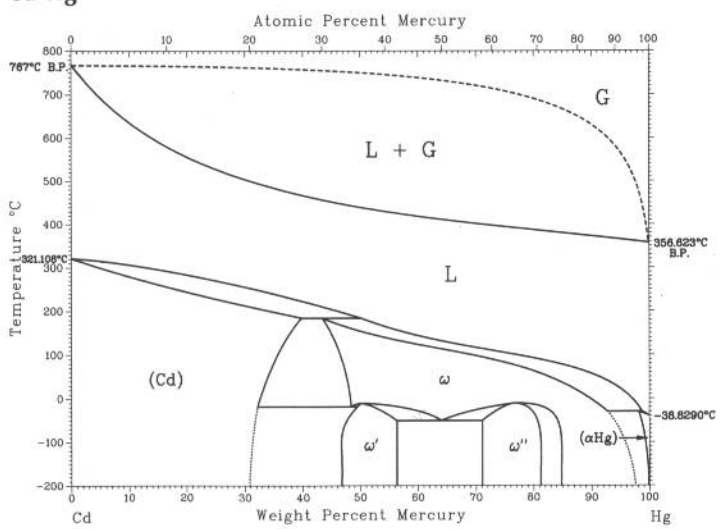

Phase	Composition, wt% Hg	Pearson symbol	Space group
(Cd)	0 to 37	*hP*2	$P6_3/mmc$
ω	42 to 94	*tI*2	*I*4/*mmm*
ω′	47 to 56	*tI*6	*I*4/*mmm*
ω″	71 to 81	*tI*6	*I*4/*mmm*
(αHg)(a)	98 to 100	*hR*1	$R\bar{3}m$
(βHg)(b)	~100	*tI*2	*I*4/*mmm*

(a) From –38.8290 to –193 °C at 100 wt% Hg. (b) Below –193 °C

Cd-In

J. Dutkiewicz, L.A. Zabdyr, W. Zakulski, Z. Moser, J. Salawa, P.J. Horrocks, F.H. Hayes, and M.H. Rand, 1992

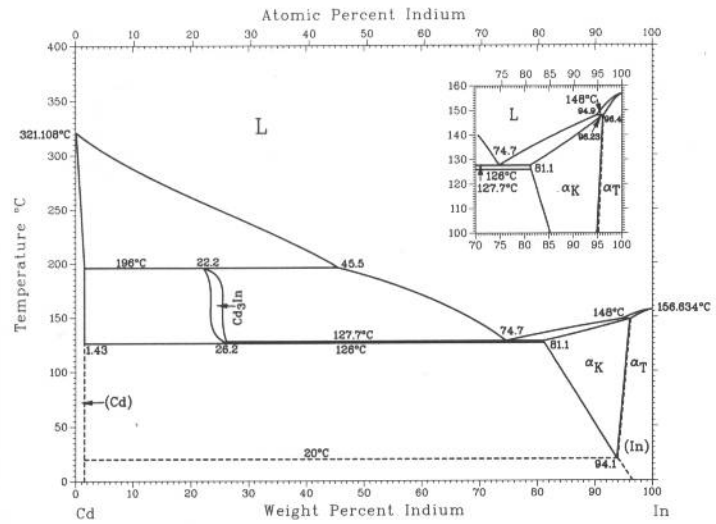

Phase	Composition, wt% In	Pearson symbol	Space group
(Cd)	0 to 1.4	*hP*2	$P6_3/mmc$
Cd_3In	22.2 to 26.2	*cP*4	$Pm\bar{3}m$
α_K	81.1 to 94	*cF*4	$Fm\bar{3}m$
(In)(α_T)	94 to 100	*tI*2	*I*4/*mmm*

Cd-La

K.A. Gschneidner, Jr. and F.W. Calderwood, 1988

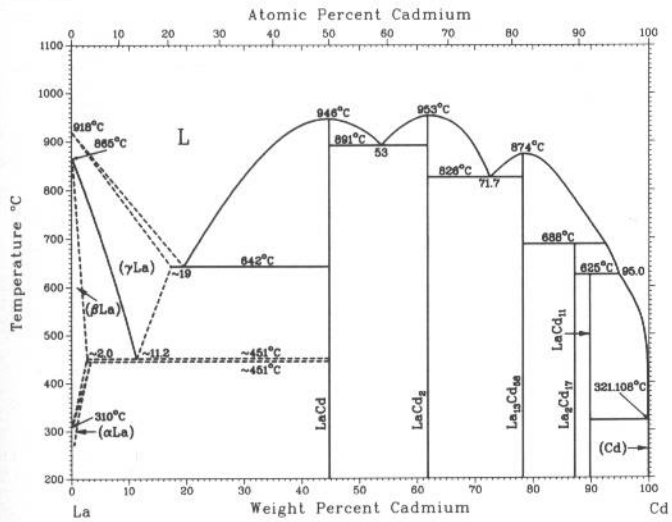

Phase	Composition, wt% Cd	Pearson symbol	Space group
(αLa)	0	*hP*4	$P6_3/mmc$
(βLa)	0 to ~2.0	*cF*4	$Fm\bar{3}m$
(γLa)	0 to ~18	*cI*2	$Im\bar{3}m$
LaCd	44.7	*cP*2	$Pm\bar{3}m$
$LaCd_2$	61.8	*hP*3	*P*3*m*1
$La_{13}Cd_{58}$	78.3	*hP*142	$P6_3/mmc$
La_2Cd_{17}	85.8	*hP*38	$P6_3/mmc$
$LaCd_{11}$	89.9	*cP*36	$Pm\bar{3}m$
(Cd)	100	*hP*2	$P6_3/mmc$

Cd-Li

A.D. Pelton, 1988

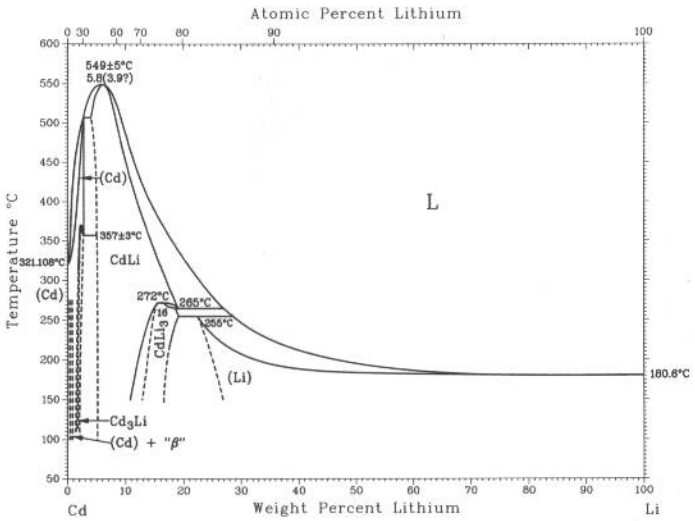

Phase	Composition, wt% Li	Pearson symbol	Space group
(Cd)	0 to 2.6	*hP*2	$P6_3/mmc$
Cd_3Li	2? to 2.5	*hP*2	$P6_3/mmc$
CdLi	3.6 to 18	*cF*16	$Fd\bar{3}m$
$CdLi_3$	10? to 18	*cF*4	$Fm\bar{3}m$
(βLi)	22 to 100	*cI*2	$Im\bar{3}m$
(αLi)(a)	100	*hP*2	$P6_3/mmc$

(a) Below –193 °C

Cd-Mg

Z. Moser, W. Gasior, J. Wypartowicz, and L. Zabdyr, 1984

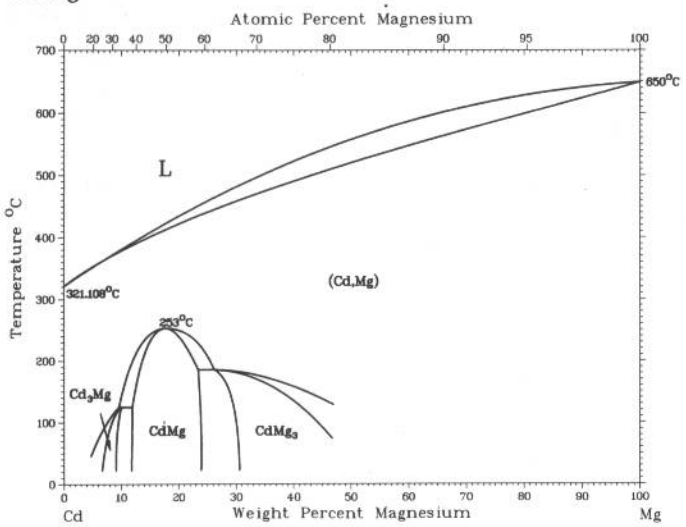

Phase	Composition, wt% Mg	Pearson symbol	Space group
(Cd, Mg)	0 to 100	*hP*2	$P6_3/mmc$
α′ or Cd_3Mg	7 to 9	*hP*8	$P6_3/mmc$
α″ or CdMg	12 to 25	*oP*4	*Pmma*
α‴ or $CdMg_3$	29 to 50	*hP*8	$P6_3/mmc$

Cd-Na

A.D. Pelton, 1988

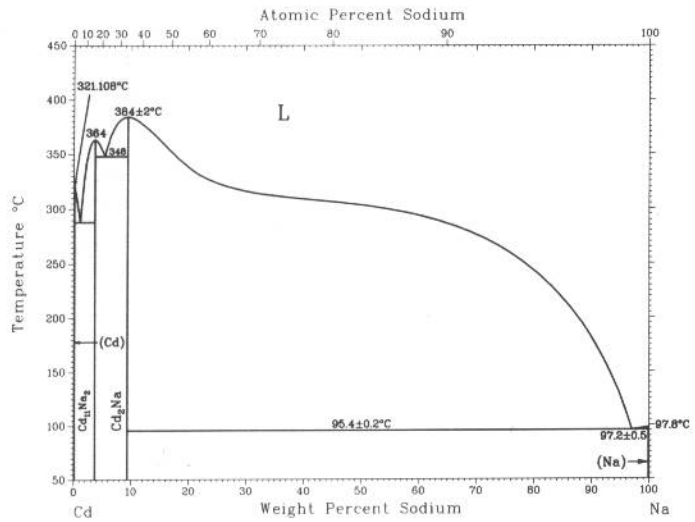

Phase	Composition, wt% Na	Pearson symbol	Space group
(Cd)	0	*hP*2	$P6_3/mmc$
$Cd_{11}Na_2$	3.9	*cP*39	$Pm\bar{3}$
Cd_2Na(a)	9.3	*cF*1192	...
(βNa)	100	*cI*2	$Im\bar{3}m$
(αNa)(b)	100	*hP*2	$P6_3/mmc$

(a) Complex cubic structure that corresponds to the formula $Cd_{1.92}Na$ at 0.070 wt% Na. (b) Below –237 °C

Cd-Ni

F.A. Shunk and P. Nash, 1991

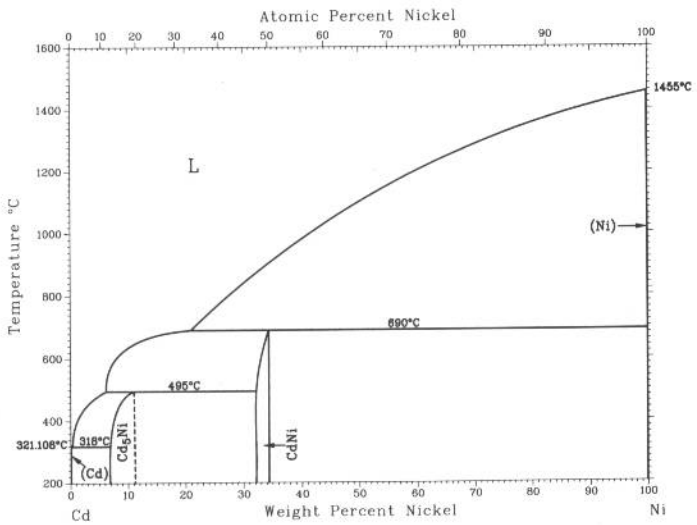

Phase	Composition, wt% Ni	Pearson symbol	Space group
(Cd)	0	*hP*2	$P6_3/mmc$
Cd_5Ni	9 to 10.6	*cP*52	$P\bar{4}3m$
CdNi	31.9 to 34.3	*cF*112	$Fd\bar{3}m$
(Ni)	100	*cF*4	$Fm\bar{3}m$

Cd-P

H. Okamoto, 1990

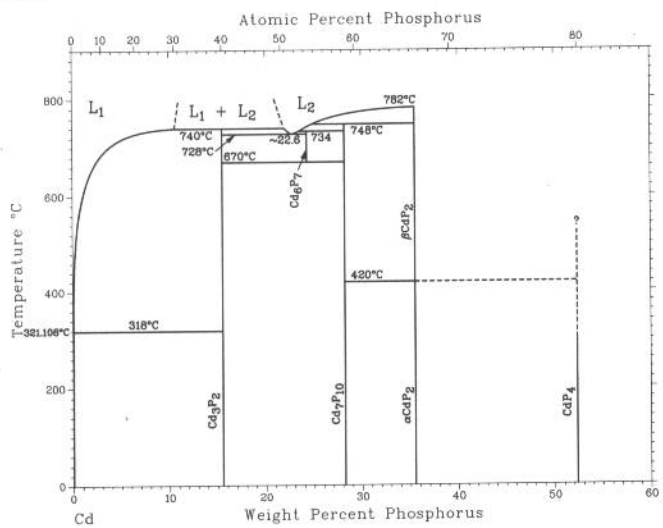

Phase	Composition, wt% P	Pearson symbol	Space group
(Cd)	0	*hP*2	$P6_3/mmc$
Cd_3P_2	16	*tI*40	$P4_2/nmc$
Cd_6P_7	24.3	*c**52	...
Cd_7P_{10}	24.3	*oF*136	*Fdd*2
βCdP_2	55.6	*tP*24	$P4_32_12$
αCdP_2	35.6	*oP*12	$Pna2_1$
CdP_4	52.4	*mP*10	$P2_1/c$

Cd-Pb

J. Dutkiewicz, Z. Moser, and W. Zakulski, 1988

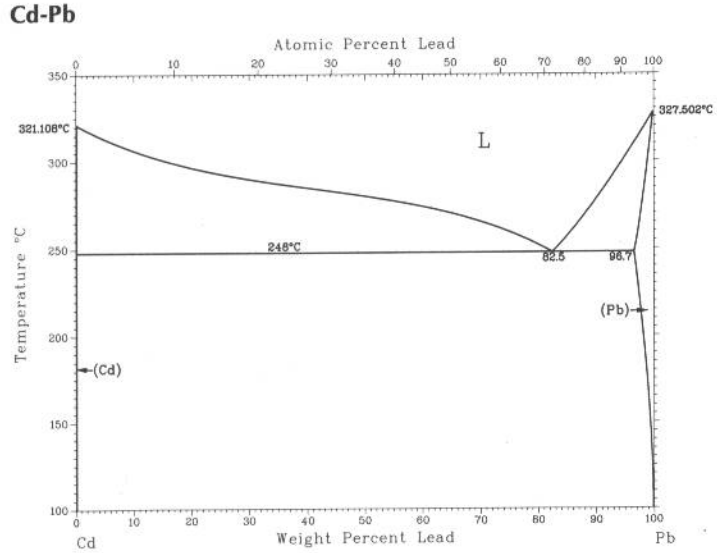

Phase	Composition, wt% Pb	Pearson symbol	Space group
(Cd)	0	*hP*2	$P6_3/mmc$
(Pb)	96.7 to 100	*cF*4	$Fm\bar{3}m$

Cd-Sb

H. Okamoto, 1990

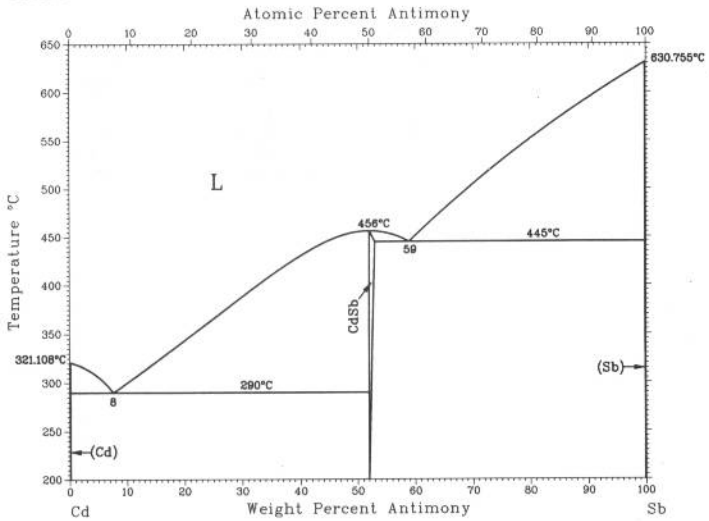

Phase	Composition, wt% Sb	Pearson symbol	Space group
(Cd)	0	*hP*2	$P6_3/mmc$
CdSb	52.0 to 53	*oP*16	*Pbca*
(Sb)	100	*hR*2	$R\bar{3}m$
Metastable phases			
Cd_3Sb_2	42	*m**20	...
Cd_4Sb_3	44.9	*hR**	...

Cd-Se

R.C. Sharma and Y.A. Chang, unpublished

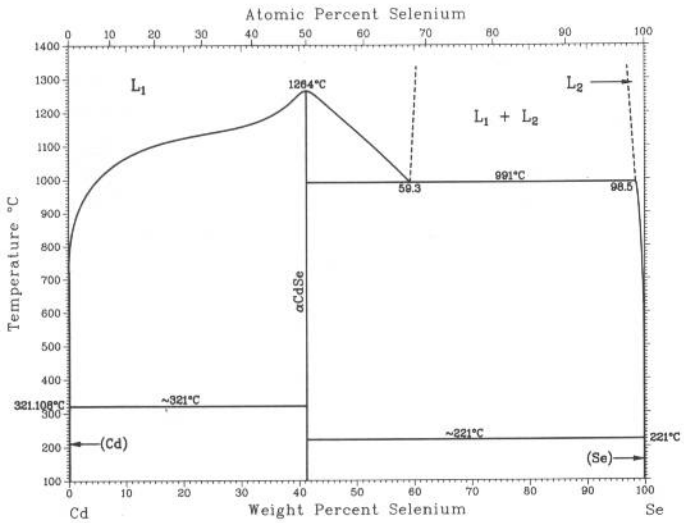

Phase	Composition, wt% Se	Pearson symbol	Space group
(Cd)	0	*hP*2	$P6_3/mmc$
αCdSe	41.3	*hP*4	$P6_3mc$
βCdSe(a)	41.3	*cF*8	$Fm\bar{3}m$
(Se)	100	*hP*3	$P3_121$

(a) High-pressure phase

Cd-Sm

K.A. Gschneidner, Jr. and F.W. Calderwood, 1988

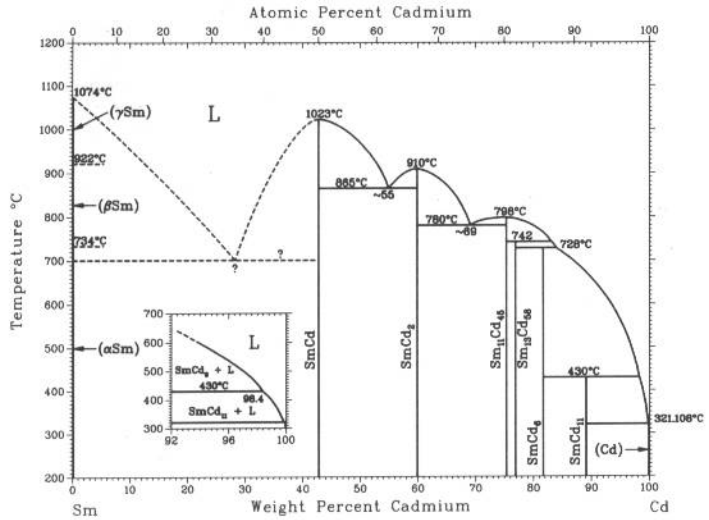

Phase	Composition, wt% Cd	Pearson symbol	Space group
(αSm)	0	*hR*3	$R\bar{3}m$
(βSm)	0	*hP*2	$P6_3/mmc$
(γSm)	0	*cI*2	$Im\bar{3}m$
SmCd	42.8	*cP*2	$Pm\bar{3}m$
$SmCd_2$	60.0	*hP*3	$P3m1$
$Sm_{11}Cd_{45}$	75.4	*cF*448	$F\bar{4}3m$
$Sm_{13}Cd_{58}$	76.9	*hP*142	$P6_3/mmc$
$SmCd_6$	81.8	*cI*168	$Im\bar{3}$
$SmCd_{11}$	89.2	*cP*36	$Pm\bar{3}m$
(Cd)	100	*hP*2	$P6_3/mmc$

Cd-Sn

J. Dutkiewicz, L.A. Zabdyr, Z. Moser, and J. Salawa, 1989

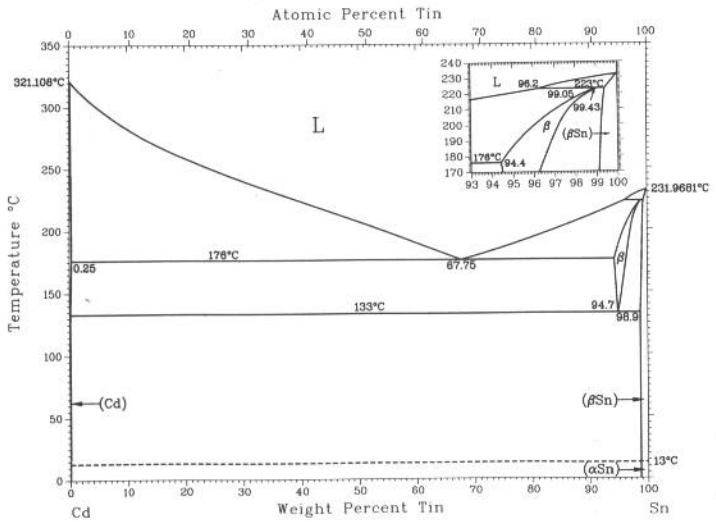

Phase	Composition, wt% Sn	Pearson symbol	Space group
(Cd)	0 to 0.25	*hP*2	$P6_3/mmc$
β	94.3 to 99.1	*hP*2	$P6_3/mmc$
(Sn)	98.9 to 100	*tI*4	$I4_1/amd$

Cd-Sr

H. Okamoto, 1990

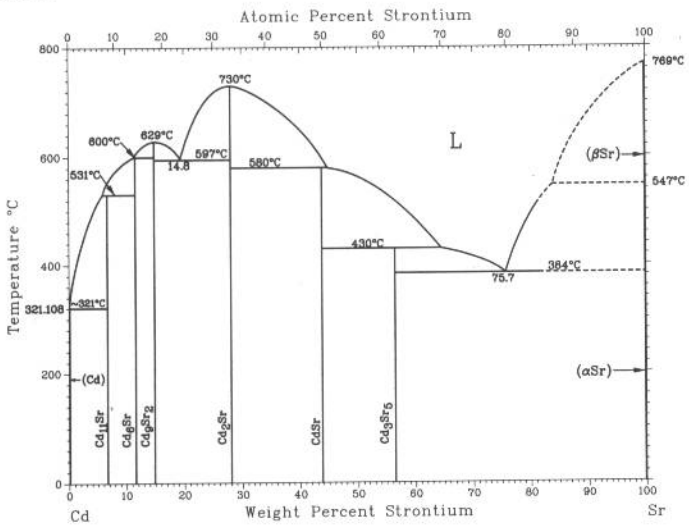

Phase	Composition, wt% Sr	Pearson symbol	Space group
(Cd)	0	*hP*2	$P6_3/mmc$
$Cd_{11}Sr$	6.6	*tI*48	$I4_1/amd$
Cd_6Sr	11.5	...	...
Cd_9Sr_2	14.8	...	...
Cd_2Sr	28.0	*oI*12	*Imma*
CdSr	43.8	*cP*2	$Pm\bar{3}m$
Cd_3Sr_5	56.5	*tI*32	*I*4/*mcm*
(βSr)	100	*cI*2	$Im\bar{3}m$
(αSr)	100	*cF*4	$Fm\bar{3}m$

Cd-Te

R.C. Sharma and Y.A. Chang, 1989

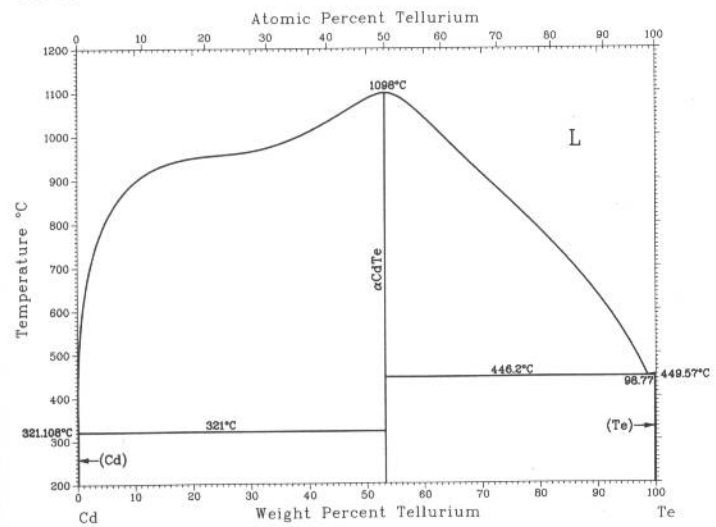

Phase	Composition, wt% Te	Pearson symbol	Space group
(Cd)	0	*hP*2	$P6_3/mmc$
αCdTe	53.2	*cF*8	$F\bar{4}3m$
βCdTe(a)	53.2	*cF*8	$Fm\bar{3}m$
γCdTe(a)	53.2	*tI*4	$I4_1/amd$
(Te)	100	*hP*3	$P3_121$

(a) High-pressure phase

Cd-Th

J. Dutkiewicz, unpublished

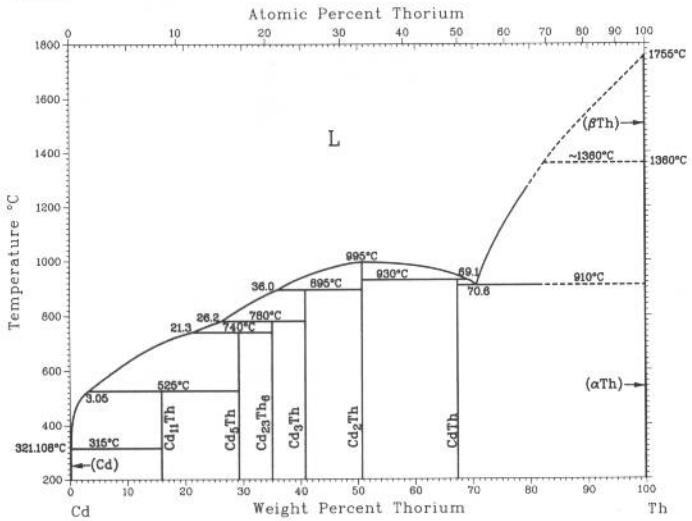

Phase	Composition, wt% Th	Pearson symbol	Space group
(Cd)	0	*hP*2	$P6_3/mmc$
$Cd_{11}Th$	15.79	*cP*36	$Pm\bar{3}m$
Cd_5Th	29.21	*hP*36	$P6_3/mmc$
$Cd_{23}Th_6$	35.00	*cF*116	$Fm\bar{3}m$
Cd_3Th	41	*hP*8	$P6_3/mmc$
Cd_2Th	50.79	*hP*3	$P6/mmm$
CdTh	67.4	*oP*24	...
(αTh)	100	*cF*4	$Fm\bar{3}m$
(βTh)	100	*cI*2	$Im\bar{3}m$

Cd-Tl

H. Okamoto, 1990

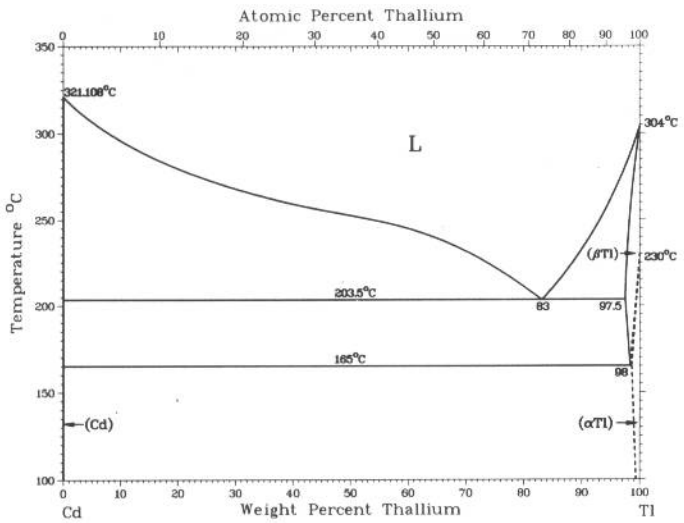

Phase	Composition, wt% Tl	Pearson symbol	Space group
(Cd)	0	*hP*2	$P6_3/mmc$
(βTl)	97.5 to 100	*cI*2	$Im\bar{3}m$
(αTl)	~98 to 100	*hP*2	$P6_3/mmc$

Cd-Y

K.A. Gschneidner, Jr. and F.W. Calderwood, 1988

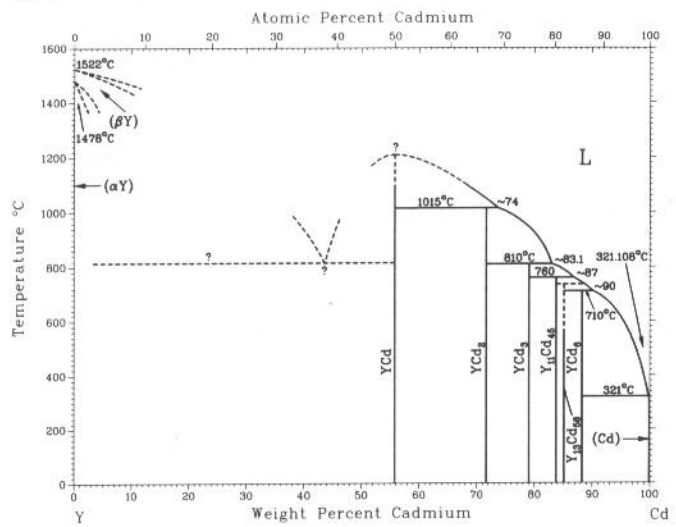

Phase	Composition, wt% Cd	Pearson symbol	Space group
(αY)	0	*hP*2	$P6_3/mmc$
(βY)	0	*cI*2	$Im\bar{3}m$
YCd	55.8	*cP*2	$Pm\bar{3}m$
YCd_2	71.7	*hP*3	$P3m1$
YCd_3	79	*oC*16	$Cmcm$
$Y_{11}Cd_{45}$	83.8	*cF*448	$F\bar{4}3m$
$Y_{13}Cd_{58}$	85.0	*hP*142	$P6_3/mmc$
YCd_6	88.3	*cI*168	$Im\bar{3}$
(Cd)	100	*hP*2	$P6_3/mmc$

Cd-Yb

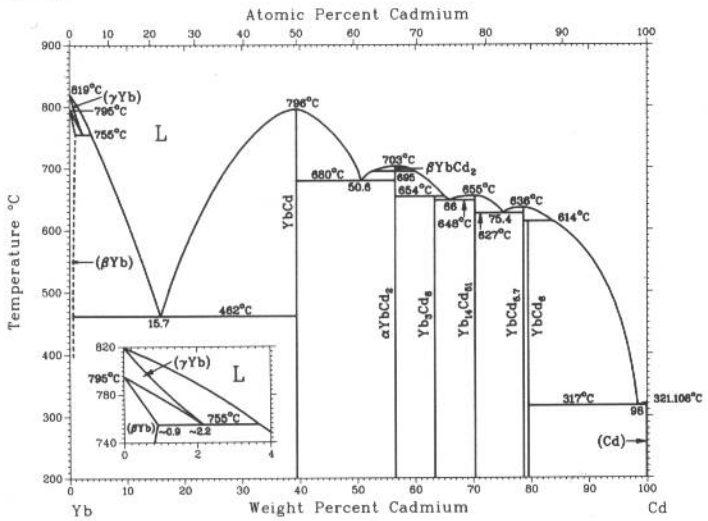

K.A. Gschneidner, Jr. and F.W. Calderwood, 1988

Phase	Composition, wt% Cd	Pearson symbol	Space group
(βYb)	0 to ~0.91	*cF*4	$Fm\bar{3}m$
(γYb)	0 to ~2.2	*cI*2	$Im\bar{3}m$
YbCd	39.4	*cP*2	$Pm\bar{3}m$
$YbCd_2$	56.5	*hP*12	$P6_3/mmc$
Yb_3Cd_8	63.4	...	...
$Yb_{14}Cd_{51}$	70.3	*hP*65	*P*6/*m*
$YbCd_{5.7}$	78.8	...	...
$YbCd_6$	79.6	*cI*168	$Im\bar{3}$
(Cd)	100	*hP*2	$P6_3/mmc$

Cd-Zn

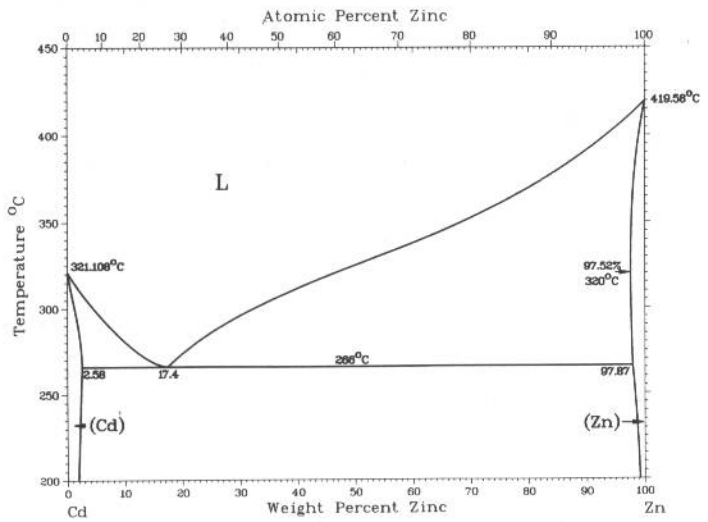

J. Dutkiewicz and W. Zakulski, 1984

Phase	Composition, wt% Zn	Pearson symbol	Space group
(Cd)	0 to 2.58	*hP*2	$P6_3/mmc$
(Zn)	97.52 to 100	*hP*2	$P6_3/mmc$

Ce-Co

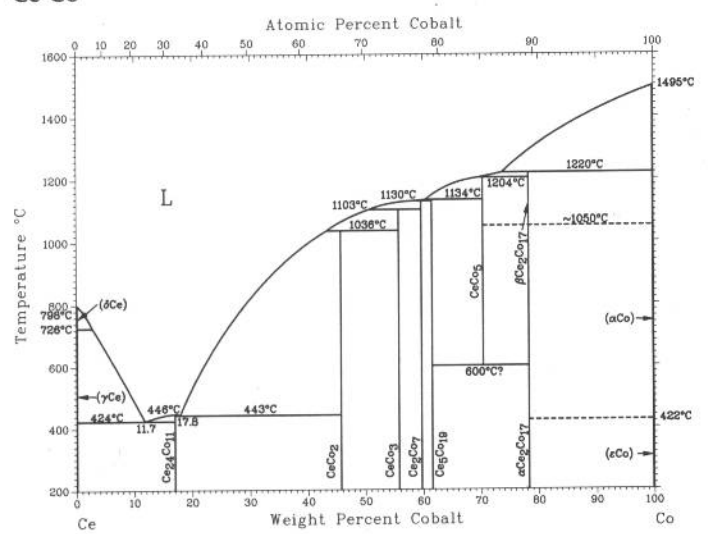

K.A. Gschneidner, Jr. and M.E. Verkade, 1974

Phase	Composition, wt% Co	Pearson symbol	Space group
(δCe)	0	*cI*2	$Im\bar{3}m$
(γCe)	0	*cF*4	$Fm\bar{3}m$
$Ce_{24}Co_{11}$	16.1	*hP*70	$P6_3/mc$
$CeCo_2$	45.7	*cF*24	$Fd\bar{3}m$
$CeCo_3$	56	*hR*12	$R\bar{3}m$
Ce_2Co_7	59.6	*hP*36	$P6_3/mmc$
Ce_5Co_{19}	61.1	*hR*24	$R\bar{3}m$
$CeCo_5$	67.7	*hP*6	*P*6/*mmm*
βCe_2Co_{17}	78.2	*hP*38	$P6_3/mmc$
αCe_2Co_{17}	78.2	*hR*19	$R\bar{3}m$
(αCo)	100	*cF*4	$Fm\bar{3}m$
(εCo)	100	*hP*2	$P6_3/mmc$

Ce-Cu

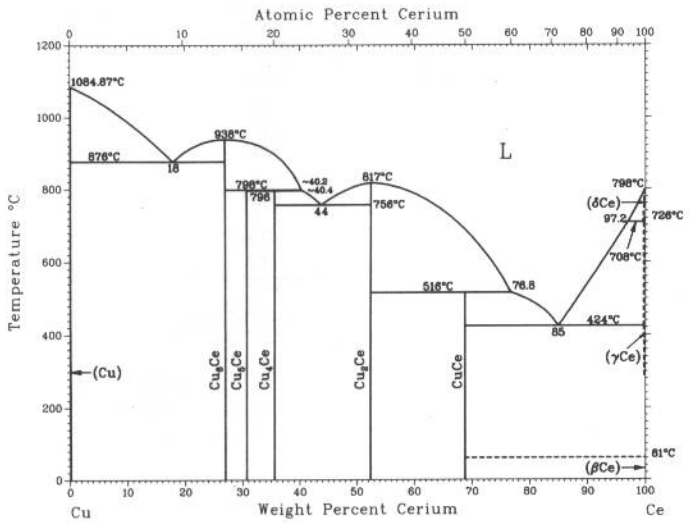

P.R. Subramanian and D.E. Laughlin, 1988

Phase	Composition, wt% Ce	Pearson symbol	Space group
(Cu)	0	*cF*4	$Fm\bar{3}m$
Cu_6Ce	~26.88	*oP*28	*Pnma*
Cu_5Ce	~30.61	*hP*6	*P6/mmm*
Cu_4Ce	~35.5	*oP*20	*Pnnm*
Cu_2Ce	~52.4	*oI*12	*Imma*
CuCe	~68.8	*oP*8	*Pnma*
(δCe)	100	*cI*2	$Im\bar{3}m$
(γCe)	100	*cF*4	$Fm\bar{3}m$
(βCe)	100	*hP*2	$P6_3/mmc$
(αCe)	100	*cF*4	$Fm\bar{3}m$

Ce-Fe

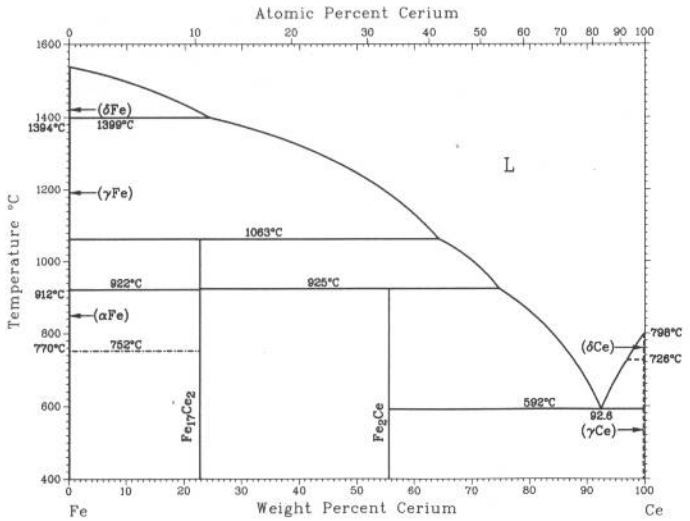

W. Zhang, G. Liu, and K. Han, 1992

Phase	Composition, wt% Ce	Pearson symbol	Space group
(δFe)	0	*cI*2	$Im\bar{3}m$
(γFe)	0	*cF*4	$Fm\bar{3}m$
(αFe)	0	*cI*2	$Im\bar{3}m$
$\alpha Fe_{17}Ce_2$	22.7	*hP*38	*P6/mmm*
$\beta Fe_{17}Ce_2$	22.7	*hR*19	$R\bar{3}m$
Fe_2Ce	55.6	*cF*24	$Fd\bar{3}m$
(δCe)	100	*cF*4	$Fm\bar{3}m$
(βCe)	100	*hP*2	$P6_3/mmc$
(αCe)	100	*cF*4	$Fm\bar{3}m$

Enlargement of the Ce-rich portion of the Fe-Ce phase diagram

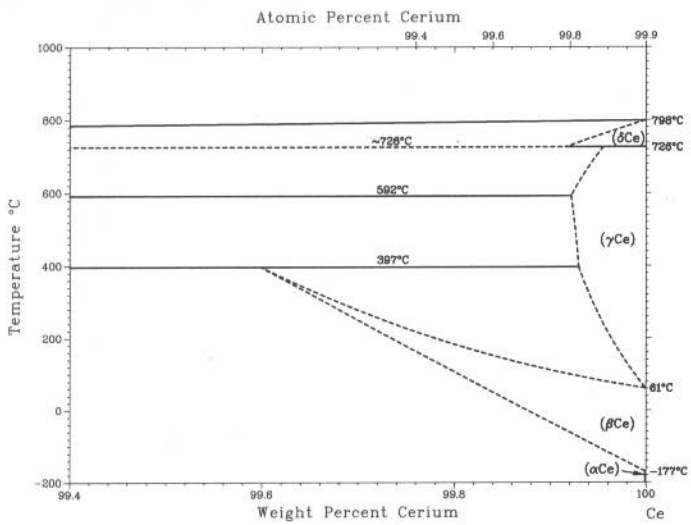

Ce-Ga

H. Okamoto, 1990

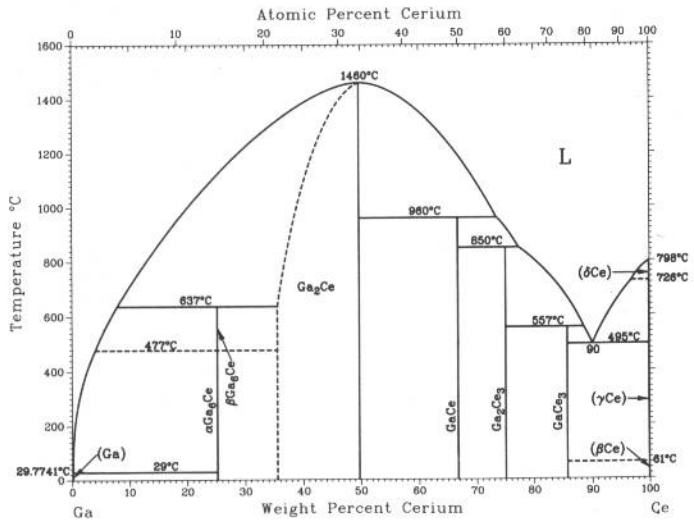

Phase	Composition, wt% Ce	Pearson symbol	Space group
(Ga)	0	*oC*8	*Cmca*
βGa_6Ce	21.1	...	...
αGa_6Ce	21.1	*tI*14	*P4/nbm*
Ga_2Ce	? to 44.6	*hP*3	*P6/mmm*
GaCe	61.7	*oC*8	*Cmcm*
Ga_2Ce_3	71	*tP*20	$P4_2/mnm$
Ga_3Ce_5(a)	73	*tI*32	*I4/mcm*
$GaCe_3$	83	*cP*4	$Pm\bar{3}m$
(δCe)	100	*cI*2	$Im\bar{3}m$
(γCe)	100	*cF*4	$Fm\bar{3}m$
(βCe)	100	*hP*4	$P6_3/mmc$

(a) Not shown in the diagram

Ce-Ge

A.B. Gokhale and G.J. Abbaschian, 1989

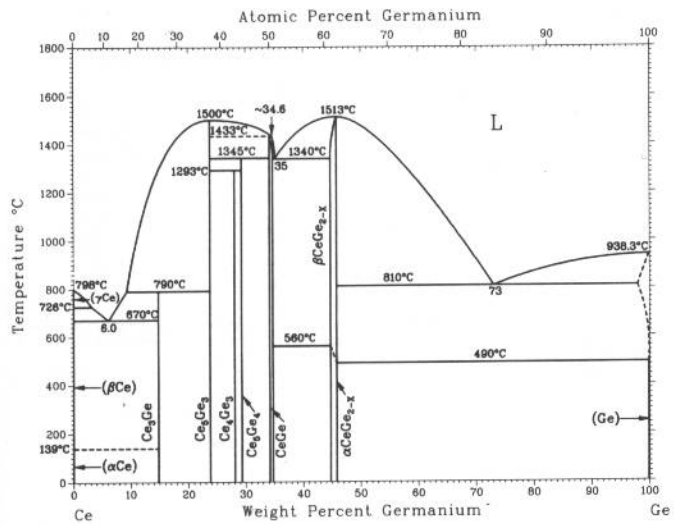

Phase	Composition, wt% Ge	Pearson symbol	Space group
(δCe)(a)	0	*cI*2	$Im\bar{3}m$
(γCe)(b)	0	*cF*4	$Fm\bar{3}m$
(βCe)(c)	0	*hP*4	$P6_3/mmc$
(αCe)(d)	0	*cF*4	$Fm\bar{3}m$
Ce_3Ge	15	...	...
Ce_5Ge_3	23.7	*hP*16	$P6_3/mcm$
Ce_4Ge_3	28.0	*cI*28	$I\bar{4}3d$
Ce_5Ge_4	29.4	...	*Pnma*
CeGe	34.1	*oP*8	*Pnma*
$\alpha CeGe_{2-x}$	44.9 to 45.94	(e)	*Imma*
$\beta CeGe_{2-x}$	44.9 to 45.94	*tI*12	$I4_1/amd$
(Ge)	100	*cF*8	$Fd\bar{3}m$

(a) From 798 to 726 °C. (b) From 726 to 61 °C (139 °C on heating, 16 °C on cooling). (c) From 61 to −177 °C. (d) Below −177 °C. (e) Orthorhombic

Ce-In

H. Okamoto, 1992

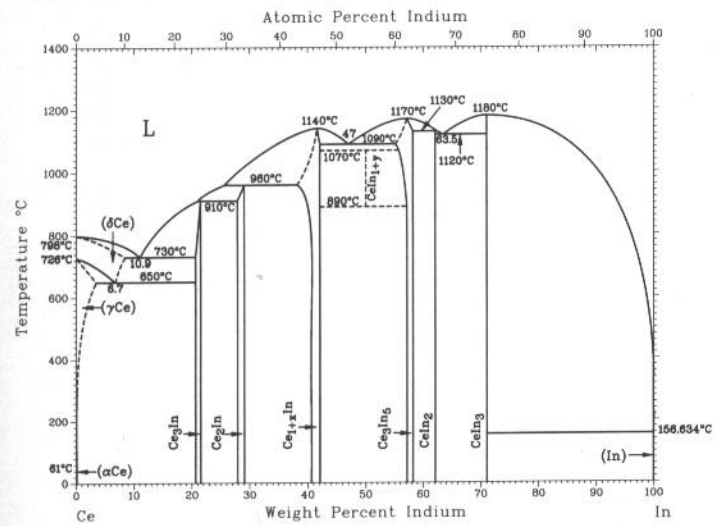

Phase	Composition, wt% In	Pearson symbol	Space group
(δCe)	0 to 8	*cI*2	$Im\bar{3}m$
(γCe)	0 to 3	*cF*4	$Fm\bar{3}m$
(βCe)	0	*hP*4	$P6_3/mmc$
(αCe)	0	*cF*4	$Fm\bar{3}m$
βCe_3In	22	*cF*4	$Fm\bar{3}m$
αCe_3In	21 to 22	*cP*4	$Pm\bar{3}m$
Ce_2In	28 to 29.0	*hP*6	$P6_3/mmc$
$Ce_{1+x}In$	38 to 42	...	...
$CeIn_{1+y}$	...	...	...
Ce_3In_5	55 to 58	*oC*32	*Cmcm*
$CeIn_2$	62.1	*oI*12	*Imma*
$CeIn_3$	71	*cP*4	$Pm\bar{3}m$
(In)	100	*tI*2	*I4/mmm*

Ce-Ir

H. Okamoto, 1991

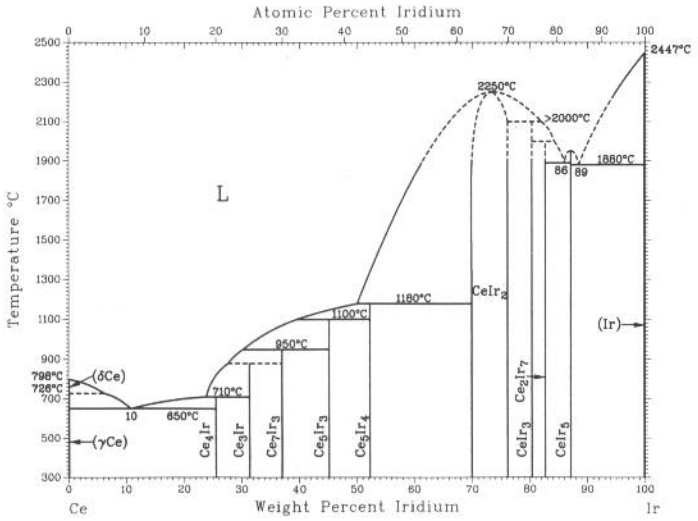

Phase	Composition, wt% Ir	Pearson symbol	Space group
(δCe)	0	*cI*2	$Im\bar{3}m$
(γCe)	0	*cF*4	$Fm\bar{3}m$
(βCe)	0	*hP*4	$P6_3/mmc$
(αCe)	0	*cF*4	$Fm\bar{3}m$
Ce_4Ir	26	...	...
Ce_3Ir	31	...	...
Ce_7Ir_3	37	*hP*20	$P6_3mc$
Ce_5Ir_3	45.1	*tP*32	$P4/ncc$
Ce_5Ir_4	52.3	*oP*36	*Pnma*
$CeIr_2$	70 to 76	*cF*24	$Fd\bar{3}m$
$CeIr_3$	81	*hR*12	$R\bar{3}m$
Ce_2Ir_7	82.8	*hR*18	$R\bar{3}m$
$CeIr_5$	87.2	*cF*24	$F4\bar{3}m$
(Ir)	100	*cF*4	$Fm\bar{3}m$

Ce-Mg

A.A. Nayeb-Hashemi and J.B. Clark, 1988

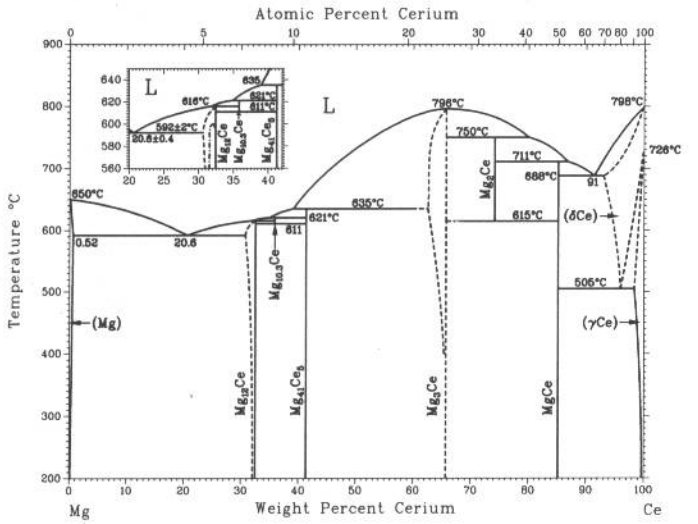

Phase	Composition, wt% Ce	Pearson symbol	Space group
(Mg)	0 to 0.52	*hP*2	$P6_3/mmc$
$Mg_{12}Ce$(I)	32.44(a,b)	*tI*26	$I4/mmm$
$Mg_{12}Ce$(II)	32.44(b)	*oI*338	(*Immm*)
$Mg_{10.3}Ce$	35.89(a)	*hP*38	$P6_3/mmc$
$Mg_{41}Ce_5$	41.28(a)	*tI*92	$I4/m$
Mg_3Ce	? to 66	*cF*16	$Fm\bar{3}m$
Mg_2Ce	74.24(a)	*cF*24	$Fd\bar{3}m$
MgCe	85.22	*cP*2	$Pm\bar{3}m$
(δCe)	? to 100	*cI*2	$Im\bar{3}m$
(γCe)	98.5 to 100	*cF*4	$Fm\bar{3}m$

(a) Appears to be a line compound. The composition range, if any, is unknown. (b) Composition has not been established with certainty. (c) The $Ni_{17}Th_2$ structure type is taken from the homologous Mg-Nd system. In the Mg-Ce system, the $Ni_{17}Th_2$ structure has not yet been found.

Ce-Mn

A. Palenzona and S. Cirafici, unpublished

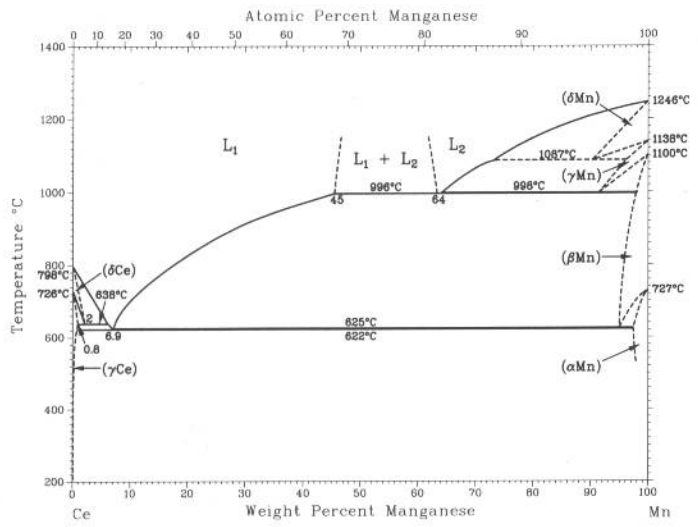

Phase	Composition, wt% Mn	Pearson symbol	Space group
(δCe)	0 to 2	*cI*2	$Im\bar{3}m$
(γCe)	0 to 0.8	*cF*4	$Fm\bar{3}m$
(βCe)	0	*hP*4	$P6_3/mmc$
(αCe)	0	*cF*4	$Fm\bar{3}m$
(δMn)	~100	*cI*2	$Im\bar{3}m$
(γMn)	~100	*cF*4	$Fm\bar{3}m$
(βMn)	~100	*cP*20	$P4_132$
(αMn)	~100	*cI*58	$I\bar{4}3m$

Ce-Ni

P. Nash and C.H. Tung, 1991

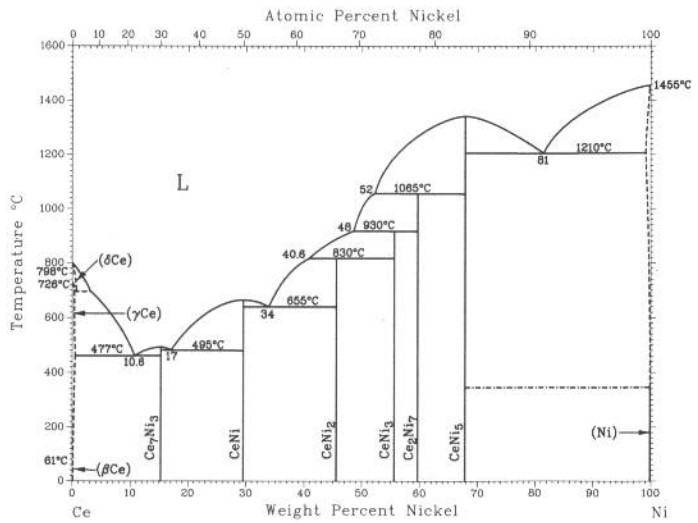

Phase	Composition, wt% Ni	Pearson symbol	Space group
(γCe)	~0	*cF*4	$Fm\bar{3}m$
(δCe)	~0	*cI*2	$Im\bar{3}m$
Ce_7Ni_3	15	*hP*20	$P6_3mc$
CeNi	29.5	*oC*8	*Cmcm*
$CeNi_2$	45.6	*cF*24	$Fd\bar{3}m$
$CeNi_3$	55.7	(a)	$P6_3/mmc$
Ce_2Ni_7	59.5	(c)	$P6_3/mmc$
$CeNi_5$	67.6	*hP*6	$P6/mmm$
(Ni)(b)	99.90 to 100	*cF*4	$Fm\bar{3}m$

(a) Hexagonal. (b) Solubility of Ce in Ni is 0.05 at.% Ce at 1200 °C and 0.04 at.% Ce at room temperature; data were obtained from pure Ni.

Ce-O

P.R. Subramanian, 1990

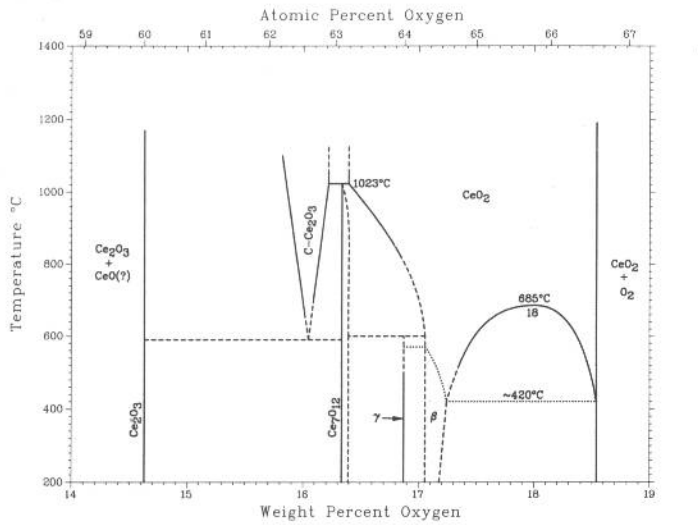

Phase	Composition, wt% O	Pearson symbol	Space group
(αCe)(a)	~0	*cF*4	$Fm\bar{3}m$
(βCe)(b)	~0	*hP*4	$P6_3/mmc$
(γCe)(c)	~0	*cF*4	$Fm\bar{3}m$
(δCe)(d)	~0	*cI*2	$Im\bar{3}m$
CeO	~10.2	*cF*8	$Fm\bar{3}m$
Ce_2O_3	~15	*hP*5	$P\bar{3}m1$
"C-C_2O_3" (e, g)	15.86 to 16.16	*cI*80	$Ia\bar{3}$
Ce_7O_{12}	16.3 to 16.43	*hR*22	$R\bar{3}$
γ(f)	~16.90	*hR*?	...
β(g)	~17.1 to 17.2	*hR*?	...
Ce_6O_{11}(h)	~17.3	*mP*?	$P2_1/n$
CeO_2	~18.6	*cF*12	$Fm\bar{3}m$
CeO_2(j)	~18.6	*hP*48	...
High-pressure phase			
CeO(k)	~10.2	*cF*?	...

(a) Below room temperature. (b) Up to 61 °C. (c) From 61 to 726 °C. (d) From 726 to 798 °C. (e) High-temperature phase; stable above ~590 °C. (f) Reported to be γ form of Ce_2O_3, perhaps a compound with stoichiometry Ce_9O_{16}, with monoclinic or lower symmetry. (g) Reported to be β form of Ce_2O_3, perhaps a compound with stoichiometry $Ce_{10}O_{18}$, with monoclinic or lower symmetry. (h) High-temperature phase; reported to be stable between 790 and 850 °C. (j) Reported to be high-temperature phase, observed at 1340 °C. (k) High-pressure phase, formed by reaction of Ce and CeO_2 at 700 °C and 15 kbar pressure

Ce-Pd

H. Okamoto, 1991

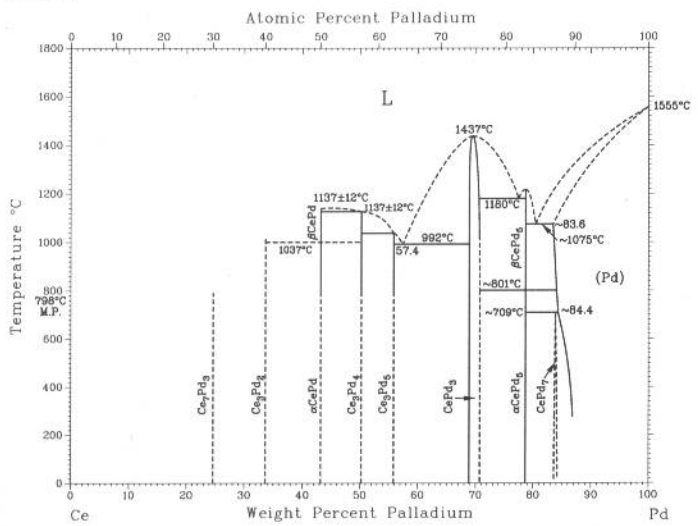

Phase	Composition, wt% Pd	Pearson symbol	Space group
(δCe)	0	*cI*2	$Im\bar{3}m$
(γCe)	0	*cF*4	$Fm\bar{3}m$
(βCe)	0	*hP*4	$P6_3/mmc$
(αCe)	0	*cF*4	$Fm\bar{3}m$
Ce_7Pd_3	25	*hP*20	$P6_3mc$
Ce_3Pd_2	34	...	...
βCePd	43.2	*oP*8	*Pnma*
αCePd	43.2	*oC*8	*Cmcm*
Ce_3Pd_4	50.3	*hR*14	$R\bar{3}m$
Ce_3Pd_5	55.9	*hP*8	$P\bar{6}2m$
$CePd_3$	69.3 to 70.9	*cP*4	$Pm\bar{3}m$
$\beta CePd_5$	79.1	*hR**	...
$\alpha CePd_5$	79.1	*cF**	...
$CePd_7$	84.2	*cF**	$Fm\bar{3}m$
(Pd)	84 to 100	*cF*4	$Fm\bar{3}m$

Ce-Pu

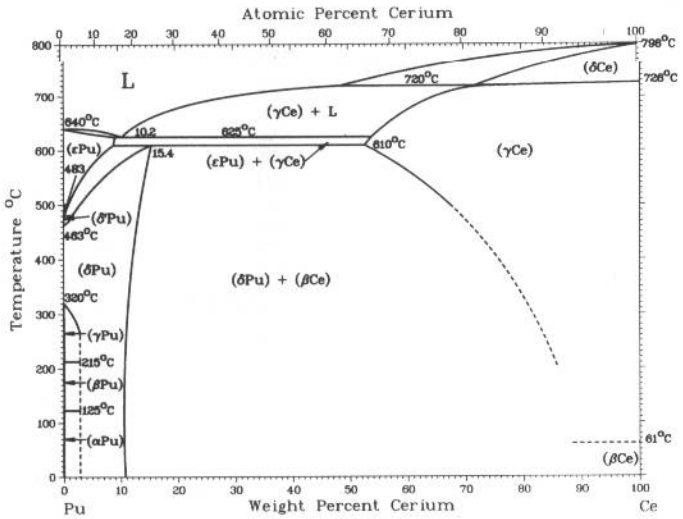

J.E. Selle and D.E. Etter, 1964

Phase	Composition, wt% Ce	Pearson symbol	Space group
(εPu)	0 to 9	*cI*2	$Im\bar{3}m$
(δ'Pu)	0	*tI*2	*I*4/*mmm*
(δPu)	0 to 15.4	*cF*4	$Fm\bar{3}m$
(γPu)	0	*oF*8	*Fddd*
(βPu)	0	*mC*34	*I*2/*m*
(αPu)	0	*mP*16	$P2_1/m$
(δCe)	72 to 100	*cI*2	$Im\bar{3}m$
(γCe)	53 to 100	*cF*4	$Fm\bar{3}m$
(βCe)	100	*hP*4	$P6_3/mmc$
(αCe)	100	*cF*4	$Fm\bar{3}m$

Ce-S

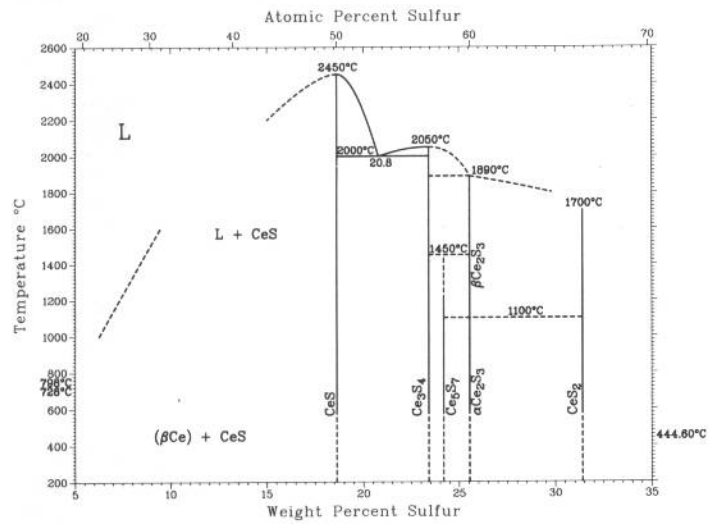

K.A. Gschneidner, Jr. and M.E. Verkade, 1974

Phase	Composition, wt% S	Pearson symbol	Space group
(γCe)	0	*cF*4	$Fm\bar{3}m$
CeS	18.6	*cF*8	$Fm\bar{3}m$
Ce_3S_4	23.3	...	...
Ce_5S_7	24.2	*tI*92	$I4_1/acd$
βCe_2S_3	26	*cI*28	$I\bar{4}3d$
αCe_2S_3	26	*oP*20	*Pnma*
CeS_2	31.4	*tP*24	*P*4/*nmm*

Ce-Si

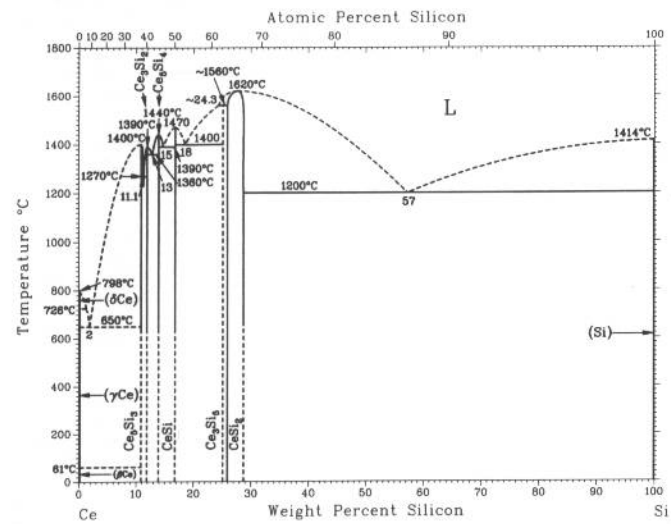

A. Munitz, A.B. Gokhale, and G.J. Abbaschian, 1989

Phase	Composition, wt% Si	Pearson symbol	Space group
δCe(a)	0	*cI*2	$Im\bar{3}m$
γCe(b)	0	*cF*4	$Fm\bar{3}m$
βCe(c)	0	*hP*4	$P6_3/mmc$
αCe(d)	0	*cF*4	$Fm\bar{3}m$
Ce_5Si_3	10.7	*tI*32	*I*4/*mcm*
Ce_3Si_2	12	*tP*10	*P*4/*mbm*
Ce_5Si_4	13.8	(e)	...
CeSi	16.7	*oP*8	*Pnma*
Ce_3Si_5	25.0	(f)	*Imma*
$CeSi_2$	26 to 28.62	*tI*12	$I4_1/amd$
Si	100	*cF*8	$Fd\bar{3}m$
SiII(H.P.)	100	*tI*4	$I4_1/amd$

(a) From 798 to >726 °C. (b) From 726 to >61 °C (139 °C on heating, 16 °C on cooling). (c) From 61 °C to ? (d) <177 °C. (e) Tetragonal. (f) Orthorhombic

Ce-Sn

H. Okamoto, 1990

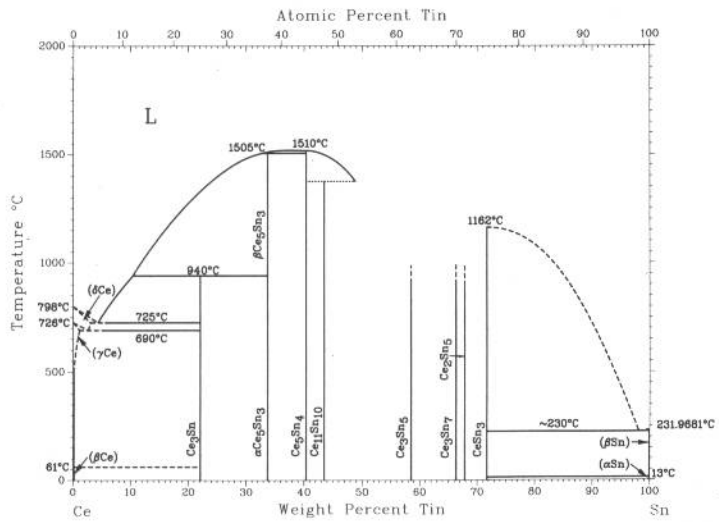

Phase	Composition, wt% Sn	Pearson symbol	Space group
(δCe)	0 to ?	*cI*2	$Im\bar{3}m$
(γCe)	0 to ?	*cF*4	$Fm\bar{3}m$
(βCe)	0	*hP*4	$P6_3/mmc$
(αCe)	0	*cF*4	$Fm\bar{3}m$
Ce_3Sn	22	*cP*4	$Pm\bar{3}m$
βCe_5Sn_3	33.7	*hP*16	$P6_3/mcm$
αCe_5Sn_3	33.7	*tI*32	$I4/mcm$
Ce_5Sn_4	40.4	*oP*36	*Pnma*
$Ce_{11}Sn_{10}$	43.5	*tI*84	$I4/mmm$
Ce_3Sn_5	58.5	*oC*32	*Cmcm*
Ce_3Sn_7	66	*o***	...
Ce_2Sn_5	67.9	*o***	...
$CeSn_3$	72	*cP*4	$Pm\bar{3}m$
(βSn)	100	*tI*4	$I4_1/amd$
(αSn)	100	*cF*8	$Fm\bar{3}m$

Ce-Te

H. Okamoto, 1990

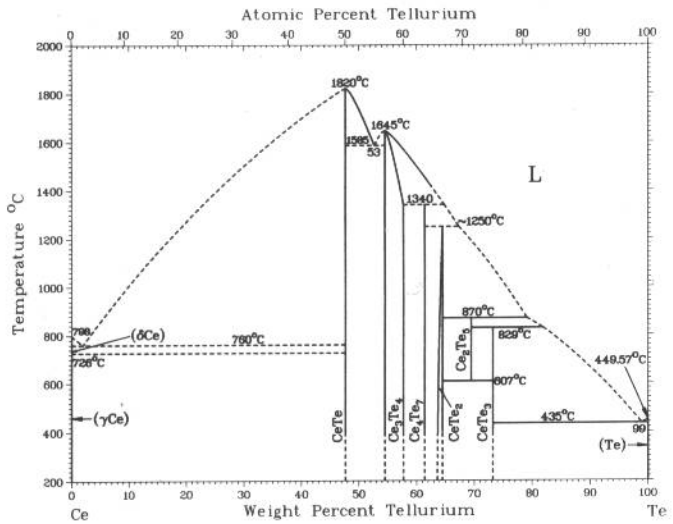

Phase	Composition, wt% Te	Pearson symbol	Space group
(δCe)	0	*cI*2	$Im\bar{3}m$
(γCe)	0	*cF*4	$Fm\bar{3}m$
(βCe)	0	*hP*4	$P6_3/mmc$
CeTe	47.7	*cF*8	$Fm\bar{3}m$
Ce_3Te_4	54.8 to 58	*cI*28	$I\bar{4}3d$
Ce_4Te_7	61.1	*tP**	...
$CeTe_2$	64.6	*tP*6	$P4/nmm$
Ce_2Te_5	69.5	*oC*28	*Cmcm*
$CeTe_3$	73	*oC*16	*Cmcm*
(Te)	100	*hP*3	$P3_121$

Ce-Ti

J.L. Murray, 1987

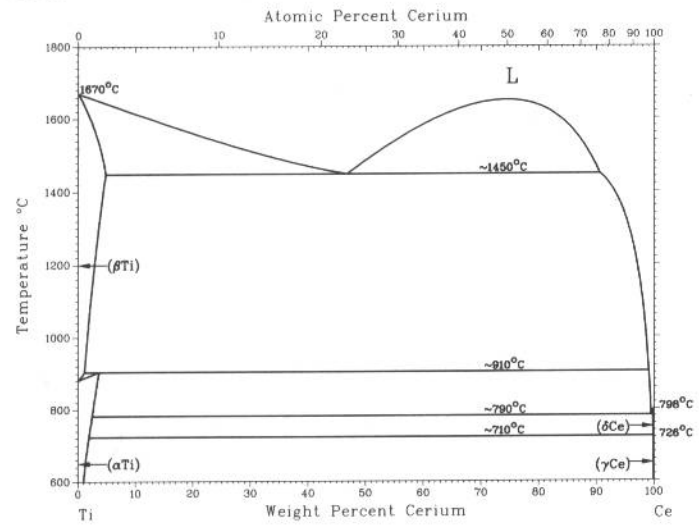

Phase	Composition, wt% Ce	Pearson symbol	Space group
(αTi)	0 to 3.4	*hP*2	$P6_3/mmc$
(βTi)	0 to 4.8	*cI*2	$Im\bar{3}m$
(δCe)	99.9 to 100	*cI*2	$Im\bar{3}m$
(γCe)	100	*cF*4	$Fm\bar{3}m$
(βCe)	100	*hP*4	$P6_3/mmc$

Ce-Tl

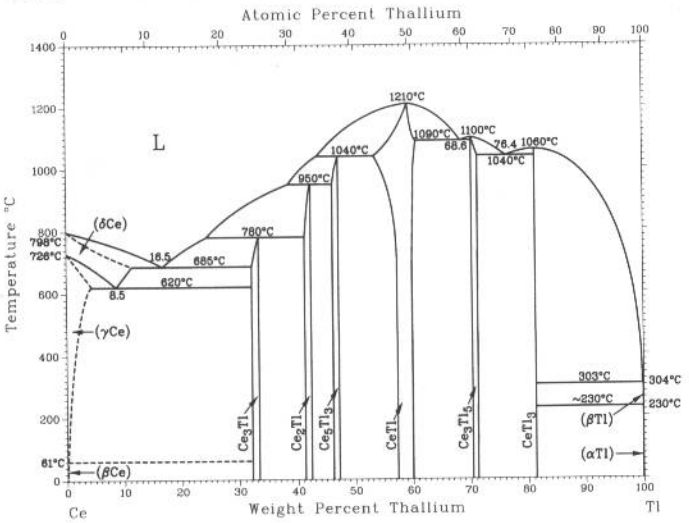

S. Delfino, A. Saccone, A. Palenzona, and R. Ferro, unpublished

Phase	Composition, wt% Tl	Pearson symbol	Space group
(αCe)	0	*cF*4	$Fm\bar{3}m$
(βCe)	0	*hP*4	$P6_3/mmc$
(γCe)	0 to 4	*cF*4	$Fm\bar{3}m$
(δCe)	0 to 13	*cI*2	$Im\bar{3}m$
Ce_3Tl(a)	~32.1 to ~33.3	*cP*4	$Pm\bar{3}m$
	~33	*cF*4	$Fm\bar{3}m$
Ce_2Tl	~42	...	...
Ce_5Tl_3	~46 to ~47	*tI*32	*I*4/*mcm*
CeTl(b)	~53 to ~60	*cP*2	$Pm\bar{3}m$
		(or *cI*2)	$Im\bar{3}m$
CeTl(c)	~53 to ~60	*tP*2	*P*4/*mmm*
Ce_3Tl_5	~70 to ~71	*oC*32	*Cmcm*
$CeTl_3$	81	*cP*4	$Pm\bar{3}m$
(βTl)	100	*cI*2	$Im\bar{3}m$
(αTl)	100	*hP*2	$P6_3/mmc$

(a) A *cP*4-*cF*4 order-disorder transformation in this phase has been suggested. (b) Cubic structure presumed to be room- and high-temperature phases. (c) Tetragonal structure presumed to be low-temperature phase

Ce-Zn

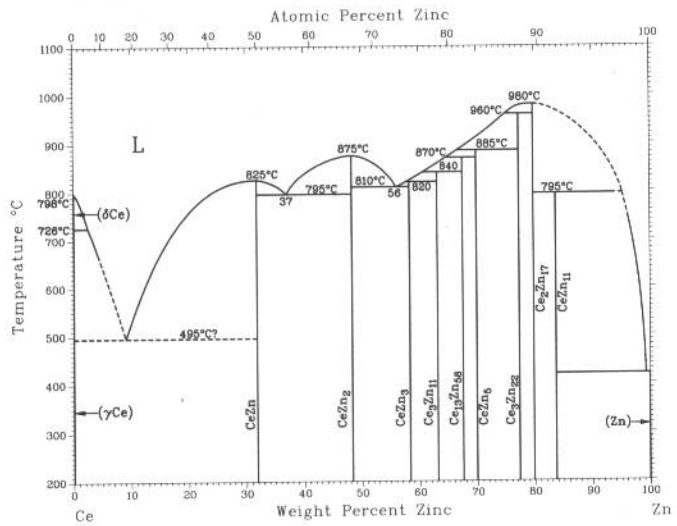

H. Okamoto, 1990

Phase	Composition, wt% Zn	Pearson symbol	Space group
(δCe)	0	*cI*2	$Im\bar{3}m$
(γCe)	0	*cF*4	$Fm\bar{3}m$
(βCe)	0	*hP*4	$P6_3/mmc$
(αCe)	0	*cF*4	$Fm\bar{3}m$
CeZn	31.8	*cP*2	$Pm\bar{3}m$
$CeZn_2$	48.3	*oI*12	*Imma*
$CeZn_3$	58	*oC*16	*Cmcm*
Ce_3Zn_{11}	63.2	*oI*28	*Immm*
$Ce_{13}Zn_{58}$	67.6	*hP*142	$P6_3mc$
$CeZn_5$	70.0	*hP*6	*P*6/*mmm*
Ce_3Zn_{22}	77	*tI*100	$I4_1/amd$
Ce_2Zn_{17}	79.9	*hR*19	$R\bar{3}m$
$CeZn_{11}$	83.8	*tI*48	$I4_1/amd$
(Zn)	100	*hP*2	$P6_3/mmc$

Cl-Cs

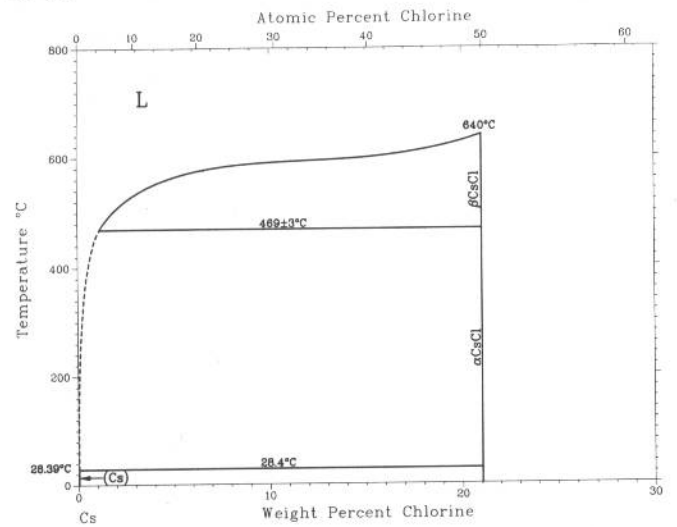

H. Okamoto, 1990

Phase	Composition, wt% Cl	Pearson symbol	Space group
(Cs)	0	*cI*2	$Im\bar{3}m$
βCsCl	21.1	*cF*8	$Fm\bar{3}m$
αCsCl	21.1	*cP*2	$Pm\bar{3}m$
(Cl)	100	*oC*8	*Cmca*

Cl-Ga

H. Okamoto, 1990

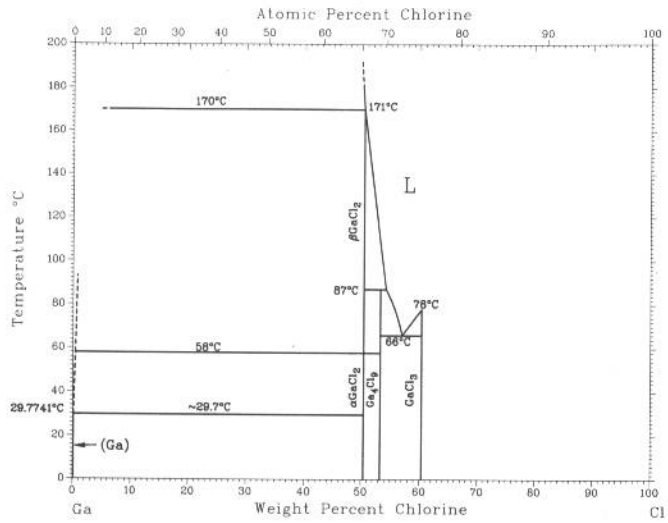

Phase	Composition, wt% Cl	Pearson symbol	Space group
(Ga)	0	*oC*8	*Cmca*
$\beta GaCl_2$	50.5	*tP*24	*Pnma*
$\alpha GaCl_2$	50.5	...	...
Ga_4Cl_9	53.3	...	...
$GaCl_3$	60	*aP*8	$P\bar{1}$
(Cl)	100	*oC*8	*Cmca*

Cl-Hg

H. Okamoto, 1990

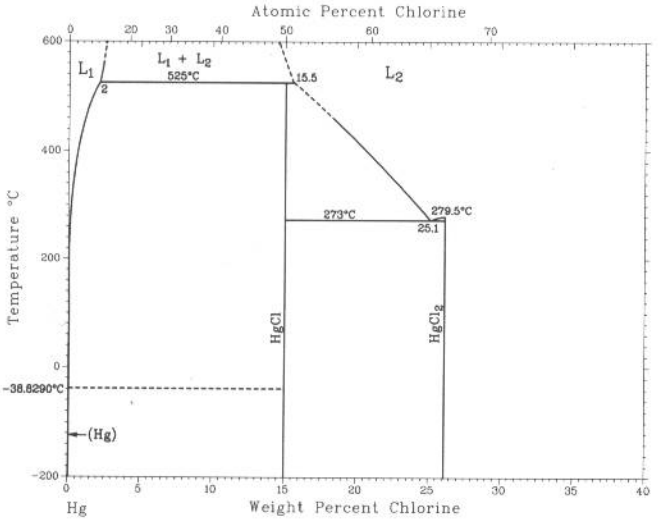

Phase	Composition, wt% Cl	Pearson symbol	Space group
(αHg)	0	*hR*1	$R\bar{3}m$
HgCl	15.0	*tI*8	*I*4/*mmm*
$HgCl_2$	26.1	*oP*12	*Pmnb*
(Cl)	100	*oC*8	*Cmca*

Cl-In

H. Okamoto, 1992

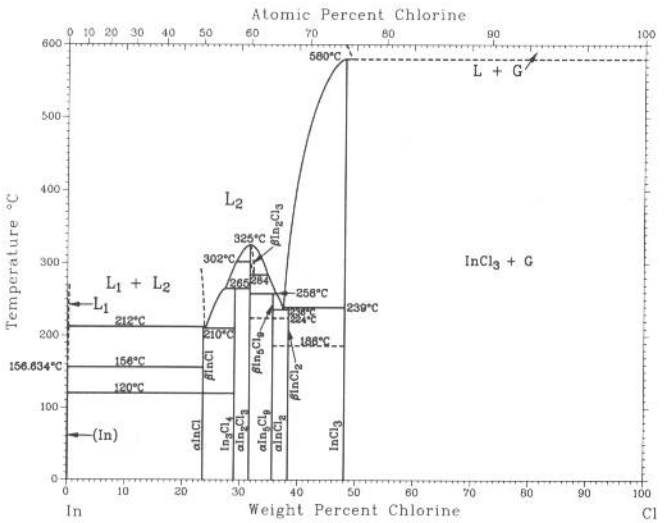

Phase	Composition, wt% Cl	Pearson symbol	Space group
(In)	0	*tI*2	*I*4/*mmm*
βInCl	23.6	*oC*8	*Cmcm*
αInCl	23.6	*cP*64	$P2_13$
In_3Cl_4	29.1	...	...
In_2Cl_3(I)	32	*o**30	...
In_2Cl_3(II)	32	*t**45	...
In_2Cl_3(III)	32	*hP**	...
βIn_5Cl_9(a)	35.7	...	...
αIn_5Cl_9(a)	35.7	...	...
$\beta InCl_2$	38.2	*oP*24	*Pnna*
$\alpha InCl_2$	38.2	*m***	...
$InCl_3$	48	*mC*16	*C*2/*m*
(Cl)	100	*oC*8	*Cmca*

(a) Or In_4Cl_7

Cl-Na

H. Okamoto, 1990

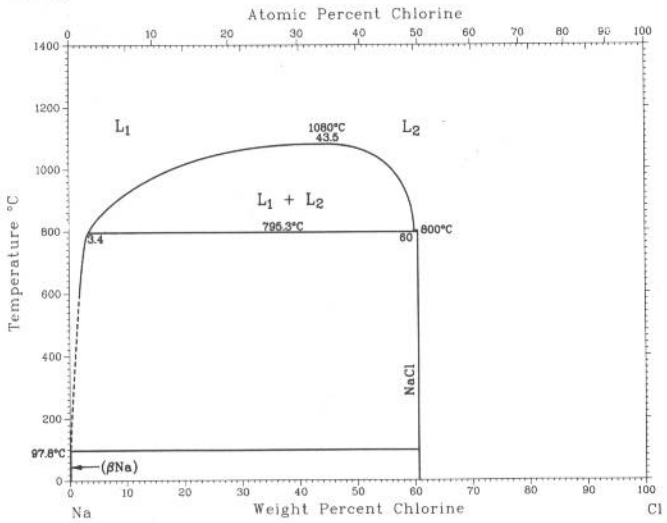

Phase	Composition, wt% Cl	Pearson symbol	Space group
(Na)	0	*cI*2	$Im\bar{3}m$
NaCl	60.7	*cF*8	$Fm\bar{3}m$
(Cl)	100	*oC*8	*Cmca*

Co-Cr

K. Ishida and T. Nishizawa, 1990

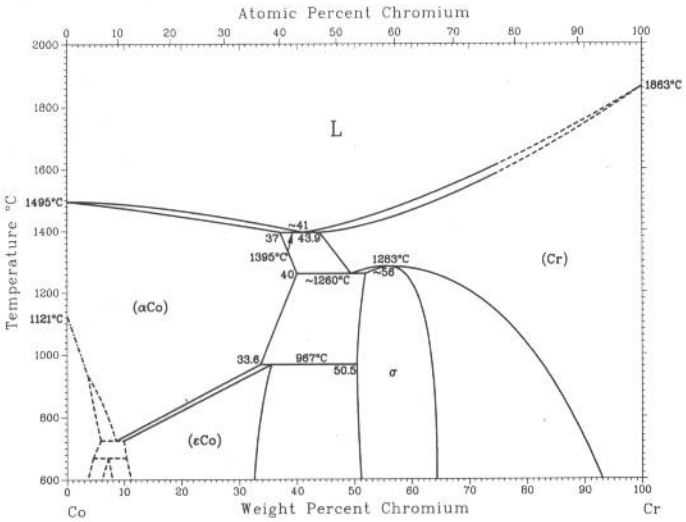

Phase	Composition, wt% Cr	Pearson symbol	Space group
(αCo)	0 to 40	*cF*4	$Fm\bar{3}m$
(εCo)	0 to 36	*hP*2	$P6_3/mmc$
(αCr)	43.9 to 100	*cI*2	$Im\bar{3}m$
σ	50.5 to 63	*tP*30	$P4_2/mnm$
Metastable phases			
(αCr)	~16	*cI*2	$Im\bar{3}m$
(αCo)	40 to 62.9	*cF*4	$Fm\bar{3}m$
(δCr)	54 to 100	*cP*8	$Pm\bar{3}n$
Co_3Cr?	23	*hP*8	$P6_3/mmc$

Co-Cu

T. Nishizawa and K. Ishida, 1984

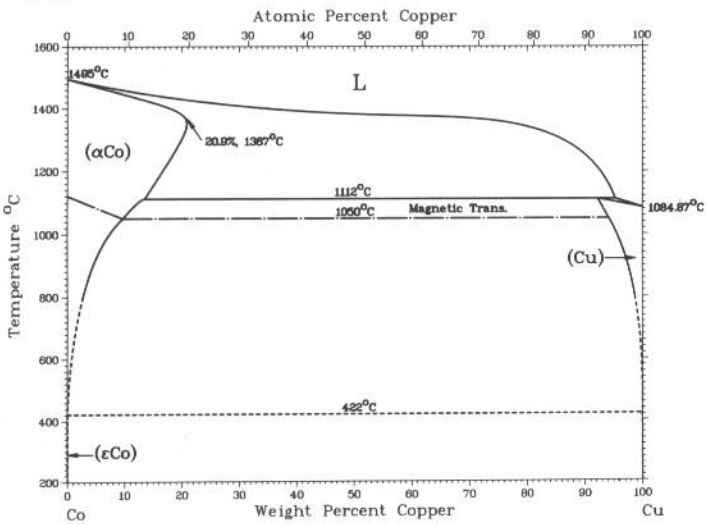

Phase	Composition, wt% Cu	Pearson symbol	Space group
(αCo)	0 to 20.9	*cF*4	$Fm\bar{3}m$
(εCo)	0 to 9(a)	*hP*2	$P6_3/mmc$
(Cu)	93 to 100	*cF*4	$Fm\bar{3}m$
Metastable phase			
ε′	9 to 10	*hR*1	$R\bar{3}m$

(a) The composition of (εCo) is between 0 and 0.3 wt% Cu in equilibrium, but is 0 to 9 wt% Cu in the metastable state, which is obtained by quenching from high temperatures.

Co-Dy

H. Okamoto, 1990

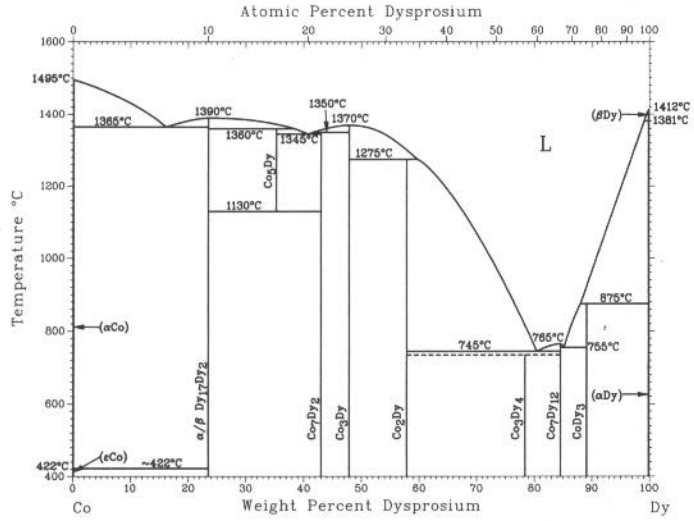

Phase	Composition, wt% Dy	Pearson symbol	Space group
(αCo)	~0	*cF*4	$Fm\bar{3}m$
(εCo)	~0	*hP*2	$P6_3/mmc$
$\beta Co_{17}Dy_2$	24.4	*hP*38	$P6_3/mmc$
$\alpha Co_{17}Dy_2$	24.4	*hR*19	$R\bar{3}m$
Co_5Dy	35.6	*hP*6	$P6/mmm$
Co_7Dy_2	44.0	*hR*18	$R\bar{3}m$
Co_3Dy	48	*hR*12	$R\bar{3}m$
Co_2Dy	57.9	*cF*24	$Fd\bar{3}m$
Co_3Dy_4	78.6	*hP*22	$P6_3/m$
Co_7Dy_{12}	82.6	*mP*38	$P2_1/c$
$CoDy_3$	89	*oP*16	*Pnma*
(βDy)	~100	*cI*2	$Im\bar{3}m$
(αDy)	~100	*hP*2	$P6_3/mmc$

Co-Er

H. Okamoto, 1990

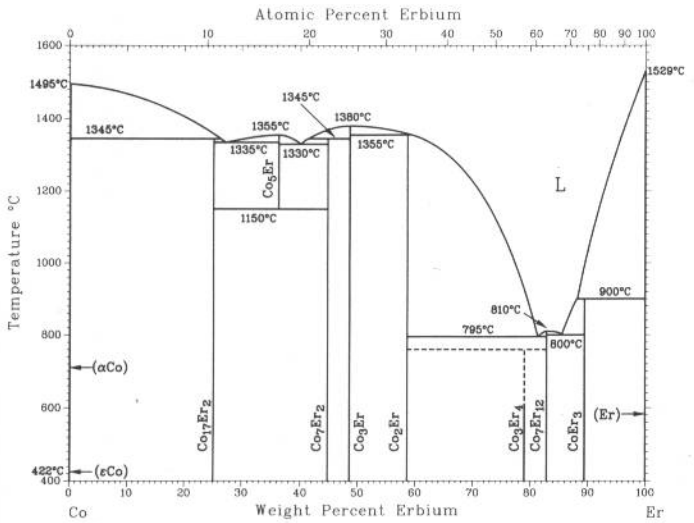

Phase	Composition, wt% Er	Pearson symbol	Space group
(αCo)	~0	*cF*4	$Fm\bar{3}m$
$Co_{17}Er_2$	25.0	*hP*38	$P6_3/mmc$
Co_5Er	36.3	*hP*6	$P6/mmm$
Co_7Er_2	44.7	*hR*18	$R\bar{3}m$
Co_3Er	49	*hR*12	$R\bar{3}m$
Co_2Er	58.6	*cF*24	$Fd\bar{3}m$
Co_3Er_4	79.1	*hP*22	$P6_3/m$
Co_7Er_{12}	83.0	*mP*38	$P2_1/c$
$CoEr_3$	99.5	*oP*16	*Pnma*
(Er)	~100	*hP*2	$P6_3/mmc$

Co-Fe

T. Nishizawa and K. Ishida, 1984

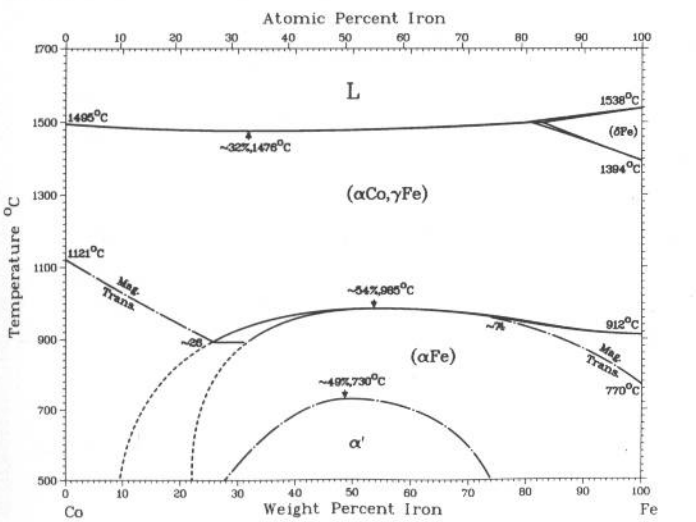

Phase	Composition, wt% Fe	Pearson symbol	Space group
(αCo, γFe)	0 to 100	*cF*4	$Fm\bar{3}m$
α′	~28 to ~74	*cP*2	$Pm\bar{3}m$
(αFe)	~22 to 100	*cI*2	$Im\bar{3}m$
(δFe)	82 to 100	*cI*2	$Im\bar{3}m$
Metastable phase			
η	0.5 to 5.7	*hP*4	$P6_3/mmc$

Co-Ga

H. Okamoto, 1990

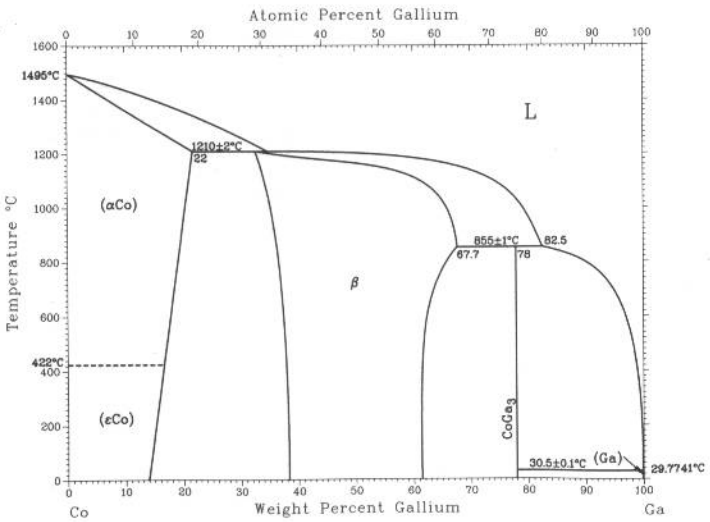

Phase	Composition, wt% Ga	Pearson symbol	Space group
(αCo)	0 to 22	*cF*4	$Fm\bar{3}m$
(εCo)	0 to 17	*hP*2	$P6_3/mmc$
β	33 to 67.7	*cP*2	$Pm\bar{3}m$
$CoGa_3$	78	*tP*16	$P\bar{4}n2$
(Ga)	100	*oC*8	*Cmca*

Co-Gd

H. Okamoto, 1990

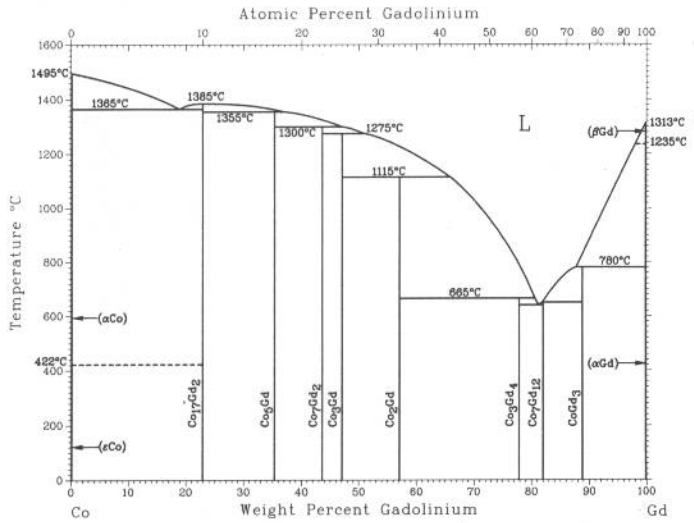

Phase	Composition, wt% Gd	Pearson symbol	Space group
(αCo)	~0	*cF*4	$Fm\bar{3}m$
(εCo)	~0	*hP*2	$P6_3/mmc$
$Co_{17}Gd_2$	~23.8	*hP*38	$P6_3/mmc$
		*hR*19	$R\bar{3}m$
Co_5Gd	~34.9	*hP*6	*P6/mmm*
Co_7Gd_2	~43.2	*hR*18	$R\bar{3}m$
		*hP*36	$P6_3/mmc$
Co_3Gd	47	*hR*12	$R\bar{3}m$
Co_2Gd	57.1	*cF*24	$Fd\bar{3}m$
Co_3Gd_4	78.0	*hP*22	$P6_3/m$
Co_7Gd_{12}	~82.1	*mP*38	$P2_1/c$
$CoGd_3$	89	*oP*16	*Pnma*
(βGd)	~100	*cI*2	$Im\bar{3}m$
(αGd)	100	*hP*2	$P6_3/mmc$
Other reported phases			
Co_8Gd	~25.0	*hP*8	*P6/mmm*
CoGd	72.7	*oP*8	*Pnma*
Co_3Gd_7	86	*o**	...
$CoGd_9$	96	*o**	...

Co-Ge

K. Ishida and T. Nishizawa, 1991

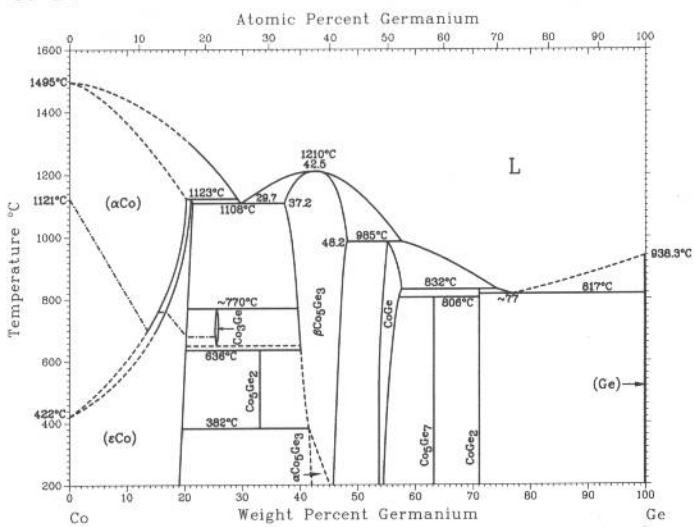

Phase	Composition, wt% Ge	Pearson symbol	Space group
(αCo)	0 to 20.7	*cF*4	$Fm\bar{3}m$
(εCo)	0 to 21	*hP*2	$P6_3/mmc$
Co_3Ge	25.2 to 26	*cP*8	$Pm\bar{3}n$?
Co_5Ge_2	33.0	(a)	...
αCo_5Ge_3	~41.5 to ~45	(b)?	*Pbnm*?
βCo_5Ge_3	37.2 to 48.2	*hP*6	$P6_3/mmc$
CoGe	53.7 to 57.7	*mC*16	*C*2/*m*
		*cP*8	$P2_13$
Co_5Ge_7	63.3	*tI*24	*I*4*mm*
$CoGe_2$	71.2	*oC*24	*Aba*2
(Ge)	~100	*cF*8	$Fd\bar{3}m$

Co-Hf

K. Ishida and T. Nishizawa, 1991

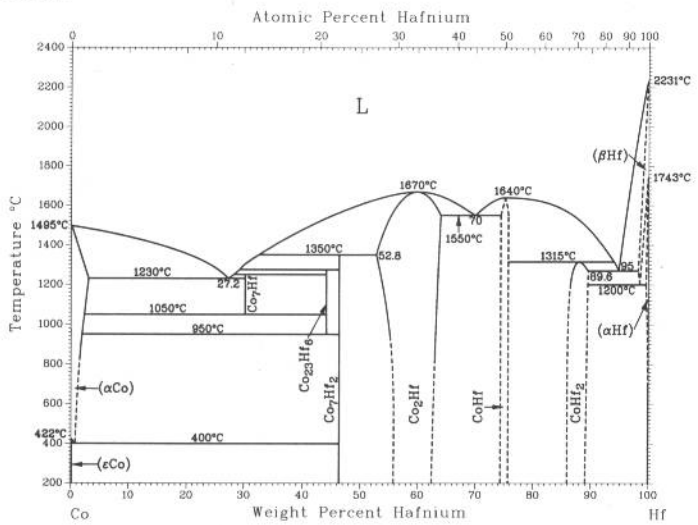

Phase	Composition, wt% Hf	Pearson symbol	Space group
(αCo)	0 to ~6	*cF*4	$Fm\bar{3}m$
(εCo)	0 to ~1.5	*hP*2	$P6_3/mmc$
Co_7Hf	30.2	*tP*32	...
$Co_{23}Hf_6$	44.2	*cF*116	$Fm\bar{3}m$
Co_7Hf_2	46.4	*o***	...
Co_2Hf	52.8 to ~63	*cF*24	$Fd\bar{3}m$
CoHf	~74 to ~76	*cP*2	$Pm\bar{3}m$
$CoHf_2$	~86 to 89.6	*cF*112	$Fd3m$
(βHf)	~98 to 100	*cI*2	$Im\bar{3}m$
(αHf)	~99 to 100	*hP*2	$P6_3/mmc$

Co-Ho

H. Okamoto, 1990

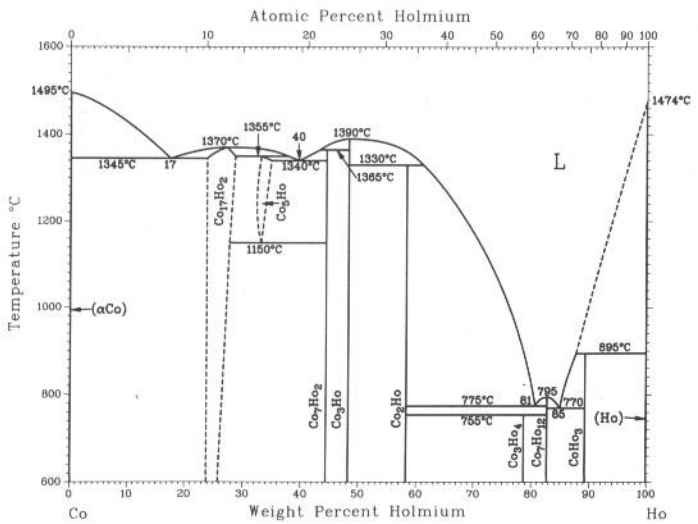

Phase	Composition, wt% Ho	Pearson symbol	Space group
(αCo)	~0	*cF*4	$Fm\bar{3}m$
(εCo)	~0	*hP*2	$P6_3/mmc$
$Co_{17}Ho_2$	24.7	*hR*19	$R\bar{3}m$
		*hP*38	$P6_3/mmc$
		*hP*52	$P6_3/mmc$
Co_5Ho	35.9	*hP*6	$P6/mmm$
Co_7Ho_2	44.4	*hR*18	$R\bar{3}m$
Co_3Ho	48	*hR*12	$R\bar{3}m$
Co_2Ho	58.3	*cF*24	$Fd\bar{3}m$
Co_3Ho_4	78.8	*hP*22	$P6_3/m$
Co_7Ho_{12}	82.8	*mP*38	$P2_1/c$
$CoHo_3$	89	*oP*16	*Pnma*
(Ho)	~100	*hP*2	$P6_3/mmc$

Co-Mn

K. Ishida and T. Nishizawa, 1990

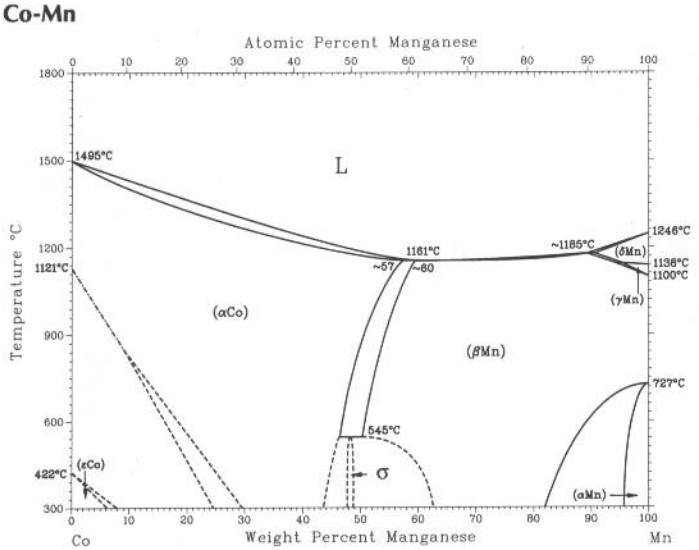

Phase	Composition, wt% Mn	Pearson symbol	Space group
(εCo)	0 to ~19	*hP*2	$P6_3/mmc$
(αCo)	0 to ~57	*cF*4	$Fm\bar{3}m$
σ	~48	*tP*30	$P4_2/mnm$
(αMn)	97 to 100	*cI*58	$I\bar{4}3m$
(βMn)	49 to 100	*cP*20	$P4_132$
(γMn)	95 to 100	*cF*4	$Fm\bar{3}m$
(δMn)	90 to 100	*cI*2	$Im\bar{3}m$
(γ'Mn)(a)	90 to 100	*tI*2	$I4/mmm$

(a) Splat quenched from the liquid state or rapid quenched from the high-temperature solid field

Co-Mo

From [Molybdenum]

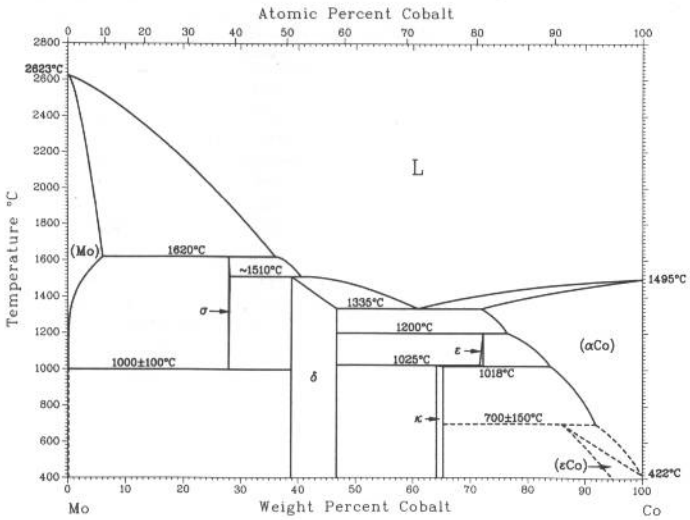

Phase	Composition, wt% Co	Pearson symbol	Space group
(Mo)	0 to ~6	*cI*2	$Im\bar{3}m$
σ	~27.8 to 28	*tP*30	$P4_2/mnm$
ε	~38.8 to ~46.7	*hR*13	$R\bar{3}m$
κ	~64.2 to ~65.4	*hP*8	$P6_3/mmc$
cph	~72	*hP*2	$P6_3/mmc$
(αCo)	~72 to 100	*cF*4	$Fm\bar{3}m$
(εCo)	~86 to 100	*hP*2	$P6_3/mmc$

Co-Nb

J.K. Pargeter and W. Hume-Rothery, 1967

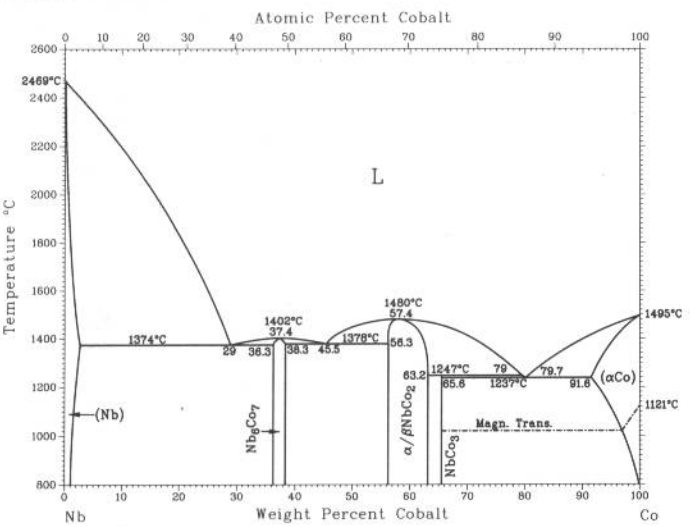

Phase	Composition, wt% Co	Pearson symbol	Space group
(Nb)	0 to ~3	*cI*2	$Im\bar{3}m$
Nb_6Co_7	36.3 to 38.3	*hR*13	$R\bar{3}m$
$\beta NbCo_2$(a)	56.3 to ?	*hP*12	$P6_3/mmc$
$\alpha NbCo_2$	56.3 to 63.2	*cF*24	$Fd\bar{3}m$
$NbCo_3$	65.3	*hP*24	$P6_3/mmc$
(αCo)	91.6 to 100	*cF*4	$Fm\bar{3}m$

(a) $\beta NbCo_2$ is stable above ~1200 °C.

Co-Nd

A.E. Ray, 1974

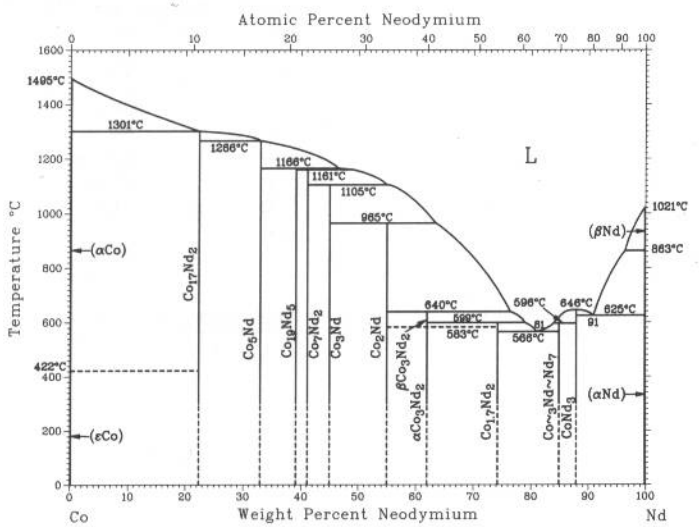

Phase	Composition, wt% Nd	Pearson symbol	Space group
(αCo)	~0	*cF*4	$Fm\bar{3}m$
(εCo)	~0	*hP*2	$P6_3/mmc$
$Co_{17}Nd_2$	~22.3	*hR*19	$R\bar{3}m$
Co_5Nd	~32.9	*hP*6	*P6/mmm*
$Co_{19}Nd_5$	~39.1	*hR*24	$R\bar{3}m$
βCo_7Nd_2	~41.1	*hR*18	$R\bar{3}m$
αCo_7Nd_2	~41.1	*hP*36	$P6_3/mmc$
Co_3Nd	45	*hR*12	$R\bar{3}m$
Co_2Nd	55.0	*cF*24	$Fd\bar{3}m$
Co_3Nd_2	62	*o***	...
$Co_{1.7}Nd_2$	~74.3	*h***	...
$Co_{\sim 3}Nd_{\sim 7}$	~85	*hP*20	$P6_3mc$
$CoNd_3$	88	*oP*16	*Pnma*
(βNd)	~100	*cI*2	$Im\bar{3}m$
(αNd)	~100	*hP*4	$P6_3/mmc$
Other reported phases			
Co_3Nd_4	~76.5	*hP*7	$P\bar{6}$
$Co_{11}Nd_{24}$	~84.2	*hP*70	$P6_3mc$
Co_2Nd_5	~85.9	*mC*28	*C*2/*c*

Co-Ni

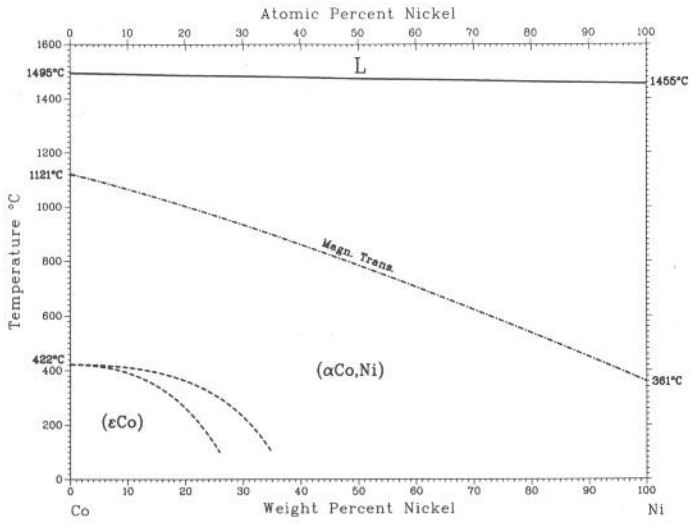

T. Nishizawa and K. Ishida, 1991

Phase	Composition, wt % Ni	Pearson symbol	Space group
(αCo,Ni)	0 to 100	*cF*4	$Fm\bar{3}m$
(εCo)	0 to 35	*hP*2	$P6_3/mmc$

Co-P

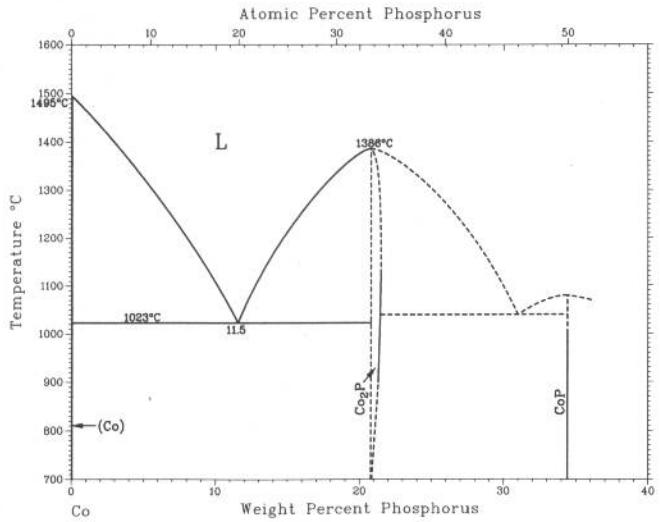

K. Ishida and T. Nishizawa, 1990

Phase	Composition, wt % P	Pearson symbol	Space group
(αCo)	~0	*cF*4	$Fm\bar{3}m$
(εCo)	~0	*hP*2	$P6_3/mmc$
Co_2P	~20.6 to 21.3	*oP*12	*Pnma*
CoP	34.5	*oP*8	*Pnma*
CoP_2	51.3	(a)	...
CoP_3	61	*cI*32	$Im\bar{3}m$
Red (P)	100	(b)	...
White (P)	100	(b)	...
Black (P)	100	*oC*8	*Cmca*

(a) Monoclinic. (b) Cubic

Co-Pd

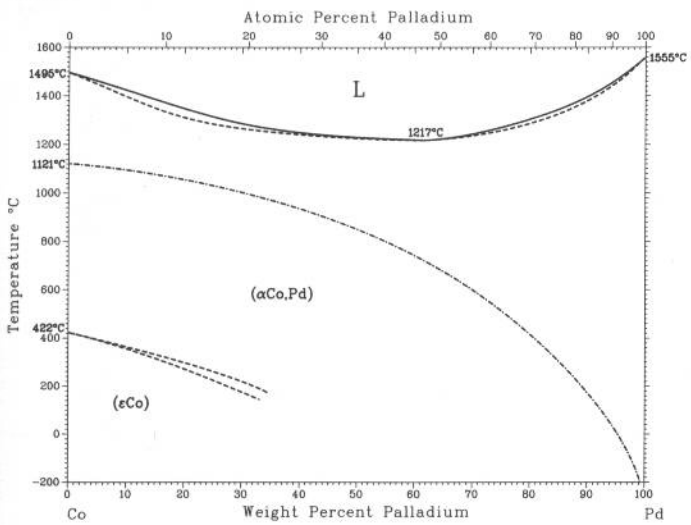

K. Ishida and T. Nishizawa, 1991

Phase	Composition, wt % Pd	Pearson symbol	Space group
(αCo,Pd)	0 to 100	*cF*4	$Fm\bar{3}m$
(εCo)	0 to ~31	*hR*2	$P6_3/mmc$
Metastable phases			
α″	~63 to ~66	*tP*4	*P*4/*mmm*
α′	73 to 94	*cP*4	$Pm\bar{3}m$

Co-Pr

A.E. Ray, 1974

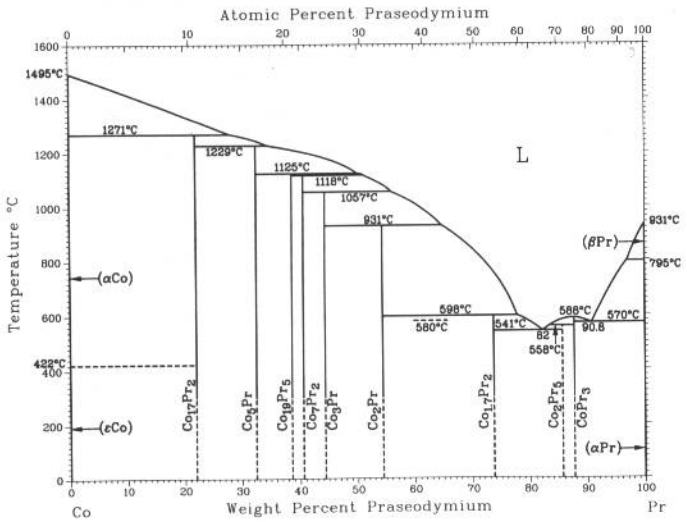

Phase	Composition, wt% Pr	Pearson symbol	Space group
(αCo)	~0	*cF*4	$Fm\bar{3}m$
(εCo)	~0	*hP*2	$P6_3/mmc$
$Co_{17}Pr_2$	21.9	*hR*19	$R\bar{3}m$
Co_5Pr	32.4	*hP*6	*P6/mmm*
$Co_{19}Pr_5$	38.6	*hR*24	$R\bar{3}m$
βCo_7Pr_2	40.6	*hR*18	$R\bar{3}m$
αCo_7Pr_2	40.6	*hP*36	$P6_3/mmc$
Co_3Pr	44	*hR*12	$R\bar{3}m$
Co_2Pr	54.4	*cF*24	$Fd\bar{3}m$
$Co_{1.7}Pr_2$	~73.8	*hP**	...
Co_2Pr_5	~85.7	*mC*28	*C2/c*
$CoPr_3$	88	*oP*16	*Pnma*
(βPr)	~100	*cI*2	$Im\bar{3}m$
(αPr)	~100	*hP*4	$P6_3/mmc$

Co-Pt

H. Okamoto, 1990

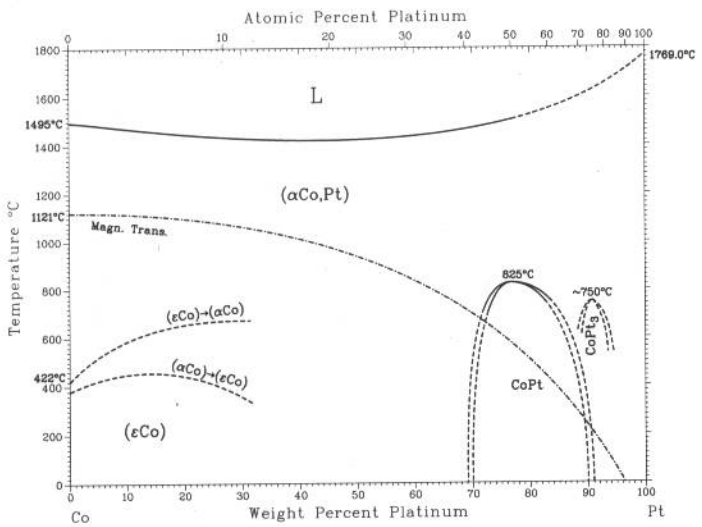

Phase	Composition, wt% Pt	Pearson symbol	Space group
(αCo, Pt)	0 to 100	*cF*4	$Fm\bar{3}m$
(εCo)	0 to ?	*hP*2	$P6_3/mmc$
CoPt	~76.8	*tP*4	*P4/mmm*
$CoPt_3$	~91	*cP*4	$Pm\bar{3}m$

Co-Pu

D.M. Poole, M.G. Bale, P.G. Mardon, J.A.C. Marples, and J.L. Nichols, 1961

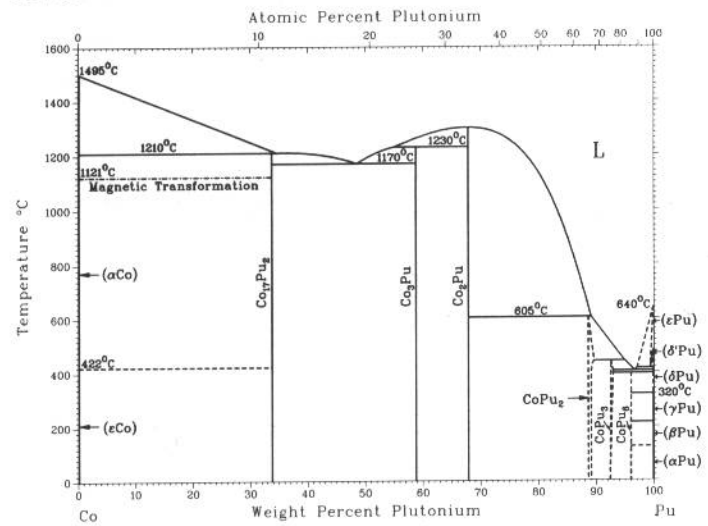

Phase	Composition, wt% Pu	Pearson symbol	Space group
(αCo)	~0	*cF*4	$Fm\bar{3}m$
(εCo)	~0	*hP*2	$P6_3/mmc$
$Co_{17}Pu_2$	34	*hP*38	$P6_3/mmc$
Co_3Pu	~58.9	*hR*12	$R\bar{3}m$
Co_2Pu	~67.4	*cF*24	$Fd\bar{3}m$
$CuPu_2$	~88.7 to 90	*hP*9	$P6_3/mmc$
$CoPu_3$	~92.6 to 93	*oC*16	*Cmcm*
$CoPu_6$	96.1	*tI*28	*I4/mcm*
(εPu)	~99.5 to 100	*cI*2	$Im\bar{3}m$
(δ'Pu)	~100	*tI*2	*I4/mmm*
(δPu)	~100	*cF*4	$Fm\bar{3}m$
(γPu)	~100	*oF*8	*Fddd*
(βPu)	~100	*mC*34	*C2/m*
(αPu)	~100	*mP*16	$P2_1/m$

Co-Re

H. Okamoto, 1990

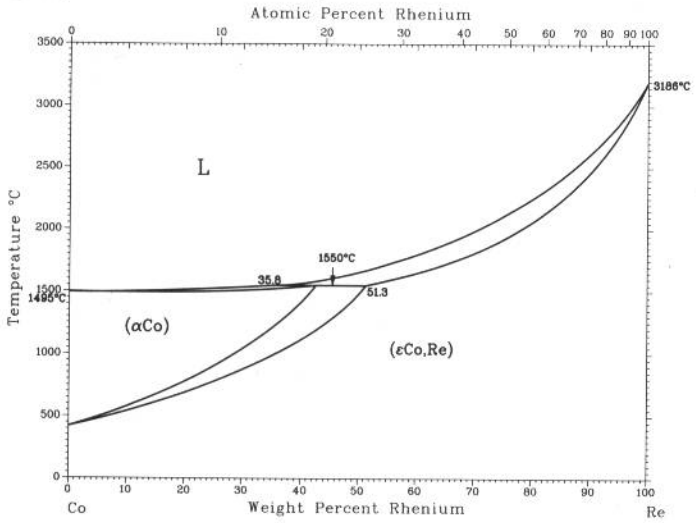

Phase	Composition, wt% Re	Pearson symbol	Space group
(αCo)	0 to 43	*cF*4	$Fm\bar{3}m$
(εCo,Re)	0 to 100	*hP*2	$P6_3/mmc$

Co-S

K. Friedrich, 1908

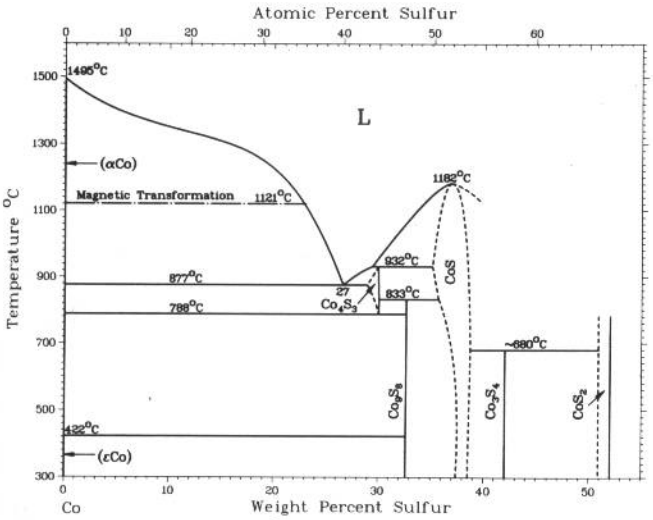

Phase	Composition, wt% S	Pearson symbol	Space group
(αCo)	0	*cF*4	$Fm\bar{3}m$
(εCo)	0	*hP*2	$P6_3/mmc$
Co_4S_3	~29.0	...	...
Co_9S_8	32.6	*cF*68	$Fm\bar{3}m$
CoS	35.2 to 40	*hP*4	$P6_3/mmc$
Co_3S_4	42.0	*cF*56	$Fd\bar{3}m$
CoS_2	52.1	*cP*12	$Pa\bar{3}$
(S)	100	*oF*128	*Fddd*

Co-Sb

H. Okamoto, 1991

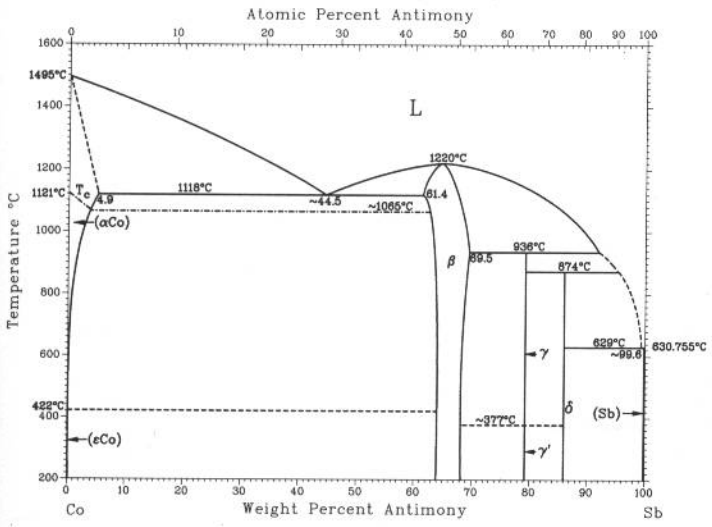

Phase	Composition, wt% Sb	Pearson symbol	Space group
(αCo)	0 to ~5.0	*cF*4	$Fm\bar{3}m$
(εCo)	0	*hP*2	$P6_3/mmc$
β	61.4 to ~69	*hP*4	$P6_3/mmc$
γ	79	*oP*6	*Pnnm*
γ′	79	*mP*12	$P2_1/c$
δ	~86	*cI*32	$Im\bar{3}$
(Sb)	~100	*hR*2	$R\bar{3}m$

Co-Se

H. Okamoto, 1990

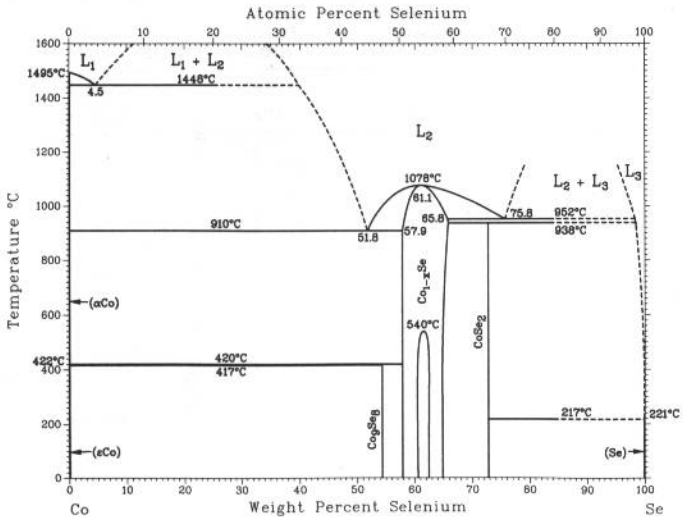

Phase	Composition, wt% Se	Pearson symbol	Space group
(αCo)	0	*cF*4	$Fm\bar{3}m$
(εCo)	0	*hP*2	$P6_3/mmc$
Co_9Se_8	54.4	*cF*68	$Fm\bar{3}m$
$Co_{1-x}Se$	57.9 to 65.8	*m***	...
$CoSe_2$	72.9	*cP*12	$Pa\bar{3}$
(Se)	100	*oC*8	*Cmca*

Co-Si

K. Ishida and T. Nishizawa, 1991

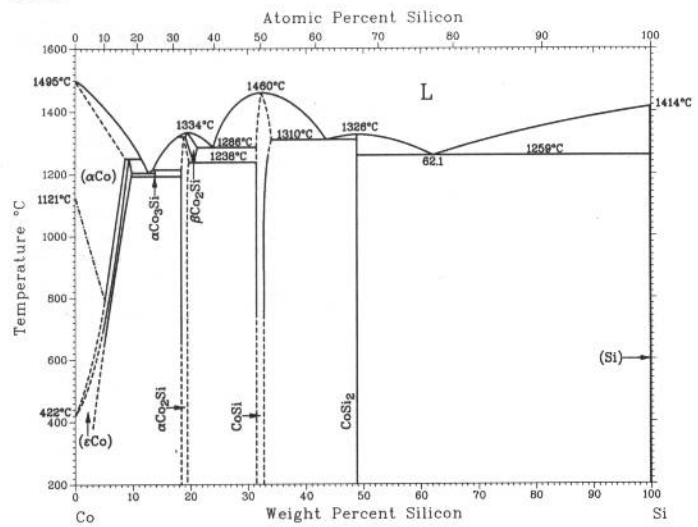

Phase	Composition, wt% Si	Pearson symbol	Space group
(αCo)	0 to 8.5	*cF*4	$Fm\bar{3}m$
(εCo)	0 to 9.7	*hP*2	$P6_3/mmc$
Co_3Si	14	*t***	...
αCo_2Si	~18 to ~20	*oP*12	*Pnma*
βCo_2Si	~18 to 21.0	...	...
CoSi	31 to ~34	*cP*8	$P2_13$
$CoSi_2$	48.8	*cF*12	$Fm\bar{3}m$
(Si)	~100	*cF*8	$Fd\bar{3}m$
Metastable phases			
Co_3Si	~4 to 14	*hP*8	$P6_3/mmc$
Co_4Si	~11	...	...
γCo_2Si(a)	~14	*o***	...
Co_2Si_3	42	*tP*20	$P\bar{4}c2$

(a) Formed by massive transformation

Co-Sm

From [Moffatt]

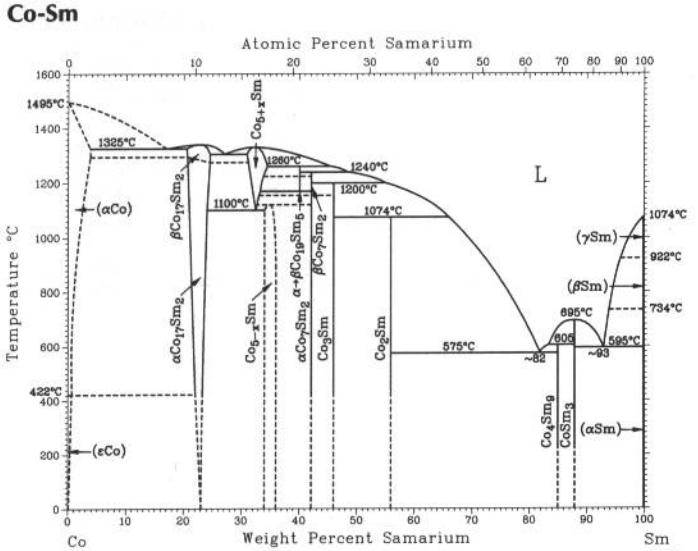

Phase	Composition, wt% Sm	Pearson symbol	Space group
(αCo)	0 to ~3.7	*cF*4	$Fm\bar{3}m$
(εCo)	~0	*hP*2	$P6_3/mmc$
$\beta Co_{17}Sm_2$	~23.0	*hP*38	$P6_3/mmc$
$\alpha Co_{17}Sm_2$	~23.0	*hR*19	$R\bar{3}m$
		*hP*8	$P6/mmm$
$Co_{5+x}Sm$	~33 to 34	...	...
$Co_{5-x}Sm$	~34 to 35	...	...
$Co_{19}Sm_5$	~40.1	*hR*24	$R\bar{3}m$
		*hP*48	$P6_3/mmc$
αCo_7Sm_2	~42.1	*hR*18	$R\bar{3}m$
βCo_7Sm_2	~42.1	*hP*36	$P6_3/mmc$
Co_3Sm	46	*hR*12	$R\bar{3}m$
Co_2Sm	56.0	*hR*4	$R\bar{3}m$
		*cF*24	$Fd\bar{3}m$
Co_4Sm_9	~85.1	*o***	...
$CoSm_3$	88	*oP*16	*Pnma*
(γSm)	~100	*cI*2	$Im\bar{3}m$
(βSm)	~100	*hP*2	$P6_3/mmc$
(αSm)	~100	*hR*3	$R\bar{3}m$
Other reported phases			
Co_5Sm	~33.8	*hP*6	$P6/mmm$
		*hP**	...
Co_2Sm_5	~86.4	*mC*28	*C*2/*c*

Co-Sn

K. Ishida and T. Nishizawa, 1991

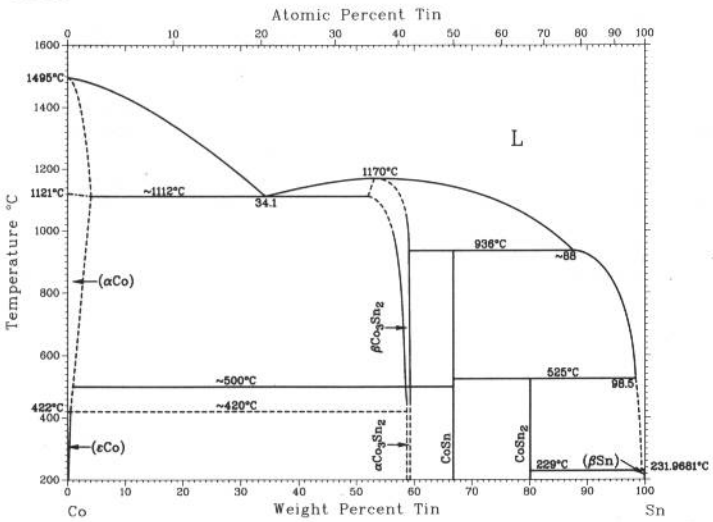

Phase	Composition, wt% Sn	Pearson symbol	Space group
(αCo)	0 to ~4	*cF*4	$Fm\bar{3}m$
(εCo)	0 to ~0.4	*hP*2	$P6_3/mmc$
βCo_3Sn_2	~52 to ~59	*hP*4	$P6_3/mmc$
αCo_3Sn_2	~58 to ~59	*oP*20	*Pnma*
CoSn	66.8	*hP*6	*P6/mmm*
$CoSn_2$	80.1	*tI*12	*I*4/*m*
(βSn)	~100	*tI*4	$I4_1/amd$
Metastable phases			
(ε′Co)	3.0 to 15.1	…	$R\bar{3}m$
Co_3Sn	40.2	*cI*2	$Im\bar{3}m$
		*cP*2	$Pm\bar{3}m$

Co-Ta

H. Okamoto, 1991

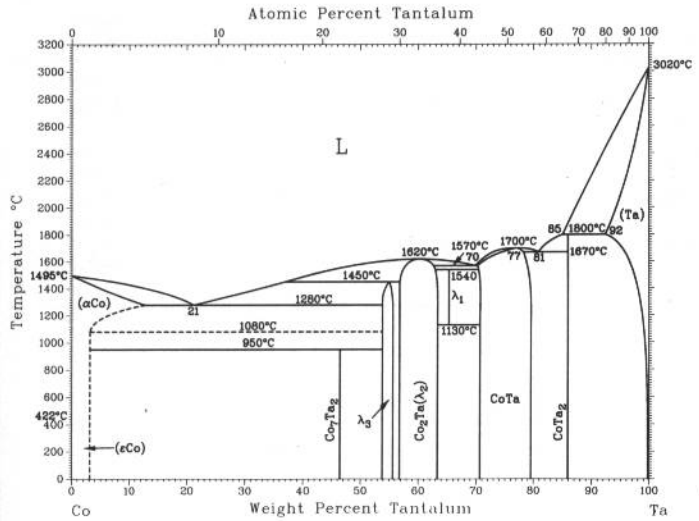

Phase	Composition, wt% Ta	Pearson symbol	Space group
(αCo)	0 to 11	*cF*4	$Fm\bar{3}m$
Co_7Ta_2	46.7	…	…
λ_3	53.8 to 56	*hP*24	$P6_3/mmc$
λ_2	56.2 to 63	*cF*24	$Fd\bar{3}m$
λ_1	~64	*hP*12	$P6_3/mmc$
Co_6Ta_7	71 to 80	*hR*13	$R\bar{3}m$
$CoTa_2$	86.0	*tI*12	*I*4/*mcm*
(Ta)	92 to 100	*cI*2	$Im\bar{3}m$

Co-Tb

H. Okamoto, 1990

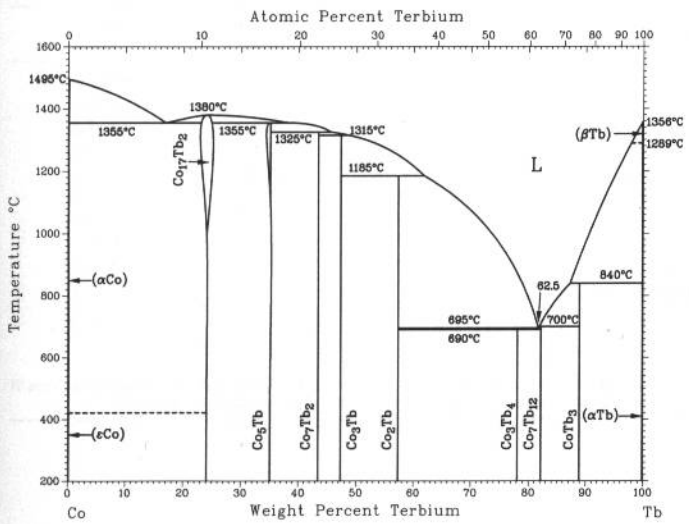

Phase	Composition, wt% Tb	Pearson symbol	Space group
(αCo)	0	*cF*4	$Fm\bar{3}m$
(εCo)	0	*hP*2	$P6_3/mmc$
$\beta Co_{17}Tb_2$	24.0	*hP*38	$P6_3/mmc$
$\alpha Co_{17}Tb_2$	24.0	*hR*19	$R\bar{3}m$
Co_5Tb	35.1	*hP*6	*P6/mmm*
Co_7Tb_2	43.5	*hR*18	$R\bar{3}m$
Co_3Tb	47	*hR*12	$R\bar{3}m$
Co_2Tb	57.4	*cF*24	*Fd*3*m*
Co_3Tb_4	78.2	*hP*22	$P6_3/m$
Co_7Tb_{12}	82.2	*mP*38	$P2_1/c$
$CoTb_3$	89	*oP*16	*Pnma*
(Tb)	100	*hP*2	$P6_3/mmc$

Co-Te

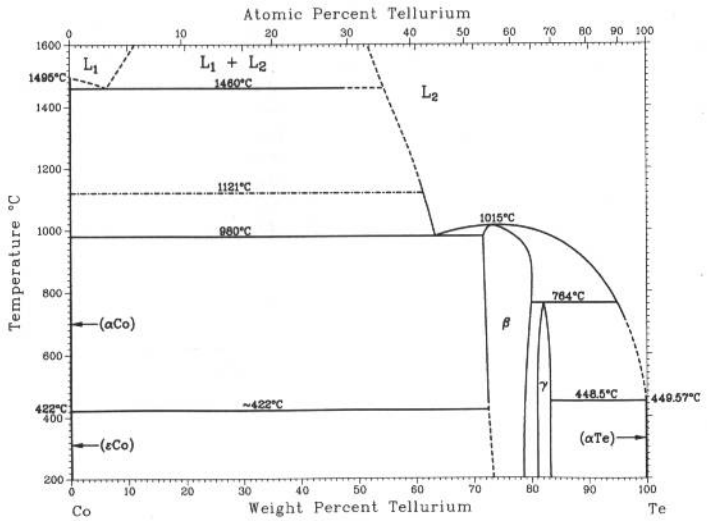

K. Ishida and T. Nishizawa, unpublished

Phase	Composition, wt% Te	Pearson symbol	Space group
(αCo)	~0	*cF*4	$Fm\bar{3}m$
(εCo)	~0	*hP*2	$P6_3/mmc$
$\beta(Co_2Te_3)$	73 to 80	*hP*4	$P6_3/mmc$
$\gamma(CoTe_2)$	81.1 to 83.3	*oP*6	*Pnn*2
$CoTe_2$(a)	81.3	*hP*3	$P\bar{3}m1$
$CoTe_2$(b)	81.3	*cP*12	$Pa\bar{3}$
(αTe)	~100	*hP*3	$P3_121$

(a) Metastable? (b) Under high pressure

Co-Th

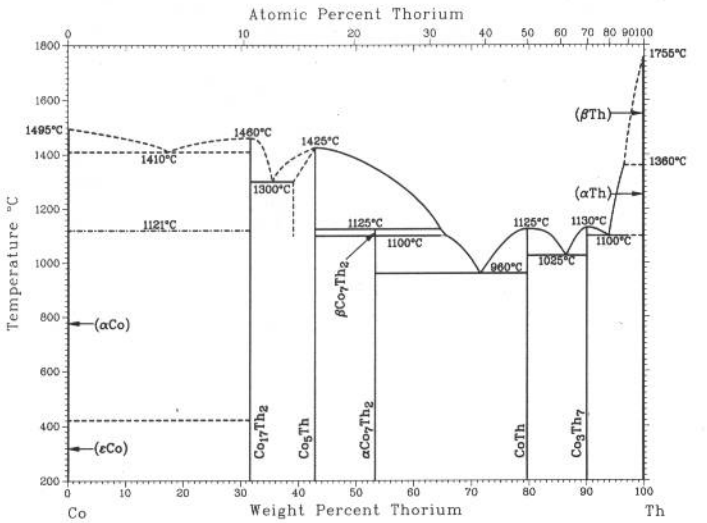

K. Ishida, T. Nishizawa, and H. Okamoto, unpublished

Phase	Composition, wt% Th	Pearson symbol	Space group
(αCo)	~0	*cF*4	$Fm\bar{3}m$
(εCo)	~0	*hP*2	$P6_3/mmc$
$Co_{17}Th_2$	31.6	*hR*19	$R\bar{3}m$
Co_5Th	44.1	*hP*6	*P6/mmm*
αCo_7Th_2	52.9	*hP*36	$P6_3/mmc$
βCo_7Th_2	52.9	*hR*18	$R\bar{3}m$
CoTh	79.7	*oC*8	*Cmcm*
Co_3Th_7	90	*hP*20	$P6_3mc$
(βTh)	~100	*cI*2	$Im\bar{3}m$
(αTh)	~100	*cF*4	$Fm\bar{3}m$

Co-Ti

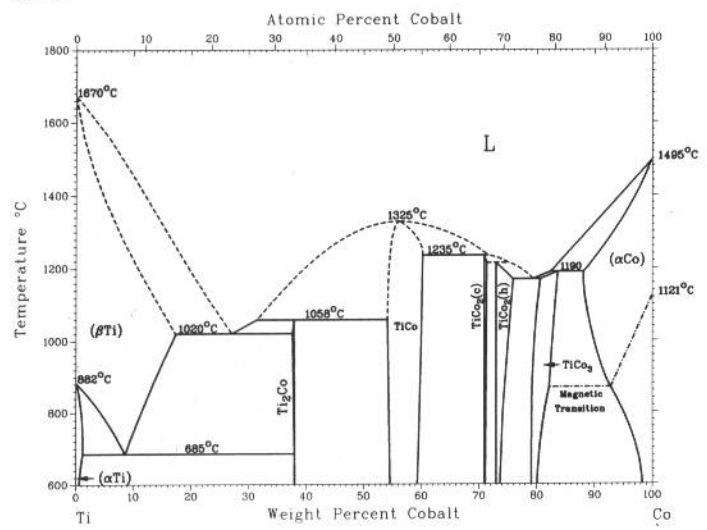

J.L. Murray, 1987

Phase	Composition, wt% Co	Pearson symbol	Space group
(αTi)	0 to 1.0	*hP*2	$P6_3/mmc$
(βTi)	0 to 17.3	*cI*2	$Im\bar{3}m$
Ti_2Co	37.6 to 38.1	*cF*96	$Fd\bar{3}m$
TiCo	54 to 60	*cP*2	$Pm\bar{3}m$
$TiCo_2$ (cubic)	71.0 to 71	*cF*24	$Fd\bar{3}m$
$TiCo_2$ (hexagonal)	73.0 to 76	*hP*24	$P6_3/mmc$
$TiCo_3$	79.1 to 83.7	*cP*4	$Pm\bar{3}m$
(εCo)	~99.2 to 100	*hP*2	$P6_3/mmc$
(αCo)	88.0 to 100	*cF*4	$Fm\bar{3}m$
Metastable phases			
ω	...	(a)	*P6/mmm*
(α″Co)	...	(b)	...

(a) The "ideal" ω structure is hexagonal, but a distorted trigonal form has also been observed in some Ti systems. The structure of ω in Ti-Co has not been definitively established. (b) Rhombohedral

Co-V

J.F. Smith, 1989

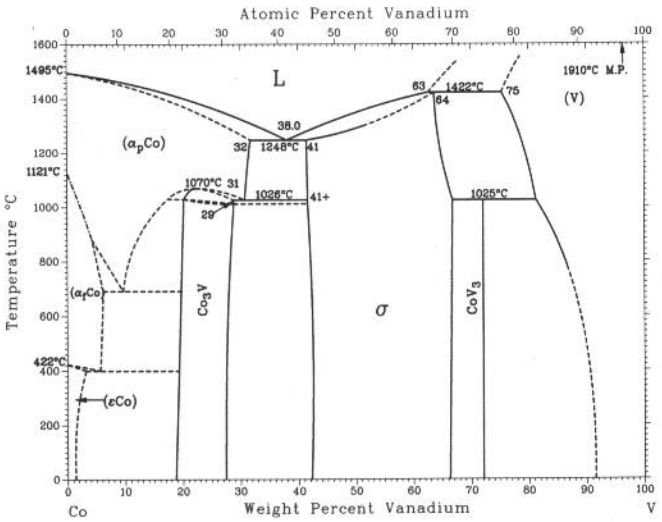

Phase	Composition, wt% V	Pearson symbol	Space group
(αCo)	0 to 32	*cF*4	$Fm\bar{3}m$
(εCo)	0 to ?	*hP*2	$P6_3/mmc$
Co_3V(hex)	~21 to 29	*hP*24	$P\bar{6}m2$
Co_3V(fcc)	~19 to 28	*cP*4	$Pm\bar{3}m$
σ	41 to ~67	*tP*30	$P4_2/mnm$
CoV_3	~72	*cP*8	$Pm\bar{3}n$
(V)	75 to 100	*cI*2	$Im\bar{3}m$

Co-W

S.V. Nagender Naidu, A.M. Sriramamurthy, and P. Rama Rao, 1986

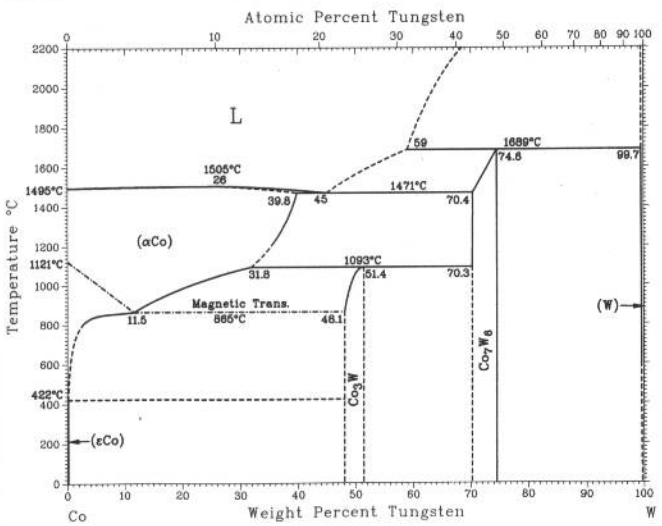

Phase	Composition, wt% W	Pearson symbol	Space group
(αCo)	0 to 39.8	*cF*4	$Fm\bar{3}m$
(εCo)	0	*hP*2	$P6_3/mmc$
Co_3W	48.1 to 51.4	*hP*8	$P6_3/mmc$
Co_7W_6	70.3 to 74.6	*hR*13	$R\bar{3}m$
(W)	99.7 to 100	*cI*2	$Im\bar{3}m$

Co-Y

H. Okamoto, 1992

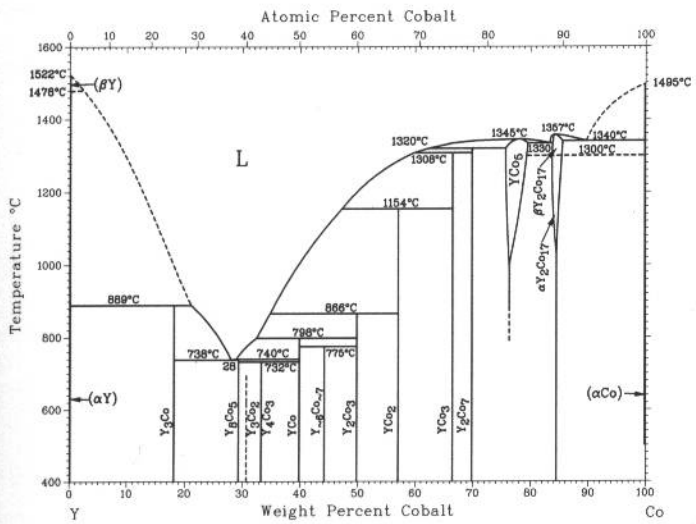

Phase	Composition, wt% Co	Pearson symbol	Space group
(βY)	0	*cI*2	$Im\bar{3}m$
(αY)	0	*hP*2	$P6_3/mmc$
Y_3Co	18	*oP*16	*Pnma*
Y_8Co_5	29.3	*mP*52	$P2_1/c$
Y_4Co_3	33.2	*hP*22	$P6_3/m$
YCo	39.9	*oC*8	*Cmcm*
Y_6Co_7	44.4	...	...
Y_2Co_3	49.9	*cP**	...
YCo_2	57.0	*cF*24	$Fd\bar{3}m$
YCo_3	67	*hR*12	$R\bar{3}m$
		*hP*24	$P6_3/mmc$
Y_2Co_7	69.9	*hR*18	$R\bar{3}m$
YCo_5	75.8 to 80	*hP*6	*P6/mmm*
βY_2Co_{17}	84 to 86	*hP*38	$P6_3/mmc$
αY_2Co_{17}	~84	*hP*19	$R\bar{3}m$
(αCo)	100	*cF*4	$Fm\bar{3}m$
(εCo)	100	*hP*2	$P6_3/mmc$
Metastable phase			
Y_3Co_2	31	*oP*20	*Pnnm*

Co-Zn

H. Okamoto, 1990

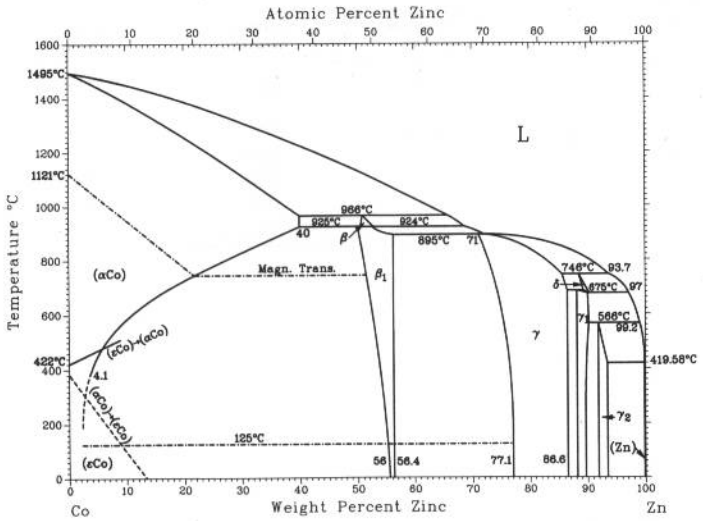

Phase	Composition, wt% Zn	Pearson symbol	Space group
(αCo)	0 to 40	*cF*4	$Fm\bar{3}m$
(εCo)	0 to ?	*hP*2	$P6_3/mmc$
β	~52 to 54	*cI*2?	$Im\bar{3}m$
β_1	50.5 to 59.0	*cP*20	$P4_132$
γ	71 to 86.6	*cP*52	$P\bar{4}3m$
γ_1	88.5 to 89.6	...	...
δ	~89 to <91	...	...
γ_2	92 to 93.5	*mC*28	*C*2/*m*
(Zn)	~100	*hP*2	$P6_3/mmc$

Cr-Cu

D.J. Chakrabarti and D.E Laughlin, 1984

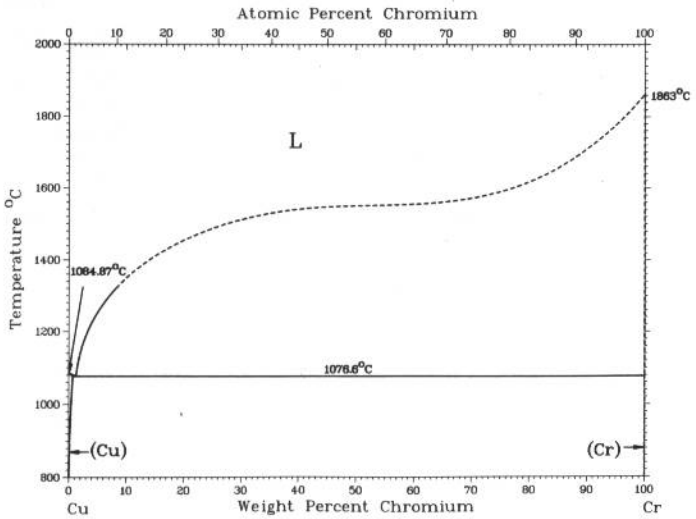

Phase	Composition, wt% Cr	Pearson symbol	Space group
(Cu)	0 to 0.73	*cF*4	$Fm\bar{3}m$
(Cr)	99.8 to 100	*cI*2	$Im\bar{3}m$

Cr-Fe

H. Okamoto, 1990

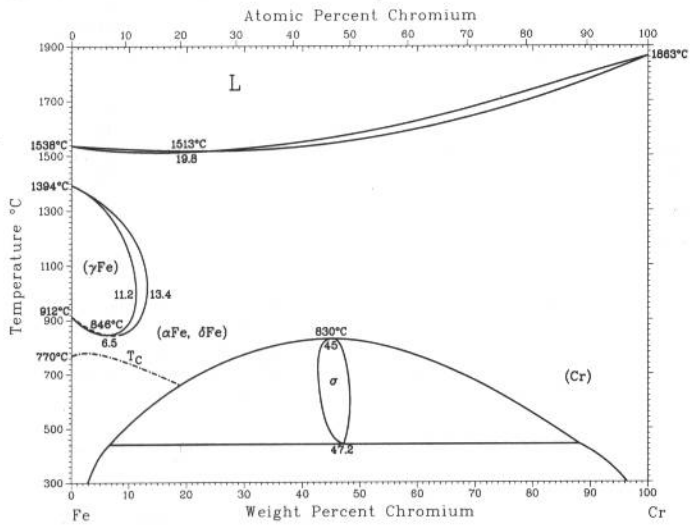

Phase	Composition, wt% Cr	Pearson symbol	Space group
(αFe,Cr)	0 to 100	*cI*2	$Im\bar{3}m$
(γFe)	0 to 11.2	*cF*4	$Fm\bar{3}m$
σ	42.7 to 48.2	*tP*30	$P4_2/mnm$

Cr-Ga

J.-D. Bornand and P. Feschotte, 1972

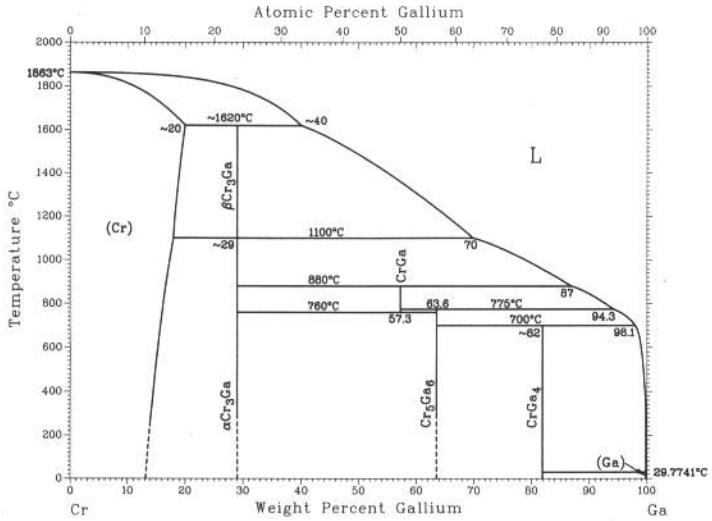

Phase	Composition, wt% Ga	Pearson symbol	Space group
(Cr)	0 to ~20	*cI*2	$Im\bar{3}m$
βCr_3Ga	~29	...	...
αCr_3Ga	~29	*cP*8	$Pm\bar{3}n$
CrGa	57.3	*hR*26	$R\bar{3}m$
Cr_5Ga_6	63.6	...	...
$CrGa_4$	~82	*cI*10	*I*432
(Ga)	~100	*oC*8	*Cmca*

Cr-Ge

A.B. Gokhale and G.J. Abbaschian, 1986

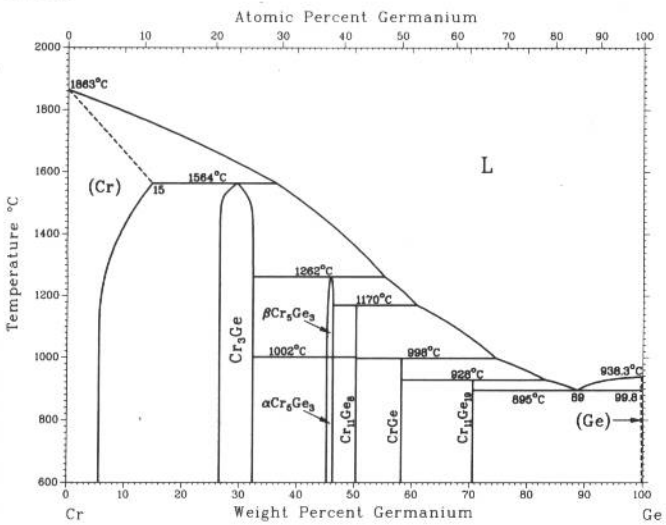

Phase	Composition, wt% Ge	Pearson symbol	Space group
(Cr)	0 to 15	*cI*2	$Im\bar{3}m$
Cr_3Ge	26.5 to 31.9	*cP*8	$Pm\bar{3}n$
Cr_5Ge_3	45.5 to 46.3	*hP*16	*I*4/*mcm*
$Cr_{11}Ge_8$	50.4	*oP*76	*Pnam*
CrGe	58.3	*cP*8	$P2_13$
$Cr_{11}Ge_{19}$	70.7	(a)	$P\bar{4}n2$
(Ge)	100	*cF*8	$Fd\bar{3}m$

(a) Tetragonal

Cr-Hf

M. Venkatraman and J.P. Neumann, 1986

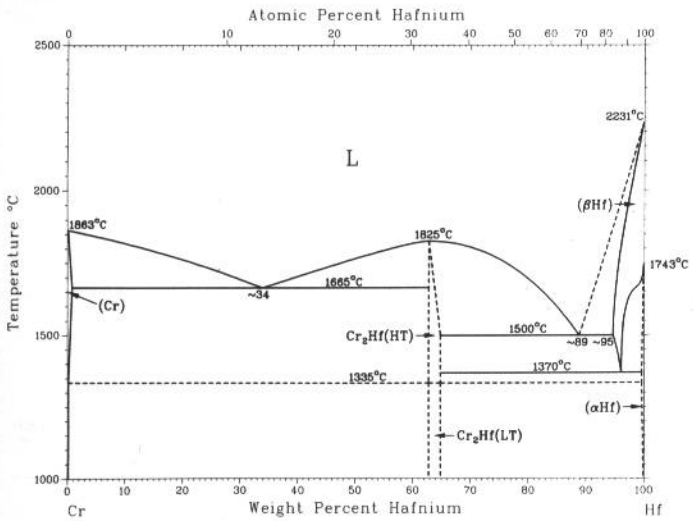

Phase	Composition, wt% Hf	Pearson symbol	Space group
(Cr)(a)	~0	*cI*2	$Im\bar{3}m$
Cr_2Hf(HT)(b)	63 to 65	*hP*12	$P6_3/mmc$
Cr_2Hf(LT)(c)	63 to 65	*cF*24	$Fd\bar{3}m$
(βHf)(d)	~95 to 100	*cI*2	$Im\bar{3}m$
(αHf)(e)	98 to 100	*hP*2	$P6_3/mmc$

(a) Stable at <1863 °C. (b) Stable at 1335 to 1825 °C. (c) Stable at <1335 °C. (d) Stable at 1740 to 2224 °C. (e) Stable at <1740 °C

Cr-Ir

M. Venkatraman and J.P. Neumann, 1990

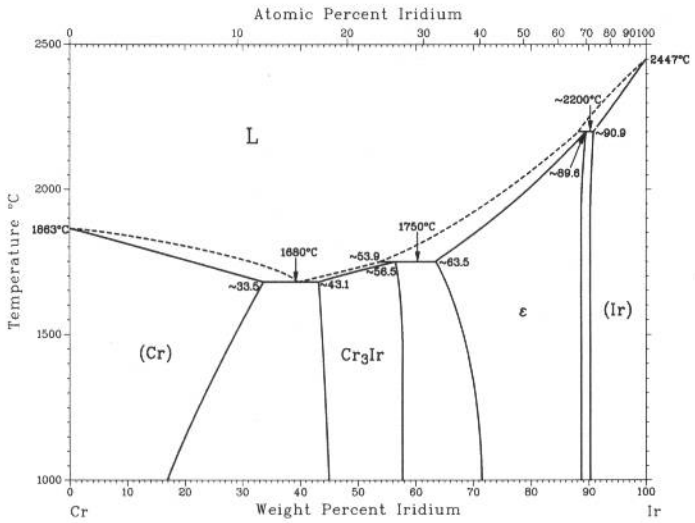

Phase	Composition, wt% Ir	Pearson symbol	Space group
(Cr)	0 to ~33.5	*cI*2	$Im\bar{3}m$
Cr_3Ir	~43.1 to 58	*cP*8	$Pm\bar{3}n$
ε	~63.5 to ~89.6	*hP*2	$P6_3/mmc$
$CrIr_3$(a)	~90 to ~95	*cP*4	$Pm\bar{3}m$
(Ir)	91 to 100	*cF*4	$Fm\bar{3}m$

(a) Order-disorder temperature has not been determined, but because it is presumably below 1000 °C, the phase is not shown in the diagram.

Cr-Lu

H. Okamoto, 1992

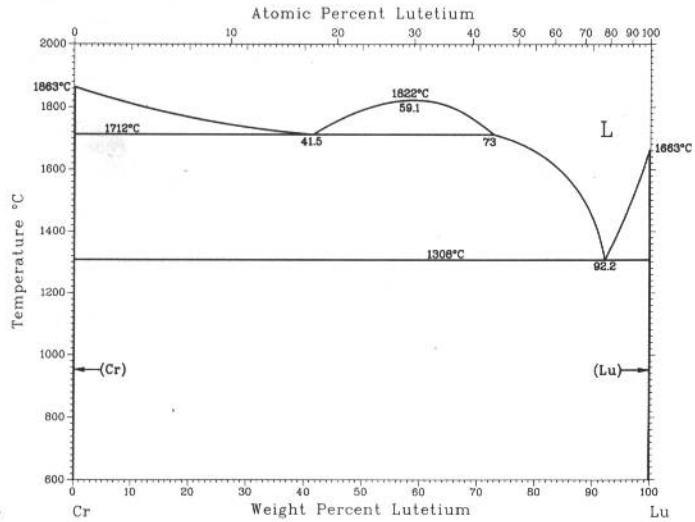

Phase	Composition, wt% Lu	Pearson symbol	Space group
(Cr)	0	*cI*2	$Im\bar{3}m$
(Lu)	100	*hP*2	$P6_3/mmc$

Cr-Mn

M. Venkatraman and J.P. Neumann, 1986

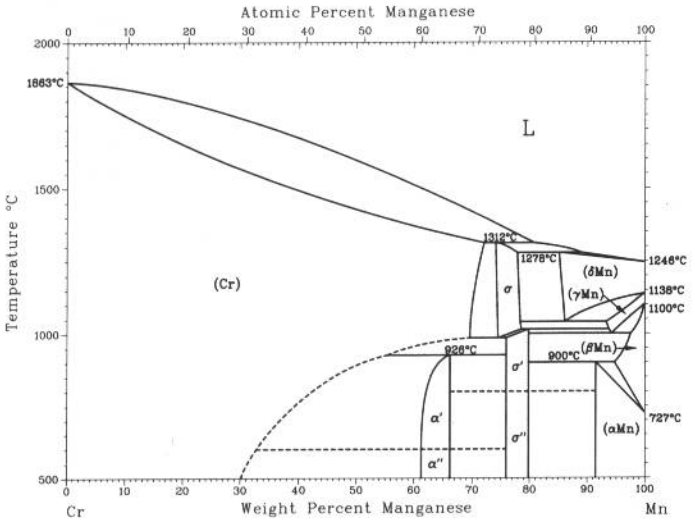

Phase	Composition, wt% Mn	Pearson symbol	Space group
(Cr)(a)	0 to 72.5	*cI*2	$Im\bar{3}m$
α′ (HT)(b)	61.5 to 66.5	...	...
α″ (LT)(c)	61.5 to 66.5	...	...
σ (HT)(d)	74 to 79	*tP*30	$P4_2/mnm$
σ′ (MT)(e)	76 to 80	*tP*30	$P4_2/mnm$
σ″ (LT)(f)	76 to 80	*tP*30	$P4_2/mnm$
(δMn)(g)	86 to 100	*cI*2	$Im\bar{3}m$
(αMn)(h)	91 to 100	*cI*58	$I\bar{4}3m$
(γMn)(j)	93 to 100	*cF*4	$Fm\bar{3}m$
(βMn)(k)	94 to 100	*cP*20	$P4_132$
Metastable phases			
"(δMn)"	73 to 84	*cI*2	$Im\bar{3}m$
"(γMn)"	85 to 100	*tI*2	$I4/mmm$

(a) Below 1863 °C. (b) From 600 to 926 °C. (c) Below 600 °C. (d) From 999 to 1312 °C. (e) From ~800 to 1006 °C. (f) Below ~800 °C. (g) From 1140 to 1246 °C. (h) Below 707 °C. (j) From 1088 to 1140 °C. (k) From 707 to 1088 °C

Cr-Mo

M. Venkatraman and J.P. Neumann, 1987

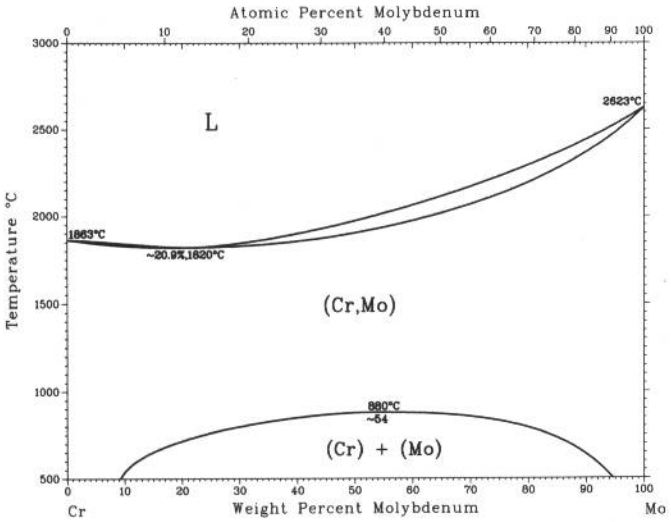

Phase	Composition, wt% Mo	Pearson symbol	Space group
(Cr,Mo)	0 to 100	*cI*2	$Im\bar{3}m$

Cr-Nb

M. Venkatraman and J.P. Neumann, 1986

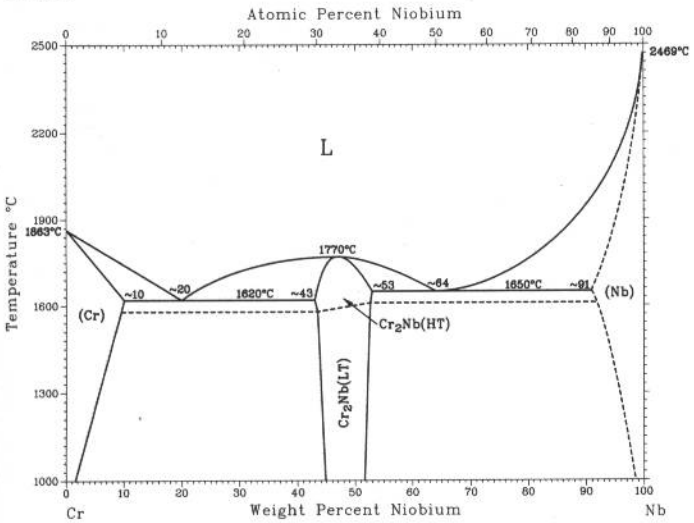

Phase	Composition, wt% Nb	Pearson symbol	Space group
(Cr)	0 to ~10	*cI*2	$Im\bar{3}m$
Cr_2Nb (HT)	~43 to ~53	*hP*12	$P6_3/mmc$
Cr_2Nb (LT)	43 to 53	*cF*24	$Fd\bar{3}m$
(Nb)	~91 to 100	*cI*2	$Im\bar{3}m$

Cr-Ni

P. Nash, 1991

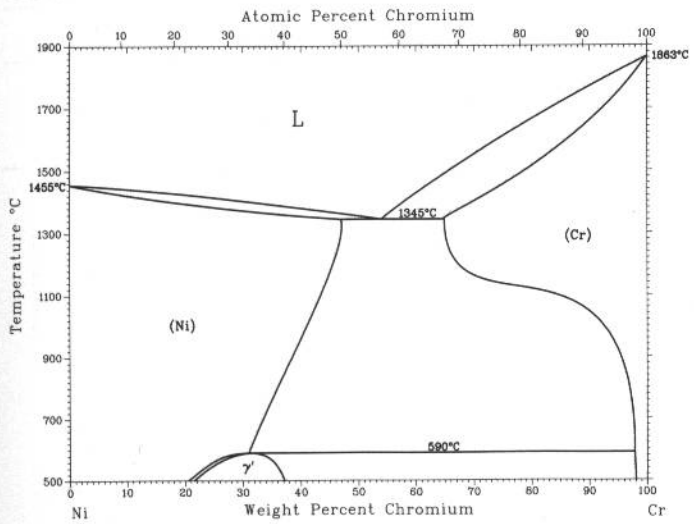

Phase	Composition, wt% Cr	Pearson symbol	Space group
(Ni)	0 to 47.0	*cF*4	$Fm\bar{3}m$
Ni_2Cr or γ′	21 to 37	*oI*6	*Immm*
(Cr)	65 to 100	*cI*2	$Im\bar{3}m$
Metastable phases			
σ	~28	*tP*30	$P4_2/mnm$
δ	100	*cP*8	$Pm\bar{3}m$

Cr-O

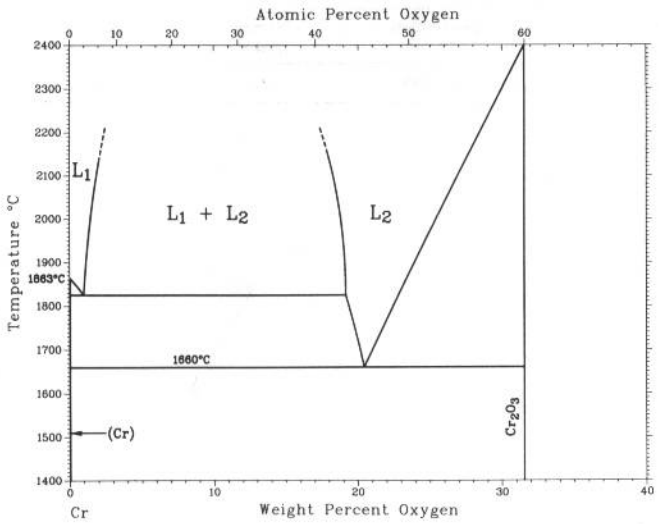

C. Banik, T. Schmitt, P. Ettmayer, and B. Lux, 1980

Phase	Composition, wt% O	Pearson symbol	Space group
(Cr)	0	*cI*2	$Im\bar{3}m$
Cr_3O_4(a)	29.1	*tI*28	$I4_1/amd$
Cr_2O_3	32	*hR*10	$R\bar{3}c$
CrO_2	38.1	*tP*6	$P4_2/mnm$
Cr_5O_{12}	42.5	*oP*68	*Pbcn*
Cr_6O_{15}	43.4	*oC*84	*Cmcm*
CrO_3	48	*oC*16	*Ama*2

(a) Metastable or high-pressure phase

Cr-Os

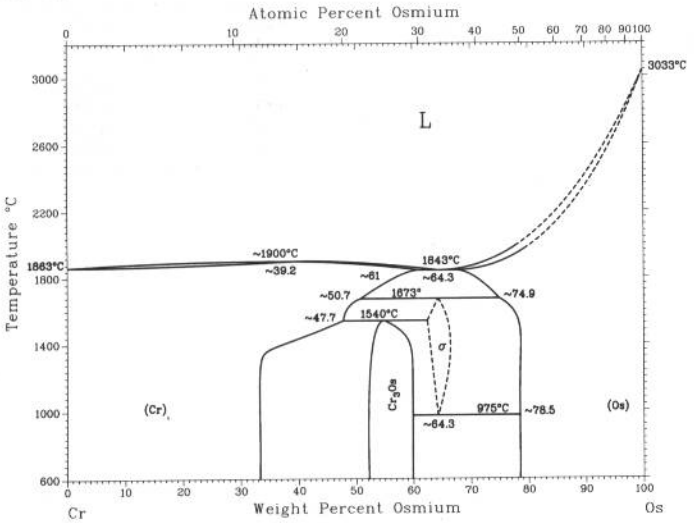

M. Venkatraman and J.P. Neumann, 1990

Phase	Composition, wt% Os	Pearson symbol	Space group
(Cr)(a)	0 to ~61	*cI*2	$Im\bar{3}m$
Cr_3Os(b)	~52 to ~60	*cP*8	$Pm\bar{3}n$
σ(c)	~61 to ~81	*tP*30	$P4_2/mnm$
(Os)(d)	~66 to 100	*hP*2	$P6_3/mmc$

(a) Below 1900 °C. (b) Below 1540 °C. (c) 975 to 1673 °C. (d) Below 3033 °C

Cr-Pd

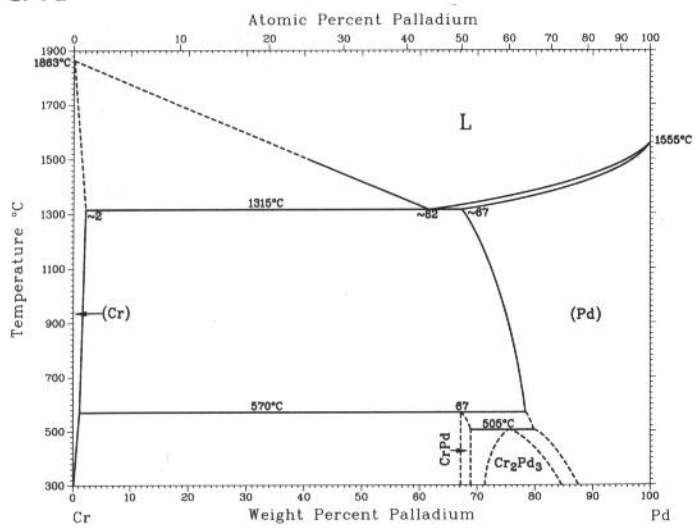

M. Venkatraman and J.P. Neumann, 1990

Phase	Composition, wt% Pd	Pearson symbol	Space group
(Cr)	0 to ~2	*cI*2	$Im\bar{3}m$
CrPd	67 to ~69	*tP*2	*P*4/*mmm*
Cr_2Pd_3	~71 to ~86	*cP*4	$Pm\bar{3}m$
(Pd)	~67 to 100	*cF*4	$Fm\bar{3}m$

Cr-Pt

M. Venkatraman and J.P. Neumann, 1990

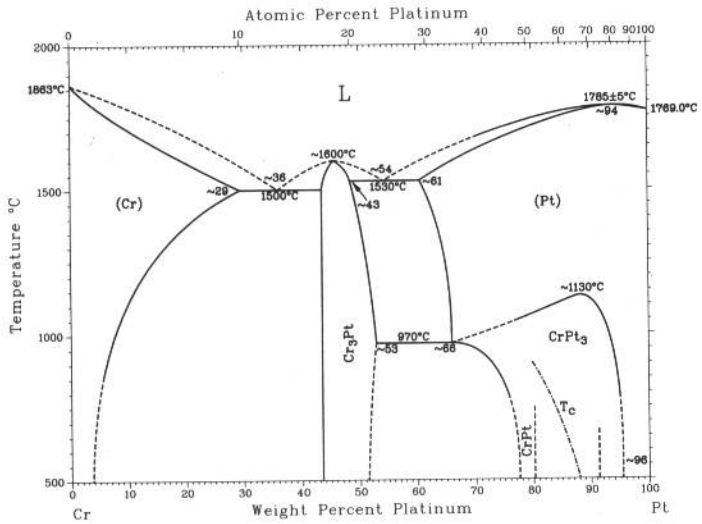

Phase	Composition, wt% Pt	Pearson symbol	Space group
(Cr)	0 to ~29	*cI*2	$Im\bar{3}m$
Cr_3Pt	44 to ~53	*cP*8	$Pm\bar{3}n$
CrPt	~78 to ~80	*tP*2	*P*4/*mmm*
$CrPt_3$	~66 to 96	*cP*4	$Pm\bar{3}m$
(Pt)	~61 to 100	*cF*4	$Fm\bar{3}m$

Cr-Re

M. Venkatraman and J.P. Neumann, 1987

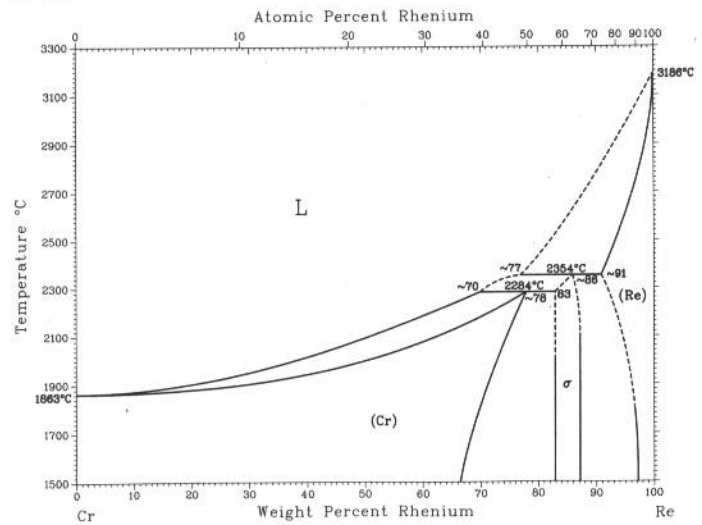

Phase	Composition, wt% Re	Pearson symbol	Space group
(Cr)	0 to ~78	*cI*2	$Im\bar{3}m$
σ (Cr_2Re_3)	83 to 87	*tP*30	$P4_2/mnm$
(Re)	~91 to 100	*hP*2	$P6_3/mmc$

Cr-Rh

M. Venkatraman and J.P. Neumann, 1987

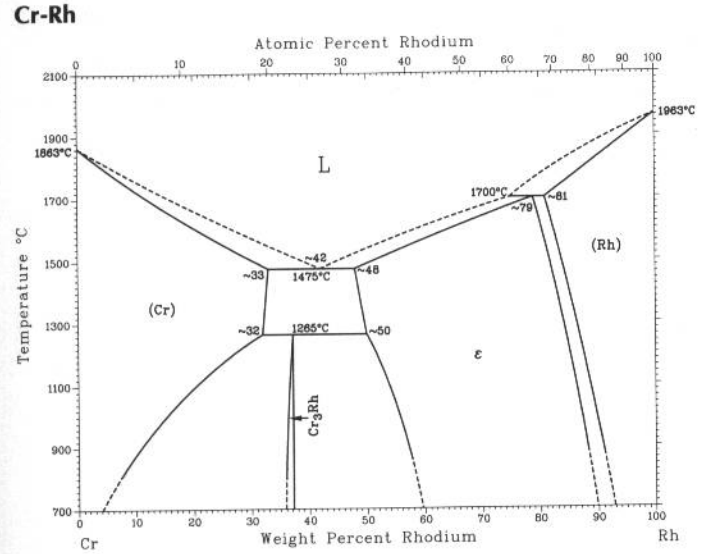

Phase	Composition, wt% Rh	Pearson symbol	Space group
(Cr)	0 to ~33	*cI*2	$Im\bar{3}m$
Cr_3Rh	36 to 37	*cP*8	$Pm\bar{3}n$
ε	~48 to 81	*hP*2	$P6_3/mmc$
(Rh)	~81 to 100	*cF*4	$Fm\bar{3}m$

Cr-Ru

M. Venkatraman and J.P. Neumann, 1987

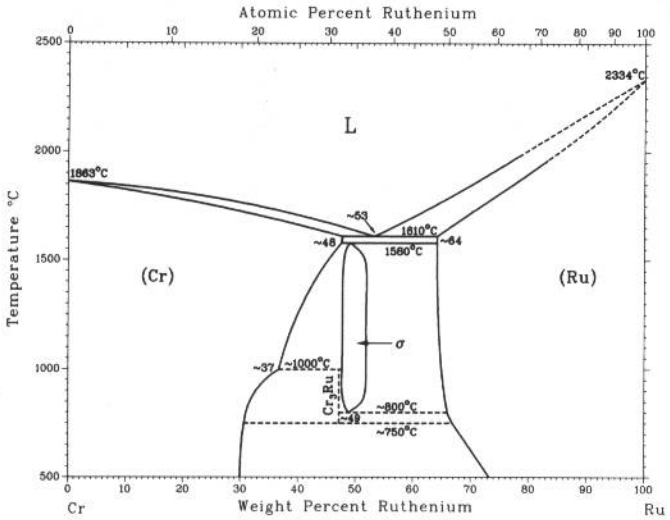

Phase	Composition, wt% Ru	Pearson symbol	Space group
(Cr)(a)	0 to ~48	*cI*2	$Im\bar{3}m$
Cr_3Ru(b)	47.2	*cP*8	$Pm\bar{3}n$
σCr_2Ru(c)	48 to 52	*tP*30	$P4_2/mnm$
(Ru)(d)	~64 to 100	*hP*2	$P6_3/mmc$

(a) Stable below 1863 °C. (b) Stable from 750 to 1000 °C; might be located at ~39.3 wt%, instead. (c) Stable from 800 to 1580 °C. (d) Stable below 2334 °C

Cr-S

M. Venkatraman and J.P. Neumann, unpublished

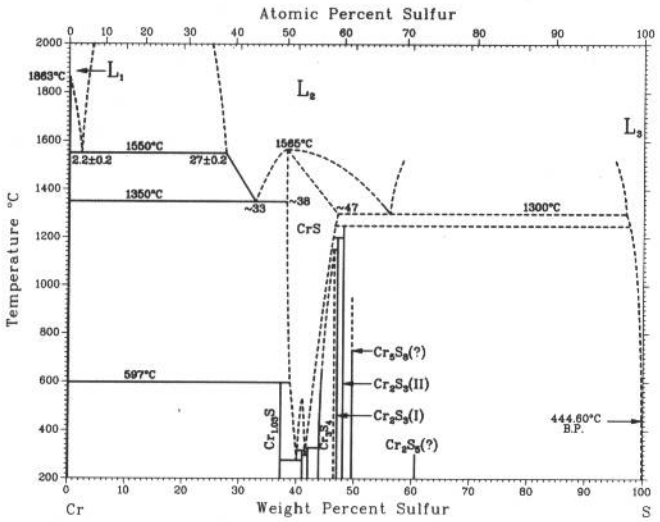

Phase	Composition, wt% S	Pearson symbol	Space group
(Cr)	0 to ~0.001	*cI*2	$Im\bar{3}m$
$Cr_{1.03}S$	~37.5	*mC*8	*C*2/*c*
CrS	~38 to ~47	*hP*4	$P6_3/mmc$
Cr_7S_8	41.2 to 41.5	*hP*4	$P\bar{3}m1$
Cr_5S_6	~42	*hP*22	$P\bar{3}1c$
Cr_3S_4	44 to ~46.2	*mC*14	*C*2/*m*
Cr_2S_3(I)	46.5 to 47.5	*hP*20	$P\bar{3}1c$
Cr_2S_3(II)	47.8 to 48.7	*hR*10	$R\bar{3}$
Cr_5S_8(a)	49.6	*mC**	*C*2/*m*
Cr_2S_5(?)	60.6	(b)	...

(a) High-pressure phase. (b) Unknown

Cr-Sb

H. Okamoto, 1992

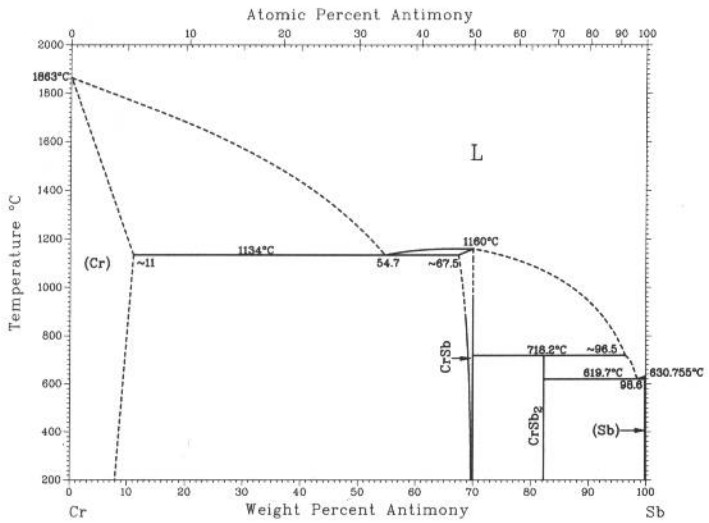

Phase	Composition, wt% Sb	Pearson symbol	Space group
(Cr)	0 to ~11	*cI*2	$Im\bar{3}m$
CrSb	~67.5 to 70.1	*hP*4	$P6_3/mmc$
$CrSb_2$	82.4	*oP*6	*Pnnm*
(Sb)	100	*hR*2	$R\bar{3}m$

Cr-Sc

M. Venkatraman and J.P. Neumann, 1985

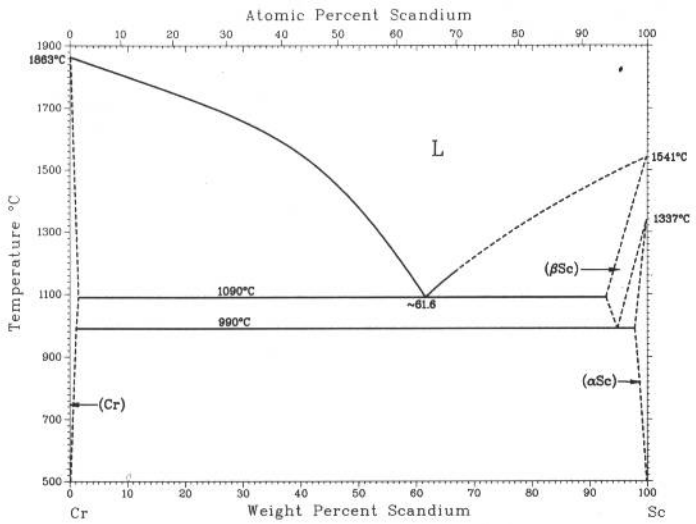

Phase	Composition, wt% Sc	Pearson symbol	Space group
(Cr)	0 to <0.09	*cI*2	$Im\bar{3}m$
(βSc)	>89 to 100	*cI*2	$Im\bar{3}m$
(αSc)	~100	*hP*2	$P6_3/mmc$
Metastable phase			
$Cr_{0.85}Sc_{2.15}B_x$	~69.0	*cF*112	$Fd\bar{3}m$

Cr-Se

M. Venkatraman and J.P. Neumann, unpublished

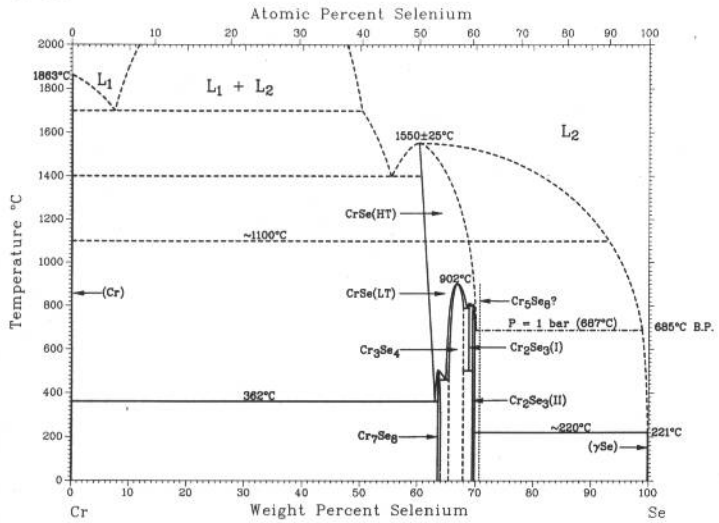

Phase	Composition, wt% Se	Pearson symbol	Space group
(Cr)	~0	*cI*2	$Im\bar{3}m$
CrSe(HT)	60.3 to ~69.5	*hP*4	$P6_3/mmc$
CrSe(LT)	~61 to ~69.9	*hP*4	$P\bar{3}m1$
Cr_7Se_8	63.6 to 64.1	*mF*60	*F*2/*m*
Cr_3Se_4	65.4 to 68.0	*mI*14	*I*2/*m*
Cr_2Se_3(I)	~69.0	*hP*20	$P\bar{3}1c$
Cr_2Se_3(II)	69.3 to 69.7	*hR*10	$R\bar{3}$
Cr_2Se_3(III)(a)	69.9 to 70.4	*mI*15	*I*2/*m*
Cr_5Se_8(b)	70.8	*mF*52	*F*2/*m*
$CrSe_2$(a)	75.3	*hP*3	$P\bar{3}m1$
(γSe)	~100	*hP*3	$P3_121$

(a) Metastable. (b) Stable at high pressure

Detailed view of the Cr-Se phase diagram in the region 59.9 to 70.5 wt% Se

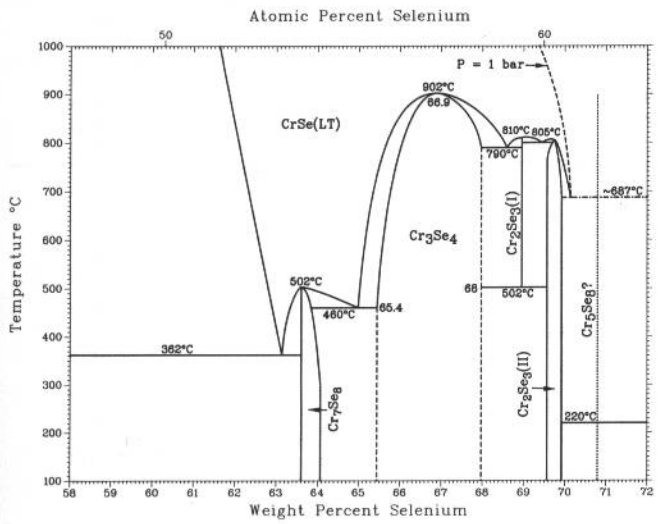

Cr-Si

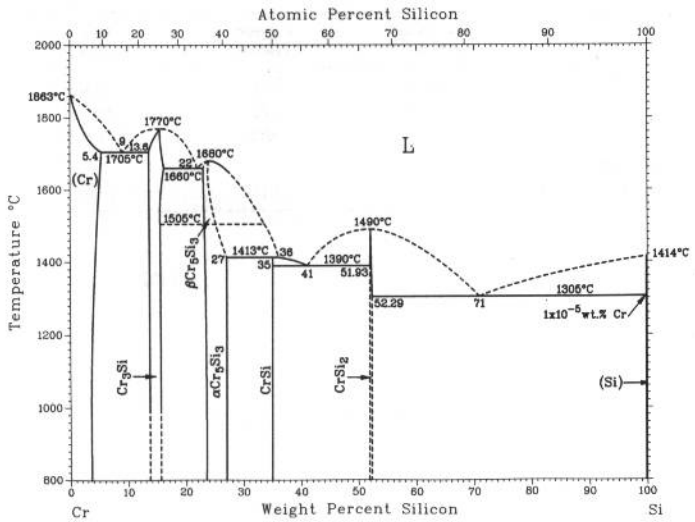

A.B. Gokhale and G.J. Abbaschian, 1987

Phase	Composition, wt% Si	Pearson symbol	Space group
(Cr)	0 to 5.4	*cI*2	$Im\bar{3}m$
Cr_3Si	13.6 to 16.2	*cP*8	$Pm\bar{3}n$
αCr_5Si_3	23 to 27	*tI*38	*I*4/*mcm*
CrSi	35	*cP*8	$P2_13$
$CrSi_2$	51.9 to 52.29	*hP*9	$P6_222$
(Si)	~100	*cF*8	$Fd\bar{3}m$

Cr-Sn

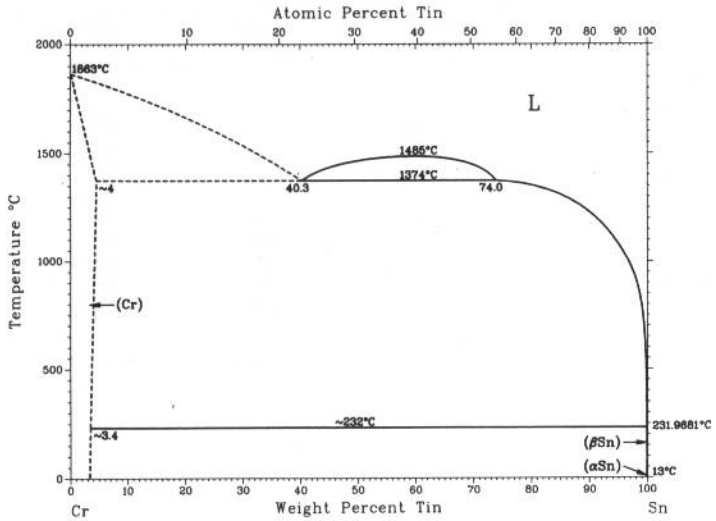

M. Venkatraman and J.P. Neumann, 1988

Phase	Composition, wt% Sn	Pearson symbol	Space group
(Cr)	0 to ~4	*cI*2	$Im\bar{3}m$
(βSn)	~100	*tI*4	$I4_1/amd$
(αSn)	~100	*cF*8	$Fd\bar{3}m$
Metastable phase			
Cr_2Sn_3	77 to 78	*oF*48	*Fddd*

Cr-Ta

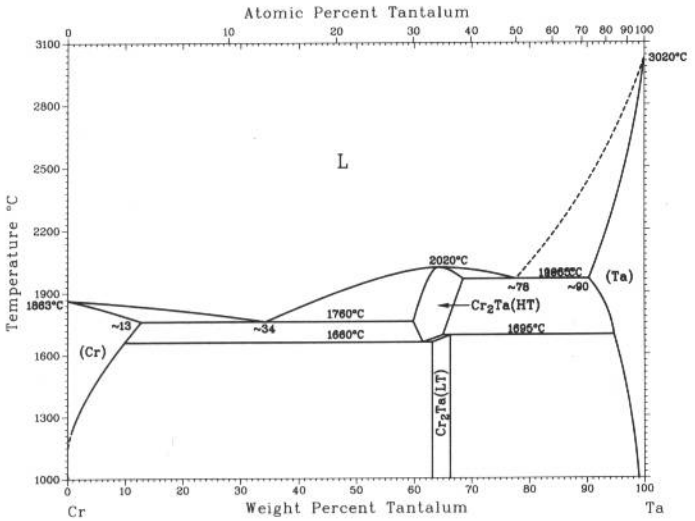

M. Venkatraman and J.P. Neumann, 1987

Phase	Composition, wt% Ta	Pearson symbol	Space group
(Cr)	0 to ~13	*cI*2	$Im\bar{3}m$
Cr_2Ta(HT)	60 to 68	*hP*12	$P6_3/mmc$
Cr_2Ta(LT)	63 to 66	*cF*24	$Fd\bar{3}m$
(Ta)	~90 to 100	*cI*2	$Im\bar{3}m$

Cr-Te

M. Venkatraman and J.P. Neumann, unpublished

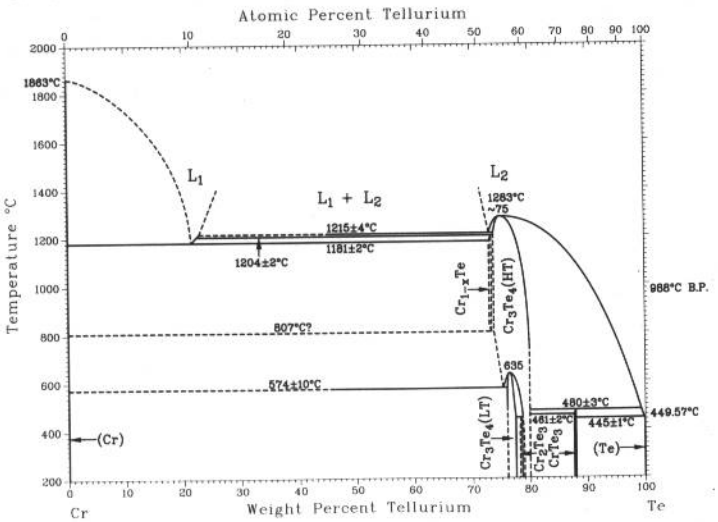

Phase	Composition, wt% Te	Pearson symbol	Space group
(Cr)	~0	*cI*2	$Im\bar{3}m$
$Cr_{1-x}Te$	73.1 to 73.8	*hP*4	$P6_3/mmc$
Cr_3Te_4(HT)	~73.9 to ~80.0	*mC*14	*C*2/*m*
Cr_3Te_4(LT)	~76 to 77.5	...	...
Cr_5Te_8-I(a)	78.4 to ~78.9	*mC*26	*C*2/*m*
Cr_5Te_8-II(a)	~79.7 to ~80.0	...	$P\bar{3}c1$ (?)
Cr_2Te_3	78.3 to 78.6	*hP*20	$P\bar{3}1c$
$CrTe_3$	~88	*mP*32	$P2_1/c$
(Te)	~100	*hP*3	$P3_121$

(a) Not shown in diagram

Cr-Ti

J.L. Murray, 1987

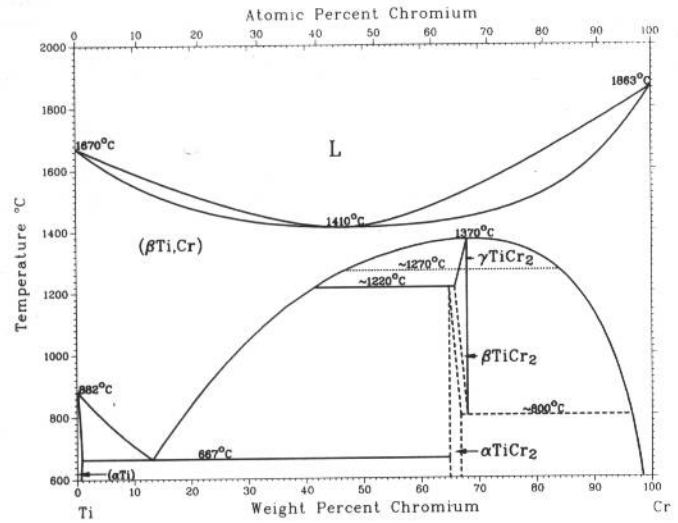

Phase	Composition, wt% Cr	Pearson symbol	Space group
(βTi,Cr)	0 to 100	*cI*2	$Im\bar{3}m$
(αTi)	0 to 0.2	*hP*2	$P6_3/mmc$
$\alpha TiCr_2$	65 to 67	*cF*24	$Fd\bar{3}m$
$\beta TiCr_2$	66 to 68	*hP*12	$P6_3/mmc$
$\gamma TiCr_2$	66 to 68	*hP*24	$P6_3/mmc$
Metastable phase			
ω	...	*hP*3	$P\bar{3}m1$

Cr-U

M. Venkatraman, J.P. Neumann, and D.E. Peterson, 1985

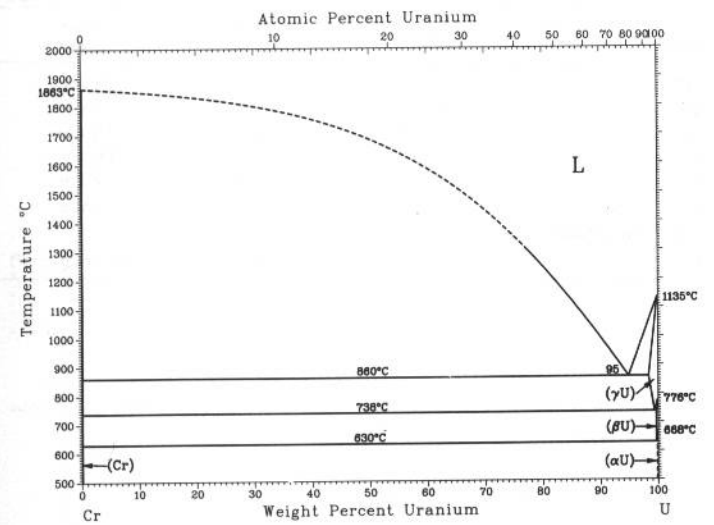

Phase	Composition, wt% U	Pearson symbol	Space group
(Cr)(a)	~0	*cI*2	$Im\bar{3}m$
(γU)(b)	99 to 100	*cI*2	$Im\bar{3}m$
(βU)(c)	99.8 to 100	*tP*30	$P4_2/mnm$
(αU)(d)	~100	*oC*4	*Cmcm*

(a) Stable below 1863 °C. (b) Stable from 775 to 1135 °C. (c) Stable from 668 to 775 °C. (d) Stable below 668 °C

Cr-V

J.F. Smith, 1989

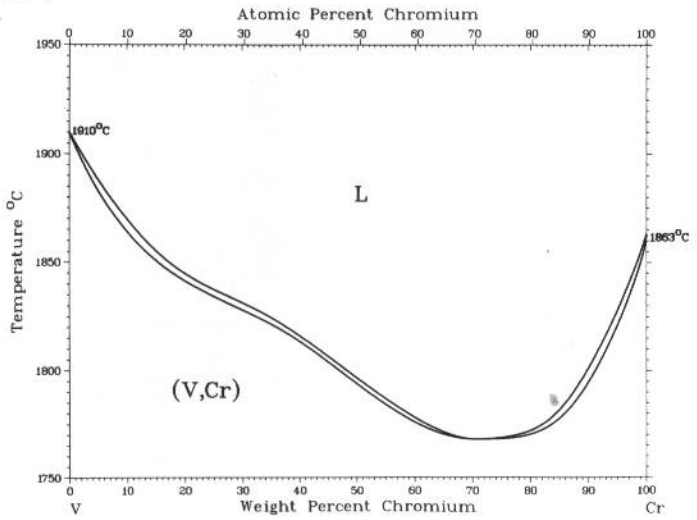

Phase	Composition, wt% Cr	Pearson symbol	Space group
(V,Cr)	0 to 100	*cI*2	$Im\bar{3}m$

Cr-W

S.V. Nagender Naidu, A.M. Sriramamurthy, and P. Rama Rao, 1984

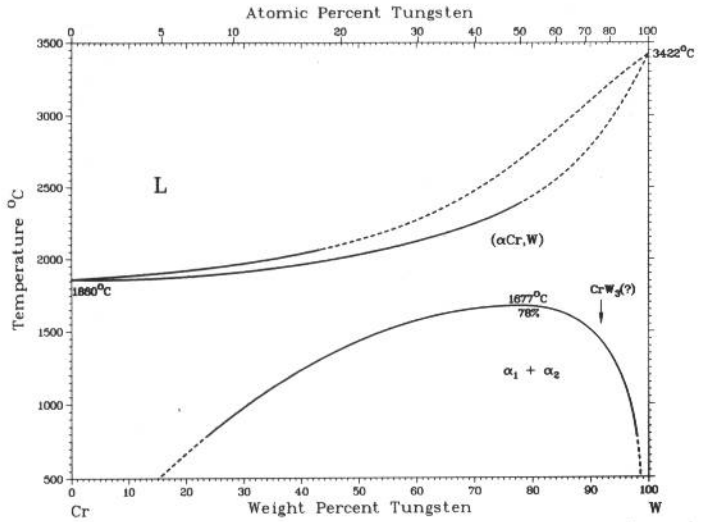

Phase	Composition, wt% W	Pearson symbol	Space group
(βCr)(a)	0	*cF*4	$Fm\bar{3}m$
(γCr)(b)	0	*cI*58	$I\bar{4}3m$
(δCr)	0	*cP*8	$Pm\bar{3}n$
(εCr)	0	*hP*2	$P6_3/mmc$
(αCr,W)	0 to 100	*cI*2	$Im\bar{3}m$
CrW_3(?)	91	*tI**	...

(a) Above 1840 °C. (b) Electrolytic

Cr-Zr

D. Arias and J.P. Abriata, 1986

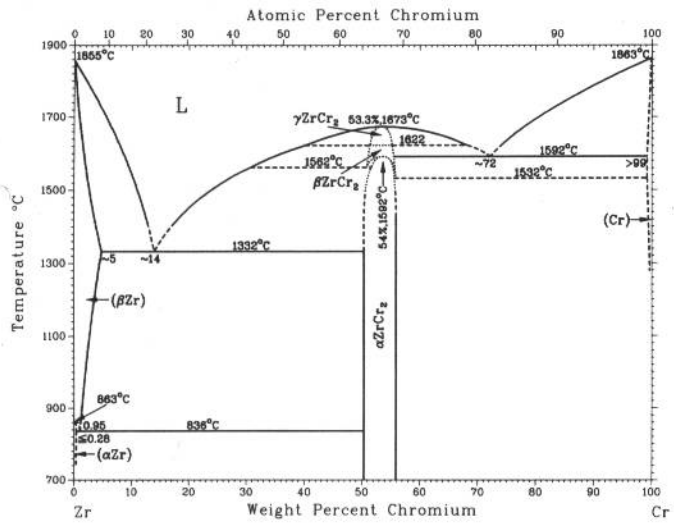

Phase	Composition, wt% Cr	Pearson symbol	Space group
(αZr)	0 to 0.28	*hP*2	$P6_3/mmc$
(βZr)	0 to ~5	*cI*2	$Im\bar{3}m$
$\gamma ZrCr_2$	50 to 56	*hP*12	$P6_3/mmc$
$\beta ZrCr_2$	50 to 56	*hP*24	$P6_3/mmc$
$\alpha ZrCr_2$	50 to 56	*cF*24	$Fd\bar{3}m$
(Cr)	>99 to 100	*cI*2	$Im\bar{3}m$
Metastable phases			
ω	...	*hP*3	$P\bar{3}m1$ (*P6/mmm*?)

Cs-Ge

H. Okamoto, 1990

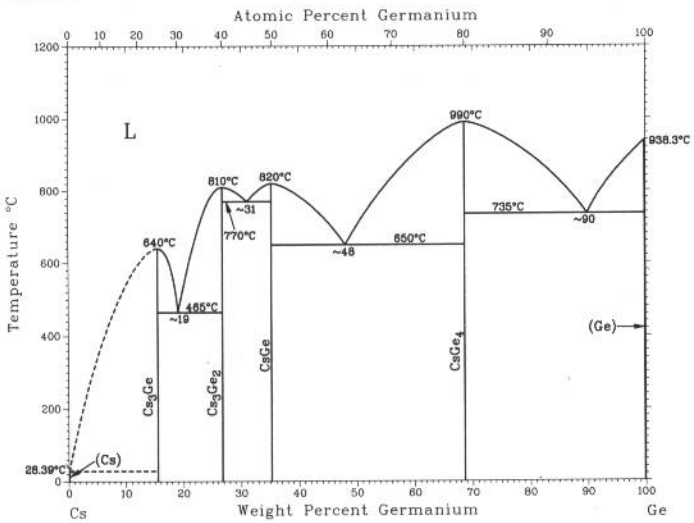

Phase	Composition, wt% Ge	Pearson symbol	Space group
(Cs)	0	*cI*2	$Im\bar{3}m$
Cs_3Ge	15	...	...
Cs_3Ge_2	27	...	...
CsGe	35.3	*cP*64	$P\bar{4}3n$
$CsGe_4$	69	*cP**	$Pm\bar{3}n$
(Ge)	100	*cF*8	$Fm\bar{3}m$

Cs-Hg

From [Hansen]

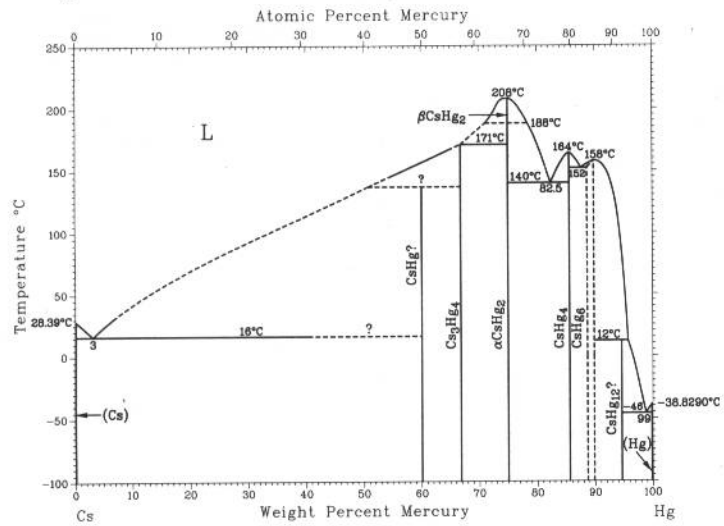

Phase	Composition, wt% Hg	Pearson symbol	Space group
(Cs)	0	*cI*2	$Im\bar{3}m$
CsHg?	60.1	...	...
Cs_3Hg_4	66.8	...	...
$\beta CsHg_2$	75.1	...	...
$\alpha CsHg_2$	75.1	...	...
$CsHg_4$	86	...	...
$CsHg_6$	90.0	...	...
$CsHg_{12}$?	~95	*c***	...
(Hg)	100	*hR*1	$R\bar{3}m$

Cs-In

A.D. Pelton and S. LaRose, 1990

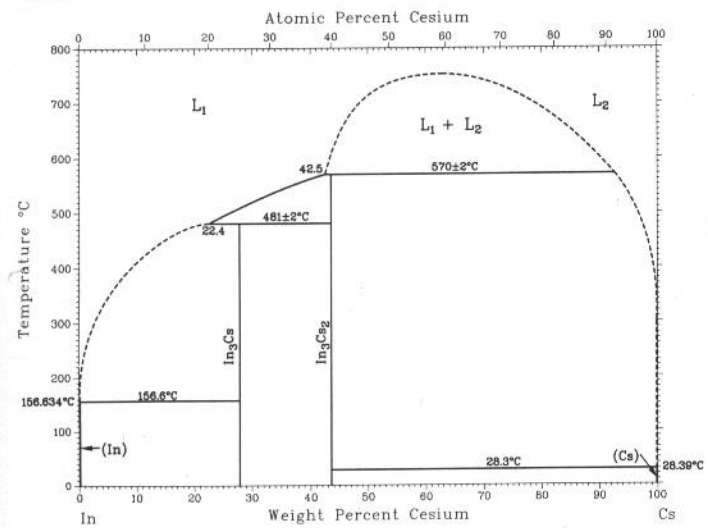

Phase	Composition, wt% Cs	Pearson symbol	Space group
(In)	0	*tI*2	*I*4/*mmm*
In_3Cs	28	*tI*24	*I*4*m*2
In_3Cs_2	44	...	*I*4*m*2
(Cs)	100	*cI*2	$Im\bar{3}m$

Cs-K

C.W. Bale and A.D. Pelton, 1983

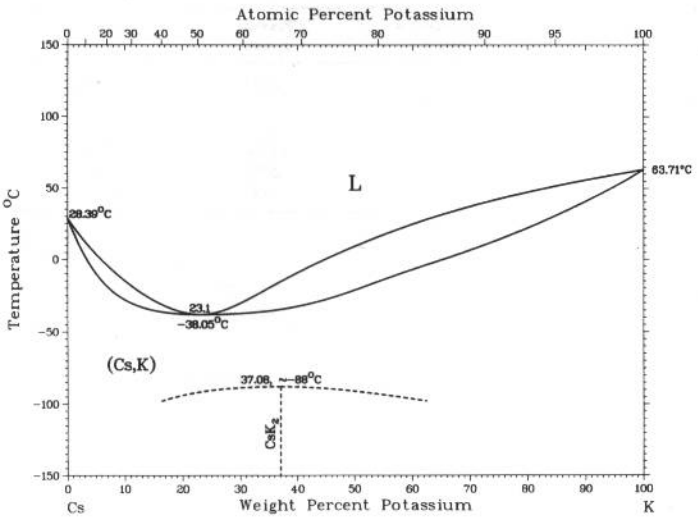

Phase	Composition, wt% K	Pearson symbol	Space group
(Cs,K)	0 to 100	*cI*2	$Im\bar{3}m$
CsK_2	37.0	*hP*2?	...
Other reported phase			
Cs_6K_7	?	...	...

Cs-Na

C.W. Bale, 1982

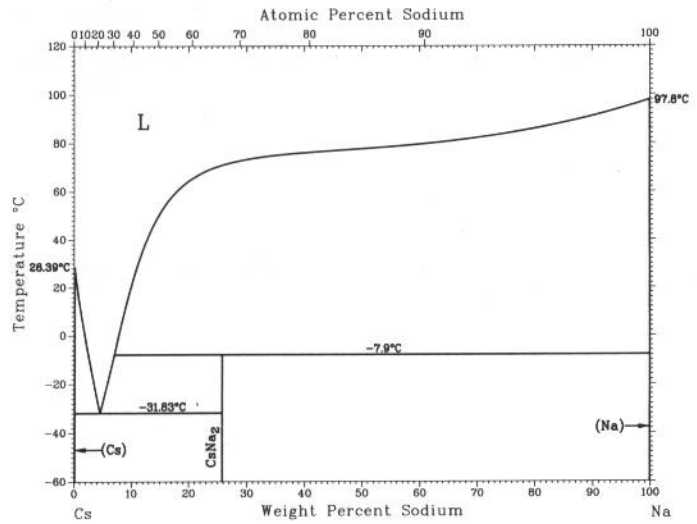

Phase	Composition, wt% Na	Pearson symbol	Space group
(Cs)	0	*cI*2	$Im\bar{3}m$
$CsNa_2$	25.7	...	...
(Na)	100	*cI*2	$Im\bar{3}m$

Cs-O

P.R. Subramanian, 1990

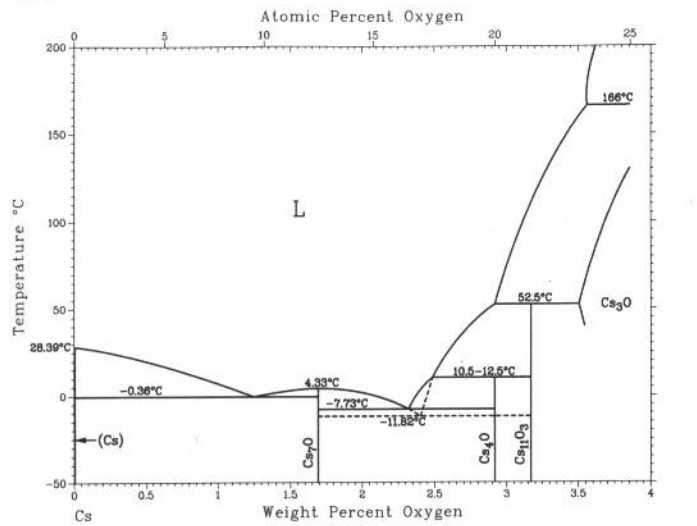

Phase	Composition, wt% O	Pearson symbol	Space group
(Cs)	~0	*cI*2	$Im\bar{3}m$
Cs_7O	~1.7	*hP*24	$P\bar{6}m2$
Cs_4O	3	...	...
$Cs_{11}O_3$(a)	~3.2	*mP*56	$P2_1/c$
Cs_3O	~4	...	...
Cs_2O	~5.7	*hR*3	$R\bar{3}m$
CsO	~10.7	*oI*8	*Immm*
Cs_2O_3	~15	*cI*28	$I\bar{4}3d$
CsO_2(LT)	~19.4	*tI*6	*I*4/*mmm*
CsO_2(HT)(b)	~19.4	*cF*8	$Fm\bar{3}m$

(a) Also reported as Cs_7O_2. (b) Above ~200 °C

Cs-Rb

C.W. Bale and A.D. Pelton, 1983

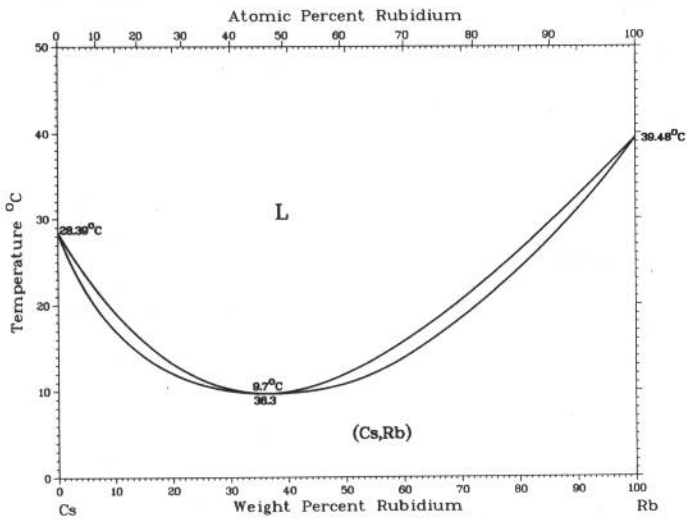

Phase	Composition, wt% Rb	Pearson symbol	Space group
(Cs,Rb)	0 to 100	*cI*2	$Im\bar{3}m$

Cs-S

From [Smithells]

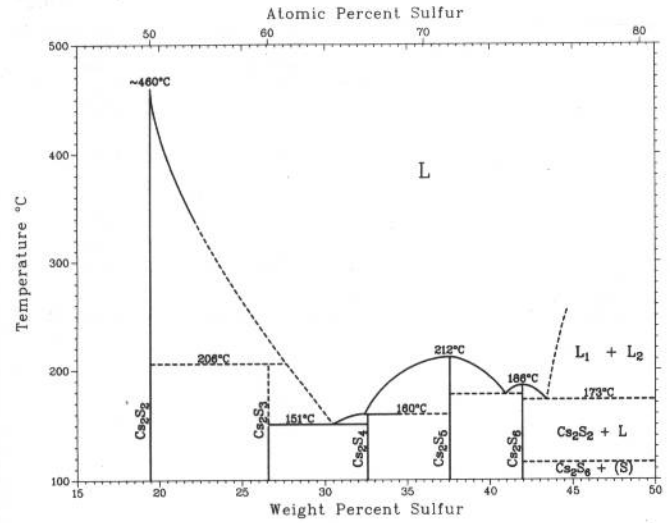

Phase	Composition, wt% S	Pearson symbol	Space group
Cs_2S_2	19.4	*oI*8	...
Cs_2S_3	27	*oC*20	$Cmc2_1$
Cs_2S_4	~34.7	...	...
Cs_2S_5	~40.0	...	...
Cs_2S_6	~42.5	...	...

Cs-Sb

F.W. Dorn and W. Klemm, 1961

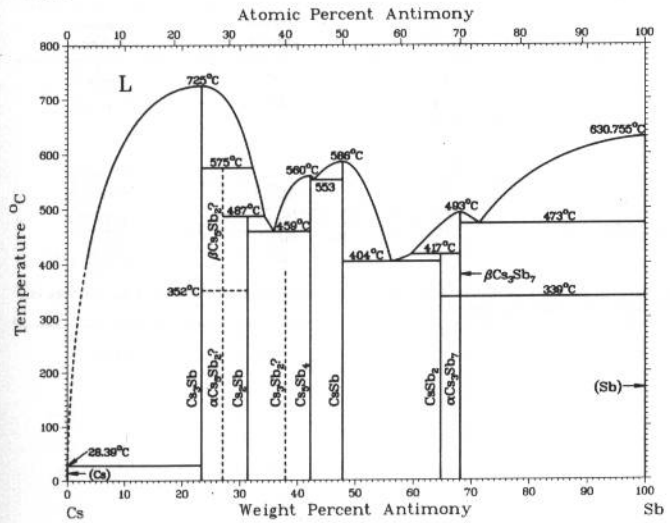

Phase	Composition, wt% Sb	Pearson symbol	Space group
(Cs)	0	*cI*2	$Im\bar{3}m$
Cs_3Sb	23	*cF*16	$Fd\bar{3}m$
αCs_5Sb_2	26.8	...	...
βCs_5Sb_2	26.8	...	...
Cs_2Sb	31	...	...
Cs_3Sb_2	38	...	...
Cs_5Sb_4	42.2	...	...
CsSb	47.8	*oP*16	$P2_12_12_1$
$CsSb_2$	64.7	...	...
αCs_3Sb_7	68	...	...
βCs_3Sb_7	68	...	...
(Sb)	100	*hR*2	$R\bar{3}m$

Cs-Se

H. Okamoto, 1990

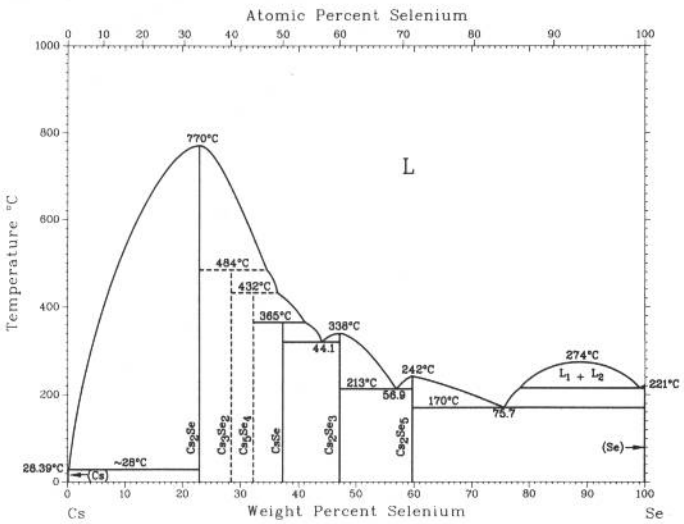

Phase	Composition, wt% Se	Pearson symbol	Space group
(Cs)	0	*cI*2	$Im\bar{3}m$
Cs_2Se	22.9	*oP*12	*Pnma*
Cs_3Se_2	28	...	...
Cs_5Se_4	32.2	...	...
CsSe	37.3	...	...
Cs_2Se_3	47	*oC*20	$Cmc2_1$
Cs_2Se_5	59.7	*oP*28	$P2_12_12_1$
(Se)	100	*hP*3	$P3_12_1$
High-pressure phase			
Cs_2Se	22.9	*oF*24	$Fdd\bar{2}$

Cs-Sn

L.Z. Melenkov, S.P. Yatsenko, K.A. Chantonov, and Yu.N. Grin, 1987

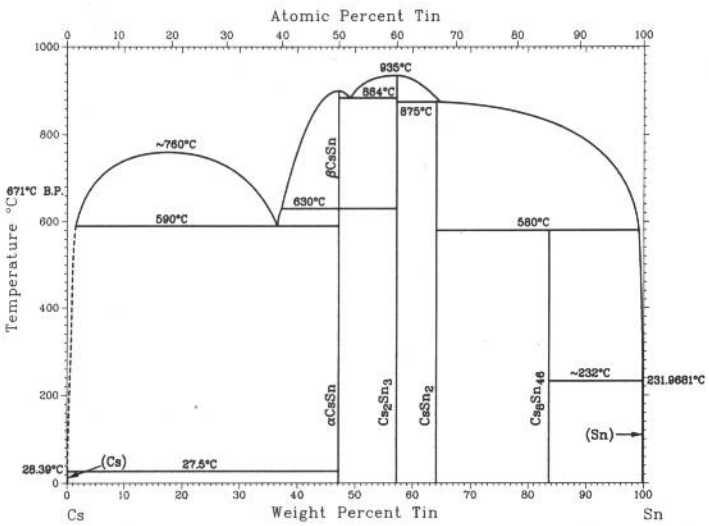

Phase	Composition, wt% Sn	Pearson symbol	Space group
(Cs)	~0	*cI*2	$Im\bar{3}m$
βCsSn	47.2	...	...
αCsSn	47.2	*tI*64	$I4_1/acd$
Cs_2Sn_3	57	...	...
$CsSn_2$	64.1	...	...
Cs_8Sn_{46}	84	...	$Pm\bar{3}n$
(βSn)(a)	~100	*tI*4	$I4_1/amd$
(αSn)(b)	~100	*cF*8	$Fd\bar{3}m$

(a) Between 13 and 231.9681 °C. (b) Below 13 °C

Cs-Te

J. Sangster and A.D. Pelton, unpublished

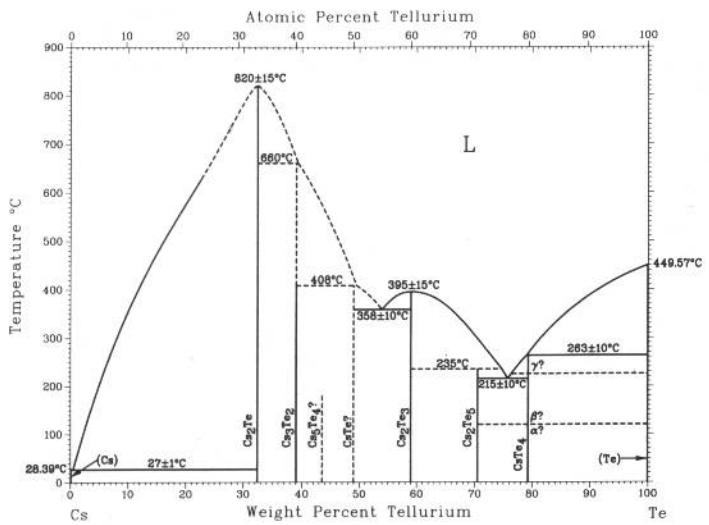

Phase	Composition, wt% Te	Pearson symbol	Space group
(Cs)	0	*cI*2	$Im\bar{3}m$
Cs_2Te	32.4	*oP*12	$P2_12_12_1$
Cs_3Te_2	39.0	...	...
Cs_5Te_4(a)	43.4	...	...
CsTe(a)	49.0	...	...
Cs_2Te_3	59	*oC*20	$Cmc2_1$
Cs_2Te_5	70.6	*oC*28	*Cmcm*
$CsTe_4$(b)	79	*mP*20	$P2_1/c$
(Te)	100	*hP*3	$P3_12_1$

(a) Might not exist. (b) Three allotropic forms have been reported to exist. If so, this is the structure of a metastable high-temperature allotrope.

Cs-Tl

V.D. Busmanov and S.P. Yatsenko, 1981

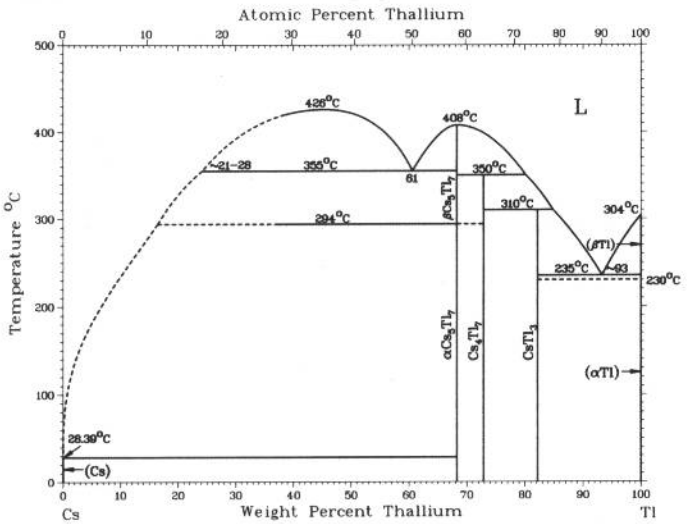

Phase	Composition, wt% Tl	Pearson symbol	Space group
(Cs)	0	*cI*2	$Im\bar{3}m$
αCs_5Tl_7	68.3	...	...
βCs_5Tl_7	68.3	...	...
Cs_4Tl_7	62.9	...	...
$CsTl_3$	82	...	...
(αTl)	100	*hP*2	$P6_3/mmc$
(βTl)	100	*cI*2	$Im\bar{3}m$

Cu-Dy

P.R. Subramanian and D.E. Laughlin, 1988

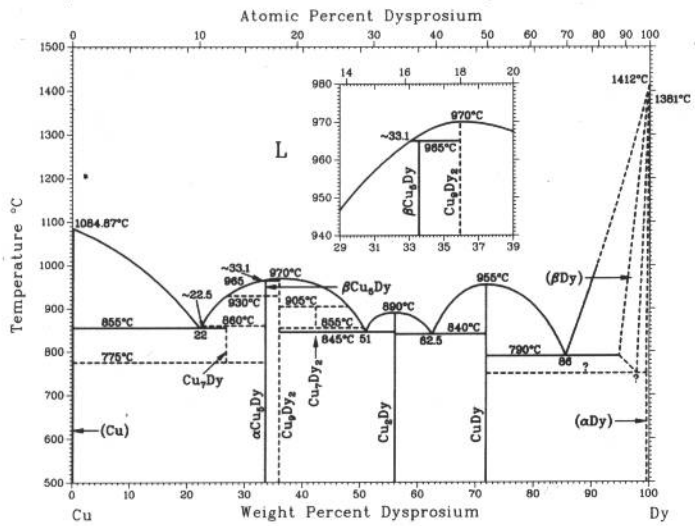

Phase	Composition, wt% Dy	Pearson symbol	Space group
(Cu)	0	*cF*4	$Fm\bar{3}m$
βCu_5Dy	~33.84	*hP*6	*P6/mmm*
αCu_5Dy	~33.84	*cF*24	$F\bar{4}3m$
Cu_2Dy	~56.1	*oI*12	*Imma*
CuDy	~72	*cP*2	$Pm\bar{3}m$
(α′Dy)	100	*oC*4	*Cmcm*
(αDy)	100	*hP*2	$P6_3/mmc$
(βDy)	100	*cI*2	$Im\bar{3}m$

Cu-Er

P.R. Subramanian and D.E. Laughlin, 1988

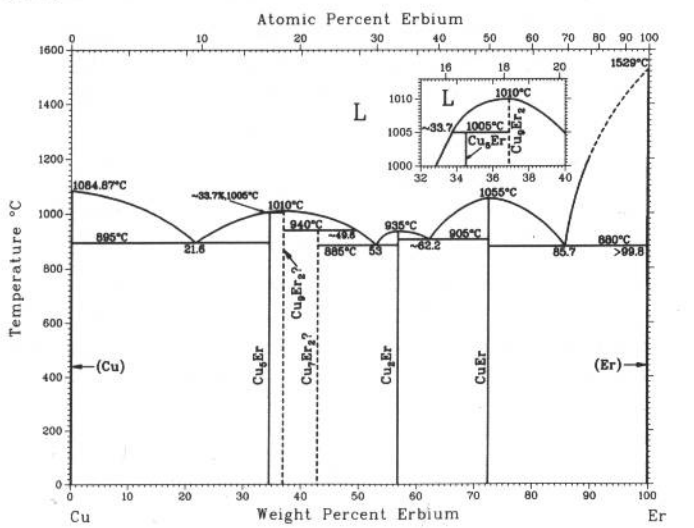

Phase	Composition, wt% Er	Pearson symbol	Space group
(Cu)	0	*cF*4	$Fm\bar{3}m$
Cu_5Er	~34.49	*cF*24	$F\bar{4}3m$
Cu_2Er	~56.8	*oI*12	*Imma*
CuEr	~73	*cP*2	$Pm\bar{3}m$
(Er)	100	*hP*2	$P6_3/mmc$

Cu-Eu

P.R. Subramanian and D.E. Laughlin, 1988

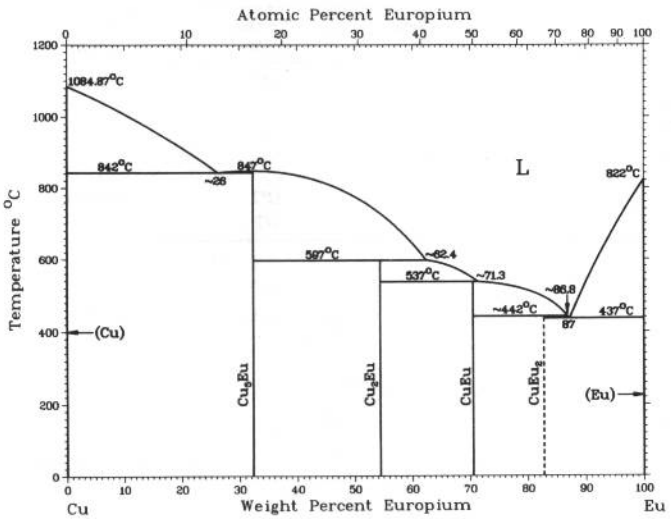

Phase	Composition, wt% Eu	Pearson symbol	Space group
(Cu)	0	*cF*4	$Fm\bar{3}m$
Cu_5Eu	~35.24	*hP*6	*P*6/*mmm*
Cu_2Eu	~57.6	*oI*12	*Imma*
CuEu	~73	*oP*8	*Pnma*
$CuEu_2$	~84.48	*oP*12	*Pnma*
(Eu)	100	*cI*2	$Im\bar{3}m$

Cu-Fe

L.J. Swartzendruber, 1992

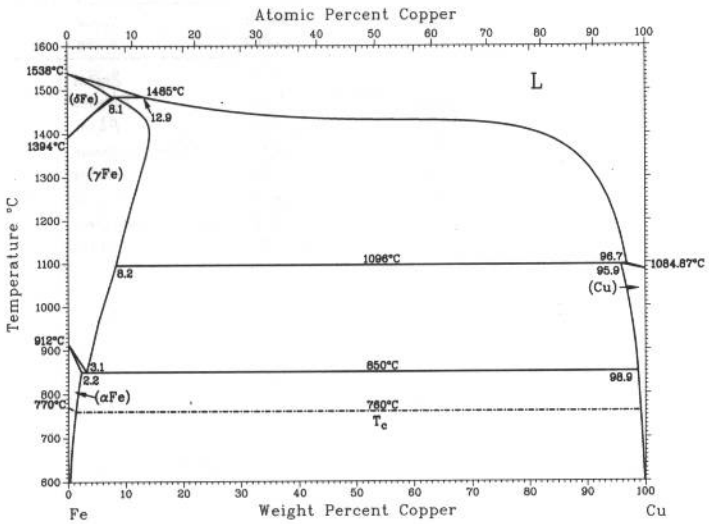

Phase	Composition, wt% Cu	Pearson symbol	Space group
(δFe)	0 to 7.6	*cI*2	$Im\bar{3}m$
(γFe)	0 to 13	*cF*4	$Fm\bar{3}m$
(αFe)	0 to 2.2	*cI*2	$Im\bar{3}m$
(Cu)	95.9 to 100	*cF*4	$Fm\bar{3}m$

Cu-Ga

P.R. Subramanian and D.E. Laughlin, unpublished

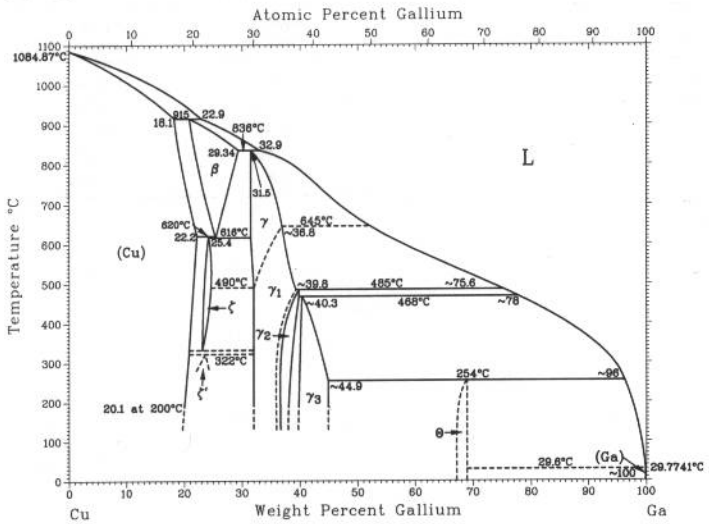

Phase	Composition, wt% Ga	Pearson symbol	Space group
(Cu)	0 to 22.2	*cF*4	$Fm\bar{3}m$
β	20.8 to 29.34	*cI*2	$Im\bar{3}m$
γ	31.5 to ~36.8	*cP*52	$P\bar{4}3m$
γ_1	31.8 to 39.8	*cP*52	$P\bar{4}3m$
γ_2	36.0 to 39.9	*cP*?(a)	$P\bar{4}3m$
γ_3	39.7 to ~44.9	*cP*?(a)	$P\bar{4}3m$
ζ	22.1 to 24.2	*hP*2	$P6_3/mmc$
ζ′	22.6 to 24.1	...	...
θ	66.7 to 68.70	*tP*3	*P*4/*mmm*
(Ga)	~100	*oC*8	*Cmca*

(a) The number of atoms/cell decreases from 52 to ~47, as the Ga contents decrease from 32.0 to 44.6 wt%.

Cu-Gd

P.R. Subramanian and D.E. Laughlin, 1988

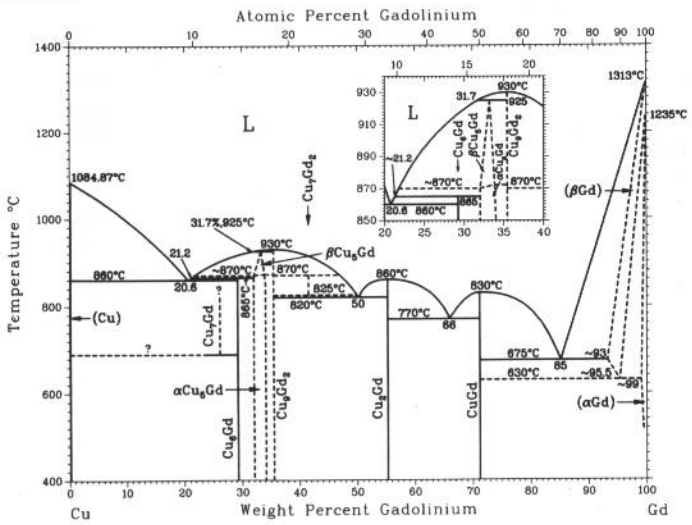

Phase	Composition, wt% Gd	Pearson symbol	Space group
(Cu)	0	*cF*4	$Fm\bar{3}m$
Cu_6Gd	~29.21	*oP*28	*Pnma*
βCu_5Gd	~32 to ~34.1	*hP*6	*P6/mmm*
αCu_5Gd	~32 to ~34.1	*cF*4	$F\bar{4}3m$
Cu_2Gd	~55.3	*oI*12	*Imma*
CuGd	~71.2	*cP*2	$Pm\bar{3}m$
(αGd)	~99.3 to 100	*hP*2	$P6_3/mmc$
(βGd)	~93 to 100	*cI*2	$Im\bar{3}m$

Cu-Ge

R.W. Olesinski and G.J. Abbaschian, 1986

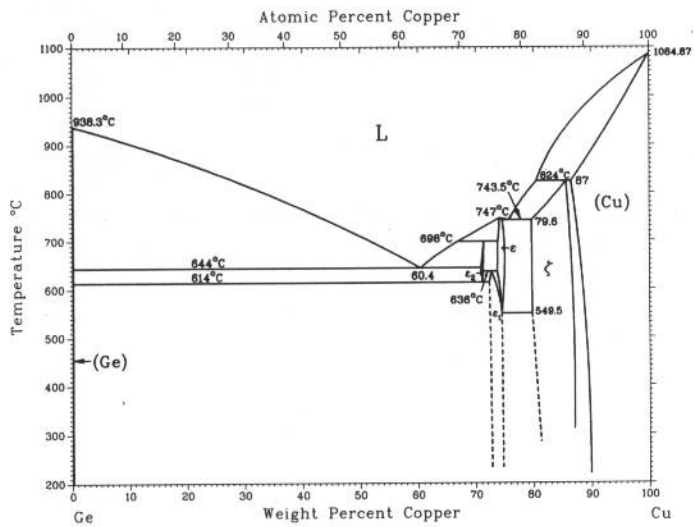

Phase	Composition, wt% Cu	Pearson symbol	Space group
(Ge)	0	*cF*8	$Fd\bar{3}m$
GeII (HP)	...	*tI*4	$I4_1/amd$
ε_2(a)	70.8 to 71.3	*cI*2	$Im\bar{3}m$
ε_1(a)	72.3 to 74.4	*oP*8	*Pmnm*
ε(a)	73.7 to 74.4	(b)	...
ζ(c)	79.6 to 87.1	*hP*2	$P6_3/mmc$
(Cu)	87 to 100	*cF*4	$Fm\bar{3}m$
Other reported phase			
γ″	75.6	(d)	...

(a) Also denoted as Cu_3Ge. (b) Rhombohedral. (c) Also denoted as Cu_5Ge. (d) Cubic

Cu-H

O.M. Barabash and Yu.N. Koval, 1986

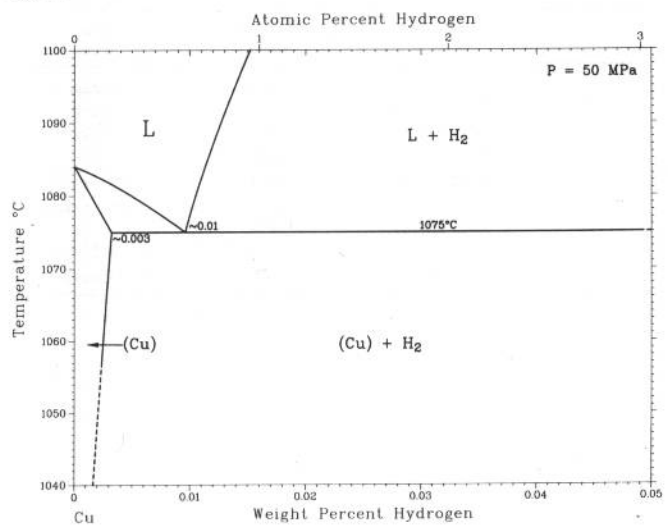

Phase	Composition, wt% H	Pearson symbol	Space group
(Cu)	0 to ~0.003	*cF*4	$Fm\bar{3}m$

Cu-Hf

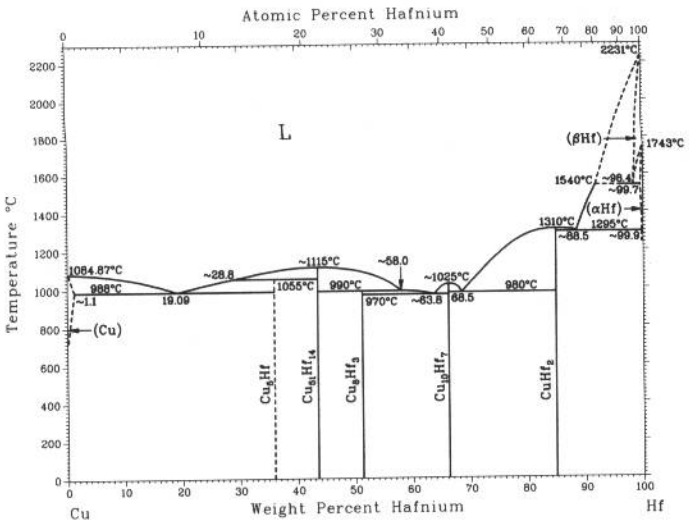

P.R. Subramanian and D.E. Laughlin, 1988

Phase	Composition, wt% Hf	Pearson symbol	Space group
(Cu)	0 to ~1.1	*cF*4	$Fm\bar{3}m$
$Cu_{51}Hf_{14}$	43.54	*hP*68	*P*6/*m*
Cu_8Hf_3	51.29	*oP*44	*Pnma*
$Cu_{10}Hf_7$	66.29	*oC*68	...
$CuHf_2$	84.89	*tI*6	*I*4/*mmm*
(αHf)	~99.7 to 100	*hP*2	$P6_3/mmc$
(βHf)	~98.4 to 100	*cI*2	$Im\bar{3}m$

Cu-Hg

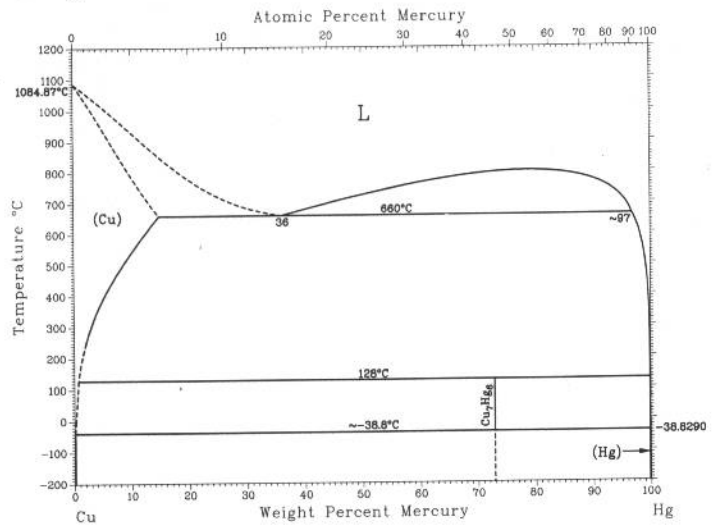

D.J. Chakrabarti and D.E. Laughlin, 1985

Phase	Composition, wt% Hg	Pearson symbol	Space group
(Cu)	0 to ?	*cF*4	$Fm\bar{3}m$
γ(a)	73	*hR*52	$R\bar{3}m$
(αHg)	100	*hR*1	$R\bar{3}m$
(βHg)	100	*tI*2	*I*4/*mmm*
(γHg)(b)	100	...	...

(a) Composition of the γ phase corresponds to stoichiometry Cu_7Hg_6. (b) Formed from αHg by strain-induced (martensitic) transformation at 4.2 K, reverting to αHg at 50 K

Cu-In

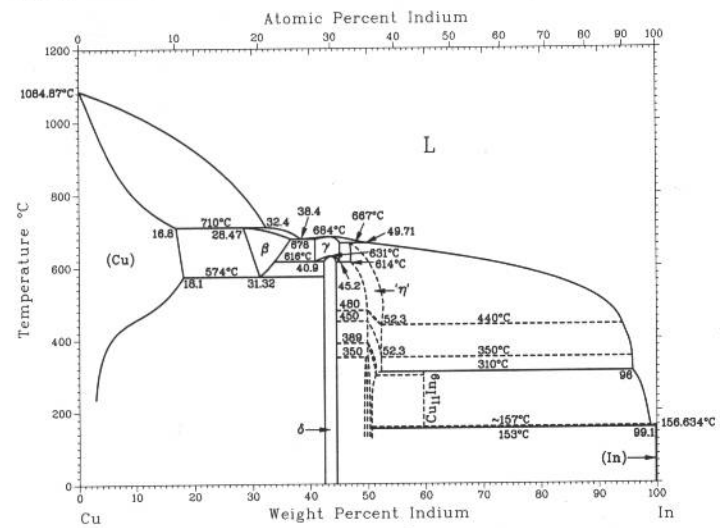

H. Okamoto, 1991

Phase	Composition, wt% In	Pearson symbol	Space group
(Cu)	0 to 18.1	*cF*4	$Fm\bar{3}m$
β	28.47 to 37.0	*cI*2	$Im\bar{3}m$
γ	40.9 to 45.2	*cP*52	$P\bar{4}3m$
δ	42.52 to 44.3	*aP*40	$P\bar{1}$
"η"	47.00 to 52.3	*hP*4	$P6_3/mmc$
		*hP*6	$P6_3/mmc$
	49.5 to 52.3	*o***	...
$Cu_{11}In_9$	~59	*mC*20	*C*2/*m*
(In)	~100	*tI*2	*I*4/*mmm*

Cu-Ir

D.J. Chakrabarti and D.E. Laughlin, 1987

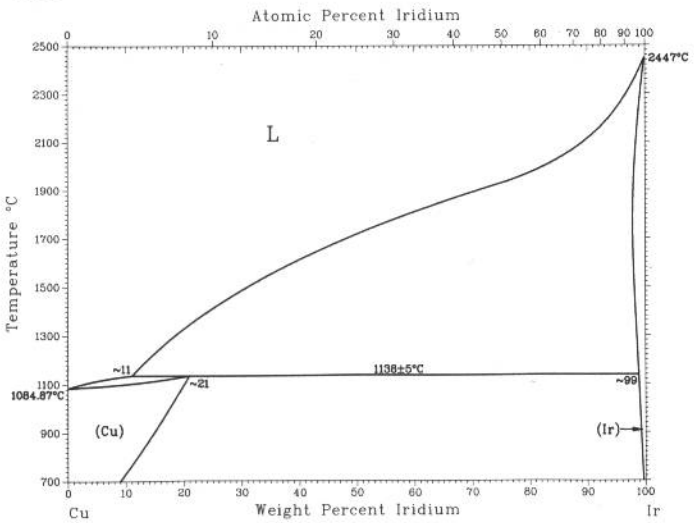

Phase	Composition, wt% Ir	Pearson symbol	Space group
(Cu)	0 to ~21	*cF*4	$Fm\bar{3}m$
(Ir)	~97.8 to 100	*cF*4	$Fm\bar{3}m$

Cu-La

H. Okamoto, 1991

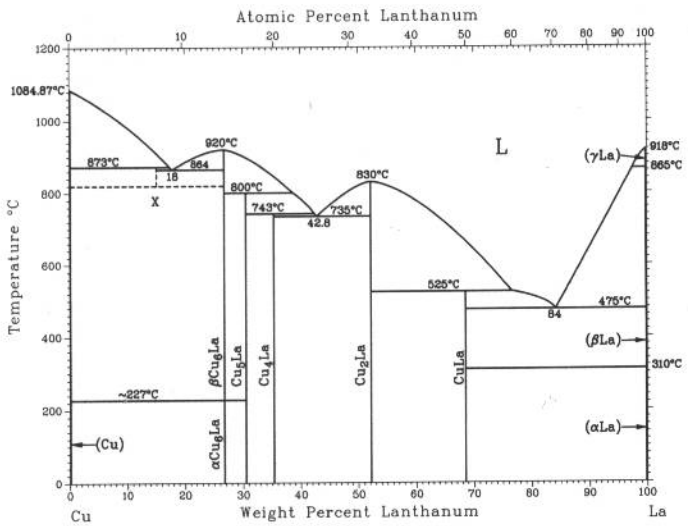

Phase	Composition, wt% La	Pearson symbol	Space group
(Cu)	~0	*cF*4	$Fm\bar{3}m$
X	15.1	...	...
βCu_6La	26.7	*oP*28	*Pnma*
αCu_6La(a)	26.7	*mP**	...
Cu_5La	30.3	*hP*6	*P6/mmm*
Cu_4La	35	*tI*90	$I\bar{4}m2$
Cu_2La	52.2	*hP*3	*P6/mmm*
CuLa	69	*oP*8	*Pnma*
(γLa)	~100	*cI*2	$Im\bar{3}m$
(βLa)	~100	*cF*4	$Fm\bar{3}m$
(αLa)	~100	*hP*4	$P6_3/mmc$

(a) Below ~227 °C

Cu-Li

A.D. Pelton, 1986

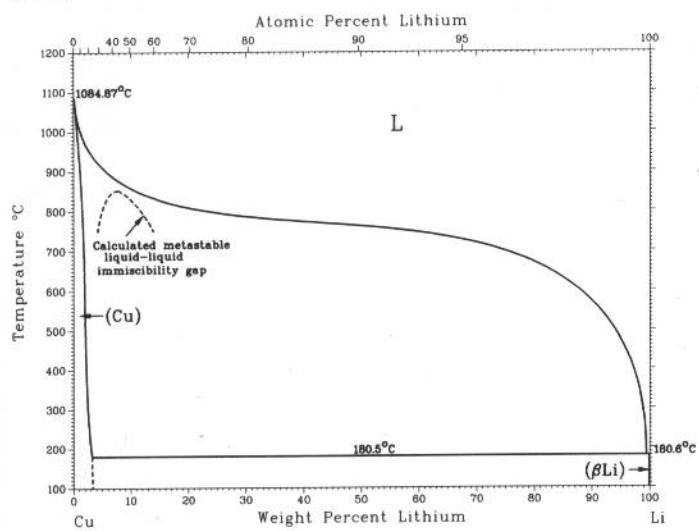

Phase	Composition, wt% Li	Pearson symbol	Space group
(Cu)	0 to 3	*cF*4	$Fm\bar{3}m$
(βLi)	100	*cI*2	$Im\bar{3}m$
(αLi)(a)	100	*hP*2	$P6_3/mmc$

(a) Below −193 °C

Cu-Mg

H. Okamoto, 1992

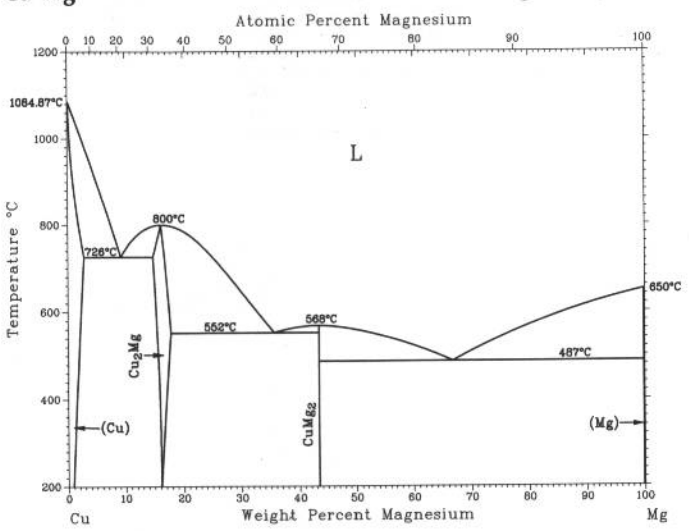

Phase	Composition, wt% Mg	Pearson symbol	Space group
(Cu)	0 to 2.77	*cF*4	$Fm\bar{3}m$
Cu_2Mg	15 to 18	*cF*24	$Fd\bar{3}m$
$CuMg_2$	43.4	*oF*48	*Fddd*
(Mg)	100	*hP*2	$P6_3/mmc$

Cu-Mn

N.A. Gokcen, unpublished

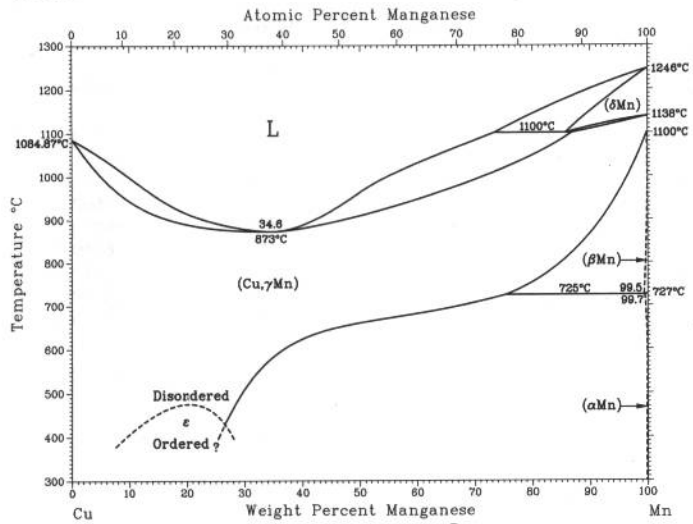

Phase	Composition, wt% Mn	Pearson symbol	Space group
(Cu,γMn)	0 to 100	*cF*4	$Fm\bar{3}m$
(δMn)	85.8 to 100	*cI*2	$Im\bar{3}m$
(βMn)	99.5 to 100	*cP*20	$P4_132$
(αMn)	99.7 to 100	*cI*58	$I\bar{4}3m$

Cu-Nb

H. Okamoto, 1991

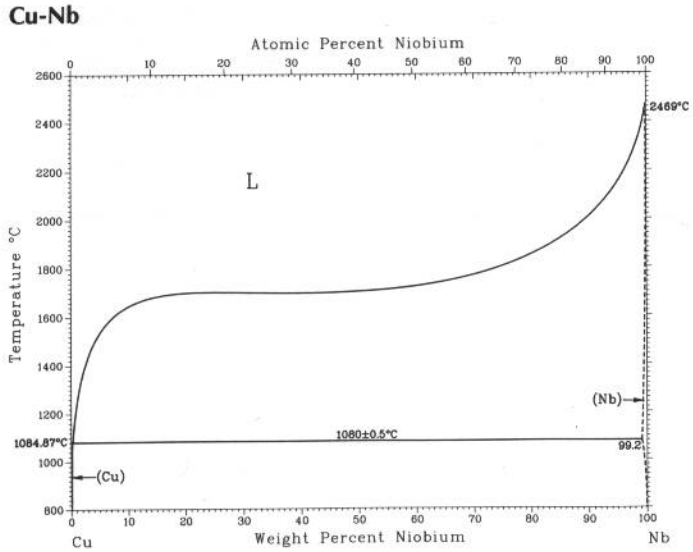

Phase	Composition, wt% Nb	Pearson symbol	Space group
(Cu) or α	0 to 0.15	*cF*4	$Fm\bar{3}m$
(Nb) or β	99.2 to 100	*cI*2	$Im\bar{3}m$

Enlargement of the Cu-rich portion of the Cu-Nb system

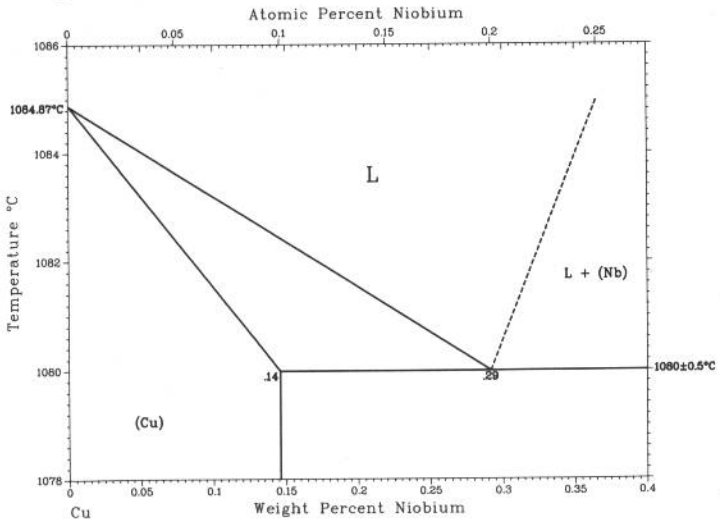

Cu-Nd

P.R. Subramanian and D.E. Laughlin, 1988

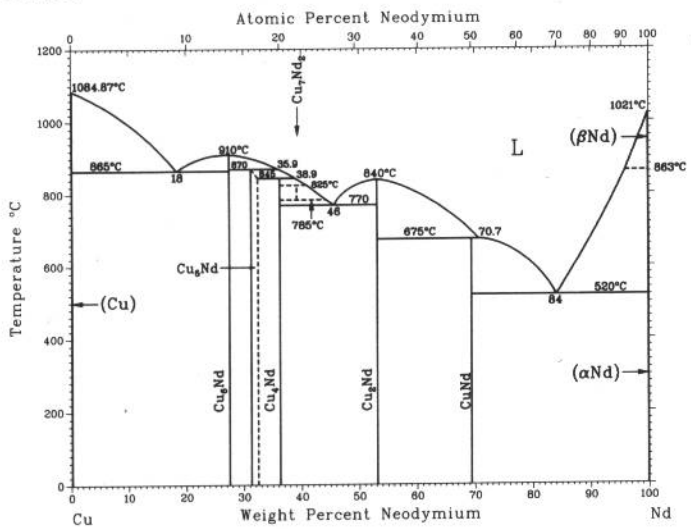

Phase	Composition, wt% Nd	Pearson symbol	Space group
(Cu)	0	*cF*4	$Fm\bar{3}m$
Cu_6Nd	~27.45	*oP*28	*Pnma*
Cu_5Nd	~31.23	*hP*6	*P6/mmm*
Cu_4Nd	~36.2	...	*Pnnm*
Cu_2Nd	~53.1	*oI*12	*Imma*
CuNd	~69	*oP*8	*Pnma*
(βNd)	100	*cI*2	$Im\bar{3}m$
(αNd)	100	*hP*4	$P6_3/mmc$

Cu-Ni

D.J. Chakrabarti, D.E. Laughlin, S.W. Chen, and Y.A. Chang, 1991

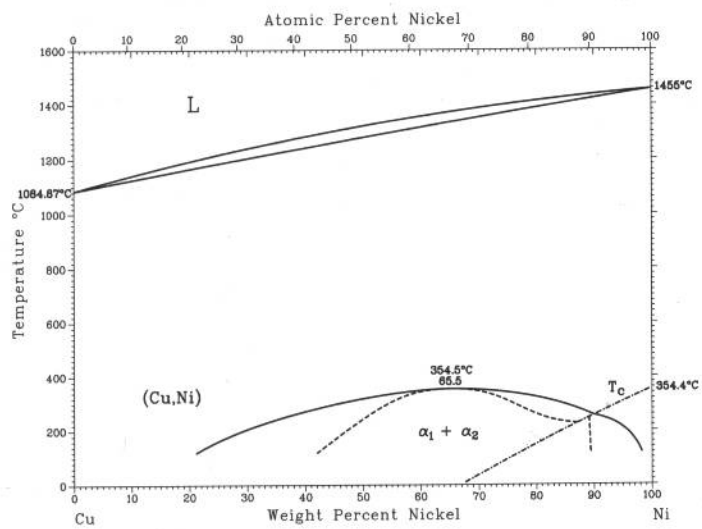

Phase	Composition, wt% Ni	Pearson symbol	Space group
(Cu,Ni)	0 to 100(a)	*cF*4	$Fm\bar{3}m$

(a) Above 354.5 °C

Cu-O

J.P. Neumann, T. Zhong, and Y.A. Chang, 1984

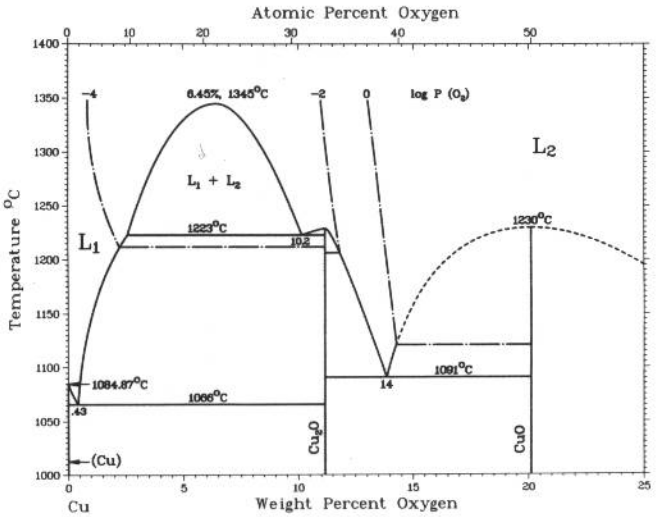

Phase	Composition, wt % O	Pearson symbol	Space group
(Cu)	0 to 0.008	*cF*4	$Fm\bar{3}m$
Cu_2O(a)	11.2	*cP*6	$Pn\bar{3}m$
CuO(b)	20	*mC*8	...
Cu_4O_3(c)	15.9	*tI*28	*I*4/*mcm*

(a) κ or cuprite. (b) τ or tenorite. (c) Additional possible phase, π or paramelaconite

Cu-O stability diagram

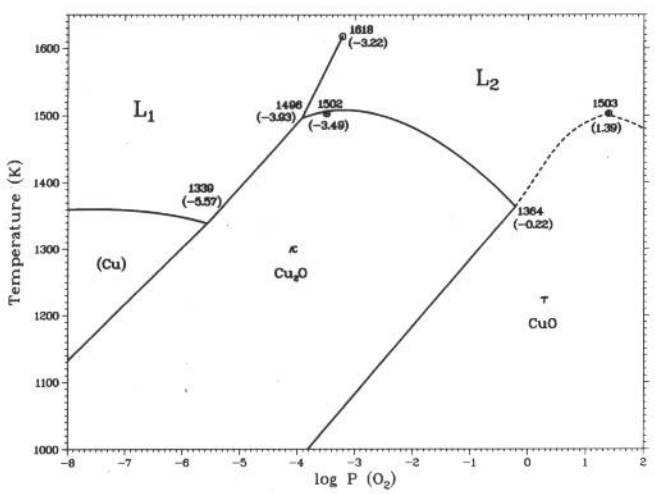

Solubility of O in (Cu)

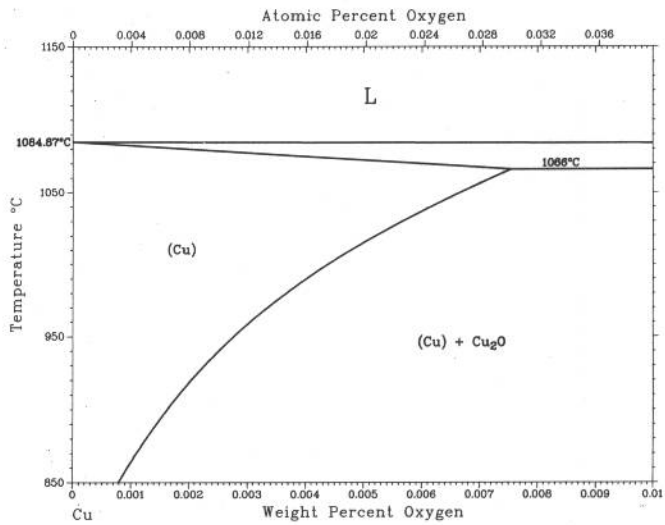

Cu-P

H. Okamoto, 1990

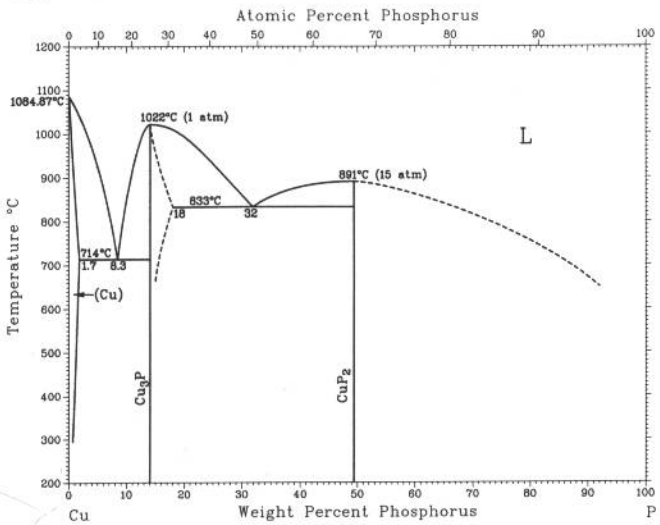

Phase	Composition, wt % P	Pearson symbol	Space group
(Cu)	0 to 1.7	*cF*4	$Fm\bar{3}m$
Cu_3P	14 to 18	*hP*24	$P6_3cm$
CuP_2	49.4	*mP*12	$P2_1/c$
Cu_2P_7(a)	63.1	*mC*72	*C*2/*m*

(a) Not shown in the diagram

Cu-Pb

D.J. Chakrabarti and D.E. Laughlin, 1984

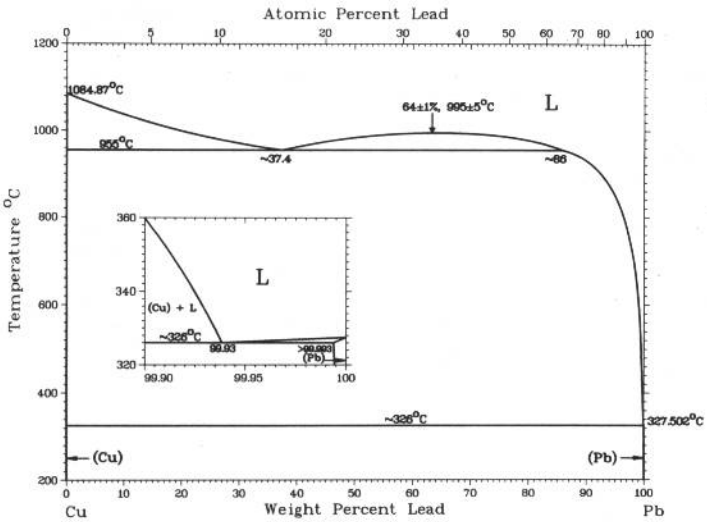

Phase	Composition, wt% Pb	Pearson symbol	Space group
(Cu)	0(a)	*cF*4	$Fm\bar{3}m$
(αPb)	100	*cF*4	$Fm\bar{3}m$
(βPb)(b)	100	*hP*2	$P6_3/mmc$

(a) Metastable solid solubility may extend up to 10.0 to 12.0 wt% Pb. (b) Above 10.3 GPa

Cu-Pd

P.R. Subramanian and D.E. Laughlin, 1991

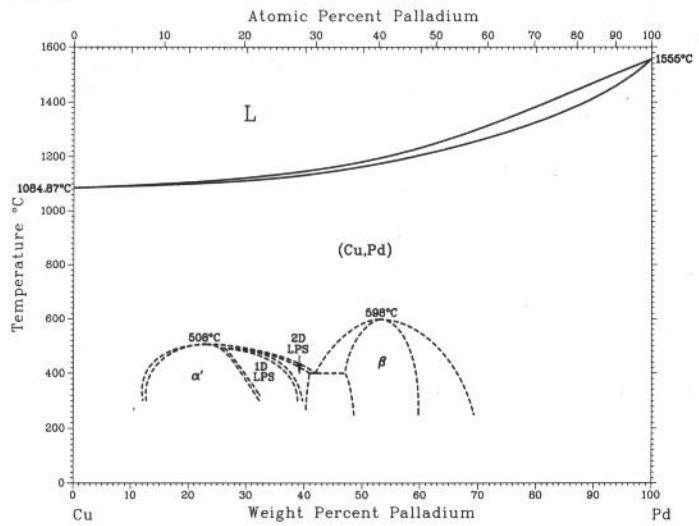

Phase	Composition, wt% Pd	Pearson symbol	Space group
(Cu,Pd)	0 to 100	*cF*4	$Fm\bar{3}m$
Cu_3Pd (α′)	~12.1 to ~32	*cP*4	$Pm\bar{3}m$
Cu_3Pd (α″)			
1D-LPS	~26 to ~39	*tP*28	*P*4*mm*
2D-LPS	~28 to ~43	...	...
CuPd (β)	~49 to ~60	*cP*2	$Pm\bar{3}m$

Cu-Pt

P.R. Subramanian and D.E. Laughlin, unpublished

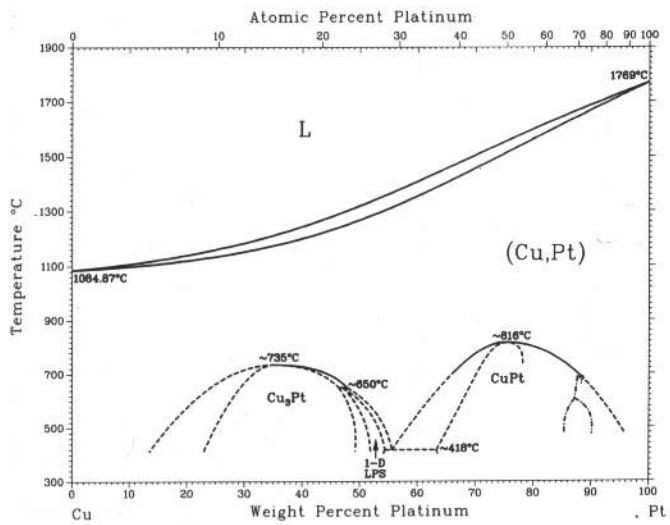

Phase	Composition, wt% Pt	Pearson symbol	Space group
(Cu,Pt)	0 to 100	*cF*4	$Fm\bar{3}m$
Cu_3Pt	~16 to ~52	*cP*4	$Pm\bar{3}m$
1D-LPS	~43 to ~56	*tP*28	*P*4*mm*
CuPt	~63 to ~81	*hR*32	$R\bar{3}m$
Cu_3Pt_5	~85 to ~88	*hR**	?
$CuPt_3$	~87 to ~90	*o***	?
$CuPt_3$	~88 to ?	*c***	?

Cu-Pu

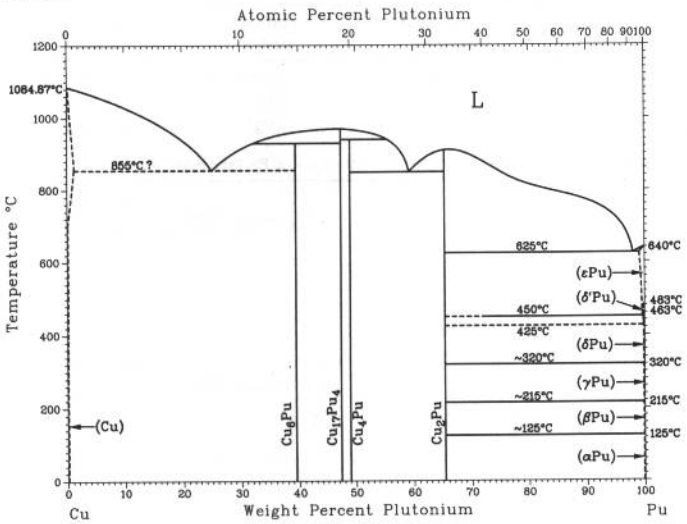

V.I. Kutaitsev, N.T. Chebotarev, I.G. Lebedev, M.A. Andrianov, V.N. Konev, and T.S. Menshikova, 1967

Phase	Composition, wt% Pu	Pearson symbol	Space group
(Cu)	0	*cF*4	$Fm\bar{3}m$
Cu_6Pu	39.1	...	...
$Cu_{17}Pu_4$	47.4	...	...
Cu_4Pu	49	*o**20	...
Cu_2Pu	65.7	*oI*12	*Imma*
(εPu)	? to 100	*cI*2	$Im\bar{3}m$
(δ'Pu)	100	*tI*2	*I*4/*mmm*
(δPu)	100	*cF*4	$Fm\bar{3}m$
(γPu)	100	*oF*8	*Fddd*
(βPu)	100	*mC*34	*C*2/*m*
(αPu)	100	*mP*16	$P2_1/m$

Cu-Rh

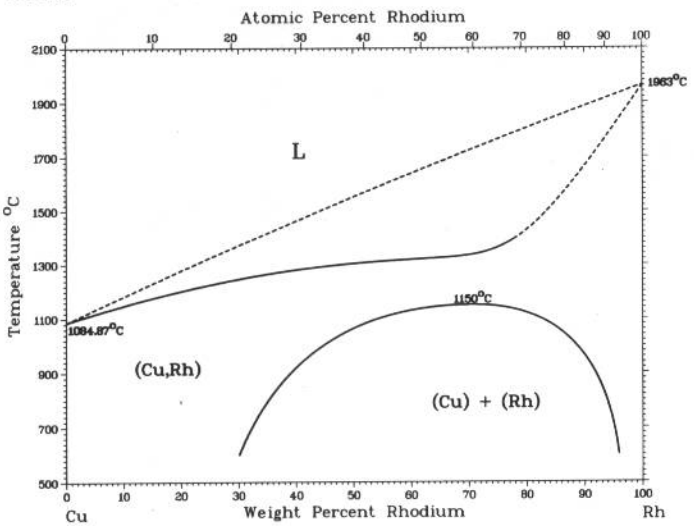

D.J. Chakrabarti and D.E. Laughlin, 1982

Phase	Composition, wt% Rh	Pearson symbol	Space group
(Cu,Rh)	0 to 100	*cF*4	$Fm\bar{3}m$

Cu-S

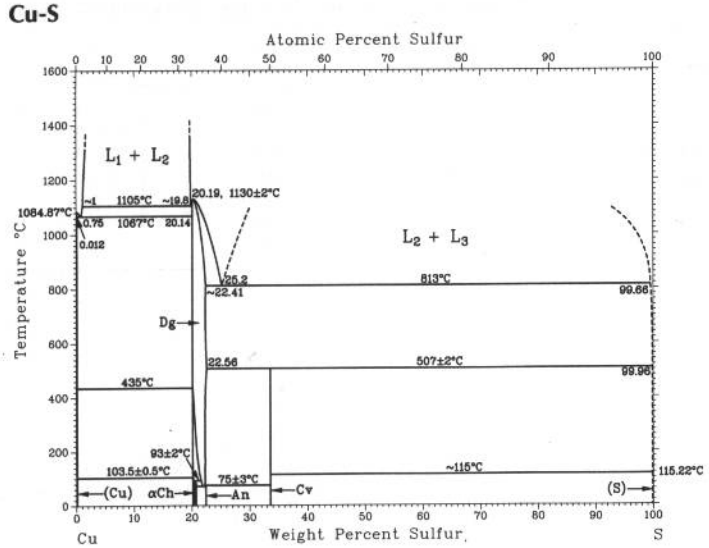

Enlargement of the Cu-S diagram from 0 to 160 °C

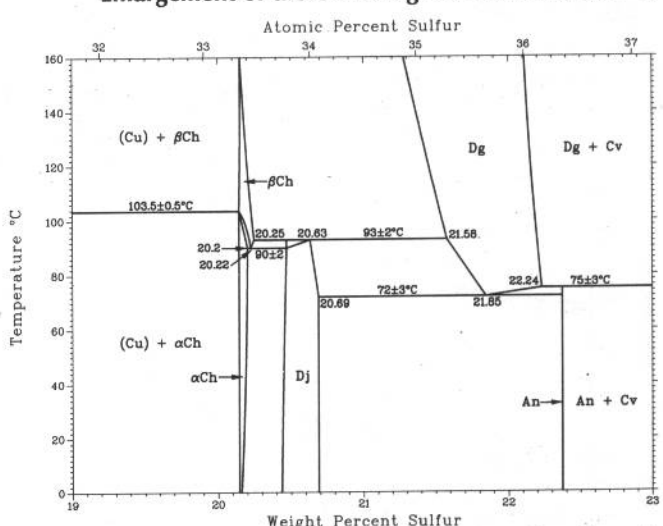

(continued)

Cu-saturated boundary of digenite

D.J. Chakrabarti and D.E. Laughlin, 1983

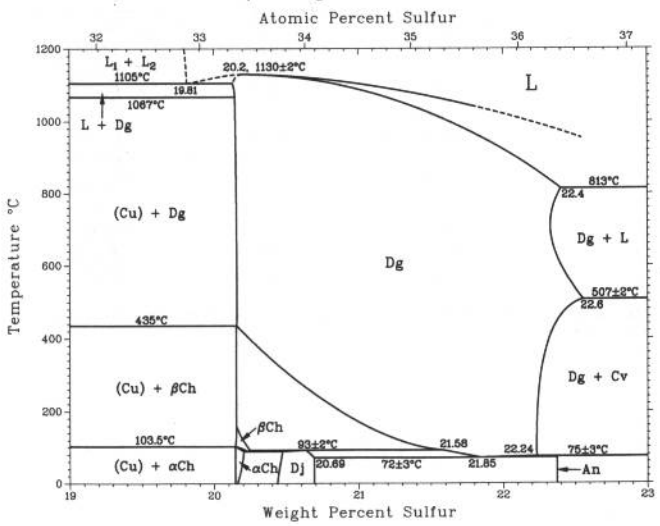

Phase	Composition, wt% S(Cu/S)	Pearson symbol	Space group
(Cu)	0 to 0.012	*cF*4	$Fm\bar{3}m$
α chalcocite (αCu_2S)	20.14 to 20.01	*mP*144(?)	$P2_1/c$
β chalcocite (βCu_2S)	20.14 to 20.22	*hP*6	$P6_3/mmc$
Djurleite ($Cu_{\sim 1.96}S$)	20.4 to 20.69	*oP*380(?)	*Pmnm* $P2_1nm$(?) $Pmn2_1$
Digenite ($Cu_{2-\delta}S$)	20.14 to 22.24	*cF*12	$Fm\bar{3}m$
Anilite($Cu_{1.75}S$)	22.38 ± 0.03	*oP*44(?)	*Pnma*
Covellite (CuS)	33.5	*hP*12	$P6_3/mmc$
(S)	~100	*oF*128 *mP*48 *hR*6	*Fddd* $P2_1/a$ $R\bar{3}$
Metastable phases			
Protodjurleite	20.4 (1.00)(a) 20.5 (0.999)(b)	...	...
Tetragonal Hexagonal-tetragonal	20.5 (0.999)	*tP*12	$P4_32_12$
Cu_xS	20.7 to 22.4 (0.98 to 0.89)	...	...
Low digenite (αDg)	21.99 to 22.22 (0.911 to 0.899)(c)	...	$R\bar{3}m$
Blaubleibender covellite I	26.5 ± 1.4 (0.71 ± 0.5)	...	...
Blaubleibender covellite II	31.6 ± 1.95 (0.6 ± 0.1)	...	...
CuS_2	50.23 (0.3)	...	*Pa*3(?)

(a) At 75 °C. (b) At 93 °C. (c) At 25 °C

Cu-Sb

P.R. Subramanian, 1990

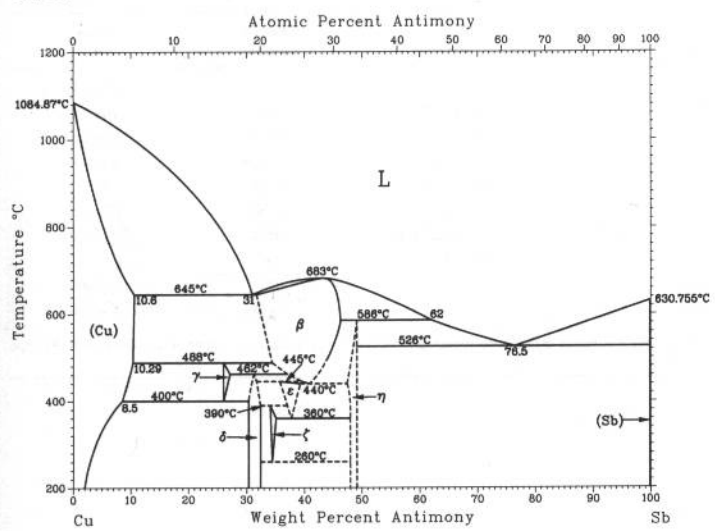

Phase	Composition, wt% Sb	Pearson symbol	Space group
(Cu)	0 to 10.6	*cF*4	$Fm\bar{3}m$
β	31.6 to 46.0	*oF*16	$Fm\bar{3}m$
γ	~26.0 to 26.7	*hP*2	$P6_3/mmc$
δ	30.3 to 32	*hP*?	$P6_3/mmc$
ε	~36.1 to 39.4	*oP*8	*Pmmn*
ζ	~34.1 to 34.5	*hP*26	$P\bar{3}$
η	~47.4 to 48.9	*tP*6	$P4/nmm$
(Sb)	~100	*hR*2	$R\bar{3}m$

Cu-Se

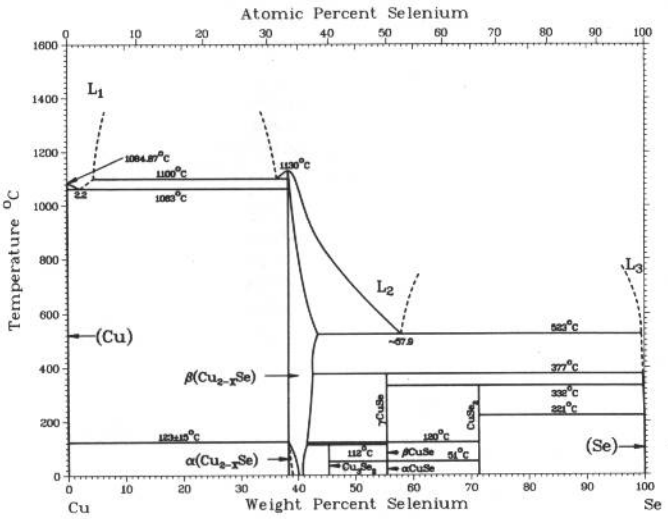

D.J. Chakrabarti and D.E. Laughlin, 1981

Phase	Composition, wt% Se	Pearson symbol	Space group
(Cu)	~0	*cF*4	$Fm\bar{3}m$
$\alpha Cu_{2-x}Se$	~38.3 to 38.8	(a)	...
$\beta Cu_{2-x}Se$	~38.3 to 41.6(b)	*cF*12	$Fm\bar{3}m$
Cu_3Se_2	45	...	$P\bar{4}2_1m$
αCuSe	55.4	...	$P6_3/mmc$
βCuSe	55.4	...	...
γCuSe	55.4	...	$P6_3/mmc$
$CuSe_2$	71.3	*oP*6	*Pnnm*
(Se)	~100	*hP*3	$P3_121$

(a) Monoclinic. (b) Homogeneity range at room temperature, $0.18 \le x \le 0.22$, and at 500 °C, $x = 0$ to −0.26

Cu-Si

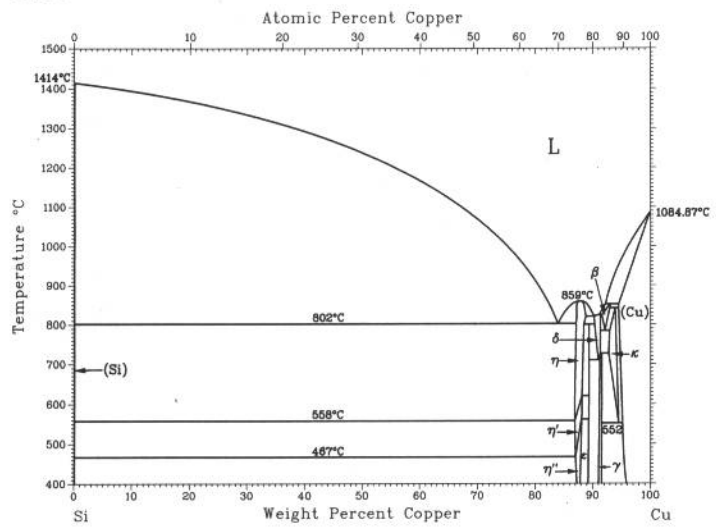

R.W. Olesinski and G.J. Abbaschian, 1986

Phase	Composition, wt% Cu	Pearson symbol	Space group
(Si)	0	*cF*8	$Fd\bar{3}m$
SiII (HP)	0	*tI*4	$I4_1/amd$
η″(a)	87.2 to 88.16	(b)	...
η′(a)	87.0 to 88.22	(c)	$R\bar{3}$
η(a)	87.2 to 88.8	(c)	$R\bar{3}m$
ε(d)	89.3 to 89.4	(e)	...
δ	90.3 to 91.4	(f)	...
γ(g)	91.4 to 91.62	*cP*20	$P4_132$
β	91.6 to 93.2	*cI*2	$Im\bar{3}m$
κ(h)	93.0 to 94.80	*hP*2	$P6_3/mmc$
(Cu)	94.6 to ~100	*cF*4	$Fm\bar{3}m$
Other reported phases			
η″(j)	...	(f)	...
Metastable	...	(f)	...

(a) Also denoted Cu_3Si. (b) Orthorhombic. (c) Rhombohedral. (d) Also denoted $Cu_{15}Si_4$. (e) Cubic. (f) Tetragonal. (g) Also denoted Cu_5Si. (h) Also denoted Cu_7Si. (j) Originally denoted η′

Cu-Sn

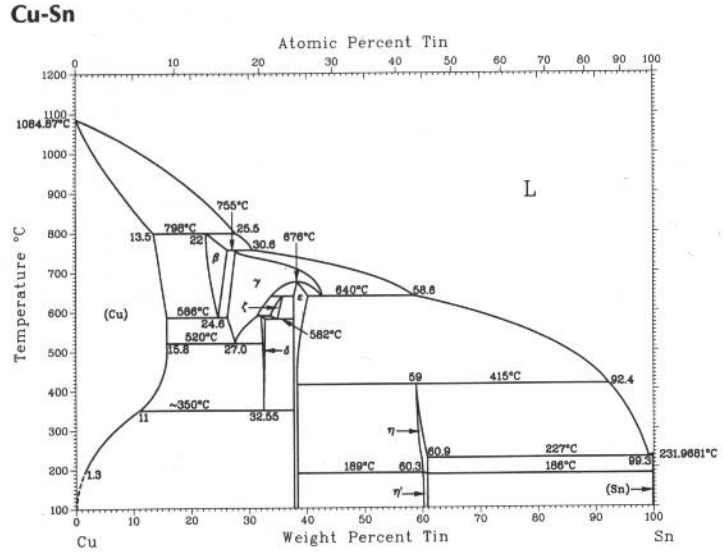

N. Saunders and A.P. Miodownik, 1990

Phase	Composition, wt% Sn	Pearson symbol	Space group
α	0 to 15.8	*cF*4	$Fm\bar{3}m$
β	22.0 to 27.0	*cI*2	$Im\bar{3}m$
γ	25.5 to 41.5	*cF*16	$Fm\bar{3}m$
δ	32 to 33	*cF*416	$F\bar{4}3m$
ζ	32.2 to 35.2	*hP*26	$P6_3$
ε	27.7 to 39.5	*oC*80	*Cmcm*
η	59.0 to 60.9	*hP*4	$P6_3/mmc$
η′	44.8 to 60.9	(a)	...
(βSn)	~100	*tI*4	$I4_1/amd$
(αSn)	100	*cF*8	$Fd\bar{3}m$

Note: Lattice parameter data can be found in [Pearson3]. (a) Hexagonal; superlattice based on NiAs-type structure

Cu-Sr

D.J. Chakrabarti and D.E. Laughlin, 1984

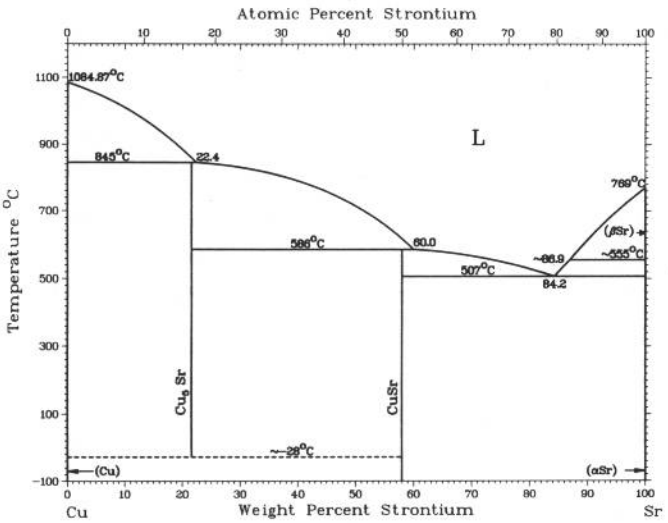

Phase	Composition, wt% Sr	Pearson symbol	Space group
(Cu)	0	*cF*4	$Fm\bar{3}m$
Cu_5Sr	21.62	*hP*6	*P*6/*mmm*
CuSr	58.0	*hP*8(?)	$P6_3/mmc$
(βSr)	100	*cI*2	$Im\bar{3}m$
(αSr)	100	*cF*4	$Fm\bar{3}m$
Pressure-stabilized form			
βSr or Sr-II	100	*cI*2	$Im\bar{3}m$

Cu-Te

H. Okamoto, unpublished

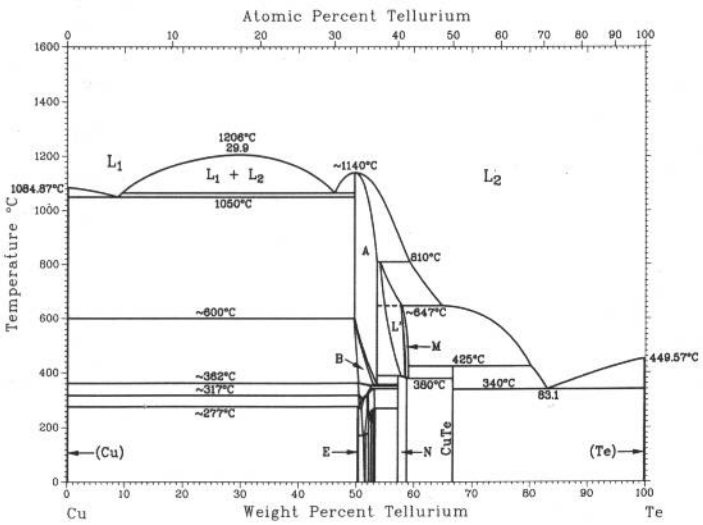

Phase	Composition, wt% Te	Pearson symbol	Space group
(Cu)	0	*cF*2	$Fm\bar{3}m$
Cu_2Te group			
A	50 to 53.6	*cF*12	$Fd\bar{3}m$
B	50 to 52.99	*hP*6	*P*6/*mmm*
C	50.4 to 52.5	*hP**	...
D	50.46 to 51.1	*o***	...
E	50.3 to 50.46	*o***	...
F	51.0 to 52	*o***	...
G	51.3 to 51.6	*o***	...
H	52.12 to 53.1	*hP*72	*P*3*m*1
I	52.23 to 52.88	...	...
J	52.23 to 52.6	*hP**	...
K	52.9 to 53.3	*hP*22	*P*3*m*1
L	54 to 58	*tP*6	*P*4/*nmm*
L'	55 to 58	...	...
M	58 to 59	...	...
N	57 to 58.8	...	...
CuTe	67	*oP*4	*Pmmn*
(Te)	100	*hP*3	$P3_121$
High-pressure phase			
$CuTe_2$	50.1	*cP*12	*Pa*3

Details of the Cu-Te phase diagram from 49.7 to 53.6 wt% Te

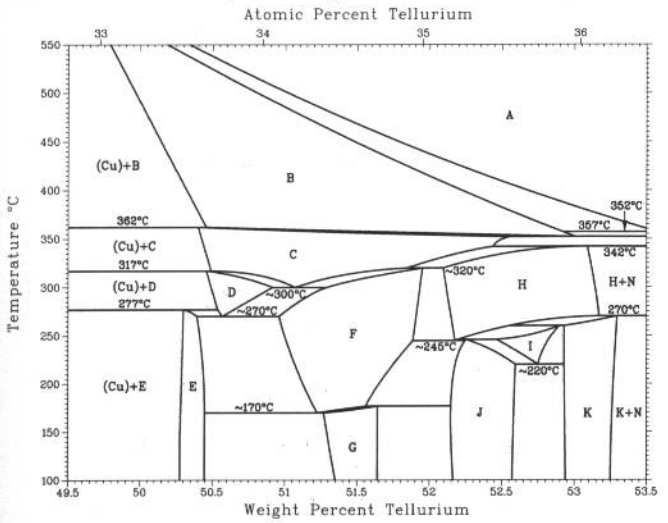

Cu-Th

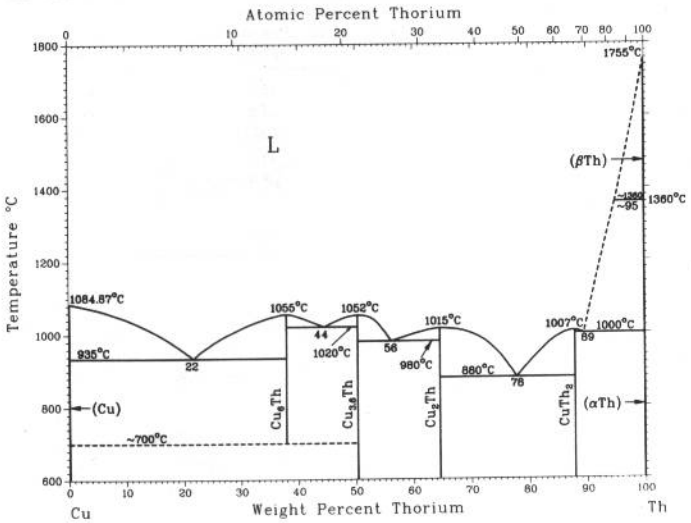

D.J. Chakrabarti, D.E. Laughlin, and D.E. Peterson, 1986

Phase	Composition, wt% Th	Pearson symbol	Space group
(Cu)	0	*cF*4	$Fm\bar{3}m$
Cu_6Th	37.84	*oP*28?	*Pnma*
$Cu_{3.6}Th$	50.36	(a)	*P6/m*
Cu_2Th	64.61	*hP*3	*P6/mmm*
CuTh(b)	79	*oC*8	*Cmcm*
$CuTh_2$	87.96	*tI*12	*I4/mcm*
(βTh)	100	*cI*2	$Im\bar{3}m$
(αTh)	100	*cF*4	$Fm\bar{3}m$

(a) Hexagonal. (b) Metastable

Cu-Ti

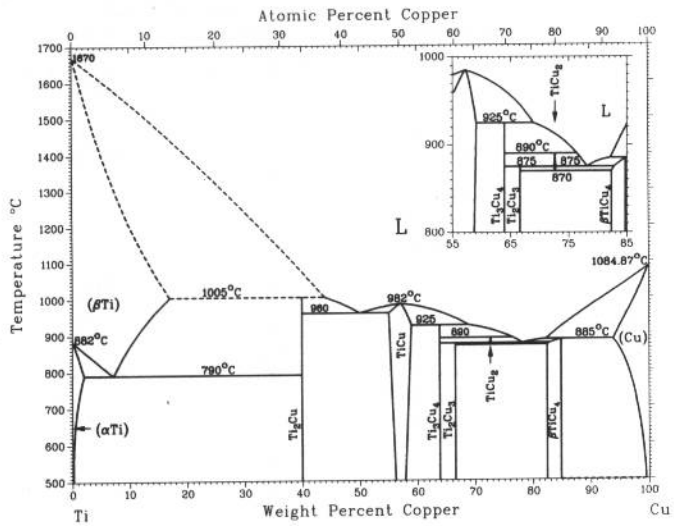

J.L. Murray, 1987

Phase	Composition, wt% Cu	Pearson symbol	Space group
(αTi)	0 to 2.1	*hP*2	$P6_3/mmc$
(βTi)	0 to 17.2	*cI*2	$Im\bar{3}m$
Ti_2Cu	39.9	*tI*6	*I4/mmm*
TiCu	55 to 59	*tP*4	*P4/nmm*
Ti_3Cu_4	63.9	*tI*14	*I4/mmm*
Ti_2Cu_3	67	*tP*10	*P4/nmm*
$TiCu_2$	72.7	*oC*12	*Amm*2
$TiCu_4$	83 to 84.9	*oP*20	*Pnma*
$\alpha TiCu_4$	~83 to 84.9	*tI*10	*I4/m*
(Cu)	94 to 100	*cF*4	$Fm\bar{3}m$
Metastable phases			
$TiCu_3$	...	*oP*8	*Pmnm*
β″	...	*tP*2	*P4/mmm*

Transformation of $\beta TiCu_4 \leftrightarrow \alpha TiCu_4$

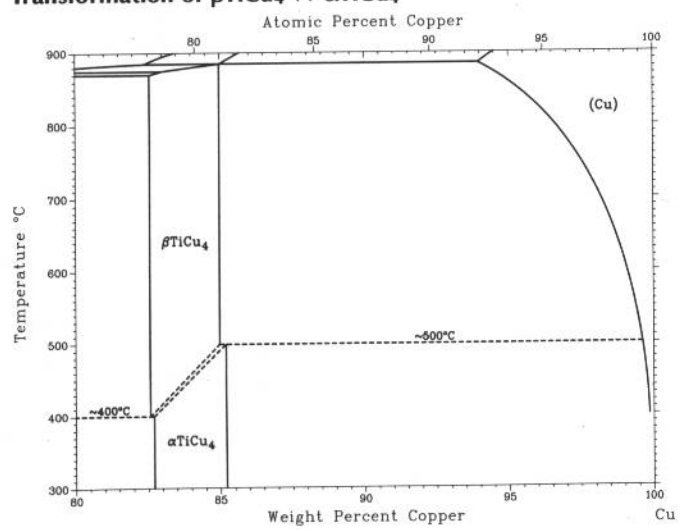

Cu-Tl

D.J. Chakrabarti and D.E. Laughlin, 1984

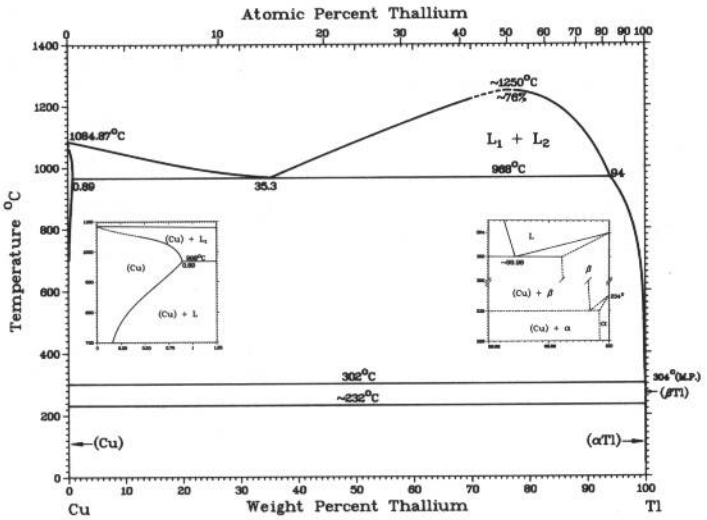

Phase	Composition, wt% Tl	Pearson symbol	Space group
(Cu)	0 to 0.89	*cF*4	$Fm\bar{3}m$
(αTl)	100	*hP*2	$P6_3/mmc$
(βTl)	100	*cI*2	$Im\bar{3}m$
Pressure-stabilized phase			
γTl	100	*cF*?	...

Cu-V

J.F. Smith and O.N. Carlson, 1989

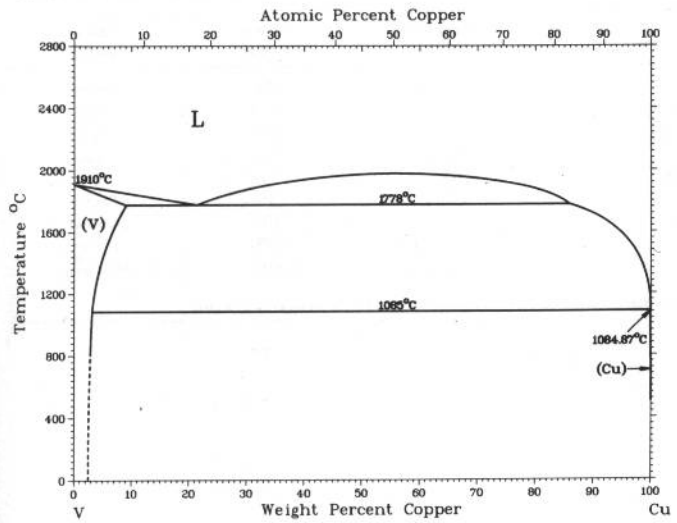

Phase	Composition, wt% Cu	Pearson symbol	Space group
(V)	0 to 9.2	*cI*2	$Im\bar{3}m$
(Cu)	99.9 to 100	*cF*4	$Fm\bar{3}m$

Cu-Yb

P.R. Subramanian and D.E. Laughlin, 1988

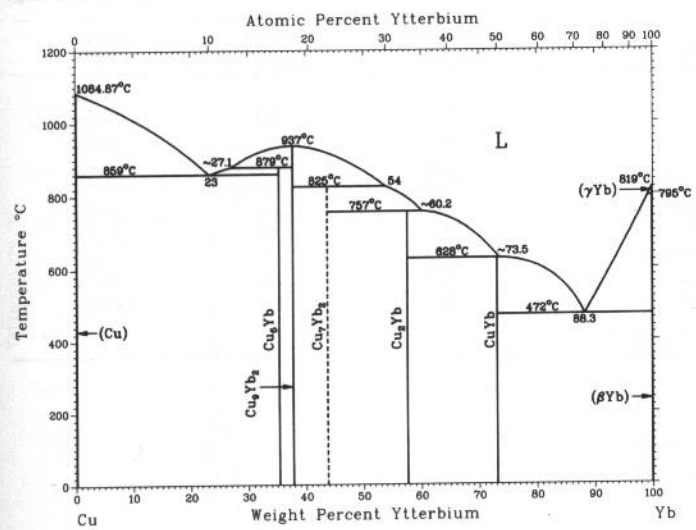

Phase	Composition, wt% Yb	Pearson symbol	Space group
(Cu)	0	*cF*4	$Fm\bar{3}m$
Cu_5Yb	~35.26	*hP*6	$P6/mmm$
Cu_2Yb	~57.6	*oI*12	*Imma*
CuYb	~73.1	*oP*8	*Pnma*
(γYb)	100	*cI*2	$Im\bar{3}m$
(βYb)	~99.99 to 100	*cF*4	$Fm\bar{3}m$
(αYb)	100	*hP*2	$P6_3/mmc$

Cu-Zn

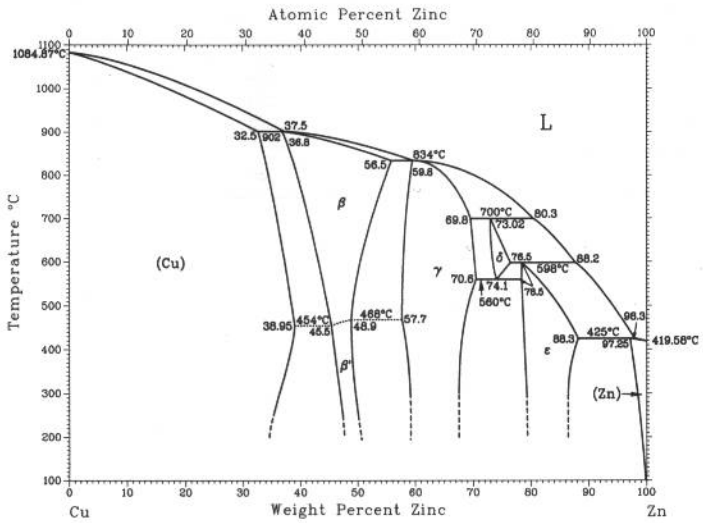

A.P. Miodownik, unpublished

Phase	Composition, wt% Zn	Pearson symbol	Space group
α or (Cu)	0 to 38.95	*cF*4	$Fm\bar{3}m$
β	36.8 to 56.5	*cI*2	$Im\bar{3}m$
β′	45.5 to 50.7	*cP*2	$Pm\bar{3}m$
γ	57.7 to 70.6	*cI*52	$I\bar{4}3m$
δ	73.02 to 76.5	*hP*3	$P\bar{6}$
ε	78.5 to 88.3	*hP*2	$P6_3/mmc$
η or (Zn)	97.25 to 100	*hP*2	$P6_3/mmc$

Cu-Zr

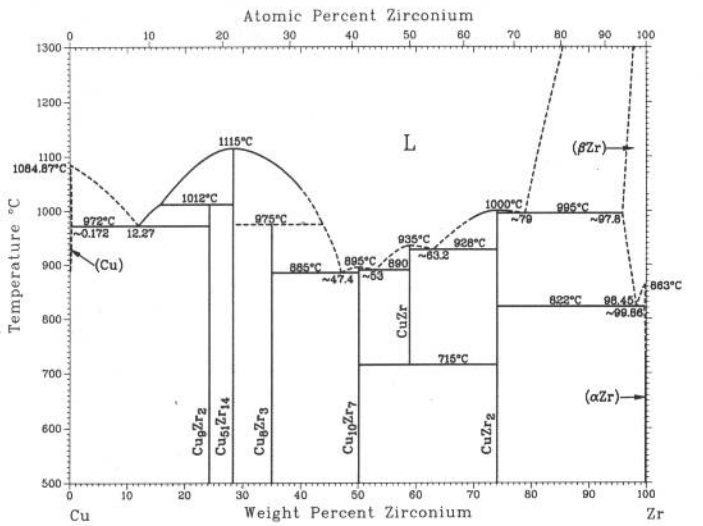

D. Arias and J.P. Abriata, 1990

Phase	Composition, wt% Zr	Pearson symbol	Space group
(Cu)	0 to ~0.172	*cF*4	$Fm\bar{3}m$
Cu_9Zr_2(a)	24.18	*tP*24	*P*4/*m*
$Cu_{51}Zr_{14}$	28.27	*hP*65	*P*6/*m*
Cu_8Zr_3	34.99	*oP*44	*Pnma*
$Cu_{10}Zr_7$	50.13	*oC*68	...
CuZr	58.9	*cP*2	$Pm\bar{3}m$
$CuZr_2$	74.17	*tI*6	*I*4/*mmm*
(βZr)	~97.8 to 100	*cI*2	$Im\bar{3}m$
(αZr)	~99.86 to 100	*hP*2	$P6_3/mmc$

(a) Tetragonal long-period superlattice derived from the $AuBe_5$-type structure

Dy-Fe

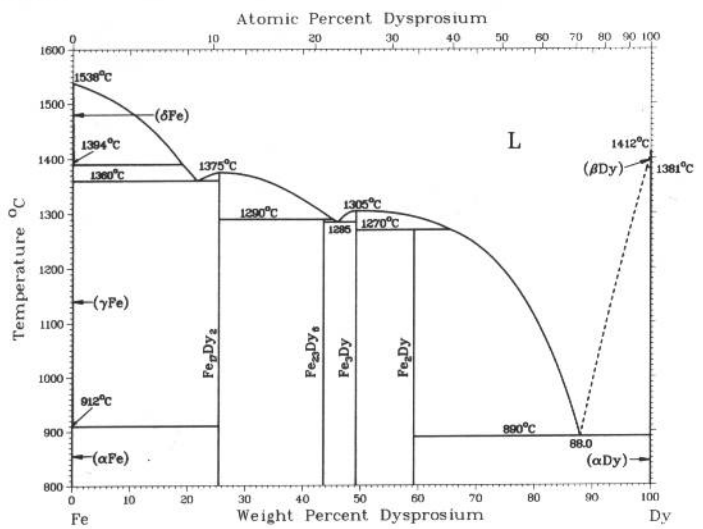

H. Okamoto, 1992

Phase	Composition, wt% Dy	Pearson symbol	Space group
(δFe)	0	*cI*2	$Im\bar{3}m$
(γFe)	0	*cF*4	$Fm\bar{3}m$
(αFe)	0	*cI*2	$Im\bar{3}m$
$Fe_{17}Dy_2$	25.4	*hP*38	$P6_3/mmc$
$Fe_{23}Dy_6$	43.2	*cF*116	$Fm\bar{3}m$
Fe_3Dy	49	*hR*12	$R\bar{3}m$
Fe_2Dy	59.2	*cF*24	$Fd\bar{3}m$
Fe_2Dy'(a)	59.2	*t***	...
(βDy)	100	*cI*2	$Im\bar{3}m$
(αDy)	100	*hP*2	$P6_3/mmc$

(a) Below ~23 °C

Dy-Ga

From [Moffatt]

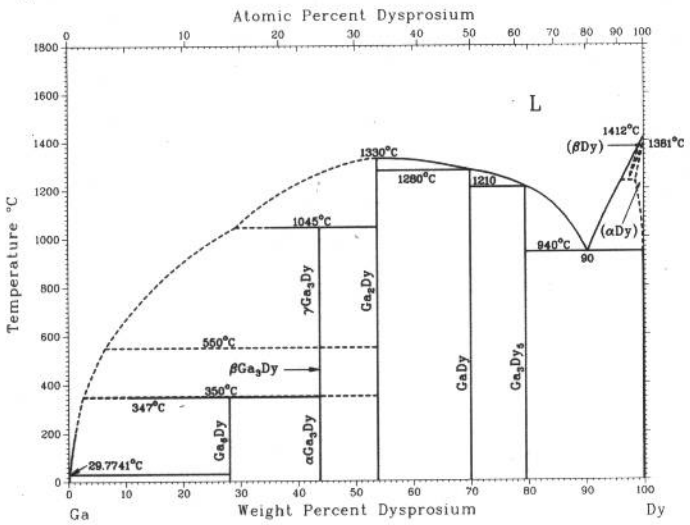

Phase	Composition, wt% Dy	Pearson symbol	Space group
(Ga)	0	*oC*8	*Cmca*
Ga_6Dy	28.0	*tP*14	*P4/nbm*
γGa_3Dy	44	*cP*4	$Pm\bar{3}m$
βGa_3Dy	44	*hP*40	$P6_3/mmc$
αGa_3Dy	44	*hP*16	$R\bar{3}m$
Ga_2Dy	53.8	*hP*3	*P6/mmm*
GaDy	70.0	*oC*8	*Cmcm*
Ga_3Dy_5	79.5	*tI*32	*I4/mcm*
(βDy)	100	*cI*2	$Im\bar{3}m$
(αDy)	100	*hP*2	$P6_3/mmc$

Dy-Ge

V.N. Eremenko, V.G. Batalin, Yu.I. Buyanov, and I.M. Obushenko, 1977

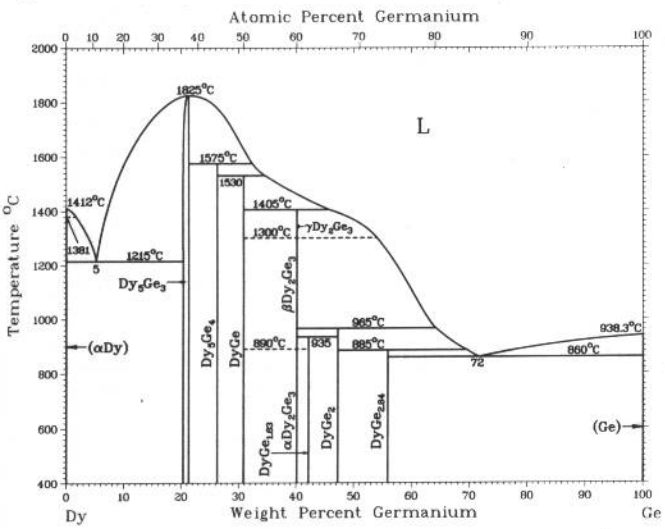

Phase	Composition, wt% Ge	Pearson symbol	Space group
(βDy)	0	*cI*2	$Im\bar{3}m$
(αDy)	0	*hP*2	$P6_3/mmc$
Dy_5Ge_3	~21.4	*hP*16	$P6_3/mcm$
Dy_5Ge_4	26.3	*oP*36	*Pnma*
DyGe	30.9	*oC*8	*Cmcm*
γDy_2Ge_3	40	...	...
βDy_2Ge_3	40	...	...
αDy_2Ge_3	40	*hP*3	*P6/mmm*
$DyGe_{1.83}$	45.0	...	...
$DyGe_2$	47.2	*tI*12	$I4_1/amd$
		*o***(a)	...
$DyGe_{2.84}$	56	...	...
(Ge)	100	*hR*2	$R\bar{3}m$

(a) High-temperature (>750 °C) phase?

Dy-In

H. Okamoto, 1992

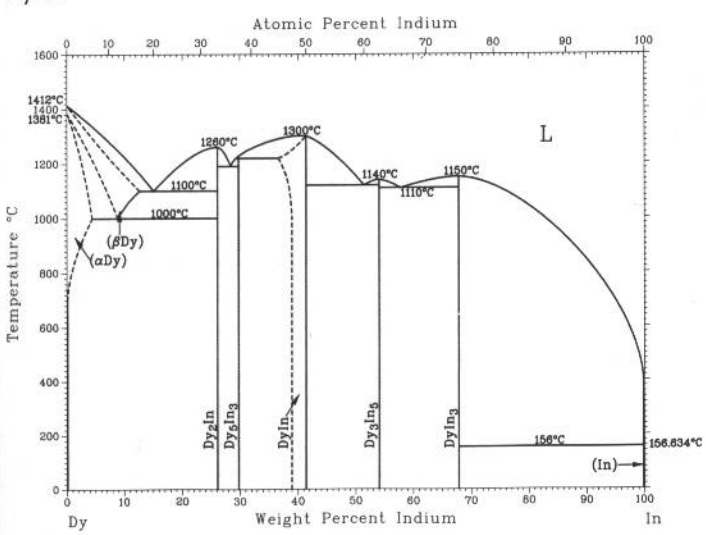

Phase	Composition, wt% In	Pearson symbol	Space group
(βDy)	0 to 13	*cI*2	$Im\bar{3}m$
(αDy)	0 to 6	*hP*2	$P6_3/mmc$
Dy_3In(a)	19	*tP*4	*P4/mmm*
Dy_2In	26.1	*hP*6	$P6_3/mmc$
Dy_5In_3	29.8	*tI*32	*I4/mcm*
DyIn	37 to 41	*cP*2	$Pm\bar{3}m$
Dy_3In_5	54.1	*oC*32	*Cmcm*
$DyIn_3$	68	*cP*4	$Pm\bar{3}m$
(In)	100	*tI*2	*I4/mmm*

(a) Not accepted in the assessed diagram

Dy-Mn

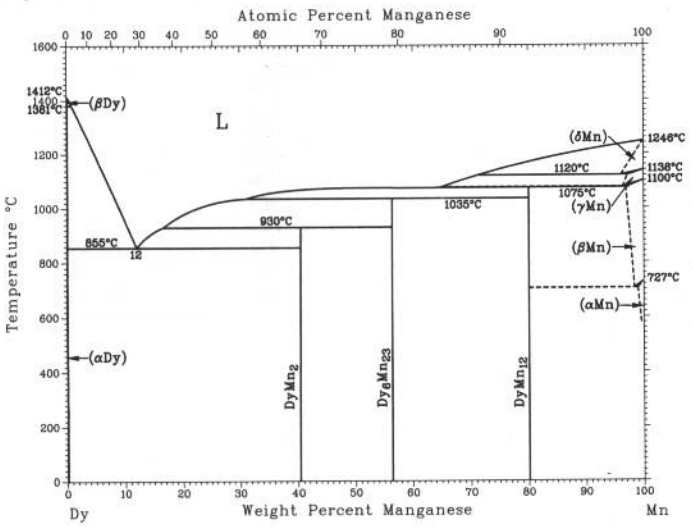

H.R. Kirchmayr and W. Lugscheider, 1967

Phase	Composition, wt% Mn	Pearson symbol	Space group
(βDy)	0	*cI*2	$Im\bar{3}m$
(αDy)	0	*hP*2	$P6_3/mmc$
$DyMn_2$	40.4	*cF*24	$Fd\bar{3}m$
Dy_6Mn_{23}	56.4	*cF*116	$Fm\bar{3}m$
$DyMn_{12}$	80.2	*tI*26	$I4/mmm$
(δMn)	100	*cI*2	$Im\bar{3}m$
(γMn)	100	*cF*4	$Fm\bar{3}m$
(βMn)	100	*cP*20	$P4_132$
(αMn)	100	*cI*58	$I\bar{4}3m$

Dy-Ni

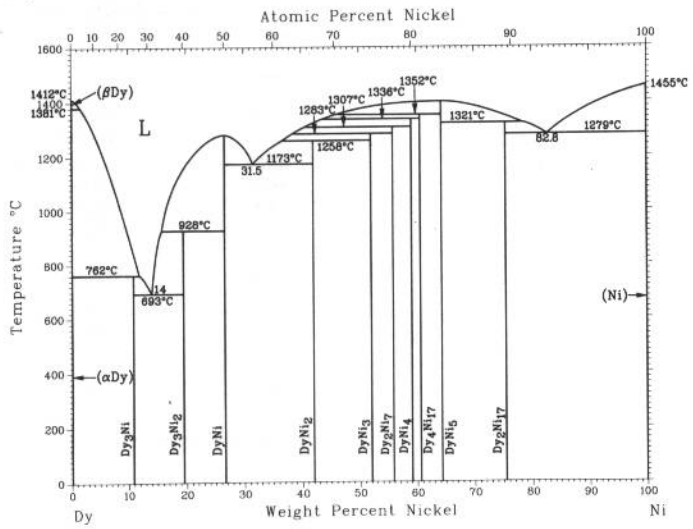

Y.Y. Pan and P. Nash, 1991

Phase	Composition, wt% Ni	Pearson symbol	Space group
(αDy)	0	*cI*2	$Im\bar{3}m$
(βDy)	0	*hP*2	$P6_3/mmc$
(α′Dy)	0	*oC*4	*Cmcm*
Dy_3Ni	10.7	*oP*16	*Pnma*
Dy_3Ni_2	19.4	*mC*20	*C*2/*m*
DyNi	26.5	*oP*8	*Pbnm*
$DyNi_2$	42.0	*cF*24	$Fd\bar{3}m$
$DyNi_3$	52.0	*hR*24	$R\bar{3}m$
Dy_2Ni_7	55.9	*hR*54	$R\bar{3}m$
		*hP*36	$P6_3/mmc$
$DyNi_4$	59.1	...	...
Dy_4Ni_{17}	61	...	...
$DyNi_5$	64.3	*hP*6	$P6_3/mmm$
Dy_2Ni_{17}	75.5	*hP*38	$P6_3/mmc$
(Ni)	100	*cF*4	$Fm\bar{3}m$

(a) Low-temperature form. (b) High-temperature form

Dy-Pb

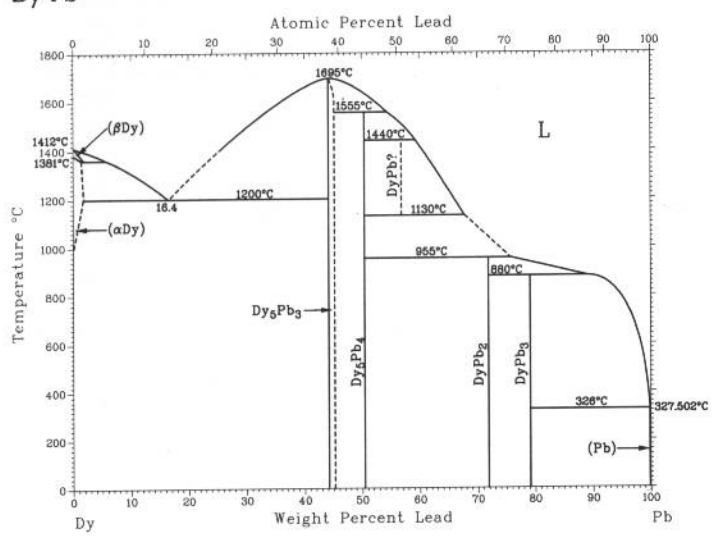

O.D. McMasters, T.J. O'Keefe, and K.A. Gschneidner, Jr., 1968

Phase	Composition, wt% Pb	Pearson symbol	Space group
(βDy)	0	*cI*2	$Im\bar{3}m$
(αDy)	0	*hP*2	$P6_3/mmc$
Dy_5Pb_3	43.3	*hP*16	$P6_3/mcm$
Dy_5Pb_4	50.5	*oP*36	*Pnma*
DyPb	56.0	...	...
$DyPb_2$	71.9	...	...
$DyPb_3$	79	*cP*4	$Pm\bar{3}m$
(Pb)	100	*cF*4	$Fm\bar{3}m$

Dy-Pd

H. Okamoto, 1990

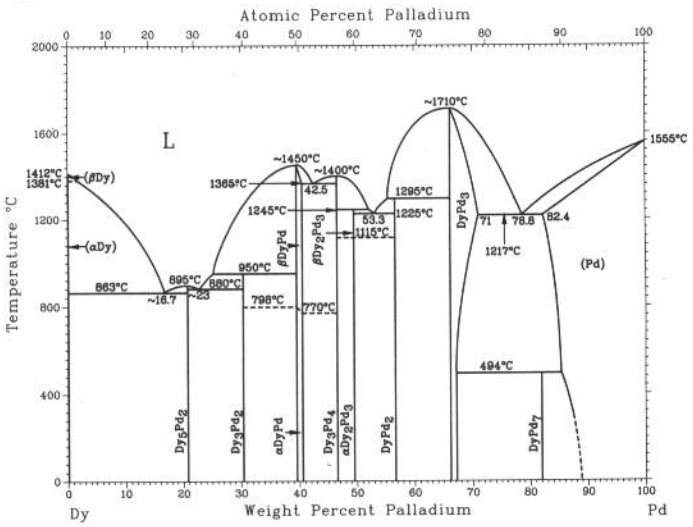

Phase	Composition, wt% Pd	Pearson symbol	Space group
(βDy)	0	*cI*2	$Im\bar{3}m$
(αDy)	0	*hP*2	$P6_3/mmc$
Dy_5Pd_2	20.8	*tI*49	$I4_1/a$
Dy_3Pd_2	30	*tP*10	$P4/mbm$
βDyPd	39.6	*cP*2	$Pm\bar{3}m$
αDyPd	39.6	*oP*8	$Pnma$
Dy_3Pd_4	46.6	*hR*14	$R\bar{3}$
$βDy_2Pd_3$	50	...	...
$αDy_2Pd_3$	50	...	...
$DyPd_2$	56.7	...	...
$DyPd_3$	66 to 71	*cP*4	$Pm\bar{3}m$
$DyPd_7$	82	*c***	...
(Pd)	82.4 to 100	*cF*4	$Fm\bar{3}m$

Dy-S

H. Okamoto, 1990

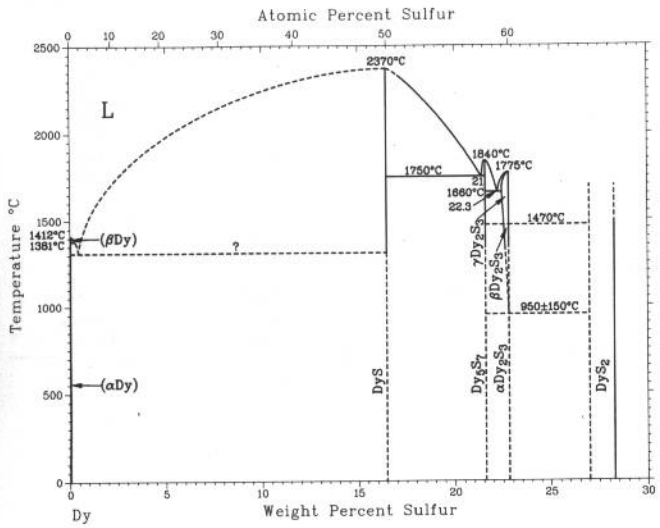

Phase	Composition, wt% S	Pearson symbol	Space group
(βDy)	0	*cI*2	$Im\bar{3}m$
(αDy)	0	*hP*2	$P6_3/mmc$
DyS	17	*cF*8	$Fm\bar{3}m$
Dy_5S_7	21.6	*mC*24	$C2/m$
$γDy_2S_3$	23	*cI*28	$I\bar{4}3d$
$βDy_2S_3$	23	*oP*20	$Pnma$
$αDy_2S_3$	23	*m***	...
DyS_2	27.2 to 28.3	*cF*24	$Fd\bar{3}m$
(S)	100	*oF*128	$Fddd$

Dy-Sb

H. Okamoto, 1990

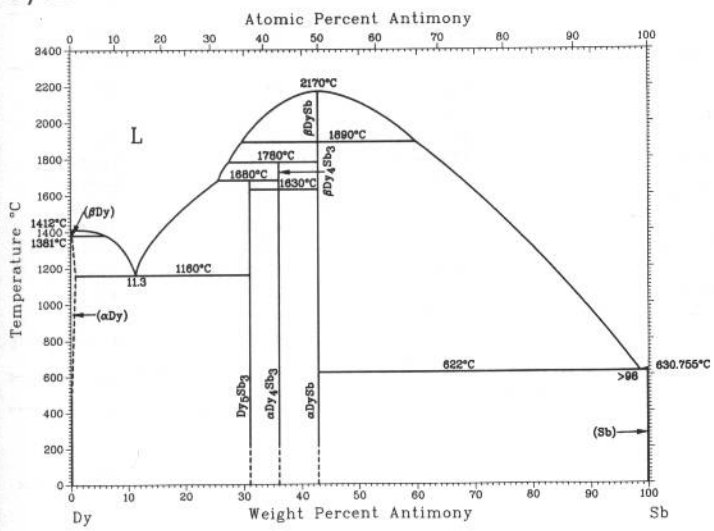

Phase	Composition, wt% Sb	Pearson symbol	Space group
(βDy)	0	*cI*2	$Im\bar{3}m$
(αDy)	0	*hP*2	$P6_3/mmc$
Dy_5Sb_3	31.0	*hP*16	$P6_3/mcm$
$βDy_4Sb_3$	36.0	...	...
$αDy_4Sb_3$	36.0	*cI*28	$I\bar{4}3d$
βDySb	42.8	...	...
αDySb	42.8	*cF*8	$Fm\bar{3}m$
α′DySb(a)	42.8	*tI*4	$I4/mmm$
(Sb)	100	*hR*2	$R\bar{3}m$
High-pressure phase			
$DySb_2$	60.1	*o**6	...

(a) Below 11 K

Dy-Sn

H. Okamoto, 1990

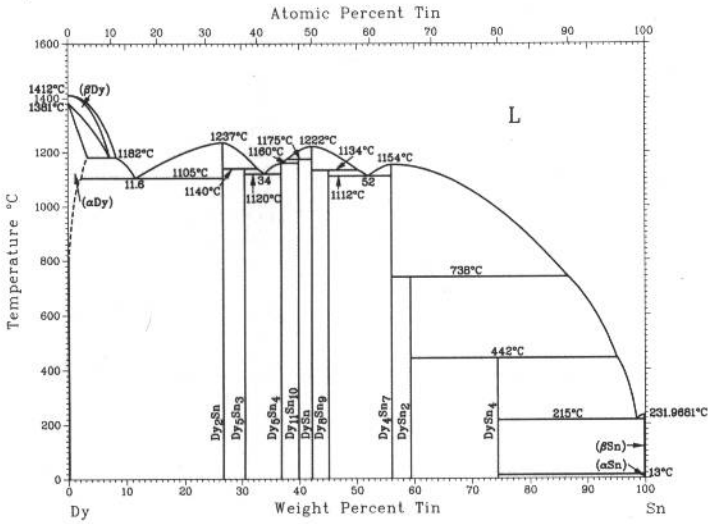

Phase	Composition, wt% Sn	Pearson symbol	Space group
(βDy)	0	*cI*2	$Im\bar{3}m$
(αDy)	0	*hP*2	$P6_3/mmc$
Dy_2Sn	26.7	...	...
Dy_5Sn_3	30.5	*hP*16	$P6_3/mcm$
Dy_5Sn_4	36.8	*oP*36	*Pnma*
$Dy_{11}Sn_{10}$	39.9	*tI*84	*I*4/*mmm*
DySn	42.2	...	...
Dy_8Sn_9	45.1	...	...
Dy_4Sn_7	56.1	...	...
$DySn_2$	59.4	*oC*12	*Cmcm*
$DySn_4$	75	...	...
(βSn)	100	*tI*4	$I4_1/amd$
(αSn)	100	*cF*8	$Fd\bar{3}m$
High-pressure phase			
$DySn_3$	69	*cP*4	$Pm\bar{3}m$

Dy-Te

H. Okamoto, 1990

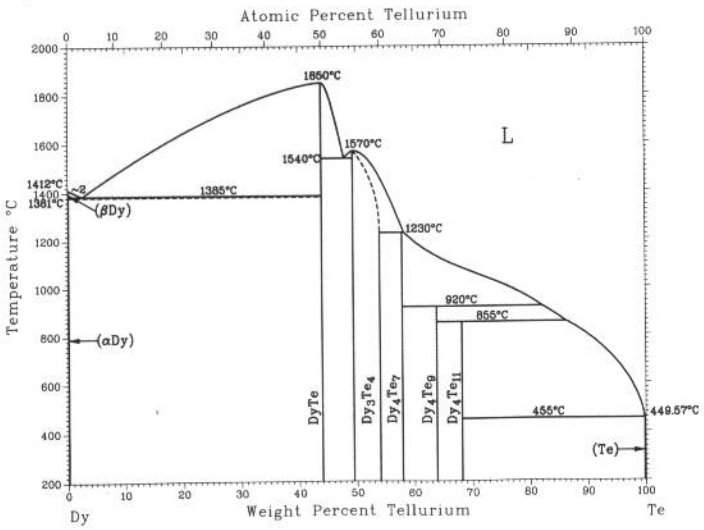

Phase	Composition, wt% Te	Pearson symbol	Space group
(βDy)	0	*cI*2	$Im\bar{3}m$
(αDy)	0	*hP*2	$P6_3/mmc$
DyTe	44.0	*cF*8	$Fm\bar{3}m$
Dy_3Te_4	51.1 to 54	*oF*80	*Fddd*
Dy_4Te_7	57.8	*tP*6	*P*4/*nmm*
Dy_4Te_9	63.8	...	...
Dy_4Te_{11}	68.3	...	...
(Te)	100	*hP*3	$P3_121$
Other phases			
Dy_2Te_5	66.2	*oC*28	*Cmcm*
$DyTe_3$	70	*oC*16	*Cmcm*
		*tP*16	$P4_2/n$

Dy-Tl

S. Delfino, A. Saccone, A. Palenzona, and R. Ferro, unpublished

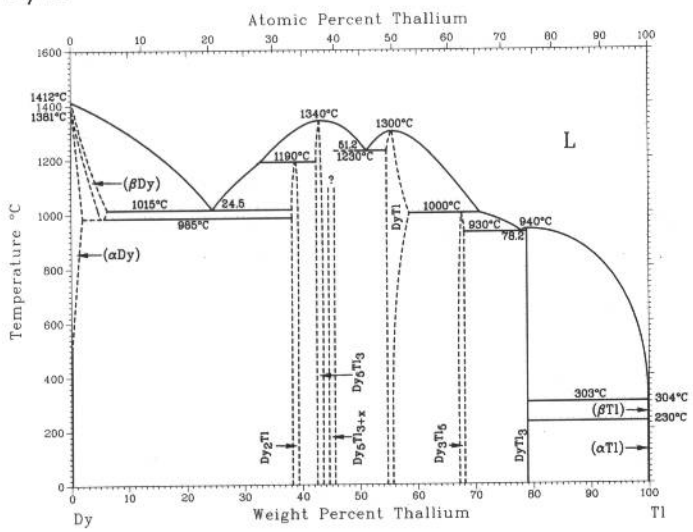

Phase	Composition, wt% Tl	Pearson symbol	Space group
(βDy)	0 to ~6	*cI*2	$Im\bar{3}m$
(αDy)	0 to ?	*hP*2	$P6_3/mmc$
Dy_2Tl	~38 to ~39	*hP*6	$P6_3/mmc$
Dy_5Tl_3	~43 to ~44	*hP*16	$P6_3/mcm$
Dy_5Tl_{3+x}	?	*tI*32	*I*4/*mcm*
DyTl(a)	55 to ~59	*cP*2	$Pm\bar{3}m$
		(or *cI*2)	$Im\bar{3}m$
DyTl(b)	~55 to ~59	*tP*2	*P*4/*mmm*
Dy_3Tl_5	~67 to ~68	*oC*32	*Cmcm*
$DyTl_3$	79	*cP*4	$Pm\bar{3}m$
(βTl)	100	*cI*2	$Im\bar{3}m$
(αTl)	100	*hP*2	$P6_3/mmc$

(a) Cubic structure presumed to be room- and higher temperature phases. (b) Tetragonal structure presumed to be lower temperature phase

Dy-Zr

J. Croni, C.E. Armantrout, and H. Kato, 1960

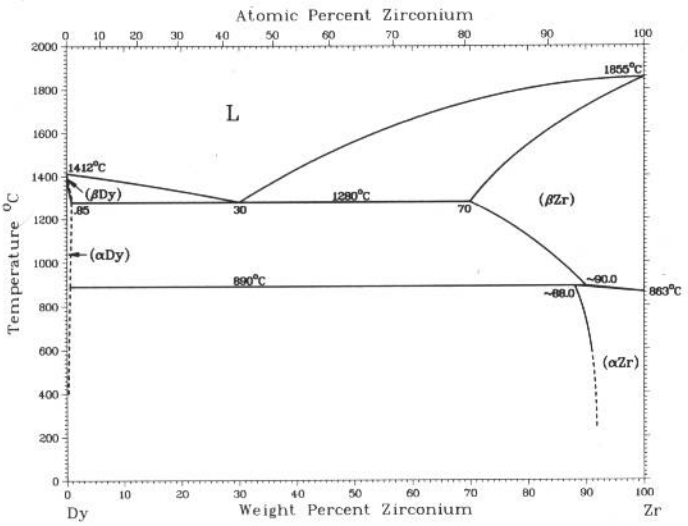

Phase	Composition, wt% Zr	Pearson symbol	Space group
(βDy)	0 to ?	*cI*2	$Im\bar{3}m$
(αDy)	0 to 0.85	*hP*2	$P6_3/mmc$
(βZr)	70 to 100	*cI*2	$Im\bar{3}m$
(αZr)	~88 to 100	*hP*2	$P6_3/mmc$

Er-Fe

H. Okamoto, 1992

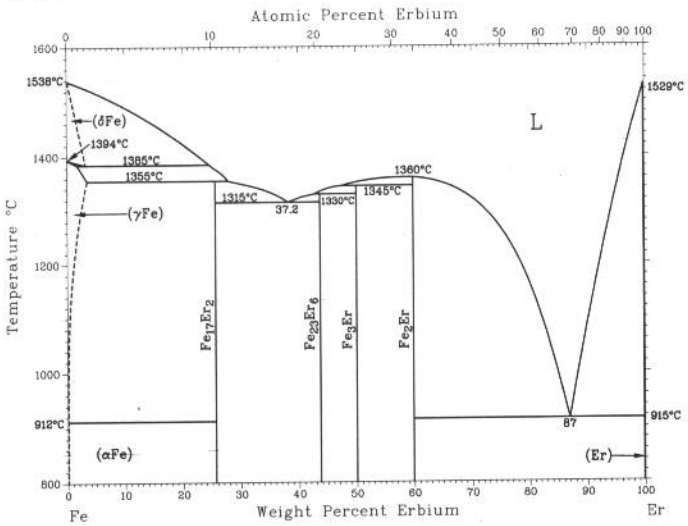

Phase	Composition, wt% Er	Pearson symbol	Space group
(δFe)	0	*cI*2	$Im\bar{3}m$
(γFe)	0	*cF*4	$Fm\bar{3}m$
(αFe)	0	*cI*2	$Im\bar{3}m$
$Fe_{17}Er_2$	26.0	*hP*38	$P6_3/mmc$
$Fe_{23}Er_6$	43.9	*cF*116	$Fm\bar{3}m$
Fe_3Er	50	*hR*12	$R\bar{3}m$
Fe_2Er	59.9	*cF*24	$Fd\bar{3}m$
(Er)	100	*hP*2	$P6_3/mmc$
Metastable phase			
	~75.0	*hP*12	$P6_3/mmc$

Er-Ga

H. Okamoto, 1990

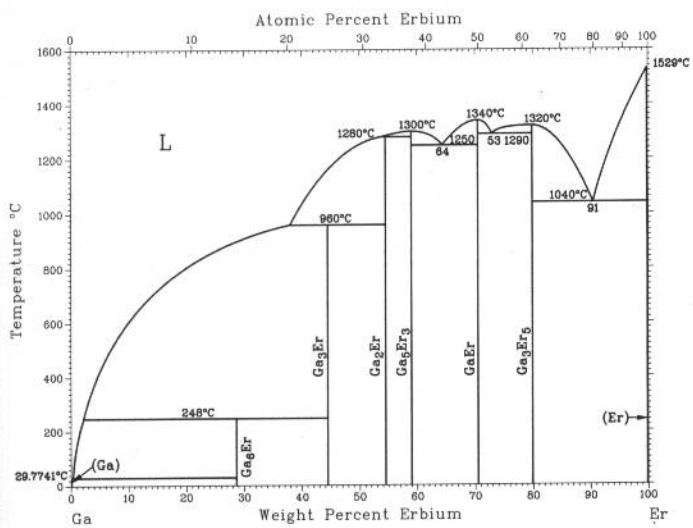

Phase	Composition, wt% Er	Pearson symbol	Space group
(Ga)	0	*oC*8	*Cmca*
Ga_6Er	28.6	*tP*14	$P4/nbm$
Ga_3Er	44	*cP*4	$Pm\bar{3}m$
Ga_2Er	54.5	*hP*3	*P6/mmm*
Ga_5Er_3	59.0	*oP*32	*Pnma*
GaEr	70.6	*oC*8	*Cmcm*
Ga_3Er_5	80.0	*hP*16	$P6_3/mcm$
(Er)	100	*hP*2	$P6_3/mmc$

Er-Ge

H. Okamoto, 1990

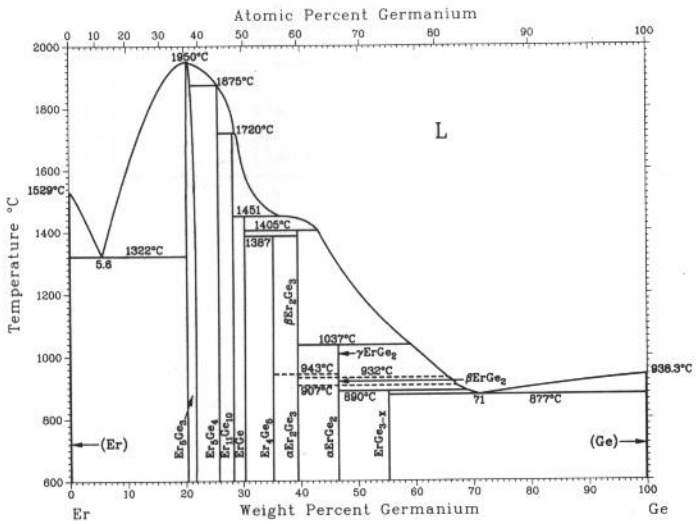

Phase	Composition, wt% Ge	Pearson symbol	Space group
(Er)	0	*hP*2	$P6_3/mmc$
Er_5Ge_3	~20.7	*hP*16	$P6_3/mcm$
Er_5Ge_4	25.7	*oP*36	*Pnma*
$Er_{11}Ge_{10}$	28.3	*tI*84	*I*4/*mmm*
ErGe	30.3	*oC*8	*Cmcm*
Er_4Ge_5	35.2	...	...
βEr_2Ge_3	39	*hP*3	*P*6/*mmm*
αEr_2Ge_3	39	...	...
$\gamma ErGe_2$	46.5	...	...
$\beta ErGe_2$	46.5	...	...
$\alpha ErGe_2$	46.5	...	...
$ErGe_{3-x}$	55	*oC*16	$C222_1$
(Ge)	100	*cF*8	$Fd\bar{3}m$

Er-In

H. Okamoto, 1992

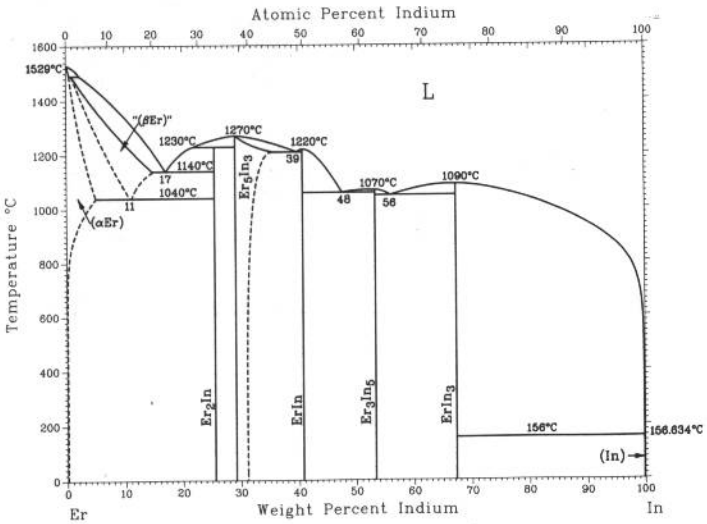

Phase	Composition, wt% In	Pearson symbol	Space group
(αEr)	0 to 5	*hP*2	$P6_3/mmc$
"(βEr)"	? to 15	*cI*2	$Im\bar{3}m$
Er_2In	25.5	*hP*6	$P6_3/mmc$
Er_5In_3	29.2 to 36	*hP*16	$P6_3/mcm$
ErIn	40.7	*cP*2	$Pm\bar{3}m$
Er_3In_5	53.4	*oC*32	*Cmcm*
$ErIn_3$	67	*cP*4	$Pm\bar{3}m$
(In)	100	*tI*2	*I*4/*mmm*

Er-Mn

H.R. Kirchmayr and W. Lugscheider, 1967

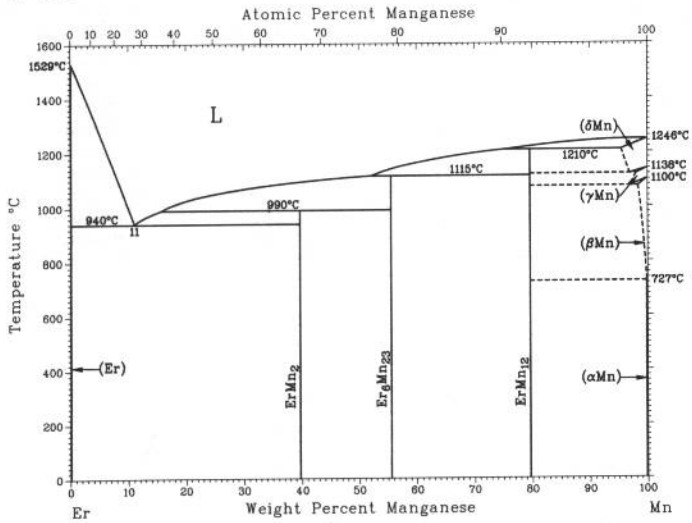

Phase	Composition, wt% Mn	Pearson symbol	Space group
(Er)	0	*hP*2	$P6_3/mmc$
$ErMn_2$	39.7	...	...
Er_6Mn_{23}	55.7	*cF*116	$Fm\bar{3}m$
$ErMn_{12}$	79.7	*tI*26	*I*4/*mmm*
(δMn)	100	*cI*2	$Im\bar{3}m$
(γMn)	100	*cF*4	$Fm\bar{3}m$
(βMn)	100	*cP*20	$P4_132$
(αMn)	100	*cI*58	$I\bar{4}3m$

Er-Ni

Y.Y. Pan and P. Nash, 1991

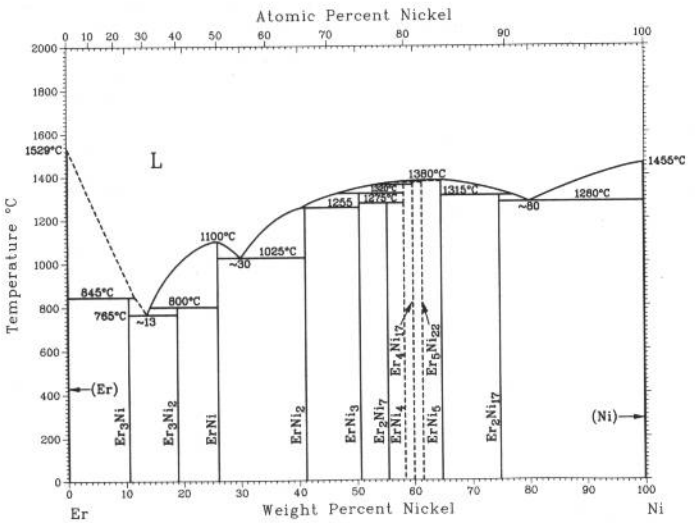

Phase	Composition, wt% Ni	Pearson symbol	Space group
(Er)	0	*hP*2	$P6_3/mmc$
Er_3Ni	10.5	*oP*16	*Pnma*
Er_3Ni_2	19.0	*hR*5	$R\bar{3}$
ErNi	26.0	*oP*8	*Pnma*
$ErNi_2$	41.3	*cF*24	$Fd\bar{3}m$
$ErNi_3$	51.3	*hR*24	$R\bar{3}m$
Er_2Ni_7	55.2	*hR*54	$R\bar{3}m$
$ErNi_4$	58.4	*hP*36	$P6_3/mmc$
Er_4Ni_{17}	60	...	...
Er_5Ni_{22}	60.7	...	...
$ErNi_5$	63.6	*hP*6	*P6/mmm*
Er_2Ni_{17}	74.9	*hP*38	$P6_3/mmc$
(Ni)	100	*cF*4	$Fm\bar{3}m$

Er-Pd

H. Okamoto, 1991

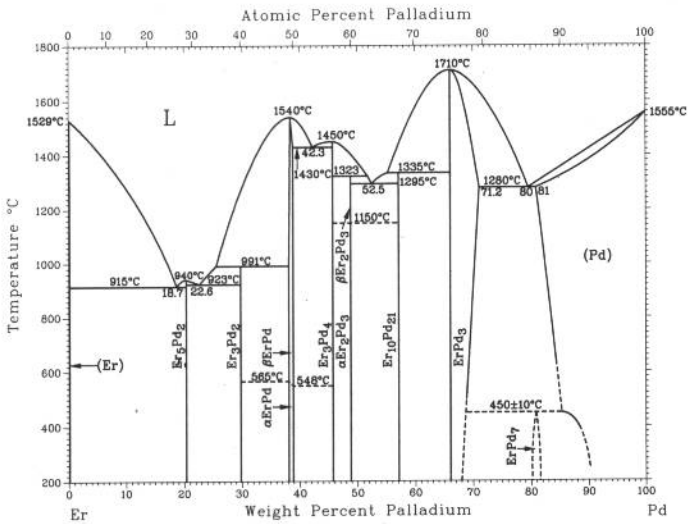

Phase	Composition, wt% Pd	Pearson symbol	Space group
(Er)	0	*hP*2	$P6_3/mmc$
Er_5Pd_2	20.3	*cF*96	$Fd\bar{3}m$
		*tI*49	$I4_1/a$
Er_3Pd_2	30	*tP*10	*P4/mbm*
βErPd	~38.9	*cP*2	$Pm\bar{3}m$
αErPd	~38.9	...	...
Er_3Pd_4	45.9	*hR*14	$R\bar{3}$
βEr_2Pd_3	49	...	...
αEr_2Pd_3	49	...	...
$Er_{10}Pd_{21}$(a)	57.1	*mC*124	*C2/m*
$ErPd_3$	66 to 71.2	*cP*4	$Pm\bar{3}m$
$ErPd_7$	81.7	*c***	...
(Pd)	100	*cF*4	$Fm\bar{3}m$

(a) Similarity to $Sm_{10}Pd_{21}$ is assumed.

Er-Pt

H. Okamoto, 1990

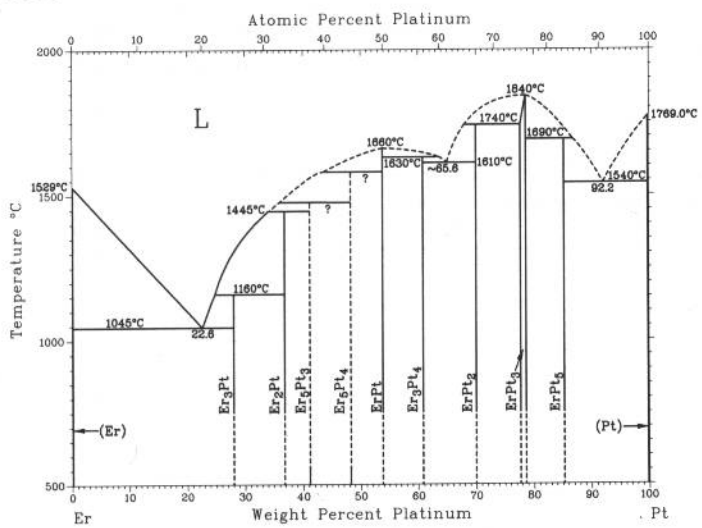

Phase	Composition, wt% Pt	Pearson symbol	Space group
(Er)	0	*hP*2	$P6_3/mmc$
Er_3Pt	28	*oP*16	*Pnma*
Er_2Pt	36.8	*oP*12	*Pnma*
Er_5Pt_3	41.2	*hP*16	$P6_3/mcm$
Er_5Pt_4	48.2	*oP*36	*Pnma*
ErPt	53.8	*oP*8	*Pnma*
Er_3Pt_4	60.8	*hR*14	$R\bar{3}m$
$ErPt_2$	70.0	*cF*24	$Fd\bar{3}m$
$ErPt_3$	~78	*cP*4	$Pm\bar{3}m$
$ErPt_5$	85.3	*o**72	...
(Pt)	100	*cF*4	$Fm\bar{3}m$

Er-Ru

H. Okamoto, 1990

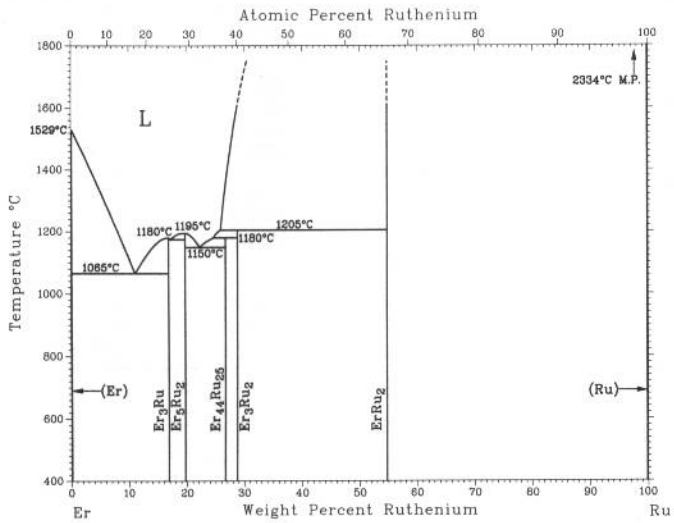

Phase	Composition, wt% Ru	Pearson symbol	Space group
(Er)	0	*hP*2	$P6_3/mmc$
Er_3Ru	17	*oP*16	*Pnma*
Er_5Ru_2	19.5	*mC*28	*C*2/*c*
$Er_{44}Ru_{25}$	25.4	*oP*276	*Pnma*
Er_3Ru_2	29	*hP*10	$P6_3/m$
$ErRu_2$	54.8	*hP*12	$P6_3/mmc$
(Ru)	100	*hP*2	$P6_3/mmc$

Er-Se

H. Okamoto, 1990

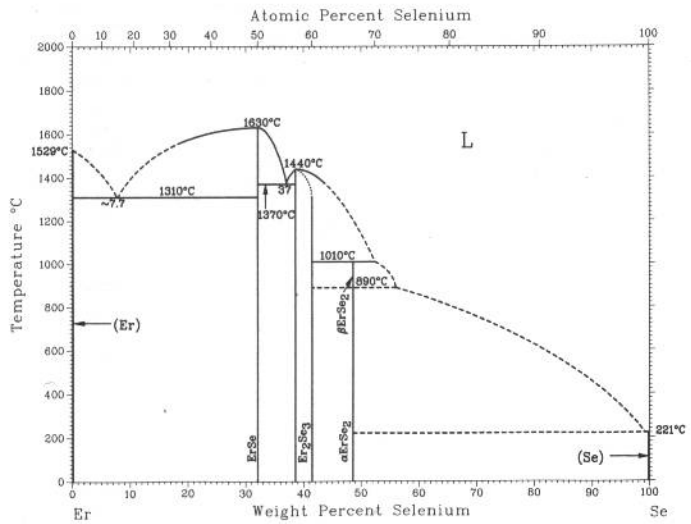

Phase	Composition, wt% Se	Pearson symbol	Space group
(Er)	0	*hP*2	$P6_3/mmc$
ErSe	32.1	*cF*8	$Fm\bar{3}m$
Er_2Se_3	38.6 to 42	*oF*80	*Fddd*
$\beta ErSe_2$	48.6	*oC*132	*Cmma*
$\alpha ErSe_2$	48.6	*oI*12	*Immm*
(Se)	100	*hP*3	$P3_121$

Er-Te

H. Okamoto, 1990

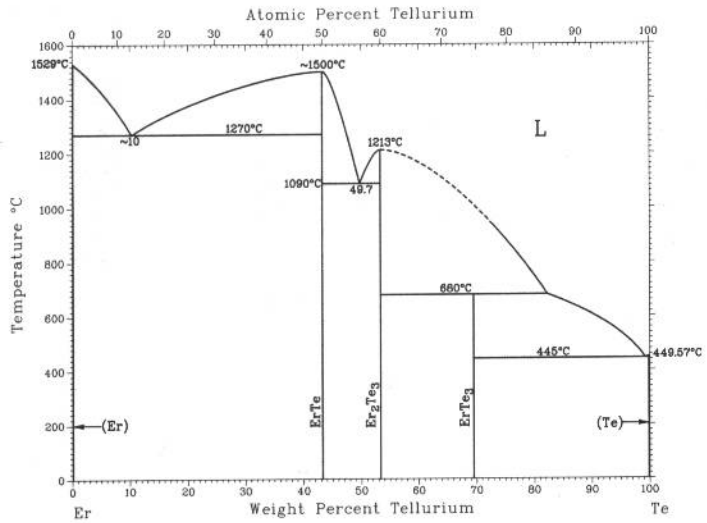

Phase	Composition, wt% Te	Pearson symbol	Space group
(Er)	0	*hP*2	$P6_3/mmc$
ErTe	43.3	*cF*8	$Fm\bar{3}m$
Er_2Te_3	53	*oF*80	*Fddd*
$ErTe_3$	70	*oC*16	*Cmcm*
(Te)	100	*hP*3	$P3_121$
High-temperature, high-pressure phase			
$ErTe_2$	60.4	*tP*6	*P*4/*nmm*

Er-Ti

J.L. Murray, 1987

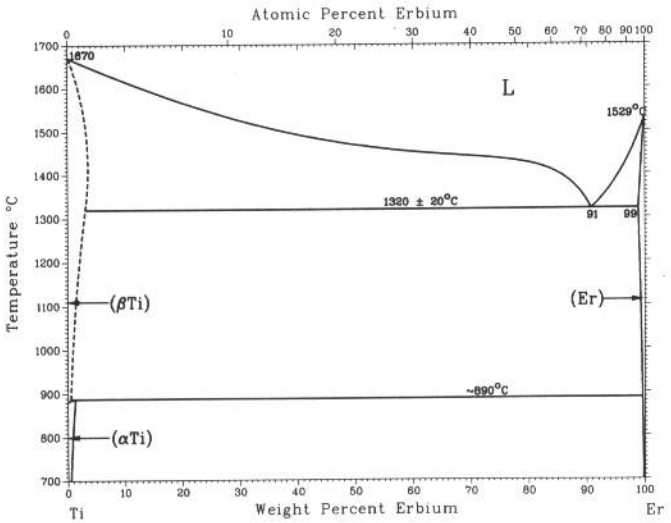

Phase	Composition, wt% Er	Pearson symbol	Space group
(βTi)	0 to ~3.1	*cI*2	$Im\bar{3}m$
(αTi)	0 to ~1.0	*hP*2	$P6_3/mmc$
(Er)	99.7 to 100	*hP*2	$P6_3/mmc$

Er-Tl

S. Delfino, A. Saccone, A. Palenzona, and R. Ferro, unpublished

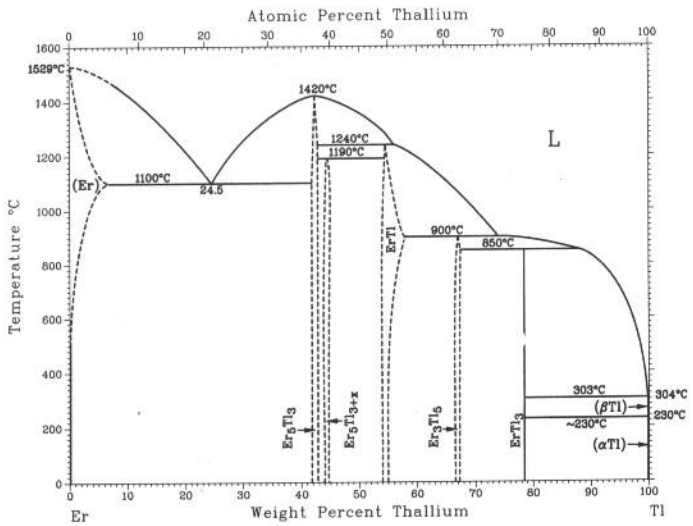

Phase	Composition, wt% Tl	Pearson symbol	Space group
(Er)	0 to ~7	*hP*2	$P6_3/mmc$
Er_5Tl_3	~42 to 43	*hP*16	$P6_3/mcm$
Er_5Tl_{3+x}	?	*tI*32	$I4/mcm$
ErTl(a)	~54 to ~58	*cP*2 (or *cI*2)	$Pm\bar{3}m$ $Im\bar{3}m$
ErTl(b)	~54 to ~58	*tP*2	$P4/mmm$
Er_3Tl_5	~67 to ~68	*oC*32	$Cmcm$
$ErTl_3$	79	*cP*4	$Pm\bar{3}m$
(βTl)	100	*cI*2	$Im\bar{3}m$
(αTl)	100	*hP*2	$P6_3/mmc$

(a) Cubic structure presumed to be room-temperature and higher temperature phases. (b) Tetragonal structure presumed to be lower temperature phase

Eu-Ga

S.P. Yatsenko, B.G. Semenov, and K.A. Chuntonov, 1978

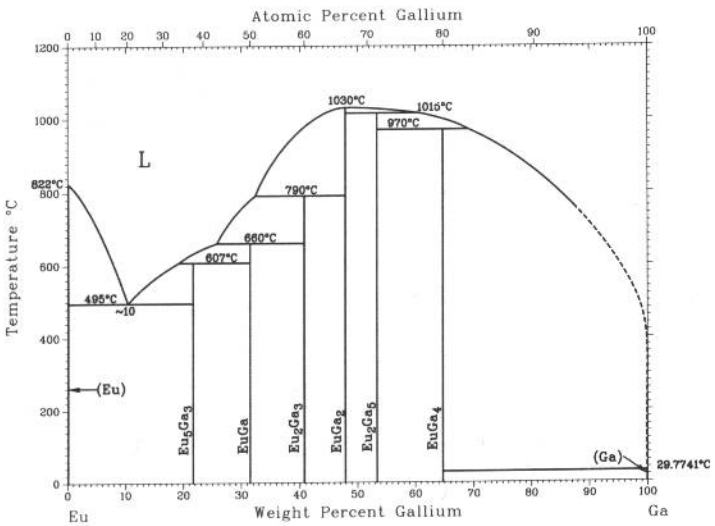

Phase	Composition, wt% Ga	Pearson symbol	Space group
(Eu)	0	*cI*2	$Im\bar{3}m$
Eu_5Ga_3	21.6	...	...
EuGa	31.5	...	...
Eu_2Ga_3	41	...	...
$\beta EuGa_2$(a)	47.9	*hP*3	$P6/mmm$
$\alpha EuGa_2$(b)	47.9	*oI*12	$Imma$
Eu_2Ga_5	53.4	...	...
$EuGa_4$	65	*tI*10	$I4/mmm$
(Ga)	100	*oC*8	$Cmca$

(a) Hexagonal structure presumed to be lower temperature phase. (b) Cubic structure presumed to be higher temperature phase

Eu-Ge

A.B. Gokhale and G.J. Abbaschian, 1991

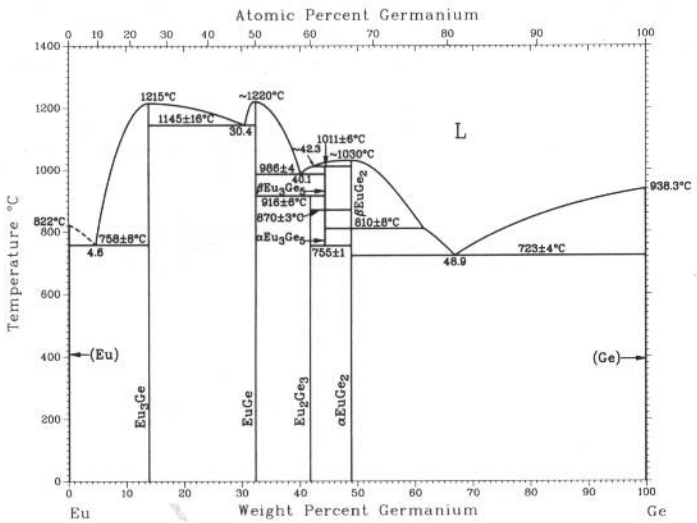

Phase	Composition, wt% Ge	Pearson symbol	Space group
(Eu)	0	*cI*2	$Im\bar{3}m$
EuGe	32.3	*oC*8	*Cmcm*
Eu_2Ge_3	41.7	...	...
βEu_3Ge_5	44.3	...	...
αEu_3Ge_5	44.3	(a)	...
$\beta EuGe_2$	48.82	...	...
$\alpha EuGe_2$	48.9	*hP*3	$P\bar{3}m1$
(Ge)	100	*cF*8	$Fd\bar{3}m$

(a) Hexagonal structure

Eu-In

H. Okamoto, 1990

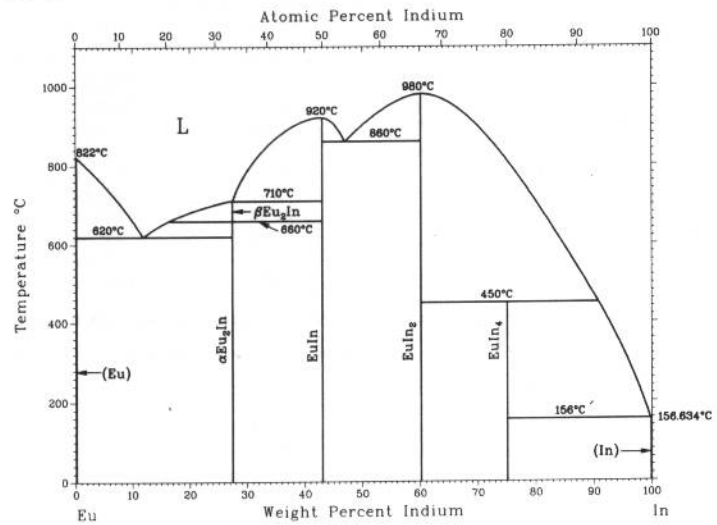

Phase	Composition, wt% In	Pearson symbol	Space group
(Eu)	0	*cI*2	$Im\bar{3}m$
βEu_2In	27.4	...	...
αEu_2In	27.4	...	...
EuIn	43.0	...	...
$EuIn_2$	60.1	*hP*6	$P6_3/mmc$
$EuIn_4$	75.1	...	...
(In)	100	*tI*2	*I*4/*mmm*

Eu-Mg

H. Okamoto, 1992

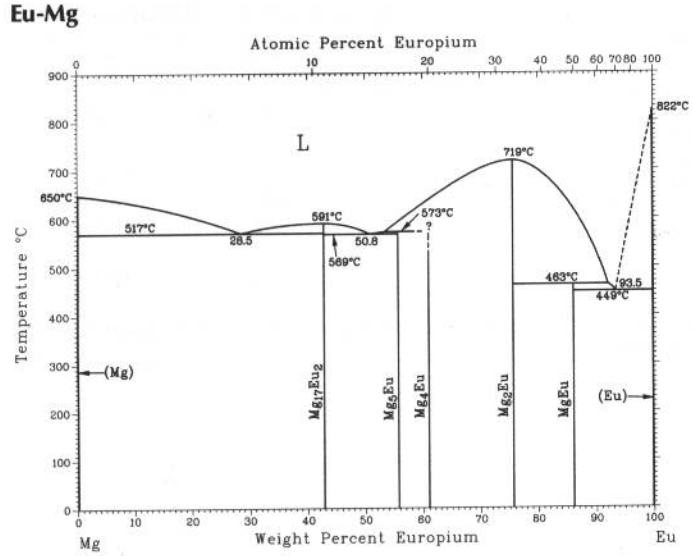

Phase	Composition, wt% Eu	Pearson symbol	Space group
(Mg)	0	*hP*2	$P6_3/mmc$
$Mg_{17}Eu_2$	42.3	*hP*38	$P6_3/mmc$
Mg_5Eu	55.6	*hP*36	$P6_3/mmc$
Mg_4Eu	61	*hP*90	$P6_3/mmc$
Mg_2Eu	75.7	*hP*12	$P6_3/mmc$
MgEu	86.2	*cP*2	$Pm\bar{3}m$
(Eu)	100	*cI*2	$Im\bar{3}m$

Eu-Pb

O.D. McMasters and K.A. Gschneidner, Jr., 1967

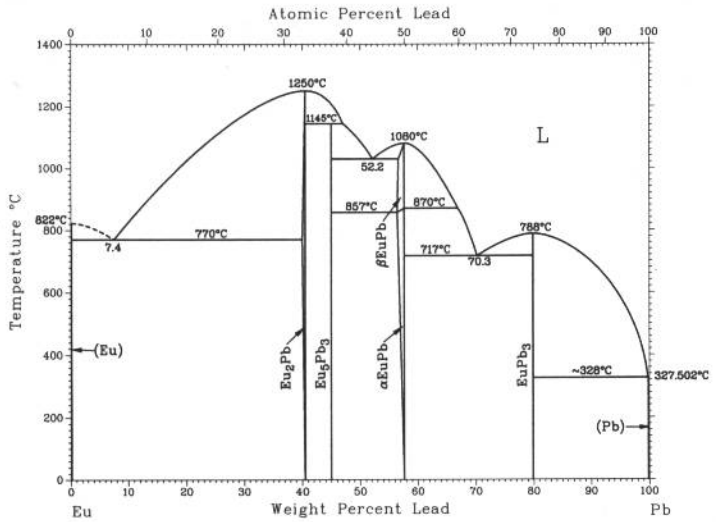

Phase	Composition, wt% Pb	Pearson symbol	Space group
(Eu)	0	*cI*2	$Im\bar{3}m$
Eu_2Pb	~40 to 40.5	*oP*12	*Pnma*
Eu_5Pb_3	45.0	*tI*32	*I4/mcm*
βEuPb	~57.7	...	...
αEuPb(a)	~57.7	*tP*2	*P4/mmm*
$EuPb_3$	80	*cP*4	$Pm\bar{3}m$
(Pb)	100	*cF*4	$Fm\bar{3}m$

(a) Crystal structure data might be for βEuPb.

Eu-Pd

H. Okamoto, 1990

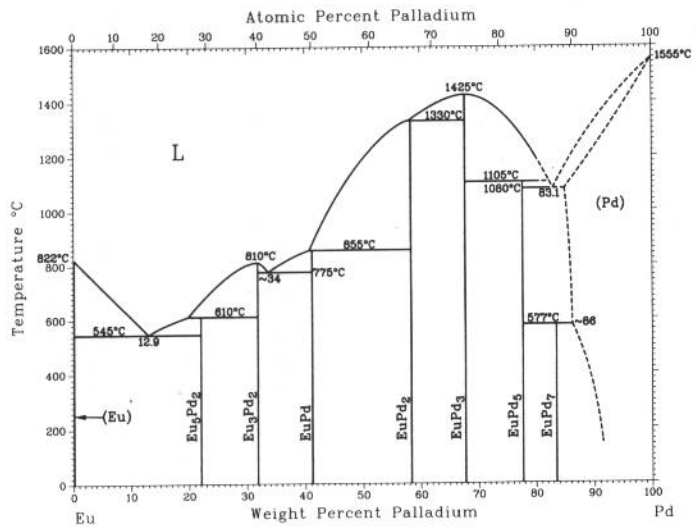

Phase	Composition, wt% Pd	Pearson symbol	Space group
(Eu)	0	*cI*2	$Im\bar{3}m$
Eu_5Pd_2	21.8	*mC*28	*C2/c*
Eu_3Pd_2	32	*hR*15	$R\bar{3}$
EuPd	41.2	*oC*8	*Cmcm*
$EuPd_2$	58.4	...	...
$EuPd_3$	68	*cP*4	$Pm\bar{3}m$
$EuPd_5$	77.7	*o*72*	...
$EuPd_7$	~83.1	*c***	...
(Pd)	~86 to 100	*cF*4	$Fm\bar{3}m$

Eu-Pt

A. Iandelli and A. Palenzona, 1981

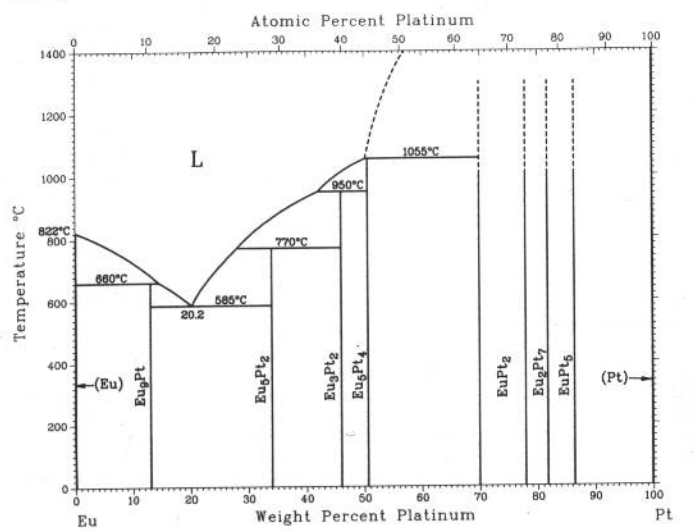

Phase	Composition, wt% Pt	Pearson symbol	Space group
(Eu)	0	*cI*2	$Im\bar{3}m$
Eu_9Pt	13	*cF**	...
Eu_5Pt_2	34.0	*mC*28	*C2/c*
Eu_3Pt_2	46	*hR*15	$R\bar{3}$
Eu_8Pt_4	50.6	*oP*36	*Pnma*
$EuPt_2$	70 to 78	*cF*24	$Fd\bar{3}m$
Eu_2Pt_7	81.8	*hP*36	$P6_3/mmc$
$EuPt_5$	86.5	*o***	...
(Pt)	100	*cF*4	$Fm\bar{3}m$

Eu-Te

O.A. Sadovskaya and E.I. Yarembash, 1970

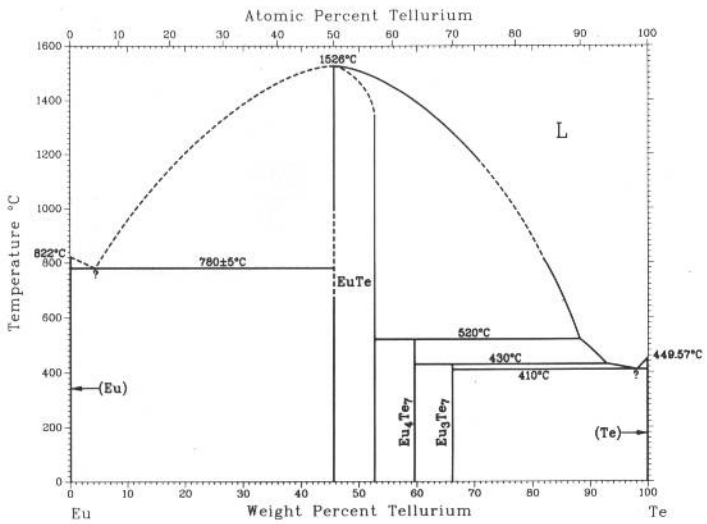

Phase	Composition, wt% Te	Pearson symbol	Space group
(Eu)	0	*cI*2	$Im\bar{3}m$
EuTe	46 to 52.8	*cF*8	$Fm\bar{3}m$
Eu_4Te_7	59.5	...	...
Eu_3Te_7	66	...	...
(Te)	100	*hP*3	$P3_121$

Fe-Ga

H. Okamoto, 1992

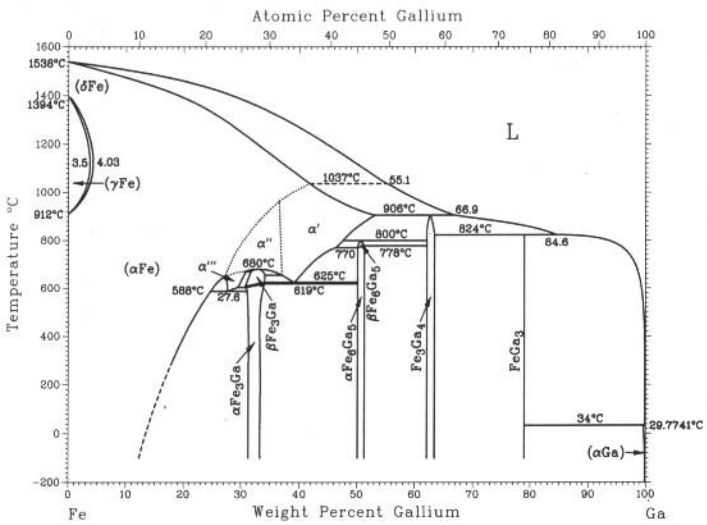

Phase	Composition, wt% Ga	Pearson symbol	Space group
(γFe)	0 to 3.5	*cF*4	$Fm\bar{3}m$
(αFe)	0 to 41	*cI*2	$Im\bar{3}m$
α′	36.5 to 53.0	*cP*2	$Pm\bar{3}m$
α″	26.9 to 37.1	*cF*16	$Fm\bar{3}m$
α‴	26.9 to 30.4	*cF*16	$Fm\bar{3}m$
βFe_3Ga	30.5 to 33.8	*hP*8	$P6_3/mmc$
αFe_3Ga	30.7 to 34.0	*cP*4	$Pm\bar{3}m$
βFe_6Ga_5	50.0 to 51.0	*hR*26	$R\bar{3}m$
αFe_6Ga_5	50.0 to 51.0	*mC*44	*C*2/*m*
Fe_3Ga_4	61.9 to 63.3	*mC*42	*C*2/*m*
		*t**63	...
$FeGa_3$	79	*tP*16	$P\bar{4}n2$
		*tP*16	$P4_2/mnm$
(αGa)	100	*oC*8	*Cmca*
Metastable phase			
$Fe_{13}Ga_9$	46.4	...	...

Fe-Gd

H. Okamoto, 1992

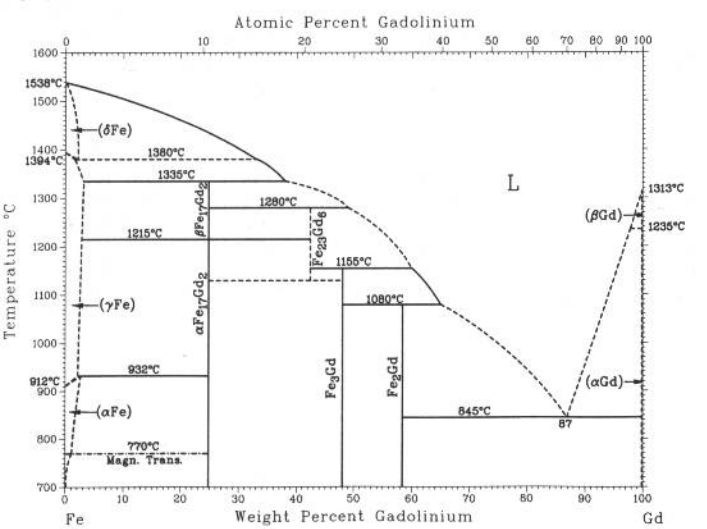

Phase	Composition, wt% Gd	Pearson symbol	Space group
(δFe)	0	*cI*2	$Im\bar{3}m$
(γFe)	0	*cF*4	$Fm\bar{3}m$
(αFe)	0	*cI*2	$Im\bar{3}m$
$\beta Fe_{17}Gd_2$	24.8	*hP*38	$P6_3/mmc$
$\alpha Fe_{17}Gd_2$	24.8	*hR*19	$R\bar{3}m$
$Fe_{23}Gd_6$	42.4	*cF*116	$Fm\bar{3}m$
Fe_3Gd	48	*hR*12	$R\bar{3}m$
Fe_2Gd	58.4	*cF*24	$Fd\bar{3}m$
(βGd)	100	*cI*2	$Im\bar{3}m$
(αGd)	100	*hP*2	$P6_3/mmc$
Questionable phases			
Fe_5Gd	24	*hP**	...
$Fe_{17}Gd_2$	24.8	*hP*8	*P*6/*mmm*
Fe_5Gd	36.1	*hP*6	*P*6/*mmm*
Fe_4Gd	41	*hP*10	...
Fe_7Gd_2	44.6	*o**18	...
Fe_3Gd_2	65	*c**30	...

Fe-Ge

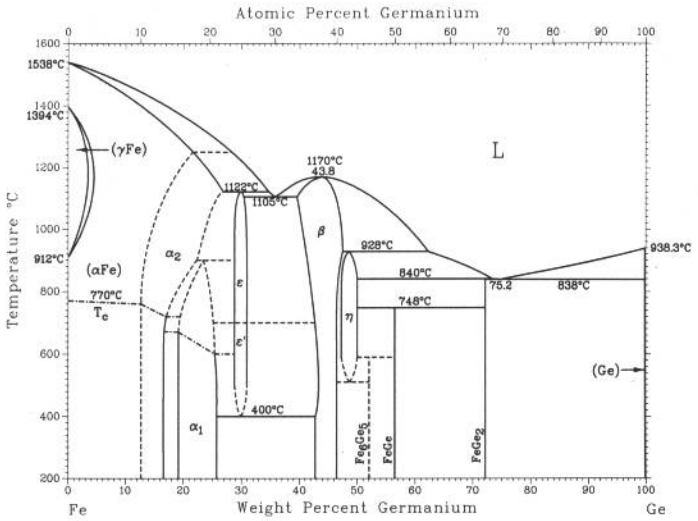

E. Kato and S. Nunoue, 1992

Phase	Composition, wt% Ge	Pearson symbol	Space group
(γFe)	0 to 4.4	*cF*4	$Fm\bar{3}m$
(αFe)	0 to 21.6	*cI*2	$Im\bar{3}m$
α_2	12.6 to 26.8	*cP*2	$Pm\bar{3}m$
α_1	18.9 to 25.7	*cF*16	$Fm\bar{3}m$
ε(Fe_3Ge)	28.8 to 31.0	*hP*8	$P6_3/mmc$
ε'(Fe_3Ge)	28.8 to 31.0	*cP*4	$Pm\bar{3}m$
β	39.6 to 47.5	*hP*4	$P6_3/mmc$
η	47.3 to 50.0	*hP*6	$P6_3/mmc$
Fe_6Ge_5	52.0	...	*C*2/*m*
FeGe	56.5	...	*C*2/*m*
		*hP*6	*P*6/*mmm*
		*cP*8	$P2_13$
$FeGe_2$	72.3	*tI*2	*I*4/*mcm*
(Ge)	100	*cF*8	$Fd\bar{3}m$

Fe-H

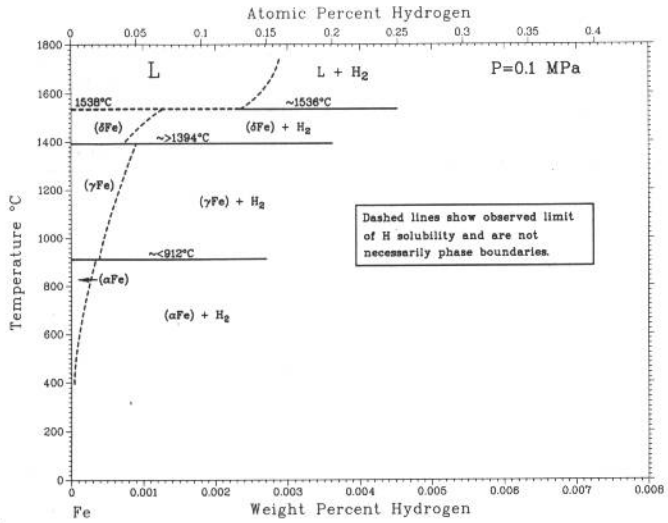

A. San-Martin and F.D. Manchester, 1992

Phase	Composition, wt% H	Pearson symbol	Space group
(δFe) or δ	0 to 0.0013	*cI*2	$Im\bar{3}m$
(γFe) or γ	0 to 0.0008	*cF*4	$Fm\bar{3}m$
(αFe) or α	0 to 0.0003	*cI*2	$Im\bar{3}m$
Metastable phases			
ε	1.2 to 1.4(a)	*hP*2	$P6_3/mmc$
		*hP*4	$P6_3/mmc$
		*hP*4	$P6_3mc$

(a) Produced under a pressure of 6.7 GPa at 250 °C

Fe-Hf

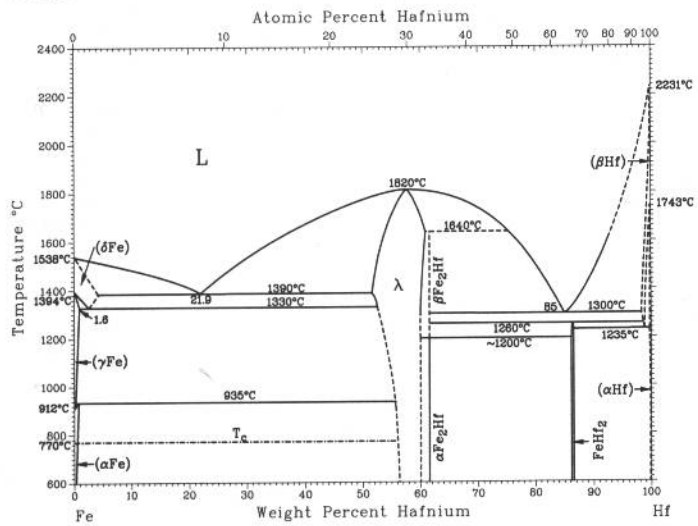

H. Okamoto, 1992

Phase	Composition, wt% Hf	Pearson symbol	Space group
(δFe)	0 to 6	*cI*2	$Im\bar{3}m$
(γFe)	0 to 1.6	*cF*4	$Fm\bar{3}m$
(αFe)	0 to 0.70	*cI*2	$Im\bar{3}m$
λ	52 to 61.2	*hP*12	$P6_3/mmc$
βFe_2Hf	61.5	*hP*24	$P6_3/mmc$
αFe_2Hf	61.5	*cF*24	$Fd\bar{3}m$
$FeHf_2$	85.6 to 86.6	*cF*96	$Fd\bar{3}m$
(βHf)	? to 100	*cI*2	$Im\bar{3}m$
(αHf)	? to 100	*hP*2	$P6_3/mmc$

Fe-Ho

H. Okamoto, 1992

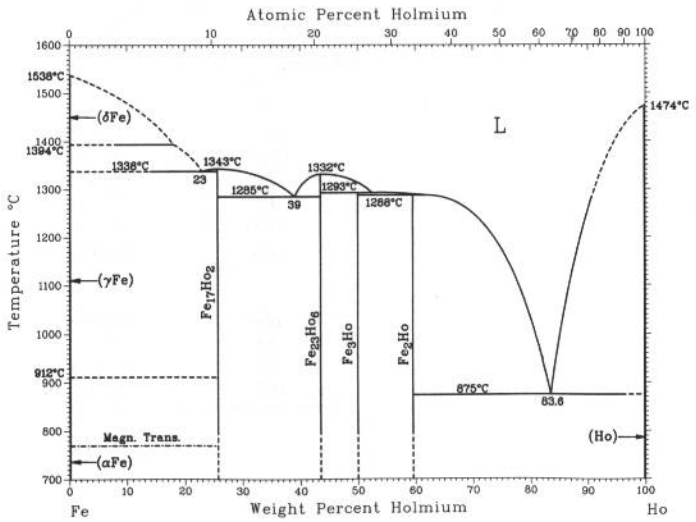

Phase	Composition, wt% Ho	Pearson symbol	Space group
(δFe)	0	*cI*2	$Im\bar{3}m$
(γFe)	0	*cF*4	$Fm\bar{3}m$
(αFe)	0	*cI*2	$Im\bar{3}m$
$Fe_{17}Ho_2$	25.7	*hP*38	$P6_3/mmc$
$Fe_{23}Ho_6$	43.5	*cF*116	$Fm\bar{3}m$
Fe_3Ho	50	*hR*12	$R\bar{3}m$
Fe_2Ho	59.6	*cF*24	$Fd\bar{3}m$
(Ho)	100	*hP*2	$P6_3/mmc$
Metastable phase			
...	~75	*hP*12	$P6_3/mmc$

Fe-Ir

L.J. Swartzendruber, 1992

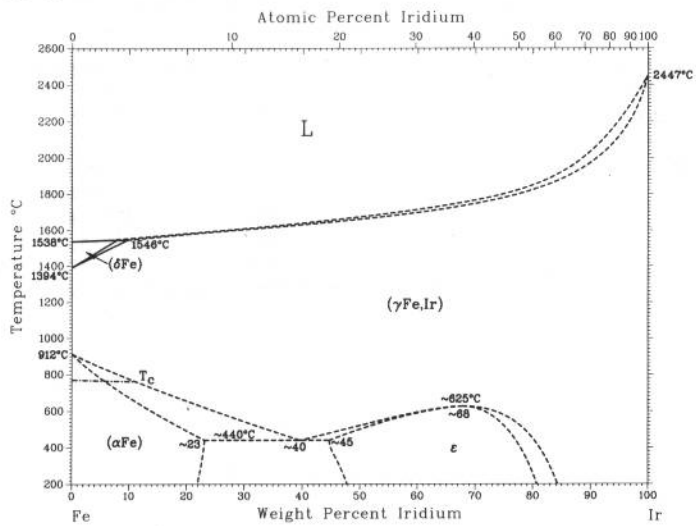

Phase	Composition, wt% Ir	Pearson symbol	Space group
(αFe)	0 to ~23	*cI*2	$Im\bar{3}m$
(γFe,Ir)	0 to 100	*cF*4	$Fm\bar{3}m$
(δFe)	0 to 7	*cI*2	$Im\bar{3}m$
ε	~45 to 80	*hP*2	$P6_3/mmc$

Fe-La

H. Okamoto, 1992

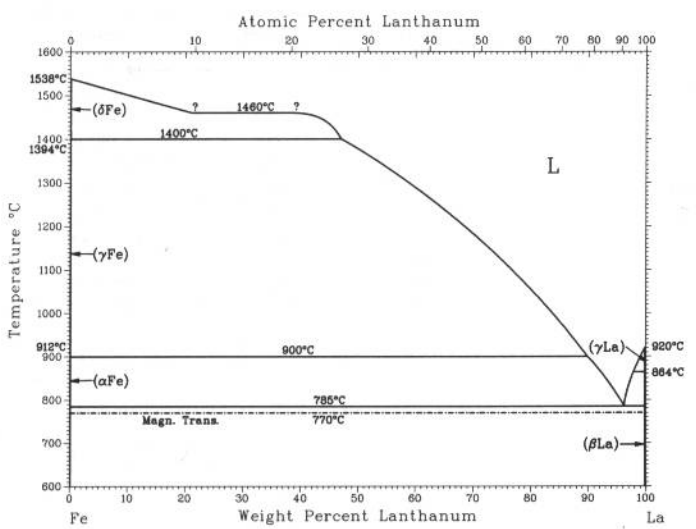

Phase	Composition, wt% La	Pearson symbol	Space group
(δFe)	0	*cI*2	$Im\bar{3}m$
(γFe)	0	*cF*4	$Fm\bar{3}m$
(αFe)	0	*cI*2	$Im\bar{3}m$
(γLa)	100	*cI*2	$Im\bar{3}m$
(βLa)	100	*cF*4	$Fm\bar{3}m$
(αLa)	100	*hP*4	$P6_3/mmc$

Fe-Lu

H. Okamoto, 1992

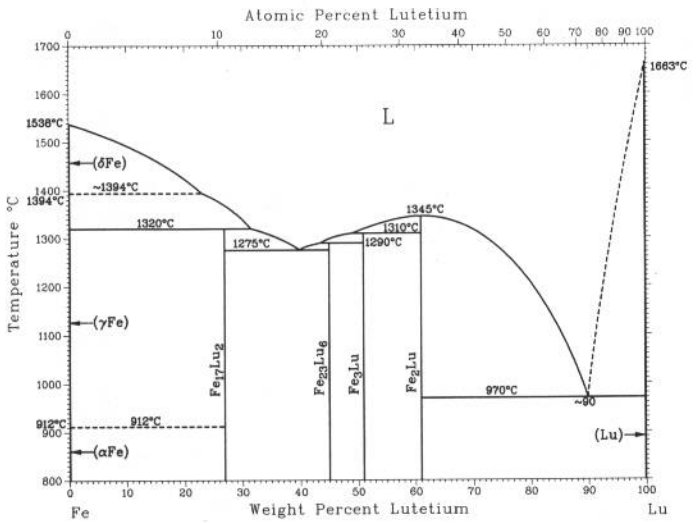

Phase	Composition, wt% Lu	Pearson symbol	Space group
(δFe)	0	*cI*2	$Im\bar{3}m$
(γFe)	0	*cF*4	$Fm\bar{3}m$
(αFe)	0	*cI*2	$Im\bar{3}m$
$Fe_{17}Lu_2$	24.7 to 26.9	*hP*38	$P6_3/mmc$
$Fe_{23}Lu_6$	45.0	*cF*116	$Fm\bar{3}m$
Fe_3Lu	51	*hR*12	$R\bar{3}m$
Fe_2Lu	61.0	*cF*24	$Fd\bar{3}m$
(Lu)	100	*hP*2	$P6_3/mmc$
Metastable phase			
...	~76	*hP*12	$P6_3/mmc$

Fe-Mn

H. Okamoto, 1992

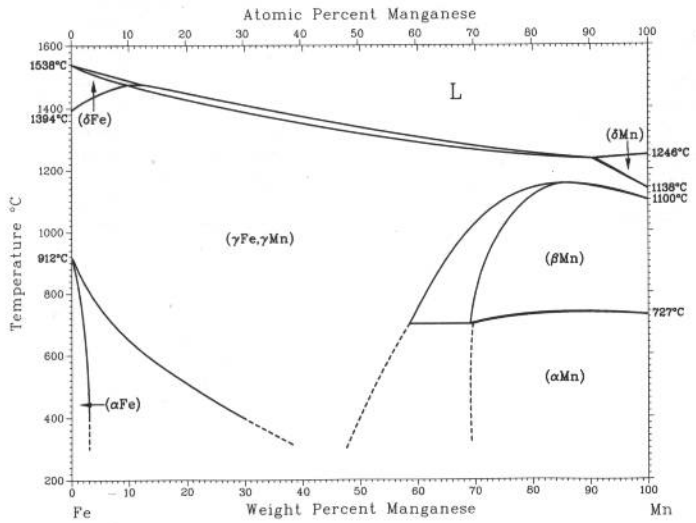

Phase	Composition, wt% Mn	Pearson symbol	Space group
(δFe)	0 to 10	*cI*2	$Im\bar{3}m$
(γFe,γMn)	0 to 100	*cF*4	$Fm\bar{3}m$
(αFe)	0 to 3	*cI*2	$Im\bar{3}m$
(δMn)	91 to 100	*cI*2	$Im\bar{3}m$
(βMn)	69.2 to 100	*cP*20	$P4_132$
(αMn)	~70 to 100	*cI*58	$I\bar{4}3m$
Metastable phases			
α′	3 to 18	*tI*2	*I*4/*mmm*
ε	12 to 30	*hP*2	$P6_3/mmc$
γ′	?	*t***	...

Fe-Mo

A. Fernández Guillermet, 1992

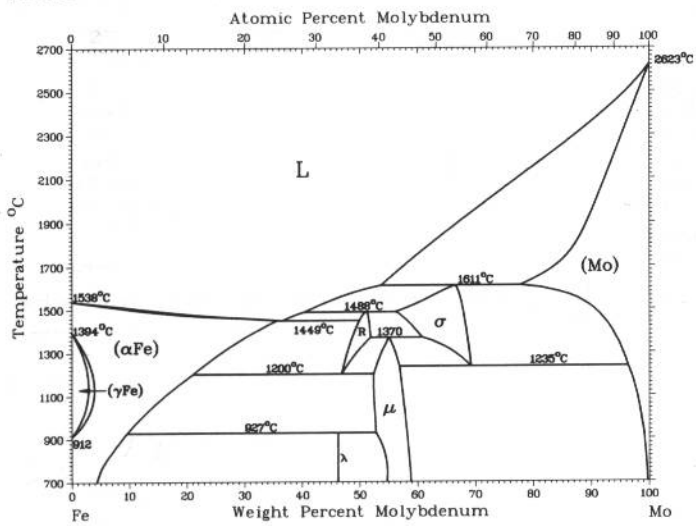

Phase	Composition, wt% Mo	Pearson symbol	Space group
(αFe)	0 to 35.7	*cI*2	$Im\bar{3}m$
(γFe)	0 to 2.9	*cF*4	$Fm\bar{3}m$
λ	46.2	*hP*12	$P6_3/mmc$
R	46.8 to 51.8	*hR*53	...
μ	52.3 to 57.4	*hR*13	$R\bar{3}m$
σ	56.3 to 69.2	*tP*30	$P4_2/mnm$
(Mo)	79.0 to 100	*cI*2	$Im\bar{3}m$

Fe-N

H.A. Wriedt, N.A. Gokcen, and R.H. Nafziger, 1992

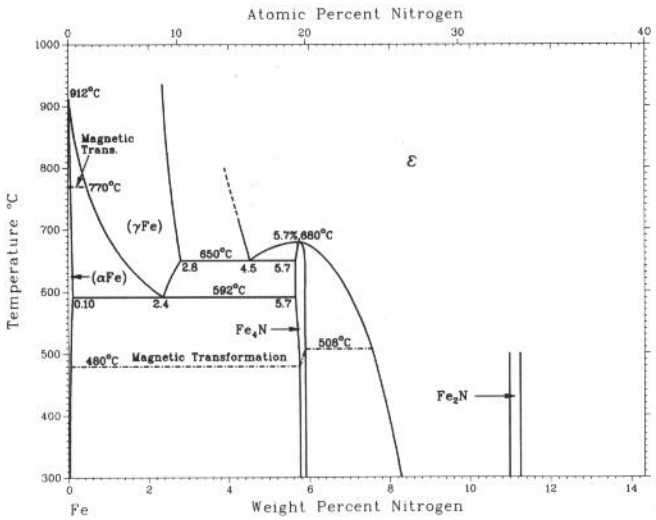

Phase	Composition, wt% N	Pearson symbol	Space group
Stable at 0.1 MPa			
(δFe)	0 to ~0.9	*cI*2	$Im\bar{3}m$
(γFe)	0 to 2.8	*cF*4	$Fm\bar{3}m$
(αFe)	0 to 0.10	*cI*2	$Im\bar{3}m$
Fe_4N	5.7 to 5.9	*cP*5	$Pm\bar{3}m$ or $P\bar{4}3m$
ε	~4 to ~11	*hP*3	$P6_3/mmc$
Fe_2N	~11.1	*o***	...
FeN_6	~61	...	...
FeN_9	~69	...	...
Other phases			
(εFe)(a)	0 to ?	*hP*2	$P6_3/mmc$
Martensite	0 to 0.6	*cI*2	$Im\bar{3}m$
	0.7 to 2.6	(b)	...
$Fe_{16}N_2$	~3.0	(b)	*I*4/*mmm*

(a) Stable at pressures >13 GPa. (b) bct

Fe-Nb

E. Paul and L.J. Swartzendruber, 1992

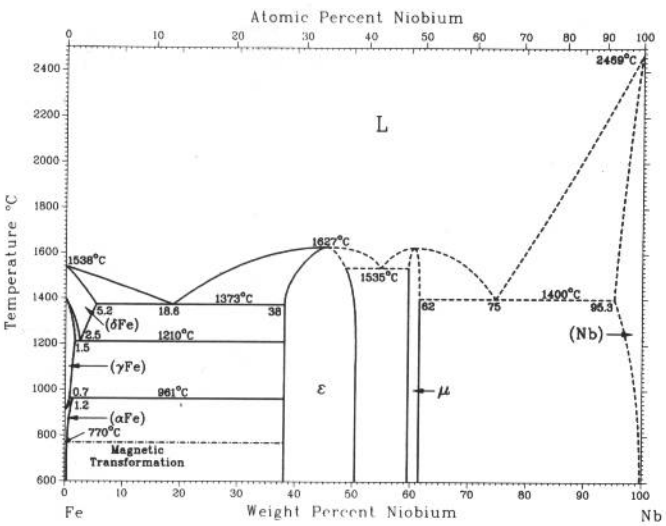

Phase	Composition, wt% Nb	Pearson symbol	Space group
δ or (δFe)	0 to 5.2	*cI*2	$Im\bar{3}m$
γ or (γFe)	0 to 1.5	*cF*4	$Fm\bar{3}m$
α or (αFe)	0 to 1.2	*cI*2	$Im\bar{3}m$
ε or Fe_2Nb	38 to 51	*hP*12	$P6_3/mmc$
μ or FeNb	60 to 62	*hR*13	$R\bar{3}m$
(Nb)	95.3 to 100	*cI*2	$Im\bar{3}m$

Fe-Nd

W. Zhang, G. Liu, and K. Han, 1992

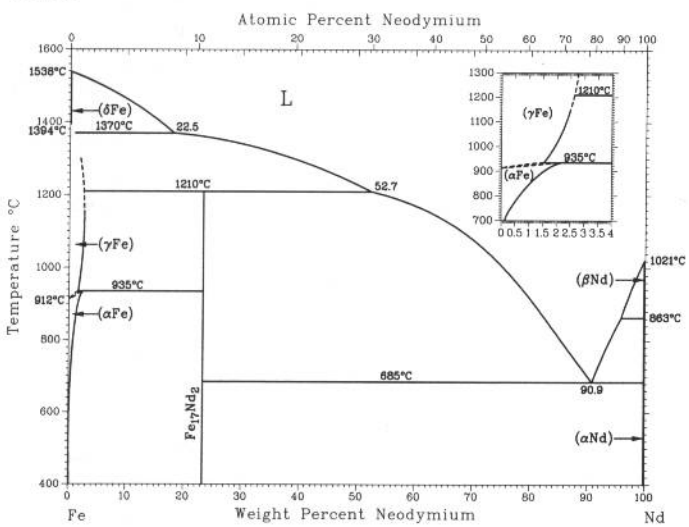

Phase	Composition, wt% Nd	Pearson symbol	Space group
(δFe)(a)	0	*cI*2	$Im\bar{3}m$
(γFe)(b)	0 to ~1	*cF*4	$Fm\bar{3}m$
(αFe)(c)	0 to ~1.1	*cI*2	$Im\bar{3}m$
$Fe_{17}Nd_2$	23.3	(d)	$R\bar{3}m$
(βNd)(e)	100	*cI*2	$Im\bar{3}m$
(αNd)(f)	100	*hP*4	$P6_3/mmc$
Metastable phase			
$Fe_{5+x}Nd$	...	*hP*6	*P*6/*mmm*

(a) From 1538 to 1394 °C. (b) From <1394 to 912 °C. (c) Below 912 °C. (d) Rhombohedral. (e) From 1021 to 863 °C. (f) Below 863 °C

Fe-Ni

L.J. Swartzendruber, V.P. Itkin, and C.B. Alcock, 1992

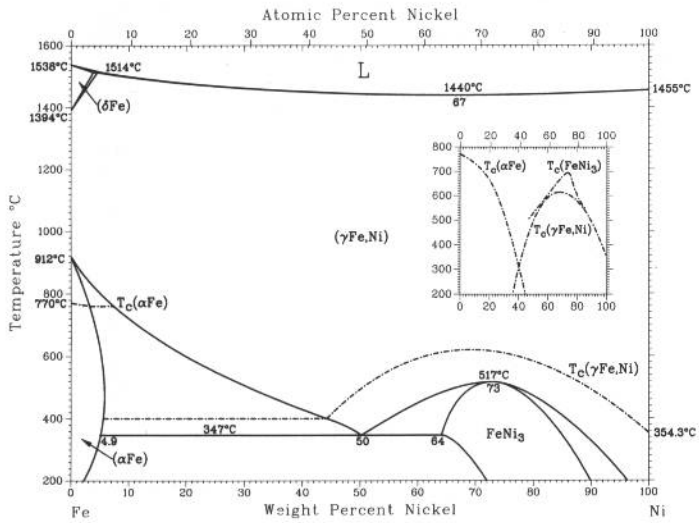

Phase	Composition, wt% Ni	Pearson symbol	Space group
(δFe)	0 to 3.7	*cI*2	$Im\bar{3}m$
(γFe, Ni)	0 to 100	*cF*4	$Fm\bar{3}m$
(αFe)	0 to 5.8	*cI*2	$Im\bar{3}m$
Fe_3Ni(a)	26	*cP*4	$Pm\bar{3}m$
FeNi(a)	51	*tP*2	*P4/mmm*
$FeNi_3$	64 to ~90	*cP*4	$Pm\bar{3}m$

(a) Metastable

Fe-O

H.A. Wriedt, 1992

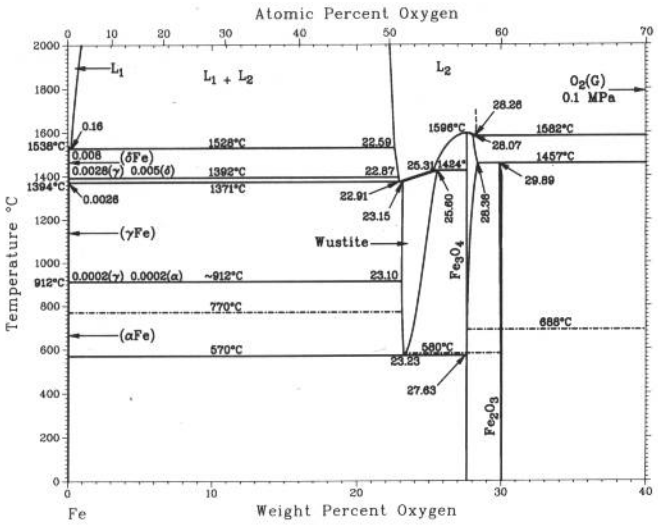

Phase	Composition, wt% O	Pearson symbol	Space group
Stable phases			
(δFe)	~0	*cI*2	$Im\bar{3}m$
(γFe)	~0	*cF*4	$Fm\bar{3}m$
(αFe)	~0	*cI*2	$Im\bar{3}m$
Wustite	23.15 to 25.60	*cF*8	$Fm\bar{3}m$
Fe_3O_4(LT)	~27.6	*mC*224	*Cc*
Fe_3O_4	27.56 to 28.36	*cF*56	$Fd\bar{3}m$
αFe_2O_3	~30.1	*hR*10	$R\bar{3}c$
Other phases			
(εFe)(a)	0 to ?	*hP*2	$P6_3/mmc$
P′(wustite)	~23.2 to ~24.8	*c***(?)(b)	...
P″(wustite)	~24 to ~25	*mP*500(?)	$P2_1/m$
P‴(wustite)	...	...	...
Wustite(LT)	23.2 to 24.6	*hR*2(c)	$R\bar{3}$
Fe_3O_4(P)(d)	~27.6	*m**14	...
βFe_2O_3	~30.1	*cI*80	$Ia\bar{3}$
γFe_2O_3	~30.1	*tP*60	$P4_32_12$
εFe_2O_3	~30.1	*m**100	...

(a) Stable at pressures >13 GPa. (b) Incommensurate or orthorhombic. (c) Magnetic reflections might indicate linear cell dimensions are doubled, corresponding to *hR*16. (d) Stable at pressures >25 GPa

Fe-O phase diagram from 22 to 31 wt% O

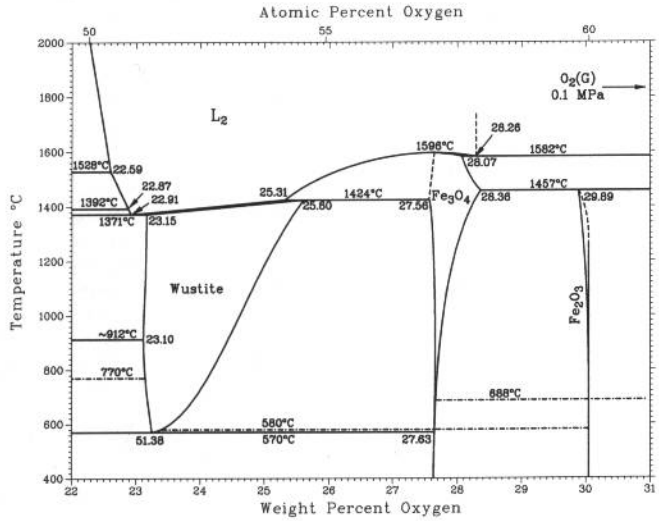

Fe-P

H. Okamoto, 1992

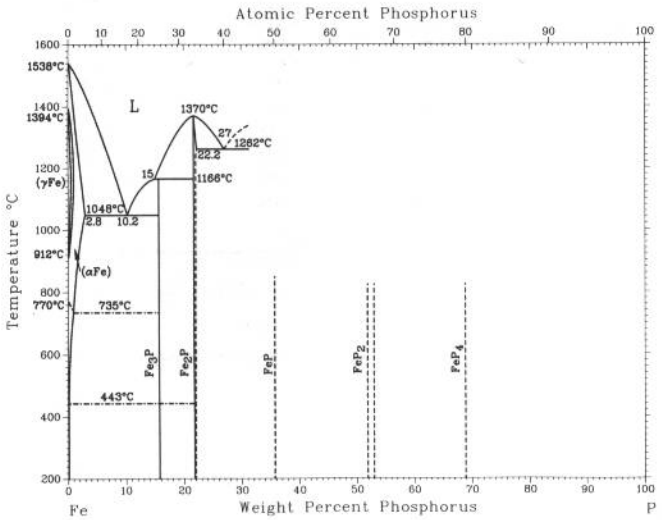

Phase	Composition, wt% P	Pearson symbol	Space group
(γFe)	0 to 0.31	*cF*4	$Fm\bar{3}m$
(αFe)	0 to 2.8	*cI*2	$Im\bar{3}m$
Fe_3P	16	*tI*32	*I*4
Fe_2P	21.7 to 22.2	*hP*9	$P\bar{6}2m$
FeP	36	*oP*8	$Pna2_1$
FeP_2	52 to 53	*oP*6	*Pnnm*
FeP_4	69	*mP*30	$P2_1/c$
(P) (white)	100	*c***	...
Metastable phases			
$Fe_{4+}P$	<12	*o***	...
(P) black	100	*oC*8	*Cmca*
High-pressure phases			
Fe_2P	21.7	*oP*12	*Pnma*
FeP_4	69	*oC*20	$C222_1$

Fe-Pd

H. Okamoto, 1992

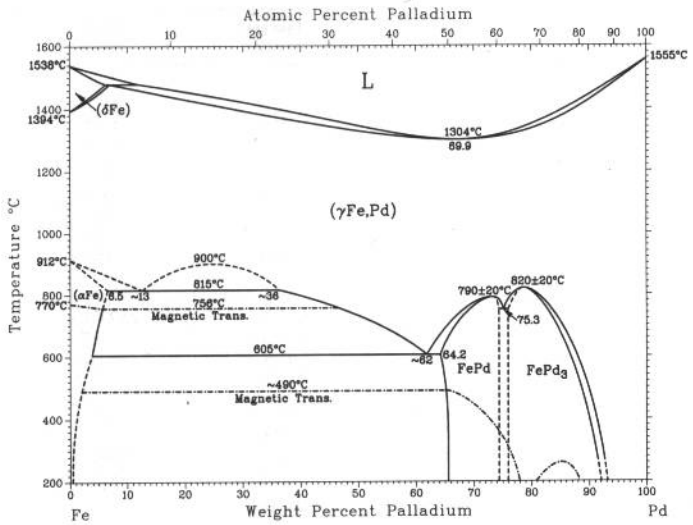

Phase	Composition, wt% Pd	Pearson symbol	Space group
(δFe)	0 to 6.1	*cI*2	$Im\bar{3}m$
(γFe, Pd)	0 to 100	*cF*4	$Fm\bar{3}m$
(αFe)	0 to 6.5	*cI*2	$Im\bar{3}m$
FePd	64.2 to 74	*tP*2	*P*4/*mmm*
$FePd_3$	76 to ?	*cP*4	$Pm\bar{3}m$

Fe-Pu

H. Okamoto, 1992

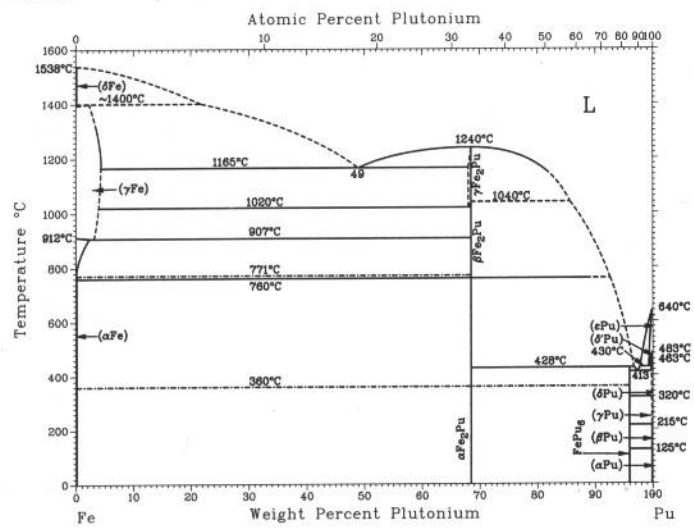

Phase	Composition, wt% Pu	Pearson symbol	Space group
(δFe)	0	*cI*2	$Im\bar{3}m$
(γFe)	0 to ~4	*cF*4	$Fm\bar{3}m$
(αFe)	0	*cI*2	$Im\bar{3}m$
γFe_2Pu	68.6	*c***	...
βFe_2Pu	68.6	*hP*24	$P6_3/mmc$
αFe_2Pu	68.6	*cF*24	$Fd\bar{3}m$
$FePu_6$	96.3	*tI*28	*I*4/*mcm*
(εPu)	99.5 to 100	*cI*2	$Im\bar{3}m$
(δ'Pu)	~100	*tI*2	*I*4/*mmm*
(δPu)	99.9 to 100	*cF*4	$Fm\bar{3}m$
(γPu)	100	*oF*8	*Fddd*
(βPu)	100	*mC*34	*C*2/*m*
(αPu)	100	*mP*16	$P2_1/m$

Fe-Rh

L.J. Swartzendruber, 1992

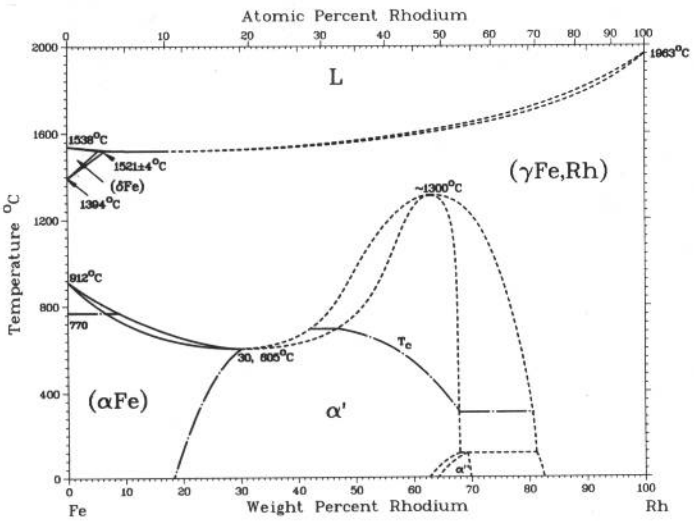

Phase	Composition, wt% Rh	Pearson symbol	Space group
(δFe)	0 to 5	*cI*2	$Im\bar{3}m$
(γFe,Rh)	0 to 100	*cF*4	$Fm\bar{3}m$
(αFe)	0 to 30	*cI*2	$Im\bar{3}m$
α′	19 to 69	*cP*2	$Pm\bar{3}m$
α″ (chemical cell)	63 to 69	*cP*2	$Pm\bar{3}m$
α″ (magnetic cell)	63 to 69	*cF*16	$Fm\bar{3}m$

Fe-S

From [Kubaschewski]

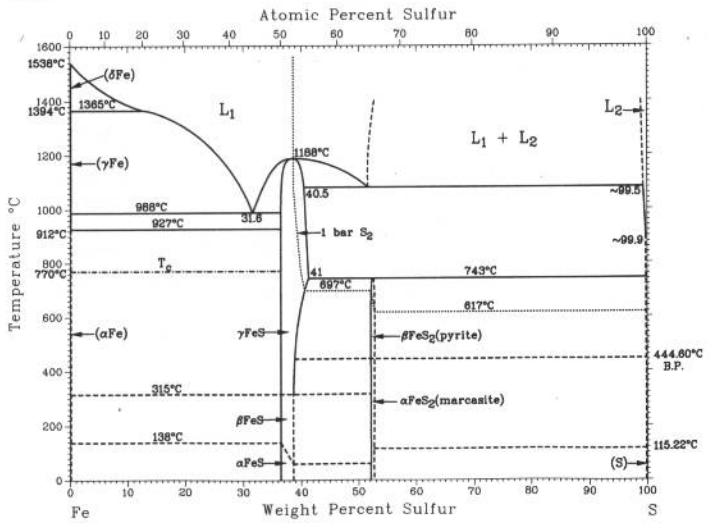

Fe-rich region of the Fe-S system

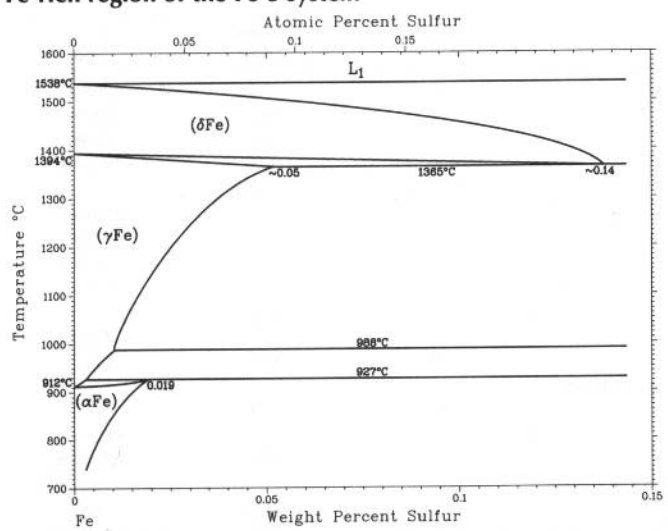

Fe-Sb

H. Okamoto, 1992

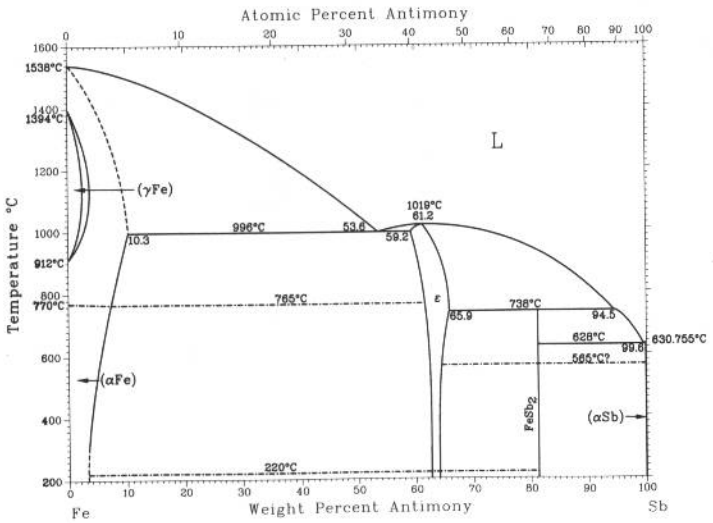

Phase	Composition, wt% Sb	Pearson symbol	Space group
(αFe)	0 to 10.3	*cI*2	$Im\bar{3}m$
(γFe)	0 to 2.4	*cF*4	$Fm\bar{3}m$
ε	59.2 to 65.9	*hP*4	$P6_3/mmc$
$FeSb_2$	81.4	*oP*6	*Pnn*2
(αSb)	100	*hR*2	$R\bar{3}m$
Metastable phase			
$FeSb_4$	90	*cP*1	$Pm\bar{3}m$

Fe-Sc

H. Okamoto, 1992

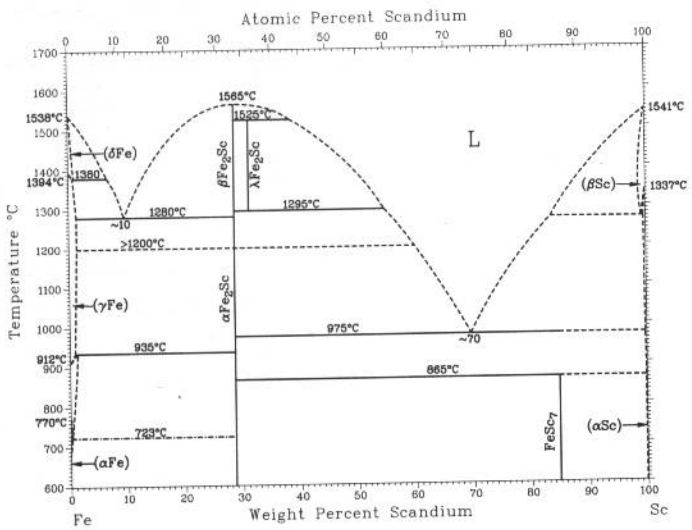

Phase	Composition, wt% Sc	Pearson symbol	Space group
(δFe)	~0	*cI*2	$Im\bar{3}m$
(γFe)	~0	*cF*4	$Fm\bar{3}m$
(αFe)	~0	*cI*2	$Im\bar{3}m$
βFe_2Sc	28.7	*hP*24	$P6_3/mmc$
αFe_2Sc	28.7	*hP*12	$P6_3/mmc$
λFe_2Sc	~31	*cF*24	$Fd\bar{3}m$
$FeSc_7$	84.9	…	…
(βSc)	~100	*cI*2	$Im\bar{3}m$
(αSc)	~100	*hP*2	$P6_3/mmc$

Fe-Se

H. Okamoto, 1992

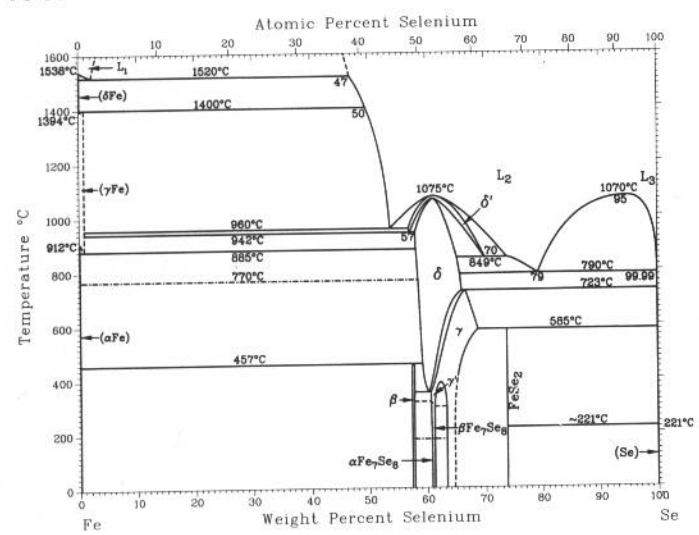

Phase	Composition, wt% Se	Pearson symbol	Space group
(δFe)	~0	*cI*12	$Im\bar{3}m$
(γFe)	~0	*cF*4	$Fm\bar{3}m$
(αFe)	~0	*cI*2	$Im\bar{3}m$
β	57.6 to 58.0	*tP*4	*P*4/*nmm*
δ′	57 to 70	…	…
δ	58.1 to 66	*hP*4	$P6_3/mmc$
γ′	?	*mC*7	*C*2/*m*
γ	? to 69	*mC*14	*C*2/*m*
βFe_7Se_8	61.7	*hP*45	$P3_121$
αFe_7Se_8	61.7	*aP*120	
$FeSe_2$	73.9	*oP*6	*Pnnm*
(γSe)	100	*hP*3	$P3_121$
Metastable phases			
FeSe	58.6	*c***	…
FeSe	58.6	*hP*4	$P6_3/mmc$
FeSe	58.6	*tP*2	*P*4/*mmm*
High-pressure phase			
$FeSe_2$	73.9	*cP*12	*Pa*3

Fe-Si

From [Kubaschewski]

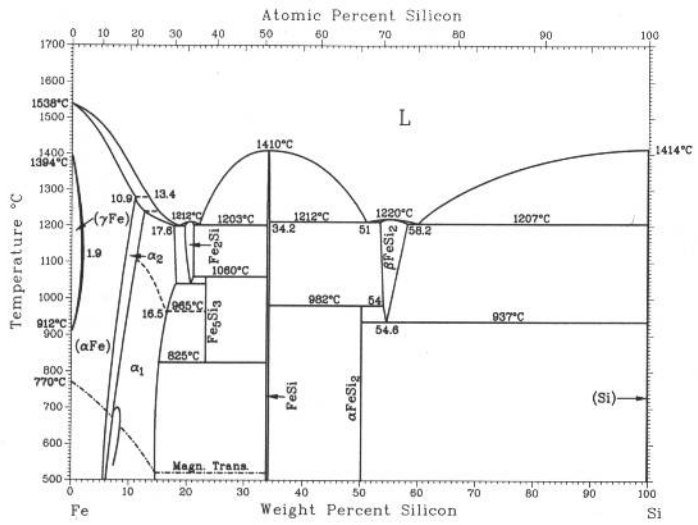

Phase	Composition, wt % Si	Pearson symbol	Space group
(γFe)	0 to 10.9	*cF*4	$Fm\bar{3}m$
(αFe)	0 to 1.63	*cI*2	$Im\bar{3}m$
α_2	~5 to 12	*cP*2	$Pm\bar{3}m$
α_1	~5 to 18	*cF*16	$Fm\bar{3}m$
Fe_2Si	~20.1	*hP*6	$P\bar{3}m1$
Fe_5Si_3	23.2	*hP*16	$P6_3/mcm$
FeSi	~34	*cP*8	$P2_13$
$\beta FeSi_2$	53.4 to 58.2	*tP*3	*P*4/*mmm*
$\alpha FeSi_2$	50.2	*oC*48	*Cmca*
(Si)	100	*cF*8	$Fd\bar{3}m$

Fe-Sm

H. Okamoto, 1992

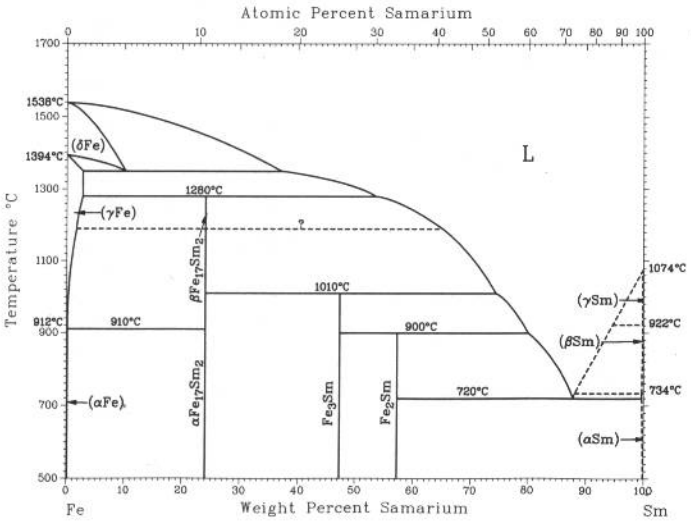

Phase	Composition, wt % Sm	Pearson symbol	Space group
(δFe)	~0	*cI*2	$Im\bar{3}m$
(γFe)	~0	*cF*4	$Fm\bar{3}m$
(αFe)	0	*cI*2	$Im\bar{3}m$
$\beta Fe_{17}Sm_2$	24.0	*hP*38	$P6_3/mmc$
$\alpha Fe_{17}Sm_2$	24.0	*hR*19	$R\bar{3}m$
Fe_3Sm	47	*hR*12	$R\bar{3}m$
Fe_2Sm	57.3	*cF*24	$Fd\bar{3}m$
(γSm)	100	*cI*2	$Im\bar{3}m$
(βSm)	~100	*hP*2	$P6_3/mmc$
(αSm)	>99.8 to 100	*hR*3	$R\bar{3}m$
Questionable phase			
Fe_5Sm	35.1	*hP*6	*P*6/*mmm*

Fe-Sn

H. Okamoto, 1992

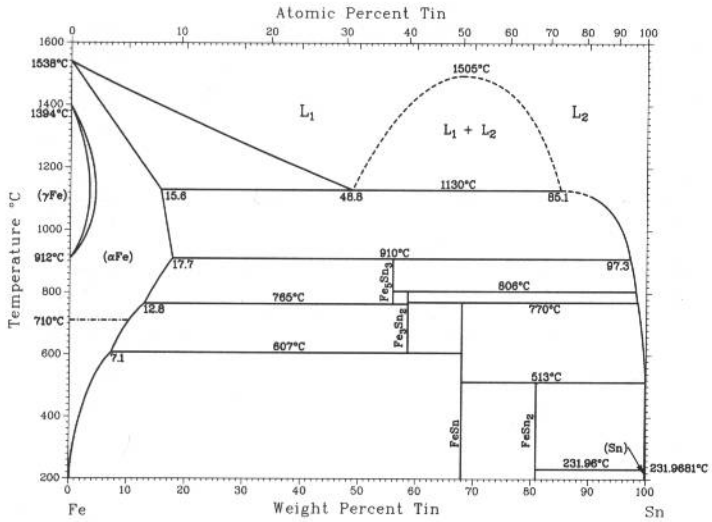

Phase	Composition, wt % Sn	Pearson symbol	Space group
(γFe)	0 to 1.7	*cF*4	$Fm\bar{3}m$
(αFe)	0 to 17.7	*cI*2	$Im\bar{3}m$
Fe_5Sn_3	56.1	*hP*6	$P6_3/mmc$
Fe_3Sn_2	59	*hR*10	$R\bar{3}m$
FeSn	68.0	*hP*6	*P*6/*mmm*
$FeSn_2$	81.0	*tI*2	*I*4/*mcm*
(βSn)	100	*tI*4	$I4_1/amd$
(αSn)	100	*cF*8	$Fm\bar{3}m$
Oxygen stabilized phase			
"Fe_3Sn"	42	*hP*8	$P6_3/mmc$

Fe-Tb

H. Okamoto, 1992

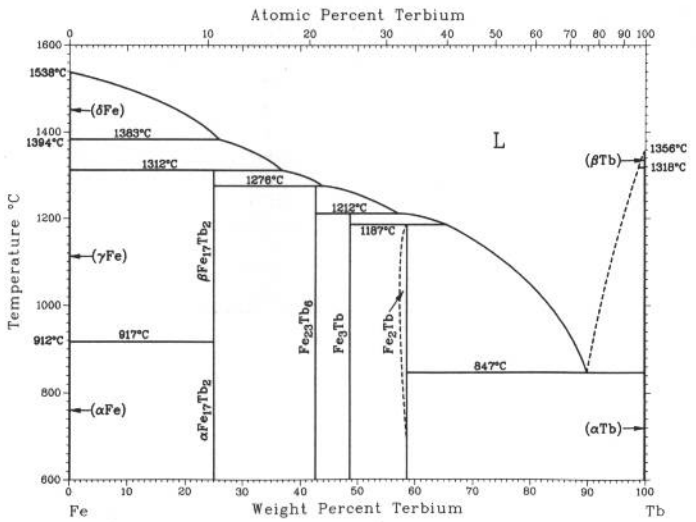

Phase	Composition, wt% Tb	Pearson symbol	Space group
(δFe)	0	*cI*2	$Im\bar{3}m$
(γFe)	~0	*cF*4	$Fm\bar{3}m$
(αFe)	0	*cI*2	$Im\bar{3}m$
$\beta Fe_{17}Tb_2$	25.0	*hP*38	$P6_3/mmc$
$\alpha Fe_{17}Tb_2$	25.0	*hR*19	$R\bar{3}m$
$Fe_{23}Tb_6$	42.6	*cF*116	$Fm\bar{3}m$
Fe_3Tb	49	*hR*12	$R\bar{3}m$
Fe_2Tb	58.7	*cF*24	$Fd\bar{3}m$
Fe_2Tb(a)	58.7	*hR*6	$R\bar{3}m$
(βTb)	100	*cI*2	$Im\bar{3}m$
(αTb)	100	*hP*2	$P6_3/mmc$

(a) Distorted Cu_2Mg type due to magnetostriction at low temperatures

Fe-Te

H. Okamoto and L.E. Tanner, 1992

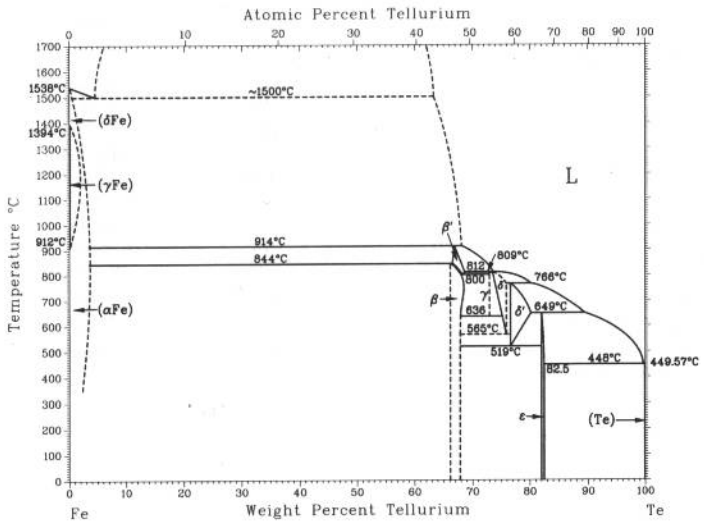

Phase	Composition, wt% Te	Pearson symbol	Space group
(δFe, αFe)	0 to 3.4	*cI*2	$Im\bar{3}m$
(γFe)	~0	*cF*4	$Fm\bar{3}m$
β′	66.5 to 68.3	*hR**	...
β	66 to 68.3	*tP*4	*P*4/*nmm*
		*tP*6	*P*4/*nmm*
β_1(a)	66 to 68	*mP**	$P2_1/m$
γ	73.0	...	...
δ	74 to 77	*mC*14	*C*2/*m*
δ′	76.9 to 80.6	*hP*4	$P6_3/mmc$
ε	82.0 to 82.5	*oP*6	*Pnn*2
$FeTe2_2I$(b)	82.1	*cP*12	$Pa\bar{3}$
(Te)	100	*hP*3	$P3_121$

(a) Low-temperature phase. (b) High-pressure phase

Fe-Th

H. Okamoto, 1992

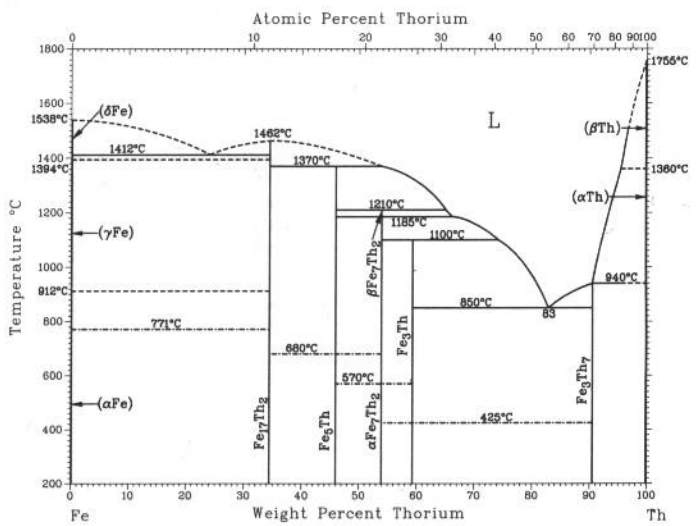

Phase	Composition, wt% Th	Pearson symbol	Space group
(δFe)	0	*cI*2	$Im\bar{3}m$
(γFe)	0	*cF*4	$Fm\bar{3}m$
(αFe)	0	*cI*2	$Im\bar{3}m$
$Fe_{17}Th_2$	32.8	*hR*19	$R\bar{3}m$
Fe_5Th	45.4	*hP*6	*P*6/*mmm*
βFe_7Th_2	54.2	*hR*18	$R\bar{3}m$
αFe_7Th_2	54.2	*hP*36	$P6_3/mmc$
Fe_3Th	58	*hR*12	$R\bar{3}m$
Fe_3Th_7	91	*hP*20	$P6_3mc$
(βTh)	100	*cI*2	$Im\bar{3}m$
(αTh)	100	*cF*4	$Fm\bar{3}m$

Fe-Ti

J.L. Murray, 1992

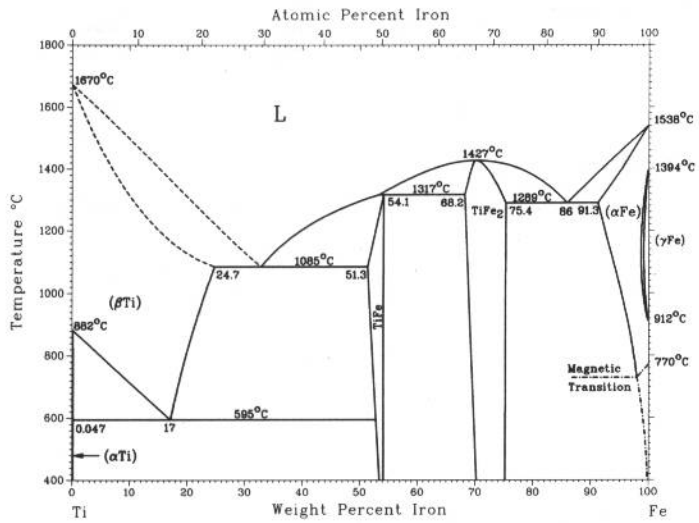

Phase	Composition, wt% Fe	Pearson symbol	Space group
(αTi)	0 to 0.047	*hP*2	$P6_3/mmc$
(βTi)	0 to 24.7	*cI*2	$Im\bar{3}m$
TiFe	51.3 to 54.1	*cP*2	$Pm\bar{3}m$
$TiFe_2$	68.2 to 75.4	*hP*12	$P6_3/mmc$
(αFe)	91.3 to 100	*cI*2	$Im\bar{3}m$
(γFe)	99.5 to 100	*cF*4	$Fm\bar{3}m$
ω	(a)	*hP*3	*P6/mmm*

(a) Metastable phase

Fe-Tm

H. Okamoto, 1992

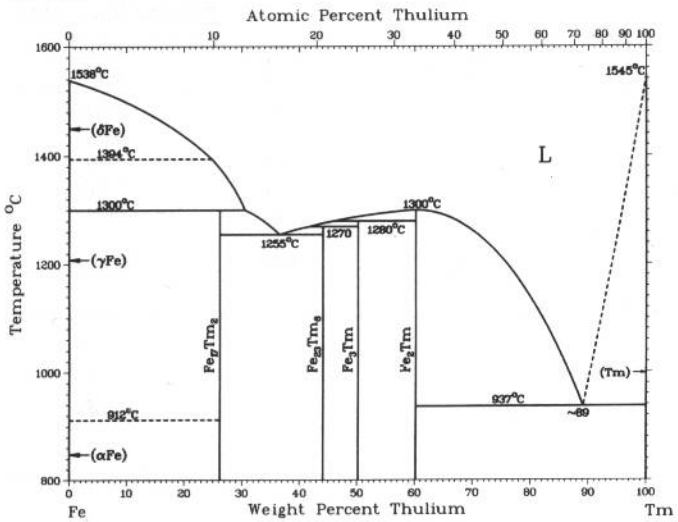

Phase	Composition, wt% Tm	Pearson symbol	Space group
(δFe)	0	*cI*2	$Im\bar{3}m$
(γFe)	0	*cF*4	$Fm\bar{3}m$
(αFe)	0	*cI*2	$Im\bar{3}m$
$Fe_{17}Tm_2$	26.2	*hP*38	$P6_3/mmc$
$Fe_{23}Tm_6$	44.1	*cF*114	$Fm\bar{3}m$
Fe_3Tm	50.2	*hR*12	$R\bar{3}m$
Fe_2Tm	60.2	*cF*24	$Fd\bar{3}m$
(Tm)	100	*hP*2	$P6_3/mmc$
Metastable phase			
...	~75	*hP*12	$P6_3/mmc$

Fe-U

H. Okamoto, 1992

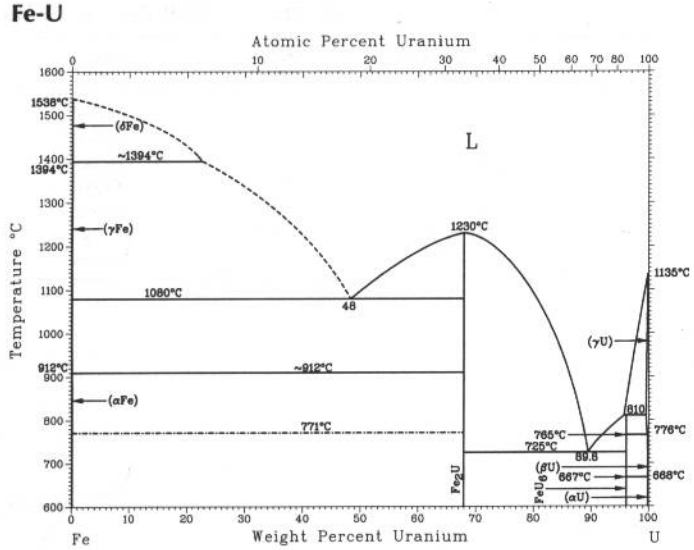

Phase	Composition, wt% U	Pearson symbol	Space group
(δFe)	0	*cI*2	$Im\bar{3}m$
(γFe)	0	*cF*4	$Fm\bar{3}m$
(αFe)	0	*cI*2	$Im\bar{3}m$
Fe_2U	68.0	*cF*24	$Fd\bar{3}m$
FeU_6	96.2	*tI*28	*I4/mcm*
(γU)	99.7 to 100	*cI*2	$Im\bar{3}m$
(βU)	99.9 to 100	*tP*30	$P4_2/mnm$
(αU)	99.99 to 100	*oC*4	*Cmcm*

Fe-V

J.F. Smith, 1992

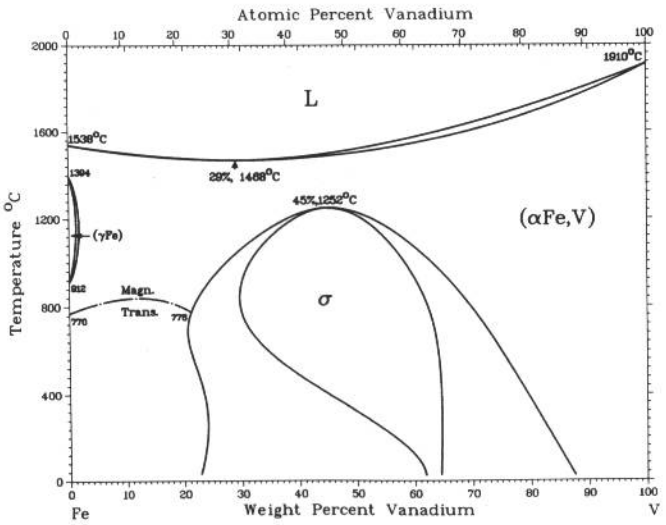

Phase	Composition, wt % V	Pearson symbol	Space group
(αFe,V)	0 to 100	*cI*2	$Im\bar{3}m$
(γFe)	0 to 1.2	*cF*4	$Fm\bar{3}m$
σ	30 to 65	*tP*30	$P4_2/mnm$
Metastable phase			
α′	47.7	*cP*2	$Pm\bar{3}m$

Fe-W

S.V. Nagender Naidu, A.M. Sriramamurthy, and P. Rama Rao, 1992

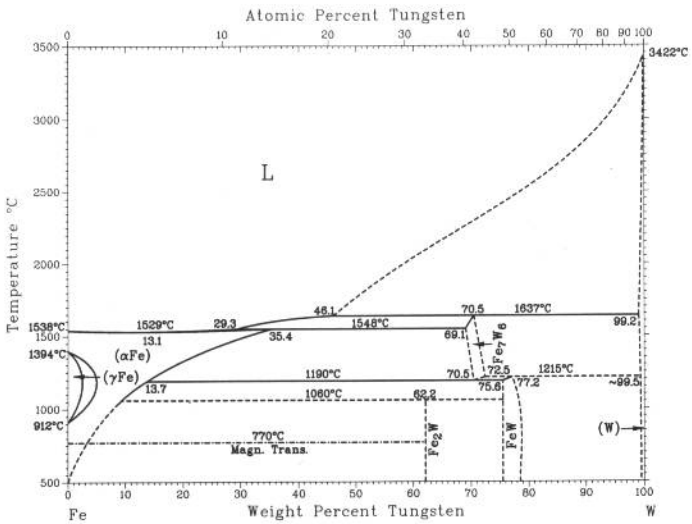

Phase	Composition, wt % W	Pearson symbol	Space group
(γFe)	0	*cF*4	$Fm\bar{3}m$
(αFe)	0	*cI*2	$Im\bar{3}m$
Fe_7W_6 (μ)	~70.5	*hR*13	$R\bar{3}m$
FeW (δ)	~77.2	(a)	$P2_12_12_1$
(W)	100	*cI*2	$Im\bar{3}m$
Metastable phase			
Fe_2W (λ)	62.2	*hP*12	$P6_3/mmc$

(a) Orthorhombic

Fe-Zn

B.P. Burton and P. Perrot, 1992

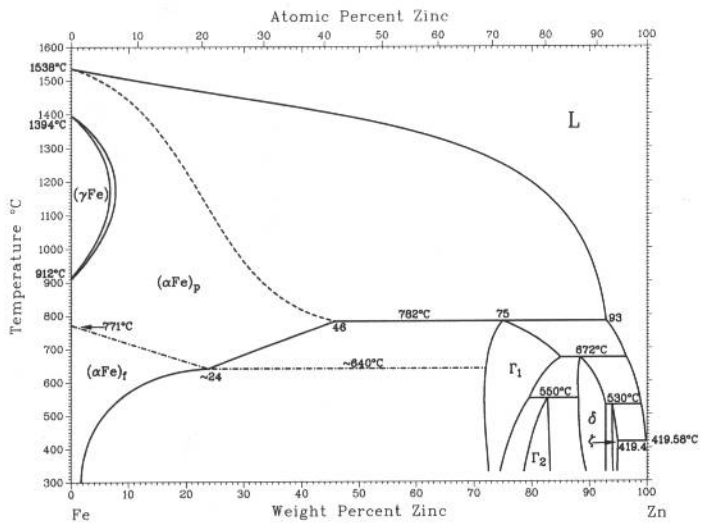

Phase	Composition, wt % Zn	Pearson symbol	Space group
(γFe)	0 to 6.59	*cF*4	$Fm\bar{3}m$
(αFe,δFe)	0 to 46	*cI*2	$Im\bar{3}m$
Γ_1	~72 to ~85	*cI*52	$I\bar{4}3m$
Γ_2	0.91 to 83	*cF*408	$F\bar{4}3m$
δ-$FeZn_{10}$	88.5 to 93.0	*hP*555	$P6_3mc$
ζ-$FeZn_{13}$	~94 to 94.8?	*mC*28	*C*2/*m*
(Zn)	~100	*hP*2	$P6_3/mmc$

Fe-Zr

D. Arias and J.P. Abriata, 1992

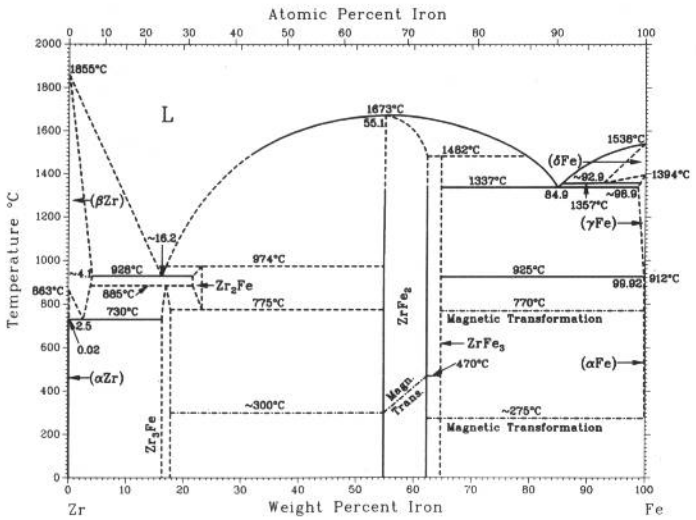

Phase	Composition, wt% Fe	Pearson symbol	Space group
(βZr)	0 to ~4.1	*cI*2	$Im\bar{3}m$
(αZr)	0 to 0.02	*hP*2	$P6_3/mmc$
Zr_3Fe	16.2 to 18.3	*oC*16	*Cmcm*
Zr_2Fe	21.6 to 23.4	*tI*12	*I*4/*mcm*
$ZrFe_2$	54.3 to 62.2	*cF*24	$Fd\bar{3}m$
$ZrFe_3$	64.7	*cF*116	$Fm\bar{3}m$
(δFe)	~92.9 to 100	*cI*2	$Im\bar{3}m$
(γFe)	~98.9 to 100	*cF*4	$Fm\bar{3}m$
(αFe)	99.91 to 100	*cI*2	$Im\bar{3}m$

Ga-Gd

A. Palenzona and S. Cirafici, 1990

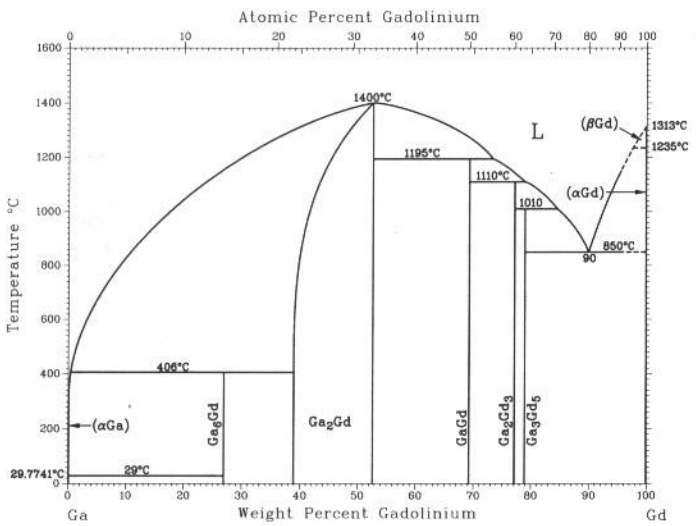

Phase	Composition, wt% Gd	Pearson symbol	Space group
(Ga)	~0	*oC*8	*Cmca*
Ga_6Gd	27.32	*tP*14	*P*4/*nbm*
Ga_2Gd	39 to 53.0	*hP*3	*P*6/*mmm*
GaGd	69.3	*oC*8	*Cmcm*
Ga_2Gd_3	77	*tI*80	*I*4/*mcm*
Ga_3Gd_5	79.0	*tI*32	*I*4/*mcm*
(βGd)	~100	*cI*2	$Im\bar{3}m$
(αGd)	~100	*hP*2	$P6_3/mmc$

Ga-Ho

H. Okamoto, 1990

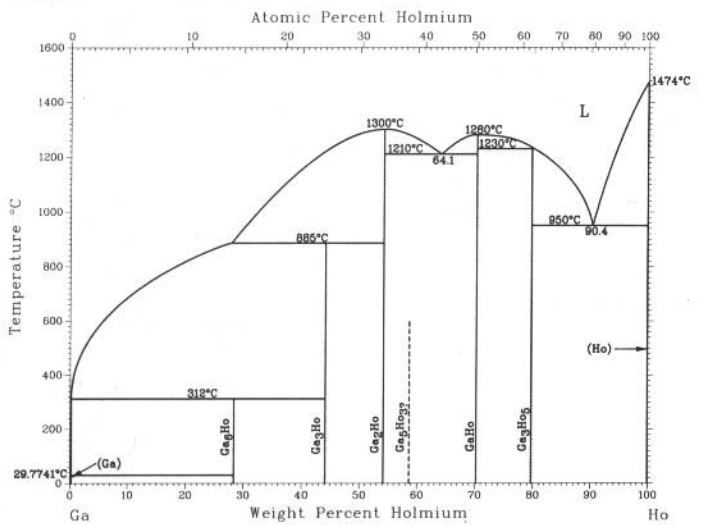

Phase	Composition, wt% Ho	Pearson symbol	Space group
(Ga)	0	*oC*8	*Cmca*
Ga_6Ho	28.3	*tP*14	*P*4/*nbm*
Ga_3Ho	44	*cP*4	$Pm\bar{3}m$
Ga_2Ho	54.1	*hP*3	*P*6/*mmm*
Ga_5Ho_3	58.7	*oP*32	*P*4/*nbm*
GaHo	70.3	*oC*8	*Cmcm*
Ga_3Ho_5	79.8	*hP*16	$P6_3/mcm$
(Ho)	100	*hP*2	$P6_3/mmc$

Ga-In

T.J. Anderson and I. Ansara, 1992

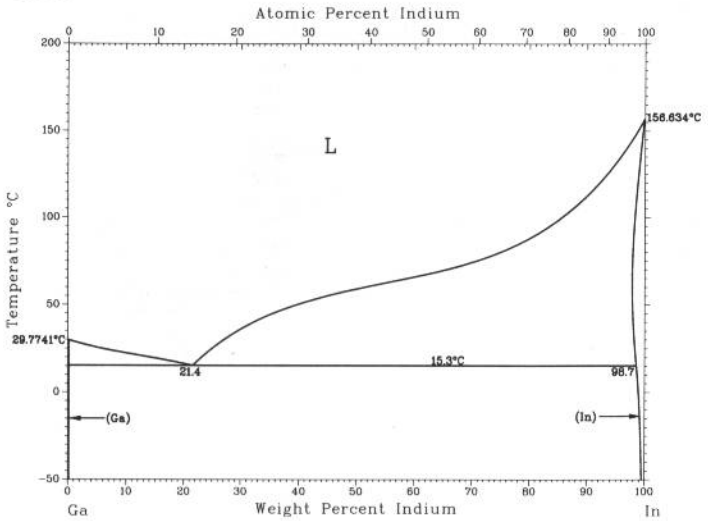

Phase	Composition, wt% In	Pearson symbol	Space group
(αGa)	0	*oC*8	*Cmca*
(βGa)	0	...	*C*2/*c*
(In)	98.6 to 100	*tI*2	*I*4/*mmm*

Ga-La

A. Palenzona and S. Cirafici, 1990

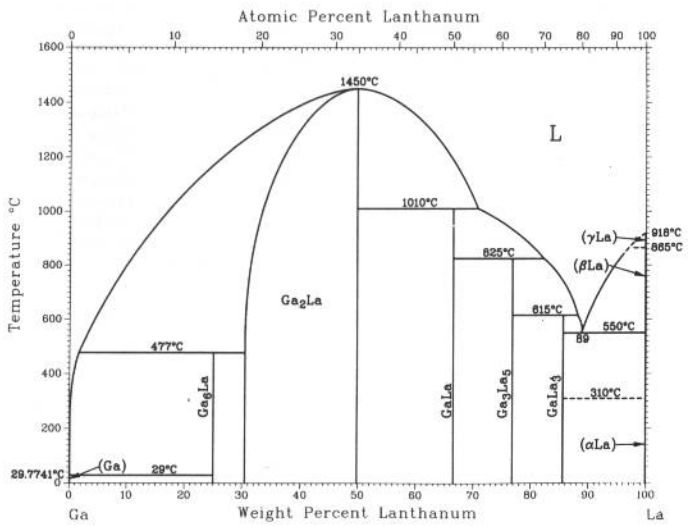

Phase	Composition, wt% La	Pearson symbol	Space group
(αGa)	~0	*oC*8	*Cmca*
Ga_6La	24.9	*tP*14	*P*4/*nbm*
Ga_4La(a)	33	*o***	...
Ga_2La	30 to 49.9	*hP*3	*P*6/*mmm*
GaLa	66.6	*oC*8	*Cmcm*
Ga_3La_5	76.9	*tI*32	*I*4/*mcm*
$GaLa_3$	86	*cP*4	$Pm\bar{3}m$
(γLa)	~100	*cI*2	$Im\bar{3}m$
(βLa)	~100	*cF*4	$Fm\bar{3}m$
(αLa)	~100	*hP*4	$P6_3/mmc$

(a) Not shown on diagram; needs further confirmation

Ga-Li

J. Sangster and A.D. Pelton, 1991

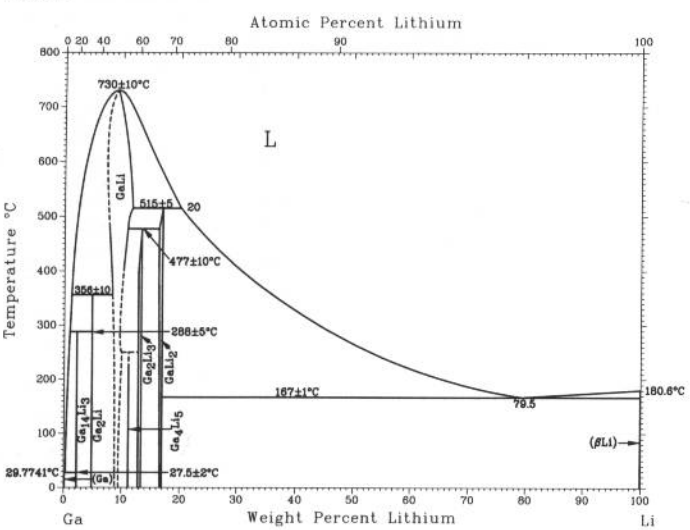

Phase	Composition, wt% Li	Pearson symbol	Space group
(Ga)	0	*oC*8	*Cmca*
$Ga_{14}Li_3$	2.1	*hR*51	$R\bar{3}m$
Ga_2Li	4.7(a)	...	...
GaLi	8 to 11(b)	*cF*16	$Fd\bar{3}m$
Ga_4Li_5	11.1	*hR*9	$P\bar{3}m1$
Ga_2Li_3	12.8 to 13.2	*hR*15	$R\bar{3}m$
$GaLi_2$	16 to 17	*oC*12	*Cmcm*
(βLi)	100	*cI*2	$Im\bar{3}m$
(αLi)(c)	100	*hP*2	$P6_3/mmc$

(a) Stoichiometry uncertain. (b) Near 400 °C. (c) Below –193 °C

Ga-Lu

S.P. Yatsenko, A.A. Semyannikov, B.G. Semenov, and K.A. Chuntonov, 1979

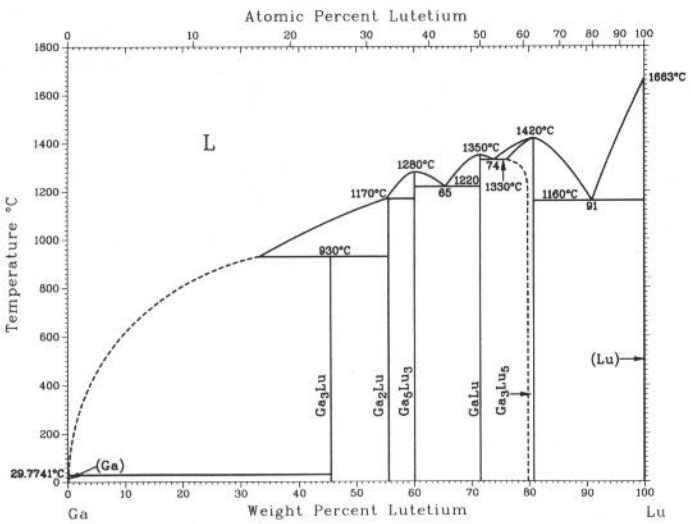

Phase	Composition, wt% Lu	Pearson symbol	Space group
(Ga)	0	*oC*8	*Cmca*
Ga_3Lu	46	*cP*4	$Pm\bar{3}m$
Ga_2Lu	55.6	*oI*12	*Imma*
Ga_5Lu_3	60.1	*oP*32	*Pnma*
GaLu	71.5	*oC*8	*Cmcm*
Ga_3Lu_5	? to 80.7	*hP*16	$P6_3/mcm$
(Lu)	100	*hP*2	$P6_3/mmc$

Ga-Mg

H. Okamoto, 1991

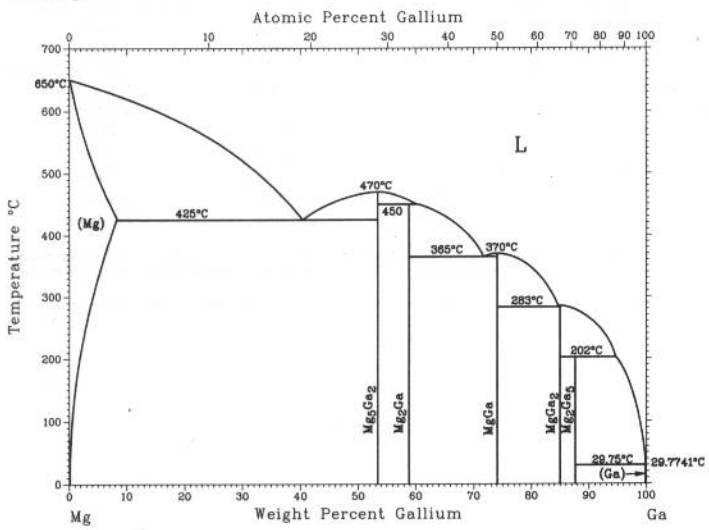

Phase	Composition, wt% Ga	Pearson symbol	Space group
(Mg)	0 to 9.4	*hP*2	$P6_3/mmc$
Mg_5Ga_2	53.43	*oI*28	*Ibam*
Mg_2Ga(a)	58.9	*hP*18	$P\bar{6}2c$
MgGa	74.2	*tI*32	$I4_1/a$
$MgGa_2$	85.15	*oP*24	*Pbam*
Mg_2Ga_5	87.76	*tI*28	*I*4/*mmm*
(Ga)	100	*oC*8	*Cmca*

(a) The structure is closely related to the Fe_2P (*hP*9) type with a small deviation.

Ga-Mn

X.S. Lu, J.K. Liang, and M.G. Zhou, 1980

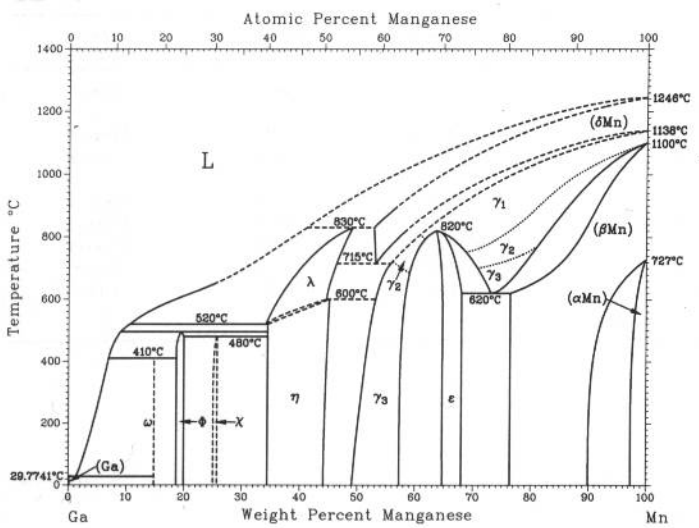

Phase	Composition, wt% Mn	Pearson symbol	Space group
(Ga)	0	*oC*8	*Cmca*
ω	15	*oC*28	*Cmcm*
φ	~18 to 20	...	...
χ	~25	*tP*14	*P*4/*mbm*
λ	~34.0 to 49	*hR*26	$R\bar{3}m$
η	34.4 to 44	...	...
(δMn)	~53 to 100	*cI*2	$Im\bar{3}m$
γ_1(γMn)	~62 to 100	*cF*4	$Fm\bar{3}m$
γ_2	~56 to 100	*tI*8	*I*4/*mmm*
γ_3	~49 to ~59	*tP*4	*P*4/*mmm*
ε	64 to 68	...	...
(βMn)	76.3 to ~100	*cP*20	$P4_132$
(αMn)	97.3 to ~100	*cI*58	$I\bar{4}3m$

Ga-Mo

From [Molybdenum]

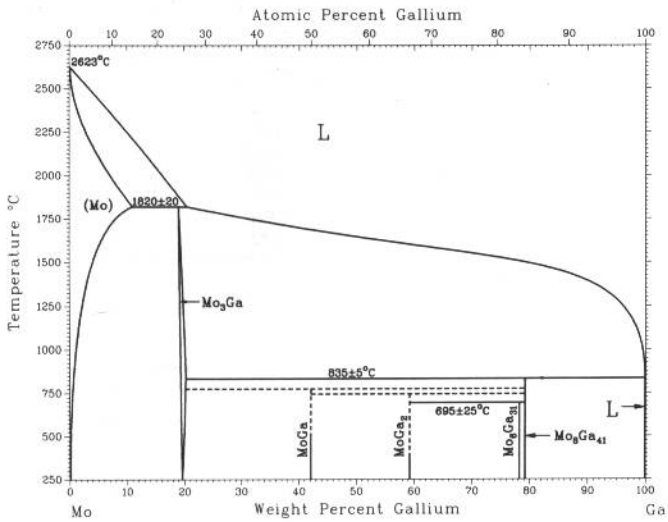

Phase	Composition, wt% Ga	Pearson symbol	Space group
(Mo)	0 to 11	*cI*2	$Im\bar{3}m$
Mo_3Ga	~20	*cP*8	$Pm\bar{3}n$
MoGa	42.1	...	...
$MoGa_2$	59.3	...	...
Mo_6Ga_{31}	~78	*mP*148	$P2_1/c$
Mo_8Ga_{41}	~79	*hR*49	$R\bar{3}$
(Ga)	100	*oC*8	*Cmca*

Ga-Na

A.D. Pelton and S. Larose, 1990

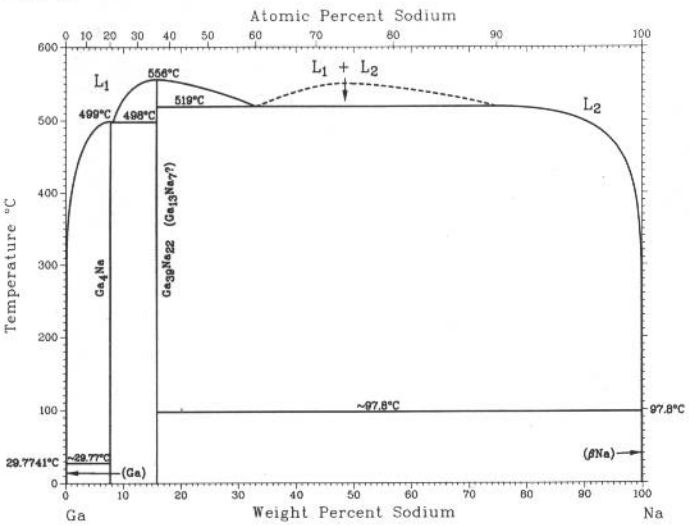

Phase	Composition, wt% Na	Pearson symbol	Space group
(Ga)	0	*oC*8	*Cmca*
Ga_4Na	8	*tI*10	*I*4/*mmm*
$Ga_{13}Na_7$(a)	15	*hR*360	$R\bar{3}m$
$Ga_{13}Na_7$(b, c)	15	*oP*240	*Pnma*
$Ga_{39}Na_{22}$(c)	15.7	*oP*244	*Pnma*
(βNa)	100	*cI*2	$Im\bar{3}m$
(αNa)	100	*hP*2	$P6_3/mmc$

(a) Structure observed when compound prepared with excess Ga. (b) Structure observed when compound prepared with excess Na. (c) Same compound with same diffractogram, although different stoichiometries have been reported

Ga-Nb

H. Okamoto, 1990

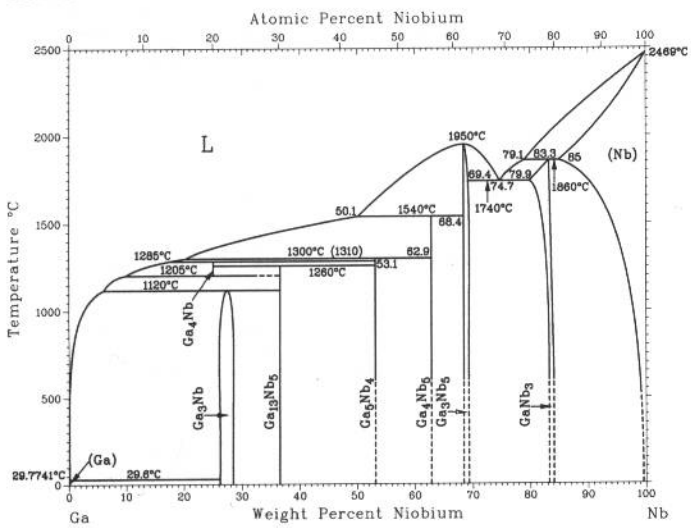

Phase	Composition, wt% Nb	Pearson symbol	Space group
(Ga)	0	*oC*8	*Cmca*
Ga_4Nb	25	...	...
Ga_3Nb	26 to 29	*tI*8	*I*4/*mmm*
$Ga_{13}Nb_5$	36.7	*oC*36	*Cmmm*
Ga_5Nb_4	53.3	*t***	...
Ga_4Nb_5	62.5	*hP*18	$P6_3/mcm$
Ga_2Nb_3(a)	67	*tP*10	*P*4/*mbm*
Ga_3Nb_5	68.4 to 69.4	*tI*32	*I*4/*mcm*
$GaNb_3$	79.9 to 84	*cP*8	$Pm\bar{3}n$
(Nb)	100	*cI*2	$Im\bar{3}m$

(a) Not in phase diagram

Ga-Nd

From [Moffatt]

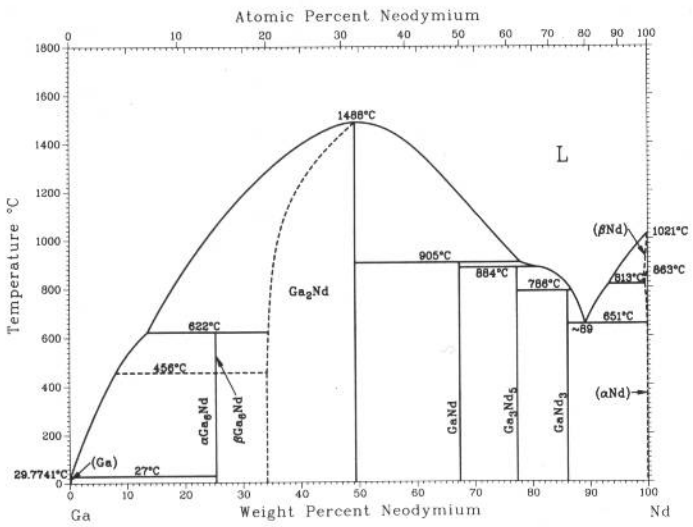

Phase	Composition, wt% Nd	Pearson symbol	Space group
(Ga)	0	*oC*8	*Cmca*
βGa_6Nd	25.7	...	...
αGa_6Nd	25.7	*tP*14	*P*4/*nbm*
Ga_2Nd	~34 to 50.8	*hP*3	*P*6/*mmm*
GaNd	67.4	*oC*8	*Cmcm*
Ga_3Nd_5	77.5	*tI*32	*I*4/*mcm*
$GaNd_3$	86	*cP*4	$Pm\bar{3}m$
(βNd)	? to 100	*cI*2	$Im\bar{3}m$
(αNd)	? to 100	*hP*4	$P6_3/mmc$

Ga-Ni

S.Y. Lee and P. Nash, 1991

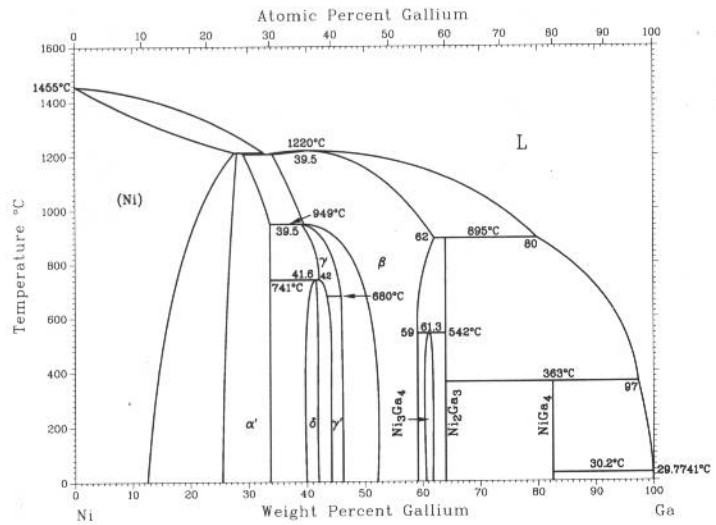

Phase	Composition, wt% Ga	Pearson symbol	Space group
(Ni)	0 to 27.6	*cF*4	$Fm\bar{3}m$
$\alpha'(Ni_3Ga)$	25.8 to 34	*cP*4	$Pm\bar{3}m$
β(NiGa)	34.2 to 62	*cP*2	$Pm\bar{3}m$
$\gamma(Ni_3Ga_2)$	39.5 to 46	*hP*4	$P6_3/mmc$
$\delta(Ni_5Ga_3)$	40.3 to 42	*oC*16	*Cmmm*
$\gamma'(Ni_3Ga_2)$	~43.4 to ~46.4	...	...
Ni_3Ga_4	~60.8 to 61.7	*cI*112	*Ia*3*d*
$\beta'(Ni_2Ga_3)$	64	*hP*5	$P\bar{3}m1$
$\varepsilon(NiGa_4)$	83	*cI*52	$I\bar{4}3m$
(Ga)	100	*oC*8	*Cmca*

Ga-Pb

I. Ansara and F. Ajersch, 1991

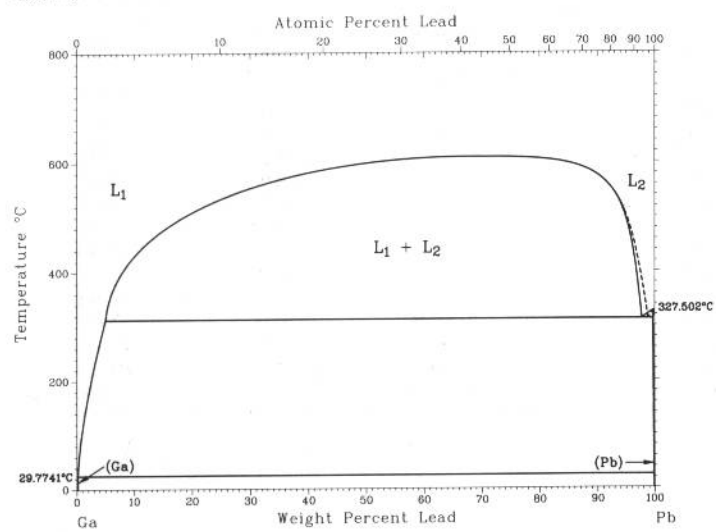

Phase	Composition, wt% Pb	Pearson symbol	Space group
(Ga)	0	*oC*8	*Cmca*
(Pb)	100	*cF*4	$Fm\bar{3}m$

Ga-Pd

H. Okamoto, 1990

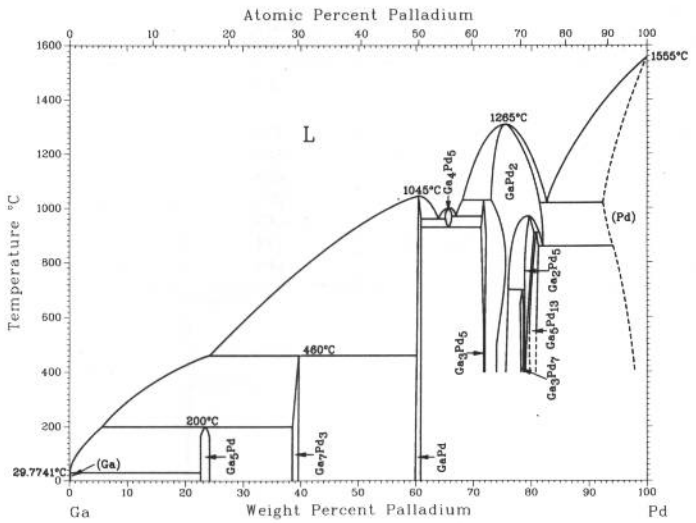

Phase	Composition, wt% Pd	Pearson symbol	Space group
(Ga)	0	*oC*8	*Cmca*
Ga_5Pd	~23.4	*tI*24	*I*4/*mcm*
Ga_7Pd_3	~40	*cI*40	$Im\bar{3}m$
GaPd	~60.4	*cP*8	$P2_13$
Ga_4Pd_5	~65.7	*cP*2	$Pm\bar{3}m$
Ga_3Pd_5	~71.8	*oP*16	*Pbam*
$GaPd_2$	73 to 82	*oP*12	*Pnma*
Ga_3Pd_7	~78	...	...
Ga_2Pd_5	79 to 80.5	*oP*28	*Pnma*
Ga_5Pd_{13}	80 to 81.3	*o***	...
(Pd)	? to 100	*cF*4	$Fm\bar{3}m$

Ga-Pr

H. Okamoto, 1990

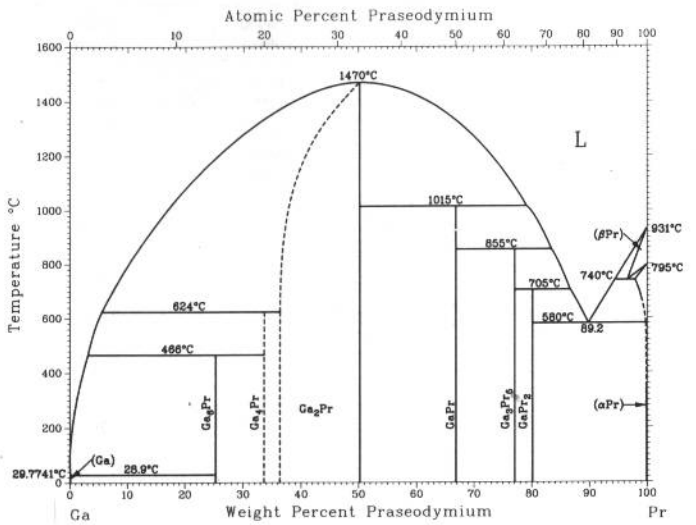

Phase	Composition, wt% Pr	Pearson symbol	Space group
(Ga)	0	*oC*8	*Cmca*
Ga_6Pr	25.2	*tI*14	*P*4/*nbm*
Ga_4Pr	34	...	...
Ga_2Pr	36 to 50.2	*hP*3	*P*6/*mmm*
GaPr	66.9	*oC*8	*Cmcm*
Ga_3Pr_5	77.1	*tP*32	*P*4/*ncc*
$GaPr_2$	80.2	*oP*12	*Pnma*
(βPr)	96 to 100	*cI*2	$Im\bar{3}m$
(αPr)	98 to 100	*hP*4	$P6_3/mmc$

Ga-Pt

H. Okamoto, 1990

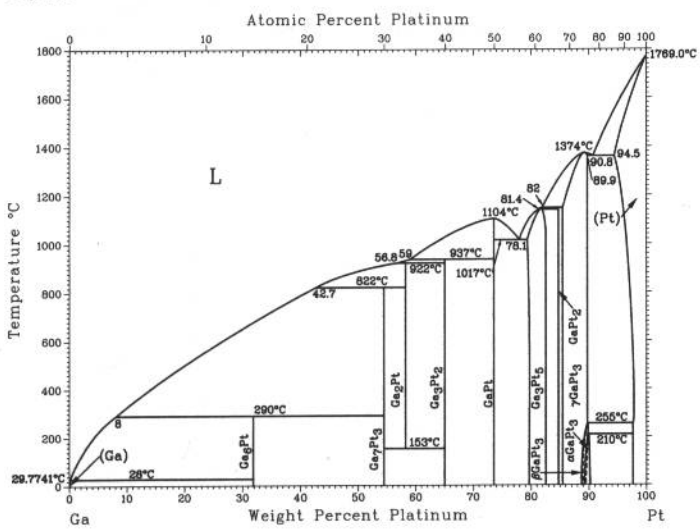

Phase	Composition, wt% Pt	Pearson symbol	Space group
(Ga)	0	*oC*8	*Cmca*
Ga_6Pt	31.8	*o***	...
Ga_7Pt_3	55	*cI*40	$Im\bar{3}m$
Ga_2Pt	58.3	*cF*12	$Fm\bar{3}m$
Ga_3Pt_2	65	*hP*5	$P\bar{3}m1$
GaPt	73.7	*cP*8	$P2_13$
Ga_3Pt_5	79 to 83	*oC*16	*Cmmm*
$\gamma GaPt_2$	84.9	*oP*16	*Pbam*
$\beta GaPt_2$	84.9	*o***	...
$\alpha GaPt_2$	84.9	*tP*2	*P*4/*mmm*
$\gamma GaPt_3$	85 to 90	*cP*4	$Pm\bar{3}m$
$\beta GaPt_3$	~89	*tI*16	*I*4/*mcm*
$\alpha GaPt_3$	~89	*tP*16	*P*4/*mbm*
(Pt)	94.5 to 100	*cF*4	$Fm\bar{3}m$

Ga-Pu

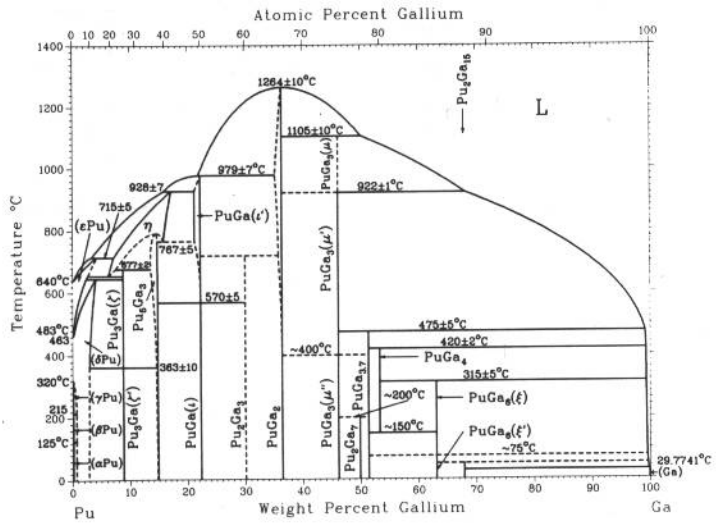

D.E. Peterson and M.E. Kassner, 1988

Phase	Composition, wt% Ga	Pearson symbol	Space group
(εPu)	0 to 4	*cI*2	$Im\bar{3}m$
(δ'Pu)	0 to 0.07	*tI*2	*I*4/*mmm*
(δPu)	0 to 3.9	*cF*4	$Fm\bar{3}m$
(γPu)	0	*oF*8	*Fddd*
(βPu)	0	*mC*34	*C*2/*m*
(αPu)	0	*mP*16	$P2_1/m$
η	6.1 to 17	...	$I2_13$(a)
$Pu_3Ga(\zeta)$	9	*cP*4	$Pm\bar{3}m$
$Pu_3Ga(\zeta')$	9	*tP*4	*P*4/*mmm*
Pu_5Ga_3	14 to 14.6	*tI*38	*I*4/*mcm*
		(b)	...
PuGa(ι')	~22.2	*cI*2	$Im\bar{3}m$
		(c)	*I*4/*mmm*
PuGa(ι)	22.2	(d)	*I*4*mm*
Pu_2Ga_3	30	(e)	...
$PuGa_2$	36.4	*hP*3	*P*6/*mmm*
$PuGa_3(\mu)$	46	...	...
$PuGa_3(\mu')$	46	*hP*8	$P6_3/mmc$
$PuGa_3(\mu'')$	46	...	$R\bar{3}m$
Pu_2Ga_7	50.0	(c)	...
$PuGa_{3.7}$	51.4	...	...
$PuGa_4$	53	*oI*20	*Imma*
$PuGa_6(\xi)$	63.1	...	*P*4/*nbm*
			*P*4/*mbm*
$PuGa_6(\xi')$	63.1	...	...
Pu_2Ga_{15}	68.1	(c)	...
(Ga)	100	*oC*8	*Cmca*

(a) Partially ordered. (b) Face-centered cubic. (c) Tetragonal. (d) Body-centered tetragonal. (e) Hexagonal

Ga-S

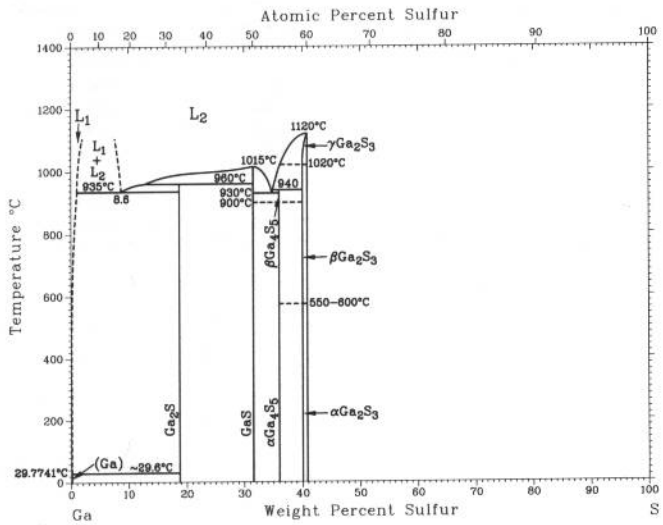

P.G. Rustamov, B.N. Mardakhaev, and M.G. Safarov, 1967

Phase	Composition, wt% S	Pearson symbol	Space group
(Ga)	0	*oC*8	*Cmca*
Ga_2S	18.7	...	...
GaS	31.5	*hP*8	$P6_3/mmc$
βGa_4S_5	36.5	...	...
αGa_4S_5	36.5	...	...
γGa_2S_3	41	*hP*4	$P6_3mc$
βGa_2S_3	41	*mC*20	*Cc*
αGa_2S_3	41	*cF*8	$F\bar{4}3m$

Ga-Sb

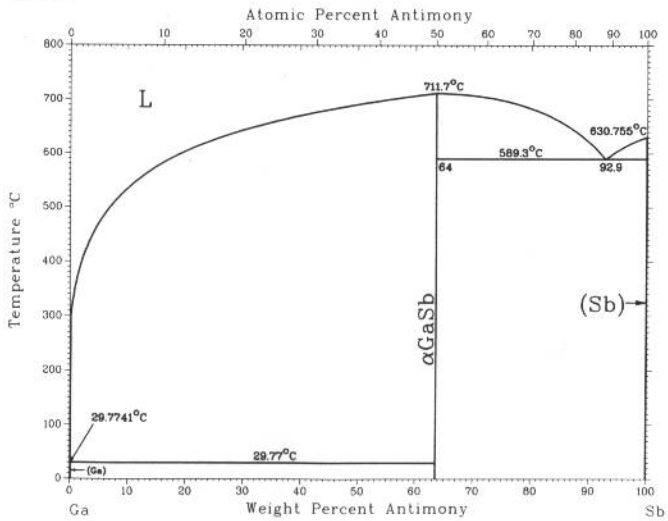

T.I. Ngai, R.C. Sharma, and Y.A. Chang, 1988

Phase	Composition, wt% Sb	Pearson symbol	Space group
(Ga)	0	*oC*8	*Cmca*
αGaSb	63.6	*cF*8	$F4\bar{3}m$
βGaSb(a)	63.6	*tI*4	$I4_1/amd$
(Sb)	100	*hR*2	$R\bar{3}m$

(a) At high pressure

Ga-Sc

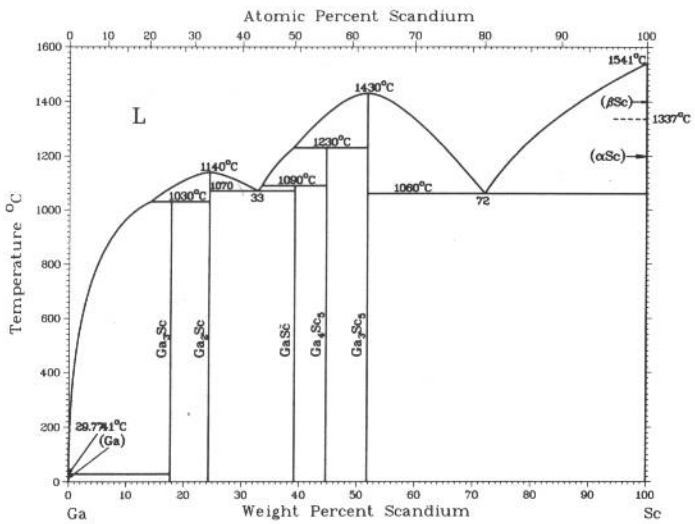

S.P. Yatsenko, A.A. Semyannikov, G.B. Semenov, and K.A. Chuntonov, 1979

Phase	Composition, wt% Sc	Pearson symbol	Space group
(Ga)	0	*oC*8	*Cmca*
Ga_3Sc	18	*cP*4	$Pm\bar{3}m$
Ga_2Sc	24.4	*oI*12	*Imma*
GaSc	39.2	*oC*8	*Cmcm*
Ga_4Sc_5	44.7	*tI*84	*I*4/*mmm*
Ga_3Sc_5	51.8	*hP*16	$P6_3/mcm$
(βSc)	100	*cI*2	$Im\bar{3}m$
(αSc)	100	*hP*2	$P6_3/mmc$
Other reported phase			
Ga_3Sc_2	30	*oP*32	*Pnma*

Ga-Se

From [Moffatt]

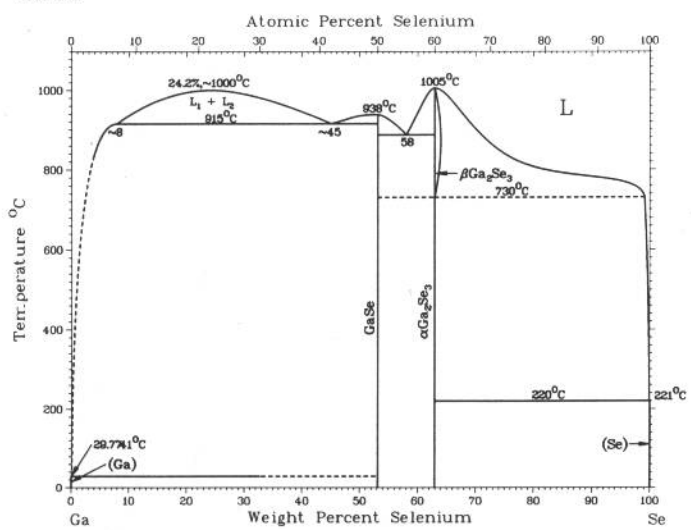

Phase	Composition, wt% Se	Pearson symbol	Space group
(Ga)	0	*oC*8	*Cmca*
GaSe	53.1	*hR*4	$R\bar{3}m$
		*hP*8	$P\bar{6}$
		*hP*16	$P6_3mc$
βGa_2Se_3	~63	*c***	...
αGa_2Se_3	63	*mC*20	*Cc*
(Se)	100	*hP*3	$P3_121$

Ga-Sm

From [Moffatt]

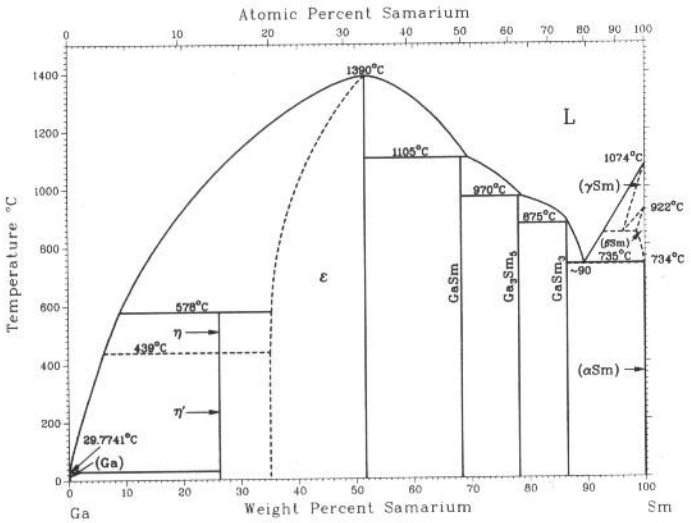

Phase	Composition, wt% Sm	Pearson symbol	Space group
(Ga)	0	*oC*8	*Cmca*
$\beta Ga_6Sm(\eta)$	26.5	...	...
$\alpha Ga_6Sm(\eta')$	26.5	*tP*14	*P4/nbm*
$Ga_2Sm(\varepsilon)$	~35 to 51.8	*hP*3	*P6/mmm*
GaSm	68.3	*oC*8	*Cmcm*
Ga_3Sm_5	78.2	*tI*32	*I4/mcm*
$GaSm_3$	87	*cP*4	$Pm\bar{3}m$
(γSm)	? to 100	*cI*2	$Im\bar{3}m$
(βSm)	? to 100	*hP*2	$P6_3/mmc$
(αSm)	100	*hR*3	$R\bar{3}m$

Ga-Sn

T.J. Anderson and I. Ansara, 1992

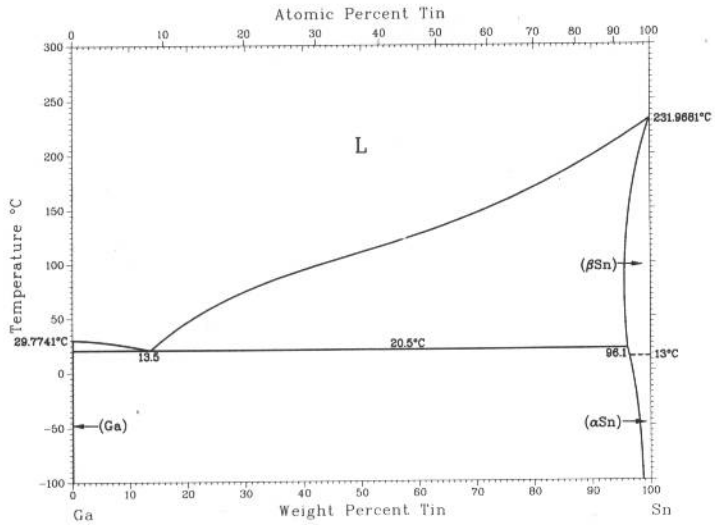

Phase	Composition, wt% Sn	Pearson symbol	Space group
(αGa)	0	*oC*8	*Cmca*
(βGa)(a)	0 to 0.03	*tI*2	*I4/mmm*
(βSn)	96.1 to 100	*tI*4	$I4_1/amd$

(a) Above 1.2 GPa

Ga-Sr

V.P. Itkin and C.B. Alcock, 1992

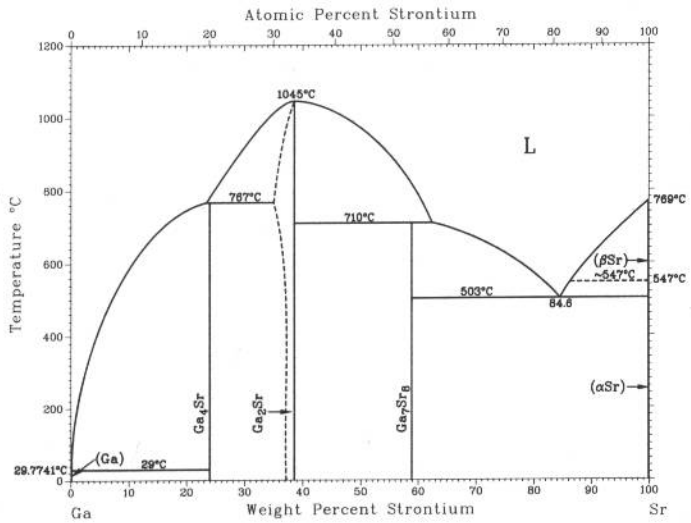

Phase	Composition, wt% Sr	Pearson symbol	Space group
(Ga)	0	*hP*2	$P6_3/mmc$
Ga_4Sr	24	*tI*10	*I4/mmm*
Ga_2Sr	35 to 38.6 (a)	*hP*3	*P6/mmm*
Ga_7Sr_8	58.9	*cP*60	$P2_13$
(αSr)	100	*cF*4	$Fm\bar{3}m$
(βSr)	100	*cI*2	$Im\bar{3}m$

(a) After annealing at 900 °C

Ga-Tb

From [Moffatt]

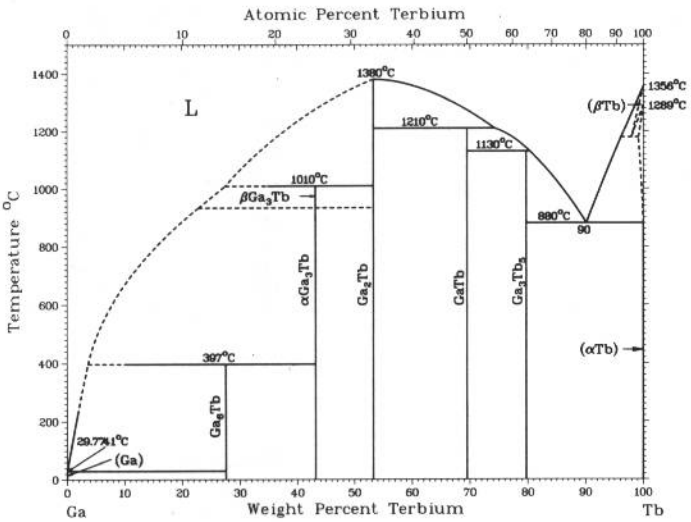

Phase	Composition, wt% Tb	Pearson symbol	Space group
(Ga)	0	*oC8*	*Cmca*
Ga_6Tb	27.6	*tP14*	*P4/nbm*
βGa_3Tb	43	*cP4*	$Pm\bar{3}m$
αGa_3Tb	43	*hP8*	$P6_3/mmc$
Ga_2Tb	53.2	*hP3*	*P6/mmm*
GaTb	69.5	*oC8*	*Cmcm*
Ga_3Tb_5	79.2	*tI32*	*I4/mcm*
(βTb)	? to 100	*cI2*	$Im\bar{3}m$
(αTb)	? to 100	*hP2*	$P6_3/mmc$

Ga-Te

U.R. Kattner, unpublished

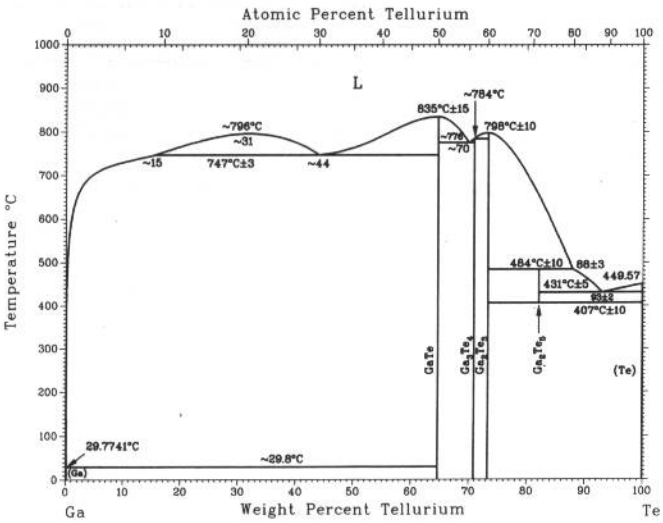

Phase	Composition, wt% Te	Pearson symbol	Space group
(Ga)	0	*oC8*	*Cmca*
GaTe	64.7	*mC24*	*C2/m*
Ga_3Te_4	70.9	*hP**	...
Ga_2Te_3	73	*cF8*	$F\bar{4}3m$
Ga_2Te_5	82.1	*tI14*	*I4/m*
(Te)	100	*hP3*	$P3_121$
Metastable (thin film)			
GaTe	64.7	*hP8*	$P6_3/mmc$

Ga-Tl

J. Klingbeil and R. Schmid-Fetzer, 1991

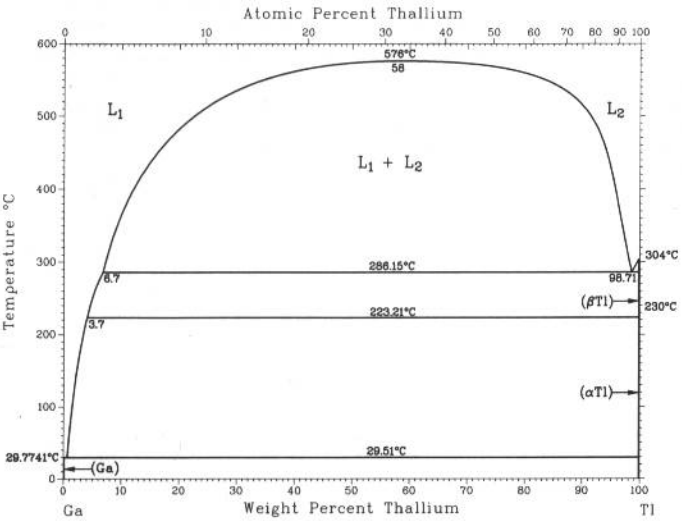

Phase	Composition, wt% Tl	Pearson symbol	Space group
(Ga)	0	*oC*	*Cmca*
(αTl)	100	*hP2*	$P6_3/mmc$
(βTl)	100	*cI2*	$Im\bar{3}m$

Ga-Tm

From [Moffatt]

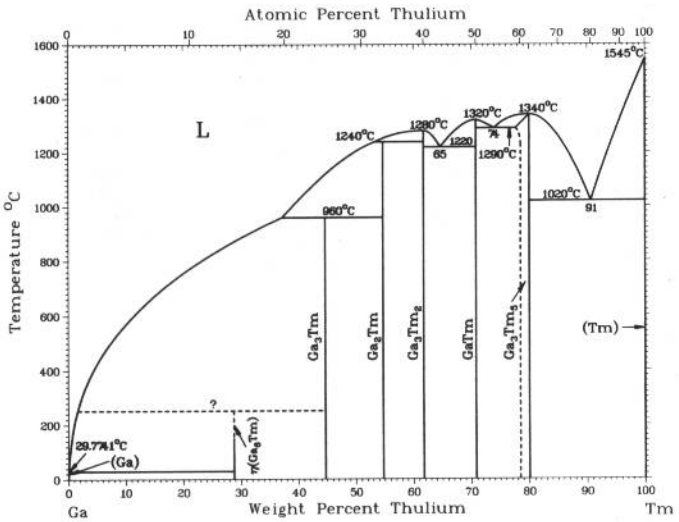

Phase	Composition, wt% Tm	Pearson symbol	Space group
(Ga)	0	*oC*8	*Cmca*
Ga_6Tm	28.8	*tP*14	*P4/nbm*
Ga_3Tm	45	*cP*4	*Pm$\bar{3}$m*
Ga_2Tm	54.7	*oI*12	*Imma*
Ga_3Tm_2	62	...	...
GaTm	70.8	*oC*8	*Cmcm*
Ga_3Tm_5	? to 80.2	*oP*32	*Pnma*
(Tm)	100	*hP*2	$P6_3/mmc$

Ga-U

K.H.J. Buschow, 1973

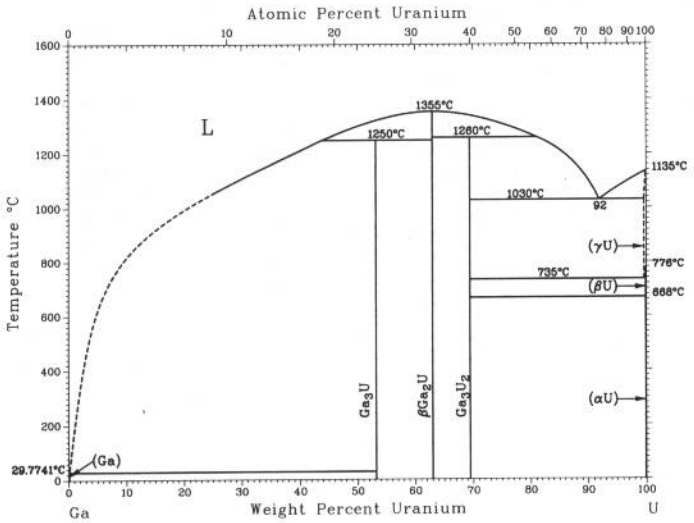

Phase	Composition, wt% U	Pearson symbol	Space group
(Ga)	0	*oC*8	*Cmca*
Ga_3U	53	*cP*4	*Pm$\bar{3}$m*
βGa_2U	63.0	*hP*3	*P6/mmm*
αGa_2U(a)	63.0	*oC**	*Cmmm*
Ga_3U_2	70	*oC*32	*Cmcm*
(γU)	? to 100	*cI*2	*Im$\bar{3}$m*
(βU)	100	*tP*30	$P4_2/mnm$
(αU)	100	*oC*4	*Cmcm*

(a) Below the Curie temperature (–148 °C)

Ga-V

J.F. Smith, 1989

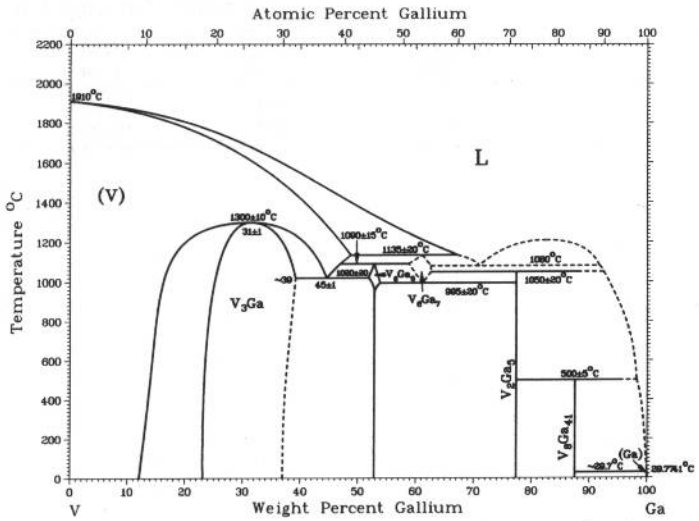

Phase	Composition, wt% Ga	Pearson symbol	Space group
(V)	0 to 49	*cI*2	*Im$\bar{3}$m*
V_3Ga	~23 to ~39	*cP*8	*Pm$\bar{3}$n*
V_6Ga_5	~53.3	*hP*22	...
V_6Ga_7	~59 to ~63	*cI*52	*I$\bar{4}$3m*
V_2Ga_5	77.4	*tP*14	...
V_8Ga_{41}	87.5	*hR*49	...
(Ga)	100	*oC*8	*Cmca*

Ga-Y

S.P. Yatsenko, 1977

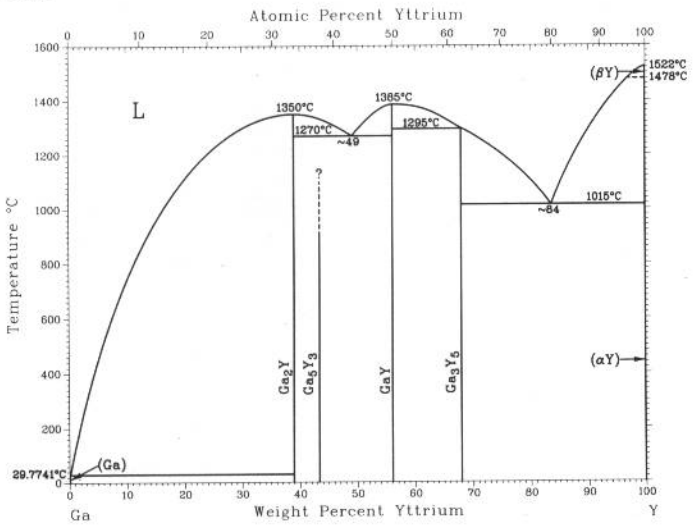

Phase	Composition, wt% Y	Pearson symbol	Space group
(Ga)	0	*oC*8	*Cmca*
Ga_2Y	38.9	...	...
Ga_5Y_3	43.3	*oP*32	*Pnma*
GaY	56.0	*oC*8	*Cmcm*
Ga_3Y_5	68.0	*hP*16	$P6_3/mcm$
(βY)	100	*cI*2	$Im\bar{3}m$
(αY)	100	*hP*2	$P6_3/mmc$

Ga-Yb

A. Palenzona and S. Cirafici, 1992

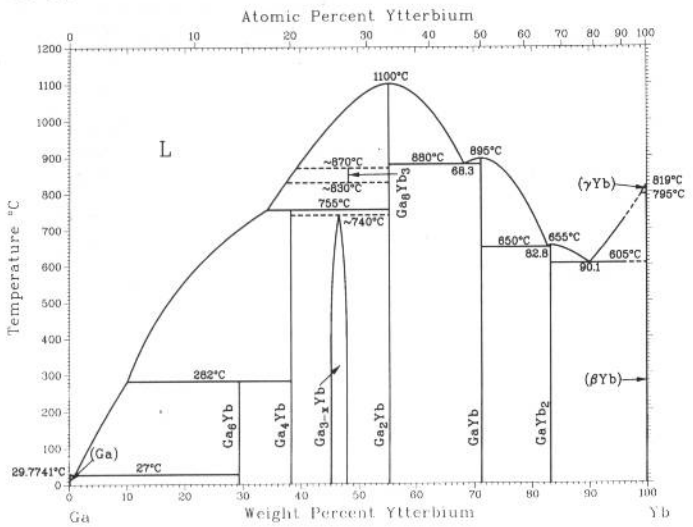

Phase	Composition, wt% Yb	Pearson symbol	Space group
(αGa)	~0	*oC*8	*Cmca*
Ga_6Yb	29.3	*tP*14	$P4/nbm$
Ga_4Yb	38	*mC*10	$C2/m$
$Ga_{3-x}Yb$(a)	45 to 48.5	*hP*54.3	$P6/mmm$
Ga_8Yb_3	48.2	*oI*22	*Immm*
Ga_2Yb	55.3	*hP*6	$P6_3/mmc$
GaYb	71.3	*tP*4	$P4/mmm$
$GaYb_2$	83.3	*oP*12	*Pnma*
(γYb)	~100	*cI*2	$Im\bar{3}m$
(βYb)	~100	*cF*4	$Fm\bar{3}m$
(αYb)	~100	*hP*2	$P6_3/mmc$

(a) $0 \le x \le 0.36$

Ga-Zn

J. Dutkiewicz, Z. Moser, L. Zabdyr, D.D. Gohil, T.G. Chart, I. Ansara, and C. Girard, 1990

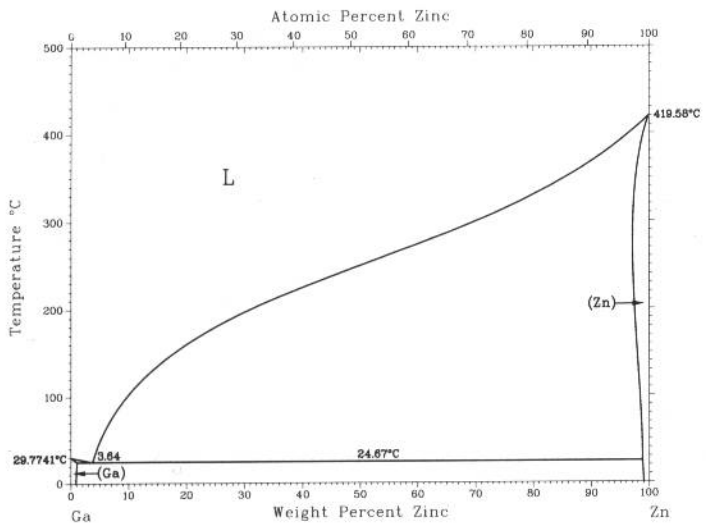

Phase	Composition, wt% Zn	Pearson symbol	Space group
(Ga)	0 to 0.75	*oC*8	*Cmca*
(Zn)	97.49 to 100	*hP*2	$P6_3/mmc$

Ga-Zr

From [Shunk]

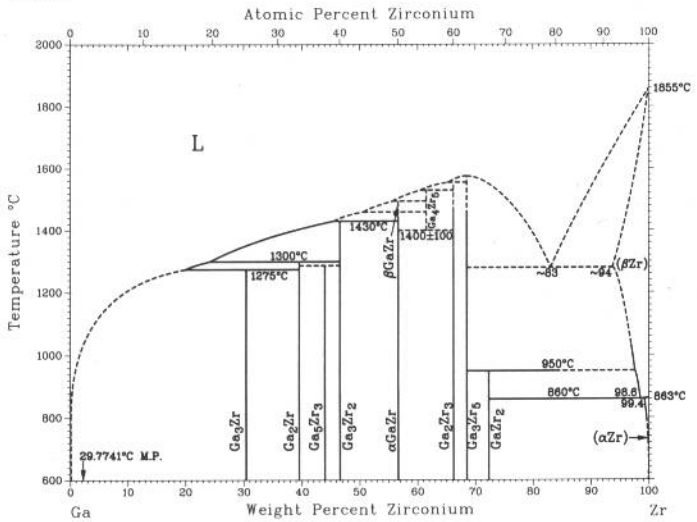

Phase	Composition, wt% Zr	Pearson symbol	Space group
(Ga)	0	*oC*8	*Cmca*
Ga_3Zr	30	*tI*16	*I4/mmm*
Ga_2Zr	39.5	*oC*12	*Cmmm*
Ga_5Zr_3	44.0	*oC*32	*Cmcm*
Ga_3Zr_2	47	*oF*40	*Fdd*2
βGaZr	56.7	...	...
αGaZr	56.7	*tI*16	$I4_1/amd$
Ga_4Zr_5	62.1	*hP*18	$P6_3/mcm$
Ga_2Zr_3	66	*tP*10	*P4/mbm*
Ga_3Zr_5	68.6	*hP*16	$P6_3/mcm$
$GaZr_2$	72.4	*tI*12	*I4/mcm*
(βZr)	~94 to 100	*cI*2	$Im\bar{3}m$
(αZr)	99.4 to 100	*hP*2	$P6_3/mmc$

Gd-Ge

A.B. Gokhale and G.J. Abbaschian, 1989

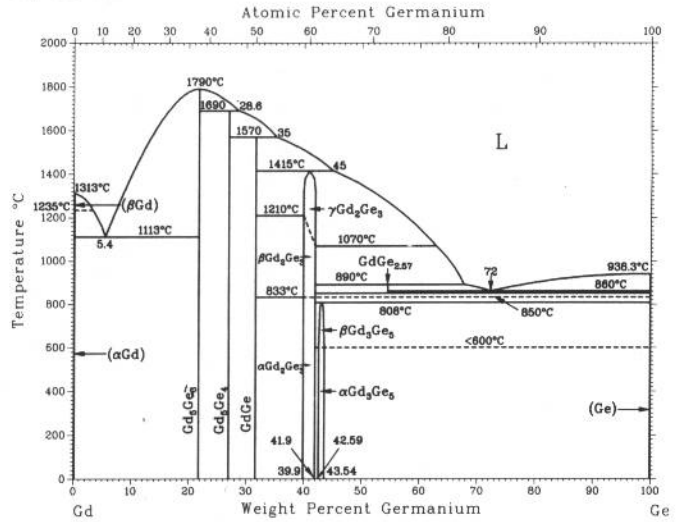

Phase	Composition, wt% Ge	Pearson symbol	Space group
βGd(a)	0	*cI*2	$Im\bar{3}m$
αGd(b)	0	*hP*2	$P6_3/mmc$
Gd_5Ge_3	21.7	*hP*16	$P6_3/mcm$
Gd_5Ge_4	27.0	(c)	*Pnma*
GdGe	31.6	*oC*8	*Cmcm*
γGd_2Ge_3	40 to 42	...	...
βGd_2Ge_3	40 to 42	...	...
αGd_2Ge_3	40 to 42	*hP*3	*P6/mmm*
βGd_3Ge_5(d)	42.59 to 43.54	(c)	*Imma*
αGd_3Ge_5	42.59 to 43.54	*tI*12	$I\bar{4}_1/amd$
$GdGe_{2.57}$	54	(c)	$C222_1$
Ge	100	*cF*8	$Fd\bar{3}m$

(a) From 1313 to >1235 °C. (b) From 1235 °C. (c) Orthorhombic. (d) Also designated "$GdGe_{2-n}$"

Gd-In

A. Palenzona and S. Cirafici, 1992

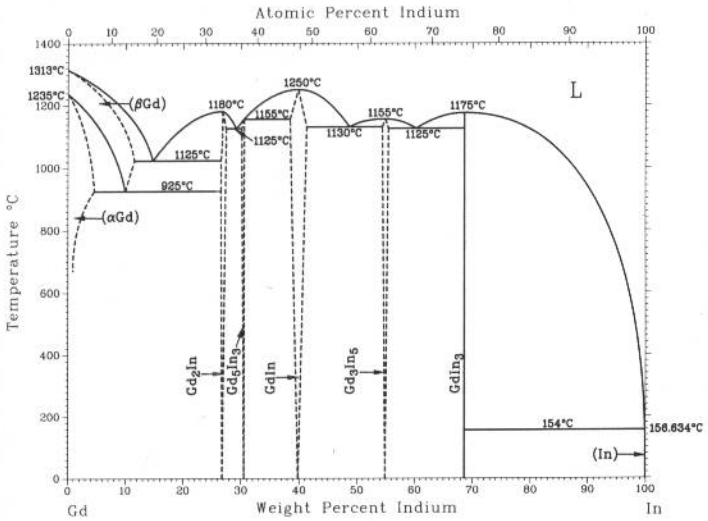

Phase	Composition, wt% In	Pearson symbol	Space group
(βGd)	0 to ~11	*cI*2	$Im\bar{3}m$
(αGd)	0 to ~5	*hP*2	$P6_3/mmc$
Gd_2In	26.7 ± ~1	*hP*6	$P6_3/mmc$
Gd_5In_3	30.5 ± ~1	*tI*32	*I4/mcm*
GdIn(a)	39 ± ~2	*cP*2 or *cI*2	$Pm\bar{3}m$ or $Im\bar{3}m$
Gd_3In_5	54.9 ± ~1	*oC*32	*Cmcm*
$GdIn_3$	69	*cP*4	$Pm\bar{3}m$
(In)	~100	*tI*2	*I4/mmm*

(a) Possibly metastable

Gd-Mg

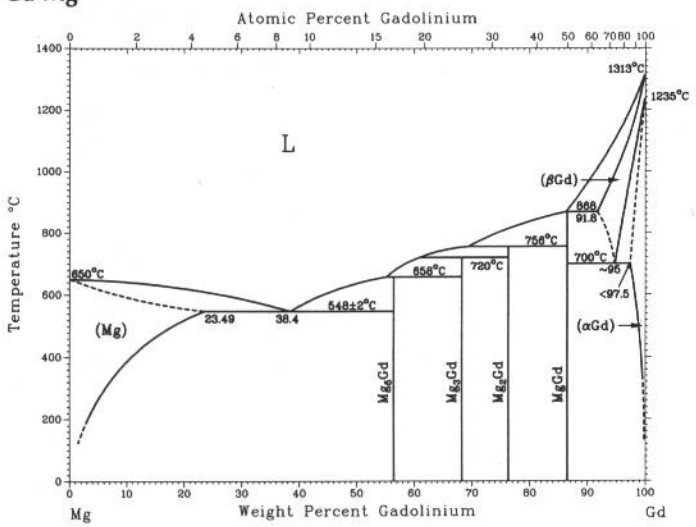

A.A. Nayeb-Hashemi and J.B. Clark, 1988

Phase	Composition, wt% Gd	Pearson symbol	Space group
(Mg)	0 to 23.49	*hP*2	$P6_3/mmc$
Mg_5Gd	56.41(a)	(b)	$F\bar{4}3m$
Mg_3Gd	68	*cF*16	$Fm\bar{3}m$
Mg_2Gd	76.38	*cF*24	$Fd\bar{3}m$
MgGd	86.6	*cP*2	$Pm\bar{3}m$
(βGd)	? to 100	*cI*2	$Im\bar{3}m$
(αGd)	<97.5 to 100	*hP*2	$P6_3/mmc$

(a) There may be a small homogeneity range. The exact stoichiometry was reported as $Mg_{5.05}Gd$, closely related to that of $Sm_{11}Cd_{45}$. (b) Cubic

Gd-Mn

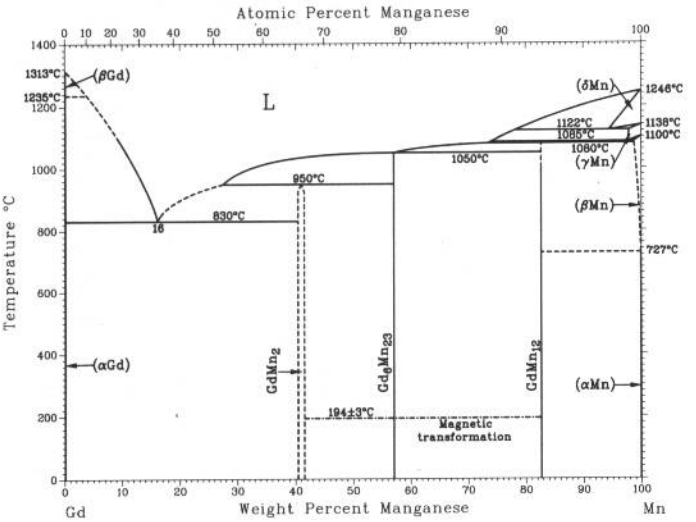

H. Okamoto, 1990

Phase	Composition, wt% Mn	Pearson symbol	Space group
(βGd)	0	*cI*2	$Im\bar{3}m$
(αGd)	0	*hP*2	$P6_3/mmc$
$GdMn_2$	~41.2	*cF*24	$Fd\bar{3}m$
Gd_6Mn_{23}	57.2	*cF*116	$Fm\bar{3}m$
$GdMn_{12}$	80.7	*tI*26	$I4/mmm$
(δMn)	~95 to 100	*cI*2	$Im\bar{3}m$
(γMn)	~97 to 100	*cF*4	$Fm\bar{3}m$
(βMn)	~100	*cP*20	$P4_132$
(αMn)	100	*cI*58	$I\bar{4}3m$

Gd-Ni

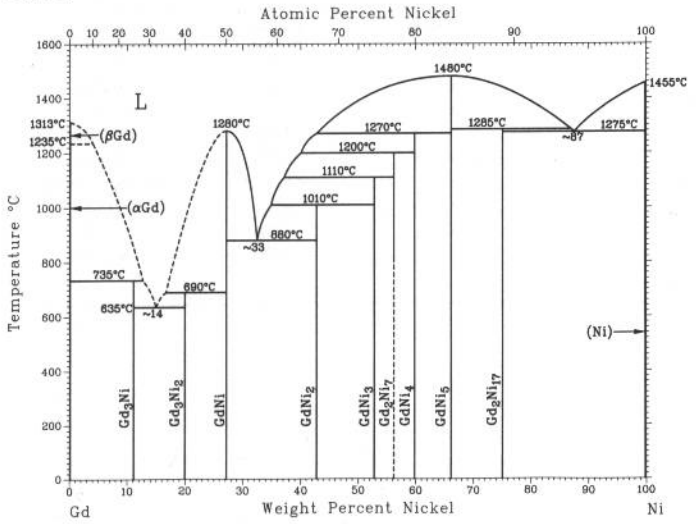

Y.Y. Pan and P. Nash, 1991

Phase	Composition, wt% Ni	Pearson symbol	Space group
(βGd)	0	*hP*2	$P6_3/mmc$
(αGd)	0	*cI*2	$Im\bar{3}m$
Gd_3Ni	11.1	*oP*16	$P6/mmm$
Gd_3Ni_2	19.9	*t***	...
GdNi	27.2	*oC*8	*Cmcm*
$GdNi_2$	42.8	*cF*24	$Fd\bar{3}m$
$GdNi_3$	52.8	*hP*24	$R\bar{3}m$
Gd_2Ni_7	56.7	*hP*36(a)	$P6_3/mmc$
		*hR*54(b)	$R\bar{3}m$
$GdNi_4$	59.9	*hP*6	...
$GdNi_5$	65.1	*hP*6	$P6/mmm$
Gd_2Ni_{17}	76.1	*hP*38	$P6_3/mmc$
(Ni)	100	*cF*4	$Fm\bar{3}m$

(a) High-temperature form. (b) Low-temperature form

Gd-Pb

A. Palenzona and S. Cirafici, 1991

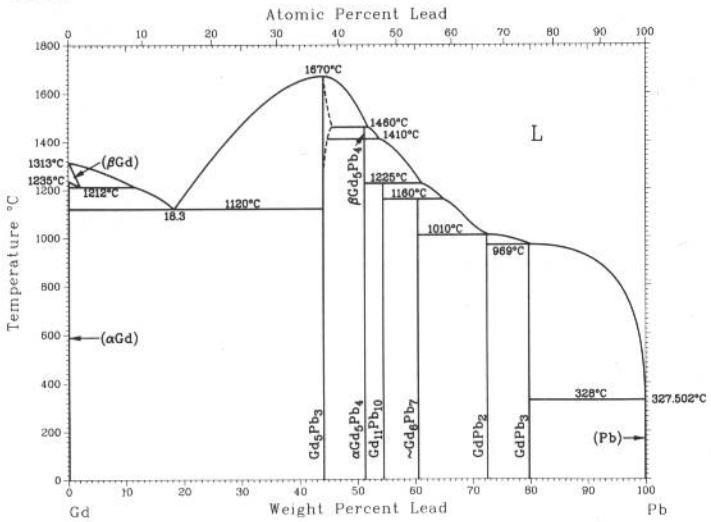

Phase	Composition, wt% Pb	Pearson symbol	Space group
(βGd)	0 to 3	*cI*2	$Im\bar{3}m$
(αGd)	0 to 1	*hP*2	$P6_3/mmc$
Gd_5Pb_3	44.2 to 46	*hP*16	$P6_3/mcm$
Gd_5Pb_4	51.3	*oP*36	*Pnma*
$Gd_{11}Pb_{10}$	54.5	...	...
$GdPb_3$	80	*cP*4	$Pm\bar{3}m$
(Pb)	>99.6 to 100	*cF*4	$Fm\bar{3}m$

Gd-Pd

H. Okamoto, 1990

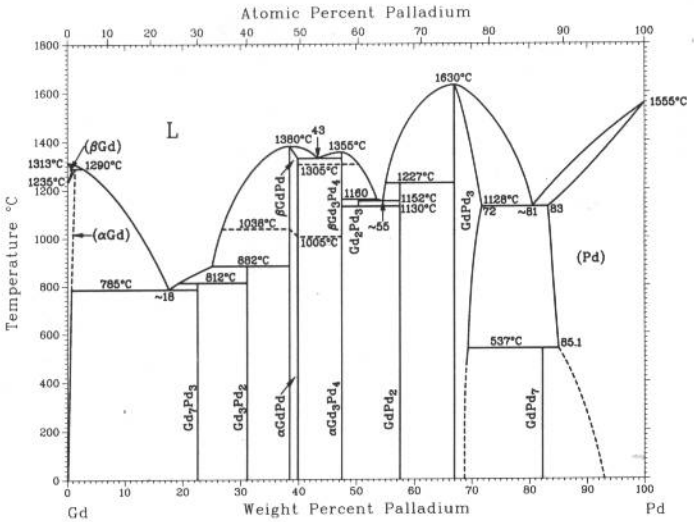

Phase	Composition, wt% Pd	Pearson symbol	Space group
(βGd)	0 to 0.68	*cI*2	$Im\bar{3}m$
(αGd)	0 to 1.4	*hP*2	$P6_3/mmc$
Gd_7Pd_3	23	*hP*20	$P6_3mc$
Gd_3Pd_2	31	*tP*10	$P4/mbm$
βGdPd	~40.4	...	...
αGdPd	~40.4	*oC*8	*Cmcm*
Gd_3Pd_4	47.4	*hR*14	$R\bar{3}$
Gd_2Pd_3	50	...	...
$GdPd_3$	67 to 72	*cP*4	$Pm\bar{3}m$
$GdPd_7$	82.6	...	...
(Pd)	83 to 100	*cF*4	$Fm\bar{3}m$

Gd-Rh

H. Okamoto, 1990

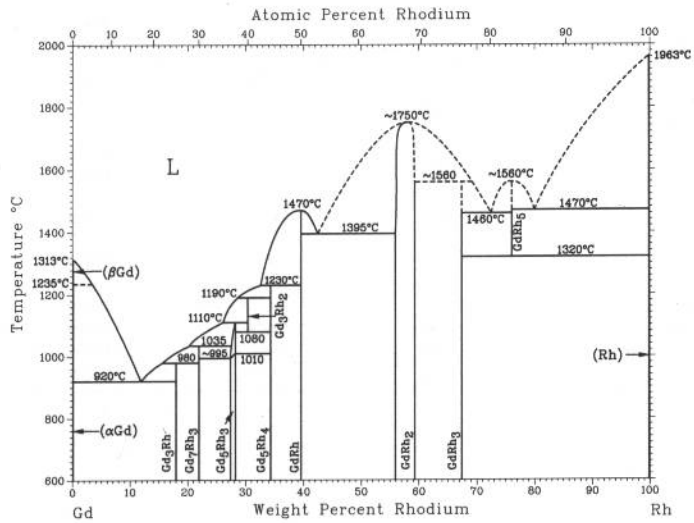

Phase	Composition, wt% Rh	Pearson symbol	Space group
(βGd)	0	*cI*2	$Im\bar{3}m$
(αGd)	0	*hP*2	$P6_3/mmc$
Gd_3Rh	18	*oP*16	*Pnma*
Gd_7Rh_3	22	*hP*20	$P6_3mc$
βGd_5Rh_3	~28.2	*hP*16	$P6_3/mcm$
αGd_5Rh_3	~28.2	...	...
Gd_3Rh_2	30	*tI*140	*I*4/*mcm*
Gd_5Rh_4	34.3	*oP*36	*Pnma*
GdRh	39.6	*cP*2	$Pd\bar{3}m$
$GdRh_2$	56 to 59	*cF*24	$Fd\bar{3}m$
$GdRh_3$	66	*hP*24	$P6_3/mmc$
$GdRh_5$	76.5	*hP*6	*P*6/*mmm*
(Rh)	100	*cF*4	$Fm\bar{3}m$

Gd-Sb

H. Okamoto, 1990

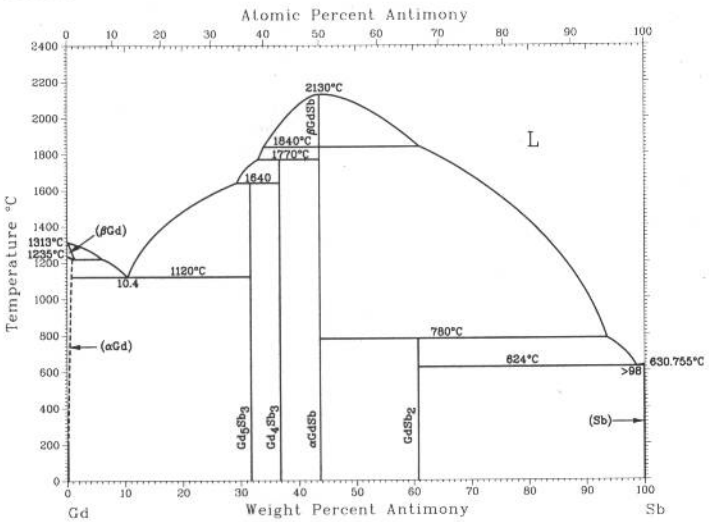

Phase	Composition, wt% Sb	Pearson symbol	Space group
(βGd)	0	*cI*2	$Im\bar{3}m$
(αGd)	0	*hP*2	$P6_3/mmc$
Gd_5Sb_3	31.7	*hP*16	$P6_3/mcm$
Gd_4Sb_3	36.8	*cI*28	$I\bar{4}3d$
βGdSb	43.6	...	...
αGdSb	43.6	*cF*8	$Fm\bar{3}m$
$GdSb_2$	60.8	*hP*12	$P6_3/mmc$
(Sb)	100	*hR*2	$R\bar{3}m$

Gd-Se

N.Yu. Pribyl'skiĭ, I.G. Vasileva, and R.S. Gamidov, 1982

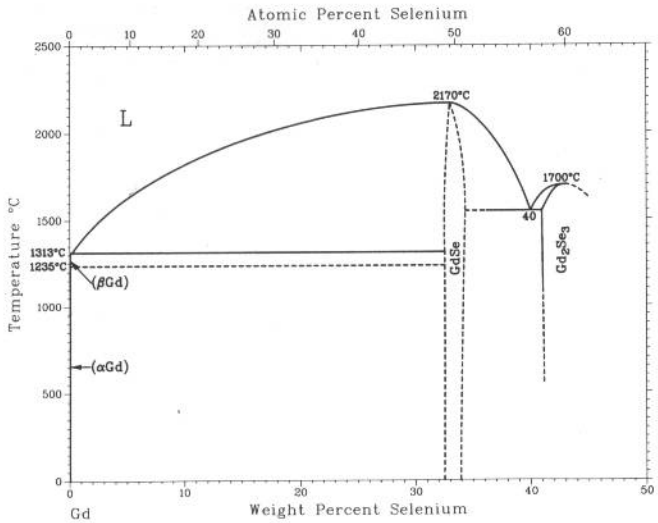

Phase	Composition, wt% Se	Pearson symbol	Space group
(βGd)	0	*cI*2	$Im\bar{3}m$
(αGd)	0	*hP*2	$P6_3/mmc$
GdSe	33 to 34	*cF*8	$Fm\bar{3}m$
Gd_2Se_3	~41 to ?	*oP*20	*Pnma*
		or *cI*28	$I\bar{4}3d$
Other reported phases			
$GdSe_2$	50.1	*oP*12	*Pnma*
		*o**144	...
		*t**24	...

Gd-Sn

A. Palenzona and S. Cirafici, 1991

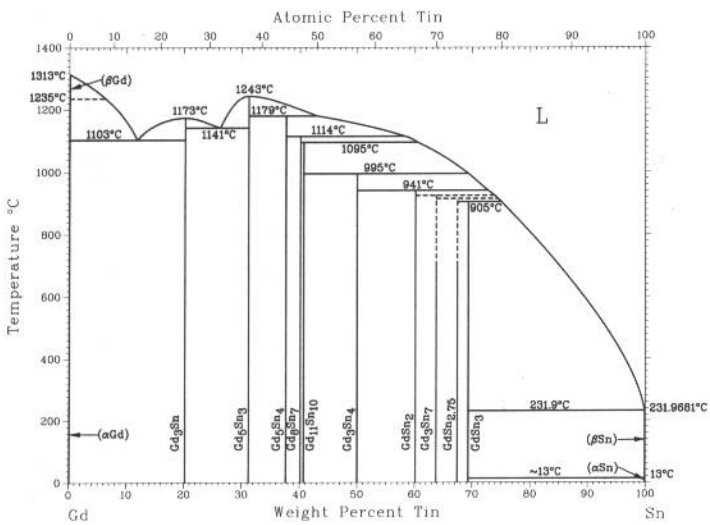

Phase	Composition, wt% Sn	Pearson symbol	Space group
(βGd)	0	*hP*2	$P6_3/mmc$
(αGd)	0	*cI*2	$Im\bar{3}m$
Gd_3Sn	20	...	...
Gd_5Sn_3	31.2	*hP*16	$P6_3/mcm$
Gd_5Sn_4	37.6	*oP*36	*Pnma*
Gd_8Sn_7	39.8	...	...
$Gd_{11}Sn_{10}$	40.7	*tI*84	*I*4/*mmm*
Gd_3Sn_4	50.1	...	...
$GdSn_2$	60.2	*oC*12	*Cmcm*
Gd_3Sn_7	64	*oC*20	*Cmmm*
$GdSn_{2.75}$	67.5	*oC*15	*Amm*2
$GdSn_3$	69	*cP*4	$Pm\bar{3}m$
(βSn)	100	*tI*4	$I4_1/amd$
(αSn)	100	*cF*8	$Fd\bar{3}m$

Gd-Te

H. Okamoto, 1990

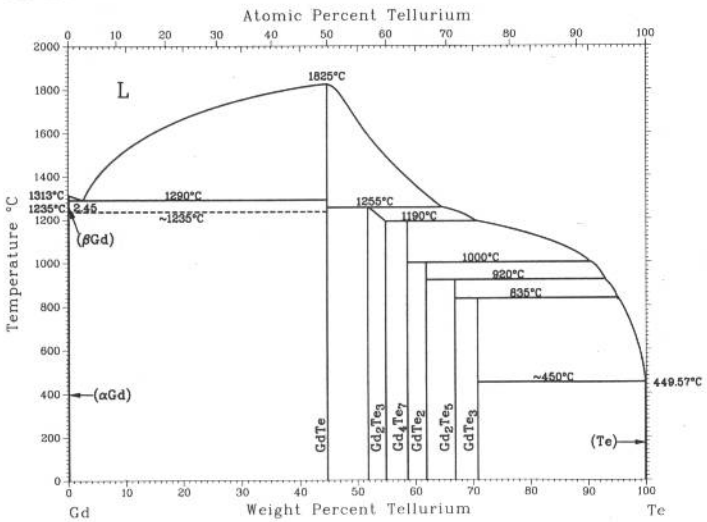

Phase	Composition, wt% Te	Pearson symbol	Space group
(βGd)	0	*cI*2	$Im\bar{3}m$
(αGd)	0	*hP*2	$P6_3/mmc$
GdTe	44.8	*cF*8	$Fm\bar{3}m$
Gd_2Te_3	52 to 55	*oP*20	*Pnma*
Gd_4Te_7	58.6	*tP*6	*P4/nmm*
$GdTe_2$	61.9	...	...
Gd_2Te_5	67.0	*oC*28	*Cmcm*
$GdTe_3$	71	*oC*16	*Cmcm*
(Te)	100	*hP*3	$P3_121$

Gd-Ti

J.L. Murray, 1987

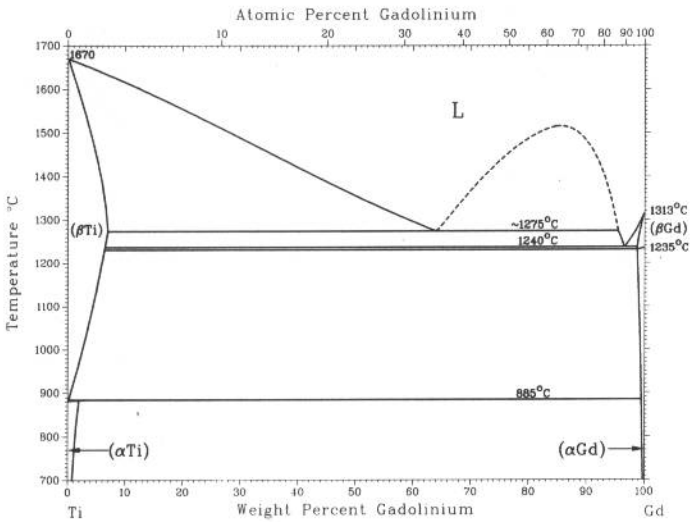

Phase	Composition, wt% Gd	Pearson symbol	Space group
(βTi)	0 to ~6	*cI*2	$Im\bar{3}m$
(αTi)	0 to ~1.9	*hP*2	$P6_3/mmc$
(βGd)	~99 to 100	*cI*2	$Im\bar{3}m$
(αGd)	~99 to 100	*hP*2	$P6_3/mmc$

Gd-Tl

S. Delfino, A. Saccone, A. Palenzona, and R. Ferro, unpublished

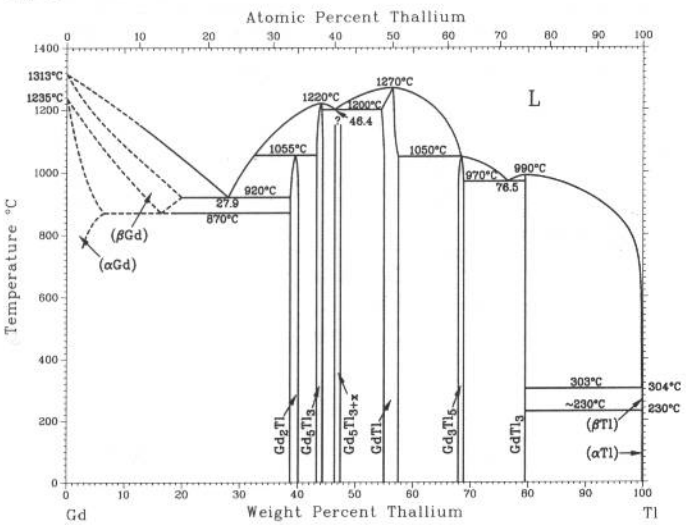

Phase	Composition, wt% Tl	Pearson symbol	Space group
(αGd)	0 to ?	*hP*2	$P6_3/mmc$
(βGd)	0 to ~20	*cI*2	$Im\bar{3}m$
Gd_2Tl	~39 to ~40	*hP*6	$P6_3/mmc$
Gd_5Tl_3	~43 to ~44	*hP*16	$P6_3/mcm$
Gd_5Tl_{3+x}	?	*tI*32	*I4/mcm*
GdTl(a)	~55 to ~58	*cP*2 (or *cI*2)	$Pm\bar{3}m$ $Im\bar{3}m$
GdTl(b)	~55 to ~58	*tP*2	*P4/mmm*
Gd_3Tl_5	~68 to ~69	*oC*32	*Cmcm*
$GdTl_3$	80	*cP*4	$Pm\bar{3}m$
(βTl)	100	*cI*2	$Im\bar{3}m$
(αTl)	100	*hP*2	$P6_3/mmc$

(a) Cubic structure presumed to be room- and higher-temperature phases. (b) Tetragonal structure presumed to be lower-temperature phase.

Ge-Ho

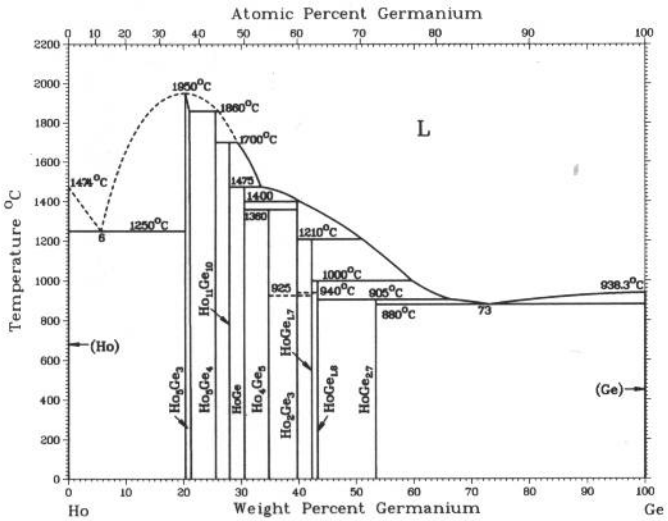

V.N. Eremenko, I.M. Obushenko, and Yu.I. Buyanov, 1980

Phase	Composition, wt% Ge	Pearson symbol	Space group
(Ho)	0	*hP*2	$P6_3/mmc$
Ho_5Ge_3	~20.9	*hP*16	$P6_3/mcm$
Ho_5Ge_4	26.0	*oP*36	*Pnma*
$Ho_{11}Ge_{10}$	28.6	*tI*84	*I*4/*mmm*
HoGe	30.6	*oC*8	*Cmcm*
Ho_4Ge_5	35.5	...	...
βHo_2Ge_3	40	*oC*12	*Cmmm*
αHo_2Ge_3	40	*hP*3	*P*6/*mmm*
$\beta HoGe_{1.7}$	43	...	...
$\alpha HoGe_{1.7}$	43	*tI*12	$I4_1/amd$
$HoGe_{1.8}$	44.2	...	...
$HoGe_{2.7}$	54	*o***	...
(Ge)	100	*cF*8	$Fd\bar{3}m$

Ge-In

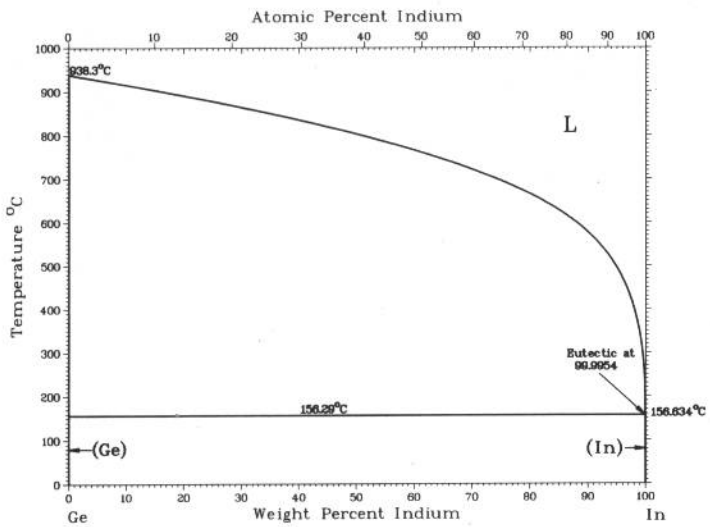

R.W. Olesinski, N. Kanani, and G.J. Abbaschian, 1992

Phase	Composition, wt% In	Pearson symbol	Space group
(Ge)	0	*cF*8	$Fd\bar{3}m$
(In)	100	*tI*2	*I*4/*mmm*

Ge-K

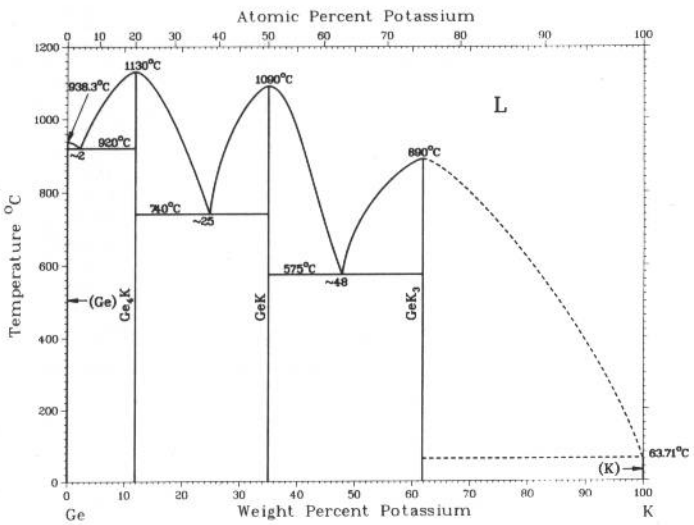

H. Okamoto, 1990

Phase	Composition, wt% K	Pearson symbol	Space group
(Ge)	0	*cF*8	$Fd\bar{3}m$
$Ge_{23}K_4$(a)	8.6	*cP*54	$Pm\bar{3}n$
Ge_4K	12	...	...
GeK	35.0	*cP*64	$P\bar{4}3m$
GeK_3	62	...	...
(K)	100	*cI*2	$Im\bar{3}m$

(a) Not shown in the phase diagram

Ge-La

A.B. Gokhale and G.J. Abbaschian, 1989

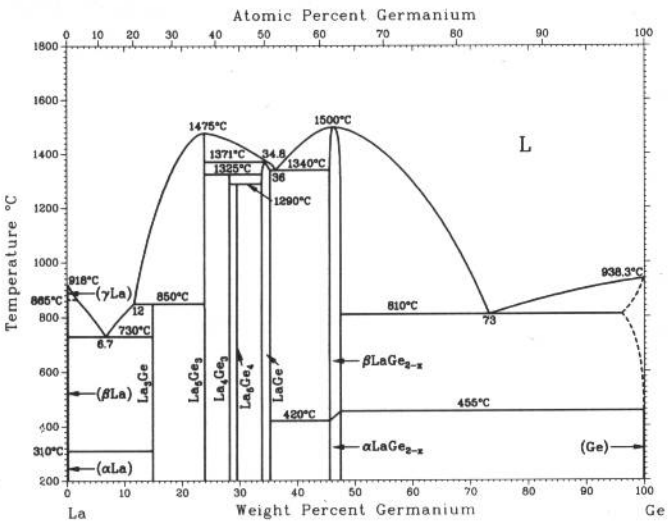

Phase	Composition, wt% Ge	Pearson symbol	Space group
(γLa)	0	*cI*2	$Im\bar{3}m$
(βLa)	0	*cF*4	$Fm\bar{3}m$
(αLa)	0	*hP*4	$P6_3/mmc$
La_3Ge	15	*t***	...
La_5Ge_3	23.9	*hP*16	$P6_3/mcm$
La_4Ge_3	28.2	*cI*28	$I\bar{4}3d$
La_5Ge_4	29.5	*oP**	*Pnma*
LaGe	33 to 35	*oP*8	*Pnma*
$\alpha LaGe_{2-x}$	45.5 to 46.4	*oI**	*Imma*
$\beta LaGe_{2-x}$	45.5 to 46.4	*tI*12	$I4_1/amd$
(Ge)	? to 100	*cF*8	$Fd\bar{3}m$

Ge-Li

H. Okamoto, 1990

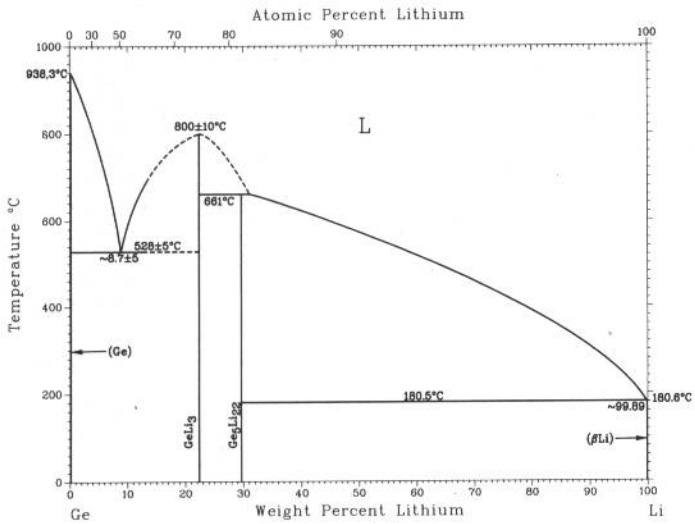

Phase	Composition, wt% Li	Pearson symbol	Space group
(Ge)	0	*cF*8	$Fd\bar{3}m$
GeLi(a)	8.7	*tI*32	$I4_1/a$
Ge_6Li_{11}(a)	14.9	*oC*68	*Cmcm*
$GeLi_2$(a)	16.1	...	...
$GeLi_3$	22	...	...
Ge_2Li_7(a)	25.1	*oC*36	*Cmmm*
Ge_4Li_{15}(a)	26.3	*cI*76	$I\bar{4}3d$
Ge_5Li_{22}	29.6	*cF*432	*F*23
(βLi)	100	*cI*2	$Im\bar{3}m$

(a) Not shown in the diagram

Ge-Lu

H. Okamoto, 1990

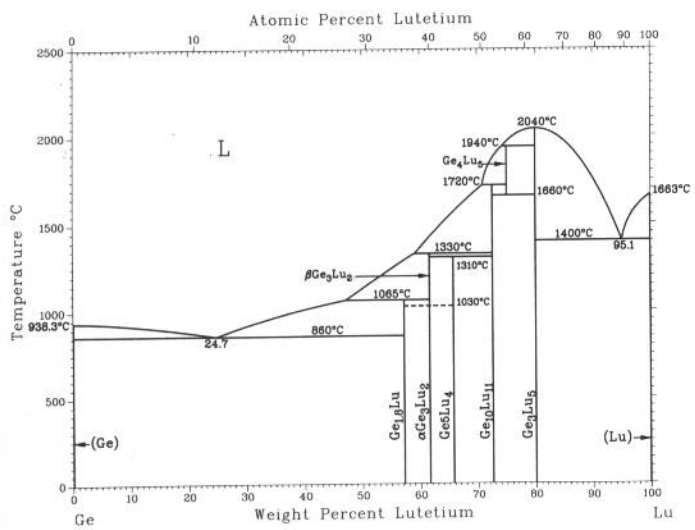

Phase	Composition, wt% Lu	Pearson symbol	Space group
(Ge)	0	*cF*8	$Fd\bar{3}m$
$Ge_{1.8}Lu$	57.2	*oC*12	*Cmcm*
Ge_3Lu_2	62	*hP*3	*P6/mmm*
Ge_5Lu_4	65.8	...	...
$Ge_{10}Lu_{11}$	72.6	*tI*84	*I4/mmm*
Ge_4Lu_5	75.1	*oP*36	*Pnma*
Ge_3Lu_5	80.1	*hP*16	$P6_3/mcm$
(Lu)	100	*hP*2	$P6_3/mmc$

Ge-Mg

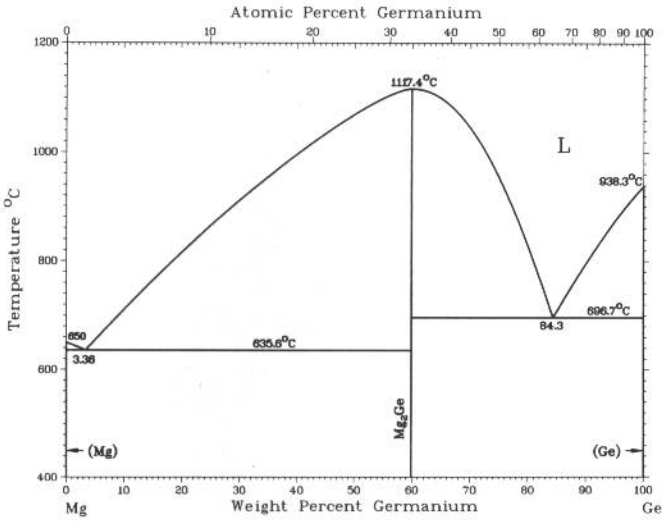

A.A. Nayeb-Hashemi, R.W. Olesinski, G.J. Abbaschian, and J.B. Clark, 1988

Phase	Composition, wt% Ge	Pearson symbol	Space group
(Mg)	~0	*hP*2	$P6_3/mmc$
Mg_2Ge	59.90	*cF*12	$Fm\bar{3}m$
(Ge)	~100	*cF*8	$Fd\bar{3}m$

Ge-Mn

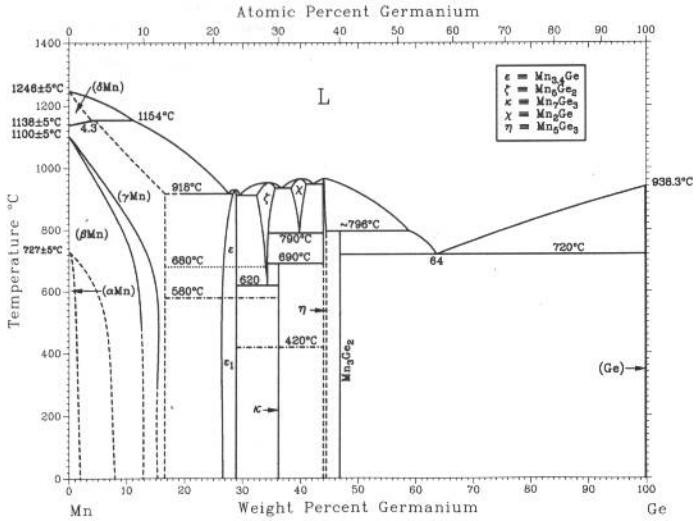

A.B. Gokhale and G.J. Abbaschian, 1990

Phase	Composition, wt% Ge	Pearson symbol	Space group
(δMn)	0 to 4.3	*cI*2	$Im\bar{3}m$
(γMn)	0 to ~16	*cF*4	$Fm\bar{3}m$
(βMn)	0 to ~13	*cP*20	$P4_132$
(αMn)	0 to ~2.0	*cI*58	$I\bar{4}3m$
ε	~28.0	*hP*8	$P6_3/mmc$
ε_1	~28.0	*tI*8	*I*4/*mmm*
ξ	~34.6	*hP*128	*P*3*c*1
κ	36	*o***	...
χ	~39.9	*hP*6	$P6_3/mmc$
η	~44.2	*hP*16	$P6_3/mcm$
Mn_3Ge_2	47	...	...
(Ge)	100	*cF*8	$Fd\bar{3}m$

Enlarged region of the Mn-Ge system

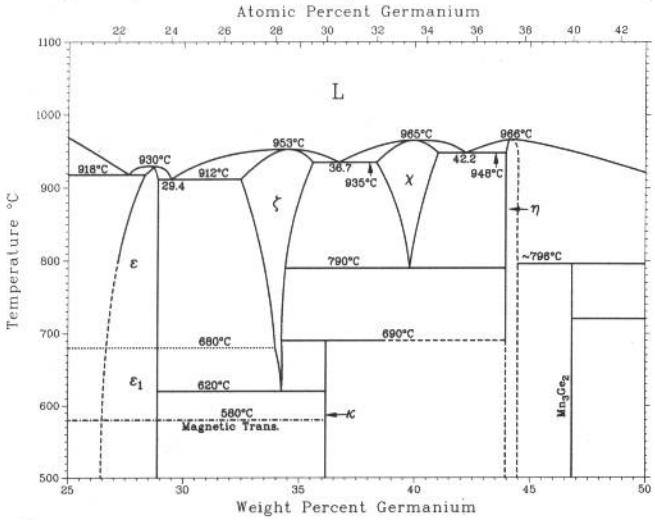

Ge-Mo

R.W. Olesinski and G.J. Abbaschian, 1987

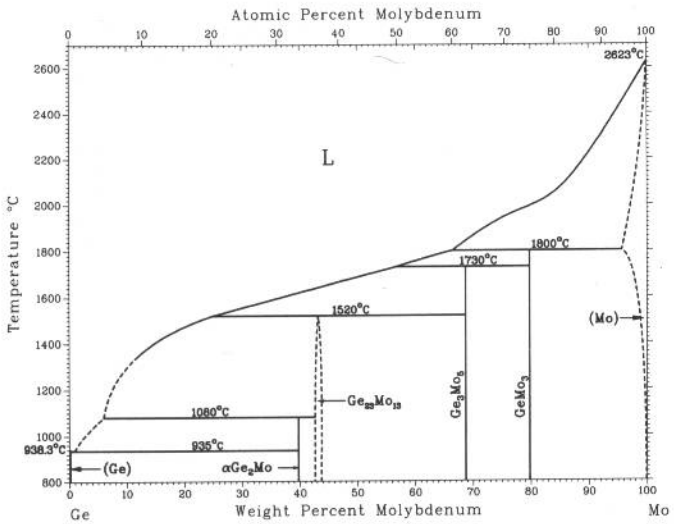

Phase	Composition, wt% Mo	Pearson symbol	Space group
(Ge)	0	*cF*8	$Fd\bar{3}m$
αGe_2Mo	39.7	*oP*12	*Pnma*
βGe_2Mo (HP)	...	*tI*8	*I*4/*mmm*
$Ge_{23}Mo_{13}$(a)	43 to 44	*tP*144	$P\bar{4}n2$
Ge_3Mo_5	68.8	*hP*16	$P6_3/mcm$
$GeMo_3$	80	*cP*8	$Pm\bar{3}n$
(Mo)	? to 100	*cI*2	$Im\bar{3}m$

(a) Also reported as $Ge_{41}Mo_{23}$ and $Ge_{16}Mo_9$ or $Ge_{1.7}Mo$

Ge-Na

H. Okamoto, 1990

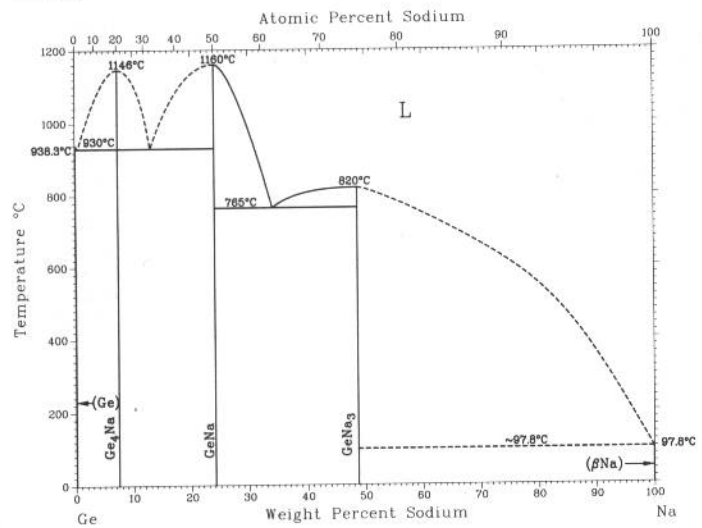

Phase	Composition, wt% Na	Pearson symbol	Space group
(Ge)	0	*cF*8	$Fd\bar{3}m$
Ge_4Na	7	*cP**	$Pm\bar{3}n$
GeNa	24.0	*mP*32	$P2_1/c$
$GeNa_3$	49	...	...
(Na)	100	*cI*2	$Im\bar{3}m$

Ge-Nb

From [Moffatt]

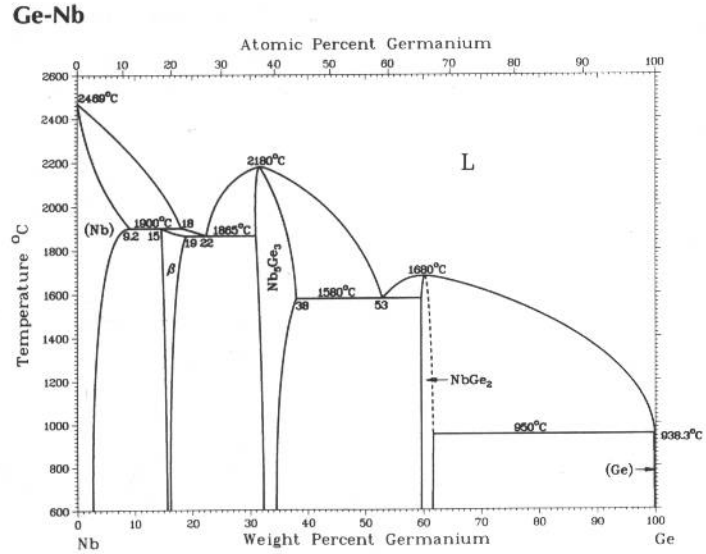

Phase	Composition, wt% Ge	Pearson symbol	Space group
(Nb)	0 to 9.2	*cI*2	$Im\bar{3}m$
β	15 to 19	*cP*8	$Pm\bar{3}n$
Nb_5Ge_3	32 to 38	*tI*32	*I*4/*mcm*
$NbGe_2$	~61.0	*hP*9	$P6_222$
(Ge)	100	*cF*8	$Fd\bar{3}m$

Ge-Nd

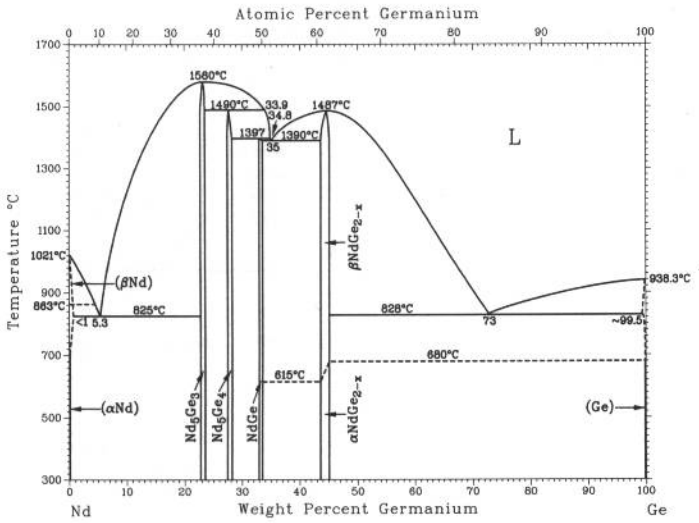

A.B. Gokhale and G.J. Abbaschian, 1989

Phase	Composition, wt% Ge	Pearson symbol	Space group
(αNd)	0 to <1	*hP*4	$P6_3/mmc$
(βNd)	0 to <1	*cI*2	$Im\bar{3}m$
Nd_5Ge_3	22.3 to 23.2	*hP*16	$P6_3/mcm$
Nd_5Ge_4	26.8 to 27.8	*oP**	*Pnma*
NdGe	33 to 33.5	*oC*8	*Cmcm*
$\alpha NdGe_{2-x}$	43 to 44.7	*oI**	*Imma*
$\beta NdGe_{2-x}$	43 to 44.7	*tI*12	$I4_1/amd$
(Ge)	100	*cF*8	$Fd\bar{3}m$

Ge-Ni

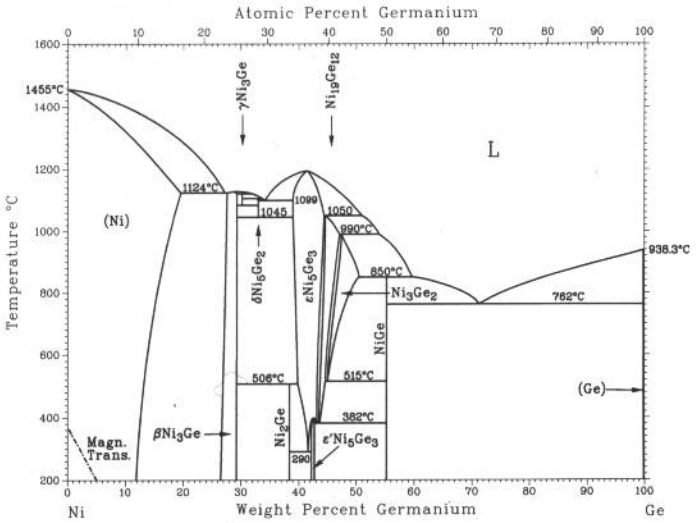

A. Nash and P. Nash, 1991

Phase	Composition, wt% Ge	Pearson symbol	Space group
(Ni)	0 to 19	*cF*4	$Fm\bar{3}m$
βNi_3Ge	26.4 to 29	*cP*4	$Pm\bar{3}m$
γNi_3Ge	29.9	...	...
δNi_5Ge_2	33	*hP*84	$P6_3/mmc$
Ni_2Ge	38.4	*oP*12	*Pnma*
$\varepsilon' Ni_5Ge_3$	~42	*mC*32	*C*2
εNi_5Ge_3	40 to 49	*hP*4	$P6_3/mmc$
$Ni_{19}Ge_{12}$	43 to 46	*mC*62	*C*2
Ni_3Ge_2(a)	46 to 48	*hP*4	$P6_3/mmc$
NiGe	55.3	*oP*8	*Pnma*
(Ge)	100	*cF*8	$Fd\bar{3}m$

Ge-P

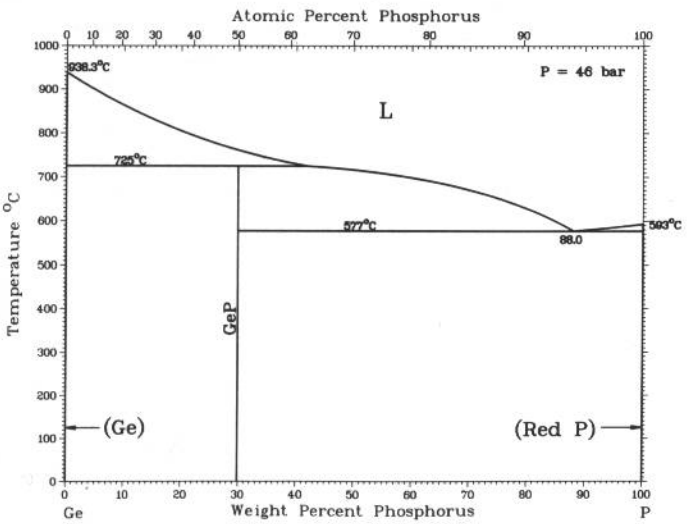

R.W. Olesinski, N. Kanani, and G.J. Abbaschian, 1985

Phase	Composition, wt% P	Pearson symbol	Space group
(Ge)	0 to 0.07	*cF*8	$Fd\bar{3}m$
GeP	29.9	(a)	*C*2/*m*
GeP(b)	29.9	(c)	*I*4/*mm*
GeP_3(b)	56	*hR*2	$R\bar{3}m$
GeP_5(b)	68.0	*hR*2	$R\bar{3}m$
Red P	100	...	...
White P	100	...	...
Black P	100	*oC*8	*Cmca*

(a) Orthorhombic. (b) High-temperature phase. (c) Tetragonal

Ge-Pb

R.W. Olesinski and G.J. Abbaschian, 1984

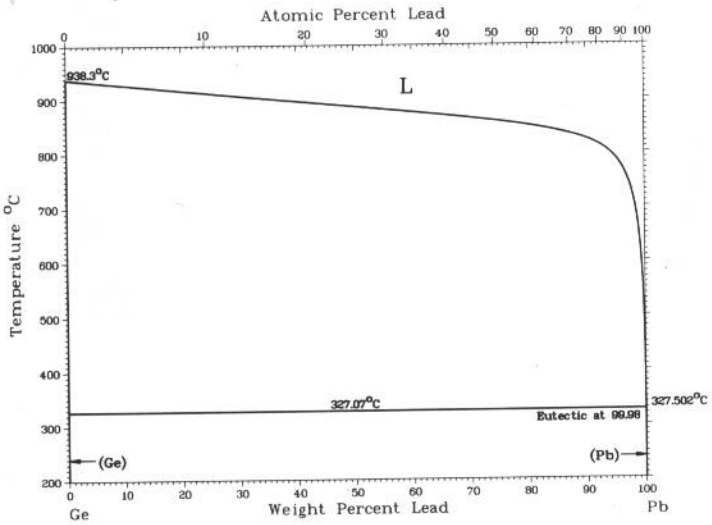

Phase	Composition, wt% Pb	Pearson symbol	Space group
(Ge)	0	*cF*8	$Fd\bar{3}m$
(Pb)	100	*cF*4	$Fm\bar{3}m$

Ge-Pd

H. Okamoto, 1992

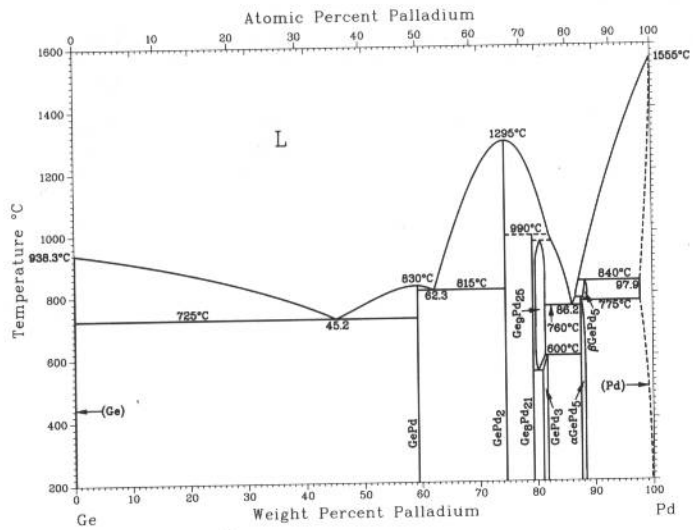

Phase	Composition, wt% Pd	Pearson symbol	Space group
(Ge)	0	*cF*8	$Fd\bar{3}m$
GePd	59.4	*oP*8	*Pnma*
$GePd_2$	74.6	*hP*9	$P\bar{6}2m$
Ge_8Pd_{21}	79.4	*tI*116	$I4_1/a$
Ge_9Pd_{25}	80 to 81.5	*hP*34	$P\bar{3}$
$GePd_3$	81.1 to 81.9	...	...
$\beta GePd_5$	88.1 to 88.9	*cI*2	$Im\bar{3}m$
$\alpha GePd_5$	87.7 to 88.5	*mC*24	*C*2
(Pd)	97.9 to 100	*cF*4	$Fm\bar{3}m$

Ge-Pr

A.B. Gokhale, A. Munitz, and G.J. Abbaschian, 1989

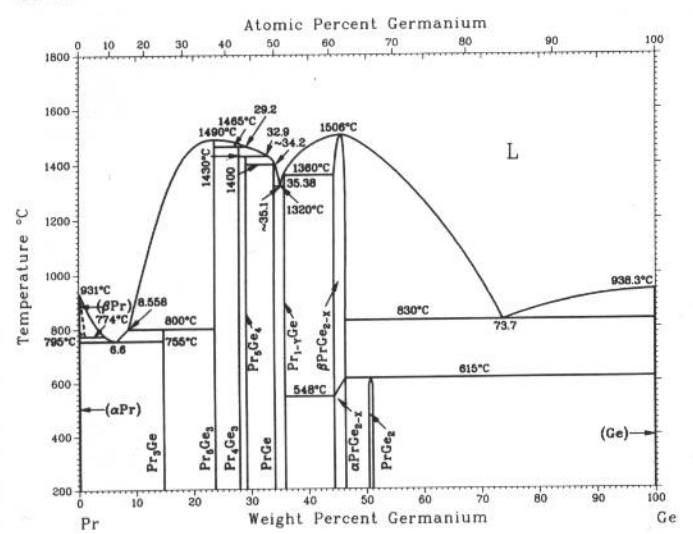

Phase	Composition, wt% Ge	Pearson symbol	Space group
(βPr)	0 to ?	*cI*2	$Im\bar{3}m$
(αPr)	0	*hP*4	$P6_3/mmc$
Pr_3Ge	15	*t***	...
Pr_5Ge_3	23.8	*hP*16	$P6_3/mcm$
Pr_4Ge_3	27.9	*cI*28	$I\bar{4}d$
Pr_5Ge_4	29.2	*oP**	*Pnma*
PrGe	34.0	*oC*8	*Cmcm*
$Pr_{1-y}Ge$	35.5	*oP*8	*Pnma*
$\alpha PrGe_{2-x}$	45 to 46.3	*oI**	*Imma*
$\beta PrGe_{2-x}$	45 to 46.3	*tI*12	$I4_1/amd$
$PrGe_2$	~50.8	*tI*12	$I4_1/amd$
(Ge)	100	*cF*8	$Fd\bar{3}m$

Ge-Pt

H. Okamoto, 1992

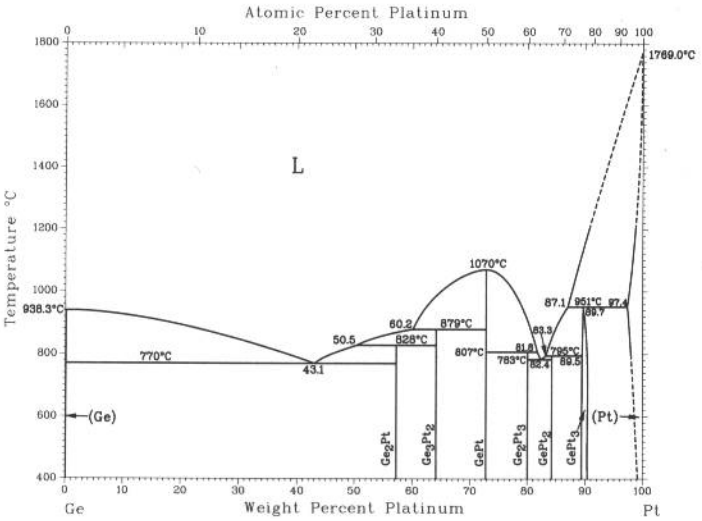

Phase	Composition, wt% Pt	Pearson symbol	Space group
(Ge)	0	*cF*8	$Fd\bar{3}m$
Ge_2Pt	57.3	*oP*6	*Pnnm*
Ge_3Pt_2	64	*oP*20	*Pnma*
GePt	72.9	*oP*8	*Pnma*
Ge_2Pt_3	80	*oP*40	*Pnma*
$GePt_2$	84.3	*hP*9	$P\bar{6}2m$
$GePt_3$	90 to 91	*mC*16	*C*2/*m*
(Pt)	97.4 to 100	*cF*4	$Fm\bar{3}m$
Metastable phase			
$GePt_3$	90 to 91	*tI*16	*I*4/*mcm*

Ge-S

C.H. Lin, A.S. Pashinkin, and A.V. Novoselova, 1963

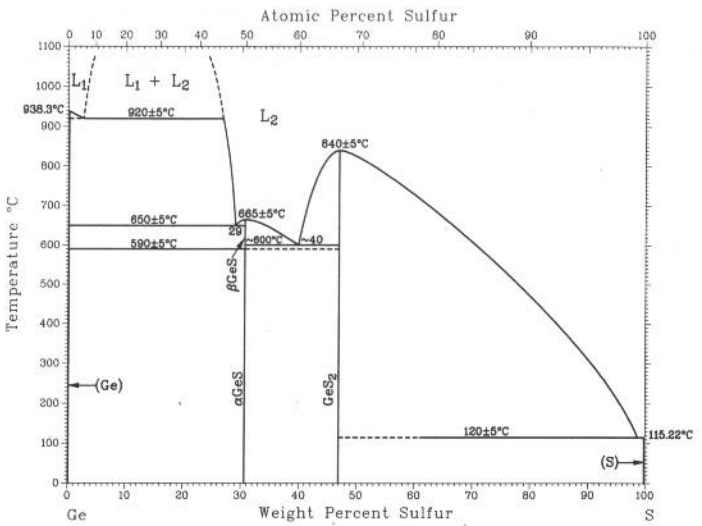

Phase	Composition, wt% S	Pearson symbol	Space group
(Ge)	0	*cF*8	$Fd\bar{3}m$
βGeS	30.6	*h***	...
αGeS	30.6	*oP*8	*Pnma*
GeS_2	46.9	*oF*72	*Fdd*2

Ge-Sb

R.W. Olesinski and G.J. Abbaschian, 1986

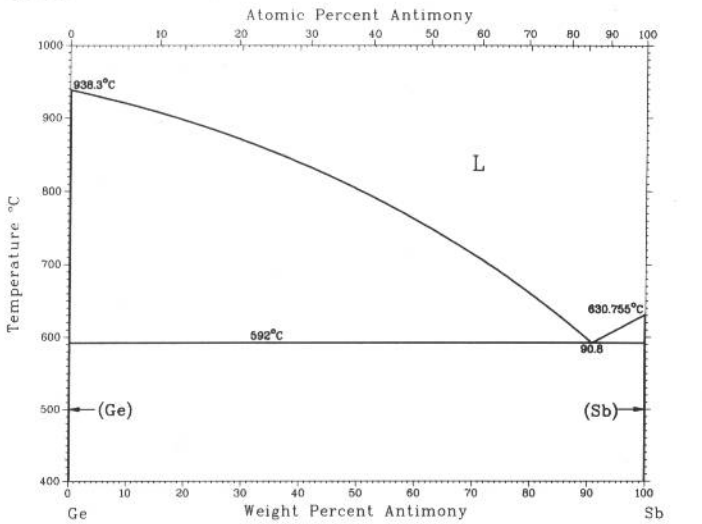

Phase	Composition, wt% Sb	Pearson symbol	Space group
(Ge)	0	*cF*8	$Fd\bar{3}m$
(Sb)	100	*hR*2	$R\bar{3}m$

Ge-Sc

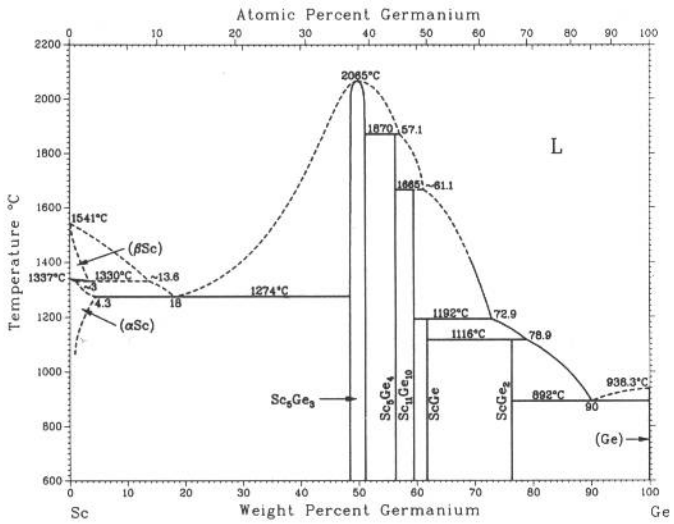

A.B. Gokhale and G.J. Abbaschian, 1986

Phase	Composition, wt% Ge	Pearson symbol	Space group
(βSc)	0 to ~3	*cI*2	$Im\bar{3}m$
(αSc)	0 to 4.3	*hP*2	$P6_3/mmc$
Sc_5Ge_3	48.1 to 50.3	*hP*16	$P6_3/mcm$
Sc_5Ge_4	56.4	...	...
$Sc_{11}Ge_{10}$	59.5	...	*I*4/*mmm*
ScGe	61.8	*oC*8	*Cmcm*
$ScGe_2$	76.4	*oC*12	*Cmcm*
(Ge)	~100	*cF*8	$Fd\bar{3}m$

Ge-Se

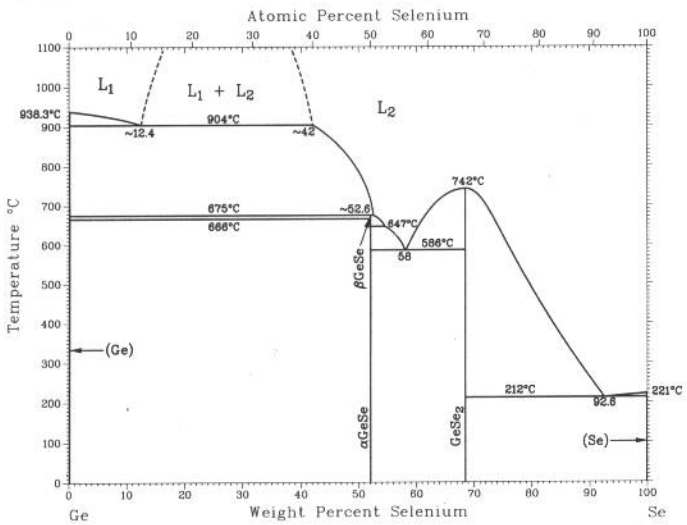

A.B. Gokhale and G.J. Abbaschian, 1990

Phase	Composition, wt% Se	Pearson symbol	Space group
(Ge)	0	*cF*8	$Fd\bar{3}m$
αGeSe	52.1	*oC*8	*Cmca*
βGeSe	52.1	*cF*8	$Fm\bar{3}m$
$GeSe_2$	68.51	...	...
(γSe)	100	*hP*3	$P3_121$

Note: Crystal structures of the low-temperature α and β forms of Se are not known.

Ge-Si

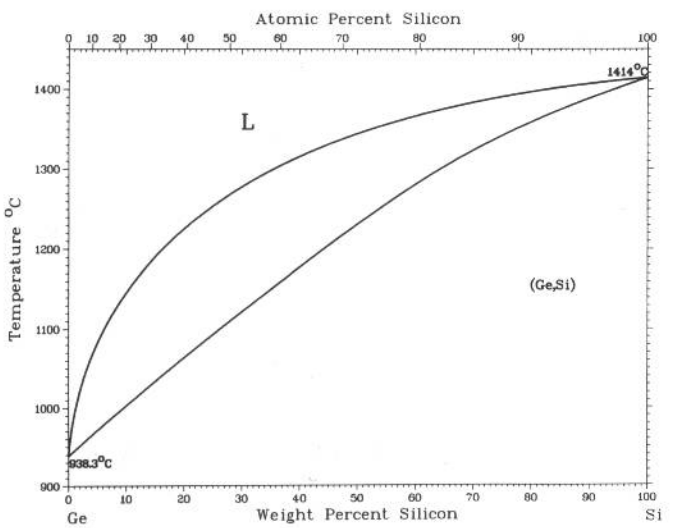

R.W. Olesinski and G.J. Abbaschian, 1984

Phase	Composition, wt% Si	Pearson symbol	Space group
(Ge,Si)	0 to 100	*cF*8	$Fd\bar{3}m$
High-pressure phases			
GeII	...	*tI*4	$I4_1/amd$
SiII	...	*tI*4	$I4_1/amd$

Ge-Sm

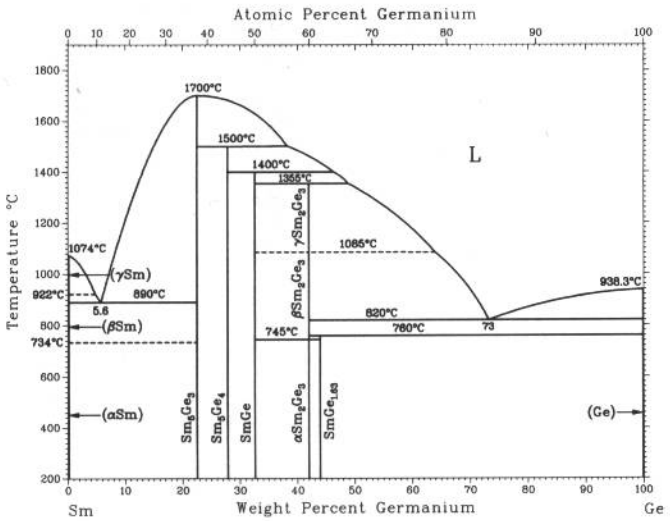

A.B. Gokhale and G.J. Abbaschian, 1988

Phase	Composition, wt% Ge	Pearson symbol	Space group
(γSm)	0	*cI*2	$Im\bar{3}m$
(βSm)	0	*hP*2	$P6_3/mmc$
(αSm)	0	*hR*3	$R\bar{3}m$
Sm_5Ge_3	22.5	*hP*16	$P6_3/mcm$
Sm_5Ge_4	27.9	*oP**	*Pnma*
SmGe	32.6	*oC*8	*Cmcm*
γSm_2Ge_3	42	...	...
βSm_2Ge_3	42	...	...
αSm_2Ge_3	42	*hP*3	*P6/mmm*
$SmGe_{1.63}$	44	*tI*12	$I4_1/amd$
(Ge)	100	*cF*8	$Fd\bar{3}m$

Ge-Sn

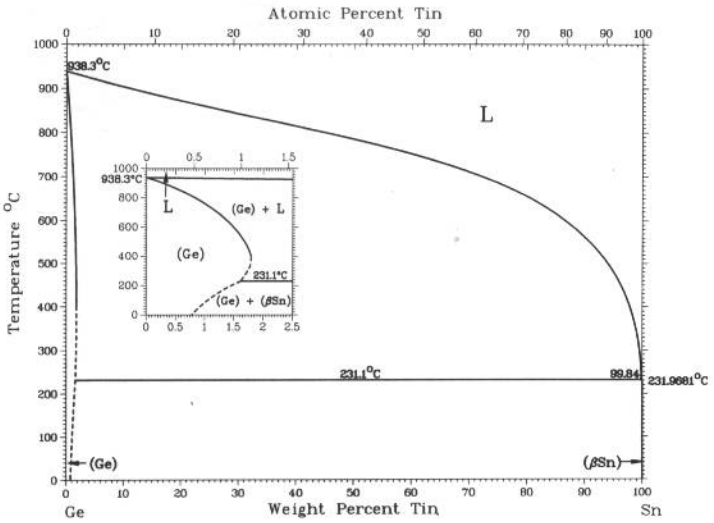

R.W. Olesinski and G.J. Abbaschian, 1984

Phase	Composition, wt% Sn	Pearson symbol	Space group
(Ge)	0 to 1.8	*cF*8	$Fd\bar{3}m$
(βSn)	100	*tI*4	$I4_1/amd$
(αSn)	100	*cF*8	$Fd\bar{3}m$
Pressure stabilized phase			
GeII	0 to 15	*tI*4	$I4_1/amd$
Crystallized from amorphous phase			
Ge_ySn_{1-y}	42 to 62.0	*cF*8	$F\bar{4}3m$

Ge-Sr

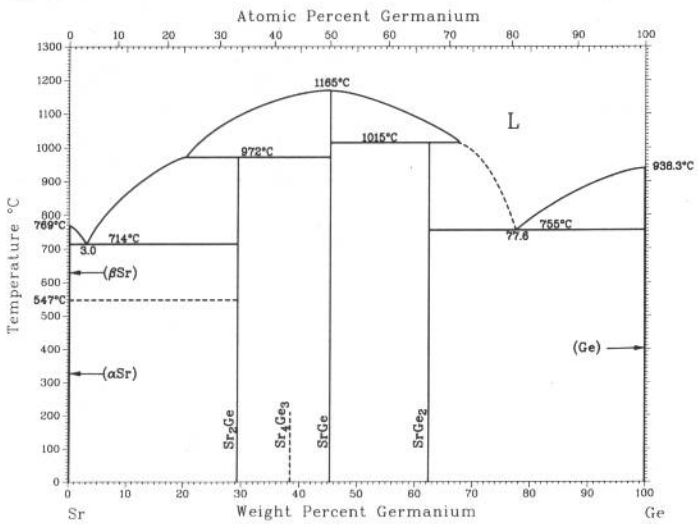

P.R. Subramanian, 1990

Phase	Composition, wt% Ge	Pearson symbol	Space group
(αSr)	0	*cF*4	$Fm\bar{3}m$
(βSr)	0	*cI*2	$Im\bar{3}m$
Sr_2Ge	29.3	*oP*12	*Pnma*
Sr_4Ge_3	~38.4	*oI*40	*Immm*
SrGe	45.3	*oC*8	*Cmcm*
$SrGe_2$	62.4	*oP*24	*Pnma*
(Ge)	100	*cF*8	$Fd\bar{3}m$

Ge-Tb

H. Okamoto, 1990

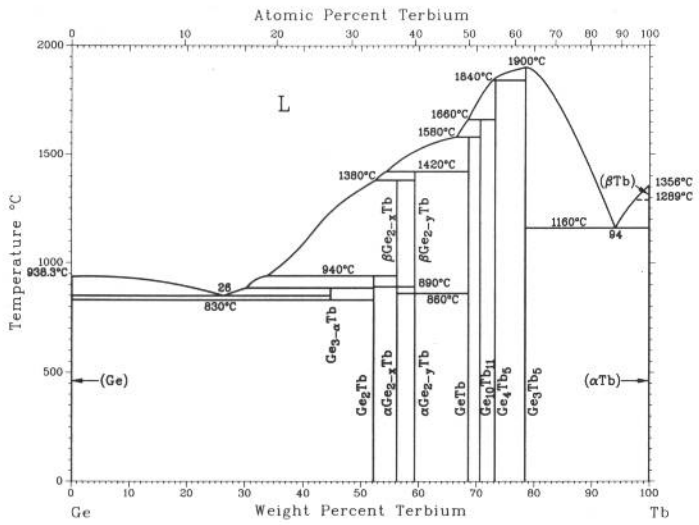

Phase	Composition, wt% Tb	Pearson symbol	Space group
(Ge)	0	*cF*8	$Fd\bar{3}m$
$Ge_{3-\alpha}Tb$	45	*oC*18	$C222_1$
Ge_2Tb	52.2	...	...
$\beta Ge_{2-x}Tb$	56	*tI*12	$I4_1/amd$
$\alpha Ge_{2-x}Tb$	56	...	...
$\beta Ge_{2-y}Tb$	59	*hP*3	*P6/mmm*
$\alpha Ge_{2-y}Tb$	59	...	...
GeTb	68.6	*oC*8	*Cmcm*
$Ge_{10}Tb_{11}$	70.7	*tI*84	*I4/mmm*
Ge_4Tb_5	73.3	*oP*36	*Pnma*
$GeTb_5$	78.5	*hP*16	$P6_3/mcm$
(Tb)	100	*hP*2	$P6_3/mmc$

Ge-Te

H. Okamoto, 1990

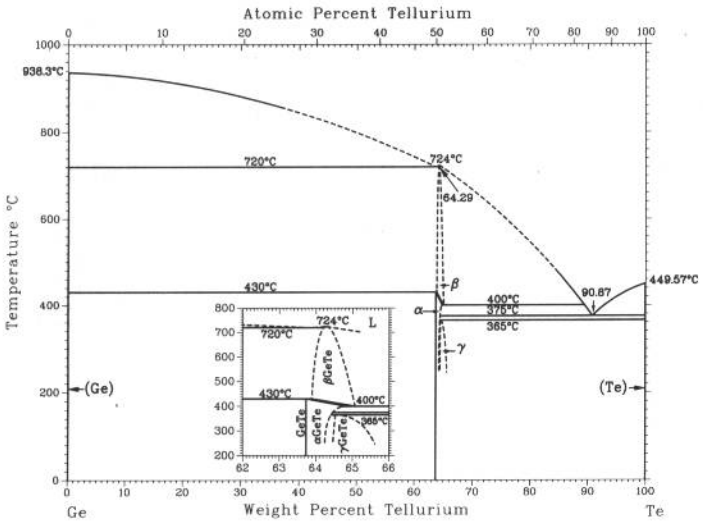

Phase	Composition, wt% Te	Pearson symbol	Space group
(Ge)	0	*cF*8	$Fd\bar{3}m$
βGeTe	~63.7 to 65	*cF*8	$Fm\bar{3}m$
αGeTe	~63.7 to 65	*hR**	$R\bar{3}m$
γGeTe	~65 to 66	*o***	...
(Te)	100	*hP*3	*P*3121

Ge-Ti

H. Okamoto, 1990

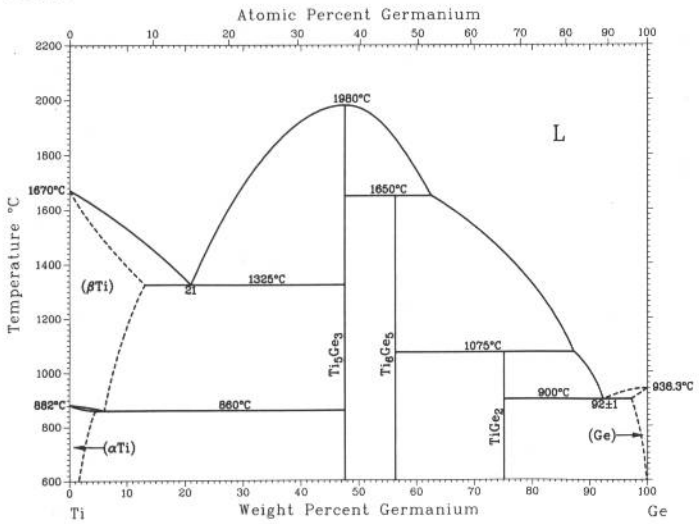

Phase	Composition, wt% Ge	Pearson symbol	Space group
(βTi)	0 to ?	*cI*2	$Im\bar{3}m$
(αTi)	0 to ?	*hP*2	$P6_3/mmc$
Ti_5Ge_3	47.6	*hP*16	$P6_3/mcm$
Ti_6Ge_5	55.9	*oI*44	*Immm*
$TiGe_2$	75.2	*oF*24	*Fddd*
(Ge)	100	*cF*8	$Fm\bar{3}m$

Ge-Tl

R.W. Olesinski and G.J. Abbaschian, 1985

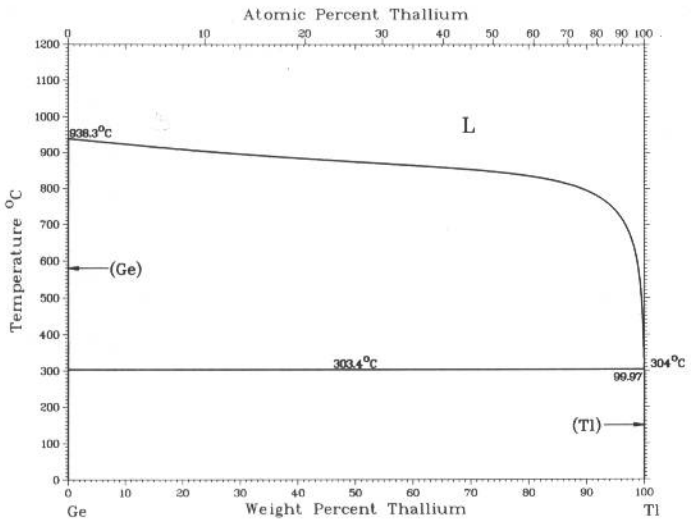

Phase	Composition, wt% Tl	Pearson symbol	Space group
(Ge)	0.06	*cF*8	$Fd\bar{3}m$
(βTl)	99.97 to 100	*cI*2	$Im\bar{3}m$
(αTl)	100	*hP*2	$P6_3/mmc$

Ge-Tm

H. Okamoto, 1990

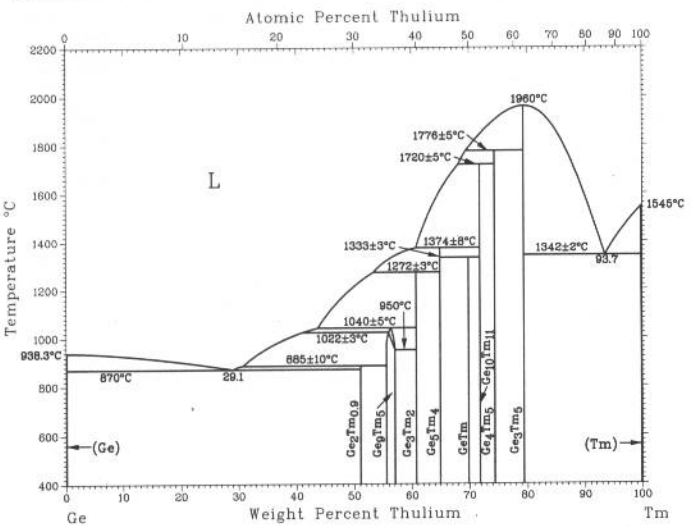

Phase	Composition, wt% Tm	Pearson symbol	Space group
(Ge)	0	*cF*8	$Fd\bar{3}m$
$Ge_2Tm_{0.9}$	51	*oC*12	*Cmcm*
βGe_9Tm_5	56.4	...	...
αGe_9Tm_5	56.4	...	...
Ge_3Tm_2	61	*hP*3	*P6/mmm*
Ge_5Tm_4	65.0	...	...
GeTm	69.9	*oC*8	*Cmcm*
$Ge_{10}Tm_{11}$	71.9	*tI*84	*I4/mmm*
Ge_4Tm_5	74.4	*oP*36	*Pnma*
Ge_3Tm_5	79.5	*hP*16	$P6_3/mcm$
(Tm)	100	*hP*2	$P6_3/mmc$

Ge-U

V.S. Lyashenko and V. Bykov, 1960

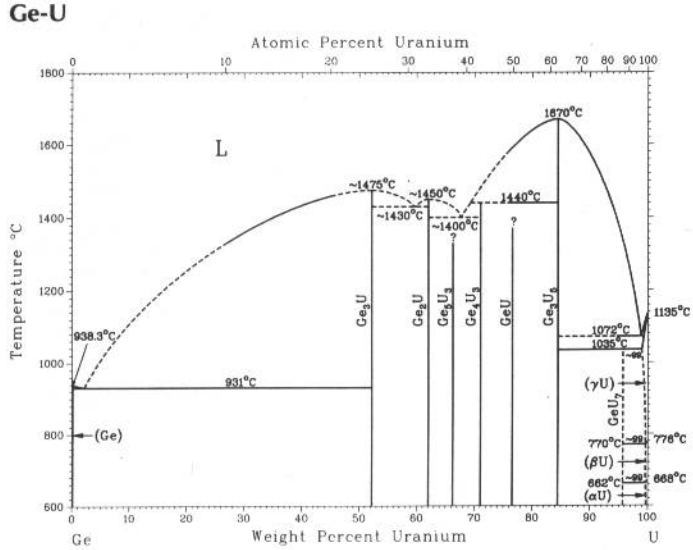

Phase	Composition, wt% U	Pearson symbol	Space group
(Ge)	0	*cF*8	$Fd\bar{3}m$
Ge_3U	52	*cP*4	$Pm\bar{3}m$
Ge_2U	62.1	*hP*3	*P6/mmm*
		or *oC*12	*Cmcm*
Ge_5U_3	66.3	...	...
Ge_4U_3	71.1	*o***	...
GeU	76.6	...	...
Ge_3U_5	84.5	*hP*16	$P6_3/mcm$
GeU_7	95.8	...	...
(γU)	~99 to 100	*cI*2	$Im\bar{3}m$
(βU)	~99 to 100	*tP*30	$P4_2/mnm$
(αU)	~99 to 100	*oC*4	*Cmcm*

Ge-Y

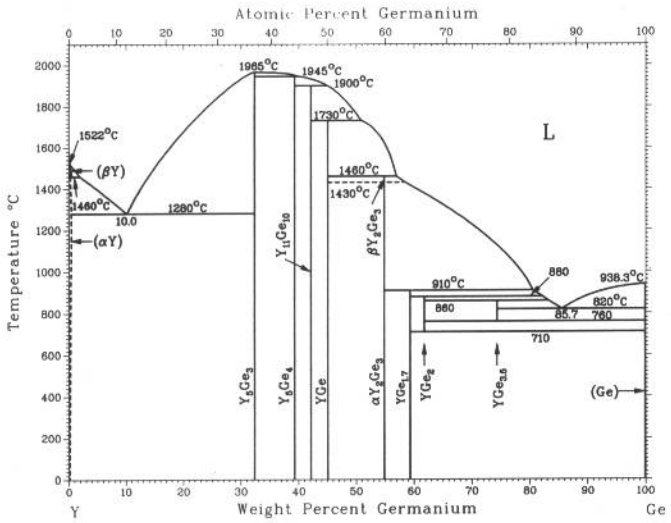

A.B. Gokhale and G.J. Abbaschian, 1988

Phase	Composition, wt% Ge	Pearson symbol	Space group
(αY)	0 to ~0.81	*hP*2	$P6_3/mmc$
(βY)	0 to ~0.81	*cI*2	$Im\bar{3}m$
Y_5Ge_3	32.9	*hP*16	$P6_3/mcm$
Y_5Ge_4	39.52	*oP*36	*Pnma*
$Y_{11}Ge_{10}$	42.6	*tI*84	*I*4/*mmm*
YGe	45.0	*oC*8	*Cmcm*
βY_2Ge_3	55	...	*Pccm*(a)
αY_2Ge_3	55	*hP*3	*P*6/*mmm*
βY_3Ge_5	57.6	*oF*72	*Fdd*2
αY_3Ge_5	57.6	*tI*12	$I4_1/amd$
YGe_2	62.03	*oC*12	*Cmcm*
Y_2Ge_7	74.09	...	$C222_1$(a)
(Ge)	0 to ~0.4	*cF*8	$Fd\bar{3}m$

(a) Tentative

Ge-Yb

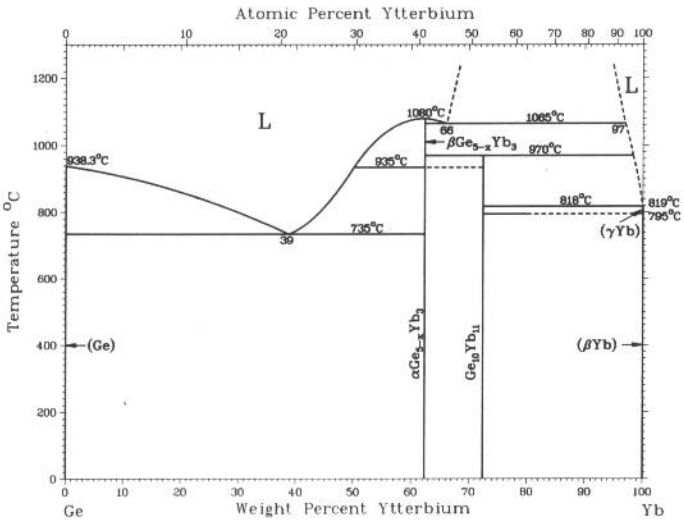

V.N. Eremenko, K.A. Meleshevich, and Yu.I. Buyanov, 1983

Phase	Composition, wt% Yb	Pearson symbol	Space group
(Ge)	0	*cF*8	$Fd\bar{3}m$
$\beta Ge_{5-x}Yb$	~61	*hP*3	*P*6/*mmm*
$\alpha Ge_{5-x}Yb$	~61	*hP*8	$P\bar{6}2m$
$Ge_{10}Yb_{11}$	72.3	*tI*84	*I*4/*mmm*
(γYb)	100	*cI*2	$Im\bar{3}m$
(βYb)	100	*cF*4	$Fm\bar{3}m$
(αYb)	100	*hP*2	$P6_3/mmc$

Ge-Zn

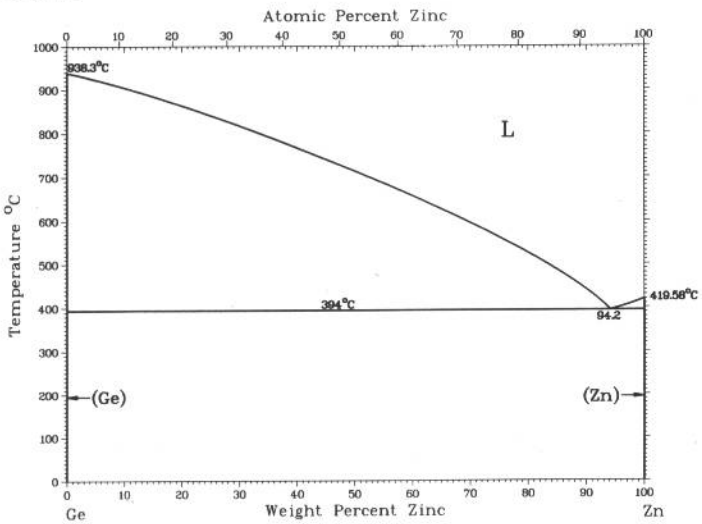

R.W. Olesinski and G.J. Abbaschian, 1985

Phase	Composition, wt% Zn	Pearson symbol	Space group
(Ge)	0	*cF*8	$Fd\bar{3}m$
(Zn)	100	*hP*2	$P6_3/mmc$

H-La

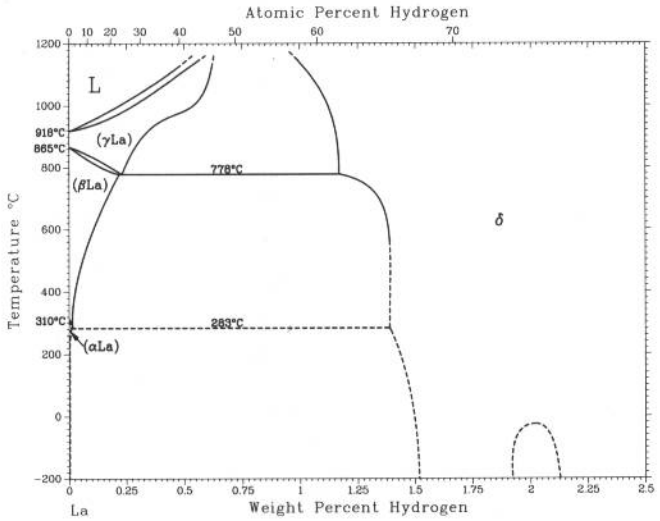

D. Khatamian and F.D. Manchester, 1990

Phase	Composition, wt% H	Pearson symbol	Space group
(γLa)(a)	0 to 0.6	*cI*2	$Im\bar{3}m$
(βLa)(b)	0 to 0.2	*cF*4	$Fm\bar{3}m$
(αLa)(c)	0 to 0.01	*hP*4	$P6_3/mmc$
δ	1 to 2	*cF*16	$Fm\bar{3}m$

(a) From 865 to 918 °C at 0 at.% H. (b) From 310 to <865 °C at 0 at.% H. (c) Up to <310 °C at 0 at.% H

H-Nb

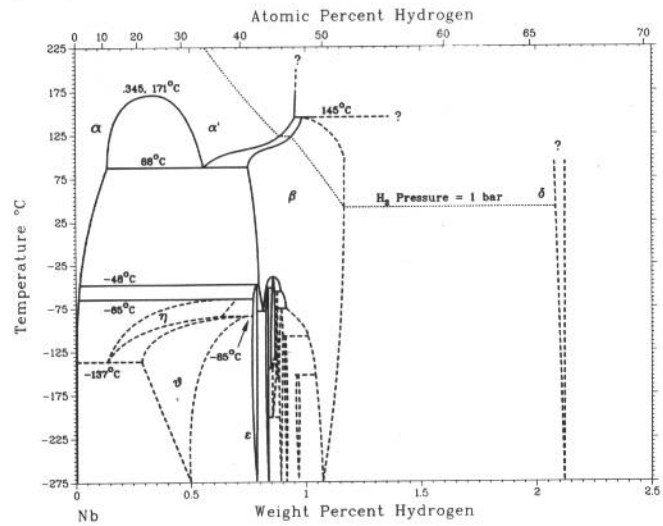

J.F. Smith, 1983

Phase	Composition, wt% H	Pearson symbol	Space group
α, α′	0 to 470.95	*cI*2	$Im\bar{3}m$
η	~0.13 to ~0.69	...	...
θ	~0.29 to ~0.75	...	...
β	0.75 to ~1.2	*oP*8	...
ε	~0.78	*oP*28	...
ι, λ, ο, μ, υ, ξ	~0.83 to 0.92	(a)	...
γ	~0.96	(b)	...
δ	~2.13	*cF*12	$Fm\bar{3}m$

(a) H-deficient β structure having ordering of H atoms. (b) Possibly a face-centered tetragonal structure

Peritectoid cascade region of the Nb-H phase diagram

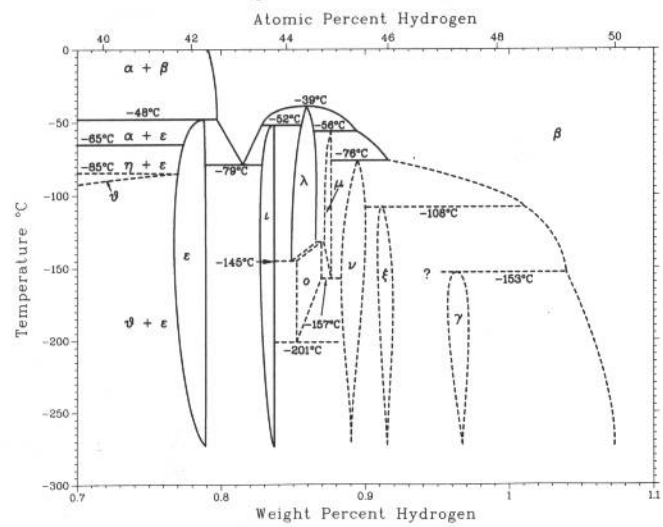

H-Nd

P.R. Subramanian, 1990

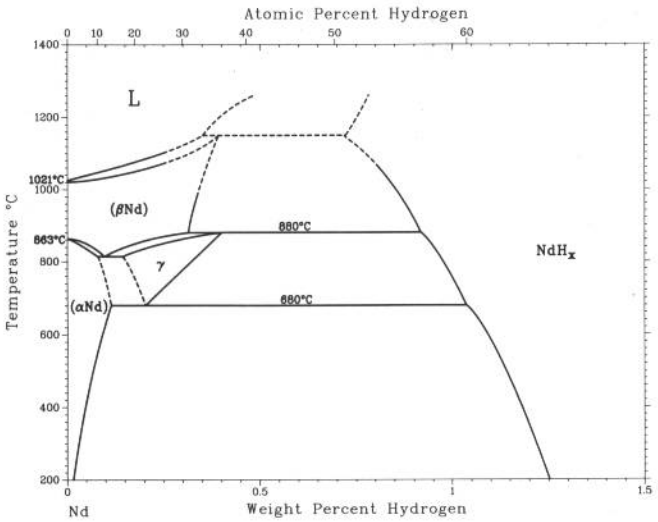

Phase	Composition, wt% H	Pearson symbol	Space group
(βNd)	0	*cI*2	$Im\bar{3}m$
(αNd)	0	*hP*4	$P6_3/mmc$
γ(a)	~0.15 to 0.43	...	...
NdH_2(b)	~1.38	*cF*12	$Fm\bar{3}m$
Nd_2H_5(b, c)	~1.6	*tI*28	$I4_1md$
		*tI*40	$I4_1md$

(a) High-temperature phase; exists between 680 and 880 °C. (b) Not shown in the phase diagram. (c) Ideal stoichiometry; structure based on neutron-diffraction studies on samples with the composition $NdD_{2.36}$

H-Ni

M.L. Wayman and G.C. Weatherly, 1991

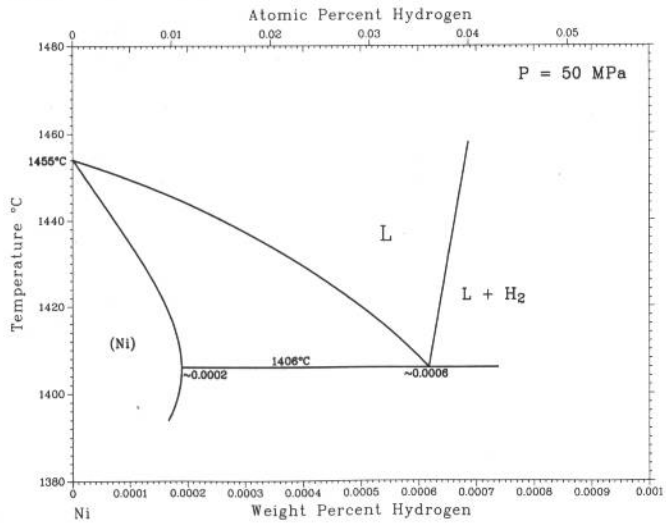

Phase	Composition, wt% H	Pearson symbol	Space group
(Ni)	0 to ~0.0002	*cF*4	$Fm\bar{3}m$

H-Pd

A. San-Martin and F.D. Manchester, unpublished

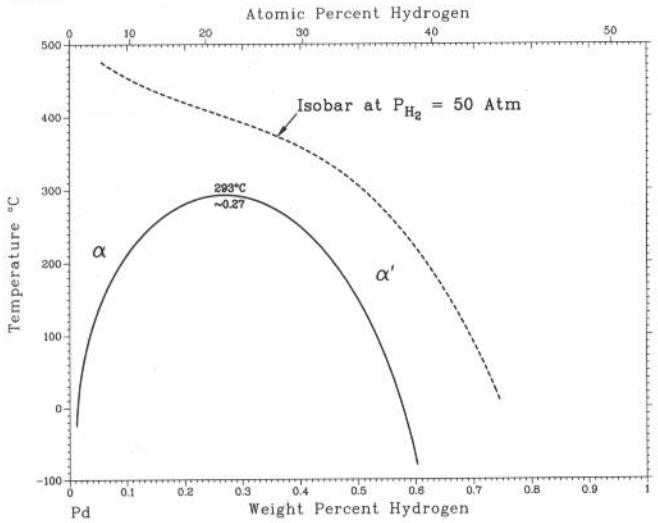

Phase	Composition, wt% H	Pearson symbol	Space group
(Pd)	0	*cF*4	$Fm\bar{3}m$
α or (Pd)	0 to 0.019(a)	*cF*8	$Fm\bar{3}m$
α′ or (Pd)	~0.567(a)	(b)	...
Low-temperature phases(c)			
A_2B_2	0.601	...	$I4_1/amd$
A_4B	0.715	*tI*10	$I4/m$

(a) At 25 °C. (b) fcc. (c) Below 100 K

H-Sr

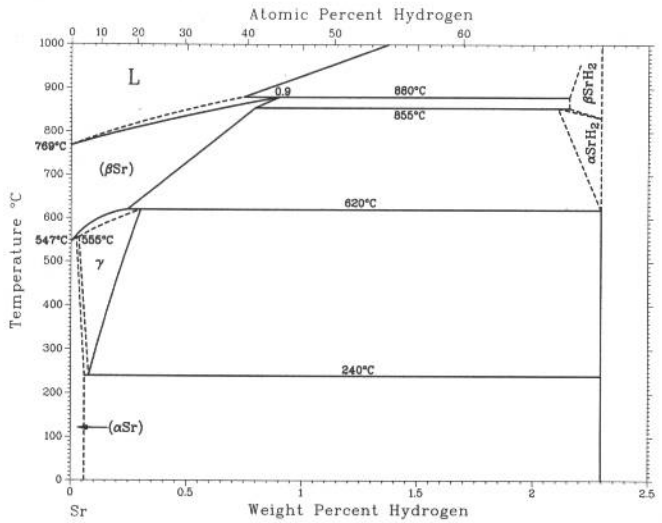

D.T. Peterson and R.P. Colburn, 1964

Phase	Composition, wt% H	Pearson symbol	Space group
(βSr)	0 to 0.9	*cI*2	$Im\bar{3}m$
(αSr)	0 to ?	*cF*4	$Fm\bar{3}m$
γ	? to 0.3	*hP**	...
βSrH_2	2.3	...	...
αSrH_2	2.3	*oP*12	*Pnma*

H-Ta

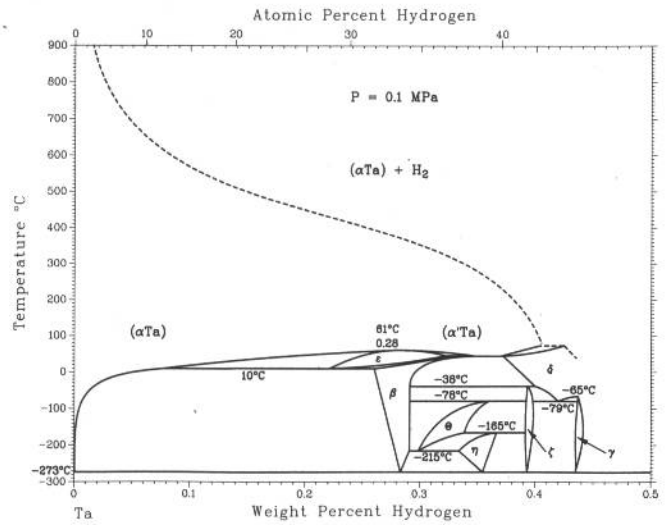

A.San-Martin and F.D. Manchester, 1991

Phase	Composition, wt% H	Pearson symbol	Space group
(αTa)	0 to 0.28	*cI*2	$Im\bar{3}m$
(α'Ta)	0.28 to 0.42	*cI*2	$Im\bar{3}m$
ε	0.22 to 0.32	*mC**	*C*222
β	0.26 to 0.35	*mC**	*C*222
θ	0.30 to 0.36	...	...
η	0.34 to ~0.37	...	...
δ	0.37 to 0.438	*oP**	*Pnnm*
ζ	0.395 to ~0.398	...	...
γ	0.436 to 0.439	...	...

H-Ti

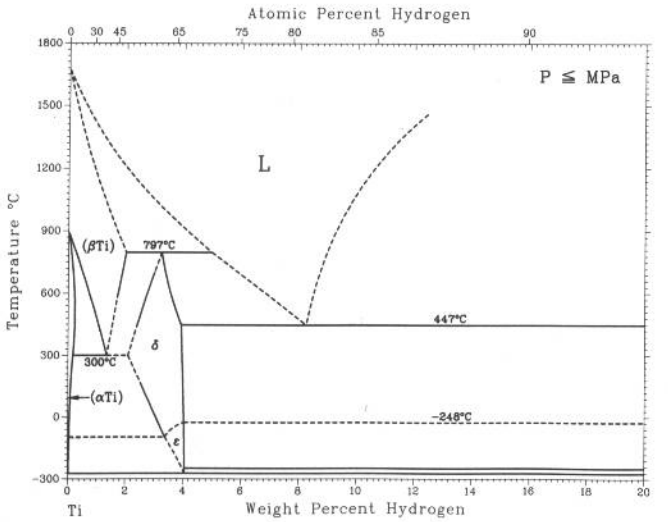

H. Okamoto, 1992

Phase	Composition, wt% H	Pearson symbol	Space group
(βTi)	0 to 2.06	*cI*2	$Im\bar{3}m$
(αTi)	0 to 0.2	*hP*2	$P6_3/mmc$
δ	2.06 to 4.05	*cF*12	$Fm\bar{3}m$
ε	3.06 to 4.05	*tI*6	*I*4/*mmm*

H-U

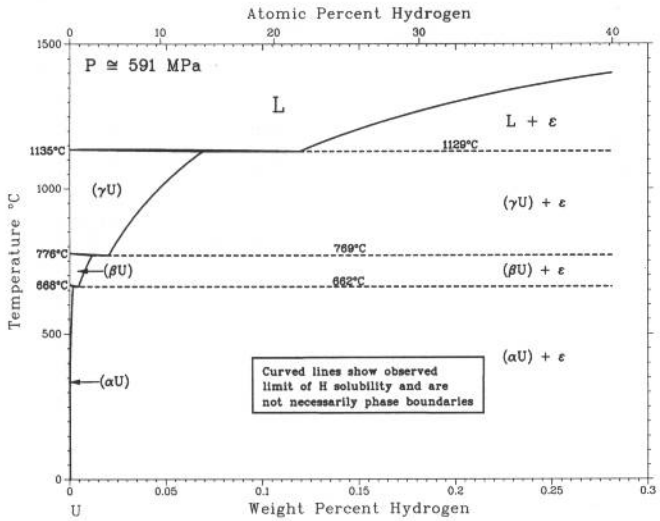

A. San-Martin and F.D. Manchester, unpublished

Phase	Composition, wt% H	Pearson symbol	Space group
(γU)	0 to 0.069	*cI*2	$Im\bar{3}m$
(βU)	0 to 0.011	*tP*30	$P4_2/mnm$
(αU)	0 to 0.0014	*oC*4	*Cmcm*
ε	1.25	*cP*32	*Pm*3*n*
δ(a)	1.25	*cP*8	*Pm*3*n*

(a) Metastable phase

H-V

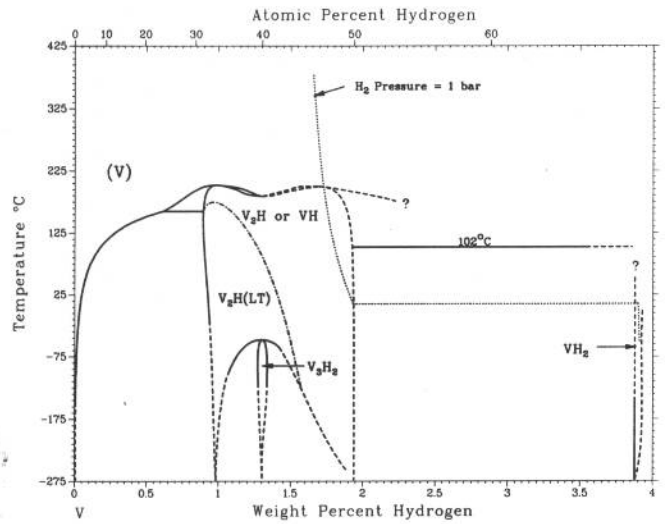

J.F. Smith and D.T. Peterson, 1989

Phase	Composition, wt% H	Pearson symbol	Space group
α or (V)	0 to ?	*cI*2	$Im\bar{3}m$
β_1 or V_2H(LT)	~0.97	*mC*6	*C*2/*m*
β_2 or V_2H or VH	~0.97 to 1.94	*tF*6, *tF*8?	...
δ or V_3H_2	~1.30	*mC*10	...
γ or VH_2	3.81	*cF*12	$Fm\bar{3}m$

H-Zr

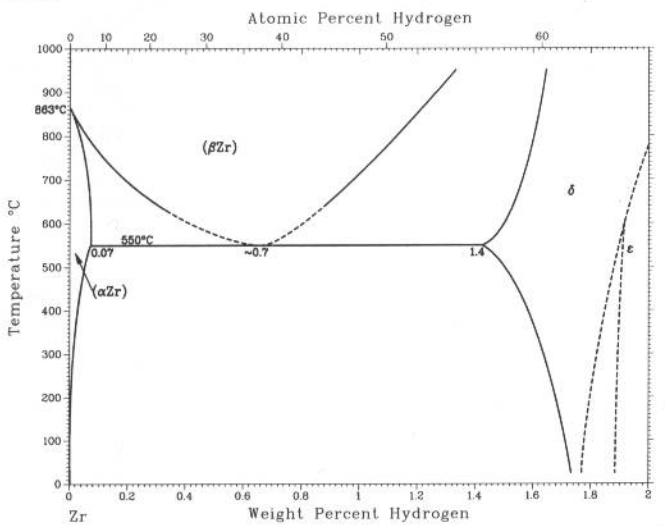

E. Zuzek, J.P. Abriata, A.San-Martin, and F.D. Manchester, 1990

Phase	Composition, wt% H	Pearson symbol	Space group
α or (αZr)	0 to 0.07	*hP*2	$P6_3/mmc$
β or (βZr)	0 to ~1.28?	*cI*2	$Im\bar{3}m$
δ	1.4 to ~2.1?	*cF*12	$Fm\bar{3}m$
ε	1.89	*tI*6	*I*4/*mmm*
Metastable phase			
γ	~0.011	*tP*6	$P4_2/n$

Hf-Ir

H. Okamoto, 1990

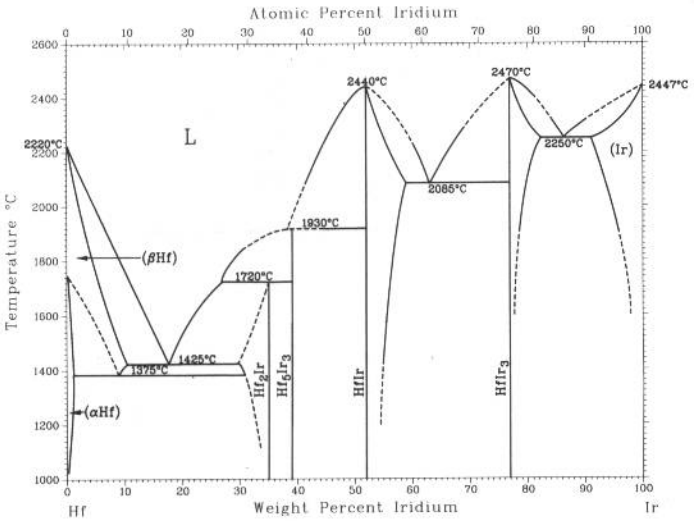

Phase	Composition, wt% Ir	Pearson symbol	Space group
(βHf)	0 to ~10.5	*cI*2	$Im\bar{3}m$
(αHf)	0 to ~ 1.5	*hP*2	$P6_3/mmc$
Hf_2Ir	~28 to 35.0	*cF*96	$Fd\bar{3}m$
Hf_5Ir_3	39.3	*hP*16	$P6_3/mcm$
HfIr	51.9 to 59	*o***	...
$HfIr_3$	76 to 82	*cP*4	$Pm\bar{3}m$
(Ir)	~91 to 100	*cF*4	$Fm\bar{3}m$

Hf-Mn

H. Okamoto, unpublished

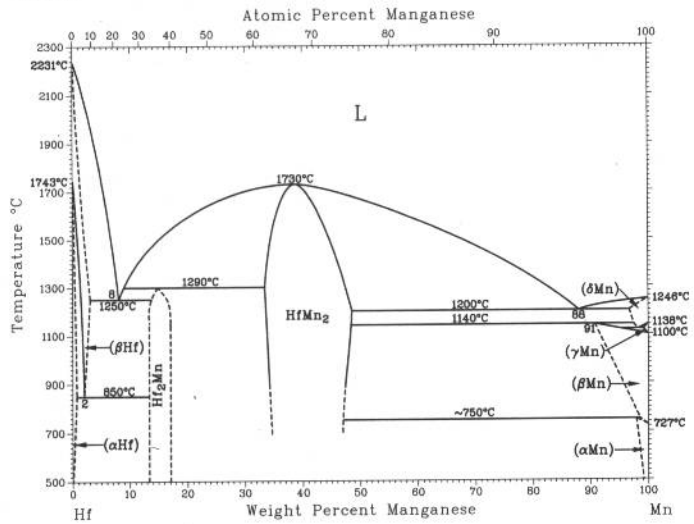

Phase	Composition, wt% Mn	Pearson symbol	Space group
(βHf)	0 to 3	*cI*2	$Im\bar{3}m$
(αHf)	0 to 0.62	*hP*2	$P6_3/mmc$
Hf_2Mn	13.3 to ?	*cF*96	$Fd\bar{3}m$
$\beta HfMn_2$	?	*hP*24	$P6_3/mmc$
$\alpha HfMn_2$	33 to 48.7	*hP*12	$P6_3/mmc$
(δMn)	97.4 to 100	*cI*2	$Im\bar{3}m$
(γMn	99.0 to 100	*cF*4	$Fm\bar{3}m$
(βMn)	91 to 100	*cP*20	$P4_132$
(αMn)	99.4 to 100	*cI*58	$I\bar{4}3m$

Hf-Mo

From [Molybdenum]

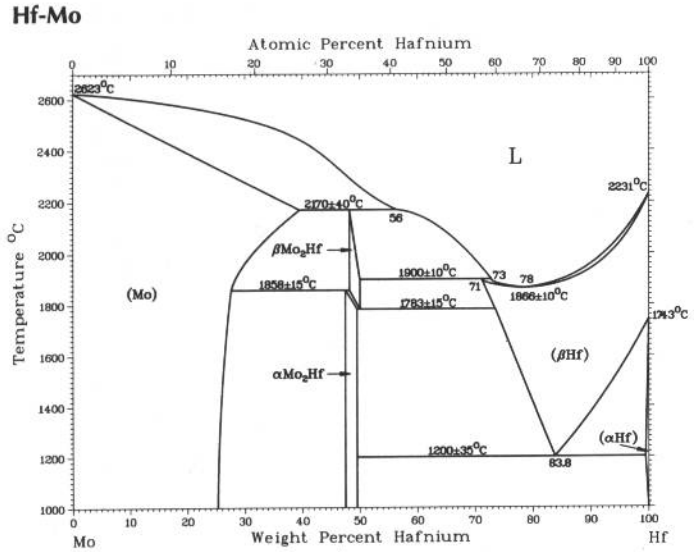

Phase	Composition, wt% Hf	Pearson symbol	Space group
(Mo)	0 to 38	*cI*2	$Im\bar{3}m$
βMo_2Hf	~48.2	*hP*24	$P6_3/mmc$
αMo_2Hf	~48.2	*cF*25	$Fd\bar{3}m$
(βHf)	71 to 100	*cI*2	$Im\bar{3}m$
(αHf)	~100	*hP*2	$P6_3/mmc$

Hf-N

H. Okamoto, 1990

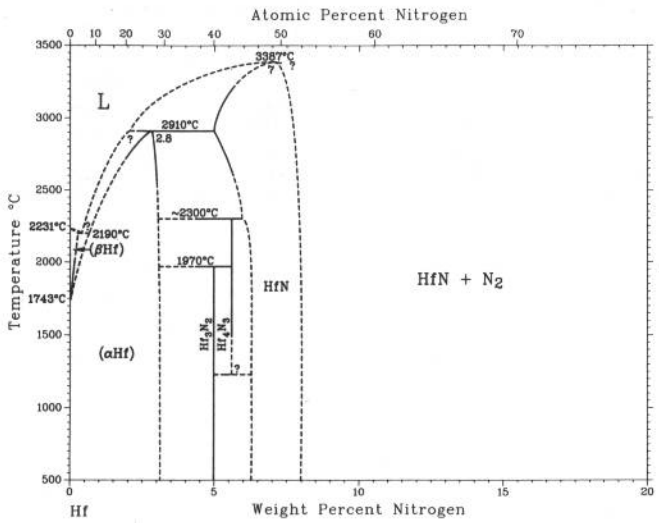

Phase	Composition, wt% N	Pearson symbol	Space group
(βHf)	0 to ?	*cI*2	$Im\bar{3}m$
(αHf)	0 to 3.1	*hP*2	$P6_3/mmc$
Hf_3N_2	4.97	*hR*6	$R\bar{3}m$
Hf_4N_3	5.57	*hR*8	$R\bar{3}m$
HfN	4.59 to 7.98	*cF*8	$Fm\bar{3}m$
(αN)	100	*cP*8	*Pa*3

Hf-Nb

H. Okamoto, 1991

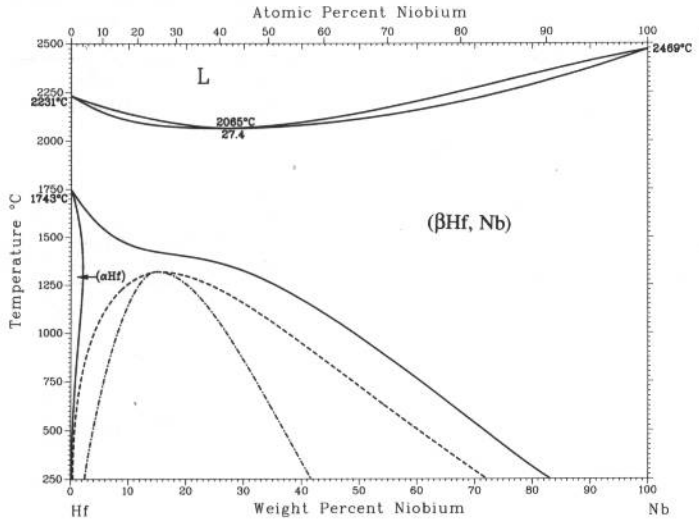

Phase	Composition, wt% Nb	Pearson symbol	Space group
(βHf,Nb)	0 to 100	*cI*2	$Im\bar{3}m$
(αHf)	0 to 2.4	*hP*2	$P6_3/mmc$

Hf-Ni

P. Nash and A. Nash, 1991

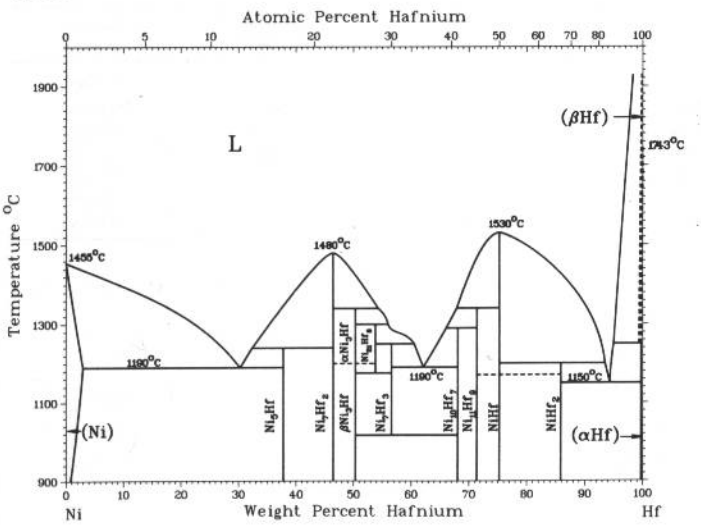

Phase	Composition, wt% Hf	Pearson symbol	Space group
(Ni)	0 to 3	*cF*4	$Fm\bar{3}m$
Ni_5Hf	37.9	*cF*24	$F\bar{4}3m$
Ni_7Hf_2	46.5	*m***	...
βNi_3Hf	50	*hP*40	$P6_3/mmc$
αNi_3Hf	50	*hR*12	$R\bar{3}m$
$Ni_{21}Hf_6$	53.7	*aP*29	$P\bar{1}$
Ni_7Hf_3	57	*aP*20	$P\bar{1}$
$Ni_{10}Hf_7$	68.1	*oC*68	*C*2*ca*
$Ni_{11}Hf_9$	71	*tI**	*I*4/*m*
NiHf	75.3	*oC*8	*Cmcm*
$NiHf_2$	85.9	*tI*12	*I*4/*mcm*
(βHf)	99.3 to 100	*cI*2	$Im\bar{3}m$
(αHf)	99.7 to 100	*hP*2	$P6_3/mmc$

Hf-O

From [Hafnium]

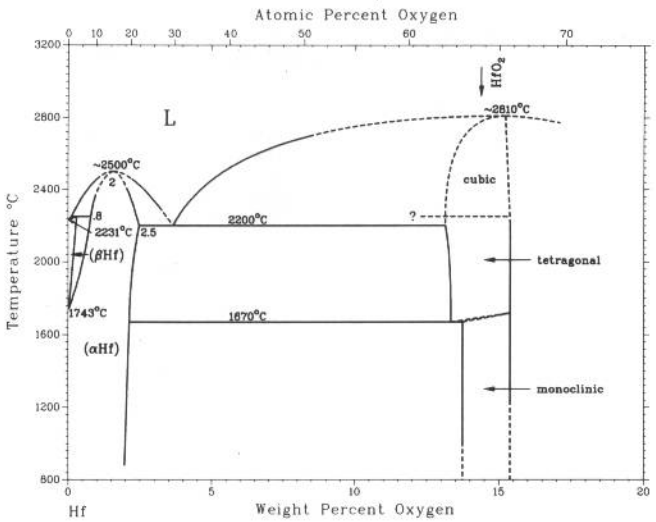

Phase	Composition, wt% O	Pearson symbol	Space group
(βHf)	0 to 0.8	*cI*2	$Im\bar{3}m$
(αHf)	0 to 2.5	*hP*2	$P6_3/mmc$
HfO_2	~13.2 to 15.4	*cF*12	$Fm\bar{3}m$
	~13.2 to 15.4	*t***	...
	~13.7 to 15.4	*mP*12	$P2_1/c$

Hf-Os

H. Okamoto, 1990

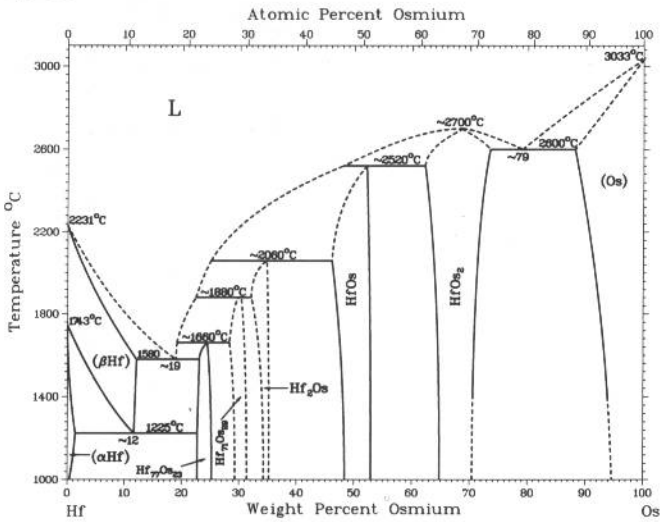

Phase	Composition, wt% Os	Pearson symbol	Space group
(βHf)	0 to 13	*cI*2	$Im\bar{3}m$
(αHf)	0 to 2	*hP*2	$P6_3/mmc$
θ	~24	...	...
ζ	~30	...	...
Hf_2Os	~35	...	...
HfOs	~47 to 54	*cP*2	$Pm\bar{3}m$
$HfOs_2$	~64 to 73	*cF*96	$Fd\bar{3}m$
		*hP*12	$P6_3/mmc$
(Os)	100	*hP*2	$P6_3/mmc$

Hf-Rh

H. Okamoto, 1990

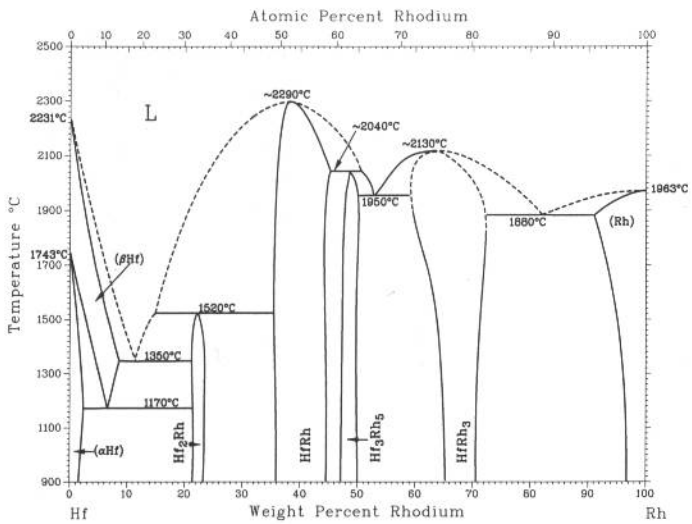

Phase	Composition, wt% Rh	Pearson symbol	Space group
(βHf)	0	*cI*2	$Im\bar{3}m$
(αHf)	0	*hP*2	$P6_3/mmc$
Hf_2Rh	22 to 23	*cF*96	$Fd\bar{3}m$
HfRh	36 to 44	*cP*2	$Pm\bar{3}m$
Hf_3Rh_5	47 to 51	*oP*16	*Pbam*
$HfRh_3$	59 to 72	*cP*4	$Pm\bar{3}m$
(Rh)	100	*cF*4	$Fm\bar{3}m$

Hf-Si

A.B. Gokhale and G.J. Abbaschian, 1989

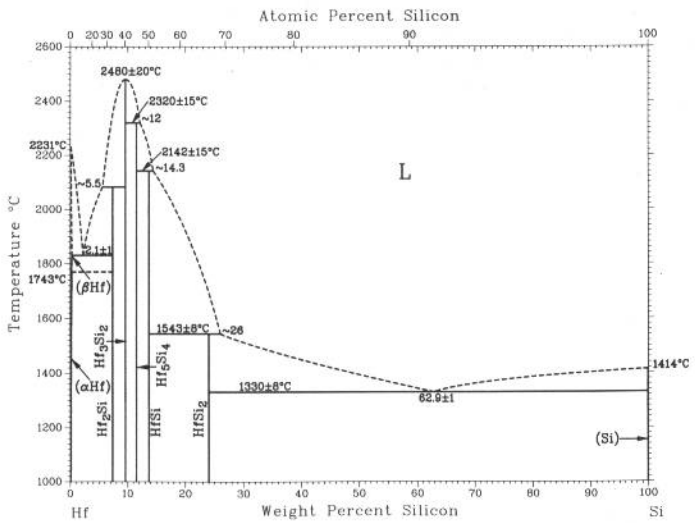

Phase	Composition, wt% Si	Pearson symbol	Space group
(αHf)	~0	*hP*2	$P6_3/mmc$
(βHf)	~0	*cI*2	$Im\bar{3}m$
Hf_2Si	7.3	*tI*12	*I*4/*mcm*
Hf_3Si_2	9	*tP*10	*P*4/*mbm*
Hf_5Si_4	11.2	...	$P4_12_12$
HfSi	13.6	*oP*8	*Pnma*
$HfSi_2$	24.0	*oC*12	*Cmcm*
(Si)	100	*cF*8	$Fd\bar{3}m$

Note: The presence of Mn_5Si_3-type ($D8_8$) Hf_5Si_3 has been reported. However, the phase occurs only in the presence of interstitial impurities.

Hf-Ta

R. Krishnan, S.P. Garg, and N. Krishnamurthy, 1989

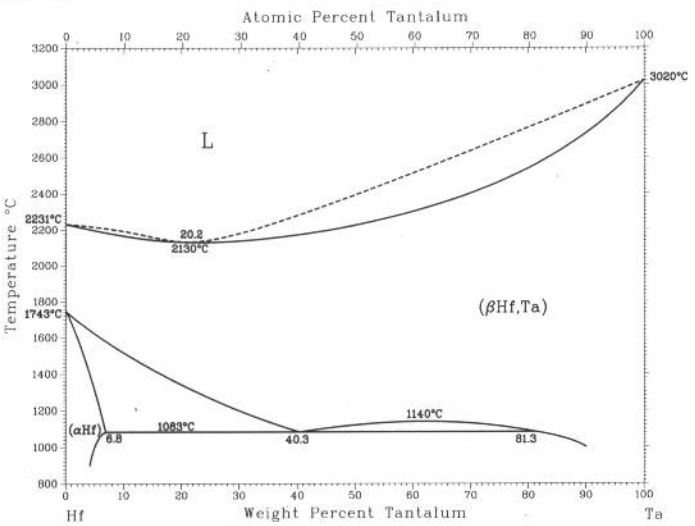

Phase	Composition, wt% Ta	Pearson symbol	Space group
(βHf,Ta)	0 to 100	*cI*2	$Im\bar{3}m$
(αHf)	0 to 6.8	*hP*2	$P6_3/mmc$

Hf-U

D.T. Peterson and D.J. Beerntsen, 1960

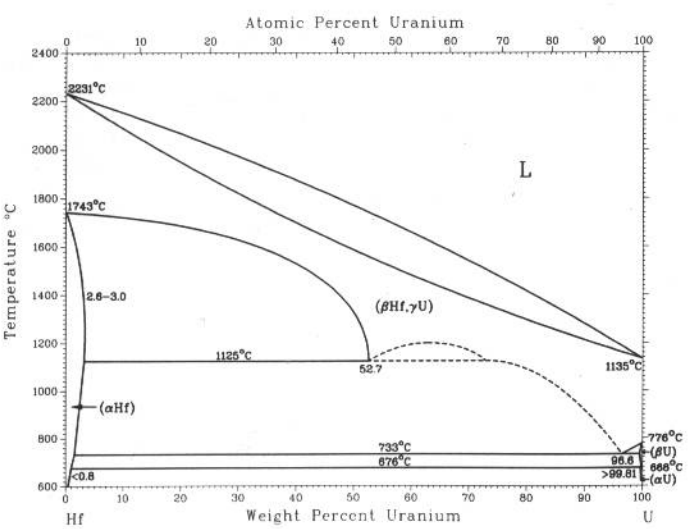

Phase	Composition, wt% U	Pearson symbol	Space group
(βHf,γU)	0 to 100	*cI*2	$Im\bar{3}m$
(αHf)	0 to ~3	*hP*2	$P6_3/mmc$
(βU)	100	*tP*30	$P4_2/mnm$
(αU)	100	*oC*4	*Cmcm*

Hf-V

J.F. Smith, 1989

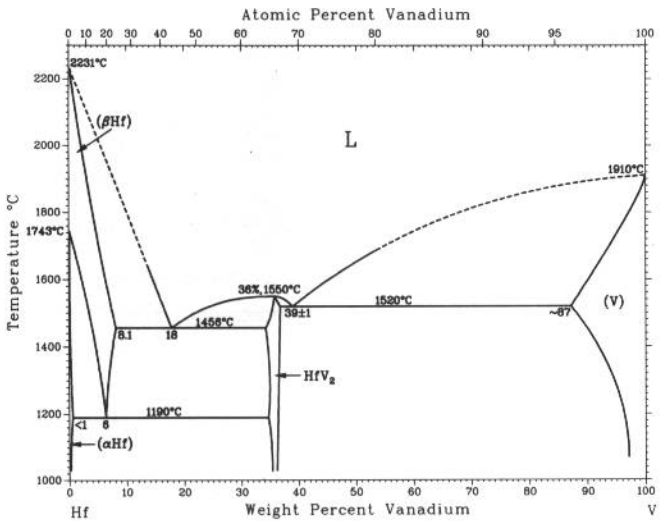

Phase	Composition, wt% V	Pearson symbol	Space group
(βHf)	0 to 8.1	*cI*2	$Im\bar{3}m$
(αHf)	0 to <1	*hP*2	$P6_3/mmc$
HfV_2	~36.4	*cF*24	$Fd\bar{3}m$
(V)	~87 to 100	*cI*2	$Im\bar{3}m$

Hf-W

S.V. Nagender Naidu and P. Rama Rao, 1991

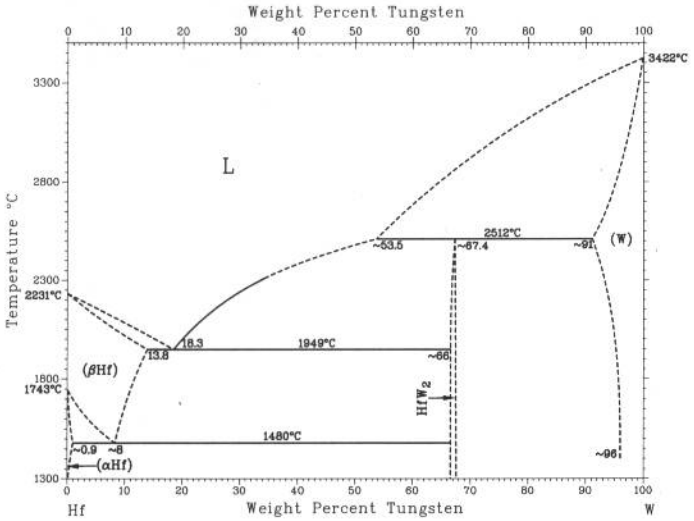

Phase	Composition, wt% W	Pearson symbol	Space group
(βHf)	0 to 13.8	*cI*2	$Im\bar{3}m$
(αHf)	0 to ~0.9	*hP*2	$P6_3/mmc$
HfW_2	~67.4	*cF*24	$Fd\bar{3}n$
(W)	~91 to 100	*cI*2	$Im\bar{3}m$

Hf-Zr

J.P. Abriata, J.C. Bolcich, and H.A. Peretti, 1982

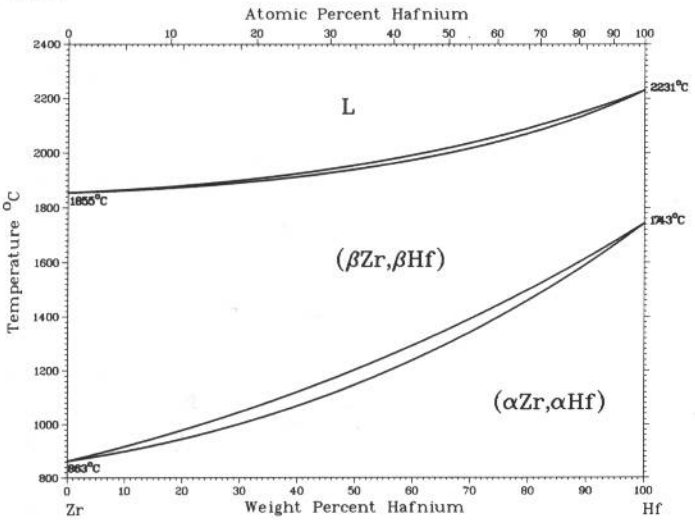

Phase	Composition, wt% Hf	Pearson symbol	Space group
(αZr,αHf)	0 to 100	*hP*2	$P6_3/mmc$
(βZr,βHf)	0 to 100	*cI*2	$Im\bar{3}m$
ω(a)	0 to 100	*hP*3	$P\bar{3}m1$ ($P6/mmm$?)

(a) Metastable at room temperature and zero pressure

Hg-In

H. Okamoto, 1992

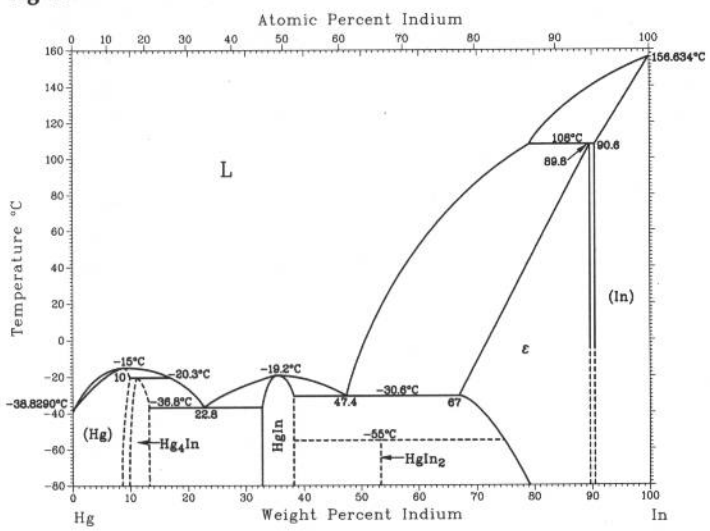

Phase	Composition, wt% In	Pearson symbol	Space group
(Hg)	0 to ~10	*hR*1	$R\bar{3}m$
Hg_4In	10 to 14	*oF*8	*Fddd*
HgIn	33 to 38	*hR*2	$R\bar{3}m$
$HgIn_2$	53.4	...	...
ε	67 to 89.8	*cF*4	$Fm\bar{3}m$
(In)	90.6 to 100	*tI*2	*I*4/*mmm*

Hg-K

A.E. Vol and I.K. Kagan, 1979

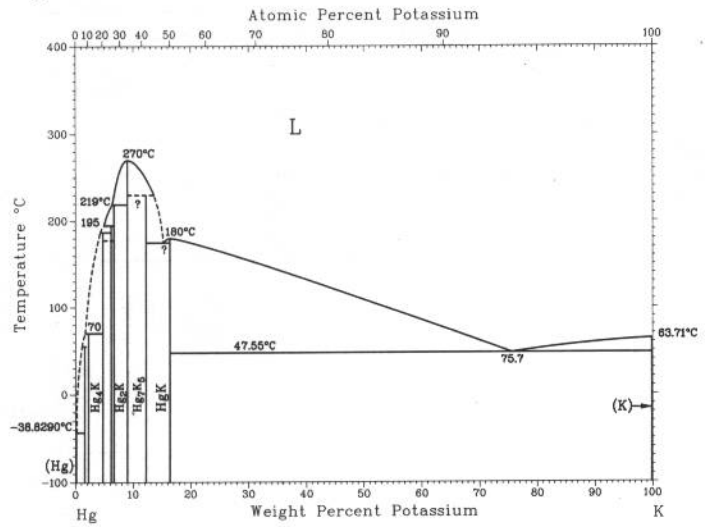

Phase	Composition, wt% K	Pearson symbol	Space group
(Hg)	0	*hR*1	$R\bar{3}m$
$Hg_{11}K$	1.7	*cP*36	$Pm\bar{3}m$
Hg_9K	2.1	...	...
Hg_4K	4.6	...	...
Hg_3K	6.1	...	...
$Hg_{2.7}K$	6.7	...	...
Hg_2K	8.9	*oI*12	*Imma*
Hg_7K_5	12.2	*oP*48	*Pbcm*
HgK	16.3	*aP*8	*P*1
(K)	100	*cI*2	$Im\bar{3}m$

Hg-La

C. Guminski, unpublished

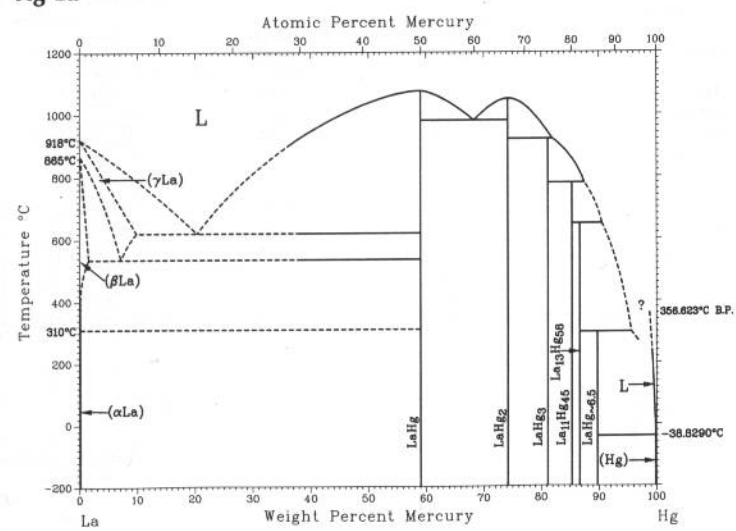

Phase	Composition, wt% Hg	Pearson symbol	Space group
(γLa)	0	*cI*2	$Im\bar{3}m$
(βLa)	0	*cF*4	$Fm\bar{3}m$
(αLa)	0	*hP*4	$P6_3/mmc$
LaHg	59.1	*cP*2	$Pm\bar{3}m$
$LaHg_2$	74.3	*hP*3	*P*6/*mmm*
$LaHg_3$	81	*hP*8	$P6_3/mmc$
$La_{11}Hg_{45}$	85.5	*cF*448	$F\bar{4}3m$
$La_{13}Hg_{58}$	87	*hP*142	$P6_3/mmc$
$LaHg_{\sim 6.5}$	91	*o***	*Cmcm* or *C*2*cm* or $Cmc2_1$
(Hg)	100	*hR*1	$R\bar{3}m$

Hg-Li

From [Hansen]

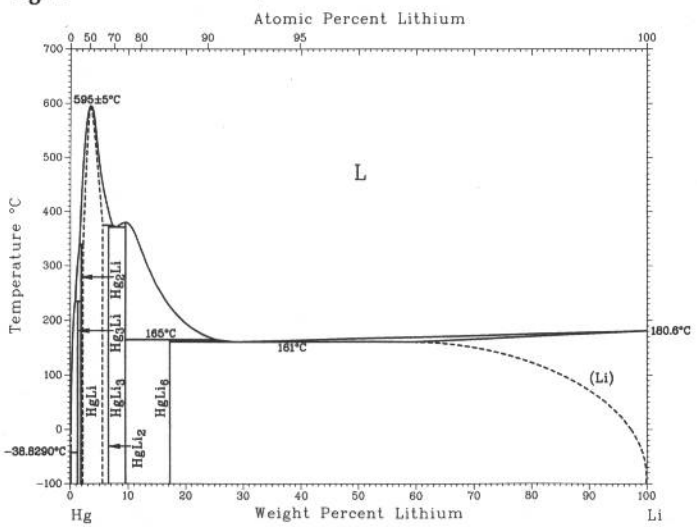

Phase	Composition, wt% Li	Pearson symbol	Space group
(Hg)	0	*hR*1	$R\bar{3}m$
Hg_3Li	1.1	*hP*8	$P6_3/mmc$
Hg_2Li	1.7	...	...
HgLi	~2.08 to 5.6	*cP*2	$Pm\bar{3}m$
$HgLi_2$	6.5	...	...
$HgLi_3$	9.4	*cF*16	$Fm\bar{3}m$
$HgLi_6$	17.2	...	...
(Li)	? to 100	*cI*2	$Im\bar{3}m$

Hg-Mg

A.A. Nayeb-Hashemi and J.B. Clark, 1988

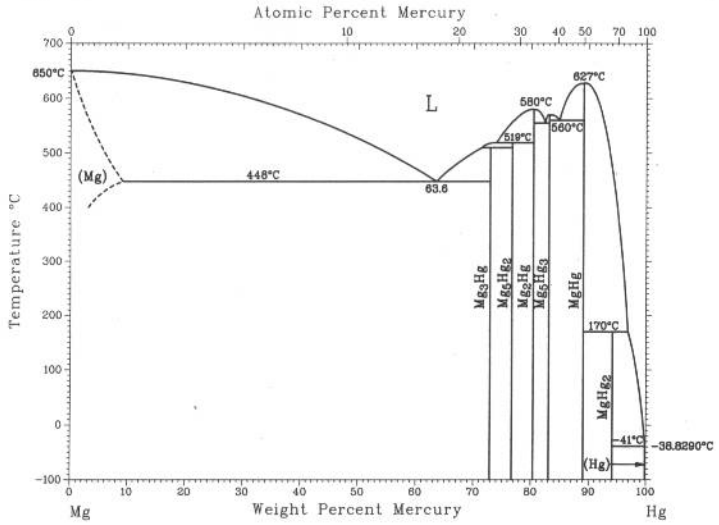

Phase	Composition, wt% Hg	Pearson symbol	Space group
(Mg)	0 to ~9.1	*hP*2	$P6_3/mmc$
Mg_3Hg	73	*hP*8	$P6_3/mmc$
Mg_5Hg_2	76.8	...	...
Mg_2Hg	80.5	...	...
Mg_5Hg_3	83.2	*hP*16	$P6_3/mmc$
MgHg	89.2	*cP*2	$Pm\bar{3}m$
$MgHg_2$	94.3	*tI*6	$I4/mmm$
(Hg)	100	*hR*1	$R\bar{3}m$

Hg-Na

H. Okamoto, 1990

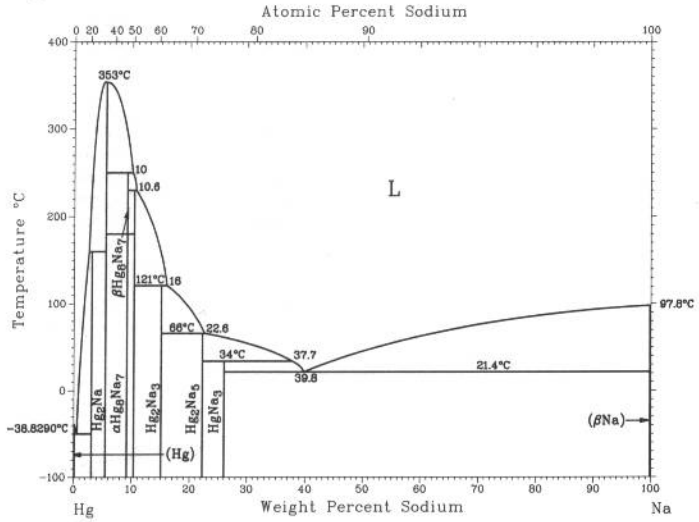

Phase	Composition, wt% Na	Pearson symbol	Space group
(Hg)	~0	*hR*1	$R\bar{3}m$
Hg_4Na	3	*h***	...
Hg_2Na	5.4	*hP*3	$P6/mmm$
βHg_8Na_7	~9.1	...	...
αHg_8Na_7	~9.1	...	...
HgNa	10.3	*oC*16	*Cmcm*
Hg_2Na_3	15	*tP*20	$P4_2/mnm$
Hg_2Na_5	~22.2	*hR**	...
$HgNa_3$	26	...	...
(βNa)	~100	*cI*2	$Im\bar{3}m$

Hg-Pb

From [Hansen]

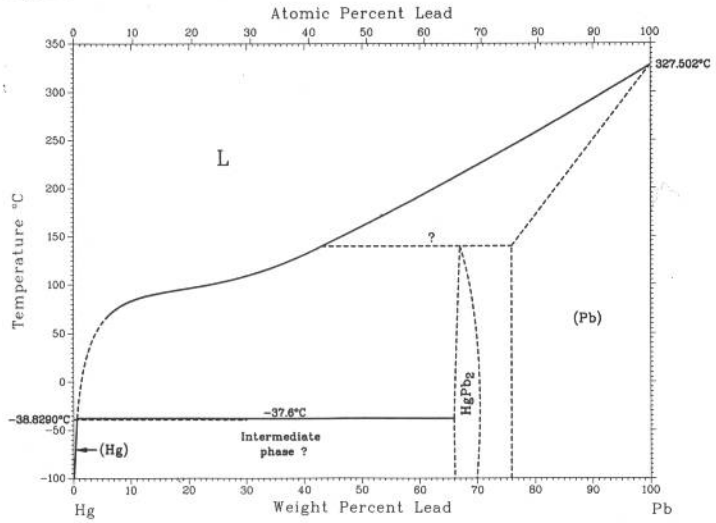

Phase	Composition, wt% Pb	Pearson symbol	Space group
(Hg)	0	*hR*1	$R\bar{3}m$
$HgPb_2$	~66 to ~71	*tP*2	$P4/mmm$
(Pb)	~76 to 100	*cF*4	$Fm\bar{3}m$

Hg-Rb

From [Hansen]

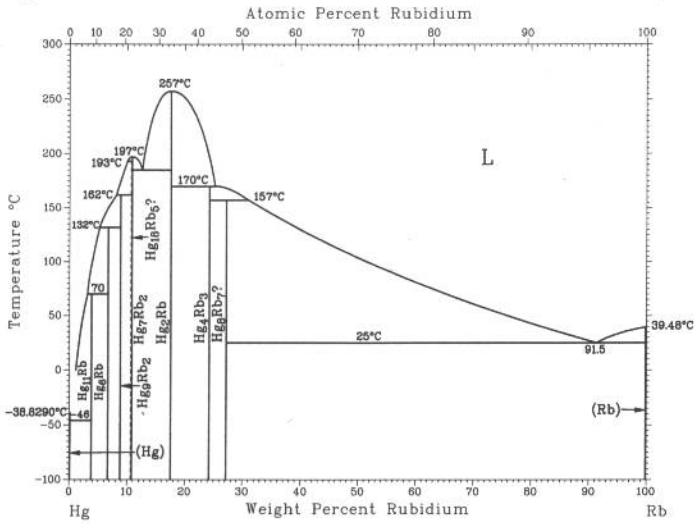

Phase	Composition, wt% Rb	Pearson symbol	Space group
(Hg)	0	*hR*1	$R\bar{3}m$
$Hg_{11}Rb$	3.7	*cP*36	$Pm\bar{3}m$
Hg_6Rb	6.6	...	...
Hg_9Rb_2	8.7	...	...
$Hg_{18}Rb_5$	10.6	...	...
Hg_7Rb_2	10.8	...	...
Hg_2Rb	17.5	...	...
Hg_4Rb_3	24.2	...	...
Hg_8Rb_7	27.2	...	...
(Rb)	100	*cI*2	$Im\bar{3}m$

Hg-S

R.C. Sharma, Y.A. Chang, and C. Guminski, 1992

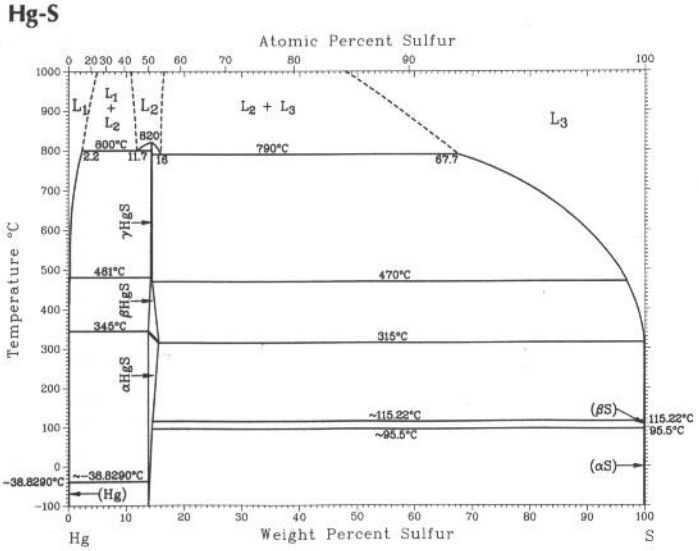

Phase	Composition, wt% S	Pearson symbol	Space group
Hg	0	*hR*1	$R\bar{3}m$
γHgS	14.19 to 14.47	(a)	...
βHgS	13.8 to 15.61	*cF*8	$F\bar{4}3m$
αHgS	13.8 to 15.5	*hP*6	$P3_121$
δHgS(b)	13.8	*cF*8	$Fm\bar{3}m$
(βS)(c)	100	*mP**	$P2_1/c$
(αS)(d)	100	*oF*128	*Fddd*

(a) Hexagonal. (b) Above 13 GPa. (c) From 95.5 to 115.22 °C. (d) At <95.5 °C

Hg-Se

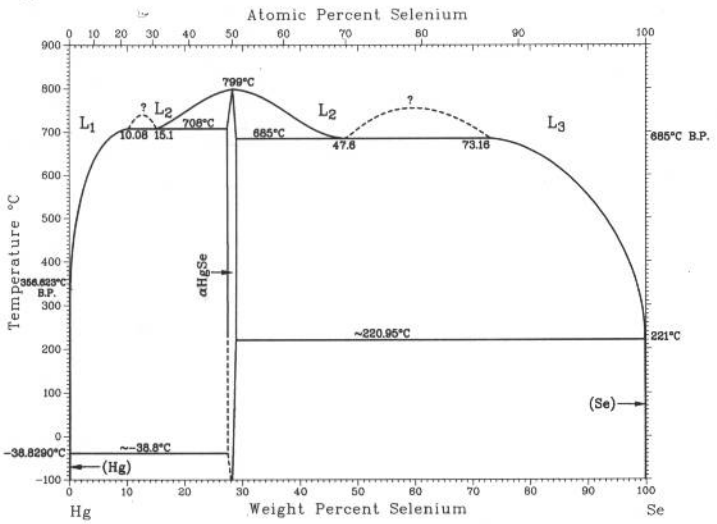

R.C. Sharma, Y.A. Chang, and C. Guminski, 1992

Phase	Composition, wt% Se	Pearson symbol	Space group
(Hg)	0	*hR*1	$R\bar{3}m$
αHgSe	27.3 to 28.86	*cF*8	$F\bar{4}3m$
(γSe)	100	*hP*3	$P3_121$
(βSe)	100	*mP*64	$P2_1/c$
(αSe)	100	*mP*32	$P2_1/n$
High-pressure phases			
βHgSe(a)	28.2	*hP*6	$P3_121$
γHgSe(b)	28.2	*cF*8	$Fm\bar{3}m$
δHgSe(c)	28.2	*tI*4	$I\bar{4}m2$

(a) Between 0.30 and ~7 GPa. (b) Between ~7 GPa and 13.3 GPa. (c) Above 13.3 GPa

Hg-Sn

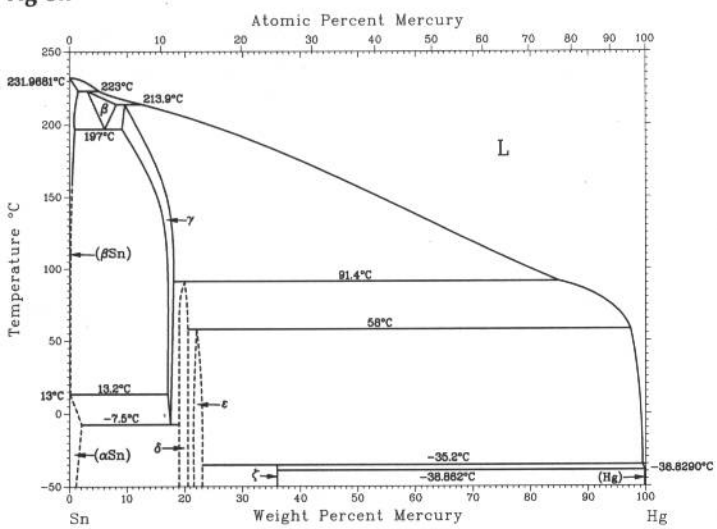

H. Okamoto, 1990

Phase	Composition, wt% Hg	Pearson symbol	Space group
(βSn)	0 to <0.8	*tI*4	$I4_1/amd$
(αSn)	0 to <2	*cF*8	$Fd\bar{3}m$
β	~3 to 8	*h***	...
γ	~10 to 19	*hP*2	$P6_3/mmc$
δ	~20	...	...
ε	~22 to 23	...	...
ζ	36	...	...
(Hg)	~100	*hR*1	$R\bar{3}m$

Hg-Sr

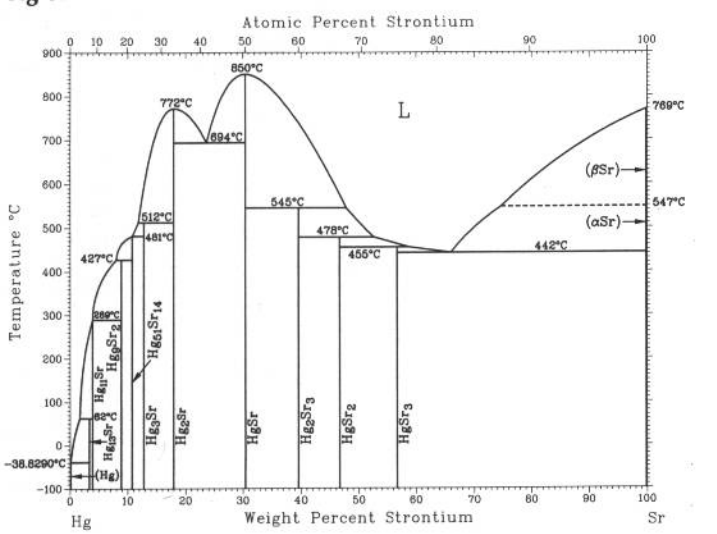

P.R. Subramanian, 1990

Phase	Composition, wt% Sr	Pearson symbol	Space group
(Hg)	0	*hR*1	$R\bar{3}m$
$Hg_{13}Sr$	~3.2	...	...
$Hg_{11}Sr$	~3.8	*cP*36	$Pm\bar{3}m$
Hg_9Sr_2	~8.8	*hP*142	$P6_3mc$
$Hg_{51}Sr_{14}$	~10.7	*hP*58	$P6/m$
Hg_3Sr	13	*hP*8	$P6_3/mmc$
Hg_2Sr	17.9	*oI*12	$Immc$
		*hP*3	$P6/mmm$
HgSr	30.4	*cP*2	$Pm\bar{3}m$
Hg_2Sr_3	40	*tP*10	$P4/mbm$
$HgSr_2$	46.7	...	...
$HgSr_3$	57	*oP*16	$Pnma$
(βSr)	100	*cI*2	$Im\bar{3}m$
(αSr)	100	*cF*4	$Fm\bar{3}m$

Hg-Te

R.C. Sharma and Y.A. Chang, unpublished

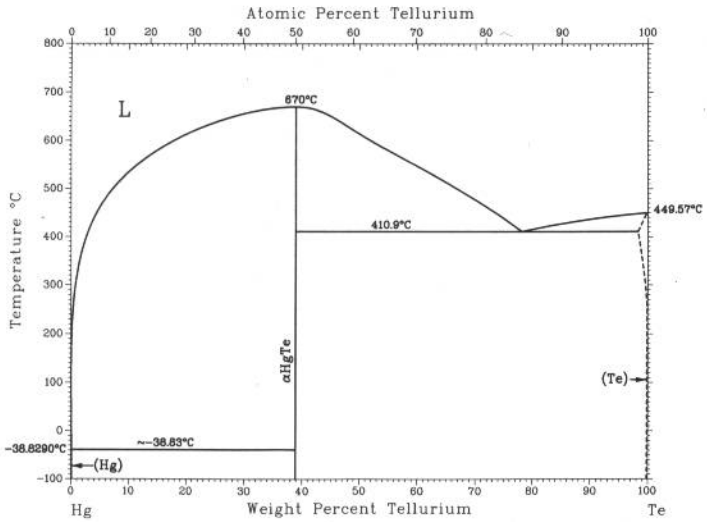

Phase	Composition, wt% Te	Pearson symbol	Space group
(Hg)	0	*hR*1	$R\bar{3}m$
αHgTe	30.9	*cF*8	$F\bar{4}3m$
βHgTe(a)	38.9	*hP*6	$P3_121$
(Te)	~98 to 100	*hP*3	$P3_121$

(a) High-pressure form

Hg-Tl

C. Guminski, unpublished

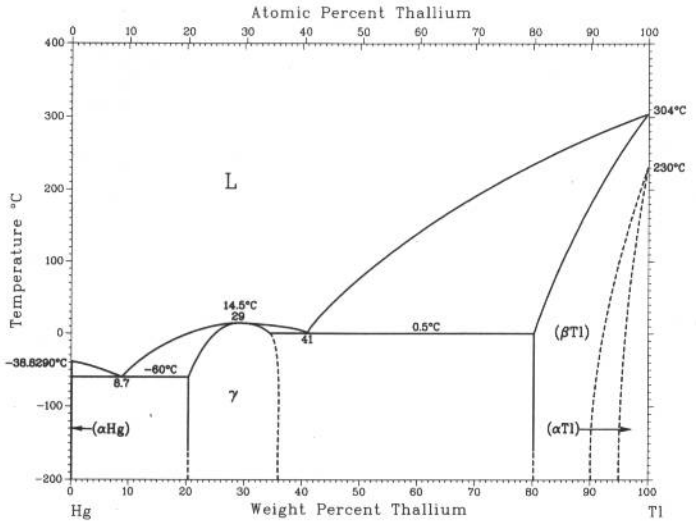

Phase	Composition, wt% Tl	Pearson symbol	Space group
(αHg)	0	*hR*1	$R\bar{3}m$
γ or Hg_5Tl_2	~29	*cF*4	$Fm\bar{3}m$
(βTl)	80 to 100	*cI*2	$Im\bar{3}m$
(αTl)	? to 100	*hP*2	$P6_3/mmc$

Hg-Zn

L.A. Zabdyr and C. Guminski, unpublished

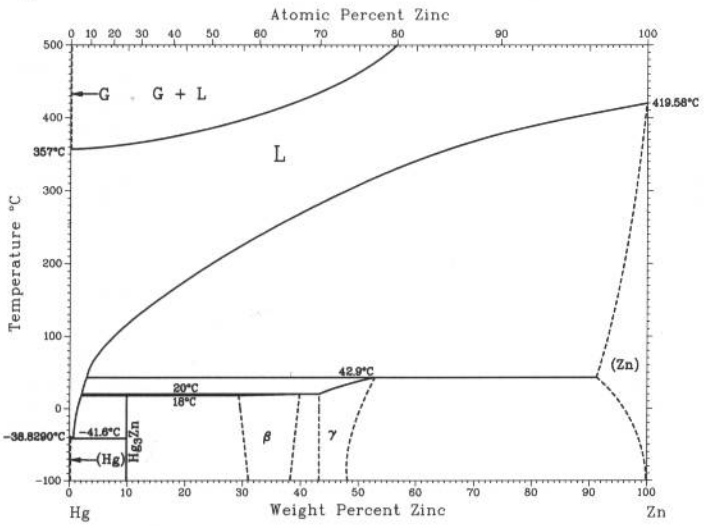

Phase	Composition, wt% Zn	Pearson symbol	Space group
(Hg)	0 to 0.1	*hR*1	$R\bar{3}m$
Hg_3Zn	10	...	...
β	~29 to ~40	...	...
γ(a)	~43 to ~52	*oC*4	$Cmc2_1$
(Zn)	~95.0 to 100	*hP*2	$P6_3/mmc$

(a) Possibly a hexagonal structure

Ho-In

H. Okamoto, 1992

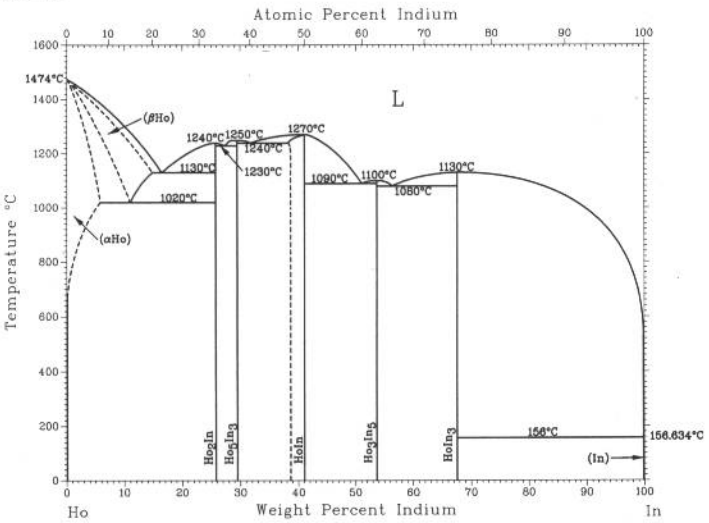

Phase	Composition, wt% In	Pearson symbol	Space group
(αHo)	0 to ~6	*hP*2	$P6_3/mmc$
(βHo)	0 to 15	*cI*2	$Im\bar{3}m$
Ho_2In	25.8	*hP*6	$P6_3/mmc$
βHo_5In_3	29.5	*hP*16	$P6_3/mcm$
αHo_5In_3	29.5	*tI*32	*I*4/*mcm*
HoIn	33 to 41.0	*cP*2	$Pm\bar{3}m$
		*t***	...
Ho_3In_5	53.7	*oC*32	*Cmcm*
$HoIn_3$	68	*cP*4	$Pm\bar{3}m$
(In)	100	*tI*2	*I*4/*mmm*

Ho-Mn

H.R. Kirchmayr and W. Lugscheider, 1967

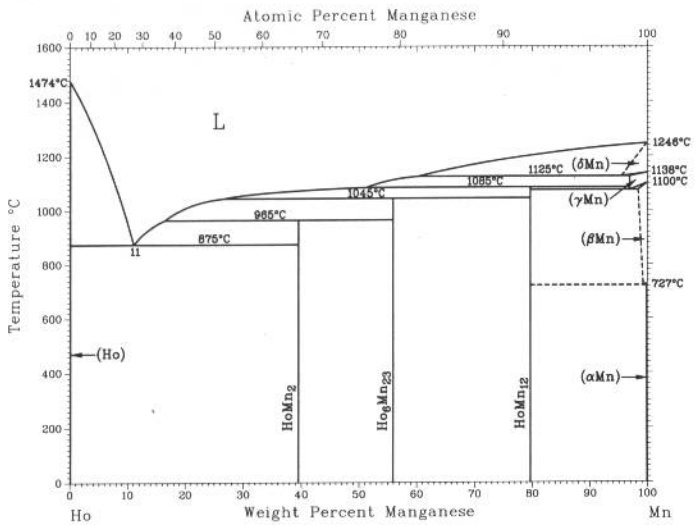

Phase	Composition, wt% Mn	Pearson symbol	Space group
(Ho)	~0	*hP*2	$P6_3/mmc$
$HoMn_2$	40.0	*cF*24	$Fd\bar{3}m$
Ho_6Mn_{23}	~56.1	*cF*116	$Fm\bar{3}m$
$HoMn_{12}$	~80.0	*tI*26	*I*4/*mmm*
(δMn)	~97 to 100	*cI*2	$Im\bar{3}m$
(γMn)	~97 to 100	*cF*4	$Fm\bar{3}m$
(βMn)	>97 to 100	*cP*20	$P4_132$
(αMn)	~100	*cI*58	$I4\bar{3}m$

Ho-Pd

H. Okamoto, 1991

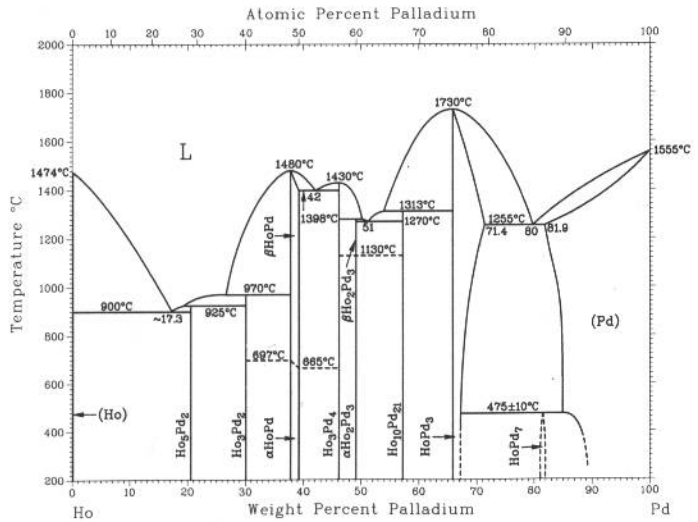

Phase	Composition, wt% Pd	Pearson symbol	Space group
(Ho)	0	*hP*2	$P6_3/mmc$
Ho_5Pd_2	20.5	*tI*49	$I4_1a$
Ho_3Pd_2	30	*tP*10	*P*4/*mbm*
βHoPd	~39.2	*cP*2	$Pm\bar{3}m$
αHoPd	~39.2	*oP*8	*Pnma*
Ho_3Pd_4	46.2	*hR*14	$R\bar{3}$
βHo_2Pd_3	49.2	...	...
αHo_2Pd_3	49.2	...	...
$Ho_{10}Pd_{21}$(a)	57.5	*mC*124	*C*2/*m*
$HoPd_3$	66 to 71.4	*cP*4	$Pm\bar{3}m$
$HoPd_7$	81.9	*c***	...
(Pd)	81.9 to 100	*cF*4	$Fm\bar{3}m$

(a) Similarity to $Sm_{10}Pd_{21}$ is assumed.

Ho-Sb

H. Okamoto, 1990

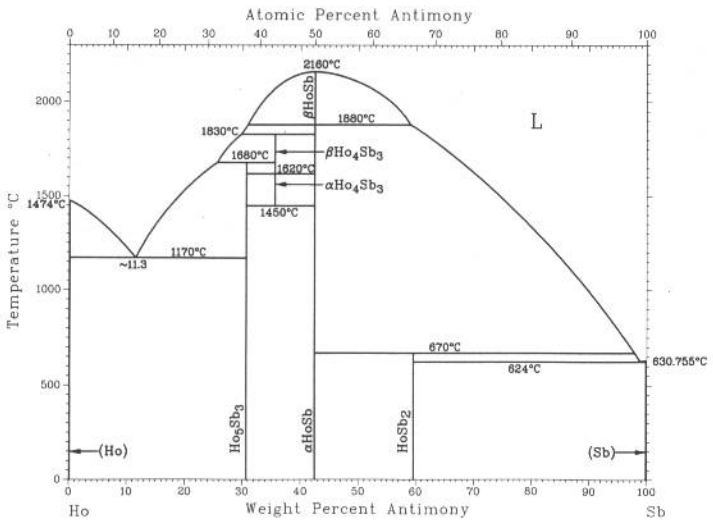

Phase	Composition, wt% Sb	Pearson symbol	Space group
(Ho)	0	*hP*2	$P6_3/mmc$
Ho_5Sb_3	30.7	*hP*16	$P6_3/mcm$
βHo_4Sb_3	35.7	...	...
αHo_4Sb_3	35.7	*cI*28	$I\bar{4}3d$
βHoSb	42.5	...	
αHoSb	42.5	*cF*8	$Fm\bar{3}m$
$HoSb_2$(a)	59.7	*oC*6	*C*222
(Sb)	100	*hR*2	$R\bar{3}m$

(a) Synthesized under high pressure

Ho-Te

E.I. Yarembash, E.S. Vigileva, A.A. Eliseev, A.V. Zachatskaya, T.G. Aminov, and M.A. Chernitsyna, 1974

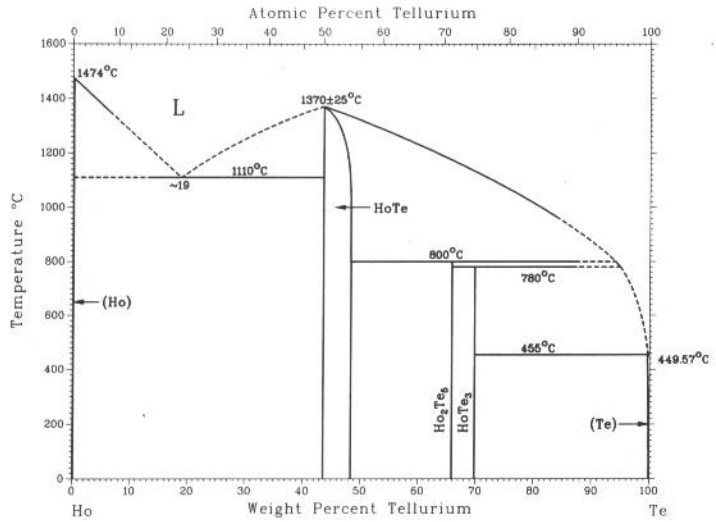

Phase	Composition, wt% Te	Pearson symbol	Space group
(Ho)	~0	*hP*2	$P6_3/mmc$
HoTe	44 to <49	*cF*8	$Fm\bar{3}m$
Ho_2Te_5	~65.9	*oC*28	*Cmcm*
$HoTe_3$	70	*oC*16	*Cmcm*
(Te)	~100	*hP*3	$P3_121$

Ho-Tl

S. Delfino, A. Saccone, A. Palenzona, and R. Ferro, unpublished

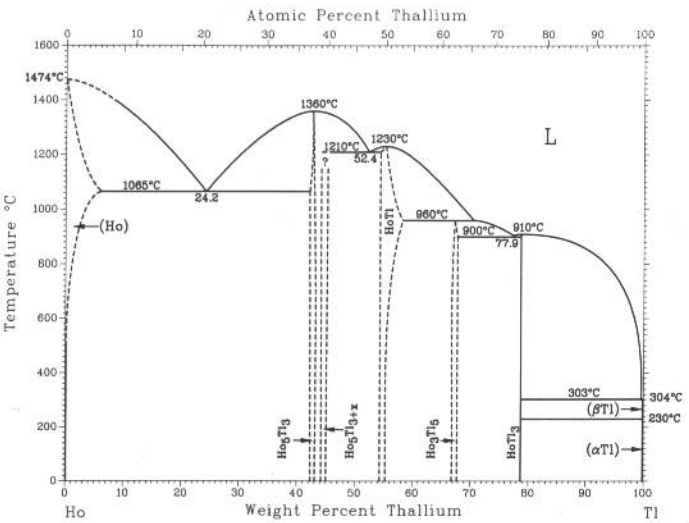

Phase	Composition, wt% Tl	Pearson symbol	Space group
(Ho)	0 to ~6	*hP*2	$P6_3/mmc$
Ho_5Tl_3	~42 to ~43	*hP*16	$P6_3/mcm$
Ho_5Tl_{3+x}	?	*tI*32	*I*4/*mcm*
HoTl(a)	~54 to ~58	*cP*2	$Pm\bar{3}m$
		(or *cI*2)	$Im\bar{3}m$
HoTl(b)	~54 to ~58	*tP*2	*P*4/*mmm*
Ho_3Tl_5	~67 to ~68	*oC*32	*Cmcm*
$HoTl_3$	79	*cP*4	$Pm\bar{3}m$
(βTl)	100	*cI*2	$Im\bar{3}m$
(αTl)	100	*hP*2	$P6_3/mmc$

(a) Cubic structure presumed to be room- and higher-temperature phase. (b) Tetragonal structure presumed to be lower-temperature phase

In-K

H. Okamoto, 1992

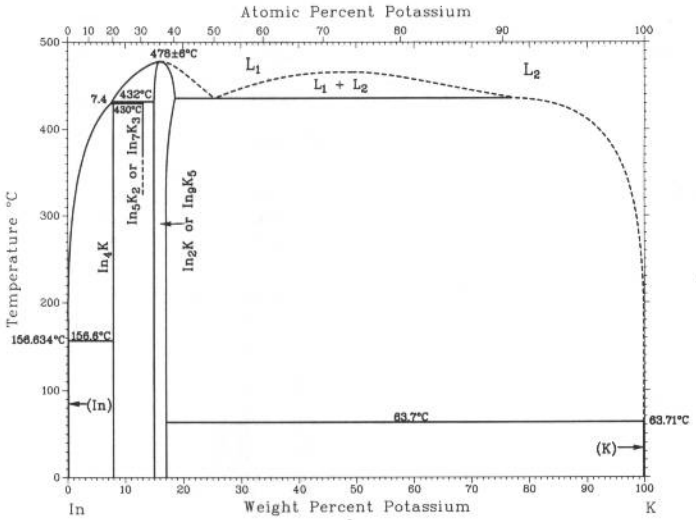

Phase	Composition, wt% K	Pearson symbol	Space group
(In)	0	*tI*2	*I*4/*mmm*
In_4K	8	*tI*10	*I*4/*mmm*
In_5K_2(a)	~13	...	...
In_2K(b)	14 to 19	...	...
(K)	100	*cI*2	$Im\bar{3}m$

(a) Or In_7K_3. (b) Or In_9K_5

In-La

A. Palenzona and S. Cirafici, 1992

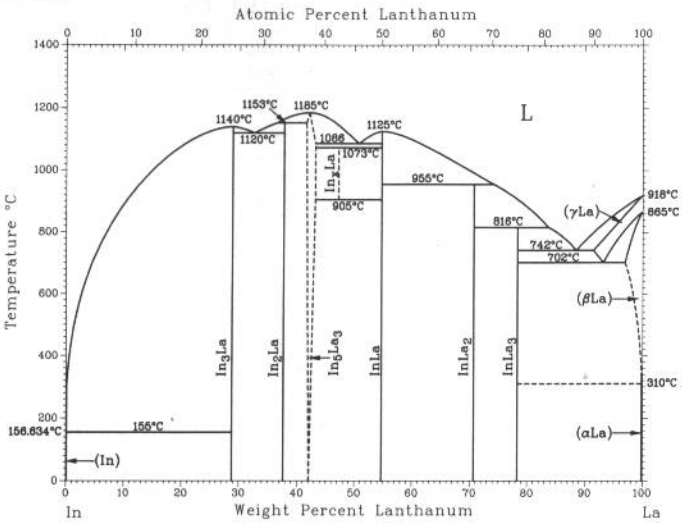

Phase	Composition, wt% La	Pearson symbol	Space group
(In)	0	*tI*2	*I*4/*mmm*
In_3La	29	*cP*4	$Pm\bar{3}m$
In_2La	37.7	*oI*12	*Imma*
In_5La_3	~42 to ~43.1	*oC*32	*Cmcm*
In_xLa	?	...	...
InLa	~54.7	*cP*2	$Pm\bar{3}m$
		...	*Pmmm*
$InLa_2$	70.8	*hP*6	$P6_3/mmc$
$InLa_3$	78	*cP*4	$Pm\bar{3}m$
(γLa)	91.4 to 100	*cI*2	$Im\bar{3}m$
(βLa)	97.1 to 100	*cF*4	$Fm\bar{3}m$
(αLa)	100	*hP*4	$P6_3/mmc$

In-Li

J. Sangster and A.D. Pelton, 1992

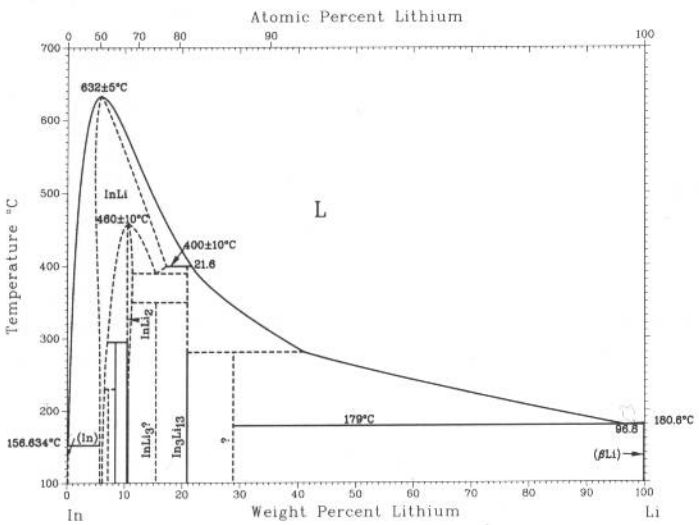

Phase	Composition, wt% Li	Pearson symbol	Space group
(In)	0 to 0.1	*tI*2	*I*4/*mmm*
InLi	5 to 9(a)	*cF*16	$Fd\bar{3}m$
In_4Li_5	~7.0	*hP*9	$P\bar{3}m1$
In_2Li_3	8	*hR*5	$R\bar{3}m$
$InLi_2$	10.3 to 11.2	*oC*12	*Cmcm*
In_3Li_{13}	20.8	*cF*128	$Fd\bar{3}m$
(αLi)(b)	100	*hP*2	$P6_3/mmc$
(βLi)	100	*cI*2	$Im\bar{3}m$

(a) At 415 °C. (b) Below −193 °C

In-Lu

H. Okamoto, 1992

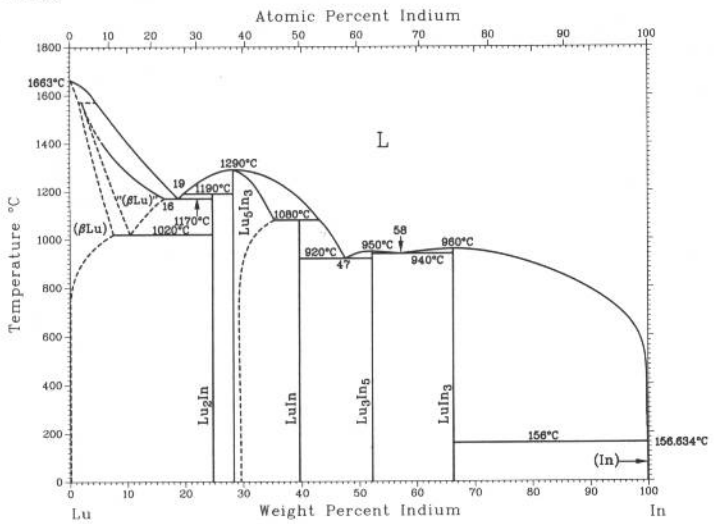

Phase	Composition, wt% In	Pearson symbol	Space group
(Lu)	0 to ?	*cI*2	$Im\bar{3}m$
Lu_2In	24.7	*hP*6	$P6_3/mmc$
Lu_5In_5	28.3 to 35	*hP*16	$P6_3/mcm$
LuIn	39.6	*cP*2	$Pm\bar{3}m$
Lu_3In_5	52.2	*oC*32	*Cmcm*
$LuIn_3$	66	*cP*4	$Pm\bar{3}m$
(In)	100	*tI*2	*I*4/*mmm*

In-Mg

A.A. Nayeb-Hashemi and J.B. Clark, 1992

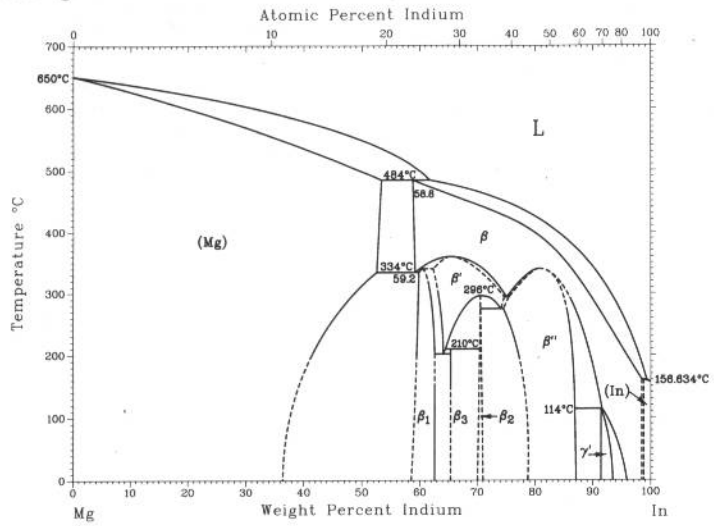

Phase	Composition, wt% In	Pearson symbol	Space group
(Mg)	0 to 53.2	*hP*2	$P6_3/mmc$
β	58.8 to 98.5	*cF*4	$Fm\bar{3}m$
β′	~62 to 74.7	*cP*4	$Pm\bar{3}m$
β_1(a)	~58.5 to 62	*hR*16	$R\bar{3}m$
β_3	65.4	*oI*28	*Ibam*
β_2	~71	*hP*9	$P\bar{6}2m$
β″	~75 to 87	*tP*2	*P*4/*mmm*
γ′	~91.5 to 93.6	*cP*4	$Pm\bar{3}m$
(In)	99 to 100	*tI*2	*I*4/*mmm*

(a) At high temperatures, β_1 has a cubic structure, space group $Pm\bar{3}m$, Pearson symbol *cP*4.

In-Mn

H. Okamoto, 1992

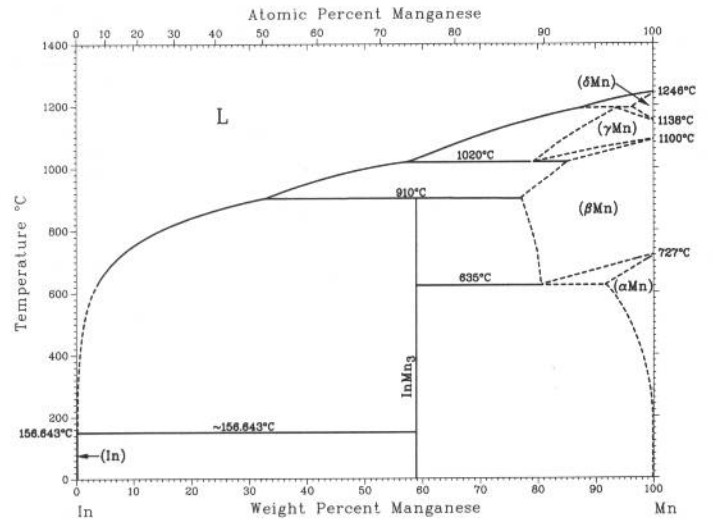

Phase	Composition, wt% Mn	Pearson symbol	Space group
(In)	0	*tI*2	*I*4/*mmm*
$InMn_3$	59 ± ?	*cP*52	$P\bar{4}3m$
(δMn)	? to 100	*cI*2	$Im\bar{3}m$
(γMn)	? to 100	*cF*4	$Fm\bar{3}m$
(βMn)	? to 100	*cP*20	$P4_132$
(αMn)	? to 100	*cI*58	$I\bar{4}3m$
Metastable phase			
...	75	*cI*2	$Im\bar{3}m$

In-Na

S. Larose and A.D. Pelton, 1992

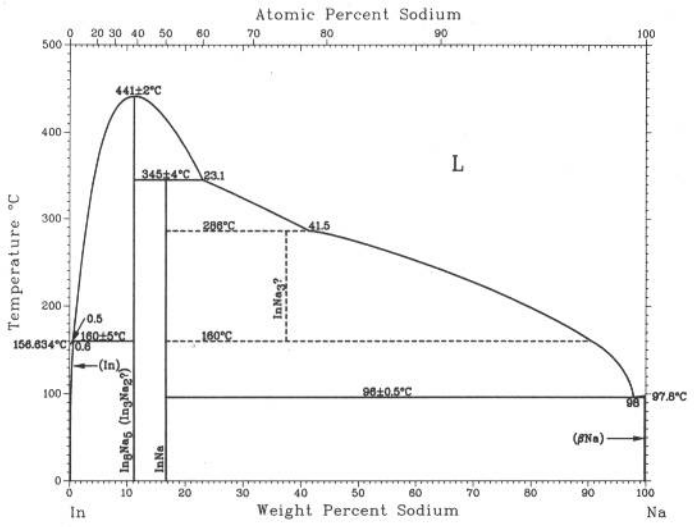

Phase	Composition, wt% Na	Pearson symbol	Space group
(In)	0 to 0.6	*tI*2	*I*4/*mmm*
In_8Na_5(b)	11.1	...	...
InNa	16.7	*cF*16	$Fd\bar{3}m$
$InNa_3$(b)	...	...	...
(βNa)	100	*cI*2	$Im\bar{3}m$
(αNa)	100	*hP*2	$P6_3/mmc$

(a) At 160 °C. (b) Stoichiometry uncertain

In-Nb

H. Okamoto, 1992

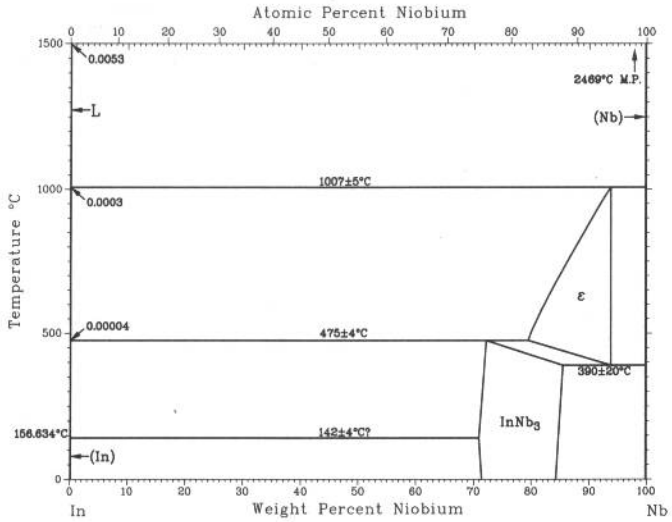

Phase	Composition, wt% Nb	Pearson symbol	Space group
(In)	0	*tI*2	*I*4/*mmm*
$InNb_3$	71 to 86	*cP*8	$Pm\bar{3}n$
ε	79 to 94	...	...
(Nb)	100	*cI*2	$Im\bar{3}m$

In-Nd

H. Okamoto, 1992

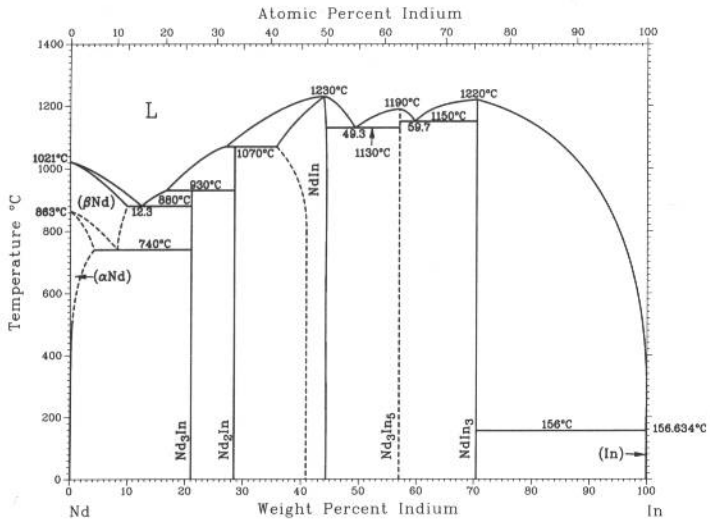

Phase	Composition, wt% In	Pearson symbol	Space group
(βNd)	0 to 10	*cI*2	$Im\bar{3}m$
(αNd)	0 to 4	*hP*4	$P6_3/mmc$
Nd_3In	21	*cP*4	$Pm\bar{3}m$
Nd_2In	28.4	*hP*6	$P6_3/mmc$
NdIn	36 to 44.3	*cP*2	$Pm\bar{3}m$
Nd_3In_5	57.0	*oC*32	*Cmcm*
$NdIn_3$	71	*cP*4	$Pm\bar{3}m$
(In)	100	*tI*2	*I*4/*mmm*

In-Ni

M.F. Singleton and P. Nash, 1992

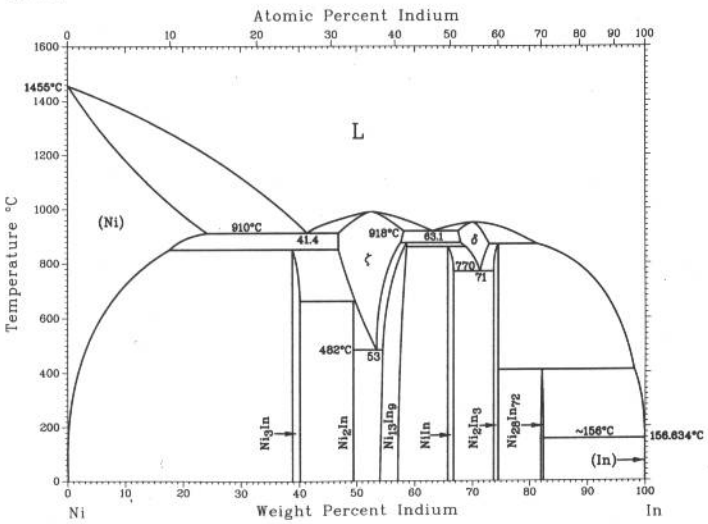

Phase	Composition, wt% In	Pearson symbol	Space group
(Ni)	0 to 24.9	*cF*4	$Fm\bar{3}m$
Ni_3In	38.8 to 40.1	*hP*8	$P6_3/mmc$
$\eta(Ni_2In)$	49.4	*hP*6	$P6_3/mmc$
ζ	47 to 58.1	*hP*4	$P6_3/mmc$
$\zeta'(Ni_{13}In_9)$	55.1 to 58.8	...	...
ε(NiIn)	65.7 to 66.6	*hP*6	*P6/mmm*
δ(NiIn)	67.5 to 73	*cP*2	$Pm\bar{3}m$
Ni_2In_3	74 to 75	*hP*5	$P\bar{3}m1$
$Ni_{28}In_{72}$	82 to 82.4	...	...
(In)	~100	*tI*2	*I4/mmm*
Metastable phase			
ε'	27.7 to 40	*cI*2	$Im\bar{3}m$

In-P

H. Okamoto, 1992

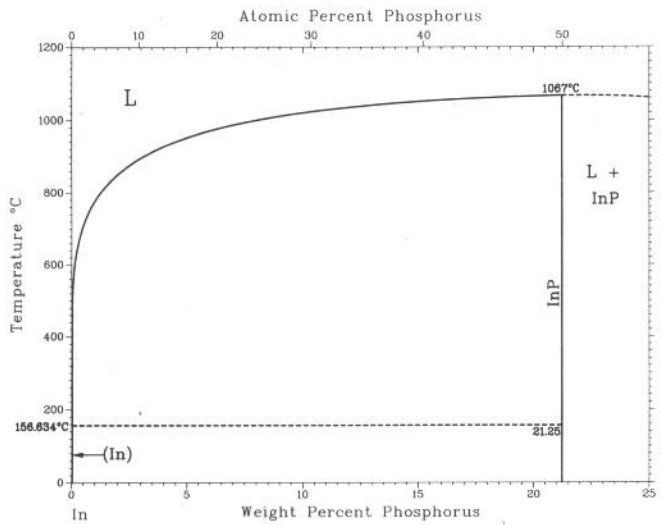

Phase	Composition, wt% P	Pearson symbol	Space group
Stable phases			
(In)	0	*tI*2	*I4/mmm*
InP	21.2	*cF*8	$F\bar{4}3m$
High-pressure phases			
InP II(a)	21.2	*cF*8	$Fm\bar{3}m$
InP III(b)	21.2	*tI*4	*I4/amd*
InP_3	45	*hR*8	$R\bar{3}m$

(a) 10.8 to 18.9 GPa. (b) >18.9 GPa

In-Pb

J.P. Nabot and I. Ansara, 1992

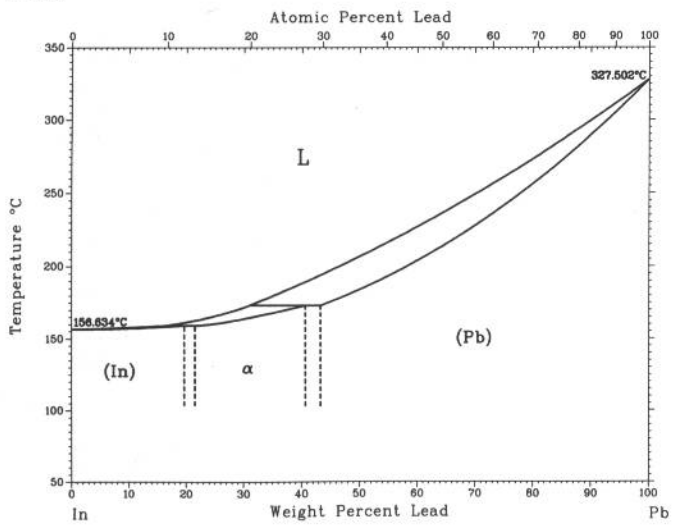

Phase	Composition, wt% Pb	Pearson symbol	Space group
(In)	0 to ?	*tI*2	*I4/mmm*
α	~24 to ~44	*tI*2	*I4/mmm*
(Pb)	? to 100	*cF*4	$Fm\bar{3}m$

In-Pd

H. Okamoto, 1992

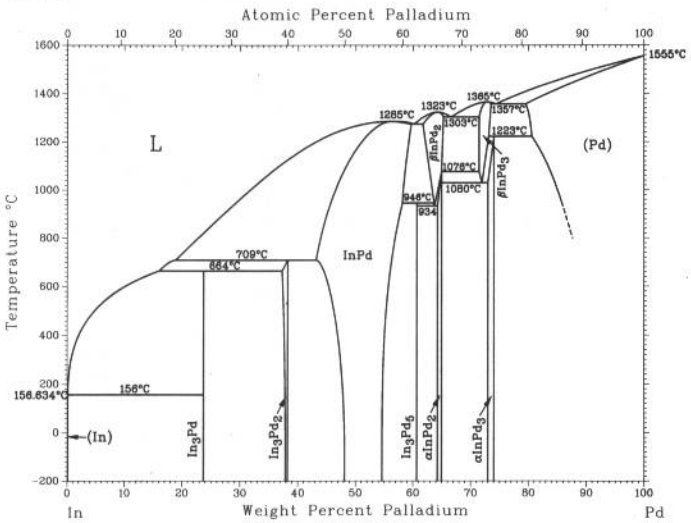

Phase	Composition, wt% Pd	Pearson symbol	Space group
(In)	0	*tI*2	*I*4/*mmm*
In_3Pd	24	*c**52	...
In_3Pd_2	37 to 38	*hP*5	$P\bar{3}m1$
InPd	43 to 59.7	*cP*2	$Pm\bar{3}m$
In_3Pd_5	60.7	*oP*16	*Pbam*
$\beta InPd_2$	61.7 to 65.5	...	...
$\alpha InPd_2$	64 to 65.0	*oP*12	*Pnma*
$\beta InPd_3$	72 to 74	...	...
$\alpha InPd_3$	73.0 to 74.1	*tI*8	*I*4/*mmm*
(Pd)	80 to 100	*cF*4	$Fm\bar{3}m$

In-Pr

H. Okamoto, 1992

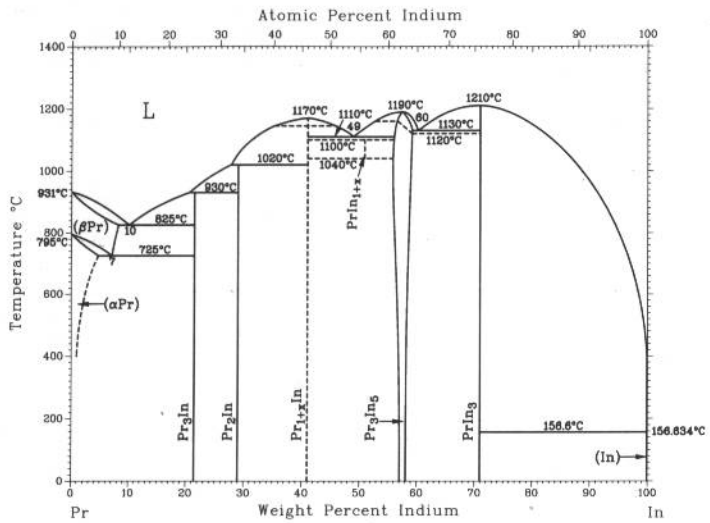

Phase	Composition, wt% In	Pearson symbol	Space group
(βPr)	0 to 8.1	*cI*2	$Im\bar{3}m$
(αPr)	0 to 4.6	*hP*4	$P6_3/mmc$
Pr_3In	21	*cP*4	$Pm\bar{3}m$
Pr_2In	28.9	*hP*6	$P6_3/mmc$
$\beta Pr_{1+x}In$	~41	...	...
$\alpha Pr_{1+x}In$	41	...	...
PrIn(a)	44.9	*cP*2	$Pm\bar{3}m$
$PrIn_{1+x}$	?	...	...
Pr_3In_5	56 to 59	*oC*32	*Cmcm*
$PrIn_3$	70	*cP*4	$Pm\bar{3}m$
(In)	100	*tI*2	*I*4/*mmm*

(a) Metastable or same as $PrIn_{1+x}$?

In-Pt

H. Okamoto, 1992

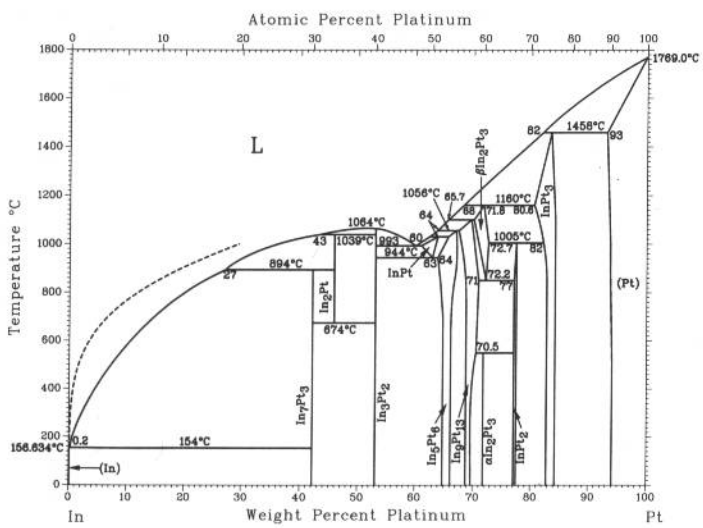

Phase	Composition, wt% Pt	Pearson symbol	Space group
(In)	0	*tI*2	*I*4/*mmm*
In_7Pt_3	42	*cI*40	$Im\bar{3}m$
In_2Pt	45.9	*cF*12	$Fm\bar{3}m$
In_3Pt_2	53	*hP*5	$P\bar{3}m1$
InPt	61 to 64	...	...
In_5Pt_6(a)	64 to 67.1	*mC*20	*C*2/*m*
In_9Pt_{13}	68 to 71	*mC*44	*C*2/*m*
βIn_2Pt_3	70 to 72.7	*hP*4	$P6_3/mmc$
αIn_2Pt_3	72	*hP*20	$P\bar{3}1c$
$InPt_2$	77.1 to 78	*oC*16	*Cmmm*
$InPt_3$	80.6 to 84.3	*cP*4	$Pm\bar{3}m$
$InPt_3$	83.6	*tP*4	*P*4/*mmm*
(Pt)	93 to 100	*cF*4	$Fm\bar{3}m$

(a) $InPt_{1+}$

In-Pu

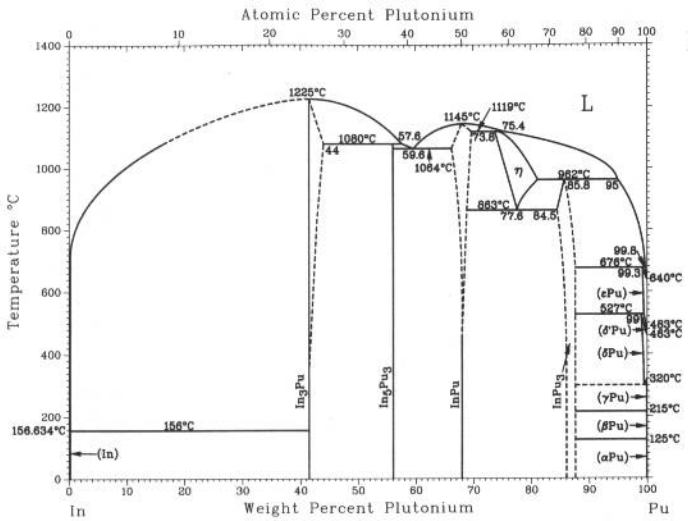

H. Okamoto, 1992

Phase	Composition, wt% Pu	Pearson symbol	Space group
(In)	0	*tI*2	*I*4/*mmm*
In_3Pu	42 to 44	*cP*4	$Pm\bar{3}m$
In_5Pu_3	56.1	...	(a)
InPu	66 to 70	*tP*2	*P*4/*mmm*
		*tI*2	*I*4/*mmm*
η	73.8 to 81	...	...
$InPu_3$	84.5 to 88	*cP*4	$Pm\bar{3}m$
		*cF*4	$Fm\bar{3}m$
(εPu)	99.3 to 100	*cI*2	$Im\bar{3}m$
(δ'Pu)	100	*tI*2	*I*4/*mmm*
(δPu)	99 to 100	*cF*4	$Fm\bar{3}m$
(γPu)	100	*oF*8	*Fddd*
(βPu)	100	*mC*34	*C*2/*m*
(αPu)	100	*mP*16	$P2_1/m$

(a) Complex

In-Rb

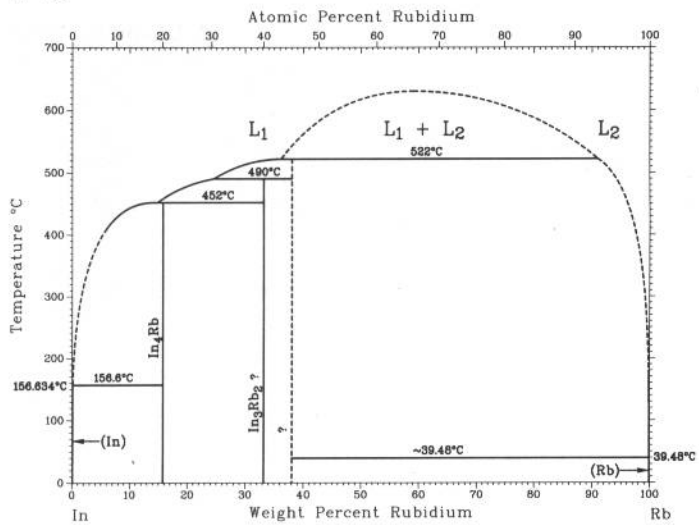

A.D. Pelton and S. Larose, 1992

Phase	Composition, wt% Rb	Pearson symbol	Space group
(In)	0	*tI*2	*I*4/*mmm*
In_4Rb	16	*tI*10	*I*4/*mmm*
In_3Rb_2(a)	~33	...	...
In_5Rb_4(b)	...	...	...
(Rb)	100	*cI*2	$Im\bar{3}m$

(a) Stoichiometry requires verification. (b) Existence and stoichiometry require verification.

In-S

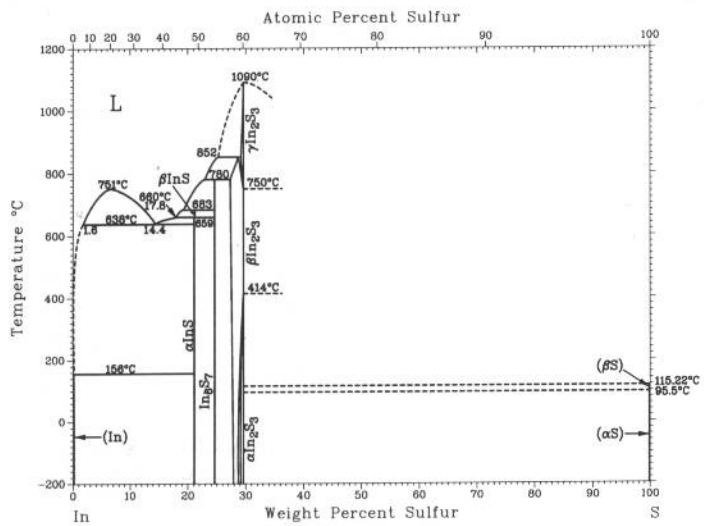

H. Okamoto, 1992

Phase	Composition, wt% S	Pearson symbol	Space group
(In)	0	*tI*2	*I*4/*mmm*
βInS	21.2	...	...
αInS	21.0	*oP*8	*Pnnm*
In_6S_7	24.5	*mP*26	$P2_1/m$
γIn_2S_3	29.5	*hP*7	$P\bar{3}m1$
βIn_2S_3	27.8 to 29.5	*cF*56	$Fd\bar{3}m$
αIn_2S_3	29.5	*tI*80	$I4_1/amd$
(βS)	100	*mP**	$P2_1/c$
(αS)	100	*oF*128	*Fddd*
Metastable phase			
InS′	21.8	...	...
High-pressure phase			
εIn_2S_3	29.5	*hR*10	$R\bar{3}c$
Questionable phases			
In_5S_4(a)	18.2	*cP*72	$Pa\bar{3}$
In_3S_4	27.1	*hP**	...
In_2S_3(b)	29.5	*cF*8	$F4\bar{3}m$
In_2S_3(c)	29.5	*o***	...
In_3S_5(c)	31.8	*hP**	...

(a) Probably a ternary compound. (b) Low-temperature phase. (c) High-temperature phase. Conflicts with γIn_2S_3

In-Sb

R.C. Sharma, T.L. Ngai, and Y.A. Chang, 1992

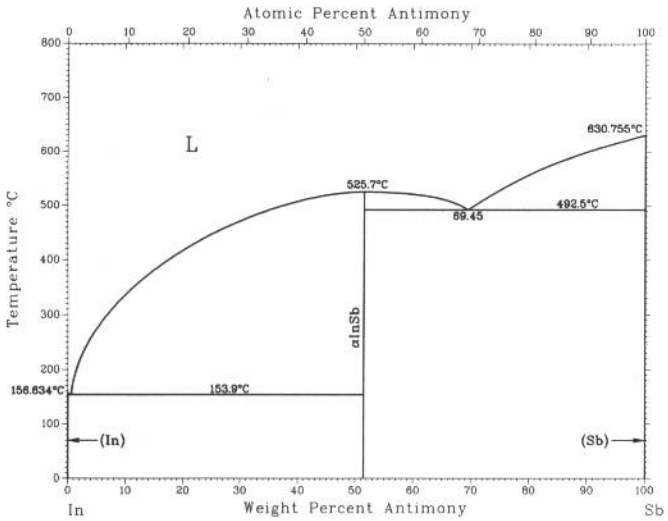

Phase	Composition, wt% Sb	Pearson symbol	Space group
(In)	0	*tI*2	*F*4/*mmm*
ω(a)	~21	*hP*6	$P6_3/mmc$
ζ(a)	~41	*tI*32	*I*4/*mcm*
γ_2(a)	49.0	*oP*4	...
αInSb	51.5	*cF*8	$F\bar{4}3m$
βInSb(a)	51.5	*tI*4	$I4_1/amd$
γ_1(a)	51.5 to 56	*oP*2	*Pmm*2
γInSb(a)	51.5	(b)	...
γInSb(a)	51.5	*oP*4	*Pmmm* or *Pmmn*
δInSb(a)	51.5	*oP*2	*Pmm*2
<<βSn>>(a)	56	*tI*4	$I4_1/amd$
π′(a)	58.9	*hR*1	$R\bar{3}m$
π(c)	61 to 71	*cP*1	$Pm\bar{3}m$
InSb (thin films)(c)	...	*hP*4	$P6_3mc$
(Sb)	100	*hR*2	$R\bar{3}m$

(a) High-pressure phase. (b) Hexagonal. (c) Metastable phase

In-Sc

H. Okamoto, 1992

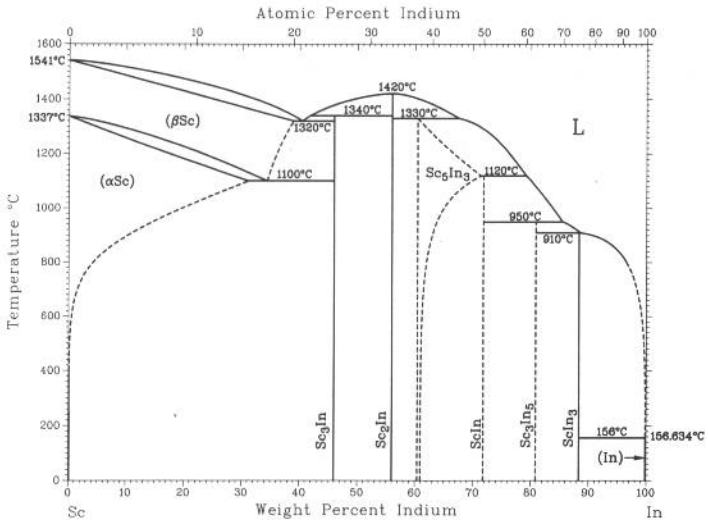

Phase	Composition, wt% In	Pearson symbol	Space group
(βSc)	0 to 39	*cI*2	$Im\bar{3}m$
(αSc)	0 to 31	*hP*2	$P6_3/mmc$
Sc_3In	46	*hP*8	$P6_3/mmc$
Sc_2In	56.0	*hP*6	$P6_3/mmc$
Sc_5In_3	60.5 to 71.9	...	...
ScIn	71.9	...	...
Sc_3In_5	81.0	...	...
$ScIn_3$	89	*cP*4	$Pm\bar{3}m$
(In)	100	*tI*2	*I*4/*mmm*

In-Se

H. Okamoto, 1992

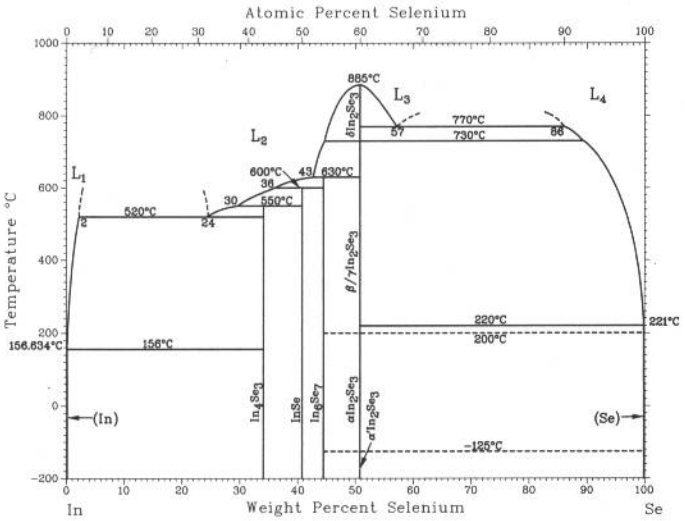

Phase	Composition, wt% Se	Pearson symbol	Space group
(In)	0	*tI*2	*I*4/*mmm*
In_4Se_3	34.1	*oP*28	*Pnnm*
αInSe	40.7	*hR*4	$R\bar{3}m$
βInSe(a)	40.7	*hP*8	$P6_3/mmc$
InSe II(b)	40.7	*mP*8	*P*2/*m*
In_6Se_7	44.5	*mP*26	$P2_1/m$
In_2Se_3	51	...	...
δ		*hP*5	$P6_1$
γ(c)		*hP*30	$P6_1$
β(c, d)		*hR*5	$R\bar{3}m$
α3(d)		*hR*5	$R\bar{3}m$
α2(d)		*hP*10	$P6_3/mmc$
α1(d)		*hP*5	...
α'(d)		*o***	...
In_2Se_3(e)	51	*hP*160	$P6_3$
(Se)	100	*hP*3	$P3_121$
Uncertain phases and structures			
In_2Se(f)	25.6	*oP*24	*Pnnm*
InSe	40.7	*hP**	...
In_6Se_7	44.5	*mP*26	$P2_1/m$
In_5Se_6	45.2	...	...
In_3Se_4	47.8	...	...
In_5Se_7	49.0	*c***	...
In_2Se_3	51	*hP*30	$P6_5$
In_2Se_3(g)	51	*m***	...
In_2Se_3(h)	51	*c***	...
$InSe_4$	51	...	...

(a) Probably metastable. (b) High-pressure phase. (c) β ↔ α transition is ambiguous. (d) Metastable. (e) Thin film. (f) Probably In_4Se_3. (g) Probably In_6Se_7. (h) Same as In_5Se_7?

In-Si

R.W. Olesinski, N. Kanani, and G.J. Abbaschian, 1992

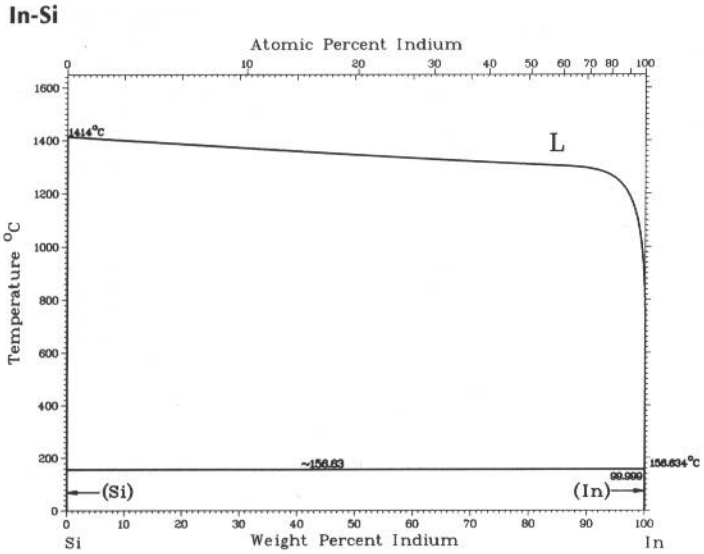

Phase	Composition, wt% In	Pearson symbol	Space group
(Si)	~0	*cF*8	$Fd\bar{3}m$
(In)	~100	*tI*2	*I*4/*mmm*

In-Sm

H. Okamoto, 1992

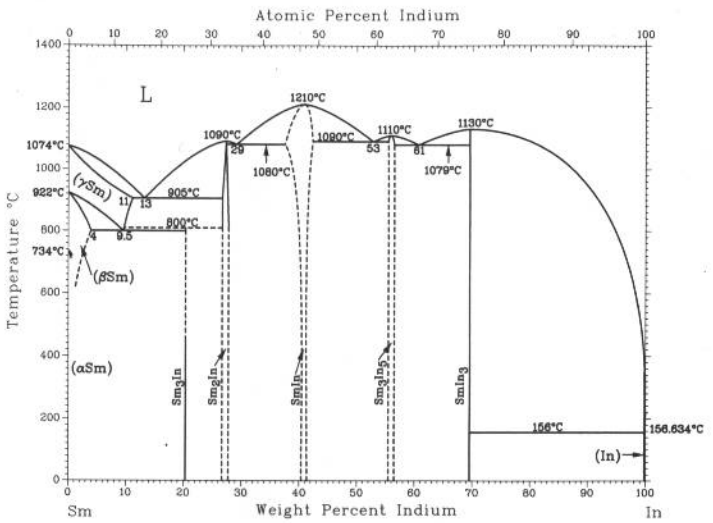

Phase	Composition, wt% In	Pearson symbol	Space group
(γSm)	0 to 11	*cI*2	$Im\bar{3}m$
(βSm)	0 to 4	*hP*2	$P6_3/mmc$
(αSm)	0	*hR*3	$R\bar{3}m$
Sm_3In	20	*cP*4	$Pm\bar{3}m$
Sm_2In	26 to 28	*hP*6	$P6_3/mmc$
SmIn	38 to 42	*cP*2	$Pm\bar{3}m$
Sm_3In_5	56 to 57	*oC*32	*Cmcm*
$SmIn_3$	70	*cP*4	$Pm\bar{3}m$
(In)	100	*tI*2	*I*4/*mmm*

In-Sn

H. Okamoto, 1992

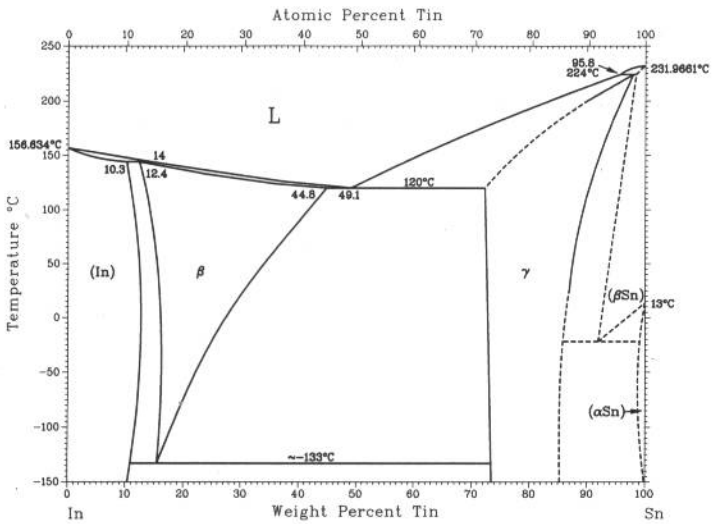

Phase	Composition, wt% Sn	Pearson symbol	Space group
(In)	0 to 12.4	*tI*2	*I*4/*mmm*
β	12.4 to 44.8	*tI*2	*I*4/*mmm*
γ	73 to ?	*hP*5	*P*6/*mmm*
(βSn)	? to 100	*tI*4	$I4_1/and$
(αSn)	100	*cF*8	$Fd\bar{3}m$

In-Sr

H. Okamoto, 1992

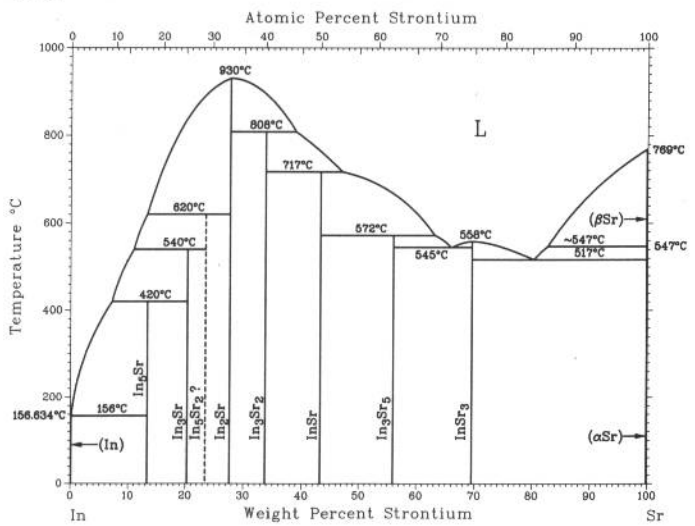

Phase	Composition, wt% Sr	Pearson symbol	Space group
(In)	0	*tI*2	*I*4/*mmm*
In_5Sr	13.3	*hP**	...
In_3Sr	20	*hP*8	$P6_3/mmc$
In_5Sr_2?	23.4	...	...
In_2Sr	27.6	*hP*6	$P6_3/mmc$
In_3Sr_2	34	...	...
InSr	43.3	*o***	...
In_3Sr_5	56.0	*tI*32	*I*4/*mcm*
$InSr_3$	70	*cF*16	$Fm\bar{3}m$
(βSr)	100	*cI*2	$Im\bar{3}m$
(αSr)	100	*cF*4	$Fm\bar{3}m$

In-Tb

H. Okamoto, 1992

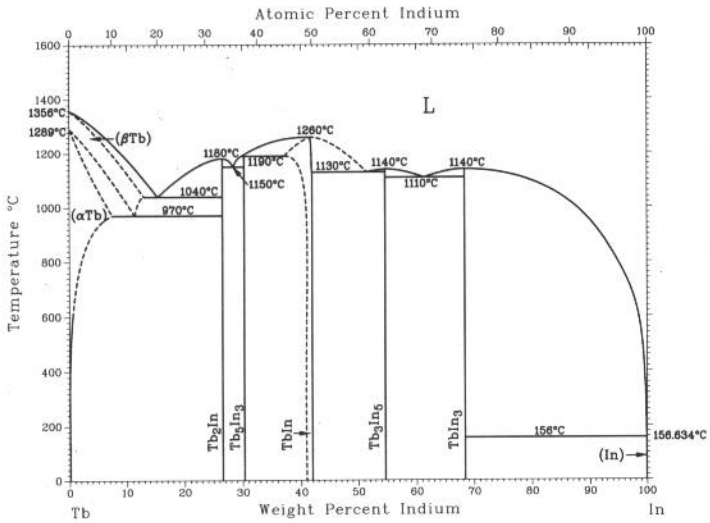

Phase	Composition, wt% In	Pearson symbol	Space group
(βTb)	0 to 13	*cI*2	$Im\bar{3}m$
(αTb)	0 to 7	*hP*2	$P6_3/mmc$
Tb_2In	26.5	*hP*6	$P6_3/mmc$
Tb_5In_3	30.2	*tI*32	$I4/mcm$
TbIn	37 to 41.9	*t***	...
Tb_3In_5	54.6	*oC*32	*Cmcm*
$TbIn_3$	68	*cP*4	$Pm\bar{3}m$
(In)	100	*tI*2	$I4/mmm$

In-Te

H. Okamoto, 1992

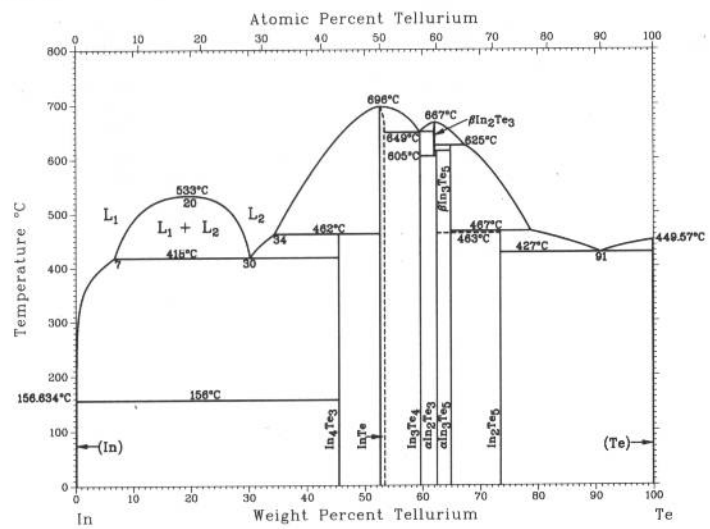

Phase	Composition, wt% Te	Pearson symbol	Space group
(In)	0	*tI*2	$I4/mmm$
In_4Te_3	45.5	*oP*28	*Pnnm*
InTe	53 to 54	*tI*16	$I4/mcm$
In_3Te_4	59.7	*hR*7	$R\bar{3}m$
In_3Te_4	59.7	*tI**	$I4/mmm$
βIn_2Te_3	62.0 to 62.6	*cF*8	$F\bar{4}3m$
αIn_2Te_3	62.5	*cF*180	$F\bar{4}3m$
βIn_3Te_5	64.9	*hP**	...
αIn_3Te_5	64.9	...	...
In_2Te_5I	73.5	*mC*28	*Cc*
(Te)	100	*hP*3	$P3_121$
Metastable or high-pressure phases			
InTeII	52.6	*cF*8	$Fm\bar{3}m$
InTeIII	52.6	*cP*2	$Pm\bar{3}m$
InTeII′	52.6	*t**8	...
$In_{2+x}Te_3$	...	*cP**	...
In_2Te_3	62.5	*oI**	*Imm*2
In_2Te_3	62.5	*tP**	$P4_2mcm$ or $P4_2nm$
In_2Te_3(a)	62.5	*hP**	...
In_2Te_3II	62.5	*hR*5	$R\bar{3}m$
In_2Te_5II	73.5	*mC*84	*C*2/*c*

(a) Thin film

In-Th

H. Okamoto, 1992

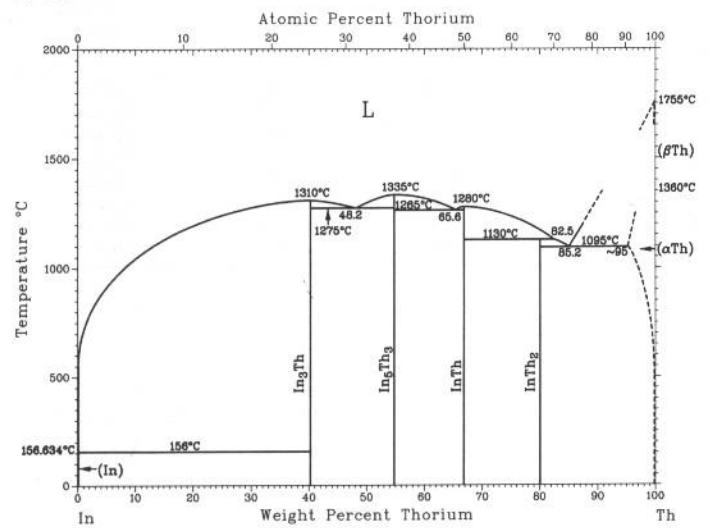

Phase	Composition, wt% Th	Pearson symbol	Space group
(In)	0	*tI*2	$I4/mmm$
In_3Th	40	*cP*4	$Pm\bar{3}m$
In_5Th_3	54.8	*oC*32	*Cmcm*
InTh	66.9	*oP*24	*Pbcm*
$InTh_2$	80.2	*tI*12	$I4/mcm$
(βTh)	? to 100	*cI*2	$Im\bar{3}m$
(αTh)	~95 to 100	*cF*4	$Fm\bar{3}m$

In-Ti

J.L. Murray, 1992

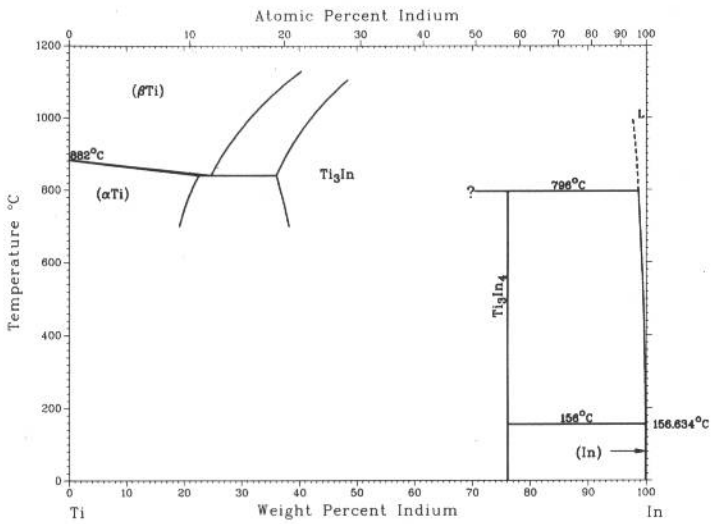

Phase	Composition, wt% In	Pearson symbol	Space group
(βTi)	0 to ?	*cI*2	$Im\bar{3}m$
(αTi)	0 to ~21	*hP*2	$P6_3/mmc$
Ti_3In	39 to ?	*hP*8	$P6_3/mmc$
Ti_3In_2	(a)	*tP*2	*P*4/*mmm*
Ti_3In_4	76.1	*tP*14	*P*4/*mbm*
(In)	~100	*tI*2	*I*4/*mmm*

(a) Unknown

In-Tl

H. Okamoto, 1992

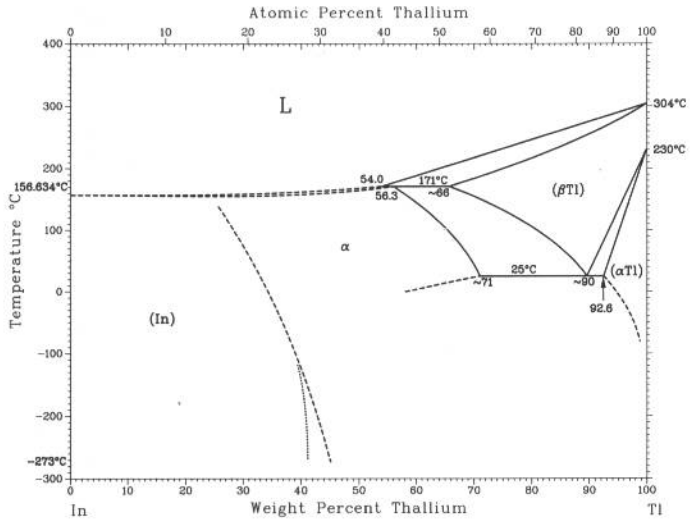

Phase	Composition, wt% Tl	Pearson symbol	Space group
(In)	0 to 44	*tI*2	*I*4/*mmm*
α	25 to ~71	*cF*4	$Fm\bar{3}m$
(βTl)	~66 to 100	*cI*2	$Im\bar{3}m$
(αTl)	92.6 to 100	*hP*2	$P6_3/mmc$

In-Tm

H. Okamoto, 1992

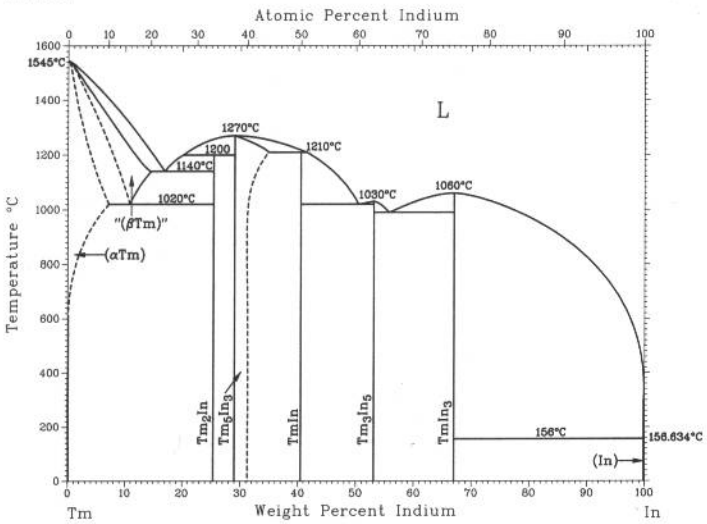

Phase	Composition, wt% In	Pearson symbol	Space group
"(βTm)"	? to 15	*cI*2	$Im\bar{3}m$
(αTm)	0 to 7	*hP*2	$P6_3/mmc$
TmIn	25.3	*hP*6	$P6_3/mmc$
Tm_5In_3	29.0 to 36	*hP*16	$P6_3/mcm$
TmIn	40.5	*cP*2	$Pm\bar{3}m$
Tm_3In_5	53.1	*oC*32	*Cmcm*
$TmIn_3$	67	*cP*4	$Pm\bar{3}m$
(In)	100	*tI*2	*I*4/*mmm*

In-V

J.F. Smith and K.J. Lee, 1992

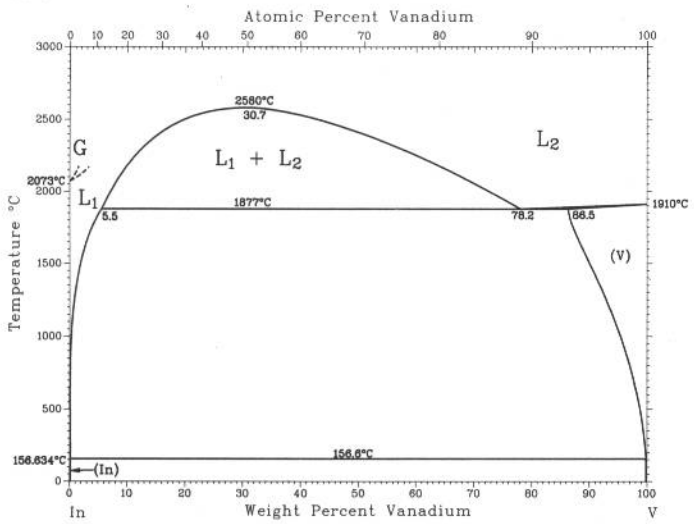

Phase	Composition, wt% V	Pearson symbol	Space group
(In)	0	*tI*2	*I*4/*mmm*
InV_3(a)	57	(b)	...
(V)	100	*cI*2	$Im\bar{3}m$

(a) Cr_3Si-type structure reported in impure sample at high pressure. (b) Tetragonal. Pressure-stabilized phase

In-Y

H. Okamoto, 1992

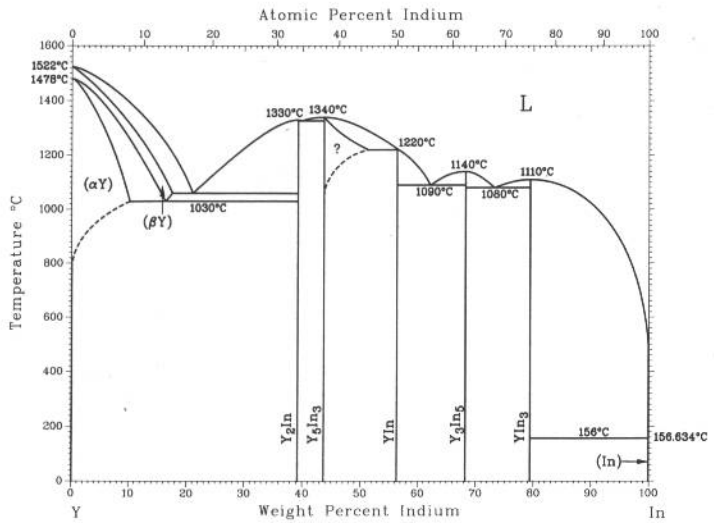

Phase	Composition, wt% In	Pearson symbol	Space group
(βY)	0 to 17.4	*cI*2	$Im\bar{3}m$
(αY)	0 to 10.1	*hP*2	$P6_3/mmc$
Y_2In	39.2	*hP*6	$P6_3/mmc$
Y_5In_3	43.7 to 51.4	*hP*16	$P6_3/mcm$
YIn	56.4	*cP*2	$Pm\bar{3}m$
Y_3In_5	68.3	*oC*32	*Cmcm*
YIn_3	79.5	*cP*4	$Pm\bar{3}m$
(In)	100	*tI*2	*I*4/*mmm*

In-Yb

A. Palenzona and S. Cirafici, 1992

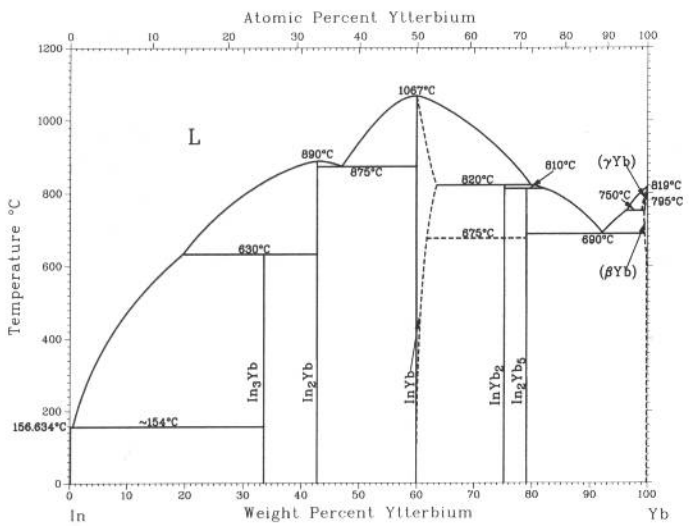

Phase	Composition, wt% Yb	Pearson symbol	Space group
(In)	~0	*tI*2	*I*4/*mmm*
In_3Yb	33.4	*cP*4	$Pm\bar{3}m$
In_2Yb	42.9	*hP*6	$P6_3/mmc$
InYb	60.1 to ~63	*cP*2	$Pm\bar{3}m$
$InYb_2$	75.1	*oP*12	*Pnma*
In_2Yb_5	~79.0	...	$R\bar{3}c$ or *R*3*c*
(γYb)	~100	*cI*2	$Im\bar{3}m$
(βYb)	~100	*cF*4	$Fm\bar{3}m$
(αYb)	~100	*hP*2	$P6_3/mmc$

In-Zn

J. Dutkiewicz and W. Zakulski, 1992

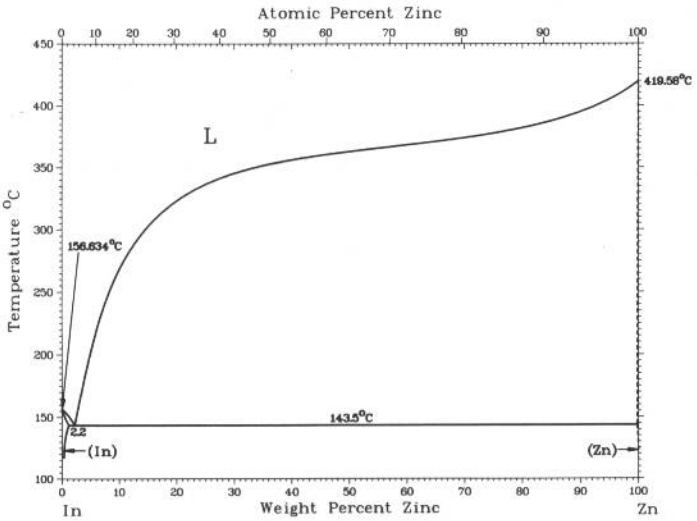

Phase	Composition, wt% Zn	Pearson symbol	Space group
(In)	0 to 1	*tI*2	*I*4/*mmm*
(Zn)	99.8 to 100	*hP*2	$P6_3/mmc$

Ir-La

H. Okamoto, 1991

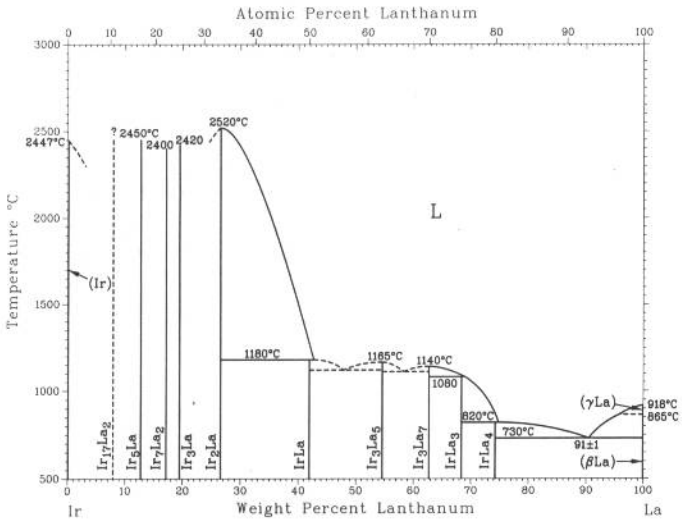

Phase	Composition, wt% La	Pearson symbol	Space group
(Ir)	0	*cF*4	$Fm\bar{3}m$
$Ir_{17}La_2$?	7.8	...	...
Ir_5La	12.7	*hP*6	*P6/mmm*
Ir_7La_2	17.1	*hP*36	$P6_3/mmc$
Ir_3La	19	*hR*12	$R\bar{3}m$
Ir_2La	26.5	*cF*24	$Fd\bar{3}m$
IrLa?	41.9	...	...
Ir_3La_5	54.6	*tP*32	*P*4/*ncc*
Ir_3La_7	63	*hP*20	$P6_3mc$
$IrLa_3$	68	*oP*16	*Pnma*
$IrLa_4$	74	...	...
(γLa)	100	*cI*2	$Im\bar{3}m$
(βLa)	100	*cF*4	$Fm\bar{3}m$
(αLa)	100	*hP*4	$P6_3/mmc$

Ir-Mo

From [Molybdenum]

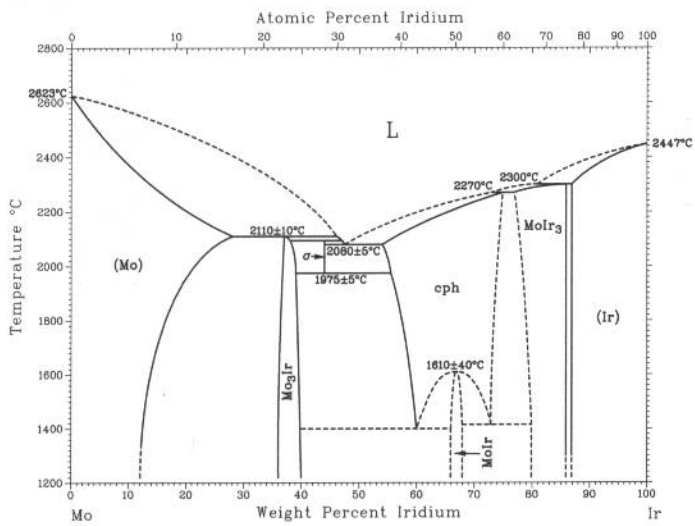

Phase	Composition, wt% Ir	Pearson symbol	Space group
(Mo)	0 to ~28	*cI*2	$Im\bar{3}m$
Mo_3Ir	<36 to 40	*cP*8	$Pm\bar{3}n$
σ	~44	*tP*30	$P4_2/mnm$
MoIr (cph)	~54 to >75	*hP*2	$P6_3/mmc$
MoIr (LT)	~66 to 68	*oP*4	*Pmma*
$MoIr_3$	~77 to 86	*hP*8	$P6_3/mmc$
(Ir)	~87 to 100	*cF*4	$Fm\bar{3}m$

Ir-Nb

H. Okamoto, unpublished

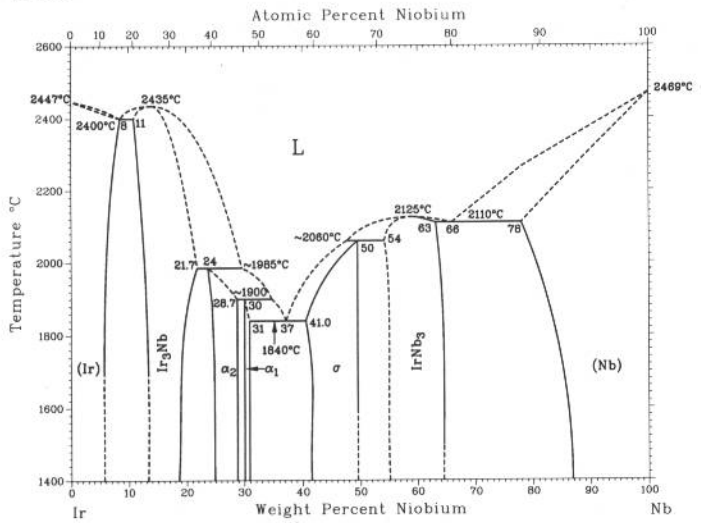

Phase	Composition, wt% Nb	Pearson symbol	Space group
(Ir)	0 to 8	*cF*4	$Fm\bar{3}m$
Ir_3Nb	11 to 21.7	*cP*4	$Pm\bar{3}m$
α_2	24 to 28.7	*oP*12	*Pmma*
α_1	30 to 31	*tP*2	*P4/mmm*
σ	41.0 to 50	*tP*30	$P4_2/mnm$
$IrNb_3$	54 to 63	*cP*8	$Pm\bar{3}n$
(Nb)	78 to 100	*cI*2	$Im\bar{3}m$

Ir-Ni

S.C. Yang, N. Chen, and P. Nash, 1991

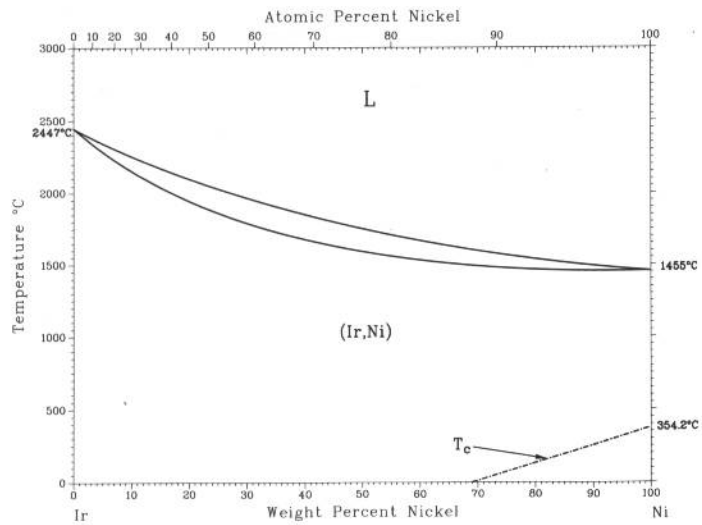

Phase	Composition, wt% Ni	Pearson symbol	Space group
(Ir,Ni)	0 to 100	*cF*4	$Fm\bar{3}m$

Ir-Pd

S.N. Tripathi, S.R. Bharadwaj, and M.S. Chandrasekharaiah, 1991

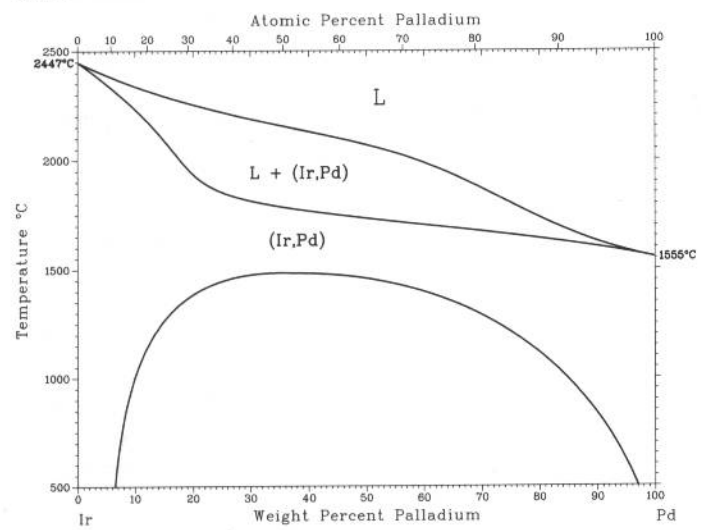

Phase	Composition, wt% Pd	Pearson symbol	Space group
(Ir,Pd)	0 to 100	*cF*4	$Fm\bar{3}m$

Ir-Pt

L. Muller, 1930; and E. Raub and W. Plate, 1956

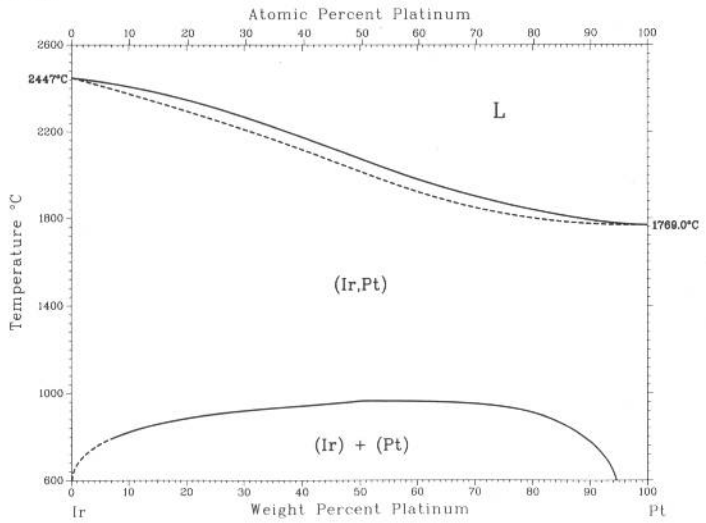

Phase	Composition, wt% Pt	Pearson symbol	Space group
(Ir,Pt)	0 to 100	*cF*4	$Fm\bar{3}m$

Ir-Rh

S.N. Tripathi, S.R. Bharadwaj, and M.S. Chandrasekharaiah, 1991

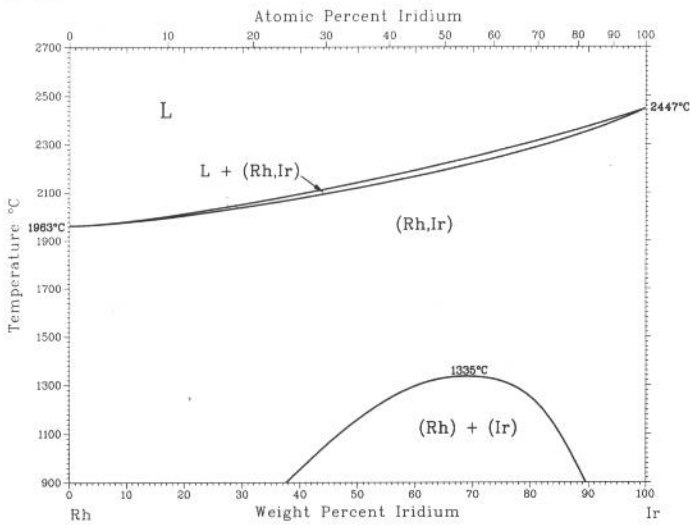

Phase	Composition, wt% Ir	Pearson symbol	Space group
(Ir,Rh)	0 to 100	*cF*4	$Fm\bar{3}m$

Ir-Ru

H. Okamoto, 1992

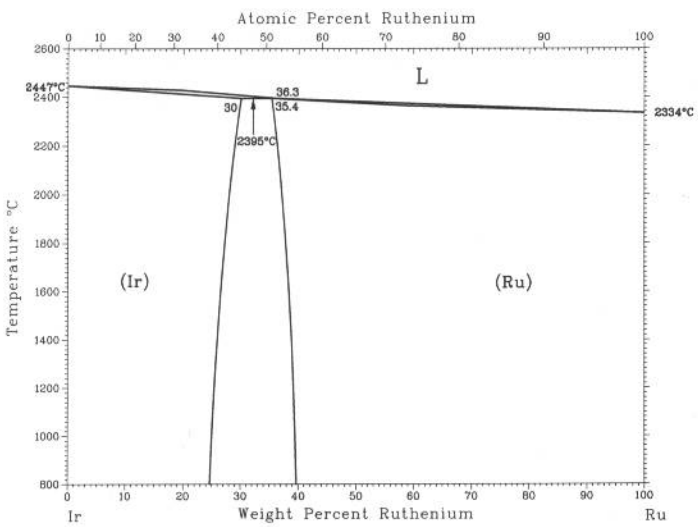

Phase	Composition, wt% Ru	Pearson symbol	Space group
(Ir)	0 to 30	*cF*4	$Fm\bar{3}m$
(Ru)	35.4 to 100	*hP*2	$P6_3/mmc$

Ir-Ta

From [Metals]

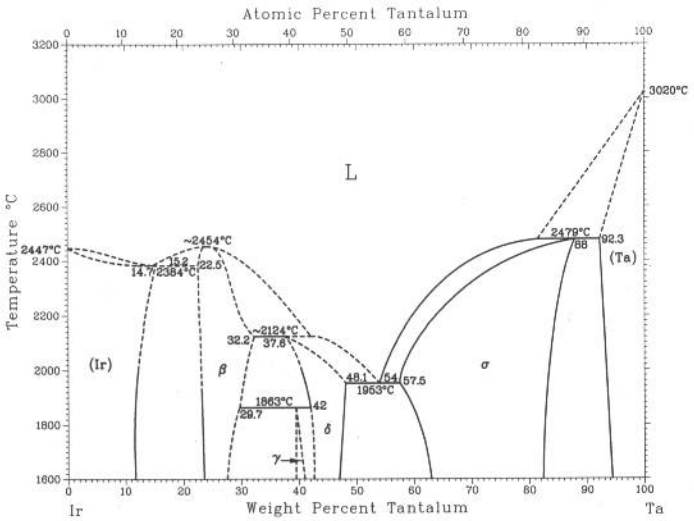

Phase	Composition, wt% Ta	Pearson symbol	Space group
(Ir)	0 to 15.2	*cF*4	$Fm\bar{3}m$
β	22.5 to 32.2	*cP*4	$Pm\bar{3}m$
γ	~41	*tI*2	*I*4/*mmm*
δ	37.6 to 48.1	*oP*12	*Pmma*
σ	57.5 to 88.0	*tP*30	$P4_2/mnm$
(Ta)	92.3 to 100	*cI*2	$Im\bar{3}m$

Ir-Th

H. Okamoto, 1991

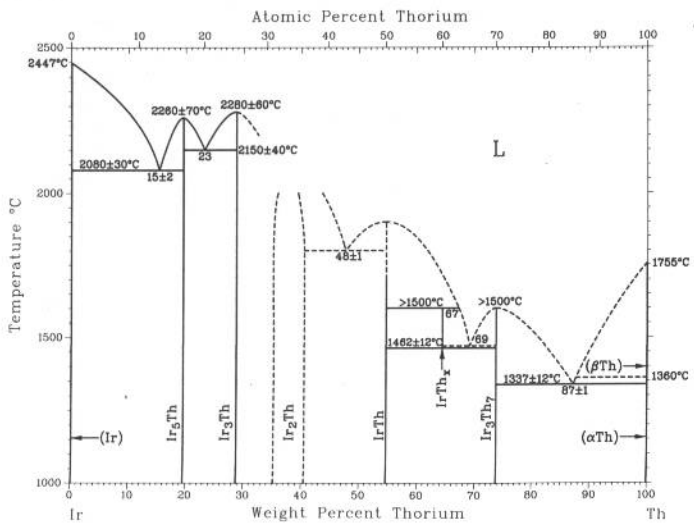

Phase	Composition, wt% Th	Pearson symbol	Space group
(Ir)	0	*cF*4	$Fm\bar{3}m$
Ir_5Th	19.5	*hP*6	*P*6/*mmm*
Ir_3Th	29	...	...
Ir_2Th	35 to 40	*cF*24	$Fd\bar{3}m$
IrTh	54.7	*oC*8	*Cmcm*
$IrTh_x$	~64	...	...
Ir_3Th_7	74	*hP*20	$P6_3mc$
(βTh)	100	*cI*2	$Im\bar{3}m$
(αTh)	100	*cF*4	$Fm\bar{3}m$

Ir-Ti

H. Okamoto, 1992

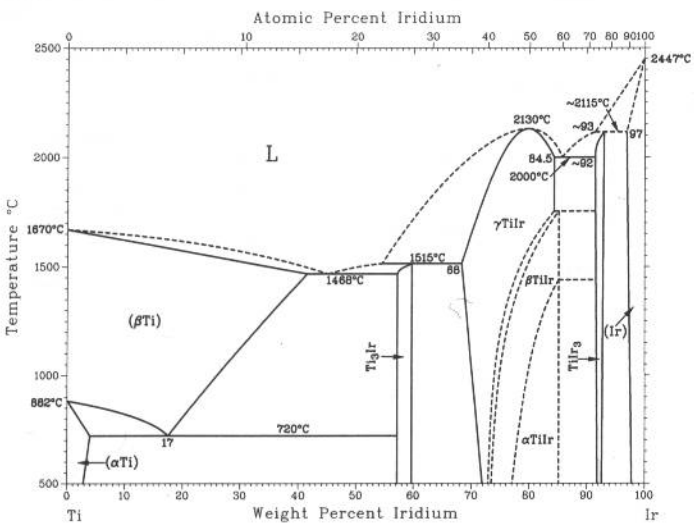

Phase	Composition, wt% Ir	Pearson symbol	Space group
(βTi)	0 to 4	*cI*2	$Im\bar{3}m$
(αTi)	0 to 40.5	*hP*2	$P6_3/mmc$
Ti_3Ir	57 to 60	*cP*8	$Pm\bar{3}n$
γTiIr	68 to 84	*cP*2	$Pm\bar{3}m$
βTiIr	73 to ?	*tP*2	*P*4/*mmm*
αTiIr	77 to ?	*c***	...
$TiIr_3$	~92 to ~93	*cP*4	$Pm\bar{3}m$
(Ir)	~97 to 100	*cF*4	$Fm\bar{3}m$

Ir-U

H. Okamoto, 1992

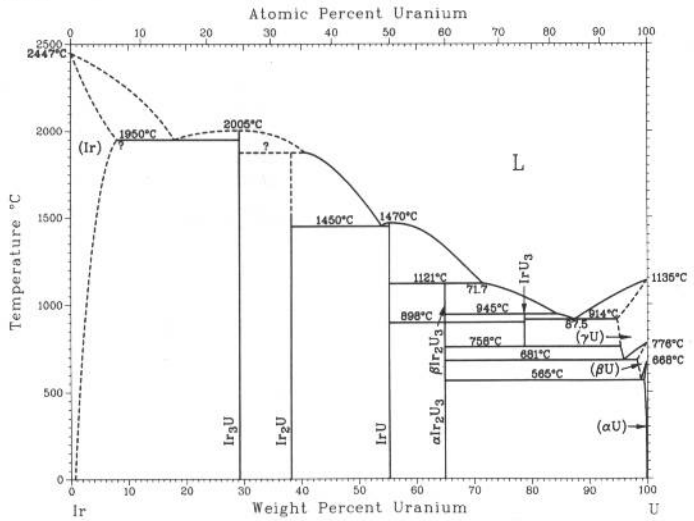

Phase	Composition, wt% U	Pearson symbol	Space group
(Ir)	0 to ?	*cF*4	$Fm\bar{3}m$
Ir_3U	29	*cP*4	$Pm\bar{3}m$
Ir_2U	38.2	*cF*24	$Fd\bar{3}m$
IrU	55.3	...	...
βIr_2U_3	65	...	...
αIr_2U_3	65	...	...
IrU_3	79	...	...
(γU)	? to 100	*cI*2	$Im\bar{3}m$
(βU)	? to 100	*tP*30	$P4_2/mnm$
(αU)	? to 100	*oC*4	*Cmcm*
Possible phase			
IrU_2	71.3	*m***	...

Ir-V

J.F. Smith, 1989

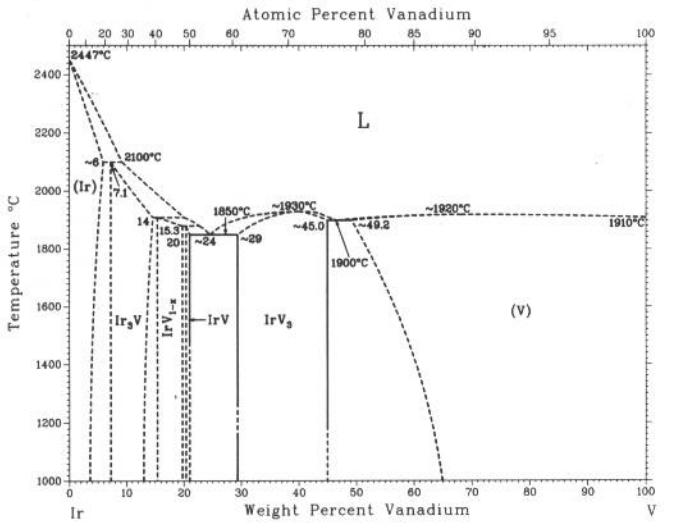

Phase	Composition, wt% V	Pearson symbol	Space group
(Ir)	0 to ~6	*cF*4	$Fm\bar{3}m$
Ir_3V	7.1 to 14	*cP*4	$Pm\bar{3}m$
IrV_{1-x}	15.3 to 20	*tP*2	*P4/mmm*
IrV	~20.9	*oC*8	*Cmmm*
IrV_3	~29 to ~45.0	*cP*8	$Pm\bar{3}n$
(V)	~49.2 to 100	*cI*2	$Im\bar{3}m$

Ir-W

S.V. Nagender Naidu, A.M. Sriramamurthy, and P. Rama Rao, 1991

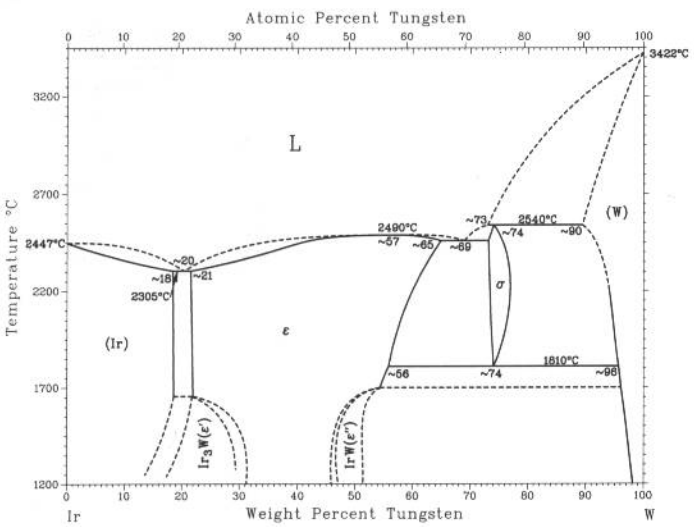

Phase	Composition, wt%W	Pearson symbol	Space group
(Ir)	0 to ~18	*cF*4	$Fm\bar{3}m$
ε	~21 to ~65	*hP*2	$P6_3/mmc$
$Ir_3W(\varepsilon')$	~24(a)	*hP*8	$P6_3/mmc$
$IrW(\varepsilon'')$	48.9(a)	*oP*4	*Pmma*
σ	74	*tP*30	$P4_2/mnm$
(W)	~90 to 100	*cI*2	$Im\bar{3}m$

(a) Ordered structure

Ir-Zr

H. Okamoto, 1992

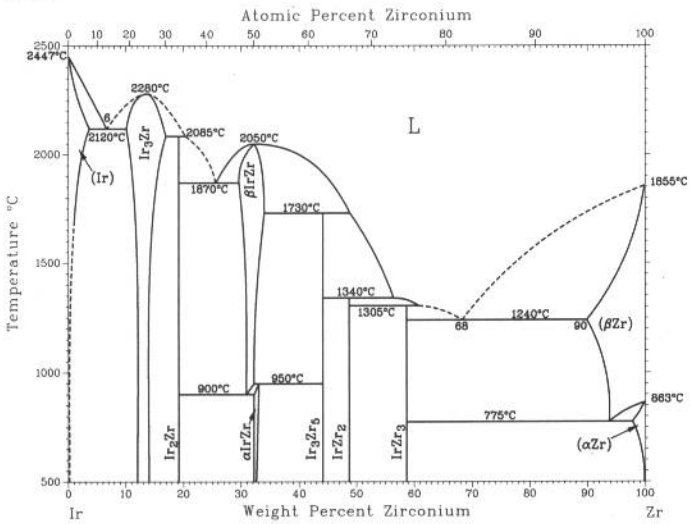

Phase	Composition, wt% Zr	Pearson symbol	Space group
(Ir)	0 to 3	*cF*4	$Fm\bar{3}m$
Ir_3Zr	10 to 17	*cP*4	$Pm\bar{3}m$
Ir_2Zr	19.2	*cF*24	$Fd\bar{3}m$
βIrZr	30 to 34	*cP*2	$Pm\bar{3}m$
αIrZr	32.2 to 33	(a)	...
Ir_3Zr_5	44.2	*hP*16	$P6_3/mcm$
$IrZr_2$	48.7	*tI*12	$I4/mcm$
$IrZr_3$	59	*tI*32	$I4_1/m$
(βZr)	90 to 100	*cI*2	$Im\bar{3}m$
(αZr)	98 to 100	*hP*2	$P6_3/mmc$

(a) Complex

K-Na

C.W. Bale, 1982

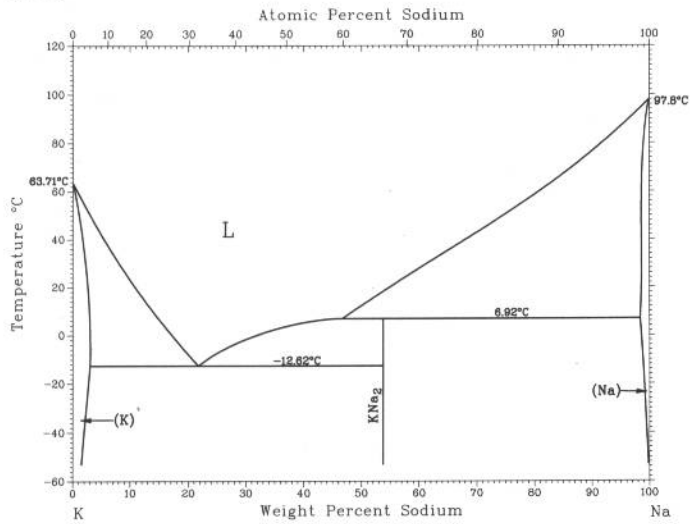

Phase	Composition, wt% Na	Pearson symbol	Space group
(K)	0	*cI*2	$Im\bar{3}m$
K_2Na(a)	22.72	...	...
KNa_2	54.05	*hP*12	$P6_3/mmc$
(Na)	100	*cI*2	$Im\bar{3}m$

(a) Possible phase (not shown in diagram)

K-Pb

H. Okamoto, 1990

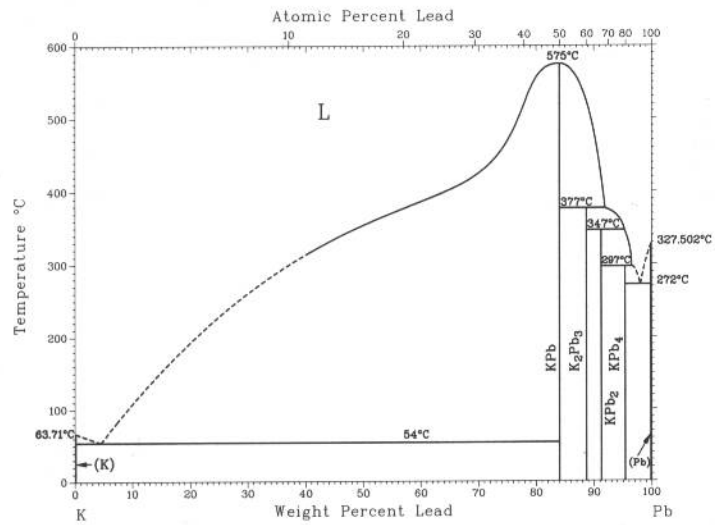

Phase	Composition, wt% Pb	Pearson symbol	Space group
(K)	0	*hP*2	$P6_3/mmc$
KPb	84.1	*tI*64	$I4_1/acd$
K_2Pb_3	89	...	...
KPb_2	91.4	*hP*12	$P6_3/mmc$
KPb_4	96	*cI**	...
(Pb)	100	*cF*4	$Fm\bar{3}m$

K-Rb

C.W. Bale and A.D. Pelton, 1983

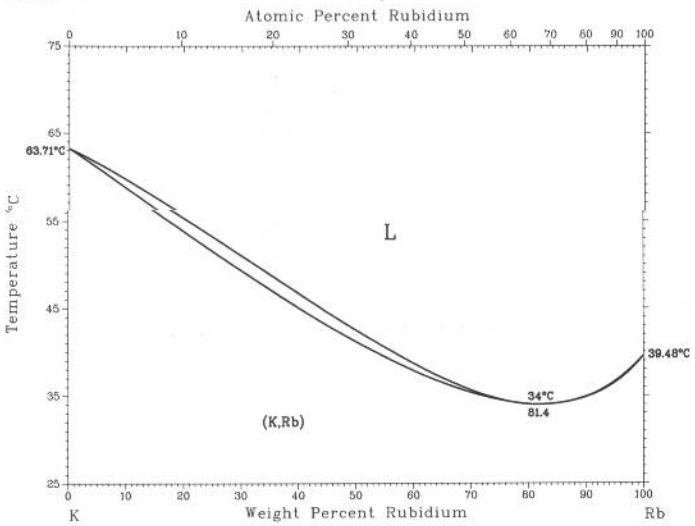

Phase	Composition, wt% Rb	Pearson symbol	Space group
(K,Rb)	0 to 100	*cI*2	$Im\bar{3}m$

K-S

H. Okamoto, 1990

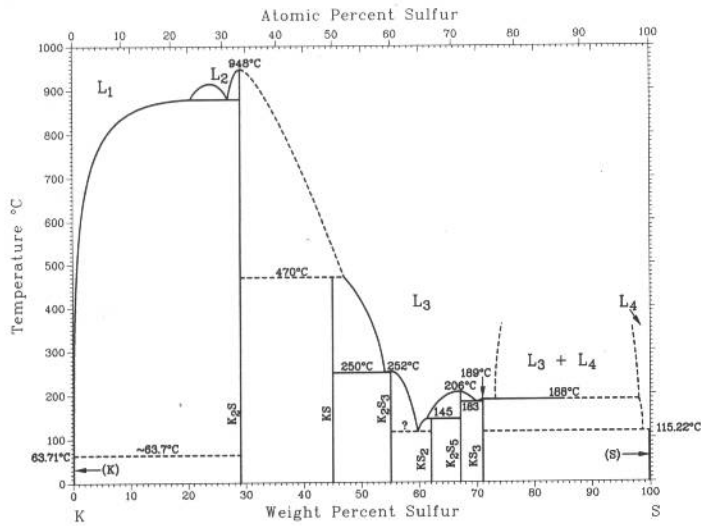

Phase	Composition, wt% S	Pearson symbol	Space group
(K)	0	*hP*2	$P6_3/mmc$
K_2S	29.1	*cF*12	$Fm\bar{3}m$
KS	45.1	*hP*12	$P6_2m$
K_2S_3	55	*oC*20	$Cmc2_1$
KS_2	62.2	*aP*42	...
K_2S_5	67.2	*oP*28	$P2_12_12_1$
KS_3	71	*aP*57	...
(S)	100	*oF*128	*Fddd*

K-Sb

F.W. Dorn and W. Klemm, 1961

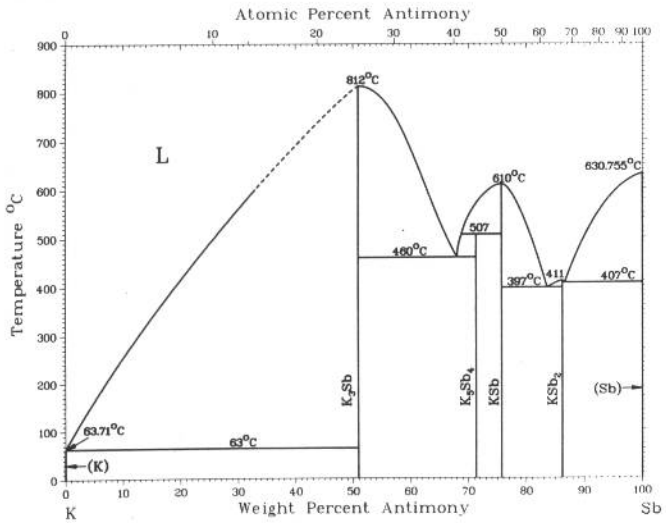

Phase	Composition, wt% Sb	Pearson symbol	Space group
(K)	~0	*cI*2	$Im\bar{3}m$
K_3Sb	51	*hP*8	$P6_3/mmc$
K_5Sb_4	71.3	...	...
KSb	75,7	*mP*16	$P2_1/c$
KSb_2	86.2	...	...
(Sb)	~100	*hR*2	$R\bar{3}m$

K-Se

H. Okamoto, 1990

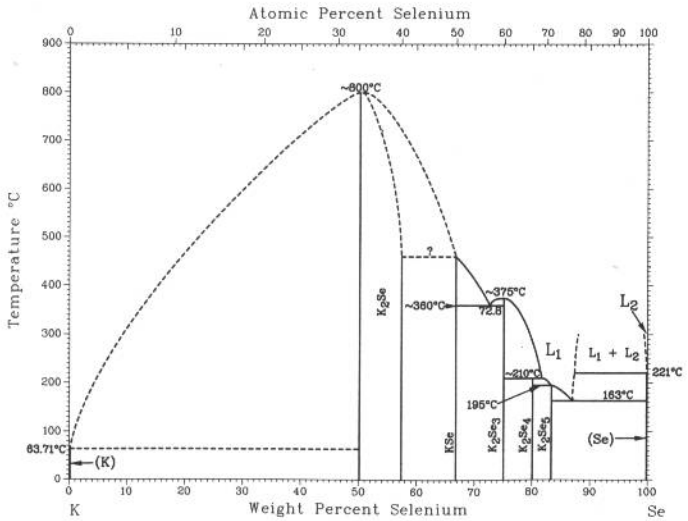

Phase	Composition, wt% Se	Pearson symbol	Space group
(K)	0	*hP*2	$P6_3/mmc$
K_2Se	50.2 to 57	*cF*12	$Fm\bar{3}m$
KSe	66.9	...	...
K_2Se_3	75	*oC*20	$Cmc2_1$
KSe_2	80.2	...	...
K_2Se_5	83.4	...	...
(Se)	100	*hP*3	$P3_121$

K-Sn

H. Okamoto, 1990

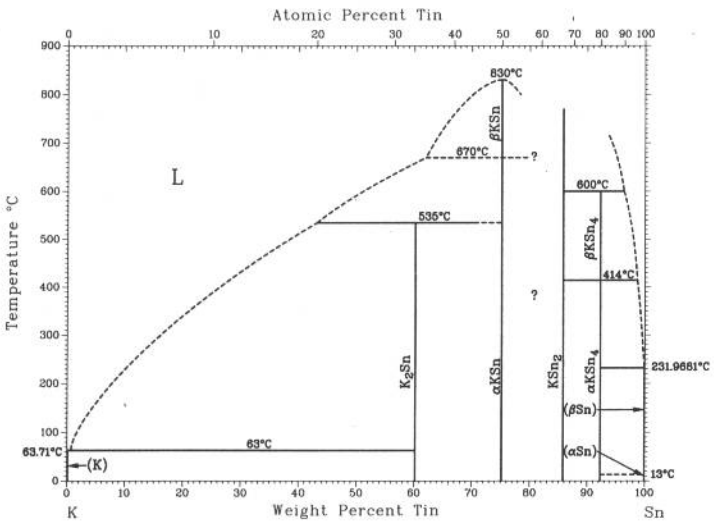

Phase	Composition, wt% Sn	Pearson symbol	Space group
(K)	~0	*cI*2	$Im\bar{3}m$
K_2Sn	~60.3	...	...
βKSn	75.2	...	...
αKSn	75.2	*tI*64	$I4_1/acd$
KSn_2	85.9	...	...
βKSn_4	92	...	...
αKSn_4	92	...	...
(βSn)	~100	*tI*4	$I4_1/amd$
(αSn)	~100	*cF*8	$Fd\bar{3}m$
Other reported phase			
K_4Sn_{23}	~94.6	*cP*54	$Pm\bar{3}n$

K-Te

A. Petric and A.D. Pelton, 1990

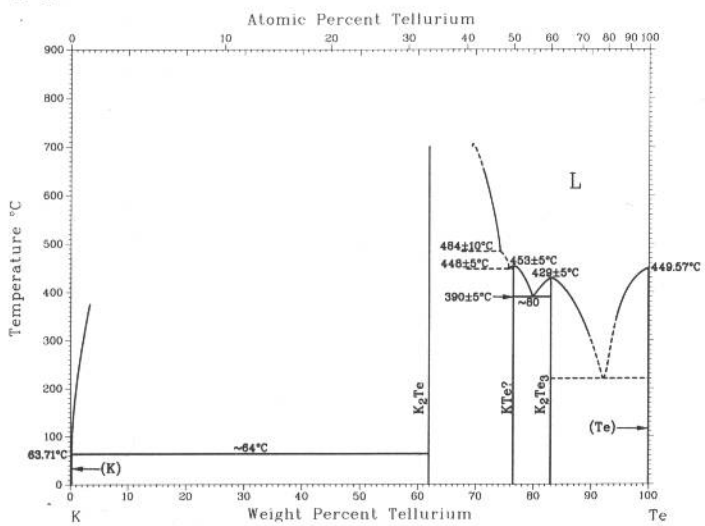

Phase	Composition, wt% Te	Pearson symbol	Space group
(K)	0	*cI*2	$Im\bar{3}m$
K_2Te	62.0 to 72.3(a)	*cF*12	$Fm\bar{3}m$
KTe	76.5	...	...
K_2Te_3	83	*oP*20	*Pnma*
(Te)	100	*hP*3	$P3_121$

(a) Homogeneity range subject to verification

K-Tl

H. Okamoto, 1990

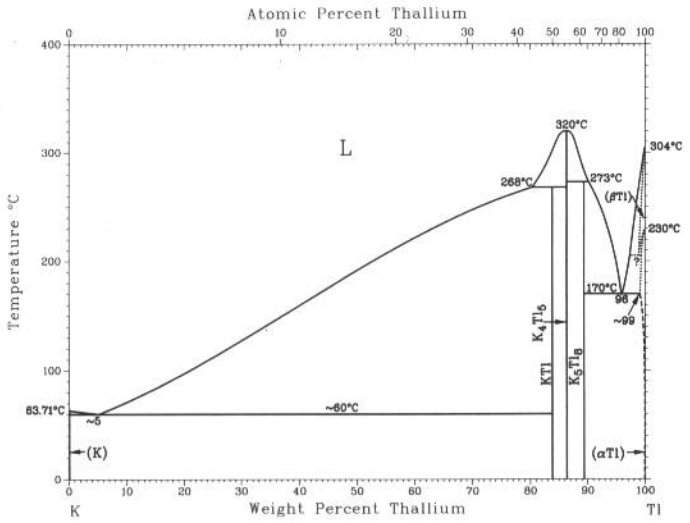

Phase	Composition, wt% Tl	Pearson symbol	Space group
(K)	0	*cI*2	$Im\bar{3}m$
KTl	83.9	(a)	...
K_4Tl_5	86.7	...	...
K_5Tl_8	89.3	...	...
(βTl)	? to 100	*cI*2	$Im\bar{3}m$
(αTl)	~99.8 to 100	*hP*2	$P6_3/mmc$

(a) Crystal structure neither the β brass or NaCl type

La-Mg

A.A. Nayeb-Hashemi and J.B. Clark, 1988

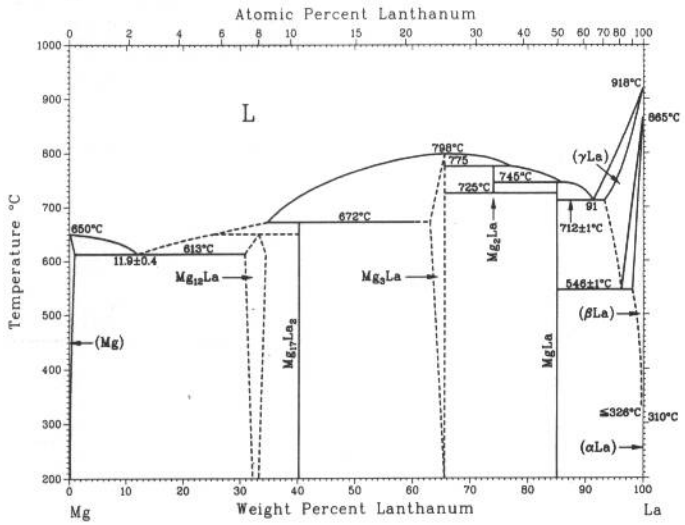

Phase	Composition, wt% La	Pearson symbol	Space group
(Mg)	0 to 0.79	*hP*2	$P6_3/mmc$
$Mg_{12}La$	30.53 to 34.18(a)	*oI*338(b)	(*Immm*)(b)
$Mg_{17}La_2$	40.21	*hP*38	$P6_3/mmc$
Mg_3La	? to 66	*cF*16	$Fm\bar{3}m$
Mg_2La	74.07	*cF*24	$Fd\bar{3}m$
MgLa	85.1	*cP*2	$Pm\bar{3}m$
(γLa)	~93 to 100	*cI*2	$Im\bar{3}m$)
(βLa)	~98.2 to 100	*cF*4	$Fm\bar{3}m$
(αLa)	? to 100	*hP*4	$P6_3/mmc$

(a) Homogeneity range estimated from lattice parameters. (b) This proposed crystal structure is based on the similarities of the lattice parameters of $Mg_{12}La$ with those of $Mg_{12}Ce$(II).

La-Mn

A. Palenzona and S. Cirafici, 1990

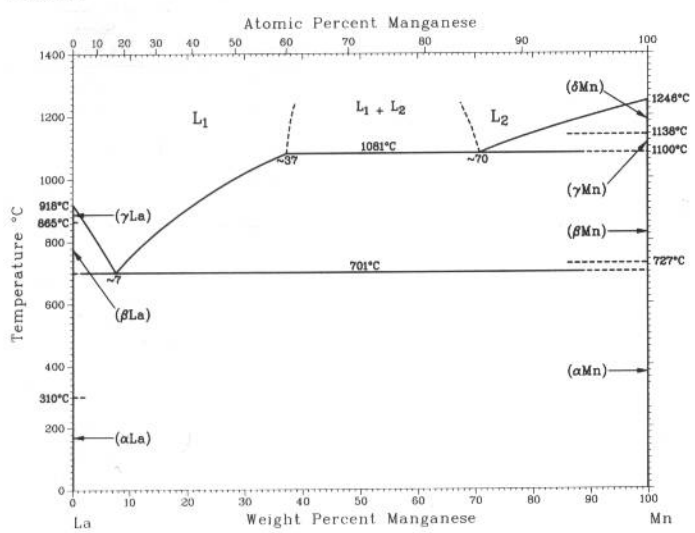

Phase	Composition, wt% Mn	Pearson symbol	Space group
(γLa)	0	*cI*2	$Im\bar{3}m$
(βLa)	0	*cF*4	$Fm\bar{3}m$
(αLa)	0	*hP*4	$P6_3/mmc$
(δMn)	~100	*cI*2	$Im\bar{3}m$
(γMn)	~100	*cI*4	$Im\bar{3}m$
(βMn)	~100	*cP*20	$P4_132$
(αMn)	~100	*cI*58	$I\bar{4}3m$

La-Ni

H. Okamoto, 1991

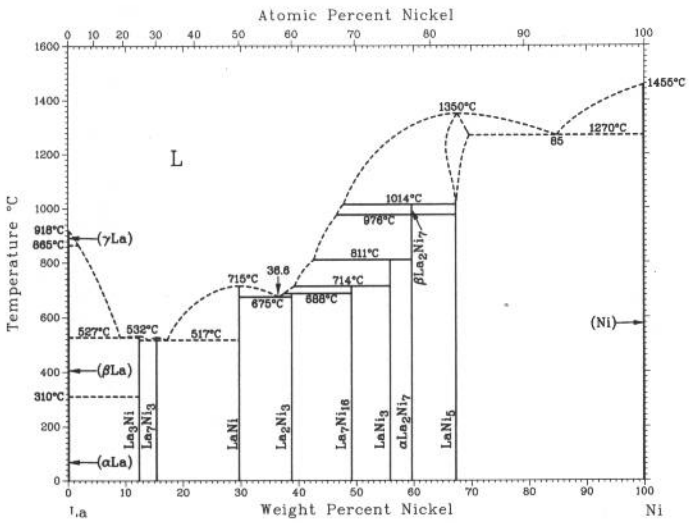

Phase	Composition, wt% Ni	Pearson symbol	Space group
(γLa)	0	*cI*2	$Im\bar{3}m$
(βLa)	0	*cF*4	$Fm\bar{3}m$
(αLa)	0	*hP*4	$P6_3/mmc$
La_3Ni	12.3	*oP*16	*Pnma*
La_7Ni_3	15.3	*hP*20	$P6_3/mc$
LaNi	29.7	*oC*8	*Cmcm*
La_2Ni_3	39.0	*oC*20	*Cmca*
La_7Ni_{16}	49.2	*tI*46	$I\bar{4}2m$
$LaNi_3$	55.9	*hR*24	$R\bar{3}m$
βLa_2Ni_7	59.7	*hR*18	$R\bar{3}m$
αLa_2Ni_7	59.7	*hP*36	$P6_3/mmc$
$LaNi_5$	67.8	*hP*6	*P6/mmm*
(Ni)	100	*cF*4	$Fm\bar{3}m$
Metastable phase			
$LaNi_2$	66.7	*cF*24	$Fd\bar{3}m$

La-Pb

A. Palenzona and S. Cirafici, 1992

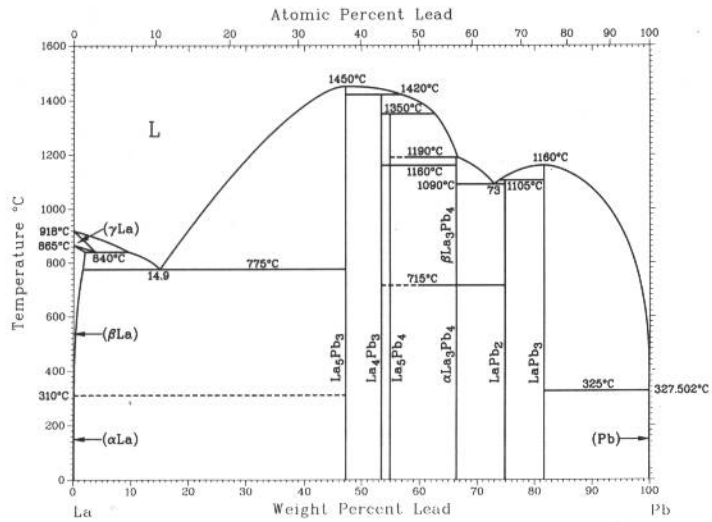

Phase	Composition, wt% Pb	Pearson symbol	Space group
(γLa)	3.7	*cI*2	$Im\bar{3}m$
(βLa)	0 to <1.5	*cF*4	$Fm\bar{3}m$
(αLa)	0	*hP*4	$P6_3/mmc$
La_5Pb_3	47.2	*hP*16	$P6_3/mcm$
La_4Pb_3(a)	52.8	*cI*28	$I\bar{4}3d$
La_5Pb_4	54.4	*oP*36	*Pnma*
βLa_3Pb_4	66.5	...	...
αLa_3Pb_4	66.5	...	...
$LaPb_2$	74.9	...	...
$LaPb_3$	81.7	*cP*4	$Pm\bar{3}m$
(Pb)	~99.9 to 100	*cF*4	$Fm\bar{3}m$

(a) Low-temperature modification

La-S

H.F. Franzen, unpublished

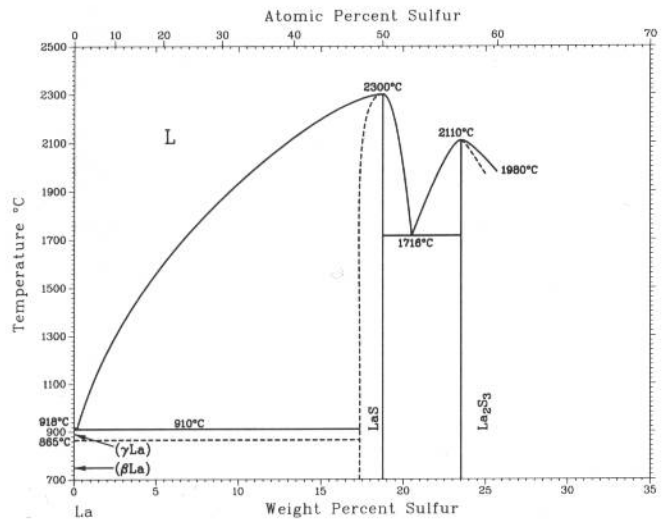

Phase	Composition, wt% S	Pearson symbol	Space group
(γLa)	0	*cI*2	$Im\bar{3}m$
(βLa)	0	*cF*4	$Fm\bar{3}m$
LaS	17 to 18.8	*cF*8	$Fm\bar{3}m$
γLa_2S_3	23.5 to 26	*cI*28	$I\bar{4}3d$

La-Sb

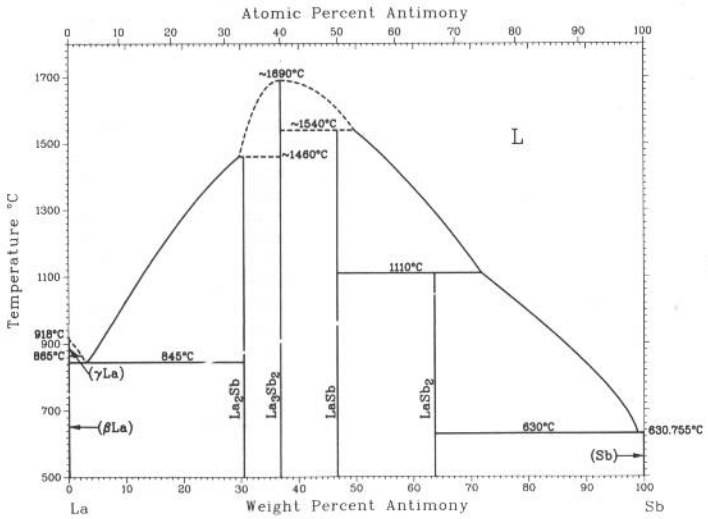

R. Vogel and H. Klose, 1954

Phase	Composition, wt% Sb	Pearson symbol	Space group
(γLa)	~0	*cI*2	$Im\bar{3}m$
(βLa)	~0	*cF*4	$Fm\bar{3}m$
La_2Sb	30.4	*tI*12	*I*4/*mmm*
La_3Sb_2	37	...	...
LaSb	46.7	*cF*8	$Fm\bar{3}m$
$LaSb_2$	63.7	*oC*24	*Cmca*
(Sb)	~100	*hR*2	$R\bar{3}m$
Other reported phases			
La_5Sb_3	34.9	*hP*16	$P6_3/mcm$
La_4Sb_3	39.7	*cI*28	$I\bar{4}3d$

La-Sc

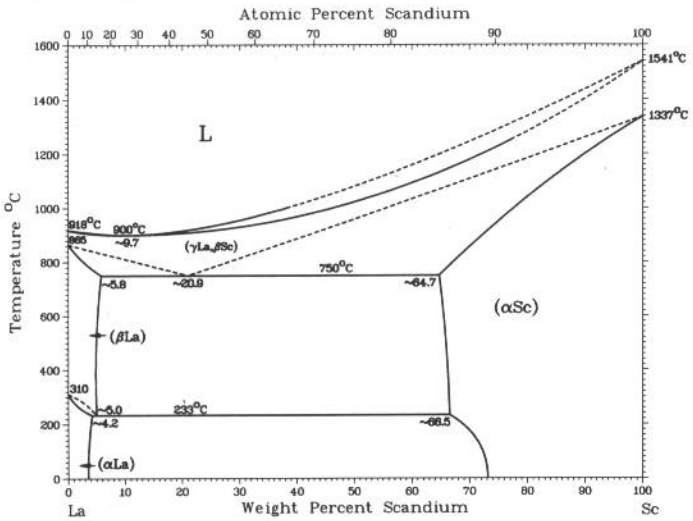

K.A. Gschneidner, Jr. and F.W. Calderwood, 1982

Phase	Composition, wt% Sc	Pearson symbol	Space group
(αLa)	0 to ~4.2	*hP*4	$P6_3/mmc$
(βLa)	0 to ~5.8	*cF*4	$Fm\bar{3}m$
(γLa,βSc)	0 to 100	*cI*2	$Im\bar{3}m$
(αSc)	~64.7 to 100	*hP*2	$P6_3/mmc$

La-Se

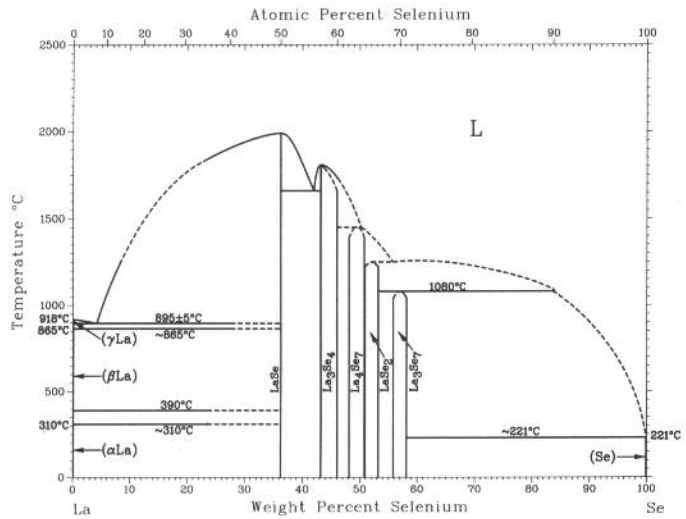

H. Okamoto, 1990

Phase	Composition, wt% Se	Pearson symbol	Space group
(γLa)	0	*cI*2	$Im\bar{3}m$
(βLa)	0	*cF*4	$Fm\bar{3}m$
(αLa)	0	*hP*4	$P6_3/mmc$
LaSe	36.2	*cF*8	$Fm\bar{3}m$
La_3Se_4	43.2 to 46	*cI*28	$I\bar{4}3d$
La_4Se_7	48 to 50.8	*mP*6	*P*2/*c*
$LaSe_2$	50.9 to 53.2	*tP*6	*P*4/*nmm*
La_3Se_7	56 to 58	*t***	...
(Se)	100	*hP*3	$P3_121$

La-Sn

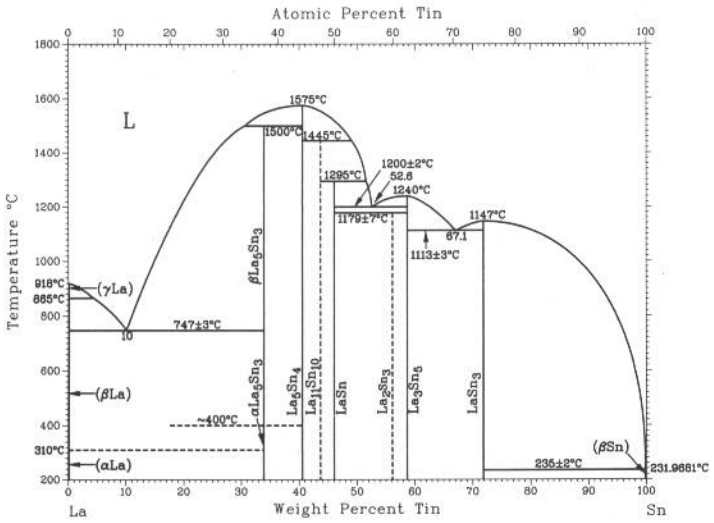

A. Palenzona and S. Cirafici, 1992

Phase	Composition, wt% Sn	Pearson symbol	Space group
γLa(a)	0	*cI*2	$Im\bar{3}m$
βLa(b)	0	*cF*4	$Fm\bar{3}m$
αLa(c)	0	*hP*4	$P6_3/mmc$
La_3Sn(d)	22	*cP*4	$Pm\bar{3}m$
βLa_5Sn_3	33.9	*hP*16	$P6_3/mcm$
αLa_5Sn_3	33.9	*tI*32	*I*4/*mcm*
La_5Sn_4	40.6	*oP*36	*Pnma*
$La_{11}Sn_{10}$(e)	43.7	*tI*84	*I*4/*mmm*
LaSn	46.1	*oC*8	*Cmcm*
La_2Sn_3	56	...	...
La_3Sn_5	58.8	*oC*32	*Cmcm*
$LaSn_3$	72	*cP*4	$Pm\bar{3}m$
βSn(f)	100	*tI*4	$I4_1/amd$
αSn(g)	100	*cF*8	$Fd\bar{3}m$

(a) From 918 to 865 °C. (b) From 865 to 310 °C. (c) Up to 310 °C. (d) High-temperature, high-pressure phase (e) Proposed structure type. (f) From 13 to 231.9681 °C. (g) Up to 13 °C

La-Tl

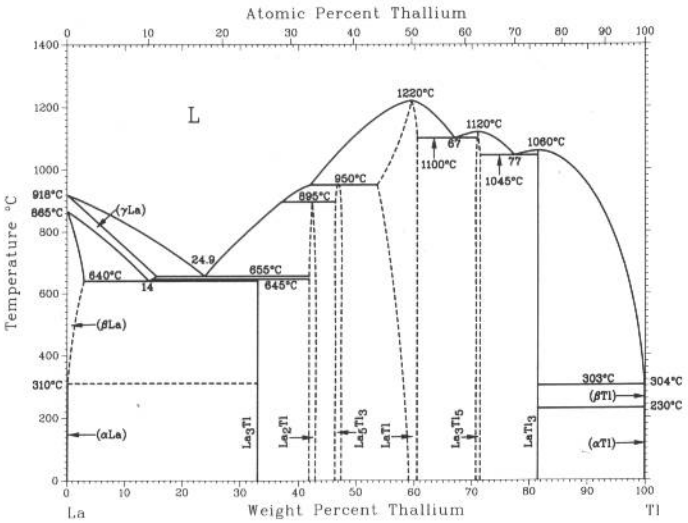

S. Delfino, A. Saccone, A. Palenzona, and R. Ferro, unpublished

Phase	Composition, wt% Tl	Pearson symbol	Space group
(γLa)	15.4	*cI*2	$Im\bar{3}m$
(βLa)	0 to 2.8	*cF*4	$Fm\bar{3}m$
(αLa)	0	*hP*4	$P6_3/mmc$
La_3Tl(a)	33	*cP*4	$Pm\bar{3}m$
	~33	*cF*4	$Fm\bar{3}m$
La_2Tl	~46.9	...	...
La_5Tl_3	~46 to 47	*tI*32	*I*4/*mcm*
LaTl(b)	~54 to ~61	*cP*2	$Pm\bar{3}m$
		*cI*2	$Im\bar{3}m$
LaTl(c)	~54 to ~61	*tP*2	*P*4/*mmm*
La_3Tl_5	~71 to ~72	*oC*32	*Cmcm*
$LaTl_3$	82	*cP*4	$Pm\bar{3}m$
(βTl)	100	*cI*2	$Im\bar{3}m$
(αTl)	100	*hP*2	$P6_3/mmc$

(a) A *cP*4-*cF*4 order-disorder transformation in this phase has been suggested. (b) Cubic structure presumed to be room- and higher-temperature phases. (c) Tetragonal structure presumed to be lower-temperature phase

La-Zn

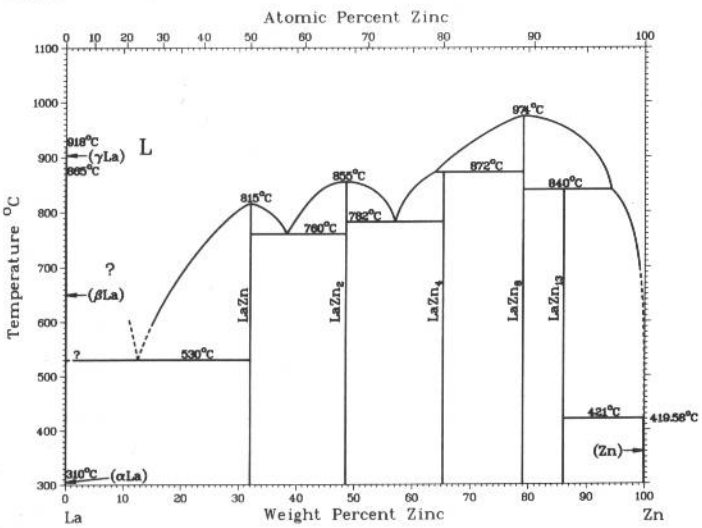

L. Rolla and A. Iandelli, 1941

Phase	Composition, wt% Zn	Pearson symbol	Space group
(γLa)	~0	*cI*2	$Im\bar{3}m$
(βLa)	~0	*cF*4	$Fm\bar{3}m$
(αLa)	~0	*hP*4	$P6_3/mmc$
LaZn	32.0	*cP*2	$Pm\bar{3}m$
$LaZn_2$	~48.5	*oI*12	*Imma*
$LaZn_4$	~65	*oC*20	*Cmcm*
$LaZn_8(La_2Zn_{17})$	~79	*hR*19	$R\bar{3}m$
$LaZn_{13}$	~86.0	*cF*112	$Fm\bar{3}c$
(Zn)	~100	*hP*2	$P6_3/mmc$
Other reported phases			
$LaZn_5$	~70.1	*hP*6	*P*6/*mmm*
La_3Zn_{22}	~78	*tI*100	$I4_1/amd$
$LaZn_{11}$	~83.9	*tI*48	$I4_1/amd$

Li-Mg

A.A. Nayeb-Hashemi, A.D. Pelton, and J.B. Clark, 1988

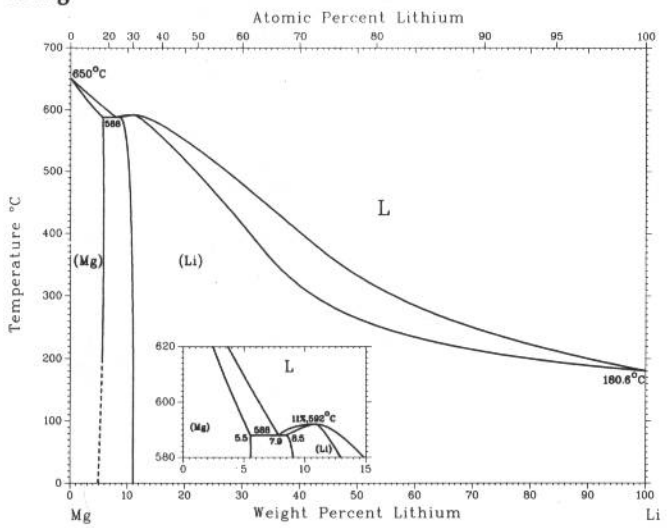

Phase	Composition, wt% Li	Pearson symbol	Space group
(Mg)	0 to 6	*hP*2	$P6_3/mmc$
(βLi)	8.5 to 100	*cI*2	$Im\bar{3}m$
(αLi)(a)	100	*hP*2	$P6_3/mmc$
Cold worked stabilized phase(b)			
(γLi)	100	*cF*4	$Fm\bar{3}m$

(a) Below −193 °C. (b) Nonequilibrium

Li-Na

C.W. Bale, 1989

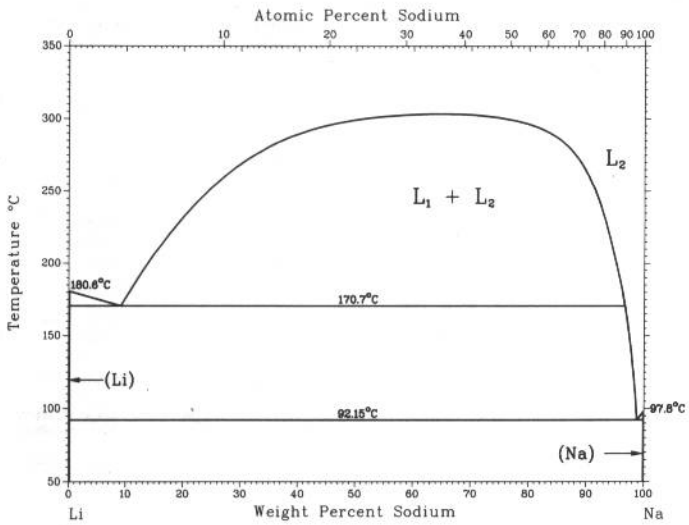

Phase	Composition, wt% Na	Pearson symbol	Space group
(βLi)	0	*cI*2	$Im\bar{3}m$
(αLi)(a)	0	*hP*2	$P6_3/mmc$
(βNa)	100	*cI*2	$Im\bar{3}m$
(αNa)	100	*hP*2	$P6_3/mmc$

(a) Below −193 °C

Li-Pb

From [Hansen]

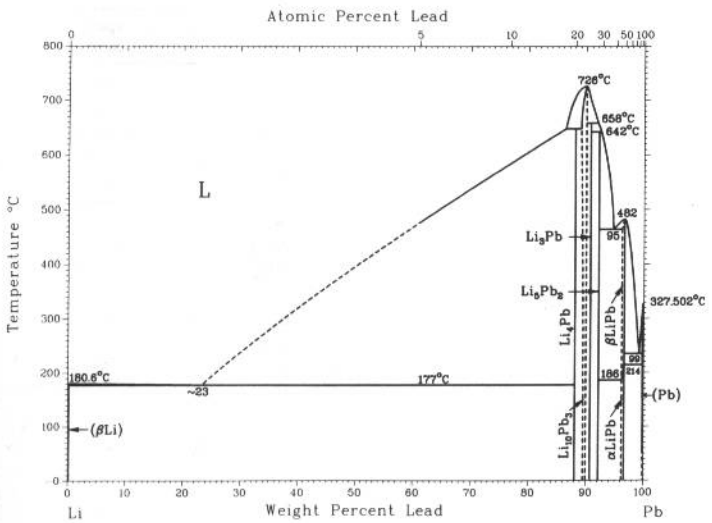

Phase	Composition, wt% Pb	Pearson symbol	Space group
(βLi)	~0	*cI*2	$Im\bar{3}m$
(αLi)(a)	0	*hP*2	$P6_3/mmc$
Li_4Pb	~88	...	...
$Li_{10}Pb_3$	~89.7 to ~90.2	*cP*52	$P\bar{4}3m$
Li_3Pb	~91	*cF*16	$Fm\bar{3}m$
Li_5Pb_2	92.3	...	...
βLiPb	<96 to 96.8	*cP*2	$Pm\bar{3}m$
αLiPb	<96 to 96.8	*hR*2	$R\bar{3}m$
(Pb)	99.9 to 100	*cF*4	$Fm\bar{3}m$
Other reported phases			
$Li_{22}Pb_5$	~87.1	*cF*432	*F*23
Li_7Pb_2	~89.5	*hP*9	*P*321
Li_8Pb_3	~91.8	*mC*22	*C*2/*m*

(a) Below −193 °C

Li-Pd

J. Sangster and A.D. Pelton, 1992

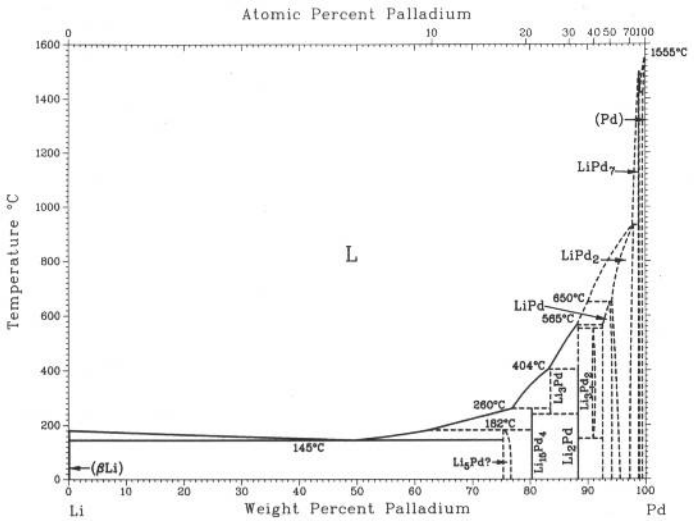

Phase	Composition, wt% Pd	Pearson symbol	Space group
(βLi)	0	*cI*2	$Im\bar{3}m$
(αLi)(a)	0	*hP*2	$P6_3/mmc$
Li_5Pd(b)	75.5(b)	*cF**	...
$Li_{15}Pd_4$	80.4	*cI*76	$I\bar{4}3d$
Li_3Pd	84	*cF*16	$Fm\bar{3}m$
Li_2Pd	88.4	*hP*3	$P6/mmm$
Li_3Pd_2	90.9 to 91.5	*cP*2(?)	$Pm\bar{3}m$
LiPd	92.7 to 94.3	*hP*2	$P\bar{6}$
$LiPd_2$	~94 to 98	*mP*8	$P2/m$
$LiPd_7$	99.1	*cF*32	$Fm\bar{3}m$
(Pd)	99.7 to 100	*cF*4	$Fm\bar{3}m$

(a) Below −193 °C. (b) Approximate composition

Li-S

H. Okamoto, unpublished

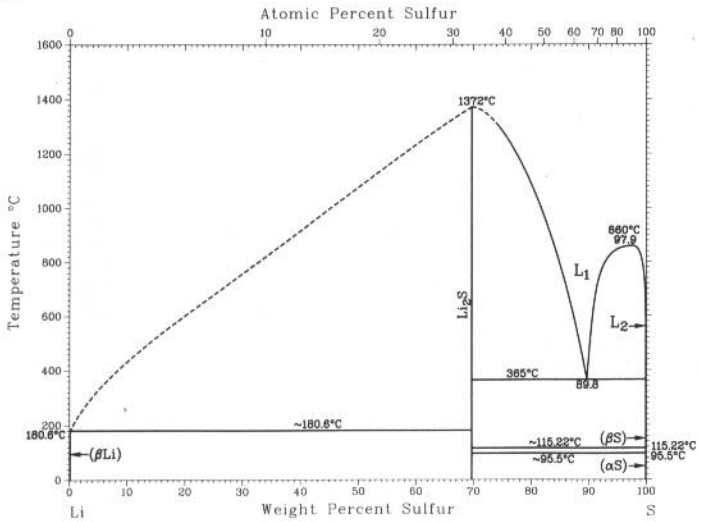

Phase	Composition, wt% S	Pearson symbol	Space group
(βLi)	0	*cI*2	$Im\bar{3}m$
(αLi)(a)	0	*hP*2	$P6_3/mmc$
Li_2S	69.8	*cF*12	$Fm\bar{3}m$
(βS)	100	*mP*48	$P2_1/a$
(αS)	100	*oF*128	*Fddd*

(a) Below −193 °C

Li-Se

P.T. Cunningham, S.A. Johnson, and E.J. Cairns, 1971

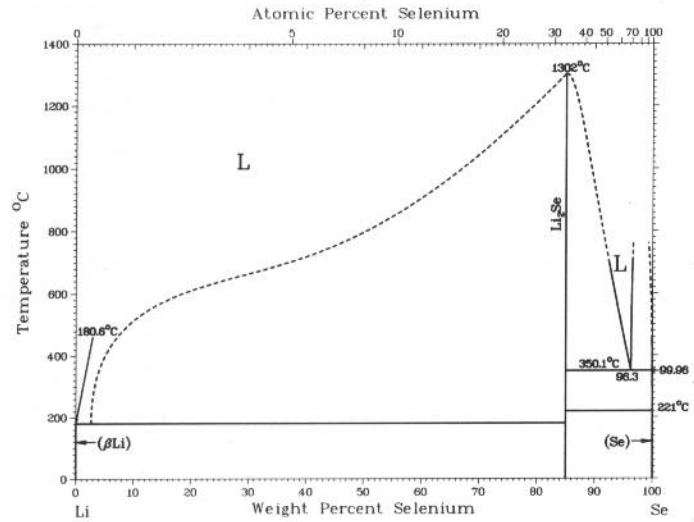

Phase	Composition, wt% Se	Pearson symbol	Space group
(βLi)	~0	*cI*2	$Im\bar{3}m$
(αLi)	0	*hP*2	$P6_3/mmc$
Li_2Se	85.0	*cF*12	$Fm\bar{3}m$
(Se)	~100	*hP*3	$P3_121$

(a) Below −193 °C

Li-Si

H. Okamoto, 1990

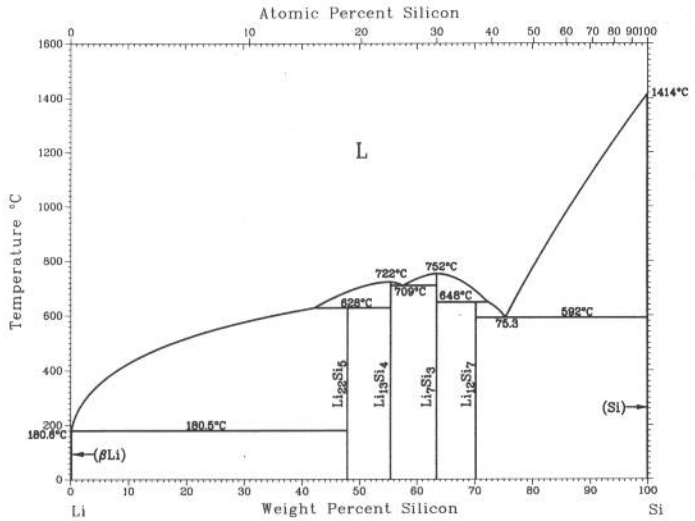

Phase	Composition, wt% Si	Pearson symbol	Space group
(βLi)	0	*cI*2	$Fm\bar{3}m$
(αLi)(a)	0	*hP*2	$P6_3/mmc$
$Li_{22}Si_5$	47.9	*cF*432	*F*23
$Li_{13}Si_4$	55.4	*oP*24	*Pbam*
Li_7Si_3	63	*hR*7	$R\bar{3}m$
$Li_{12}Si_7$	70.2	*oP*152	*Pnma*
(Si)	100	*cF*8	$Fd\bar{3}m$
Questionable phases			
Li_4Si	50	*oP*250	?
Li_7Si_2	53.6	*oP*36	*Pbam*
$Li_{10}Si_3$	54.9	*cF*416	?
Li_2Si	66.9	*mC*12	*C*2/*m*
$Li_{13}Si_7$	69	*oP*160	*Pnma*

(a) Below –193 °C

Li-Sn

From [Moffatt]

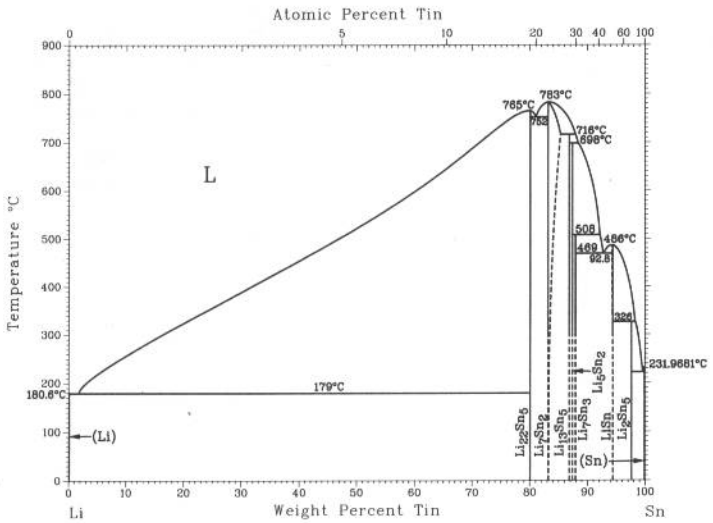

Phase	Composition, wt% Sn	Pearson symbol	Space group
(βLi)	0	*cI*2	$Im\bar{3}m$
(αLi)(a)	0	*hP*2	$P6_3/mmc$
$Li_{22}Sn_5$	79.5	*cF*432	*F*23
Li_7Sn_2	83.0 to ?	*oC*36	*Cmmm*
$Li_{13}Sn_5$	86.8	*hP*18	$P\bar{3}m1$
Li_5Sn_2	87.3	*hR*7	$R\bar{3}m$
Li_7Sn_3	88	*mP*20	$P2_1/m$
LiSn	94.5	*mP*6	*P*2/*m*
Li_2Sn_5	97.7	*tI*14	*P*4/*mbm*
(βSn)	100	*tI*4	$I4_1/amd$
(αSn)	100	*cF*8	$Fd\bar{3}m$

(a) Below –193 °C

Li-Sr

C.W. Bale and A.D. Pelton, 1989

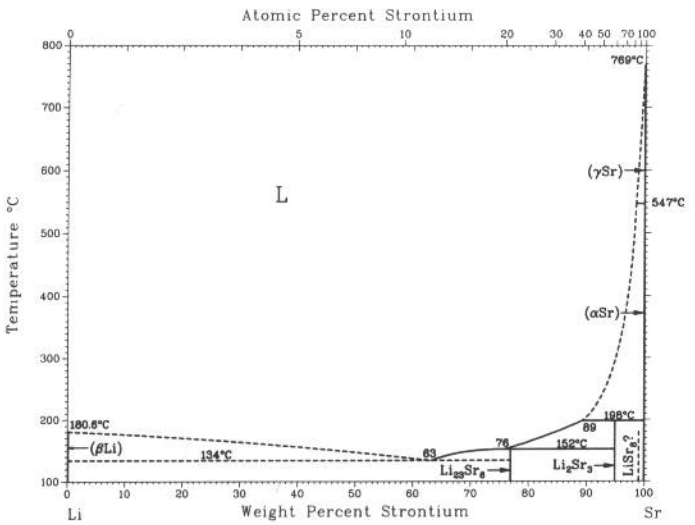

Phase	Composition, wt% Sr	Pearson symbol	Space group
(βLi)	0	*cI*2	$Im\bar{3}m$
(αLi)(a)	0	*hP*2	$P6_3/mmc$
$Li_{23}Sr_6$	76.7	*cF*116	$Fm\bar{3}m$
Li_2Sr_3	95	*tP*20	$P4_2/mnm$
$LiSr_7$(?)	98.9	*t***	...
$LiSr_8$(?)	99.0	*t***	...
		*hP**	...
(γSr)	100	*cI*2	$Im\bar{3}m$
(αSr)	100	*cF*4	$Fm\bar{3}m$

(a) Below –193 °C

Li-Te

J. Sangster and A.D. Pelton, 1992

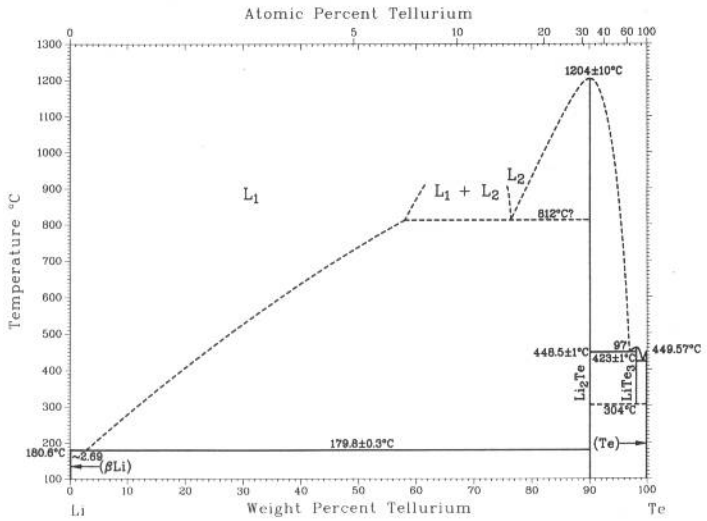

Phase	Composition, wt% Te	Pearson symbol	Space group
(βLi)	0	*cI*2	$Im\bar{3}m$
(αLi)(a)	0	*hP*2	$P6_3/mmc$
Li_2Te	90.2	*cF*12	$Fm\bar{3}m$
$LiTe_3$	98.2	*hP*48(b)	$P\bar{3}c1$
(αTe)	100	*hP*3	$P3_121$

(a) Below −193 °C. (b) Rhombohedrally centered hexagonal supercell, which is imposed on a cubic pseudocell

Li-Tl

G. Grube and G. Schaufler, 1934

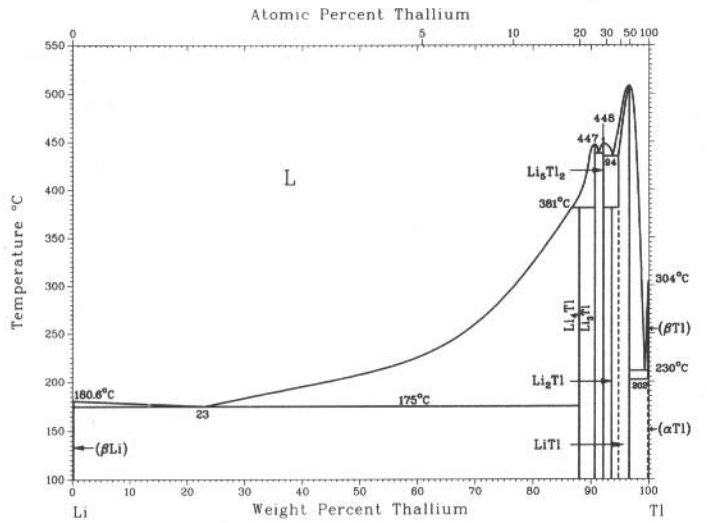

Phase	Composition, wt% Tl	Pearson symbol	Space group
(βLi)	~0	*cI*2	$Im\bar{3}m$
(αLi)(a)	0	*hP*2	$P6_3/mmc$
Li_4Tl	88	...	...
Li_3Tl	91	*cF*16	$Fm\bar{3}m$
Li_5Tl_2	~92.1	*hR*7	$R\bar{3}m$
Li_2Tl	93.6	*oC*12	*Cmcm*
LiTl	~94.9 to 96.7	*cP*2	$Pm\bar{3}m$
(βTl)	>99.9 to 100	*cI*2	$Im\bar{3}m$
(αTl)	~99.9 to 100	*hP*2	$P6_3/mmc$
Other reported phase			
$Li_{22}Tl_5$	87.0	*cF*432	*F*23

(a) Below −193 °C

Li-Zn

A.D. Pelton, 1991

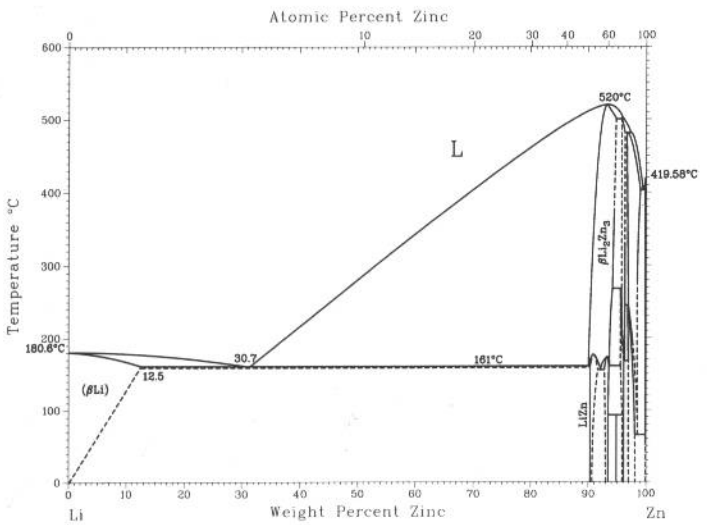

Phase	Composition, wt% Zn	Pearson symbol	Space group
(βLi)	0 to 12.5	*cI*2	$Im\bar{3}m$
(αLi)(a)	0	*hP*2	$P6_3/mmc$
LiZn	~90.4 to 92	*cF*16	$Fd\bar{3}m$
βLi_2Zn_3	~90.4 to 95	...	...
αLi_2Zn_3	~93 to 93	*c***?	...
$LiZn_2$	94.97	...	...
βLi_2Zn_5(b)	95.8 to 99.1	...	...
αLi_2Zn_5(b)	95.6 to 96.2	*h***(c)	...
$\beta LiZn_4$	~96.6 to 98.8	*hP*2	$P6_3/mmc$(d)
$\alpha LiZn_4$	~96.9 to 98.2	*h***(e)	...
(Zn)	99.9 to 100	*hP*2	$P6_3/mmc$

(a) Below −193 °C. (b) Possibly Li_3Zn_8 is a better designation. (c) Pseudocell. (d) Disordered—random distribution. (e) Ordered

Lu-Pb

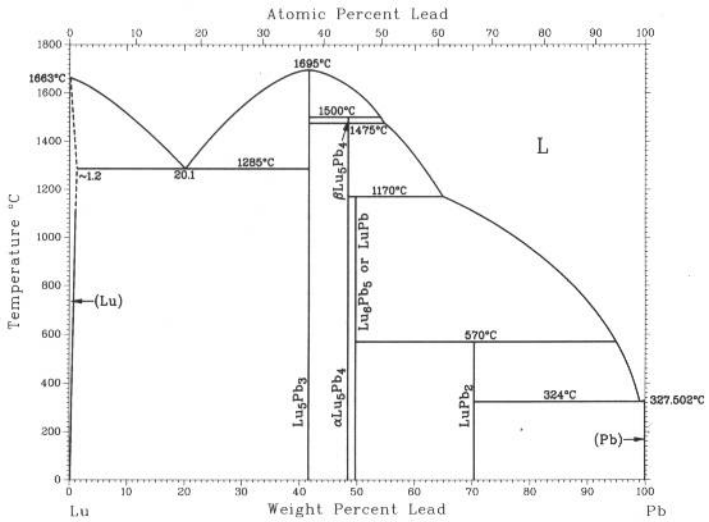

O.D. McMasters and K.A. Gschneidner, Jr., 1969

Phase	Composition, wt% Pb	Pearson symbol	Space group
(Lu)	0 to ~1.2	*hP*2	$P6_3/mmc$
Lu_5Pb_3	41.5	*hP*16	$P6_3/mcm$
βLu_5Pb_4	48.6	...	...
αLu_5Pb_4	48.6	*oP**	*Pnma*
Lu_6Pb_5 or LuPb	49.7	*oI**	*Ibam*
$LuPb_2$	70.3	*tI*6	$I4/mmm$
(Pb)	~100	*cF*4	$Fm\bar{3}m$

Lu-Tl

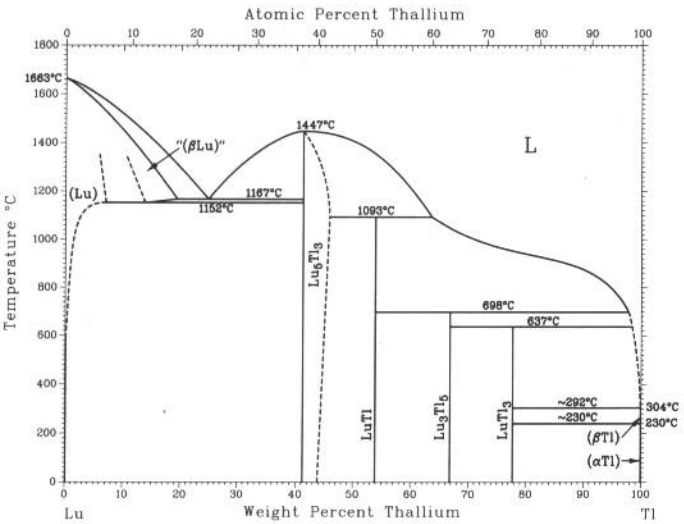

H. Okamoto, 1990

Phase	Composition, wt% Tl	Pearson symbol	Space group
(Lu)	~0	*hP*6	$P6_3/mmc$
Lu_5Tl_3	41.2	*hP*16	$P6_3/mcm$
LuTl	53.9	...	...
Lu_3Tl_5	66.1	*oC*32	*Cmcm*
$LuTl_3$	78	*cP*4	$Pm\bar{3}m$
(βTl)	~100	*cI*2	$Im\bar{3}m$
(αTl)	~100	*hP*2	$P6_3/mmc$

Mg-Mn

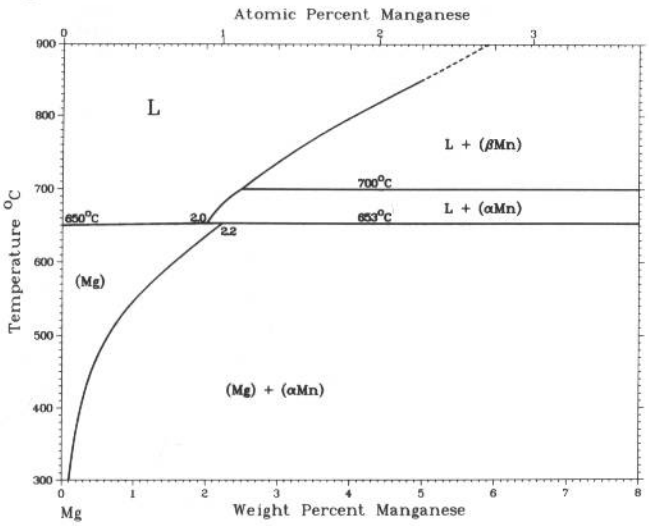

A.A. Nayeb-Hashemi and J.B. Clark, 1988

Phase	Composition, wt% Mn	Pearson symbol	Space group
(Mg)	0 to 2.2	*hP*2	$P6_3/mmc$
(αMn)	100	*cI*58	$I\bar{4}3m$
(βMn)	100	*cP*20	$P4_132$
(γMn)	100	*cF*4	$Fm\bar{3}m$
(δMn)	100	*cI*2	$Im\bar{3}m$

Mg-Ni

A.A. Nayeb-Hashemi and J.B. Clark, 1991

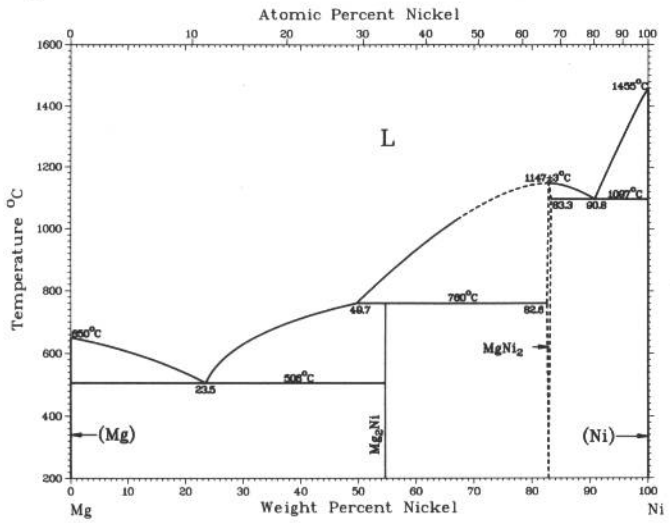

Phase	Composition, wt% Ni	Pearson symbol	Space group
(Mg)	0	*hP*2	$P6_3/mmc$
Mg_2Ni	54.7	*hP*18	$P6_222$
$MgNi_2$	82.9	*hP*24	$P6_3/mmc$
(Ni)	100	*cF*4	$Fm\bar{3}m$

Mg-Pb

A.A. Nayeb-Hashemi and J.B. Clark, 1988

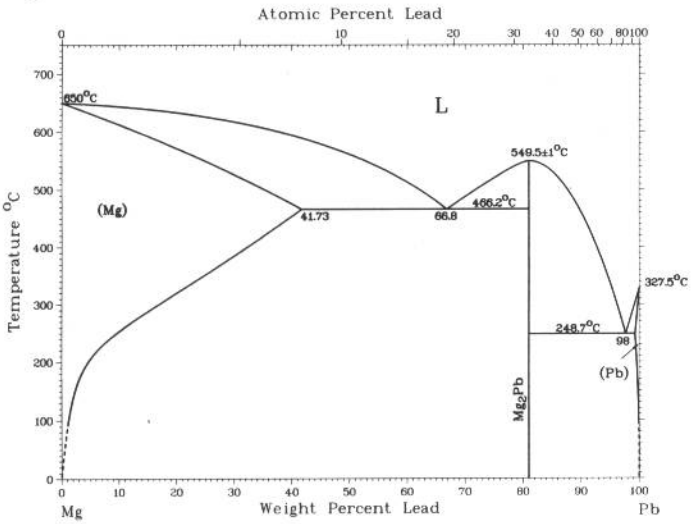

Phase	Composition, wt% Pb	Pearson symbol	Space group
(Mg)	0 to 41.73	*hP*2	$P6_3/mmc$
Mg_2Pb	81.00	*cF*12	$Fm\bar{3}m$
(Pb)	~99 to 100	*cF*4	$Fm\bar{3}m$

Mg-Sb

A.A. Nayeb-Hashemi and J.B. Clark, 1988

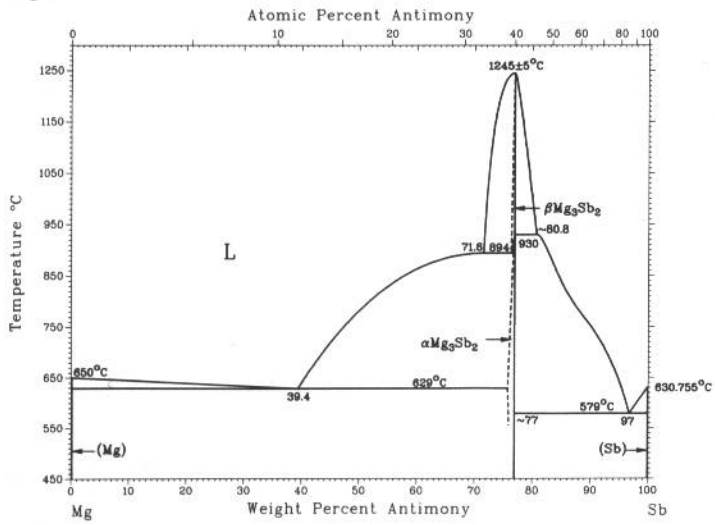

Phase	Composition, wt% Sb	Pearson symbol	Space group
(Mg)	0	*hP*2	$P6_3/mmc$
βMg_3Sb_2	~77	*cI*80	$Ia\bar{3}$
αMg_3Sb_2	~77	*hP*5	$P\bar{3}m1$
(Sb)	100	*hR*2	$R\bar{3}m$

Mg-Sc

A.A. Nayeb-Hashemi and J.B. Clark, 1988

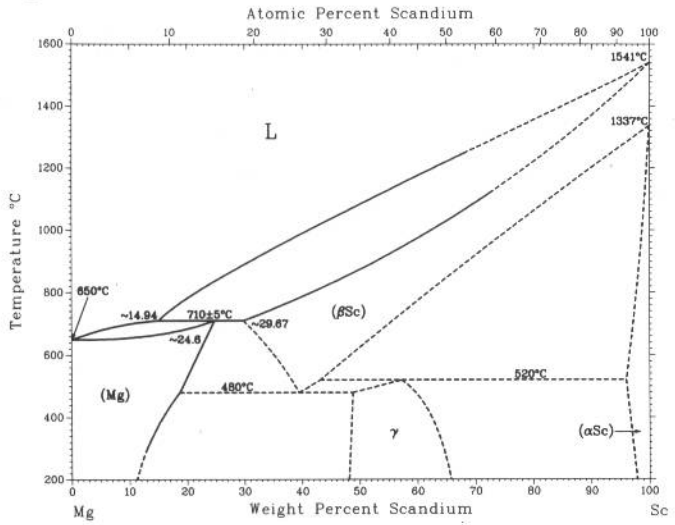

Phase	Composition, wt% Sc	Pearson symbol	Space group
(Mg)	0 to ~24.6	*hP*2	$P6_3/mmc$
γ	? to ?	*cP*2	$Pm\bar{3}m$
(βSc)	~29.67 to 100	*cI*2	$Im\bar{3}m$
(αSc)	? to 100	*hP*2	$P6_3/mmc$

Mg-Si

A.A. Nayeb-Hashemi and J.B. Clark, 1988

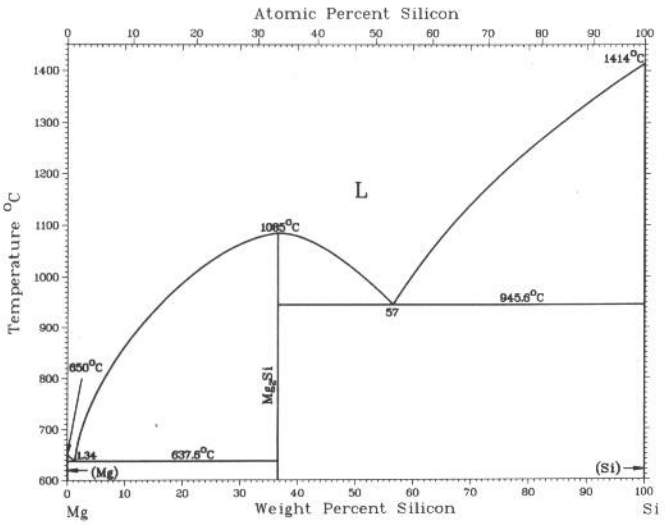

Phase	Composition, wt% Si	Pearson symbol	Space group
(Mg)	~0	*hP*2	$P6_3/mmc$
Mg_2Si	36.61	*cF*12	$Fm\bar{3}m$
(Si)	~100	*cF*8	$Fd\bar{3}m$
High-pressure phases			
Mg_2Si(a)	36.61	...	...
SiII	100	...	...

(a) Above ~2.5 GPa and 900 °C, it forms a hexagonal structure.

Mg-Sm

A.A. Nayeb-Hashemi and J.B. Clark, 1988

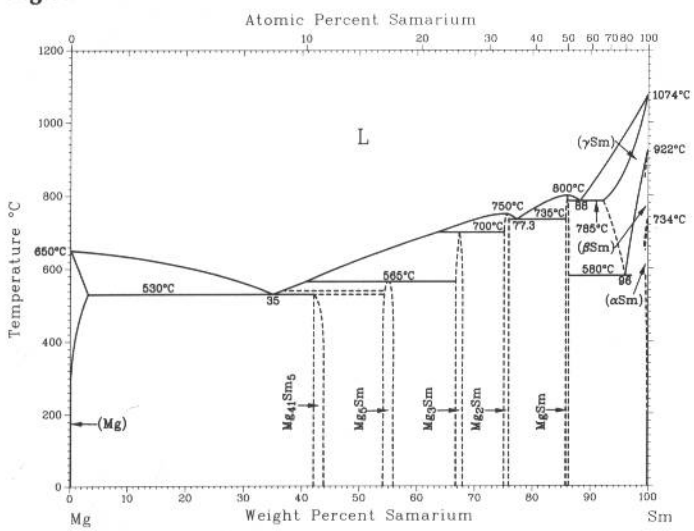

Phase	Composition, wt% Sm	Pearson symbol	Space group
(Mg)	0 to ~6	*hP*2	$P6_3/mmc$
$Mg_{41}Sm_5$	43.1	*tI*92	$I4/m$
Mg_5Sm	55.4	*cF*440-448	$F\bar{4}3m$
Mg_3Sm	67	*cF*16	$Fm\bar{3}m$
Mg_2Sm	75.57	*cF*24	$Fd\bar{3}m$
MgSm	86.1	*cP*2	$Pm\bar{3}m$
(γSm)	~96 to 100	*cI*2	$Im\bar{3}m$
(βSm)	100	*hP*2	$P6_3/mmc$
(αSm)	100	*hR*3	$R\bar{3}m$

Mg-Sn

A.A. Nayeb-Hashemi and J.B. Clark, 1988

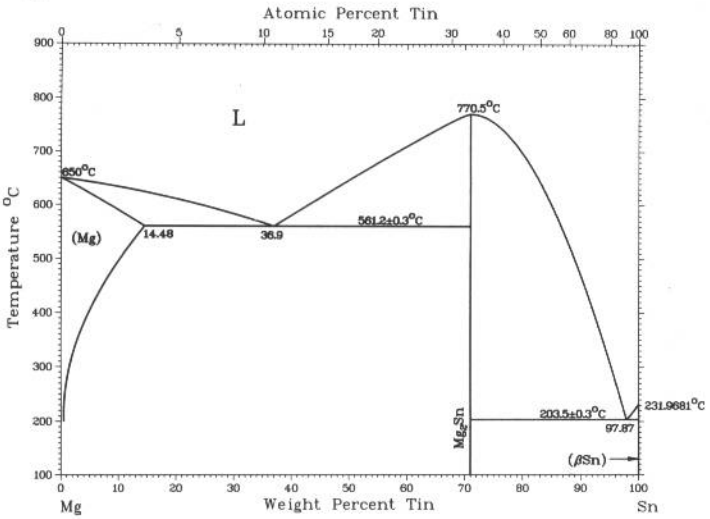

Phase	Composition, wt% Sn	Pearson symbol	Space group
(Mg)	0 to 14.48	*hP*2	$P6_3/mmc$
Mg_2Sn	70.9	*cF*12	$Fm\bar{3}m$
(βSn)	100	*tI*4	$I4_1/amd$
(αSn)	100	*cF*8	$Fd\bar{3}m$
High-pressure phases			
Mg_2Sn	70.9	*h***	...
SnII	100	*tI*2	...
SnIII	100	*cI*2	...

Mg-Sr

A.A. Nayeb-Hashemi and J.B. Clark, 1988

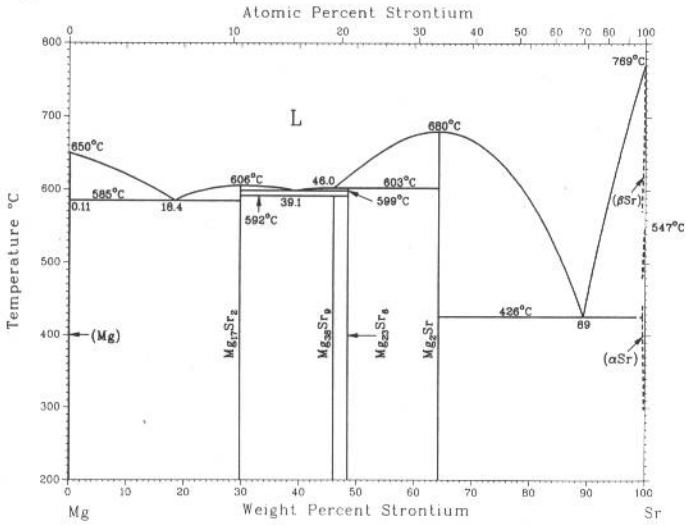

Phase	Composition, wt% Sr	Pearson symbol	Space group
(Mg)	0 to 0.11	*hP*2	$P6_3/mmc$
$Mg_{17}Sr_2$	29.79	*hP*38	$P6_3/mmc$
$Mg_{38}Sr_9$ or Mg_4Sr	46.06	*hP*94 or *hP*90	$P6_3/mmc$
$Mg_{23}Sr_6$	48.47	*cF*116	$Fm\bar{3}m$
Mg_2Sr	64.31	*hP*12	$P6_3/mmc$
(γSr)	100	*cI*2	$Im\bar{3}m$
(αSr)	? to 100	*cF*4	$Fm\bar{3}m$

Mg-Th

A.A. Nayeb-Hashemi and J.B. Clark, 1988

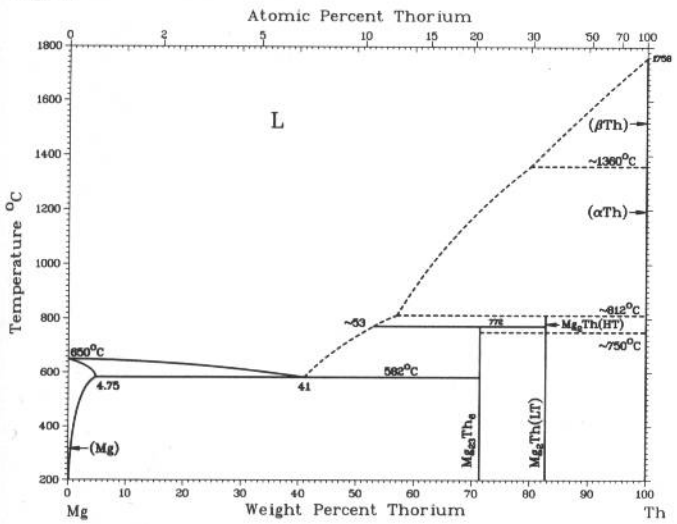

Phase	Composition, wt% Th	Pearson symbol	Space group
(Mg)	0 to 4.75	*hP*2	$P6_3/mmc$
$Mg_{23}Th_6$	71.35	*cF*116	$Fm\bar{3}m$
Mg_2Th (HT)	82.68	*cF*4	$Fd\bar{3}m$
Mg_2Th (LT)	82.68	*hP*4	$P6_3/mmc$
(βTh)	100	*cI*2	$Im\bar{3}m$
(αTh)	100	*cF*4	$Fm\bar{3}m$

Mg-Tl

A.A. Nayeb-Hashemi and J.B. Clark, 1988

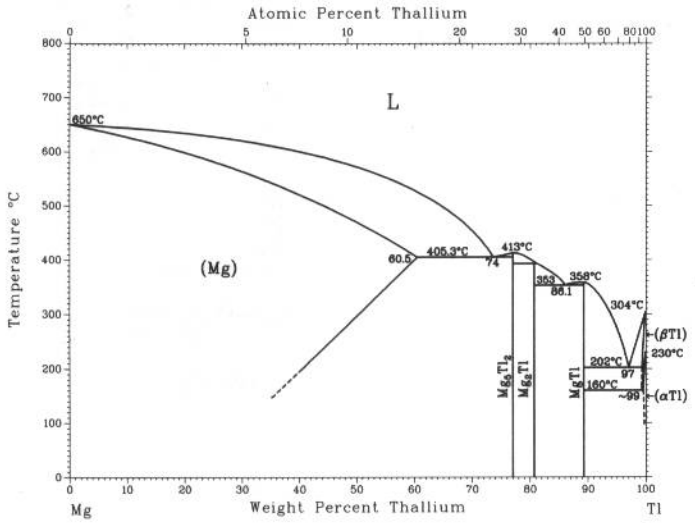

Phase	Composition, wt% Tl	Pearson symbol	Space group
(Mg)	0 to 60.5	*hP*2	$P6_3/mmc$
Mg_5Tl_2	77.08	*oI*28	*Ibam*
Mg_2Tl	80.78	*hP*9	$P\bar{6}2m$
MgTl	89.4	*cP*2	$Pm\bar{3}m$
(βTl)	100	*cI*2	$Im\bar{3}m$
(αTl)	100	*hP*2	$P6_3/mmc$

Mg-Y

H. Okamoto, 1991

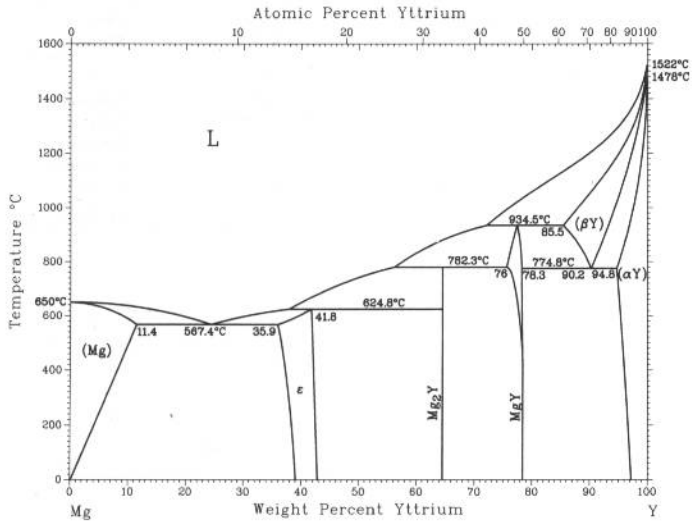

Phase	Composition, wt% Y	Pearson symbol	Space group
(Mg)	0 to 11.4	*hP*2	$P6_3/mmc$
ε	35.9 to 41.8	*cI*58	$I\bar{4}3m$
Mg_2Y	64.6	*hP*12	$P6_3/mmc$
MgY	76 to 78.3	*cP*2	$Pm\bar{3}m$
(βY)	85.5 to 100	*cI*2	$Im\bar{3}m$
(αY)	94.8 to 100	*hP*2	$P6_3/mmc$

Mg-Yb

A.A. Nayeb-Hashemi and J.B. Clark, 1988

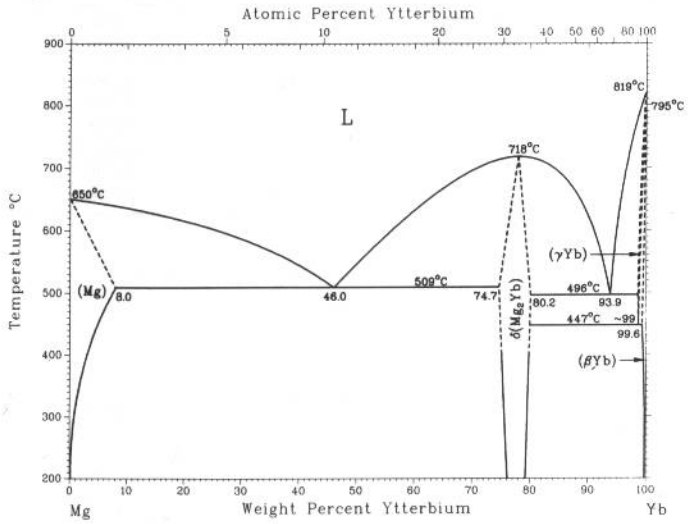

Phase	Composition, wt% Yb	Pearson symbol	Space group
(Mg)	0 to 8.0	*hP*2	$P6_3/mmc$
(δ(Mg_2Yb)	74.7 to 80.2	*hP*12	$P6_3/mmc$
(γYb)	~99 to 100	*cI*2	$Im\bar{3}m$
(βYb)	99.6 to 100	*cF*4	$Fm\bar{3}m$
(αYb)	100	*hP*2	$P6_3/mmc$

Mg-Zn

J.B. Clark, L. Zabdyr, and Z. Moser, 1988

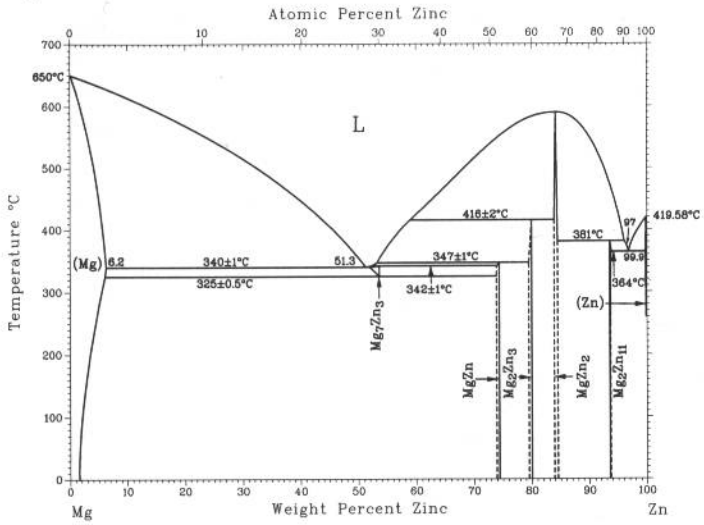

Phase	Composition, wt% Zn	Pearson symbol	Space group
(Mg)	0 to 6.2	*hP*2	$P6_3/mmc$
Mg_7Zn_3	53.6	*oI*142	*Immm*
MgZn	74.0	...	...
Mg_2Zn_3	80.1	*mC*110	*C*2/*m*
$MgZn_2$	84 to 84.6	*hP*12	$P6_3/mmc$
Mg_2Zn_{11}	93.7	*cP*39	$P\bar{m}\bar{3}$
(Zn)	99.9 to 100	*hP*2	$P6_3/mmc$

Mg-Zr

A.A. Nayeb-Hashemi and J.B. Clark, 1988

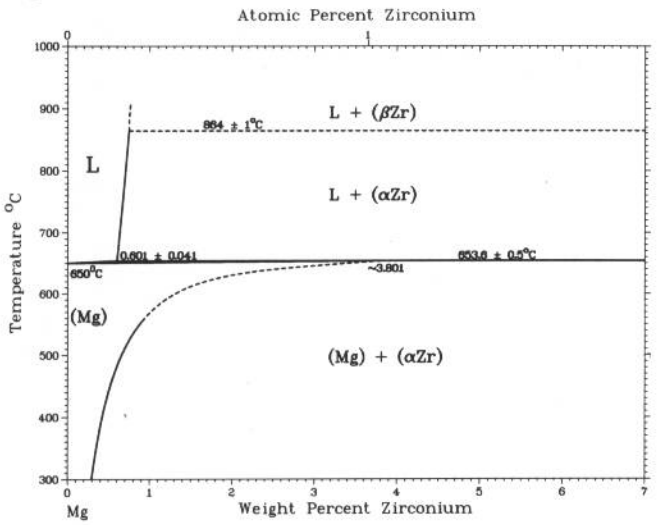

Phase	Composition, wt% Zr	Pearson symbol	Space group
(Mg)	0 to ~3.801	*hP*2	$P6_3/mmc$
(αZr)	100	*hP*2	$P6_3/mmc$
(βZr)	100	*cI*2	$Im\bar{3}m$

Mn-Mo

From [Molybdenum]

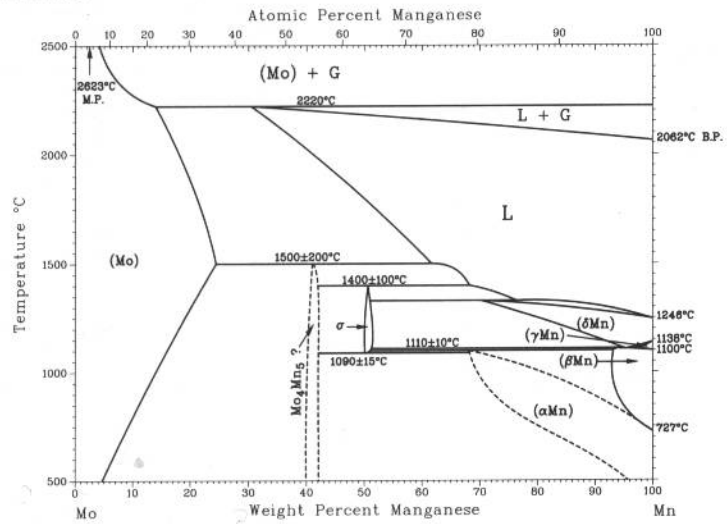

Phase	Composition, wt% Mn	Pearson symbol	Space group
(Mo)	0 to 25	*cI*2	$Im\bar{3}m$
Mo_4Mn_5	~42	*hR*39?	...
σ	~50	*tP*30	$P4_2/mnm$
(δMn)	71 to 100	*cI*2	$Im\bar{3}m$
(γMn)	97 to 100	*cF*4	$Fm\bar{3}m$
(βMn)	78 to 100	*cP*20	$P4_132$
(αMn)	~68 to 100	*cI*58	$I\bar{4}3m$

Mn-N

N.A. Gokcen, 1990

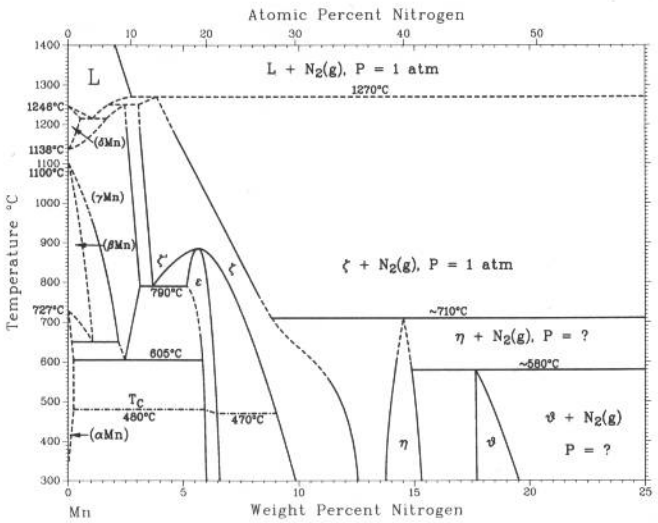

Phase	Composition, wt% N	Pearson symbol	Space group
(δMn)	0 to ~0.5	*cI*2	$Im\bar{3}m$
(γMn)	0 to 3.2	*cF*4	$Fm\bar{3}m$
(βMn)	0 to ~1	*cP*20	$P4_132$
(αMn)	0 to ~0.13	*cI*58	$I\bar{4}3m$
ε or Mn_4N	5.1 to 6.6	*cF*5	$Fm\bar{3}m$
ζ′	~13	*hP*12	$P6_322$
ζ or $Mn_{12}N_5$	~9	*hP*12	$P6_322$
ζ or Mn_2N	11.0	*hP*3	$P6_3/mmc$
ζ or Mn_2N	~11.2	*oP*12	*Pbcn*
η or Mn_6N_4	~14 to 15	...	*I*4/*mmm*
θ or Mn_6N_5	~17.7 to 20	...	...

Mn-Nd

H. Okamoto, 1992

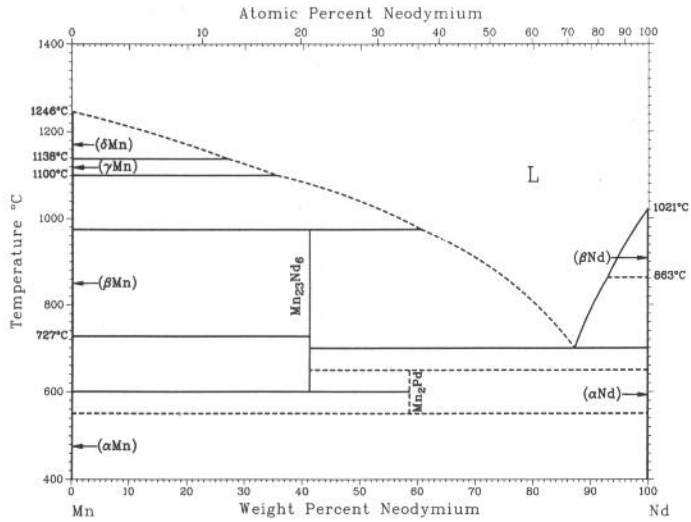

Phase	Composition, wt% Nd	Pearson symbol	Space group
(δMn)	0	*cI*2	$Im\bar{3}m$
(γMn)	0	*cF*4	$Fm\bar{3}m$
(βMn)	0	*cP*20	$P4_132$
(αMn)	0	*cI*58	$I\bar{4}3m$
$Mn_{23}Nd_6$	40.7	*cF*116	*I*4/*mmm*
βMn_2Nd	56.7	*hP*12	$P6_3/mmc$
αMn_2Nd	56.7	*m***	...
(βNd)	100	*cI*2	$Im\bar{3}m$
(αNd)	100	*hP*4	$P6_3/mmc$

Mn-Ni

N.A. Gokcen, 1991

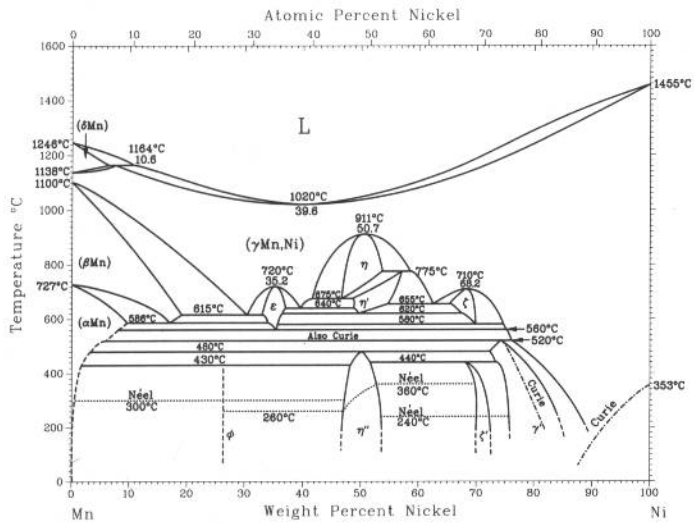

Phase	Composition, wt% Ni	Pearson symbol	Space group
(δMn)	0 to 6	*cI*2	$Im\bar{3}m$
(γMn, Ni)	0 to 100	*cF*4	$Fm\bar{3}m$
(βMn)	0 to 19	*cP*20	$P4_132$
(αMn)	0 to 10	*cI*58	$I\bar{4}3m$
φ	26	...	...
ε	34 to 38	...	...
η(a)	47 to 54	*cP*2	$Pm\bar{3}m$
η′	49 to 57.1	*tP*4	*P*4/*mmm*
ζ	66 to 70	...	...
ζ′	~71	...	...
γ′	72 to 86	*cP*4	$Pm\bar{3}m$

(a) At 745 °C; this phase cannot be retained by quenching.

Mn-O

H. Okamoto, 1990

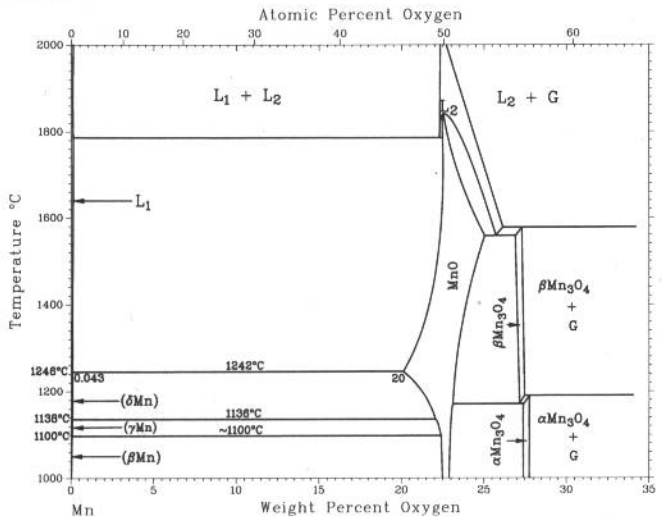

Phase	Composition, wt% O	Pearson symbol	Space group
(δMn)	0	*cI*2	$Im\bar{3}m$
(γMn)	0	*cF*4	$Fm\bar{3}m$
(βMn)	0	*cP*20	$P4_132$
(αMn)	0	*cI*58	$I\bar{4}3m$
MnO	20 to 25	*cF*8	$Fm\bar{3}m$
βMn_3O_4	~28	...	...
αMn_3O_4	~28	*tI*28	$I4_1/amd$

Mn-P

J. Berak and T. Heumann, 1950

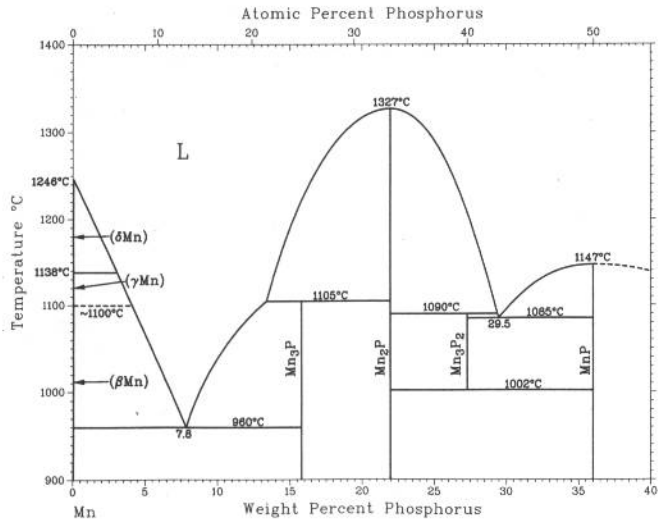

Phase	Composition, wt% P	Pearson symbol	Space group
(δMn)	~0	*cI*2	$Im\bar{3}m$
(γMn)	~0	*cF*4	$Fm\bar{3}m$
(βMn)	~0	*cP*20	$P4_132$
Mn_3P	16	*tI*32	$I\bar{4}$
Mn_2P	22.0	*hP*9	$P\bar{6}2m$
Mn_3P_2	27	...	...
MnP	36.1	*oP*8	*Pnma*
Other reported phase			
MnP_4	69	*aP*10	$P\bar{1}$
		*aP*30	$P\bar{1}$

Mn-Pd

From [Hansen]

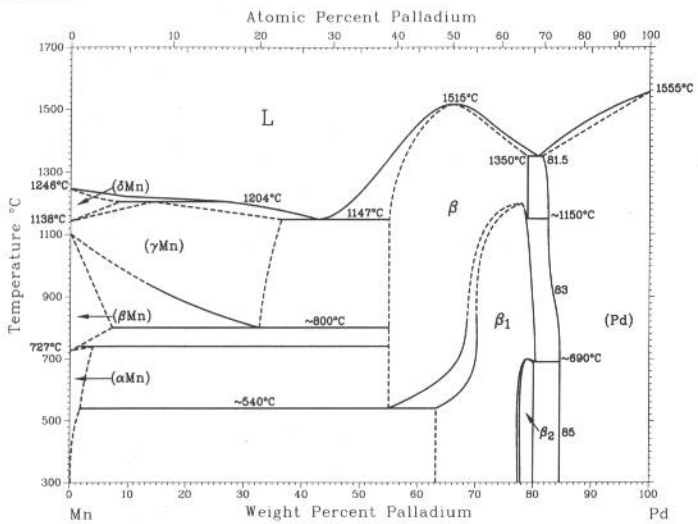

Phase	Composition, wt% Pd	Pearson symbol	Space group
(δMn)	0 to ~9	*cI*2	$Im\bar{3}m$
(γMn)	0 to ~35	*cF*4	$Fm\bar{3}m$
(βMn)	0 to ~8	*cP*20	$P4_132$
(αMn)	0 to ~4	*cI*58	$I\bar{4}3m$
β(MnPd)	~54 to <79	*cP*2	$Pm\bar{3}m$
β_1	~63 to <81	...	...
β_2	~77.5 to 80.1	...	...
(Pd)	81.5 to 100	*cF*4	$Fm\bar{3}m$
Other reported phases			
Mn_2Pd_3(HT)	~74	*tP*2	*P4/mmm*
Mn_2Pd_3(LT)	~74	*t***	...
Mn_3Pd_5	~76.4	*oC*16	*Cmmm*
$Mn_{11}Pd_{21}$	~78.6	*tP*32	*P4/mmm*
$MnPd_3$	85	*tI*16	*I4mm*

Mn-Pr

H. Okamoto, 1990

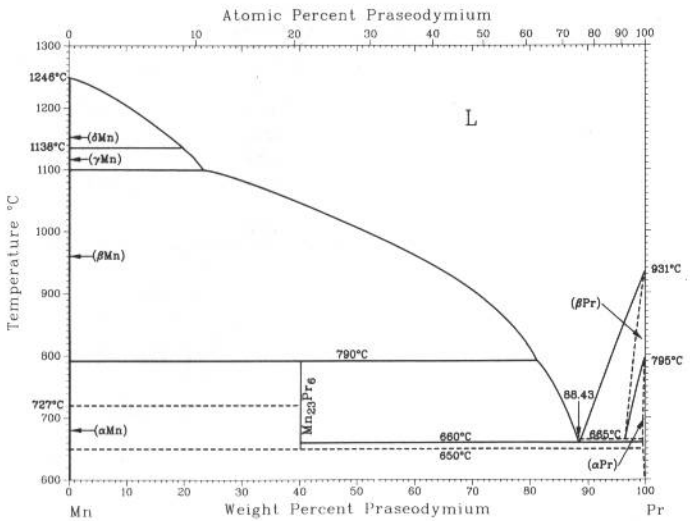

Phase	Composition, wt% Pr	Pearson symbol	Space group
(δMn)	0	*cI*2	$Im\bar{3}m$
(γMn)	0	*cF*4	$Fm\bar{3}m$
(βMn)	0	*cP*20	$P4_132$
(αMn)	0	*cI*58	$I\bar{4}3m$
$Mn_{23}Pr_6$	40.1	*cF*116	$Fm\bar{3}m$
(βPr)	~96.5 to 100	*cI*2	$Im\bar{3}m$
(αPr)	? to 100	*hP*4	$P6_3/mmc$
Metastable phase			
Mn_2Pr	56.1	*hP*12	$P6_3/mmc$

Mn-Pu

S.T. Konobeevsky, 1955

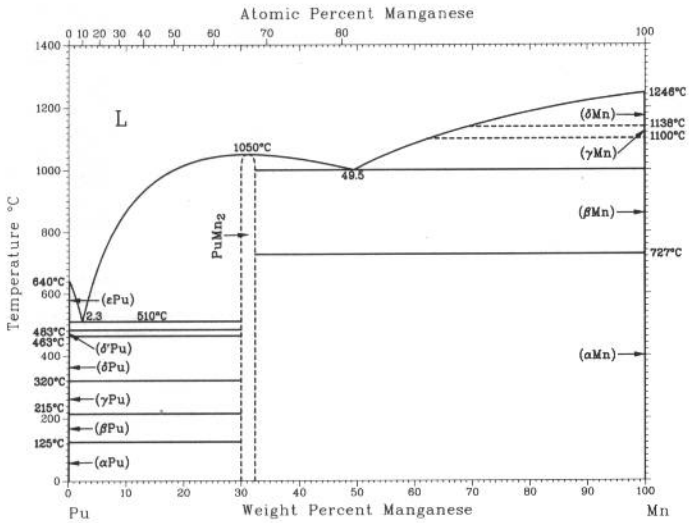

Phase	Composition, wt% Mn	Pearson symbol	Space group
(εPu)	~0	*cI*2	$Im\bar{3}m$
(δ'Pu)	~0	*tI*2	*I*4/*mmm*
(δPu)	~0	*cF*4	$Fm\bar{3}m$
(γPu)	~0	*oF*8	*Fddd*
(βPu)	~0	*mC*34	*C*2/*m*
(αPu)	~0	*mP*16	$P2_1/m$
$PuMn_2$	~31.1	*cF*24	$Fd\bar{3}m$
(δMn)	~100	*cI*2	$Im\bar{3}m$
(γMn)	~100	*cF*4	$Fm\bar{3}m$
(βMn)	~100	*cP*20	$P4_132$
(αMn)	~100	*cI*58	$I\bar{4}3m$

Mn-Sb

H. Okamoto, 1990

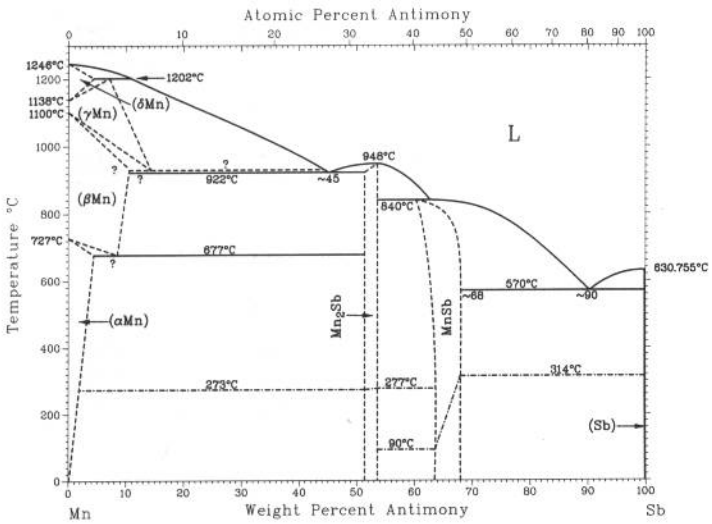

Phase	Composition, wt% Sb	Pearson symbol	Space group
(δMn)	0 to ?	*cI*2	$Im\bar{3}m$
(γMn)	0 to ?	*cF*4	$Fm\bar{3}m$
(βMn)	0 to ?	*cP*20	$P4_132$
(αMn)	0 to ?	*cI*58	$I\bar{4}3m$
Mn_2Sb	~52.5	*tP*6	*P*4/*nmm*
MnSb	~61 to ~68	*hP*4	$P6_3/mmc$
(Sb)	100	*hR*2	$R\bar{3}m$

Mn-Si

H. Okamoto, 1991

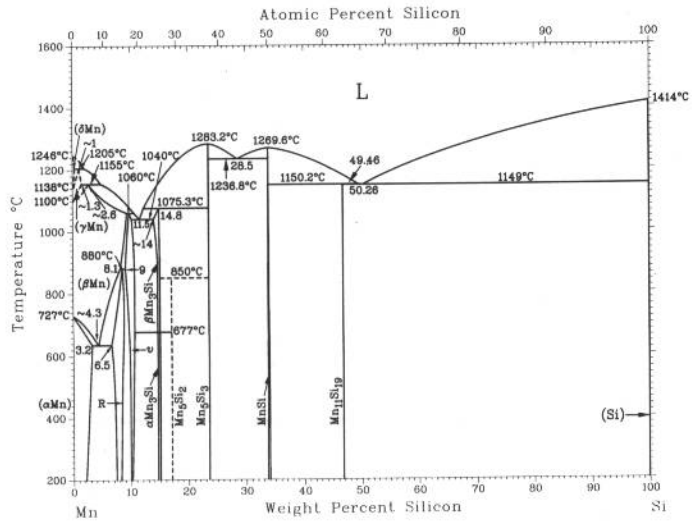

Phase	Composition, wt% Si	Pearson symbol	Space group
(δMn)	0 to ~0.1	*cI*2	$Im\bar{3}m$
(γMn)	0 to ~1.3	*cF*4	$Fm\bar{3}m$
(βMn)	0 to ~9.3	*cP*20	$P4_132$
(αMn)	0 to 3.2	*cI*58	$I\bar{4}3m$
R	6.5 to 8.72	*hR*53	$R\bar{3}$
ν	9.0 to 10.55	*oI*186	*Immm*
βMn_3Si	~14 to 15.0	*cF*16	$Fm\bar{3}m$
αMn_3Si	14.6 to 15.0		
Mn_5Si_2	17.0	*tP*56	$P4_12_12$
Mn_5Si_3	23.5	*hP*16	$P6_3/mcm$
MnSi	33.4 to 34.0	*cP*8	$P2_13$
$Mn_{11}Si_{19}$	~46.9	*tP*120	$P\bar{4}n2$
(Si)	100	*cF*8	$Fd\bar{3}m$

Mn-Sm

H.R. Kirchmayr and W. Lugscheider, 1970

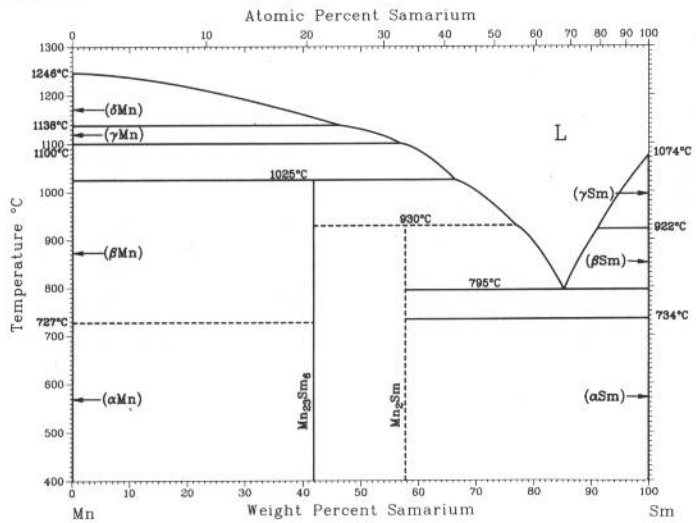

Phase	Composition, wt% Sm	Pearson symbol	Space group
(δMn)	~0	*cI*2	$Im\bar{3}m$
(γMn)	~0	*cF*4	$Fm\bar{3}m$
(βMn)	~0	*cP*20	$P4_132$
(αMn)	~0	*cI*58	$I\bar{4}3m$
$Mn_{23}Sm_6$	~41.7	*cF*116	$Fm\bar{3}m$
Mn_2Sm	57.7	*hP*12	$P6_3/mmc$
		*cF*24	$Fd\bar{3}m$
(δSm)	~100	*cI*2	$Im\bar{3}m$
(βSm)	~100	*hP*2	$P6_3/mmc$
(αSm)	~100	*hR*13	$R\bar{3}m$

Mn-Sn

H. Okamoto, 1990

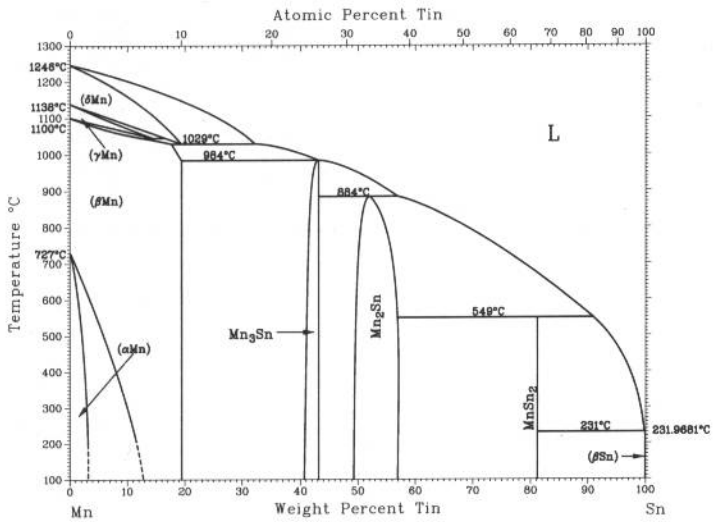

Phase	Composition, wt% Sn	Pearson symbol	Space group
(δMn)	0 to 19	*cI*2	$Im\bar{3}m$
(γMn)	0 to 14	*cF*4	$Fm\bar{3}m$
(βMn)	0 to 21	*cP*20	$P4_132$
(αMn)	0 to 2	*cI*58	$I\bar{4}3m$
Mn_3Sn	41 to 43	*hP*8	$P6_3/mmc$
Mn_2Sn	49 to 57	*hP*6	$P6_3/mmc$
$MnSn_2$	81.2	*tI*12	$I4/mcm$
(βSn)	100	*tI*2	$I4_1/amd$
(αSn)	100	*cF*8	$Fd\bar{3}m$

Mn-Ti

J.L. Murray, 1987

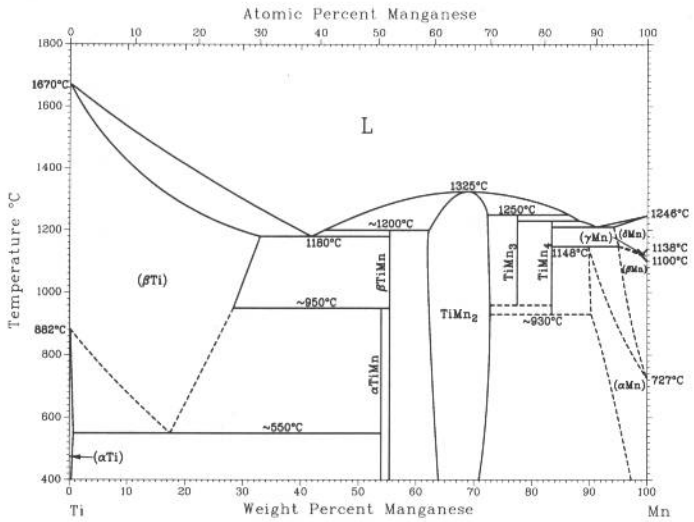

Phase	Composition, wt% Mn	Pearson symbol	Space group
(βTi)	0 to 33	*cI*2	$Im\bar{3}m$
(αTi)	0 to 0.5	*hP*2	$P6_3/mmc$
αTiMn	53.9	*t**58	...
βTiMn	55	(a)	...
$TiMn_2$	63 to 73	*hP*12	$P6_3/mmc$
$TiMn_3$	78	(b)	...
$TiMn_4$	83.5	*hR*53	$R\bar{3}m$
(δMn)	92 to 100	*cI*2	$Im\bar{3}m$
(γMn)	99.5 to 100	*cF*4	$Fm\bar{3}m$
(βMn)	95 to 100	*cP*20	$P4_132$
(αMn)	89 to 100	*cI*58	$I\bar{4}3m$
(α′Ti)	(c)	*hP*2	$P6_3/mmc$
ω	(c)	*hP*3	*P*6/*mmm*

(a) Undetermined. (b) Orthorhombic. (c) Metastable phase

Mn-U

From [Hansen]

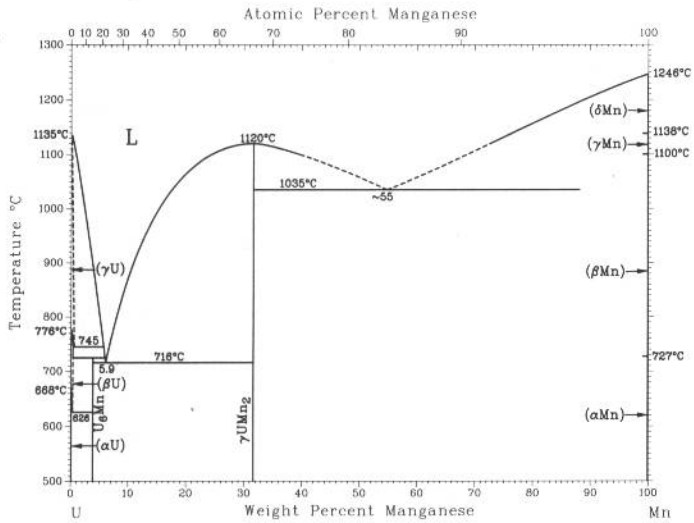

Phase	Composition, wt% Mn	Pearson symbol	Space group
(γU)	0 to ~0.5	*cI*2	$Im\bar{3}m$
(βU)	0 to ~0.4	*tP*30	$P4_2/mnm$
(αU)	~0	*oC*4	*Cmcm*
U_6Mn	~3.7	*tI*28	*I*4/*mcm*
γUMn_2	31.6	*oI*12	*Imma*
βUMn_2	31.6	*cF*24	$Fd\bar{3}m$
αUMn_2	31.6	*mC*24	*C*2/*m*
(δMn)	~100	*cI*2	$Im\bar{3}m$
(γMn)	~100	*cF*4	$Fm\bar{3}m$
(βMn)	~100	*cP*20	$P4_132$
(αMn)	~100	*cI*58	$I\bar{4}3m$

Mn-V

H. Okamoto, 1992

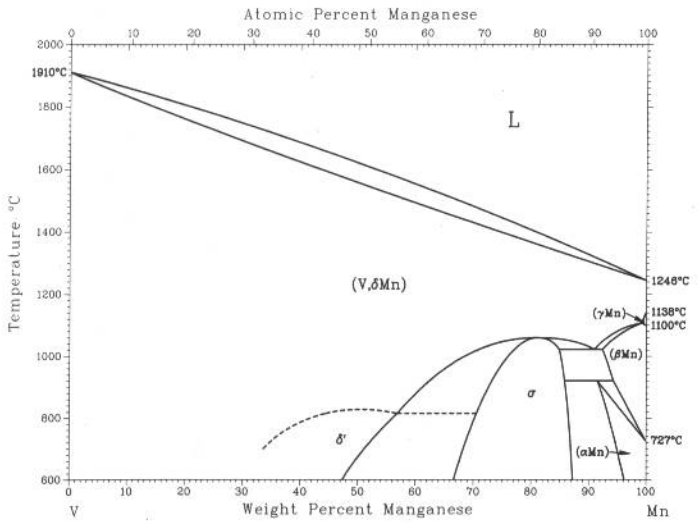

Phase	Composition, wt% Mn	Pearson symbol	Space group
(V, δMn)	0 to 100	*cI*2	$Im\bar{3}m$
δ′	? to ~57	*cP*2	$Pm\bar{3}m$
σ	? to ?	*tP*30	$P4_2/mnm$
(γMn)	99 to 100	*cF*4	$Fm\bar{3}m$
(βMn)	93 to 100	*cP*20	$P4_132$
(αMn)	92 to 100	*cI*58	$I\bar{4}3m$

Mn-Y

A. Palenzona and S. Cirafici, 1991

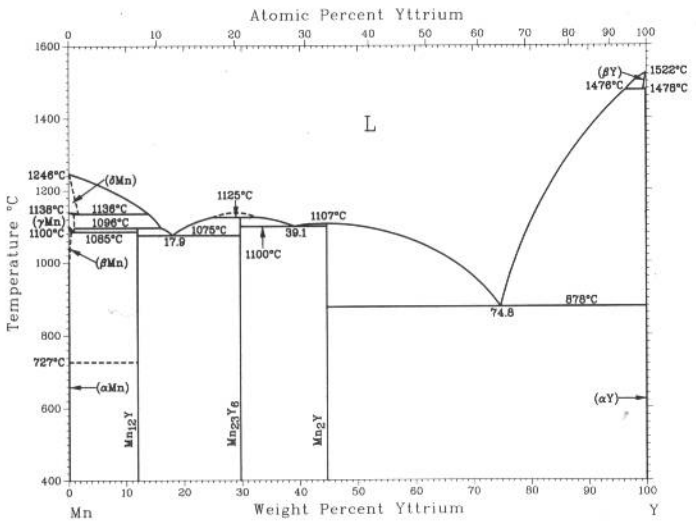

Phase	Composition, wt% Y	Pearson symbol	Space group
(δMn)	0	*cI*2	$Im\bar{3}m$
(γMn)	0	*cF*4	$Fm\bar{3}m$
(βMn)	0	*cP*20	$P4_132$
(αMn)	0	*cI*58	$I\bar{4}3m$
$Mn_{12}Y$	11.9	*tI*26	*I*4/*mmm*
$Mn_{23}Y_6$	29.7	*cF*116	$Fm\bar{3}m$
Mn_2Y	44.7	*cF*24	$Fd\bar{3}m$
(βY)	100	*cI*2	$Im\bar{3}m$
(αY)	100	*hP*2	*P*6$_3$/*mmc*
Other phases			
Mn_2Y(a)	44.7	*hP*12	*P*6$_3$/*mmc*
Mn_2Y(b)	44.7	...	...

(a) Synthesized under high temperature (1300 °C) and high pressure (40 kbar). (b) Distorted tetragonal Cu_2Mg type obtained below 100 K

Mn-Zn

H. Okamoto and L.E. Tanner, 1990

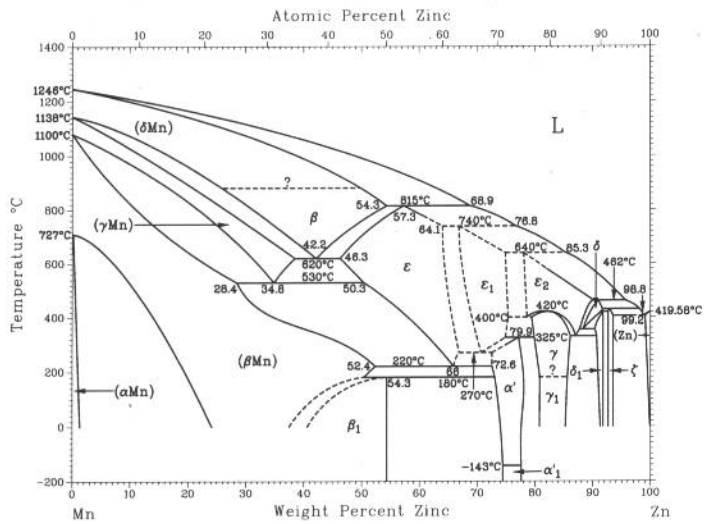

Phase	Composition, wt% Zn	Pearson symbol	Space group
(δMn)	0 to 54.3	*cI*2	$Im\bar{3}m$
(γMn)	0 to 38	*cF*4	$Fm\bar{3}m$
(γMn_1)	0 to ?	*tI*2	*I*4/*mmm*
(βMn)	0 to 52.4	*cP*20	$P4_131$
(αMn)	0 to 2.0	*cI*58	$I\bar{4}3m$
β	? to 54.3	*cP*2	$Pm\bar{3}m$
β_1	47.8 to 54.3	*cP*2	$Pm\bar{3}m$
ε	46.3 to 67	*hP*2	*P*6$_3$/*mmc*
ε_1	67 to 75	*hP*8	*P*6$_3$/*mmc*
ε_2	78 to 90.2	*hP**	...
α′	72.6 to 78	*cP*4	$Pm\bar{3}m$
α_1'	74 to 78	*tP*2	*P*4/*mmm*
γ	79.9 to 86.6	*cI*52	...
γ_1	...	*cI*550 ± 8	...
δ	88.4 to 92.0	*hP**	...
δ_1	90.5 to 92.2	*hP**	...
ζ($MnZn_{13}$)	93.7 to 94.0	*mC*28	*P*2/*m*
(Zn)	99.2 to 100	*hP*2	*P*6$_3$/*mmc*

Mn-Zr

M. Lasocka, unpublished

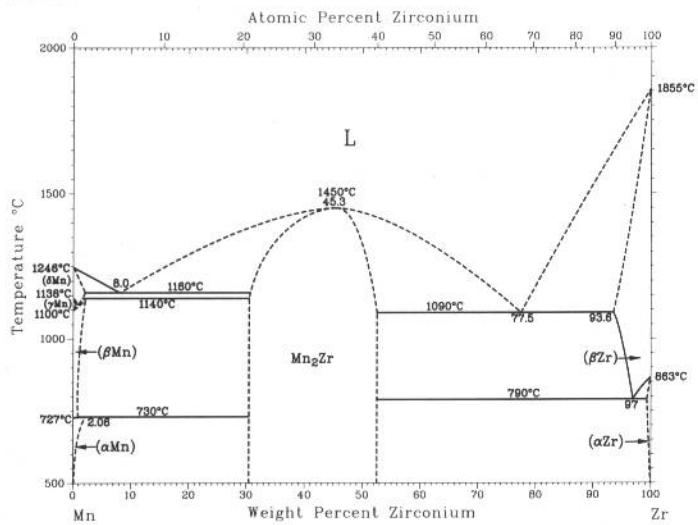

Phase	Composition, wt% Zr	Pearson symbol	Space group
(δMn)	0 to 2.06	*cI*2	$Im\bar{3}m$
(γMn)	0	*cF*4	$Fm\bar{3}m$
(βMn)	0 to ~2	*cP*20	$P4_132$
(αMn)	0 to 2.06	*cI*58	$I\bar{4}3m$
Mn_2Zr	30.40 to 53	*hP*12	*P*6$_3$/*mmc*
(βZr)	93.6 to 100	*cI*2	$Im\bar{3}m$
(αZr)	100	*hP*2	*P*6$_3$/*mmc*

Mo-N

P.R. Subramanian, 1990

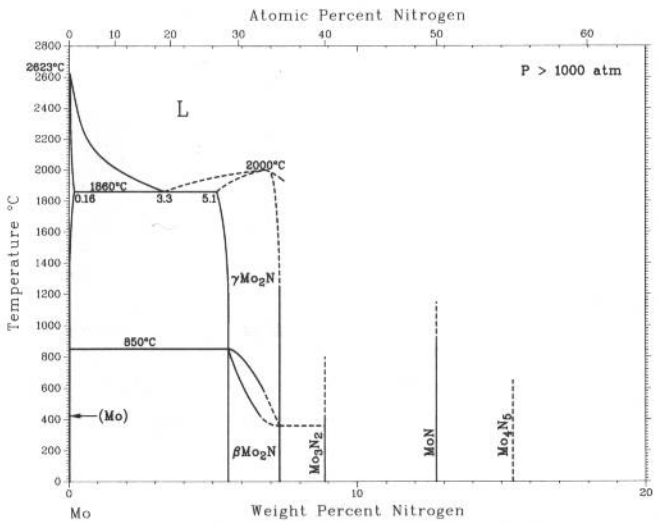

Phase	Composition, wt% N	Pearson symbol	Space group
(Mo)	0 to 0.16	*cI*2	$Im\bar{3}m$
γMo_2N	5.1 to 7	*cF*8	$Fm\bar{3}m$
βMo_2N	5.6 to 7	*tI*12	$I4_1/amd$
Mo_3N_2	~9	*cP*8	$Pm\bar{3}m$
MoN	12.7	*hP*16	$P6_3/mmc$
Mo_4N_5	~15.5	*hP*8	$P6_3/mmc$

Mo-Nb

H. Okamoto, 1991

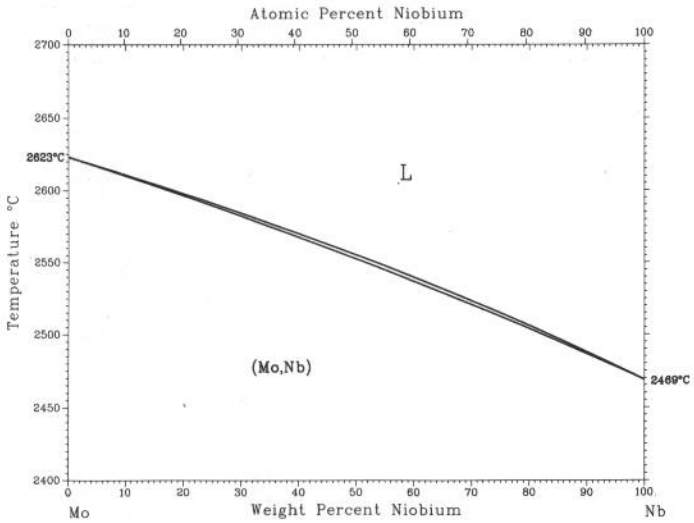

Phase	Composition, wt% Nb	Pearson symbol	Space group
(Mo,Nb)	0 to 100	*cI*2	$Im\bar{3}m$

Mo-Ni

H. Okamoto, 1991

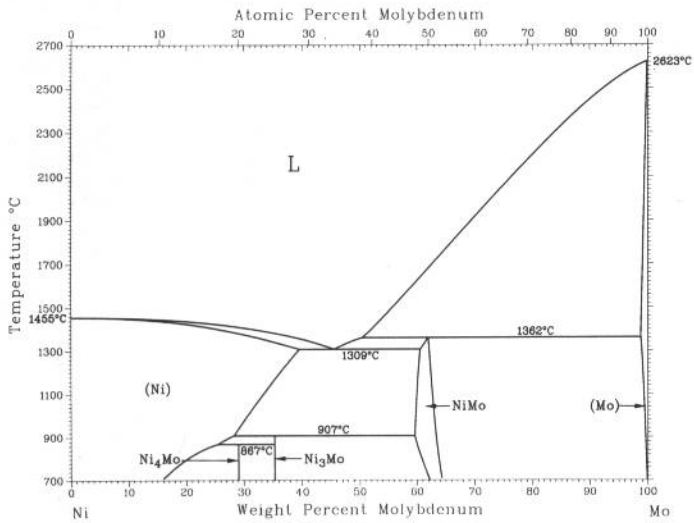

Phase	Composition, wt% Mo	Pearson symbol	Space group
(Ni)	0 to 38(a)	*cF*4	$Fm\bar{3}m$
Ni_4Mo	29.0	*tI*10	$I4/m$
Ni_3Mo	35.3	*oP*8	$Pmnn$
NiMo	63.9 to 65.7	*oP*112	$P2_12_12_1$
(Mo)	98.9 to 100(b)	*cI*2	$Im\bar{3}m$
Metastable phases			
Ni_2Mo	...	*oI*6	...
Ni_3Mo	...	*tI*8	$I4/mmm$
Ni_4Mo	...	*tI*10, *cF*4	...
$Ni_{17}Mo_5$	...	...	...

(a) At 1317 °C. (b) At 1362 °C

Mo-O

L. Brewer and R.H. Lamoreaux, 1980

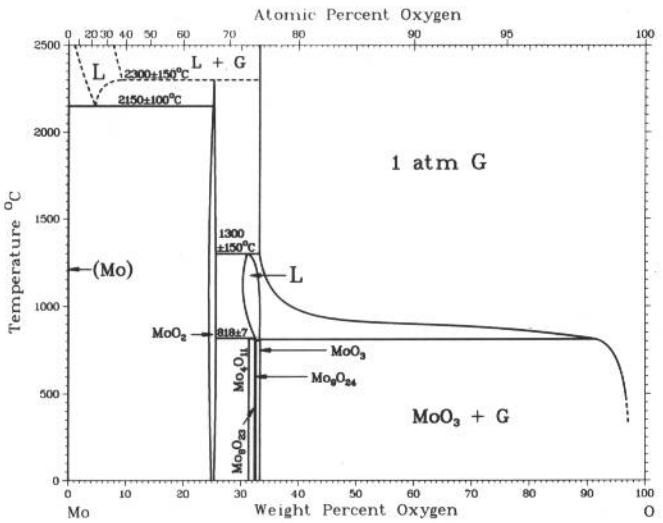

Phase	Composition, wt% O	Pearson symbol	Space group
(Mo)	0	*cI*2	$Im\bar{3}m$
MoO_2	~25.0	*mP*12	$P2_1/c$(a)
		*tP*6	$P4_2/mnn$
Mo_4O_{11}	31.4	*oP*60	$Pna2_1$
Mo_8O_{23}	32.4	*mP*124	*Pc*
		*mP*62	*P*2/*c*
Mo_9O_{24}(b)	32.5	*mC*280	*C*2/*c*
		*mP*70	*P*2/*c*
MoO_3	33	*oP*128	*Pba*2

(a) Or $P2_1$. (b) Might be Mo_9O_{26}

Mo-Os

From [Molybdenum]

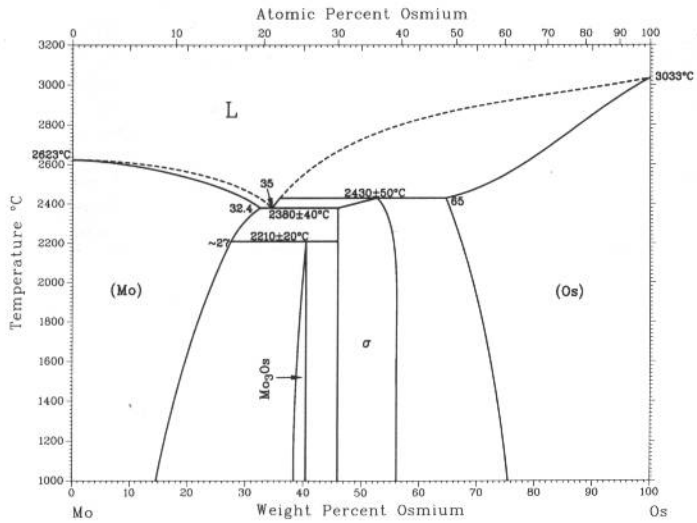

Phase	Composition, wt% Os	Pearson symbol	Space group
(Mo)	0 to 32.4	*cI*2	$Im\bar{3}m$
Mo_3Os	~40	*cP*8	$Pm\bar{3}n$
σ (Mo_2Os)	46 to 56	*tP*30	$P4_2/mnm$
(Os)	65 to 100	*hP*2	$P6_3/mmc$

Mo-P

From [Molybdenum]

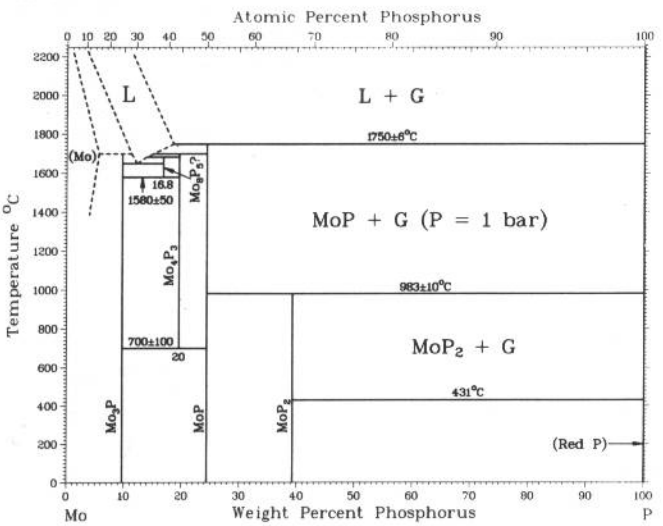

Phase	Composition, wt% P	Pearson symbol	Space group
(Mo)	0 to >5	*cI*2	$Im\bar{3}m$
Mo_3P	10	*tI*32	$I\bar{4}2m$
Mo_8P_5	16.8	*mP*13	*Pm*
Mo_4P_3	20	*oP*56	*Pnma*
MoP	24.4	*hP*2	$P\bar{6}m2$
MoP_2	39.3	*oC*12	$Cmc2_1$
(P) (red)	~100	...	...
Other reported phase			
Mo_5P_3	~16.2	*h***	...

Mo-Pd

H. Okamoto, 1992

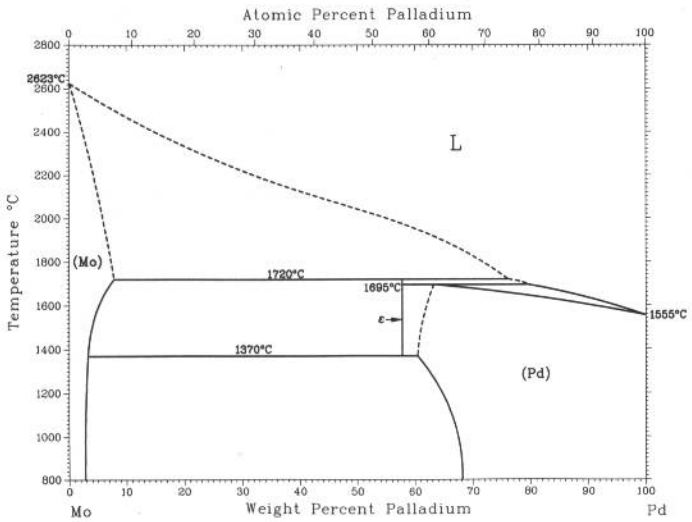

Phase	Composition, wt% Pd	Pearson symbol	Space group
(Mo)	0 to 8	*cI*2	$Im\bar{3}m$
ε	~58	*hP*2	$P6_3/mmc$
(Pd)	61 to 100	*cF*4	$Fm\bar{3}m$

Mo-Pt

L. Brewer and R.H. Lamoreaux, 1980

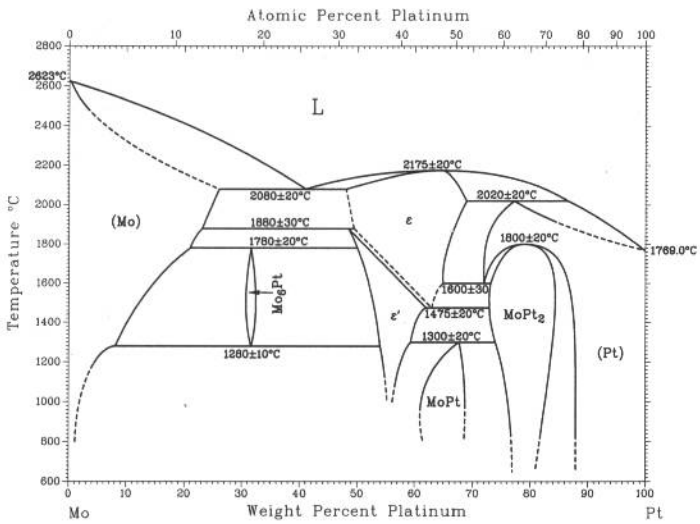

Phase	Composition, wt% Pt	Pearson symbol	Space group
(Mo)	0 to 26 ± 2	*cI*2	$Im\bar{3}m$
Mo_6Pt	31.6 ± 0.7	*cP*8	$Pm\bar{3}n$
ε?	48 ± 1 to 71 ± 2	*hP*2	$P6_3/mmc$
ε′	48.4 ± 1 to 62 ± 2	*hP*8	$P6_3/mmc$
MoPt	61 ± 2 to 70 ± 2	*oP*4	*Pmma*
$MoPt_2$	74 ± 2 to 84 ± 1	*oI*6	*Immm*
(Pt)	72 ± 2 to 100	*cF*4	$Fm\bar{3}m$

Mo-Pu

From [Molybdenum]

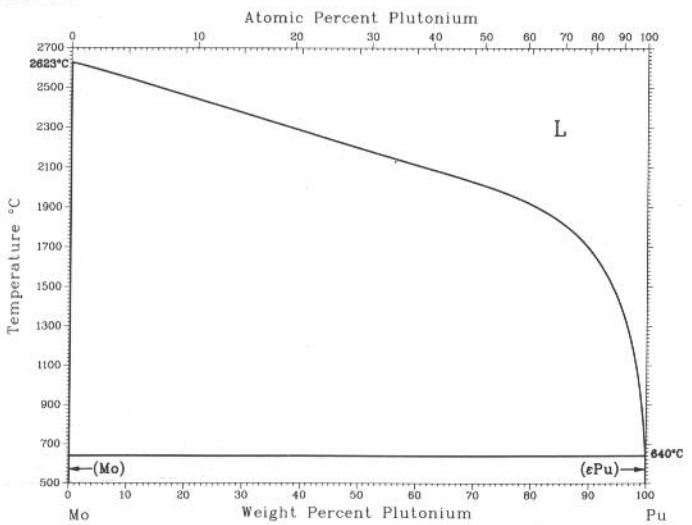

Phase	Composition, wt% Pu	Pearson symbol	Space group
(Mo)	0	*cI*2	$Im\bar{3}m$
(εPu)	100	*cI*2	$Im\bar{3}m$

Mo-Rh

From [Molybdenum]

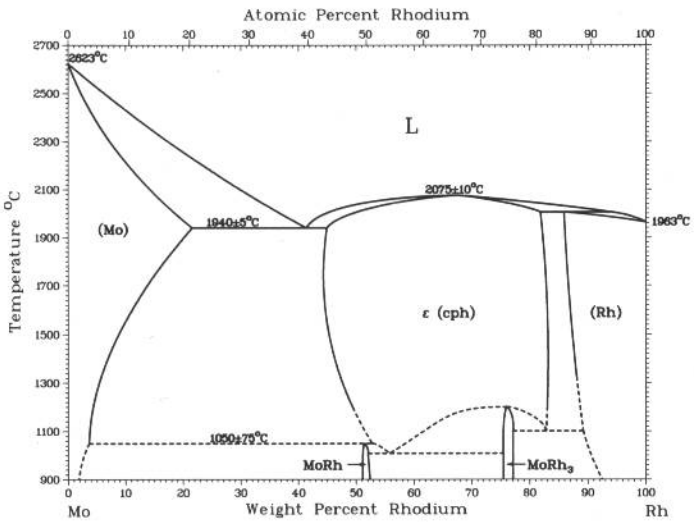

Phase	Composition, wt% Rh	Pearson symbol	Space group
(Mo)	0 to 21	*cI*2	$Im\bar{3}m$
MoRh	~51.8	*oP*4	*Pmma*
ε	~44 to 83	*hP*2	$P6_3/mmc$
$MoRh_3$	~76	...	...
(Rh)	86 to 100	*cF*4	$Fm\bar{3}m$

Mo-Ru

H. Okamoto, 1990

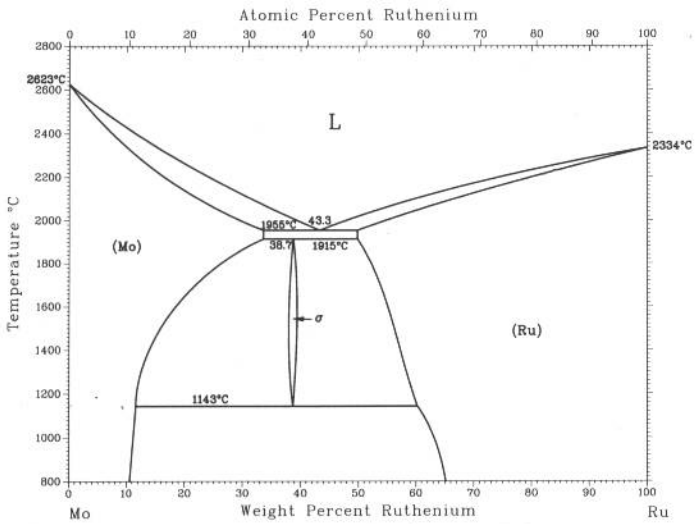

Phase	Composition, wt% Ru	Pearson symbol	Space group
(Mo)	0 to 33.6	*cI*2	$Im\bar{3}m$
σ	37.9 to 40.7	*tP*30	$P4_2/mnm$
(Ru)	49.8 to 100	*hP*2	$P6_3/mmc$

Mo-S

L. Brewer and R.H. Lamoreaux, 1980

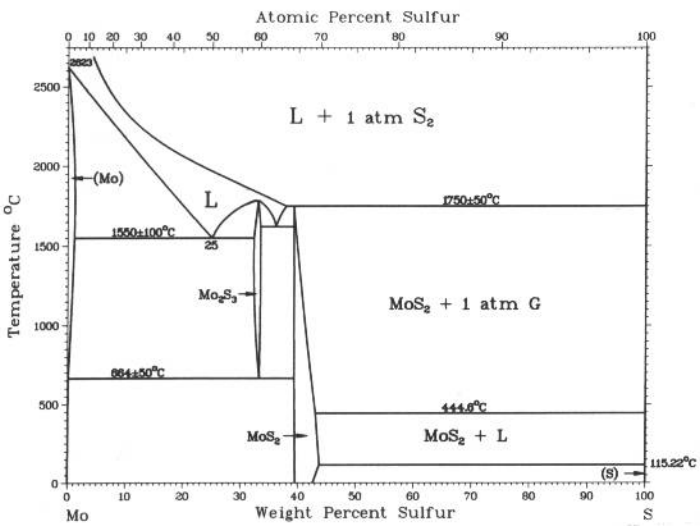

Phase	Composition, wt% S	Pearson symbol	Space group
(Mo)	0 to 1	*cI*2	$Im\bar{3}m$
Mo_2S_3	~33	*mP*10	$P2_1/m$
MoS_2	39 to 44	*hP*6	$P6_3/mmc$
		*hR*3	$R\bar{3}m$
(βS)	100	*mP**	$P2_1/c$
(αS)(a)	100	*oF*128	*Fddd*

(a) Below 95.5 °C

Mo-Si

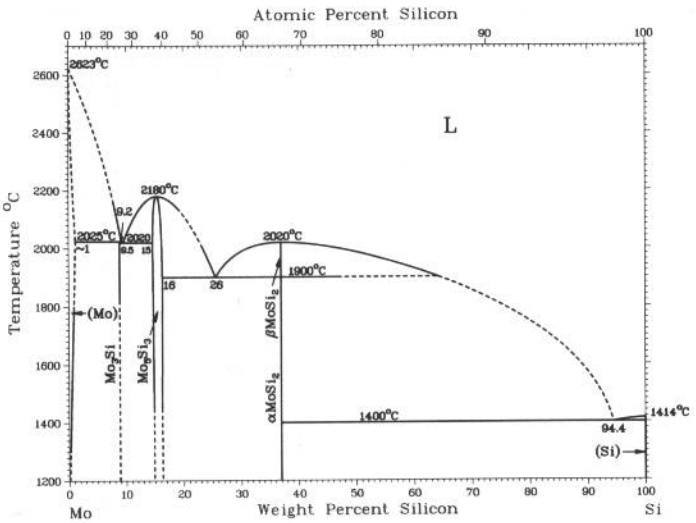

A.B. Gokhale and G.J. Abbaschian, 1991

Phase	Composition, wt% Si	Pearson symbol	Space group
(Mo)	0 to ~1	*cI*2	$Im\bar{3}m$
Mo_3Si	9	*cP*8	$Pm\bar{3}n$
Mo_5Si_3	~14.9	*tI*38	*I*4/*mcm*
$\beta MoSi_2$	37.0	...	$C6_22$
$\alpha MoSi_2$	37.0	*tI*6	*I*4/*mmm*
(Si)	100	*cF*8	$Fd\bar{3}m$

Mo-Ta

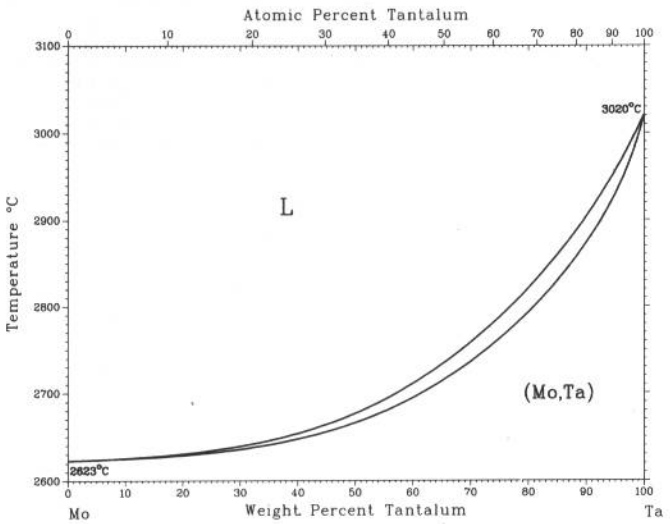

R. Krishnan, S.P. Garg, and N. Krishnamurthy, 1986

Phase	Composition, wt% Ta	Pearson symbol	Space group
(Mo,Ta)	0 to 100	*cI*2	$Im\bar{3}m$

Mo-Ti

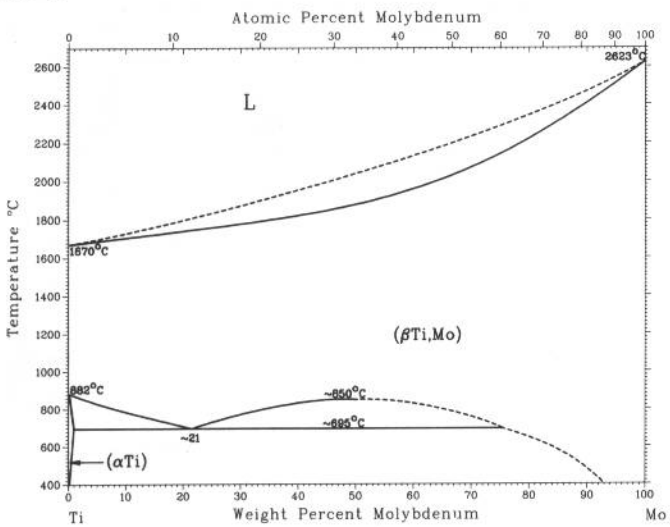

J.L. Murray, 1987

Phase	Composition, wt% Mo	Pearson symbol	Space group
(βTi,Mo)	0 to 100	*cI*2	$Im\bar{3}m$
(αTi)	0 to 0.8	*hP*2	$P6_3/mmc$
α′	(a)	*hP*2	$P6_3/mmc$
α″	(a)	*oC*4	*Cmcm*
ω	(a)	*hP*3	*P*6/*mmm*

(a) Metastable

Mo-U

H. Okamoto, 1990

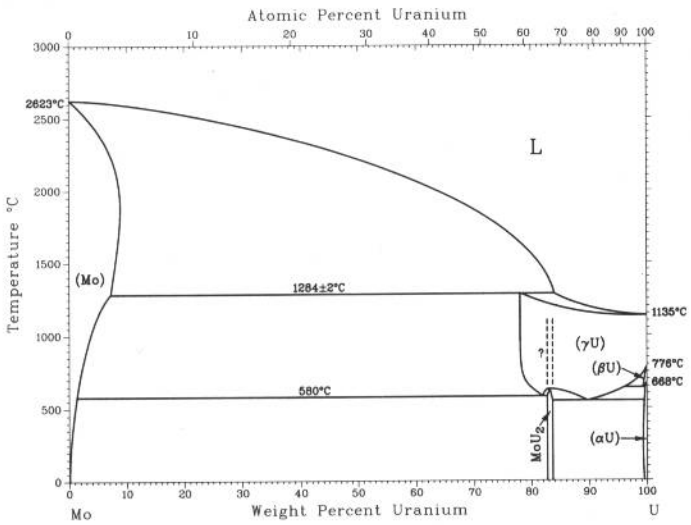

Phase	Composition, wt% U	Pearson symbol	Space group
(Mo)	0 to 9	*cI*2	$Im\bar{3}m$
MoU_2	83.2	*tI*6	*I*4/*mmm*
(γU)	98 to 100	*cI*2	$Im\bar{3}m$
(βU)	99 to 100	*tP*30	$P4_2/mnm$
(αU)	99 to 100	*oC*4	*Cmcm*

Mo-V

J.F. Smith, 1989

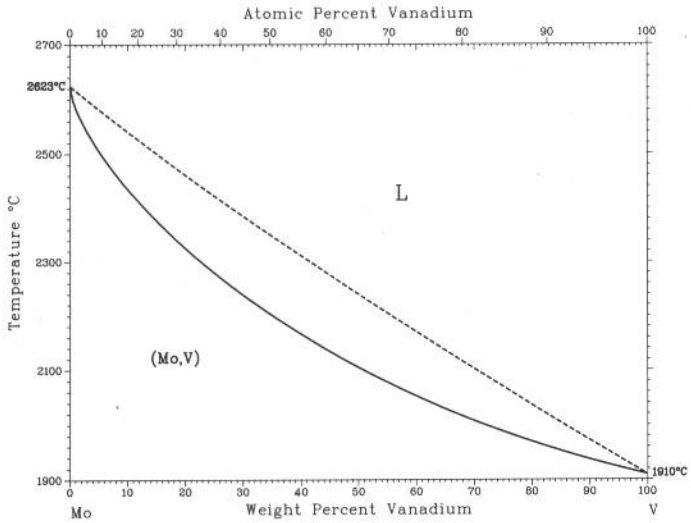

Phase	Composition, wt% V	Pearson symbol	Space group
(Mo,V)	0 to 100	*cI*2	$Im\bar{3}m$

Mo-W

S.V. Nagender Naidu, A.M. Sriramamurthy, and P. Rama Rao, 1984

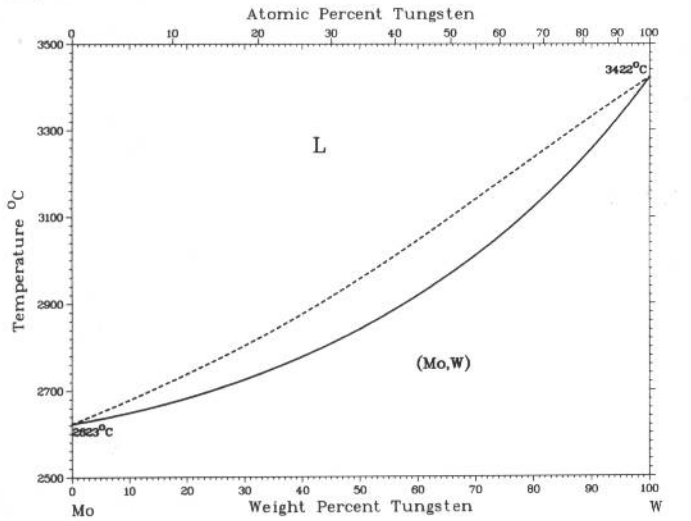

Phase	Composition, wt% W	Pearson symbol	Space group
(Mo,W)	0 to 100	*cI*2	$Im\bar{3}m$

Mo-Zr

From [Zirconium]

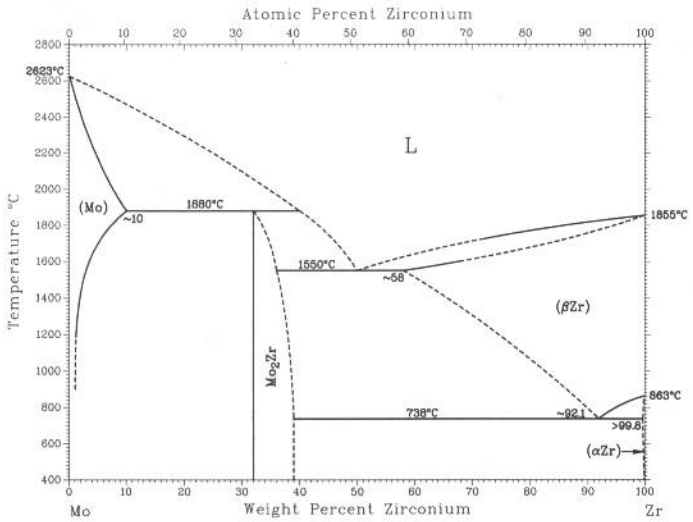

Phase	Composition, wt% Zr	Pearson symbol	Space group
(Mo)	0 to ~10	*cI*2	$Im\bar{3}m$
Mo_2Zr	32 to 39	*cF*24	$Fd\bar{3}m$
(βZr)	~58 to 100	*cI*2	$Im\bar{3}m$
(αZr)	~100	*hP*2	$P6_3/mmc$

N-Nb

Yu.V. Levinskiy, 1974

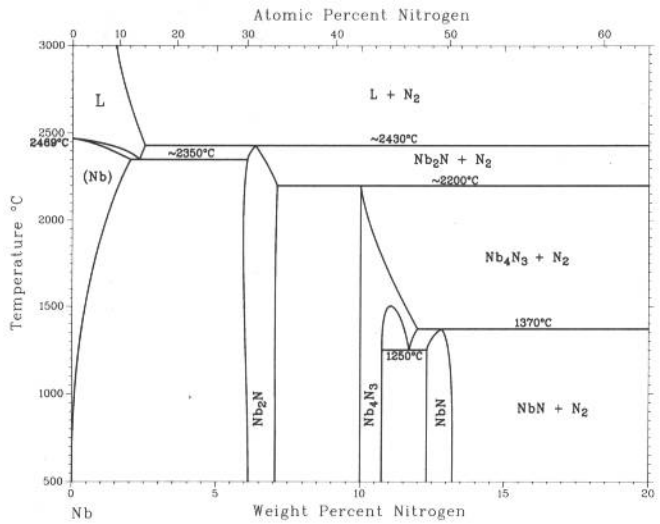

Phase	Composition, wt% N	Pearson symbol	Space group
(Nb)	0 to <3	*cI*2	$Im\bar{3}m$
Nb_2N	~5.9 to 7	*hP*9	$P\bar{3}1m$
Nb_4N_3	~10.2	*tI*14	*I*4/*mmm*
NbN	~13.1	*hP*8	$P6_3/mmc$
Other reported phases			
Nb_3N	5	*tP*58	*P*4/*m*
$Nb_{10}N_9$	12.0	*hP*2	$P\bar{6}m2$
NbN	13.1	*hP*4	$P6_3/mmc$
Nb_5N_6	15.3	*hP*22	$P6_3/mcm$
Nb_4N_5	15.9	*tI*18	*I*4/*m*

N-Ni

H.A. Wriedt, 1991

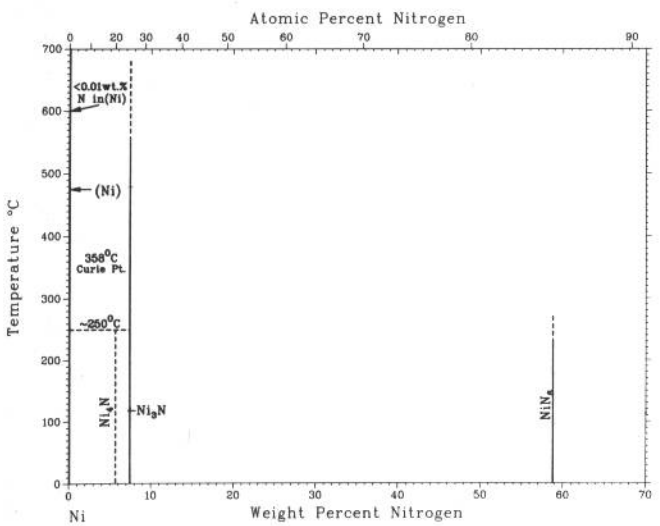

Phase	Composition, wt% N	Pearson symbol	Space group
Stable phases			
(Ni)(a)	~0	*cF*4	$Fm\bar{3}m$
Ni_3N	7	*hP**	$P6_322$ or $P312$
$Ni(N_3)_2$	58.9	...	...
Other phases			
Ni_4N,I	6	*c***	...
Ni_4N,II	6	*t***	...
Ni_2N	10.6	*t***	...
Ni_3N_2(b)	14	...	...

(a) At 25 °C. (b) Existence questionable

N-Ta

J. Gatterer, D. Dufek, P. Ettmayer, and R. Kieffer, 1975

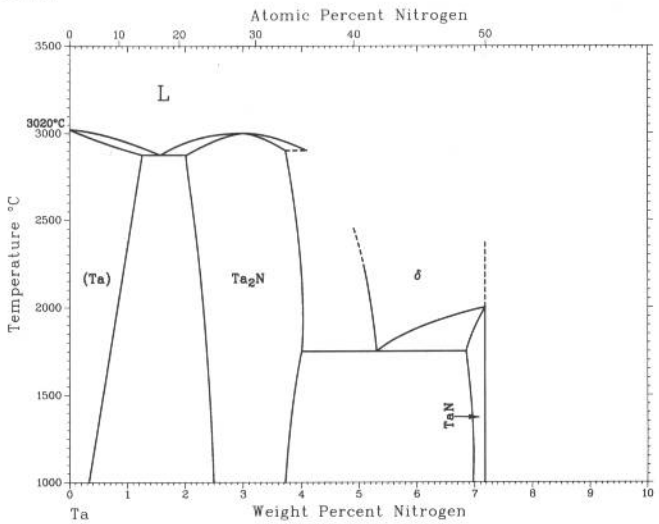

Phase	Composition, wt% N	Pearson symbol	Space group
(Ta)	0 to 1.5	*cI*2	$Im\bar{3}m$
Ta_2N	2.1 to 4.0	*hP*3	$P6_3/mmc$
δ	~4.9 to 7.2	*cF*8	$Fm\bar{3}m$
TaN	7.2	*c***	...
Other reported phases			
Ta_9N_2	~1.7	*c***	...
Ta_4(HT?)	~1.9	*o***	...
Ta_2N	~3.7	*hP*9	$P\bar{3}1m$
TaN	7.2	*hP*8	$P6_3/mmc$
Ta_5N_6	~8.5	*hP*22	$P6_3/mcm$
Ta_4N_5	~8.8	*tI*18	$I4/m$
Ta_3N_5	~11.4	*t***	...
		*oC*32	*Cmcm*
		*mC*32	*C*2/*m*

N-Th

H. Okamoto, 1990

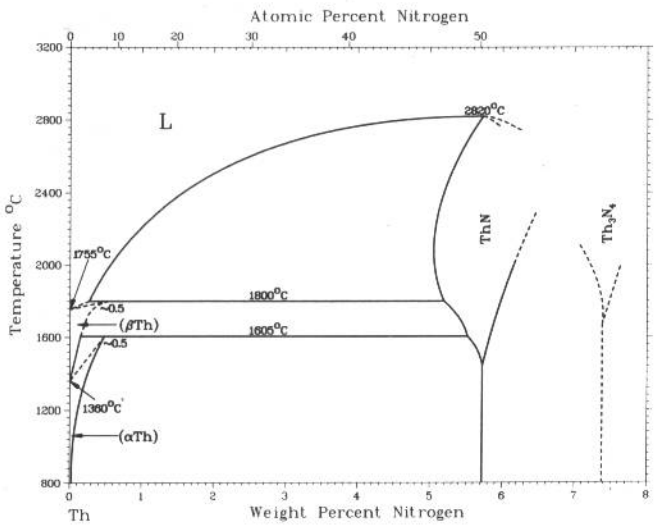

Phase	Composition, wt% N	Pearson symbol	Space group
(βTh)	0	*cI*2	$Im\bar{3}m$
(αTh)	0	*cF*4	$Fm\bar{3}m$
ThN	~5.7	*cF*8	$Fm\bar{3}m$
Th_3N_4	~7.4	*mC*4	*Cm*
		*o**18	...
		*hR*7	$R\bar{3}m$
Th_2N_3	8.3	*hP*5	$P\bar{3}m1$

N-Ti

H.A. Wriedt and J.L. Murray, 1987

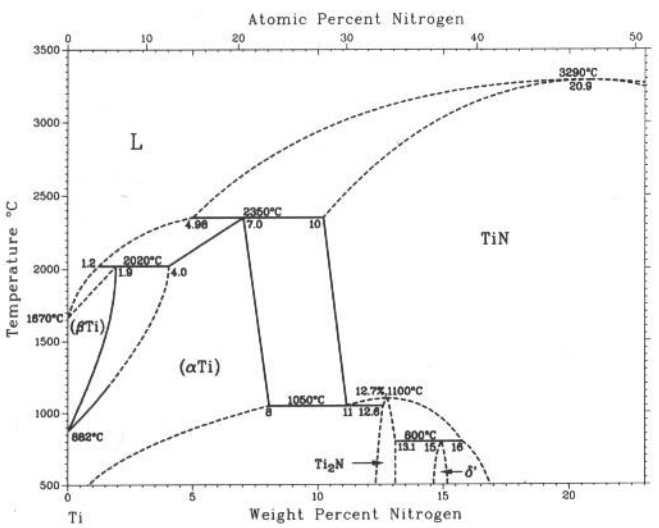

Phase	Composition, wt% N	Pearson symbol	Space group
Stable phases			
(αTi)	0 to 8	*hP*2	$P6_3/mmc$
(βTi)	0 to 1.9	*cI*2	$Im\bar{3}m$
Ti_2N	~13	*tP*6	$P4_2/mnm$
TiN	10 to >22.6	*cF*8	$Fm\bar{3}m$
δ′	~15	*tI*12	$I4_1/amd$
ω	~0	*h***	...
Metastable phase			
α′	...	*tP*6	$P4_2/mnm$

N-U

From [Metals]

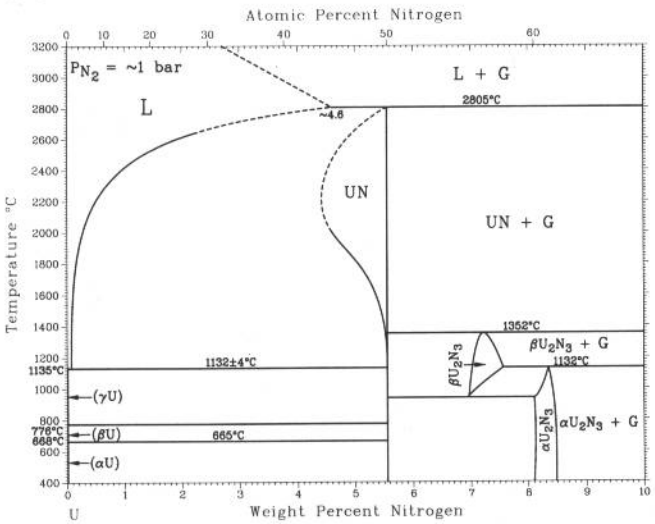

Phase	Composition, wt% N	Pearson symbol	Space group
(γU)	~0	*cI*2	$Im\bar{3}m$
(βU)	~0	*tP*30	$P4_2/mnm$
(αU)	~0	*oC*4	*Cmcm*
UN	~4.4 to 5.6	*cF*8	$Fm\bar{3}m$
βU_2N_3	~7 to 7.5	*hP*5	$P\bar{3}m1$
αU_2N_3	~8 to 8.4	*cI*80	$Ia\bar{3}$
Other reported phases			
U_4N_7	~9.3	*hR**	...
UN_2	~10.5	*cF*12	$Fm\bar{3}m$

N-Zr

From [Zirconium]

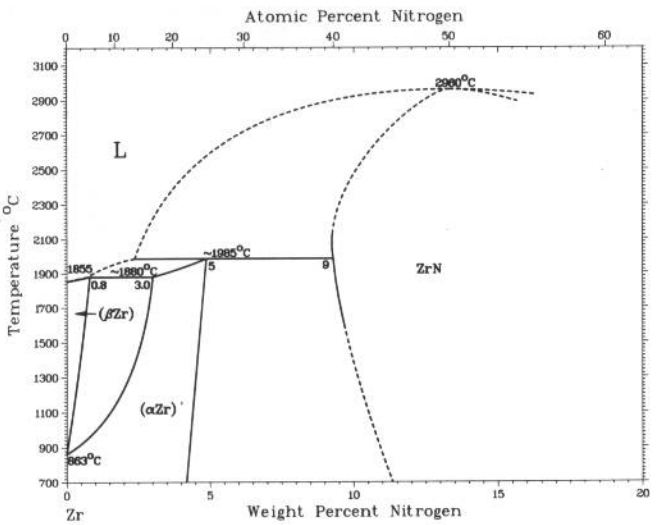

Phase	Composition, wt% N	Pearson symbol	Space group
(βZr)	0 to 0.7	*cI*2	$Im\bar{3}m$
(αZr)	0 to 5	*hP*2	$P6_3/mmc$
ZrN	9 to ?	*cF*8	$Fm\bar{3}m$

Na-O

H.A. Wriedt, 1987

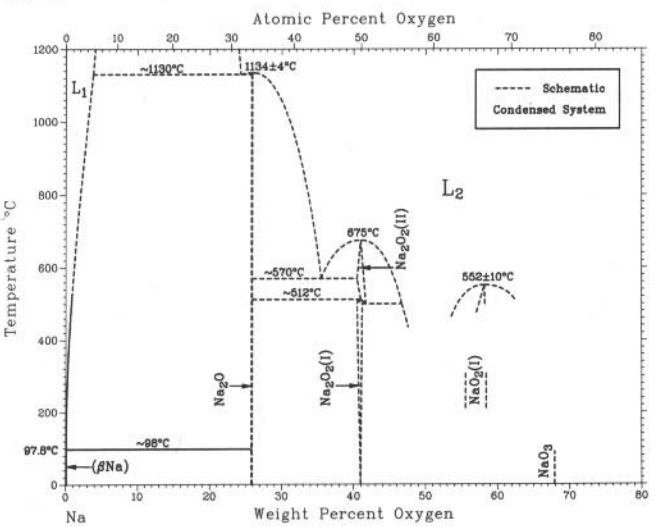

Phase	Composition, wt% O	Pearson symbol	Space group
(βNa)	0	*cI*2	$Im\bar{3}m$
(αNa)	0	*hP*2	$P6_3/mmc$
Na_2O	25.8	*cF*12	$Fm\bar{3}m$
Na_2O_2-II	41.0	...	...
Na_2O_2-I	41.0	*hP*9	$P\bar{6}2m$(a)
NaO_2 (I)	58.2	*cF*8	$Fm\bar{3}m$
NaO_2 (II)	58.2	*cP*12	$Pa\bar{3}$
NaO_2 (III)	58.2	*oP*6	*Pnnm*
NaO_3	68	bct	*I*4/*mmm*
Other phase			
Na_2O_2-Q(b)	41.0	...	...

(a) Might be $C\bar{6}2m$. (b) Noncubic

Na-Pb

From [Metals]

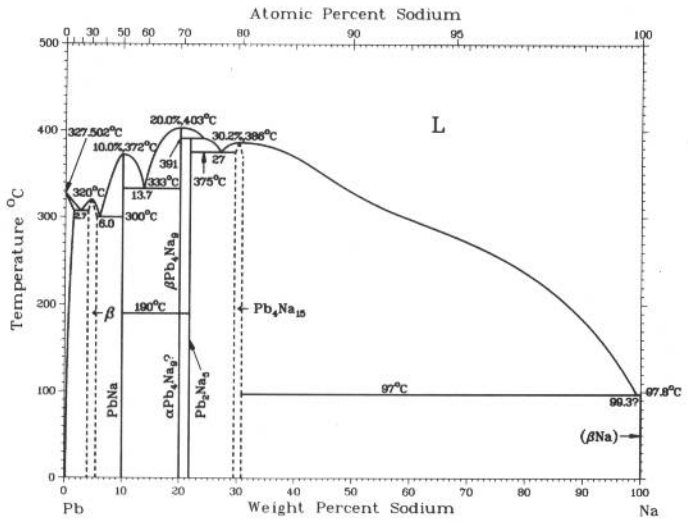

Phase	Composition, wt% Na	Pearson symbol	Space group
(Pb)	0 to 2.7	*cF*4	$Fm\bar{3}m$
β(Pb_3Na)	>4 to >5	*cP*4	$Pm\bar{3}m$
PbNa	10.0	*tI*64	$I4_1/acd$
Pb_4Na_9	~20.0	*hP*26	$P6_3/mmc$
Pb_2Na_5	~21.7	*hR*7	$R\bar{3}m$
Pb_4Na_{15}	~29 to 31	*cI*76	$I\bar{4}3d$
(βNa)	~100	*cI*2	$Im\bar{3}m$
Other reported phases			
Pb_5Na_{13}	~22.4	*hP*36	$P6_3/mmc$
$PbNa_5$	~36.5	*hP**	...

Na-Rb

C.W. Bale, 1982

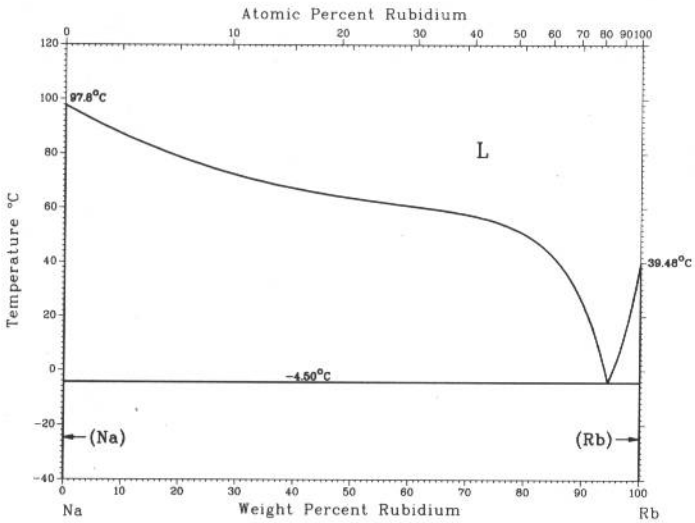

Phase	Composition, wt% Rb	Pearson symbol	Space group
(Na)	0	*cI*2	$Im\bar{3}m$
(Rb)	100	*cI*2	$Im\bar{3}m$

Na-S

H. Okamoto, 1990

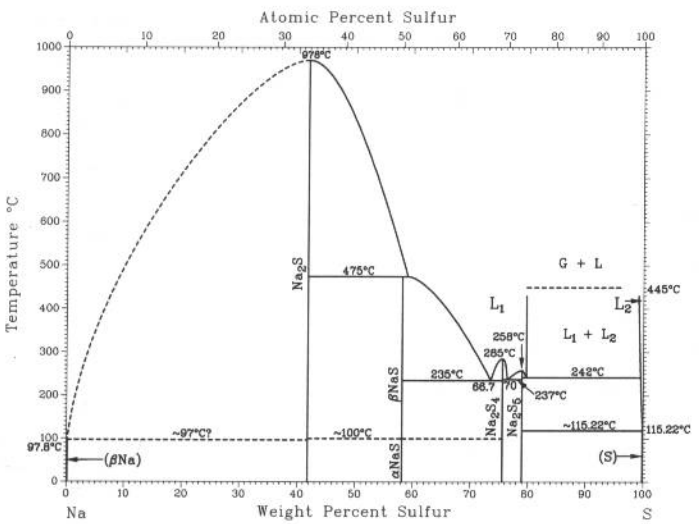

Phase	Composition, wt% S	Pearson symbol	Space group
(βNa)	0	*cI*2	$Im\bar{3}m$
Na_2S	41.0	*cF*12	$Fm\bar{3}m$
βNaS	58.2	*hP*8	$P6_3/mmc$
αNaS	58.2	*hP*12	$P\bar{6}2m$
Na_2S_4	73.6	*tI*48	$I\bar{4}2d$
Na_2S_5	~78	*oP*28	*Pnma*
(S)	0	*mP*64	$P2_1/c$

Na-Sb

C.H. Mathewson, 1906

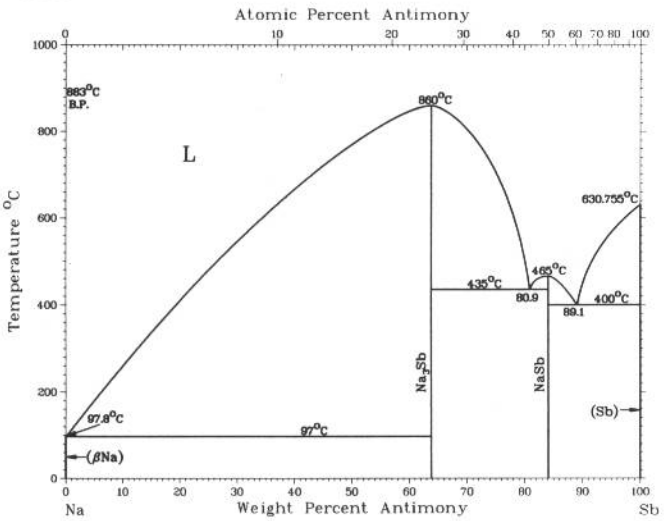

Phase	Composition, wt% Sb	Pearson symbol	Space group
(βNa)	~0	*cI*2	$Im\bar{3}m$
Na_3Sb	64	*hP*8	$P6_3/mmc$
NaSb	84.1	*mP*16	$P2_1/c$
(Sb)	~100	*hR*2	$R\bar{3}m$

Na-Se

H. Okamoto, 1990

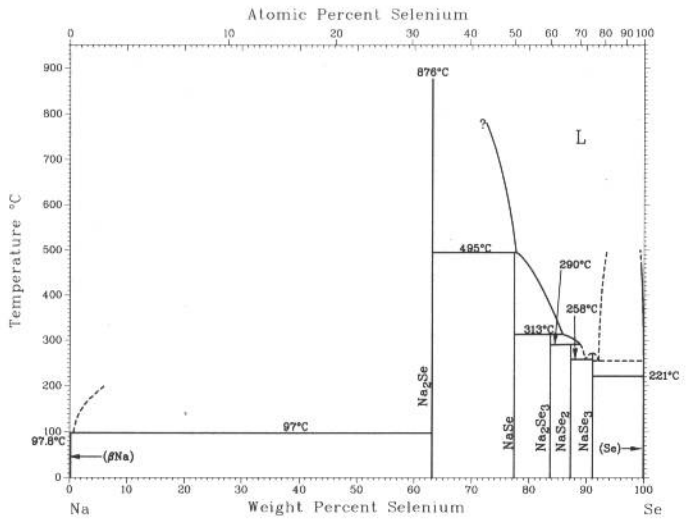

Phase	Composition, wt% Se	Pearson symbol	Space group
(βNa)	0	*cI*2	$Im\bar{3}m$
Na_2Se	63.2	*cF*12	$Fm\bar{3}m$
NaSe	77.4	*hP*8	$P6_3/mmc$
Na_2Se_3	84	...	...
$NaSe_2$	87.3	...	...
$NaSe_3$	91	...	...
(Se)	100	*hP*3	$P3_121$

Na-Sn

H. Okamoto, 1990

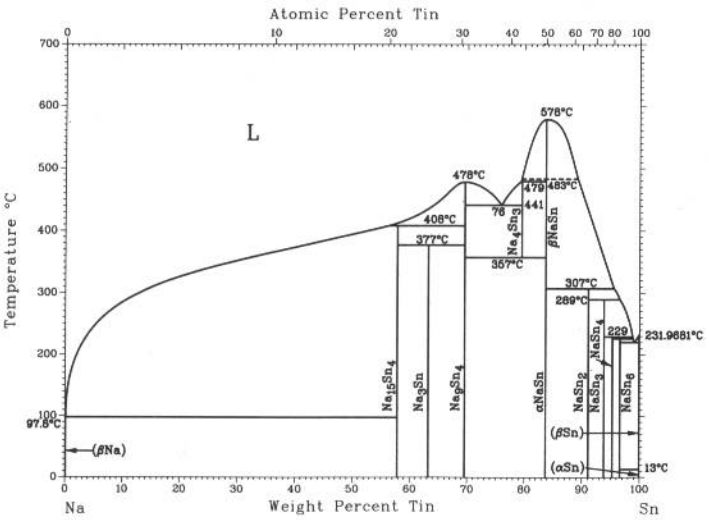

Phase	Composition, wt% Sn	Pearson symbol	Space group
(βNa)	0	*cI*2	$Im\bar{3}m$
$Na_{15}Sn_4$	58	*cI*76	$I\bar{4}3d$
		*oP*40	*Pnma*
Na_3Sn	63	...	...
Na_9Sn_4	69.7	*oC*52	*Cmcm*
Na_4Sn_3	79.5	...	...
βNaSn	83.8	...	...
αNaSn	83.8	*tI*64	$I4_1/acd$
$NaSn_2$	91.2	...	...
$NaSn_3$	94	...	...
$NaSn_4$	95	...	...
$NaSn_6$	96.9	...	...
(βSn)	100	*tI*2	$I4_1/amd$
(αSn)	100	*cF*8	$Fd\bar{3}m$

Na-Sr

A.D. Pelton, 1985

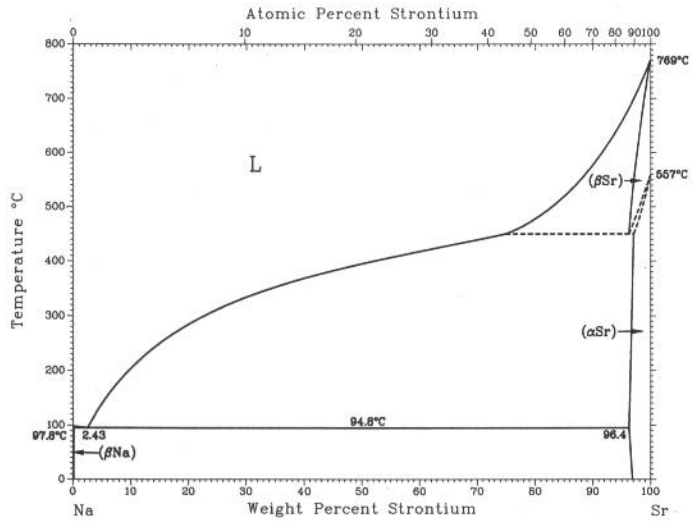

Phase	Composition, wt% Sr	Pearson symbol	Space group
(βNa)	0	*cI*2	$Im\bar{3}m$
(αNa)	0	*hP*2	$P6_3/mmc$
(βSr)	97.2 to 100	*cI*2	$Im\bar{3}m$
(αSr)	96.4 to 100	*cF*4	$Fm\bar{3}m$

Na-Te

A.D. Pelton and A. Petric, 1990

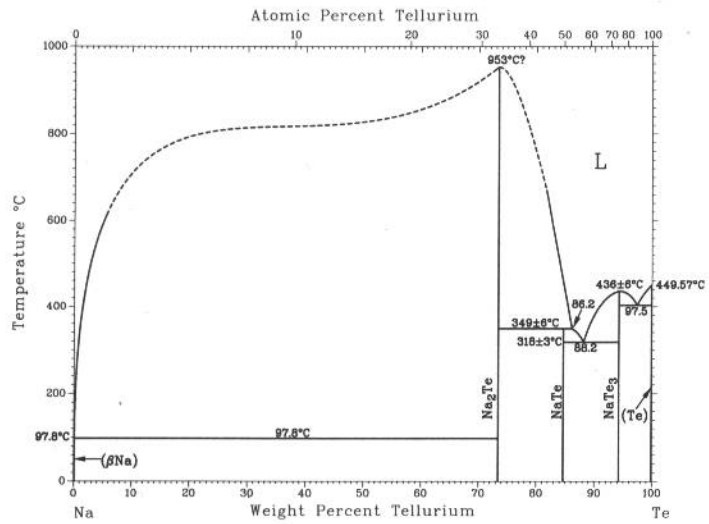

Phase	Composition, wt% Te	Pearson symbol	Space group
(βNa)	0	*cI*2	$Im\bar{3}m$
(αNa)	0	*hP*2	$P6_3/mmc$
Na_2Te	73.5	*cF*12	$Fm\bar{3}m$
NaTe	84.7	...	...
$NaTe_3$	94	...	...
(Te)	100	*hP*3	$P3_121$

Na-Tl

G. Grube and A. Schmidt, 1936

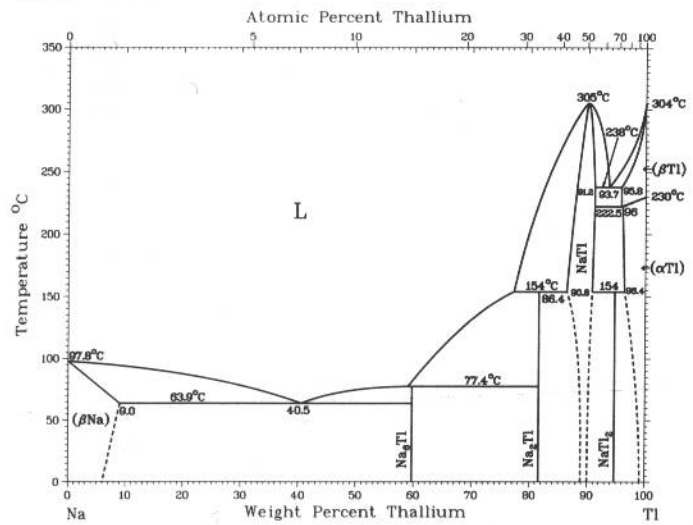

Phase	Composition, wt% Tl	Pearson symbol	Space group
(βNa)	0 to 9.0	*cI*2	$Im\bar{3}m$
Na_6Tl	~59.7	*cF*400	$F\bar{4}3m$
Na_2Tl	81.6	*oC*48	$C222_1$
NaTl	86.4 to 91.2	*cF*16	$Fd\bar{3}m$
$NaTl_2$	94.7	...	...
(βTl)	95.8 to 100	*cI*2	$Im\bar{3}m$
(αTl)	96 to 100	*hP*2	$P6_3/mmc$

Nb-Ni

H. Okamoto, 1992

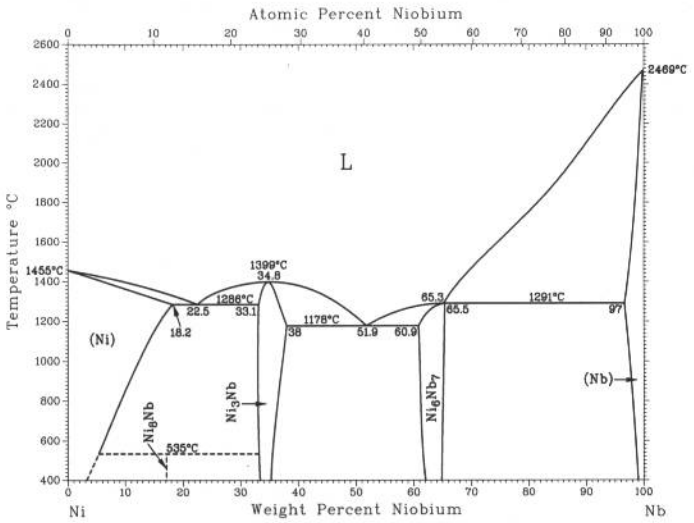

Phase	Composition, wt% Nb	Pearson symbol	Space group
(Ni)	0 to 18.2	*cF*4	$Fm\bar{3}m$
Ni_8Nb	16.5	*tI*36	...
Ni_3Nb	33.1 to 38.0	*oP*8	*Pmmn*
Ni_6Nb_7	60.9 to 65.5	*hR*13	$R\bar{3}m$
(Nb)	97 to 100	*cI*2	$Im\bar{3}m$

Nb-Os

R.M. Waterstrat and R.C. Manuszewski, 1977

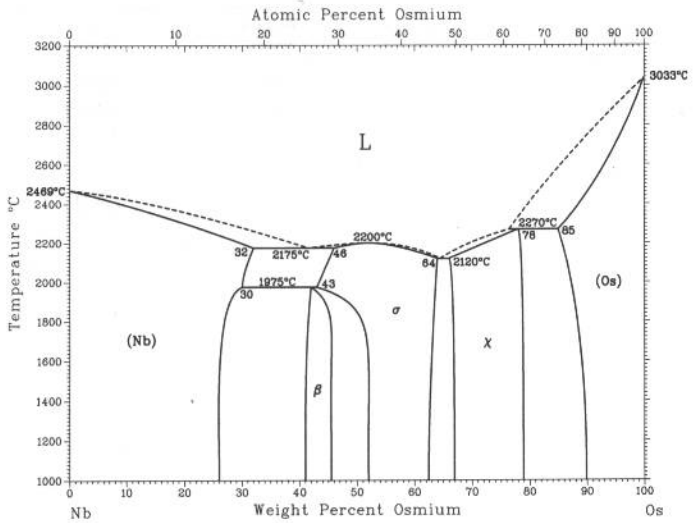

Phase	Composition, wt% Os	Pearson symbol	Space group
(Nb)	0 to 32	*cI*2	$Im\bar{3}m$
β	>41 to ~46	*cP*8	$Pm\bar{3}n$
σ	43 to 64	*tP*30	$P4_2/mnm$
χ	66 to 78	*cI*58	$I\bar{4}3m$
(Os)	85 to 100	*hP*2	$P6_3/mmc$

Nb-Pd

M.S. Chandrasekharaiah, 1988

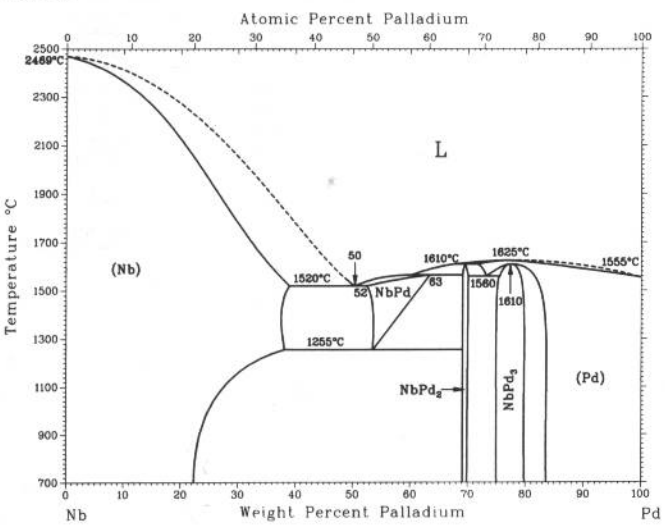

Phase	Composition, wt% Pd	Pearson symbol	Space group
(Nb)	0 to 39	*cI*2	$Im\bar{3}m$
NbPd(a)	52 to 63	*cF*4	$Fm\bar{3}m$
$NbPd_2$	69.2 to 70.1	*oI*14	*Immm*
$\alpha NbPd_3$	78(b)	*tI*8	*I*4/*mmm*
$\beta NbPd_3$	76 to 78	...	*Pmmn*
(Pd)	73 to 100	*cF*4	$Fm\bar{3}m$

(a) Data from rapidly quenched samples. (b) At 1300 °C

Nb-Pt

H. Okamoto, 1990

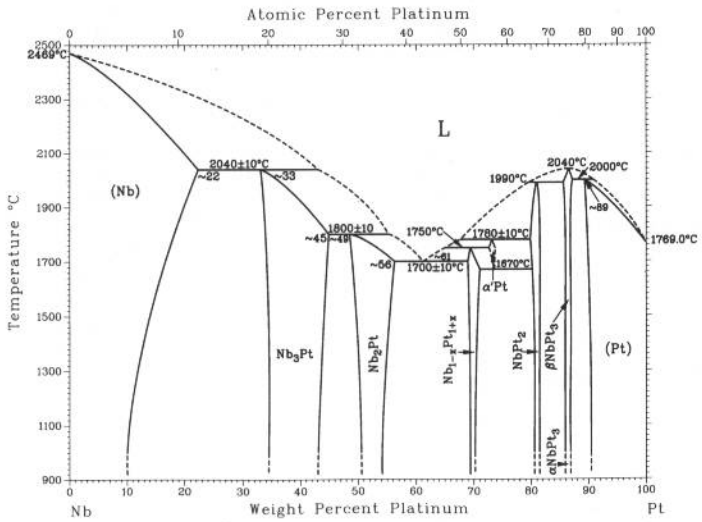

Phase	Composition, wt% Pt	Pearson symbol	Space group
(Nb)	0 to ~22	*cI*2	$Im\bar{3}m$
Nb_3Pt	~33 to ~45	*cP*8	$Pm\bar{3}n$
Nb_2Pt	~49 to ~56	*tP*30	$P4_2/mnm$
$Nb_{1-x}Pt_{1+x}$	69 to 70	*oP*4	*Pmma*
α'Pt	~74	...	...
$NbPt_2$	~81	*oI*6	*Immm*
$\beta NbPt_3$	~87	*mP*48	$P2_1/m$
$\alpha NbPt_3$	~87	*oP*8	*Pmmn*
(Pt)	~89 to 100	*cF*4	$Fm\bar{3}m$

Nb-Rh

D.L. Ritter, B.C. Giessen, and N.J. Grant, 1964

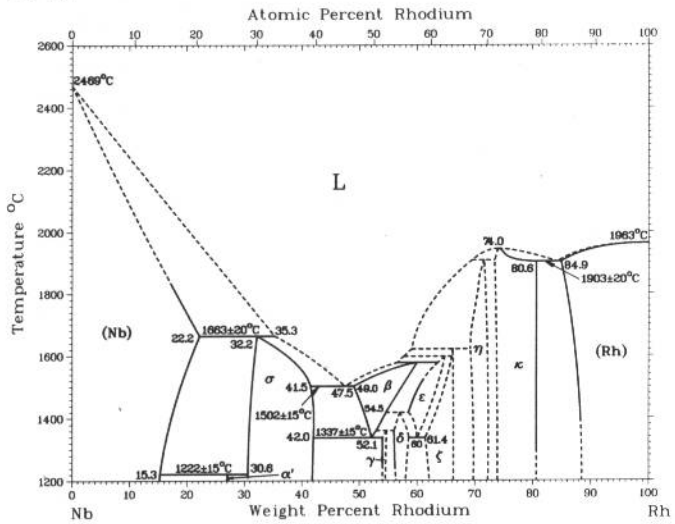

Phase	Composition, wt% Rh	Pearson symbol	Space group
(Nb)	0 to 22.2	*cI*2	$Im\bar{3}m$
α'(Nb_3Rh)	27	*cP*8	$Pm\bar{3}n$
σ($Nb_{13}Rh_7$)	30.6 to 42.0	*tP*30	$P4_2/mnm$
β	49.0 to ~61	...	...
γ	~54.0 to 55	*tP*2	*P*4/*mmm*
δ	~56.0 to 59	*o***	...
ε(Nb_2Rh_3)	~59 to 64	*oP*4	*Pmma*
ζ(Nb_2Rh_3)	61 to ~66	*mP*18	*P*2/*m*
η($Nb_{13}Rh_{27}$)	~69 to 72	*hP*24	$P\bar{6}m2$
κ($NbRh_3$)	~73 to 80.6	*cP*4	$Pm\bar{3}m$
(Rh)	84.9 to 100	*cF*4	$Fm\bar{3}m$
Other reported phases			
NbRh	~52.6	*tP*2	*P*4/*mmm*
		*oP*4	*Pnma*
Nb_9Rh_{11}	58	*oP*12	*Pnma*

Nb-Ru

H. Okamoto, 1990

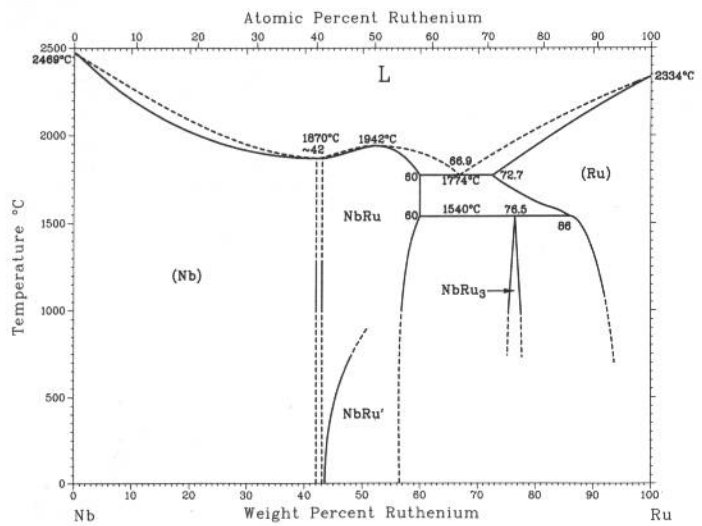

Phase	Composition, wt% Ru	Pearson symbol	Space group
(Nb)	0	*cI*2	$Im\bar{3}m$
NbRu	43 to 60	*cP*2	$Pm\bar{3}m$
NbRu'	?	*tP*2	*P*4/*mmm*
$NbRu_3$	76.5	*cP*4	$Pm\bar{3}m$
(Ru)	72.7 to 100	*hP*2	$P6_3/mmc$

Nb-Si

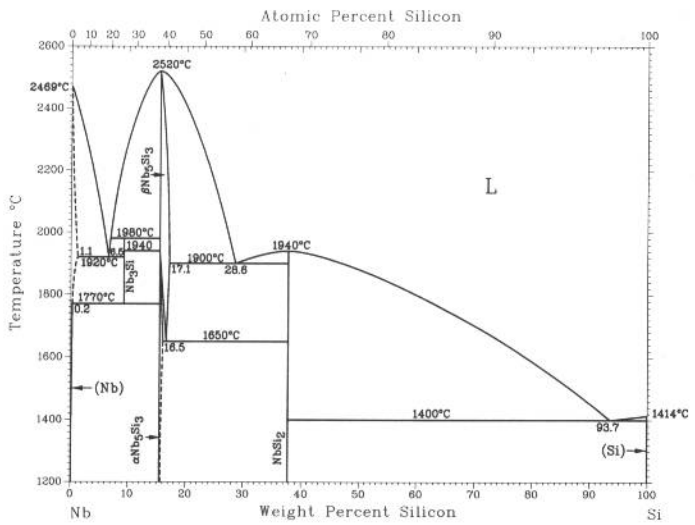

H. Okamoto, A.B. Gokhale, and G.J. Abbaschian, unpublished

Phase	Composition, wt% Si	Pearson symbol	Space group
(Nb)	0 to 1.1	*cI*2	$Im\bar{3}m$
Nb_3Si	9	*tP*32	$P4_2/n$
βNb_5Si_3	15.4 to 17.1	*tI*32	*I*4/*mcm*
αNb_5Si_3	15.4 to 15.9	*tI*32	*I*4/*mcm*
$NbSi_2$	37.7	*hP*9	$P6_422$
(Si)	100	*cF*8	$Fd\bar{3}m$
Metastable phases			
Nb_7Si	2.9 to 4.3	*c***	...
Nb_3Si·m	3.2 to 7.9	*cP*8	$Pm\bar{3}n$
Nb_3Si·m′	3.2 to 10.1	*cF*4	$Fm\bar{3}m$
Nb_3Si·m″	9.2	*cF*4	$Pm\bar{3}m$
γNb_5Si_3	15.4	*hP*16	$P6_3/mcm$
High-pressure phase			
Nb_3Si-I	9.2	*t***	...

Nb-Ta

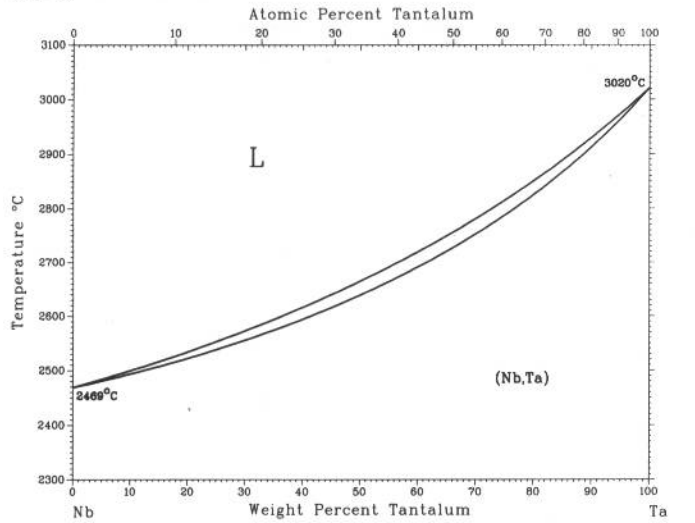

R. Krishnan, S.P. Garg, and N. Krishnamurthy, 1982

Phase	Composition, wt% Ta	Pearson symbol	Space group
(Nb,Ta)	0 to 100	*cI*2	$Im\bar{3}m$

Nb-Th

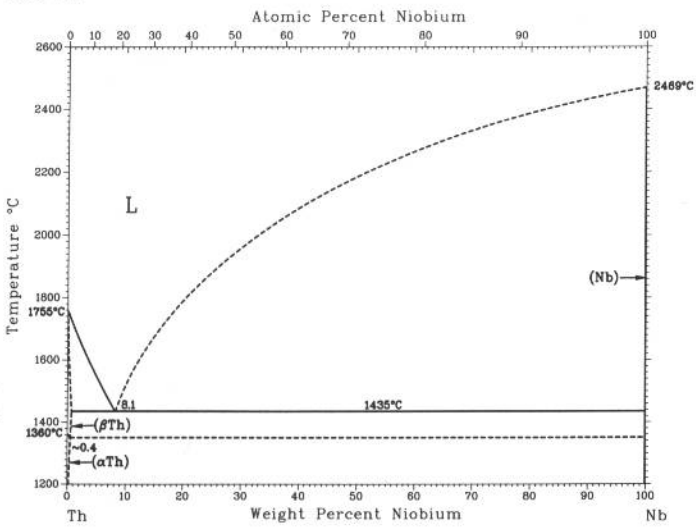

O.N. Carlson, J.M. Dickerson. H.E. Lunt, and H.A. Wilhelm, 1956

Phase	Composition, wt% Nb	Pearson symbol	Space group
(βTh)	0 to ~0.6	*cI*2	$Im\bar{3}m$
(αTh)	0 to ~0.4	*cF*4	$Fm\bar{3}m$
(Nb)	100	*cI*2	$Im\bar{3}m$

Nb-Ti

J.L. Murray, 1987

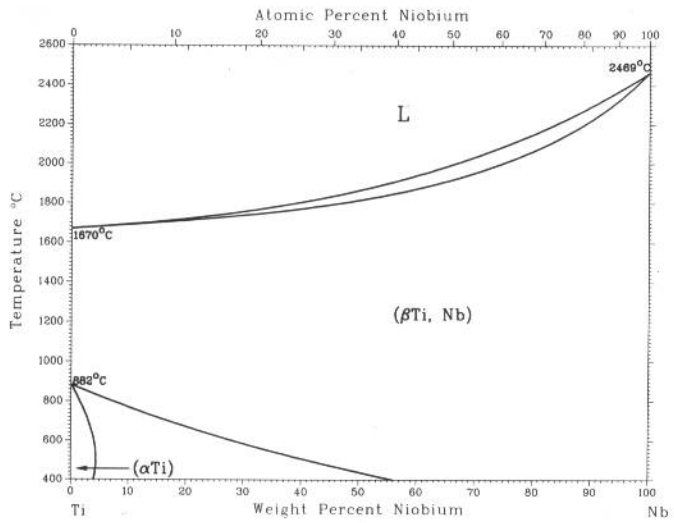

Phase	Composition, wt% Nb	Pearson symbol	Space group
(βTi,Nb)	0 to 100	*cI*2	$Im\bar{3}m$
(αTi)	0 to 4.7	*hP*2	$P6_3/mmc$
Metastable phases			
(α′Ti)	0 to ~9	*hP*2	$P6_3/mmc$
(α″Ti)	~14 to 43	*oC*4	*Cmcm*
ω	16 to 45	*hP*3	*P*6/*mmm*
τ	26 to 41	(a)	...

(a) bct

Nb-U

H. Okamoto, 1990

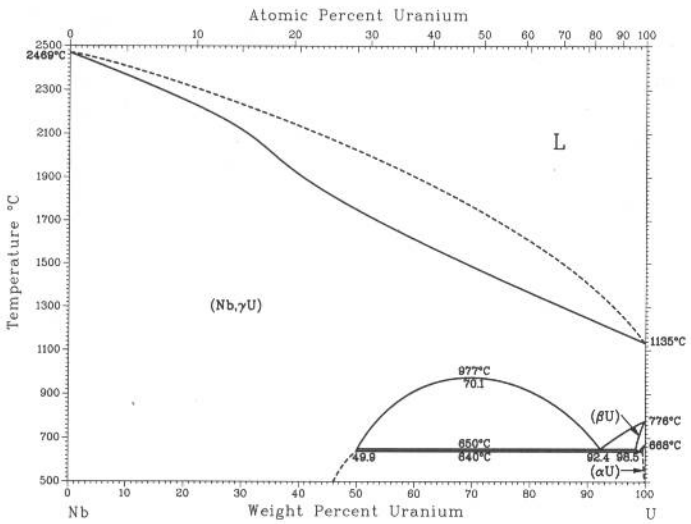

Phase	Composition, wt% U	Pearson symbol	Space group
(Nb,γU)	0 to 100	*cI*2	$Im\bar{3}m$
(βU)	98.5 to 100	*cF*4	$Fm\bar{3}m$
(αU)	~100	*hP*2	$P6_3/mmc$

Nb-V

J.F. Smith and O.N. Carlson, 1989

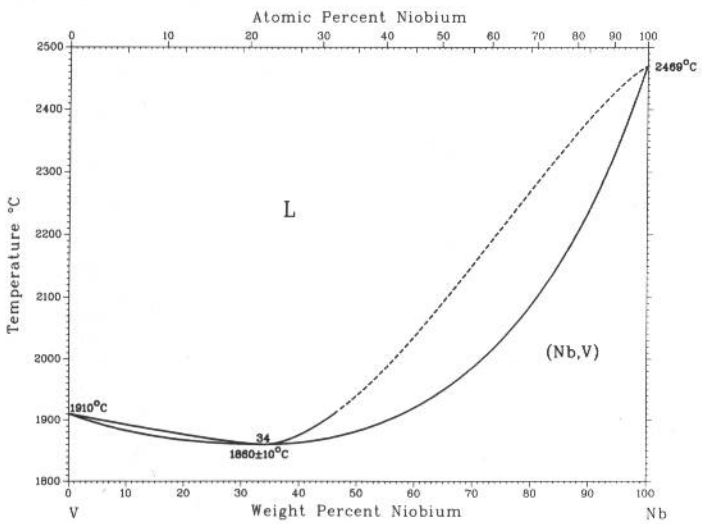

Phase	Composition, wt% Nb	Pearson symbol	Space group
(V,Nb)	0 to 100	*cI*2	$Im\bar{3}m$

Nb-W

S.V. Nagender Naidu, A.M. Sriramamurthy, and P. Rama Rao, 1988

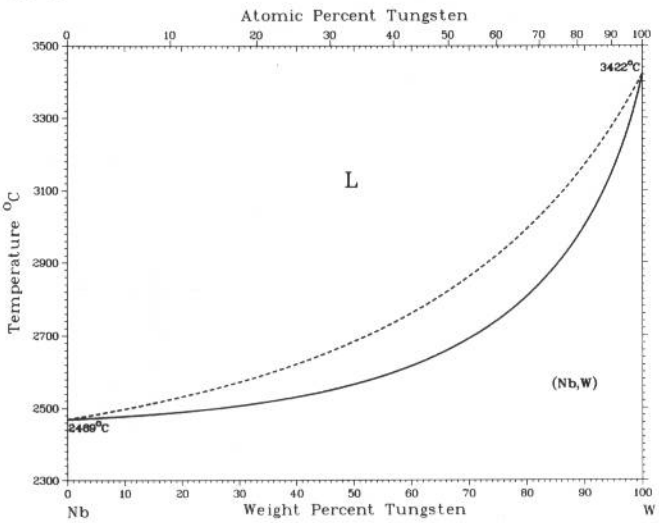

Phase	Composition, wt% W	Pearson symbol	Space group
(Nb,W)	0 to 100	*cI*2	$Im\bar{3}m$

Nb-Zr

H. Okamoto, 1992

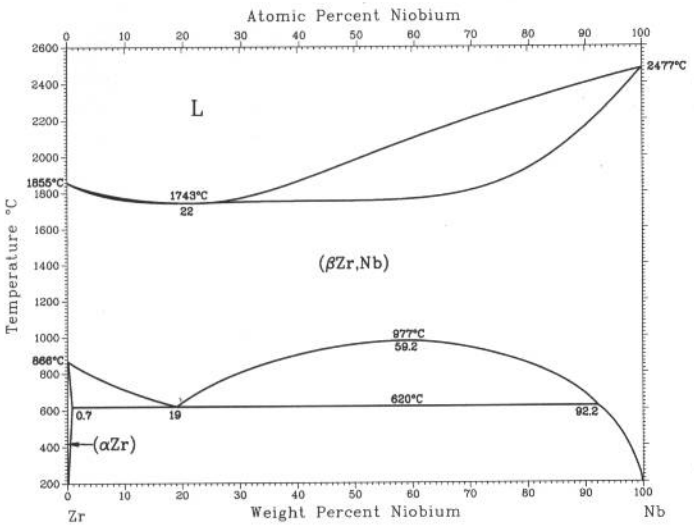

Phase	Composition, wt% Nb	Pearson symbol	Space group
(βZr,Nb)	0 to 100	*cI*2	$Im\bar{3}m$
(αZr)	0 to 0.7	*hP*2	$P6_3/mmc$
Metastable phase			
ω	...	*hP*3	(a)

(a) Changes from $P6/mmm$ to $P\bar{3}m1$ with increasing Nb content

Nd-Ni

H. Okamoto, 1992

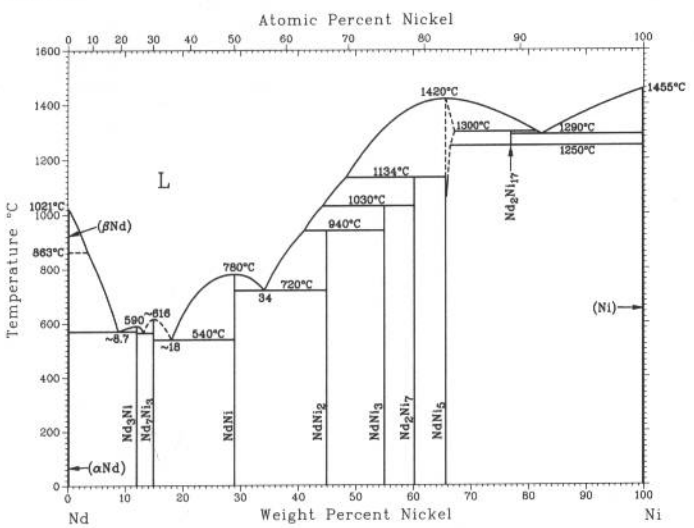

Phase	Composition, wt% Ni	Pearson symbol	Space group
(βNd)	0	*cI*2	$Im\bar{3}m$
(αNd)	0	*hP*4	$P6_3/mmc$
Nd_3Ni	11.9	*oP*16	*Pnma*
Nd_7Ni_3	14.8	*hP*20	$P6_3mc$
NdNi	28.9	*oC*8	*Cmcm*
$NdNi_2$	44.9	*cF*24	$Fd\bar{3}m$
$NdNi_3$	55.0	*hR*12	$R\bar{3}m$
Nd_2Ni_7	58.8	*hP*36	$P6_3/mmc$
		*hR*18	$R\bar{3}m$
$NdNi_5$	67.0	*hP*6	$P6/mmm$
Nd_2Ni_{17}	77.6	*hP*38	$P6_3/mmc$
(Ni)	100	*cF*4	$Fm\bar{3}m$

Nd-Pt

H. Okamoto, 1990

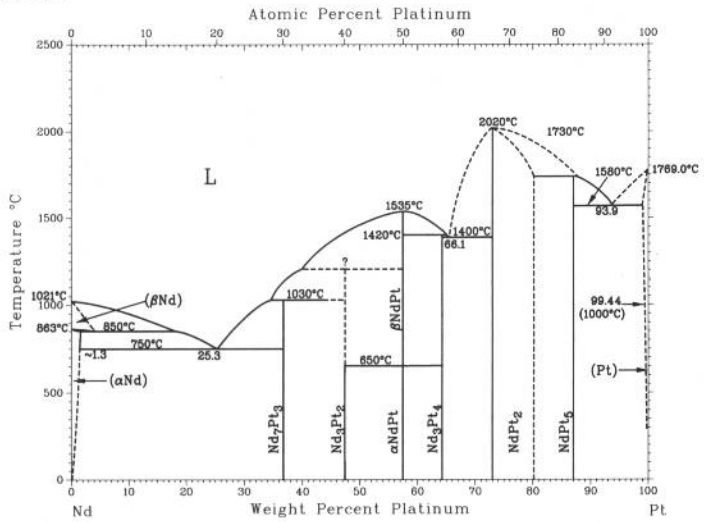

Phase	Composition, wt% Pt	Pearson symbol	Space group
(βNd)	0 to ~4	*cI*2	$Im\bar{3}m$
(αNd)	0 to ~1.3	*hP*4	$P6_3/mmc$
Nd_7Pt_3	37	*hP*20	$P6_3mc$
Nd_3Pt_2	47	*hR*15	$R\bar{3}$
βNdPt	57.5	*oC*8	*Cmcm*
αNdPt	57.5	*oP*8	*Pnma*
Nd_3Pt_4	64.3	*hR*14	$R\bar{3}$
$NdPt_2$	73.0 to 80	*cF*24	$Fd\bar{3}m$
$NdPt_5$	87.1	*hP*6	$P6/mmm$
(Pt)	~100	*cF*4	$Fm\bar{3}m$

Nd-Rh

H. Okamoto, 1990

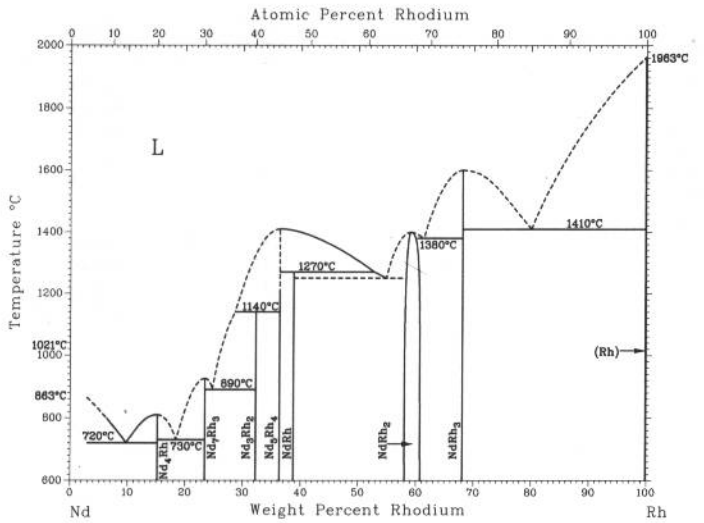

Phase	Composition, wt% Rh	Pearson symbol	Space group
(βNd)	0	*cI*2	$Im\bar{3}m$
(αNd)	0	*hP*4	$P6_3/mmc$
Nd_4Rh	15	*oP*16	*Pnma*
Nd_7Rh_3	23	*hP*20	$P6_3mc$
βNd_3Rh_2	32	...	...
αNd_3Rh_2	32	*hR*15	$R\bar{3}$
Nd_5Rh_4	36.3	*oP*36	*Pnma*
NdRh	39	*oC*8	*Cmcm*
$NdRh_2$	58 to 60.8	*cF*24	$Fd\bar{3}m$
$NdRh_3$	68	*hP*24	$P6_3/mmc$
(Rh)	100	*cF*4	$Fm\bar{3}m$

Nd-Sb

H. Okamoto, 1990

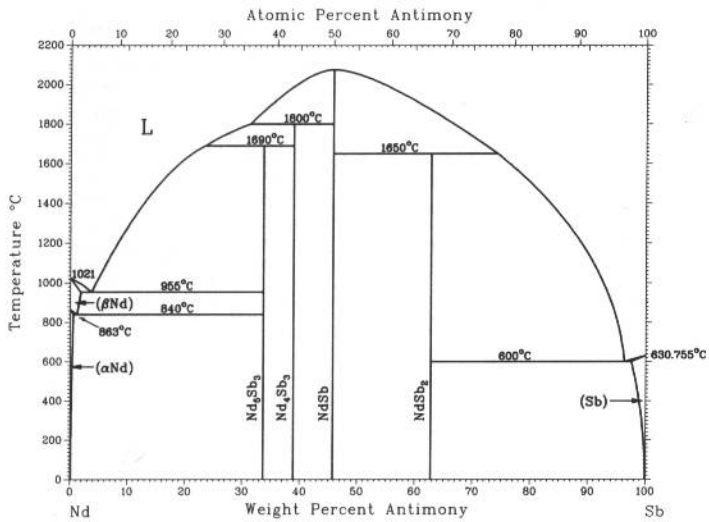

Phase	Composition, wt% Sb	Pearson symbol	Space group
(βNd)	0 to 1.7	*cI*2	$Im\bar{3}m$
(αNd)	0 to 0.8	*hP*4	$P6_3/mmc$
Nd_5Sb_3	33.6	*hP*16	$P6_3/mcm$
Nd_4Sb_3	38.8	*cI*28	$I\bar{4}3d$
NdSb	45.8	*cF*8	$Fm\bar{3}m$
$NdSb_2$	62.8	*oC*24	*Cmca*
(Sb)	97.6 to 100	*hR*2	$R\bar{3}m$

Nd-Si

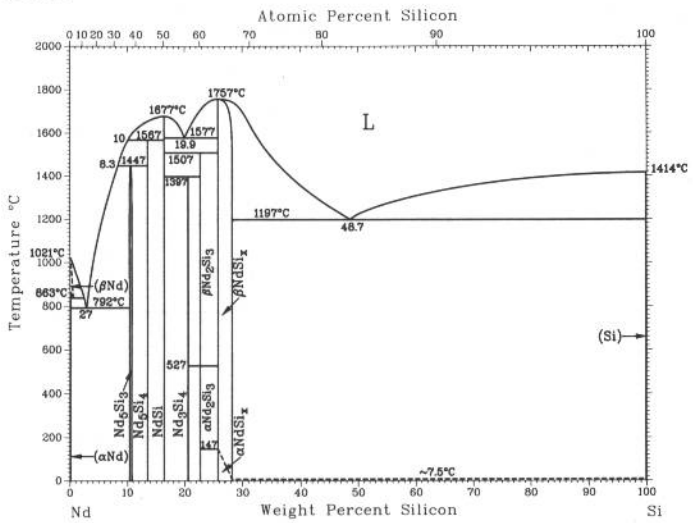

A.B. Gokhale, A. Munitz, and G.J. Abbaschian, 1989

Phase	Composition, wt% Si	Pearson symbol	Space group
(βNd)	0	*cI*2	$Im\bar{3}m$
(αNd)	0	*hP*4	$P6_3/mmc$
Nd_5Si_3	~10.3 to ~10.7	*tI*32	$I4/mcm$
Nd_5Si_4	13.48	...	$P4_12_12$
NdSi	16.3	*oP*8	*Pnma*
Nd_3Si_4	21	...	...
βNd_2Si_3	23	...	...
αNd_2Si_3	22.6	*hP*3	*P6/mmm*
$\beta NdSi_x$	28.14	*tI*12	$I4_1/amd$
$\alpha NdSi_x$	25.7 to 28.14	...	*Imma*
(Si)	100	*cF*8	$Fd\bar{3}m$

Nd-Sn

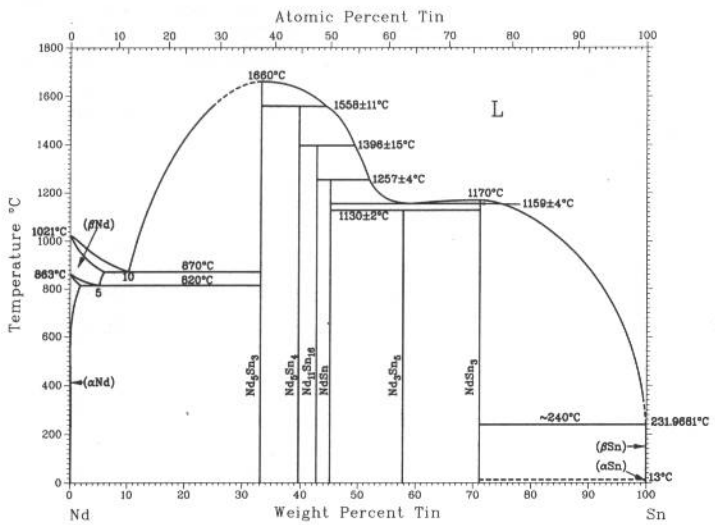

H. Okamoto, 1990

Phase	Composition, wt% Sn	Pearson symbol	Space group
(βNd)	0 to 6	*cI*2	$Im\bar{3}m$
(αNd)	0 to 2	*hP*4	$P6_3/mmc$
Nd_5Sn_3	33.1	*hP*16	$P6_3/mcm$
Nd_5Sn_4	39.7	*oP*36	*Pnma*
$Nd_{11}Sn_{10}$	42.8	*tI*84	$I4/mmm$
NdSn	45.1	...	...
Nd_3Sn_5	57.8	...	...
$NdSn_3$	71	*cP*4	$Pm\bar{3}m$
(βSn)	100	*tI*4	$I4_1/amd$
(αSn)	100	*cF*8	$Fd\bar{3}m$

Nd-Te

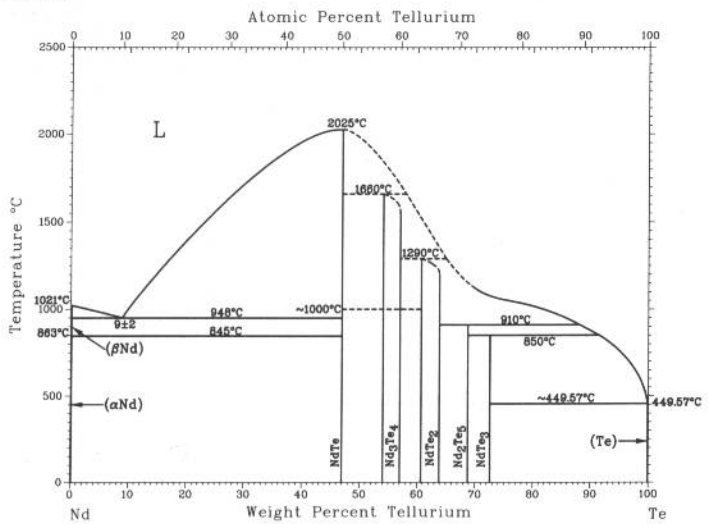

H. Okamoto, 1990

Phase	Composition, wt% Te	Pearson symbol	Space group
(βNd)	0	*cI*2	$Im\bar{3}m$
(αNd)	0	*hP*4	$P6_3/mmc$
NdTe	46.9	*cF*8	$Fm\bar{3}m$
Nd_3Te_4(a)	54 to 57?	*cI*28	$I\bar{4}3d$
Nd_2Te_3(a)	57	*oP*20	*Pnma*
$NdTe_2$	60.7 to 63.9	*tP*6	*P4/nmm*
Nd_2Te_5	68.8	*oC*28	*Cmcm*
$NdTe_3$	73	*oP*16	*Cmcm*
(Te)	100	*hP*3	$P3_121$

(a) The phase relationships between Nd_3Te_4 and Nd_2Te_3, and the homogeneity range of each, are unknown.

Nd-Ti

J.L. Murray, 1987

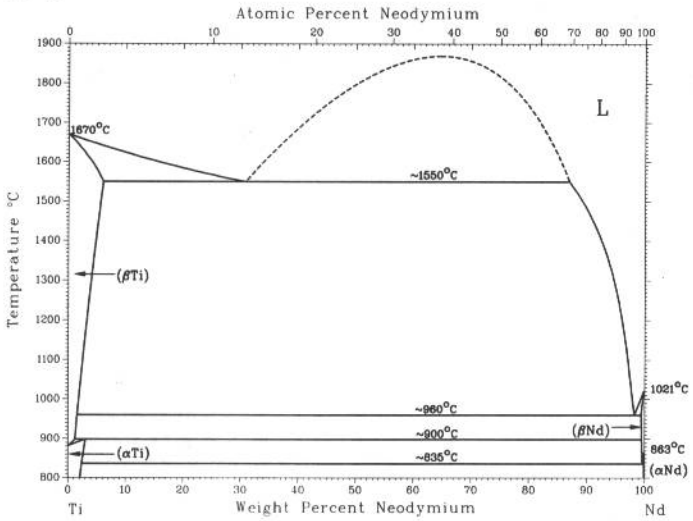

Phase	Composition, wt% Nd	Pearson symbol	Space group
(βTi)	0 to ~9	*cI*2	$Im\bar{3}m$
(αTi)	0 to ~3	*hP*2	$P6_3/mmc$
(βNd)	? to 100	*cI*2	$Im\bar{3}m$
(αNd)	~100	*hP*2	$P6_3/mmc$

Nd-Tl

S. Delfino, A. Saccone, A. Palenzona, and R. Ferro, unpublished

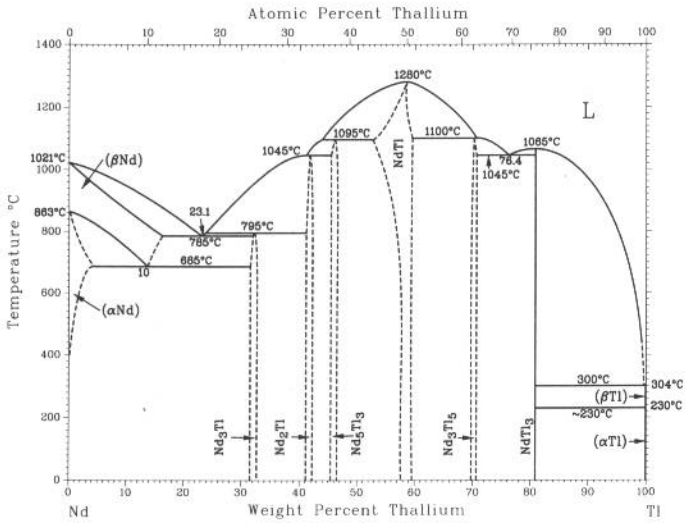

Phase	Composition, wt% Tl	Pearson symbol	Space group
(βNd)	0 to ~16	*cI*2	$Im\bar{3}m$
(αNd)	0 to ~4	*hP*4	$P6_3/mmc$
Nd_3Tl(a)	~31.5 to 32.7	*cP*4	$Pm\bar{3}m$
	~32.1	*cF*4	$Fm\bar{3}m$
Nd_2Tl	~41 to ~42	*hP*6	$P6_3/mmc$
Nd_5Tl_3	~45 to ~47	*tI*32	*I*4/*mcm*
NdTl(b)	~53 to ~60	*cP*2	$Pm\bar{3}m$
		(or *cI*2)	$Im\bar{3}m$
NdTl(c)	~53 to ~60	*tP*2	*P*4/*mmm*
Nd_3Tl_5	~70 to ~71	*oC*32	*Cmcm*
$NdTl_3$	81	*cP*4	$Pm\bar{3}m$
(βTl)	100	*cI*2	$Im\bar{3}m$
(αTl)	100	*hP*2	$P6_3/mmc$

(a) A *cP*4-*cF*4 order-disorder transformation in this phase has been suggested. (b) Cubic structure presumed to be room- and higher-temperature phases. (c) Tetragonal structure presumed to be lower-temperature phase

Nd-Zn

J.T. Mason and P. Chiotti, 1972

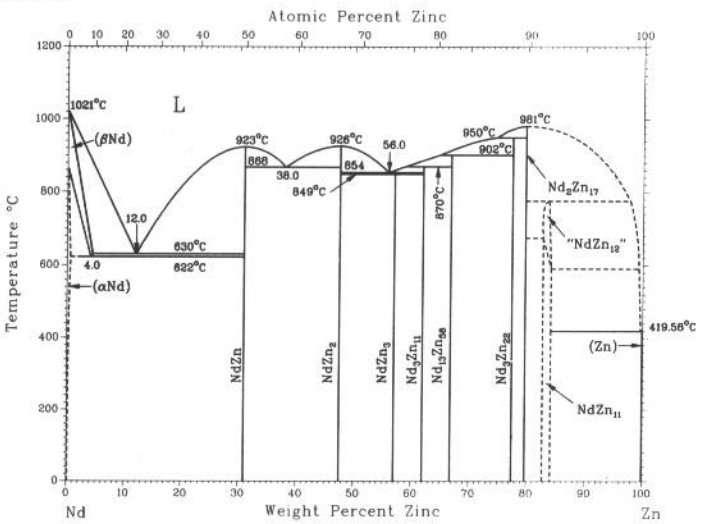

Phase	Composition, wt% Zn	Pearson symbol	Space group
(βNd)	0 to 4.0	*cI*2	$Im\bar{3}m$
(αNd)	0 to >0.5	*hP*4	$P6_3/mmc$
NdZn	31.2	*cP*2	$Pm\bar{3}m$
$NdZn_2$	47.6	*oI*12	*Imma*
$NdZn_3$	~57.0	*oP*16	*Pnma*
Nd_3Zn_{11}	~62.5	*oI*28	*Immm*
$Nd_{13}Zn_{58}$	~66.9	*hP*142	$P6_3mc$
Nd_3Zn_{22}	>77	*tI*100	$I4_1/amd$
Nd_2Zn_{17}	~79.4	*hP*38	$P6_3/mmc$
		*hR*19	$R\bar{3}m$
$NdZn_{11}$	~83.4	*tI*48	$I4_1/amd$
"$NdZn_{12}$"	~84.5	...	...
(Zn)	~100	*hP*2	$P6_3/mmc$
Other reported phase			
$NdZn_5$	~69.3	*hP*6	*P*6/*mmm*

Ni-O

J.P. Neumann, T. Zhong, and Y.A. Chang, 1991

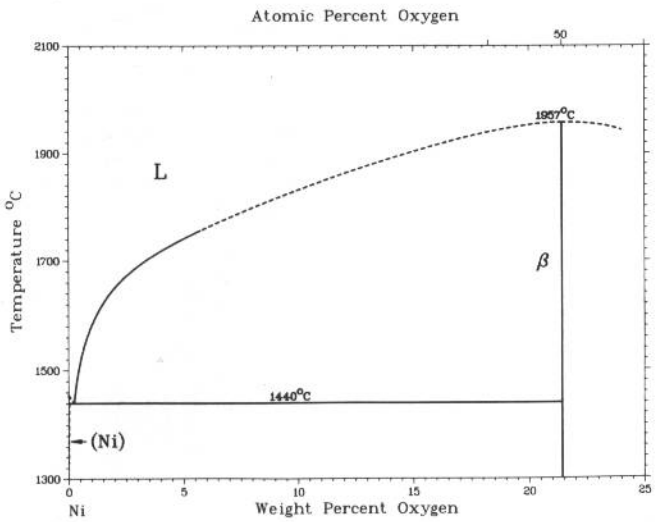

Phase	Composition, wt% O	Pearson symbol	Space group
(Ni)	0 to 0.01	*cF*4	$Fm\bar{3}m$
NiO(HT) or β	21.4	*cF*8	$Fm\bar{3}m$
NiO(LT)	21.4	*rP*2(a)	...
Ni_3O_4	27	...	...
Ni_2O_3	29	...	...
NiO_2	35.3	...	...

(a) The *rP*2 designation for NiO(LT) is an alternative to *hR*2.

Ni-rich region of the Ni-O phase diagram

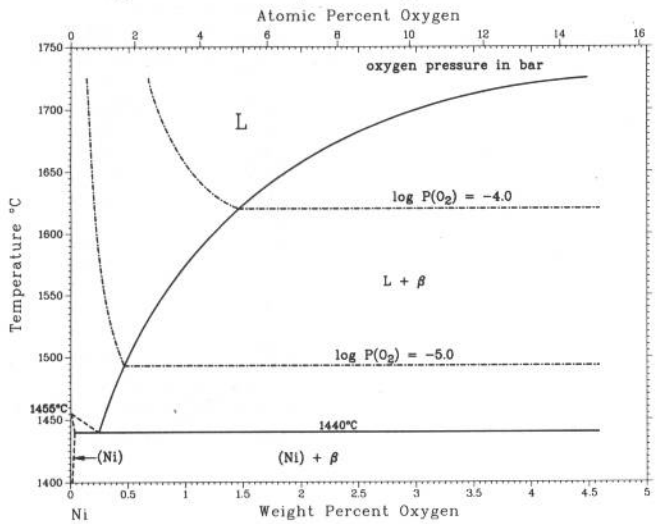

Ni-Os

P. Nash, 1991

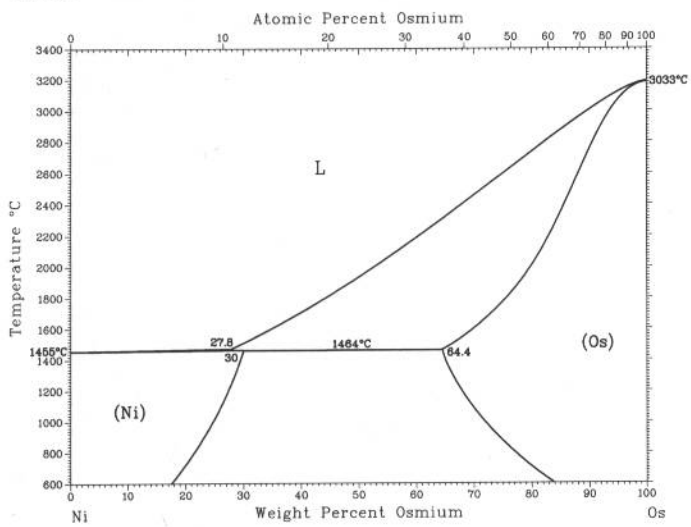

Phase	Composition, wt% Os	Pearson symbol	Space group
(Ni)	0 to 30	*cF*4	$Fm\bar{3}m$
(Os)	64.4 to 100	*hP*2	$P6_3/mmc$

Ni-P

K.J. Lee and P. Nash, 1991

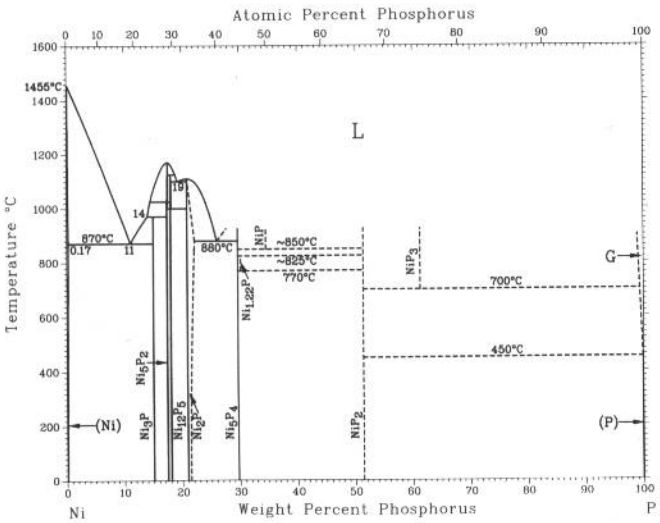

Phase	Composition, wt% P	Pearson symbol	Space group
(Ni)	0 to 0.17	*cF*4	$Fm\bar{3}m$
Ni_3P	15	*tI*32	$I\bar{4}$
βNi_5P_2	17.5	...	...
αNi_5P_2	17.5	*hP*168(a)	$P\bar{3}$
$\delta Ni_{12}P_5$	18.0	...	...
$\gamma Ni_{12}P_5$	18.0	*tI*34	$I4/m$
Ni_2P	20.9 to ?	*hP*9	$P\bar{6}2m$ $P3_21$
Ni_5P_4	29.6	*hP*36	$P6_3mc$
$Ni_{1.22}P$	30.2	...	...
NiP	34.5	*oP*16	*Pcba*
NiP_2	51.4	*mC*12	$C2/c$
NiP_3	61	*cI*32	$Im\bar{3}$
P (red)	100	...	...
High-pressure phase			
NiP_2	51.4	*cP*12	$Pa\bar{3}$
Metastable phases			
"Ni_5P_2"	11 to 18	*h***	...
α	8 to 15	*c***	...
α_1	8 to 15	*h***	...
α_2	8 to 15	*h***	...
α_3	8 to 15	*h***	...
"αNi_3P"	15	*t***	...
"βNi_3P"	15	*h***	...
"γNi_3P"	15	*c***	...
α (amorphous)	~15	(b)	...
β (amorphous)	~15	(c)	...

(a) Might be *hP*336. (b) Liquid-like. (c) Molecular cluster

Ni-Pb

P. Nash, 1991

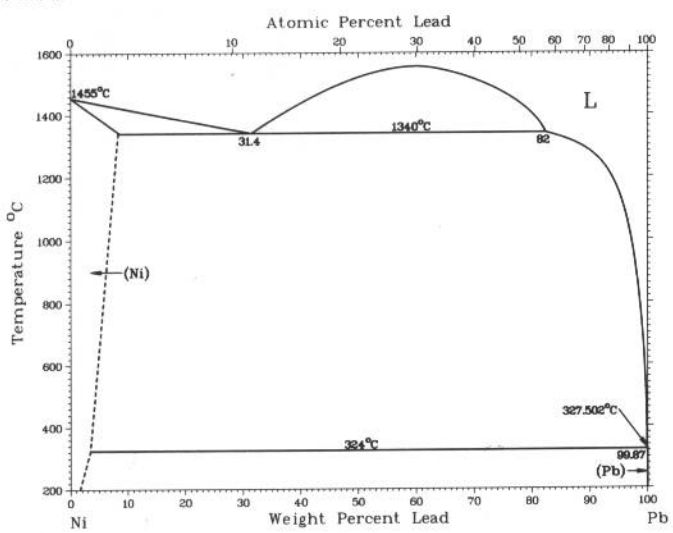

Phase	Composition, wt% Pb	Pearson symbol	Space group
(Ni)	0 to ~4.1	*cF*4	$Fm\bar{3}m$
(Pb)	99.9 to 100	*cF*4	$Fm\bar{3}m$
Metastable phase			
NiPb	77.9	*hP*4	$P6_3/mmc$

Ni-Pd

A. Nash and P. Nash, 1991

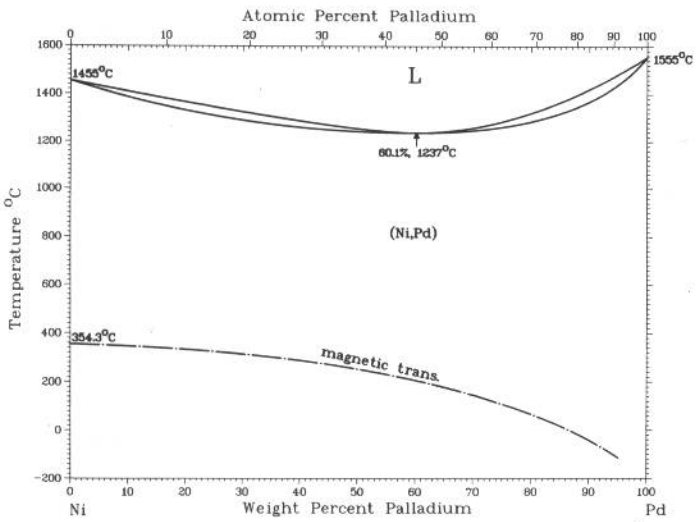

Phase	Composition, wt% Pd	Pearson symbol	Space group
(Ni,Pd)	0 to 100	*cF*4	$Fm\bar{3}m$

Ni-Pr

Y.Y. Pan and P. Nash, 1991

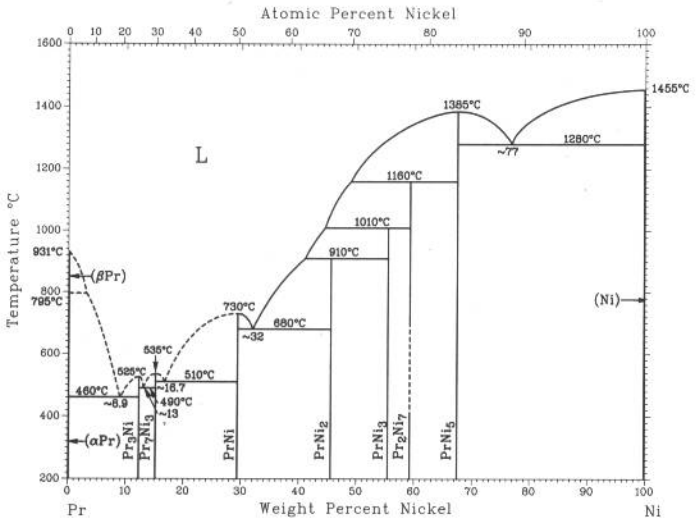

Phase	Composition, wt% Ni	Pearson symbol	Space group
(βPr)	0	*hP*4	$P6_3/mmc$
(αPr)	0	*cI*2	$Im\bar{3}m$
Pr_3Ni	12.2	*oP*16	*Pnma*
Pr_7Ni_3	15.1	*hP*20	$P6_3mc$
PrNi	29.4	*oC*8	*Cmcm*
$PrNi_2$	45.5	*cF*24	$Fd\bar{3}m$
$PrNi_3$	55.5	*hR*24	$R\bar{3}m$
Pr_2Ni_7	59.3	*hP*36	$P6_3/mmc$
		*hR*54	$R\bar{3}m$
$PrNi_5$	67.5	*hP*6	*P6/mmm*
(Ni)	100	*cF*4	$Fm\bar{3}m$

Ni-Pt

P. Nash and M.F. Singleton, 1991

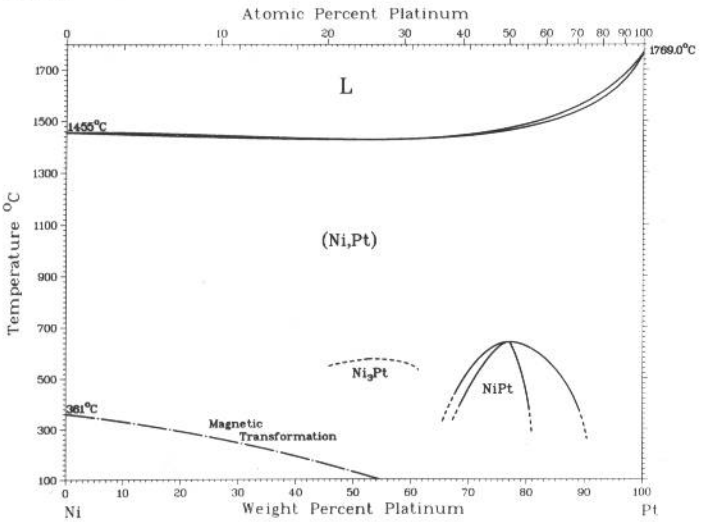

Phase	Composition, wt% Pt	Pearson symbol	Space group
(Ni,Pt)	0 to 100	*cF*4	$Fm\bar{3}m$
Ni_3Pt	~53	*cP*4	$Pm\bar{3}m$
NiPt	~76.9	*tP*4	*P4/mmm*

Ni-Pu

D.E. Peterson, 1991

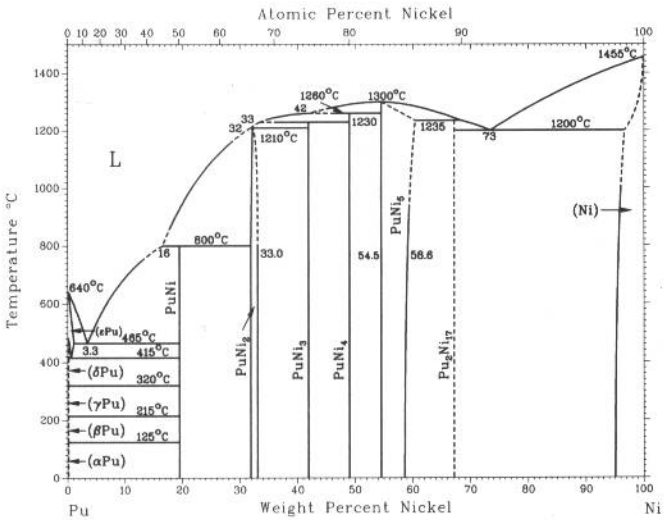

Phase	Composition, wt% Ni	Pearson symbol	Space group
(εPu)	0 to 1.1	*cI*2	$Im\bar{3}m$
(δ′Pu)	0 to 0.04	*tI*2	*I*4/*mmm*
(δPu)	0 to 0.1	*cF*4	$Fm\bar{3}m$
(γPu)	0	*oF*8	*Fddd*
(βPu)	0	*mC*34	*C*2/*m*
(αPu)	0	*mP*16	$P2_1/m$
PuNi	19.4	*oC*8	*Cmcm*
$PuNi_2$	32.5 to 34	*cF*24	$Fd\bar{3}m$
$PuNi_3$	42	*hR*12	$R\bar{3}m$
$PuNi_4$	49	*mC*30	*C*2/*m*
$PuNi_5$	54.5 to 60	*hP*6	*P*6/*mmm*
Pu_2Ni_{17}	67.2	*hP*38	$P6_3/mmc$
(Ni)	92.9 to 100	*cF*4	$Fm\bar{3}m$

Pu-rich region of the Pu-Ni phase diagram

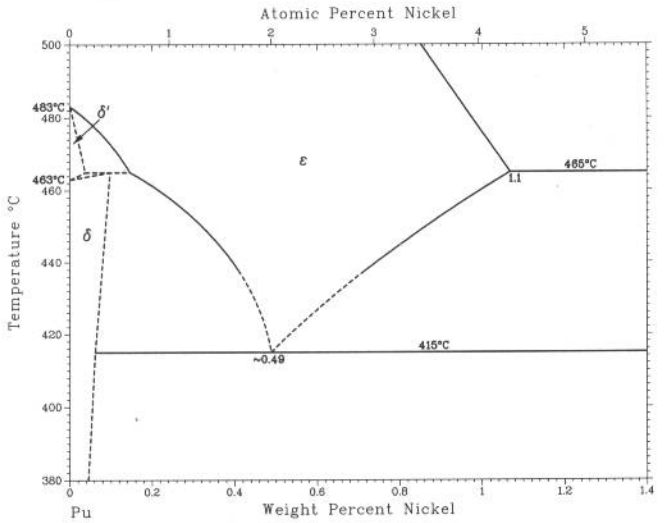

Ni-Re

H. Okamoto, 1992

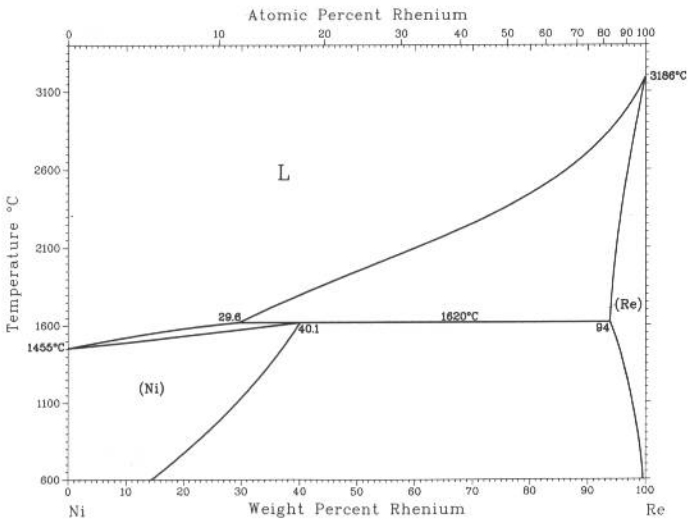

Phase	Composition, wt% Re	Pearson symbol	Space group
(Ni)	0 to 40.1	*cF*4	$Fm\bar{3}m$
(Re)	94 to 100	*hP*2	$P6_3/mmc$

Ni-Rh

A. Nash and P. Nash, 1991

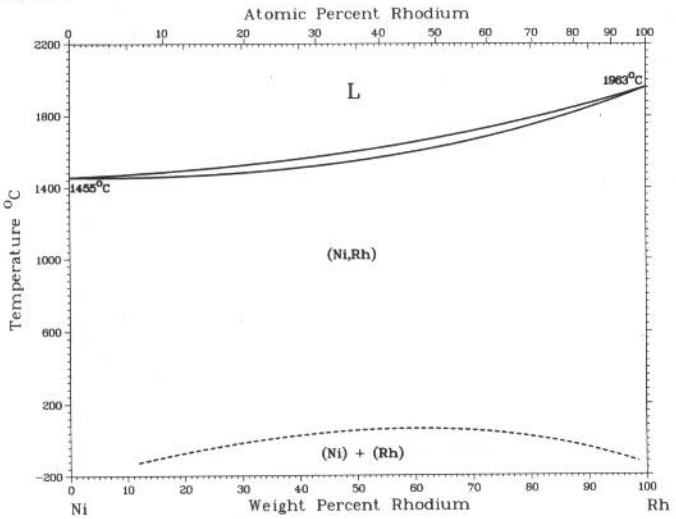

Phase	Composition, wt% Rh	Pearson symbol	Space group
(Ni,Rh)	0 to 100	*cF*4	$Fm\bar{3}m$

Ni-Ru

P. Nash, 1991

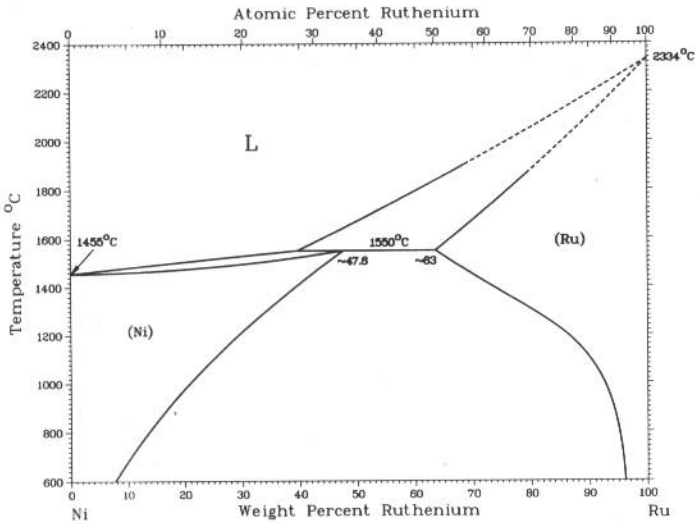

Phase	Composition, wt% Ru	Pearson symbol	Space group
(Ni)	0 to ~47.6	*cF*4	$Fm\bar{3}m$
(Ru)	~63 to 100	*hP*2	$P6_3/mmc$
Metastable phase			
η	?	*t***	...

Ni-S

M. Singleton, P. Nash, and K.J. Lee, 1991

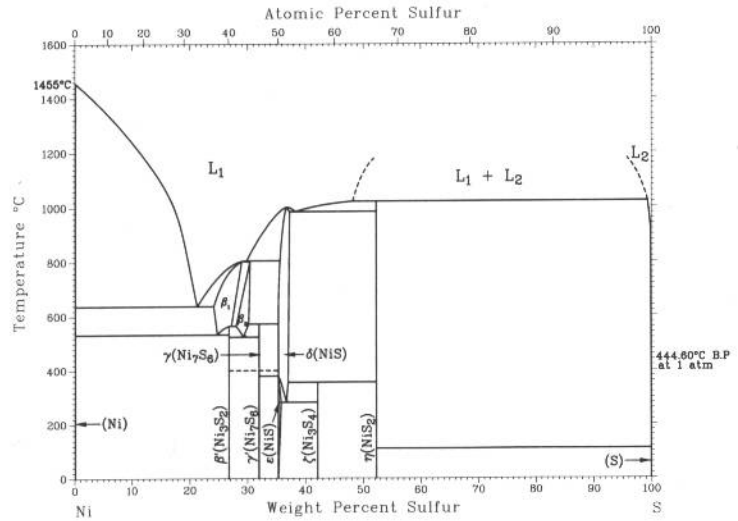

Phase	Composition, wt% S	Pearson symbol	Space group
(Ni)	0	*cF*4	$Fm\bar{3}m$
$\beta'(Ni_3S_2)$	27	*hR*5	*R*32
$\beta_1(Ni_3S_2)$	24.1 to ~28	(a)	...
$\beta_2(Ni_4S_3)$	28 to 30	...	...
$\gamma(Ni_7S_6)$	31.9	(a)	...
$\gamma'(Ni_7S_6)$	31.9	...	...
ε(NiS)	35.3 to 35.8	*hR*6	$R\bar{3}m$
δ(NiS)	35.1 to 37.7	*hP*4	$P6_3/mmc$
$\zeta(Ni_3S_4)$	42.1	*cF*56	$Fd\bar{3}m$
$\eta(NiS_2)$	52.3	*cP*12	*Pa*3
(S)	100	*oF*128	*Fddd*

(a) Hexagonal

Ni-Sb

G.H. Cha, S.Y. Lee, and P. Nash, 1991

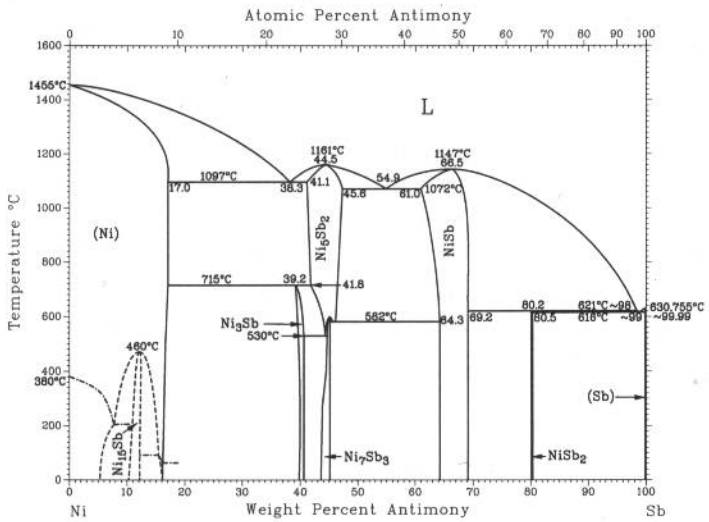

Phase	Composition, wt% Sb	Pearson symbol	Space group
(Ni)	0 to 17.0	*cF*4	$Fm\bar{3}m$
$Ni_{15}Sb$	12.2	...	...
Ni_3Sb	39.2 to 41	*oP*8	*Pmmm*
Ni_5Sb_2	41.1 to 45.6	*mC*28	...
Ni_7Sb_3	45	*t***	...
NiSb	61.0 to 69.2	*hP*4	$P6_3/mmc$
$NiSb_2$	80.2 to 80.5	*oP*6	*Pnnm*
(Sb)	~100	*hR*2	$R\bar{3}m$

Ni-Sc

P. Nash and Y.Y. Pan, 1991

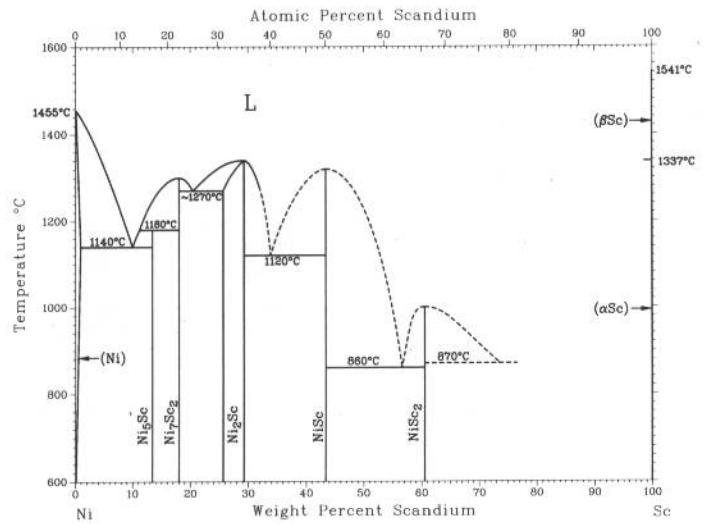

Phase	Composition, wt% Sc	Pearson symbol	Space group
(Ni)	~0	*cF*4	$Fm\bar{3}m$
Ni_5Sc(HT)	13.3	*hP*6	*P6/mmm*
Ni_5Sc(LT)	13.3	...	...
Ni_7Sc_2	17.9	*hP*36	$P6_3/mmc$
Ni_2Sc	26 to 29	*cF*24	$Fd\bar{3}m$
NiSc	43.4	*cP*2	$Pm\bar{3}m$
$NiSc_2$	60.5	*cF*96	$Fd\bar{3}m$
(βSc)	100	*cI*2	$Im\bar{3}m$
(αSc)	100	*hP*2	$P6_3/mmc$

Ni-Se

S.Y. Lee and P. Nash, 1991

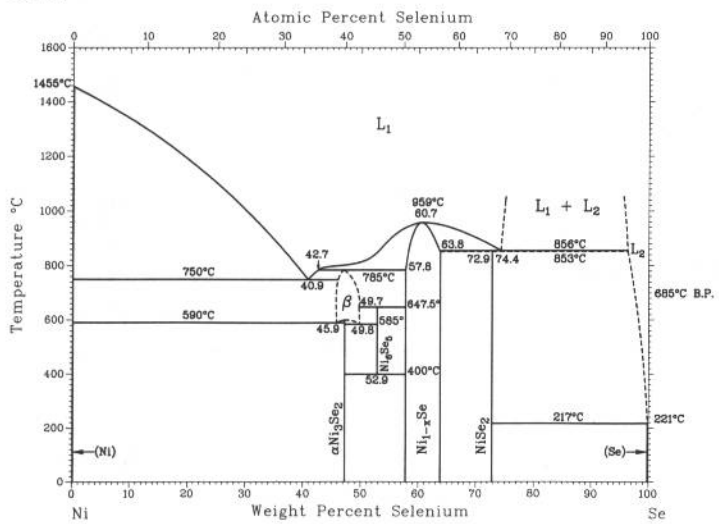

Phase	Composition, wt% Se	Pearson symbol	Space group
(Ni)	~0	*cF*4	$Fm\bar{3}m$
$\beta Ni_{3\pm x}Se_2$	45.9 to 49.8	*c***	...
αNi_3Se_2	47	*hR*5	*R*32
Ni_6Se_5	52.9	*oP*88	$Pca2_1$
		*oC*48	*Cmcm*
$Ni_{1-x}Se$	57.8 to 63.8	*hP*4	$P6_3/mmc$
$NiSe_2$	72.9	*cP*12	*Pa*3
(γSe)	~100	*hP*2	$P3_121$
Metastable phase			
$\alpha' Ni_3Se_2$	47	*tI**	...

Ni-Si

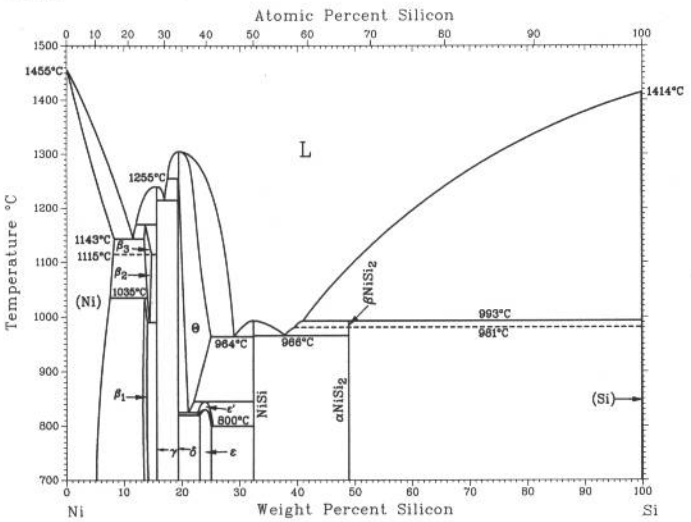

P. Nash and A. Nash, 1991

Phase	Composition, wt% Si	Pearson symbol	Space group
(Ni)	0 to 8.2	*cF*4	$Fm\bar{3}m$
β_1 (Ni_4Si)	12.4 to 13.4	*cP*4	$Pm\bar{3}m$
β_3 (Ni_3Si)	~13.4 to 14.1	*mC*16	...
β_2 (Ni_3Si)	~13.4 to 14.1	*mC*16	...
γ ($Ni_{31}Si_{12}$)	15.6	*hP*14	...
θ (Ni_2Si)	19.4 to 25	*hP*6	...
δ (Ni_2Si)	19.3	*oP*12	...
ε (Ni_3Si_2)	23 to 25	*oP*80	...
NiSi	32.4	*oP*8	*Pnma*
$\beta NiSi_2$	48.9	?	...
$\alpha NiSi_2$	48.9	*cF*12	$Fm\bar{3}m$
(Si)	~100	*cF*8	$Fd\bar{3}m$

Ni-Sm

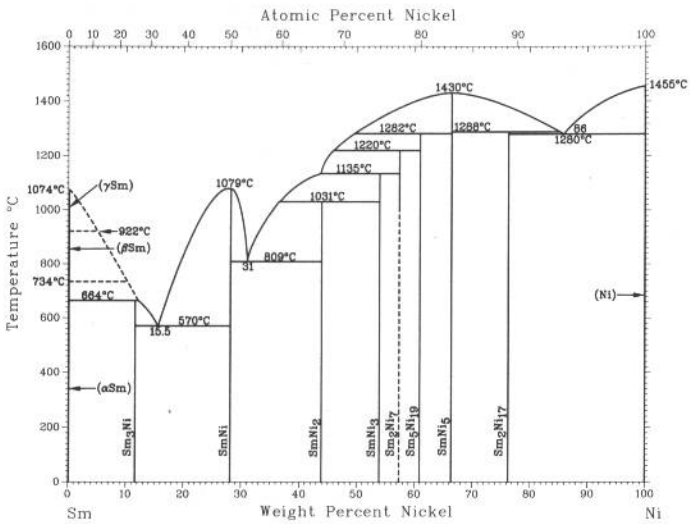

Y.Y. Pan and P. Nash, 1991

Phase	Composition, wt% Ni	Pearson symbol	Space group
(γSm)	0	*cI*2	$Im\bar{3}m$
(βSm)	0	*hP*2	$P6_3/mmc$
(αSm)	0	*hR*3	$R\bar{3}m$
Sm_3Ni	11.5	*oP*16	*Pnma*
SmNi	28.1	*oC*8	*Cmcm*
$SmNi_2$	43.9	*cF*24	$Fd\bar{3}m$
$SmNi_3$	53.9	*hR*24	$R\bar{3}m$
Sm_2Ni_7	57.8	*hP*36(a)	$P6_3/mmc$
		*hR*54(b)	$R\bar{3}m$
Sm_5Ni_{19}	59.8	(c)	$P\bar{3}m1$
$SmNi_5$	66.1	*hP*6	$P6/mmm$
Sm_2Ni_{17}	76.9	*hP*38	$P6_3/mmm$
(Ni)	100	*cF*4	$Fm\bar{3}m$

(a) High-temperature form. (b) Low-temperature form. (c) Trigonal

Ni-Sn

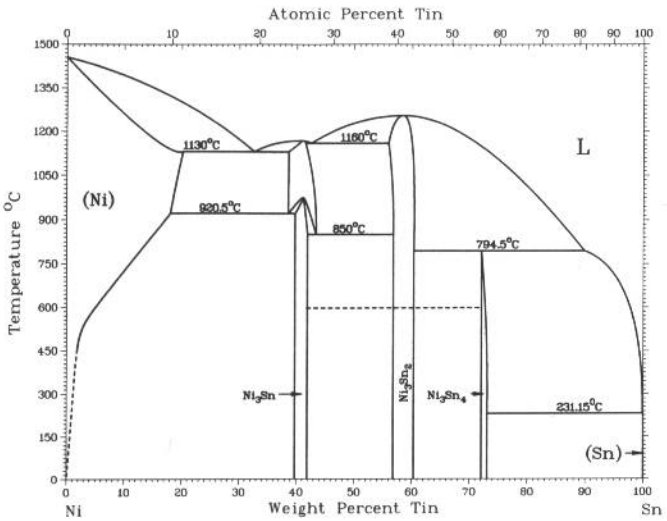

P. Nash and A. Nash, 1991

Phase	Composition, wt% Sn	Pearson symbol	Space group
(Ni)	0 to 19.3	*cF*4	$Fm\bar{3}m$
Ni_3Sn(HT)	37.9 to 43.0	(a)	...
Ni_3Sn(LT)	39 to 41.7	*hP*8	$P6_3/mmc$
Ni_3Sn_2(HT)	54.8 to 57.9	(a)	...
		(b)	...
Ni_3Sn_2(LT)	55.9 to 59.9	*hP*4	$P6_3/mmc$
Ni_3Sn_4	71.6 to 73	*mC*14	*C*2/*m*
(βSn)	~100	*tI*4	$I4_1/amd$
Metastable phase			
Ni_3Sn	40	*oP*8	*Pmmn*

(a) Hexagonal. (b) Orthorhombic

Ni-Ta

A. Nash and P. Nash, 1991

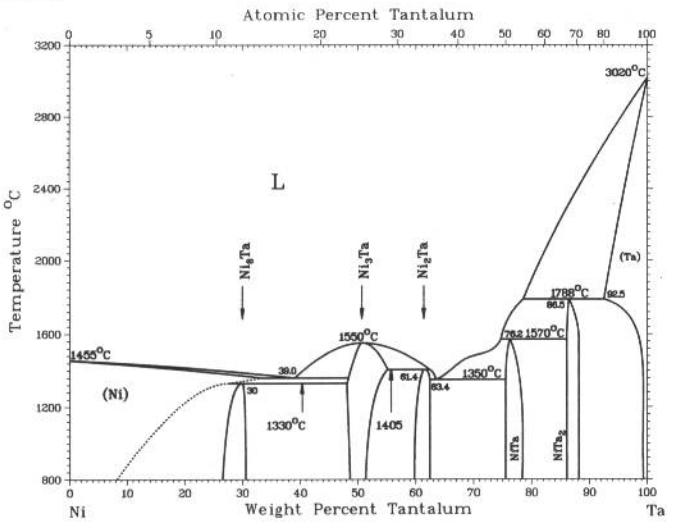

Phase	Composition, wt% Ta	Pearson symbol	Space group
(Ni)	0 to 33	*cF*4	$Fm\bar{3}m$
Ni_8Ta	27.8	*tI*36	...
$Ni_3Ta(12)S$	47.2 to 55.1	*mP*48	$P2_1/m$
Ni_2Ta	59.7 to 62	*tI*6	*I*4/*mmm*
NiTa	75.5 to 78	*hR*13	$R\bar{3}m$
$NiTa_2$	86.1 to 88	*tI*12	*I*4/*mcm*
(Ta)	92.5 to 100	*cI*2	$Im\bar{3}m$
Metastable phases			
ζ	45	...	...
$Ni_3Ta(2)S$	51	*mP*8	*Pmmm*
$Ni_3Ta(3)S$	51	*tI*8	*I*4/*mmm*

Note: Number in parentheses indicates stacking period; *S* identifies the orthogonal layer type.

Ni-Te

S.Y. Lee and P. Nash, 1991

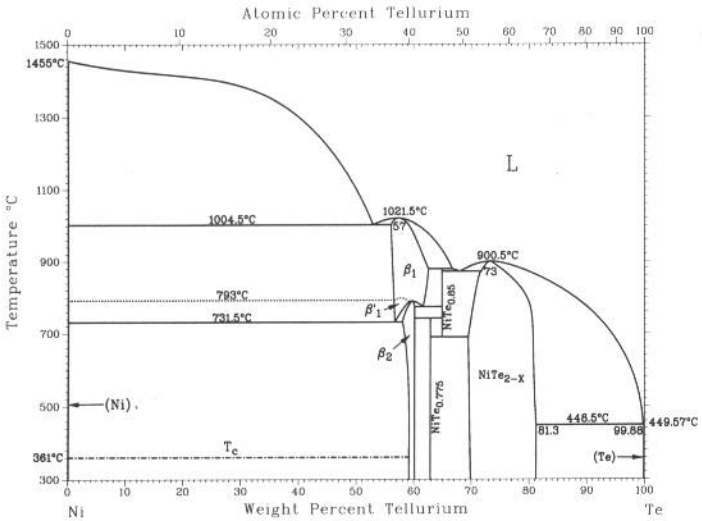

Phase	Composition, wt% Te	Pearson symbol	Space group
(Ni)	~0	*cF*4	$Fm\bar{3}m$
β_1	55.9 to 62.4	*cF**	...
β_2	58.0 to 59.7	*m***	...
	59.7 to 60.1	*o***	...
	60.0 to 60.4	*t***	...
β'_1	56.5 to 58	...	...
$NiTe_{0.775}$	62.7	*o***	...
$NiTe_{0.85}$	64.8	...	...
$NiTe_{2-x}$	69.4 to 81.3	*hP*4	$P6_3/mmc$
		*hP*3	$P\bar{3}m1$
(Te)	~100	*hP*3	$P3_121$

Ni-Ti

J.L. Murray, 1991

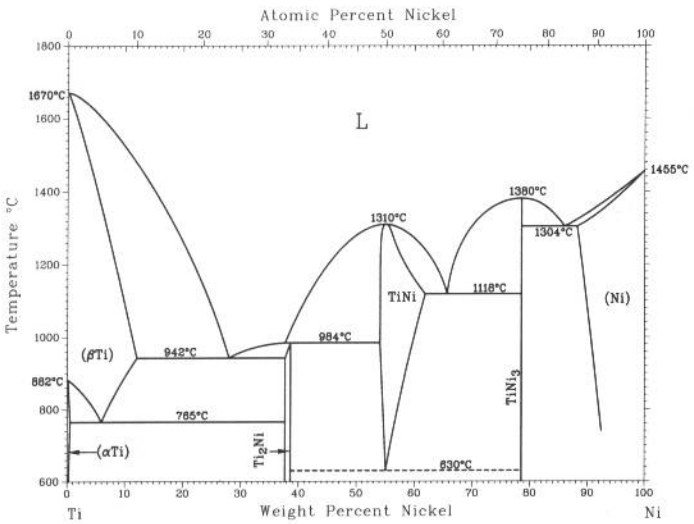

Phase	Composition, wt% Ni	Pearson symbol	Space group
(βTi)	0 to 12	*cI*2	$Im\bar{3}m$
(αTi)	0 to 0.3	*hP*2	$P6_3/mmc$
ω(a)	~10	*hP*3	*P*6/*mmm* or $P\bar{3}m1$
Ti_2Ni	38.0	*cF*96	$Fd\bar{3}m$
TiNi′(a)	~54 to 58	*mP*4	$P2_1/m$
TiNi	54.6 to 62	*cP*2	$Pm\bar{3}m$
γ″$TiNi_3$(a)	~77	*hR*21	$R\bar{3}m$
$TiNi_3$	79	*hP*16	$P6_3/mmc$
γ′$TiNi_3$(a)	~86 to 90	*cP*4	$Pm\bar{3}m$
(Ni)	88.4 to 100	*cF*4	$Fm\bar{3}m$

(a) Metastable

Ni-U

D.E. Peterson, 1991

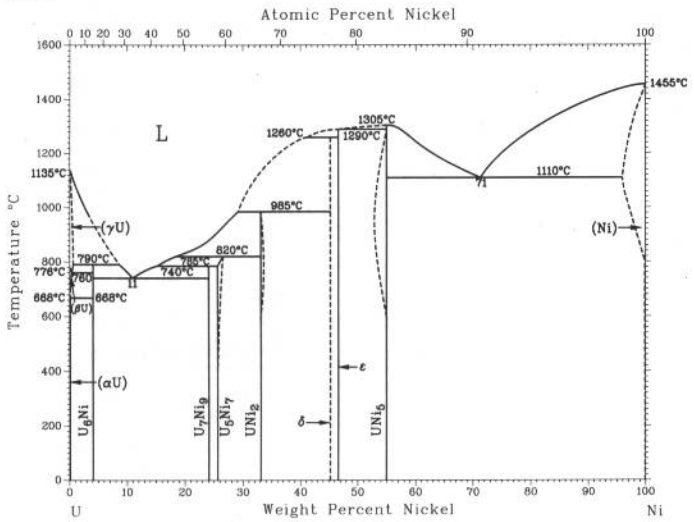

Phase	Composition, wt% Ni	Pearson symbol	Space group
(γU)	0 to 0.5	*cI*2	$Im\bar{3}m$
(βU)	0 to 0.2	*tP*30	$P4_2/mnm$
(αU)	0	*oC*4	*Cmcm*
U_6Ni	4.0	*tI*28	*I*4/*mcm*
U_7Ni_9	24.0	...	...
U_5Ni_7	25.6 to 26.6	...	...
UNi_2	33.1 to 33.4	*hP*12	$P6_3/mmc$
δ	45.2	...	...
ε	46.6	...	...
η(a)	52.9	...	...
UNi_5	53.8 to 55.2	*cF*24	$F\bar{4}3m$
(Ni)	93.1 to 100	*cF*4	$Fm\bar{3}m$

(a) Existence tentative

Ni-V

J.F. Smith, O.N. Carlson, and P. Nash, 1991

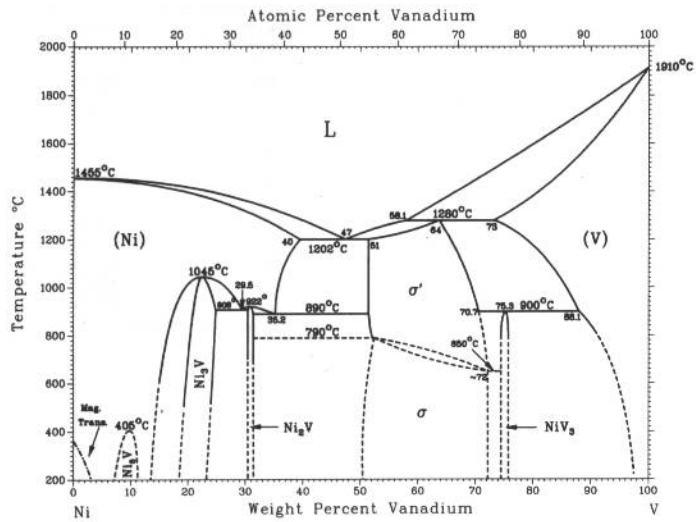

Phase	Composition, wt% V	Pearson symbol	Space group
(Ni)	0 to 40	*cF*4	$Fm\bar{3}m$
Ni_8V	~9.8	*tI*18	...
Ni_3V	~19 to 23.0	*tI*8	*I*4/*mmm*
Ni_2V	~30.2	*oI*6	...
σ′	51 to ~72	...	...
σ	54.0 to ~72	*tP*30	$P4_2/mnm$
NiV_3	74.9 to 76.0	*cP*8	$Pm\bar{3}n$
(V)	73 to 100	*cI*2	$Im\bar{3}m$

Ni-W

H. Okamoto, 1991

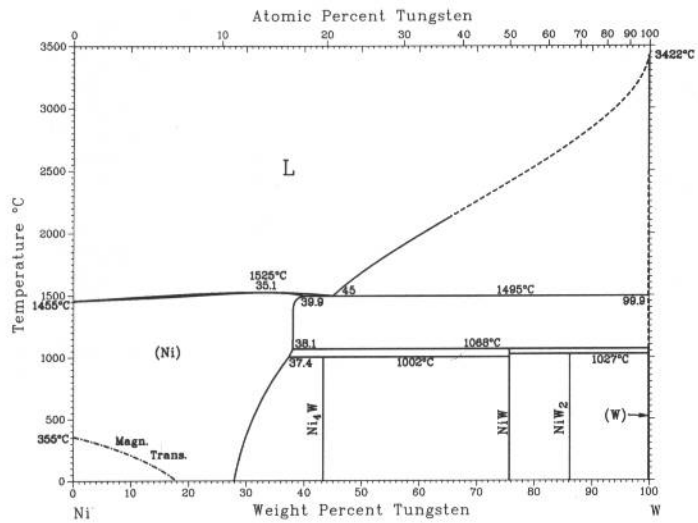

Phase	Composition, wt% W	Pearson symbol	Space group
(Ni)	0 to 39.9	*cF*4	$Fm\bar{3}m$
Ni_4W	~44	*tI*10	*I*4/*m*
NiW	~75.8	*o***	...
NiW_2	86.3	*tI*96	*I*4
(W)	99.9 to 100	*cI*2	$Im\bar{3}m$

Ni-Y

P. Nash, 1991

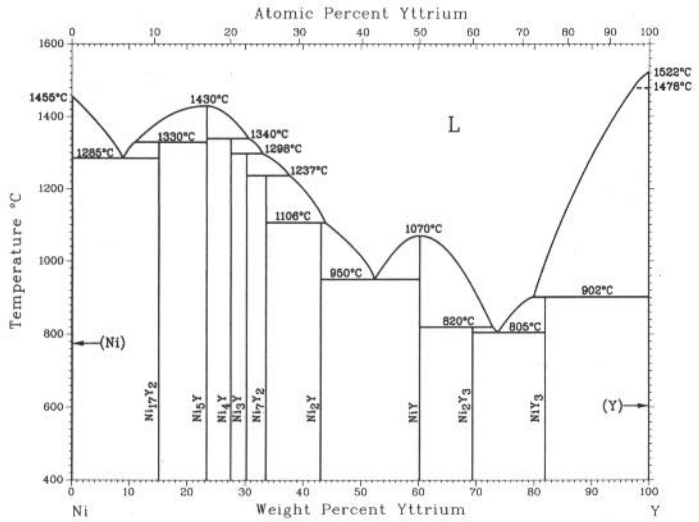

Phase	Composition, wt% Y	Pearson symbol	Space group
(Ni)	0	*cF*4	$Fm\bar{3}m$
$Ni_{17}Y_2$	15.1	*hP**	$P6_3/mmc$
Ni_5Y	23.3	*hP*6	$P6/mmm$
Ni_4Y	27.5	...	...
Ni_7Y_2	30.2	*hR**	$R\bar{3}m$
Ni_3Y	33.6	*hP***	$P6_3/mmc$
		*hR**	$R\bar{3}m$
Ni_2Y	43.1	*cF*24	$Fd\bar{3}m$
NiY	60.2	*oP*8	*Pnma*
Ni_2Y_3	69.4	*t***	$P4_12_12$
NiY_3	82.0	*oP*16	*Pnma*
(βY)	100	*cF*4	$Fm\bar{3}m$
(αY)	100	*hP*2	$P6_3/mmc$

Ni-Yb

P. Nash, 1991

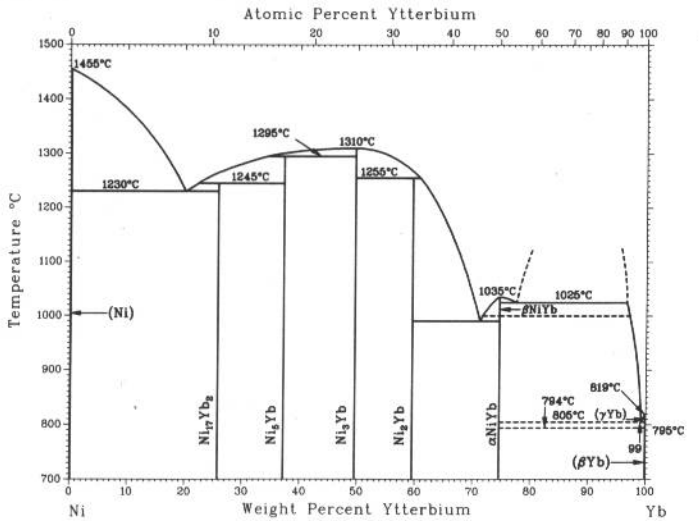

Phase	Composition, wt% Yb	Pearson symbol	Space group
(Ni)	0	*cF*4	$Fm\bar{3}m$
$Ni_{17}Yb_2$	25.7	*hP*38	$P6_3/mmc$
Ni_5Yb	37.2	*hP*6	$P6/mmm$
Ni_3Yb	49.6	*hR*12	$R\bar{3}m$
Ni_2Yb	59.5	*cF*24	$Fd\bar{3}m$
αNiYb	74.7	*oP*8	*Pnma*
(γYb)	100	*cI*2	$Im\bar{3}m$
(βYb)	100	*cF*4	$Fm\bar{3}m$
(αYb)	100	*hP*2	$P6_3/mmc$

Ni-Zn

P. Nash and Y.Y. Pan, 1991

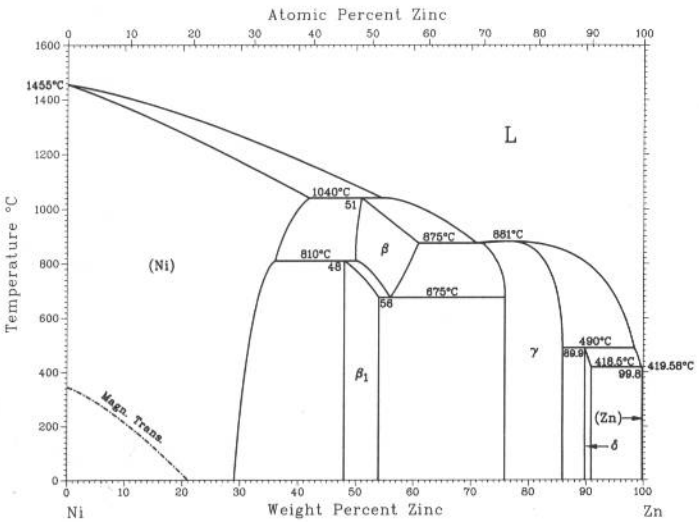

Phase	Composition, wt% Zn	Pearson symbol	Space group
(Ni)	0 to 41.9	*cF*4	$Fm\bar{3}m$
β	50.0 to 60.9	*cP*2	$Pm\bar{3}m$
β_1	48.0 to 54.5	*tP*2	*P*4/*mmm*
γ(a)	72 to 86	*cI*52	$I\bar{4}3m$
δ	~90	*mC*6	*C*2/*m*
(Zn)	100	*hP*2	$P6_3/mmc$

(a) Might have orthorhombic structure

Ni-Zr

P. Nash and C.S. Jayanth, 1991

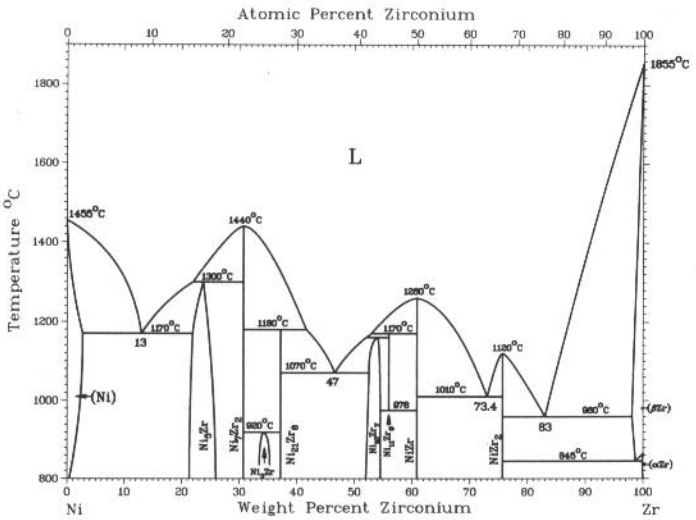

Phase	Composition, wt% Zr	Pearson symbol	Space group
(Ni)	0 to 2.74	*cF*4	$Fm\bar{3}m$
Ni_5Zr	21.32 to 25.95	*cF*24	$F\bar{4}3m$
Ni_7Zr_2	30.75	*mC*36	*C*2/*m*
Ni_3Zr	33.5 to 35.3	*hP*8	$P6_3/mmc$
$Ni_{21}Zr_8$	37.2	(a)	...
$Ni_{10}Zr_7$	52.0 to 54.52	*oC*68	*C*2*ca*(b) *Pbca*(c)
$Ni_{11}Zr_9$	56.0	*tI*40	*I*4/*m*
NiZr	60.9	*oC*8	*Cmcm*
$NiZr_2$	75.7	*tI*12	*I*4/*mcm*
(βZr)	98.10 to 100	*cI*2	$Im\bar{3}m$
(αZr)	99.9 to 100	*hP*2	$P6_3/mmc$

(a) Triclinic. (b) Stoichiometric. (c) Zr-rich

Np-Pu

R.I. Sheldon and D.E. Peterson, 1985

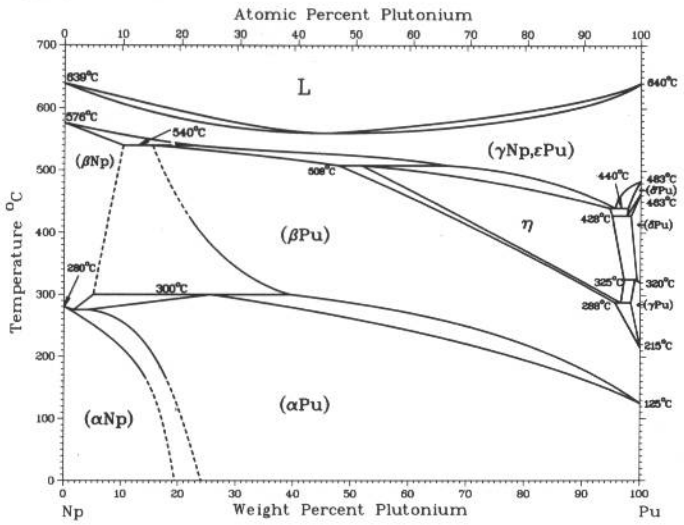

Phase	Composition, wt% Pu	Pearson symbol	Space group
(γNp,εPu)	0 to 100	*cI*2	$Im\bar{3}m$
(βNp)	0 to 10.3	*tP*4	$P4_12$
(αNp)	0 to 19.5	*oP*8	*Pnma*
η	52 to 97.1	(a)	...
(δ′Pu)	97.7 to 100	*tI*2	*I*4/*mmm*
(δPu)	98.3 to 100	*cF*4	$Fm\bar{3}m$
(γPu)	98.3 to 100	*oF*8	*Fddd*
(βPu)	15.4 to 100	*mC*34	*C*2/*m*
(αPu)	4.1 to 100	*mP*16	$P2_1/m$

(a) Orthorhombic (tentative)

Np-U

R.I. Sheldon and D.E. Peterson, 1985

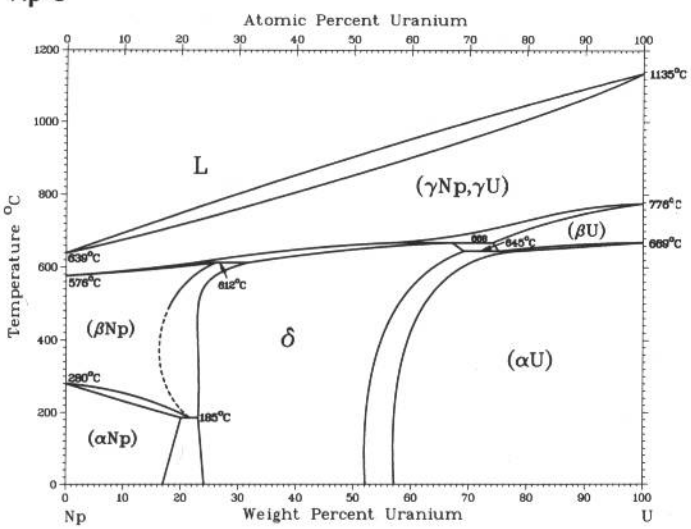

Phase	Composition, wt% U	Pearson symbol	Space group
(γNp,γU)	0 to 100	*cI*2	$Im\bar{3}m$
(βNp)	0 to 26	*tP*4	$P4_12$
(αNp)	0 to 20	*oP*8	*Pnma*
δ	23 to 69	*cP*58(a)	...
(βU)	74 to 100	*tP*30	$P4_2/mmm$
(αU)	57 to 100	*oC*4	*Cmcm*

(a) Tentative

O-Pb (condensed system, 0.1 MPa)

H.A. Wriedt, 1988

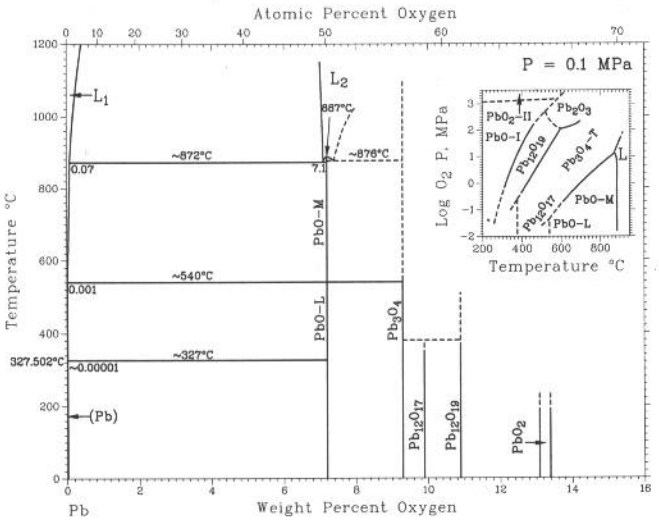

Inset shows equilibrium phase fields under identical hydrostatic and partial O_2 gas pressures

Phase	Composition, wt% O	Pearson symbol	Space group
Stable (0.1 MPa)			
(Pb)	0	*cF*4	$Fm\bar{3}m$
PbO-M	7.2	*oP*8	*Pbma*
PbO-L	7.2	*tP*4	*P4/nmm*
Pb_3O_4-T	9.3	*tP*28	$P4_2/mbc$
Pb_3O_4-R	9.3	*oP*28	*Pbam*
$Pb_{12}O_{17}$	9.9	*oP*58?	$Pmc2_1$?
$Pb_{12}O_{19}$	10.9	*mP*62	*Pc*? or $P2_1/c$
PbO_2-I	13.1 to 13.4(a)	*tP*6	$P4_2/mnm$
Other			
(εPb)(b)	0	*hP*2	$P6_3/mmc$
Pb_2O_3(b)	10.4	*mP*20	$P2_1/a$
PbO_2-II(b)	13.4	*oP*12	*Pbcn*
PbO_2-III(b)	13.4	*cF*12	$Fm\bar{3}m$
PbOα	7.2	(c)	...
PbO	7.2	(d)	$P2_1$ or $P2_1/m$
PbO_n	9.3 to 10.8	(c)	...
Pb_3O_4	9.3	(c)	...
$Pb_{12}O_{17}$	9.9	(e)	...
$Pb_{12}O_{19}$(II)	10.9	(d)	...
$Pb_{12}O_{19}$	10.9	(e)	...

(a) Contains a small amount of hydrogen. (b) Stable at hydrostatic pressures elevated from 0.1 MPa. (c) Orthorhombic. (d) Monoclinic. (e) Pseudocubic?

O-Pr

P.R. Subramanian, 1990

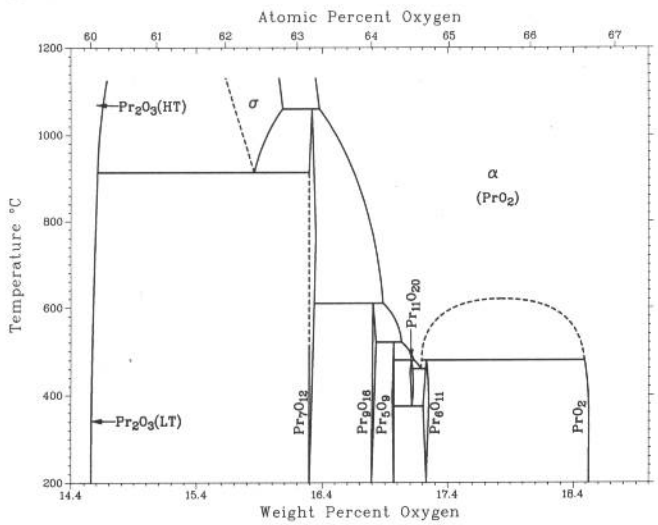

Phase	Composition, wt% O	Pearson symbol	Space group
(βPr)	0	*cI*2	$Im\bar{3}m$
(αPr)	0	*hP*4	$P6_3/mmc$
Pr_2O_3(HT)	~15	*hP*5	$P\bar{3}m1$
Pr_2O_3(LT)	~15	*cI*80	$Ia\bar{3}$
σ(a)	~16.0	*cI*80	$Ia\bar{3}$
Pr_7O_{12}	~16.3	*hR*19	$R\bar{3}$
Pr_9O_{16}	~17	*aP**	$P\bar{1}$
Pr_5O_9	~17.0	*mP*112	$P2_1/c$
$Pr_{11}O_{20}$	~17.1	*m***	...
Pr_6O_{11}	~17.2	*c***	...
PrO_2(α)	~18.5	*cF*12	$Fm\bar{3}m$
High-pressure phase			
PrO(b)	10.2	*cF**	...

(a) Reported to be a high-temperature phase; stable above ~920 °C. (b) Obtained by reduction of Pr_2O_3 by Pr at 800 °C and 50 kbar

O-Pu (condensed system)

H.A. Wriedt, 1990

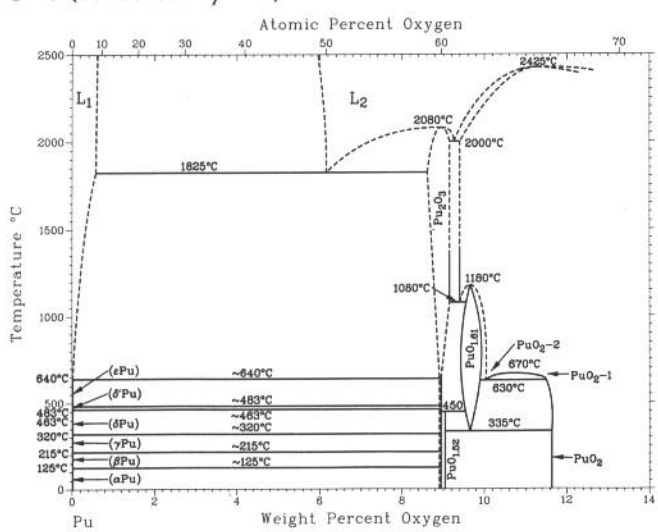

Phase	Composition, wt% O	Pearson symbol	Space group
Stable			
(αPu)	~0	*mP*16	$P2_1/m$
(βPu)	~0	*mC*34	*C2/m*
(γPu)	~0	*oF*8	*Fddd*
(δPu)	~0	*cF*4	$Fm\bar{3}m$
(δ'Pu)	~0	*tI*2	*I4/mmm*
(εPu)	~0	*cI*2	$Im\bar{3}m$
P_2O_3(a)	~8.9 to ~9.0	*hP*5	$P\bar{3}m1$
$PuO_{1.52}$(b)	~9.1	*cI*80	$Ia\bar{3}$
$PuO_{1.61}$(b)	~9.6 to ~10.0	*cI*80	$Ia\bar{3}$
PuO_2	~9 to 11.6(c)	*cF*12	$Fm\bar{3}m$
Other			
Pu	...	*hP*2	$P6_3/mmc$

(a) The lower limit at 1100 °C might be 58.8 at.% O. (b) Possibly unconnected ranges of the same phase. (c) At 0.1 MPa O_2 pressure

O-Sn

From [Hansen]

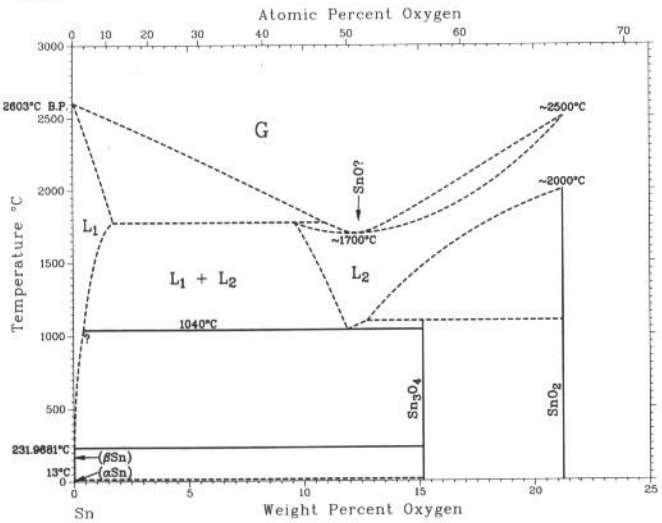

Phase	Composition, wt% O	Pearson symbol	Space group
(βSn)	0	*tI*4	$I4_1/amd$
(αSn)	0	*cF*8	$Fd\bar{3}m$
SnO(?)	11.9	*tP*4	*P*4/*nmm*
Sn_3O_4	15.2	*a***	...
SnO_2	21.3	*tP*6	$P4_2/mnm$

O-Ti

J.L. Murray and H.A. Wriedt, 1987

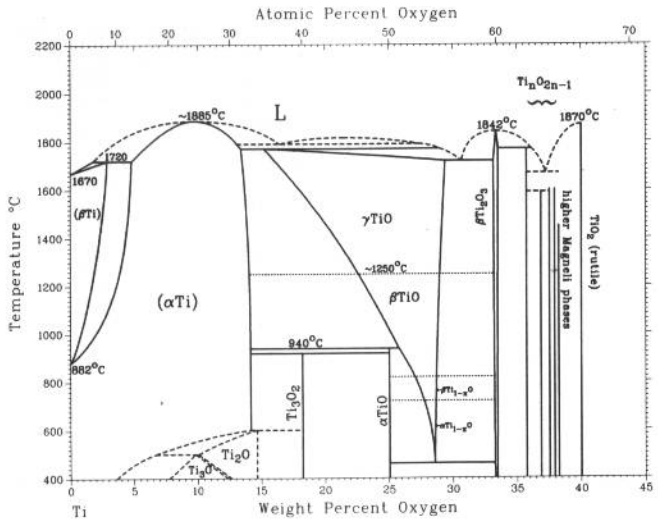

Phase	Composition, wt% O	Pearson symbol	Space group
(βTi)	0 to 3	*cI*2	$Im\bar{3}m$
(αTi)	0 to 13.5	*hP*2	$P6_3/mmc$
Ti_3O	~8 to ~13	*hP*~16	$P\bar{3}1c$
Ti_2O	~10 to 14.4	*hP*3	$P\bar{3}m1$
γTiO	15.2 to 29.4	*cF*8	$Fm\bar{3}m$
Ti_3O_2	~18	*hP*~5	*P*6/*mmm*
βTiO	~24 to ~29.4	*c***	...
αTiO	~25.0	*mC*16	*A*2/*m* or *B***/*
$\beta Ti_{1-x}O$	~29.5	*oI*12	*I*222
$\alpha Ti_{1-x}O$	~29.5	*tI*18	*I*4/*m*
βTi_2O_3	33.2 to 33.6	*hR*30	$R\bar{3}c$
αTi_2O_3	33.2 to 33.6	*hR*30	$R\bar{3}c$
βTi_3O_5	35.8	*m***	...
αTi_3O_5	35.8	*mC*32	*C*2/*m*
$\alpha' Ti_3O_5$	35.8	*mC*32	*Cc*
γTi_4O_7	36.9	*aP*44	$P\bar{1}$
βTi_4O_7	36.9	*aP*44	$P\bar{1}$
αTi_4O_7	36.9	*aP*44	$P\bar{1}$
γTi_5O_9	37.6	*aP*28	$P\bar{1}$
βTi_6O_{11}	38.0	*aC*68	$A\bar{1}$
Ti_7O_{13}	38.3	*aP*40	$P\bar{1}$
Ti_8O_{15}	38.5	*aC*92	$A\bar{1}$
Ti_9O_{17}	38.7	*aP*52	$P\bar{1}$
Rutile	40.1	*tP*6	$P4_2/mnm$
Metastable phases			
Anatase	...	*tI*12	$I4_1/amd$
Brookite	...	*oP*24	*Pbca*
High-pressure phases			
TiO_2-II	...	*oP*12	*Pbcn*
TiO_2-III	...	*hP*~48	...

O-V

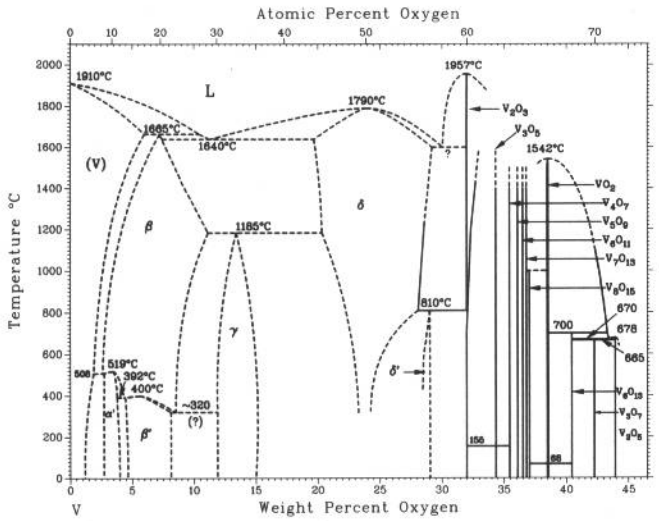

H.A. Wriedt, 1989

Phase	Composition, wt% O	Pearson symbol	Space group
(V)	0 to 6	*cI*2	$Im\bar{3}m$
α′	2.7 to 4.0	*tI*216(a)	…
β	2.6 to 11.1	*tI*2.5(b)	*I*4/*mmm*
β′	4 to 8	*tI*76(c)	*I*4/*mmm*
γ	12 to 15	*mC*20(d)	*C*2/*m*
δ	19 to 29.4	*cF*8	$Fm\bar{3}m$
δ′	27 to 28.6	*tI*116	$I4_1/amd$
h-V_2O_3(e)	32.0 to 32.5	*hR*10	$R\bar{3}c$
l-V_2O_3(f)	32	*mI*20	*I*2*a*
h-V_3O_5(e)	~34.4	*mI*32	*I*2/*c*
l-V_3O_5(f)	34.4 to 34.38	*mP*32	*P*2/*c*
V_4O_7	35.4	*aP*22	$P\bar{1}$
V_5O_9	36.1	*aP*28	$P\bar{1}$
V_6O_{11}	36.5	*aP*34	$P\bar{1}$
V_7O_{13}	36.8	*aP*40	$P\bar{1}$
V_8O_{15}	37.0	*aP*46	$P\bar{1}$
βVO_2(e)	38.5 to 38.8	*tP*6	$P4_2/mnm$
αVO_2(f)	38.6	*mP*12	$P2_1/c$
h-V_6O_{13}(e)	~40.5	*mC*38	*C*2/*m*
l-V_6O_{13}(f)	~40.5	*mP*38	$P2_1/a$
V_3O_7	~42	*mC*120	*C*2/*c*
V_2O_5	~43.9	*oP*14	*Pmnm*
Other phases			
Martensite-A	2.2 to 2.9	*tI**(g)	…
Martensite-B	2.0 to 2.2	*tI**(g)	…
ε	8 to 11	*mP**	$P2_1/c$
$VO_{1.17}$	~27	…	$I4_1/a$
V_9O_{17}	~37.3	*aP*52	*P*1
VO_2-B	~38.6	*tI*288(?)	…
VO_2-M_2	~38.6	*mC*24	*C*2/*m*
VO_2-T_2	~38.6	*tP*6	$P4_2/mnm$
VO_2-M_3	38.7 to 39.2	*mP*6	*P*2/*m*
VO_2-M_4(h)	~38.6	*mC*24	*C*2/*m*
VO_2-D	~38.6	*oP*12	*Pbnm*
V_6O_{13}-C	~40.5	*cP*76(?)	…
V_6O_{13}-D	~40.5	*mC*38	*C*2/*m*
V_4O_9	~41.4	*oP*52	*Pnma*
V_4O_9-E	~41.1	*oP*104(?)	…
V_2O_5	~44.1	…	…

(a) At V_8O. (b) At V_4O. (c) At $V_{16}O_3$. (d) At V_7O_3. (e) Above T_{trs}. (f) Below transformation temperature, T_{trs}. (g) 2 atoms V/unit cell. (h) Also called VO_2(*B*)

O-W (condensed system, 0.1 MPa)

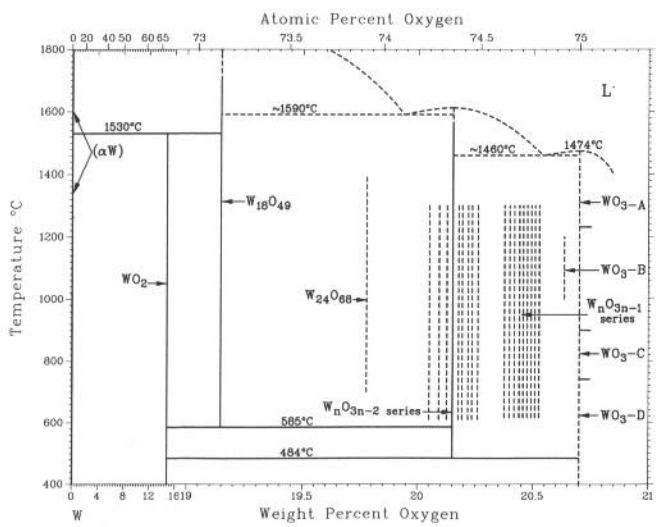

H.A. Wriedt, 1989

Phase	Composition, wt% O	Pearson symbol	Space group
(αW)	~0	*cI*2	$Im\bar{3}m$
WO_2	~14.8	*mP*12	$P2_1/c$
$W_{18}O_{49}$	~19.1	*mP*67	*P*2/*m*
$W_{24}O_{68}$	~19.8	*m**92	…
$W_{20}O_{58}$(a)	20.2	*mP*78	*P*2/*m*
$W_{24}O_{70}$(a)	20.3	*mP*94	…
$W_{25}O_{73}$(a)(b)	20.3	*mP*98	*P*2/*c*
$W_{25}O_{74}$(c)	20.4	*mP*99	*P*2/*m*
WO_3-M	~20.7	…	…
WO_3-J	~20.7	…	…
WO_3-K	~20.7	…	…
WO_3-H	~20.7	…	…
WO_3-G	~20.7	*mP*16	*Pc*
WO_3-F	~20.7	*aP*32	$P\bar{1}$
WO_3-E(d)	~20.7	*mP*32	$P2_1/n$
WO_3-D(d)	~20.7	*oP*32	*Pmnb*
WO_3-C(d)	~20.7	*tP*8	*P*4/*nmn*
WO_3-B	~20.7	*tP*8	*P*4/*nmm*
WO_3-A	~20.7	*tP*8(?)	*P*4/*nmm*(?)
Other			
(βW)	0 to ?	*cP*8	$Pm\bar{3}n$
$W_{40}O_{118}$(a)	20.4	*mP*158	*P*2
WO_3(e)	20.7	*hP*24	*P*6/*mmm*(?)
WO_3(f)	20.7	*c**4	…

(a) Member W_nO_{3n-2} series. (b) Identified as $WO_{2.96}$(α). (c) Probable member W_nO_{3n-1} series, called $WO_{2.96}$(β). (d) Often described as a slightly distorted ReO_3 ($D0_9$). (e) Hexagonal. (f) Cubic

O-Y

O.N. Carlson, 1990

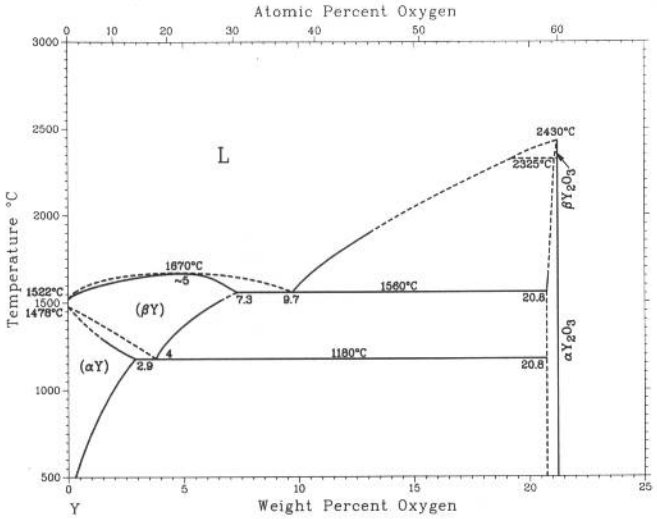

Phase	Composition, wt% O	Pearson symbol	Space group
(βY)	0 to 7.3	*cI*2	$Im\bar{3}m$
(αY)	0 to 2.9	*hP*2	$P6_3/mmc$
αY_2O_{3-x}	20.8 to 21	*cI*80	$Ia\bar{3}$
βY_2O_{3-x}	~21	*hP*(?)	$P\bar{3}m1$
γY_2O_3(a)	~21	*mC*(?)	*C*2/*m*

(a) High-pressure phase

O-Zr

J.P. Abriata, R. Versaci, and J. Garcés, 1986

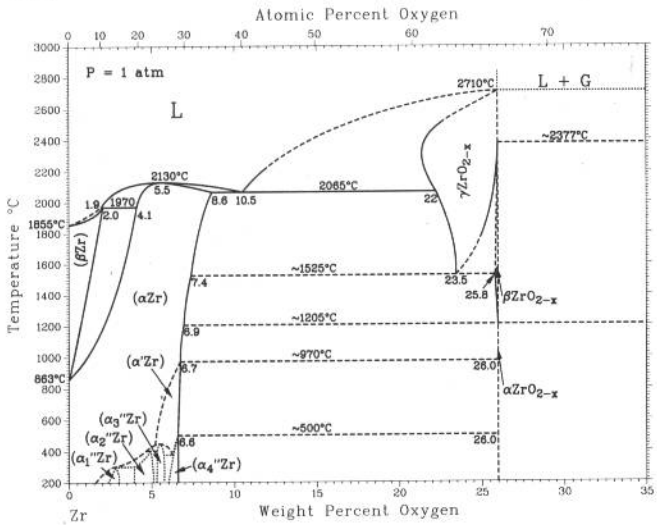

Phase	Composition, wt% O	Pearson symbol	Space group
(αZr)	0 to 8.6	*hP*2	$P6_3/mmc$
(βZr)	0 to 2.0	*cI*2	$Im\bar{3}m$
γZrO_{2-x}	22 to 25.9	*cF*12	$Fm\bar{3}m$
βZrO_{2-x}	25.8 to 25.9	*tP*6	$P4_2/nmc$
αZrO_{2-x}	25.9	*mP*12	$P2_1/c$

Os-Pt

H. Okamoto, 1990

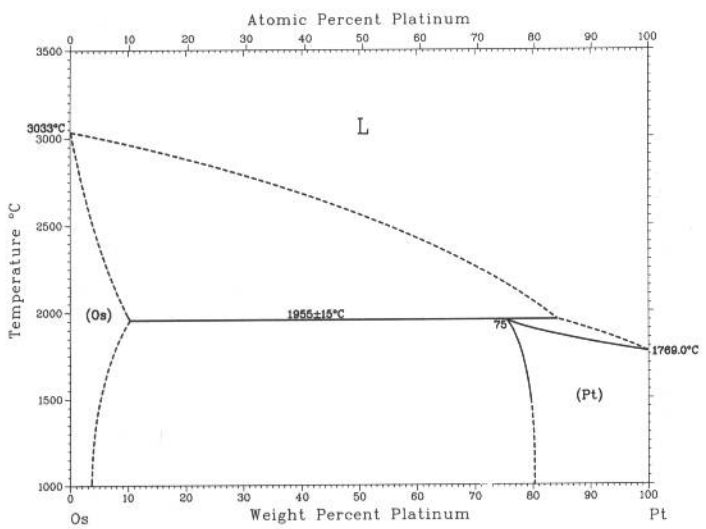

Phase	Composition, wt% Pt	Pearson symbol	Space group
(Os)	0 to ~11	*hP*2	$P6_3/mmc$
(Pt)	75 to 100	*cF*2	$Fm\bar{3}m$

Os-Pu

S.T. Konobeevsky, 1955

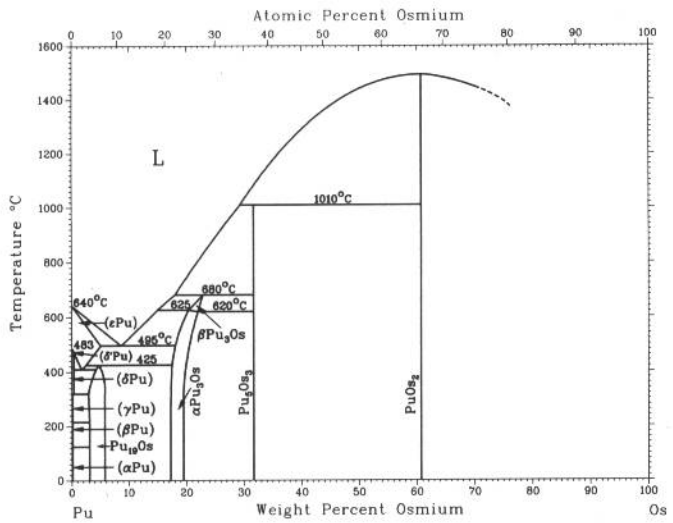

Phase	Composition, wt% Os	Pearson symbol	Space group
(εPu)	0 to ~5	*cI*2	$Im\bar{3}m$
(δ'Pu)	0 to ~0.4	*tI*2	*I*4/*mmm*
(δPu)	0 to ~0.4	*cF*4	$Fm\bar{3}m$
(γPu)	~0	*oF*8	*Fddd*
(βPu)	~0	*mC*34	*C*2/*m*
(αPu)	~0	*mP*16	$P2_1/m$
$\beta Pu_{19}Os$	3 to >6	*oP*52	*Pnna*
$\alpha Pu_{19}Os$	3 to >6	*oC*40	*Cmca*
βPu_3Os	~21 to <22	...	...
αPu_3Os	~17 to >22	...	...
Pu_5Os_3	~31.9	*tI*32	*I*4/*mcm*
$PuOs_2$	61.0	*hP*12	$P6_3/mmc$
Other reported phase			
$PuOs_2$	61.0	*cF*24	$Fd\bar{3}m$

Os-Re

M.A. Tylkina, V.P. Polyakova, and E.M. Savitskii, 1962

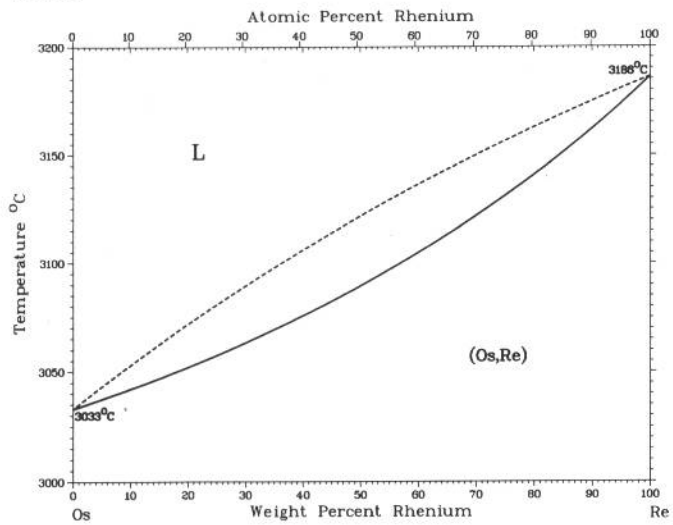

Phase	Composition, wt% Re	Pearson symbol	Space group
(Os,Re)	0 to 100	*hP*2	$P6_3/mmc$

Os-Rh

H. Okamoto, 1990

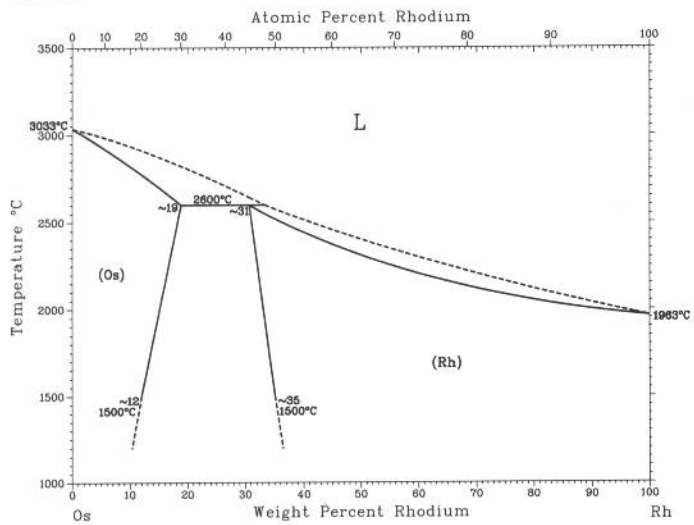

Phase	Composition, wt% Rh	Pearson symbol	Space group
(Os)	0 to ~19	*hP*2	$P6_3/mmc$
(Rh)	~31 to 100	*cF*2	$Fm\bar{3}m$

Os-Ru

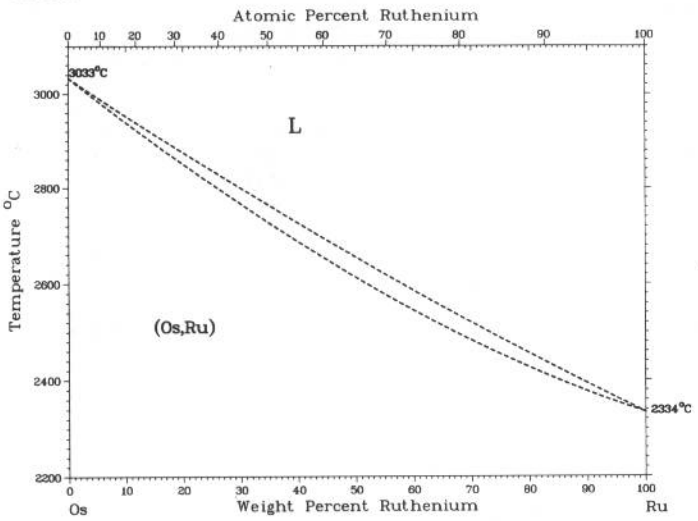

M.A. Tylkina, V.P. Polyakova, and E.M. Savitskii, 1962

Phase	Composition, wt% Ru	Pearson symbol	Space group
(Os,Ru)	0 to 100	*hP*2	$P6_3/mmc$

Os-Si

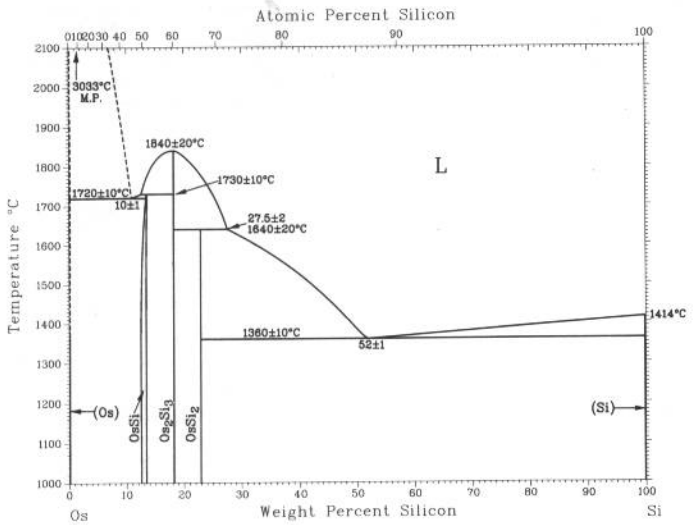

H. Okamoto, 1990

Phase	Composition, wt% Si	Pearson symbol	Space group
(Os)	0	*hP*2	$P6_3/mmc$
OsSi	12.9	*cP*8	$P2_13$
Os_2Si_3	18	*oP*40	*Pbcn*
$OsSi_2$	22.8	*oC*48	*Cmca*
(Si)	100	*cF*8	$Fd\bar{3}m$
Metastable phase			
$OsSi_2$·m	22.8	*mC*12	*C*2/*m*

Os-Ti

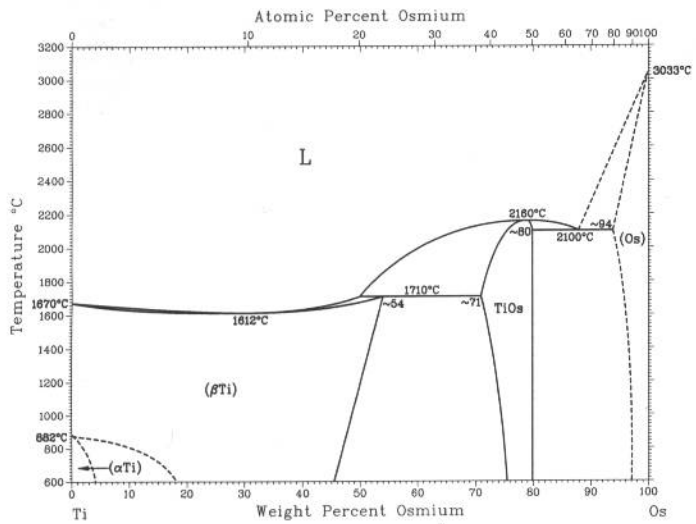

J.L. Murray, 1990

Phase	Composition, wt% Os	Pearson symbol	Space group
(βTi)	0 to 54	*cI*2	$Im\bar{3}m$
(αTi)	0 to 4	*hP*2	$P6_3/mmc$
TiOs	~71 to ~80	*cP*2	$Pm\bar{3}m$
(Os)	~94 to 100	*hP*2	$P6_3/mmc$

Os-U

From [Shunk]

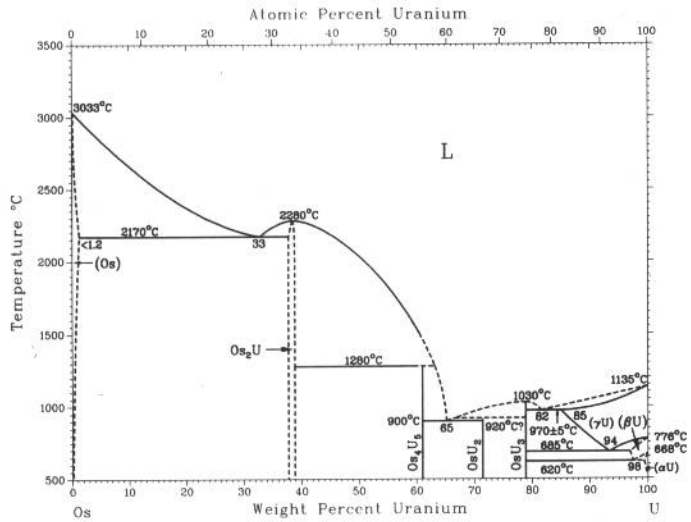

Phase	Composition, wt% U	Pearson symbol	Space group
(Os)	0 to <1.2	*hP*2	$P6_3/mmc$
Os_2U	~37.6 to 39	*cF*24	$Fd\bar{3}m$
Os_4U_5	~61.0	...	...
OsU_2	~71.5	*m**12	...
OsU_3	79	...	...
(γU)	85 to 100	*cI*2	$Im\bar{3}m$
(βU)	>97 to 100	*tP*30	$P4_2/mnm$
(αU)	>99 to 100	*oC*4	*Cmcm*

Os-V

J.F. Smith, 1989

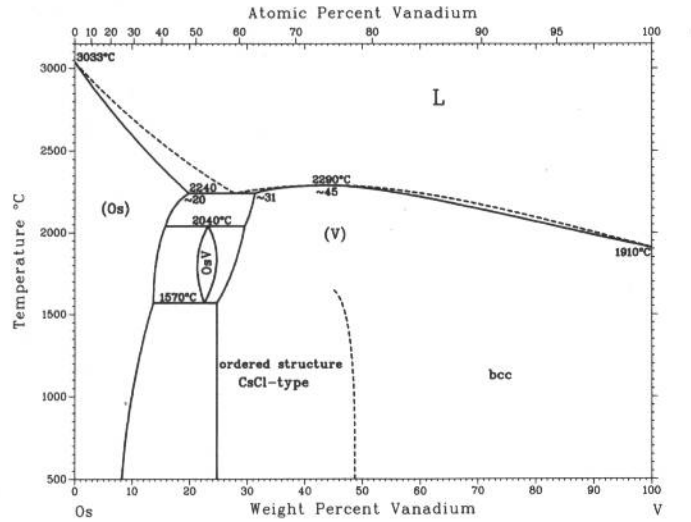

Phase	Composition, wt% V	Pearson symbol	Space group
(Os)	0 to ~20	*hP*2	$P6_3/mmc$
OsV	~21.1 to 25	*cP*8	$Pm\bar{3}n$
(V)	25 to ?	*cP*2	$Pm\bar{3}m$
	? to 100	*cI*2	$Im\bar{3}m$

Os-W

S.V. Nagender Naidu and P. Rama Rao, 1991

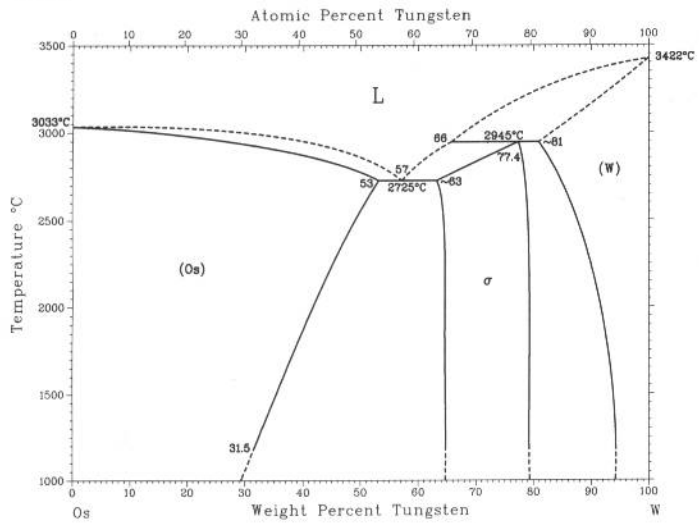

Phase	Composition, wt% W	Pearson symbol	Space group
(Os)	0 to 53	*hP*2	$P6_3/mmc$
σ	~63 to ~80	*tP*30	$P4_2/mnm$
(W)	~81 to 100	*cI*2	$Im\bar{3}m$

Os-Zr

H. Okamoto, 1990

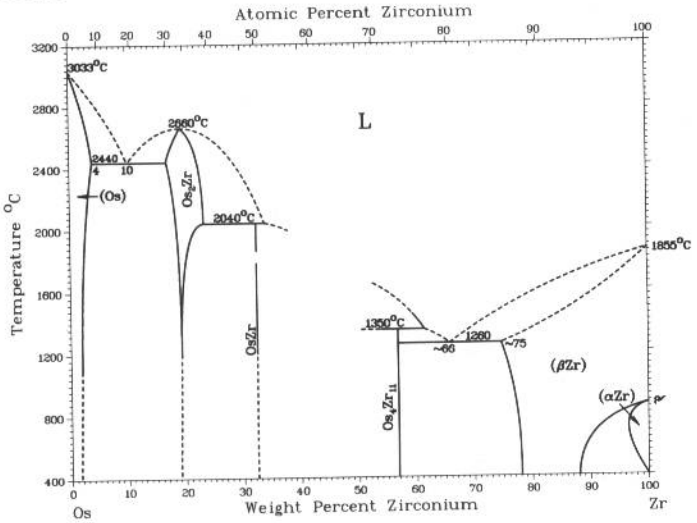

Phase	Composition, wt% Zr	Pearson symbol	Space group
(Os)	0 to 4	*hP*2	$P6_3/mmc$
Os_2Zr	~17 to <24	*hP*12	$P6_3/mmc$
OsZr	32.4	*cP*2	$Pm\bar{3}m$
Os_4Zr_{11}	~56.8	*cF*120	$Fm\bar{3}m$
(βZr)	~75 to 100	*cI*2	$Im\bar{3}m$
(αZr)	98 to 100	*hP*2	$P6_3/mmc$

P-Pd

H. Okamoto, unpublished

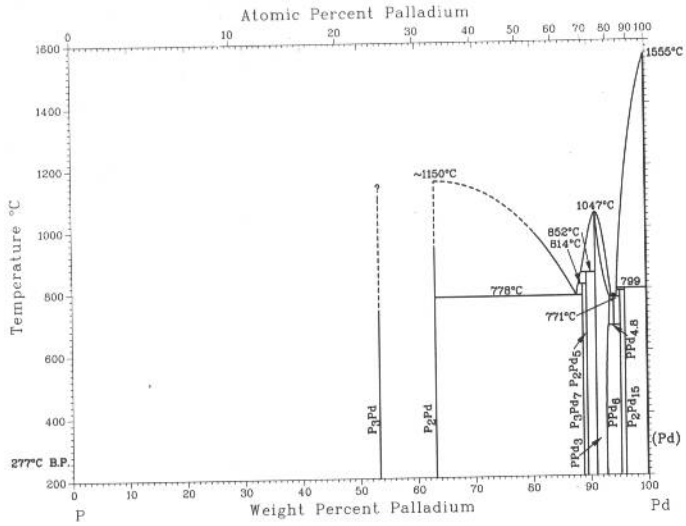

Phase	Composition, wt% Pd	Pearson symbol	Space group
P (white)	0	*c***	...
P_3Pd	53	*cI*32	$Im\bar{3}$
P_2Pd	63.2	*mC*12	*C*2/*c*
P_3Pd_7	88.9	*hR*20	$R\bar{3}$
P_2Pd_5	89.6	...	...
PPd_3	91 to 93.5	*oP*16	*Pnma*
$PPd_{4.8}$	94.3	*mP*24	$P2_1$
PPd_6	95.4	*mP*28	$P2_1/c$
P_2Pd_{15}	96.3	*hR*17	$R\bar{3}$
(Pd)	100	*cF*4	$Fm\bar{3}m$

P-Pr

From [Moffatt]

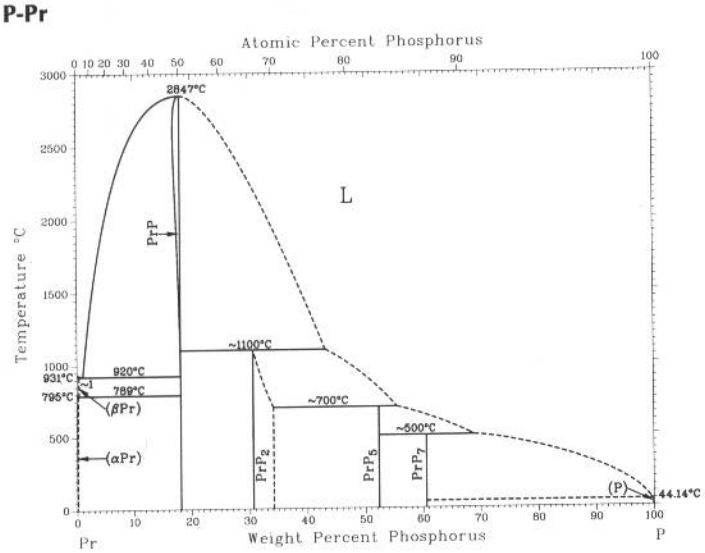

Phase	Composition, wt% P	Pearson symbol	Space group
(βPr)	0 to 0.2	*cI*2	$Im\bar{3}m$
(αPr)	0 to ~0.07	*hP*4	$P6_3/mmc$
PrP	~17 to 18.0	*cF*8	$Fm\bar{3}m$
PrP_2	30.6 to ?	*mP*12	$P2_1/c$
PrP_5	52.3	*mP*12	$P2_1/m$
PrP_7	60.6	...	...
(αP)	100	*c***	...

P-Ru

H. Okamoto, 1990

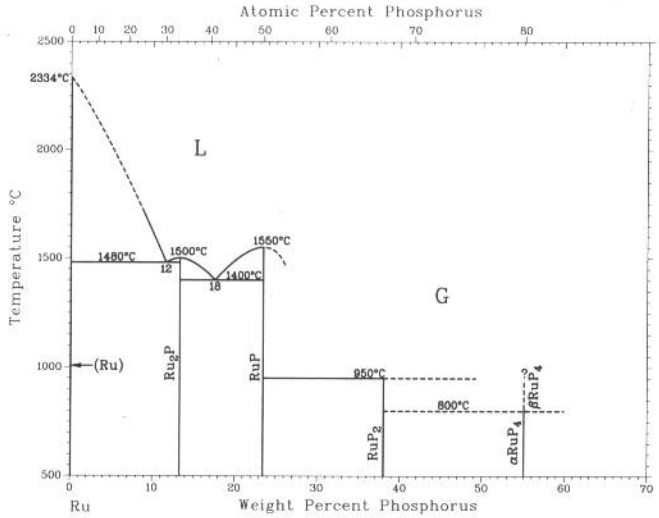

Phase	Composition, wt% P	Pearson symbol	Space group
(Ru)	0	*hP*2	$P6_3/mmc$
Ru_2P	13.3	*oP*12	*Pnma*
RuP	23.5	*oP*8	*Pnma*
RuP_2	38.0	*oP*6	*Pnnm*
βRuP_4	55	*aP*15	$P\bar{1}$
αRuP_4	55	*mP*10	$P2_1/c$

P-Sn

A.C. Vivian, 1920

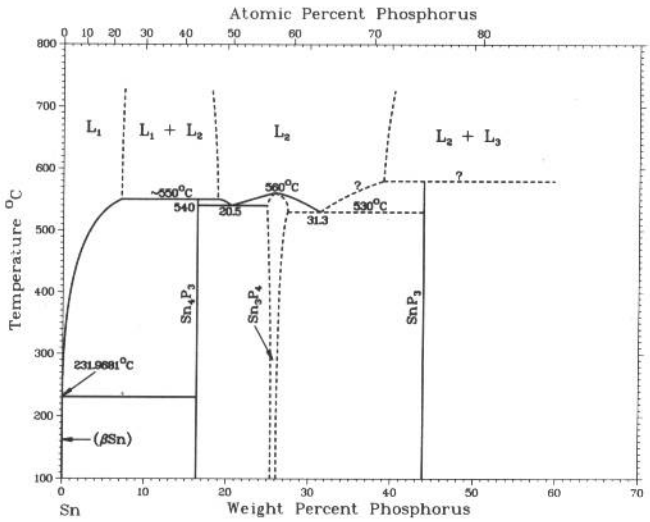

Phase	Composition, wt% P	Pearson symbol	Space group
(βSn)	0	*tI*4	$I4_1/amd$
(αSn)	0	*cF*8	$Fd\bar{3}m$
Sn_4P_3	16.4	*hR*7	$R\bar{3}m$
Sn_3P_4	~25.8	*hR*7	$R\bar{3}m$
SnP_3	44	*hR*8	$R\bar{3}m$
Metastable/high-pressure phases			
SnP	20.7	*cF*8	$Fm\bar{3}m$
	20.7	*hP*16	*P*321
	20.7	*tI*4	*I*4*mm*
Sn_7P_{10}	27.1	*h***	...

P-Ti

J.L. Murray, 1987

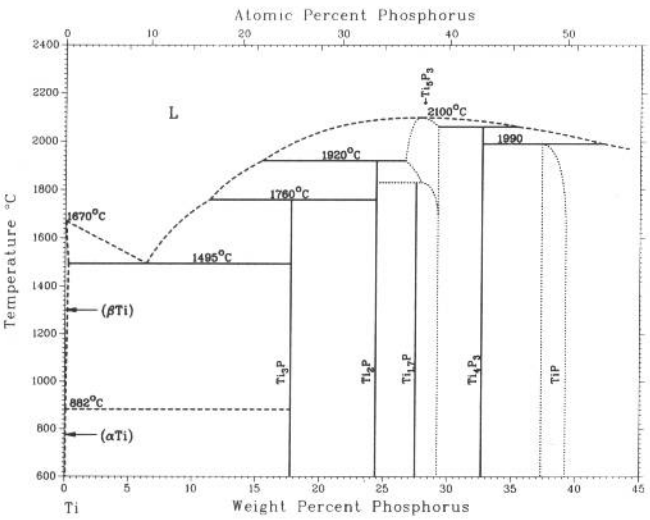

Phase	Composition, wt% P	Pearson symbol	Space group
(βTi)	0 to 0.2	*cI*2	$Im\bar{3}m$
(αTi)	0 to ?	*hP*2	$P6_3/mmc$
Ti_3P	18	*tP*32	$P4_2/n$
Ti_2P	24.4	*h***	...
		(a)	...
Ti_5P_3	~27 to ~29	*hP*16	$P6_3/mcm$
$Ti_{1.7}P$	27.5	*oP**	$P2_12_12_1$
Ti_4P_3	32.7	*c***	...
Ti_3P_2(b)	28	*t***	...
TiP	37 to 39.3	*hP*8	$P6_3/mmc$
TiP_2	56.4	*tI*12	$I4/mcm$

(a) Trigonal. (b) Not shown in diagram

P-Zn

J. Dutkiewicz, 1991

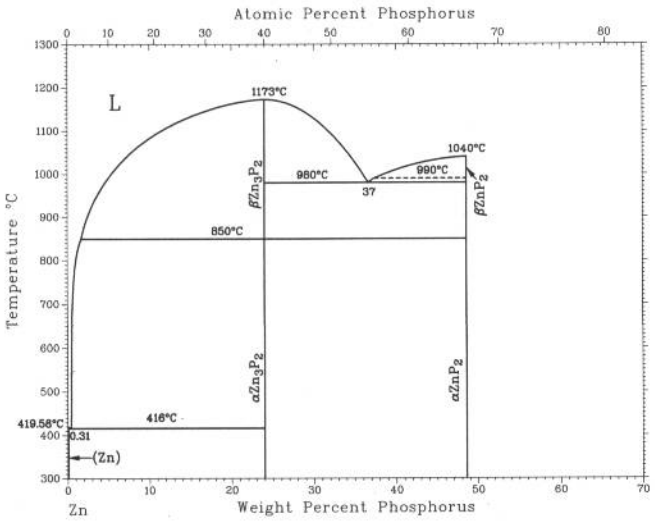

Phase	Composition, wt% P	Pearson symbol	Space group
(Zn)	0	*hP*2	$P6_3/mmc$
βZn_3P_2	24	*c***	...
αZn_3P_2	24	*tP*40	$P4_2/nmc$
βZnP_2	48.7	*mP*24	$P2_1/c$
αZnP_2	48.7	*tP*24	$P4_12_12$

Pb-Pd

H. Okamoto, 1990

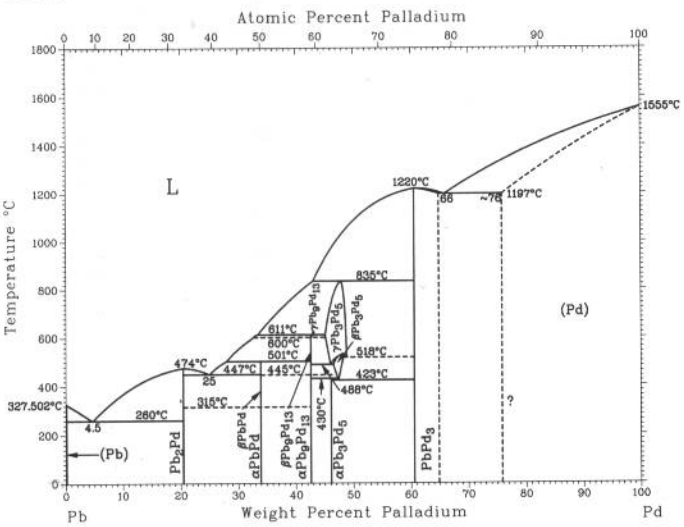

Phase	Composition, wt% Pd	Pearson symbol	Space group
(Pb)	0	*cF*4	$Fm\bar{3}m$
Pb_2Pd	20.4	*tI*12	*I*4/*mcm*
PbPd	33.9	*aP*32	$P\bar{1}$
γPb_9Pd_{13}	42.6	...	...
βPb_9Pd_{13}	42.6	*hP*5	...
αPb_9Pd_{13}	42.6	*mC*88	*C*2/*c*
γPb_3Pd_5	45 to 48	...	...
βPb_3Pd_5	46 to 47	*hP*4	$P6_3/mmc$
αPb_3Pd_5	46.1	*mC*32	*C*2
$PbPd_3$	61 to 66	*cP*4	$Pm\bar{3}m$
(Pd)	~76 to 100	*cF*4	$Fm\bar{3}m$

Pb-Pr

H. Okamoto, 1990

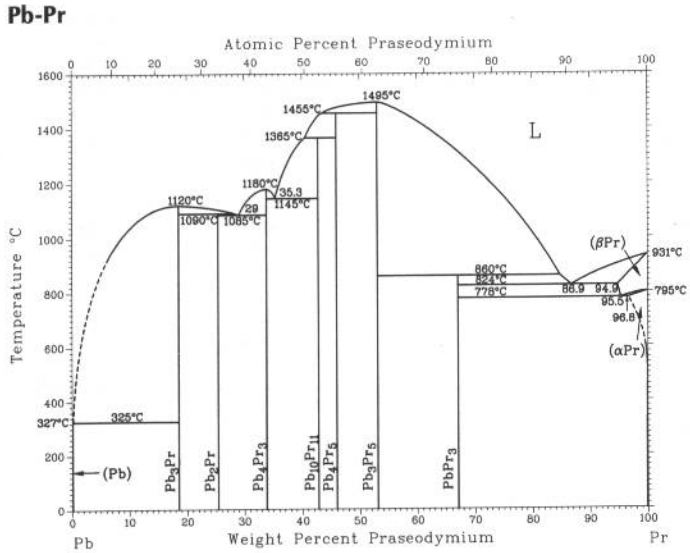

Phase	Composition, wt% Pr	Pearson symbol	Space group
(Pb)	0	*cF*4	$Fm\bar{3}m$
Pb_3Pr	19	*cP*4	$Pm\bar{3}m$
Pb_2Pr	25.3	*tI*24	$I4_1/amd$
Pb_4Pr_3	33.8	...	...
$Pb_{10}Pr_{11}$	42.8	*tI*84	*I*4/*mmm*
Pb_4Pr_5	46.0	*oP*36	*Pnma*
Pb_3Pr_5	53.1	*hP*16	$P6_3/mcm$
$PbPr_3$	67	*cP*4	$Pm\bar{3}m$
(βPr)	94.9 to 100	*cI*2	$Im\bar{3}m$
(αPr)	96.8 to 100	*hP*4	$P6_3/mmc$

Pb-Pt

From [Hansen]

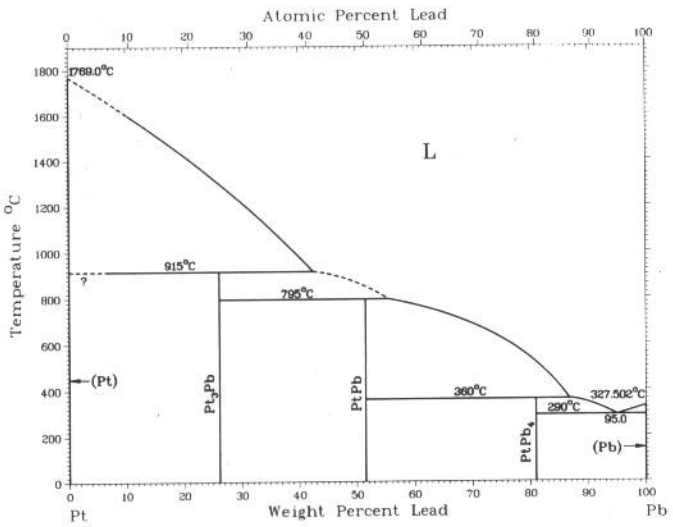

Phase	Composition, wt% Pb	Pearson symbol	Space group
(Pt)	0	*cF*4	$Fm\bar{3}m$
Pt_3Pb	26	*cP*4	$Pm\bar{3}m$
PtPb	51.5	*hP*4	$P6_3/mmc$
$PtPb_4$	81	*tP*10	$P4/nbm$
(Pb)	100	*cF*4	$Fm\bar{3}m$

Pb-Pu

E.M. Foltyn and D.E. Peterson, 1988

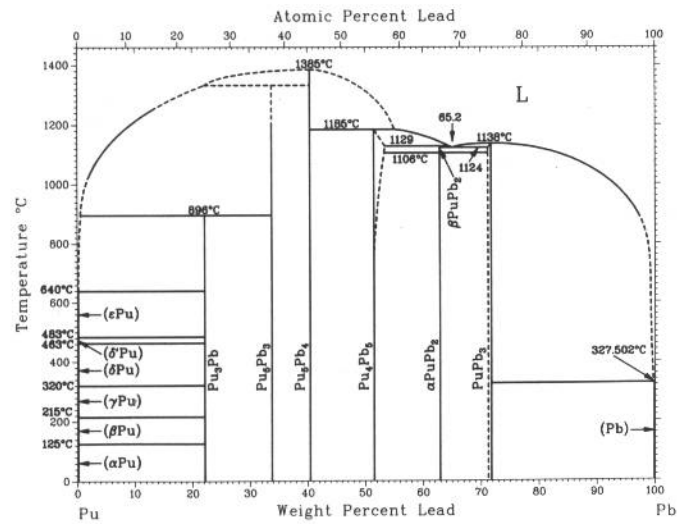

Phase	Composition, wt% Pb	Pearson symbol	Space group
(εPu)	0	*cI*2	$Im\bar{3}m$
(δ'Pu)	0	*tI*2	*I*4/*mmm*
(δPu)	0	*cF*4	$Fm\bar{3}m$
(γPu)	0	*oF*8	*Fddd*
(βPu)	0	*mC*34	*C*2/*m*
(αPu)	0	*mP*16	$P2_1/m$
Pu_3Pb	22	*cP*4	$Pm\bar{3}m$
Pu_5Pb_3	33.7	*tI*38	*I*4/*mcm*
Pu_5Pb_4	40.4	...	$P6_3/mcm$
Pu_4Pb_5	51.5 to 53.5	...	$P6_322$
$\beta PuPb_2$	63.0	...	...
$PuPb_2$	63.0	*tI*24	$I4_1/amd$
$PuPb_3$	71 to 72	*cP*4	$Pm\bar{3}m$
(Pb)	100	*cF*4	$Fm\bar{3}m$

Pb-Rb

A.N. Kuznetsov, K.A. Chuntonov, and S.P. Yatsenko, 1977

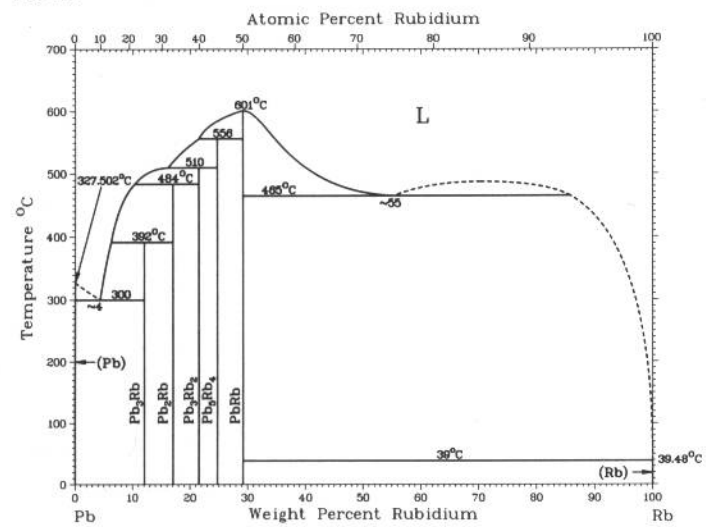

Phase	Composition, wt% Rb	Pearson symbol	Space group
(Pb)	0	*cF*4	$Fm\bar{3}m$
Pb_3Rb	12	...	...
Pb_2Rb	17.1	...	...
Pb_3Rb_2	22	...	...
Pb_5Rb_4	24.8	...	...
PbRb	29.2	*tI*64	$I4_1/acd$
(Rb)	100	*cI*2	$Im\bar{3}m$

Pb-Rh

H. Okamoto, 1990

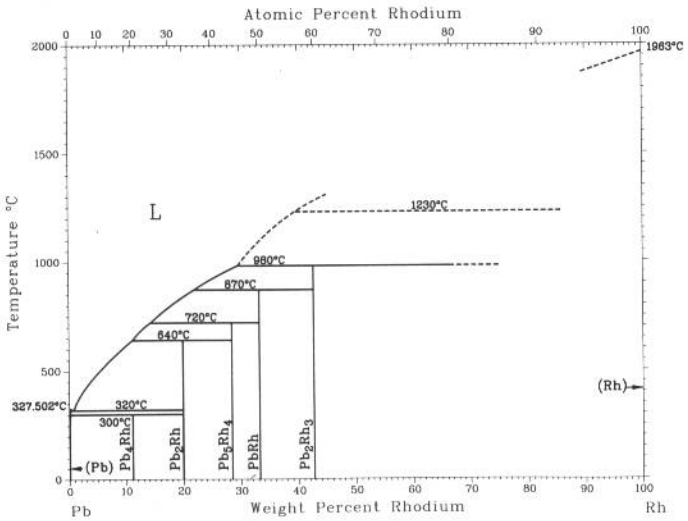

Phase	Composition, wt% Rh	Pearson symbol	Space group
(Pb)	0	*cF*4	$Fm\bar{3}m$
Pb_4Rh	11	...	...
Pb_2Rh	19.9	*tI*12	*I*4/*mcm*
Pb_5Rh_4	28.4	*oF*72	*Fmmm*
PbRh	33.2	*hP*6	*P*6/*mmm*
Pb_2Rh_3	43	*hP*4	$P6_3/mmc$
(Rh)	100	*cF*4	$Fm\bar{3}m$

Pb-S

J.-C. Lin, R.C Sharma, and Y.A. Chang, 1986

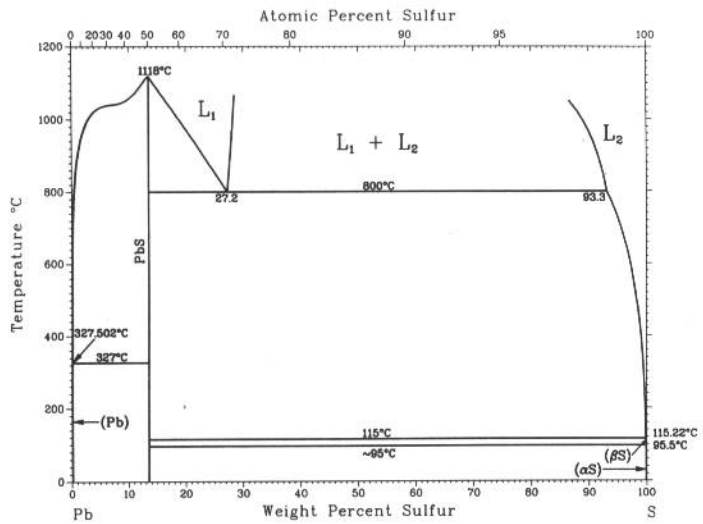

Phase	Composition, wt% S	Pearson symbol	Space group
(Pb)	~0	*cF*4	$Fm\bar{3}m$
PbS	13.4	*cF*8	$Fm\bar{3}m$
PbS(a)	13.4	*oP*8	*Pnma*
(βS)	100	*mP**	$P2_1/c$
(αS)	100	*oF*128	*Fddd*

(a) High-pressure phase

Pb-Sb

S. Ashtakala, A.D. Pelton, and C.W. Bale, 1981

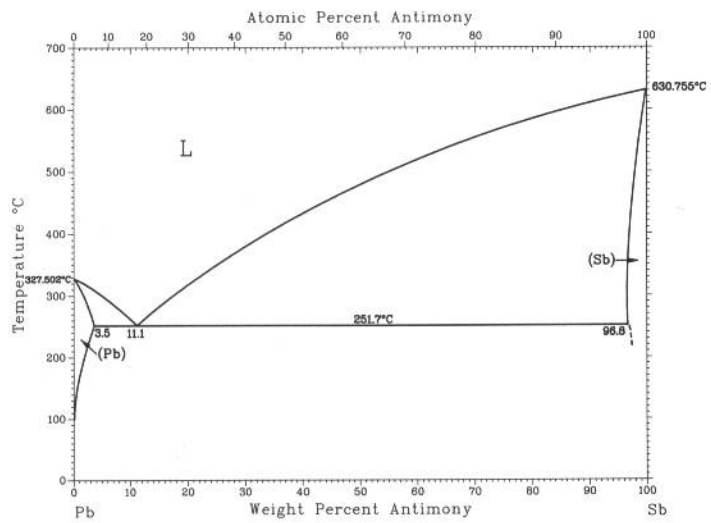

Phase	Composition, wt% Sb	Pearson symbol	Space group
(Pb)	0 to 3.5	*cF*4	$Fm\bar{3}m$
(Sb)	? to 100	*hR*2	$R\bar{3}m$

Pb-Se

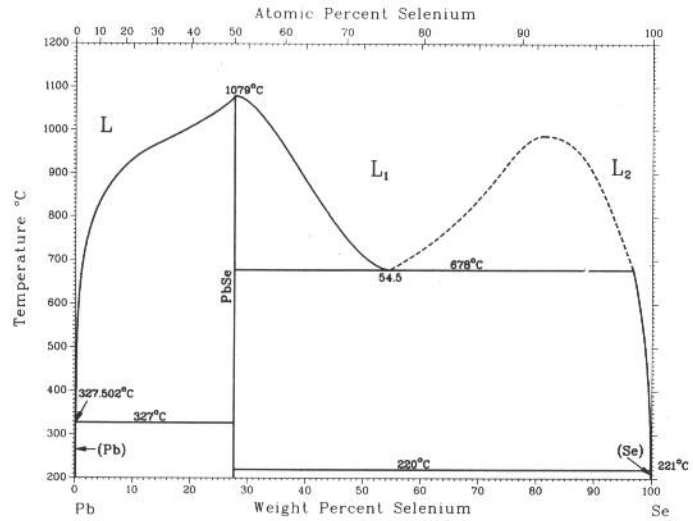

J.-C. Lin, R.C. Sharma, and Y.A. Chang, unpublished

Phase	Composition, wt% Se	Pearson symbol	Space group
(Pb)	~0	*cF*4	$Fm\bar{3}m$
PbSe	27.6	*cF*8	$Fm\bar{3}m$
PbSe(HP)	27.6	*oP*87	*Pnma*
(Se)	~100	*hP*3	$P3_121$

Pb-Sn

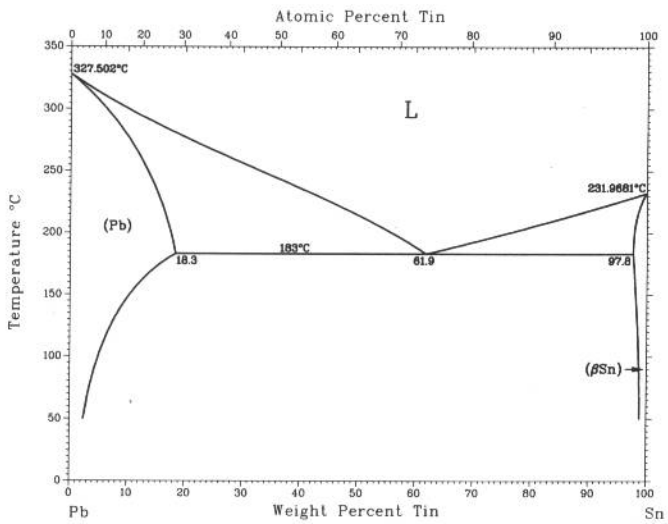

I. Karakaya and W.T. Thompson, 1988

Phase	Composition, wt% Sn	Pearson symbol	Space group
(Pb)	0 to 18.3	*cF*4	$Fm\bar{3}m$
(βSn)	97.8 to 100	*tI*4	$I4_1/amd$
(αSn)	100	*cF*8	$Fd\bar{3}m$
High-pressure phases			
ε(a)	52 to 74	*hP*1	*P6/mmm*
ε′(b)	52	*hP*2	$P6_3/mmc$

(a) From phase diagram calculated at 2500 MPa. (b) This phase was claimed for alloys at 350 °C and 5500 MPa.

Pb-Sr

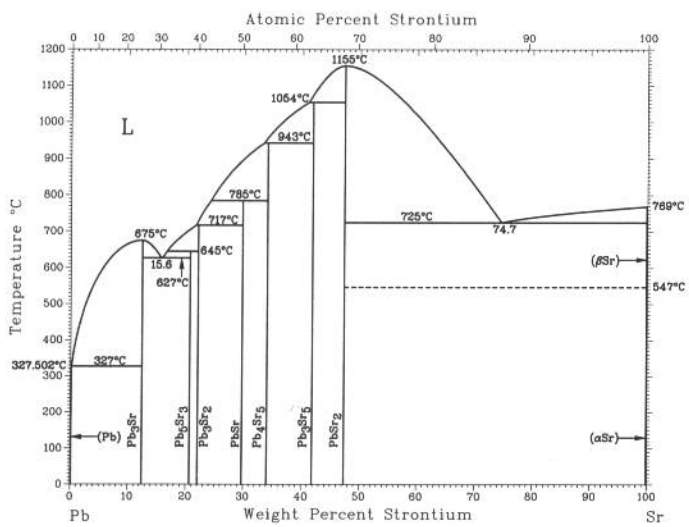

G. Bruzzone, E. Franceschi, and F. Merlo, 1981

Phase	Composition, wt% Sr	Pearson symbol	Space group
(Pb)	0	*cF*4	$Fm\bar{3}m$
Pb_3Sr	12	*tP*4	*P4/mmm*
Pb_5Sr_3	20.2	*t***	...
Pb_3Sr_2	22	*t***	...
PbSr	29.7	*oC*8	*Cmcm*
Pb_4Sr_5	34.6	*oP*36	*Pnma*
Pb_3Sr_5	41.3	*tI*32	*I4/mcm*
$PbSr_2$	45.9	*oP*12	*Pnma*
(βSr)	100	*cI*2	$Im\bar{3}m$
(αSr)	100	*cF*4	$Fm\bar{3}m$

Pb-Te

J.-C. Lin, K.C. Hsieh, R.C. Sharma, and Y.A. Chang, 1989

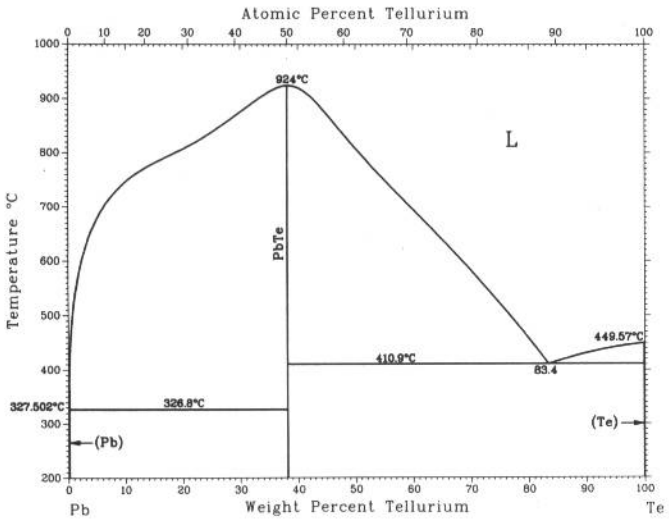

Phase	Composition, wt% Te	Pearson symbol	Space group
(Pb)	0	*cF*4	$Fm\bar{3}m$
PbTe	38.1	*cF*8	$Fm\bar{3}m$
PbTe(HP)	38.1	*oP*8	*Pnma*
(Te)	100	*hP*3	$P3_121$

Pb-Tl

From [Hultgren,B]

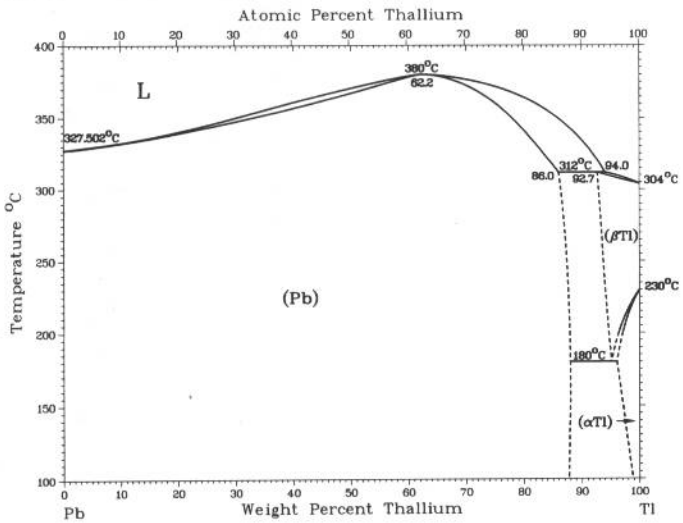

Phase	Composition, wt% Tl	Pearson symbol	Space group
(Pb)	0 to 88	*cF*4	$Fm\bar{3}m$
(βTl)	92.7 to 100	*cI*2	$Im\bar{3}m$
(αTl)	96 to 100	*hP*2	$P6_3/mmc$

Pb-Y

O.N. Carlson, F.A. Schmidt, and D.E. Diesburg, 1967

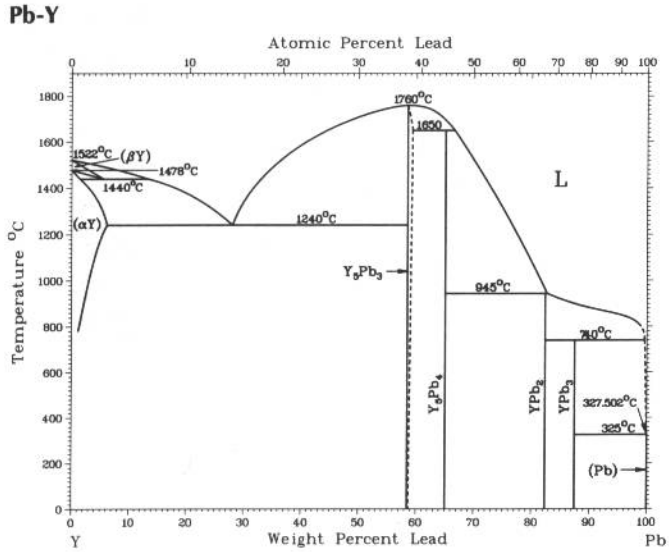

Phase	Composition, wt% Pb	Pearson symbol	Space group
(βY)	0 to 5.6	*cI*2	$Im\bar{3}m$
(αY)	0 to 5.6	*hP*2	$P6_3/mmc$
Y_5Pb_3	~58.3	*hP*16	$P6_3/mcm$
Y_5Pb_4	65.1	*oP*6	*Pnma*
YPb_2	82.3	*oC*12	*Cmcm*
YPb_3	87.5	*cP*4	$Pm\bar{3}m$
(Pb)	100	*cF*4	$Fm\bar{3}m$

Pb-Yb

A. Palenzona and S. Cirafici, 1991

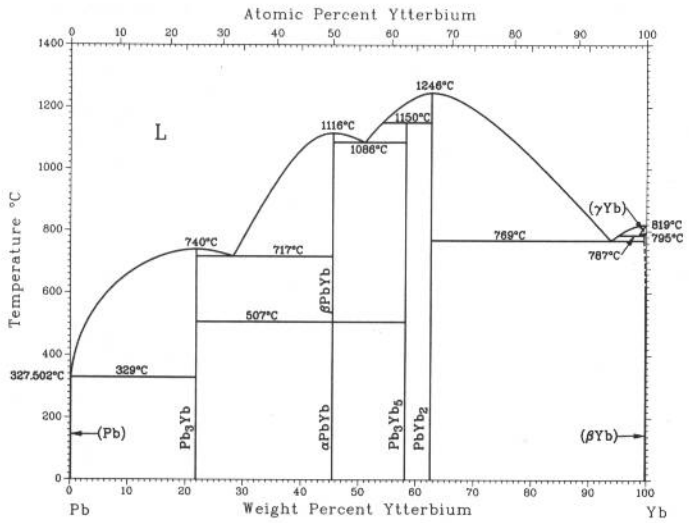

Phase	Composition, wt% Yb	Pearson symbol	Space group
(Pb)	~0	*cF*4	$Fm\bar{3}m$
Pb_3Yb	22	*cP*4	$Pm\bar{3}m$
PbYb	45.5	*tP*4(a)	*P*4/*mmm*(a)
Pb_3Yb_5	58.2	*hP*16	$P6_3/mcm$
$PbYb_2$	62.6	*oP*12	*Pnma*
(γYb)	~100	*cI*2	$Im\bar{3}m$
(βYb)	~100	*cF*4	$Fm\bar{3}m$
(αYb)	~100	*hP*2	$P6_3/mmc$

(a) Low-temperature modification

Pb-Zn

From [Hansen]

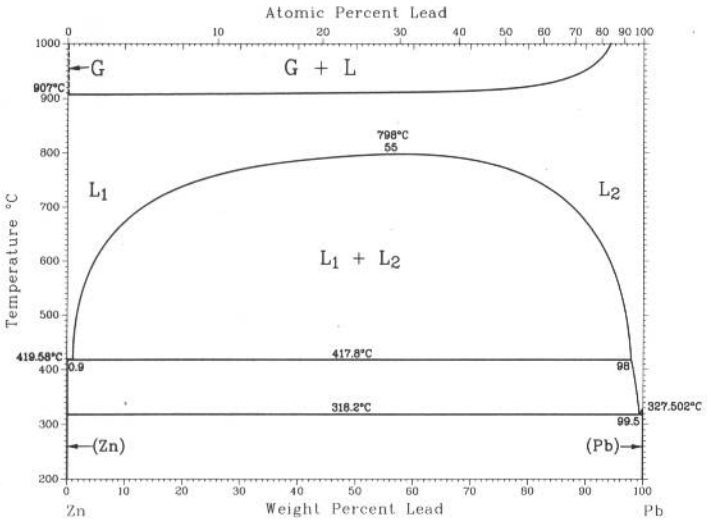

Phase	Composition, wt% Pb	Pearson symbol	Space group
(Zn)	0	*hP*2	$P6_3/mmc$
(Pb)	100	*cF*4	$Fm\bar{3}m$

Pd-Pt

H. Okamoto, 1991

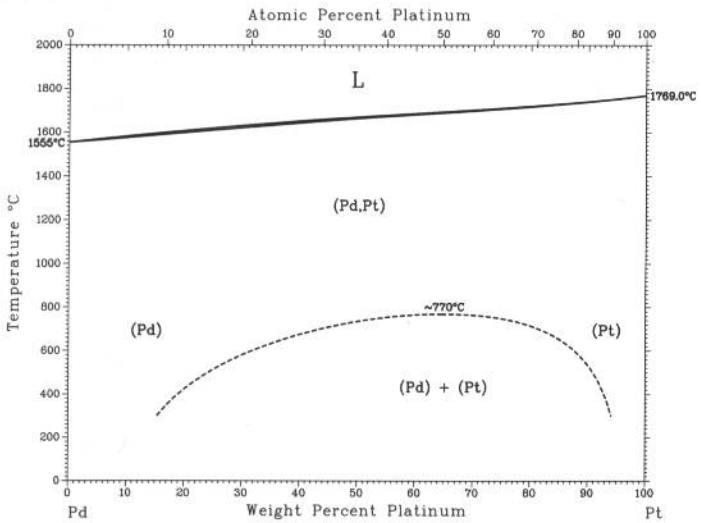

Phase	Composition, wt% Pt	Pearson symbol	Space group
(Pd,Pt)	0 to 100	*cF*4	$Fm\bar{3}m$

Pd-Pu

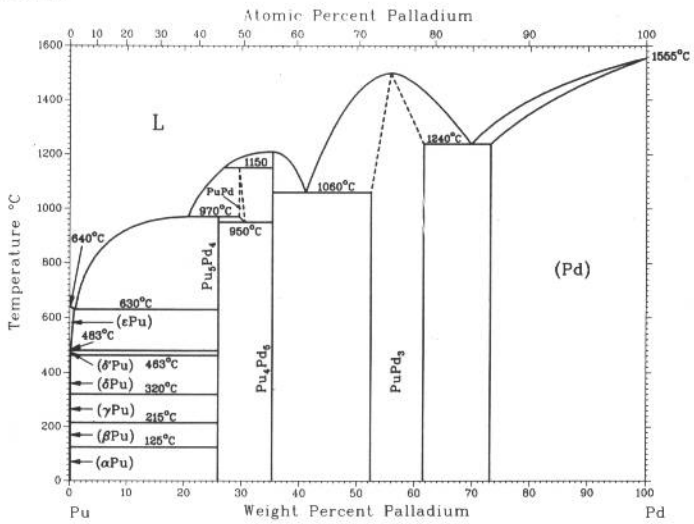

V.I. Kutaitsev, N.T. Chebotarev, I.G. Lebedev, M.A. Andrianov, V.N. Konev, and T.S. Menshikova, 1967

Phase	Composition, wt% Pd	Pearson symbol	Space group
(εPu)	0 to 0.7	*cI*2	$Im\bar{3}m$
(δ'Pu)	0	*tI*2	*I*4/*mmm*
(δPu)	0	*cF*4	$Fm\bar{3}m$
(γPu)	0	*oF*8	*Fddd*
(βPu)	0	*mC*34	*C*2/*m*
(αPu)	0	*mP*16	$P2_1/m$
Pu_5Pd_4	25.8	...	...
PuPd	~30 to 30.4	*oP*8	*Pnma*
Pu_4Pd_5	35.3	...	...
$PuPd_3$	~52.2 to 61.4	*cP*4	$Pm\bar{3}m$
(Pd)	~73 to 100	*cF*4	$Fm\bar{3}m$

Pd-Rh

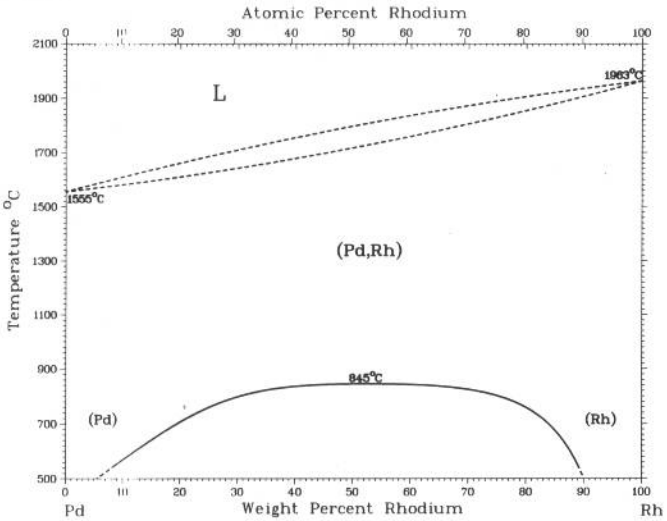

H. Okamoto, 1990

Phase	Composition, wt% Rh	Pearson symbol	Space group
(Pd,Rh)	0 to 100	*cF*4	$Fm\bar{3}m$

Pd-Ru

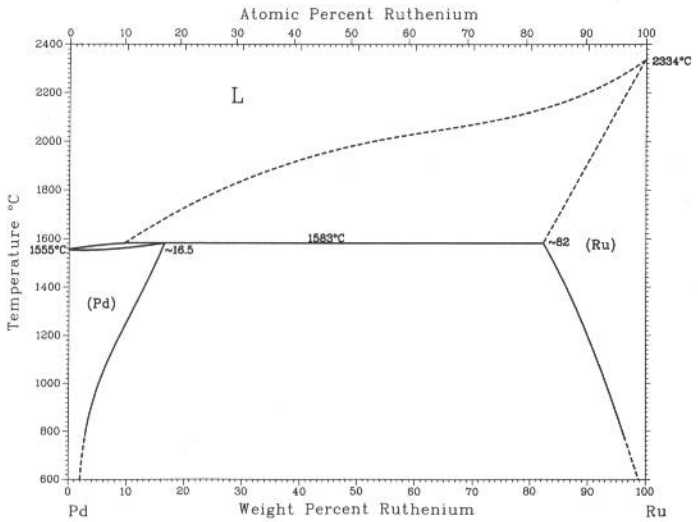

H. Okamoto, 1990

Phase	Composition, wt% Ru	Pearson symbol	Space group
(Pd)	0 to ~16.5	*cF*4	$Fm\bar{3}m$
(Ru)	~82 to 100	*hP*2	$P6_3/mmc$

Pd-S

H. Okamoto, 1992

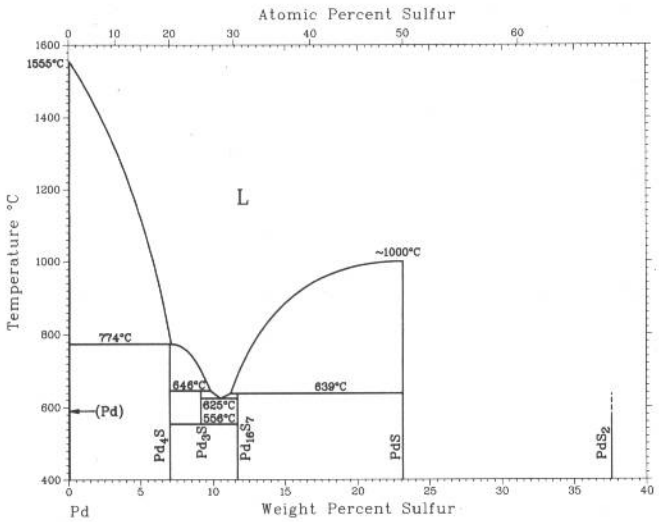

Phase	Composition, wt% S	Pearson symbol	Space group
(Pd)	0	*cF*4	$Fm\bar{3}m$
Pd_4S	7	*tP*10	$P\bar{4}2_1c$
Pd_3S	9	*oC*16	*Ama*2
$Pd_{17}S_7$	11.6	*cP*64	$Pm\bar{3}m$
PdS	23.2	*tP*16	$P4_2/m$
PdS_2	37.6	*oP*12	*Pbca*

Pd-Sb

H. Okamoto, 1992

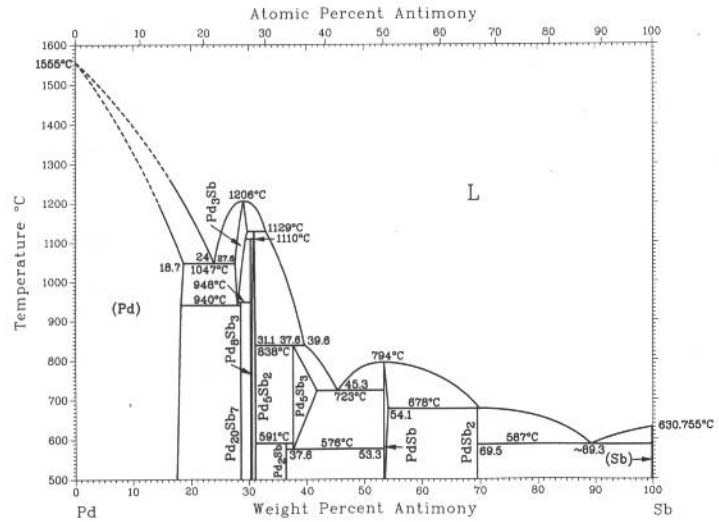

Phase	Composition, wt% Sb	Pearson symbol	Space group
(Pd)	0 to 18.7	*cF*4	$Fm\bar{3}m$
Pd_3Sb	27.6 to 29.7	*cF*16	$Fd\bar{3}m$
$Pd_{20}Sb_7$	28.6	*hR*27	$R\bar{3}$
Pd_8Sb_3	30.3	*hR*44	$R\bar{3}c$
Pd_5Sb_2	30.5 to 31.1	*hP*84	$P6_3/mmc$
Pd_2Sb	36.4	*oC*24	$Cmc2_1$
Pd_5Sb_3	37.4 to 41.7	*hP*4	$P6_3/mmc$
PdSb	53.4 to 44.2	*hP*4	$P6_3/mmc$
$PdSb_2$	69.6	*cP*12	*Pa*3
(Sb)	100	*hR*2	$R\bar{3}m$

Pd-Se

H. Okamoto, 1992

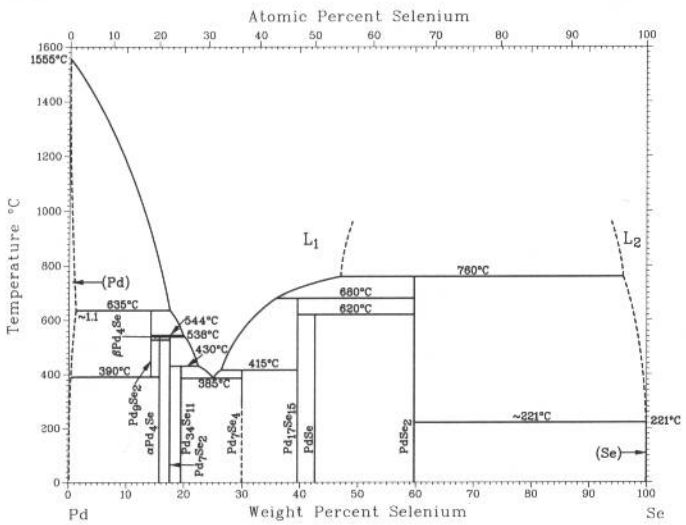

Phase	Composition, wt% Se	Pearson symbol	Space group
(Pd)	0 to ~1.1	*cF*4	$Fm\bar{3}m$
Pd_9Se_2	14.2	*hP**	...
βPd_4Se	16	...	...
αPd_4Se	16	*tP*10	$P\bar{4}2_1c$
Pd_7Se_2	17.5	*m**18	...
$Pd_{34}Se_{11}$	19.3	*mP**	$P2_1/n$
Pd_7Se_4	29.8	*oP*22	$P2_122_1$
$Pd_{17}Se_{15}$	39.6	*cP*64	$Pm\bar{3}m$
PdSe	42.6	*tP*16	$P4_2/m$
$PdSe_2$	59.8	*oP*12	*Pbca*
(γSe)	100	*hP*3	$P3_121$

Pd-Si

H.C. Baxi and T.B. Massalski, 1991

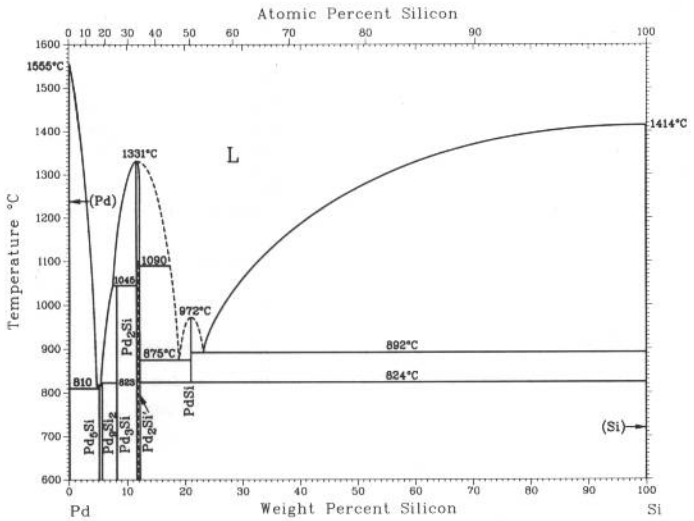

Phase	Composition, wt% Si	Pearson symbol	Space group
(Pd)	0	*cF*4	$Fm\bar{3}m$
Pd_9Si	5.02	*mP*24	$P2_1$
Pd_9Si_2	5.54	*oP*44	*Pnma*
Pd_3Si	8.1	*oP*16	*Pnma*
Pd_2Si	11.5 to 12.1	*hP*9	$P\bar{6}2m$
Pd_2Si'(a)	11.7 to 12.1	(b)	...
PdSi(c)	20.9	*oP*8	*Pnma*
(Si)	100	*cF*8	$Fd\bar{3}m$

(a) Below 1090 °C. (b) Hexagonal superstructure based on the Pd_2Si unit cell. (c) From 972 to 612 °C

Pd-Sm

H. Okamoto, 1990

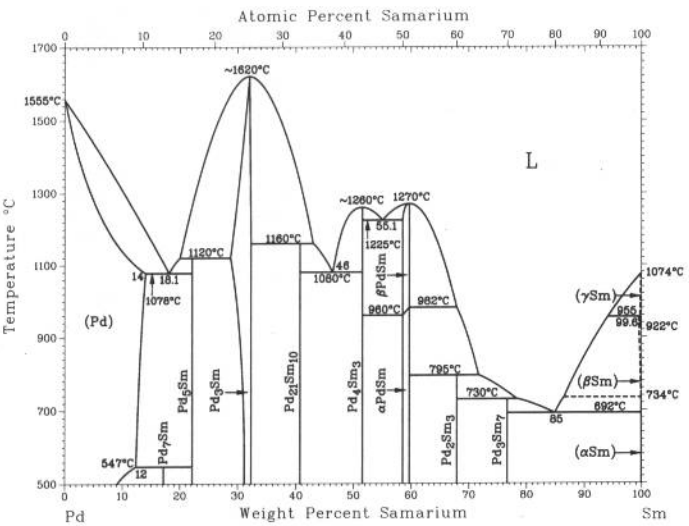

Phase	Composition, wt% Sm	Pearson symbol	Space group
(Pd)	0 to 14	*cF*4	$Fm\bar{3}m$
Pd_7Sm	16.8	*c***	...
Pd_9Sm	22.1	*o**72	...
Pd_3Sm	29.1 to 32	*cP*4	$Pm\bar{3}m$
$Pd_{21}Sm_{10}$	40.3	*mC*124	*C*2/*m*
Pd_4Sm_3	51.5	*hR*14	$R\bar{3}$
βPdSm	58.6	...	...
αPdSm	58.6	*oC*8	*Cmcm*
Pd_2Sm_3	68	...	...
Pd_2Sm_7	77	*hP*20	$P6_3mc$
(γSm)	100	*cI*2	$Im\bar{3}m$
(βSm)	100	*hP*2	$P6_3/mmc$
(αSm)	100	*hR*3	$R\bar{3}m$

Pd-Sn

H. Okamoto, 1990

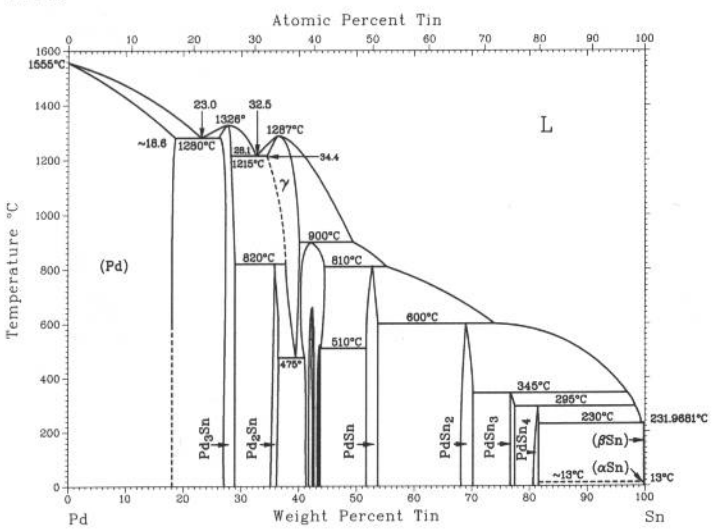

Phase	Composition, wt% Sn	Pearson symbol	Space group
(Pd)	0 to ~18.6	*cF*4	$Fm\bar{3}m$
Pd_3Sn	26 to 28.1	*cP*4	$Pm\bar{3}m$
Pd_2Sn	35.8	*oP*12	*Pnma*
γ	34 to 40.1	*hP*4	$P6_3/mmc$
$Pd_{20}Sn_{13}$	41 to 45	*hP*66	$P3_121$
βPd_3Sn_2	42.4	...	...
αPd_3Sn_2	43	...	...
δ	44	...	...
PdSn	~52.7	*oP*8	*Pnma*
$PdSn_2$	~69.1	*oC*24	*Aba*2
$PdSn_3$	~77	*oC*32	*Cmca*
$PdSn_4$	~82	*oC*20	*Aba*2
(βSn)	100	*tI*4	$I4_1/amd$
(αSn)	100	*cF*8	$Fd\bar{3}m$

(continued)

Pd-Sn phase diagram from 39 to 45 wt% Sn

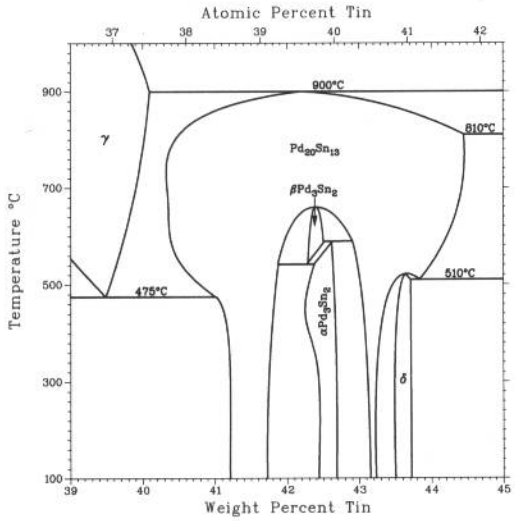

Pd-Te

H. Okamoto, 1992

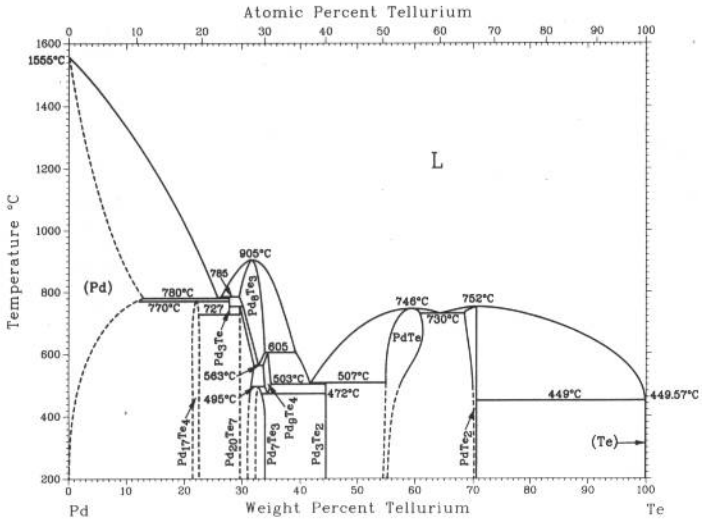

Phase	Composition, wt% Te	Pearson symbol	Space group
(Pd)	0 to 13	*cF*2	$Fm\bar{3}m$
$Pd_{17}Te_4$	~22	...	...
Pd_3Te	27.8	*cI*2	$Im\bar{3}m$
$Pd_{20}Te_7$	30 to 34	*hR*27	*R*3
Pd_8Te_3	30 to 39	*o***	...
Pd_7Te_3	33 to 34	*m***	...
Pd_9Te_4	39 to 40	*mP*52	$P2_1/c$
Pd_3Te_2	44	*oC*20	*Cmcm*
PdTe	54.5 to 59	*hP*4	$P6_3/mmc$
$PdTe_2$	68.5 to 70.6	*hP*3	$P\bar{3}m1$
(Te)	100	*hP*3	$P3_121$
Questionable phases			
Pd_4Te	23 to 26	*cF*104	$F\bar{4}3m$
Pd_3Te_2	44	*oP*45	$P222_1$

Pd-Ti

J.L. Murray, 1987

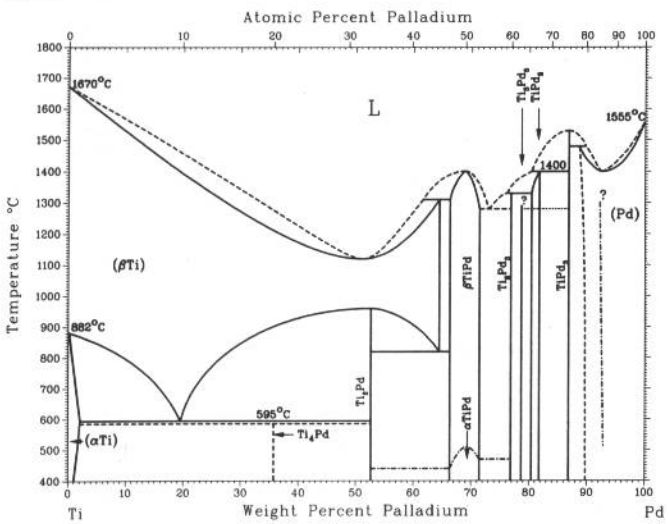

Phase	Composition, wt% Pd	Pearson symbol	Space group
(βTi)	0 to 65	*cI*2	$Im\bar{3}m$
(αTi)	0 to ~2	*hP*2	$P6_3/mmc$
Ti_4Pd	36	*cP*8	$Pm\bar{3}n$
Ti_2Pd	52.6	*tI*6	*I*4/*mmm*
βTiPd	66 to 72	*cP*2	$Pm\bar{3}m$
αTiPd	66 to 72	*oP*4	*Pmma*
Ti_2Pd_3	77	*oC*20	*Cmcm*
Ti_3Pd_5	78.7	*tP*8	*P*4/*mmm*
$TiPd_{2-}$	81 to 82	*tI*6	*I*4/*mmm*
$TiPd_2$	81 to 82	(a)	...
$TiPd_3$	87	*hP*16	$P6_3/mmc$
γ(b)	87 to 92	*cP*4	*P*4/*mmm*
(Pd)	93 to 100	*cF*4	$Fm\bar{3}m$

(a) Orthorhombic distortion of $MoSi_2$. (b) Possibly an ordered metastable phase. The dot-dash lines show the observed limits of ordering.

Pd-Tl

H. Okamoto, 1990

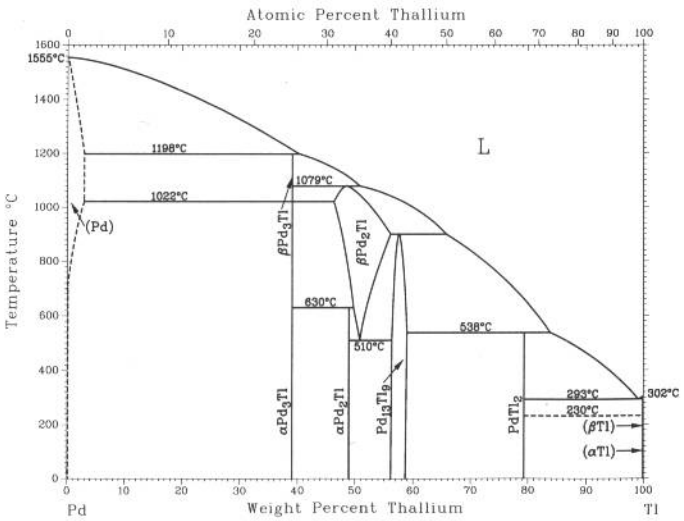

Phase	Composition, wt% Tl	Pearson symbol	Space group
(Pd)	0	*cF*4	$Fm\bar{3}m$
βPd_3Tl	39	*tI*8	*I*4/*mmm*
αPd_3Tl	39	*tI*16	*I*4/*mmm*
βPd_2Tl	45 to 56	*hP*6	$P6_3/mmc$
αPd_2Tl	48.9	*oP*12	*Pnma*
$Pd_{13}Tl_9$	56 to 59	*hP*20	$P\bar{3}1c$
$PdTl_2$	79.4	*tI*12	*I*4/*mcm*
(βTl)	100	*cI*2	$Im\bar{3}m$
(αTl)	100	*hP*2	$P6_3/mmc$

Pd-U

H. Okamoto, 1992

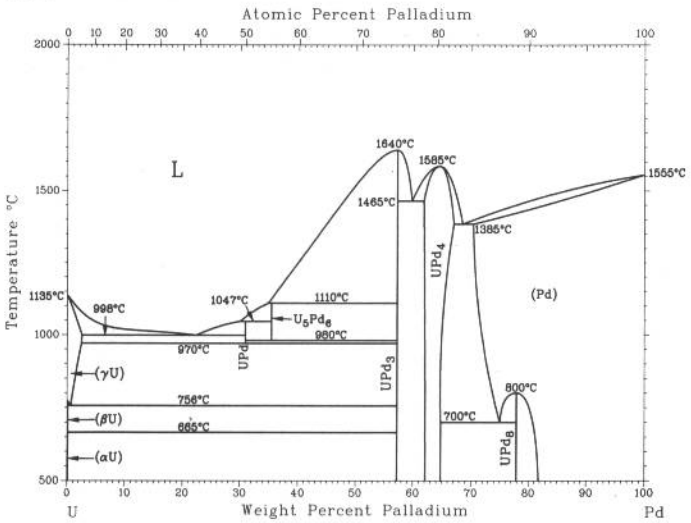

Phase	Composition, wt% Pd	Pearson symbol	Space group
(γU)	0 to 2	*cI*2	$Im\bar{3}m$
(βU)	0	*tP*30	$P4_2/mmm$
(αU)	0	*oC*4	*Cmcm*
UPd	30.9	...	...
U_5Pd_6	34.9	...	...
UPd_3	57	*hP*16	$P6_3/mmc$
UPd_4	61 to 66	*cP*4	$Pm\bar{3}m$
UPd_8	78.2	...	...
(Pd)	70 to 100	*cF*4	$Fm\bar{3}m$

Pd-V

J.F. Smith, 1989

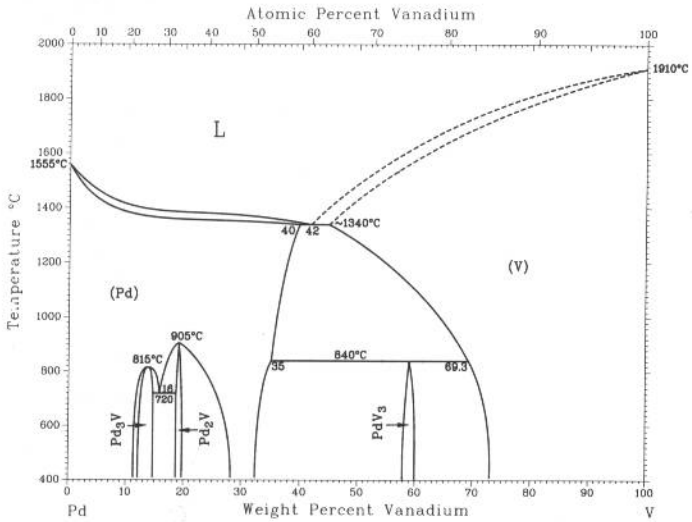

Phase	Composition, wt% V	Pearson symbol	Space group
(Pd)	0 to 40	*cF*4	$Fm\bar{3}m$
Pd_3V	~14	*tI*8	*I*4/*mmm*
Pd_2V	~19.3	*oI*6	*Immm*
PdV_3	~59	*cP*8	$Pm\bar{3}n$
(V)	~44.4 to 100	*cI*2	$Im\bar{3}m$

Pd-W

S.V. Nagender Naidu and P. Rama Rao, 1991

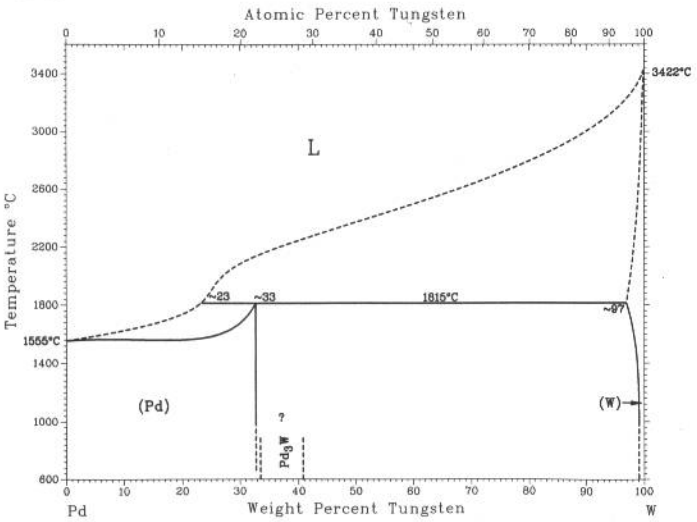

Phase	Composition, wt% W	Pearson symbol	Space group
(Pd)	0 to 33	*cF*4	$Fm\bar{3}m$
(W)	~97 to 100	*cI*2	$Im\bar{3}m$

Pd-Y

H. Okamoto, 1990

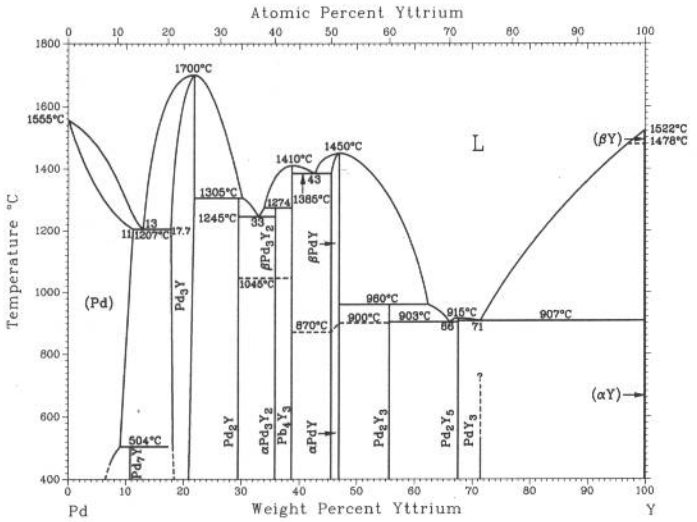

Phase	Composition, wt% Y	Pearson symbol	Space group
(Pd)	0 to 11	*cF*4	$Fm\bar{3}m$
Pd_7Y	10.7	*c***	...
Pd_3Y	17.7 to 22	*cP*4	$Pm\bar{3}m$
Pd_2Y	29.4	...	...
βPd_3Y_2	36	...	...
αPd_3Y_2	36	...	...
Pd_4Y_3	38.6	*hR*14	$R\bar{3}$
βPdY	45.5 to ~47	...	...
αPdY	45.5 to ~47	...	...
Pd_2Y_3	56	*hR*15	$R\bar{3}$
Pd_2Y_5	67.6	*cF*144	$Fd\bar{3}m$
PdY_3	72	*oP*16	*Pnma*
(βY)	100	*cI*2	$Im\bar{3}m$
(αY)	100	*hP*2	$P6_3/mmc$

Pd-Yb

A. Iandelli and A. Palenzona, 1973

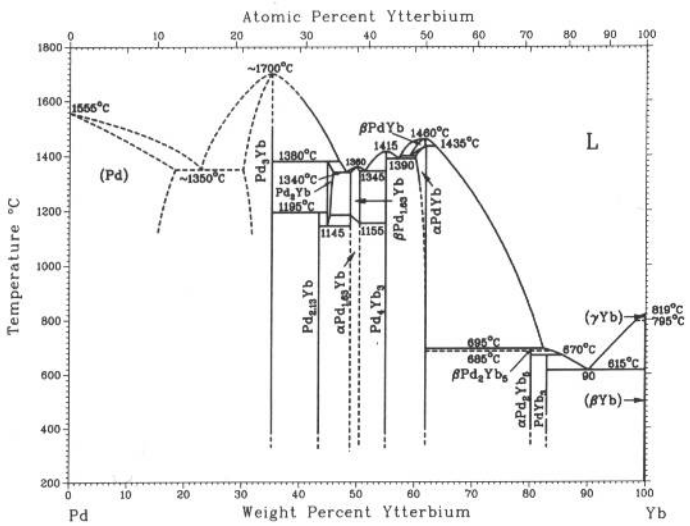

Phase	Composition, wt% Yb	Pearson symbol	Space group
(Pd)	0 to 18	*cF*4	$Fm\bar{3}m$
Pd_3Yb	30 to 35	*cP*4	$Pm\bar{3}m$
$Pd_{2.13}Yb$	43	...	...
Pd_2Yb	44.8 to 46.1	...	...
$\beta Pd_{1.63}Yb$	49 to 50.4	...	...
$\alpha Pd_{1.63}Yb$	49 to 50.4	...	...
Pd_4Yb_3	55	*hR*14	$R\bar{3}$
βPdYb	59 to ~61.9	...	...
αPdYb	60 to 61.9	*cP*2	$Pm\bar{3}m$
βPd_2Yb_5	~80.2	...	...
αPd_2Yb_5	~80.2	...	...
$PdYb_3$	83	...	...
(γYb)	100	*cI*2	$Im\bar{3}m$
(βYb)	100	*cF*4	$Fm\bar{3}m$

Pd-Zn

H. Okamoto, 1990

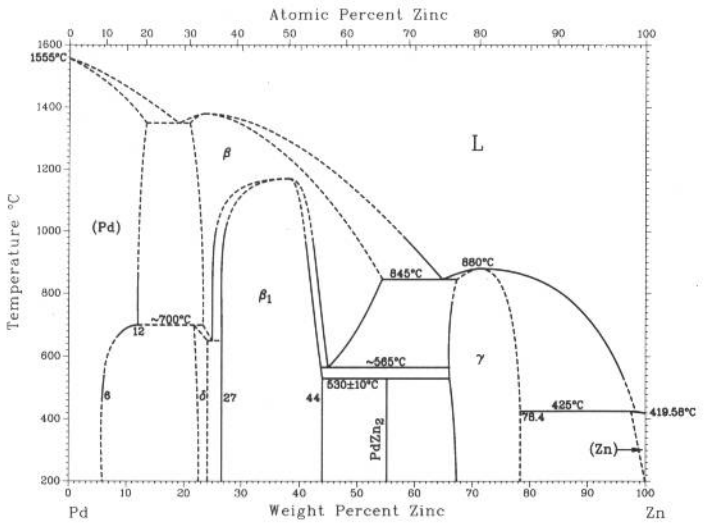

Phase	Composition, wt% Zn	Pearson symbol	Space group
(Pd)	0 to 13	*cF*4	$Fm\bar{3}m$
δ	~23	*oP*12	*Pnma*
β	21 to 53	*cP*2	$Pm\bar{3}m$
β_1	27 to 44	*tP*4	*P*4/*mmm*
$PdZn_2$	55.2	*oC*48	*Cmmm*
γ	66 to 78.4	*cI*52	$I\bar{4}3m$
(Zn)	? to 100	*hP*2	$P6_3/mmc$

Pr-Sb

H. Okamoto, 1990

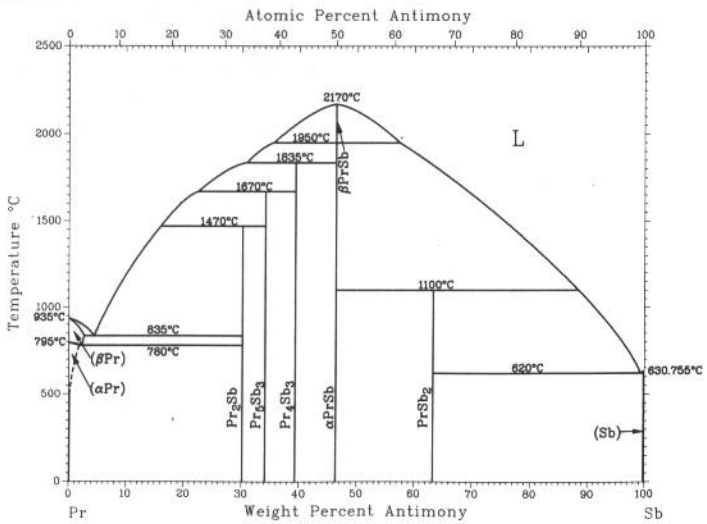

Phase	Composition, wt% Sb	Pearson symbol	Space group
(βPr)	0	*cI*2	$Im\bar{3}m$
(αPr)	0	*hP*4	$P6_3/mmc$
Pr_2Sb	30.1	*tI*12	*I*4/*mmm*
Pr_5Sb_3	34.1	*hP*16	$P6_3/mcm$
Pr_4Sb_3	39.4	*cI*28	$I\bar{4}3d$
βPrSb	46.4	...	...
αPrSb	46.4	*cF*8	$Fm\bar{3}m$
$PrSb_2$	63.4	*oC*24	*Cmca*
(Sb)	100	*hR*2	$R\bar{3}m$

Pr-Se

E.I. Yarembach, 1970

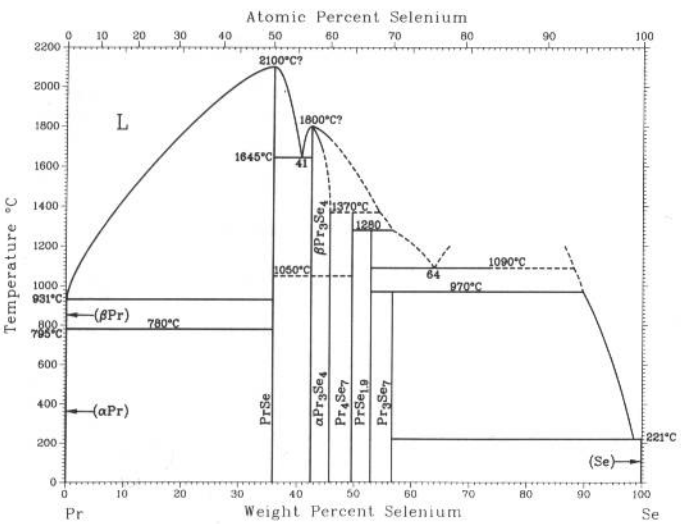

Phase	Composition, wt% Se	Pearson symbol	Space group
(βPr)	0	*cI*2	$Im\bar{3}m$
(αPr)	0	*hP*4	$P6_3/mmc$
PrSe	35.9	*cF*8	$Fm\bar{3}m$
βPr_3Se_4	~42.2 to 46	*cI*28	$I\bar{4}3d$
αPr_3Se_4	~42.2 to 46	*tI*28	*I*4/*mcm*
Pr_4Se_7	49.5	*tP*22	*P*4/*mmm*
$PrSe_{1.9}$	~52.9	*tP*6	*P*4/*mmm*
Pr_3Se_7	57	...	...
(Se)	100	*hP*3	$P3_121$

Pr-Si

H. Okamoto, 1990

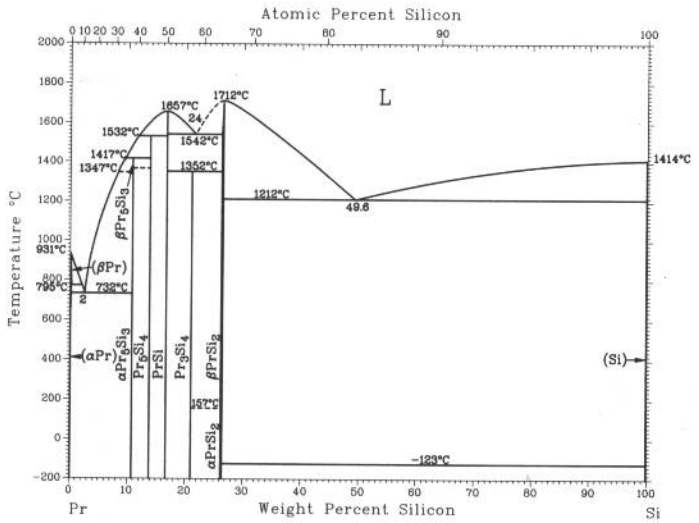

Phase	Composition, wt% Si	Pearson symbol	Space group
(βPr)	0	*cI*2	$Im\bar{3}m$
(αPr)	0	*hP*4	$P6_3/mmc$
βPr_5Si_3	10.7	...	...
αPr_5Si_3	10.7	*tI*32	$I4/mcm$
Pr_5Si_4	13.7	*tP*36	$P4_12_12$
PrSi	16.6	*oP*8	*Pnma*
Pr_3Si_4	21.0	...	...
$\beta PrSi_2$	26.4	*tI*12	$I4_1/amd$
$\alpha PrSi_2$	26.4	*oI*12	*Imma*
(Si)	100	*cF*8	$Fd\bar{3}m$

Pr-Sn

H. Okamoto, 1990

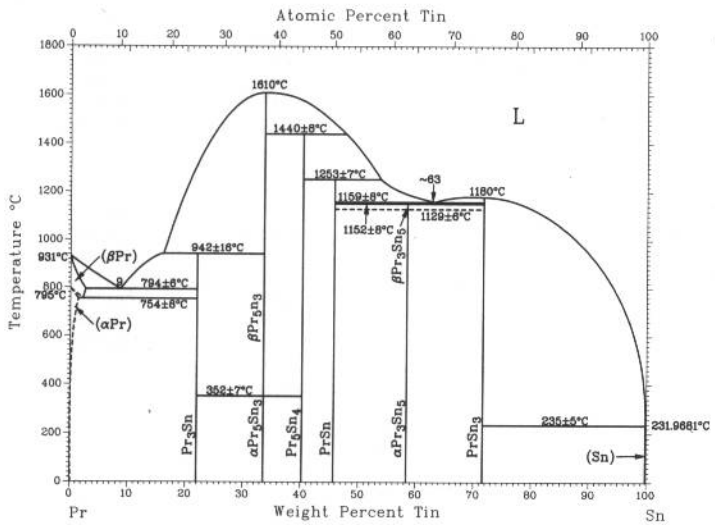

Phase	Composition, wt% Sn	Pearson symbol	Space group
(βPr)	0 to ~3	*cI*2	$Im\bar{3}m$
(αPr)	0 to ~1.3	*hP*4	$P6_3/mmc$
Pr_3Sn	22	*cP*4	$Pm\bar{3}m$
βPr_5Sn_3	33.6	*hP*16	$P6_3/mcm$
αPr_5Sn_3	33.6	*tI*32	$I4/mcm$
Pr_5Sn_4	40.2	*oP*36	*Pnma*
PrSn	45.7	...	...
βPr_3Sn_5	58.4	...	...
αPr_3Sn_5	58.4	...	...
$PrSn_3$	72	*cP*4	$Pm\bar{3}m$
(βSn)	100	*tI*4	$I4_1/amd$
(αSn)	100	*cF*8	$Fd\bar{3}m$

Pr-Te

E.I. Yarembach, 1970

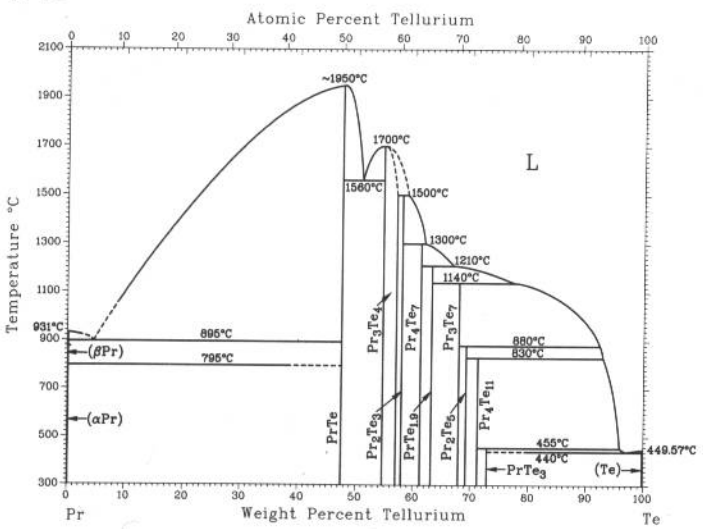

Phase	Composition, wt% Te	Pearson symbol	Space group
(βPr)	0	*cI*2	$Im\bar{3}m$
(αPr)	0	*hP*4	$P6_3/mmc$
PrTe	47.5	*cF*8	$Fm\bar{3}m$
Pr_3Te_4	54.7 to ~57	*cI*28	$I\bar{4}3d$
Pr_2Te_3	58	...	...
Pr_4Te_7	~61.3	...	...
$PrTe_{1.9}$	~63.2	...	...
Pr_3Te_7	68	...	...
Pr_2Te_5	69.3	*oC*28	*Cmcm*
Pr_4Te_{11}	71.3	...	...
$PrTe_3$	73	*tP*16	$P4_2/n$
(Te)	100	*hP*3	$P3_121$

Pr-Tl

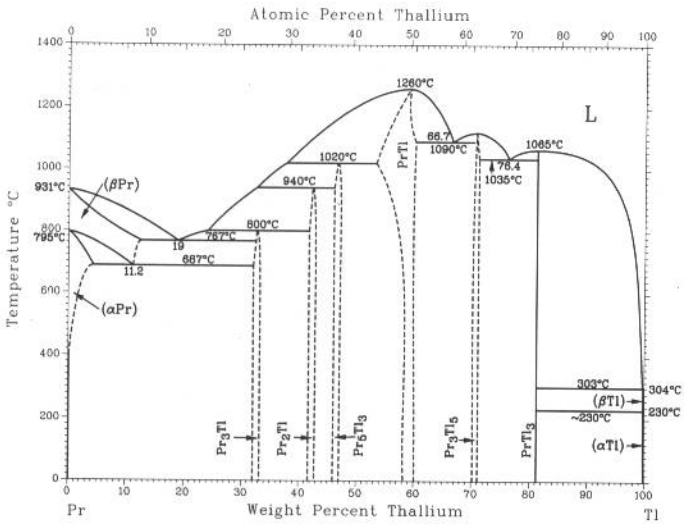

S. Delfino, A. Saccone, A. Palenzona, and R. Ferro, unpublished

Phase	Composition, wt% Tl	Pearson symbol	Space group
(βPr)	0 to 12.5	*cI*2	$Im\bar{3}m$
(αPr)	0 to 3.6	*hP*4	$P6_3/mmc$
Pr_3Tl(a)	~32.0 to ~33.2	*cP*4	$Pm\bar{3}m$
	~33	*cF*4	$Fm\bar{3}m$
Pr_2Tl	~42 to ~43	*hP*6	$P6_3/mmc$
Pr_5Tl_3	~46 to ~47	*tI*32	$I4/mcm$
PrTl(b)	~53 to ~60	*cP*2	$Pm\bar{3}m$
		or *cI*2	$Im\bar{3}m$
PrTl(c)	~53 to ~60	*tP*2	$P4/mmm$
Pr_3Tl_5	~70 to ~71	*oC*32	$Cmcm$
$PrTl_3$	81	*cP*4	$Pm\bar{3}m$
(βTl)	100	*cI*2	$Im\bar{3}m$
(αTl)	100	*hP*2	$P6_3/mmc$

(a) A *cP*4-*cF*4 order-disorder transformation in this phase has been suggested. (b) Cubic structure presumed to be room- and higher-temperature phases. (c) Tetragonal structure presumed to be lower-temperature phase

Pr-Zn

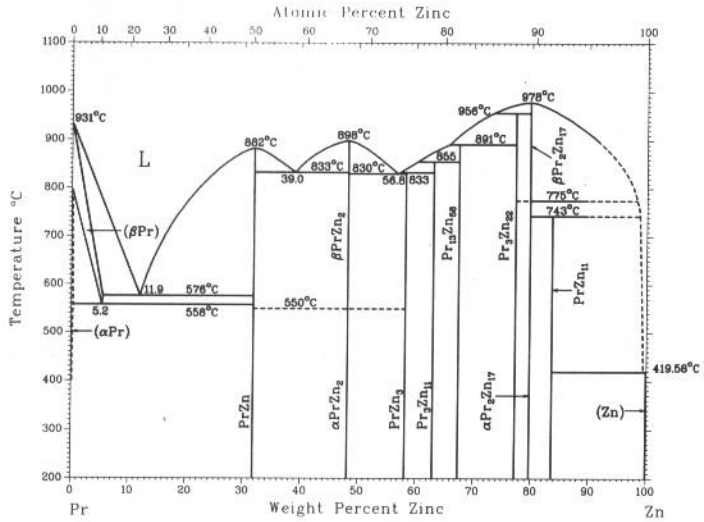

J.T. Mason and P. Chiotti, 1970

Phase	Composition, wt% Zn	Pearson symbol	Space group
(βPr)	0 to 5	*cI*2	$Im\bar{3}m$
(αPr)	0 to 0.2	*hP*4	$P6_3/mmc$
PrZn	31.7	*cP*2(a)	$Pm\bar{3}m$
$\beta PrZn_2$	48.2	...	...
$\alpha PrZn_2$	48.2	*oI*12	*Imma*
$PrZn_3$	58	*oP*16	*Pnma*
Pr_3Zn_{11}	62.9	*oI*28	*Immm*
$Pr_{13}Zn_{58}$	67.3	*hP*142	$P6_3/mc$
Pr_3Zn_{22}	77	*tI*100	$I4_1/amd$
βPr_2Zn_{17}	79.6	*hR*19	$R\bar{3}m$
αPr_2Zn_{17}	79.6	*hP*38	$P6_3/mmc$
$PrZn_{11}$	83.5	*tI*48	$I4_1/amd$
(Zn)	100	*hP*2	$P6_3/mmc$

(a) t^{**} below 45 K

Pt-Rh

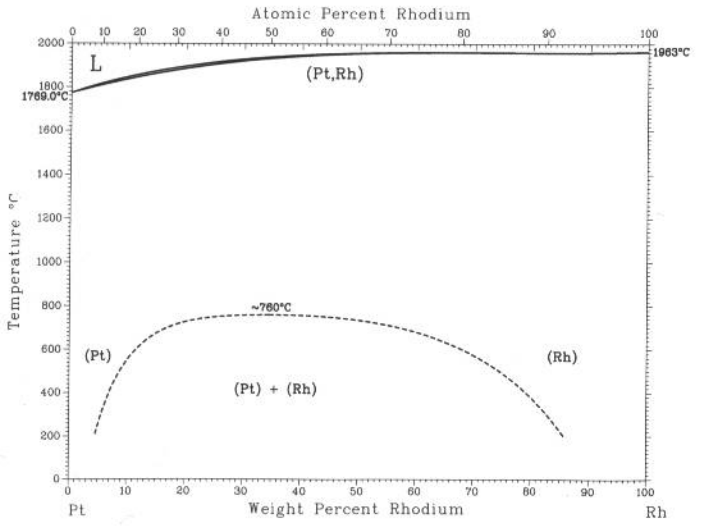

H. Okamoto, 1992

Phase	Composition, wt% Rh	Pearson symbol	Space group
(Pt,Rh)	0 to 100	*cF*4	$Fm\bar{3}m$

Pt-Si

H. Okamoto and L.E. Tanner, 1991

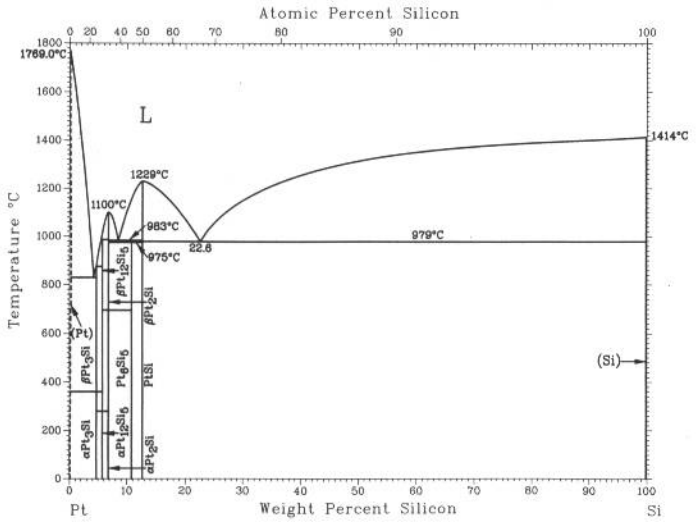

Phase	Composition, wt% Si	Pearson symbol	Space group
(Pt)	0 to 0.2	*cF*4	$Fm\bar{3}m$
γPt_3Si(a)	5	*tI*16	*I*4/*mcm*
βPt_3Si	5	*oP*16	*Pnma*
αPt_3Si	5	*mC*16	*C*2/*m*
$\beta Pt_{12}Si_5$	5.7	*tI*34	*I*4/*m*
$\alpha Pt_{12}Si_5$	5.7	*tP*68	*P*4/*n*
βPt_2Si	6.7	*hP*9	$P\bar{6}2m$
αPt_2Si	6.7	*tI*6	*I*4/*mmm*
Pt_6Si_5	10.7	*mP*22	$P2_1/m$
PtSi	12.6	*oP*8	*Pnma*
Pt_2Si_3(b)	18	*hP*10	$P6_3/mmc$
Pt_4Si_9(b)	24.4	?	?
(Si)	100	*cF*8	$Fd\bar{3}m$

(a) Impurity stabilized. (b) Metastable

Pt-Sn

From [Hansen]

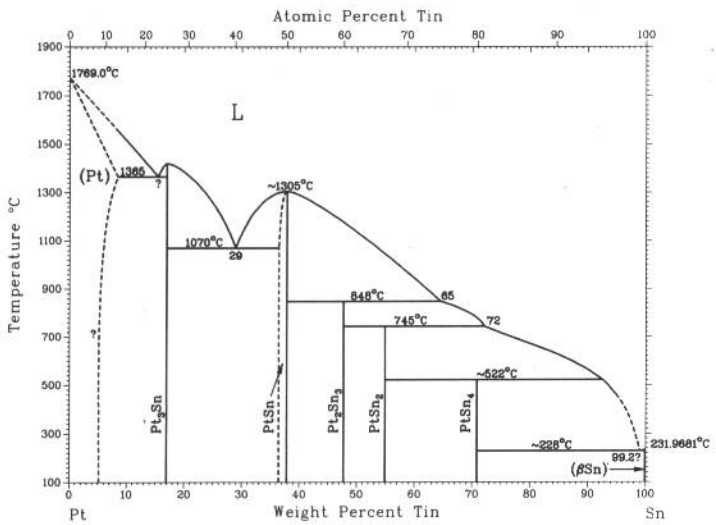

Phase	Composition, wt% Sn	Pearson symbol	Space group
(Pt)	0 to ?	*cF*4	$Fm\bar{3}m$
Pt_3Sn	17	*cP*4	$Pm\bar{3}m$
PtSn	>36 to 37.8	*hP*4	$P6_3/mmc$
Pt_2Sn_3	48	*hP*10	$P6_3/mmc$
$PtSn_2$	54.9	*cF*12	$Fm\bar{3}m$
$PtSn_4$	71	*oC*20	*Aba*2
(βSn)	100	*tI*4	$I4_1/amd$
(αSn)	100	*cF*8	$Fd\bar{3}m$

Pt-Te

H. Okamoto, 1990

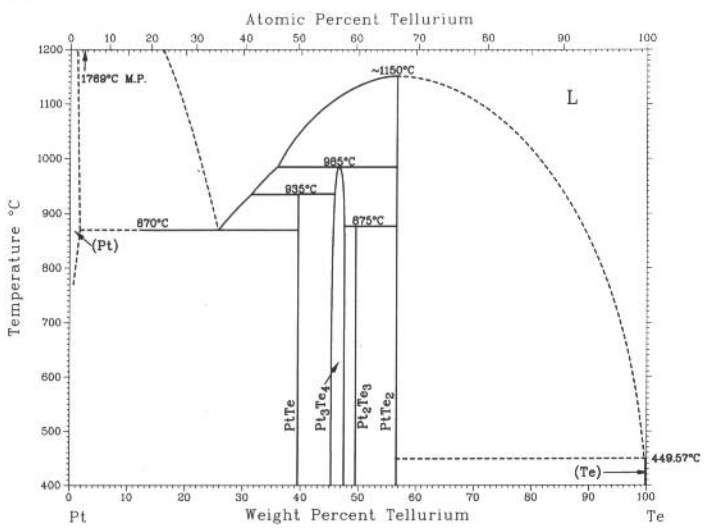

Phase	Composition, wt% Te	Pearson symbol	Space group
(Pt)	0 to ?	*cF*4	$Fm\bar{3}m$
PtTe	39.5	*mC*8	*C*2/*m*
Pt_3Te_4	~46.5	*mC*14	*C*2/*m*
Pt_2Te_3	50	*mC*20	*C*2/*m*
$PtTe_2$	56.7	*hP*3	$P\bar{3}m1$
(Te)	100	*hP*3	$P3_121$

Pt-Ti

J.L. Murray, 1987

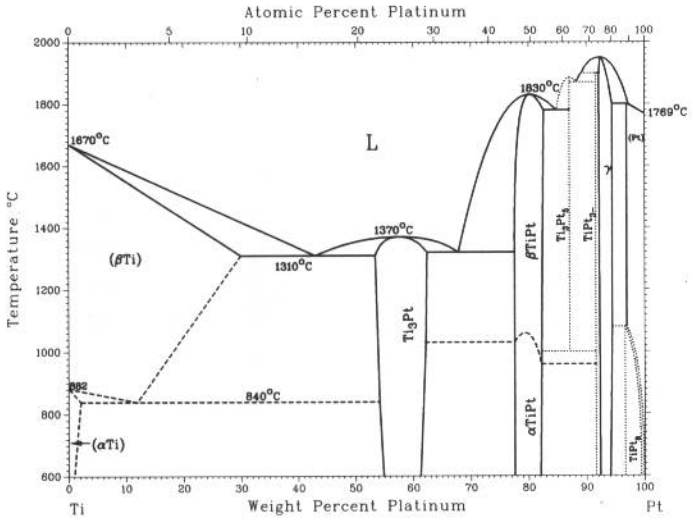

Phase	Composition, wt% Pt	Pearson symbol	Space group
(βTi)	0 to 31	*cI*2	$Im\bar{3}m$
(αTi)	0 to 2.0	*hP*2	$P6_3/mmc$
Ti_3Pt	54 to 63	*cP*8	$Pm\bar{3}n$
βTiPt	78 to 83	*oP*2	*Pmma*
αTiPt	78 to 83	*oP*4	*Pmma*
Ti_3Pt_5	87.2	*oI*32	*Ibam*
$TiPt_{3-}$	<92	*hP*16	$P6_3/mmc$
γ	92 to 95	*tP*4	$Pm\bar{3}m$
$TiPt_8$	97 to 99.5	*tI*18	*I*4/*m*
(Pt)	95 to 100	*cF*4	$Fm\bar{3}m$

Pt-Tl

H. Okamoto, 1990

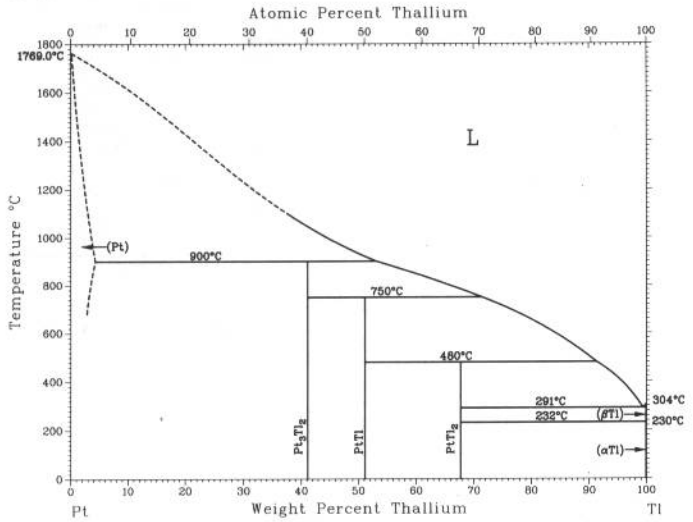

Phase	Composition, wt% Tl	Pearson symbol	Space group
(Pt)	0 to ?	*cF*4	$Fm\bar{3}m$
Pt_3Tl_2	41	*hP*20	$P\bar{3}1c$
PtTl	51.2	*hP*6	*P*6/*mmm*
$PtTl_2$	67.7	*tI*12	*I*4/*mcm*
(βTl)	100	*cI*2	$Im\bar{3}m$
(αTl)	100	*hP*2	$P6_3/mmc$

Pt-U

B.A.S. Ross and D.E. Peterson, 1990

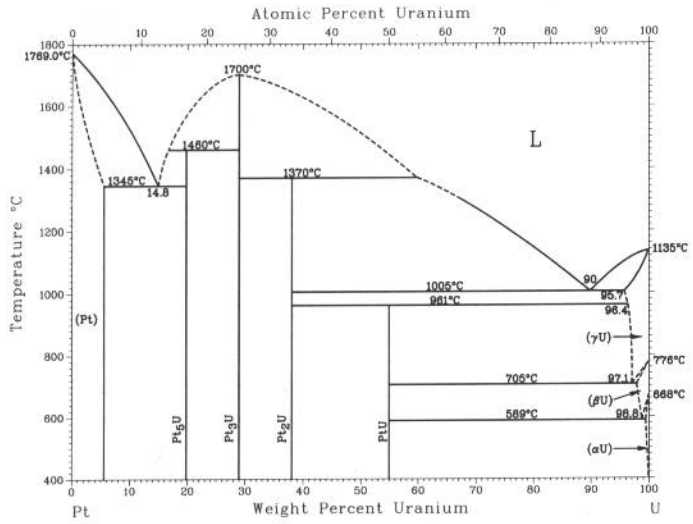

Phase	Composition, wt% U	Pearson symbol	Space group
(Pt)	0 to 5	*cF*4	$Fm\bar{3}m$
Pt_5U	19.7	*cF*24	$F\bar{4}3m$
Pt_3U	29	*hP*8	$P6_3/mmc$
Pt_2U(a)	37.9	*oC*12	*Ama*2
PtU	55.0	*oC*8	*Cmcm*
(γU)	99.7 to 100	*cI*2	$Im\bar{3}m$
(βU)	98.1 to 100	*tP*30	$P4_2/mnm$
(αU)	99.2 to 100	*oC*4	*Cmcm*

(a) Distorted structure

Pt-V

J.F. Smith, 1989

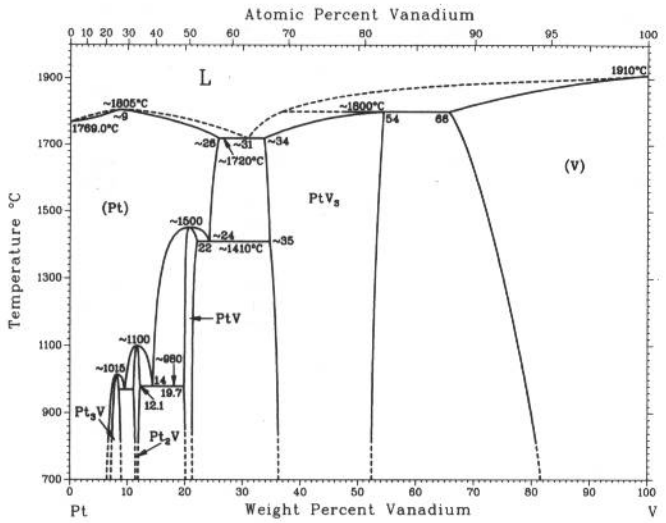

Phase	Composition, wt% V	Pearson symbol	Space group
(Pt)	0 to ~26	*cF*4	$Fm\bar{3}m$
Pt_3V	7 to 8	*tI*8	*I*4/*mmm*
Pt_2V	11 to 21.1	*oI*6	*Immm*
PtV	19.7 to 22	*oP*4	*Pmma*
PtV_3	~34 to 54	*cP*8	$Pm\bar{3}n$
(V)	66 to 100	*cI*2	$Im\bar{3}m$
Metastable phases			
Pt_8V(a)	~3.2	*tI*18	*I*4/*mmm*
Pt_3V(b)	6.9 to 7.2	*cP*4	$Pm\bar{3}m$
PtV	20.7 to 23.5	*tP*2	*P*4/*mmm*
PtV_3	~44	*cP*4	$Pm\bar{3}m$

(a) Possibly misclassified because neither its stability nor metastability is conclusive. (b) Stabilized by oxygen and possibly also by nitrogen and/or carbon

Pt-Zr

H. Okamoto, 1990

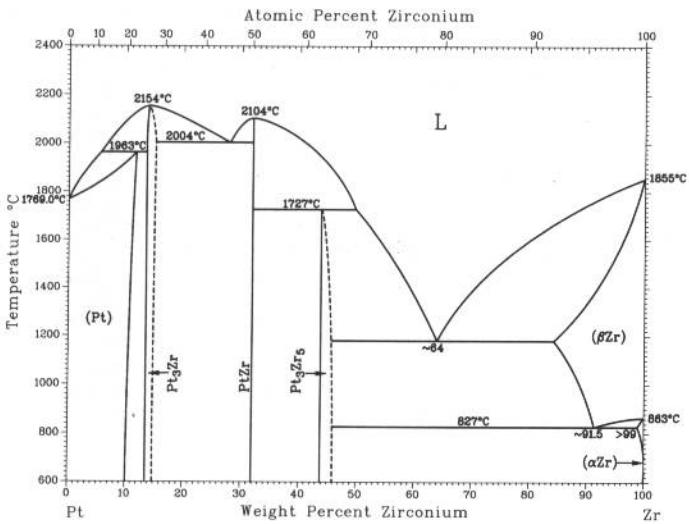

Phase	Composition, wt% Zr	Pearson symbol	Space group
(Pt)	0 to ~12	*cF*4	$Fm\bar{3}m$
Pt_3Zr	14	*cP*4	$Pm\bar{3}m$
		*hP*16	$P6_3/mmc$
$Pt_{11}Zr_9$(a)	28	*tI*40	*I*4/*m*
βPtZr	31.9	*cP*2	$Pm\bar{3}m$
αPtZr	31.9	*oC*8	*Cmcm*
Pt_3Zr_5	43.8	*hP*16	$P6_3/mcm$
(βZr)	~84.3 to 100	*cI*2	$Im\bar{3}m$
(αZr)	>99 to 100	*hP*2	$P6_3/mmc$

Note: The polymorphic transformation temperature of PtZr is unknown. (a) Not shown in the diagram

Pu-Sc

H. Okamoto, 1990

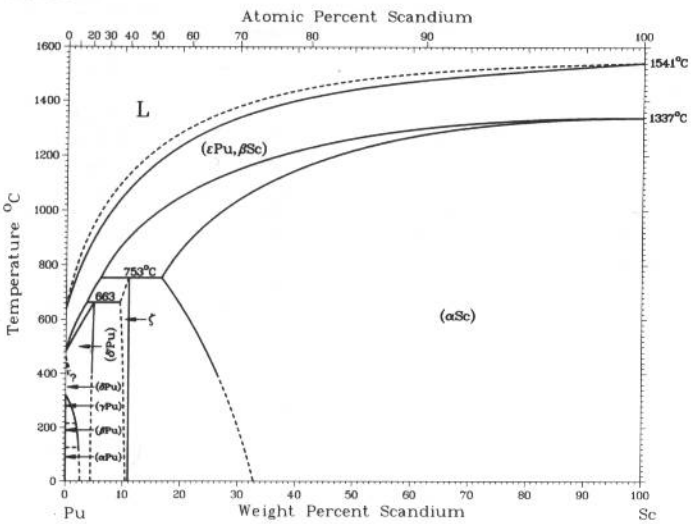

Phase	Composition, wt% Sc	Pearson symbol	Space group
(εPu,βSc)	0 to 100	*cI*2	$Im\bar{3}m$
(δ'Pu)	0 to ?	*tI*2	*I*4/*mmm*
(δPu)	0 to ?	*cF*4	$Fm\bar{3}m$
(γPu)	0 to ?	*oF*8	*Fddd*
(βPu)	0 to ?	*mC*34	*C*2/*m*
(αPu)	0 to ?	*mP*16	$P2_1/m$
ζ	? to 11	...	...
(αSc)	17 to 100	*hP*2	$P6_3/mmc$

Pu-U

H. Okamoto, 1992

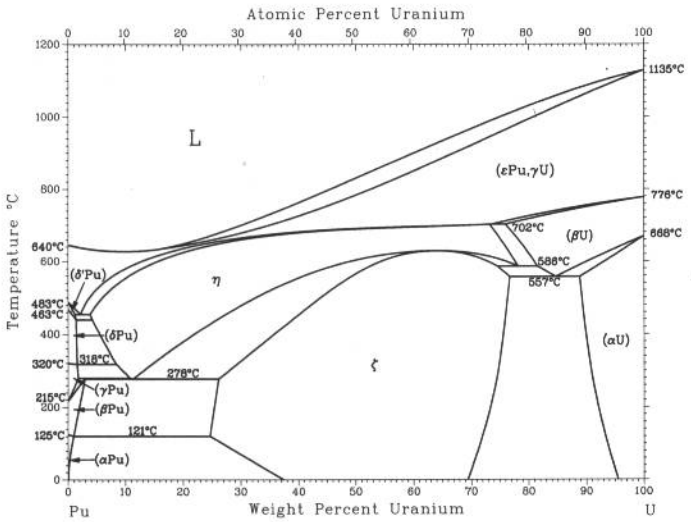

Phase	Composition, wt% U	Pearson symbol	Space group
(εPu,γU)	0 to 100	*cI*2	$Im\bar{3}m$
(δ'Pu)	0 to 2	*tI*2	*I*4/*mmm*
(δPu)	0 to 2	*cF*4	$Fm\bar{3}m$
(γPu)	0 to 2	*oF*8	*Fddd*
(βPu)	0 to 3	*mC*34	*C*2/*m*
(αPu)	0	*mP*16	$P2_1/m$
ζ	25 to 77	*cP*58	...
η	4 to 80	*tP*52	...
(βU)	77 to 100	*tP*30	$P4_2/mnm$
(αU)	89 to 100	*oC*4	*Cmcm*

Pu-Zn

From [Chiotti]

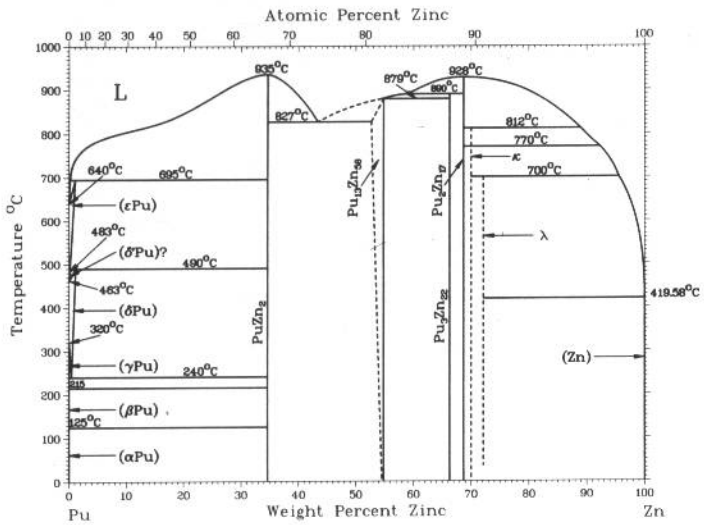

Phase	Composition, wt% Zn	Pearson symbol	Space group
(εPu)	0 to 0.96	*cI*2	$Im\bar{3}m$
(δ'Pu)	0	*tI*2	*I*4/*mmm*
(δPu)	0 to 1.1	*cF*4	$Fm\bar{3}m$
(γPu)	0	*oF*8	*Fddd*
(βPu)	0	*mC*34	*C*2/*m*
(αPu)	0	*mP*16	$P2_1/m$
$PuZn_2$	34.9	*cF*24	$Fd\bar{3}m$
Pu_3Zn_{58}	~52.5 to 55	*hP*142	$P6_3mc$
Pu_3Zn_{22}	66	*tI*100	$I4_1/amd$
Pu_2Zn_{17}	69.5	*hR**	$R\bar{3}m$
κ (HT)	~71	*hP**	*P*6/*mmm*
κ (LT)	~71	*hP*38	$P6_3/mmc$
λ	~71.8	*hP**	$P6_322$
(Zn)	100	*hP*2	$P6_3/mmc$

Pu-Zr

From [Elliott]

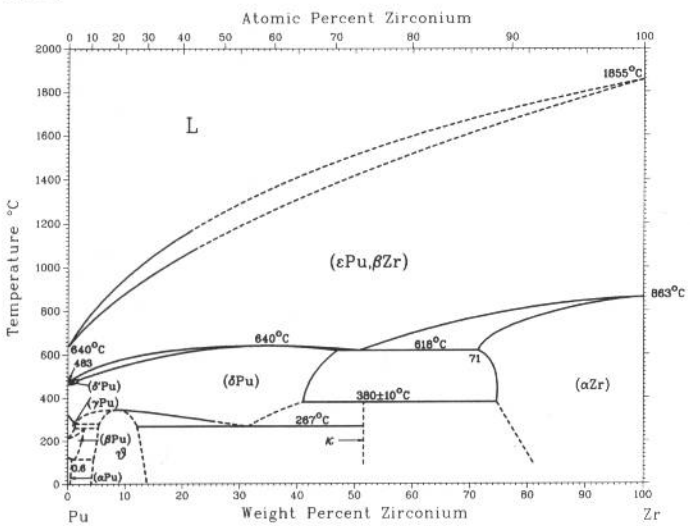

Phase	Composition, wt% Zr	Pearson symbol	Space group
(εPu,βZr)	0 to 100	*cI*2	$Im\bar{3}m$
(δ'Pu)	0 to 0.76	*tI*2	*I*4/*mmm*
(δPu)	0 to 47	*cF*4	$Fm\bar{3}m$
(γPu)	0 to 1.1	*oF*8	*Fddd*
(βPu)	0 to 2.7	*mC*34	*C*2/*m*
(αPu)	0 to 0.57	*mP*16	$P2_1/m$
θ (or Pu_4Zr)	4 to 14	*tP*80	*P*4/*ncc*
κ (or $PuZr_3$)	52	*hP*3	*P*6/*mmm*
(αZr)	71 to 100	*hP*2	$P6_3/mmm$

Rb-Sb

F.W. Dorn and W. Klemm, 1961

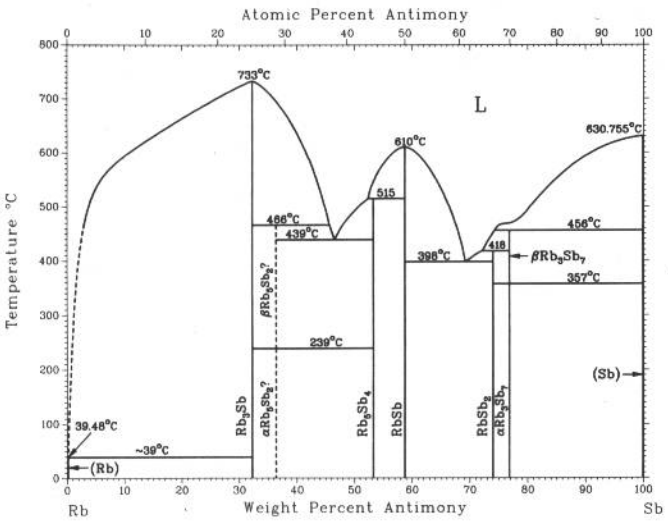

Phase	Composition, wt% Sb	Pearson symbol	Space group
(Rb)	0	*cI*2	$Im\bar{3}m$
Rb_3Sb	30	*hP*8	$P6_3/mm$
βRb_5Sb_2	36.3	...	...
αRb_5Sb_2	36.3	...	...
Rb_5Sb_4	53.2	...	...
RbSb	58.8	*oP*16	$P2_12_12_1$
$RbSb_2$	74.0	...	...
βRb_3Sb_7	77	...	...
αRb_3Sb_7	77	...	...
(Sb)	100	*hR*2	$R\bar{3}m$

Rb-Se

H. Okamoto, 1990

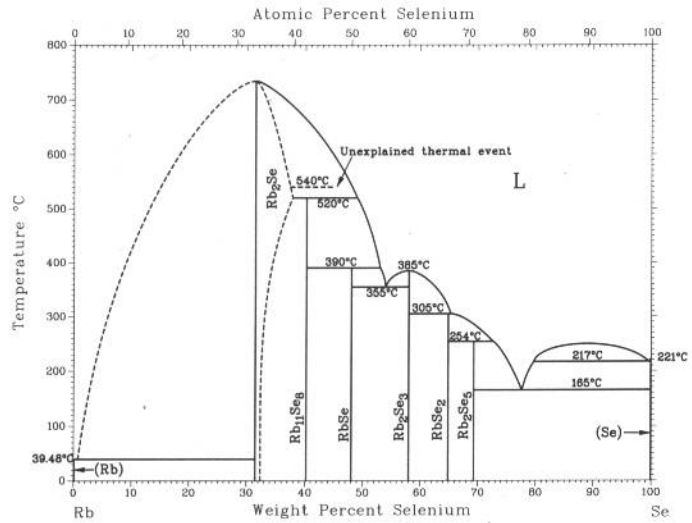

Phase	Composition, wt% Se	Pearson symbol	Space group
(Rb)	0	*cI*2	$Im\bar{3}m$
Rb_2Se	31.6 to ~38	*cF*12	$Fm\bar{3}m$
$Rb_{11}Se_8$	40.2	...	...
RbSe	48.0	...	...
Rb_2Se_3	58	*oC*20	$Cmc2_1$
$RbSe_2$	64.9	...	...
Rb_2Se_5	69.8	*oP*28	$P2_12_12_1$
(Se)	100	*hP*3	$P3_121$

Rb-Tl

R. Thümmel and W. Klemm, 1970

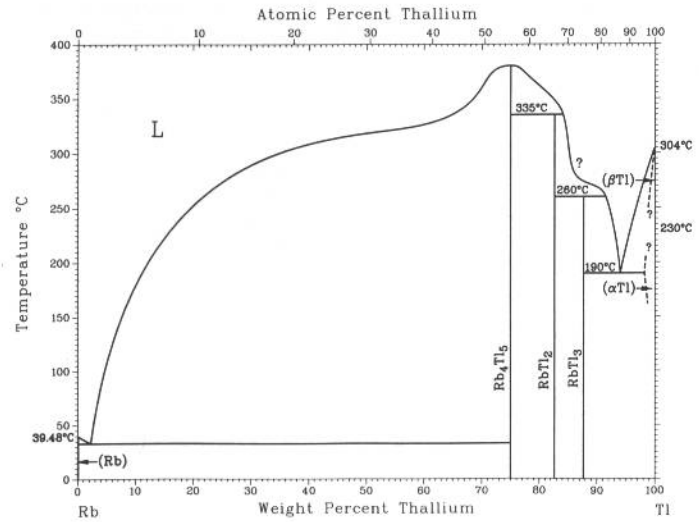

Phase	Composition, wt% Tl	Pearson symbol	Space group
(Rb)	0	*cI*2	$Im\bar{3}m$
Rb_4Tl_5	74.9	...	...
$RbTl_2$	82.7	...	...
$RbTl_3$	88	...	...
(βTl)	? to 100	*cI*2	$Im\bar{3}m$
(αTl)	? to 100	*hP*2	$P6_3/mmc$

Re-Ru

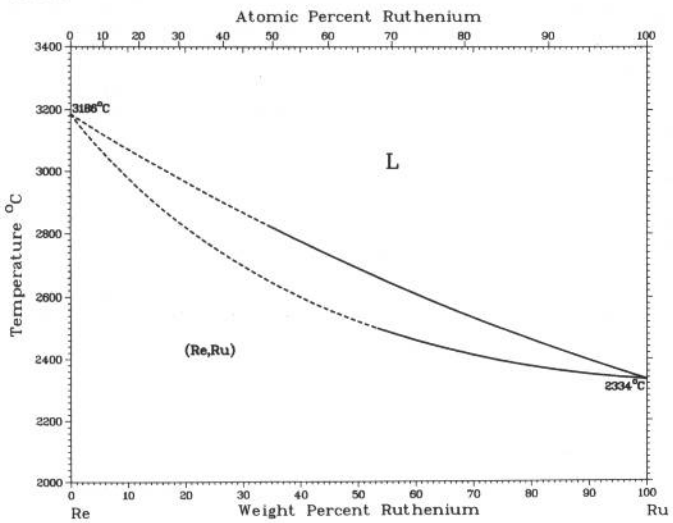

E. Rudy, B. Kietter, and H. Froelich, 1962

Phase	Composition, wt% Ru	Pearson symbol	Space group
(Re,Ru)	0 to 100	*hP*2	$P6_3/mmc$

Re-Si

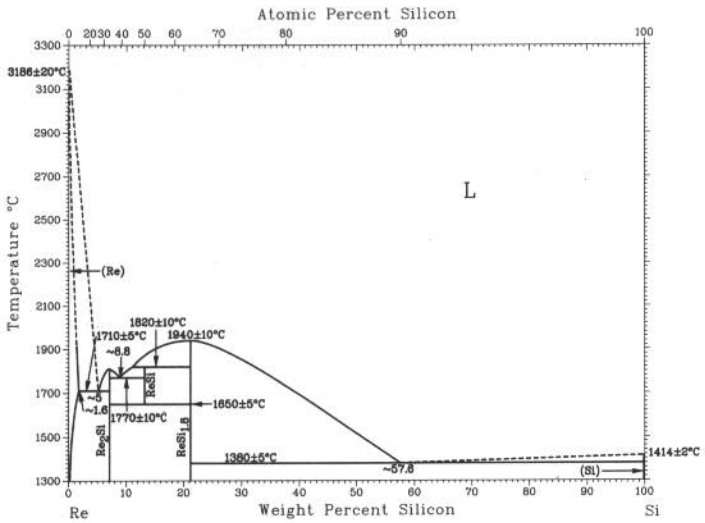

A.B. Gokhale and G.J. Abbaschian, unpublished

Phase	Composition, wt% Si	Pearson symbol	Space group
(Re)	0 to ~1.6	*hP*2	$P6_3/mmc$
Re_2Si	7.0	(a)	$P2_1/b$
ReSi	13.1	*cP*8	$P2_13$
$ReSi_{1.8}$	21.4	*tI*6	$I4/mmm$
(Si)	100	*cF*8	$Fd\bar{3}m$

(a) Monoclinic

Re-Te

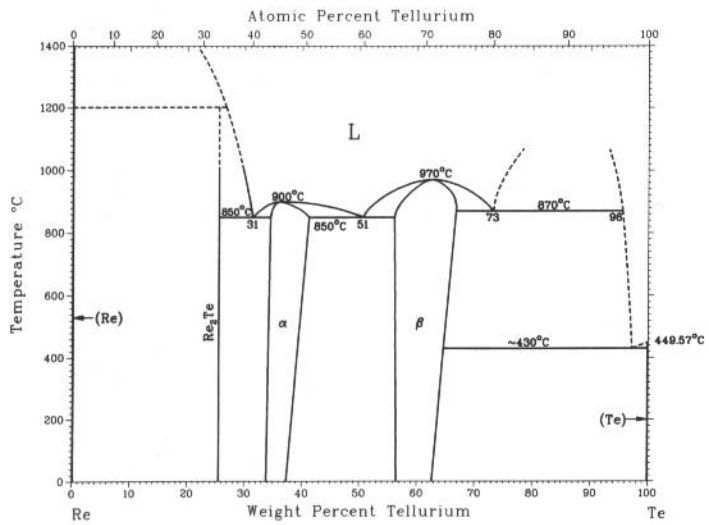

T.Kh. Kurbanov, R.A. Dovlyatshina, I.A. Dzhavodova, and F.A. Akhmenov, 1977

Phase	Composition, wt% Te	Pearson symbol	Space group
(Re)	0	*hP*2	$P6_3/mmc$
Re_2Te	25.5	...	...
α	~33.9 to 42.1	...	...
β	~56.5 to 67	*oP*84	*Pbca*
(Te)	100	*hP*3	$P3_121$

Re-U

H. Okamoto, 1990

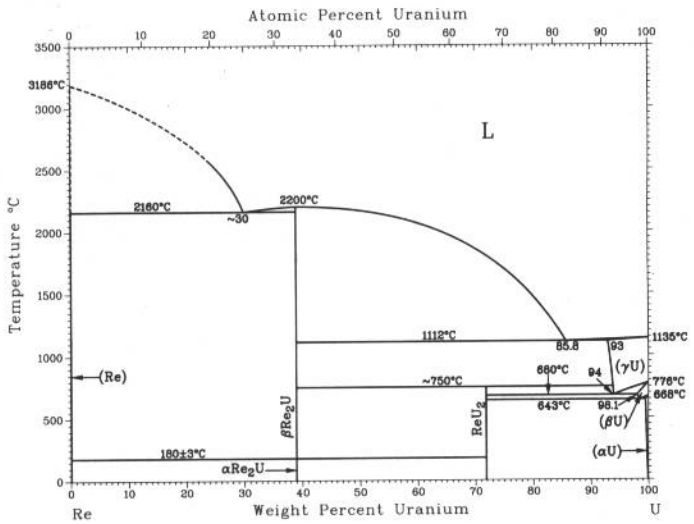

Phase	Composition, wt% U	Pearson symbol	Space group
(Re)	0	*hP*2	$P6_3/mmc$
Re_2U	39.0	*hP*12	$P6_3/mmc$
Re_2U	39.0	*oC*24	*Cmcm*
ReU_2	71.9	...	...
(γU)	93 to 100	*cI*2	$Im\bar{3}m$
(βU)	98.1 to 100	*tP*30	$P4_2/mnm$
(αU)	~100	*oC*4	*Cmcm*

Re-V

J.F. Smith, 1989

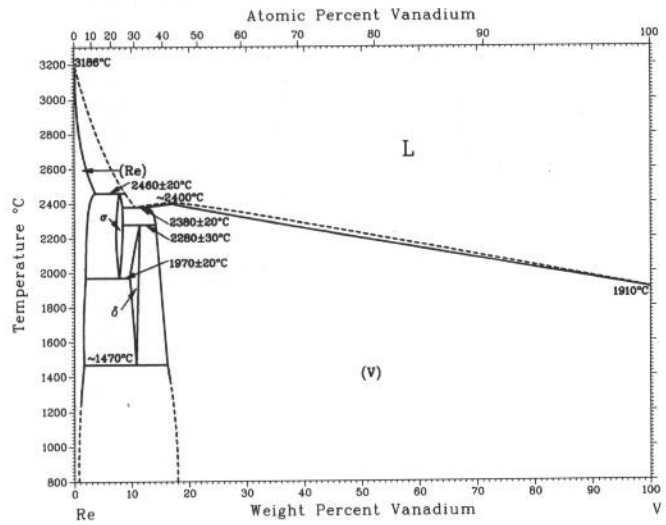

Phase	Composition, wt% V	Pearson symbol	Space group
(Re)	0 to 4	*hP*2	$P6_3/mmc$
σ	~8.0 to 8.3	*tP*30	$P4_2/mnm$
δ	9.6 to 11.4	*cP*8	$Pm\bar{3}n$
(V)	12.8 to 100	*cI*2	$Im\bar{3}m$

Rh-Se

H. Okamoto, 1990

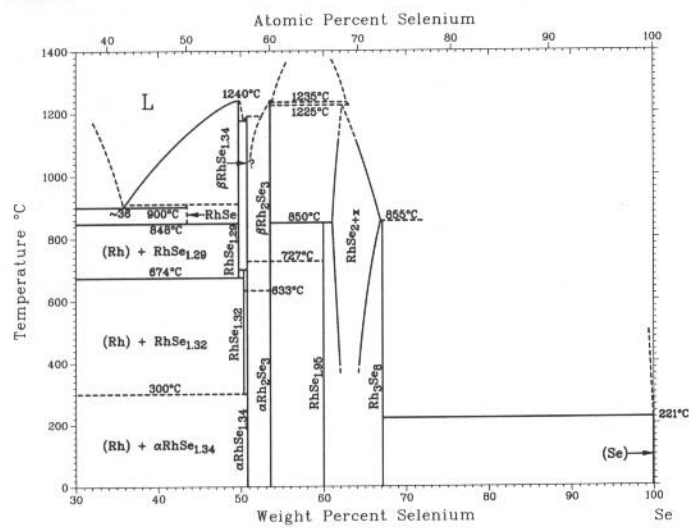

Phase	Composition, wt% Se	Pearson symbol	Space group
(Rh)	0	*cF*4	$Fm\bar{3}m$
RhSe	43.4	*hP*4	$P6_3/mmc$
$RhSe_{1.29}$	49.7	...	...
$RhSe_{1.32}$	50.3	*o***	...
$\beta RhSe_{1.34}$	50.7	...	...
$\alpha RhSe_{1.34}$	50.7	*hP**	...
βRh_2Se_3	54	...	...
αRh_2Se_3	54	*oP*20	*Pbcn*
$RhSe_{1.95}$	59.9	*oP*24	*Pnma*
$RhSe_{2+x}$	61.0 to 66.9	*cP*12	$Pa\bar{3}$
Rh_3Se_8	67.1	*hR*11	$R\bar{3}$
(Se)	100	*hP*3	$P3_121$

Rh-Ta

B.C. Giessen, H. Ibach, and N.J. Grant, 1964

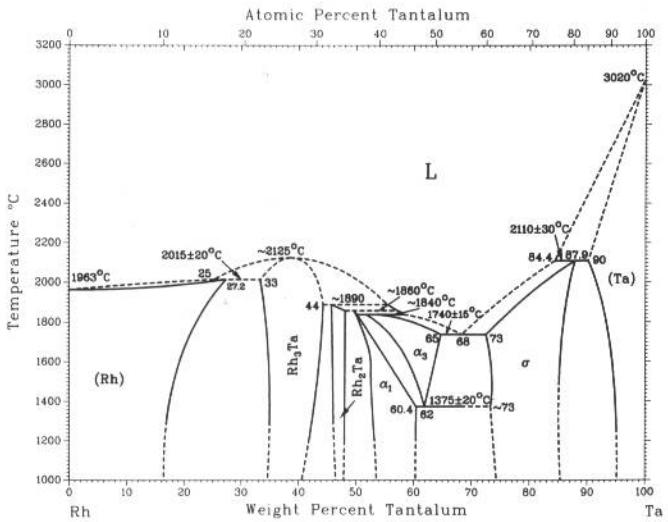

Phase	Composition, wt% Ta	Pearson symbol	Space group
(Rh)	0 to 27.2	*cF*4	$Fm\bar{3}m$
Rh_3Ta	33 to 44	*cP*4	$Pm\bar{3}m$
Rh_2Ta	45 to 48	*oP*12	*Pnma*
α_3	54 to 65	...	...
α_1	51 to 60.4	...	*Pmcm*?
σ	73 to 87.9	*tP*30	$P4_2/mnm$
(Ta)	90 to 100	*cI*2	$Im\bar{3}m$

Rh-Ti

J.L. Murray, 1987

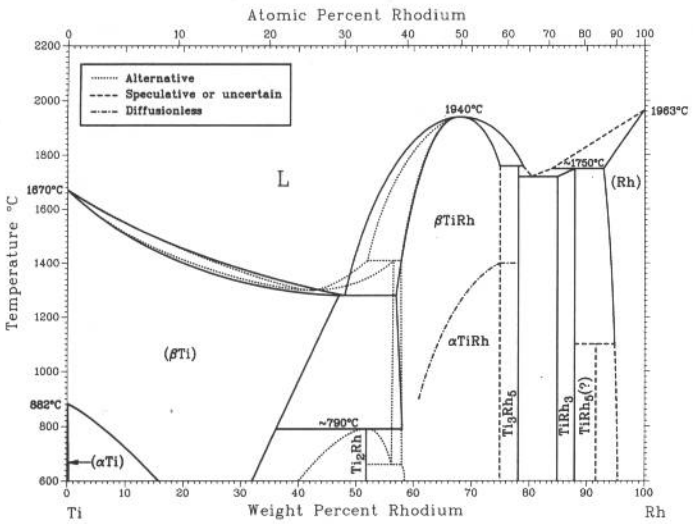

Phase	Composition, wt% Rh	Pearson symbol	Space group
(βTi)	0 to 47	*cI*2	$Im\bar{3}m$
(αTi)	0 to 0.161	*hP*2	$P6_3/mmc$
Ti_2Rh	51.8	*tI*6	*I*4/*mmm*
βTiRh	~57 to 75	*cP*2	$Pm\bar{3}m$
αTiRh	~57 to 75	*tP*2	$Pm\bar{3}m$
Ti_3Rh_5	78.2	*oP*16	*Pbam*
$TiRh_3$	85 to 88	*cP*4	$Pm\bar{3}m$
$TiRh_5$	~91.7	...	...
(Rh)	93 to 100	*cF*4	$Fm\bar{3}m$

Rh-U

From [Ivanov]

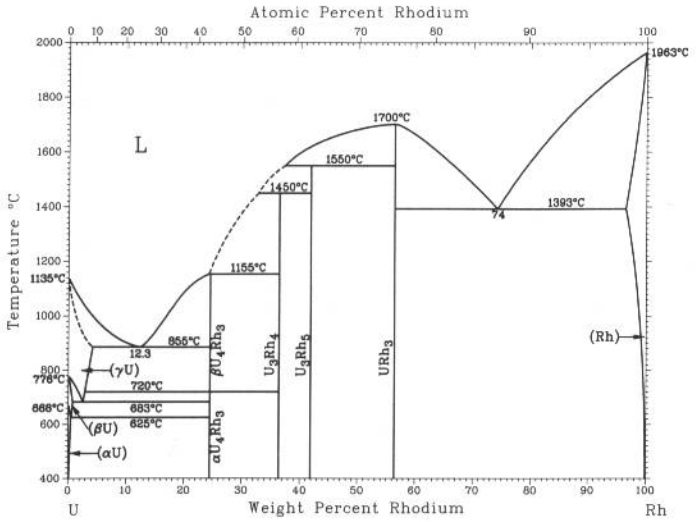

Phase	Composition, wt% Rh	Pearson symbol	Space group
(γU)	0 to 0.41	*oC*4	*Cmcm*
(βU)	0 to 0.87	*tP*30	$P\bar{4}n2$
(αU)	0 to 0.43	*cI*2	$Im\bar{3}m$
βU_4Rh_3	25	...	...
αU_4Rh_3	25	...	...
U_3Rh_4	36	...	...
U_3Rh_5	~42	...	...
URh_3	57	*cP*4	$Pm\bar{3}m$
(Rh)	96 to 100	*cF*4	$Fm\bar{3}m$

Rh-V

J.F. Smith, 1989

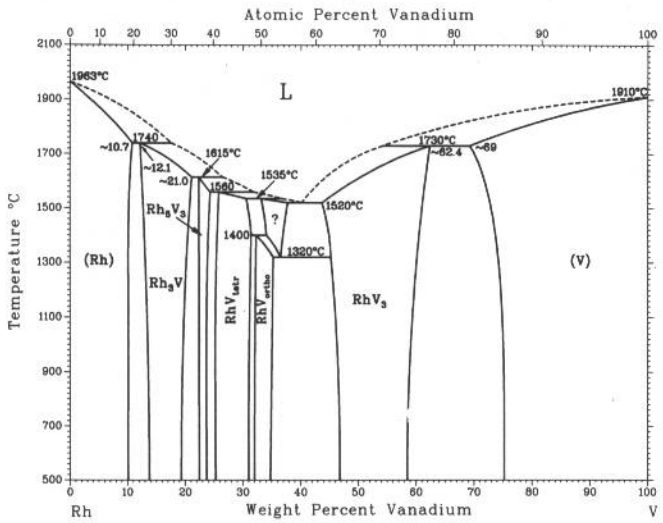

Phase	Composition, wt% V	Pearson symbol	Space group
(Rh)	0 to ~10.7	*cF*4	$Fm\bar{3}m$
Rh_3V	~12.1 to ~21.0	*cP*4	$Pm\bar{3}m$
Rh_5V_3	~23 to 24.3	*oC*16	*Cm2m* or *Cmcm*
RhV_{tetr}	25.2 to 31	*tP*4	*P4/mmm*
RhV_{ortho}	32 to 35.2	*oC*8	*Cmmm*
RhV_3	44 to ~62.4	*cP*8	$Pm\bar{3}n$
(V)	~69 to 100	*cI*2	$Im\bar{3}m$

Ru-Si

H. Okamoto, 1990

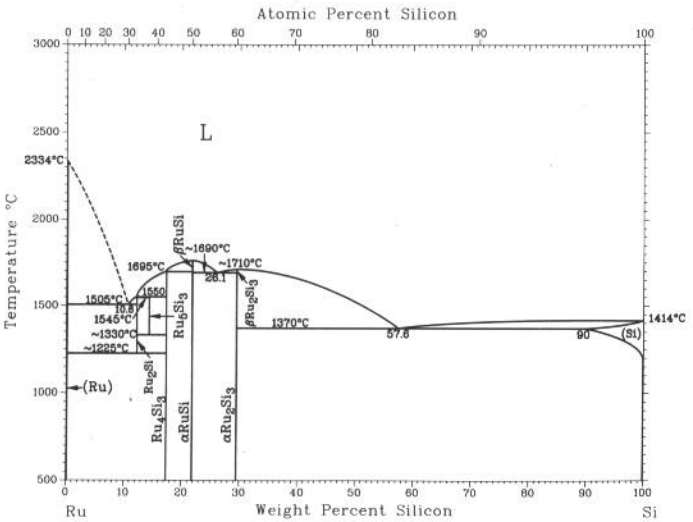

Phase	Composition, wt% Si	Pearson symbol	Space group
(Ru)	0	*hP*2	$P6_3/mmc$
Ru_2Si	12.2	*oP*12	*Pnma*
Ru_5Si_3	14.3	*oP*16	*Pbam*
Ru_4Si_3	17.3	*oP*28	*Pnma*
βRuSi	21.7	*cP*2	$Pm\bar{3}m$
αRuSi	21.7	*cP*8	$P2_13$
βRu_2Si_3	29	*tP*80	$P\bar{4}c2$
αRu_2Si_3	29	*oP*40	*Pbcn*
(Si)	90 to 100	*cF*8	$Fd\bar{3}m$

Ru-Ta

H. Okamoto, 1991

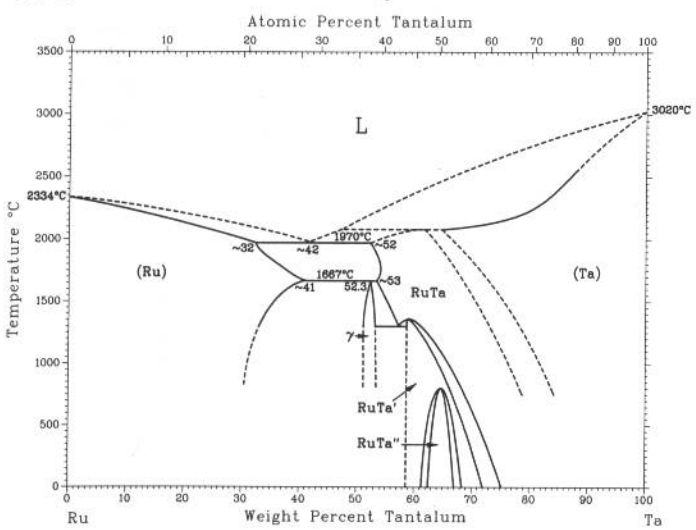

Phase	Composition, wt% Ta	Pearson symbol	Space group
(Ru)	0 to ~41	*hP*2	$P6_3/mmc$
γ	~52.3	*c***	...
RuTa	~52.3 to ?	*cP*2	$Pm\bar{3}m$
RuTa′	~58 to 73	*tP*2	*P4/mmm*
RuTa″	~62 to 67	*oC*4	*Cmmm*
(Ta)	65 to 100	*cI*2	$Im\bar{3}m$

Ru-Ti

J.L. Murray, 1987

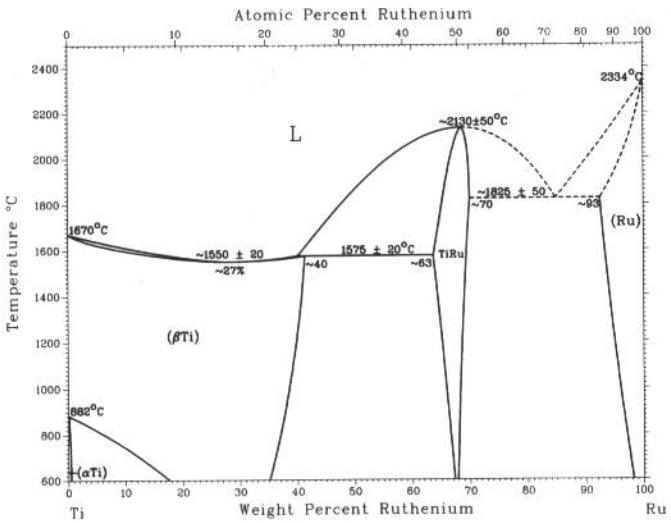

Phase	Composition, wt% Ru	Pearson symbol	Space group
(βTi)	0 to ~40	*cI*2	$Im\bar{3}m$
(αTi)	0 to >0.2	*hP*2	$P6_3/mmc$
TiRu	~63 to ~70	*cP*2	$Pm\bar{3}m$
(Ru)	~93 to 100	*hP*2	$P6_3/mmc$
Metastable phases			
(α″Ti)	...	*hP*2	$P6_3/mmc$
(α‴Ti)	...	*oC*4	*Cmcm*
ω	...	*hP*3	*P6/mmm*

Ru-U

P. Chiotti, V.V. Akhachinskij, I. Ansara, and M.H. Rand, 1982

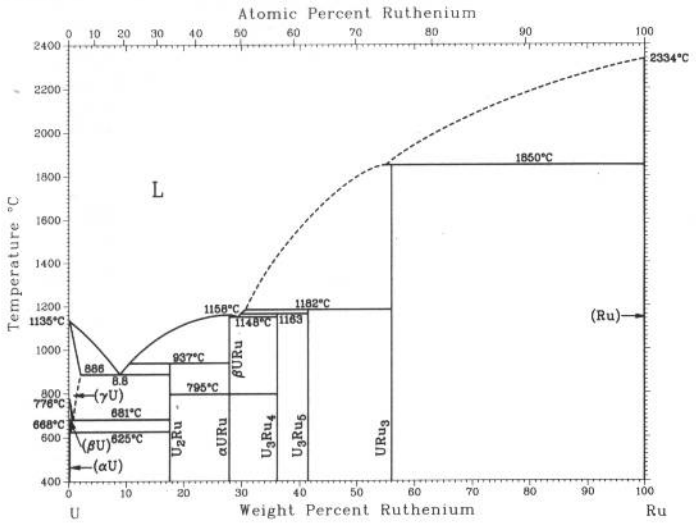

Phase	Composition, wt% Ru	Pearson symbol	Space group
(γU)	0 to 2.0	*cI*2	$Im\bar{3}m$
(βU)	0 to 0.86	*tP*30	$P4_2/mnm$
(αU)	~0	*oC*4	*Cmcm*
U_2Ru	17.5	*mP*12	$P2/m$ or $P2_1/m$
URu	27.5	...	...
U_3Ru_4	36	...	...
U_3Ru_5	41.4	...	...
URu_3	56	*cP*4	$Pm\bar{3}m$
(Ru)	98 to 100	*hP*2	$P6_3/mmc$

Ru-V

J.F. Smith, 1989

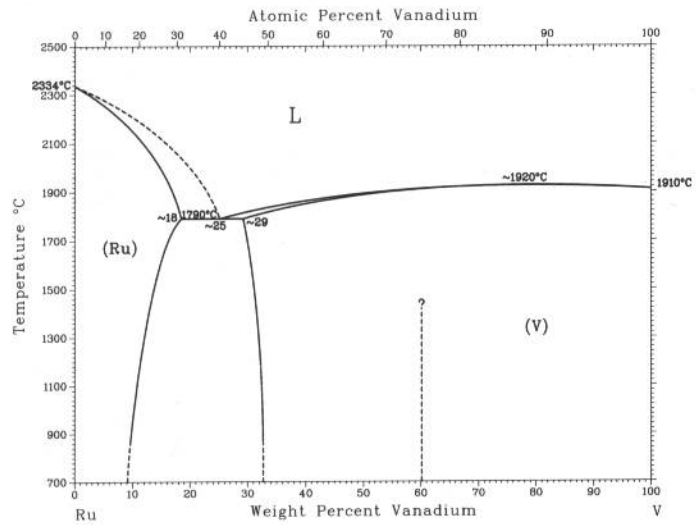

Phase	Composition, wt% V	Pearson symbol	Space group
(Ru)	0 to ~18	*hP*2	$P6_3/mmc$
RuV	33.5	*t***	...
RuV	~29 to 60	*cP*2	$Pm\bar{3}m$
(V)	60 to 100	*cI*2	$Im\bar{3}m$

S-Se

R.C. Sharma and Y.A. Chang, unpublished

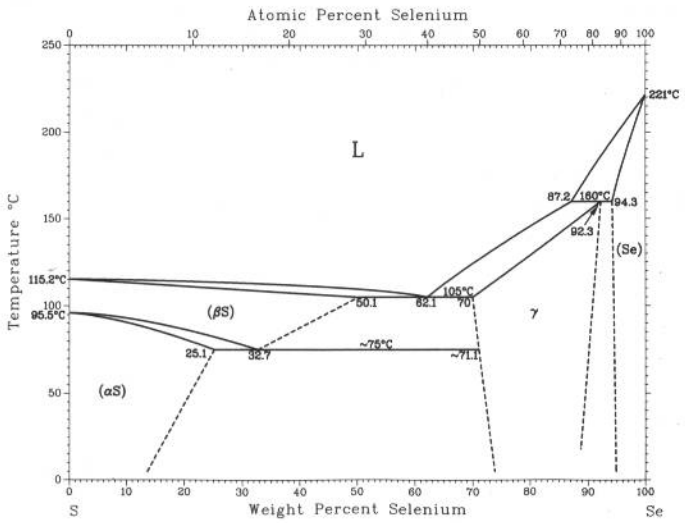

Phase	Composition, wt% Se	Pearson symbol	Space group
(βS)	0 to 50.1	*mP**	$P2_1/c$
(αS)	0 to 25.1	*oF*128	*Fddd*
γ	70 to 92.3	(a)	...
(Se)	94.3 to 100	*hP*3	$P3_121$
High-pressure phase			
$S_{0.555}Se_{0.445}$	66.4	(b)	$P3_1$ or $P3_2$

(a) Monoclinic. (b) Trigonal

S-Sn

R.C. Sharma and Y.A. Chang, 1986

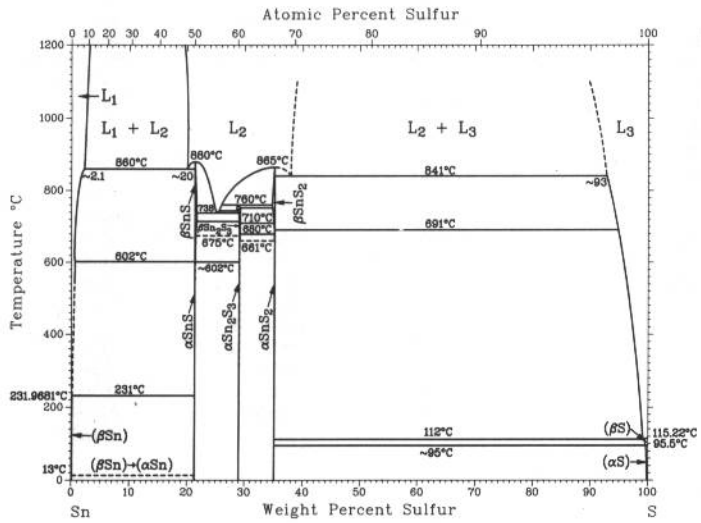

Phase	Composition, wt% S	Pearson symbol	Space group
(βSn)	0	*tI*4	$I4_1/amd$
βSnS	21.3	*cC*8	*Cmcm*
αSnS	21.3	*oP*8	*Pnma*
δSn_2S_3	29	...	...
γSn_2S_3	29	...	...
βSn_2S_3	29	...	...
αSn_2S_3	29	*oP*20	*Pnma*
SnS_2	35.1	*hP**	$P6_3mc$
		*hP*3	$P\bar{3}m1$
Metastable phases			
SnS (thin film)	21.3	*cF*8	$Fm\bar{3}m$
Sn_4S_5	25.3	...	...
Sn_3S_4	26.4	*t***	...

S-Sn phase diagram between 18 and 35 wt%

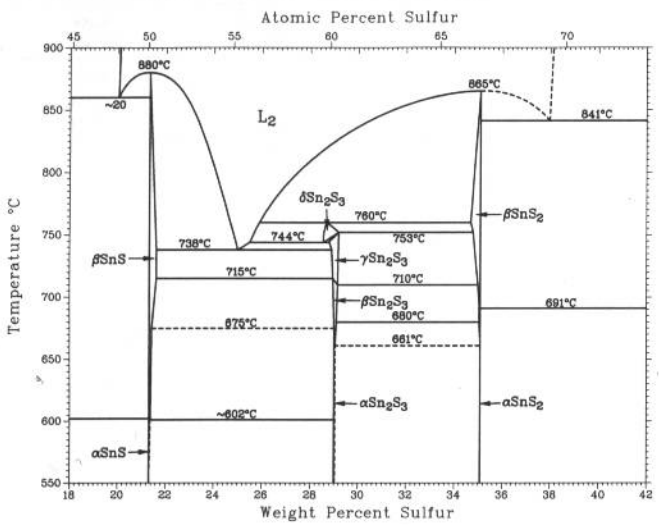

S-Te

D.T. Li, R.C. Sharma, and Y.A. Chang, 1989

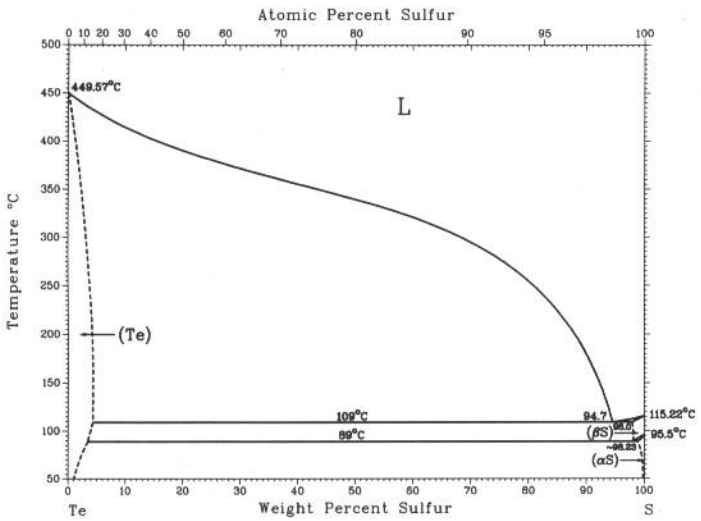

Phase	Composition, wt% S	Pearson symbol	Space group
(Te)	0 to 40.3	*hP*3	$P3_121$
Te_7S_{10}(a)	...	(b)	...
(βS)	98.0 to 100	*mP**	$P2_1/c$
(αS)	~98.23 to 100	*oF*128	*Fddd*

(a) High-pressure phase. (b) Pseudo-orthorhombic

S-Ti

J.L. Murray, 1987

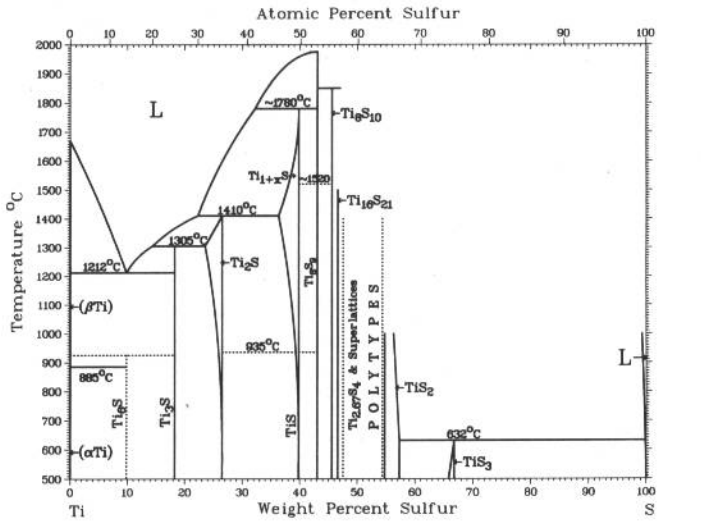

Phase	Composition, wt% S	Pearson symbol	Space group
(βTi)	0 to 0.007	*cI*2	$Im\bar{3}m$
(αTi)	0 to 0.013	*hP*2	$P6_3/mmc$
Ti_6S	~10	(a)	...
Ti_3S	18	*t**24	...
Ti_2S	23 to 27	(b)	...
$Ti_{1+x}S$	36 to 39.8	*hP*2	*P*6*m*2
TiS	~39.8	*hP*4	$P6_3/mmc$
Ti_8S_9	~42.6	*hR*18	$R\bar{3}m$
Ti_8S_{10}	~45.6	*hP*18	$P6_3/mmc$
$Ti_{16}S_{21}$	~45.6	*hR*37.1	$R\bar{3}m$
$Ti_{2.67}S_4$	47.9 to 51.6	*hP*6.8	$P6_3mc$
$(4H)_2$	49.9 to 50.4	*mC*40.14	*Cc*
$(4H)_3$	...	*mC*59.8	*Cc*
Ti_7S_{12}	~53.1	*hR*19.1	$R\bar{3}m$
TiS_2	54.8 to 57.3	*hP*3	$P\bar{3}m$
TiS_3	~67	*mP*8	$P2_1/m$
(S)	100	*oF*128	*Fddd*

(a) Hexagonal. (b) Unknown low symmetry

Sb-Se

H. Okamoto, 1990

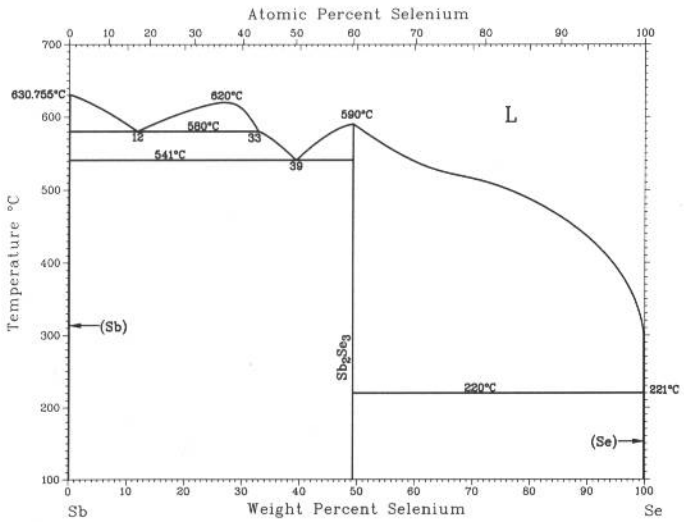

Phase	Composition, wt% Se	Pearson symbol	Space group
(Sb)	0	*hR*2	$R\bar{3}m$
Sb_2Se_3	49	*oP*20	*Pnma*
(Se)	100	*hP*3	$P3_121$

Sb-Si

R.W. Olesinski and G.J. Abbaschian, 1985

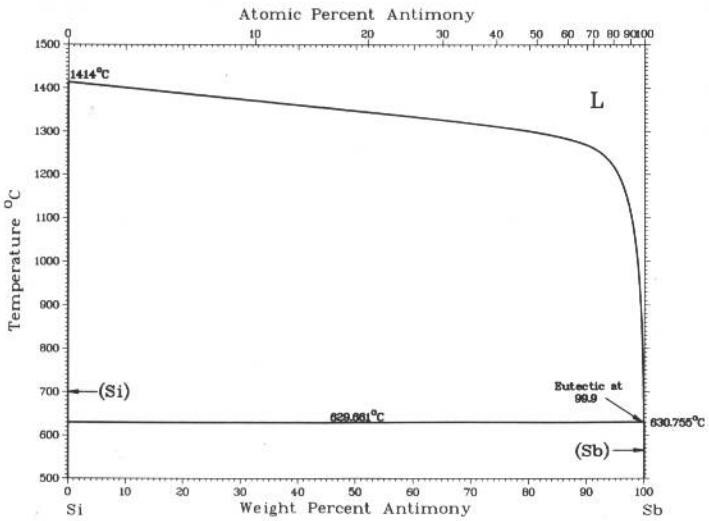

Phase	Composition, wt% Sb	Pearson symbol	Space group
(Si)	0 to 0.09	*cF*8	$Fd\bar{3}m$
(Sb)	100	*hR*2	$R\bar{3}m$

Sb-Sm

H. Okamoto, 1990

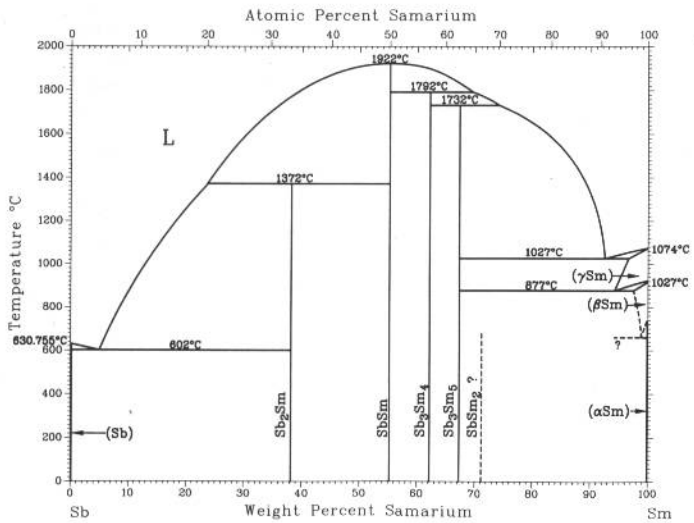

Phase	Composition, wt% Sm	Pearson symbol	Space group
(Sb)	0	*hR*2	$R\bar{3}m$
Sb_2Sm	38.1	*oC*24	*Cmca*
SbSm	55.3	*cF*8	$Fm\bar{3}m$
Sb_3Sm_4	62.2	*cI*28	$I\bar{4}3d$
Sb_3Sm_5	67.3	*hP*16	$P6_3/mcm$
$SbSm_2$	71.2	*tI*12	$I4/mmm$
(γSm)	100	*cI*2	$Im\bar{3}m$
(βSm)	100	*hP*2	$P6_3/mmc$
(αSm)	100	*hR*3	$R\bar{3}m$

Sb-Sn

B. Predel and W. Schwermann, 1971

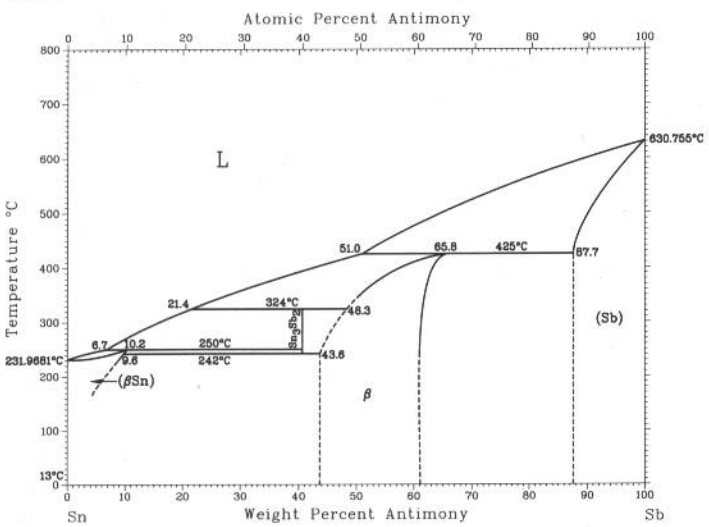

Phase	Composition, wt% Sb	Pearson symbol	Space group
(βSn)	0 to 9.6	*tI*4	$I4_1/amd$
Sn_3Sb_2	43.6	...	...
β	43.6 to 65.8	*cF*8	$Fm\bar{3}m$
(Sb)	87.7 to 100	*hR*2	$R\bar{3}m$

Sb-Sr

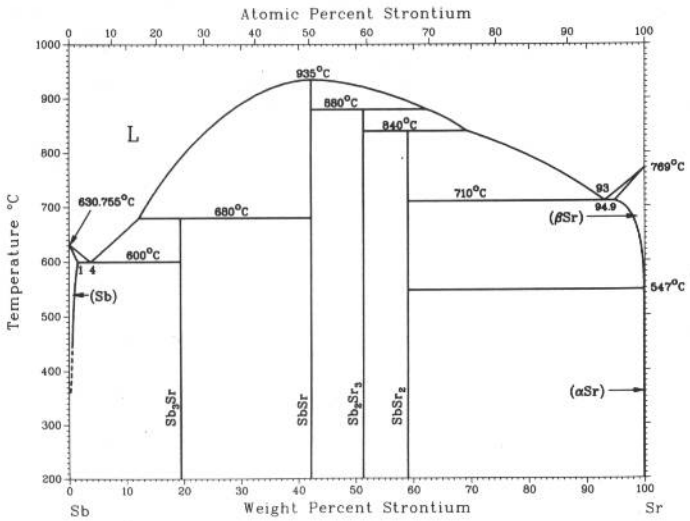

A.V. Vakhobov, Z.V. Niyazova, and B.N. Polev, 1975

Phase	Composition, wt% Sr	Pearson symbol	Space group
(Sb)	0 to 1	*hR*2	$R\bar{3}m$
Sb_3Sr	19	...	...
SbSr	41.8	...	...
Sb_2Sr_3	52	...	...
$SbSr_2$	59	*tI*12	*I*4/*mmm*
(βSr)	94.9 to 100	*cI*2	$Im\bar{3}m$
(αSr)	100	*cF*4	$Fm\bar{3}m$

Sb-Tb

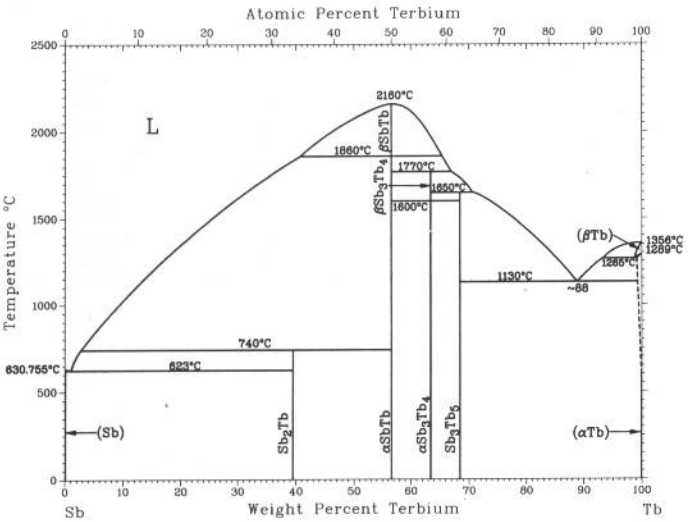

H. Okamoto, 1990

Phase	Composition, wt% Tb	Pearson symbol	Space group
(Sb)	0	*hR*2	$R\bar{3}m$
Sb_2Tb	39.5	*oC*24	*Cmca*
βSbTb	56.6	...	...
αSbTb	56.6	*cF*8	$Fm\bar{3}m$
βSb_3Tb_4	63.5	*cI*28	$I\bar{4}3d$
αSb_3Tb_4	63.5	...	...
Sb_3Tb_5	68.5	*hP*16	$P6_3/mcm$
(βTb)	100	*cI*2	$Im\bar{3}m$
(αTb)	100	*hP*2	$P6_3/mmc$

Sb-Te

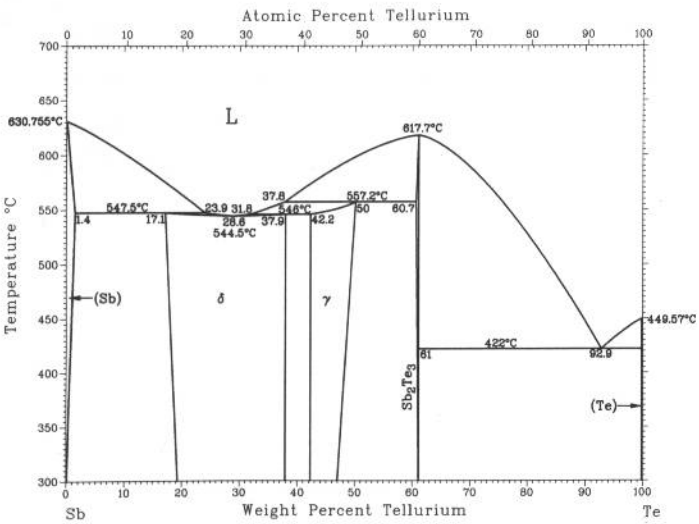

H. Okamoto, 1990

Phase	Composition, wt% Te	Pearson symbol	Space group
(Sb)	0 to 1.4	*hR*2	$R\bar{3}m$
δ	17.1 to 37.9	...	...
γ	42.2 to 50	...	...
Sb_2Te_3	60.7 to 61	*hR*5	$R\bar{3}m$
(Te)	100	*hP*3	$P3_121$

Sb-Tl

R.C. Sharma and Y.A. Chang, unpublished

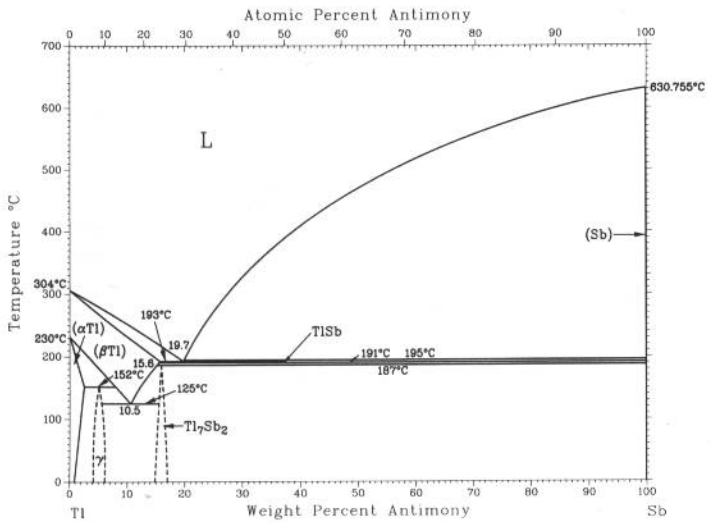

Phase	Composition, wt% Sb	Pearson symbol	Space group
(βTl)	0 to 15.6	*cI*2	$Im\bar{3}m$
(αTl)	0 to 2	*hP*2	$P6_3/mmc$
γ	4.0 to 6.0	*cF**	...
Tl_7Sb_2	14.7 to 16.9	*cI*54	$Im\bar{3}m$
TlSb	37.3	...	...
(Sb)	100	*hR*2	$R\bar{3}m$

Sb-U

P. Chiotti, 1980

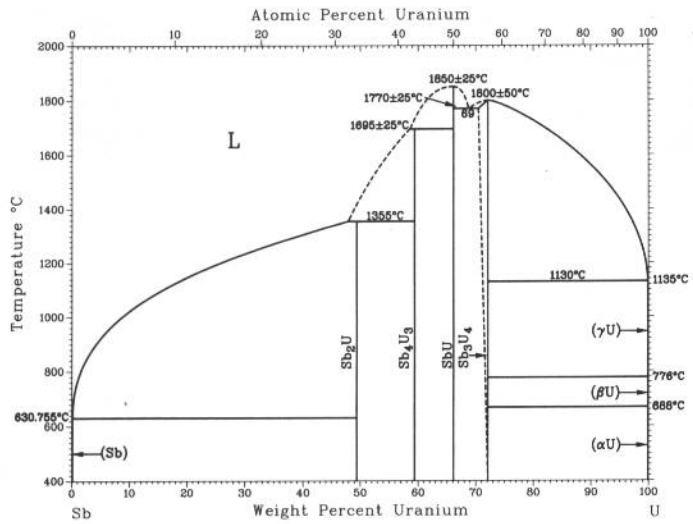

Phase	Composition, wt% U	Pearson symbol	Space group
(Sb)	0	*hR*2	$R\bar{3}m$
Sb_2U	49.4	*tP*6	*P4/nmm*
Sb_4U_3(a)	59.5	*cI*28	$I\bar{4}3d$
SbU	66.2	*cF*8	$Fm\bar{3}m$
Sb_3U_4	72.2	...	$P6_3/mcm$
(γU)	100	*cI*2	$Im\bar{3}m$
(βU)	100	*tP*30	$P4_2/mnm$
(αU)	100	*oC*4	*Cmcm*

(a) Evidence for ferromagnetic ordering of Sb_4U_3 has been presented.

Sb-Y

F.A. Schmidt and O.D. McMasters, 1970

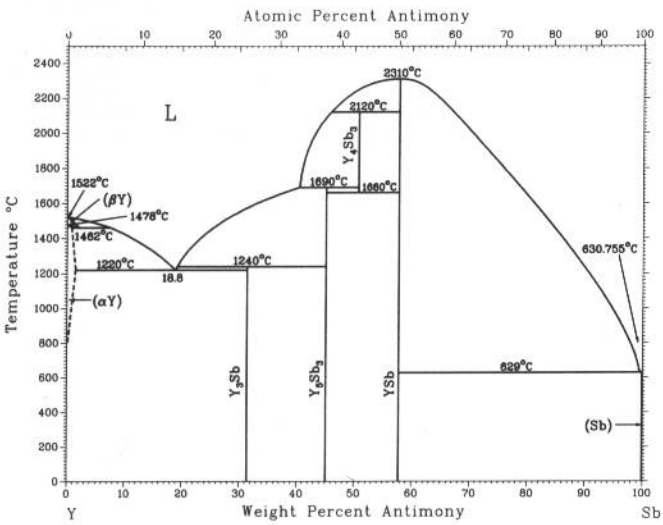

Phase	Composition, wt% Sb	Pearson symbol	Space group
(βY)	0 to 2.7	*cI*2	$Im\bar{3}m$
(αY)	0 to 1.4	*hP*2	$P6_3/mmc$
Y_3Sb	31	*tP*32	$P4_2/n$
Y_5Sb_3	45.1	*hP*16	$P6_3/mcm$
Y_4Sb_3	50.7	*cI*28	$I\bar{4}3d$
YSb	57.8	*cF*8	$Fm\bar{3}m$
(Sb)	100	*hR*2	$R\bar{3}m$

Sb-Zn

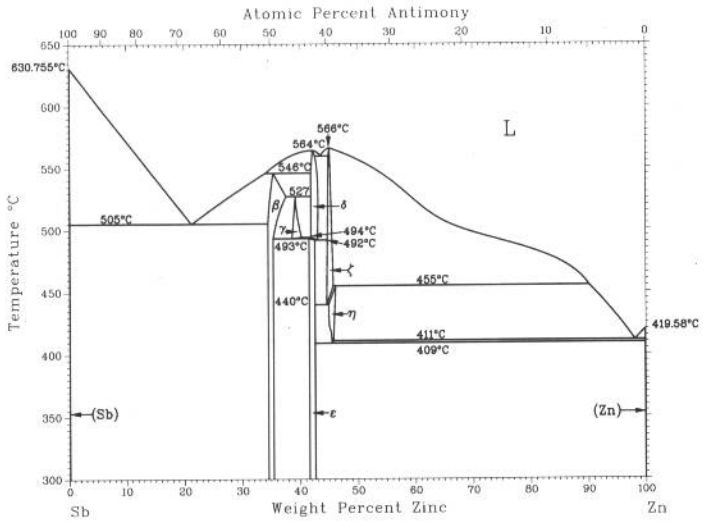

G. Vuillard and J.P. Piton, 1966; and T. Takei, 1927

Phase	Composition, wt% Zn	Pearson symbol	Space group
(Sb)	0	*hR*2	$R\bar{3}m$
β	~34.9 to ~38	*oP*16	*Pbca*
γ	39 to 41	...	...
ε	42 to 43	(a)	...
δ	42 to ~43.1	(a)	...
ζ	45 to 46	*oI**	...
η	45 to ~46	*oP*30	*Pmnn*
(Zn)	100	*hP*2	$P6_3/mmc$

(a) Sb_3Zn_4 (δ,ε?): *hR*22 or *oP*28 or *mC**?

Sc-Ti

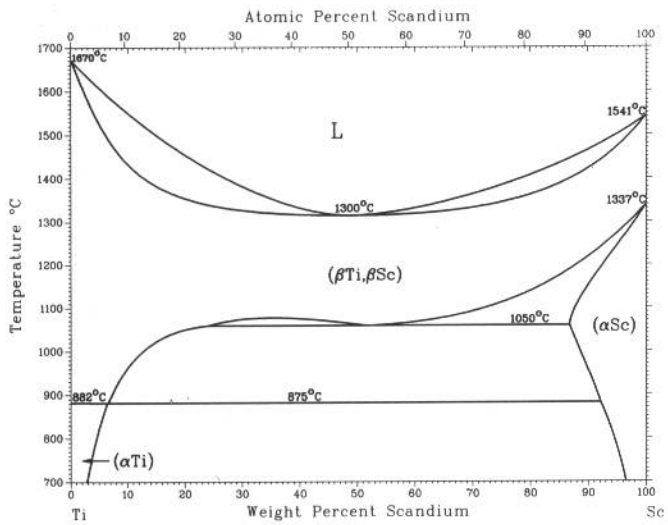

J.L. Murray, 1987

Phase	Composition, wt% Sc	Pearson symbol	Space group
(βTi,βSc)	0 to 100	*cI*2	$Im\bar{3}m$
(αTi)	0 to 7.4	*hP*2	$P6_3/mmc$
(αSc)	88.2 to 100	*hP*2	$P6_3/mmc$

Sc-Y

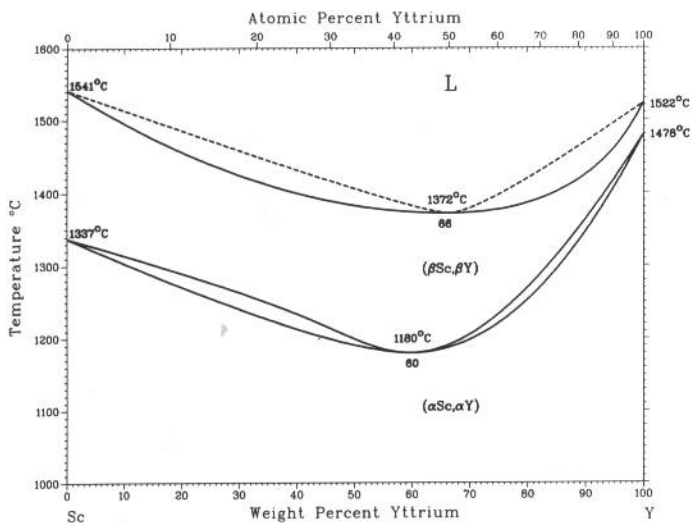

K.A. Gschneidner, Jr. and F.W. Calderwood, 1983

Phase	Composition, wt% Y	Pearson symbol	Space group
(βSc,βY)	0 to 100	*cI*2	$Im\bar{3}m$
(αSc,αY)	0 to 100	*hP*2	$P6_3/mmc$

Sc-Zr

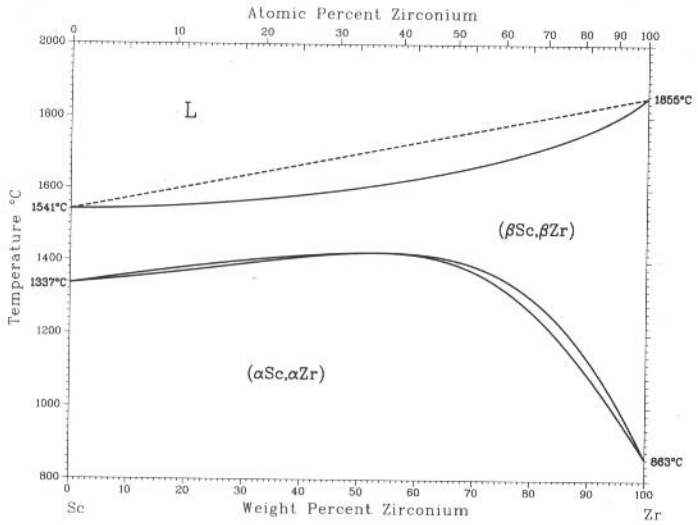

A. Palenzona and S. Cirafici, 1991

Phase	Composition, wt% Zr	Pearson symbol	Space group
(βSc,βZr)	0 to 100	*cI*2	$Im\bar{3}m$
(αSc,αZr)	0 to 100	*hP*2	$P6_3/mmc$

Se-Sn

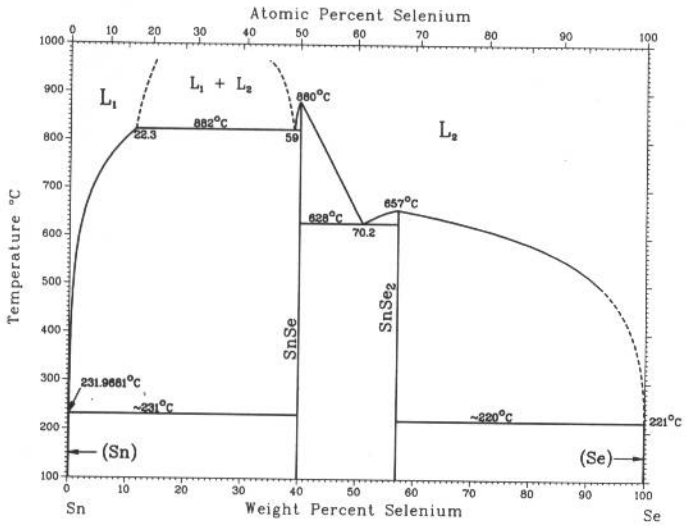

R.C. Sharma and Y.A. Chang, 1986

Phase	Composition, wt% Se	Pearson symbol	Space group
(Sn)	0	*tI*4	$I4_1/amd$
SnSe	39.9	*oP*8	*Pnma*
$SnSe_2$	57.1	*hP*3	$P\bar{3}m1$
(Se)	100	*hP*3	$P3_121$

Se-Sr

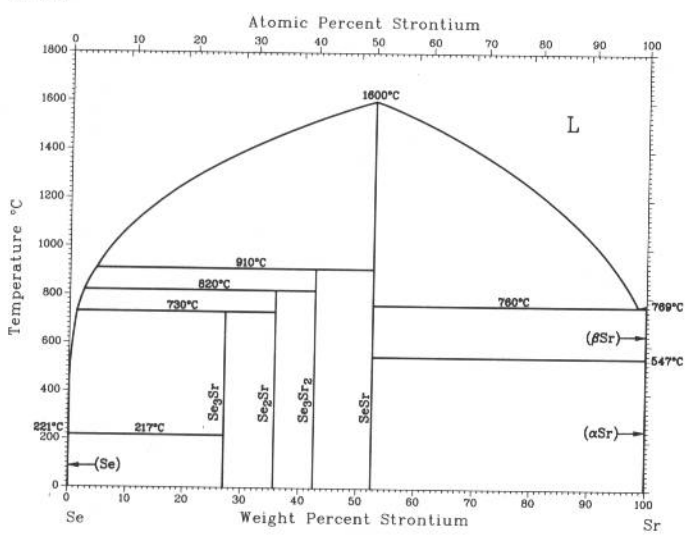

Yu.B. Lyskova and A.V. Vakhobov, 1975

Phase	Composition, wt% Sr	Pearson symbol	Space group
(Se)	0	*hP*3	$P3_121$
Se_3Sr	27	...	...
Se_2Sr	35.7	...	...
Se_3Sr_2	43	...	...
SeSr	52.6	*cF*8	$Fm\bar{3}m$
(βSr)	100	*cI*2	$Im\bar{3}m$
(αSr)	100	*cF*4	$Fm\bar{3}m$

Se-Te

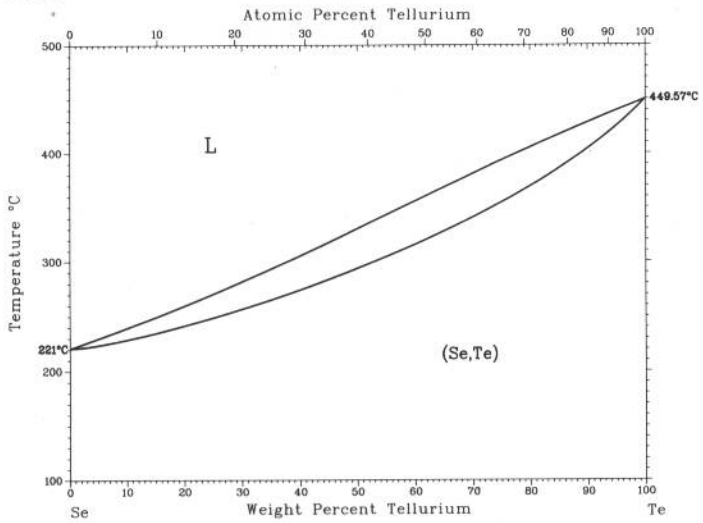

R.C. Sharma, D.T. Li, and Y.A. Chang, unpublished

Phase	Composition, wt% Te	Pearson symbol	Space group
(Se,Te)	0 to 100	*hP*3	$P3_121$

Se-Tl

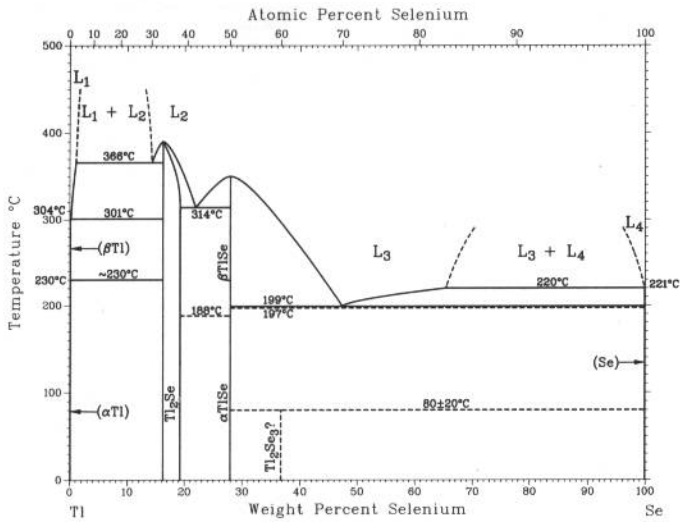

G. Morgant, B. Legendre, S. Mareglier-Lacordaire, and C. Souleau, 1981

Phase	Composition, wt% Se	Pearson symbol	Space group
(βTl)	0	*cI*2	$Im\bar{3}m$
(αTl)	0	*hP*2	$P6_3/mmc$
Tl_2Se	16.5 to 19	*tP*32	$P4/ncc$
βTlSe	27.9	*tI*16	$I4/mcm$
αTlSe	27.9	...	...
Tl_2Se_3?	37	*hP*4	$P6_3mc$
(Se)	100	*hP*3	$P3_121$

Se-Tm

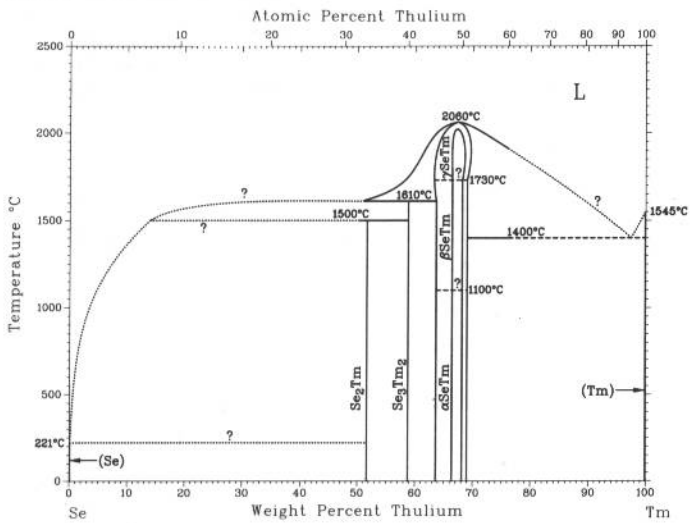

H. Okamoto, 1990

Phase	Composition, wt% Tm	Pearson symbol	Space group
(γSe)	0	*hP*3	$P3_121$
Se_2Tm	51.6	*tP*6	$P4/nmm$
Se_3Tm_2	59	*oF*80	$Fddd$
γSeTm	64 to 69	*cF*8	$Fm\bar{3}m$
βSeTm	65 to 69	...	...
αSeTm	65 to 69	...	...
(Tm)	100	*hP*2	$P6_3/mmc$

Note: "SeTm" is Se_6Tm_5 on the Se-rich side and $SeTm_{1.05}$ on the Tm-rich side.

Se-U

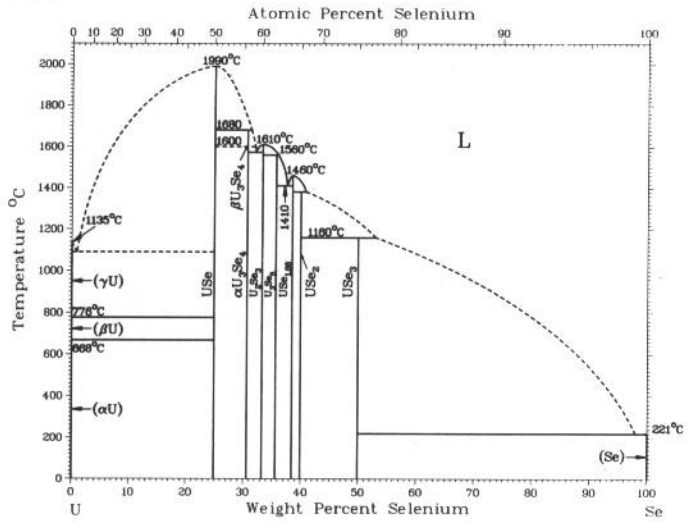

G.V. Ellert, V.G. Sevast'yanov, and V.K. Slovyanskikh, 1975

Phase	Composition, wt% Se	Pearson symbol	Space group
(γU)	0	*cI*2	$Im\bar{3}m$
(βU)	0	*tP*30	$P4_2/mnm$
(αU)	0	*oC*4	*Cmcm*
USe	24.9	*cF*8	$Fm\bar{3}m$
βU_3Se_4	31	...	...
αU_3Se_4	31	*cI*28	$I\bar{4}3d$
U_2Se_3	33	*oP*20	*Pnma*
U_3Se_5	35.6	*oP*32	*Pnma*
$USe_{1.88}$	38.4	*hP*20	$P6_3/m$
USe_2	39.9	*oP*12	*Pnma*
USe_3	49.9	*mP*8	$P2_1/m$
(Se)	100	*hP*3	$P3_121$

Si-Sn

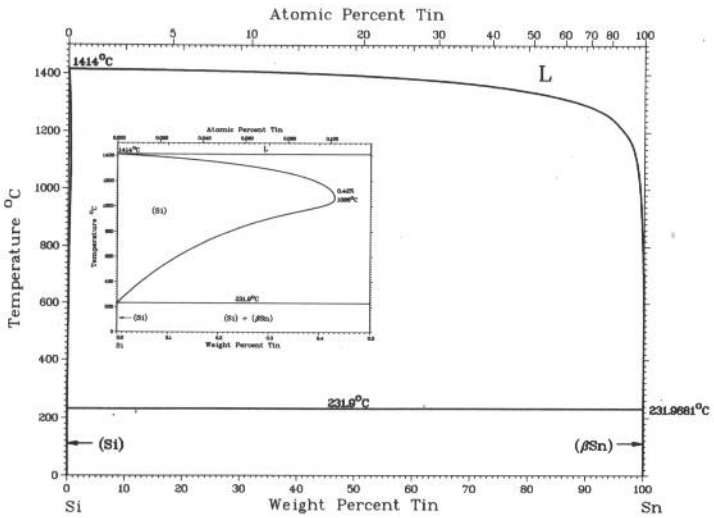

R.W. Olesinski and G.J. Abbaschian, 1984

Phase	Composition, wt% Sn	Pearson symbol	Space group
(Si)	0 to 0.42	*cF*8	$Fd\bar{3}m$
(βSn)	100	*tI*4	$I4_1/amd$
(αSn)	100	*cF*8	$Fd\bar{3}m$

Si-Sr

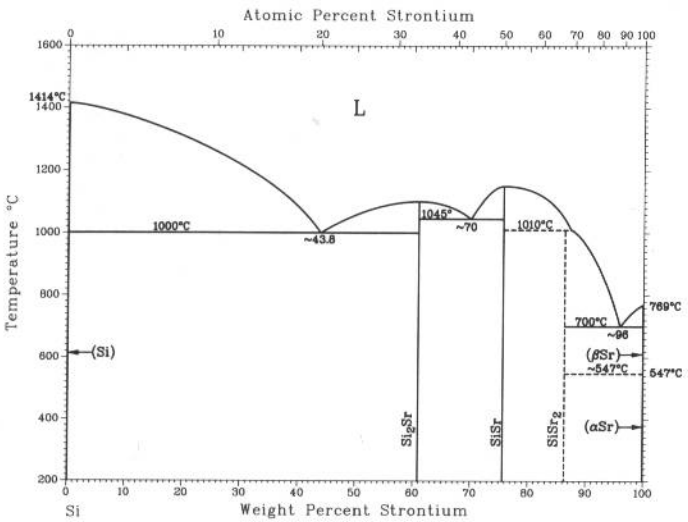

V.P. Itkin and C.B. Alcock, 1989

Phase	Composition, wt% Sr	Pearson symbol	Space group
(Si)	0	*cF*8	$Fd\bar{3}m$
Si_2Sr	60.9	*cP*12	$P4_332$
SiSr	75.7	*oC*8	*Cmcm*
$SiSr_2$	86.2	*oP*12	*Pnma*
(βSr)	100	*cI*2	$Im\bar{3}m$
(αSr)	100	*cF*4	$Fm\bar{3}m$
Other possible phases			
Si_7Sr_4	64.0 to 68(a)	*tI*12	$I4_1/amd$
αSiSr	75.7	*oI*40	*Immm*
Si_3Sr_5	83.9	*tI*32	*I*4*cm*
High-pressure, metastable phase			
Si_2Sr(II)	60.9	*tI*12	$I4_1/amd$

(a) Possible speculative homogeneity range

Si-Ta

M.E. Schlesinger, unpublished

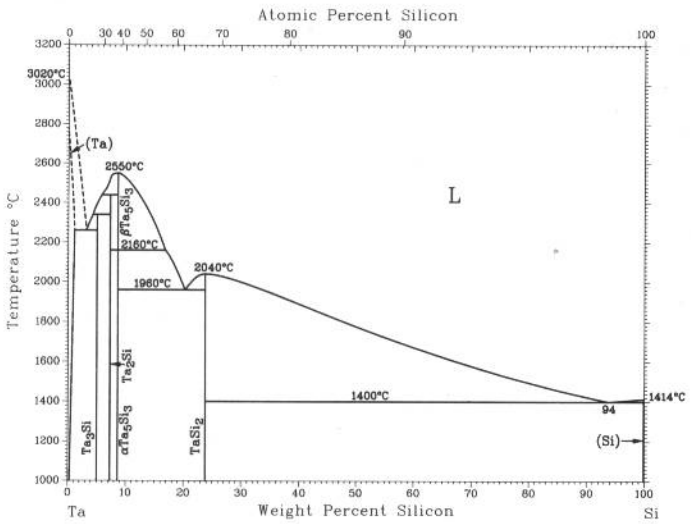

Phase	Composition, wt % Si	Pearson symbol	Space group
(Ta)	0 to ~1	*cI*2	$Im\bar{3}m$
Ta_3Si	5	*tP*32	$P4_2/n$
Ta_2Si	7.2	*tI*12	$I4/m$
βTa_5Si_3	8.5	*tI*32	$I4/mcm$
αTa_5Si_3	8.5	*tI*32	$I4/mcm$
$TaSi_2$	23.7	*hP*9	$P6_222$
Si	100	*cF*8	$Fd\bar{3}m$
Metastable phases			
$Ta_{4.5}Si$	3.5	*hP*8	$P6_3/mmc$
Ta_5Si_3	8.5	*hP*16	$P6_3/mcm$

Si-Te

T.G. Davey and E.H. Baker, 1980

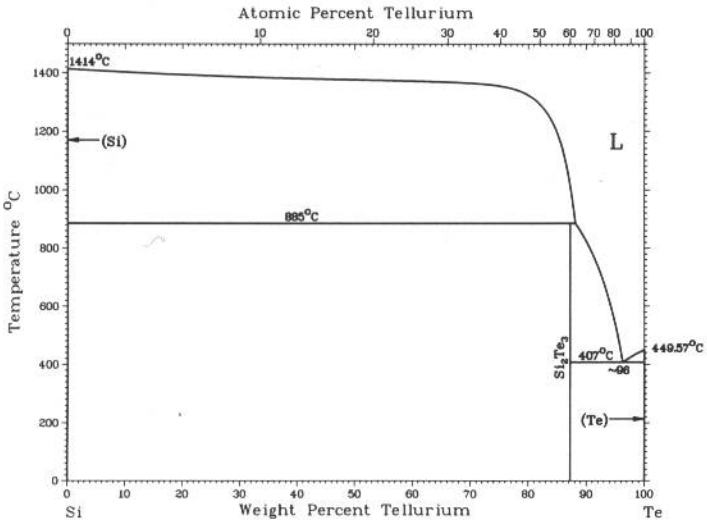

Phase	Composition, wt % Te	Pearson symbol	Space group
(Si)	0	*cF*8	$Fd\bar{3}m$
Si_2Te_3	87	*hP*40	$P\bar{3}1c$
(Te)	100	*hP*3	$P3_121$

Si-Th

From [Thorium]

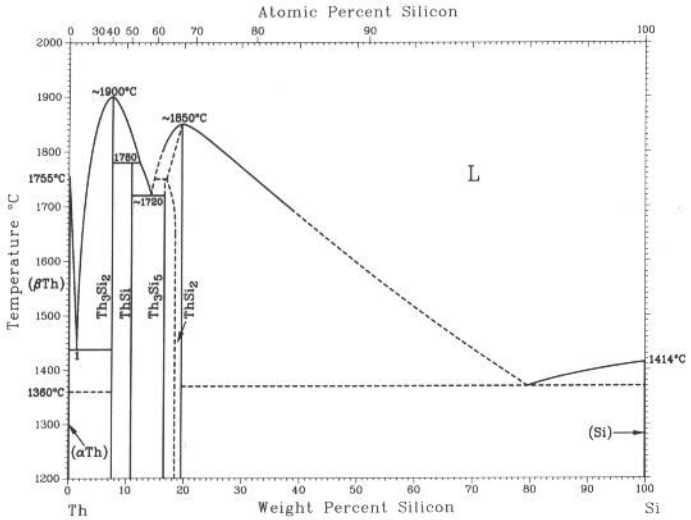

Phase	Composition, wt % Si	Pearson symbol	Space group
(βTh)	0	*cI*2	$Im\bar{3}m$
(αTh)	0	*cF*4	$Fm\bar{3}m$
Th_3Si_2	8	*tP*10	$P4/mbm$
ThSi	10.8	*oP*8	$Pnma$
Th_3Si_5	16.8	*hP*3	$P6/mmm$
$ThSi_2$	~18 to 19.5	*tI*12	$I4_1/amd$
(Si)	100	*cF*8	$Fd\bar{3}m$

Si-Ti

J.L. Murray, 1987

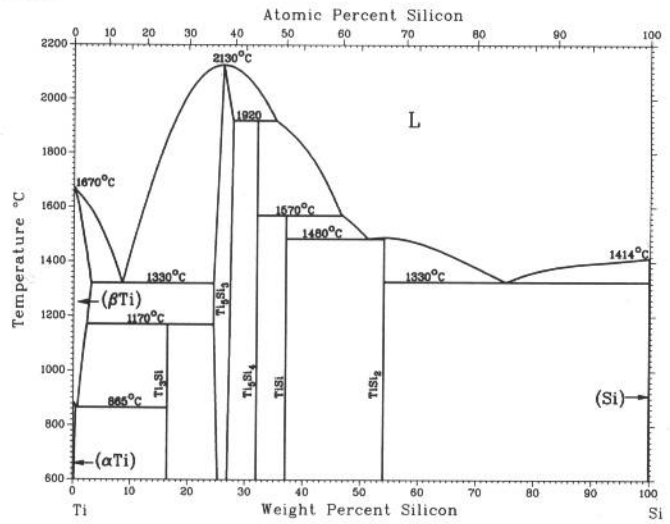

Phase	Composition, wt% Si	Pearson symbol	Space group
(βTi)	0 to 2.1	*cI*2	$Im\bar{3}m$
(αTi)	0 to 0.3	*hP*2	$P6_3/mmc$
Ti_3Si	16	*tP*32	$P4_2/n$
Ti_5Si_3	24.4 to 27.7	*hP*16	$P6_3/mcm$
Ti_5Si_4	31.9	*tP*36	$P4_12_12$
Ti_6Si_5(a)	32.9	(b)	...
TiSi	37.0	*oP*8	*Pmm*2
		*oP*8	*Pnma*
$TiSi_2$	54.0	*oF*24	*Fddd*
(Si)	100	*cF*8	$Fd\bar{3}m$

(a) Not shown in diagram. (b) Tetragonal,related to σ ($D8_8$)

Si-U

H. Okamoto, 1990

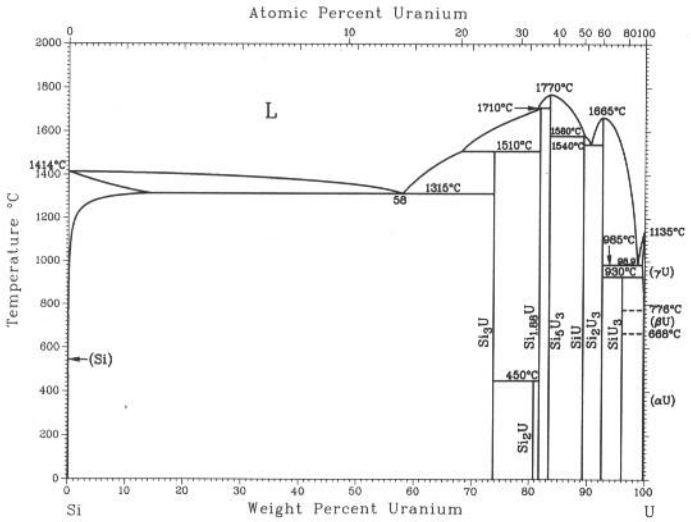

Phase	Composition, wt% U	Pearson symbol	Space group
(Si)	0	*cF*8	$Fd\bar{3}m$
Si_3U	74	*cP*4	$Pm\bar{3}m$
Si_2U	80.9	*hP*3	*P*6/*mmm*
$Si_{1.88}U$	81.8	*tI*12	$I4_1/amd$
Si_5U_3	83.6	*hP*3	*P*6/*mmm*
SiU	89.4	*oP*8	*Pnma*
Si_2U_3	93	*tP*19	*P*4/*mbm*
SiU_3	96	*cP*4	$Pm\bar{3}m$
(γU)	100	*cI*2	$Im\bar{3}m$
(βU)	100	*tP*30	$P4_2/mnm$
(αU)	100	*oC*4	*Cmcm*

Si-V

J.F. Smith, 1989

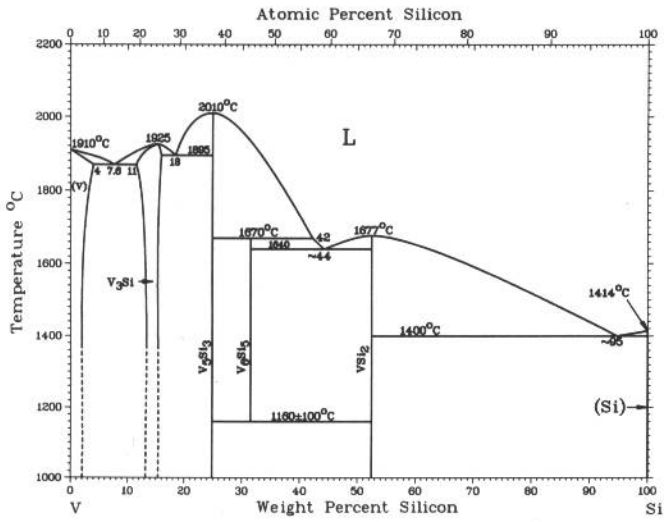

Phase	Composition, wt% Si	Pearson symbol	Space group
(V)	0 to 4	*cI*2	$Im\bar{3}m$
V_3Si	11 to ~15.9	*cP*8	$Pm\bar{3}n$
V_5Si_3	24.9	*tI*32	*I*4/*mcm*
V_5Si_3	(a)	*hP*16	$P6_3/mcm$
V_6Si_5	~31	*oI*44	*Immm*
VSi_2	52.5	*hP*9	$P6_222$
(Si)	100	*cF*8	$Fm\bar{3}m$

(a) Carbon-stabilized

Si-Zn

R.W. Olesinski and G.J. Abbaschian, 1985

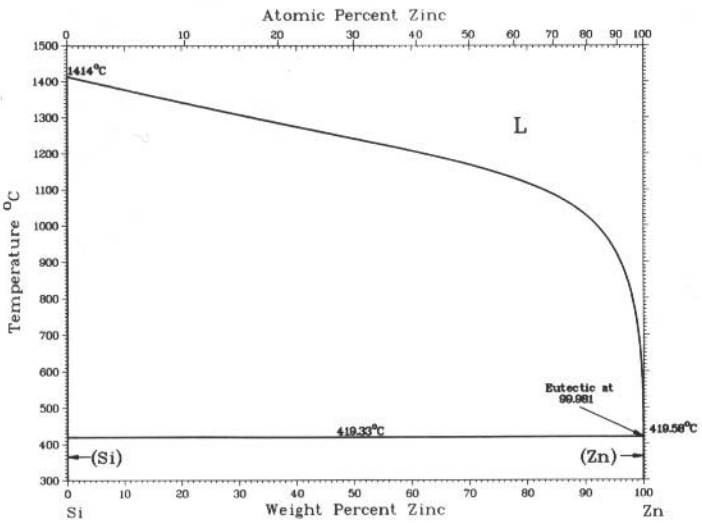

Phase	Composition, wt% Zn	Pearson symbol	Space group
(Si)	0	$cF8$	$Fd\bar{3}m$
(Zn)	100	$hP2$	$P6_3/mmc$

Si-Zr

H. Okamoto, 1990

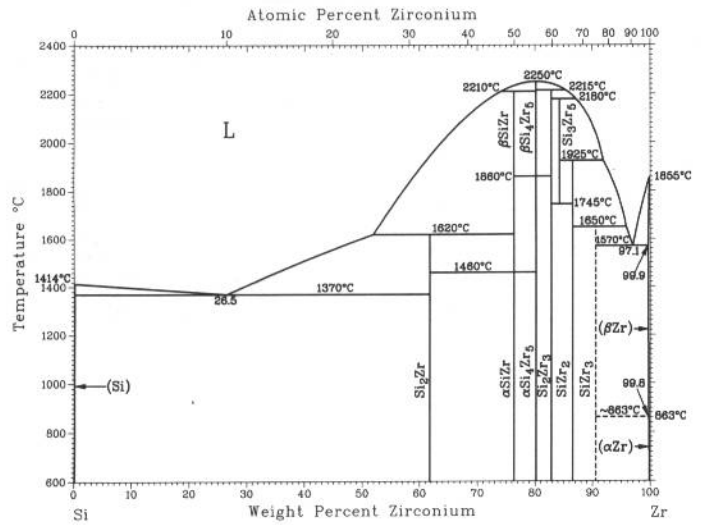

Phase	Composition, wt% Zr	Pearson symbol	Space group
(Si)	0	$cF8$	$Fd\bar{3}m$
Si_2Zr	61.9	$oC12$	$Cmcm$
βSiZr	76.5	$oC8$	$Cmcm$
αSiZr	76.5	$oP8$	$Pnma$
βSr_4Zr_5	80.3	...	...
αSr_4Zr_5	80.3	$tP36$	$P4_12_12$
Si_2Zr_3	83	$tP10$	$P4/mbm$
Si_3Zr_5	84.4	$hP16$	$P6_3/mcm$
$SiZr_2$	86.7	$tI12$	$I4/mcm$
$SiZr_3$	~91	$tP32$	$P4_2/n$
		$tI32$	$I\bar{4}$
(βZr)	100	$cI2$	$Im\bar{3}m$
(αZr)	100	$hP2$	$P6_3/mmc$

Sm-Sn

G. Borzone, A. Borsese, and R. Ferro, 1982

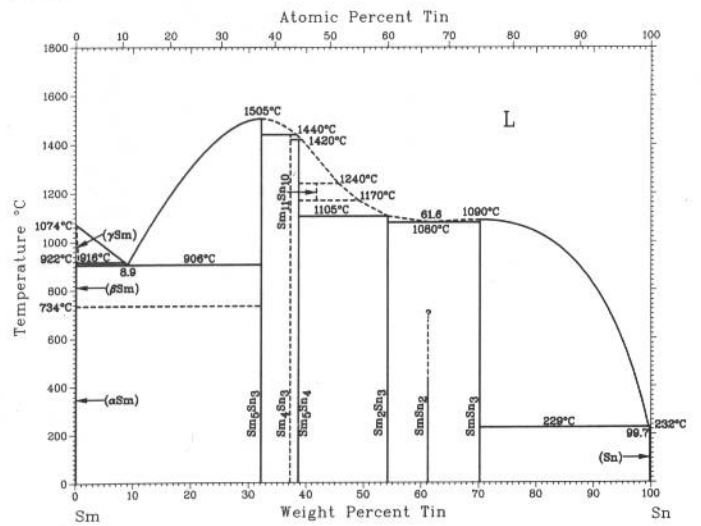

Phase	Composition, wt% Sn	Pearson symbol	Space group
(γSm)	0 to 0.4	$cI2$	$Im\bar{3}m$
(βSm)	0	$hP2$	$P6_3/mmc$
(αSm)	0	$hR3$	$R\bar{3}m$
Sm_5Sn_3	32.1	$hP16$	$P6_3/mcm$
Sm_4Sn_3	37	$cI28$	$I\bar{4}3d$
Sm_5Sn_4	38.8	$oP36$	$Pnma$
$Sm_{11}Sn_{10}$	~42	$tI84$	$I4/mmm$
Sm_2Sn_3	54	t^{**}	...
$SmSn_2$	61.3	...	...
$SmSn_3$	70	$cP4$	$Pm\bar{3}m$
(βSn)	100	$tI4$	$I4_1/amd$
(αSn)	100	$cF8$	$Fd\bar{3}m$

Sm-Tl

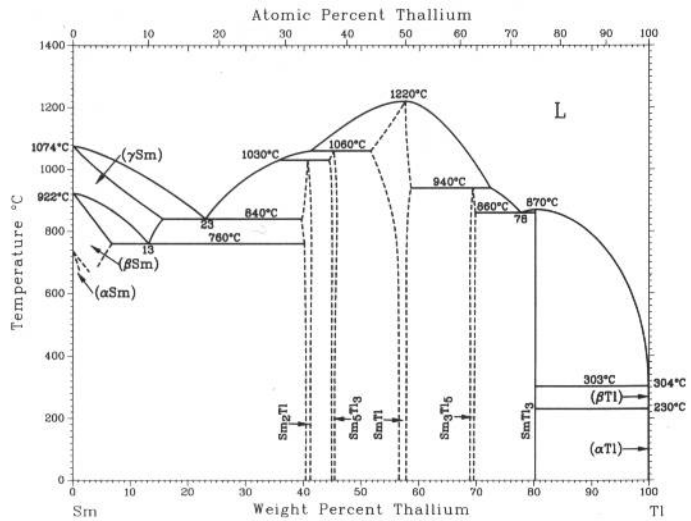

S. Delfino, A. Saccone, A. Palenzona, and R. Ferro, unpublished

Phase	Composition, wt% Tl	Pearson symbol	Space group
(βSm)	0 to ~3.4	*hP*2	$P6_3/mmc$
(αSm)	0 to ?	*hR*2	$R\bar{3}m$
(γSm)	0 to ~16	*cI*2	$Im\bar{3}m$
Sm_2Tl	~40 to ~41	*hP*6	$P6_3/mmc$
Sm_5Tl_3	~44 to ~45	*tI*32	$I4/mcm$
SmTl(a)	~52 to ~59	*tP*2 (or *cI*2)	$Pm\bar{3}m$ $Im\bar{3}m$
SmTl(b)	~52 to ~59	*tP*2	$P4/mmm$
Sm_3Tl_5	~69 to ~70	*oC*32	$Cmcm$
$SmTl_3$	80	*cP*4	$Pm\bar{3}m$
(βTl)	100	*cI*2	$Im\bar{3}m$
(αTl)	100	*hP*2	$P6_3/mmc$

(a) Cubic structure presumed to be room- and high-temperature phases. (b) Tetragonal structure presumed to be low-temperature phase.

Sm-Zn

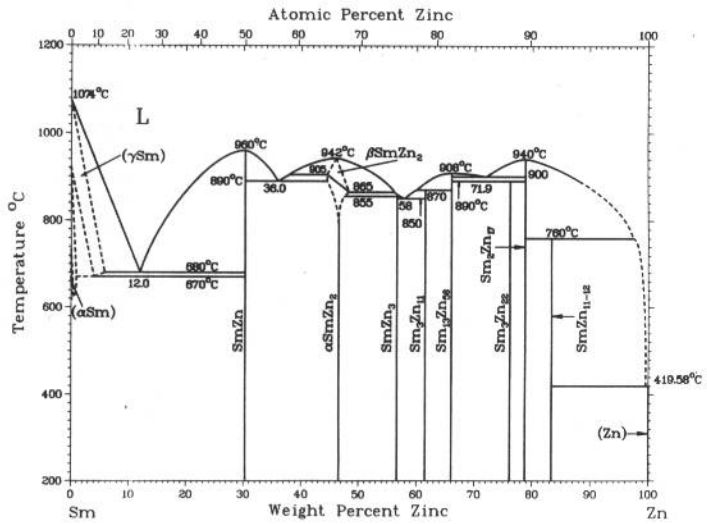

From [Moffatt]

Phase	Composition, wt% Zn	Pearson symbol	Space group
(γSm)	0 to ?	*cI*2	$Im\bar{3}m$
(βSm)	0 to ?	*hP*2	$P6_3/mmc$
(αSm)	0 to ?	*hR*3	$R\bar{3}m$
SmZn	30.3	*cP*2	$Pm\bar{3}m$
$\beta SmZn_2$	45.2 to 48	*oI*12	$Imma$
$\alpha SmZn_2$	~46.6	*oI*12	$Imma$
$SmZn_3$	57	*oP*16	$Pnma$
Sm_3Zn_{11}	~61.5	*oI*28	$Immm$
$Sm_{13}Zn_{58}$	~66.2	*hP*142	$P6_3mc$
Sm_3Zn_{22}	76	*tI*100	$I4_1/amd$
Sm_2Zn_{17}	~78.8	...	...
$SmZn_{11-12}$	83	*tI*26	$I4/mmm$
(Zn)	100	*hP*2	$P6_3/mmc$

Sn-Sr

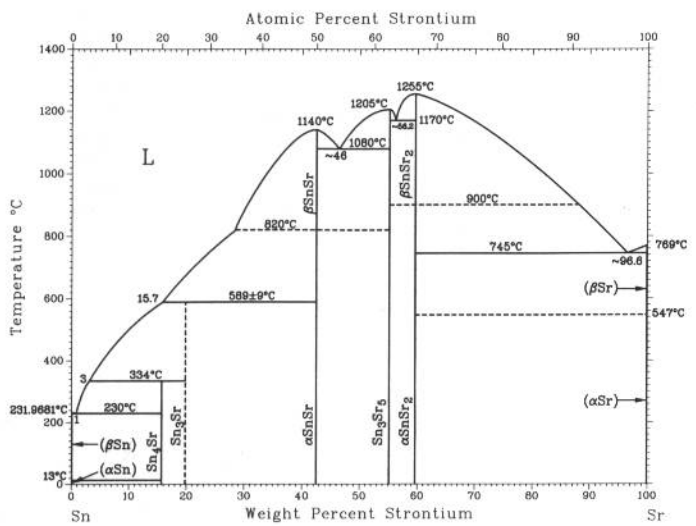

P.R. Subramanian, 1990

Phase	Composition, wt% Sr	Pearson symbol	Space group
(βSn)	0	*tI*4	$I4_1/amd$
(αSn)	0	*cF*8	$Fd\bar{3}m$
Sn_4Sr	15.6	...	...
Sn_3Sr	19.7	...	...
βSnSr	42.5	...	...
αSnSr	42.5	*oC*8	$Cmcm$
Sn_3Sr_5	55.2	*tI*32	$I4/mcm$
$\beta SnSr_2$	59.6	...	...
$\alpha SnSr_2$	59.6	*oP*12	$Pnma$
(βSr)	100	*cI*2	$Im\bar{3}m$
(αSr)	100	*cF*4	$Fm\bar{3}m$

Sn-Te

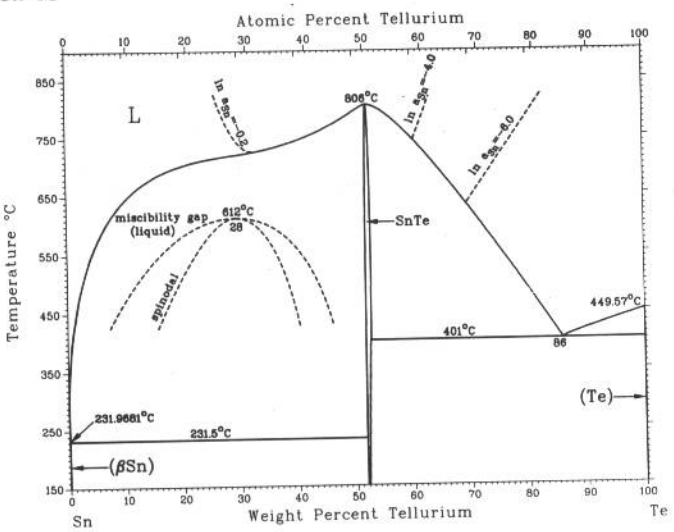

R.C. Sharma and Y.A. Chang, 1986

Phase	Composition, wt% Te	Pearson symbol	Space group
(Sn)	~0	*tI*4	$I4_1/amd$
SnTe	51.8	*cF*8	$Fm\bar{3}m$
SnTe(HP)	51.8	*oP*8	*Pnma*
(Te)	100	*hP*3	$P3_121$

Sn-Ti

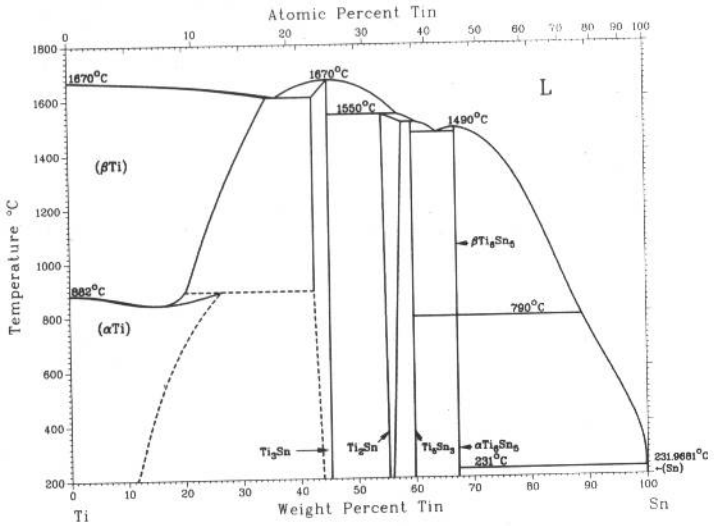

J.L. Murray, 1987

Phase	Composition, wt% Sn	Pearson symbol	Space group
(βTi)	0 to 34	*cI*2	$Im\bar{3}m$
(αTi)	0 to >16.7	*hP*2	$P6_3/mmc$
Ti_3Sn	43 to 45	*hP*8	$P6_3/mmc$
Ti_2Sn	54.6 to 58.1	*hP*6	$P6_3/mmc$
Ti_5Sn_3	59.8	*hP*16	$P6_3/mcm$
βTi_6Sn_5	67.4	*hP*22	$P6_3/mmc$
			$P\bar{3}1c$
αTi_6Sn_5	67.4	*oI*44	*Immm*
(Sn)	99.99 to 100	*tI*4	$I4_1/amd$

Sn-Tl

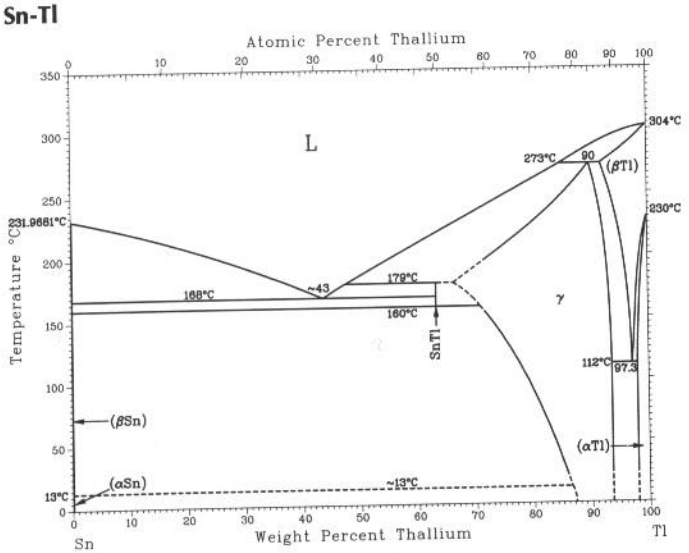

H. Okamoto, 1990

Phase	Composition, wt% Tl	Pearson symbol	Space group
(βSn)	0	*tI*4	$I4_1/amd$
(αSn)	0	*cF*8	$Fd\bar{3}m$
SnTl	63.3	*tP*2	*P*4/*mmm*
γ	68 to 94	*cF*4	$Fm\bar{3}m$
(βTl)	92 to 100	*cI*2	$Im\bar{3}m$
(αTl)	98 to 100	*hP*2	$P6_3/mmc$

Sn-U

R.I. Sheldon, E.M. Foltyn, and D.E. Peterson, 1987

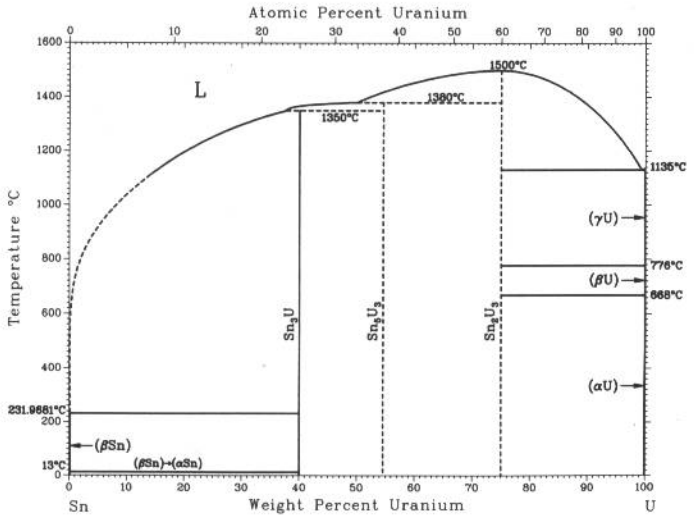

Phase	Composition, wt% U	Pearson symbol	Space group
(βSn)	0	*tI*4	$I4_1/amd$
(αSn)	0	*cF*8	$Fd\bar{3}m$
Sn_3U(a)	40.1	*cP*4	$Pm\bar{3}m$
Sn_5U_3	54.6	...	...
Sn_2U_3	75.0	...	...
(γU)	100	*cI*2	$Im\bar{3}m$
(βU)	100	*tP*30	$P4_2/mnm$
(αU)	100	*oC*4	*Cmcm*

(a) No tendency to disorder was observed.

Sn-Y

H. Okamoto, 1990

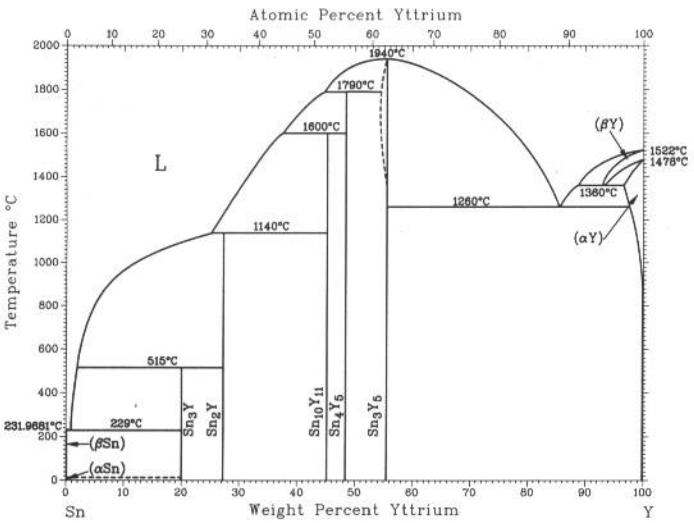

Phase	Composition, wt% Y	Pearson symbol	Space group
(βSn)	0	*tI*4	$I4_1/amd$
(αSn)	0	*cF*8	$Fd\bar{3}m$
Sn_3Y	20	*cP*4	$Pm\bar{3}m$
Sn_2Y	27.2	*oC*12	*Cmcm*
$Sn_{10}Y_{11}$	45.2	*tI*84	*I*4/*mmm*
Sn_4Y_5	48.4	*oP*36	*Pnma*
Sn_3Y_5	55.5	*hP*16	$P6_3/mcm$
(βY)	100	*cI*2	$Im\bar{3}m$
(αY)	100	*hP*2	$P6_3/mmc$

Sn-Yb

A. Palenzona and S. Cirafici, 1991

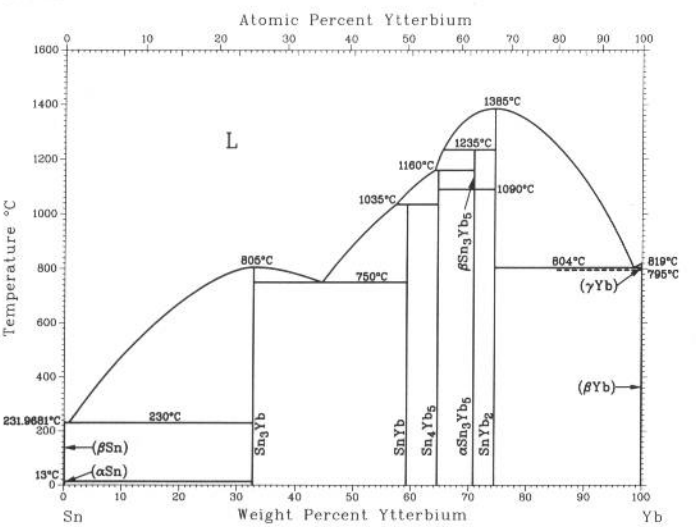

Phase	Composition, wt% Yb	Pearson symbol	Space group
(βSn)	0	*tI*4	$I4_1/amd$
(αSn)	0	*cF*8	$Fd\bar{3}m$
Sn_3Yb	32.7	*cP*4	$Pm\bar{3}m$
SnYb	59.3	*tP*2	*P*4/*mmm*
Sn_4Yb_5	64.6	*oP*36	*Pnma*
βSn_3Yb_5	70.8	*tI*32	*I*4/*mcm*
αSn_3Yb_5	70.8	*hP*16	$P6_3/mcm$
$SnYb_2$	74.5	*hP*6	$P6_3/mmc$
(γYb)	100	*cI*2	$Im\bar{3}m$
(βYb)	100	*cF*4	$Fm\bar{3}m$
(αYb)	100	*hP*2	$P6_3/mmc$

Sn-Zn

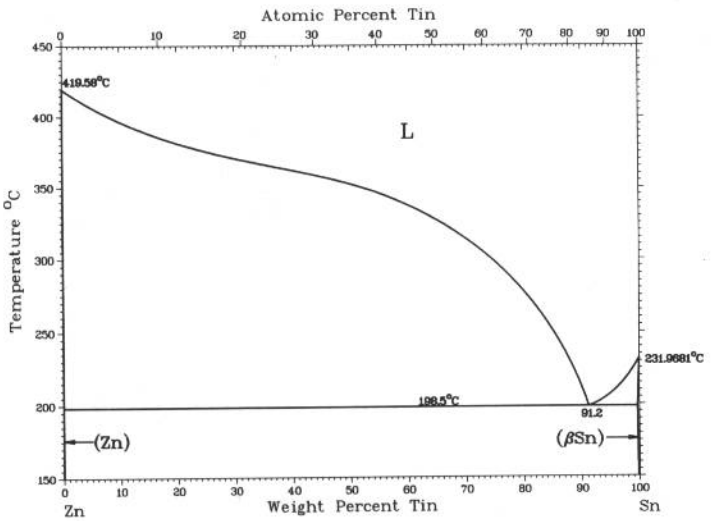

Z. Moser, J. Dutkiewicz, W. Gasior, and J. Salawa, 1985

Phase	Composition, wt% Sn	Pearson symbol	Space group
(Zn)	0	*hP*2	$P6_3/mmc$
(βSn)	~100	*tI*4	$I4_1/amd$

Sn-Zr

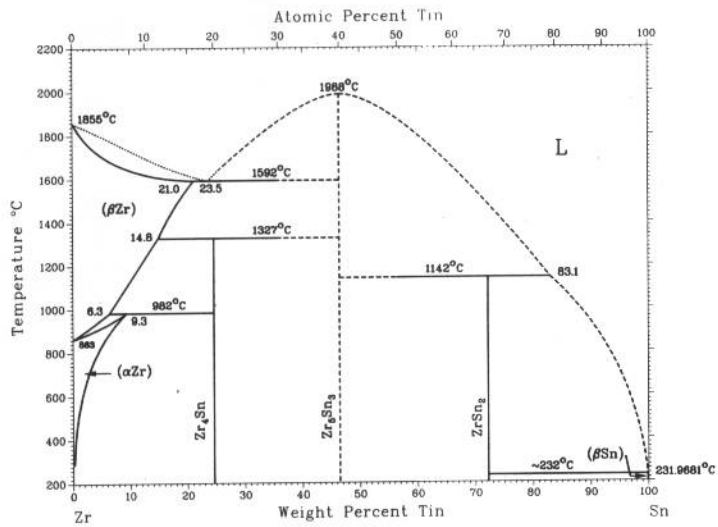

J.P. Abriata, J.C. Bolcich, and D. Arias, 1983

Phase	Composition, wt% Sn	Pearson symbol	Space group
(βZr)	0 to 21.0	*cI*2	$Im\bar{3}m$
(αZr)	0 to 9.3	*hP*2	$P6_3/mmc$
Zr_4Sn	~25	*cP*8	$Pm\bar{3}n$
Zr_5Sn_3	40 to ~47	*hP*16	$P6_3/mcm$
$ZrSn_2$	72.8	*oF*24	*Fddd*
(βSn)	100	*tI*4	$I4_1/amd$
(αSn)	100	*cF*8	$Fd\bar{3}m$
Possible additional phase			
Zr_5Sn_4	~52	*hP*18	...

Sr-Te

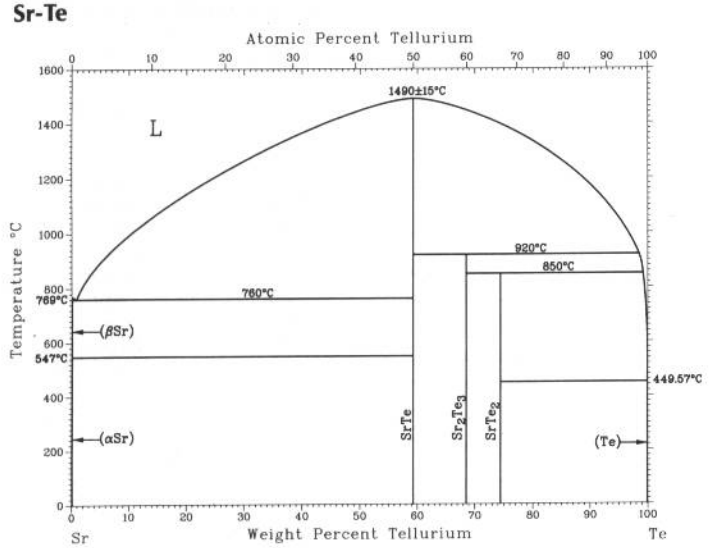

Yu.B. Lyskova and A.V. Vakhobov, 1975

Phase	Composition, wt% Te	Pearson symbol	Space group
(βSr)	0	*cI*2	$Im\bar{3}m$
(αSr)	0	*cF*4	$Fm\bar{3}m$
SrTe	59.3	*cF*8	$Fm\bar{3}m$
Sr_2Te_3	69	...	...
$SrTe_2$	74.5	...	...
(Te)	100	*hP*3	$P3_121$

Sr-Tl

H. Okamoto, 1990

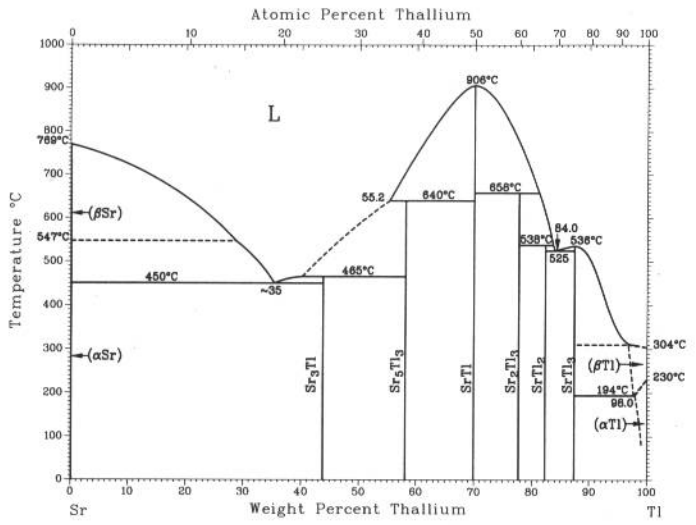

Phase	Composition, wt% Tl	Pearson symbol	Space group
(βSr)	0	*cI*2	$Im\bar{3}m$
(αSr)	0	*cF*4	$Fm\bar{3}m$
Sr_3Tl	44	...	...
Sr_5Tl_3	58.3	*tI*32	*I*4/*mcm*
SrTl	70.0	*cP*2	$Pm\bar{3}m$
Sr_2Tl_3	78	...	...
$SrTl_2$	82.4	*hP*6	$P6_3/mmc$
$SrTl_3$	88	...	...
(βTl)	? to 100	*cI*2	$Im\bar{3}m$
(αTl)	98.0 to 100	*hP*2	$P6_3/mmc$

Sr-Zn

P.R. Subramanian, 1990

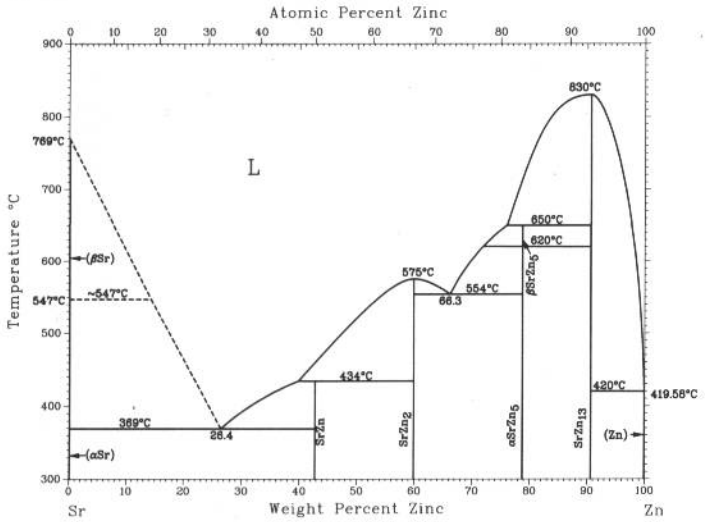

Phase	Composition, wt% Zn	Pearson symbol	Space group
(βSr)	0	*cI*2	$Im\bar{3}m$
(αSr)	0	*cF*4	$Fm\bar{3}m$
SrZn	42.7	*oP*8	*Pnma*
$SrZn_2$	59.9	*oI*12	*Imma*
$SrZn_5$(HT)	78.8	*hP*6	*P*6/*mmm*
$SrZn_5$(LT)	78.8	*oP*24	*Pnma*
$SrZn_{13}$	~90.7	*cF*112	$Fm\bar{3}c$
(Zn)	100	*hP*2	$P6_3/mmc$

Ta-Th

R. Krishnan, S.P. Garg, and N. Krishnamurthy, 1989

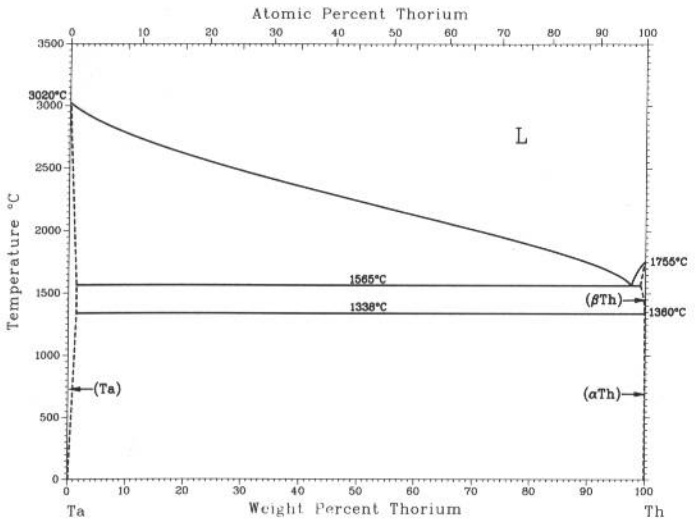

Phase	Composition, wt% Th	Pearson symbol	Space group
(Ta)	0 to <1	*cI*2	$Im\bar{3}m$
(βTh)	99.85 to 100	*cI*2	$Im\bar{3}m$
(αTh)	>99.9 to 100	*cF*4	$Fm\bar{3}m$

Ta-Ti

J.L. Murray, 1987

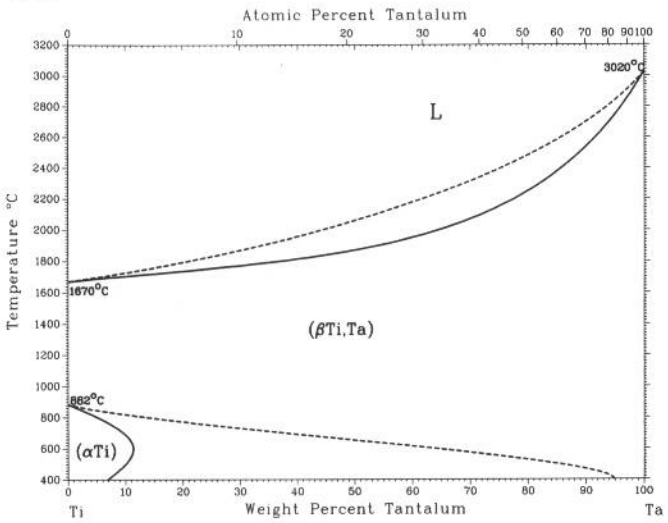

Phase	Composition, wt% Ta	Pearson symbol	Space group
(βTi,Ta)	0 to 100	*cI*2	$Im\bar{3}m$
(αTi)	0 to 12.4	*hP*2	$P6_3/mmc$
Metastable phases			
(α′)	...	*hP*2	$P6_3/mmc$
(α″)	...	*oC*4	*Cmcm*
ω	...	*hP*3	*P6/mmm* or $P\bar{3}m1$

Ta-U

R. Krishnan, S.P. Garg, and N. Krishnamurthy, 1988

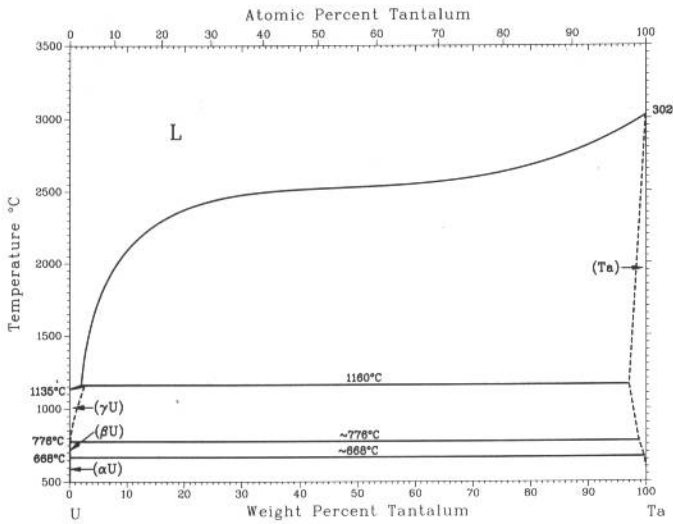

Phase	Composition, wt% Ta	Pearson symbol	Space group
(γU)	0 to ~2	*cI*2	$Im\bar{3}m$
(βU)	0	*tP*30	$P4_2/mnm$
(αU)	0	*oC*4	*Cmcm*
(Ta)	? to 100	*cI*2	$Im\bar{3}m$

Ta-V

J.F. Smith and O.N. Carlson, 1989

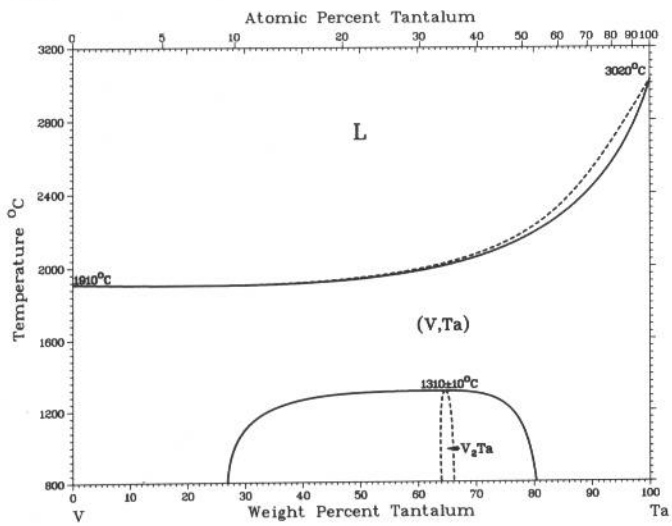

Phase	Composition, wt% Ta	Pearson symbol	Space group
(V,Ta)	0 to 100	*cI*2	$Im\bar{3}m$
V_2Ta(a)	~64 to ~67	*cF*24	$Fd\bar{3}m$

(a) A high-temperature polymorph of V_2Ta has been reported to be a hexagonal $MgZn_2$-type structure, with *hP*12 and $P6_3/mmc$.

Ta-W

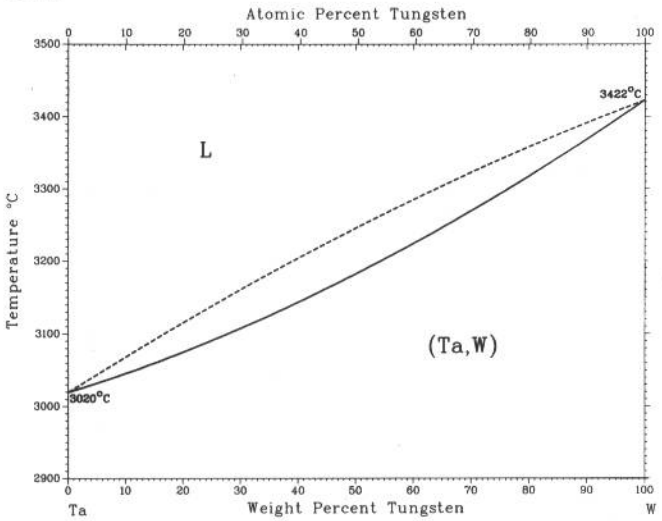

R. Krishnan, S.P. Garg, and N. Krishnamurthy, 1985

Phase	Composition, wt% W	Pearson symbol	Space group
(Ta,W)	0 to 100	*cI*2	$Im\bar{3}m$

Ta-Zr

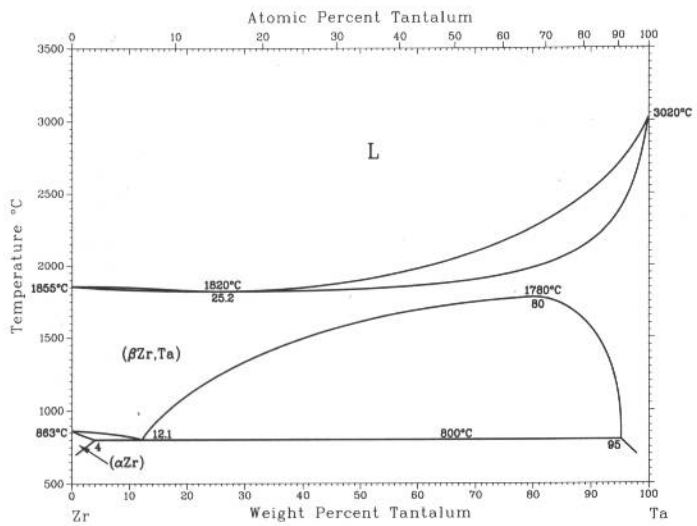

R. Krishnan, S.P. Garg, S. Banerjee, and N. Krishnamurthy, 1989

Phase	Composition, wt% Ta	Pearson symbol	Space group
(βZr,Ta)	0 to 100	*cI*2	$Im\bar{3}m$
(αZr)	0 to 4	*hP*2	$P6_3/mmc$

Tb-Tl

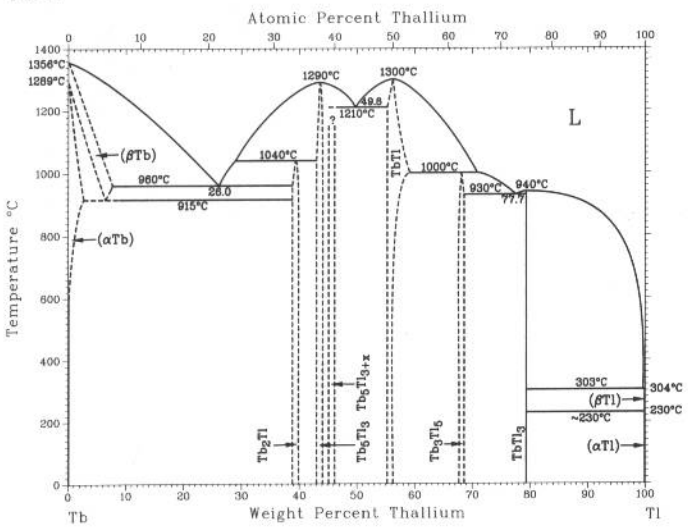

S. Delfino, A. Saccone, A. Palenzona, and R. Ferro, unpublished

Phase	Composition, wt% Tl	Pearson symbol	Space group
(βTb)	0 to ~6	*cI*2	$Im\bar{3}m$
(αTb)	0 to ?	*hP*2	$P6_3/mmc$
Tb_2Tl	~39 to ~40	*hP*6	$P6_3/mmc$
βTb_5Tl_3	~43 to ~44	*hP*16	$P6_3/mcm$
αTb_5Tl_3	~43 to ~44	*tI*32	*I*4/*mcm*
Tb_5Tl_{3+x}	?	*tI*32	*I*4/*mcm*
TbTl	~55 to ~59	*cP*2(a)	$Pm\bar{3}m$
		(or *cI*2)	$Im\bar{3}m$
	~55 to ~59	*tP*2(b)	*P*4/*mmm*
Tb_3Tl_5	~68 to ~69	*oC*32	*Cmcm*
$TbTl_3$	79	*cP*4	$Pm\bar{3}m$
(βTl)	100	*cI*2	$Im\bar{3}m$
(αTl)	100	*hP*2	$P6_3/mmc$

(a) High-temperature phase (>250 K). (b) Low-temperature phase

Te-Tl

H. Okamoto, 1991

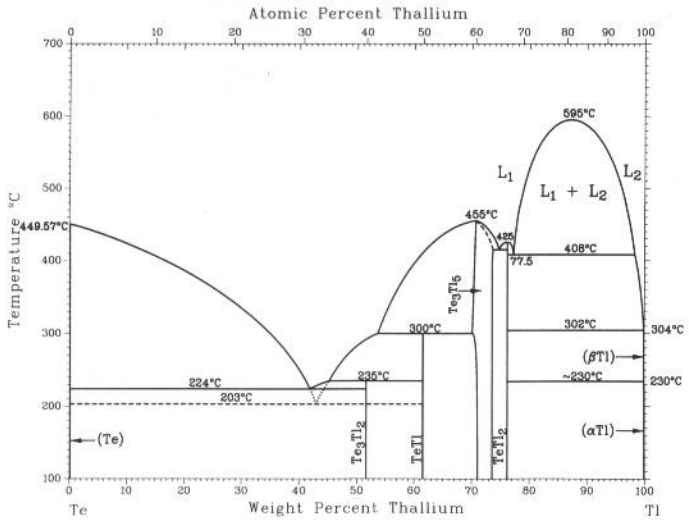

Phase	Composition, wt% Tl	Pearson symbol	Space group
(Te)	0	*hP*3	$P3_121$
Te_3Tl_2	52	*mC*20	*Cc*
TeTl	61.6	*tI*32	*I*4/*mcm*
Te_3Tl_5	72.7	*tI*32	*I*4/*m*
$TeTl_2$	76.2	...	...
(βTl)	100	*cI*2	$Im\bar{3}m$
(αTl)	100	*hP*2	$P6_3/mmc$

Te-U

From [Moffatt]

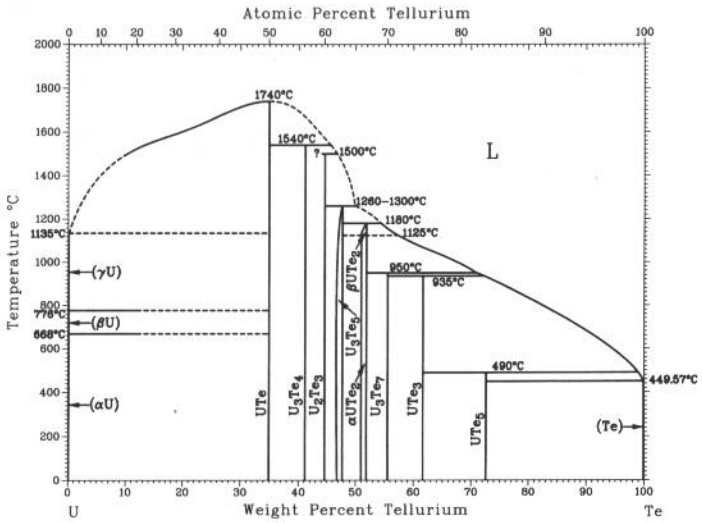

Phase	Composition, wt% Te	Pearson symbol	Space group
(γU)	0	*cI*2	$Im\bar{3}m$
(βU)	0	*tP*30	$P4_2mnm$
(αU)	0	*oC*4	*Cmcm*
UTe	34.9	*cF*8	$Fm\bar{3}m$
U_3Te_4	~41.0	*cI*28	$I\bar{4}3d$
U_2Te_3	45	*hP*16	$P6_3/mcm$
U_3Te_5	47 to 48	*oP*32	*Pnma*
β/αUTe_2	51 to 52	*oI*12	*Immm*
		*tP*6	*P*4/*nmm*
U_3Te_7	56	...	...
UTe_3	62	*t***	...
UTe_5	73.1	...	...
(Te)	100	*hP*3	$P3_121$

Te-Yb

H. Okamoto, 1990

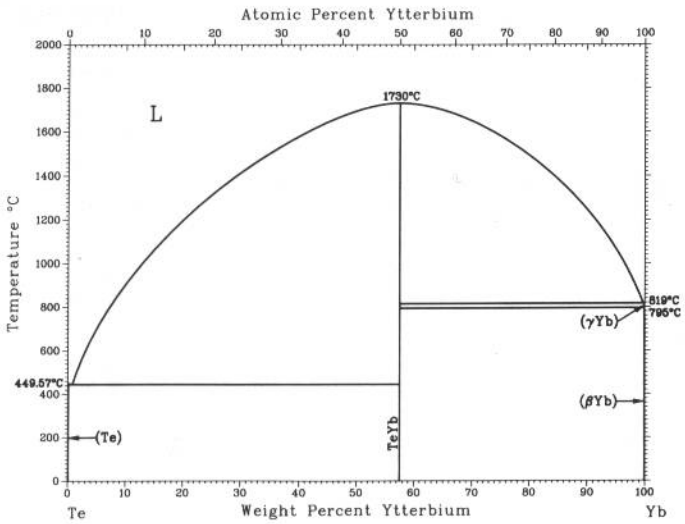

Phase	Composition, wt% Yb	Pearson symbol	Space group
(Te)	0	*hP*3	$P3_121$
TeYb	57.6	*cF*8	$Fm\bar{3}m$
(γYb)	100	*cI*2	$Im\bar{3}m$
(βYb)	100	*cF*4	$Fm\bar{3}m$
(αYb)	100	*hP*2	$P6_3/mmc$

Te-Zn

R.C. Sharma and Y.A. Chang, 1987

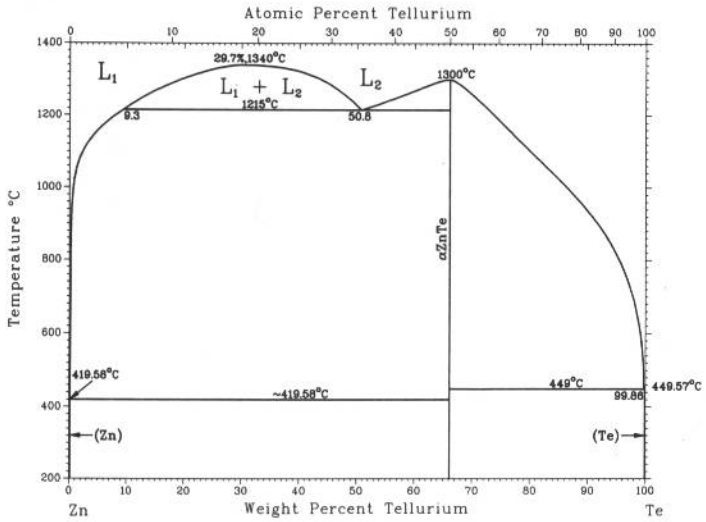

Phase	Composition, wt% Te	Pearson symbol	Space group
(Zn)	0	*hP*2	$P6_3/mmc$
αZnTe	66.1	*cF*8	$F\bar{4}3m$
(Te)	100	*hP*3	$P3_121$

Th-Ti

J.L. Murray, 1987

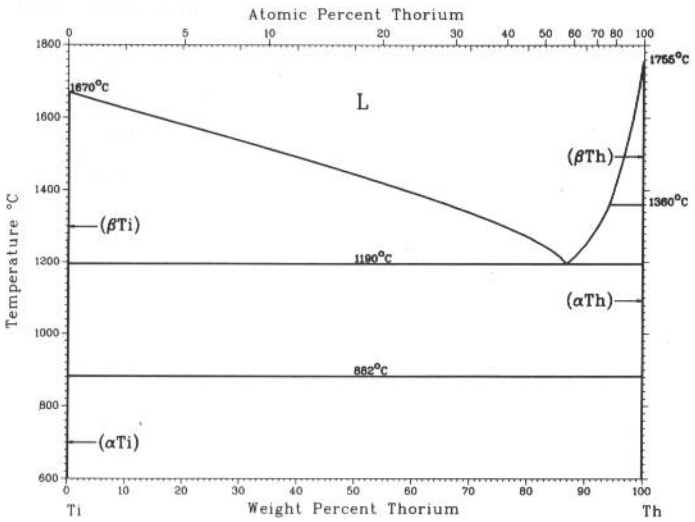

Phase	Composition, wt% Th	Pearson symbol	Space group
(βTi)	0	*cI*2	$Im\bar{3}m$
(αTi)	0	*hP*2	$P6_3/mmc$
(βTh)	100	*cI*2	$Im\bar{3}m$
(αTh)	100	*cF*4	$Fm\bar{3}m$

Th-Tl

H. Okamoto, 1990

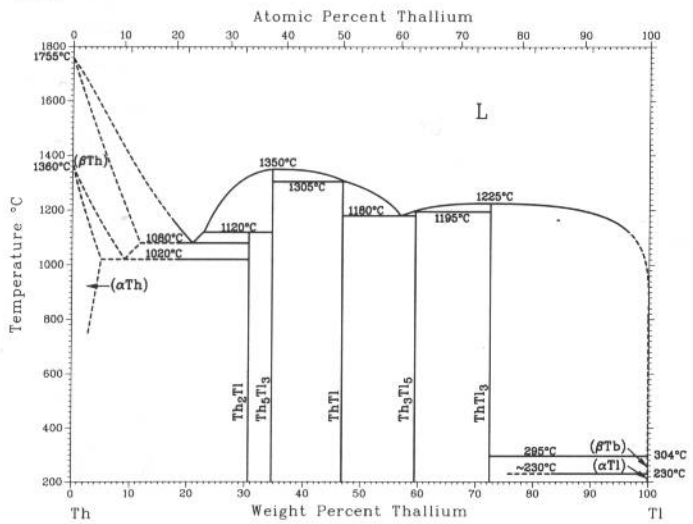

Phase	Composition, wt% Tl	Pearson symbol	Space group
(βTh)	0 to ?	*cI*2	$Im\bar{3}m$
(αTh)	0 to ?	*cF*4	$Fm\bar{3}m$
Th_2Tl	30.5	*tI*12	*I*4/*mcm*
Th_5Tl_3	34.6	*hP*16	$P6_3/mcm$
ThTl	46.8	*oP*24	*Pbcm*
Th_3Tl_5	59.5	*oC*32	*Cmcm*
$ThTl_3$	73	*cP*4	$Pm\bar{3}m$
(βTl)	100	*cI*2	$Im\bar{3}m$
(αTl)	100	*hP*2	$P6_3/mmc$

Th-Zn

P. Chiotti and K.J. Gill, 1961

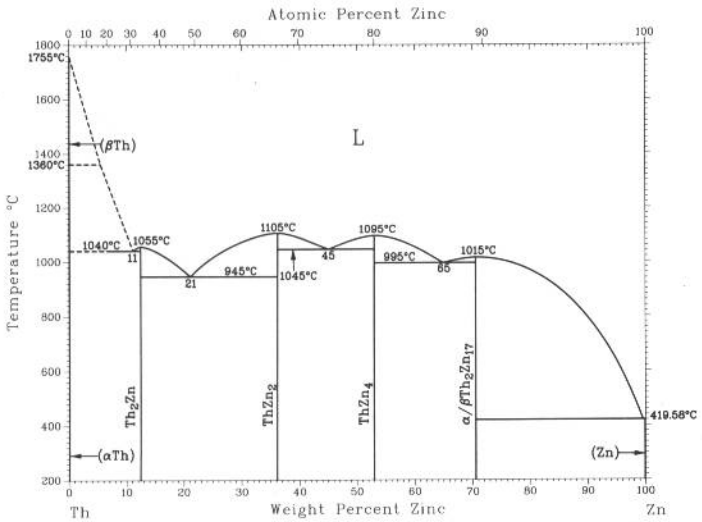

Phase	Composition, wt% Zn	Pearson symbol	Space group
(βTh)	0	*cI*2	$Im\bar{3}m$
(αTh)	0	*cF*2	$Fm\bar{3}m$
Th_2Zn	12.3	*tI*12	*I*4/*mcm*
$ThZn_2$	36.1	*hP*3	*P*6/*mmm*
$ThZn_4$	53	*tI*10	*I*4/*mmm*
βTh_2Zn_{17}	70.6	*hR*19	$R\bar{3}m$
αTh_2Zn_{17}	70.6	*hP*38	$P6_3/mmc$
(Zn)	100	*hP*2	$P6_3/mmc$

Th-Zr

E.D. Gibson, B.A. Loomis, and O.N. Carlson, 1958; R.H. Johnson and R.W.K. Honeycombe, 1961

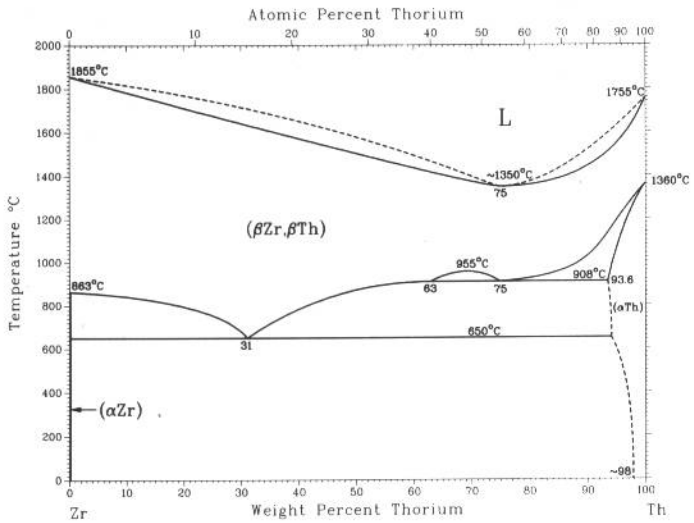

Phase	Composition, wt% Th	Pearson symbol	Space group
(βZr,βTh)	0 to 100	*cI*2	$Im\bar{3}m$
(αZr)	0	*hP*2	$P6_3/mmc$
(αTh)	93.6 to 100	*cF*4	$Fm\bar{3}m$

Ti-U

J.L. Murray, 1987

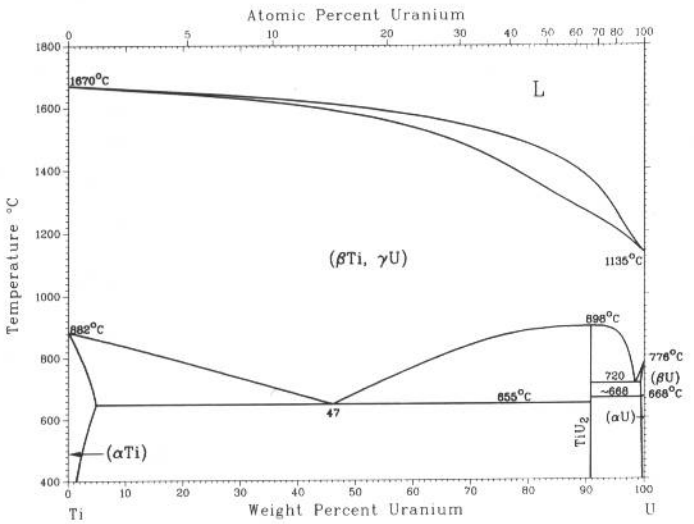

Phase	Composition, wt% U	Pearson symbol	Space group
(βTi,γU)	0 to 100	*cI*2	$Im\bar{3}m$
(αTi)	0 to ~5	*hP*2	$P6_3/mmc$
TiU_2	90.9	*hP*3	*P*6/*mmm*
(βU)	~99.6 to 100	*tP*30	$P4_2nm$
(αU)	~99.6 to 100	*oC*4	*Cmcm*
α_b''(a)	38	(b)	...

(a) Metastable. (b) Monoclinic

Ti-V

J.L. Murray, 1989

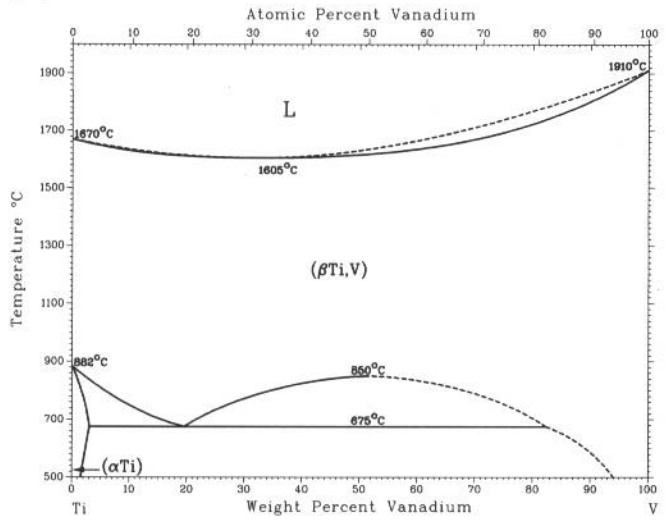

Phase	Composition, wt% V	Pearson symbol	Space group
(βTi,V)	0 to 100	*cI*2	$Im\bar{3}m$
(αTi)	0 to ~3	*hP*2	$P6_3/mmc$
Metastable phases			
α′	0 to 5	*hP*2	$P6_3/mmc$
α″	5 to 16	*oC*4	*Cmcm*
ω	12 to ~51.5	*hP*3	$P6/mmm$ or $P\bar{3}m1$

Ti-W

J.L. Murray, 1987

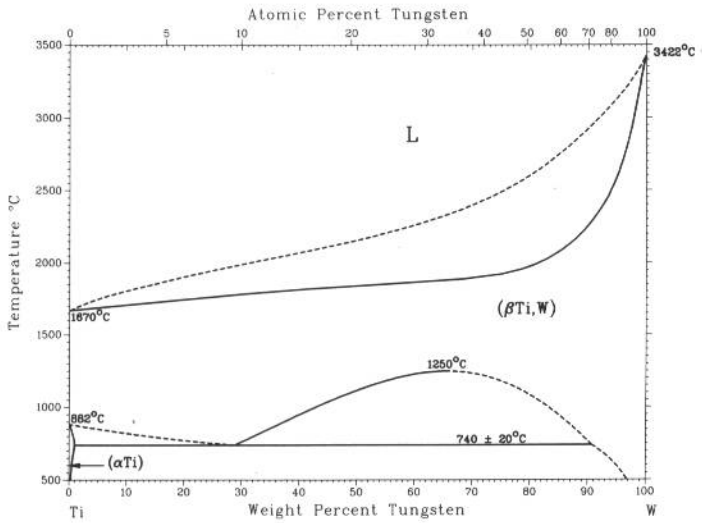

Phase	Composition, wt% W	Pearson symbol	Space group
(βTi,W)	0 to 100	*cI*2	$Im\bar{3}m$
(αTi)	0 to 0.8	*hP*2	$P6_3/mmc$
α′(a)	0 to 7	*hP*2	$P6_3/mmc$
α″(a)	7 to 18.3	*oC*4	*Cmcm*
ω(a)	20 to 30	*hP*3	*P6/mmm*

(a) Metastable

Ti-Y

J.L. Murray, 1987

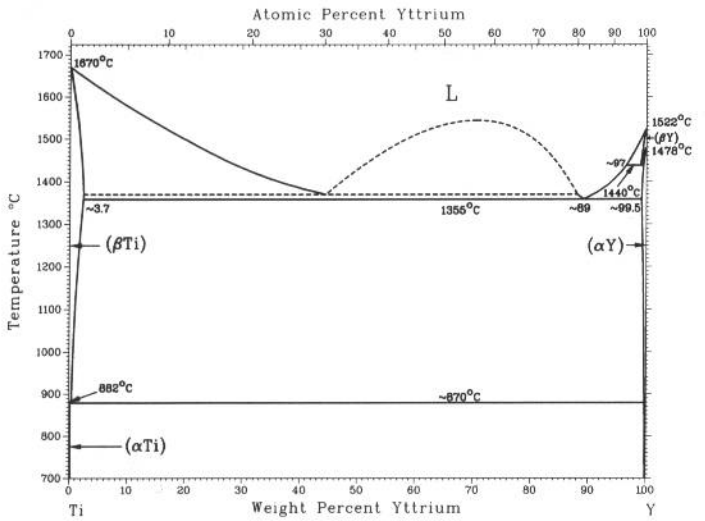

Phase	Composition, wt% Y	Pearson symbol	Space group
(βTi)	0 to ~3.7	*cI*2	$Im\bar{3}m$
(αTi)	0 to ~0.02	*hP*2	$P6_3/mmc$
(βY)	~99.5 to 100	*cI*2	$Im\bar{3}m$
(αY)	~99.5 to 100	*hP*2	$P6_3/mmc$

Ti-Zr

J.L. Murray, 1987

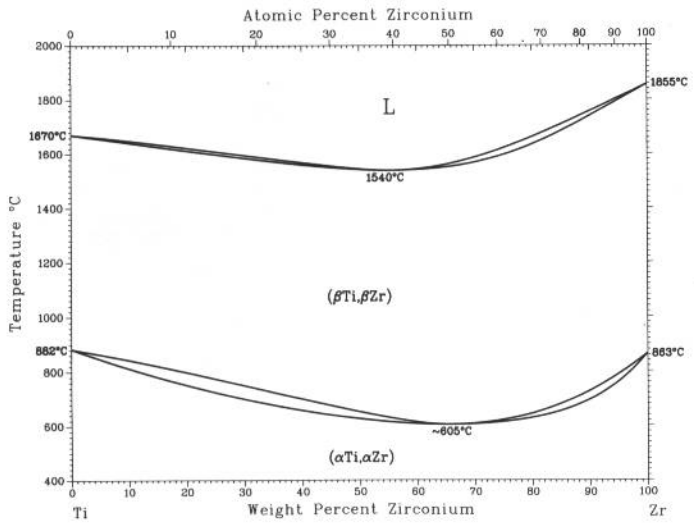

Phase	Composition, wt% Zr	Pearson symbol	Space group
(βTi,βZr)	0 to 100	*cI*2	$Im\bar{3}m$
(αTi,αZr)	0 to 100	*hP*2	$P6_3/mmc$
Metastable phases			
α′	...	*hP*2	$P6_3/mmc$
ω	...	*hP*3	$P6/mmm$ or $P\bar{3}m1$

Tl-Yb

S. Delfino, A. Saccone, A. Palenzona, and R. Ferro, unpublished

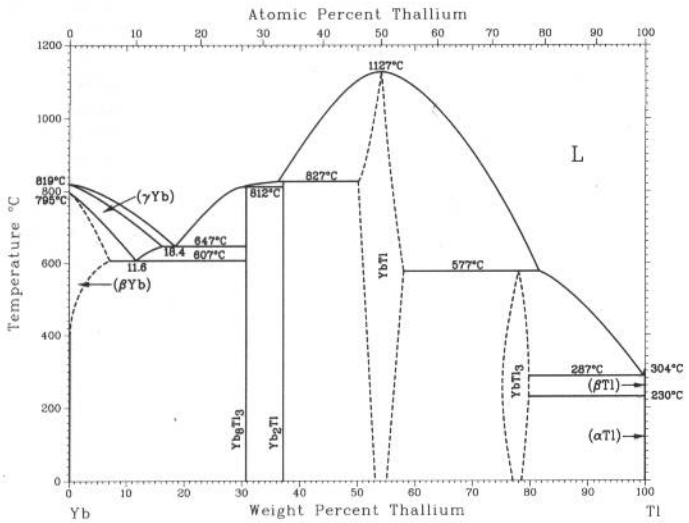

Phase	Composition, wt% Tl	Pearson symbol	Space group
(βYb)	0 to ~7	*cF*2	$Fm\bar{3}m$
(γYb)	0 to ~16	*cI*2	$Im\bar{3}m$
Yb_8Tl_3	30.69	*aP*22	$P\bar{1}$
Yb_2Tl	37.13	*oP*12	*Pnma*
YbTl	~50 to ~58	*cP*2	$Pm\bar{3}m$
		(or *cI*2)	$Im\bar{3}m$
$YbTl_3$	~75 to ~80	*cP*4	$Pm\bar{3}m$
(βTl)	100	*cI*2	$Im\bar{3}m$
(αTl)	100	*hP*2	$P6_3/mmc$

Tl-Zn

A.V. Vegesack, 1907; and W. Seith, H. Johnson, and J. Wagner, 1952

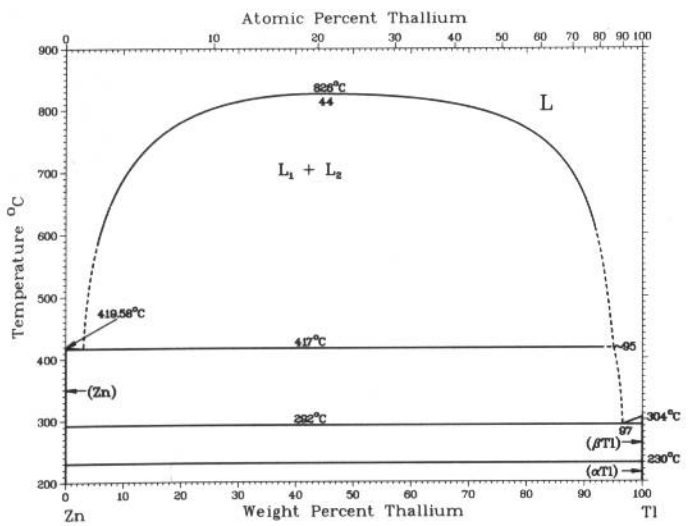

Phase	Composition, wt% Tl	Pearson symbol	Space group
(Zn)	0	*hP*2	$P6_3/mmc$
(βTl)	100	*cI*2	$Im\bar{3}m$
(αTl)	100	*hP*2	$P6_3/mmc$

U-Zr

H. Okamoto, 1992

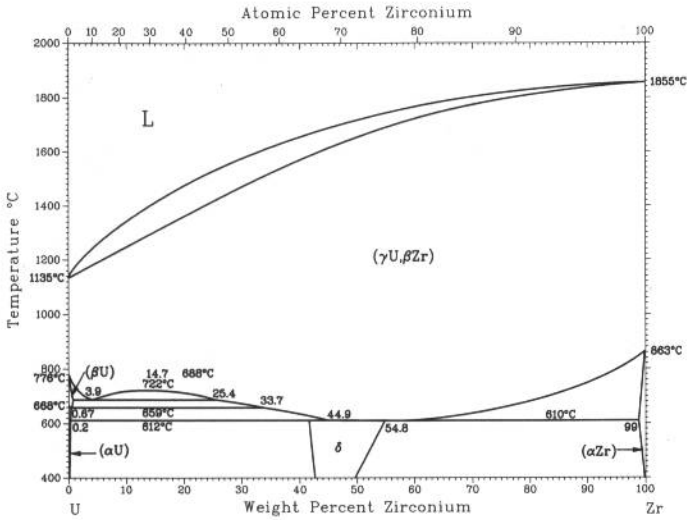

Phase	Composition, wt% Zr	Pearson symbol	Space group
(γU,βZr)	0 to 100	*cI*2	$Im\bar{3}m$
(BU)	0 to 0.4	*tP*30	$P4_2/mnm$
(αU)	0 to 0.2	*oC*4	*Cmcm*
δ	42 to 55	*hP*3	*P6/mmm*
(αZr)	99 to 100	*hP*2	$P6_3/mmc$

V-W

S.V. Nagender Naidu, A.M. Sriramamurthy, M. Vijayakumar, and P. Rama Rao, 1989

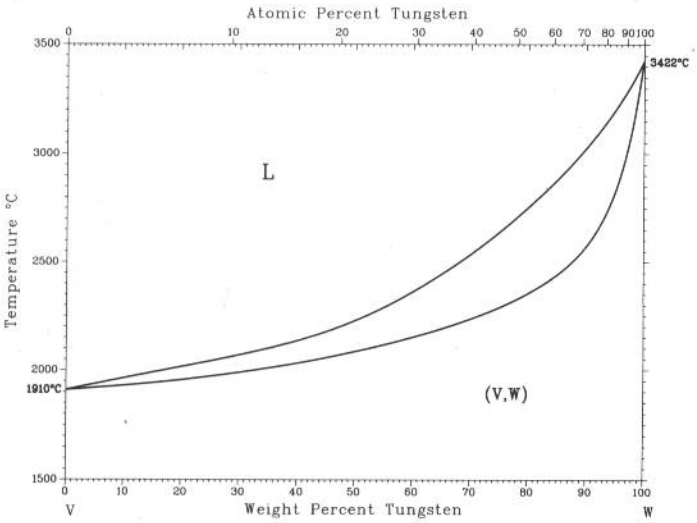

Phase	Composition, wt% W	Pearson symbol	Space group
(V,W)	0 to 100	*cI*2	$Im\bar{3}m$

V-Zr

J.F. Smith, 1989

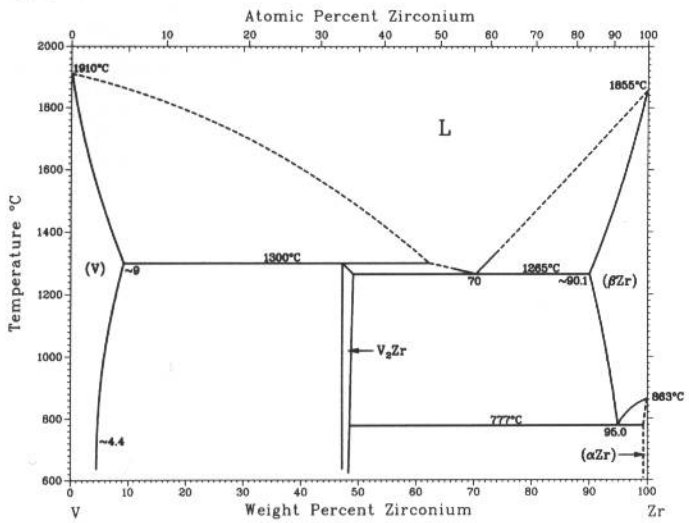

Phase	Composition, wt% Zr	Pearson symbol	Space group
(V)	0 to ~9	*cI*2	$Im\bar{3}m$
V_2Zr	~47.2	*cF*24	$Fd\bar{3}m$
(βZr)	~90.1 to 100	*cI*2	$Im\bar{3}m$
(αZr)	~100	*hP*2	$P6_3/mmc$

W-Zr

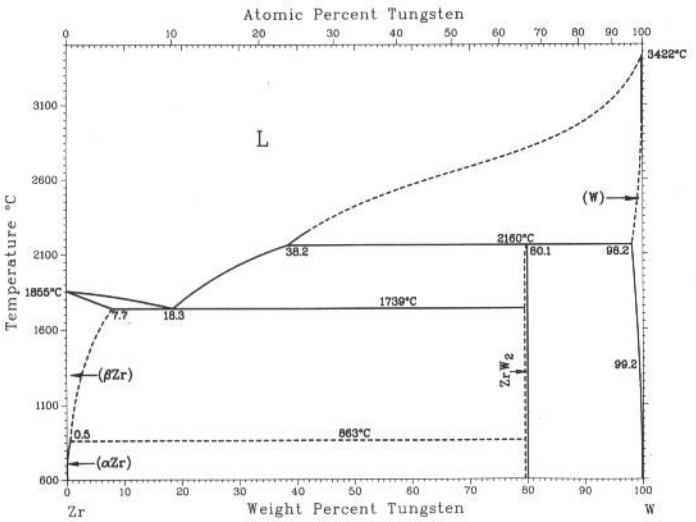

S.V. Nagender Naidu and P. Rama Rao, 1991

Phase	Composition, wt% W	Pearson symbol	Space group
(βZr)	0 to 7.7	*cI*2	$Im\bar{3}m$
(αZr)	0 to 0.50	*hP*2	$P6_3/mmc$
ZrW_2	~80.1	*cF*24	$Fd\bar{3}m$
(W)	98.2 to 100	*cI*2	$Im\bar{3}m$

Y-Zn

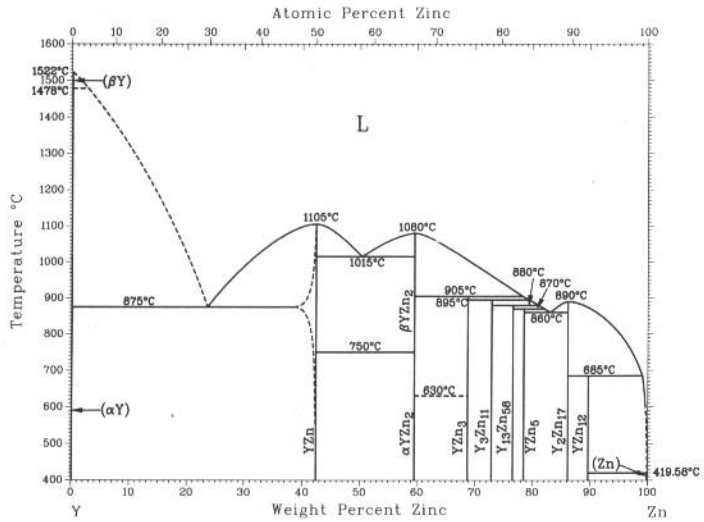

H. Okamoto, 1990

Phase	Composition, wt% Zn	Pearson symbol	Space group
(βY)	0	*cI*2	$Im\bar{3}m$
(αY)	0	*hP*2	$P6_3/mmc$
YZn	? to 42.4	*cP*2	$Pm\bar{3}m$
βYZn_2	59.6	...	...
αYZn_2	59.6	*oI*12	*Imma*
YZn_3	69	*oP*16	*Pnma*
Y_3Zn_{11}	73.0	*oI*28	*Immm*
$Y_{13}Zn_{58}$	76.7	*hP*142	$P6_3mc$
YZn_5	76.6	*hP*36	$P6_3/mmc$
Y_2Zn_{17}	86.2	*hP*38	$P6_3/mmc$
YZn_{12}	89.8	*tI*26	*I*4/*mmm*
(Zn)	100	*hP*2	$P6_3/mmc$

Y-Zr

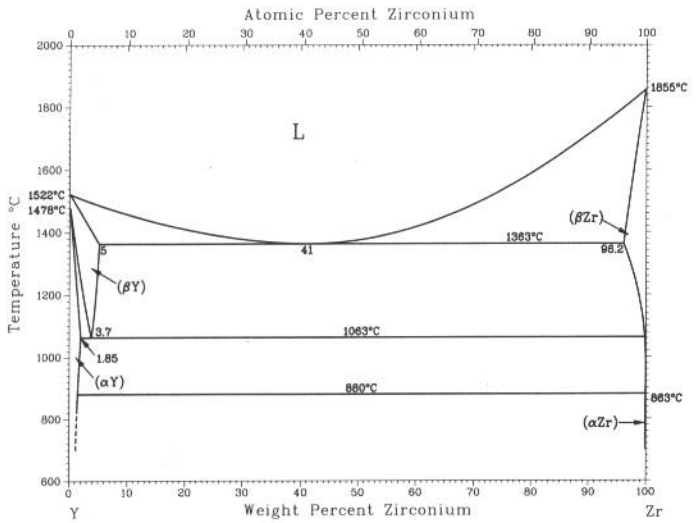

A. Palenzona and S. Cirafici, 1991

Phase	Composition, wt% Zr	Pearson symbol	Space group
(βY)	0 to 5	*cI*2	$Im\bar{3}m$
(αY)	0 to 1.85	*hP*2	$P6_3/mmc$
(βZr)	96.2 to 100	*cI*2	$Im\bar{3}m$
(αZr)	100	*hP*2	$P6_3/mmc$

Yb-Zn

J.T. Mason and P. Chiotti, 1968

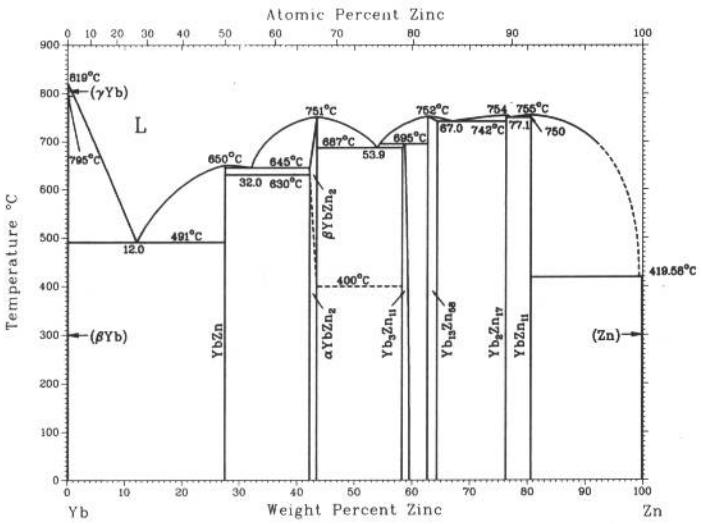

Phase	Composition, wt % Zn	Pearson symbol	Space group
(γYb)	0	*cI*2	$Im\bar{3}m$
(βYb)	0	*cF*4	$Fm\bar{3}m$
YbZn	27.4	*cP*2	$Pm\bar{3}m$
$\beta YbZn_2$	~42 to 43	...	...
$\alpha YbZn_2$	~42 to 43	*oI*12	*Imma*
Yb_3Zn_{11}	~58.0 to 59.4	*oI*28	*Immm*
$Yb_{13}Zn_{58}$	~62.5 to 64.0	*hP*142	$P6_3mc$
Yb_2Zn_{17}	76.3	...	...
$YbZn_{11}$	80.3	*tI*48	$I4_1/amd$
(Zn)	100	*hP*2	$P6_3/mmc$
Other reported phases			
Yb_3Zn_{17}	68	*cI*160	$Im\bar{3}$
$YbZn_{13}$	83.2	*cF*112	$Fm\bar{3}c$

Section 3
Ternary Alloy Phase Diagrams

Introduction ..... 3•3
Ternary Phase Diagrams ..... 3•5-58
Ternary References ..... 3•59-60
List of Systems Included:

Ag-Au-Cu.....3•5
Ag-Cd-Cu.....3•5-6
Ag-Cd-Zn.....3•6-7
Ag-Cu-Zn.....3•7
Ag-Pb-Sn.....3•7-8
Al-Cr-Fe .....3•8
Al-Cr-Mg.....3•8-9
Al-Cr-Mn.....3•9
Al-Cr-Ni .....3•9
Al-Cr-Ti.....3•9
Al-Cu-Fe .....3•9-10
Al-Cu-Mn....3•10-11
Al-Cu-Ni .....3•11-12
Al-Cu-Si .....3•12
Al-Cu-Zn.....3•12-13
Al-Fe-Mn.....3•13-14
Al-Fe-Ni .....3•14-15
Al-Fe-Si.....3•15-16
Al-Fe-Zn.....3•16
Al-Mg-Mn.....3•17
Al-Mg-Si .....3•17-18
Al-Mg-Zn....3•18-19
Al-Mn-Si .....3•19
Al-Mo-Ni .....3•20
Al-Mo-Ti.....3•20
Al-Ni-Ti .....3•20-21
Al-Si-Zn .....3•21-22
Al-Ti-V.....3•22
Au-Cu-Ni ....3•22-23
B-C-Fe.....3•23-24
C-Cr-Fe .....3•24-25
C-Cr-Mo.....3•25-26
C-Cr-N.....3•26
C-Cr-V.....3•26-27
C-Cr-W.....3•27
C-Cu-Fe.....3•27-28
C-Fe-Mn.....3•28-30
C-Fe-Mo.....3•30-31
C-Fe-N.....3•31-32
C-Fe-Ni .....3•32
C-Fe-Si .....3•33-34
C-Fe-V.....3•34
C-Fe-W.....3•35
Cd-Sb-Sn.....3•35-36
Co-Cr-Fe .....3•36-37
Co-Cr-Ni .....3•37
Co-Cr-Ti.....3•38
Co-Cr-W.....3•38
Co-Fe-Mo....3•38-39
Co-Fe-Ni .....3•39-40
Co-Fe-W.....3•40-41
Co-Mo-Ni.....3•41
Co-Ni-Ti.....3•41
Cr-Fe-Mo.....3•42
Cr-Fe-N .....3•43
Cr-Fe-Ni .....3•43-44
Cr-Fe-W .....3•45
Cr-Mo-Ni.....3•45
Cr-Mo-W.....3•46
Cr-Nb-Ni .....3•46-47
Cr-Nb-W .....3•47
Cr-Ni-Ti.....3•47-48
Cr-Ni-W .....3•48
Cr-Ti-W.....3•49
Cu-Fe-Ni .....3•49-50
Cu-Ni-Sn .....3•50
Cu-Ni-Zn.....3•51
Cu-Pb-Zn.....3•51-52
Cu-Sb-Sn.....3•52
Cu-Sn-Zn.....3•52
Fe-Mn-Ni.....3•53
Fe-Mo-Nb....3•53-54
Fe-Mo-Ni.....3•54-55
Fe-Ni-W .....3•55
Mo-Nb-Ti.....3•56
Mo-Ni-Ti.....3•56
Mo-Ni-W.....3•56
Mo-Ti-W.....3•57
Nb-Ti-W.....3•57
Pb-Sb-Sn .....3•57-58
Pb-Sn-Zn .....3•58

Introduction to Ternary Alloy Phase Diagrams

THE 80 TERNARY SYSTEMS covered in this Section were selected for their commercial importance from the thousands of systems scheduled for inclusion in the *Handbook of Ternary Alloy Phase Diagrams*, to be published by ASM in 1994. The 313 diagrams shown here were chosen from the more than 12,000 assembled for that project. Wherever a recent compilation of diagrams assessed under the International Programme covered one of these systems, priority was given to those evaluated diagrams in preference to older, unassessed work. The remaining diagrams, although not yet assessed, were selected as the best available.

When a single source covered a system, a set of compatible diagrams was selected from it. For some systems, however, diagrams from more than one source were needed. Except for occasional conversion of composition scale from atomic to weight percent or change in orientation or labeling, each author's diagram has been redrawn, but shown as originally presented. *Therefore, the diagrams do not, in all instances, agree with one another and with the binary diagrams published in this Volume.* The reference source for each diagram is identified by a code consisting of two numbers (indicating the year of publication) followed by the first three letters of the first author's (or editor's) surname. The complete citation for each source code is listed at the end of this Section.

Because this Handbook is designed to be used primarily by engineers to solve industrial problems, the composition scale is plotted in weight percent. Conversions between weight and atomic composition can be made using the standard atomic weights listed in the Appendix. For the sake of clarity, grid lines are not superimposed on the phase diagrams. However, tick marks are provided along the composition scales as well as the temperature scale,which is shown in degrees Celsius. Celsius temperatures can be easily converted to degrees Fahrenheit using the table in the Appendix. When an arrowhead appears on a temperature trough line in a liquidus projection, it indicates the direction of decreasing temperature in the trough. Dashed lines are used to denote uncertain or speculative boundaries. Dotted lines indicate the limit of the investigated region.

The diagrams presented in this Section are for stable equilibrium conditions, with the exception of metastable conditions for some diagrams involving carbon and iron. These latter ternary diagrams can be identified by the presence of Fe_3C on the Fe-C binary portion of the diagram. In some ternary diagrams involving carbon and iron, the symbol M is used to represent both iron and the other metallic element when the two metals substitute for each other in a carbide phase—for example, M_3C.

Ag-Au-Cu liquidus projection [90Pri]

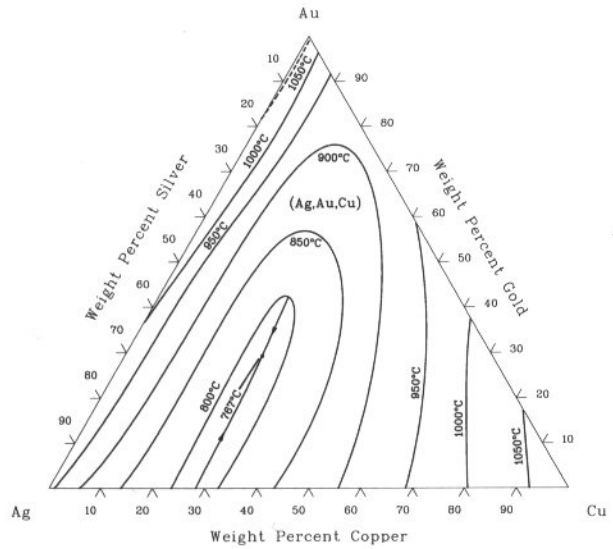

Ag-Au-Cu isothermal section at 775 °C [90Pri]

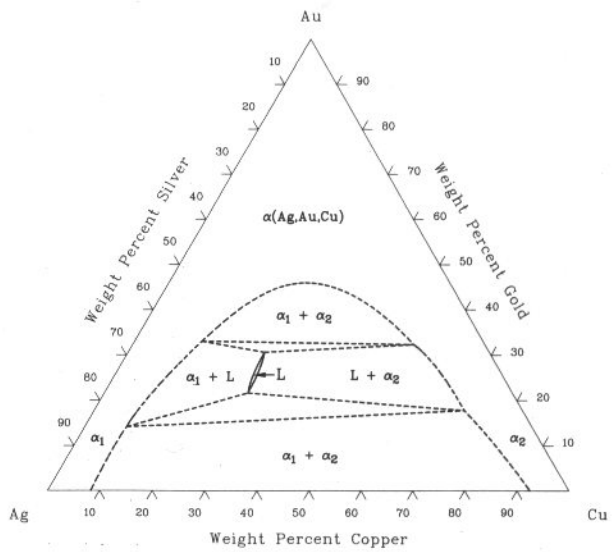

Ag-Au-Cu isothermal section at 950 °C [90Pri]

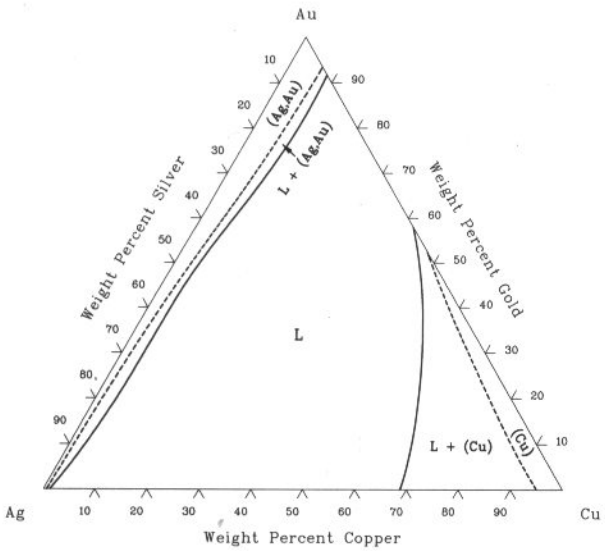

Ag-Au-Cu isothermal section at 300 °C [90Pri]

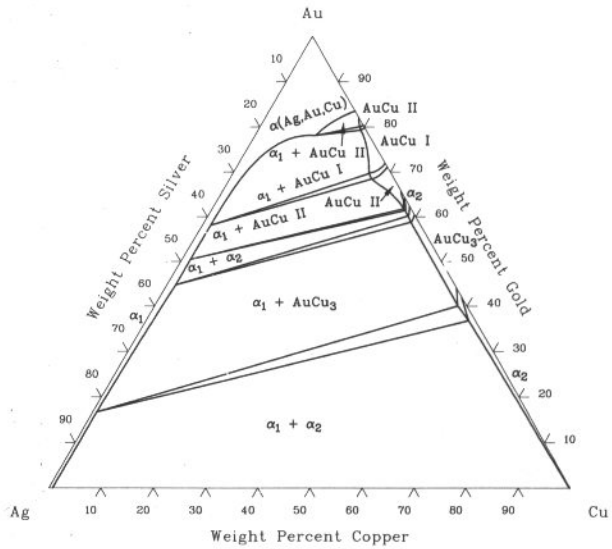

Ag-Au-Cu isothermal section at 850 °C [90Pri]

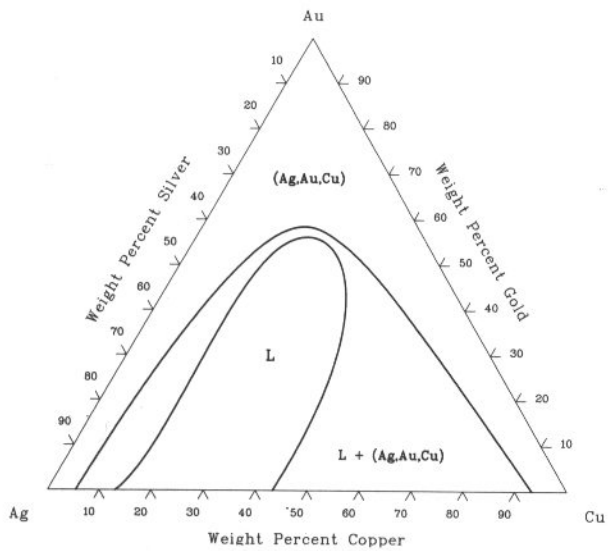

Ag-Cd-Cu liquidus projection [88Pet]

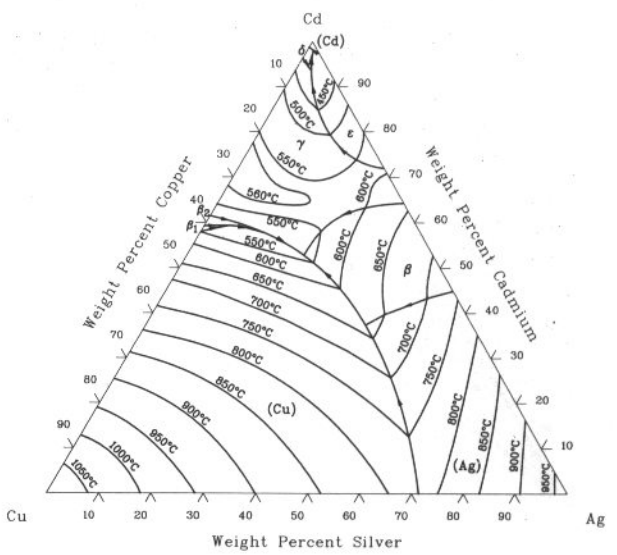

Ag-Cd-Cu isothermal section at 600 °C [88Pet]

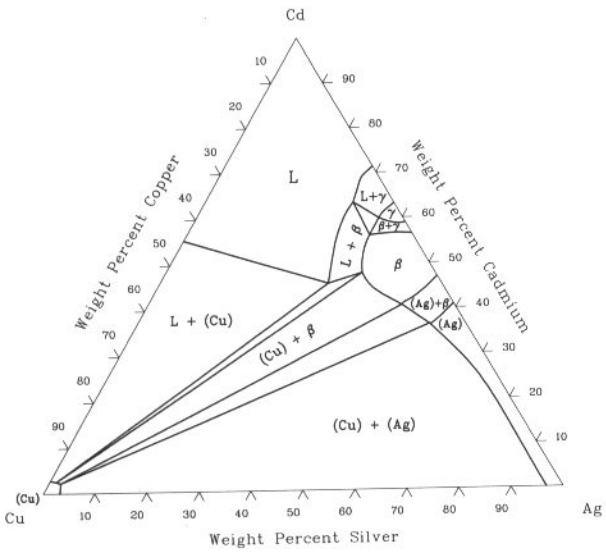

Ag-Cd-Cu isothermal section at 500 °C [88Pet]

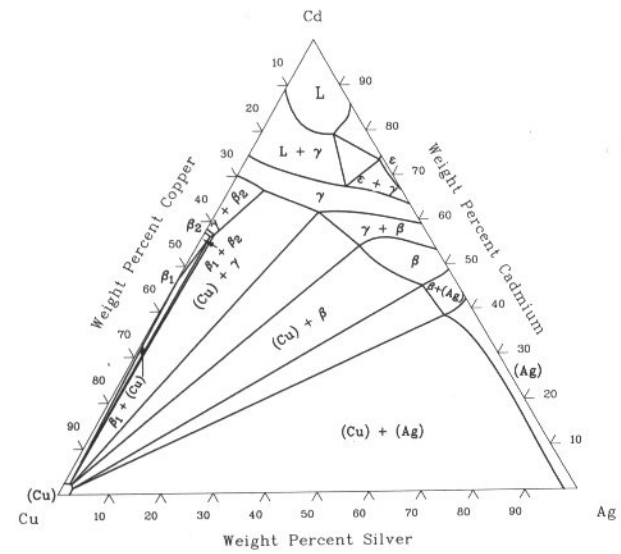

Ag-Cd-Cu isothermal section at 300 °C [88Pet]

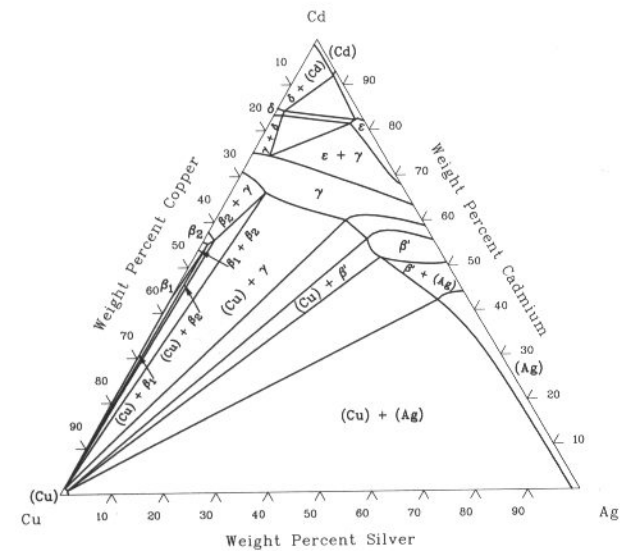

Ag-Cd-Zn liquidus projection with regions of primary crystallization [88Pet]

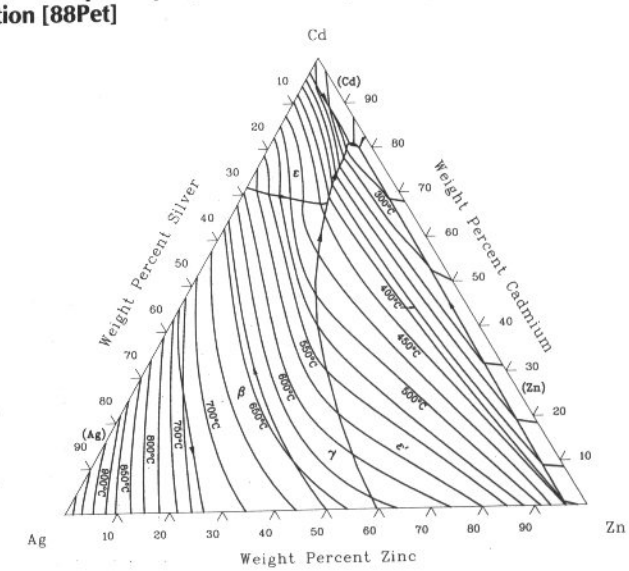

Ag-Cd-Zn isothermal section at 600 °C [88Pet]

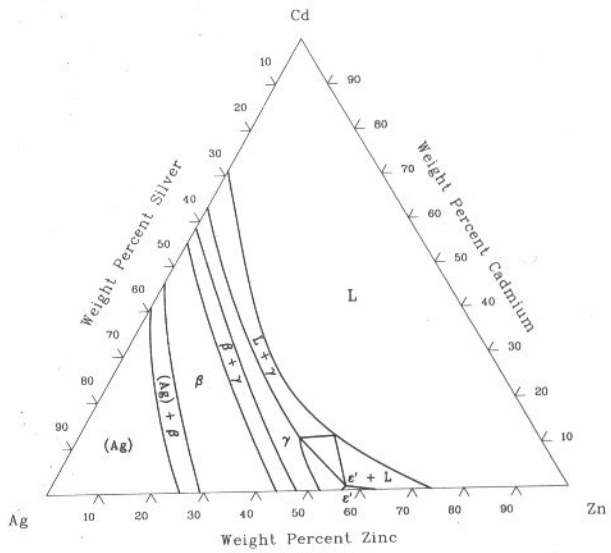

Ag-Cd-Zn isothermal section at 400 °C [88Pet]

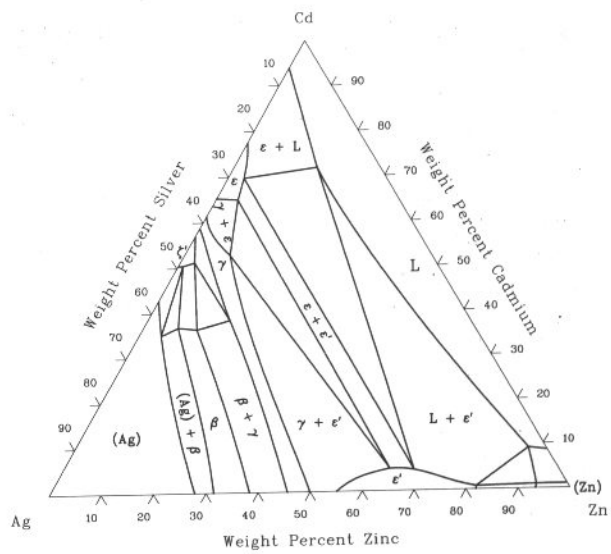

Ag-Cd-Zn isothermal section at 200 °C [88Pet]

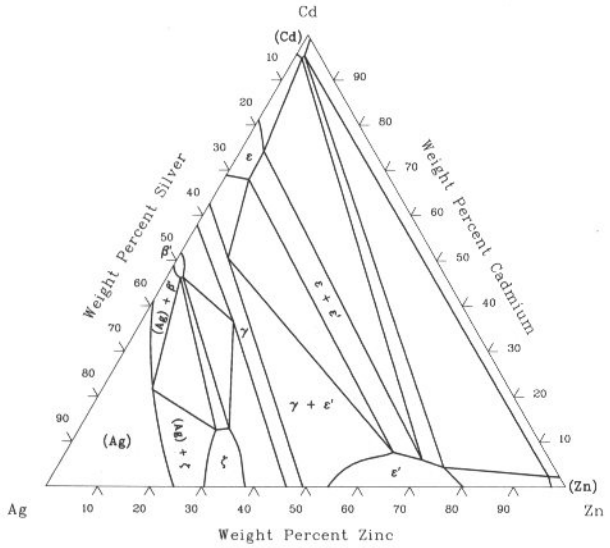

Ag-Cu-Zn isothermal section at 350 °C [88Pet]

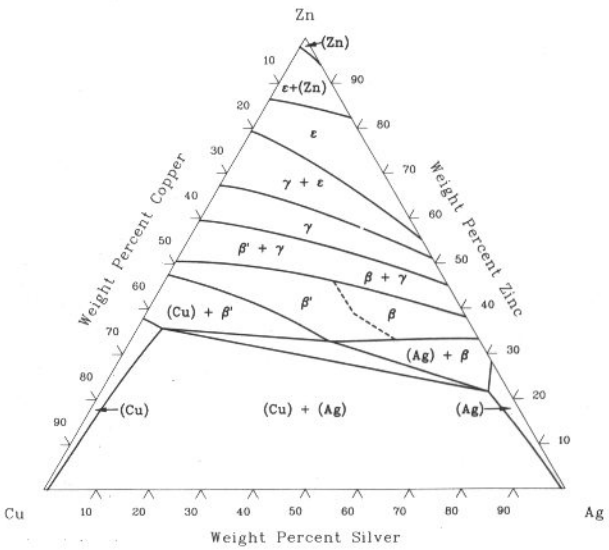

Ag-Cu-Zn liquidus projection [88Pet]

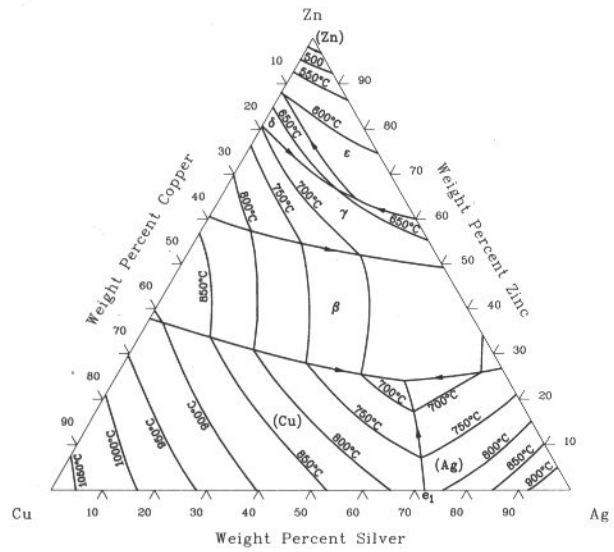

Ag-Pb-Sn [11Par]

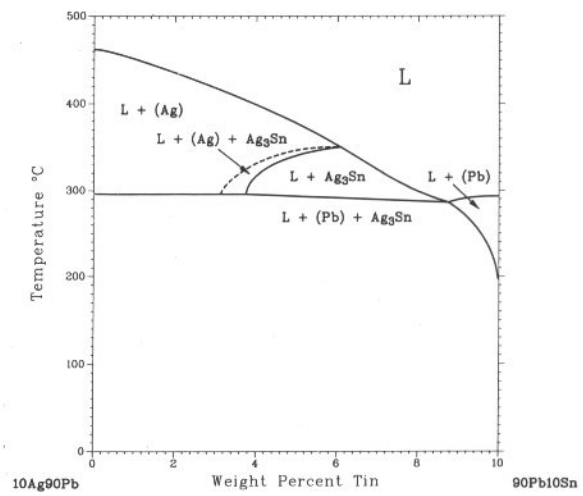

Ag-Cu-Zn isothermal section at 600 °C [88Pet]

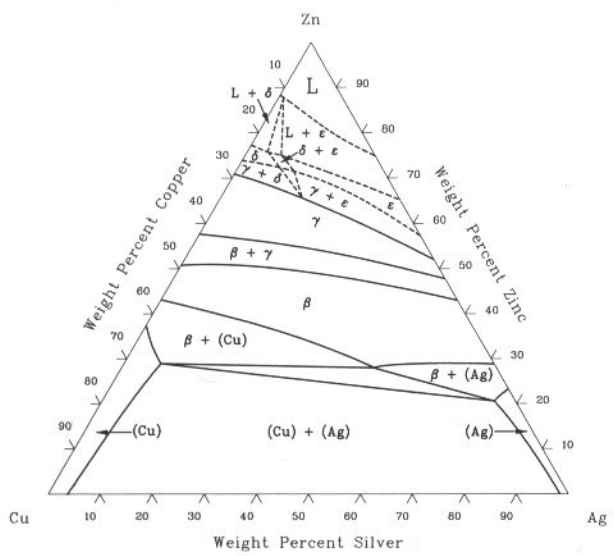

Ag-Pb-Sn [11Par]

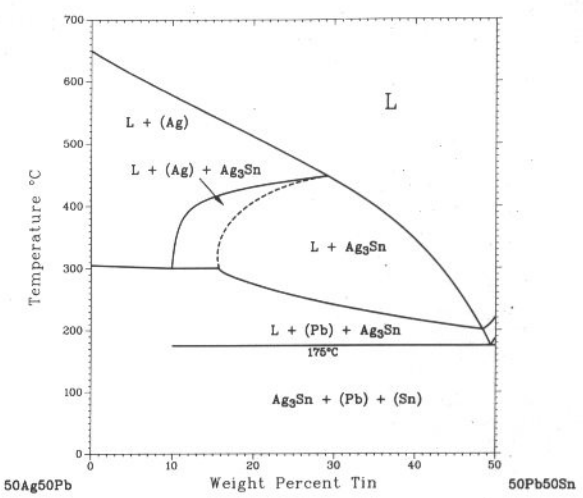

Ag-Pb-Sn [11Par]

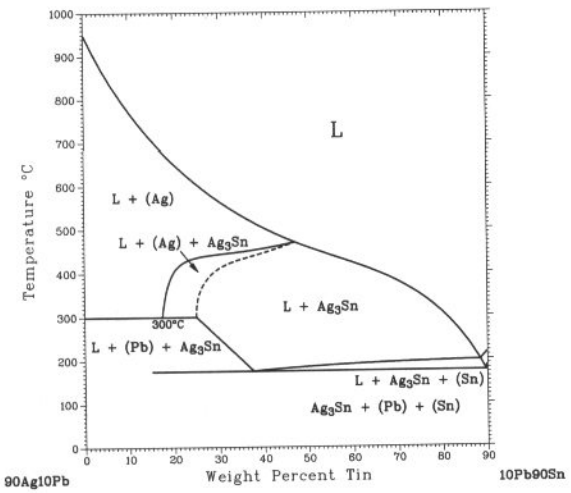

Al-Cr-Fe liquidus projection [88Ray]

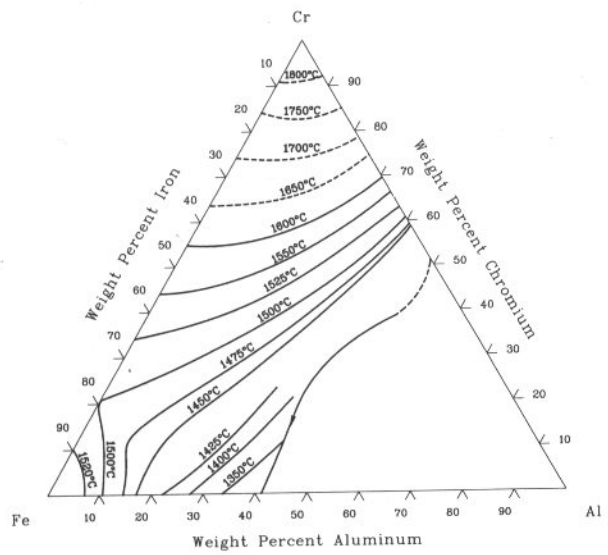

Al-Cr-Fe isothermal section at 900 °C [88Ray]

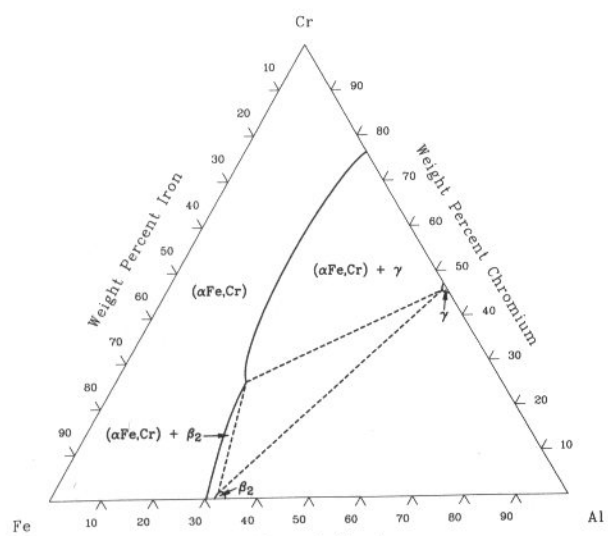

Al-Cr-Fe isothermal section at 750 °C [88Ray]

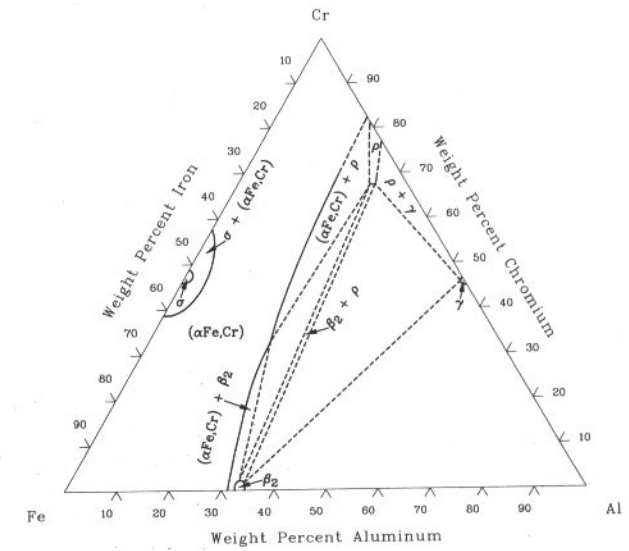

Al-Cr-Fe isothermal section at 600 °C [88Ray]

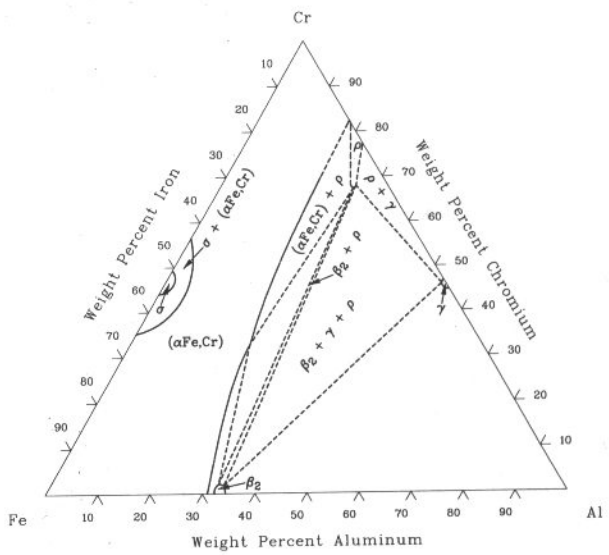

Al-Cr-Mn isothermal section at 690 °C [73Wil]

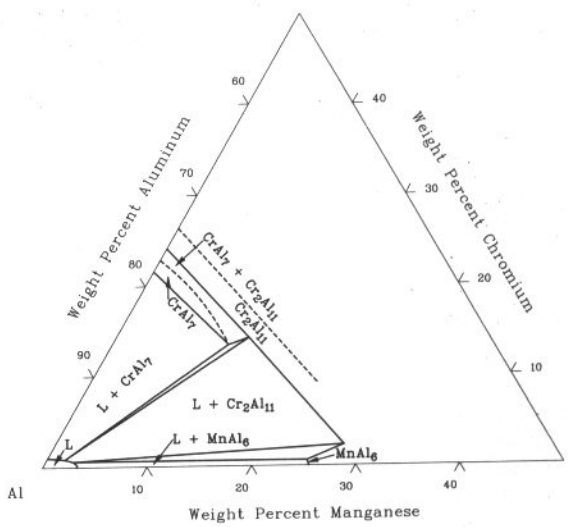

Al-Cr-Mn isothermal section at 600 °C [73Wil]

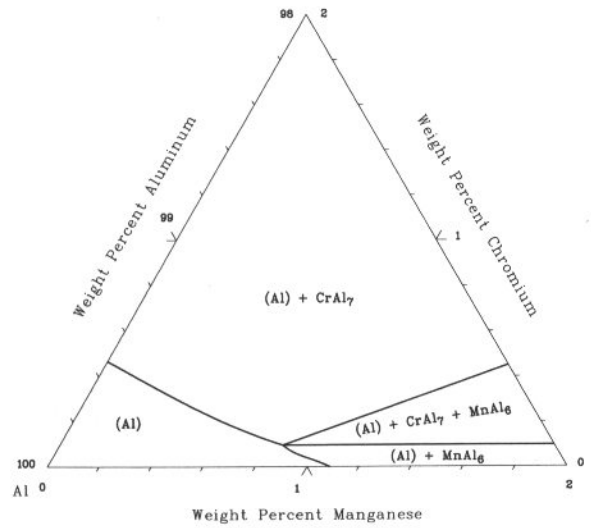

Al-Cr-Mn isothermal section at 550 °C [73Wil]

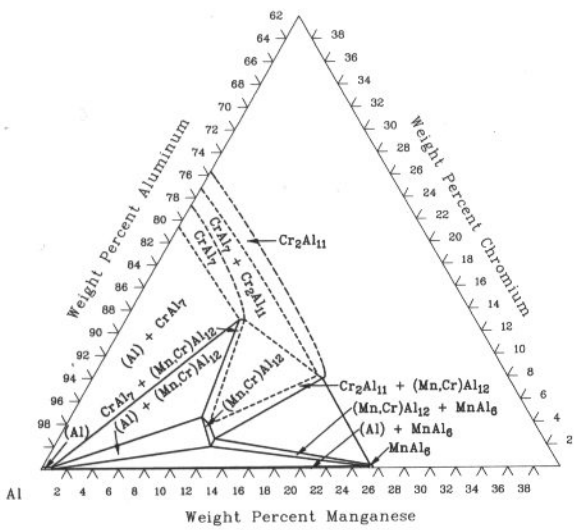

Al-Cr-Mn (Al) isothermal section at 550 °C [73Wil]

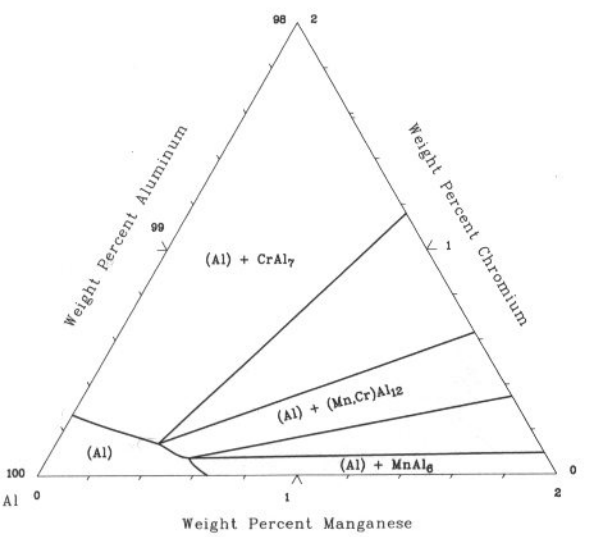

Al-Cr-Ni isothermal section at 1150 °C [87Ofo]

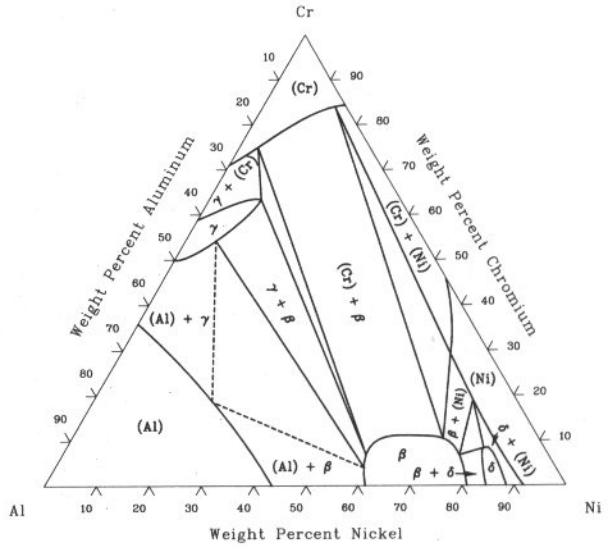

Al-Cr-Ti isothermal section at 760 °C [56Zwi]

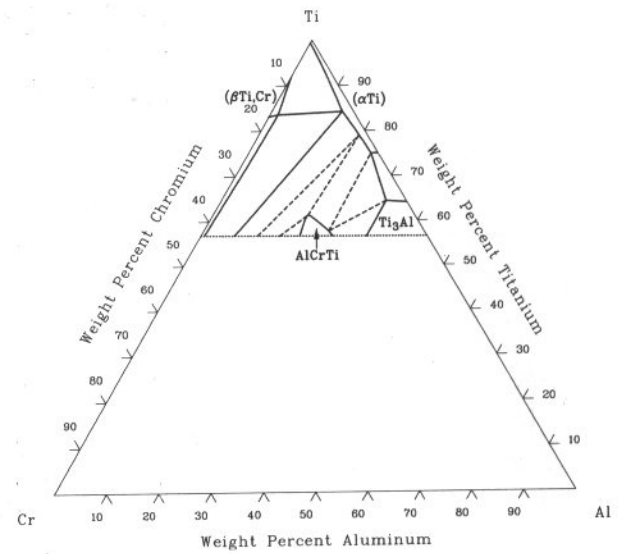

Al-Cu-Fe liquidus projection [73Wil]

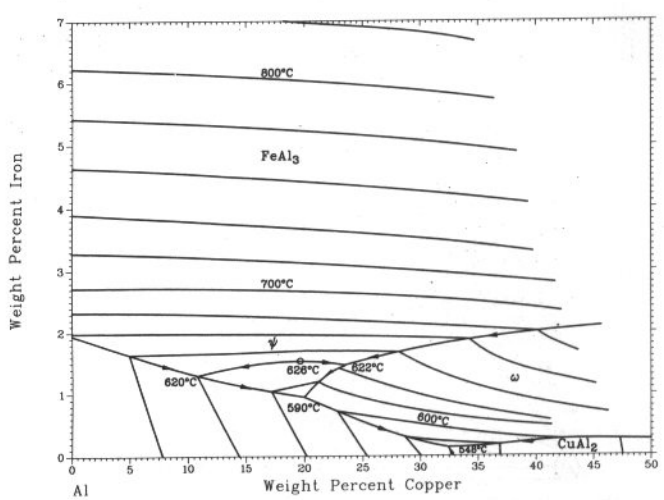

Al-Cu-Fe solidus projection [73Wil]

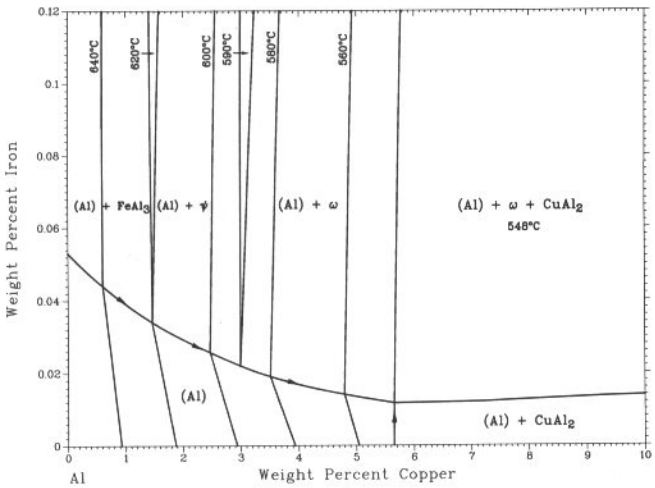

Al-Cu-Mn liquidus projection [73Wil]

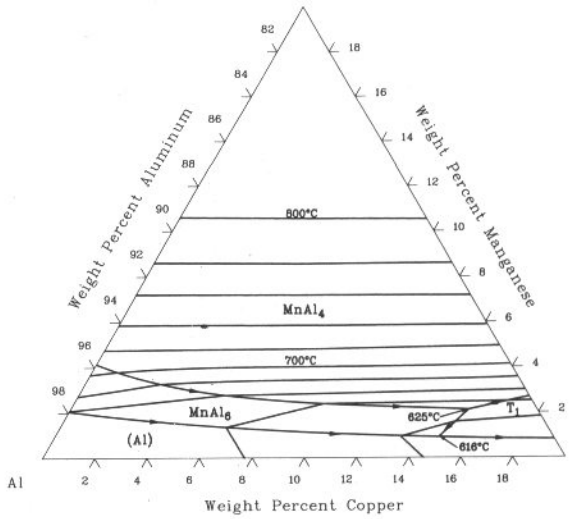

Al-Cu-Fe solvus projection [73Wil]

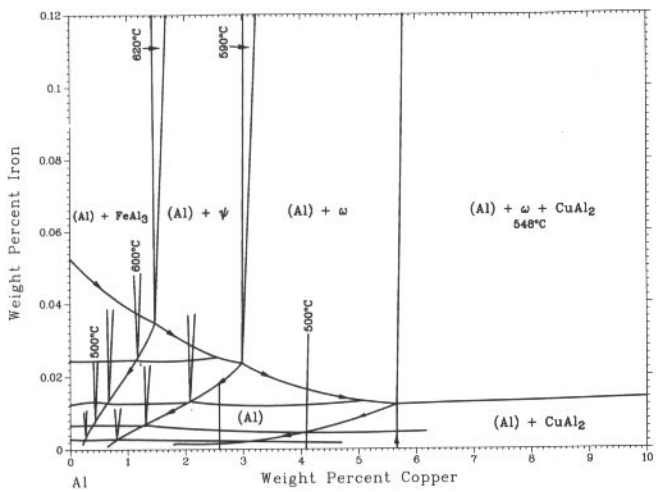

Al-Cu-Mn solidus projection [73Wil]

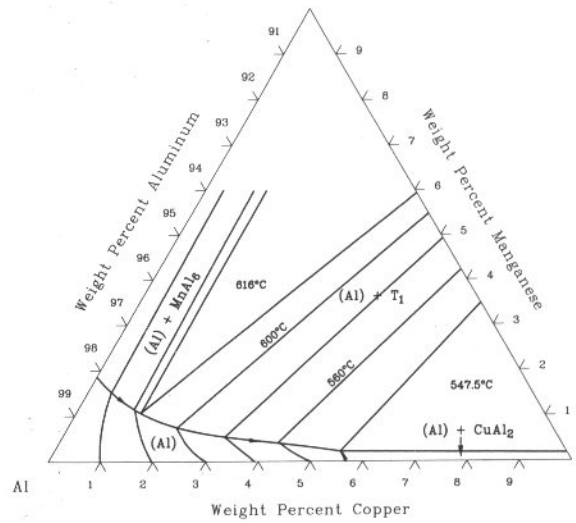

Al-Cu-Fe isothermal section at 600 °C [71Pre]

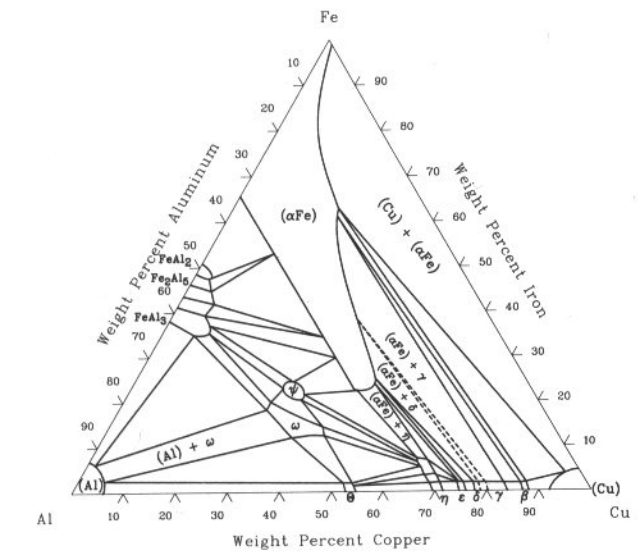

Al-Cu-Mn solvus projection [73Wil]

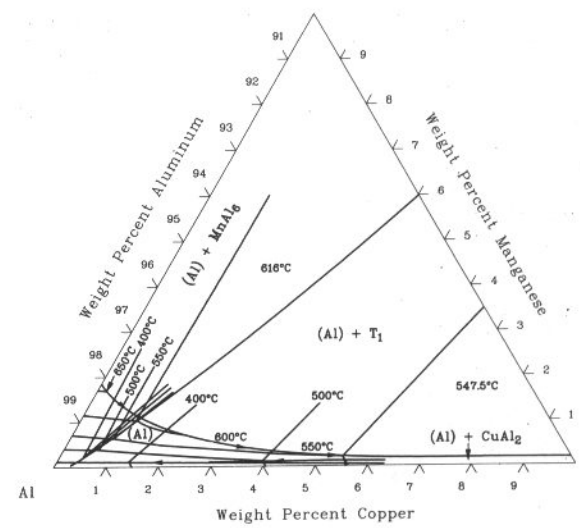

Al-Cu-Mn isothermal section at 950 °C [66Kos]

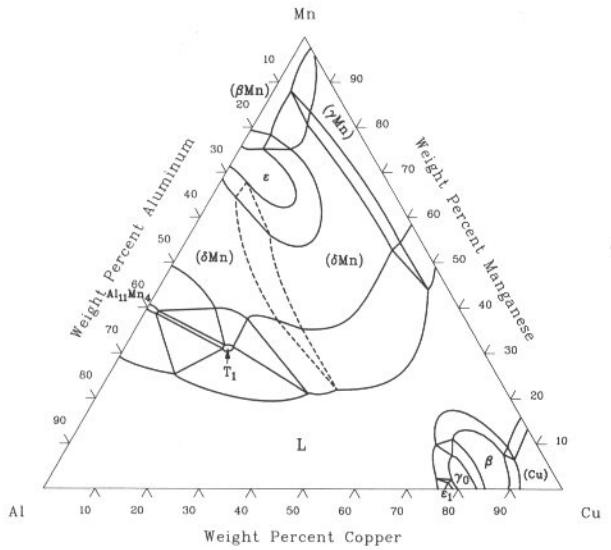

Al-Cu-Ni liquidus projection [73Wil]

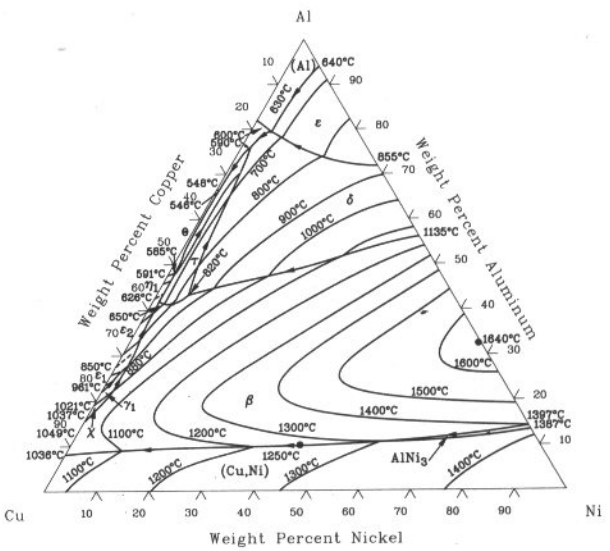

Al-Cu-Mn isothermal section at 700 °C [66Kos]

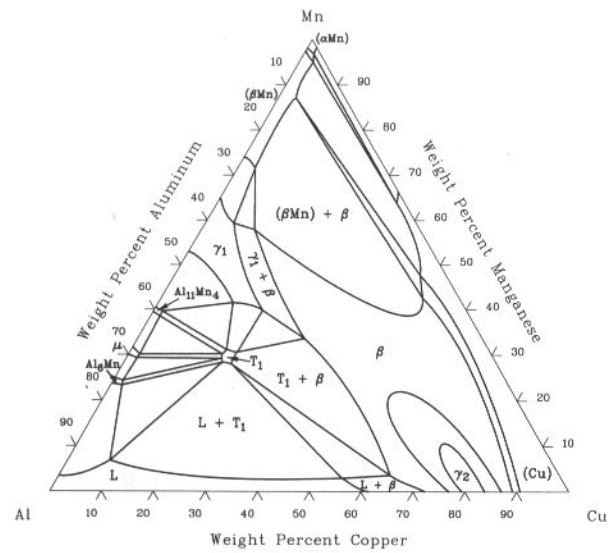

Al-Cu-Ni isothermal section at 900 °C [48Kos]

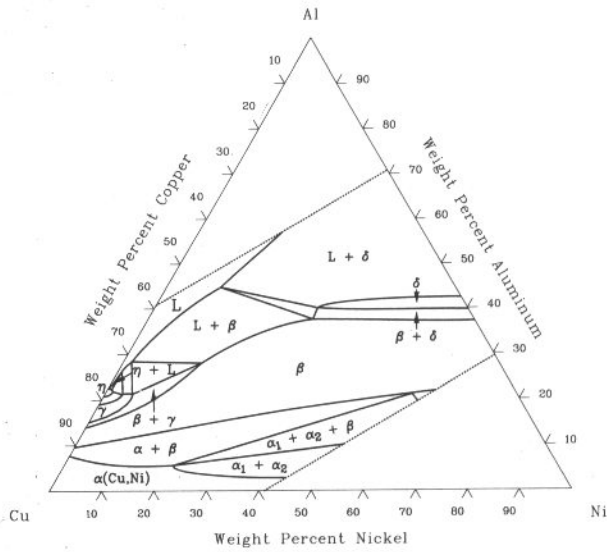

Al-Cu-Mn isothermal section at 25 °C [66Kos]

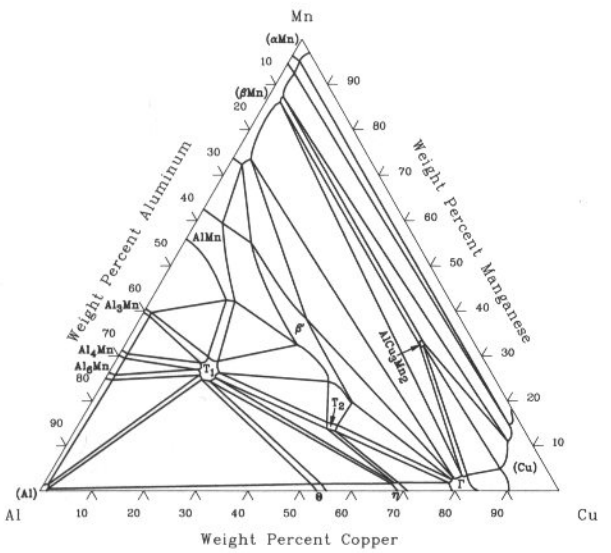

Al-Cu-Ni isothermal section at 700 °C [48Kos]

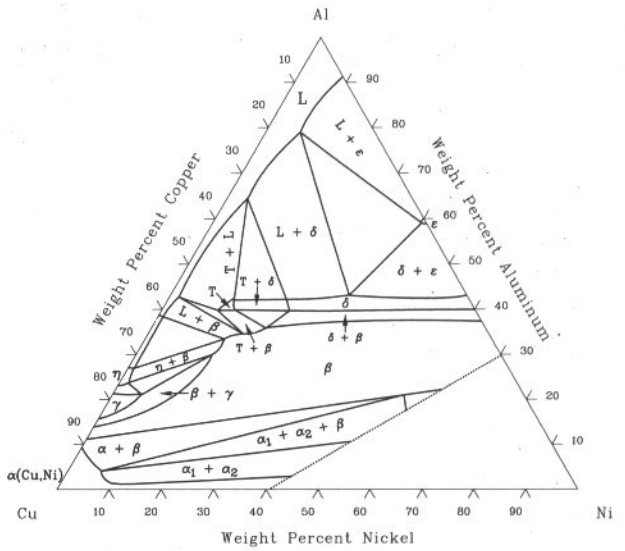

Al-Cu-Ni isothermal section at 500 °C [73Wil]

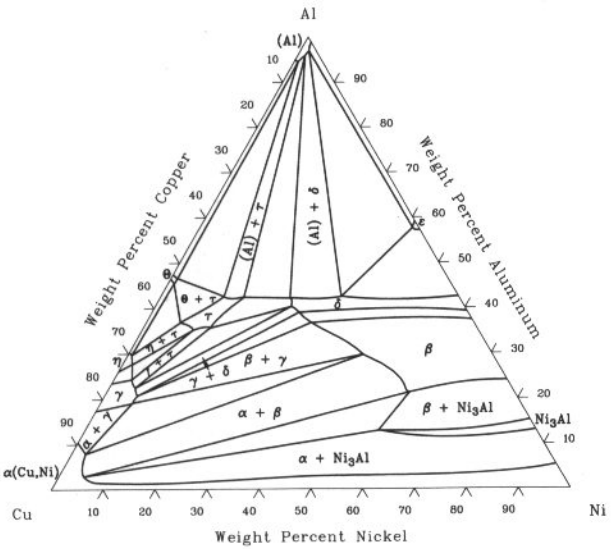

Al-Cu-Si isothermal section at 750 °C [48Wil]

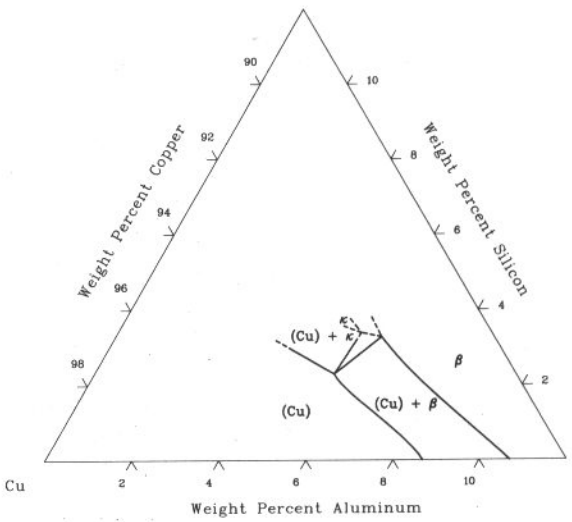

Al-Cu-Si liquidus projection [79Cha]

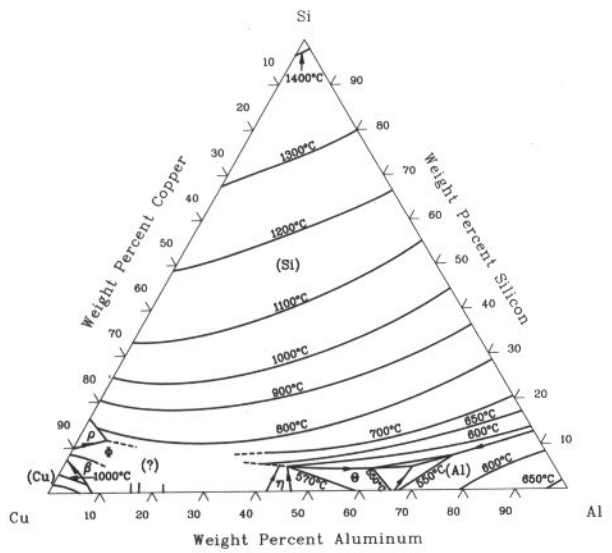

Al-Cu-Si isothermal section at 400 °C [48Wil]

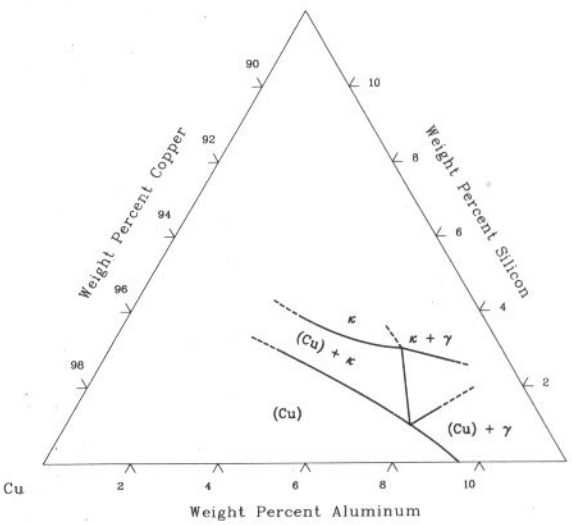

Al-Cu-Si isothermal section at 955 °C [48Wil]

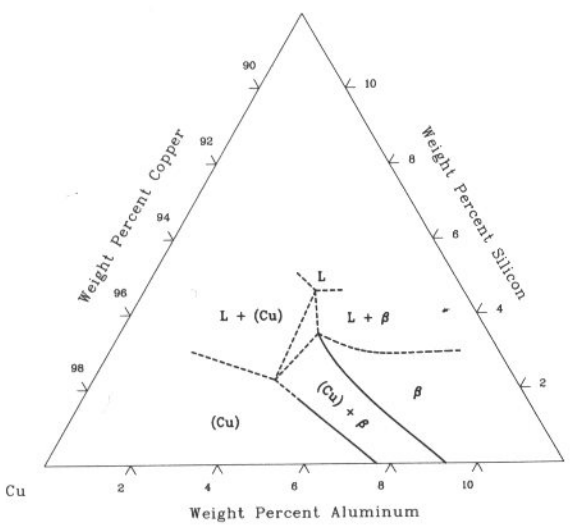

Al-Cu-Zn liquidus projection [73Wil]

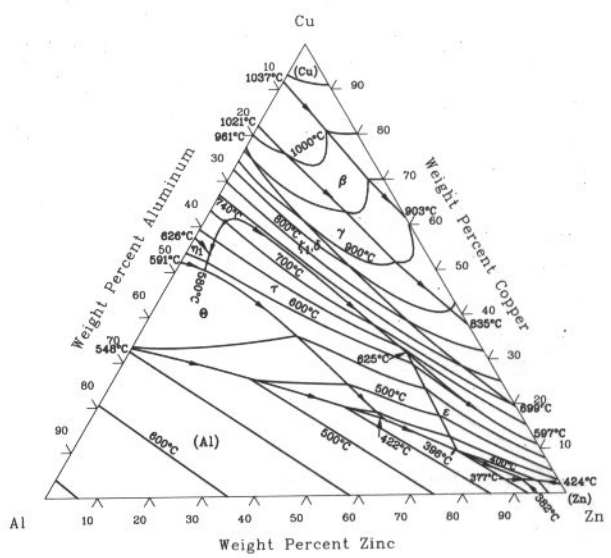

Al-Cu-Zn isothermal section at 700 °C [73Wil]

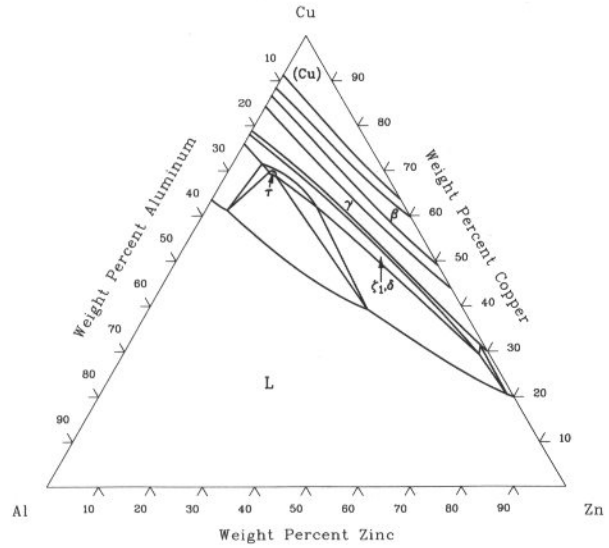

Al-Cu-Zn isothermal section at 200 °C [73Wil]

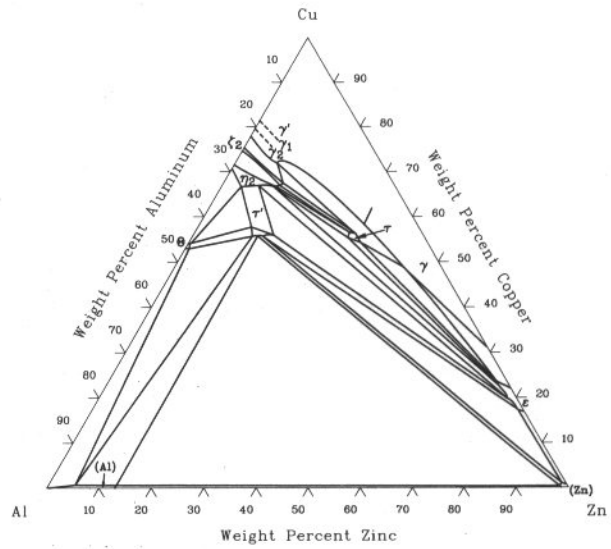

Al-Cu-Zn isothermal section at 550 °C [73Wil]

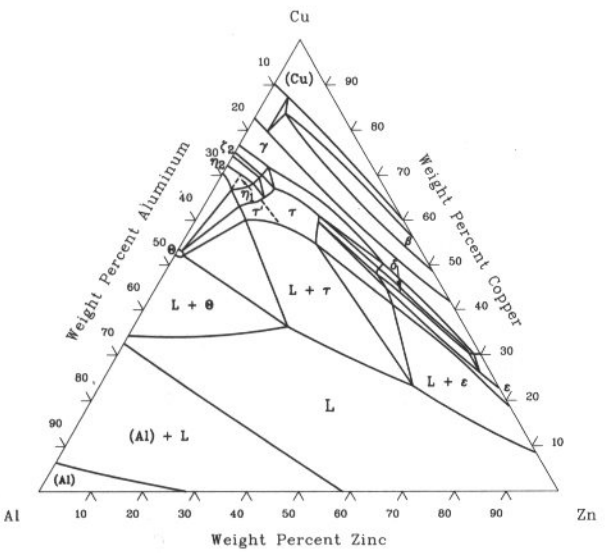

Al-Fe-Mn (Al) liquidus projection [88Ray]

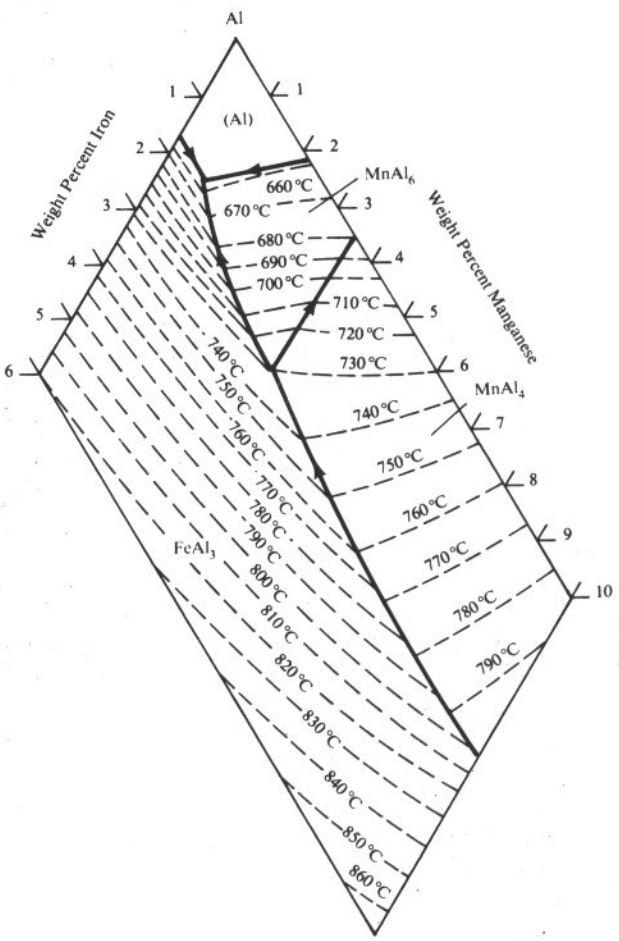

Al-Cu-Zn isothermal section at 350 °C [73Wil]

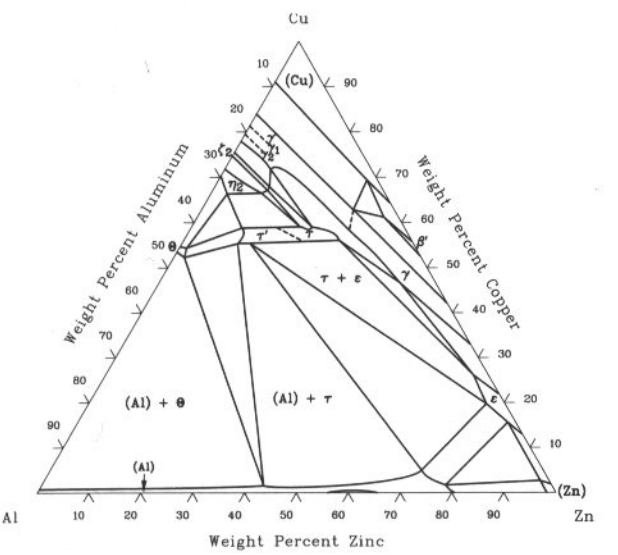

Al-Fe-Mn liquidus projection [88Ray]

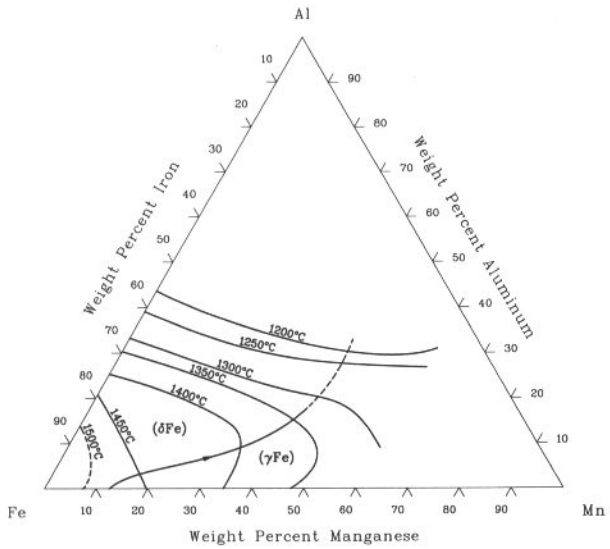

Al-Fe-Ni liquidus projection [88Ray]

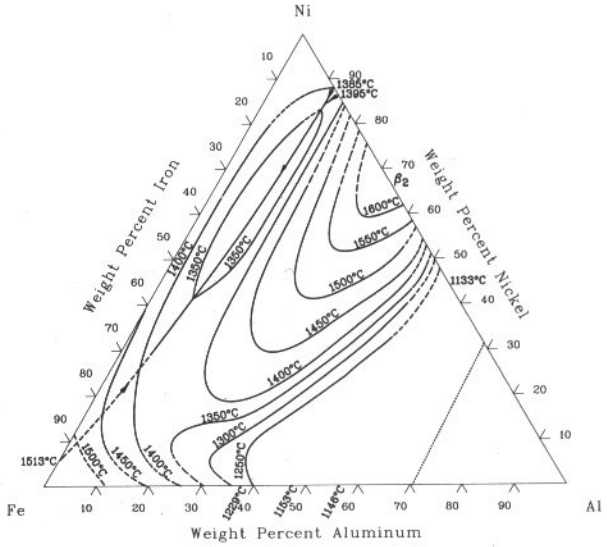

Al-Fe-Mn isothermal section at 1000 °C [88Ray]

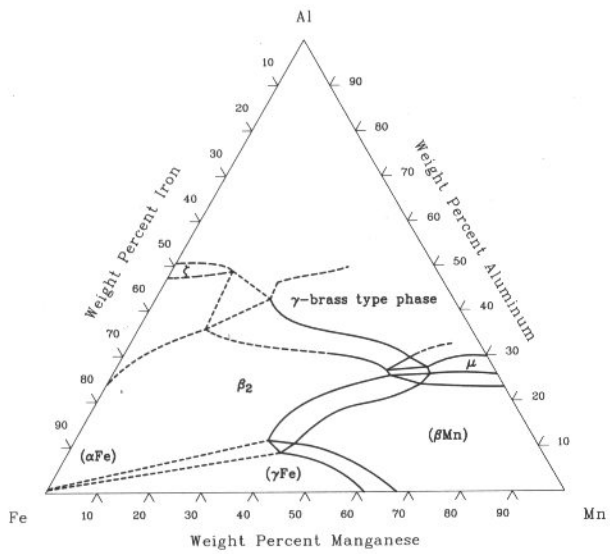

Al-Fe-Ni (Al) liquidus projection [88Ray]

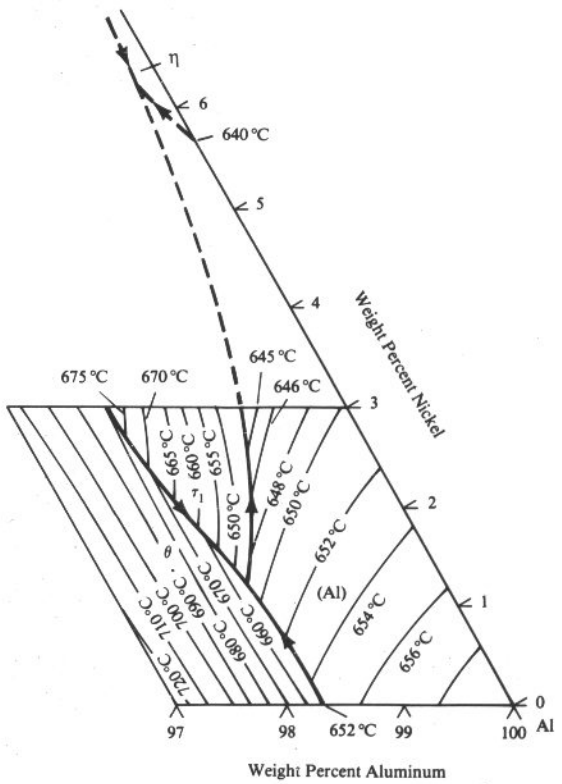

Al-Fe-Mn isothermal section at 600 °C [88Ray]

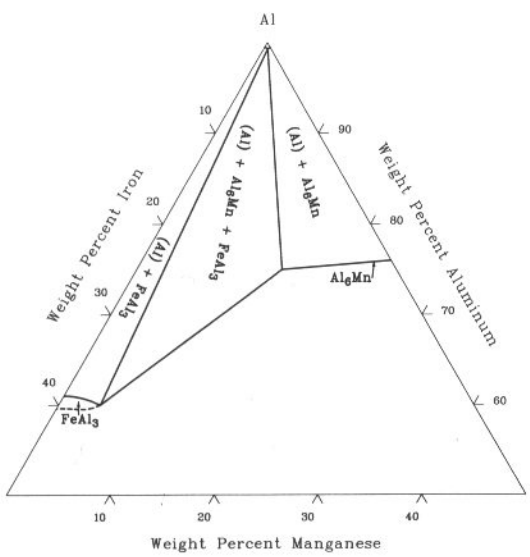

Al-Fe-Ni isothermal section at 1250 °C [88Ray]

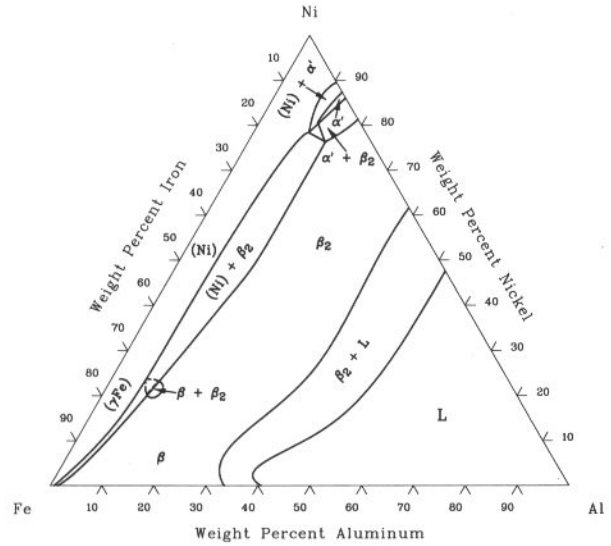

Al-Fe-Ni isothermal section at 600 °C [88Ray]

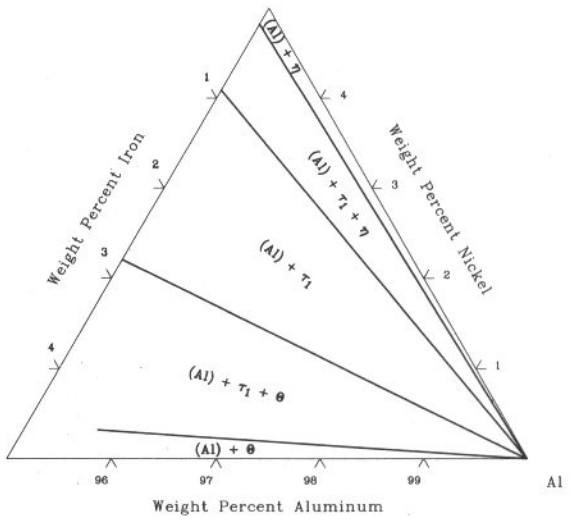

Al-Fe-Ni isothermal section at 950 °C [88Ray]

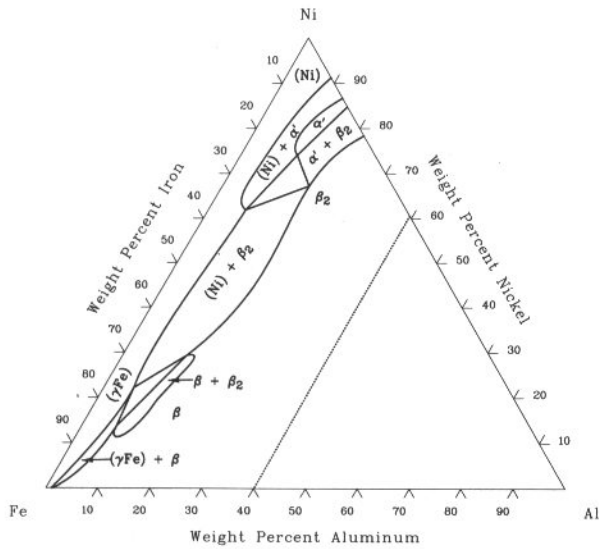

Al-Fe-Si liquidus projection [88Ray]

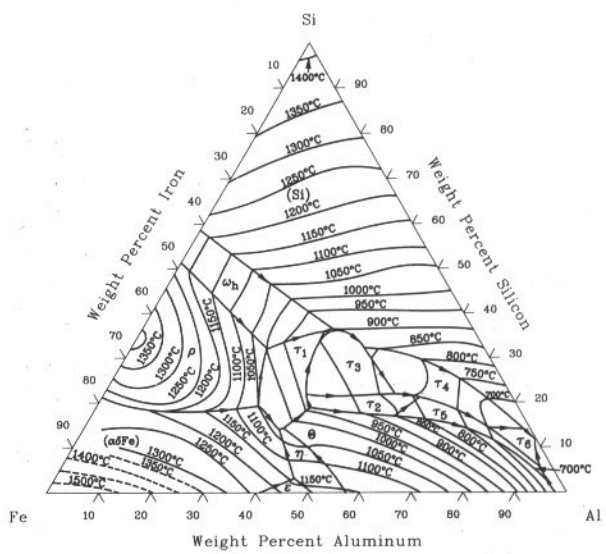

Al-Fe-Ni isothermal section at 750 °C [88Ray]

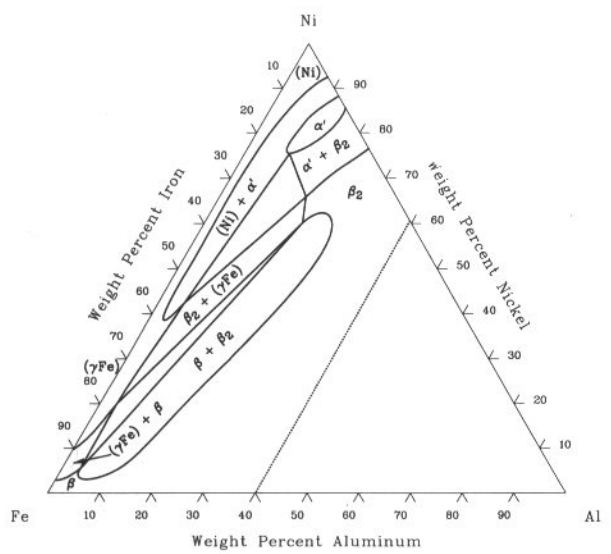

Al-Fe-Si isothermal section at 1000 °C [88Ray]

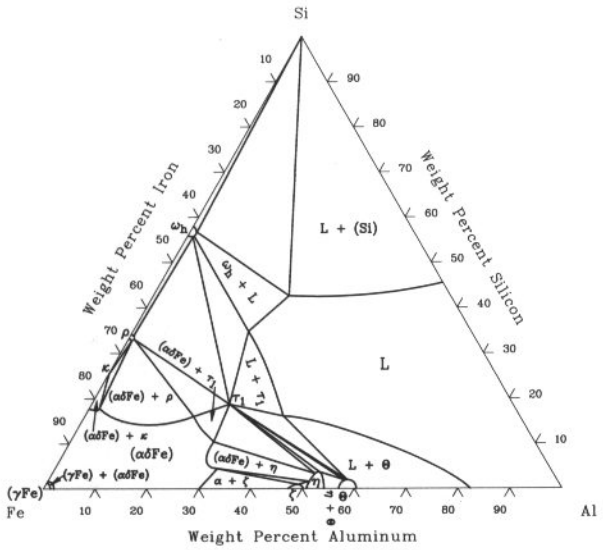

Al-Fe-Si isothermal section at 550 °C [88Ray]

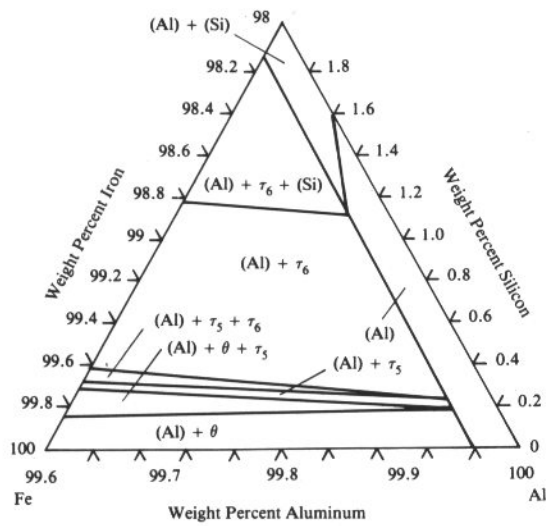

Al-Fe-Si isothermal section at 450 °C [88Ray]

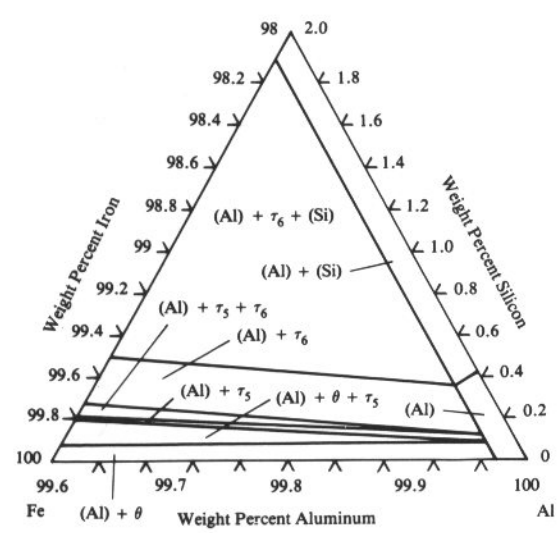

Al-Fe-Zn isothermal section at 700 °C [70Kos]

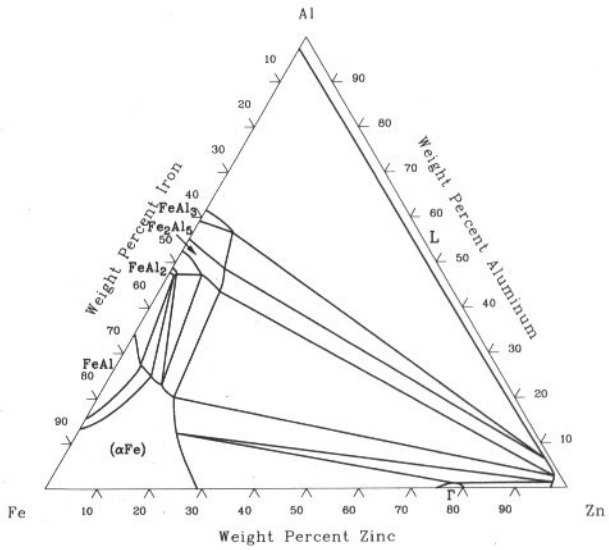

Al-Fe-Zn isothermal section at 500 °C [70Kos]

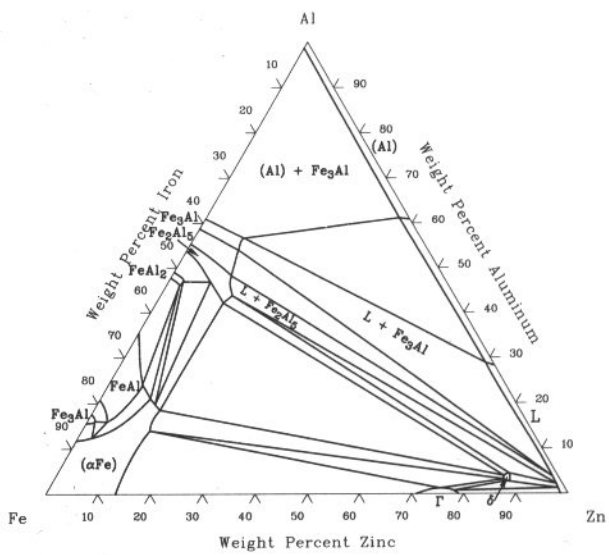

Al-Fe-Zn isothermal section at 330 °C [70Kos]

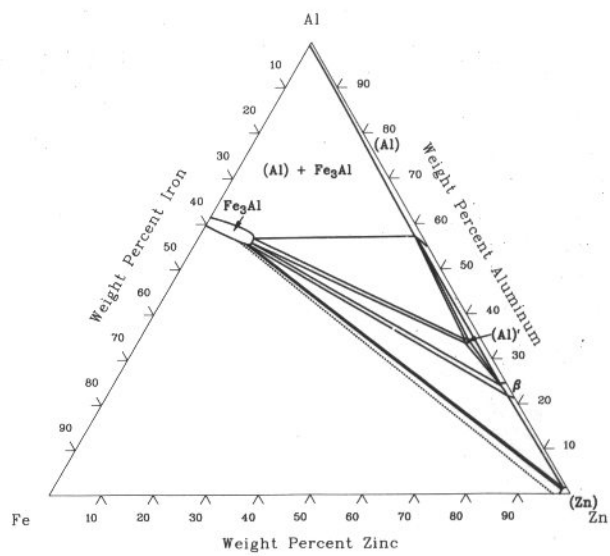

Al-Mg-Mn liquidus projection [73Wil]

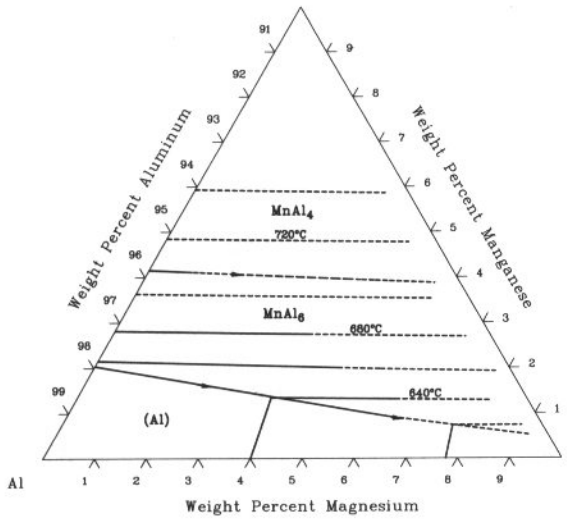

Al-Mg-Mn isothermal section at 400 °C [73Wil]

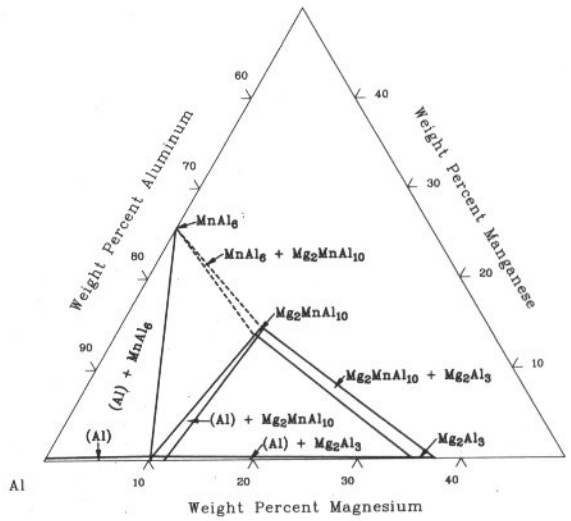

Al-Mg-Mn isothermal section at 750 °C [88Sim]

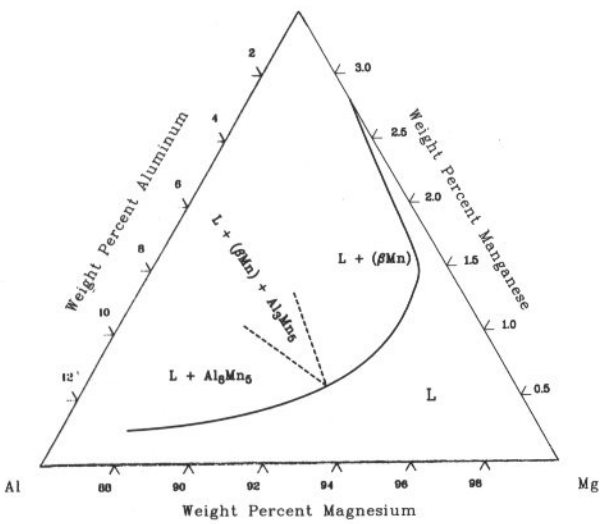

Al-Mg-Si liquidus projection [73Wil]

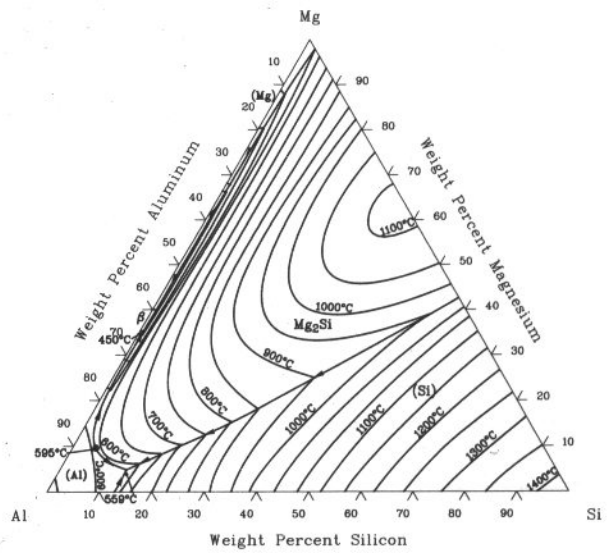

Al-Mg-Mn isothermal section at 670 °C [88Sim]

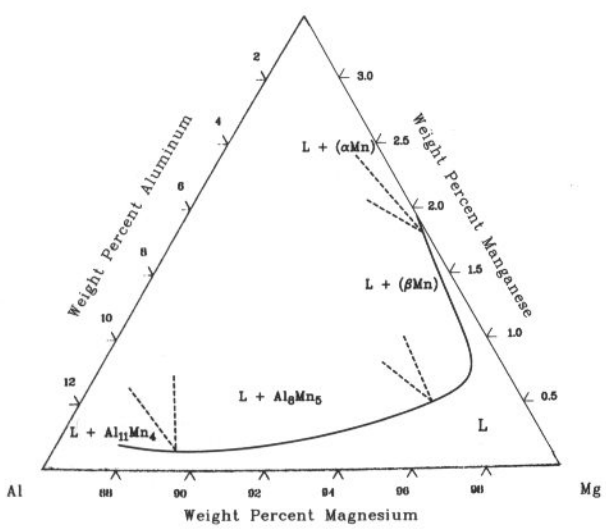

Al-Mg-Si solidus projection [73Wil]

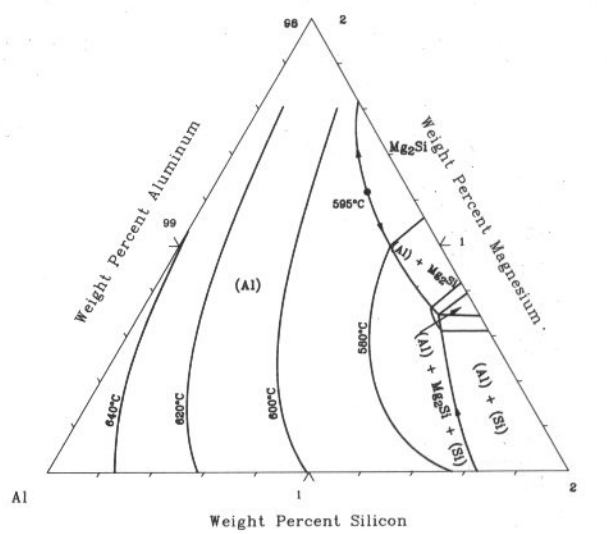

Al-Mg-Si solvus projection [73Wil]

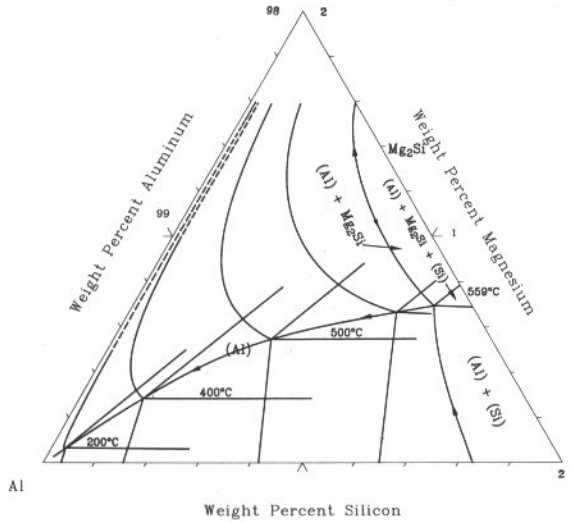

Al-Mg-Si isothermal section at 800 °C [88Rok]

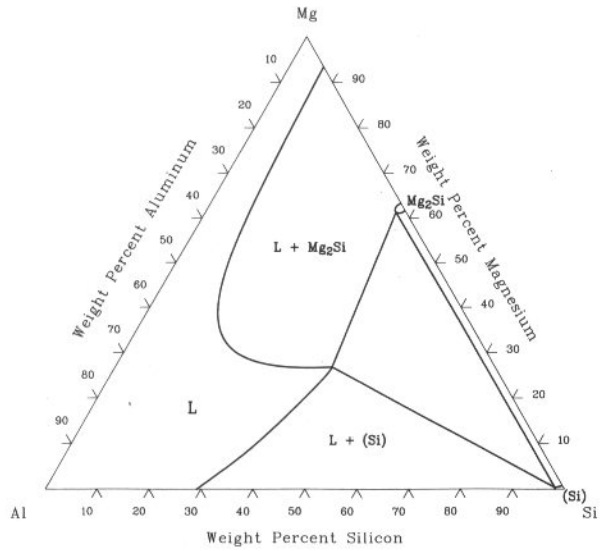

Al-Mg-Si isothermal section at 430 °C [88Rok]

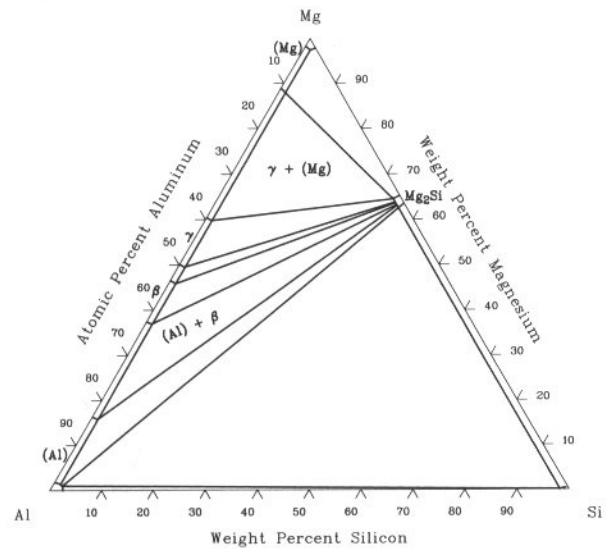

Al-Mg-Zn liquidus projection [73Wil]

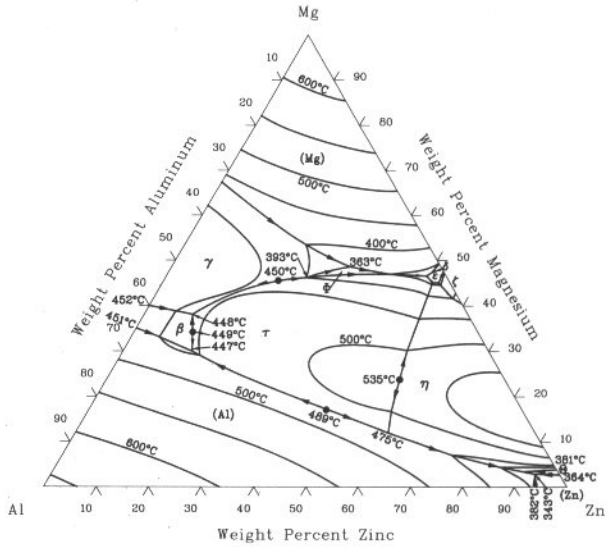

Al-Mg-Zn solvus projection [73Wil]

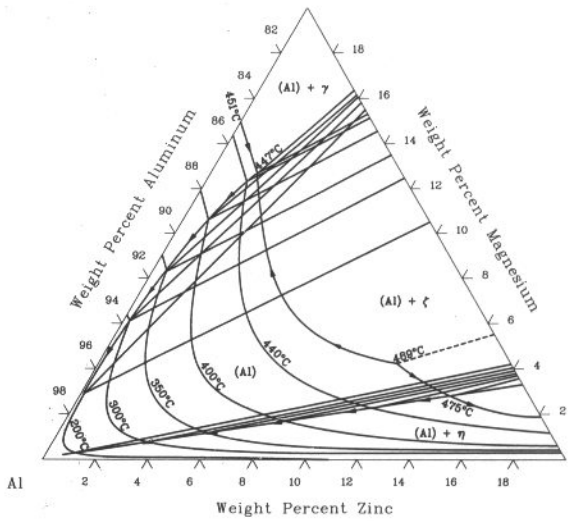

Al-Mg-Zn solidus projection [73Wil]

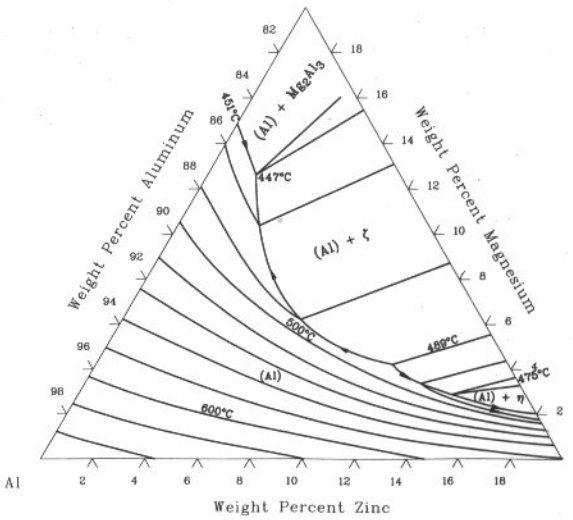

Al-Mg-Zn isothermal section at 335 °C [73Wil]

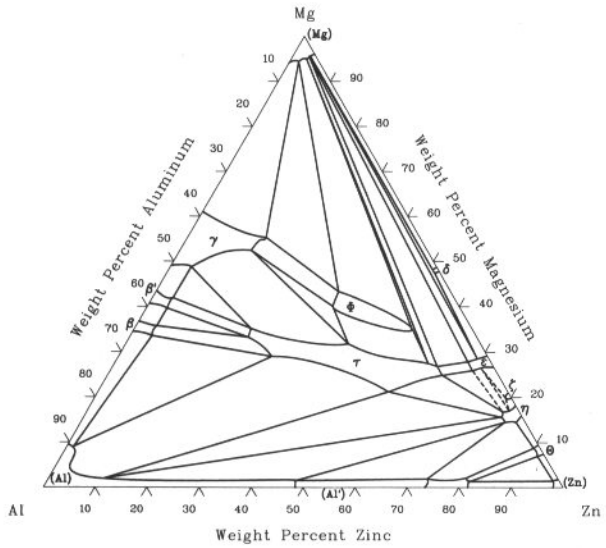

Al-Mn-Si solidus projection {73Will]

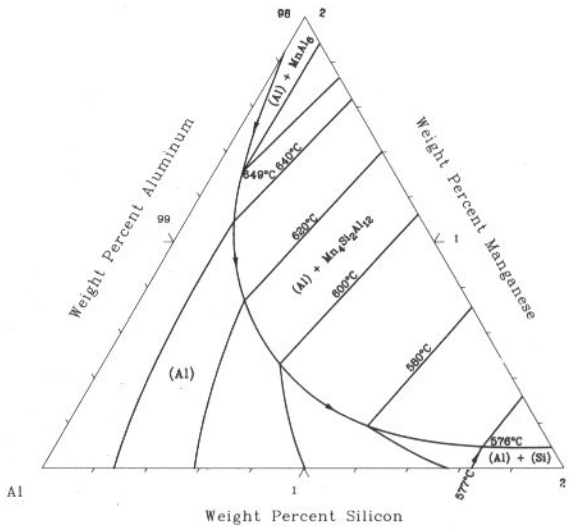

Al-Mg-Zn isothermal section at 20 °C [36Kos]

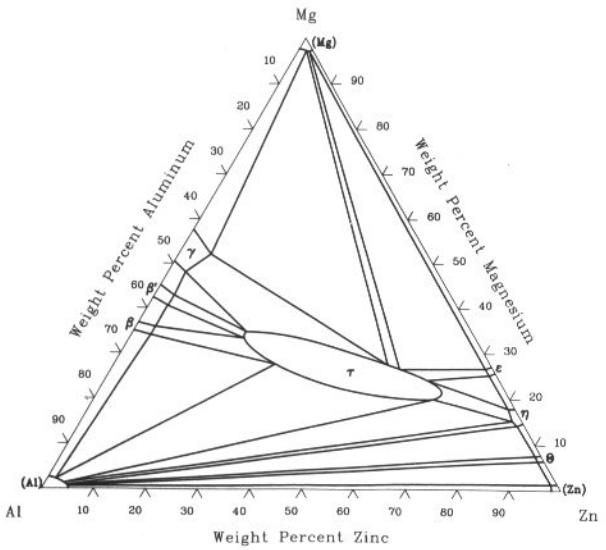

Al-Mn-Si isothermal section at 800 °C [64Kus]

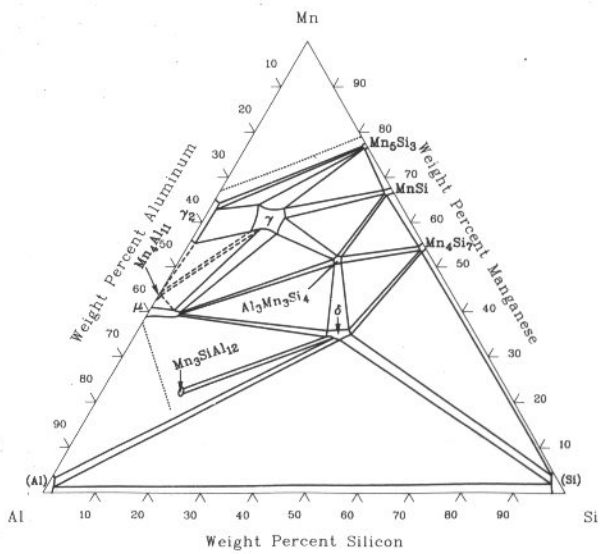

Al-Mn-Si liquidus projection [73Wil]

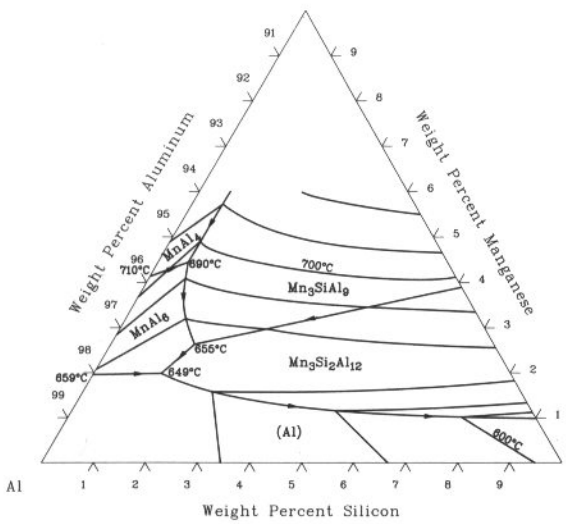

Al-Mn-Si isothermal section at 460 °C [73Wil]

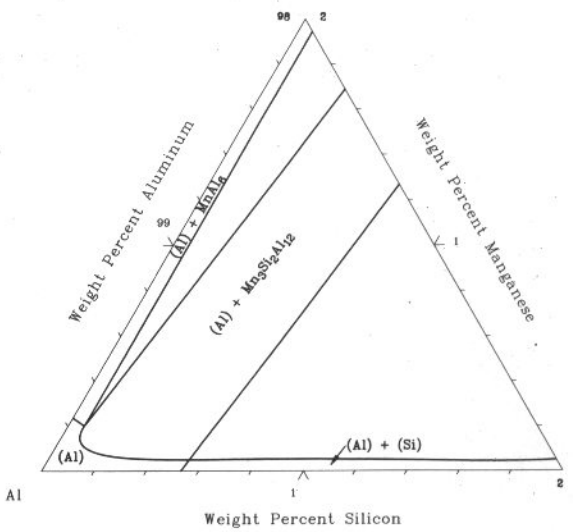

Al-Mo-Ni isothermal section at 1260 °C [84Mir]

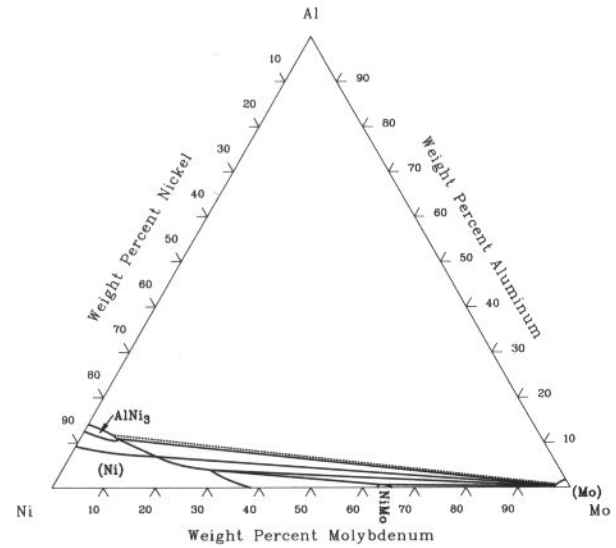

Al-Mo-Ni isothermal section at 1093 °C [84Mir]

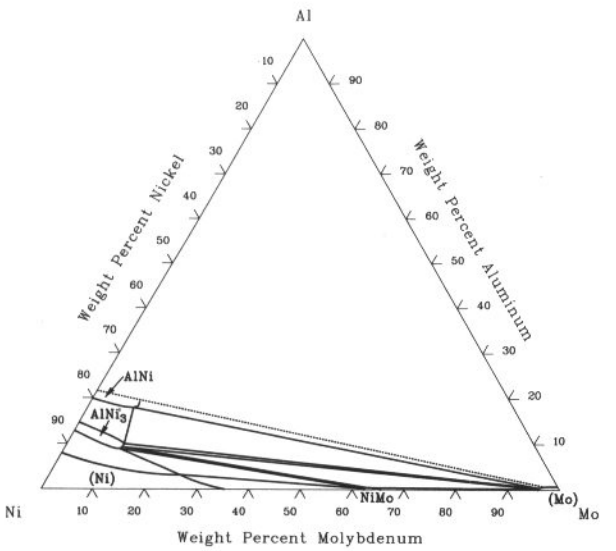

Al-Mo-Ni isothermal section at 927 °C [84Mir]

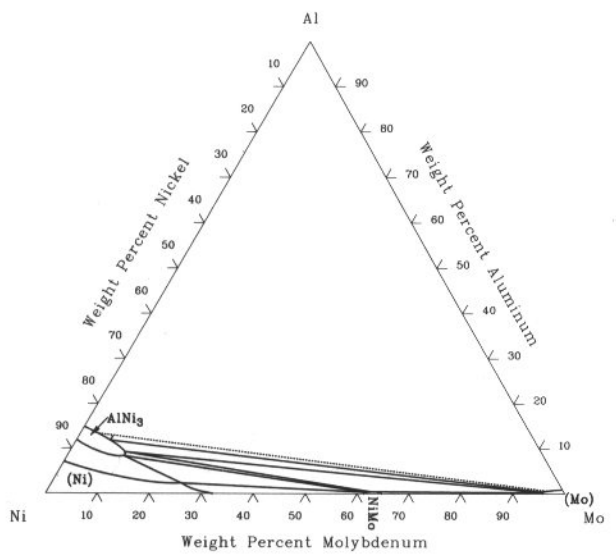

Al-Mo-Ti isothermal section at 925 °C [70Han]

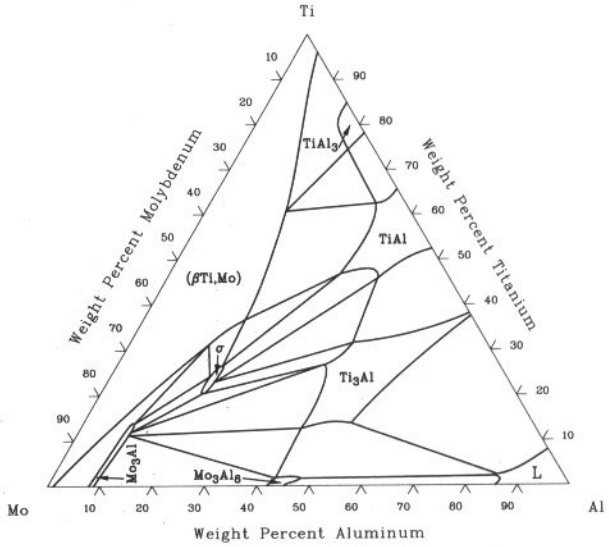

Al-Ni-Ti liquidus projection [85Nas]

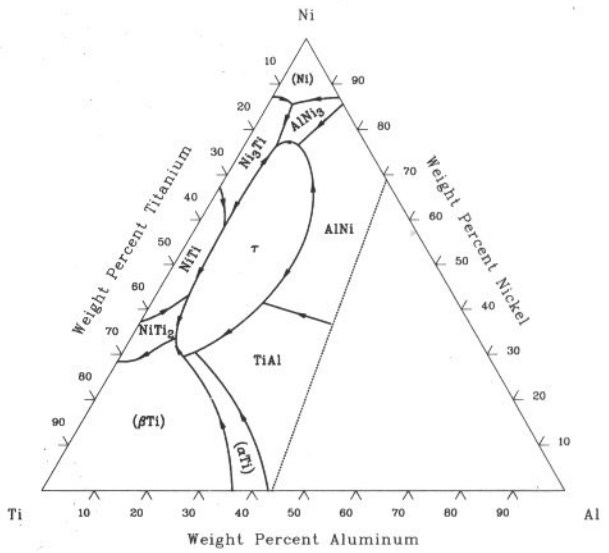

Al-Ni-Ti isothermal section at 900 °C [85Nas]

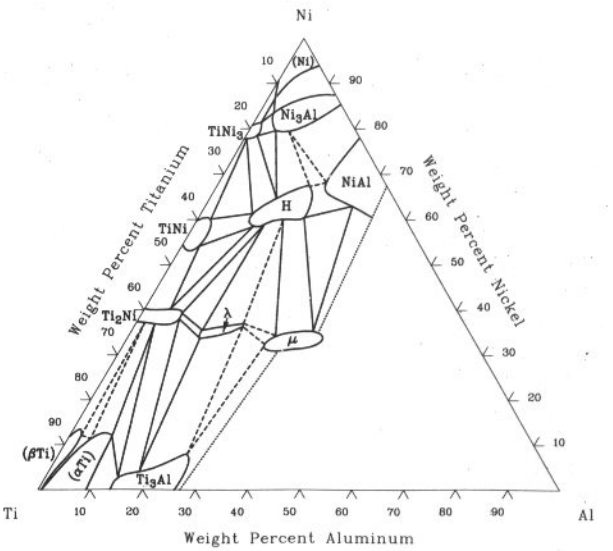

Al-Ni-Ti isothermal section at 800 °C [73Mar]

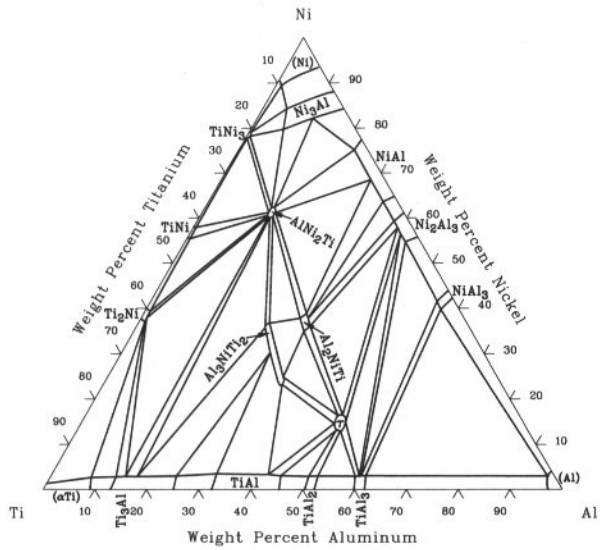

Al-Ni-Ti isothermal section at 600 °C [85Oma]

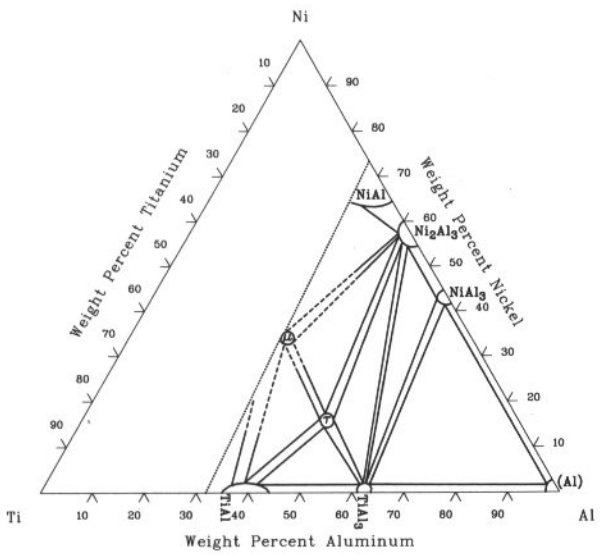

Al-Si-Zn liquidus projection [86Mey]

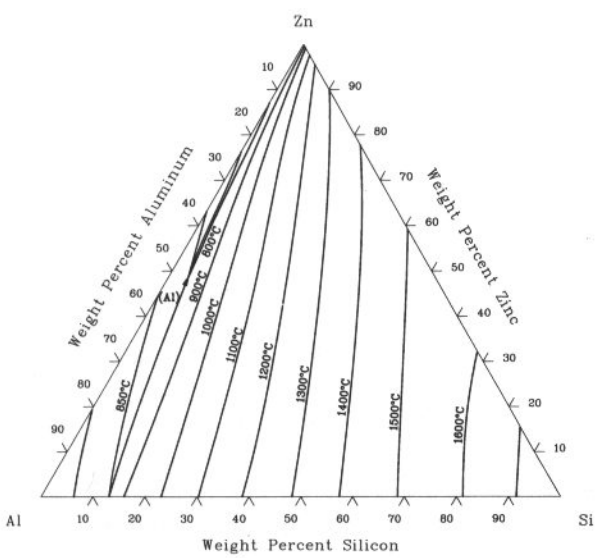

Al-Si-Zn schematic liquidus projection

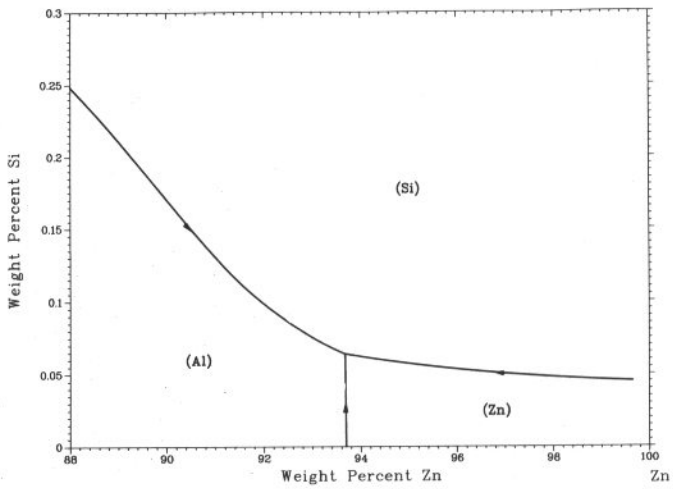

Al-Si-Zn isothermal section at 527 °C [86Mey]

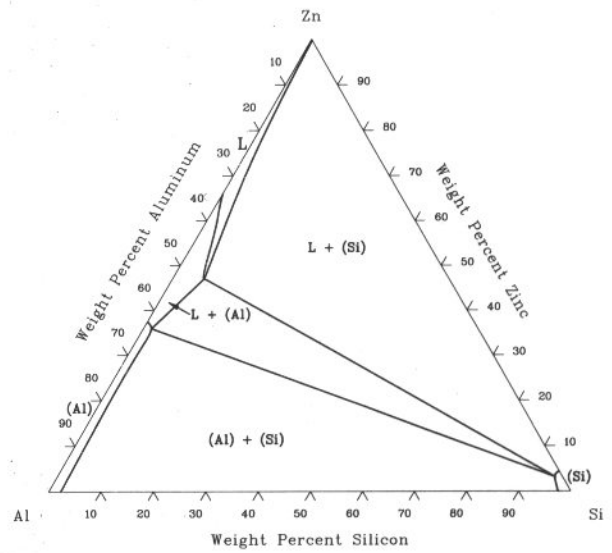

Al-Si-Zn isothermal section at 357 °C [86Mey]

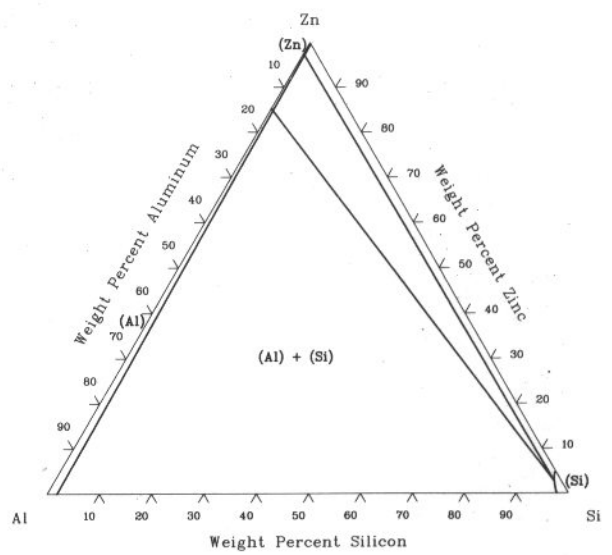

Al-Si-Zn isothermal section at 307 °C [86Mey]

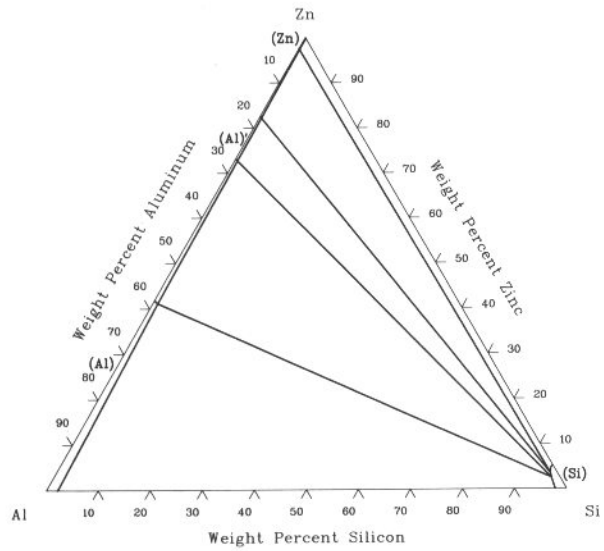

Al-Ti-V isothermal section at 980 °C [56Zwi]

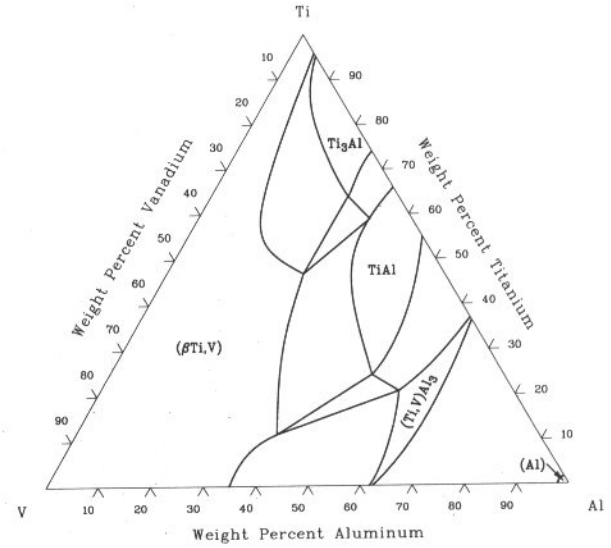

Al-Ti-V isothermal section at 1400 °C [61Far]

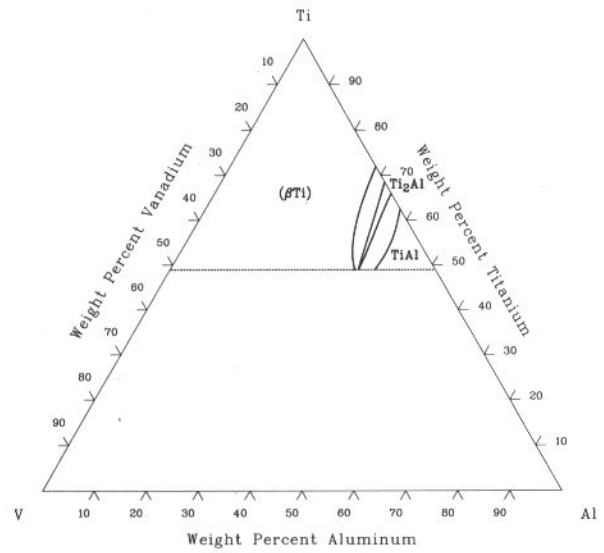

Al-Ti-V isothermal section at 900 °C [61Far]

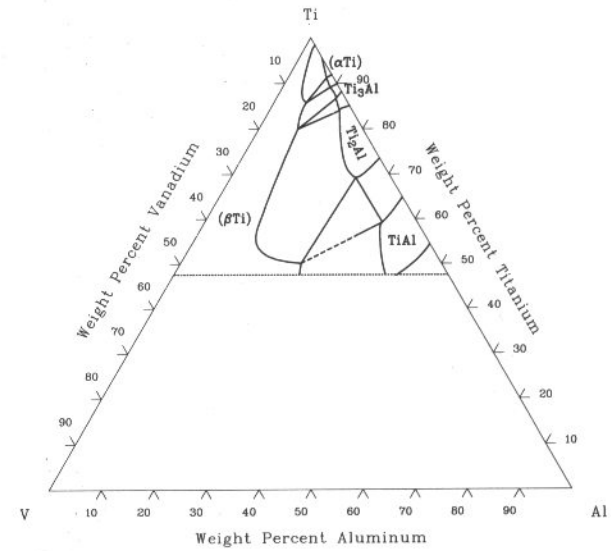

Al-Ti-V isothermal section at 1200 °C [61Far]

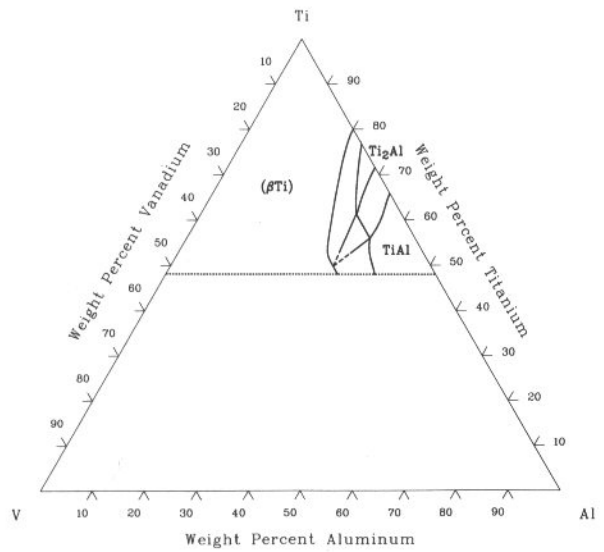

Au-Cu-Ni liquidus projection [90Pri]

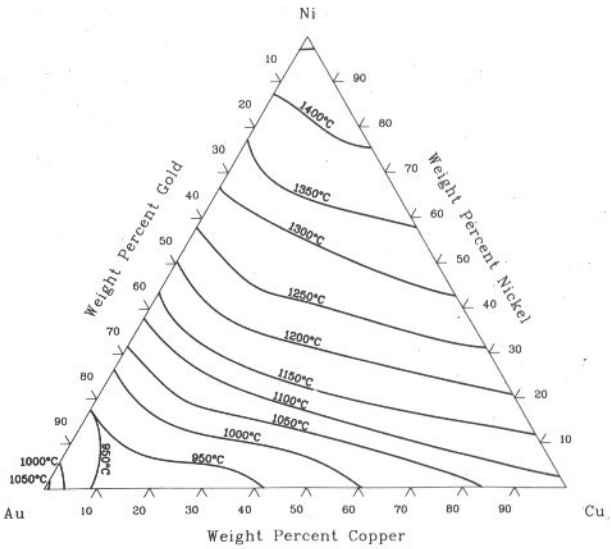

Au-Cu-Ni boundaries of solid-state miscibility gap [90Pri]

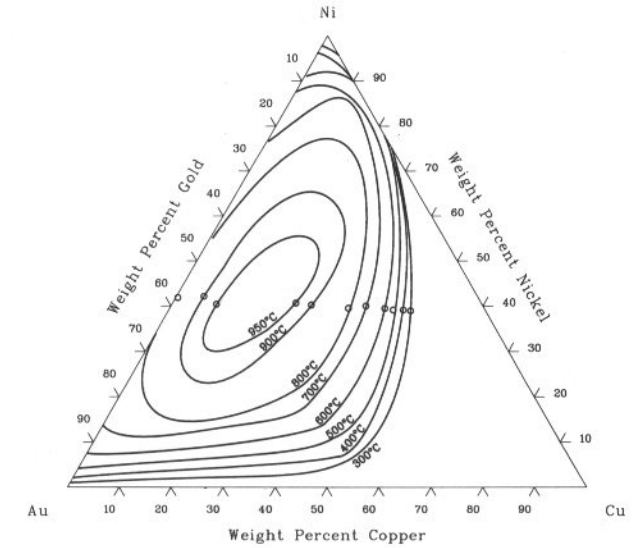

The open circles represent the compositions at which the gap closes.

Au-Cu-Ni boundary of miscibility gap at 400 °C, with tie lines [90Pri]

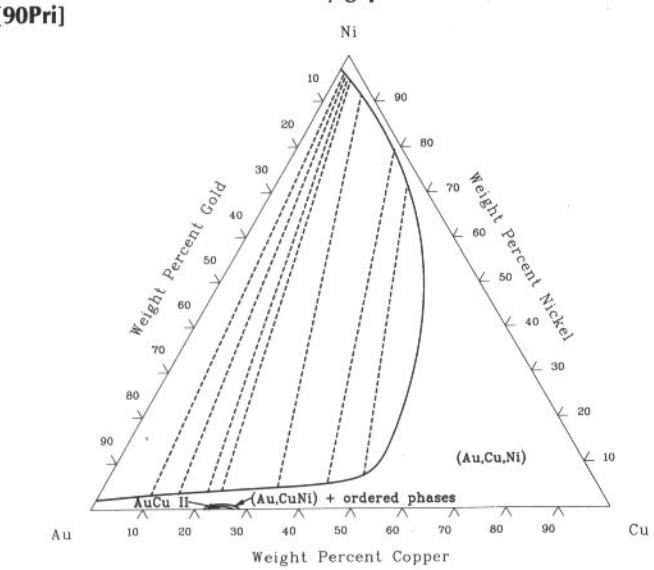

Au-Cu-Ni boundary of miscibility gap at 700 °C, with tie lines [90Pri]

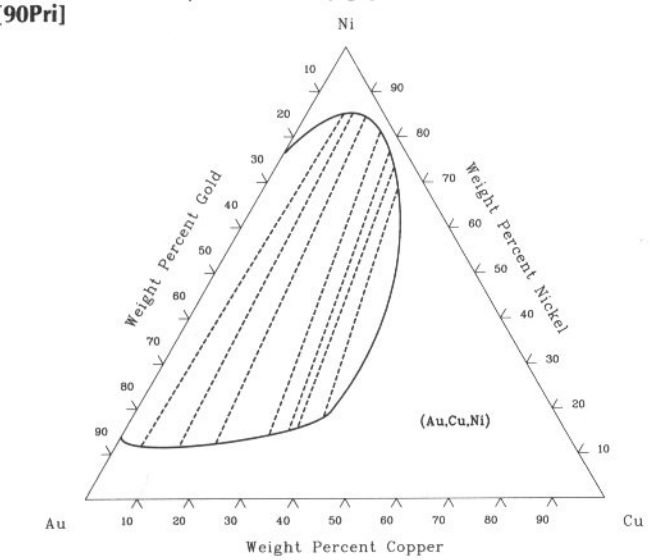

B-C-Fe liquidus projection [63Sta]

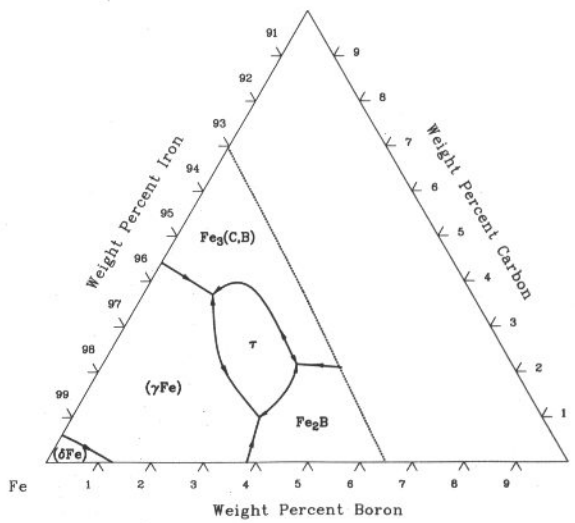

B-C-Fe isothermal section at 1000 °C [73Bre]

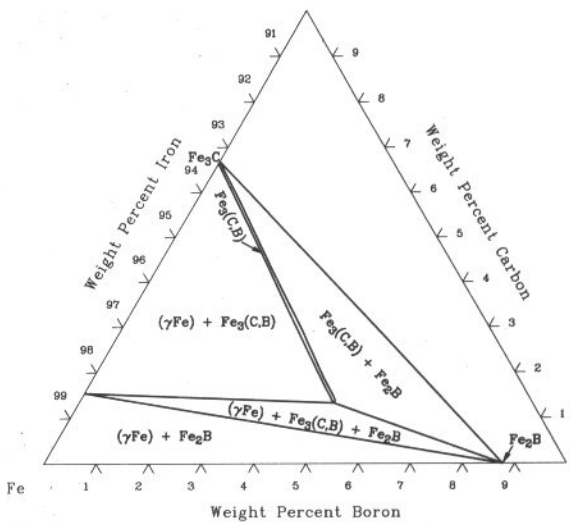

B-C-Fe isothermal section at 900 °C [73Bre]

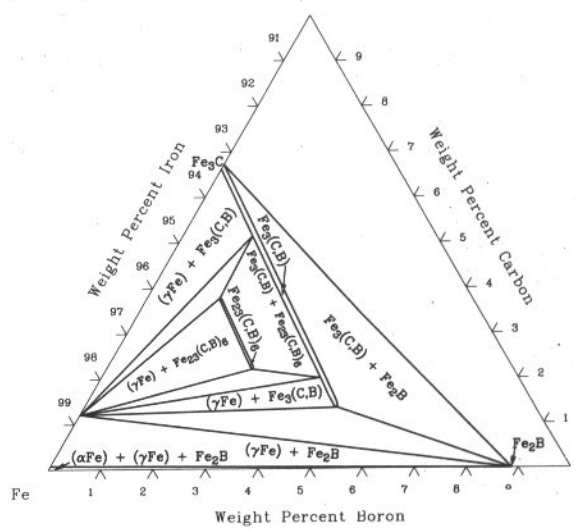

B-C-Fe isothermal section at 800 °C [73Bre]

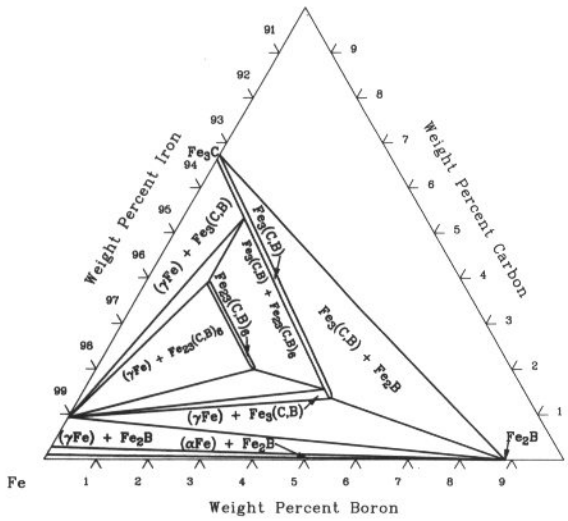

C-Cr-Fe isothermal section at 1000 °C [88Ray]

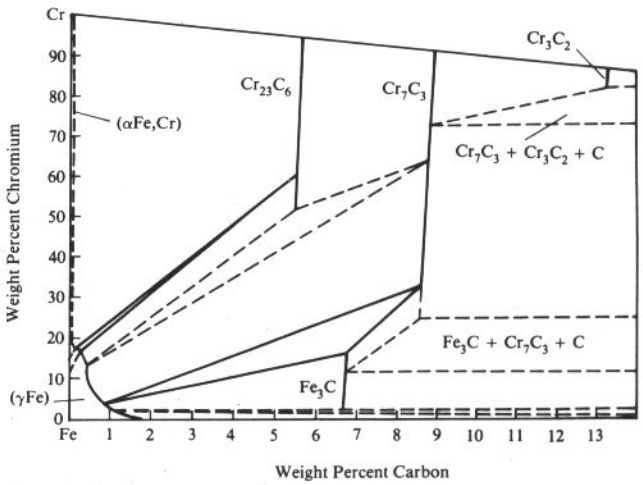

B-C-Fe isothermal section at 700 °C [73Bre]

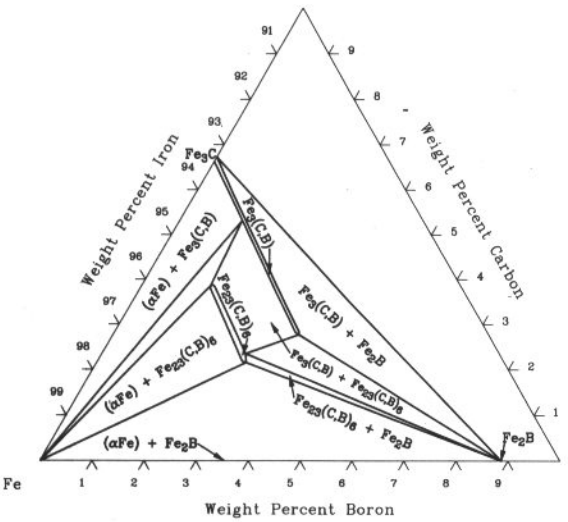

C-Cr-Fe isothermal section at 870 °C [88Ray]

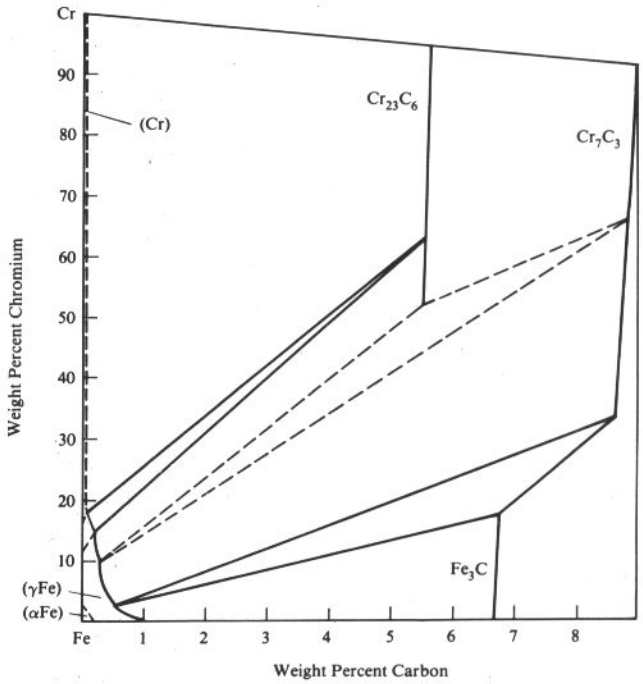

C-Cr-Fe liquidus projection [88Ray]

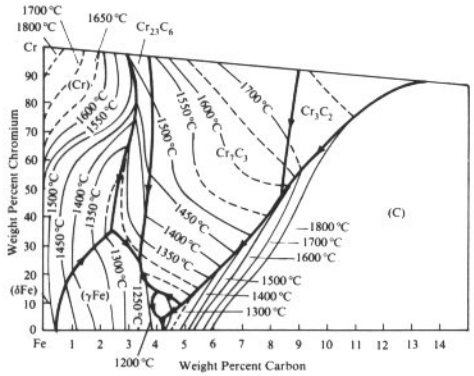

C-Cr-Fe isothermal section at 700 °C [88Ray]

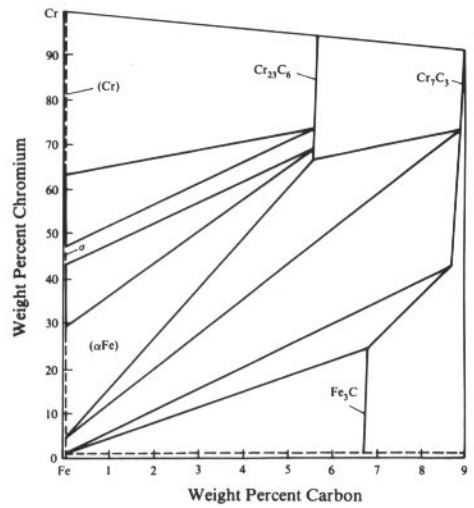

C-Cr-Fe isothermal section at 900 °C [88Ray]

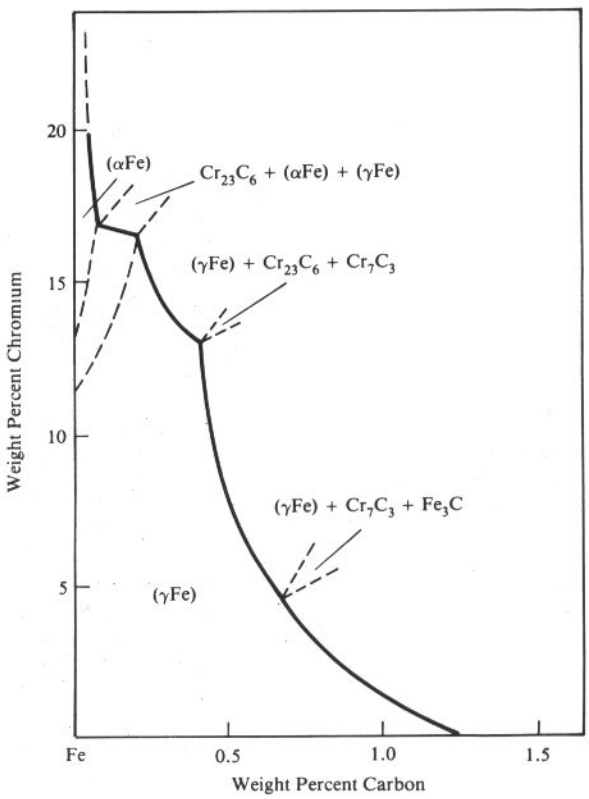

C-Cr-Fe (Fe) isothermal section at 1100 °C [88Ray]

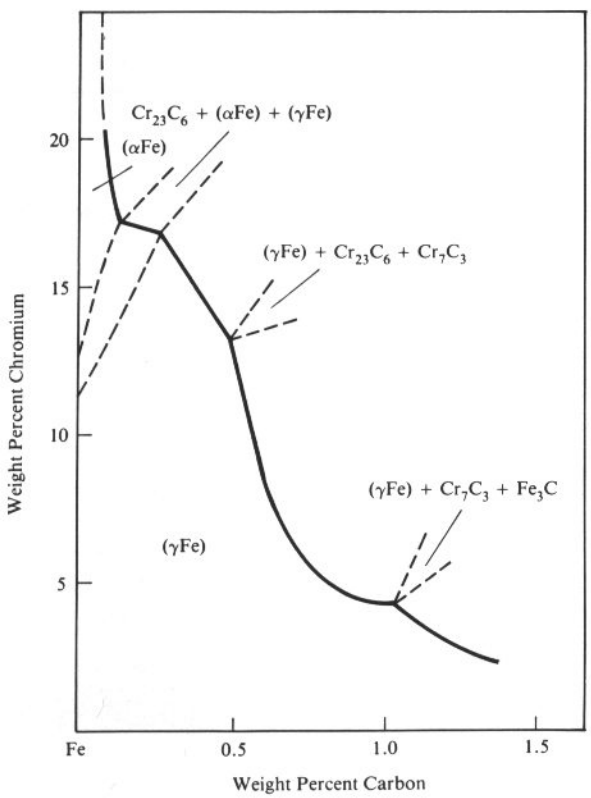

C-Cr-Mo liquidus projection [87Ere]

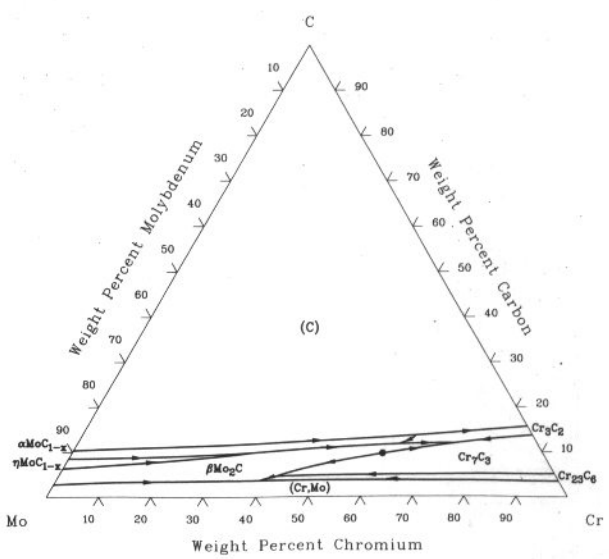

C-Cr-Mo isothermal section at 1350 °C [65Kuz]

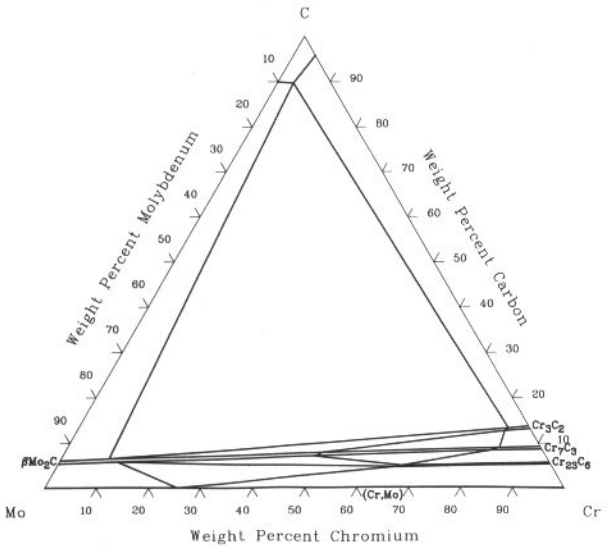

C-Cr-N isothermal section at 1400 °C [73Bre]

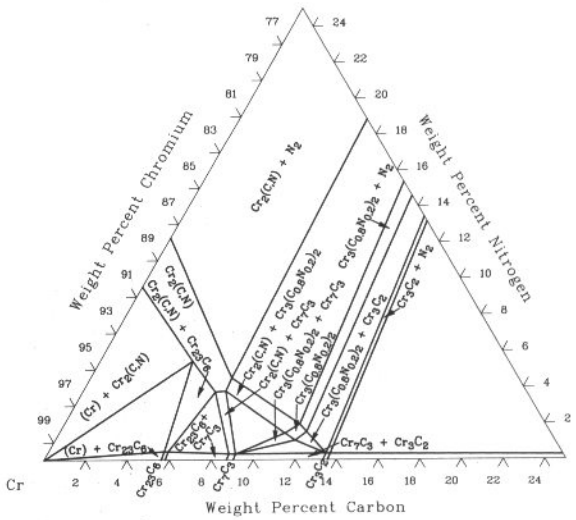

Nitrogen pressure: ~3 MPa.

C-Cr-N isothermal section at 1400 °C [73Bre]

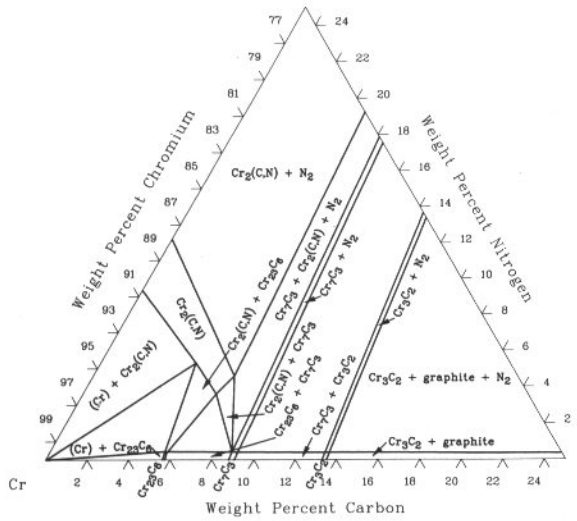

Nitrogen pressure: ≤0.1 MPa.

C-Cr-N isothermal section at 1100 °C [73Bre]

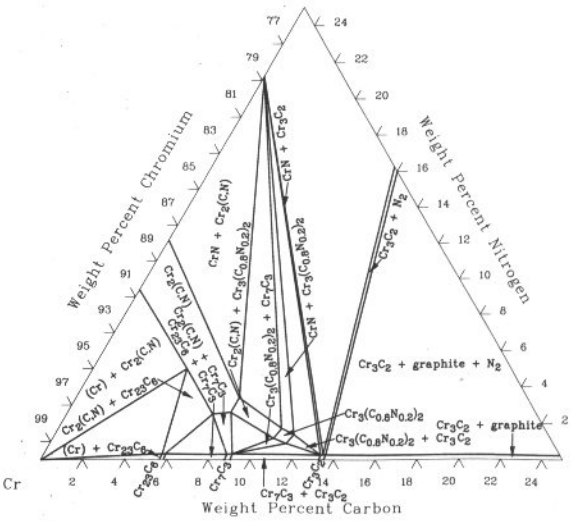

Nitrogen pressure: 0.2 to 3 MPa.

C-Cr-N isothermal section at 1100 °C [73Bre]

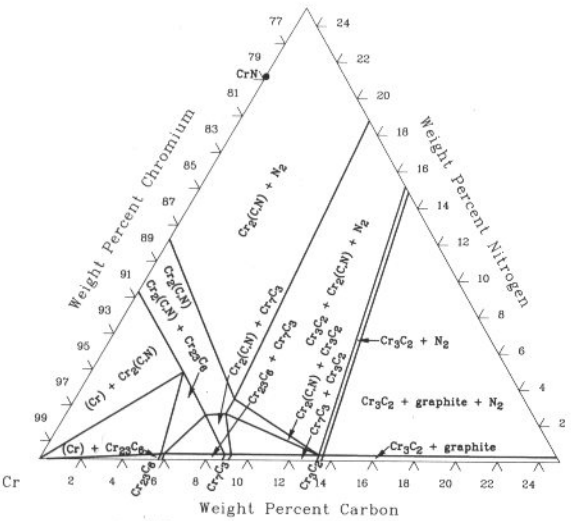

Nitrogen pressure: ≤0.1 MPa.

C-Cr-V liquidus projection [66Kie]

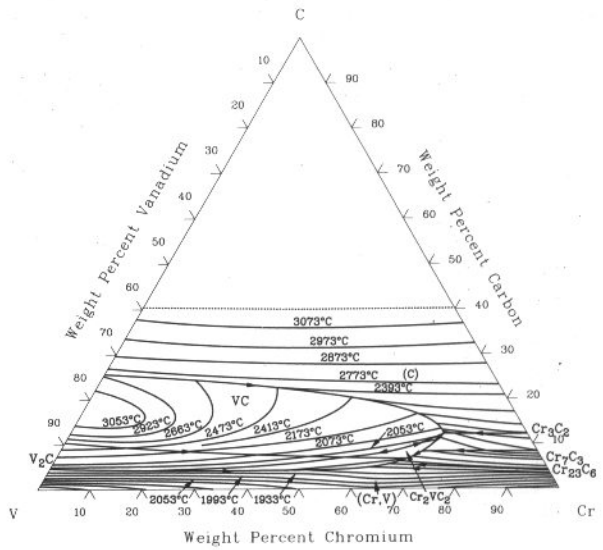

C-Cr-V isothermal section at 1350 °C [66Kie]

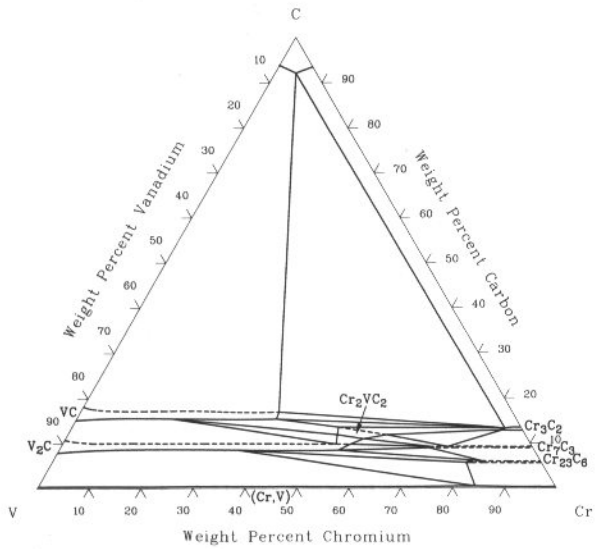

C-Cr-W isothermal section at 1600 °C [86Ere]

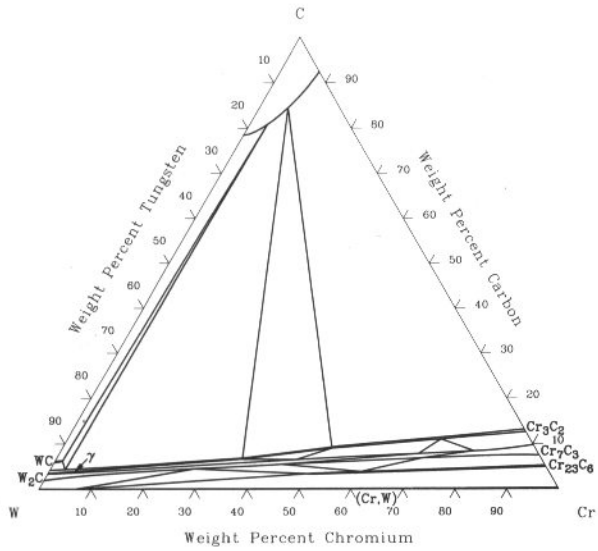

C-Cr-W isothermal section at 1350 °C [64Ste]

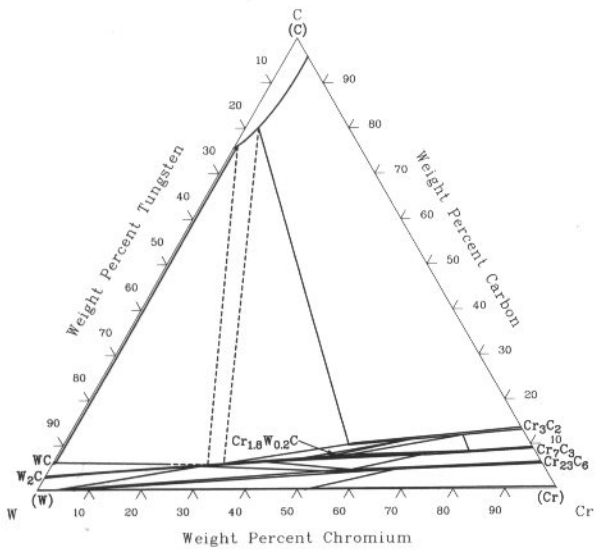

C-Cu-Fe liquidus projection [88Ray]

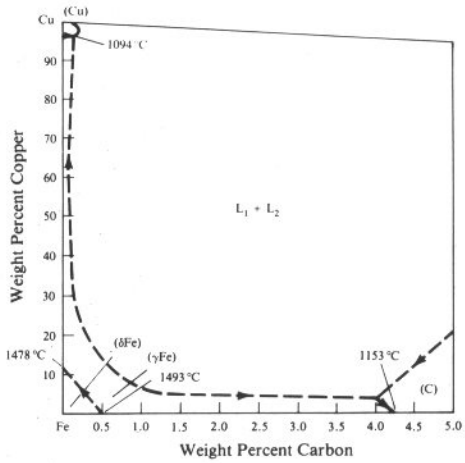

C-Cu-Fe isothermal section at 1172 °C [88Ray]

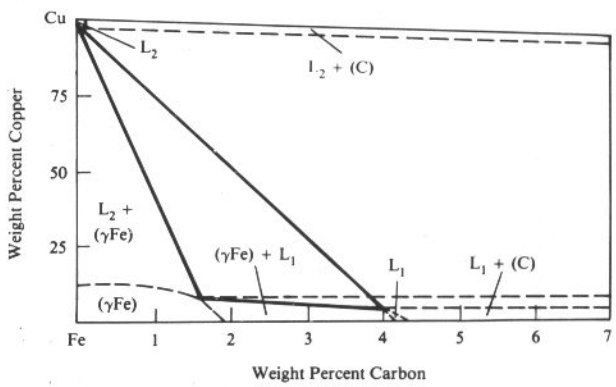

C-Cu-Fe isothermal section at 1050 °C [88Ray]

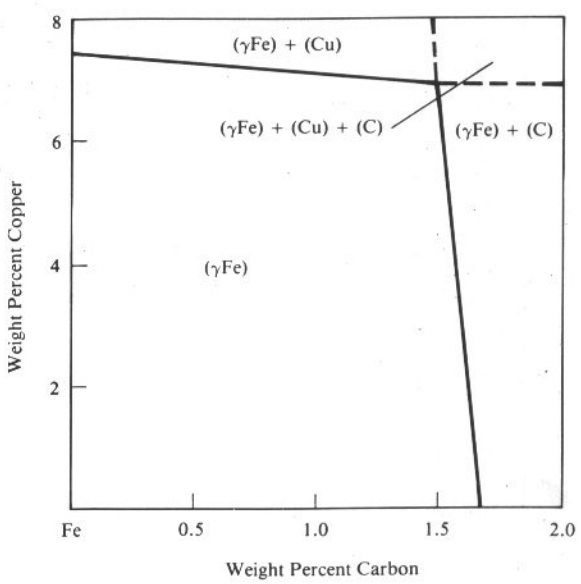

C-Cu-Fe isothermal section at 925 °C [88Ray]

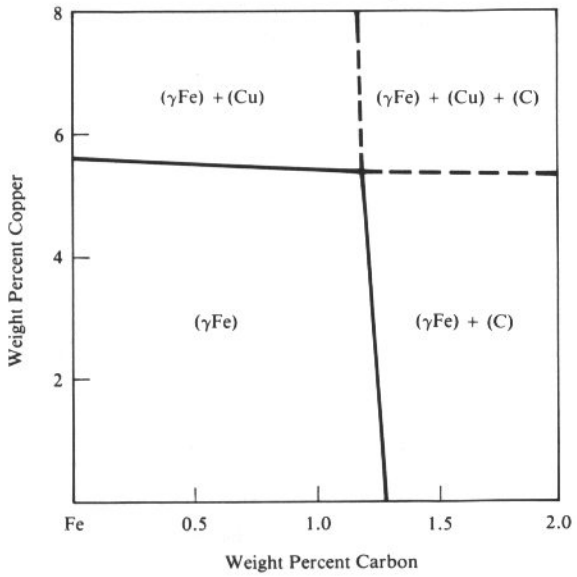

C-Cu-Fe isothermal section at 850 °C [88Ray]

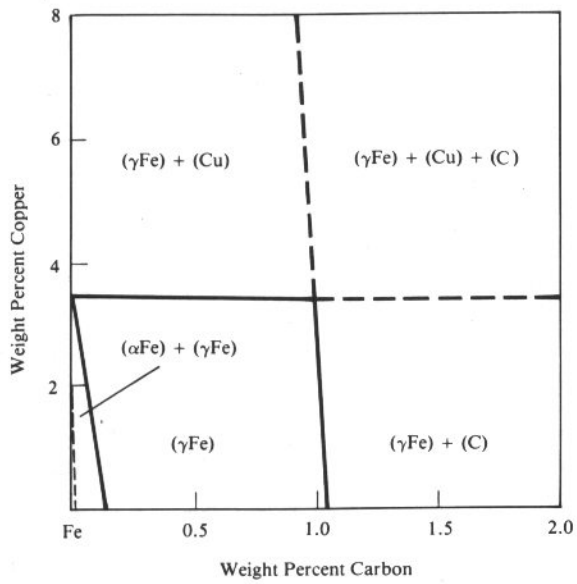

C-Cu-Fe schematic isothermal section at 850 °C [88Ray]

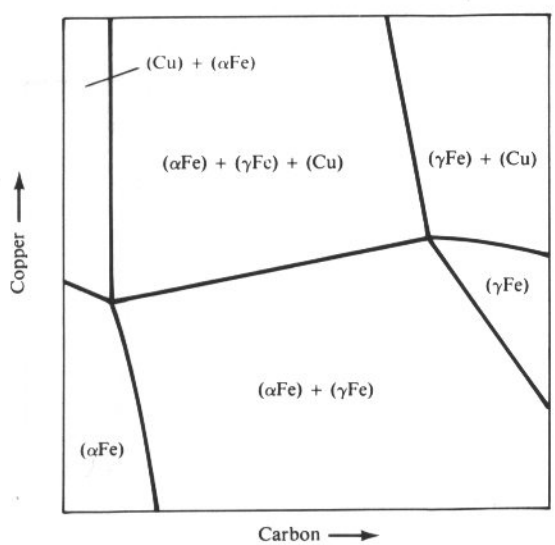

C-Fe-Mn liquidus projection [88Ray]

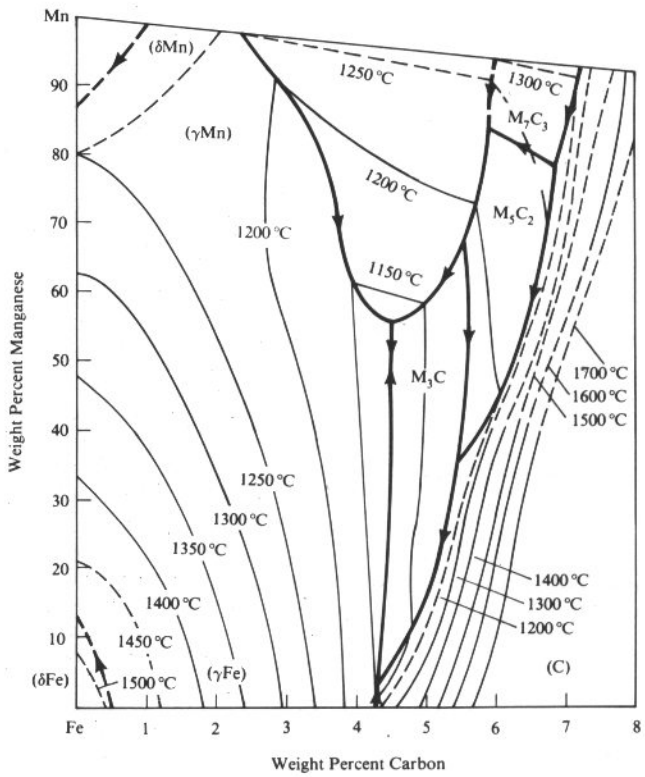

C-Fe-Mn isothermal section at 1100 °C [73Ben]

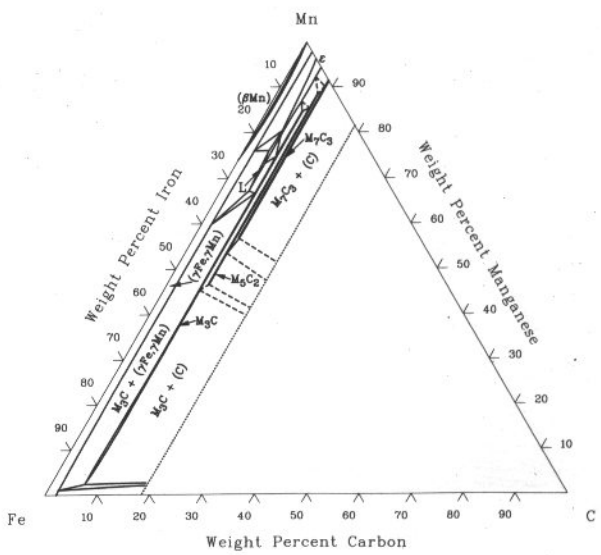

C-Fe-Mn isothermal section at 1000 °C [73Ben]

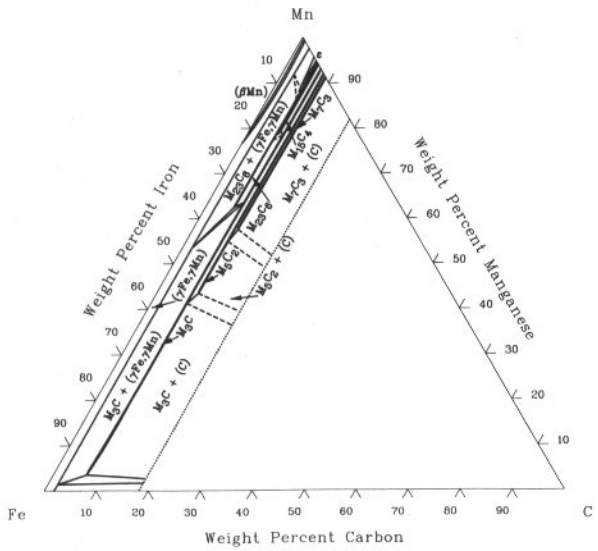

C-Fe-Mn isothermal section at 600 °C [73Ben]

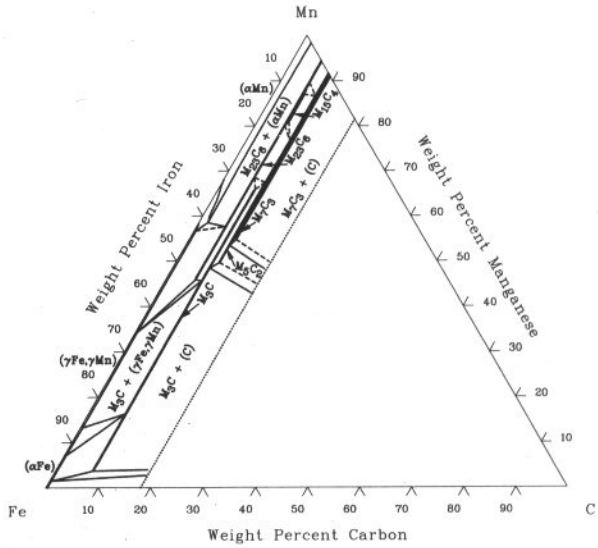

C-Fe-Mn isothermal section at 900 °C [73Ben]

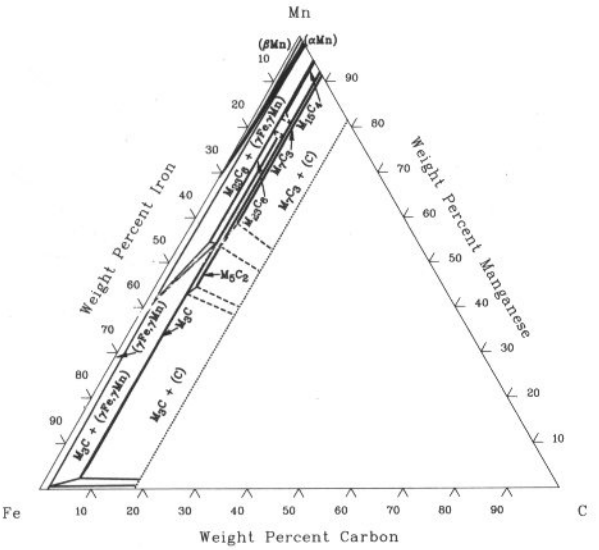

C-Fe-Mn [73Bre]

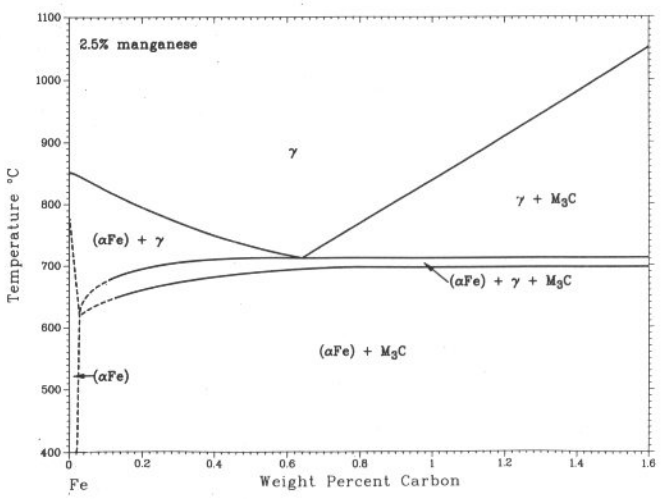

C-Fe-Mn isothermal section at 800 °C [73Ben]

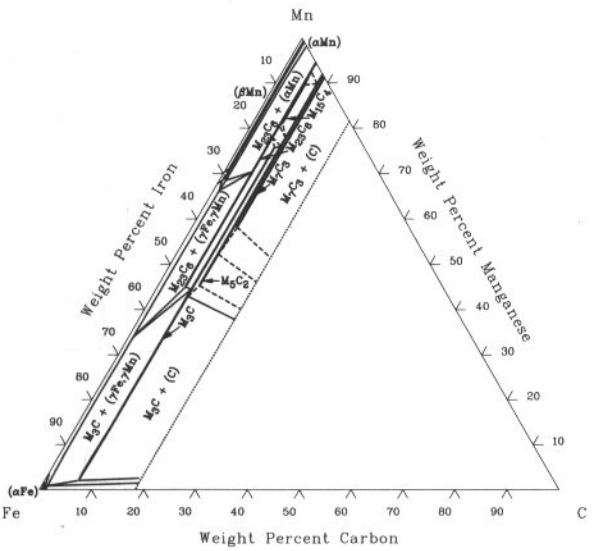

C-Fe-Mn [73Bre]

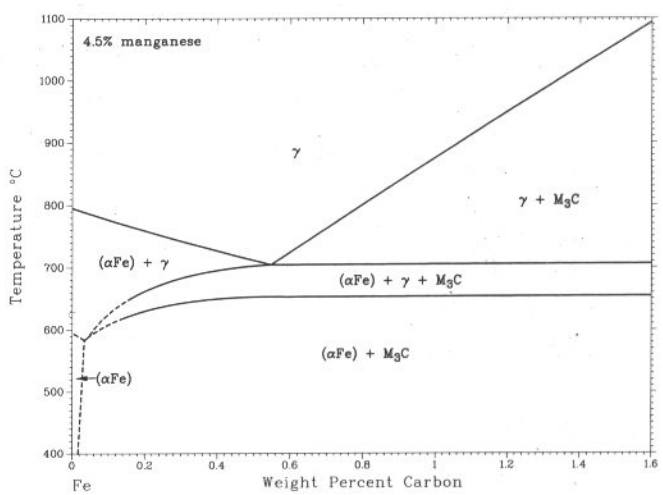

C-Fe-Mn [73Bre]

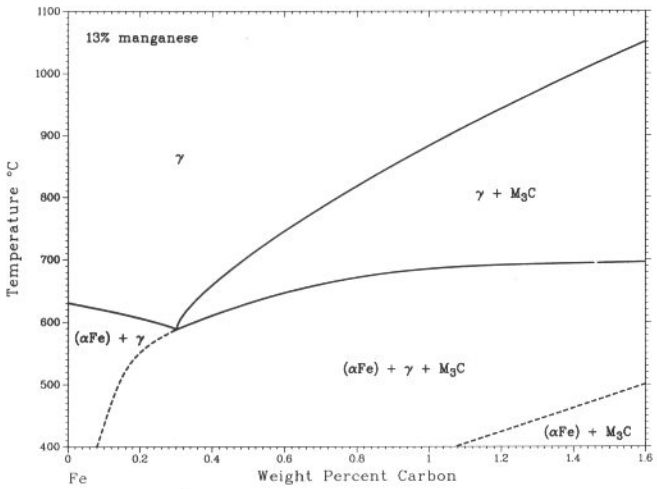

C-Fe-Mo isothermal section at 1000 °C [88Ray]

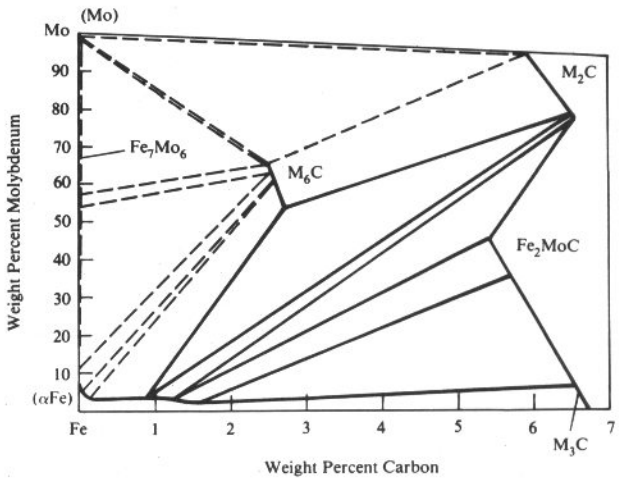

C-Fe-Mo (Fe) isothermal section at 1000 °C [88Ray]

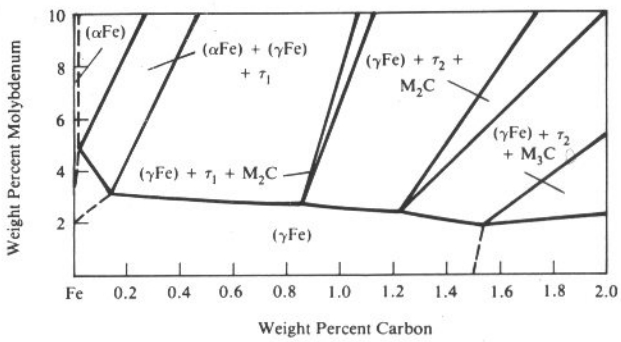

C-Fe-Mo liquidus projection [88Ray]

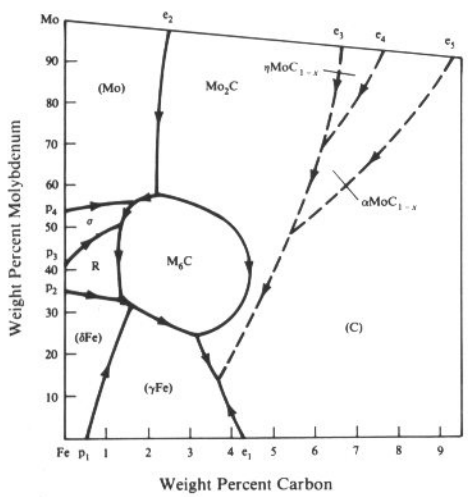

C-Fe-Mo isothermal section at 700 °C (calculated) [88Ray]

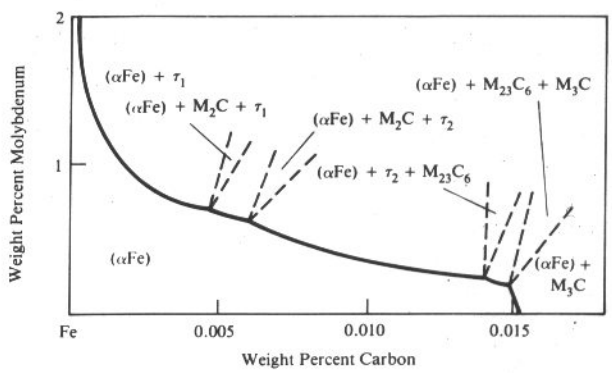

C-Fe-Mo (Fe) isothermal section at 700 °C [Ray]

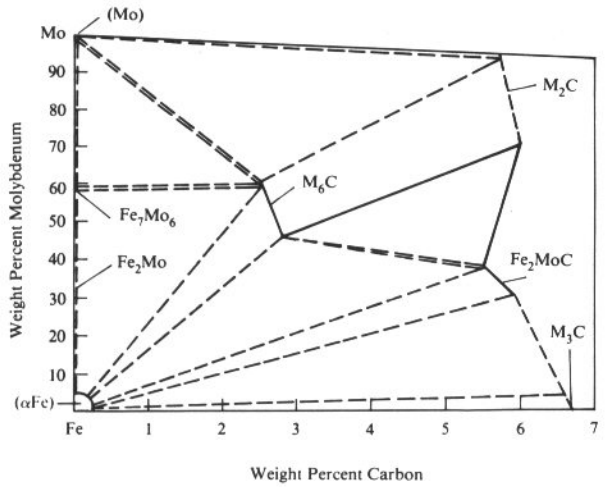

C-Fe-Mo [88Ray]

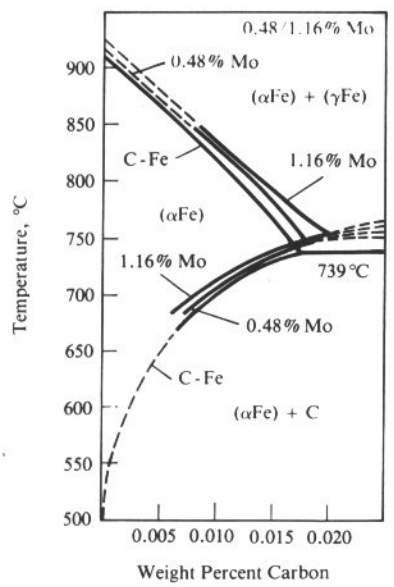

C-Fe-N isothermal section at 700 °C [87Rag]

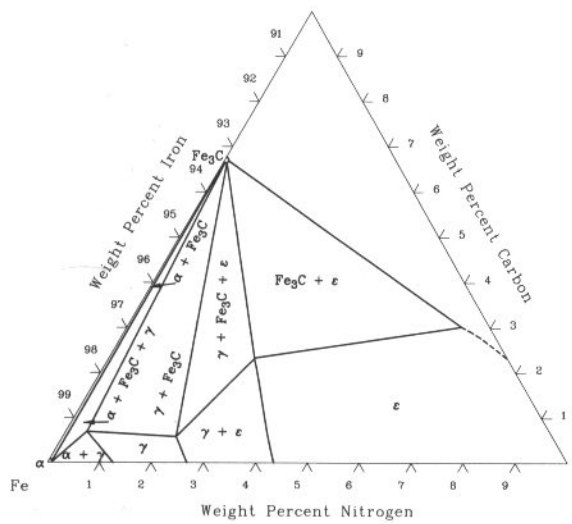

C-Fe-N isothermal section at 600 °C [87Rag]

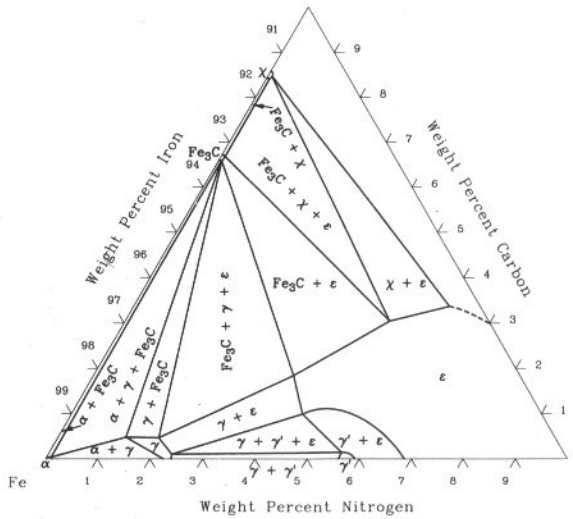

C-Fe-N isothermal section at 575 °C [87Rag]

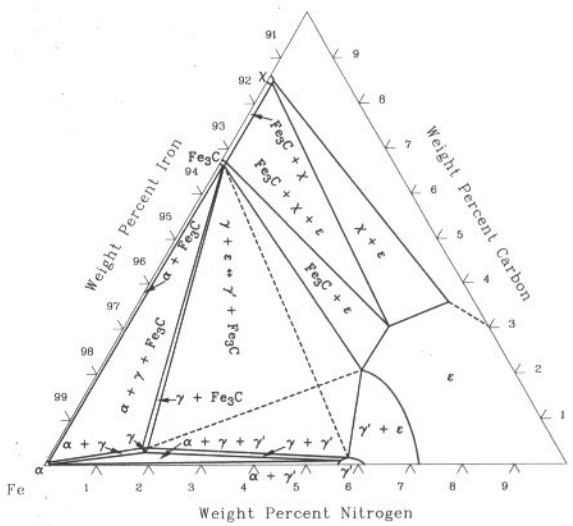

C-Fe-N isothermal section at 565 °C [87Rag]

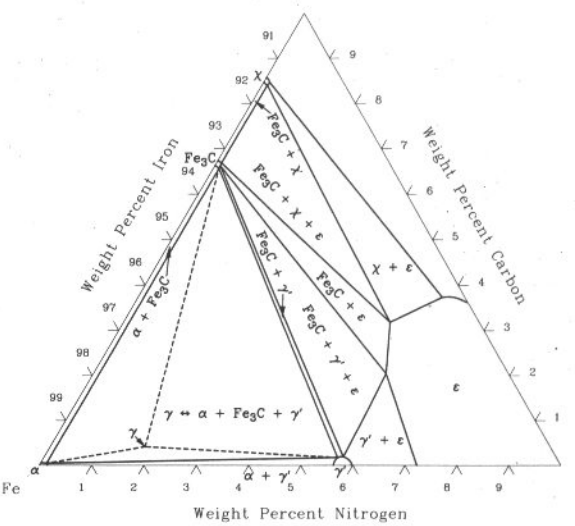

C-Fe-N isothermal section at 500 °C [87Rag]

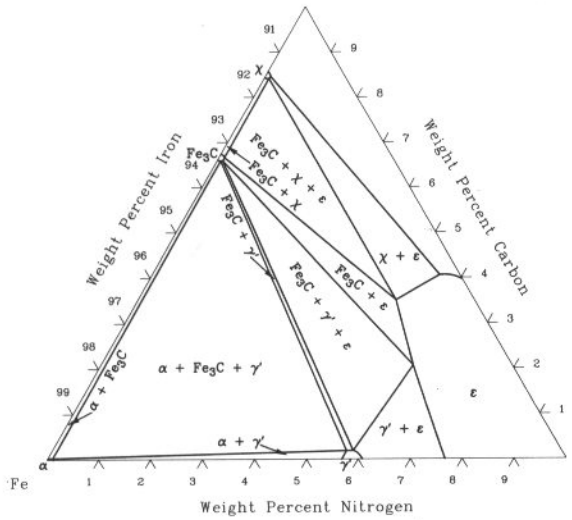

C-Fe-Ni liquidus projection [88Ray]

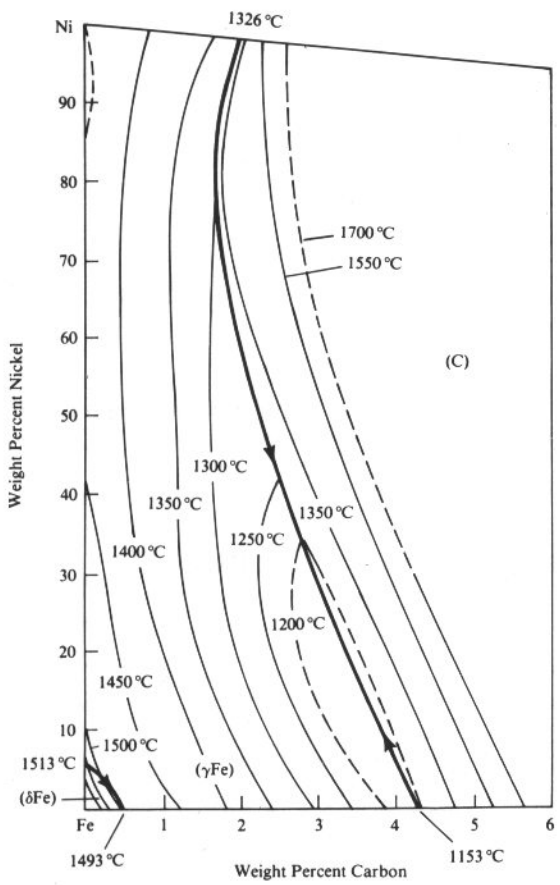

C-Fe-Ni solidus projection [88Ray]

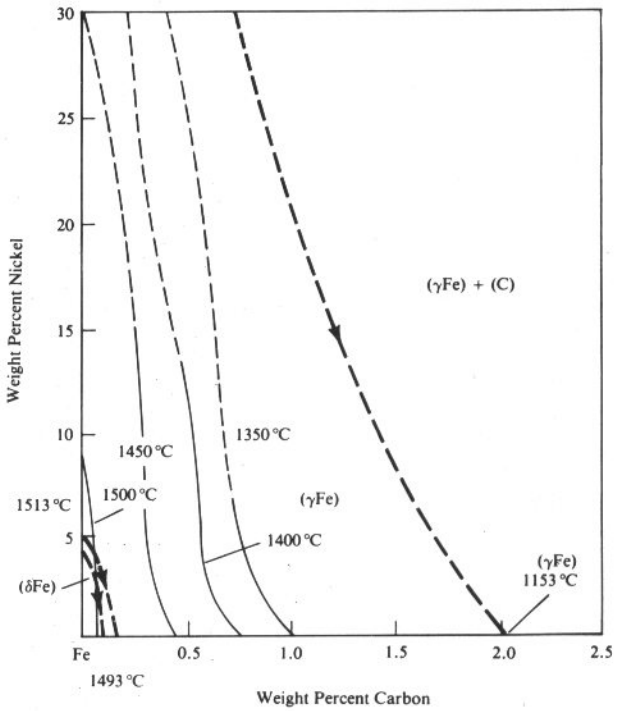

C-Fe-Ni γFe/ (γFe + C) boundary at 800 and 1000 °C [88Ray]

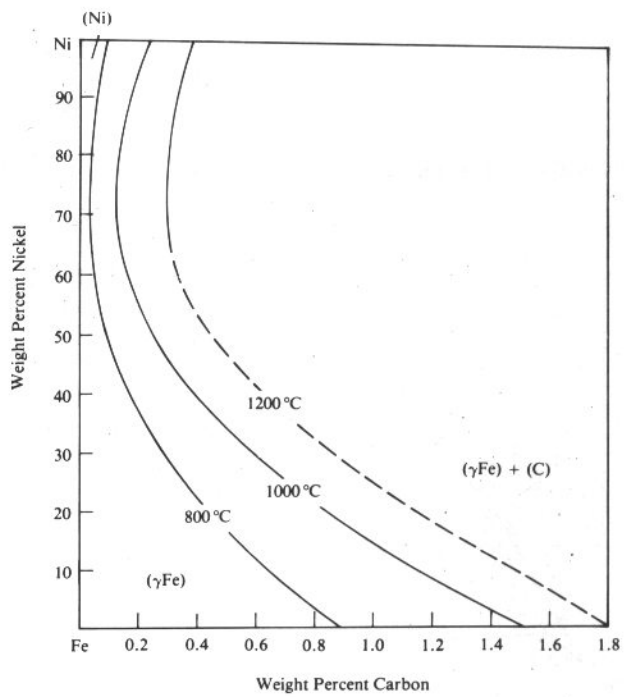

Note that at 800 °C the (αFe) phase will also appear at low Ni contents.

C-Fe-Si liquidus projection (stable equilibrium) [86Rag]

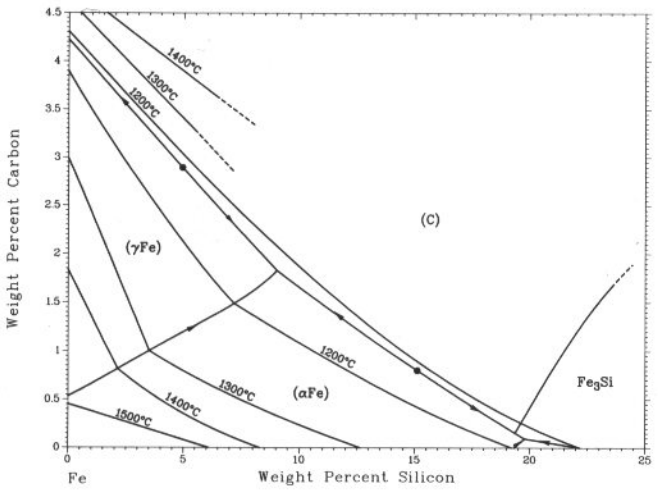

C-Fe-Si isothermal section at 1150 °C (stable equilibrium) [86Rag]

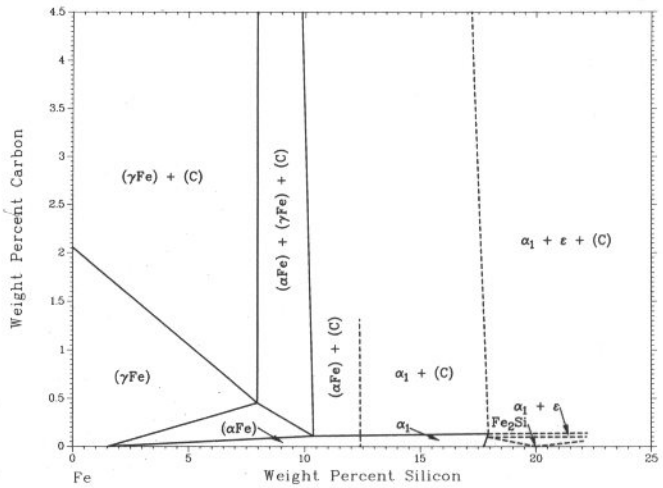

C-Fe-Si liquidus projection (metastable equilibrium) [86Rag]

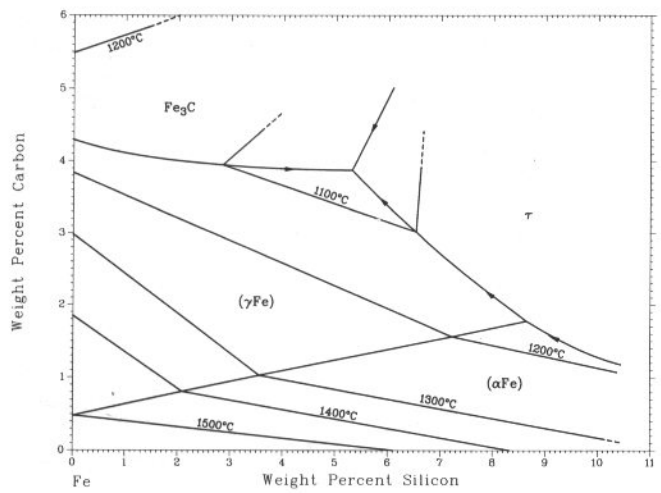

C-Fe-Si isothermal section at 1100 °C (metastable equilibrium) [86Rag]

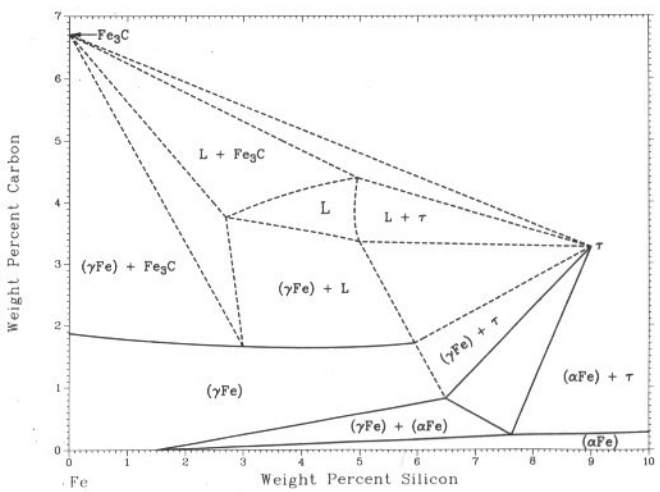

C-Fe-Si isothermal section at 1300 °C (stable equilibrium) [86Rag]

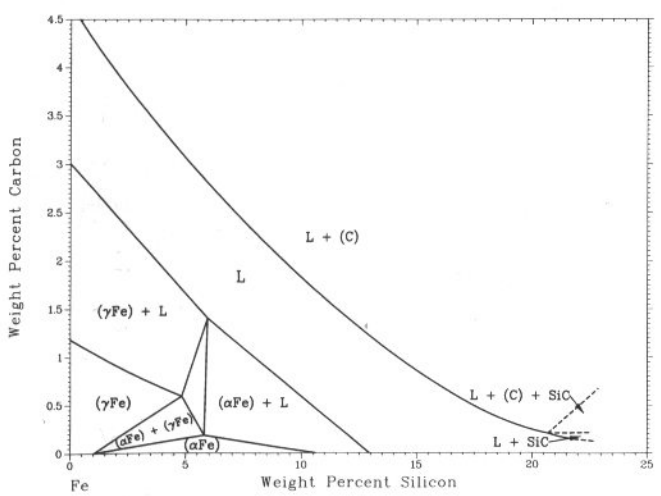

C-Fe-Si isothermal section at 1000 °C (stable equilibrium) [86Rag]

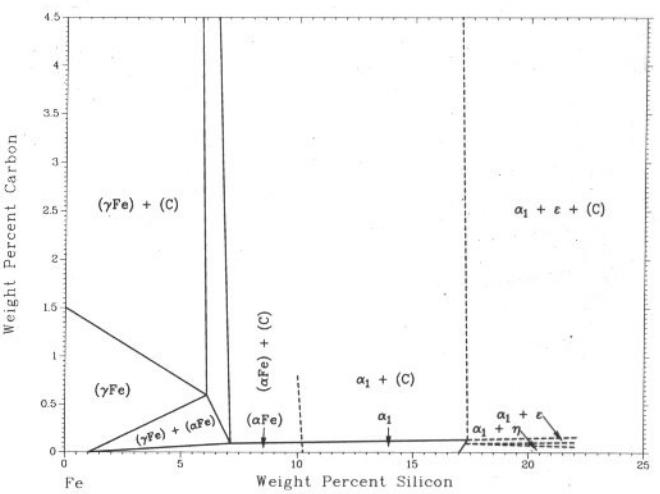

C-Fe-Si isothermal section at 900 °C (metastable equilibrium) [86Rag]

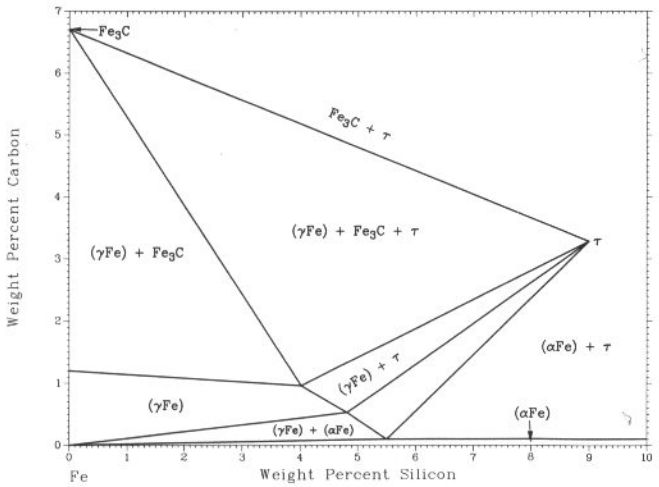

C-Fe-Si isothermal section at 800 °C (metastable equilibrium) [86Rag]

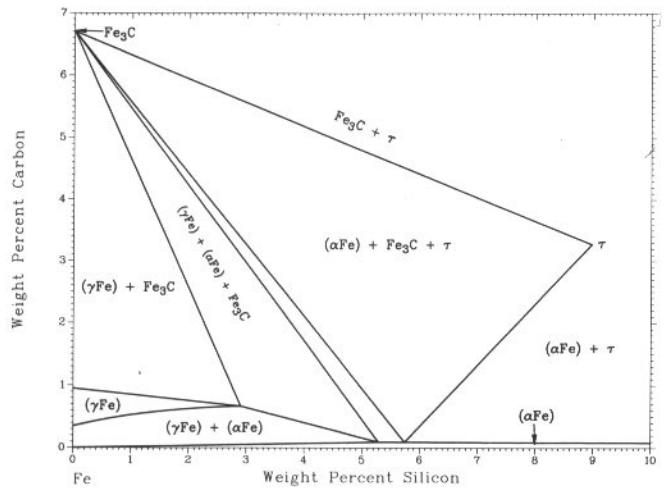

C-Fe-V liquidus projection [87Rag]

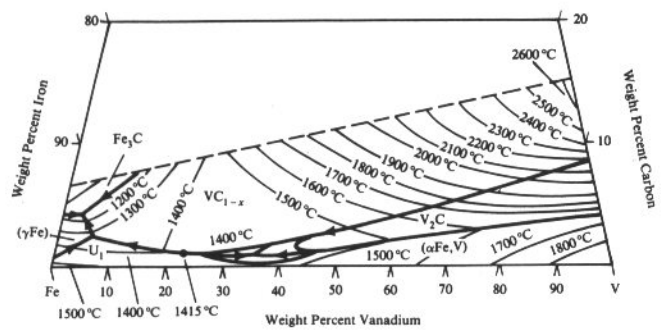

C-Fe-V isothermal section at 1100 °C [87Rag]

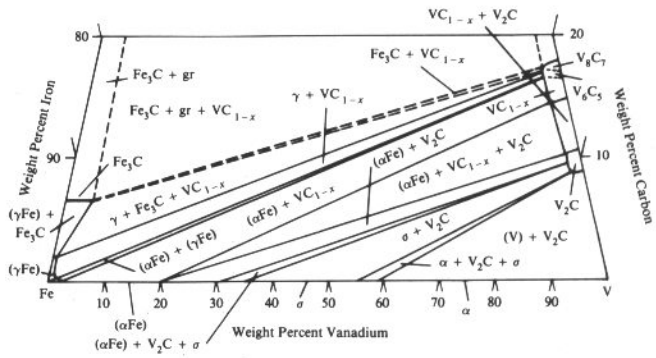

C-Fe-V isothermal section at 1000 °C [87Rag]

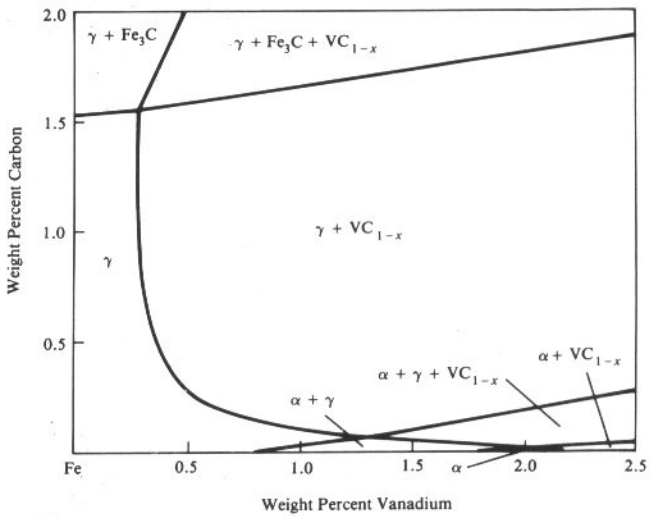

C-Fe-V isothermal section at 500 °C [87Rag]

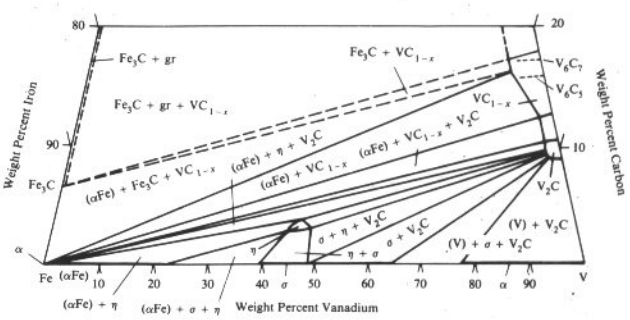

C-Fe-W liquidus projection [88Ray]

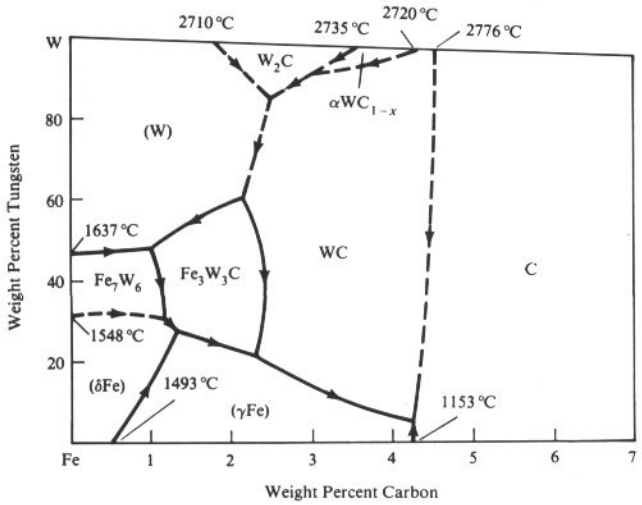

C-Fe-W isothermal section at 1000 °C [88Ray]

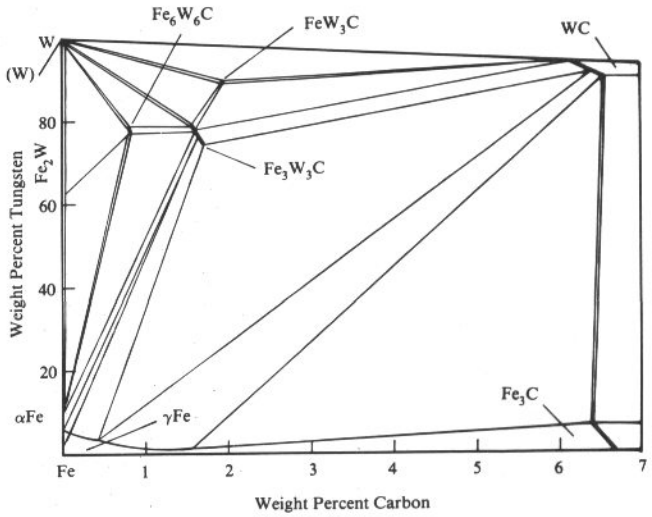

C-Fe-W isothermal section at 1250 °C [88Ray]

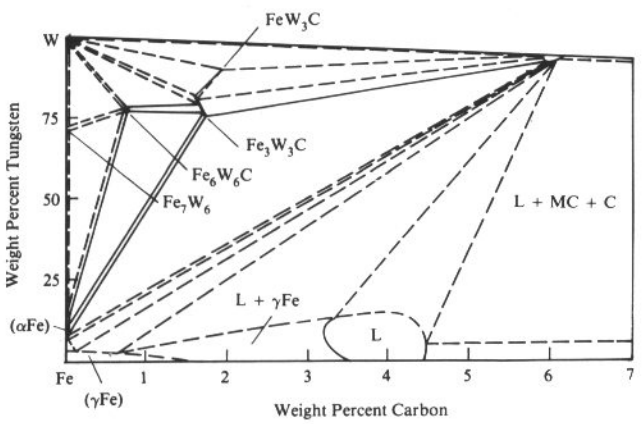

C-Fe-W (Fe) isothermal section at 1000 °C [88Ray]

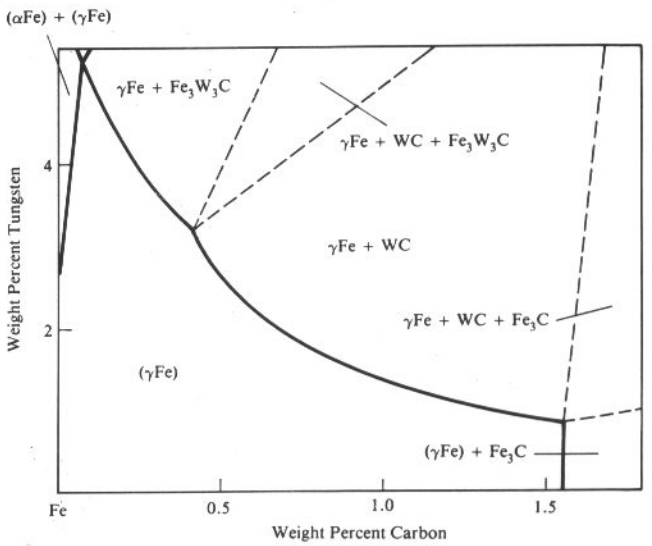

C-Fe-W (Fe) isothermal section at 1250 °C [88Ray]

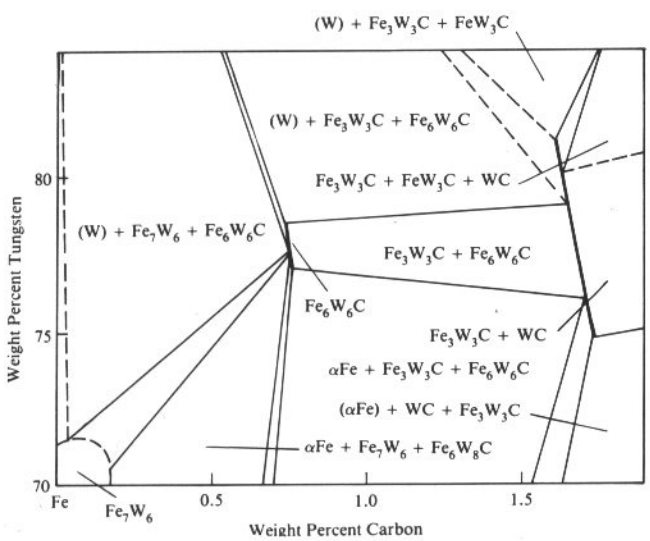

Cd-Sb-Sn liquidus projection [73Pel]

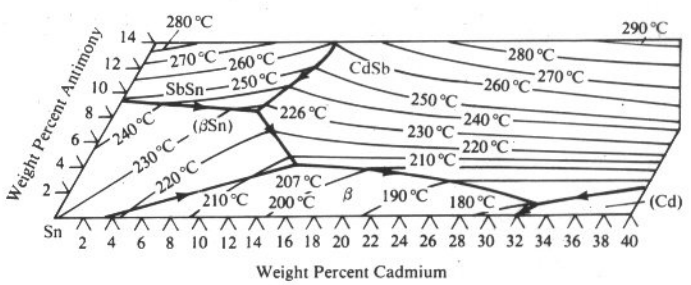

Cd-Sb-Sn isothermal section at 212 °C [73Pel]

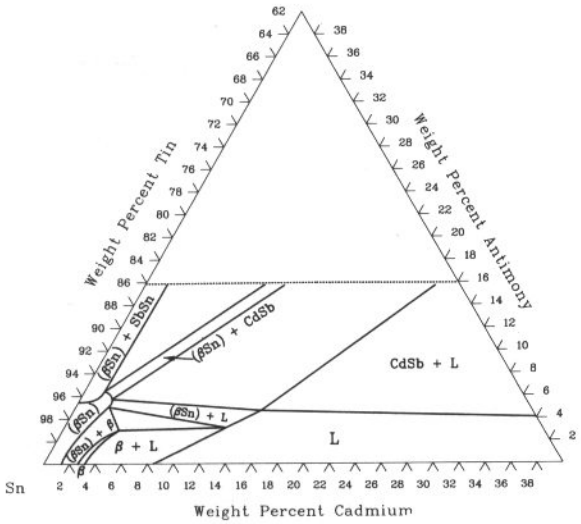

Cd-Sb-Sn [73Pel]

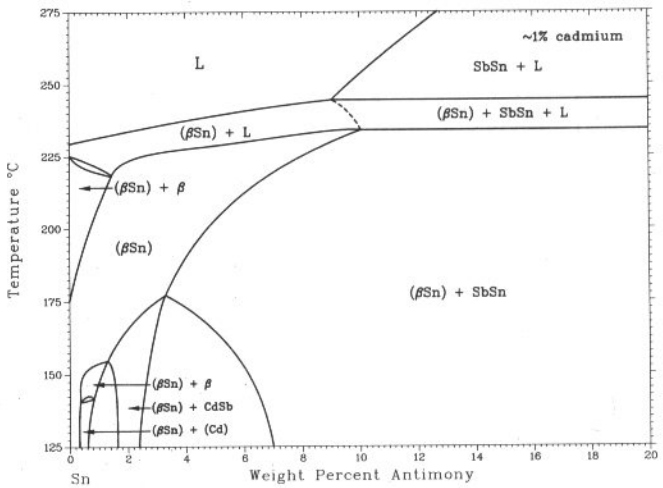

Cd-Sb-Sn isothermal section at 175 °C [73Pel]

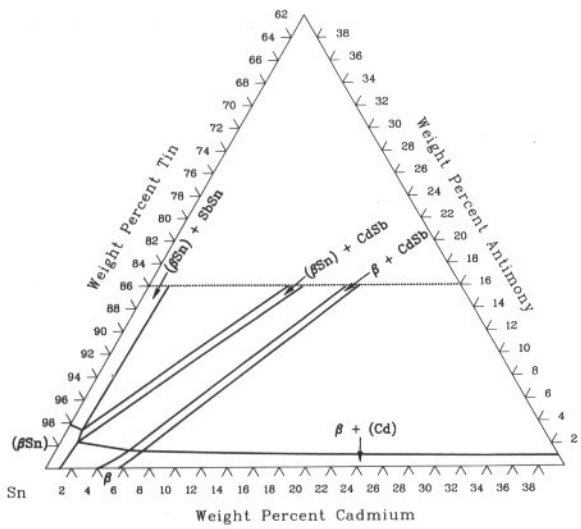

Cd-Sb-Sn [73Pel]

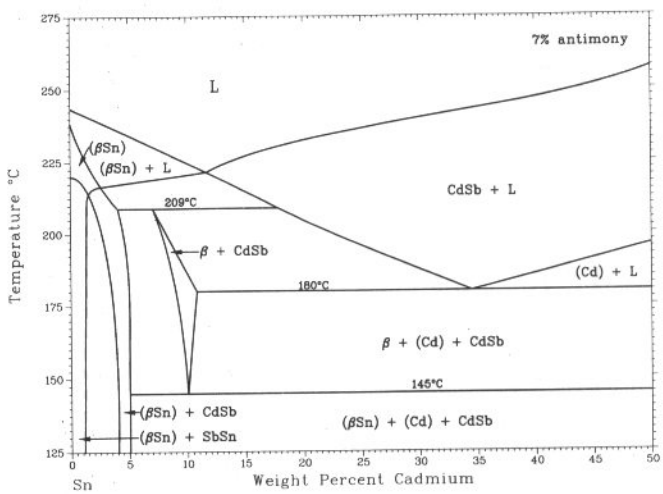

Cd-Sb-Sn isothermal section at 20 °C [73Pel]

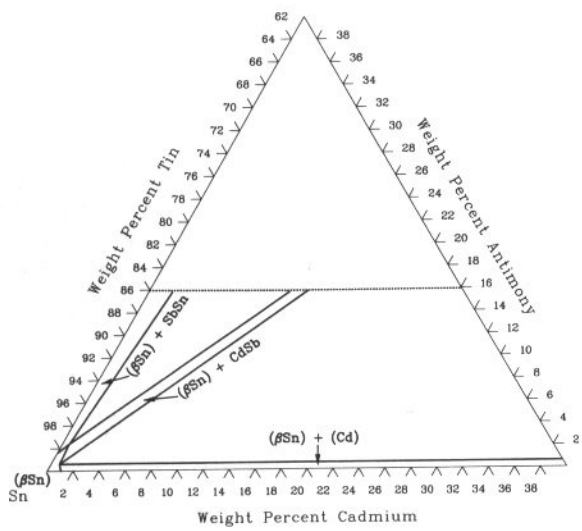

Co-Cr-Fe liquidus projection [88Ray]

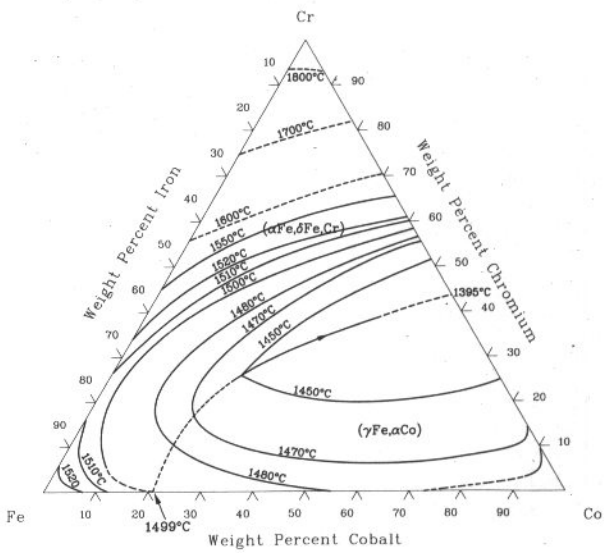

Co-Cr-Fe solidus projection [88Ray]

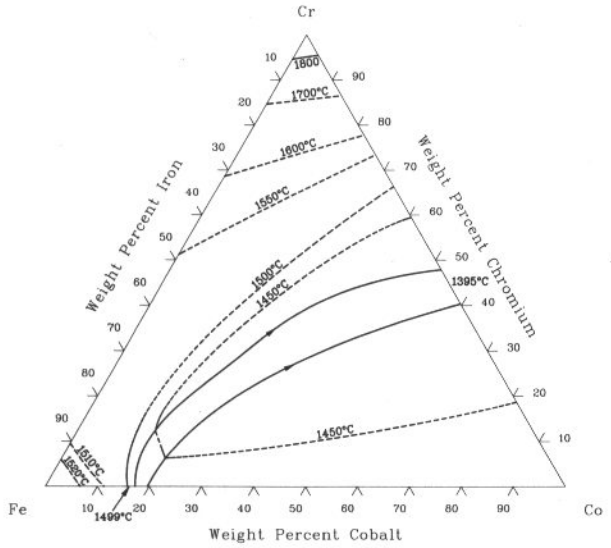

Co-Cr-Fe isothermal section at 800 °C [88Ray]

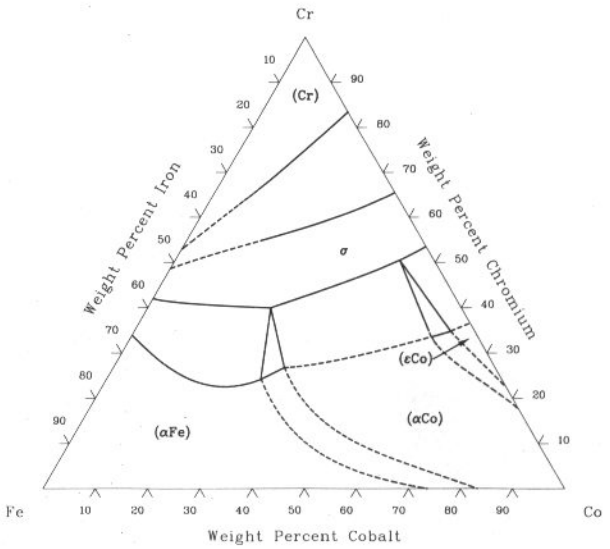

Co-Cr-Fe isothermal section at 1200 °C [88Ray]

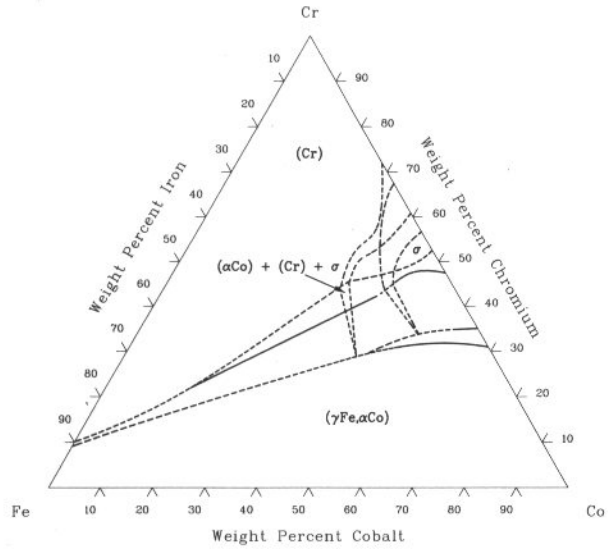

Co-Cr-Fe isothermal section at 600 °C [88Ray]

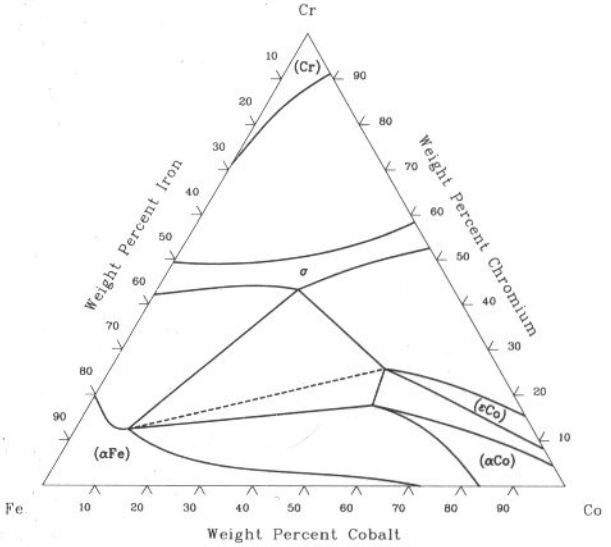

Co-Cr-Fe isothermal section at 1000 °C [88Ray]

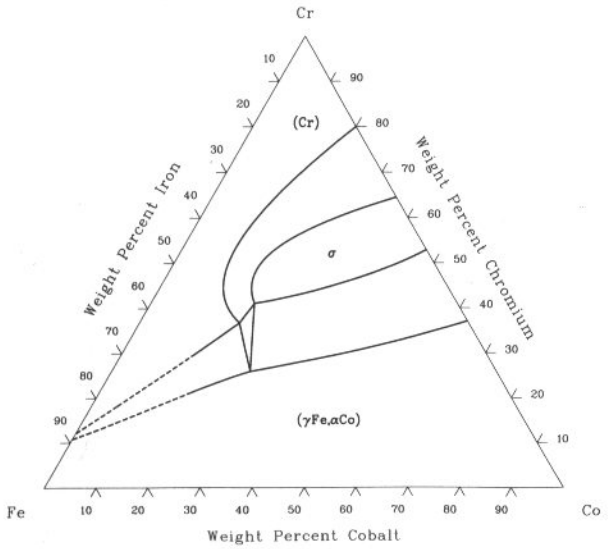

Co-Cr-Ni isothermal section at 1200 °C [81Zha]

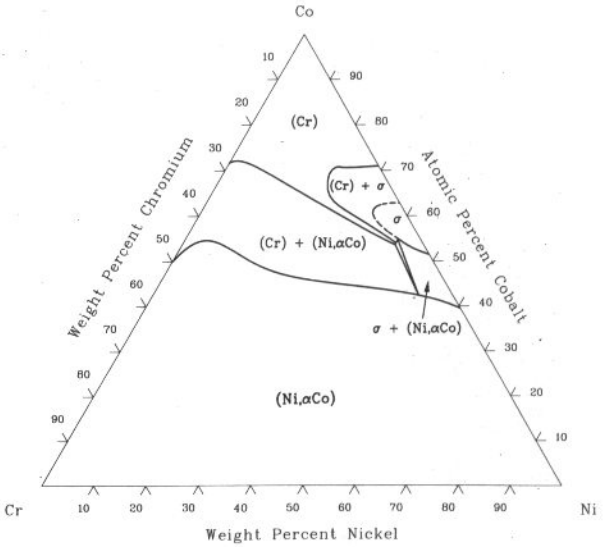

Co-Cr-Ti liquidus projection [62Zak]

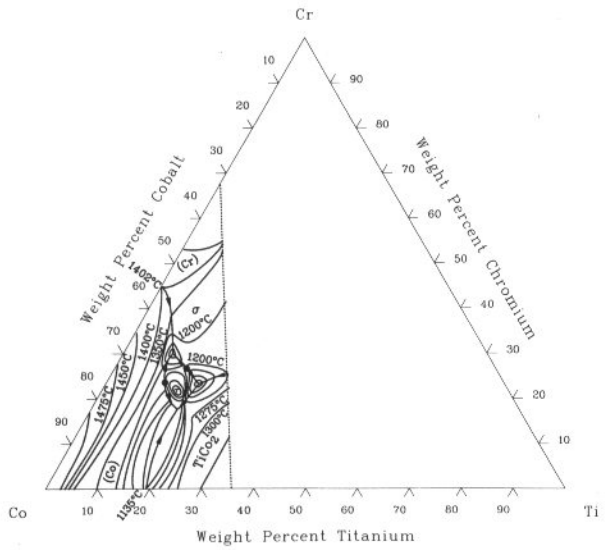

Co-Cr-Ti solidus projection [62Zak]

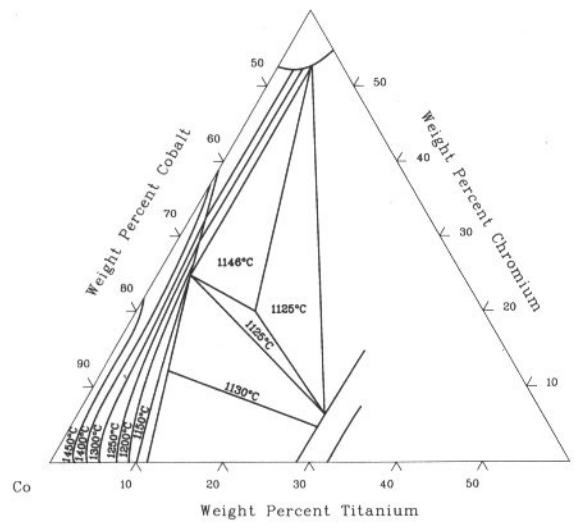

Co-Cr-Ti isothermal section at 1050 °C [58Liv]

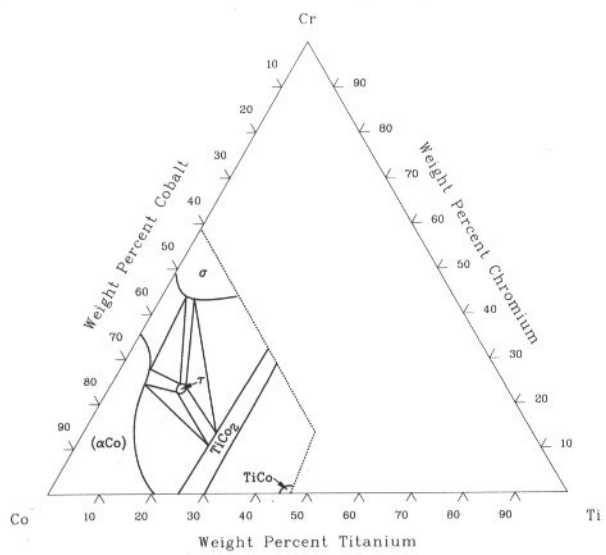

Co-Cr-W isothermal section at 1350 °C [73Dra]

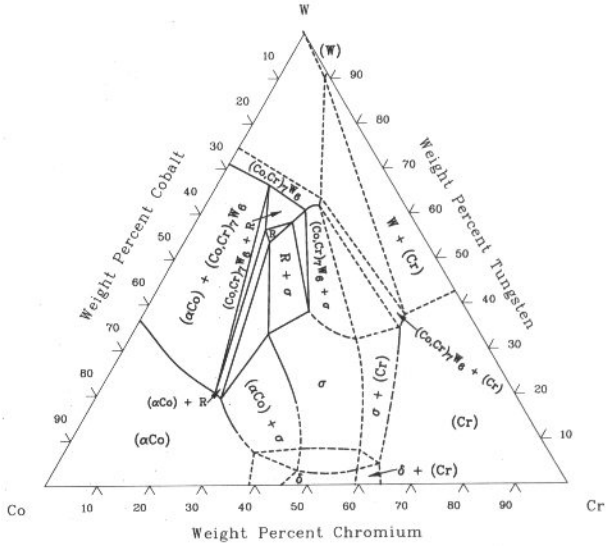

Co-Cr-W isothermal section at 700 °C [73Dra]

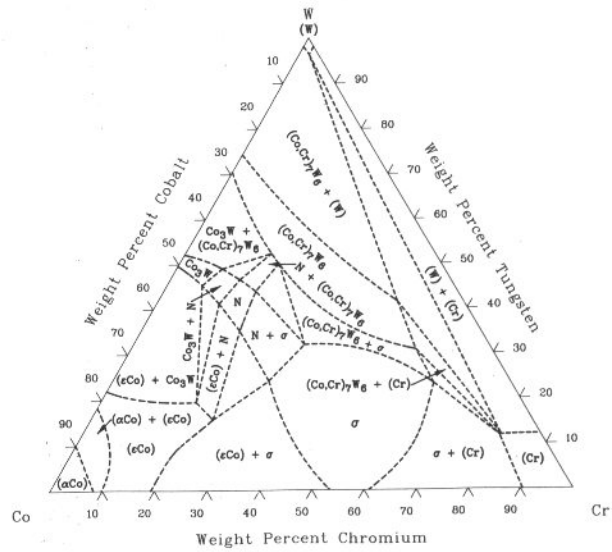

Co-Fe-Mo liquidus projection [88Ray]

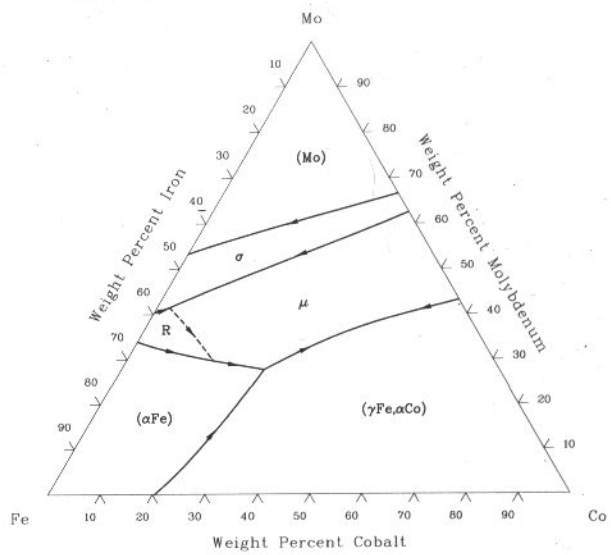

Co-Fe-Mo isothermal section at 1300 °C [88Ray]

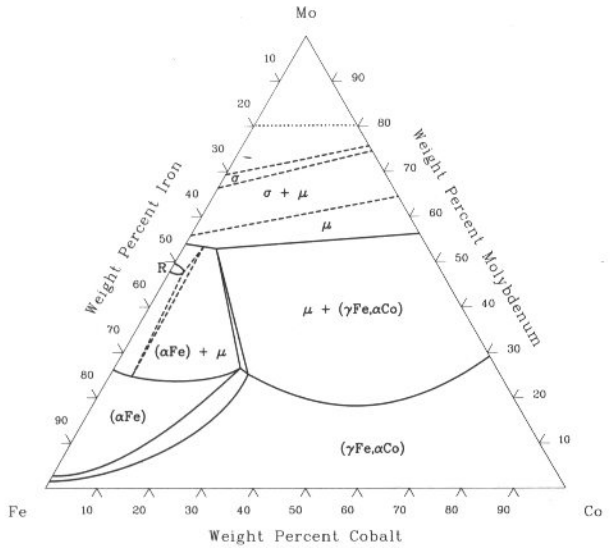

Co-Fe-Mo isothermal section at 800 °C [88Ray]

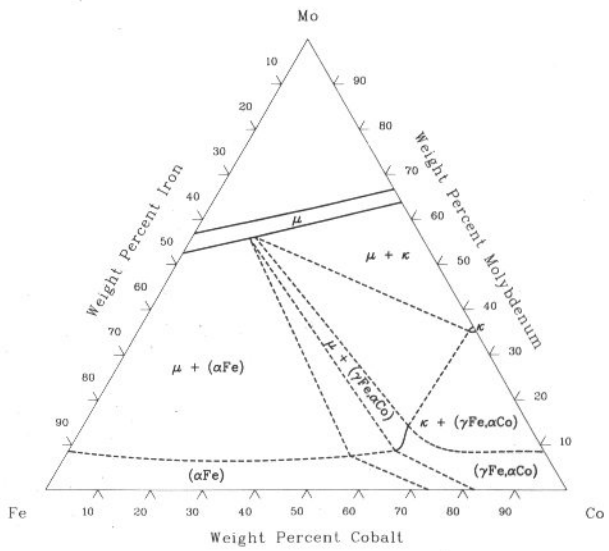

Co-Fe-Mo isothermal section at 1093 °C [88Ray]

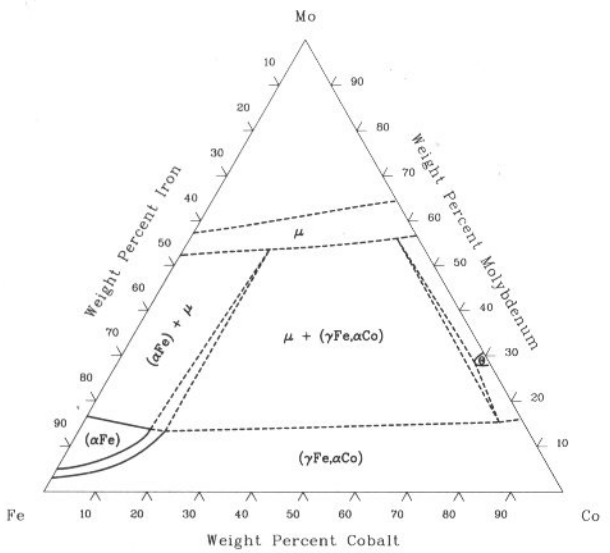

Co-Fe-Mo isothermal section at 20 °C [88Ray]

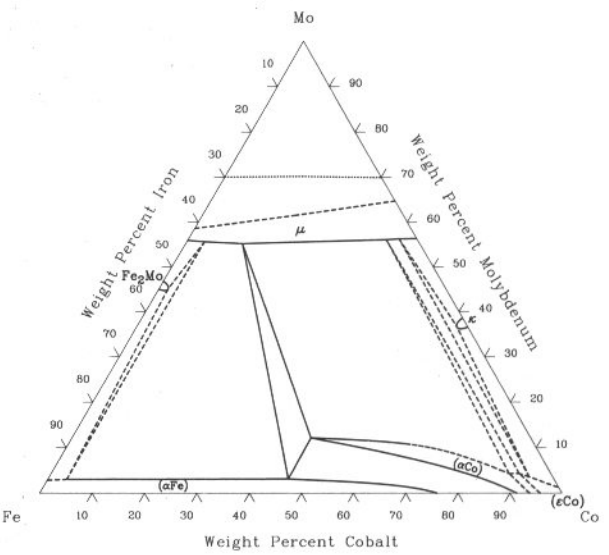

Co-Fe-Mo isothermal section at 982 °C [88Ray]

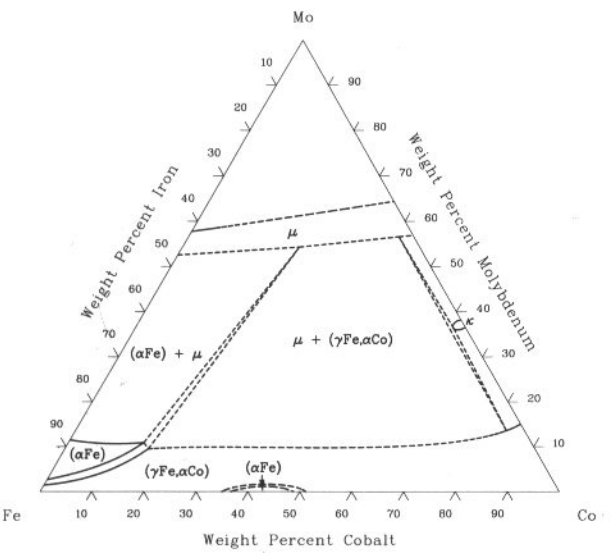

Co-Fe-Ni liquidus projection [88Ray]

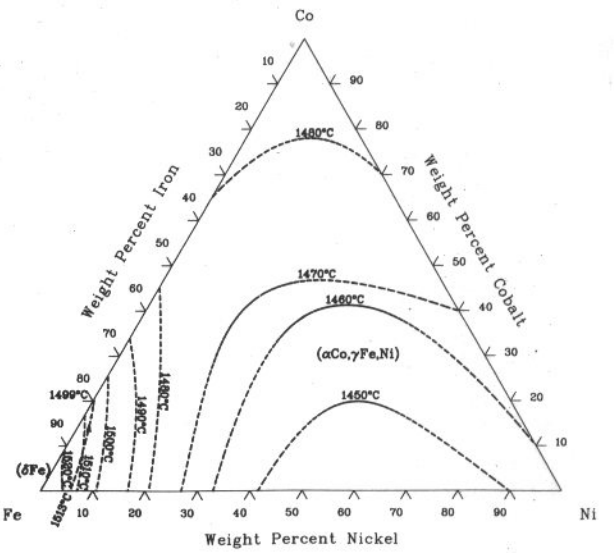

Co-Fe-Ni solidus projection [88Ray]

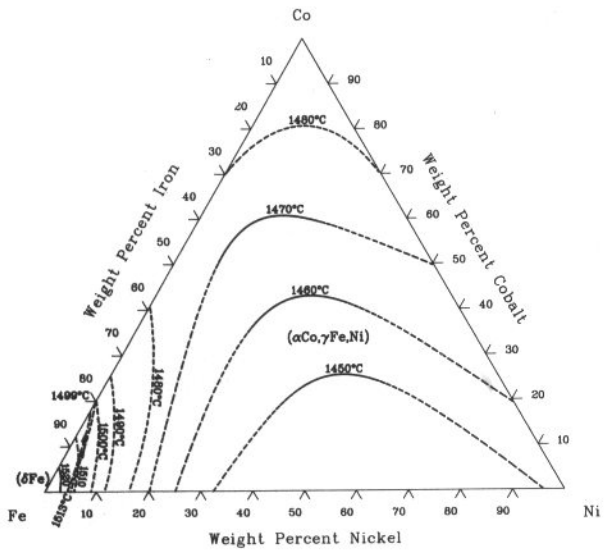

Co-Fe-W liquidus and solidus projections [88Ray]

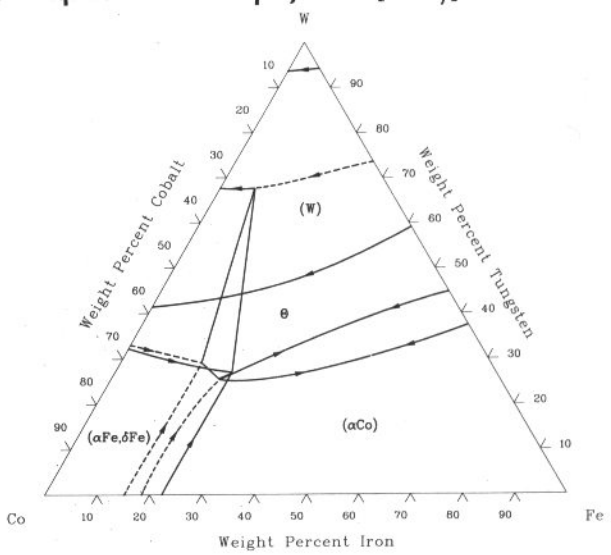

Co-Fe-Ni isothermal section at 800 °C [88Ray]

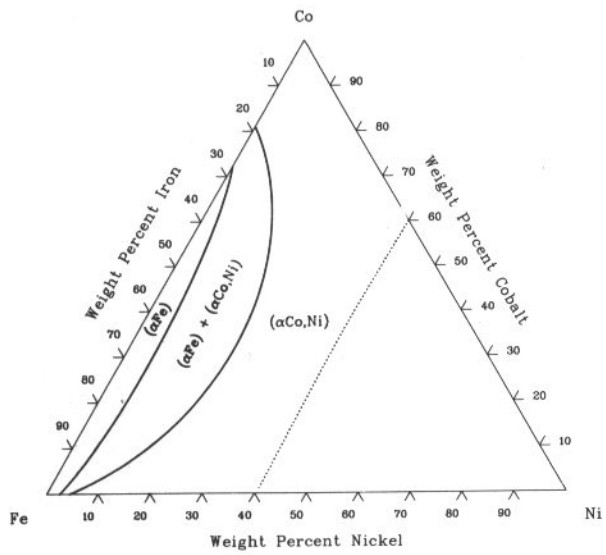

Co-Fe-W isothermal section at 1200 °C [88Ray]

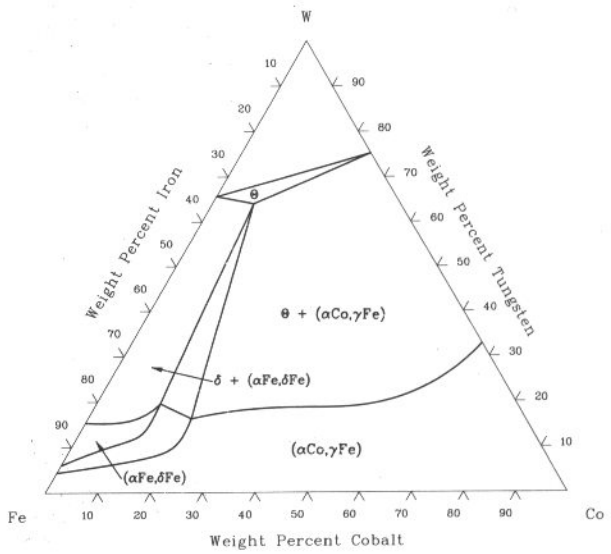

Co-Fe-Ni isothermal section at 600 °C [88Ray]

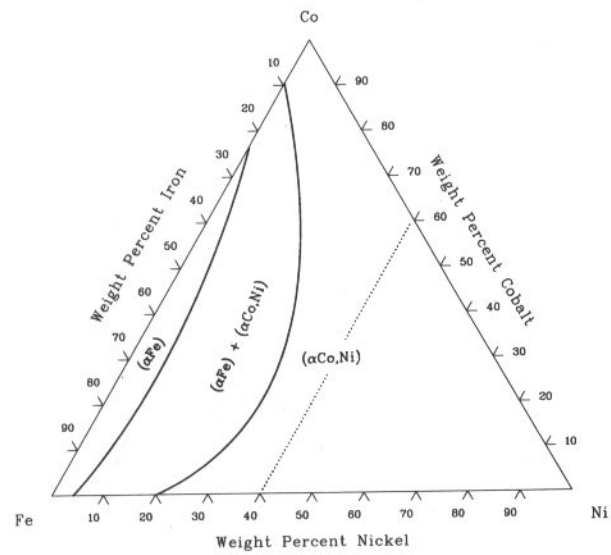

Co-Fe-W isothermal section at 1000 °C [88Ray]

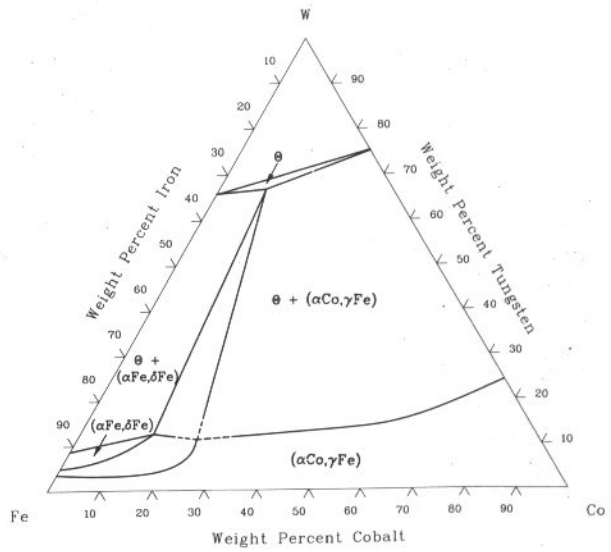

Co-Fe-W isothermal section at 800 °C [88Ray]

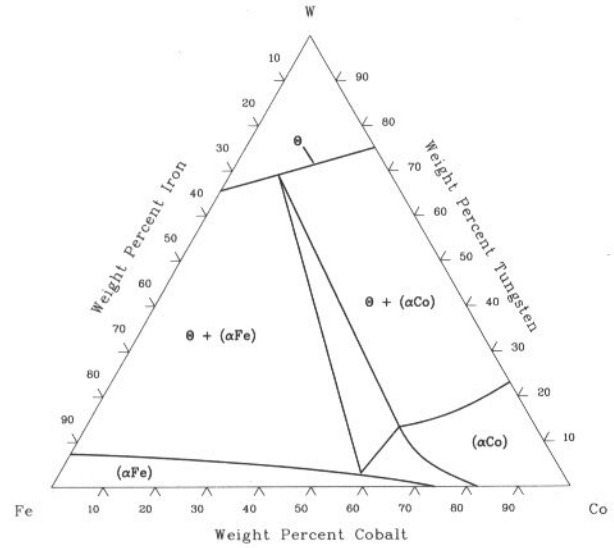

Co-Mo-Ni isothermal section at 1100 °C [80Loo]

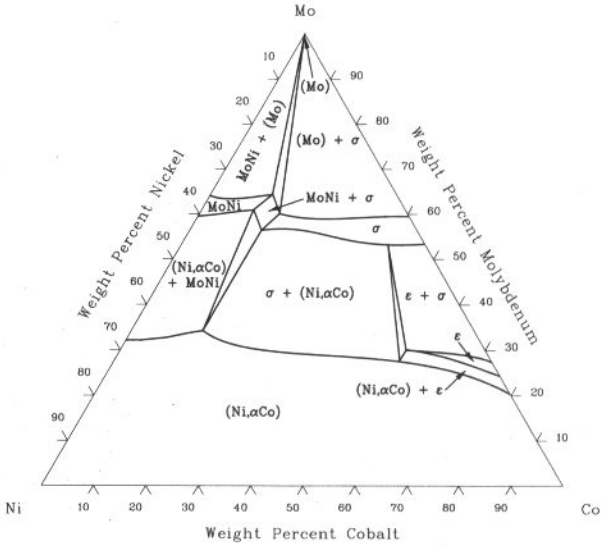

Co-Mo-Ni liquidus projection [84Gup]

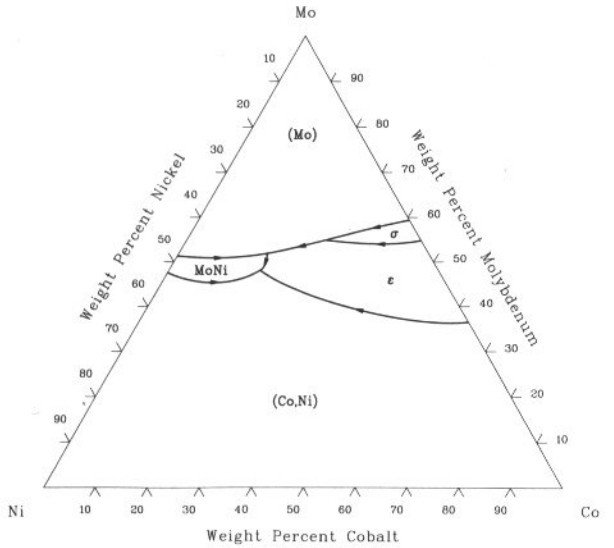

Co-Ni-Ti isothermal section at 1000 °C [83Gry]

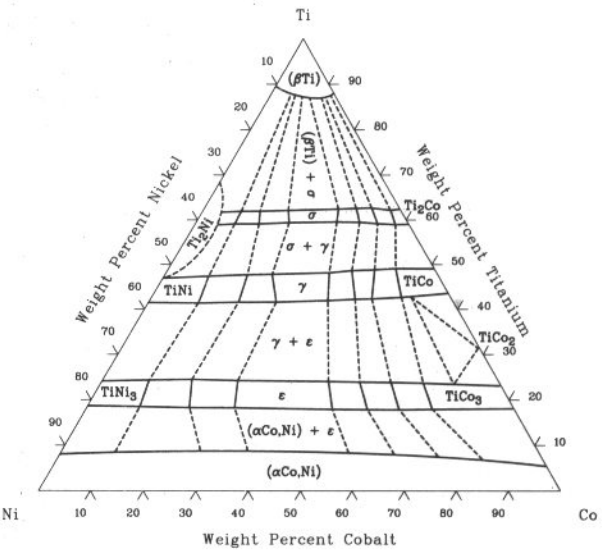

Co-Mo-Ni isothermal section at 1200 °C [52Das]

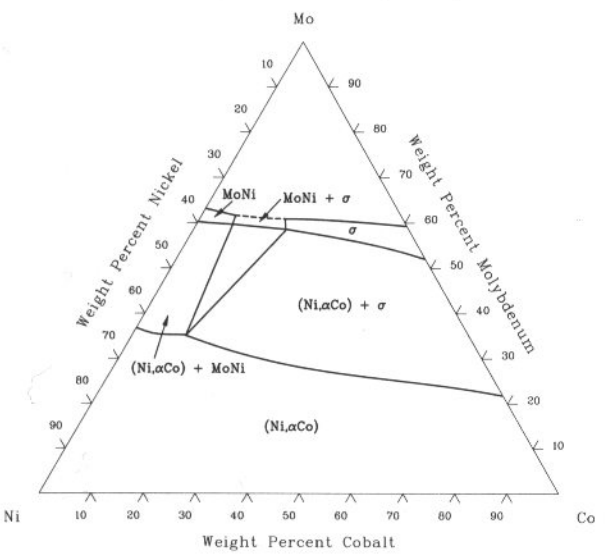

Co-Ni-Ti isothermal section at 800 °C [80Gry]

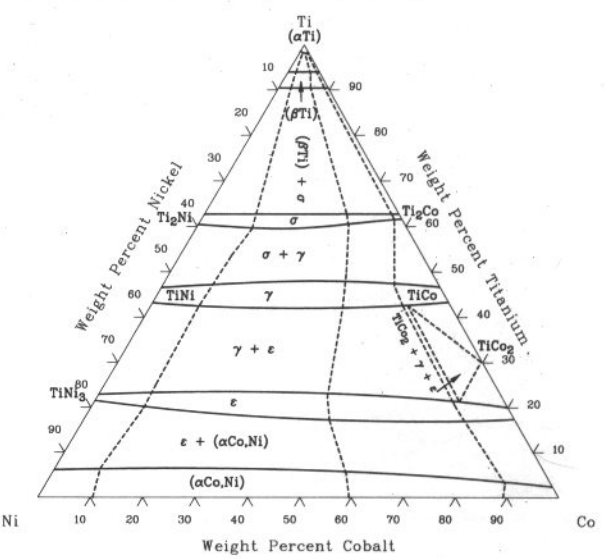

Cr-Fe-Mo liquidus projection [88Ray]

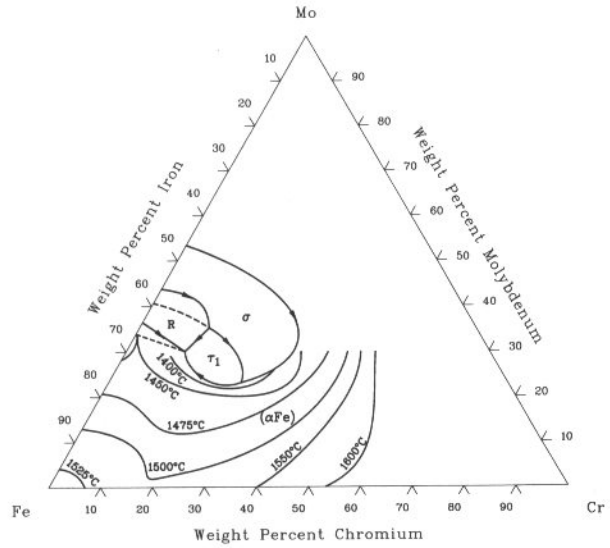

Cr-Fe-Mo isothermal section at 815 °C [88Ray]

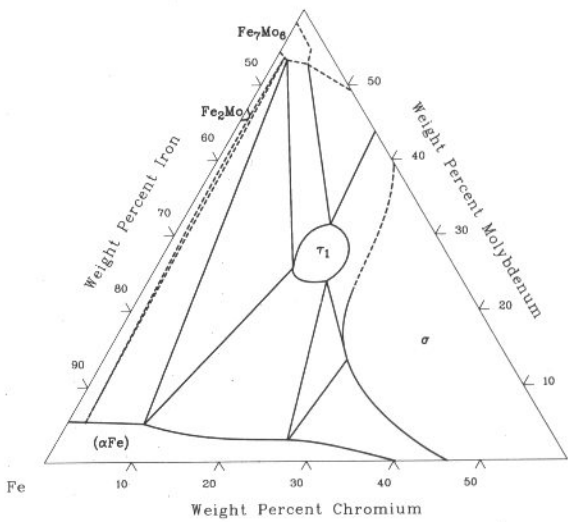

Cr-Fe-Mo isothermal section at 1250 °C [88Ray]

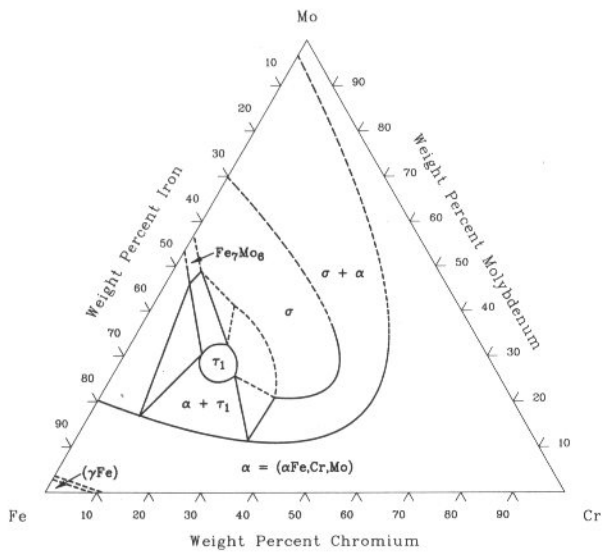

Cr-Fe-Mo [88Ray]

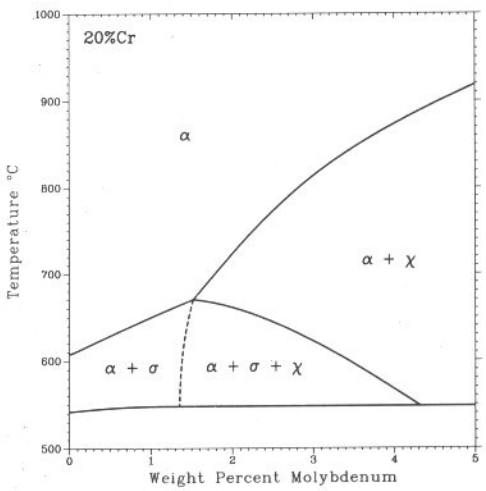

Cr-Fe-Mo isothermal section at 1100 °C [88Ray]

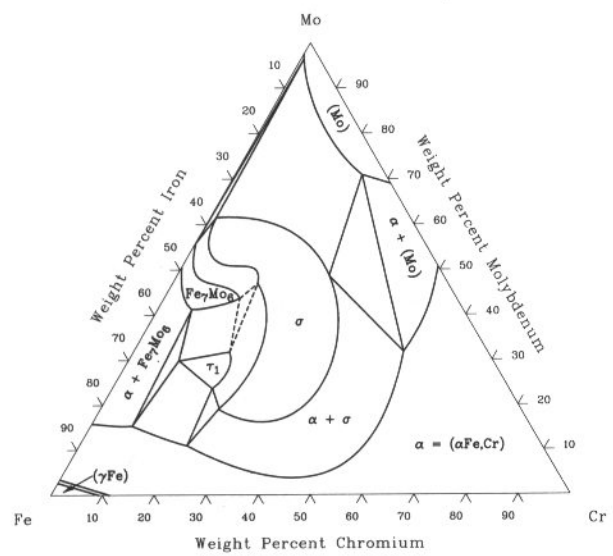

Cr-Fe-Mo [88Ray]

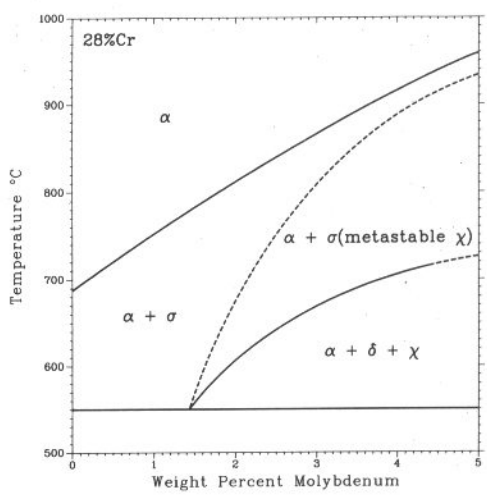

Cr-Fe-N liquidus projection [87Rag]

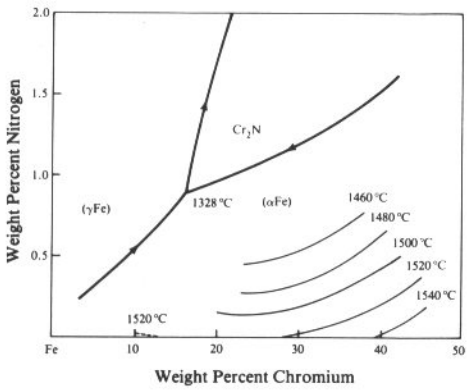

Cr-Fe-N isothermal section at 700 °C [87Rag]

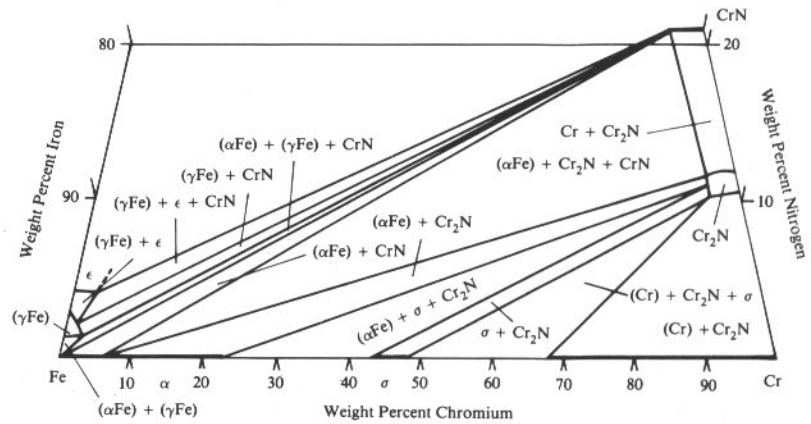

Cr-Fe-N isothermal section at 1200 °C [87Rag]

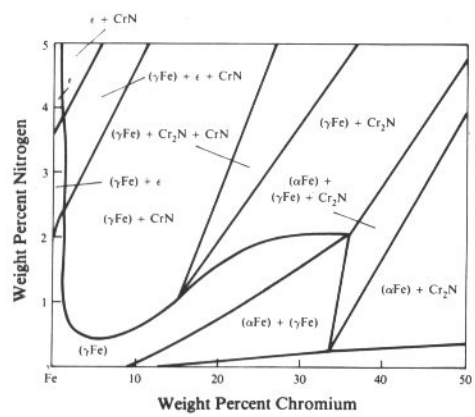

Cr-Fe-N isothermal section at 567 °C [87Rag]

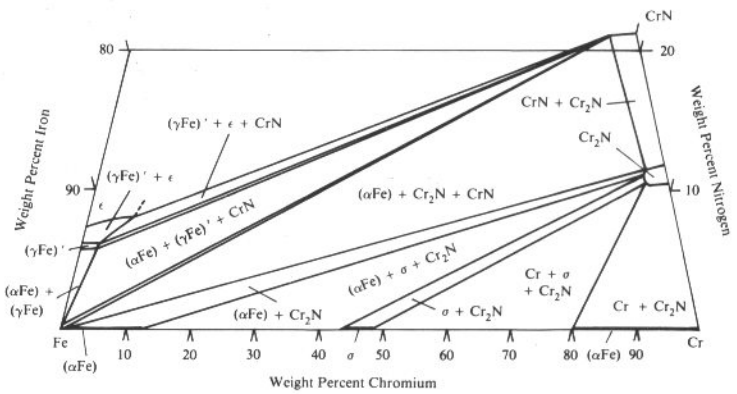

Cr-Fe-N isothermal section at 1000 °C [87Rag]

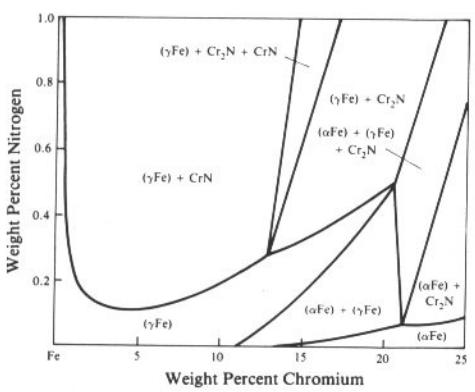

Cr-Fe-Ni liquidus projection [88Ray]

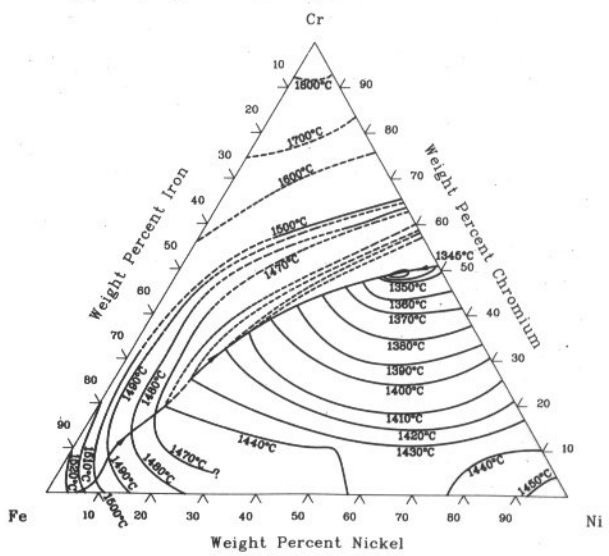

Cr-Fe-Ni solidus projection [88Ray]

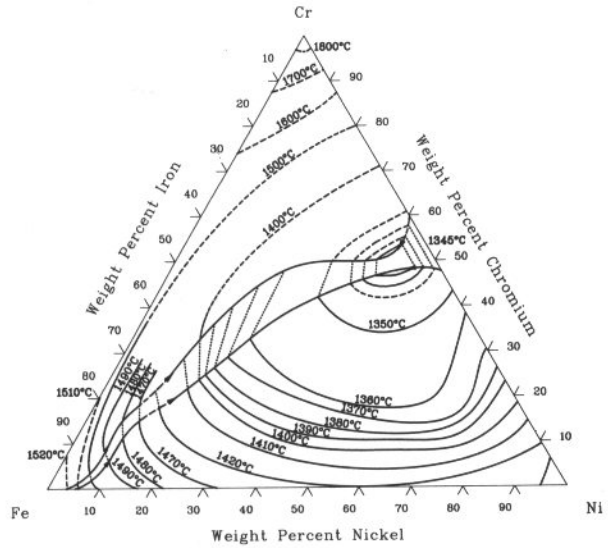

Cr-Fe-Ni isothermal section at 900 °C [88Ray]

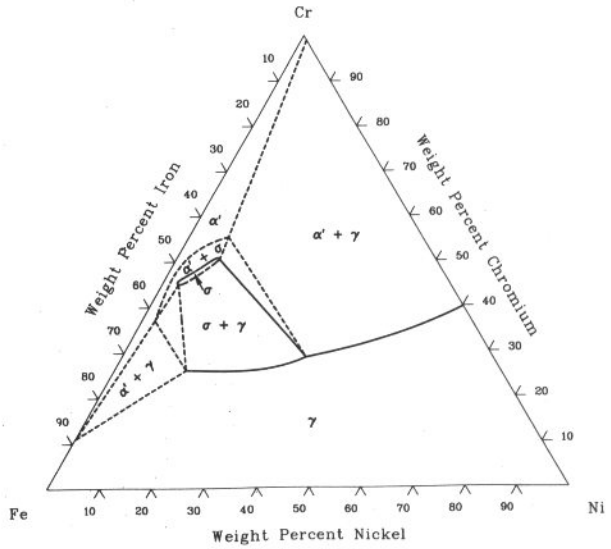

Note: α = (αFe,Cr); γ = (γFe,Ni)

Cr-Fe-Ni isothermal section at 1300 °C [88Ray]

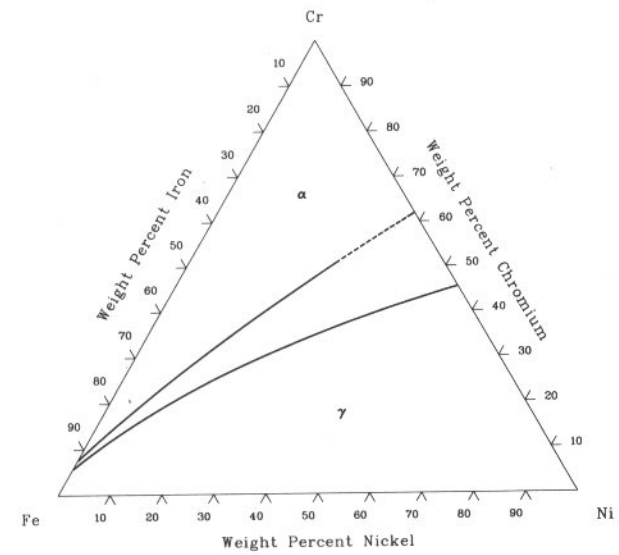

Note: α = (αFe,Cr); γ = (γFe,Ni)

Cr-Fe-Ni isothermal section at 800 °C [88Ray]

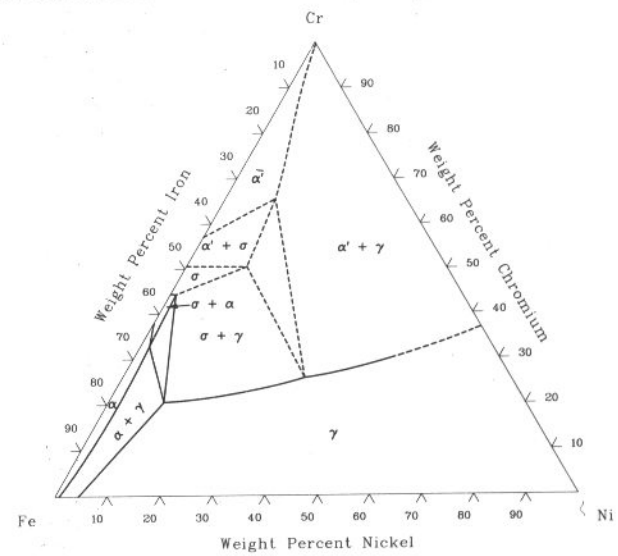

Note: α = (αFe,Cr); γ = (γFe,Ni)

Cr-Fe-Ni isothermal section at 1000 °C [88Ray]

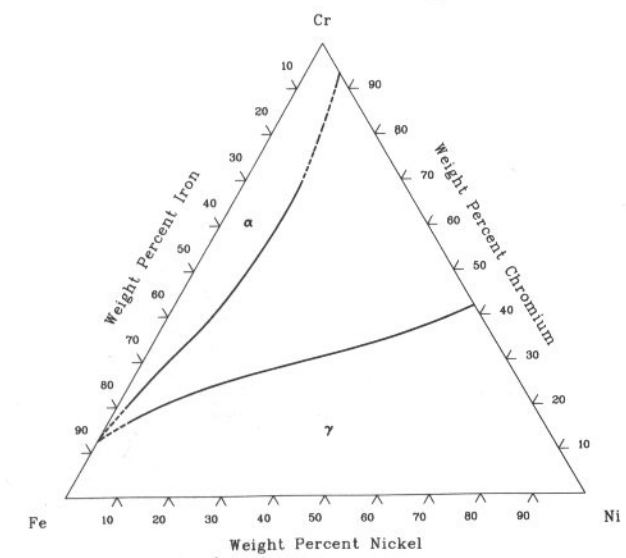

Note: α = (αFe,Cr); γ = (γFe,Ni)

Cr-Fe-Ni isothermal section at 650 °C [88Ray]

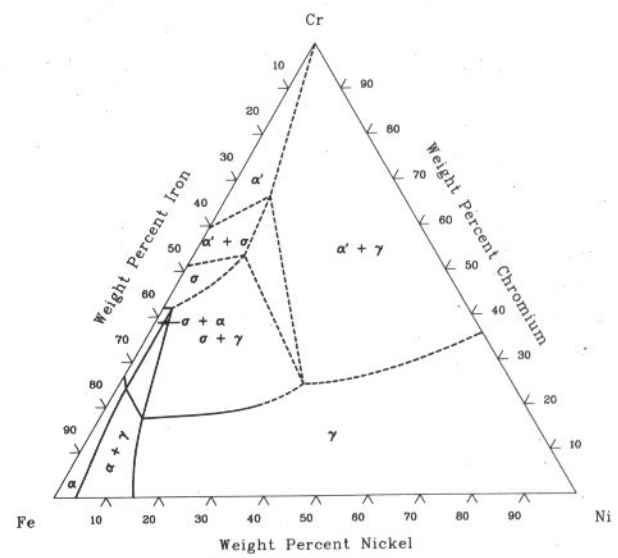

Note: α = (αFe,Cr); γ = (γFe,Ni)

Cr-Fe-W isothermal section at 1200 °C [88Ray]

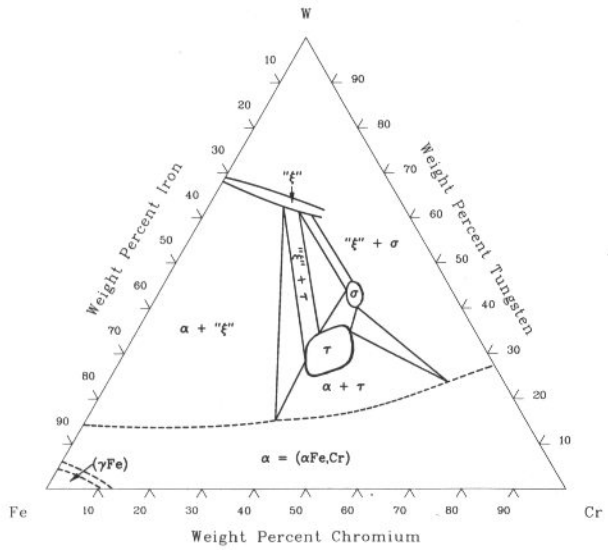

Cr-Mo-Ni isothermal section at 1250 °C [90Gup]

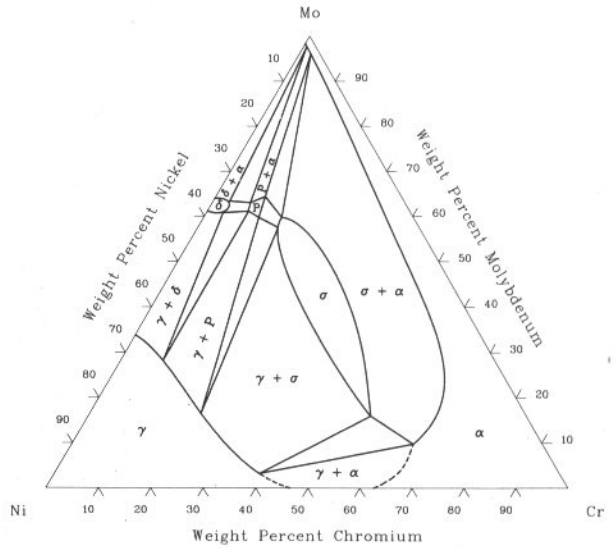

Cr-Fe-W isothermal section at 600 °C [88Ray]

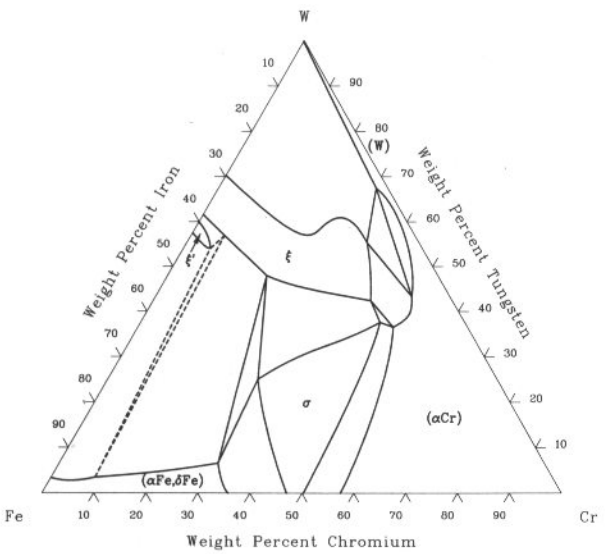

Cr-Mo-Ni isothermal section at 1200 °C [90Gup]

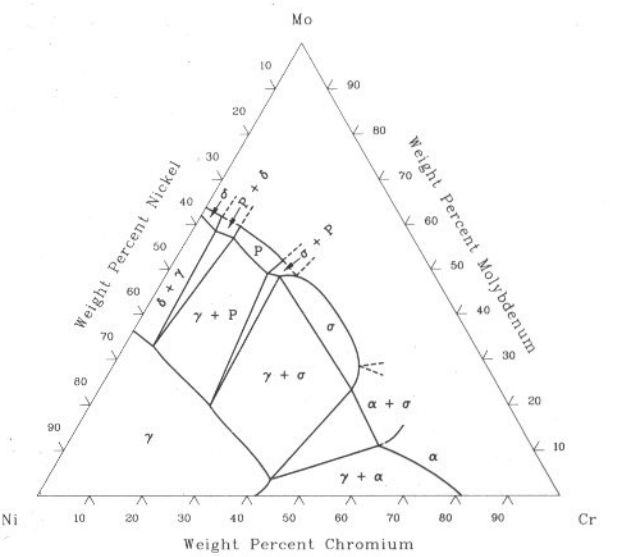

Cr-Mo-Ni liquidus projection [90Gup]

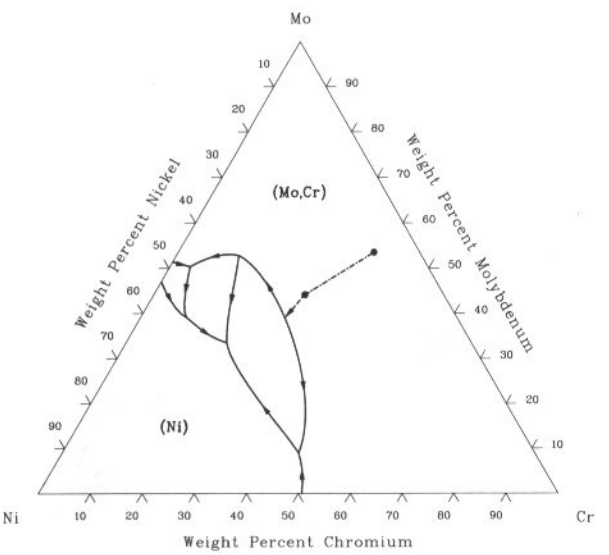

Cr-Mo-Ni isothermal section at 600 °C [90Gup]

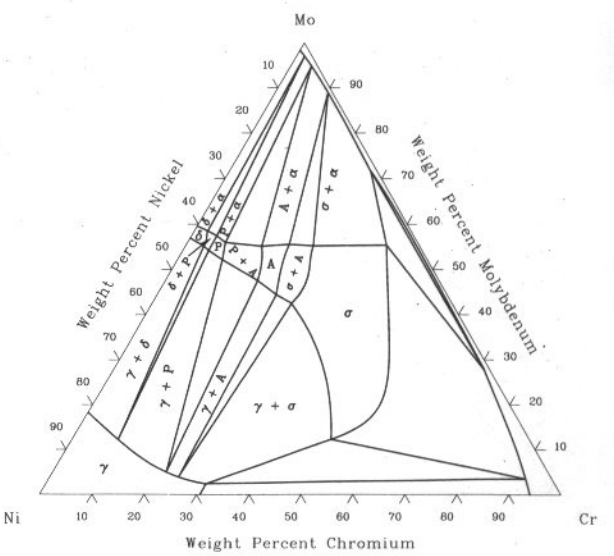

Cr-Mo-W isothermal section at 2227 °C [75Kau]

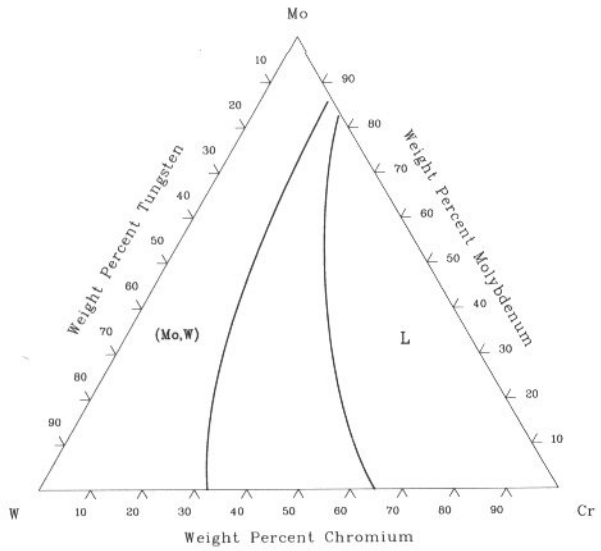

Cr-Nb-Ni liquidus projection [90Gup]

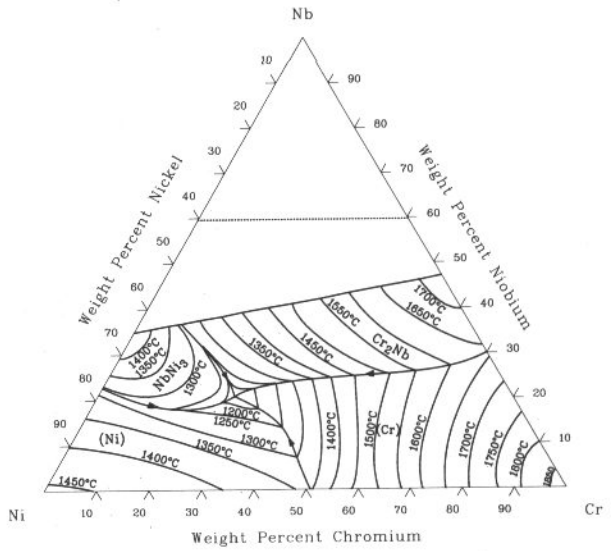

Cr-Mo-W isothermal section at 1300 °C [75Kau]

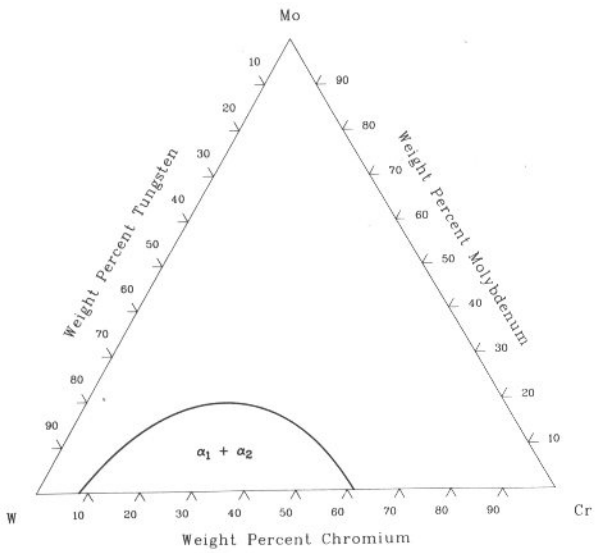

Cr-Nb-Ni isothermal section at 1200 °C [90Gup]

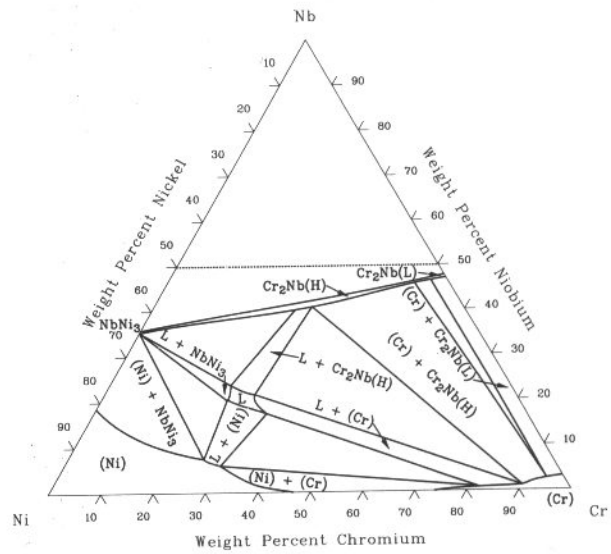

Cr-Mo-W isothermal section at 1000 °C [75Kau]

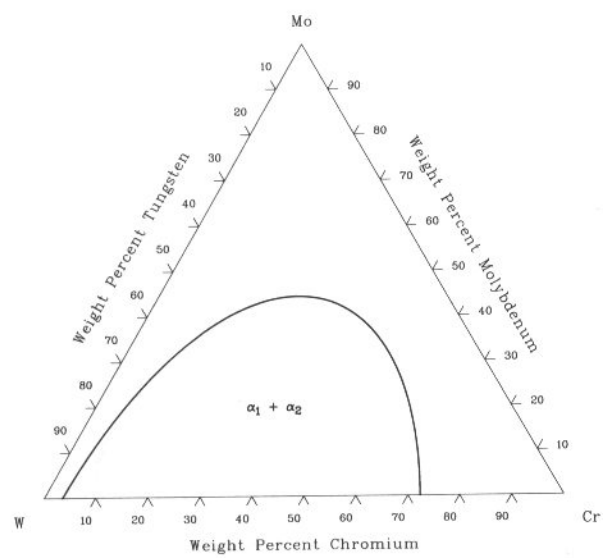

Cr-Nb-Ni isothermal section at 1175 °C [90Gup]

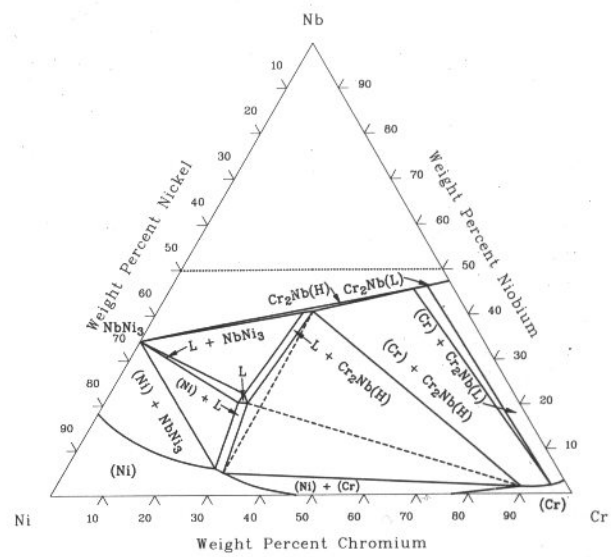

Cr-Nb-Ni isothermal section at 1100 °C [90Gup]

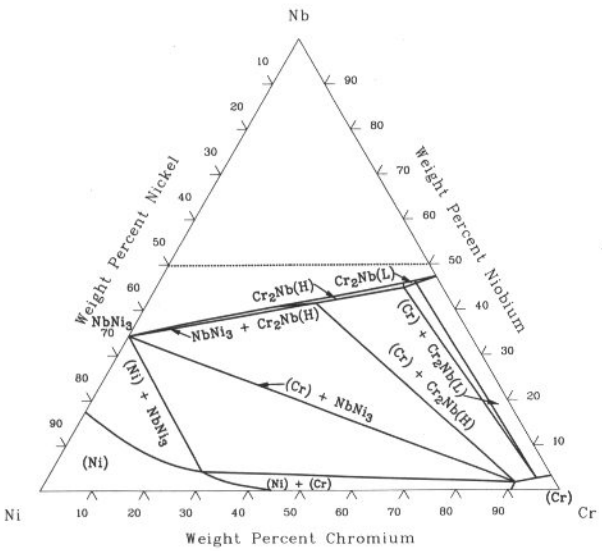

Cr-Ni-Ti liquidus projection [90Gup]

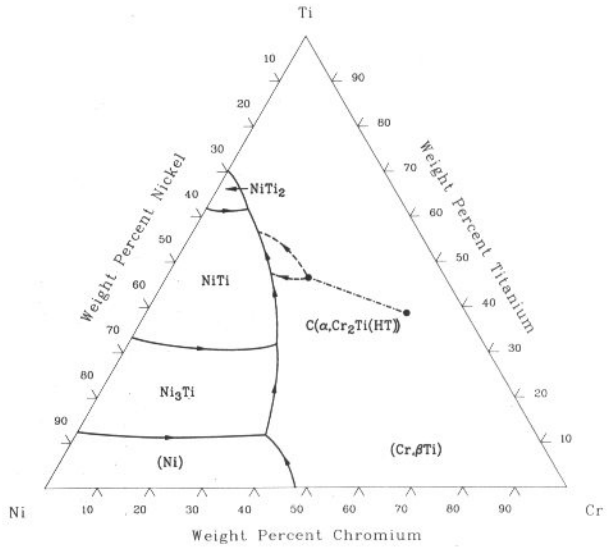

Cr-Nb-W isothermal section at 1500 °C [61Eng]

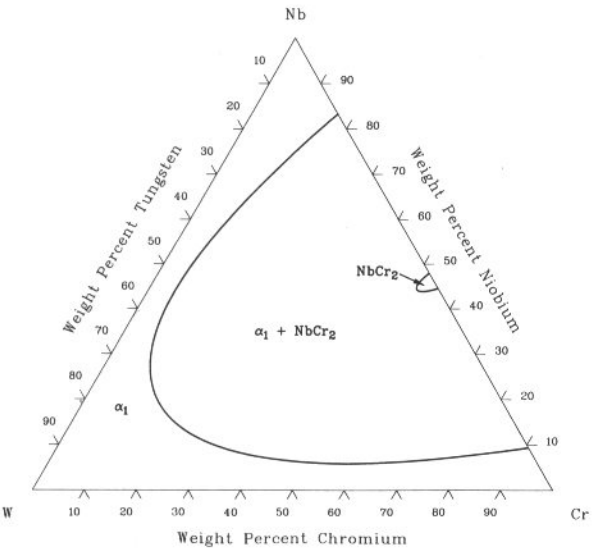

Cr-Ni-Ti isothermal section at 1352 °C [74Kau]

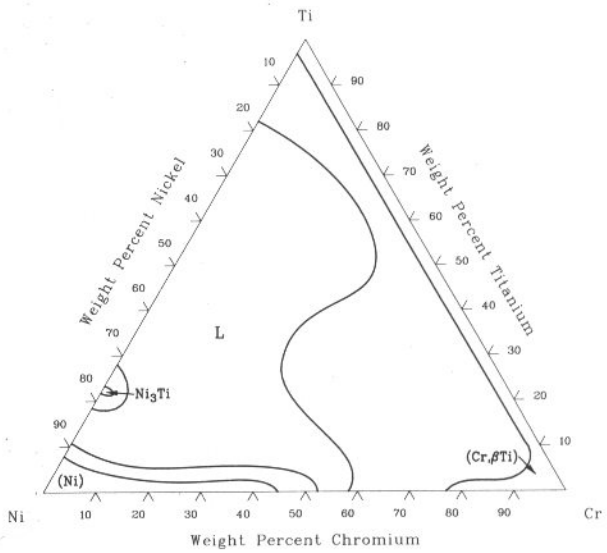

Cr-Nb-W isothermal section at 1000 °C [61Eng]

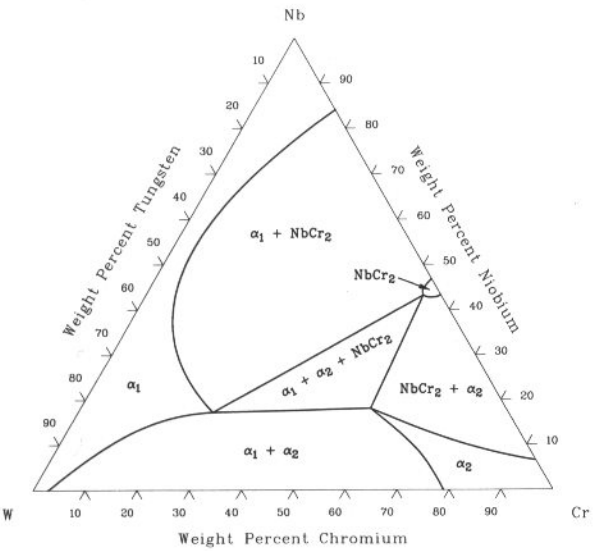

Cr-Ni-Ti isothermal section at 1277 °C [74Kau]

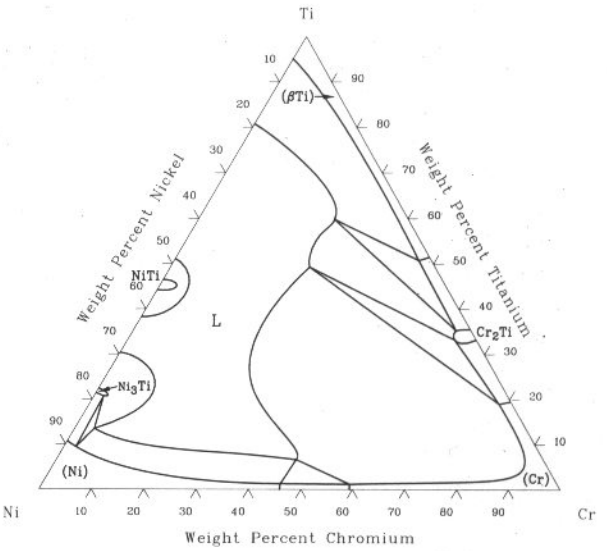

Cr-Ni-Ti isothermal section at 1027 °C [74Kau]

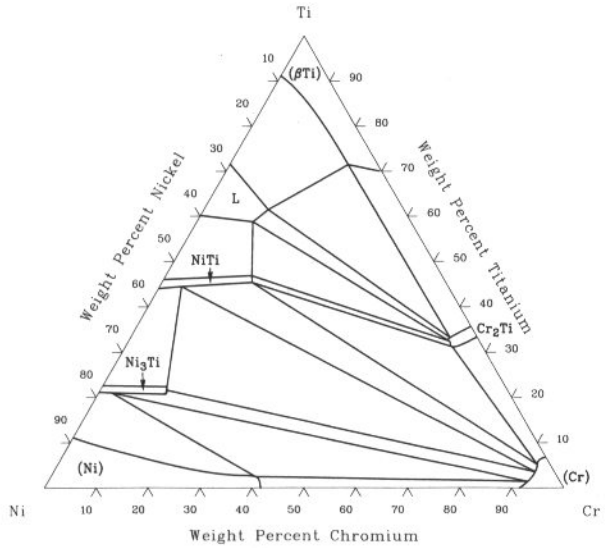

Cr-Ni-W isothermal section at 1000 °C [90Gup]

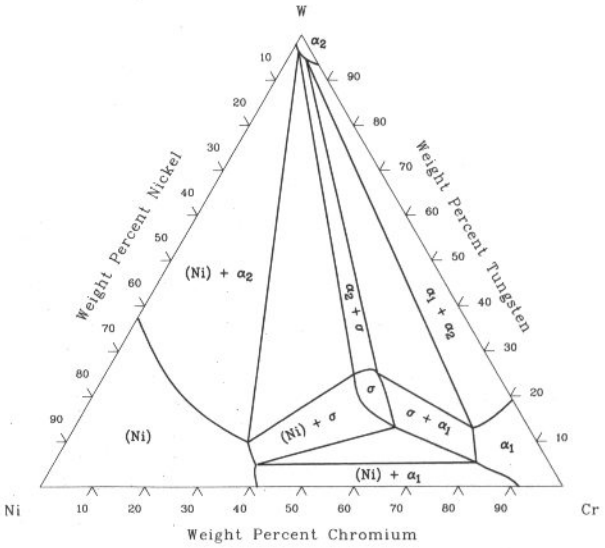

Cr-Ni-W liquidus projection [90Gup]

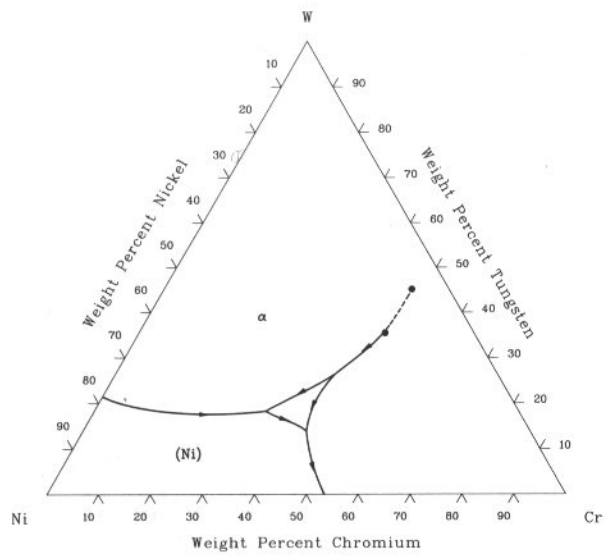

Cr-Ni-W isothermal section at 900 °C [90Gup]

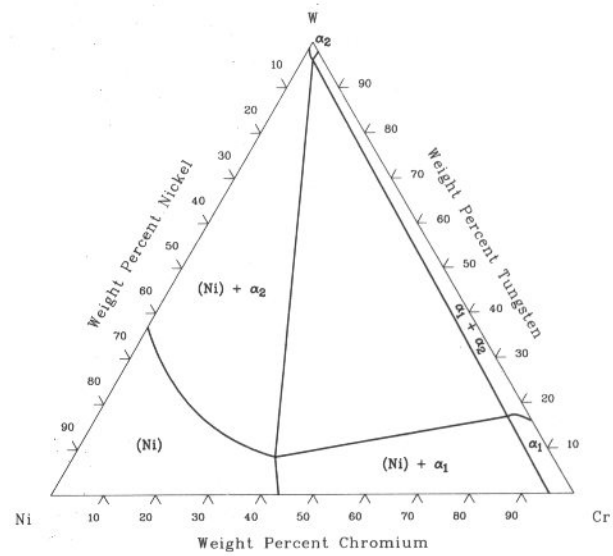

Cr-Ni-W isothermal section at 1250 °C [90Gup]

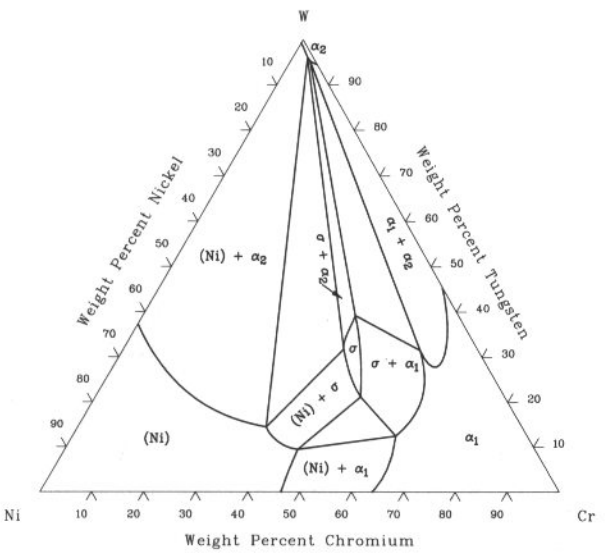

Cr-Ni-W isothermal section at 800 °C [990Gup]

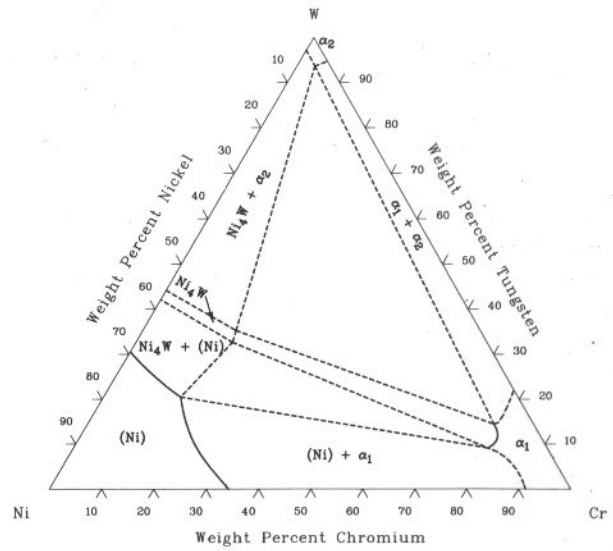

Cr-Ti-W isothermal section at 800 °C [58Bag]

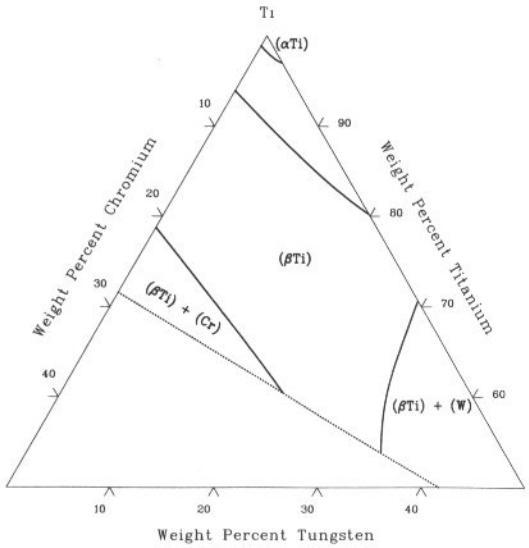

Cr-Ti-W isothermal section at 750 °C [58Bag]

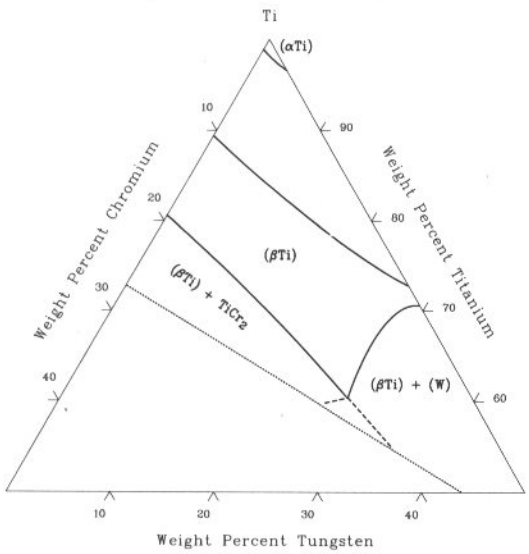

Cr-Ti-W isothermal section at 600 °C [58Bag]

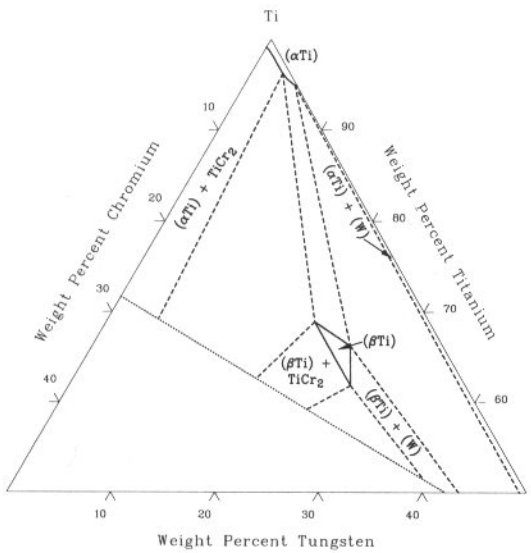

Cu-Fe-Ni liquidus projection [90Gup]

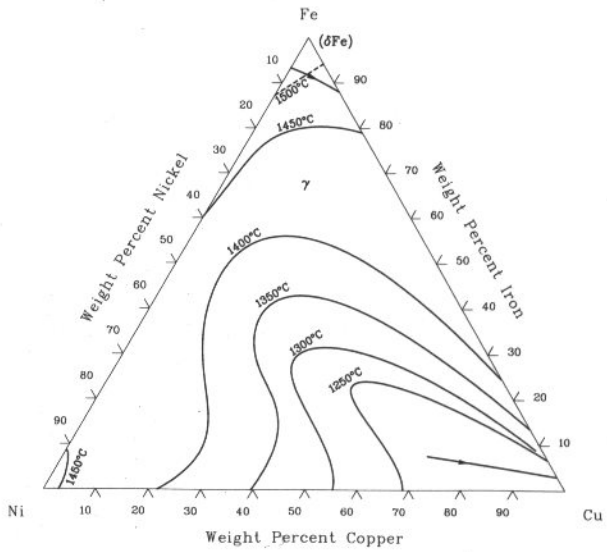

Cu-Fe-Ni miscibility gap [90Gup]

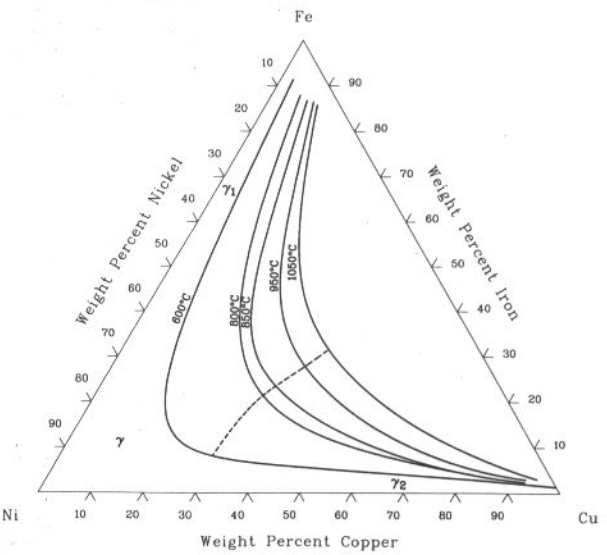

Cu-Fe-Ni isothermal section at 400 °C [90Gup]

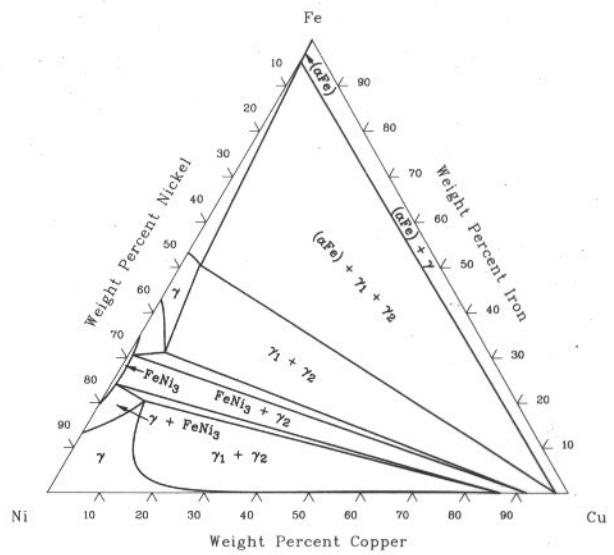

Cu-Fe-Ni isothermal section at 20 °C [90Gup]

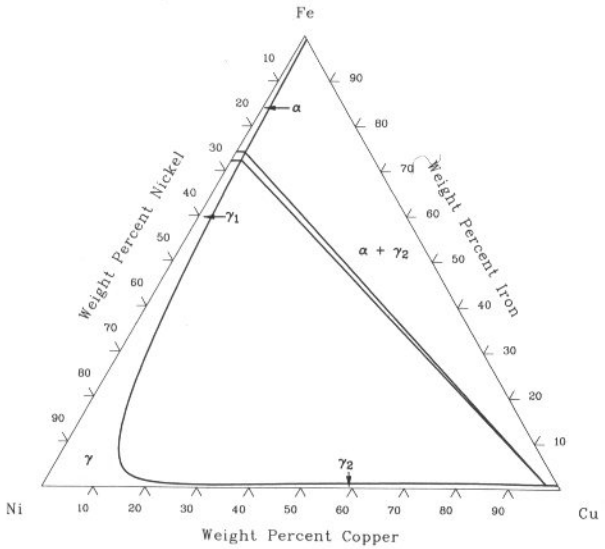

Cu-Fe-Ni [90Gup]

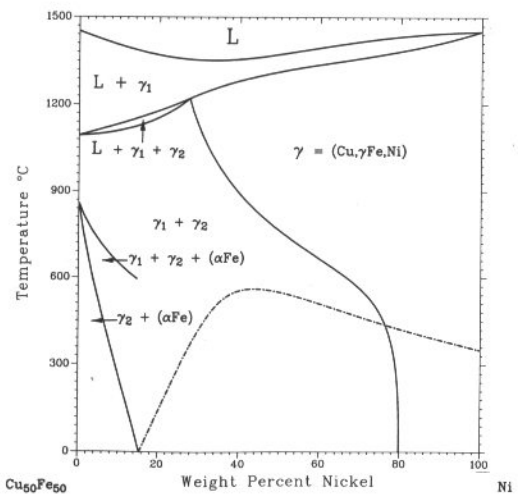

Cu-Ni-Sn liquidus projection [90Gup]

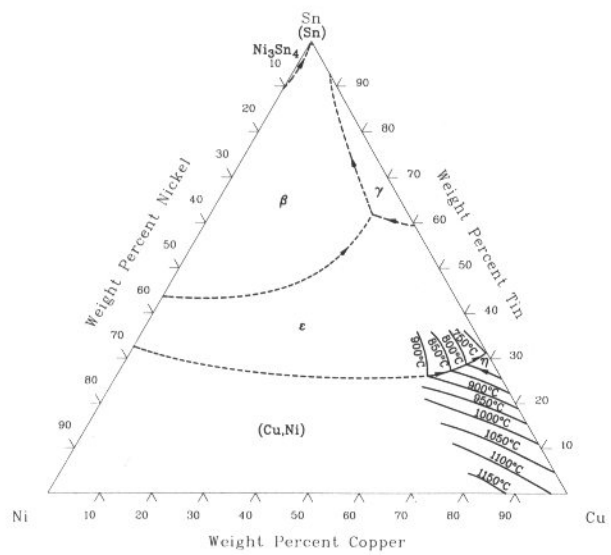

Cu-Ni-Sn solidus projection [90Gup]

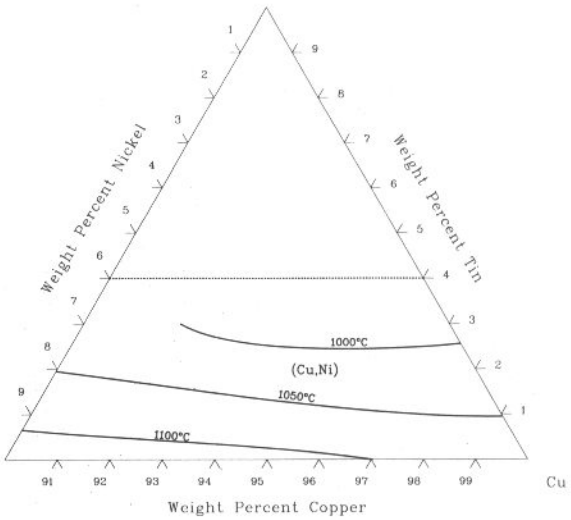

Cu-Ni-Sn isothermal section at 700 °C [90Gup]

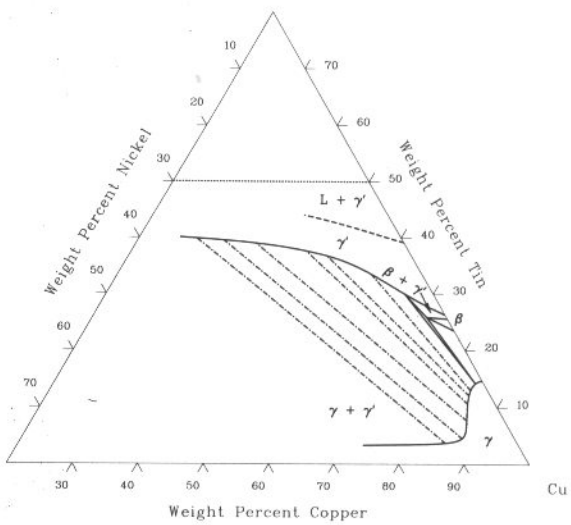

Cu-Ni-Sn isothermal section at 550 °C [90Gup]

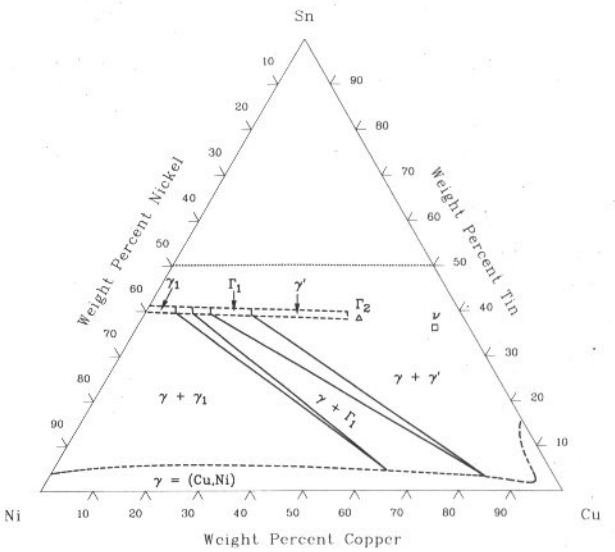

Cu-Ni-Zn liquidus projection [79Cha]

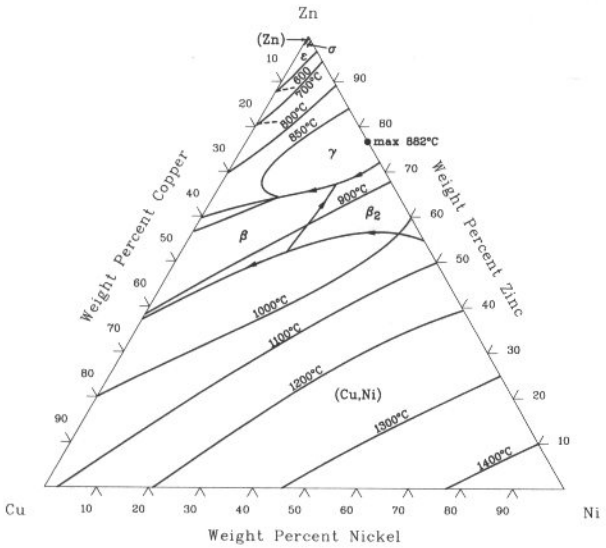

Cu-Ni-Zn isothermal section at 20 °C [73Lev]

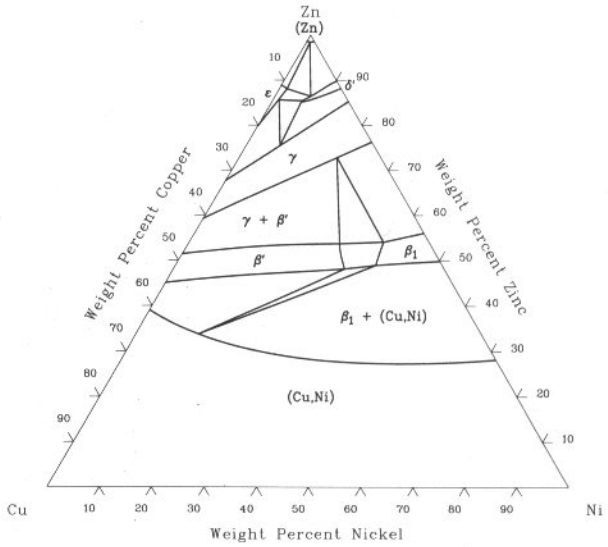

Cu-Ni-Zn isothermal section at 775 °C [79Cha]

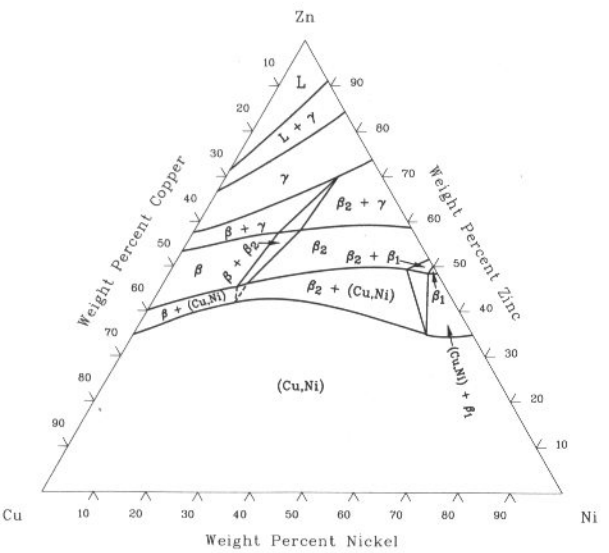

Cu-Pb-Zn liquidus projection [79Cha]

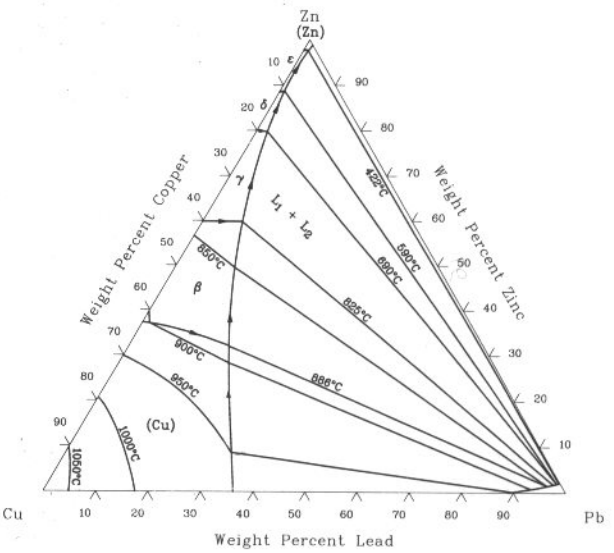

Cu-Ni-Zn isothermal section at 650 °C [73Lev]

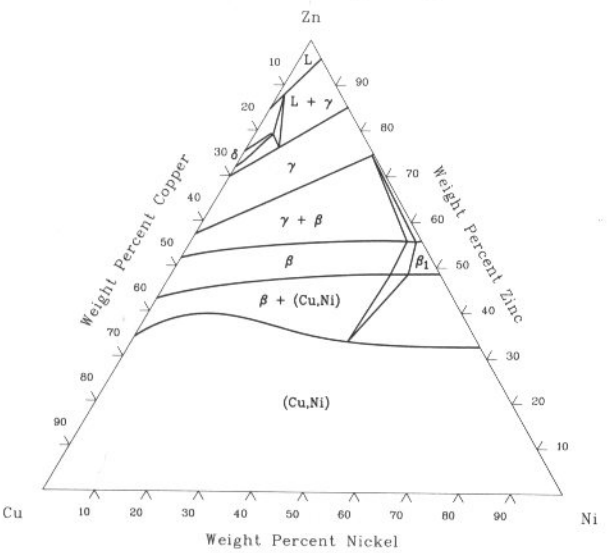

Cu-Pb-Zn (Pb) liquidus projection [79Cha]

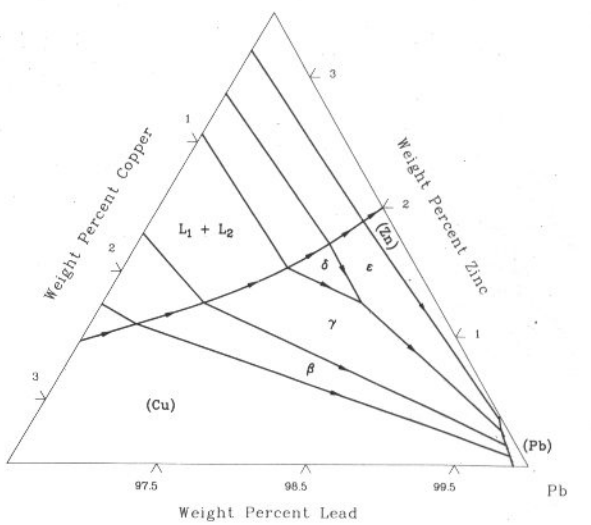

Cu-Pb-Zn isothermal section at 25 °C [29Bau]

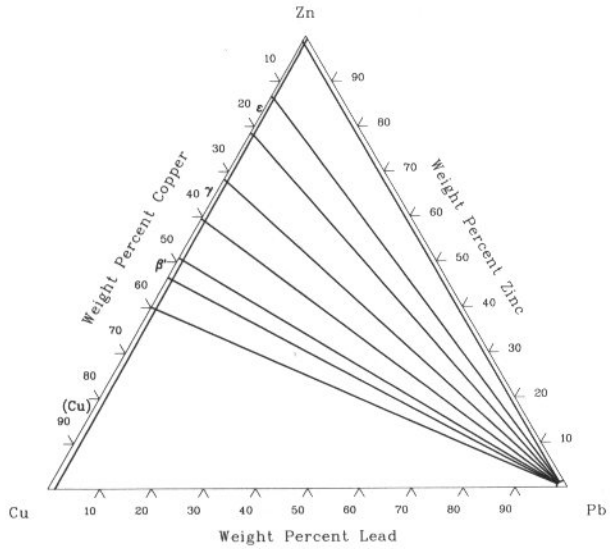

Cu-Sb-Sn phases present at temperatures below the reactions in the solid state [73Bla]

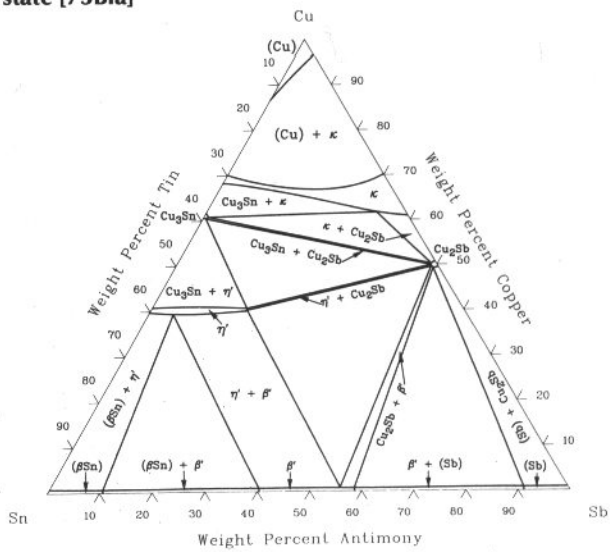

Cu-Sb-Sn liquidus projection [73Bla]

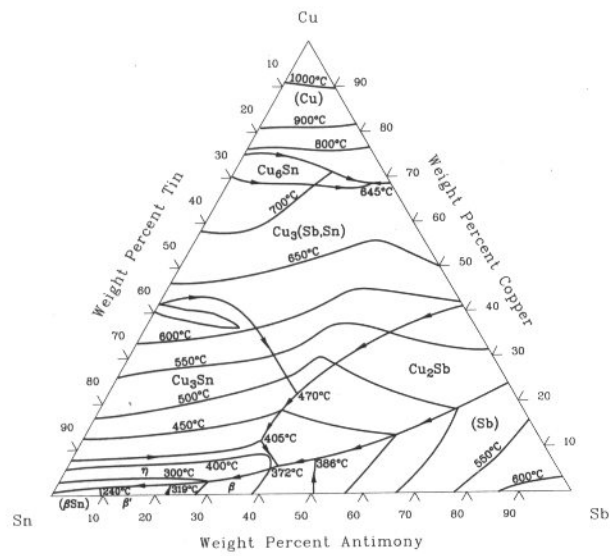

Cu-Sn-Zn liquidus projection [73Smi]

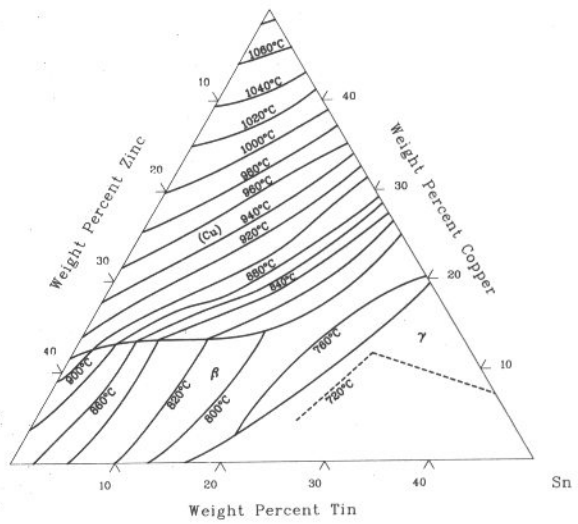

Cu-Sb-Sn (Sn) liquidus projection [73Bla]

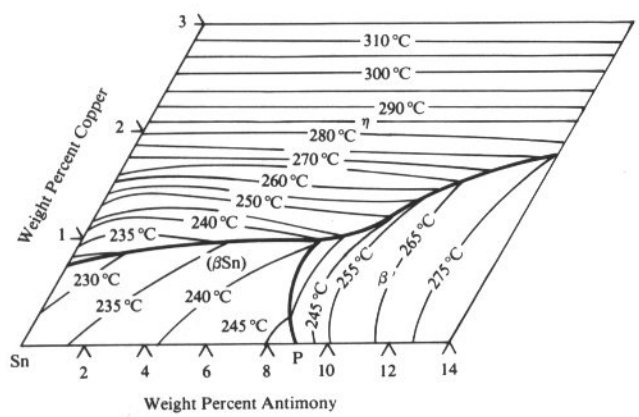

Cu-Sn-Zn isothermal section at 500 °C [73Smi]

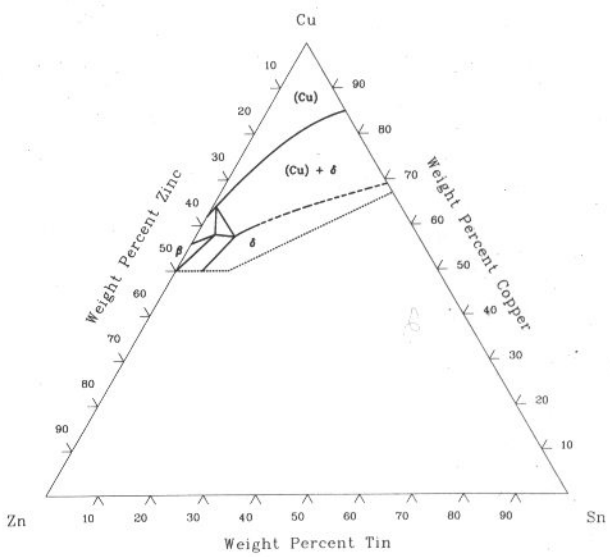

Fe-Mn-Ni liquidus projection [88Ray]

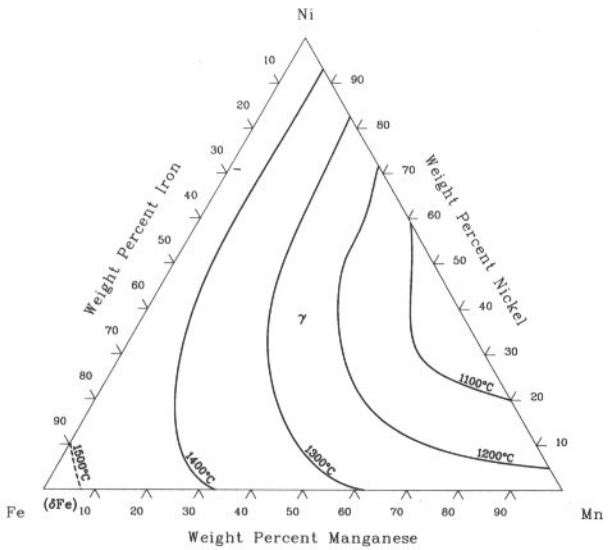

Fe-Mn-Ni isothermal section at 650 °C [89Har]

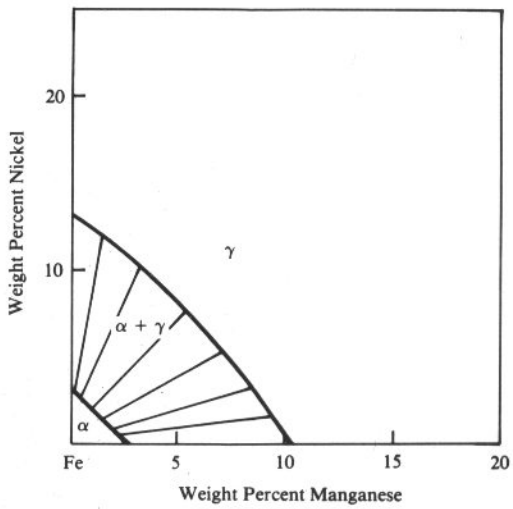

Fe-Mn-Ni isothermal section at 850 °C [89Har]

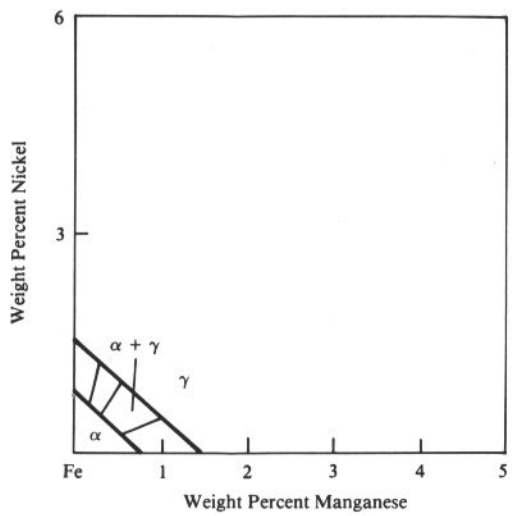

Fe-Mn-Ni isothermal section at 550 °C [89Har]

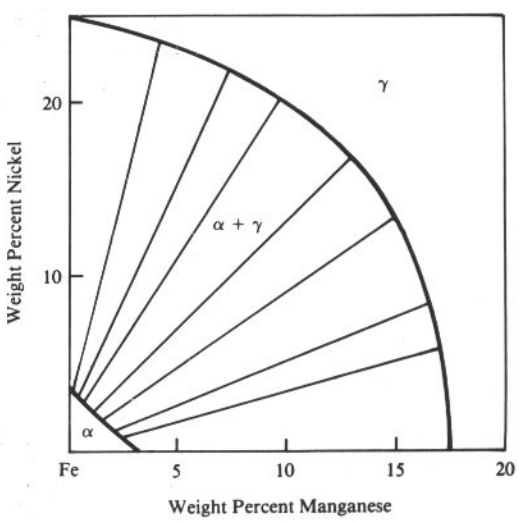

Fe-Mn-Ni isothermal section at 750 °C [89Har]

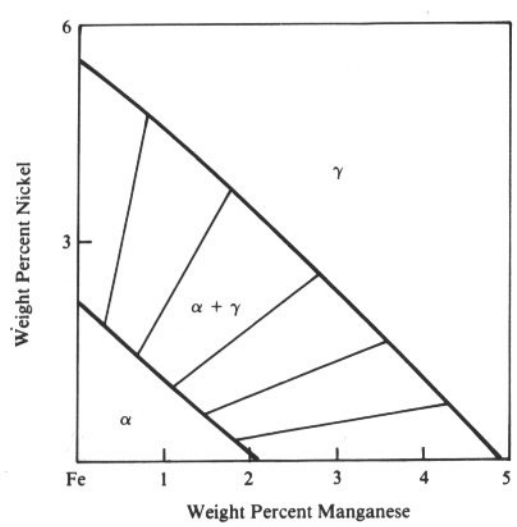

Fe-Mo-Nb isothermal section at 1250 °C [89Har]

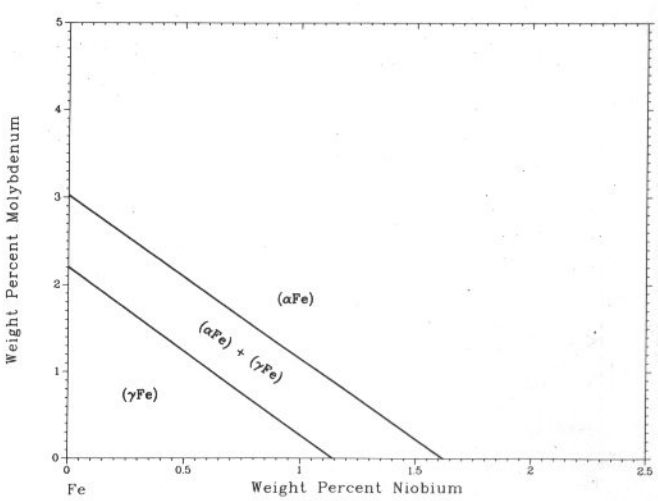

Fe-Mo-Nb isothermal section at 1150 °C [89Har]

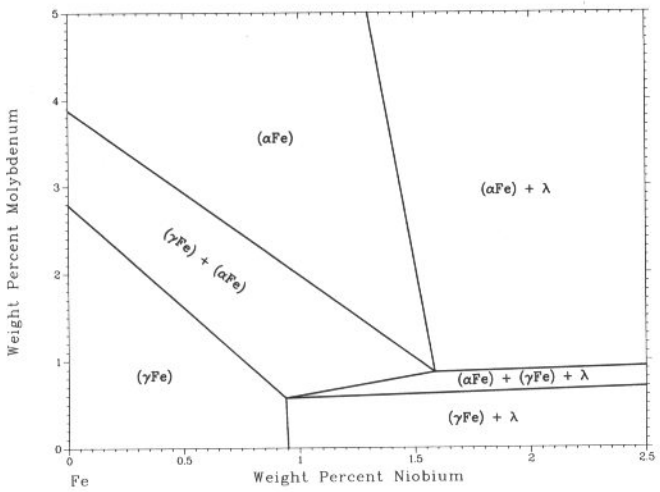

Fe-Mo-Nb isothermal section at 900 °C [87Smi]

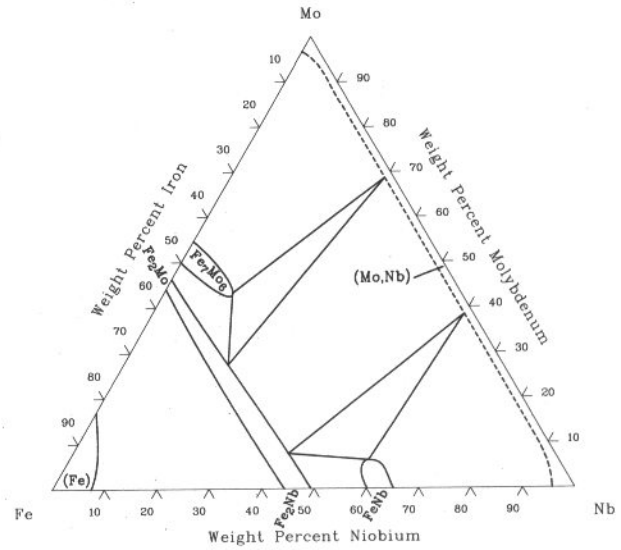

Fe-Mo-Nb isothermal section at 1050 °C [89Har]

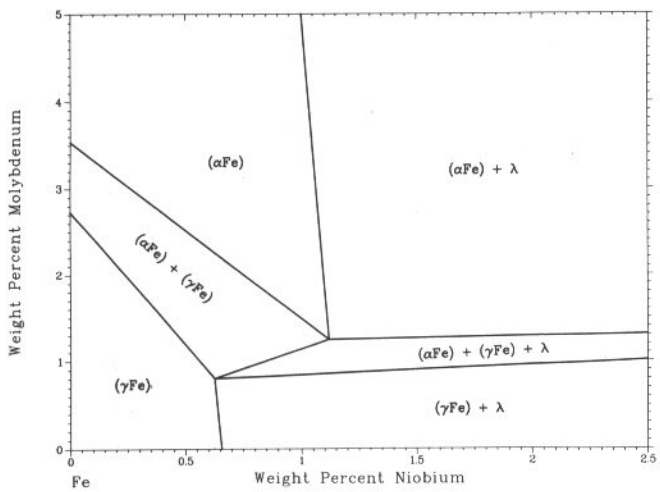

Fe-Mo-Ni liquidus projection [34Kos]

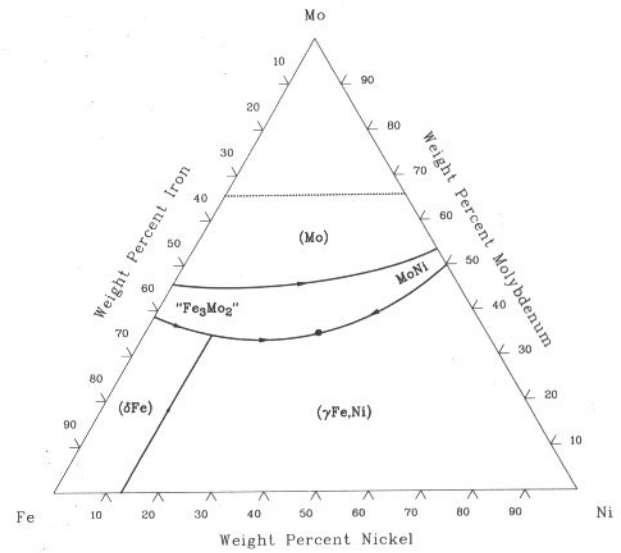

Fe-Mo-Nb isothermal section at 950 °C [89Har]

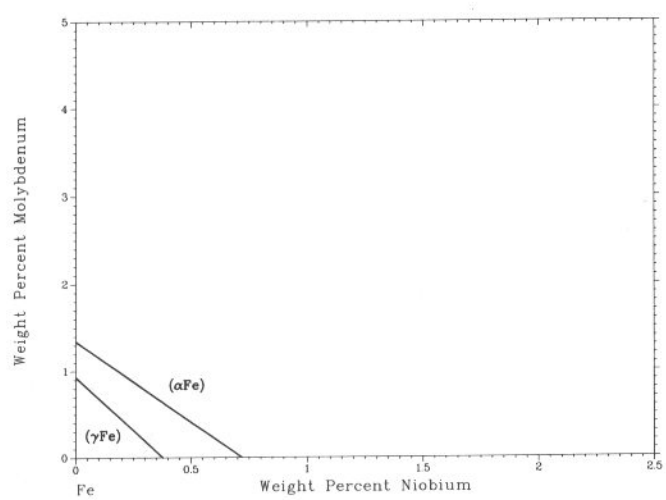

Fe-Mo-Ni isothermal section at 1200 °C [52Das]

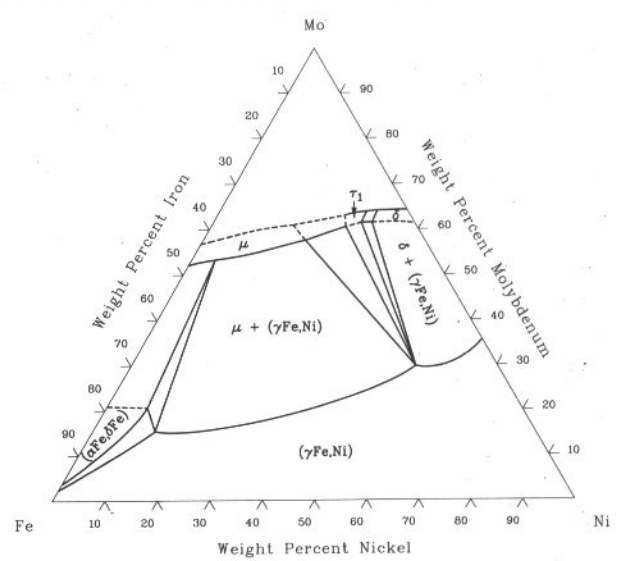

Fe-Mo-Ni isothermal section at 1100 °C [88Ray]

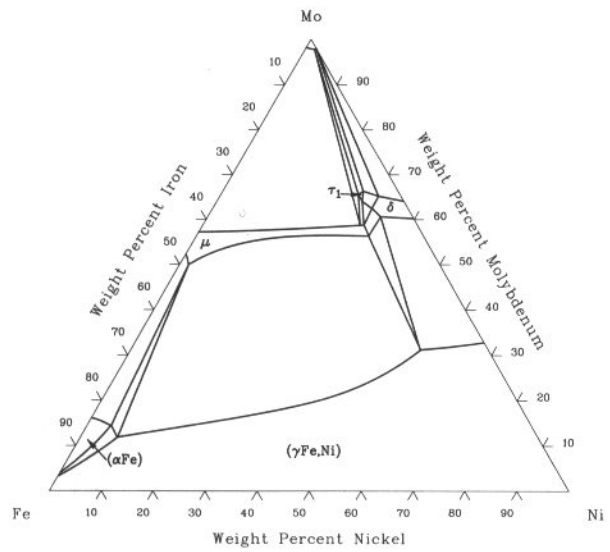

Fe-Ni-W isothermal section at 1465 °C [88Ray]

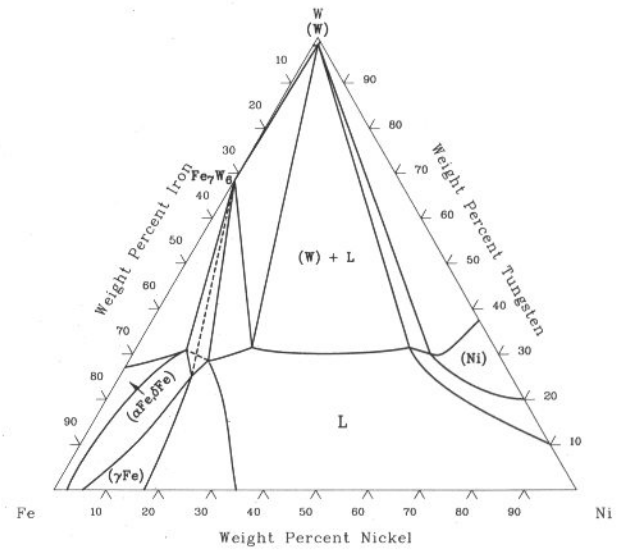

Fe-Ni-W liquidus and solidus projections [88Ray]

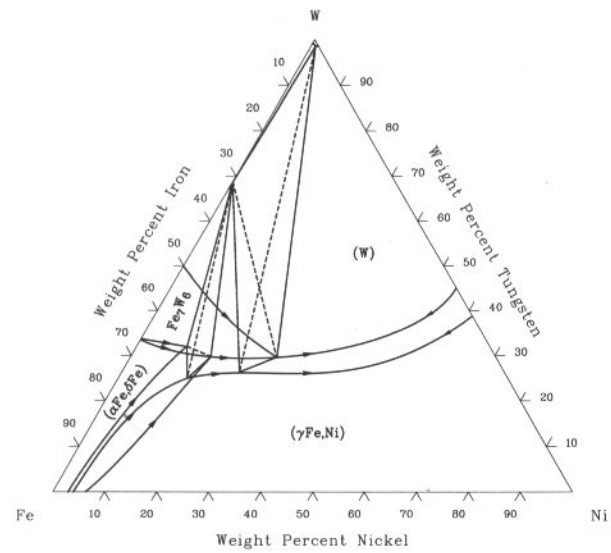

Fe-Ni-W isothermal section at 1455 °C [88Ray]

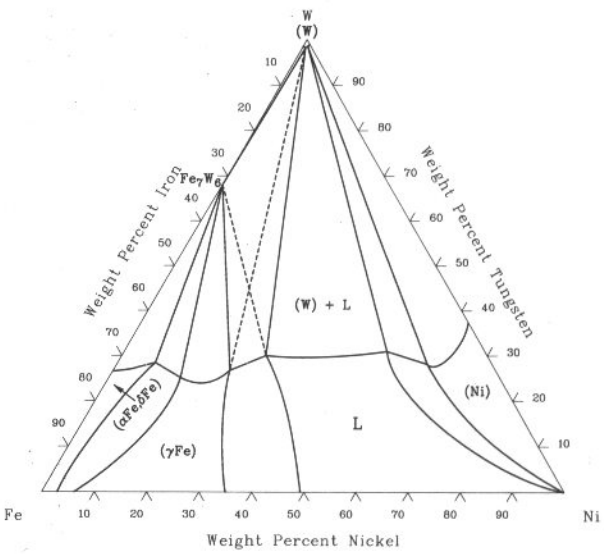

Fe-Ni-W isothermal section at 1500 °C [88Ray]

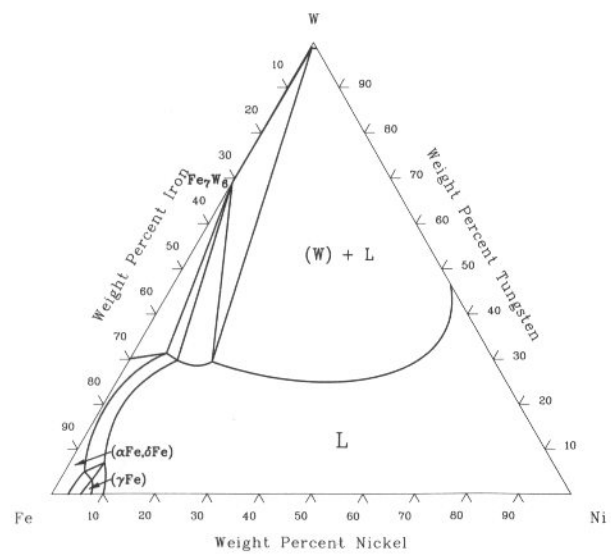

Fe-Ni-W isothermal section at 1400 °C [88Ray]

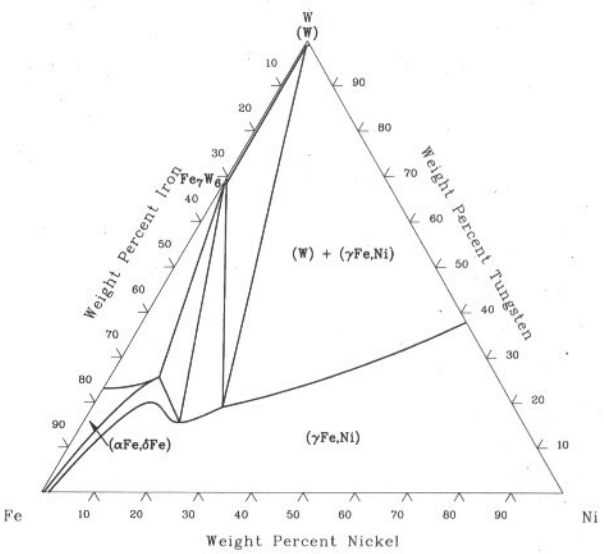

Mo-Nb-Ti isothermal section at 1100 °C [58Kor]

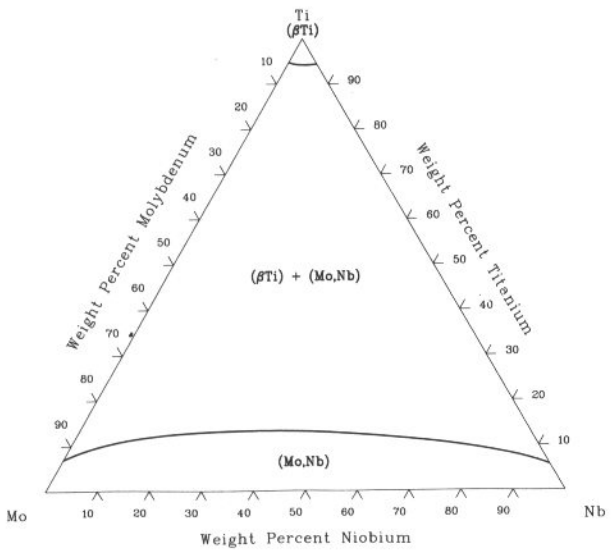

Mo-Nb-Ti isothermal section at 600 °C [58Kor]

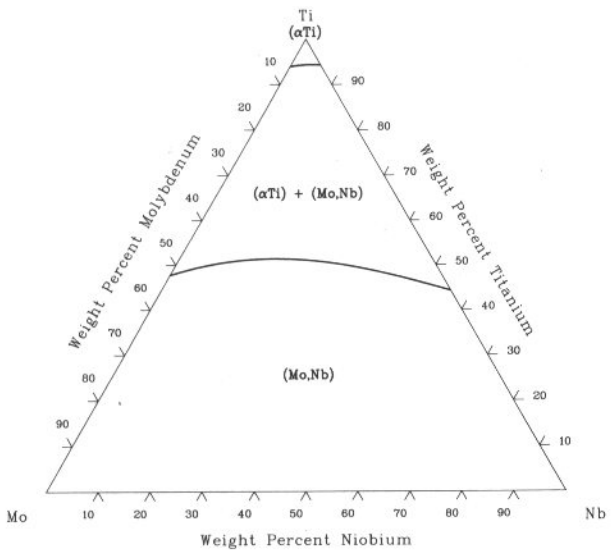

Mo-Ni-Ti isothermal section at 1200 °C [86Pri]

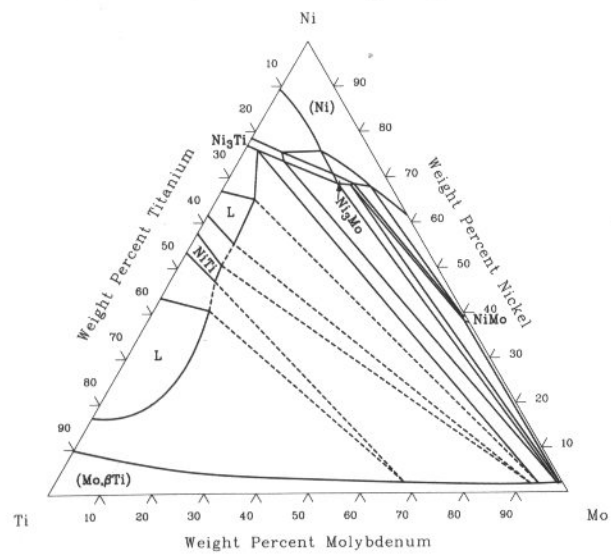

Mo-Ni-Ti isothermal section at 900 °C [84Ere]

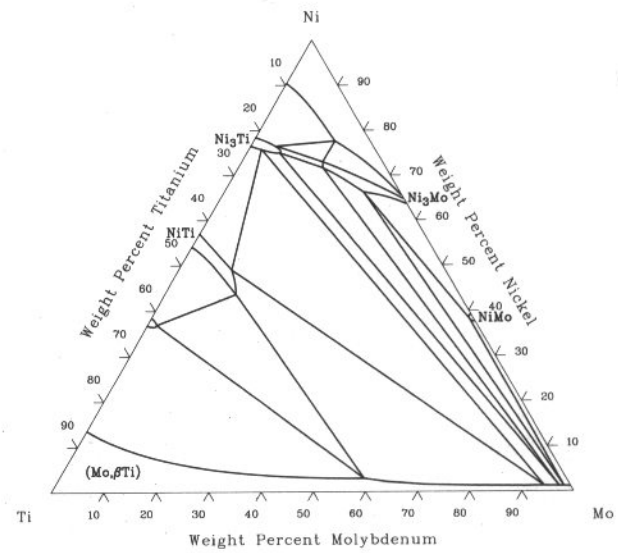

Mo-Ni-W isothermal section at 1000 °C [80Mas]

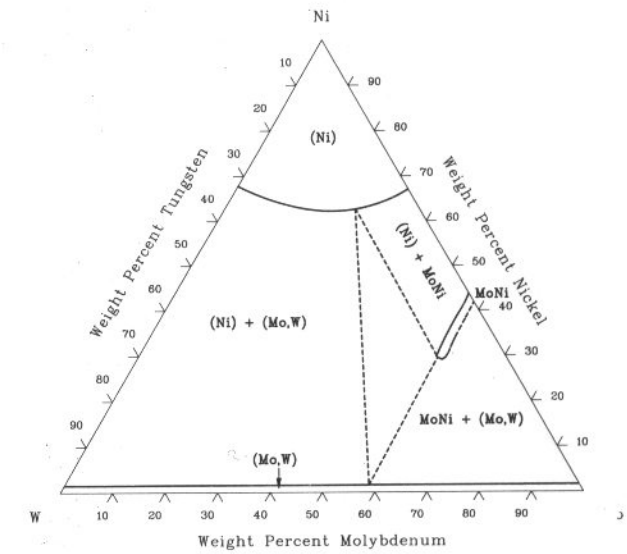

Mo-Ni-W isothermal section at 700 °C [85Mes]

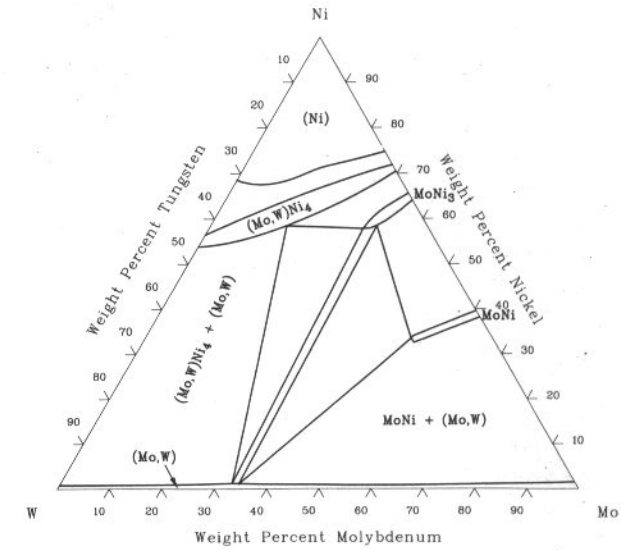

Mo-Ti-W isothermal section at 2227 °C [75Kau]

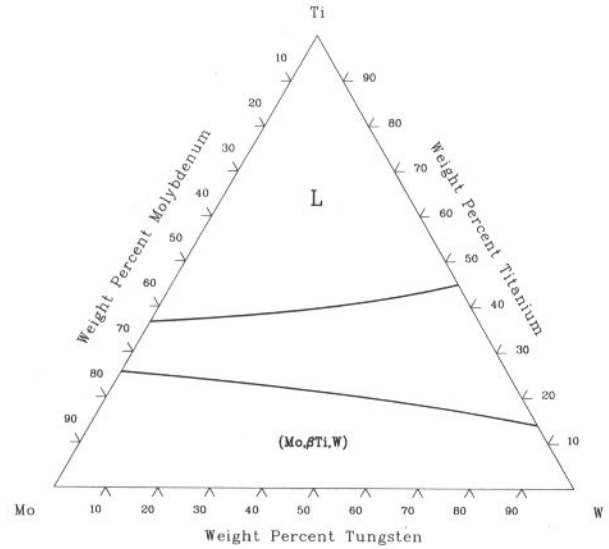

Nb-Ti-W isothermal section at 600 °C [77Lev]

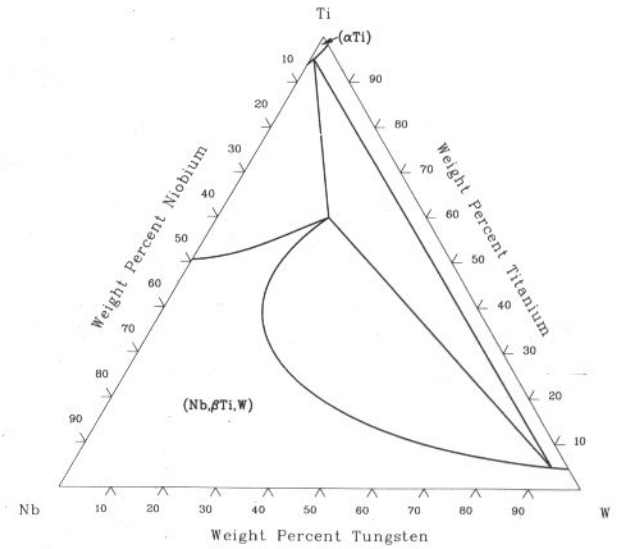

Mo-Ti-W isothermal section at 1000 °C [75Kau]

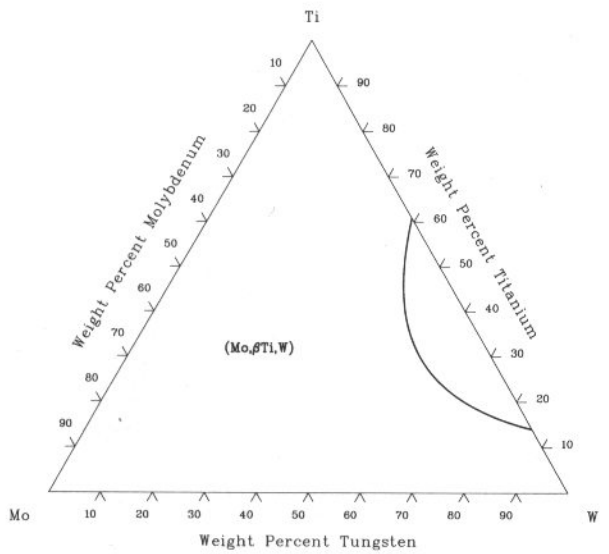

Pb-Sb-Sn liquidus projection [73Bre]

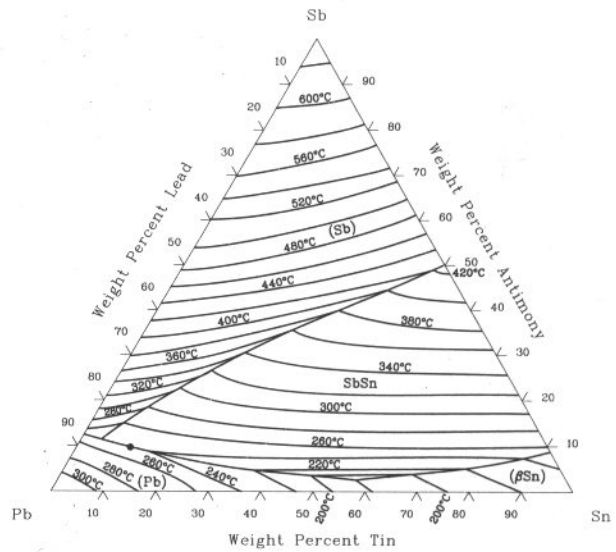

Nb-Ti-W isothermal section at 1000 °C [75Kau]

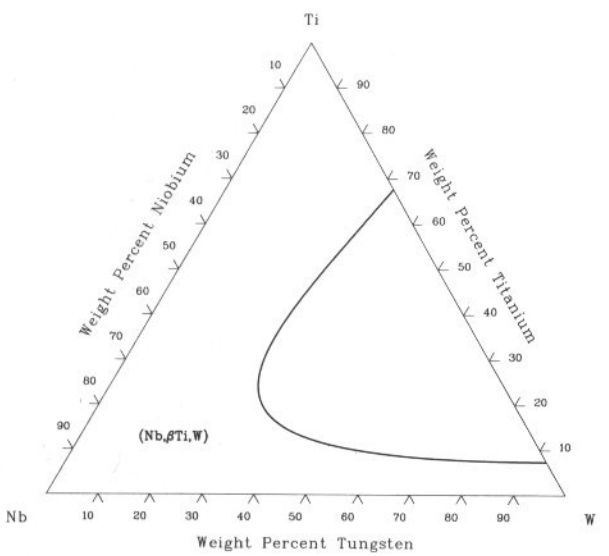

Pb-Sb-Sn isothermal section at 240 °C [85Osa]

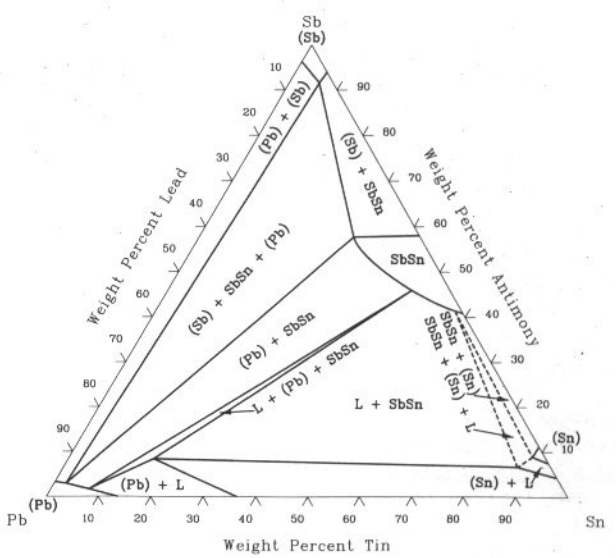

Pb-Sb-Sn (Pb) liquidus projection [73Bre]

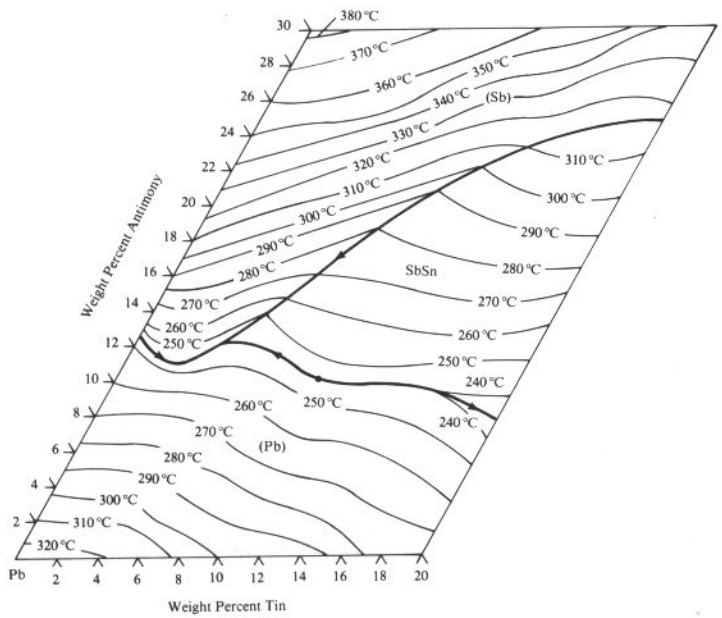

Pb-Sb-Sn [85Osa]

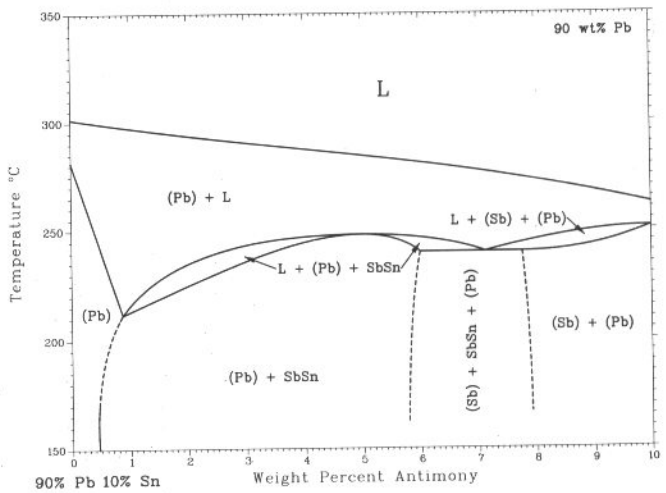

Pb-Sn-Zn liquidus projection [51Lin]

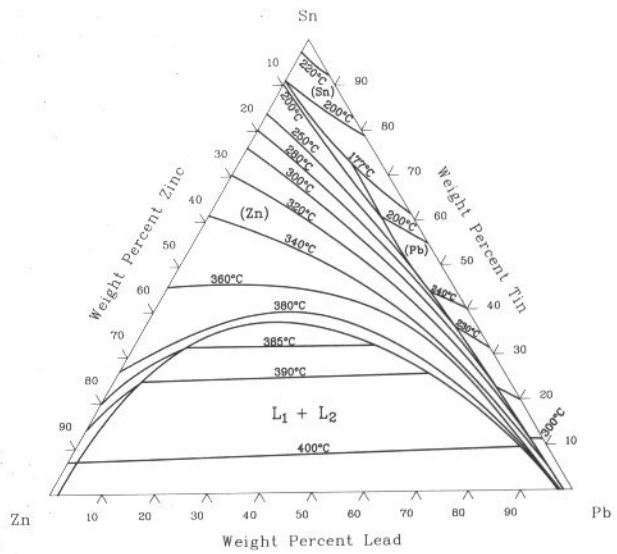

Pb-Sb-Sn isothermal section at 189 °C [85Osa]

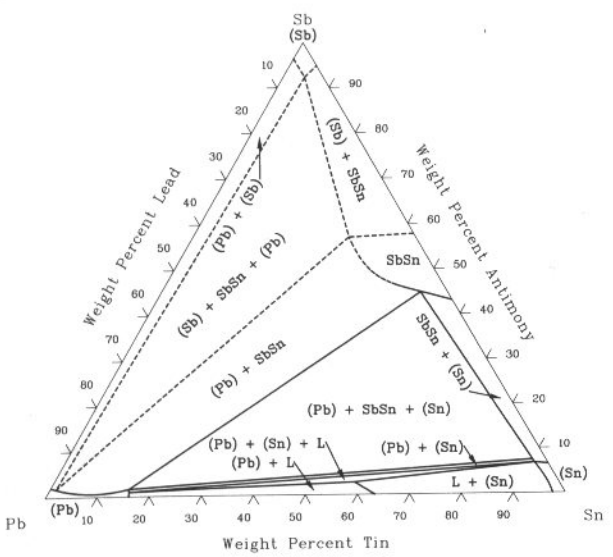

Pb-Sn-Zn isothermal section at 532 °C [67Pta]

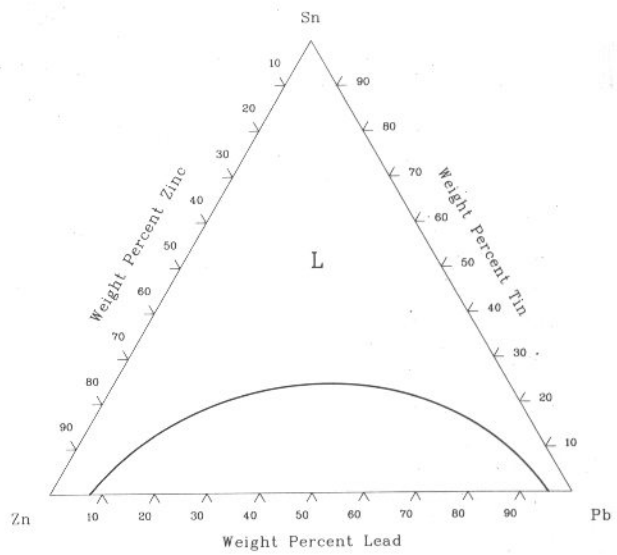

Ternary System References

11Par: N. Parravano, "Das Ternäre System Silber-Zinn-Blei," *Z. Metallkd.*, Vol 1, 1911, p 89-108

29Bau: O. Bauer and M. Hansen, "Der Einfluss von dritten Metallen auf die Konstitution der Messingle ierungen. I. Der Einfluss von Blei," *Z. Metallkd.*, Vol 21, 1929, p 190-196

36Kos: W. Köster and W. Dullenkopf, "Das Dreistoffsystem Aluminium-Magnesium-Zink. III. Der Teilbereich Mg-Al_3Mg_4-$Al_2Mg_3Zn_3$ -$MgZn_2$-Mg," *Z. Metallkd.*, Vol 28, 1936, p 363-367

48Kos: W. Köster, U. Zwicker, and K. Moeller, "Mikroskopische und röntgenographische Untersuchungen zur Kenntnis des Systems Kupfer-Nickel-Aluminium," *Z. Metallkd.*, Vol 39, 1948, p 225-231

48Wil: F.H. Wilson, "The Copper-Rich Corner of the Copper-Aluminum-Silicon Diagram," *Trans. AIME*, Vol 175, 1948, p 262-273

51Lin: E. Linder, "Eine Methode zur Erforschung von Vierstoffsystemen Dargestellt am System Blei-Zink-Kadmium-Zinn," *Z. Metallkd.*, Vol 43, 1951, p 377-387

52Das: D.K. Das, S.P. Rideout, and P.A. Beck, "Intermediate Phases in the Mo-Fe-Co, Mo-Fe-Ni, and Mo-Ni-Co Ternary Systems," *Trans. AIME*, Vol 194, 1952, p 1071-1075

56Zwi: U. Zwicker, "Die Systeme Titan-Aluminium-Chrom und Titan-Aluminium-Vanadin und die technishcen Titanlegierungen mit 5% Cr und 3% Al sowie mit 6% Al und 4% V," *Z. Metallkd.*, Vol 47, 1956, p 535-548

58Bag: Yu.A. Bagaryatskiy, G.I. Nosova, and T.V. Tagunova, "Study of the Phase Diagrams of the Alloys Titanium-Chromium, Titanium-Tungsten, and Titanium-Chromium-Tungsten, Prepared by the Method of Powder Metallurgy, *Russ. J. Inorganic Chem.;* TR: *Zh. Neorg. Khim.*, Vol 3 (No. 3), 1958, p 330-341

58Kor: I.I. Kornilov and R.S. Polyakov, Phase Diagram of the Ternary Sytem Titanium-Niobium-Molybdenum, *Russ. J. Inorganic Chem.*, Tr. *Zh. Neorg. Khim.*, Vol 3 (No. 4), 1958, p 62-74

58Liv: B. G. Livshits and Ya.D. Khorin, "Study of Equilibrium Phase Diagram of the System Co-Cr-Ti," *Russ. J. Inorganic Chem.*; TR: *Zh. Neorg. Khim.*, Vol 3 (No. 3), 1958, p 193-205

59Cla: J.W.H. Clare, "The Constitution of Aluminium-Rich Alloys of the Aluminium-Chromium-Manganese System," *Trans. AIME*, Vol 215, 1959, p 429-433

61Eng: J.J. English, "Binary and Ternary Phase Diagrams of Niobium, Molybdenum and Tungsten (1961)," Available as NTIS Document AD 257,739

61Far: P. Farrar and H. Margolin, "The Titanium Rich Region of the Titanium-Aluminium-Vanadium System," *Trans. AIME*, Vol 221, 1961, p 1214-1221

62Zak: E.K. Zakharov and B.G. Livshits, "Phase Composition Diagram of the Cobalt-Chromium-Titanium Ternary System," *Russ. Metall. Fuels*, (No. 5), 1962, p 88-97

63Sta: H.H. Stadelmaier and R.A. Gregg, "Die Ternäre Phase $Fe_{23}C_3B_3$ im Dreistoffsystem EisenKohlenstoff-Bor," *Metall. Berlin*, Vol 17, 1963, p 412-414

64Kus: J.B. Kusma and H. Nowotny, "Untersuchungen im Dreistoff: Mn-Al-Si," *Monatsh. Chem.*, Vol 95, 1964, p 1266-1271

64Ste: P. Stecher, F. Benesovsky, and H. Nowotny, "Untersuchungen im System Chrom-Wolfram-Kohlenstoff," Vol. 12, 1964, p 89-95

65Kuz: Yu.B. Kuz'ma and T.F. Fedorov, "Phase Equilibria in the System Molybdenum-Chromium-Carbon," *Sov. Powder Metall. Met. Ceram.;* TR: *Poroshk. Metall. Kiev*, Vol 4, 1965, p 920-922

66Kie: R. Kieffer and H. Rassaerts, "Über das System Vanadium-Chrom-Kohlenstoff und über den Einsatz von Vanadin- und Chromcarbiden in Hartmetallen, Teil I," *Metall, Berlin*, Vol 20, 1966, p 691-695

66Kos: W. Köster and T. Gödecke, "Das Dreistoffsystem Kupfer-Mangan-Aluminium," *Z. Metallkd.*, Vol 57, 1966, p 889-901

67Pta: W. Ptak and Z. Moser, "The Range of Occurrence of Two Liquid Phases in Zn-Sn-Cd-Pb Alloys," *Bull. Acad. Pol. Sci. Ser. Sci. Tech.*, Vol 15 (No. 9), 1967, p 809-815

70Han: R.C. Hansen and A. Raman, "Alloy Chemistry of sigma (beta-U)-Related Phases. III. sigma-Phases with Non-Transition Elements," *Z. Metallkd.*, Vol 61, 1970, p 115-120

70Kos: W. Köster and T. Gödecke, "Das Dreistoffsystem Eisen-Aluminum-Zink," *Z. Metallkd.*, Vol 61, 1970, p 649-658

71Pre: A.P. Prevarskiy, "Investigation of Fe-Cu-Al Alloys," *Russ. Metall.;* TR: *Izv. Akad. Nauk SSSR, Metall.*, (No. 4), 1971 , p 154-156

73Ben: R. Benz, J.F. Elliott, and J. Chipman, "Thermodynamics of the Solid Phases in the System Fe-Mn-C," *Metall. Trans.*, Vol 4, 1973, p 1975-1986

73Bla: J.M. Blalock, Jr., J.V. Harding, and W.T. Pell-Walpole, *Metallography, Structures and Phase Diagrams*, Vol 8, *Metals Handbook*, 8th ed., American Society for Metals, Metals, Park, OH, 1973

73Bre: L. Brewer and S.-G. Chang, *Metallography, Structures and Phase Diagrams*, Vol 8, *Metals Handbook*, 8th ed., American Society for Metals, Metals Park, OH, 1973

73Dra: J.M. Drapier and D. Coutsouradis, *Metallography, Structures and Phase Diagrams*, Vol 8, *Metals Handbook*, 8th ed., American Society for Metals, Metals Park, OH 1973

73Lev: E.D. Levine, *Metallography, Structures and Phase Diagrams*, Vol 8, *Metals Handbook*, 8th ed., American Society for Metals, Metals Park, OH 1973

73Mar: V.Ya. Markiv, V.V. Burnashova, and V.R. Ryabov, "The Systems Titanium-Iron-Aluminium, Titanium-Nickel-Aluminium, and Titanium-Copper-Aluminium," *Met. Allofizika, Kiev (Akad. Nauk Ukr. SSSR, Metallofiz.*, Vol 46, 1973, p 103-109

73Pel: W.T. Pell-Walpole and C.T. Thwaites, *Metallography, Structures and Phase Diagrams*, Vol 8, *Metals Handbook*, 8th ed., American Society for Metals, Metals Park, OH 1973

73Smi: C.S. Smith and E.D. Levine, *Metallography, Structures and Phase Diagrams*, Vol 8, *Metals Handbook*, 8th ed., American Society for Metals, Metals Park, OH 1973

73Wil: L.A. Willey, *Metallography, Structures and Phase Diagrams*, Vol 8, *Metals Handbook*, 8th ed., American Society for Metals, Metals Park, OH 1973

74Kau: L. Kaufman and H. Nesor, "Calculation of Superalloy Phase Diagrams: Part I, " *Metall. Trans.*, Vol 5, 1974, p 1617-1621

75Kau: L. Kaufman and H. Nesor, "Calculation of Superalloy Phase Diagrams: Part IV," *Metall. Trans. A*, Vol 6, 1975, p 2123-2131

77Lev: V.I. Levanov, V.S. Mikheyev, and A.I. Chernitysn, "Investigation of the Ti-Nb-W System (Nb + W up to 50 wt.%)," *Russ. Metall.*; TR: *Izv. Akad. Nauk SSSR, Met.*, (No. 1), 1977, p 186-191

79Cha: Y.A. Chang, J.P. Neumann, A. Mikula, and D. Goldberg, *Phase Diagrams and Thermodynamic Properties of Ternary Copper-Metal Systems*, INCRA Monograph VI, International Copper Research Association, 1979

80Gry: V.I. Gryzunov and A.S. Sagyndykov, "Mutual Diffusion in the System Ti-Ni-Co," *Phys. Met. Metallogr.*, Tr: *Fiz. Met. Metalloved.*, Vol 49 (No. 5), 1980, p 178-182

80Loo: F.J.J. van Loo, G.F. Bastin, J.W.G.A. Vrolijk, and J.J.M. Hendriks, "Phase Rela-

tions in the Systems Fe-Ni-Mo, Fe-Co-Mo and Ni-Co-Mo at 1100 °C," *J. Less-Common Met.*, Vol 72, 1980, p 225-230

80Mas: S.B. Maslenkov and E.A. Nikandrova, "Examination of the Ni-Mo-W Phase Diagram," *Russ. Metall.*, Tr: *Izv. Akad. Nauk SSSR, Met.*, (No. 2), 1980, p 184-187

81Zha: Jin Zhanpeng, "A Study of the Range of Stability of sigma Phase in Some Ternary Systems," *Scand. J. Metall.*, Vol 10, 1981, p 279-287

83Gry: V.I. Gryzunov, G.V. Shcherbedinskiy, Ye.M. Sokolovskaya, B.K. Aytbayev, and A.S. Sagyndykov, "Kinetics of Phase Growth During Mutual Diffusion in Ternary Multiphase Metallic Systems," *Phys. Met. Metallogr.;* TR: *Fiz. Met. Metalloved.*, Vol 56 (No. 1), 1983, p 183-186

84Ere: V.N. Eremenko, L.A. Tret'yachenko, S.B. Prima, and E.L. Semenova, "Constitution Diagrams of Titanium-Nickel-Groups IV-VIII Transition Metal Systems," *Sov. Powder Metall. Met. Ceram.*; TR: *Poroshk. Metall. Kiev*, Vol 23 (No. 8), 1984, p 613-621

84Gup: K.P. Gupta, S.B. Rajendraprasad, A.K. Jena, and R.C. Sharma, "The Co-Mo-Ni System," *Trans. Indian Inst. Met.*, Vol 37 (No. 6), 1984, p 691-697

84Mir: D.B. Miracle, K.A. Lark, V. Srinivasan, and H.A. Lipsitt, "Nickel-Aluminium-Molybdenum Phase Equilibria," *Metall. Trans. A*, Vol 15, 1984, p 481-486

85Mes: L.L. Meshkov, S.N. Nesterenko, and T.V. Ishchenko, "Structural Features of Phase Diagrams Formed by Molybdenum and Tungsten with Iron-Group Metals," *Russ. Metall.;* TR: *Izv. Akad Nauk SSSR, Met.*, (No. 2), 1985, p 204-207

85Nas: P. Nash and W.W. Liang, Phase Equilibria in the Ni-Al-Ti System at 1173 K," *Metall. Trans. A*, Vol 16, 1985, p 319-322

85Oma: A.K. Omarov, S.V. Sejtzhanov, and A.I. Idirisov, "Isothermal Sections of the Ternary System Al-Ni-Ti for the Temperature Range 1150-600 °C," *Izv. Akad. Nauk Kazakh. SSSR, Khim*, (No. 1), 1985, p 36-42

85Osa: K. Osamura, "The Pb-Sb-Sn (Lead-Antimony-Tin) System," *Bull. Alloy Phase Diagrams*, Vol 6 (No. 4), 1985, p 372-379

86Ere: V.N. Eremenko, T.Ja. Velikanova, and A.A. Bondar, "The Ternary Phase Diagram Cr-W-C System," *Dop. Akad. Nauk Ukr. RSR, A, Fiz.- Mat. Tekh.*, Vol 48 (No. 11), 1986, p 74-78

86Mey: S.a. Mey and K. Hack, "A Thermochemical Evaluation of the Silicon-Zinc, Aluminum-Silicon, and Aluminum-Silicon-Zinc Systems," *Z. Metallkd.*, Vol 77 (No. 7), 1986, p 454-459

86Pri: S.B. Prima, L.A. Tret'yachenko, and V.N. Eremenko, "Investigation of Phase Equilibria in the Ti-Ni-Mo System at 1200 °C," *Russ. Metall.;* TR: *Izv. Akad. Nauk SSSR, Met.*, (No. 2), 1986, p 205-210

86Rag: V. Raghavan, "The Carbon-Iron-Silicon System," *J. Alloy Phase Diagrams, India*, Vol 2 (No. 2), 1986, p 97-107

87Ere: V.N. Eremenko, T.Ya. Velikanova, and A.A. Bondar, "The Phase Diagram of the Cr-Mo-C System, II. Phase Equilibria in the Partial System Mo_2C-Cr_7C_3-C," *Sov. Powder Metall. Met. Ceram.*, TR: *Poroshk. Metall. Kiev*, Vol 26 (No. 6), 1987, p 506-511

87Ofo: N.C. Oforka and C.W. Haworth, "Phase Equilibria of Aluminum-Chromium-Nickel System at 1423 K," *Scand. J. Metall.*, Vol 16, 1987, p 184-188

87Rag: V. Raghavan, *Phase Diagrams of Ternary Iron Alloys*, The Indian Institute of Metals, Calcutta, India, (No. 1), 1987

87Smi: S.V. Smirnova, L.L. Meshkov, and O.N. Kosolapova, "Physicochemical Interaction and Magnetic Properties on the Phases in the Iron-Molybdenum-Niobium System," *Moscow Univ. Chem. Bull.*, Tr: *Vest. Mosk. Univ. Khim.*, Vol 42 (No. 1), 1987, p 84-87

88Pet: G. Petzow and G. Effenberg, *Ternary Alloys*, VCH Verlagsgesellschaft, Weinheim, Germany, Vol 1, 1988

88Ray: G.V. Raynor and V.G. Rivlin, *Phase Equilibria in Iron Ternary Alloys*, The Institute of Metals, London, (No. 4), 1988

88Rok: L.L. Rokhlin and A.G. Pepelyan, "Phase Equilibria in the Mg-Rich Region of the Mg-Al-Si System," *Russ. Metall.*, Tr: *Izv. Akad. Nauk SSSR, Met.*, (No. 6), 1988, p 172-174

88Sim: C.J. Simensen, B.C. Oberländer, J. Svalestuen, and A. Thornvaldsen, "The Phase Diagram for Magnesium-Aluminum-Manganese Above 650 °C," *Z. Metallkd.*, Vol 79 (No. 11), 1988, p 696-699

89Har: K.C. Harikumar and V. Raghavan, "BCC-FCC Equilibrium in Ternary Iron Alloys II, " *J. Alloy Phase Diagrams*, India, Vol 5 (No. 2), 1989, p 77-96

90Gup: K.P. Gupta, *Phase Diagrams of Ternary Nickel Alloys*, Indian Institute of Metals, Calcutta, (No. 1), 1990

90Pri: A. Prince, G.V. Raynor, and D.S. Evans, *Phase Diagrams of Ternary Gold Alloys*, The Institute of Metals, London, 1990

Section 4
Appendix

Symbols for the Chemical Elements ..... 4•3
Standard Atomic Weights of the Elements (periodic chart) ..... 4•4
Melting and Boiling Points of the Elements at Atmospheric Pressure ..... 4•5
Allotropic Transformations of the Elements at Atmospheric Pressure ..... 4•7
Magnetic Phase Transition Temperatures of the Elements ..... 4•9
Crystal Structure and Lattice Parameters of Allotropes of the Metallic Elements ..... 4•10
Crystal Structure Nomenclature, Arranged Alphabetically by Pearson Symbol Designation ..... 4•13
Temperature Conversions (tables) ..... 4•17
Abbreviations ..... 4•19
Greek Alphabet ..... 4•19

Symbols for the Chemical Elements

Actinium	Ac
Aluminum	Al
Americium	Am
Antimony	Sb
Argon	Ar
Arsenic	As
Astatine	At
Barium	Ba
Berkelium	Bk
Beryllium	Be
Bismuth	Bi
Boron	B
Bromine	Br
Cadmium	Cd
Calcium	Ca
Californium	Cf
Carbon	C
Cerium	Ce
Cesium	Cs
Chlorine	Cl
Chromium	Cr
Cobalt	Co
Columbium (Niobium)	Nb
Copper	Cu
Curium	Cm
Dysprosium	Dy
Einsteinium	Es
Erbium	Er
Europium	Eu
Fermium	Fm
Fluorine	F
Francium	Fr
Gadolinium	Gd
Gallium	Ga
Germanium	Ge
Gold	Au
Hafnium	Hf
Helium	He
Holmium	Ho
Hydrogen	H
Indium	In
Iodine	I
Iridium	Ir
Iron	Fe
Krypton	Kr
Lanthanum	La
Lawrencium	Lr
Lead	Pb
Lithium	Li
Lutetium	Lu
Magnesium	Mg
Manganese	Mn
Mendelevium	Md
Mercury	Hg
Molybdenum	Mo
Neodymium	Nd
Neon	Ne
Neptunium	Np
Nickel	Ni
Niobium	Nb
Nitrogen	N
Nobelium	No
Osmium	Os
Oxygen	O
Palladium	Pd
Phosphorus	P
Platinum	Pt
Plutonium	Pu
Polonium	Po
Potassium	K
Praseodymium	Pr
Promethium	Pm
Protactinium	Pa
Radium	Ra
Radon	Rn
Rhenium	Re
Rhodium	Rh
Rubidium	Rb
Ruthenium	Ru
Samarium	Sm
Scandium	Sc
Selenium	Se
Silicon	Si
Silver	Ag
Sodium	Na
Strontium	Sr
Sulfur	S
Tantalum	Ta
Technetium	Tc
Tellurium	Te
Terbium	Tb
Thallium	Tl
Thorium	Th
Thulium	Tm
Tin	Sn
Titanium	Ti
Tungsten	W
Uranium	U
Vanadium	V
Xenon	Xe
Ytterbium	Yb
Yttrium	Y
Zinc	Zn
Zirconium	Zr

Standard Atomic Weights of the Elements

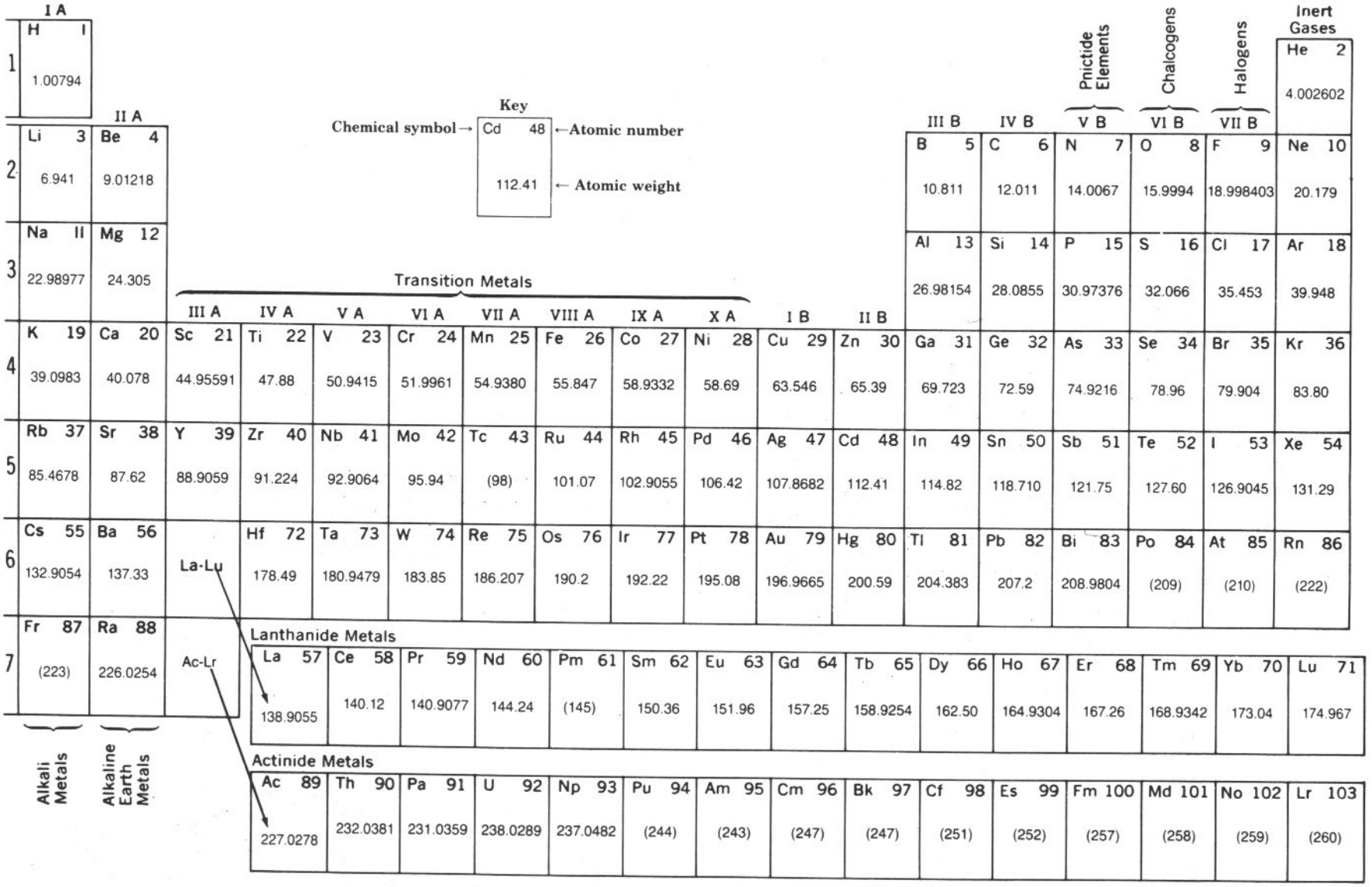

Melting and Boiling Points of the Elements at Atmospheric Pressure

Symbol	Melting point			Boiling point	
	°C	K	Error limits	°C	K
Ac	1051	1324	±50	3200	3473(a)
Ag	961.93	1235.08	...	2163	2436
Al	660.452	933.602	...	2520	2793
Am	1176	1449	...	...	...
Ar	–189.352(T.P.)	83.798(T.P.)	...	–185.9	87.3
As	614(S.P.)	887(S.P.)	...	...	...
At	(302)	(575)	...	...	...
Au	1064.43	1337.58	...	2857	3130
B	2092	2365	...	4002	4275
Ba	727	1000	±2	1898	2171
Be	1289	1562	±5	2472	2745
Bi	271.442	544.592	...	1564	1837
Bk	1050	1323	...	...	...
Br	–7.25(T.P.)	265.90(T.P.)	...	59.10	332.25
C	3827(S.P.)	4100(S.P.)	±50	...	...
Ca	842	1115	±2	1484	1757
Cd	321.108	594.258	...	767	1040
Ce	798	1071	±3	3426	3699
Cf	900	1173	...	...	...
Cl	–100.97(T.P.)	172.18(T.P.)	...	–34.05	239.10
Cm	1345	1618	...	...	...
Co	1495	1768	...	2928	3201
Cr	1863	2136	±20	2672	2945
Cs	28.39	301.54	±0.05	671	944
Cu	1084.87	1358.02	±0.04	2563	2836
Dy	1412	1685	...	2562	2835
Er	1529	1802	...	2863	3136
Es	860	1133	...	...	...
Eu	822	1095	...	1597	1870
F	–219.67(T.P.)	53.48(T.P.)	...	–188.20	84.95
Fe	1538	1811	...	2862	3135
Fm	(1527)	(1800)	...	...	...
Fr	(27)	(300)	...	...	...
Ga	29.7741(T.P.)	302.9241(T.P.)	±0.001	2205	2478
Gd	1313	1586	...	3266	3539
Ge	938.3	1211.5	...	2834	3107
H	–259.34(T.P.)	13.81(T.P.)	...	–252.882	20.268
He	–271.69(T.P.)	1.46(T.P.)	(b)	–268.935	4.215
Hf	2231	2504	±20	4603	4876
Hg	–38.836	234.210	...	356.623	629.773
Ho	1474	1747	...	2695	2968
I	113.6	386.8	...	185.25	458.40
In	156.634	429.784	...	2073	2346
Ir	2447	2720	...	4428	4701
K	63.71	336.86	±0.5	759	1032
Kr	–157.385	115.765	±0.001	–153.35	119.80
La	918	1191	...	3457	3730
Li	180.6	453.8	±0.5	1342	1615
Lr	(1627)	(1900)	...	...	...
Lu	1663	1936	...	3395	3668
Md	(827)	(1100)	...	...	...
Mg	650	923	±0.5	1090	1363
Mn	1246	1519	±5	2062	2335
Mo	2623	2896	...	4639	4912
N	–210.0042(T.P.)	63.1458(T.P.)	±0.0002	–195.80	77.35
Na	97.8	371.0	±0.1	883	1156
Nb	2469	2742	...	4744	5017

(continued)

Symbol	Melting point		Error limits	Boiling point	
	°C	K		°C	K
Nd	1021	1294	...	3068	3341
Ne	–248.587(T.P.)	24.563(T.P.)	±0.002	–246.054	27.096
Ni	1455	1728	...	2914	3187
No	(827)	(1100)	...	...	...
Np	639	912	±2	...	...
O	–218.789(T.P.)	54.361(T.P.)	...	–182.97	90.18
Os	3033	3306	±20	5012	5285
P(white)	44.14	317.29	±0.1	277	550
P(red)	589.6(T.P.)	862.8(T.P.)	(c)	431	704
Pa	1572	1845	...	...	...
Pb	327.502	600.652	...	1750	2023
Pd	1555	1828	±0.4	2964	3237
Pm	1042	1315	...	...	...
Po	254	527	...	...	...
Pr	931	1204	...	3512	3785
Pt	1769.0	2042.2	...	3827	4100
Pu	640	913	±1	3230	3503
Ra	700	973	...	...	...
Rb	39.48	312.63	±0.5	688	961
Re	3186	3459	±20	5596	5869
Rh	1963	2236	...	3697	3970
Rn	–71	202	...	–62	211
Ru	2334	2607	±10	4150	4423
S	115.22	388.37	...	444.60	717.75
Sb	630.755	903.905	...	1587	1860
Sc	1541	1814	...	2831	3104
Se	221	494	...	685	958
Si	1414	1687	±2	3267	3540
Sm	1074	1347	...	1791	2064
Sn	231.9681	505.1181	...	2603	2876
Sr	769	1042	...	1382	1655
Ta	3020	3293	...	5458	5731
Tb	1356	1629	...	3223	3496
Tc	2155	2428	±50	4265	4538
Te	449.57	722.72	±0.3	988	1261
Th	1755	2028	±10	4788	5061
Ti	1670	1943	±6	3289	3562
Tl	304	577	±2	1473	1746
Tm	1545	1818	...	1947	2220
U	1135	1408	...	4134	4407
V	1910	2183	±6	3409	3682
W	3422	3695	...	5555	5828
Xe	–111.7582(T.P.)	161.3918(T.P.)	±0.0002	–108.12	165.03
Y	1522	1795	...	3338	3611
Yb	819	1092	...	1194	1467
Zn	419.58	692.73	...	907	1180
Zr	1855	2128	±5	4409	4682

Note: T.P. = triple point; S.P. = sublimation point at atmospheric pressure. Measurements in parentheses are approximate. **(a)** ±300. **(b)** There are various triple points. **(c)** Red P sublimes without melting at atmospheric pressure.

Allotropic Transformations of the Elements at Atmospheric Pressure

Allotropic transformation of the chemical elements is discussed in the Introduction to Alloy Phase Diagrams, page 1•1 of this Handbook.

Element	Atomic number	Transformation	Temperature, °C
Ag	47	L ↔ S	0961.93
Al	13	L ↔ S	660.452
Am	95	L ↔ γ	1176
		γ ↔ β	1077
β ↔ α	769		
Ar	18	L ↔ S	83.798 K
Au	79	L ↔ S	1064.43
B	5	L ↔ β	2092
Ba	56	L ↔ S	727
Be	4	L ↔ β	1289
		β ↔ α	1270
Bi	83	L ↔ S	271.442
Bk	97	L ↔ S	1050
Br	35	L ↔ S	265.9 K
Ca	20	L ↔ β	842
		β ↔ α	443
Cd	48	L ↔ S	321.108
Ce	58	L ↔ δ	798
		δ ↔ γ	726
		γ ↔ β	61
		β ↔ α	...
Cf	98	L ↔ β	900
		β ↔ α	590
Cl	17	L ↔ S	172.16 K
Cm	96	L ↔ β	1345
		β ↔ γ	1277
Co	27	L ↔ α	1495
		α ↔ ε	422
Cr	24	L ↔ S	1863
Cs	55	L ↔ S	28.39
Cu	29	L ↔ S	1084.87
Dy	66	L ↔ β	1412
		β ↔ α	1381
		α ↔ α′	–187
Er	68	L ↔ S	1529
Es	99	L ↔ S	860
Eu	63	L ↔ S	822
F	9	L ↔ β	53.48 K
		β ↔ α	45.55 K
Fe	26	L ↔ δ	1538
		δ ↔ γ	1394
		γ ↔ α	912
Ga	31	L ↔ S	29.7741
Gd	64	L ↔ β	1313
		β ↔ α	1235
Ge	32	L ↔ S	938.3
H	1	L ↔ S	13.81 K
Hf	72	L ↔ β	2231
		β ↔ α	1743
Hg	80	L ↔ α	–38.290
Ho	67	L ↔ S	1474
I	53	L ↔ S	113.6
In	49	L ↔ S	156.634
Ir	77	L ↔ S	2447
K	19	L ↔ S	63.71
Kr	36	L ↔ S	115.65 K
La	57	L ↔ γ	918
		γ ↔ β	865
		β ↔ α	310
Li	3	L ↔ β	180.6
		β ↔ α	–193
Lu	71	L ↔ S	1663
Mg	12	L ↔ S	650
Mb	25	L ↔ δ	1246
		δ ↔ γ	1138
		γ ↔ β	1100
		β ↔ α	727
Mo	42	L ↔ S	2623
N	7	L ↔ β	63.146 K
		β ↔ α	35.61 K
Na	11	L ↔ β	97.8
		β ↔ α	–233
Nb	41	L ↔ S	2469
Nd	60	L ↔ β	1021
		β ↔ α	863
Ne	10	L ↔ S	24.563 K (T.P.)
Ni	28	L ↔ S	1455
Np	93	L ↔ γ	639
		γ ↔ β	576
		β ↔ α	280
O	8	L ↔ γ	54.361 K
		γ ↔ β	43.801 K
		β ↔ α	23.867 K
Os	76	L ↔ S	3033
P (white α)	15	L ↔ α	44.14
Pa	91	L ↔ β	1572
		β ↔ α	1170
Pb	82	L ↔ S	327.502
Pd	46	L ↔ S	1555
Pm	61	L ↔ β	1042
		β ↔ α	890
Po	84	L ↔ β	254
		β ↔ α	54
Pr	59	L ↔ β	931
		β ↔ α	795
Pt	78	L ↔ S	1769.0
Pu	94	L ↔ ε	640
		ε ↔ δ′	483
		δ′ ↔ δ	463
		δ ↔ γ	320
		γ ↔ β	215
		β ↔ α	125
Rb	37	L ↔ S	39.48
Re	75	L ↔ S	3186
Rh	45	L ↔ S	1963
Rn	86	L ↔ S	–71

(continued)

Element	Atomic number	Transformation	Temperature, °C
Ru	44	$L \leftrightarrow S$	2334
S	16	$L \leftrightarrow \beta$	115.22
		$\beta \leftrightarrow \alpha$	95.5
Sb	51	$L \leftrightarrow S$	630.755
Sc	21	$L \leftrightarrow \beta$	1541
		$\beta \leftrightarrow \alpha$	1337
Se	34	$L \leftrightarrow S$	221
Si	14	$L \leftrightarrow S$	1414
Sm	62	$L \leftrightarrow \gamma$	1074
		$\gamma \leftrightarrow \beta$	922
		$\beta \leftrightarrow \alpha$	734
Sn	50	$L \leftrightarrow \beta$	231.9681
		$\beta \leftrightarrow \alpha$	13
Sr	38	$L \leftrightarrow \beta$	769
		$\beta \leftrightarrow \alpha$	547
Ta	73	$L \leftrightarrow S$	3020
Tb	65	$L \leftrightarrow \beta$	1356
		$\beta \leftrightarrow \alpha$	1289
		$\alpha \leftrightarrow \alpha'$	–53
Te	52	$L \leftrightarrow S$	449.57
Th	90	$L \leftrightarrow \beta$	1755
		$\beta \leftrightarrow \alpha$	1360
Ti	22	$L \leftrightarrow \beta$	1670
		$\beta \leftrightarrow \alpha$	882
Tl	81	$L \leftrightarrow \beta$	304
		$\beta \leftrightarrow \alpha$	230
T	69	$L \leftrightarrow S$	1545
U	92	$L \leftrightarrow \gamma$	1135
		$\gamma \leftrightarrow \beta$	776
		$\beta \leftrightarrow \alpha$	668
V	23	$L \leftrightarrow S$	1910
W	74	$L \leftrightarrow S$	3422
Xe	54	$L \leftrightarrow S$	161.918 (T.P.)
Y	39	$L \leftrightarrow \beta$	1522
		$\beta \leftrightarrow \alpha$	1478
Yb	70	$L \leftrightarrow \gamma$	819
		$\gamma \leftrightarrow \beta$	795
		$\beta \leftrightarrow \alpha$	–3
Zn	30	$L \leftrightarrow S$	419.58
Zr	40	$L \leftrightarrow \beta$	1855
		$\beta \leftrightarrow \alpha$	863

Note: T.P. = triple point.

Magnetic Phase Transition Temperatures of the Elements

Magnetic phase transition, and other higher-order transitions of the chemical elements, is discussed in the Introduction to Alloy Phase Diagrams, page 1•1 of this Handbook.

Chemical symbol	Atomic number	Allotrope	Phase transition temperature (T_{c}), K	Type of magnetic ordering(a)	Phase transition temperature (T_{c2}), K	Type of magnetic ordering(a)	Phase transition temperature (T_{c3}), K	Type of magnetic ordering(a)	Saturation magnetic moment, μB
Ce(b)	58	β-dcph	13.7	AC?	12.5	AC?	...	...	2.61
		γ-fcc	14.4	AC?	...	...	...	...	
Cm	96	α-dcph	52	AC	...	...	...	...	...
Co	27	fcc	1388(1115 °C)	FM	...	...	...	...	1.715
Cr	24	bcc	312.7(39.5 °C)	AI	...	...	...	...	0.45
Dy	66	α-cph	179.0	AI	89.0	FM	...	...	10.33
Er	68	cph	85.0	AI	53	AC	20.0	CF	9.1
Eu	63	bcc	90.4	AC	...	...	...	...	5.9
Fe(c)	26	α-bcc	1044(771 °C)	FM	...	...	...	...	2.216
		γ-fcc	67	AC	...	...	...	...	0.75
Gd	64	α-cph	293.4(20.2 °C)	FM	...	...	...	...	0.75
Ho	67	cph	132.0	AI	20.0	CF	...	...	10.34
Mn	25	α-bcc	100	AC	...	...	...	...	(d)
Nd	60	α-dcph	19.9	AI	7.5	AC	...	...	1.84
Ni	28	fcc	627.4(354.2 °C)	FM	...	...	...	...	0.616
Pm	61	α-dcph	98	FM?	...	...	...	...	0.24
Pr	59	α-dcph	0.06	AC	...	...	...	...	0.36
Sm	62	α-rhomb	106	h, A(e)	13.8	c, A(e)	...	...	0.1
Tb	65	α-cph	230.0	AI	219.5	FM	...	...	9.34
Tm	69	cph	58.0	AI	40 to 32	FI	...	...	7.14

(a) Type of magnetic ordering indicated by symbols in the table below and the chart on the reverse side: FM = transition from paramagnetic to ferromagnetic state, AC = transition to periodic (antiferromagnetic) state that is commensurate with the lattice periodicity *(e.g.*, spins on three atom layers directed up followed by three layers down, *etc.*), AI = transition to periodic (antiferromagnetic) state that is generally not commensurate with the lattice periodicity (*e.g.*, helical spin ordering), CF = transition to conical ferromagnetic state (combination of planar helical antiferromagnetic plus ferromagnetic component), and FI = transition to ferromagnetic periodic structure (unequal number of up and down spin layers). **(b)** Ce exists in five crystal structures, two of which are magnetic (γ–fcc; and β–dcph). γCe is estimated to be antiferromagnetic below 14.4 K by extrapolation from fcc Ce-La alloys. (αCe does not exist in pure form below ~100 K.) βCe is thought to exhibit antiferromagnetism on the hexagonal lattice sites below 13.7 K and on the cubic sites below 12.5 K. **(c)** Magnetic measurements quoted in table for γFe are for fcc Fe precipitated in copper. **(d)** The magnetic moment assignments of Mn are complex. **(e)** h, A; c, A = indicate that sites of hexagonal and cubic point symmetry order antiferromagnetically, but at different temperatures.

Source: J.J. Rhyne, *Bull. Alloy Phase Diagrams*, *3*(3), 402 (1982).

Crystal Structures and Lattice Parameters of Allotropes of the Metallic Elements

The crystal structure of the allotropic forms of the metallic elements are presented here in terms of the Pearson symbol, space group, and prototype of the structure. The temperatures of the phase transformations are listed in degrees Celsius and the pressures are in GPa. A consistent nomenclature is used, whereby all allotropes are labeled by Greek letters. The lattice parameters of the unit cells are given in nanometers (nm) and are considered to be accurate ± 2 in the last reported digit. Both crystal structure and lattice parameters are discussed in the Introduction to Alloy Phase Diagrams, page 1•1 of this Handbook.

This compilation is restricted to changes in crystal structure that occur as a result of a change in temperature or pressure. Low-temperature structures are included for the diatomic and rare gases, which show many similarities with respect to the metallic elements.

Note that there may be differences between values quoted below and similar values given in another table in this Handbook that has been reproduced from another source. For example, the allotropic transformation temperatures of Mn may differ by as much as 23 °C, etc.

Element	Temperature, °C	Pressure, GPa	Pearson symbol	Space group	Prototype	Lattice parameters, nm a	b	c	Comment, c/a, or α or β
Ac	25	atm	*cF*4	$Fm\bar{3}m$	Cu	0.5311	...	...	...
Ag	25	atm	*cF*4	$Fm\bar{3}m$	Cu	0.40857	...	...	...
αAl	25	atm	*cF*4	$Fm\bar{3}m$	Cu	0.40496	...	...	...
βAl	25	>20.5	*hP*2	$P6_3/mmc$	Mg	0.2693	...	0.4398	1.6331
αAm	25	atm	*hP*4	$P6_3/mmc$	αLa	0.34681	...	1.1241	2 × 1.621
βAm	>769	atm	*cF*4	$Fm\bar{3}m$	Cu	0.4894	...	...	...
γAm	>1077	atm	*cI*2	$Im\bar{3}m$	W	?	...	...	...
δAm	25	>15	*oC*4	*Cmcm*	αU	0.3063	0.5968	0.5169	...
αAr	<–189.2	atm	*cF*4	$Fm\bar{3}m$	Cu	0.53109	...	...	...
As	25	atm	*hR*2	$R\bar{3}m$	αAs	0.41319	...	...	α = 54.12°
Au	25	atm	*cF*4	$Fm\bar{3}m$	Cu	0.40782	...	...	...
βB	25	atm	*hR*105	$R\bar{3}m$	βB	1.017	...	...	α = 65.12°
αBa	25	atm	*cI*2	$Im\bar{3}m$	W	0.50227	...	...	...
βBa	25	>5.33	*hP*2	$P6_3/mmc$	Mg	0.3901	...	0.6154	1.5775
γBa	25	>23	?	?	...	...	...	...	...
αBe	25	atm	*hP*2	$P6_3/mmc$	Mg	0.22859	...	0.35845	1.5681
βBe	>1270	atm	*cI*2	$Im\bar{3}m$	W	0.25515	...	...	...
BeII	25	>28.3	*hP**	...	...	0.4328	...	0.3416	0.7893
αBi	25	atm	*hR*2	$R\bar{3}m$	αAs	0.47460	...	...	α = 57.23°
βBi	25	>2.6	*mC*4	*C*2/*m*	βBi	0.6674	0.6117	0.3304	β = 110.33°
γBi	25	>3.0	*mP*4	$P2_1/m$	...	0.665	0.420	0.465	β = 85.33°
δBi	25	>4.3	?	?	...	...	...	...	...
ζBi	25	>9.0	*cI*2	$Im\bar{3}m$	W	0.3800	...	...	...
αBk	25	atm	*hP*4	$P6_3/mmc$	αLa	0.3416	...	1.1069	2 × 1.620
βBk	>977	atm	*cF*4	$Fm\bar{3}m$	Cu	0.4997	...	...	...
Br	<–7.25	atm	*oC*8	*Cmca*	I_2	0.668	0.449	0.874	...
C(graphite)	25	atm	*hP*4	$P6_3/mmc$	C(graphite)	0.24612	...	0.6709	2.7258
C(diamond)	25	>60	*cF*8	$Fd\bar{3}m$	C(diamond)	0.35669	...	...	...
αCa	25	atm	*cF*4	$Fm\bar{3}m$	Cu	0.55884	...	...	...
βCa	>443	atm	*cI*2	$Im\bar{3}m$	W	0.4480	...	...	...
γCa	25	>1.5	?	...	...	...	...	...	...
Cd	25	atm	*hP*2	$P6_3/mmc$	Mg	0.29793	...	0.56196	1.8862
αCe	<–177	atm	*cF*4	$Fm\bar{3}m$	Cu	0.485	...	...	...
βCe	25	atm	*hP*4	$P6_3/mmc$	αLa	0.36810	...	1.1857	2 × 1.611
γCe	>61	atm	*cF*4	$Fm\bar{3}m$	Cu	0.51610	...	...	...
δCe	>726	atm	*cI*2	$Im\bar{3}m$	W	0.412	...	...	
α′Ce	25	>5.4	*oC*4	*Cmcm*	αU	0.3049	0.5998	0.5215	...
αCf	25	atm	*hP*4	$P6_3/mmc$	αLa	0.339	...	1.1015	2 × 1.625
βCf	>590	atm	*cF*4	$Fm\bar{3}m$	Cu	?	...	...	...
Cl	<–100.97	atm	*oC*8	*Cmca*	I_2	0.624	0.448	0.826	...
αCm	25	atm	*hP*4	$P6_3/mmc$	αLa	0.3496	...	1.1331	2 × 1.621
βCm	>1277	atm	*cF*4	$Fm\bar{3}m$	Cu	0.4382	...	...	...
εCo	25	atm	*hP*2	$P6_3/mmc$	Mg	0.25071	...	0.40686	1.6228
αCo	>422	atm	*cF*4	$Fm\bar{3}m$	Cu	0.35447	...	...	...
αCr	25	atm	*cI*2	$Im\bar{3}m$	W	0.28848	...	...	...
α′Cr	25	HP	*tI*2	*I*4/*mmm*	α′Cr	0.2882	...	0.2887	1.002
αCs	25	atm	*cI*2	$Im\bar{3}m$	W	0.6141	...	...	...
βCs	25	>2.37	*cF*4	$Fm\bar{3}m$	Cu	0.6465	...	...	...

(continued)

Element	Temperature, °C	Pressure, GPa	Pearson symbol	Space group	Prototype	Lattice parameters, nm a	b	c	Comment, c/a, or α or β
β′Cs	25	>4.22	*cF*4	$Fm\bar{3}m$	Cu	0.5800	…	…	…
γCs	25	>4.27	?	…	…	…	…	…	…
Cu	25	atm	*cF*4	$Fm\bar{3}m$	Cu	0.36146	…	…	…
α′Dy	<–187	atm	*oC*4	*Cmcm*	α′Dy	0.3595	0.6184	0.5678	…
αDy	25	atm	*hP*2	$P6_3/mmc$	Mg	0.35915	…	0.56501	1.5732
βDy	>1381	atm	*cI*2	$Im\bar{3}m$	W	(0.398)	…	…	…
γDy	25	>7.5	*hR*3	$R\bar{3}m$	$CdCl_2$	0.3436	…	2.483	4.5 × 1.606
Er	25	atm	*hP*2	$P6_3/mmc$	Mg	0.35592	…	0.55850	1.5692
αEs	25	atm	*hP*4	$P6_3/mmc$	αLa	?	…	…	…
βEs	?	atm	*cF*4	$Fm\bar{3}m$	Cu	?	…	…	…
Eu	25	atm	*cI*2	$Im\bar{3}m$	W	0.45827	…	…	…
αF	<–227.60	atm	*mC*8	*C*2/*c*	αF	0.550	0.338	0.728	β = 102.17°
βF	<–219.67	atm	*cP*16	$Pm\bar{3}n$	γO	0.667	…	…	…
αFe	25	atm	*cI*2	$Im\bar{3}m$	W	0.28665	…	…	…
γFe	>912	atm	*cF*4	$Fm\bar{3}m$	Cu	0.36467	…	…	…
δFe	>1394	atm	*cI*2	$Im\bar{3}m$	W	0.29315	…	…	…
εFe	25	>13	*hP*2	$P6_3/mmc$	Mg	0.2468	…	0.396	1.603
αGa	25	atm	*oC*8	*Cmca*	αGa	0.45186	0.76570	0.45258	…
βGa	25	>1.2	*tI*2	*I*4/*mmm*	In	0.2808	…	0.4458	1.588
γGa	–53	>3.0	*oC*40	Cmcm	γGa	1.0593	1.3523	0.5203	…
αGd	25	atm	*hP*2	$P6_3/mmc$	Mg	0.36336	…	0.57810	1.5910
βGd	>1235	atm	*cI*2	$Im\bar{3}m$	W	0.406	…	…	…
γGd	25	>3.0	*hR*3	$R\bar{3}m$	αSm	0.361	…	2.603	4.5 × 1.60
αGe	25	atm	*cF*8	$Fd\bar{3}m$	C(diamond)	0.56574	…	…	…
βGe	25	>12	*tI*4	$I4_1/amd$	βSn	0.4884	…	0.2692	0.551
γGe	25	>12 → atm	*tP*12	$P4_12_12$	γGe	0.593	…	0.698	1.18
δGe	LT	>12	*cI*16	$Im\bar{3}m$	γSi	0.692	…	…	…
αH	<–271.9	atm	*cF*4	$Fm\bar{3}m$	Cu	0.5338	…	…	…
βH_3	<–259.34	atm	*hP*2	$P6_3/mmc$	Mg	0.3776	…	0.6162	1.632
He_4	–269.67	0.163	*hP*2	$P6_3/mmc$	Mg	0.3501	…	0.5721	1.634
He^3	–269.2	0.129	*hP*2	$P6_3/mmc$	Mg	0.3470	…	0.5540	1.597
αHf	25	atm	*hP*2	$P6_3/mmc$	Mg	0.31946	…	0.50510	1.5811
βHf	>1743	atm	*cI*2	$Im\bar{3}m$	W	0.3610	…	…	…
αHg	<–38.836	atm	*hR*1	$R\bar{3}m$	αHg	0.3005	…	…	α = 70.53°
βHg	<–194	HP	*tI*2	*I*4/*mmm*	βHg	0.3995	…	0.2825	0.707
αHo	25	atm	*hP*2	$P6_3/mmc$	Mg	0.35778	…	0.56178	1.5702
βHo	25	>7.5	*hR*3	$R\bar{3}m$	αSm	0.334	…	2.45	4.5 × 1.63
I	25	atm	*oC*8	*Cmca*	I_2	0.72697	0.47903	0.97942	…
In	25	atm	*tI*2	*I*4/*mmm*	In	0.3253	…	0.49470	1.5210
Ir	25	atm	*cF*4	$Fm\bar{3}m$	Cu	0.38392	…	…	…
K	25	atm	*cI*2	$Im\bar{3}m$	W	0.5321	…	…	…
Kr	<–157.385	atm	*cF*4	$Fm\bar{3}m$	Cu	0.5810	…	…	…
αLa	25	atm	*hP*4	$P6_3/mmc$	αLa	0.37740	…	1.2171	2 × 1.6125
βLa	>310	atm	*cF*4	$Fm\bar{3}m$	Cu	0.5303	…	…	…
γLa	>865	atm	*cI*2	$Im\bar{3}m$	W	0.426	…	…	…
β′La	25	>2.0	*cF*4	$Fm\bar{3}m$	Cu	0.517	…	…	…
αLi	<–193	atm	*hP*2	$P6_3/mmc$	Mg	0.3111	…	0.5093	1.637
βLi	25	atm	*cI*2	$Im\bar{3}m$	W	0.35093	…	…	…
Lu	25	atm	*hP*2	$P6_3/mmc$	Mg	0.35052	…	0.55494	1.5832
Mg	25	atm	*hP*2	$P6_3/mmc$	Mg	0.32094	…	0.52107	1.6236
αMn	25	atm	*cI*58	$I\bar{4}3m$	αMn	0.89126	…	…	…
βMn	>727	atm	*cP*20	$P4_132$	βMn	0.63152	…	…	…
γMn	>1100	atm	*cF*4	$Fm\bar{3}m$	Cu	0.3860	…	…	…
δMn	>1138	atm	*cI*2	$Im\bar{3}m$	W	0.3080	…	…	…
Mo	25	atm	*cI*2	$Im\bar{3}m$	W	0.31470	…	…	…
αN	<–237.54	atm	*cP*8	*Pa*3	αN	0.5661	…	…	…
βN	<–210.004	atm	*hP*4	$P6_3/mmc$	βN	0.4050	…	0.6604	1.631
γN	<–253	>3.3	*tP*4	$P4_2/mnm$	γN	0.3957	…	0.5109	1.291
αNa	<–233	atm	*hP*2	$P6_3/mmc$	Mg	0.3767	…	0.6154	1.634
βNa	25	atm	*cI*2	$Im\bar{3}m$	W	0.42906	…	…	…
Nb	25	atm	*cI*2	$Im\bar{3}m$	W	0.33004	…	…	…
αNd	25	atm	*hP*4	$P6_3/mmc$	αLa	0.36582	…	1.17966	2 × 1.6124
βNd	>863	atm	*cI*2	$Im\bar{3}m$	W	0.413	…	…	…
γNd	25	>5.0	*cF*4	$Fm\bar{3}m$	Cu	0.480	…	…	…
Ne	<–248.587	atm	*cF*4	$Fm\bar{3}m$	Cu	0.4462	…	…	…
Ni	25	atm	*cF*4	$Fm\bar{3}m$	Cu	0.35240	…	…	…
αNp	25	atm	*oP*8	*Pnma*	αNp	0.6663	0.4723	0.4887	…
βNp	>280	atm	*tP*4	$P42_12$	βNp	0.4883	…	0.3389	0.694
γNp	>576	atm	*cI*2	$Im\bar{3}m$	W	0.352	…	…	…
αO	<–249.283	atm	*mC*4	*C*2*m*	αO	0.5403	0.3429	0.5086	β = 132.53°
βO	<–229.349	atm	*hR*2	$R\bar{3}m$	βO	0.4210	…	…	α = 46.27°
γO	<–218.789	atm	*cP*16	$Pm\bar{3}n$	γO	0.683	…	…	…
Os	25	atm	*hP*2	$P6_3/mmc$	Mg	0.27341	…	0.43198	1.5800
αP(white)	25	atm	*c***	…	P(white)	0.718	…	…	…
P(black)	25	atm	*oC*8	*Cmca*	P(black)	0.33136	1.0478	0.43763	…
αPa	25	atm	*tI*2	*I*4/*mmm*	αPa	0.3921	…	0.3235	0.825
βPa	>1170	atm	*cI*2	$Im\bar{3}m$	W	0.381	…	…	…
αPb	25	atm	*cF*4	$Fm\bar{3}m$	Cu	0.49502	…	…	…
βPb	25	>10.3	*hP*2	$P6_3/mmc$	Mg	0.3265	…	0.5387	1.650
Pd	25	atm	*cF*4	$Fm\bar{3}m$	Cu	0.38903	…	…	…
αPm	25	atm	*hP*4	$P6_3/mmc$	αLa	0.365	…	1.165	2 × 1.60

(continued)

Element	Temperature, °C	Pressure, GPa	Pearson symbol	Space group	Prototype	Lattice parameters, nm a	b	c	Comment, c/a, or α or β
βPm	>890	atm	*cI*2	$Im\bar{3}m$	W	?	...	...	...
αPo	25	atm	*cP*1	$Pm\bar{3}m$	αPo	0.3366	...	...	...
βPo	>54	atm	*hR*1	$R\bar{3}m$	βPo	0.3373	...	...	α = 98.08°
αPr	25	atm	*hP*4	$P6_3/mmc$	αLa	0.36721	...	1.18326	2 × 1.6111
βPr	>795	atm	*cI*2	$Im\bar{3}m$	W	0.413	...	...	...
γPr	25	>4.0	*cF*4	$Fm\bar{3}m$	Cu	0.488	...	...	...
Pt	25	atm	*cF*4	$Fm\bar{3}m$	Cu	0.39236	...	...	...
αPu	25	atm	*mP*16	$P2_1/m$	αPu	0.6183	0.4822	1.0963	β = 101.97°
βPu	>125	atm	*mC*34	*C*2/*m*	βPu	0.9284	1.0463	0.7859	β = 92.13°
γPu	>215	atm	*oF*8	*Fddd*	γPu	0.31587	0.57682	1.0162	...
δPu	>320	atm	*cF*4	$Fm\bar{3}m$	Cu	0.46371	...	...	...
δ′Pu	>463	atm	*tI*2	*I*4/*mmm*	In	0.33261	...	0.44630	1.3418
εPu	>483	atm	*cI*2	$Im\bar{3}m$	W	0.36343	...	...	...
Ra	25	atm	*cI*2	$Im\bar{3}m$	W	0.5148	...	...	...
αRb	25	atm	*cI*2	$Im\bar{3}m$	W	0.5705	...	...	...
βRb	25	>1.08	?	...	...	...	...	...	...
γRb	25	>2.05	?	...	...	...	...	...	...
Re	25	atm	*hP*2	$P6_3/mmc$	Mg	0.27609	...	0.4458	1.6145
Rh	25	atm	*cF*4	$Fm\bar{3}m$	Cu	0.38032	...	...	...
Ru	25	atm	*hP*2	$P6_3/mmc$	Mg	0.27058	...	0.42816	1.5824
αS	25	atm	*oF*128	*Fddd*	αS	1.0464	1.28660	2.44860	...
βS	>95.5	atm	*mP*64	$P2_1/c$	βS	1.102	1.096	1.090	β = 96.7°
αSb	25	atm	*hR*2	$R\bar{3}m$	αAs	0.45067	...	...	α = 57.11°
βSb	25	>5.0	*cP*1	$Pm\bar{3}m$	αPo	0.2992	...	...	...
γSb	25	>7.5	*hP*2	$P6_3/mmc$	Mg	0.3376	...	0.5341	1.582
δSb	25	>14.0	*mP*3	?	...	0.556	0.404	0.422	β = 86.0°
αSc	25	atm	*hP*2	$P6_3/mmc$	Mg	0.33088	...	0.52680	1.5921
βSc	>1337	atm	*cI*2	$Im\bar{3}m$	W	0.373	...	...	...
γSe	25	atm	*hP*3	$P3_121$	γSe	0.43659	...	0.49537	1.1346
αSi	25	atm	*cF*8	$Fd\bar{3}m$	C(diamond)	0.54306	...	...	...
βSi	25	>9.5	*tI*4	$I4_1/amd$	βSn	0.4686	...	0.2585	0.552
γSi	25	>16.0	*cI*16	$Im\bar{3}m$	γSi	0.6636	...	...	...
δSi	25	>16 → atm	*hP*4	$P6_3/mmc$	αLa	0.380	...	0.628	1.653
αSm	25	atm	*hR*3	$R\bar{3}m$	αSm	0.36290	...	2.6207	4.5 × 1.6048
βSm	>734	atm	*hP*2	$P6_3/mmc$	Mg	0.36630	...	0.58448	1.5956
γSm	>922	atm	*cI*2	$Im\bar{3}m$	W	?	...	...	...
δSm	25	>4.0	*hP*4	$P6_3/mmc$	αLa	0.3618	...	1.166	2 × 1.611
αSn	<13	atm	*cF*8	$Fd\bar{3}m$	C(diamond)	0.64892	...	...	...
βSn	25	atm	*tI*4	$I4_1/amd$	βSn	0.58318	...	0.31818	0.5456
γSn	25	>9.0	*tI*2	?	γSn	0.370	...	0.337	0.91
αSr	25	atm	*cF*4	$Fm\bar{3}m$	Cu	0.6084	...	...	...
βSr	>547	atm	*cI*2	$Im\bar{3}m$	W	0.487	...	...	...
β′Sr	25	>3.5	*cI*2	$Im\bar{3}m$	W	0.4437	...	...	...
Ta	25	atm	*cI*2	$Im\bar{3}m$	W	0.33030	...	...	...
αTb	<–53	atm	*oC*4	*Cmcm*	α′Dy	0.3605	0.6244	0.5706	...
α′Tb	25	atm	*hP*2	$P6_3/mmc$	Mg	0.36055	...	0.56966	1.5800
βTb	>1289	atm	*cI*2	$Im\bar{3}m$	W	(0.402)	...	...	...
γTb	25	>6.0	*hR*3	$R\bar{3}m$	αSm	0.341	...	2.45	4.5 × 1.60
Tc	25	atm	*hP*2	$P6_3/mmc$	Mg	0.2738	...	0.4393	1.604
αTe	25	atm	*hP*3	$P3_121$	γSe	0.44566	...	0.59264	1.3298
βTe	25	>2.0	*hR*2	$R\bar{3}m$	αAs	0.469	...	...	α = 53.30°
γTe	25	>7.0	*hR*1	$R\bar{3}m$	βPo	0.3002	...	...	α = 103.3°
αTh	25	atm	*cF*4	$Fm\bar{3}m$	Cu	0.50842	...	...	...
βTh	>1360	atm	*cI*2	$Im\bar{3}m$	W	0.411	...	...	...
αTi	25	atm	*hP*2	$P6_3/mmc$	Mg	0.29506	...	0.46835	1.5873
βTi	>882	atm	*cI*2	$Im\bar{3}m$	W	0.33065	...	...	...
ωTi	25	HP → atm	*hP*3	*P*6/*mmm*	ωTi	0.4625	...	0.2813	0.6082
αTl	25	atm	*hP*2	$P6_3/mmc$	Mg	0.34566	...	0.55248	1.5983
βTl	>230	atm	*cI*2	$Im\bar{3}m$	W	0.3879	...	...	...
γTl	25	HP	*cF*4	$Fm\bar{3}m$	Cu	?	...	...	...
Tm	25	atm	*hP*2	$P6_3/mmc$	Mg	0.35375	...	0.55540	1.5700
αU	25	atm	*oC*4	*Cmcm*	αU	0.28537	0.58695	0.49548	...
βU	>668	atm	*tP*30	$P4_2/mnm$	βU	1.0759	...	0.5656	0.526
γU	>776	atm	*cI*2	$Im\bar{3}m$	W	0.3524	...	...	...
V	25	atm	*cI*2	$Im\bar{3}m$	W	0.30240	...	...	...
W	25	atm	*cI*2	$Im\bar{3}m$	W	0.31652	...	...	...
Xe	<–111.758	atm	*cF*4	$Fm\bar{3}m$	Cu	0.6350	...	...	...
αY	25	atm	*hP*2	$P6_3/mmc$	Mg	0.36482	...	0.57318	1.5711
βY	>1478	atm	*cI*2	$Im\bar{3}m$	W	(0.407)	...	...	...
αYb	<–3	atm	*hP*2	$P6_3/mmc$	Mg	0.38799	...	0.63859	1.6459
βYb	25	atm	*cF*4	$Fm\bar{3}m$	Cu	0.54848	...	...	...
γYb	>795	atm	*cI*2	$Im\bar{3}m$	W	0.444	...	...	...
Zn	25	atm	*hP*2	$P6_3/mmc$	Mg	0.26650	...	0.49470	1.8563
αZr	25	atm	*hP*2	$P6_3/mmc$	Mg	0.32316	...	0.51475	1.5929
βZr	>863	atm	*cI*2	$Im\bar{3}m$	W	0.36090	...	...	...
ωZr	25	HP → atm	*hP*2	*P*6/*mmm*	ωTi	0.5036	...	0.3109	0.617

Note: Values in parentheses are estimated.

Crystal Structure Nomenclature

The various designation systems for describing crystal structure are discussed in the Introduction to Alloy Phase Diagrams, page 1•1 of this Handbook.

Arranged Alphabetically by Pearson-Symbol Designation

Pearson symbol	Prototype	Strukturbericht designation	Space group
*cF*4	Cu	*A*1	$Fm\bar{3}m$
*cF*8	C(diamond)	*A*4	$Fd\bar{3}m$
	NaCl	*B*1	$Fm\bar{3}m$
	ZnS(sphalerite)	*B*3	$F\bar{4}3m$
*cF*12	CaF_2	*C*1	$Fm\bar{3}m$
	MgAgAs	$C1_b$	$F\bar{4}3m$
*cF*16	$AlCu_2Mn$	$L2_1$	$Fm\bar{3}m$
	BiF_3	$D0_3$	$Fm\bar{3}m$
	NaTl	*B*32	$Fd\bar{3}m$
*cF*24	$AuBe_5$	$C15_b$	$F\bar{4}3m$
	SiO_2(β cristobalite)	*C*9	$Fd\bar{3}m$
	Cu_2Mg	*C*15	$Fd\bar{3}m$
*cF*32	$CuPt_3$	$L1_a$	$Fm\bar{3}c$
*cF*52	UB_{12}	$D2_f$	$Fm\bar{3}m$
*cF*56	Al_2MgO_4	$H1_1$	$Fd\bar{3}m$
	Co_3S_4	$D7_2$	$Fd\bar{3}m$
*cF*68	Co_9S_8	$D8_9$	$Fm\bar{3}m$
*cF*80	Sb_2O_3(senarmontite)	$D5_4$	$Fd\bar{3}m$
*cF*112	Fe_3W_3C	$E9_3$	$Fd\bar{3}m$
	$NaZn_{13}$	$D2_3$	$Fm\bar{3}c$
*cF*116	$Cr_{23}C_6$	$D8_4$	$Fm\bar{3}m$
	$Mn_{23}Th_6$	$D8_a$	$Fm\bar{3}m$
*cI*2	W	*A*2	$Im\bar{3}m$
*cI*16	CoU	B_a	$I2_13$
*cI*28	Th_3P_4	$D7_3$	$I\bar{4}3d$
*cI*32	$CoAs_3$	$D0_2$	$Im\bar{3}$
*cI*40	Ge_7Ir_3	$D8_f$	$Im\bar{3}m$
	Pu_2C_3	$D5_c$	$I\bar{4}3d$
*cI*52	Cu_5Zn_8	$D8_2$	$I\bar{4}3m$
	Fe_3Zn_{10}	$D8_1$	$Im\bar{3}m$
*cI*54	Sb_2Tl_7	$L2_2$	$Im\bar{3}m$
*cI*58	αMn	*A*12	$I\bar{4}3m$
*cI*76	$Cu_{15}Si_4$	$D8_6$	$I\bar{4}3d$
*cI*80	Mn_2O_3	$D5_3$	$Ia\bar{3}$
*cI*96	$AlLi_3N_2$	$E9_d$	$Ia\bar{3}$
*cI*162	$Mg_{32}(Al,Zn)_{49}$	$D8_e$	$Im\bar{3}$
*cP*1	αPo	A_h	$Pm\bar{3}m$
*cP*2	CsCl	*B*2	$Pm\bar{3}m$
*cP*4	$AuCu_3$	$L1_2$	$Pm\bar{3}m$
	ReO_3	$D0_9$	$Pm\bar{3}m$
*cP*5	$AlFe_3C$	$L'1_2$	$Pm\bar{3}m$
	$CaTiO_3$	$E2_1$	$Pm\bar{3}m$
	Fe_4N	$L'1$	$P\bar{4}3m$
*cP*6	Ag_2O	*C*3	$Pn\bar{3}m$
*cP*7	CaB_6	$D2_1$	$Pm\bar{3}m$
*cP*8	Cr_3Si	*A*15	$Pm\bar{3}n$
	FeSi	*B*20	$P2_13$
	Cu_3VS_4	$H2_4$	$P\bar{4}3m$
*cP*12	FeS_2(pyrite)	*C*2	$Pa3$
	NiSbS	$F0_1$	$P2_13$
*cP*20	βMn	*A*13	$P4_132$
*cP*36	$BaHg_{11}$	$D2_e$	$Pm\bar{3}m$
*cP*39	Mg_2Zn_{11}	$D8_c$	$Pm\bar{3}$
*cP*52	Cu_9Al_4	$D8_3$	$P\bar{4}3m$
*hP*1	$HgSn_{6-10}$	A_f	$P6/mmm$
*hP*2	Mg	*A*3	$P6_3/mmc$
*hP*2(continued)	WC	B_h	$P\bar{6}m2$
*hP*3	AlB_2	*C*32	$P6/mmm$
	CdI_2	*C*6	$P\bar{3}m1$
	Fe_2N	*L'*3	$P6_3/mmc$
	$LiZn_2$	C_k	$P6_3/mmc$
	γSe	*A*8	$P3_121$
*hP*4	αLa	*A*3′	$P6_3/mmc$
	BN	B_k	$P6_3/mmc$
	C(graphite)	*A*9	$P6_3/mmc$
	NiAs	$B8_1$	$P6_3/mmc$
	ZnS(wurtzite)	*B*4	$P6_3mc$
*hP*5	La_2O_3	$D5_2$	$P\bar{3}m1$
	Ni_2Al_3	$D5_{13}$	$P\bar{3}m1$
*hP*6	$CaCu_5$	$D2_d$	$P6/mmm$
	CoSn	*B*35	$P6/mmm$
	Cu_2Te	C_h	$P6/mmm$
	HgS	*B*9	$P3_121$
	MoS_2	*C*7	$P6_3/mmc$
	Ni_2In	$B8_2$	$P6_3/mmc$
*hP*8	Na_3As	$D0_{18}$	$P6_3/mmc$
	Ni_3Sn	$D0_{19}$	$P6_3/mmc$
	TiAs	B_i	$P6_3/mmc$
*hP*9	$CrSi_2$	*C*40	$P6_222$
	Fe_2P	*C*22	$P\bar{6}2m$
	ζAgZn	B_b	$P\bar{3}$
	SiO_2(high quartz)	*C*8	$P6_222$
*hP*10	Pt_2Sn_3	$D5_b$	$P6_3/mmc$
*hP*12	CuS	*B*18	$P6_3/mmc$
	$MgZn_2$	*C*14	$P6_3/mmc$
	SiO_2(βtridymite)	*C*10	$P6_3/mmc$
*hP*14	W_2B_5	$D8_h$	$P6_3/mmc$
*hP*16	Mn_5Si_3	$D8_8$	$P6_3/mcm$
	Ni_3Ti	$D0_{24}$	$P6_3/mmc$
*hP*18	Al_4C_4Si	$E9_4$	$P6_3mc$
	$Al_8FeMg_3Si_6$	$E9_b$	$P\bar{6}2m$
	Mg_2Ni	C_a	$P6_222$
*hP*20	Fe_3Th_7	$D10_2$	$P6_3mc$
	Th_7S_{12}	$D8_k$	$P6_3/m$
*hP*24	Cu_3P	$D0_{21}$	$P6_3cm$
	$MgNi_2$	*C*36	$P6_3/mmc$
*hP*28	Co_2Al_5	$D8_{11}$	$P6_3/mmc$
*hR*1	αHg	*A*10	$R\bar{3}m$
	βPo	A_i	$R\bar{3}m$
*hR*2	αAs	*A*7	$R\bar{3}m$
*hR*3	αSm	*C*19	$R\bar{3}m$
*hR*4	$NaCrS_2$	$F5_1$	$R\bar{3}m$
*hR*5	Bi_2Te_3	*C*33	$R\bar{3}m$
	Ni_3S_2	$D5_e$	*R*32
*hR*6	$CaSi_2$	*C*12	$R\bar{3}m$
	NiS	B13	$R\bar{3}m$
*hR*7	Al_4C_3	$D7_1$	$R\bar{3}m$
	Mo_2B_5	$D8_i$	$R\bar{3}m$
*hR*10	αAl_2O_3	$D5_1$	$R\bar{3}c$
*hR*13	Fe_7W_6	$D8_5$	$R\bar{3}m$

(continued)

Arranged Alphabetically by Pearson-Symbol Designation (continued)

Pearson symbol	Prototype	Strukturbericht designation	Space group
*hR*15	B_4C	$D1_g$	$R\bar{3}m$
*hR*26	Cr_5Al_8	$D8_{10}$	$R\bar{3}m$
*hR*32	CuPt	$L1_1$	$R\bar{3}m$
*mC*6	$AuTe_2$(calaverite)	*C*34	*C*2/*m*
*mC*8	CuO	*B*26	*C*2/*c*
*mC*12	ThC_2	C_g	*C*2/*c*
*mC*14	δNi_3Sn_4	$D7_a$	*C*2/*m*
*mC*16	$FeKS_2$	$F5_a$	*C*2/*c*
*mP*12	$AgAuTe_4$	$E1_b$	*P*2/*c*
	ZrO_2	*C*43	$P2_1/c$
*mP*20	As_2S_3	$D5_f$	$P2_1/c$
*mP*22	Co_2Al_9	$D8_d$	$P2_1/c$
*mP*24	FeAsS	$E0_7$	$P2_1/c$
*mP*32	AsS	B_l	$P2_1/c$
	βSe	A_l	$P2_1/c$
*mP*64	αSe	A_k	$P2_1/c$
*oC*4	αU	*A*20	*Cmcm*
*oC*8	CaSi	B_c	*Cmmc*
	αGa	*A*11	*Cmca*
	CrB	B_f	*Cmcm*
	I_2	*A*14	*Cmca*
	P(black)	*A*17	*Cmca*
*oC*12	$ZrSi_2$	*C*49	*Cmcm*
*oC*16	BRe_3	$E1_a$	*Cmcm*
*oC*20	$PdSn_4$	$D1_c$	*Aba*2
*oC*24	$PdSn_2$	C_e	*Aba*2
*oC*28	Al_6Mn	$D2_h$	*Cmcm*
*oF*24	$TiSi_2$	*C*54	*Fddd*
*oF*40	Mn_4B	$D1_f$	*Fddd*
*oF*48	$CuMg_2$	C_b	*Fddd*
*oF*72	GeS_2	*C*44	*Fdd*2
*oF*128	αS	*A*16	*Fddd*
*oI*12	SiS_2	*C*42	*Ibam*
*oI*14	Ta_3B_4	$D7_b$	*Immm*
*oI*20	Al_4U	$D1_b$	*Imma*
*oI*28	Ga_2Mg_5	$D8_g$	*Ibam*
*oP*4	AuCd	*B*19	*Pmma*
*oP*6	FeS_2(marcasite)	*C*18	*Pnnm*
	$CaCl_2$	*C*35	*Pnnm*
*oP*8	αNp	A_c	*Pnma*
	ηNiSi	B_d	*Pbnm*
	βCu_3Ti	$D0_a$	*Pmmn*
	FeB	*B*27	*Pnma*
	GeS	*B*16	*Pnma*
	SnS	*B*29	*Pmcn*
	MnP	*B*31	*Pnma*
	TiB	B_m	*Pnma*
*oP*12	Co_2Si	*C*23	*Pnma*
	Co_2Si	*C*37	*Pbnm*
	$HgCl_2$	*C*28	*Pmnb*
*oP*16	Al_3Ni	$D0_{20}$	*Pnma*
	$AsMn_3$	$D0_d$	*Pmmn*
	BaS_3	$D0_{17}$	$P42_1m$
	CdSb	B_e	*Pbca*
*oP*16 (continued)	CuS_2Sb	$F5_6$	*Pnma*
	Fe_3C	$D0_{11}$	*Pnma*
*oP*20	Cr_3C_2	$D5_{10}$	*Pnma*
	Sb_2S_3	$D5_8$	*Pnma*
*oP*24	$AuTe_2$(krennerite)	*C*46	*Pma*2
	$CuFe_2S_3$	$E9_e$	*Pnma*
	TiO_2(brookite)	*C*21	*Pbca*
*oP*20	Sb_2O_3(valentinite)	$D5_{11}$	*Pccn*
*oP*40	Cr_7C_3	$D10_1$	*Pnma*
*tI*2	αPa	A_a	*I*4/*mmm*
	In	*A*6	*I*4/*mmm*
*tI*4	βSn	*A*5	$I4_1/amd$
*tI*6	CaC_2	$C11_a$	*I*4/*mmm*
	$FeCu_2SnS_4$	*H*26	$I\bar{4}2m$
	$MoSi_2$	$C11_b$	*I*4/*mmm*
	ThH_2	$L'2_b$	*I*4/*mmm*
*tI*8	Al_3Ti	$D0_{22}$	*I*4/*mmm*
*tI*10	Al_4Ba	$D1_3$	*I*4/*mmm*
	$MoNi_4$	$D1_a$	*I*4/*m*
*tI*12	Al_2Cu	*C*16	*I*4/*mcm*
	$ThSi_2$	C_c	$I4_1/amd$
*tI*14	Al_2CdS_4	*E*3	$I\bar{4}$
*tI*16	Al_3Zr	$D0_{23}$	*I*4/*mmm*
	$CuFeS_2$	$E1_1$	$I\bar{4}2d$
	Ir_3Si	$D0'_c$	*I*4/*mcm*
	MoB	B_g	$I4_1/amd$
	SiU_3	$D0_c$	*I*4/*mcm*
	TlSe	*B*37	*I*4/*mcm*
*tI*18	Fe_8N	$D2_g$	*I*4/*mmm*
*tI*26	$Mn_{12}Th$	$D2_b$	*I*4/*mmm*
*tI*28	MnU_6	$D2_c$	*I*4/*mcm*
*tI*32	Cr_5B_3	$D8_l$	*I*4/*mcm*
	Ni_3P	$D0_e$	$I\bar{4}$
	W_5Si_3	$D8_m$	*I*4/*mcm*
*tP*2	AuCu	$L1_0$	*P*4/*mmm*
	δCuTi	$L2_a$	*P*4/*mmm*
*tP*4	βNp	A_d	$P42_12$
	$CuTi_3$	$L6_0$	*P*4/*mmm*
	γCuTi	*B*11	*P*4/*nmm*
	PbO	*B*10	*P*4/*nmm*
	PtS	*B*17	$P4_2/mmc$
*tP*6	Cu_2Sb	*C*38	*P*4/*nmm*
	PbFCl	$E0_1$	*P*4/*nmm*
	TiO_2(rutile)	*C*4	$P4_2/mnm$
*tP*10	Pb_4Pt	$D1_d$	*P*4/*nbm*
	Si_2U_3	$D5_a$	*P*4/*mbm*
*tP*16	PdS	*B*34	$P4_2/m$
*tP*20	B_4Th	$D1_e$	*P*4/*mbm*
*tP*30	βU	A_b	$P4_2/mnm$
	σCrFe	$D8_b$	$P4_2/mnm$
*tP*40	Al_7Cu_2Fe	$E9_a$	*P*4/*mnc*
	Zn_3P_2	$D5_9$	$P4_2/nmc$
*tP*50	γB	A_g	$P4_2/nnm$

Arranged Alphabetically by Strukturbericht Designation

Strukturbericht designation	Prototype	Pearson symbol	Space group
A_a	αPa	*tI*2	*I*4/*mmm*
A_b	βU	*tP*30	$P4_2/mnm$
A_c	αNp	*oP*8	*Pnma*
A_d	βNp	*tP*4	$P42_12$
A_f	$HgSn_{6-10}$	*hP*1	*P*6/*mmm*
A_g	γB	*tP*50	$P4_2/nnm$
A_h	αPo	*cP*1	$Pm\bar{3}m$
A_i	βPo	*hR*1	$R\bar{3}m$
A_k	αSe	*mP*64	$P2_1/c$
A_l	βSe	*mP*32	$P2_1/c$
*A*1	Cu	*cF*4	$Fm\bar{3}m$
*A*2	W	*cI*2	$Im\bar{3}m$
*A*3	Mg	*hP*2	$P6_3/mmc$
*A*3′	αLa	*hP*4	$P6_3/mmc$
*A*4	C(diamond)	*cF*8	$Fd\bar{3}m$

(continued)

Arranged Alphabetically by Strukturbericht Designation (continued)

Struktur-bericht designation	Prototype	Pearson symbol	Space group
$A5$	βSn	$tI4$	$I4_1/amd$
$A6$	In	$tI2$	$I4/mmm$
$A7$	αAs	$hR2$	$R\bar{3}m$
$A8$	γSe	$hP3$	$P3_121$
$A9$	C(graphite)	$hP4$	$P6_3/mmc$
$A10$	αHg	$hR1$	$R\bar{3}m$
$A11$	αGa	$oC8$	$Cmca$
$A12$	αMn	$cI58$	$I\bar{4}3m$
$A13$	βMn	$cP20$	$P4_132$
$A14$	I_2	$oC8$	$Cmca$
$A15$	Cr_3Si	$cP8$	$Pm\bar{3}n$
$A16$	αS	$oF128$	$Fddd$
$A17$	P(black)	$oC8$	$Cmca$
$A20$	αU	$oC4$	$Cmcm$
B_a	CoU	$cI16$	$I2_13$
B_b	ζAgZn	$hP9$	$P\bar{3}$
B_c	CaSi	$oC8$	$Cmmc$
B_d	ηNiSi	$oP8$	$Pbnm$
B_e	CdSb	$oP16$	$Pbca$
B_f	CrB	$oC8$	$Cmcm$
B_g	MoB	$tI16$	$I4_1/amd$
B_h	WC	$hP2$	$P\bar{6}m2$
B_i	TiAs	$hP8$	$P6_3/mmc$
B_k	BN	$hP4$	$P6_3/mmc$
B_l	AsS	$mP32$	$P2_1/c$
B_m	TiB	$oP8$	$Pnma$
$B1$	NaCl	$cF8$	$Fm\bar{3}m$
$B2$	CsCl	$cP2$	$Pm\bar{3}m$
$B3$	ZnS(sphalerite)	$cF8$	$F\bar{4}3m$
$B4$	ZnS(wurtzite)	$hP4$	$P6_3mc$
$B8_1$	NiAs	$hP4$	$P6_3/mmc$
$B8_2$	Ni_2In	$hP6$	$P6_3/mmc$
$B9$	HgS	$hP6$	$P3_121$
$B10$	PbO	$tP4$	$P4/nmm$
$B11$	γCuTi	$tP4$	$P4/nmm$
$B13$	NiS	$hR6$	$R\bar{3}m$
$B16$	GeS	$oP8$	$Pnma$
$B17$	PtS	$tP4$	$P4_2/mmc$
$B18$	CuS	$hP12$	$P6_3/mmc$
$B19$	AuCd	$oP4$	$Pmma$
$B20$	FeSi	$cP8$	$P2_13$
$B26$	CuO	$mC8$	$C2/c$
$B27$	FeB	$oP8$	$Pnma$
$B29$	SnS	$oP8$	$Pmcn$
$B31$	MnP	$oP8$	$Pnma$
$B32$	NaTl	$cF16$	$Fd\bar{3}m$
$B34$	PdS	$tP16$	$P4_2/m$
$B35$	CoSn	$hP6$	$P6/mmm$
$B37$	TlSe	$tI16$	$I4/mcm$
C_a	Mg_2Ni	$hP18$	$P6_222$
C_b	$CuMg_2$	$oF48$	$Fddd$
C_c	$ThSi_2$	$tI12$	$I4_1/amd$
C_e	$PdSn_2$	$oC24$	$Aba2$
C_g	ThC_2	$mC12$	$C2/c$
C_h	Cu_2Te	$hP6$	$P6/mmm$
C_k	$LiZn_2$	$hP3$	$P6_3/mmc$
$C1$	CaF_2	$cF12$	$Fm\bar{3}m$
$C1_b$	MgAgAs	$cF12$	$F\bar{4}3m$
$C2$	FeS_2(pyrite)	$cP12$	$Pa3$
$C3$	Ag_2O	$cP6$	$Pn\bar{3}m$
$C4$	TiO_2(rutile)	$tP6$	$P4_2/mnm$
$C6$	CdI_2	$hP3$	$P\bar{3}m1$
$C7$	MoS_2	$hP6$	$P6_3/mmc$
$C8$	SiO_2(high quartz)	$hP9$	$P6_222$
$C9$	SiO_2(β cristobalite)	$cF24$	$Fd\bar{3}m$
$C10$	SiO_2(β tridymite)	$hP12$	$P6_3/mmc$
$C11_a$	CaC_2	$tI6$	$I4/mmm$
$C11_b$	$MoSi_2$	$tI6$	$I4/mmm$
$C12$	$CaSi_2$	$hR6$	$R\bar{3}m$
$C14$	$MgZn_2$	$hP12$	$P6_3/mmc$
$C15$	Cu_2Mg	$cF24$	$Fd\bar{3}m$
$C15_b$	$AuBe_5$	$cF24$	$F\bar{4}3m$
$C16$	Al_2Cu	$tI12$	$I4/mcm$
$C18$	FeS_2(marcasite)	$oP6$	$Pnnm$
$C19$	αSm	$hR3$	$R\bar{3}m$
$C21$	TiO_2(brookite)	$oP24$	$Pbca$
$C22$	Fe_2P	$hP9$	$P\bar{6}2m$
$C23$	Co_2Si	$oP12$	$Pnma$
$C28$	$HgCl_2$	$oP12$	$Pmnb$
$C32$	AlB_2	$hP3$	$P6/mmm$
$C33$	Bi_2Te_3	$hR5$	$R\bar{3}m$
$C34$	$AuTe_2$(calaverite)	$mC6$	$C2/m$
$C35$	$CaCl_2$	$oP6$	$Pnnm$
$C36$	$MgNi_2$	$hP24$	$P6_3/mmc$
$C37$	Co_2Si	$oP12$	$Pbnm$
$C38$	Cu_2Sb	$tP6$	$P4/nmm$
$C40$	$CrSi_2$	$hP9$	$P6_222$
$C42$	SiS_2	$oI12$	$Ibam$
$C43$	ZrO_2	$mP12$	$P2_1/c$
$C44$	GeS_2	$oF72$	$Fdd2$
$C46$	$AuTe_2$(krennerite)	$oP24$	$Pma2$
$C49$	$ZrSi_2$	$oC12$	$Cmcm$
$C54$	$TiSi_2$	$oF24$	$Fddd$
$D0_a$	$βCu_3Ti$	$oP8$	$Pmmn$
$D0_c$	SiU_3	$tI16$	$I4/mcm$
$D0_c'$	Ir_3Si	$tI16$	$I4/mcm$
$D0_d$	$AsMn_3$	$oP16$	$Pmmn$
$D0_e$	Ni_3P	$tI32$	$I\bar{4}$
$D0_2$	$CoAs_3$	$cI32$	$Im\bar{3}$
$D0_3$	BiF_3	$cF16$	$Fm\bar{3}m$
$D0_9$	ReO_3	$cP4$	$Pm\bar{3}m$
$D0_{11}$	Fe_3C	$oP16$	$Pnma$
$D0_{17}$	BaS_3	$oP16$	$P42_1m$
$D0_{18}$	Na_3As	$hP8$	$P6_3/mmc$
$D0_{19}$	Ni_3Sn	$hP8$	$P6_3/mmc$
$D0_{20}$	Al_3Ni	$oP16$	$Pnma$
$D0_{21}$	Cu_3P	$hP24$	$P6_3cm$
$D0_{22}$	Al_3Ti	$tI8$	$I4/mmm$
$D0_{23}$	Al_3Zr	$tI16$	$I4/mmm$
$D0_{24}$	Ni_3Ti	$hP16$	$P6_3/mmc$
$D1_a$	$MoNi_4$	$tI10$	$I4/m$
$D1_b$	Al_4U	$oI20$	$Imma$
$D1_c$	$PdSn_4$	$oC20$	$Aba2$
$D1_d$	Pb_4Pt	$tP10$	$P4/nbm$
$D1_e$	B_4Th	$tP20$	$P4/mbm$
$D1_f$	Mn_4B	$oF40$	$Fddd$
$D1_g$	B_4C	$hR15$	$R\bar{3}m$
$D1_3$	Al_4Ba	$tI10$	$I4/mmm$
$D2_b$	$Mn_{12}Th$	$tI26$	$I4/mmm$
$D2_c$	MnU_6	$tI28$	$I4/mcm$
$D2_d$	$CaCu_5$	$hP6$	$P6/mmm$
$D2_e$	$BaHg_{11}$	$cP36$	$Pm\bar{3}m$
$D2_f$	UB_{12}	$cF52$	$Fm\bar{3}m$
$D2_g$	Fe_8N	$tI18$	$I4/mmm$
$D2_h$	Al_6Mn	$oC28$	$Cmcm$
$D2_1$	CaB_6	$cP7$	$Pm\bar{3}m$
$D2_3$	$NaZn_{13}$	$cF112$	$Fm\bar{3}c$
$D5_a$	Si_2U_3	$tP10$	$P4/mbm$
$D5_b$	Pt_2Sn_3	$hP10$	$P6_3/mmc$
$D5_c$	Pu_2C_3	$cI40$	$I\bar{4}3d$
$D5_e$	Ni_3S_2	$hR5$	$R32$
$D5_f$	As_2S_3	$mP20$	$P2_1/c$
$D5_1$	$αAl_2O_3$	$hR10$	$R\bar{3}c$
$D5_2$	La_2O_3	$hP5$	$P\bar{3}m1$
$D5_3$	Mn_2O_3	$cI80$	$Ia\bar{3}$
$D5_4$	Sb_2O_3(senarmontite)	$cF80$	$Fd\bar{3}m$
$D5_8$	Sb_2S_3	$oP20$	$Pnma$
$D5_9$	Zn_3P_2	$tP40$	$P4_2/nmc$
$D5_{10}$	Cr_3C_2	$oP20$	$Pnma$
$D5_{11}$	Sb_2O_3(valentinite)	$oP20$	$Pccn$
$D5_{13}$	Ni_2Al_3	$hP5$	$P\bar{3}m1$
$D7_a$	$δNi_3Sn_4$	$mC14$	$C2/m$
$D7_b$	Ta_3B_4	$oI14$	$Immm$
$D7_1$	Al_4C_3	$hR7$	$R\bar{3}m$
$D7_2$	Co_3S_4	$cF56$	$Fd\bar{3}m$
$D7_3$	Th_3P_4	$cI28$	$I\bar{4}3d$
$D8_a$	$Mn_{23}Th_6$	$cF116$	$Fm\bar{3}m$
$D8_b$	σCrFe	$tP30$	$P4_2/mnm$
$D8_c$	Mg_2Zn_{11}	$cP39$	$Pm\bar{3}$
$D8_d$	Co_2Al_9	$mP22$	$P2_1/c$
$D8_e$	$Mg_{32}(Al,Zn)_{49}$	$cI162$	$Im\bar{3}$
$D8_f$	Ge_7Ir_3	$cI40$	$Im\bar{3}m$
$D8_g$	Ga_2Mg_5	$oI28$	$Ibam$
$D8_h$	W_2B_5	$hP14$	$P6_3/mmc$
$D8_i$	Mo_2B_5	$hR7$	$R\bar{3}m$
$D8_k$	Th_7S_{12}	$hP20$	$P6_3/m$
$D8_l$	Cr_5B_3	$tI32$	$I4/mcm$
$D8_m$	W_5Si_3	$tI32$	$I4/mcm$
$D8_1$	Fe_3Zn_{10}	$cI52$	$Im\bar{3}m$
$D8_2$	Cu_5Zn_8	$cI52$	$I\bar{4}3m$
$D8_3$	Cu_9Al_4	$cP52$	$P\bar{4}3m$
$D8_4$	$Cr_{23}C_6$	$cF116$	$Fm\bar{3}m$
$D8_5$	Fe_7W_6	$hR13$	$R\bar{3}m$
$D8_6$	$Cu_{15}Si_4$	$cI76$	$I\bar{4}3d$

(continued)

Arranged Alphabetically by Strukturbericht Designation (continued)

Struktur-bericht designation	Prototype	Pearson symbol	Space group	Struktur-bericht designation	Prototype	Pearson symbol	Space group
$D8_8$	Mn_5Si_3	*hP*16	$P6_3/mcm$	$E9_4$	Al_4C_4Si	*hP*18	$P6_3mc$
$D8_9$	Co_9S_8	*cF*68	$Fm\bar{3}m$	$F5_a$	$FeKS_2$	*mC*16	$C2/c$
$D8_{10}$	Cr_5Al_8	*hR*26	$R\bar{3}m$	$F0_1$	NiSbS	*cP*12	$P2_13$
$D8_{11}$	Co_2Al_5	*hP*28	$P6_3/mmc$	$F5_1$	$NaCrS_2$	*hR*4	$R\bar{3}m$
$D10_1$	Cr_7C_3	*oP*40	*Pnma*	$F5_6$	CuS_2Sb	*oP*16	*Pnma*
$D10_2$	Fe_3Th_7	*hP*20	$P6_3mc$	$H1_1$	Al_2MgO_4	*cF*56	$Fd\bar{3}m$
$D8_{11}$	Co_2Al_5	*hP*28	$P6_3/mmc$	$H2_4$	Cu_3VS_4	*cP*8	$P\bar{4}3m$
$E0_1$	PbFCl	*tP*6	$P4/nmm$	$H2_6$	$FeCu_2SnS_4$	*tI*16	$I\bar{4}2m$
$E0_7$	FeAsS	*mP*24	$P2_1/c$	$L'1$	Fe_4N	*cF*5	$Fm\bar{3}m$
$E1_a$	$MgCuAl_2$	*oC*16	*Cmcm*	$L'1_2$	$AlFe_3C$	*cP*5	$Pm\bar{3}m$
$E1_b$	$AgAuTe_4$	*mP*12	$P2/c$	$L'2$	ThH_2	*tI*6	$I4/mmm$
$E1_1$	$CuFeS_2$	*tI*16	$I\bar{4}2d$	$L'3$	Fe_2N	*hP*3	$P6_3/mmc$
$E2_1$	$CaTiO_3$	*cP*5	$Pm\bar{3}m$	$L1_a$	$CuPt_3$	*cF*32	$Fm\bar{3}c$
$E3$	Al_2CdS_4	*tI*14	$I\bar{4}$	$L1_0$	AuCu	*tP*2	$P4/mmm$
$E9_a$	Al_7Cu_2Fe	*tP*40	$P4/mnc$	$L1_1$	CuPt	*hR*32	$R\bar{3}m$
$E9_b$	$Al_8FeMg_3Si_6$	*hP*18	$P\bar{6}2m$	$L1_2$	$AuCu_3$	*cP*4	$Pm\bar{3}m$
$E9_d$	$AlLi_3N_2$	*cI*96	$Ia\bar{3}$	$L2_a$	δCuTi	*tP*2	$P4/mmm$
$E9_e$	$CuFe_2S_3$	*oP*24	*Pnma*	$L2_1$	$AlCu_2Mn$	*cF*16	$Fm\bar{3}m$
$E9_c$	Mn_3Al_9Si	*hP*26	$P6_3/mmc$	$L2_2$	Sb_2Tl_7	*cI*54	$Im\bar{3}m$
$E9_3$	Fe_3W_3C	*cF*112	$Fd\bar{3}m$	$L6_0$	$CuTi_3$	*tP*4	$P4/mmm$

Temperature Conversions

The general arrangement of this table was devised by Sauveur and Boylston more than 40 years ago. The middle column of figures (in **boldface** type) contains the readings (°F or °C) to be converted. If converting from degrees Fahrenheit to degrees Celsius, read the Celsius equivalent in the column headed "C". If converting from Celsius to Fahrenheit, read the Fahrenheit equivalent in the column headed "F".

F		C	F		C	F		C	F		C	F		C
.....	−458	−272.22	.....	−308	−188.89	−252.4	−158	−105.56	+17.6	−8	−22.22	287.6	142	61.11
.....	−456	−271.11	.....	−306	−187.78	−248.8	−156	−104.44	+21.2	−6	−21.11	291.2	144	62.22
.....	−454	−270.00	.....	−304	−186.67	−245.2	−154	−103.33	+24.8	−4	−20.00	294.8	146	63.33
.....	−452	−268.89	.....	−302	−185.56	−241.6	−152	−102.22	+28.4	−2	−18.89	298.4	148	64.44
.....	−450	−267.78	.....	−300	−184.44	−238.0	−150	−101.11	+32.0	±0	−17.78	302.0	150	65.56
.....	−448	−266.67	.....	−298	−183.33	−234.4	−148	−100.00	+35.6	+2	−16.67	305.6	152	66.67
.....	−446	−265.56	.....	−296	−182.22	−230.8	−146	−98.89	+39.2	+4	−15.56	309.2	154	67.78
.....	−444	−264.44	.....	−294	−181.11	−227.2	−144	−97.78	+42.8	+6	−14.44	312.8	156	68.89
.....	−442	−263.33	.....	−292	−180.00	−223.6	−142	−96.67	+46.4	+8	−13.33	316.4	158	70.00
.....	−440	−262.22	.....	−290	−178.89	−220.0	−140	−95.56	+50.0	+10	−12.22	320.0	160	71.11
.....	−438	−261.11	.....	−288	−177.78	−216.4	−138	−94.44	+53.6	+12	−11.11	323.6	162	72.22
.....	−436	−260.00	.....	−286	−176.67	−212.8	−136	−93.33	+57.2	+14	−10.00	327.2	164	73.33
.....	−434	−258.89	.....	−284	−175.56	−209.2	−134	−92.22	+60.8	+16	−8.89	330.8	166	74.44
.....	−432	−257.78	.....	−282	−174.44	−205.6	−132	−91.11	+64.4	+18	−7.78	334.4	168	75.56
.....	−430	−256.67	.....	−280	−173.33	−202.0	−130	−90.00	+68.0	+20	−6.67	338.0	170	76.67
.....	−428	−255.56	.....	−278	−172.22	−198.4	−128	−88.89	+71.6	+22	−5.56	341.6	172	77.78
.....	−426	−254.44	.....	−276	−171.11	−194.8	−126	−87.78	+75.2	+24	−4.44	345.2	174	78.89
.....	−424	−253.33	.....	−274	−170.00	−191.2	−124	−86.67	+78.8	+26	−3.33	348.8	176	80.00
.....	−422	−252.22	−457.6	−272	−168.89	−187.6	−122	−85.56	+82.4	+28	−2.22	352.4	178	81.11
.....	−420	−251.11	−454.0	−270	−167.78	−184.0	−120	−84.44	+86.0	+30	−1.11	356.0	180	82.22
.....	−418	−250.00	−450.4	−268	−166.67	−180.4	−118	−83.33	+89.6	+32	±0.00	359.6	182	83.33
.....	−416	−248.89	−446.8	−266	−165.56	−176.8	−116	−82.22	+93.2	+34	+1.11	363.2	184	84.44
.....	−414	−247.78	−443.2	−264	−164.44	−173.2	−114	−81.11	+96.8	+36	+2.22	366.8	186	85.56
.....	−412	−246.67	−439.6	−262	−163.33	−169.6	−112	−80.00	+100.4	+38	+3.33	370.4	188	86.67
.....	−410	−245.56	−436.0	−260	−162.22	−166.0	−110	−78.89	+104.0	+40	+4.44	374.0	190	87.78
.....	−408	−244.44	−432.4	−258	−161.11	−162.4	−108	−77.78	107.6	42	5.56	377.6	192	88.89
.....	−406	−243.33	−428.8	−256	−160.00	−158.8	−106	−76.67	111.2	44	6.67	381.2	194	90.00
.....	−404	−242.22	−425.2	−254	−158.89	−155.2	−104	−75.56	114.8	46	7.78	384.8	196	91.11
.....	−402	−241.11	−421.6	−252	−157.78	−151.6	−102	−74.44	118.4	48	8.89	388.4	198	92.22
.....	−400	−240.00	−418.0	−250	−156.67	−148.0	−100	−73.33	122.0	50	10.00	392.0	200	93.33
.....	−398	−238.89	−414.4	−248	−155.56	−144.4	−98	−72.22	125.6	52	11.11	395.6	202	94.44
.....	−396	−237.78	−410.8	−246	−154.44	−140.8	−96	−71.11	129.2	54	12.22	399.2	204	95.56
.....	−394	−236.67	−407.2	−244	−153.33	−137.2	−94	−70.00	132.8	56	13.33	402.8	206	96.67
.....	−392	−235.56	−403.6	−242	−152.22	−133.6	−92	−68.89	136.4	58	14.44	406.4	208	97.78
.....	−390	−234.44	−400.0	−240	−151.11	−130.0	−90	−67.78	140.0	60	15.56	410.0	210	98.89
.....	−388	−233.33	−396.4	−238	−150.00	−126.4	−88	−66.67	143.6	62	16.67	413.6	212	100.00
.....	−386	−232.22	−392.8	−236	−148.89	−122.8	−86	−65.56	147.2	64	17.78	417.2	214	101.11
.....	−384	−231.11	−389.2	−234	−147.78	−119.2	−84	−64.44	150.8	66	18.89	420.8	216	102.22
.....	−382	−230.00	−385.6	−232	−146.67	−115.6	−82	−63.33	154.4	68	20.00	424.4	218	103.33
.....	−380	−228.89	−382.0	−230	−145.56	−112.0	−80	−62.22	158.0	70	21.11	428.0	220	104.44
.....	−378	−227.78	−378.4	−228	−144.44	−108.4	−78	−61.11	161.6	72	22.22	431.6	222	105.56
.....	−376	−226.67	−374.8	−226	−143.33	−104.8	−76	−60.00	165.2	74	23.33	435.2	224	106.67
.....	−374	−225.56	−371.2	−224	−142.22	−101.2	−74	−58.89	168.8	76	24.44	438.8	226	107.78
.....	−372	−224.44	−367.6	−222	−141.11	−97.6	−72	−57.78	172.4	78	25.56	442.4	228	108.89
.....	−370	−223.33	−364.0	−220	−140.00	−94.0	−70	−56.67	176.0	80	26.67	446.0	230	110.00
.....	−368	−222.22	−360.4	−218	−138.89	−90.4	−68	−55.56	179.6	82	27.78	449.6	232	111.11
.....	−366	−221.11	−356.8	−216	−137.78	−86.8	−66	−54.44	183.2	84	28.89	453.2	234	112.22
.....	−364	−220.00	−353.2	−214	−136.67	−83.2	−64	−53.33	186.8	86	30.00	456.8	236	113.33
.....	−362	−218.89	−349.6	−212	−135.56	−79.6	−62	−52.22	190.4	88	31.11	460.4	238	114.44
.....	−360	−217.78	−346.0	−210	−134.44	−76.0	−60	−51.11	194.0	90	32.22	464.0	240	115.56
.....	−358	−216.67	−342.4	−208	−133.33	−72.4	−58	−50.00	197.6	92	33.33	467.6	242	116.67
.....	−356	−215.56	−338.8	−206	−132.22	−68.8	−56	−48.89	201.2	94	34.44	471.2	244	117.78
.....	−354	−214.44	−335.2	−204	−131.11	−65.2	−54	−47.78	204.8	96	35.56	474.8	246	118.89
.....	−352	−213.33	−331.6	−202	−130.00	−61.6	−52	−46.67	208.4	98	36.67	478.4	248	120.00
.....	−350	−212.22	−328.0	−200	−128.89	−58.0	−50	−45.56	212.0	100	37.78	482.0	250	121.11
.....	−348	−211.11	−324.4	−198	−127.78	−54.4	−48	−44.44	215.6	102	38.89	485.6	252	122.22
.....	−346	−210.00	−320.8	−196	−126.67	−50.8	−46	−43.33	219.2	104	40.00	489.2	254	123.33
.....	−344	−208.89	−317.2	−194	−125.56	−47.2	−44	−42.22	222.8	106	41.11	492.8	256	124.44
.....	−342	−207.78	−313.6	−192	−124.44	−43.6	−42	−41.11	226.4	108	42.22	496.4	258	125.56
.....	−340	−206.67	−310.0	−190	−123.33	−40.0	−40	−40.00	230.0	110	43.33	500.0	260	126.67
.....	−338	−205.56	−306.4	−188	−122.22	−36.4	−38	−38.89	233.6	112	44.44	503.6	262	127.78
.....	−336	−204.44	−302.8	−186	−121.11	−32.8	−36	−37.78	237.2	114	45.56	507.2	264	128.89
.....	−334	−203.33	−299.2	−184	−120.00	−29.2	−34	−36.67	240.8	116	46.67	510.8	266	130.00
.....	−332	−202.22	−295.6	−182	−118.89	−25.6	−32	−35.56	244.4	118	47.78	514.4	268	131.11
.....	−330	−201.11	−292.0	−180	−117.78	−22.0	−30	−34.44	248.0	120	48.89	518.0	270	132.22
.....	−328	−200.00	−288.4	−178	−116.67	−18.4	−28	−33.33	251.6	122	50.00	521.6	272	133.33
.....	−326	−198.89	−284.8	−176	−115.56	−14.8	−26	−32.22	255.2	124	51.11	525.2	274	134.44
.....	−324	−197.78	−281.2	−174	−114.44	−11.2	−24	−31.11	258.8	126	52.22	528.8	276	135.56
.....	−322	−196.67	−277.6	−172	−113.33	−7.6	−22	−30.00	262.4	128	53.33	532.4	278	136.67
.....	−320	−195.56	−274.0	−170	−112.22	−4.0	−20	−28.89	266.0	130	54.44	536.0	280	137.78
.....	−318	−194.44	−270.4	−168	−111.11	−0.4	−18	−27.78	269.6	132	55.56	539.6	282	138.89
.....	−316	−193.33	−266.8	−166	−110.00	+3.2	−16	−26.67	273.2	134	56.67	543.2	284	140.00
.....	−314	−192.22	−263.2	−164	−108.89	+6.8	−14	−25.56	276.8	136	57.78	546.8	286	141.11
.....	−312	−191.11	−259.6	−162	−107.78	+10.4	−12	−24.44	280.4	138	58.89	550.4	288	142.22
.....	−310	−190.00	−256.0	−160	−106.67	+14.0	−10	−23.33	284.0	140	60.00	554.0	290	143.33

Temperature Conversions (continued)

F		C	F		C	F		C	F		C	F		C
557.6	292	144.44	870.8	466	241.11	1832.0	1000	537.78	3398.0	1870	1021.1	4964.0	2740	1504.4
561.2	294	145.56	874.4	468	242.22	1850.0	1010	543.33	3416.0	1880	1026.7	4982.0	2750	1510.0
564.8	296	146.67	878.0	470	243.33	1868.0	1020	548.89	3434.0	1890	1032.2	5000.0	2760	1515.6
568.4	298	147.78	881.6	472	244.44	1886.0	1030	554.44	3452.0	1900	1037.8	5018.0	2770	1521.1
572.0	300	148.89	885.2	474	245.56	1904.0	1040	560.00	3470.0	1910	1043.3	5036.0	2780	1526.7
575.6	302	150.00	888.8	476	246.67	1922.0	1050	565.56	3488.0	1920	1048.9	5054.0	2790	1532.2
579.2	304	151.11	892.4	478	247.78	1940.0	1060	571.11	3506.0	1930	1054.4	5072.0	2800	1537.8
582.8	306	152.22	896.0	480	248.89	1958.0	1070	576.67	3524.0	1940	1060.0	5090.0	2810	1543.3
586.4	308	153.33	899.6	482	250.00	1976.0	1080	582.22	3542.0	1950	1065.6	5108.0	2820	1548.9
590.0	310	154.44	903.2	484	251.11	1994.0	1090	587.78	3560.0	1960	1071.1	5126.0	2830	1554.4
593.6	312	155.56	906.8	486	252.22	2012.0	1100	593.33	3578.0	1970	1076.7	5144.0	2840	1560.0
597.2	314	156.67	910.4	488	253.33	2030.0	1110	598.89	3596.0	1980	1082.2	5162.0	2850	1565.6
600.8	316	157.78	914.0	490	254.44	2048.0	1120	604.44	3614.0	1990	1087.8	5180.0	2860	1571.1
604.4	318	158.89	917.6	492	255.56	2066.0	1130	610.00	3632.0	2000	1093.3	5198.0	2870	1576.7
608.0	320	160.00	921.2	494	256.67	2084.0	1140	615.56	3650.0	2010	1098.9	5216.0	2880	1582.2
611.6	322	161.11	924.8	496	257.78	2102.0	1150	621.11	3668.0	2020	1104.4	5234.0	2890	1587.8
615.2	324	162.22	928.4	498	258.89	2120.0	1160	626.67	3686.0	2030	1110.0	5252.0	2900	1593.3
618.8	326	163.33	932.0	500	260.00	2138.0	1170	632.22	3704.0	2040	1115.6	5270.0	2910	1598.9
622.4	328	164.44	935.6	502	261.11	2156.0	1180	637.78	3722.0	2050	1121.1	5288.0	2920	1604.4
626.0	330	165.56	939.2	504	262.22	2174.0	1190	643.33	3740.0	2060	1126.7	5306.0	2930	1610.0
629.6	332	166.67	942.8	506	263.33	2192.0	1200	648.89	3758.0	2070	1132.2	5324.0	2940	1615.6
633.2	334	167.78	946.4	508	264.44	2210.0	1210	654.44	3776.0	2080	1137.8	5342.0	2950	1621.1
636.8	336	168.89	950.0	510	265.56	2228.0	1220	660.00	3794.0	2090	1143.3	5360.0	2960	1626.7
640.4	338	170.00	953.6	512	266.67	2246.0	1230	665.56	3812.0	2100	1148.9	5378.0	2970	1632.2
644.0	340	171.11	957.2	514	267.78	2264.0	1240	671.11	3830.0	2110	1154.4	5396.0	2980	1637.8
647.6	342	172.22	960.8	516	268.89	2282.0	1250	676.67	3848.0	2120	1160.0	5414.0	2990	1643.3
651.2	344	173.33	964.4	518	270.00	2300.0	1260	682.22	3866.0	2130	1165.6	5432.0	3000	1648.9
654.8	346	174.44	968.0	520	271.11	2318.0	1270	687.78	3884.0	2140	1171.1	5450.0	3010	1654.4
658.4	348	175.56	971.6	522	272.22	2336.0	1280	693.33	3902.0	2150	1176.7	5468.0	3020	1660.0
662.0	350	176.67	975.2	524	273.33	2354.0	1290	698.89	3920.0	2160	1182.2	5486.0	3030	1665.6
665.6	352	177.78	978.8	526	274.44	2372.0	1300	704.44	3938.0	2170	1187.8	5504.0	3040	1671.1
669.2	354	178.89	982.4	528	275.56	2390.0	1310	710.00	3956.0	2180	1193.3	5522.0	3050	1676.7
672.8	356	180.00	986.0	530	276.67	2408.0	1320	715.56	3974.0	2190	1198.9	5540.0	3060	1682.2
676.4	358	181.11	989.6	532	277.78	2426.0	1330	721.11	3992.0	2200	1204.4	5558.0	3070	1687.8
680.0	360	182.22	993.2	534	278.89	2444.0	1340	726.67	4010.0	2210	1210.0	5576.0	3080	1693.3
683.6	362	183.33	996.8	536	280.00	2462.0	1350	732.22	4028.0	2220	1215.6	5594.0	3090	1698.9
687.2	364	184.44	1000.4	538	281.11	2480.0	1360	737.78	4046.0	2230	1221.1	5612.0	3100	1704.4
690.8	366	185.56	1004.0	540	282.22	2498.0	1370	743.33	4064.0	2240	1226.7	5702.0	3150	1732.2
694.4	368	186.67	1007.6	542	283.33	2516.0	1380	748.89	4082.0	2250	1232.2	5792.0	3200	1760.0
698.0	370	187.78	1011.2	544	284.44	2534.0	1390	754.44	4100.0	2260	1237.8	5882.0	3250	1787.7
701.6	372	188.89	1014.8	546	285.56	2552.0	1400	760.00	4118.0	2270	1243.3	5972.0	3300	1815.5
705.2	374	190.00	1018.4	548	286.67	2570.0	1410	765.56	4136.0	2280	1248.9	6062.0	3350	1843.3
708.8	376	191.11	1022.0	550	287.78	2588.0	1420	771.11	4154.0	2290	1254.4	6152.0	3400	1871.1
712.4	378	192.22	1040.0	560	293.33	2606.0	1430	776.67	4172.0	2300	1260.0	6242.0	3450	1898.8
716.0	380	193.33	1058.0	570	298.89	2624.0	1440	782.22	4190.0	2310	1265.6	6332.0	3500	1926.6
719.6	382	194.44	1076.0	580	304.44	2642.0	1450	787.78	4208.0	2320	1271.1	6422.0	3550	1954.4
723.2	384	195.56	1094.0	590	310.00	2660.0	1460	793.33	4226.0	2330	1276.7	6512.0	3600	1982.2
726.8	386	196.67	1112.0	600	315.56	2678.0	1470	798.89	4244.0	2340	1282.2	6602.0	3650	2010.0
730.4	388	197.78	1130.0	610	321.11	2696.0	1480	804.44	4262.0	2350	1287.8	6692.0	3700	2037.7
734.0	390	198.89	1148.0	620	326.67	2714.0	1490	810.00	4280.0	2360	1293.3	6782.0	3750	2065.5
737.6	392	200.00	1166.0	630	332.22	2732.0	1500	815.56	4298.0	2370	1298.9	6872.0	3800	2093.3
741.2	394	201.11	1184.0	640	337.78	2750.0	1510	821.11	4316.0	2380	1304.4	6962.0	3850	2121.1
744.8	396	202.22	1202.0	650	343.33	2768.0	1520	826.67	4334.0	2390	1310.0	7052.0	3900	2148.8
748.4	398	203.33	1220.0	660	348.89	2786.0	1530	832.22	4352.0	2400	1315.6	7142.0	3950	2176.6
752.0	400	204.44	1238.0	670	354.44	2804.0	1540	837.78	4370.0	2410	1321.1	7232.0	4000	2204.4
755.6	402	205.56	1256.0	680	360.00	2822.0	1550	843.33	4388.0	2420	1326.7	7322.0	4050	2232.2
759.2	404	206.67	1274.0	690	365.56	2840.0	1560	848.89	4406.0	2430	1332.2	7412.0	4100	2260.0
762.8	406	207.78	1292.0	700	371.11	2858.0	1570	854.44	4424.0	2440	1337.8	7502.0	4150	2287.7
766.4	408	208.89	1310.0	710	376.67	2876.0	1580	860.00	4442.0	2450	1343.3	7592.0	4200	2315.5
770.0	410	210.00	1328.0	720	382.22	2894.0	1590	865.56	4460.0	2460	1348.9	7682.0	4250	2343.3
773.6	412	211.11	1346.0	730	387.78	2912.0	1600	871.11	4478.0	2470	1354.4	7772.0	4300	2371.1
777.2	414	212.22	1364.0	740	393.33	2930.0	1610	876.67	4496.0	2480	1360.0	7862.0	4350	2398.8
780.8	416	213.33	1382.0	750	398.89	2948.0	1620	882.22	4514.0	2490	1365.6	7952.0	4400	2426.6
784.4	418	214.44	1400.0	760	404.44	2966.0	1630	887.78	4532.0	2500	1371.1	8042.0	4450	2454.4
788.0	420	215.56	1418.0	770	410.00	2984.0	1640	893.33	4550.0	2510	1376.7	8132.0	4500	2482.2
791.6	422	216.67	1436.0	780	415.56	3002.0	1650	898.89	4568.0	2520	1382.2	8222.0	4550	2510.0
795.2	424	217.78	1454.0	790	421.11	3020.0	1660	904.44	4586.0	2530	1387.8	8312.0	4600	2537.7
798.8	426	218.89	1472.0	800	426.67	3038.0	1670	910.00	4604.0	2540	1393.3	8402.0	4650	2565.5
802.4	428	220.00	1490.0	810	432.22	3056.0	1680	915.56	4622.0	2550	1398.9	8492.0	4700	2593.3
806.0	430	221.11	1508.0	820	437.78	3074.0	1690	921.11	4640.0	2560	1404.4	8582.0	4750	2621.1
809.6	432	222.22	1526.0	830	443.33	3092.0	1700	926.67	4658.0	2570	1410.0	8672.0	4800	2648.8
813.2	434	223.33	1544.0	840	448.89	3110.0	1710	932.22	4676.0	2580	1415.6	8762.0	4850	2676.6
816.8	436	224.44	1562.0	850	454.44	3128.0	1720	937.78	4694.0	2590	1421.1	8852.0	4900	2704.4
820.4	438	225.56	1580.0	860	460.00	3146.0	1730	943.33	4712.0	2600	1426.7	8942.0	4950	2732.2
824.0	440	226.67	1598.0	870	465.56	3164.0	1740	948.89	4730.0	2610	1432.2	9032.0	5000	2760.0
827.6	442	227.78	1616.0	880	471.11	3182.0	1750	954.44	4748.0	2620	1437.8	9122.0	5050	2787.7
831.2	444	228.89	1634.0	890	476.67	3200.0	1760	960.00	4766.0	2630	1443.3	9212.0	5100	2815.5
834.8	446	230.00	1652.0	900	482.22	3218.0	1770	965.56	4784.0	2640	1448.9	9302.0	5150	2843.3
838.4	448	231.11	1670.0	910	487.78	3236.0	1780	971.11	4802.0	2650	1454.4	9392.0	5200	2871.1
842.0	450	232.22	1688.0	920	493.33	3254.0	1790	976.67	4820.0	2660	1460.0	9482.0	5250	2898.8
845.6	452	233.33	1706.0	930	498.89	3272.0	1800	982.22	4838.0	2670	1465.6	9572.0	5300	2926.6
849.2	454	234.44	1724.0	940	504.44	3290.0	1810	987.78	4856.0	2680	1471.1	9662.0	5350	2954.4
852.8	456	235.56	1742.0	950	510.00	3308.0	1820	993.33	4874.0	2690	1476.7	9752.0	5400	2982.2
856.4	458	236.67	1760.0	960	515.56	3326.0	1830	998.89	4892.0	2700	1482.2	9842.0	5450	3010.0
860.0	460	237.78	1778.0	970	521.11	3344.0	1840	1004.4	4910.0	2710	1487.8	9932.0	5500	3037.7
863.6	462	238.89	1796.0	980	526.67	3362.0	1850	1010.0	4928.0	2720	1493.3	10022.0	5550	3065.5
867.2	464	240.00	1814.0	990	532.22	3380.0	1860	1015.6	4946.0	2730	1498.9	10112.0	5600	3093.3

Abbreviations

antiphase structure ..... APS
atomic percent ..... at.%
body-centered cubic ..... bcc
body-centered tetragonal ..... bct
boiling point ..... B.P.
Celsius ..... °C
close-packed hexagonal ..... cph
components ..... *c*
composition ..... *X*
Curie temperature ..... T_C
degree (Angular) ..... °
degrees of freedom ..... *f*
differential ..... d
edge length ..... *a*,*b*,*c*
enthalpy ..... *H*
entropy ..... *S*
face-centered cubic ..... fcc
Fahrenheit ..... °F
gas ..... G
Gibbs energy ..... *G*
gigapascal ..... GPa
greater than ..... >
heat capacity ..... *C*
heat energy ..... *Q*
high temperature ..... HT
increment (finite) ..... δ
increment (infinitesimally small) ..... Δ
interaxial angle ..... A, B, Γ
internal energy ..... *E*
Kelvin ..... K
kilobar ..... kbar
kilopascal ..... kPa
less than ..... <
liquid L
low temperature ..... LT
megapascal ..... MPa
melting point ..... M.P.
metallic element ..... M
nanometer ..... nm
percent ..... %
pressure ..... P
room temperature ..... RT
solid ..... S
stable phases ..... *p*
sublimation point ..... S.P.
temperature ..... *T*
transformation temperature ... A
triple point ..... T.P.
unknown ....
volume ..... *V*
weight percent ..... wt.%
work energy ..... *W*

Greek Alphabet

Greek letter	Name	English equivalent	Greek letter	Name	English equivalent	Greek letter	Name	English equivalent
A, α	Alpha	A, a	I, ι	Iota	I, i	P, ρ	Rho	R, r
B, β	Beta	B, b	K, κ	Kappa	K, k	Σ, σ	Sigma	S, s
Γ, γ	Gamma	G, g	Λ, λ	Lambda	L, l	T, τ	Tau	T, t
Δ, δ	Delta	D, d	M, μ	Mu	M, m	Y, υ	Upsilon	U, u
E, ε	Epsilon	E, e	N, ν	Nu	N, n	Φ, φ	Phi	Ph
Z, ζ	Zeta	Z, ζ	Ξ, ξ	Xi	X, x	X, χ	Chi	Ch
H, η	Eta	E, e	O, o	Omicron	O, o	Ψ, ψ	Psi	Ps
Θ, θ	Theta	Th	Π, π	Pi	P, p	Ω, ω	Omega	O, o

Au-Rb ..... 2•75
Au-Sb ..... 2•75
Au-Se ..... 2•76
Au-Si ..... 2•76
Au-Sn ..... 2•76
Au-Sr ..... 2•77
Au-Te ..... 2•77
Au-Th ..... 2•77
Au-Ti ..... 2•78
Au-Tl ..... 2•78
Au-U ..... 2•78
Au-V ..... 2•79
Au-Yb ..... 2•79
Au-Zn ..... 2•79
Au-Zr ..... 2•80
B-C ..... 2•80
B-C-Fe ..... 3•23-24
B-Co ..... 2•80
B-Cr ..... 2•81
B-Cu ..... 2•81
B-Fe ..... 2•81
B-Mn ..... 2•82
B-Mo ..... 2•82
B-Nb ..... 2•82
B-Ni ..... 2•83
B-Pd ..... 2•83
B-Pt ..... 2•83
B-Re ..... 2•84
B-Ru ..... 2•84
B-Sc ..... 2•84
B-Si ..... 2•85
B-Ta ..... 2•85
B-Ti ..... 2•85
B-V ..... 2•86
B-W ..... 2•86
B-Y ..... 2•86
B-Zr ..... 2•87
Ba-Ca ..... 2•87
Ba-Cd ..... 2•87
Ba-Cu ..... 2•88
Ba-Ga ..... 2•88
Ba-Ge ..... 2•88
Ba-H ..... 2•89
Ba-Hg ..... 2•89
Ba-In ..... 2•89
Ba-Li ..... 2•90
Ba-Mg ..... 2•90
Ba-Na ..... 2•90
Ba-P ..... 2•91
Ba-Pb ..... 2•91
Ba-Se ..... 2•91
Ba-Si ..... 2•92
Ba-Te ..... 2•92
Ba-Tl ..... 2•92
Ba-Zn ..... 2•93
Be-Co ..... 2•93
Be-Cr ..... 2•93
Be-Cu ..... 2•94
Be-Fe ..... 2•94
Be-Hf ..... 2•95
Be-Nb ..... 2•95
Be-Ni ..... 2•95
Be-Pd ..... 2•96
Be-Si ..... 2•96
Be-Th ..... 2•96
Be-Ti ..... 2•97
Be-W ..... 2•97
Be-Zr ..... 2•97
Bi-Ca ..... 2•98
Bi-Cd ..... 2•98
Bi-Cs ..... 2•98
Bi-Cu ..... 2•99
Bi-Ga ..... 2•99
Bi-Ge ..... 2•99
Bi-Hg ..... 2•100
Bi-In ..... 2•100
Bi-K ..... 2•100
Bi-La ..... 2•101
Bi-Li ..... 2•101
Bi-Mg ..... 2•101
Bi-Mn ..... 2•102
Bi-Na ..... 2•102
Bi-Nd ..... 2•102
Bi-Ni ..... 2•103
Bi-Pb ..... 2•103
Bi-Pd ..... 2•103
Bi-Pt ..... 2•104
Bi-Rb ..... 2•104
Bi-S ..... 2•104
Bi-Sb ..... 2•105
Bi-Se ..... 2•105
Bi-Sm ..... 2•106
Bi-Sn ..... 2•106
Bi-Sr ..... 2•106
Bi-Te ..... 2•107
Bi-Tl ..... 2•107
Bi-U ..... 2•107
Bi-Y ..... 2•108
Bi-Yb ..... 2•108
Bi-Zn ..... 2•108
Bi-Zr ..... 2•109
C-Co ..... 2•109
C-Cr ..... 2•109
C-Cr-Fe ..... 3•24-25
C-Cr-Mo ..... 3•25-26
C-Cr-N ..... 3•26
C-Cr-V ..... 3•26-27
C-Cr-W ..... 3•27
C-Cu ..... 2•110
C-Cu-Fe ..... 3•27-28
C-Fe ..... 2•110
C-Fe-Mn ..... 3•28-30
C-Fe-Mo ..... 3•30-31
C-Fe-N ..... 3•31-32
C-Fe-Ni ..... 3•32
C-Fe-Si ..... 3•33-34
C-Fe-V ..... 3•34
C-Fe-W ..... 3•35
C-Hf ..... 2•111
C-La ..... 2•111
C-Mn ..... 2•111
C-Mo ..... 2•112
C-Ni ..... 2•112
C-Pr ..... 2•112
C-Sc ..... 2•113
C-Si ..... 2•113
C-Ta ..... 2•113
C-Th ..... 2•114
C-Ti ..... 2•114
C-U ..... 2•114
C-V ..... 2•115
C-W ..... 2•115
C-Y ..... 2•115
C-Zr ..... 2•116
Ca-Cd ..... 2•116
Ca-Cu ..... 2•116
Ca-Ga ..... 2•117
Ca-Ge ..... 2•117
Ca-Hg ..... 2•117
Ca-In ..... 2•118
Ca-Li ..... 2•118
Ca-Mg ..... 2•118
Ca-Na ..... 2•119
Ca-Nd ..... 2•119
Ca-Ni ..... 2•119
Ca-O ..... 2•120
Ca-Pb ..... 2•120
Ca-Pd ..... 2•120
Ca-Pt ..... 2•121
Ca-Sb ..... 2•121
Ca-Si ..... 2•121
Ca-Sr ..... 2•122
Ca-Tl ..... 2•122
Ca-Yb ..... 2•122
Ca-Zn ..... 2•123
Cd-Cu ..... 2•123
Cd-Eu ..... 2•123
Cd-Ga ..... 2•124
Cd-Gd ..... 2•124
Cd-Ge ..... 2•124
Cd-Hg ..... 2•125
Cd-In ..... 2•125
Cd-La ..... 2•125
Cd-Li ..... 2•126
Cd-Mg ..... 2•126
Cd-Na ..... 2•126
Cd-Ni ..... 2•127
Cd-P ..... 2•127
Cd-Pb ..... 2•127
Cd-Sb ..... 2•128
Cd-Sb-Sn ..... 3•35-36
Cd-Se ..... 2•128
Cd-Sm ..... 2•128
Cd-Sn ..... 2•129
Cd-Sr ..... 2•129
Cd-Te ..... 2•129
Cd-Th ..... 2•130
Cd-Tl ..... 2•130
Cd-Y ..... 2•130
Cd-Yb ..... 2•131
Cd-Zn ..... 2•131
Ce-Co ..... 2•131
Ce-Cu ..... 2•132
Ce-Fe ..... 2•132
Ce-Ga ..... 2•133
Ce-Ge ..... 2•133
Ce-In ..... 2•133
Ce-Ir ..... 2•134
Ce-Mg ..... 2•134
Ce-Mn ..... 2•134
Ce-Ni ..... 2•135
Ce-O ..... 2•135
Ce-Pd ..... 2•135
Ce-Pu ..... 2•136
Ce-S ..... 2•136
Ce-Si ..... 2•136
Ce-Sn ..... 2•137
Ce-Te ..... 2•137
Ce-Ti ..... 2•137
Ce-Tl ..... 2•138
Ce-Zn ..... 2•138
Cl-Cs ..... 2•138
Cl-Ga ..... 2•139
Cl-Hg ..... 2•139
Cl-In ..... 2•139
Cl-Na ..... 2•140
Co-Cr ..... 2•140
Co-Cr-Fe ..... 3•36-37
Co-Cr-Ni ..... 3•37
Co-Cr-Ti ..... 3•38
Co-Cr-W ..... 3•38
Co-Cu ..... 2•140
Co-Dy ..... 2•141
Co-Er ..... 2•141
Co-Fe ..... 2•141
Co-Fe-Mo ..... 3•38-39

Co-Fe-Ni ..... 3•39-40
Co-Fe-W ..... 3•40-41
Co-Ga ..... 2•142
Co-Gd ..... 2•142
Co-Ge ..... 2•142
Co-Hf ..... 2•143
Co-Ho ..... 2•143
Co-Mn ..... 2•143
Co-Mo ..... 2•144
Co-Mo-Ni ..... 3•41
Co-Nb ..... 2•144
Co-Nd ..... 2•144
Co-Ni ..... 2•145
Co-Ni-Ti ..... 3•41
Co-P ..... 2•145
Co-Pd ..... 2•145
Co-Pr ..... 2•146
Co-Pt ..... 2•146
Co-Pu ..... 2•146
Co-Re ..... 2•147
Co-S ..... 2•147
Co-Sb ..... 2•147
Co-Se ..... 2•148
Co-Si ..... 2•148
Co-Sm ..... 2•148
Co-Sn ..... 2•149
Co-Ta ..... 2•149
Co-Tb ..... 2•149
Co-Te ..... 2•150
Co-Th ..... 2•150
Co-Ti ..... 2•150
Co-V ..... 2•151
Co-W ..... 2•151
Co-Y ..... 2•151
Co-Zn ..... 2•152
Cr-Cu ..... 2•152
Cr-Fe ..... 2•152
Cr-Fe-Mo ..... 3•42
Cr-Fe-N ..... 3•43
Cr-Fe-Ni ..... 3•43-44
Cr-Fe-W ..... 3•45
Cr-Ga ..... 2•153
Cr-Ge ..... 2•153
Cr-Hf ..... 2•153
Cr-Ir ..... 2•154
Cr-Lu ..... 2•154
Cr-Mn ..... 2•154
Cr-Mo ..... 2•155
Cr-Mo-Ni ..... 3•45
Cr-Mo-W ..... 3•46
Cr-Nb ..... 2•155
Cr-Nb-Ni ..... 3•46-47
Cr-Nb-W ..... 3•47
Cr-Ni ..... 2•155
Cr-Ni-Ti ..... 3•47-48
Cr-Ni-W ..... 3•48
Cr-O ..... 2•156
Cr-Os ..... 2•156
Cr-Pd ..... 2•156
Cr-Pt ..... 2•157
Cr-Re ..... 2•157
Cr-Rh ..... 2•157
Cr-Ru ..... 2•158
Cr-S ..... 2•158
Cr-Sb ..... 2•158
Cr-Sc ..... 2•159
Cr-Se ..... 2•159
Cr-Si ..... 2•160
Cr-Sn ..... 2•160
Cr-Ta ..... 2•160
Cr-Te ..... 2•161
Cr-Ti ..... 2•161
Cr-Ti-W ..... 3•49
Cr-U ..... 2•161
Cr-V ..... 2•162
Cr-W ..... 2•162
Cr-Zr ..... 2•162
Cs-Ge ..... 2•163
Cs-Hg ..... 2•163
Cs-In ..... 2•163
Cs-K ..... 2•164
Cs-Na ..... 2•164
Cs-O ..... 2•164
Cs-Rb ..... 2•165
Cs-S ..... 2•165
Cs-Sb ..... 2•165
Cs-Se ..... 2•166
Cs-Sn ..... 2•166
Cs-Te ..... 2•166
Cs-Tl ..... 2•167
Cu-Dy ..... 2•167
Cu-Er ..... 2•167
Cu-Eu ..... 2•168
Cu-Fe ..... 2•168
Cu-Fe-Ni ..... 3•49-50
Cu-Ga ..... 2•168
Cu-Gd ..... 2•169
Cu-Ge ..... 2•169
Cu-H ..... 2•169
Cu-Hf ..... 2•170
Cu-Hg ..... 2•170
Cu-In ..... 2•170
Cu-Ir ..... 2•171
Cu-La ..... 2•171
Cu-Li ..... 2•171
Cu-Mg ..... 2•172
Cu-Mn ..... 2•172
Cu-Nb ..... 2•172
Cu-Nd ..... 2•173
Cu-Ni ..... 2•173
Cu-Ni-Sn ..... 3•50
Cu-Ni-Zn ..... 3•51
Cu-O ..... 2•174
Cu-P ..... 2•174
Cu-Pb ..... 2•175
Cu-Pb-Zn ..... 3•51-52
Cu-Pd ..... 2•175
Cu-Pt ..... 2•175
Cu-Pu ..... 2•176
Cu-Rh ..... 2•176
Cu-S ..... 2•176
Cu-Sb ..... 2•177
Cu-Sb-Sn ..... 3•52
Cu-Se ..... 2•178
Cu-Si ..... 2•178
Cu-Sn ..... 2•178
Cu-Sn-Zn ..... 3•52
Cu-Sr ..... 2•179
Cu-Te ..... 2•179
Cu-Th ..... 2•180
Cu-Ti ..... 2•180
Cu-Tl ..... 2•181
Cu-V ..... 2•181
Cu-Yb ..... 2•181
Cu-Zn ..... 2•182
Cu-Zr ..... 2•182
Dy-Fe ..... 2•182
Dy-Ga ..... 2•183
Dy-Ge ..... 2•183
Dy-In ..... 2•183
Dy-Mn ..... 2•184
Dy-Ni ..... 2•184
Dy-Pb ..... 2•184
Dy-Pd ..... 2•185
Dy-S ..... 2•185
Dy-Sb ..... 2•185
Dy-Sn ..... 2•186
Dy-Te ..... 2•186
Dy-Tl ..... 2•186
Dy-Zr ..... 2•187
Er-Fe ..... 2•187
Er-Ga ..... 2•187
Er-Ge ..... 2•188
Er-In ..... 2•188
Er-Mn ..... 2•188
Er-Ni ..... 2•189
Er-Pd ..... 2•189
Er-Pt ..... 2•189
Er-Ru ..... 2•190
Er-Se ..... 2•190
Er-Te ..... 2•190
Er-Ti ..... 2•191
Er-Tl ..... 2•191
Eu-Ga ..... 2•191
Eu-Ge ..... 2•192
Eu-In ..... 2•192
Eu-Mg ..... 2•192
Eu-Pb ..... 2•193
Eu-Pd ..... 2•193
Eu-Pt ..... 2•193
Eu-Te ..... 2•194
Fe-Ga ..... 2•194
Fe-Gd ..... 2•194
Fe-Ge ..... 2•195
Fe-H ..... 2•195
Fe-Hf ..... 2•195
Fe-Ho ..... 2•196
Fe-Ir ..... 2•196
Fe-La ..... 2•196
Fe-Lu ..... 2•197
Fe-Mn ..... 2•197
Fe-Mn-Ni ..... 3•53
Fe-Mo ..... 2•197
Fe-Mo-Nb ..... 3•53-54
Fe-Mo-Ni ..... 3•54-55
Fe-N ..... 2•198
Fe-Nb ..... 2•198
Fe-Nd ..... 2•198
Fe-Ni ..... 2•199
Fe-Ni-W ..... 3•55
Fe-O ..... 2•199
Fe-P ..... 2•200
Fe-Pd ..... 2•200
Fe-Pu ..... 2•200
Fe-Rh ..... 2•201
Fe-S ..... 2•201
Fe-Sb ..... 2•202
Fe-Sc ..... 2•202
Fe-Se ..... 2•202
Fe-Si ..... 2•203
Fe-Sm ..... 2•203
Fe-Sn ..... 2•203
Fe-Tb ..... 2•204
Fe-Te ..... 2•204
Fe-Th ..... 2•204
Fe-Ti ..... 2•205
Fe-Tm ..... 2•205
Fe-U ..... 2•205
Fe-V ..... 2•206
Fe-W ..... 2•206
Fe-Zn ..... 2•206
Fe-Zr ..... 2•207
Ga-Gd ..... 2•207
Ga-Ho ..... 2•207
Ga-In ..... 2•208
Ga-La ..... 2•208

Ga-Li ..... 2•208
Ga-Lu ..... 2•209
Ga-Mg ..... 2•209
Ga-Mn ..... 2•209
Ga-Mo ..... 2•210
Ga-Na ..... 2•210
Ga-Nb ..... 2•210
Ga-Nd ..... 2•211
Ga-Ni ..... 2•211
Ga-Pb ..... 2•211
Ga-Pd ..... 2•212
Ga-Pr ..... 2•212
Ga-Pt ..... 2•212
Ga-Pu ..... 2•213
Ga-S ..... 2•213
Ga-Sb ..... 2•214
Ga-Sc ..... 2•214
Ga-Se ..... 2•214
Ga-Sm ..... 2•215
Ga-Sn ..... 2•215
Ga-Sr ..... 2•215
Ga-Tb ..... 2•216
Ga-Te ..... 2•216
Ga-Tl ..... 2•216
Ga-Tm ..... 2•217
Ga-U ..... 2•217
Ga-V ..... 2•217
Ga-Y ..... 2•218
Ga-Yb ..... 2•218
Ga-Zn ..... 2•218
Ga-Zr ..... 2•219
Gd-Ge ..... 2•219
Gd-In ..... 2•219
Gd-Mg ..... 2•220
Gd-Mn ..... 2•220
Gd-Ni ..... 2•220
Gd-Pb ..... 2•221
Gd-Pd ..... 2•221
Gd-Rh ..... 2•221
Gd-Sb ..... 2•222
Gd-Se ..... 2•222
Gd-Sn ..... 2•222
Gd-Te ..... 2•223
Gd-Ti ..... 2•223
Gd-Tl ..... 2•223
Ge-Ho ..... 2•224
Ge-In ..... 2•224
Ge-K ..... 2•224
Ge-La ..... 2•225
Ge-Li ..... 2•225
Ge-Lu ..... 2•225
Ge-Mg ..... 2•226
Ge-Mn ..... 2•226
Ge-Mo ..... 2•227
Ge-Na ..... 2•227
Ge-Nb ..... 2•227
Ge-Nd ..... 2•228
Ge-Ni ..... 2•228
Ge-P ..... 2•228
Ge-Pb ..... 2•229
Ge-Pd ..... 2•229
Ge-Pr ..... 2•229
Ge-Pt ..... 2•230
Ge-S ..... 2•230
Ge-Sb ..... 2•230
Ge-Sc ..... 2•231
Ge-Se ..... 2•231
Ge-Si ..... 2•231
Ge-Sm ..... 2•232
Ge-Sn ..... 2•232
Ge-Sr ..... 2•232
Ge-Tb ..... 2•233
Ge-Te ..... 2•233
Ge-Ti ..... 2•233
Ge-Tl ..... 2•234
Ge-Tm ..... 2•234
Ge-U ..... 2•234
Ge-Y ..... 2•235
Ge-Yb ..... 2•235
Ge-Zn ..... 2•235
H-La ..... 2•236
H-Nb ..... 2•236
H-Nd ..... 2•237
H-Ni ..... 2•237
H-Pd ..... 2•237
H-Sr ..... 2•238
H-Ta ..... 2•238
H-Ti ..... 2•238
H-U ..... 2•239
H-V ..... 2•239
H-Zr ..... 2•239
Hf-Ir ..... 2•240
Hf-Mn ..... 2•240
Hf-Mo ..... 2•240
Hf-N ..... 2•241
Hf-Nb ..... 2•241
Hf-Ni ..... 2•241
Hf-O ..... 2•242
Hf-Os ..... 2•242
Hf-Rh ..... 2•242
Hf-Si ..... 2•243
Hf-Ta ..... 2•243
Hf-U ..... 2•243
Hf-V ..... 2•244
Hf-W ..... 2•244
Hf-Zr ..... 2•244
Hg-In ..... 2•245
Hg-K ..... 2•245
Hg-La ..... 2•245
Hg-Li ..... 2•246
Hg-Mg ..... 2•246
Hg-Na ..... 2•246
Hg-Pb ..... 2•247
Hg-Rb ..... 2•247
Hg-S ..... 2•247
Hg-Se ..... 2•248
Hg-Sn ..... 2•248
Hg-Sr ..... 2•248
Hg-Te ..... 2•249
Hg-Tl ..... 2•249
Hg-Zn ..... 2•249
Ho-In ..... 2•250
Ho-Mn ..... 2•250
Ho-Pd ..... 2•250
Ho-Sb ..... 2•251
Ho-Te ..... 2•251
Ho-Tl ..... 2•251
In-K ..... 2•252
In-La ..... 2•252
In-Li ..... 2•252
In-Lu ..... 2•253
In-Mg ..... 2•253
In-Mn ..... 2•253
In-Na ..... 2•254
In-Nb ..... 2•254
In-Nd ..... 2•254
In-Ni ..... 2•255
In-P ..... 2•255
In-Pb ..... 2•255
In-Pd ..... 2•256
In-Pr ..... 2•256
In-Pt ..... 2•256
In-Pu ..... 2•257
In-Rb ..... 2•257
In-S ..... 2•257
In-Sb ..... 2•258
In-Sc ..... 2•258
In-Se ..... 2•259
In-Si ..... 2•259
In-Sm ..... 2•260
In-Sn ..... 2•260
In-Sr ..... 2•260
In-Tb ..... 2•261
In-Te ..... 2•261
In-Th ..... 2•261
In-Ti ..... 2•262
In-Tl ..... 2•262
In-Tm ..... 2•262
In-V ..... 2•263
In-Y ..... 2•263
In-Yb ..... 2•263
In-Zn ..... 2•264
Ir-La ..... 2•264
Ir-Mo ..... 2•264
Ir-Nb ..... 2•265
Ir-Ni ..... 2•265
Ir-Pd ..... 2•265
Ir-Pt ..... 2•266
Ir-Rh ..... 2•266
Ir-Ru ..... 2•266
Ir-Ta ..... 2•267
Ir-Th ..... 2•267
Ir-Ti ..... 2•267
Ir-U ..... 2•268
Ir-V ..... 2•268
Ir-W ..... 2•268
Ir-Zr ..... 2•269
K-Na ..... 2•269
K-Pb ..... 2•269
K-Rb ..... 2•270
K-S ..... 2•270
K-Sb ..... 2•270
K-Se ..... 2•271
K-Sn ..... 2•271
K-Te ..... 2•271
K-Tl ..... 2•272
La-Mg ..... 2•272
La-Mn ..... 2•272
La-Ni ..... 2•273
La-Pb ..... 2•273
La-S ..... 2•273
La-Sb ..... 2•274
La-Sc ..... 2•274
La-Se ..... 2•274
La-Sn ..... 2•275
La-Tl ..... 2•275
La-Zn ..... 2•275
Li-Mg ..... 2•276
Li-Na ..... 2•276
Li-Pb ..... 2•276
Li-Pd ..... 2•277
Li-S ..... 2•277
Li-Se ..... 2•277
Li-Si ..... 2•278
Li-Sn ..... 2•278
Li-Sr ..... 2•278
Li-Te ..... 2•279
Li-Tl ..... 2•279
Li-Zn ..... 2•279
Lu-Pb ..... 2•280
Lu-Tl ..... 2•280
Mg-Mn ..... 2•280
Mg-Ni ..... 2•281
Mg-Pb ..... 2•281
Mg-Sb ..... 2•281
Mg-Sc ..... 2•282

Mg-Si ... 2•282
Mg-Sm ... 2•282
Mg-Sn ... 2•283
Mg-Sr ... 2•283
Mg-Th ... 2•283
Mg-Tl ... 2•284
Mg-Y ... 2•284
Mg-Yb ... 2•284
Mg-Zn ... 2•285
Mg-Zr ... 2•285
Mn-Mo ... 2•285
Mn-N ... 2•286
Mn-Nd ... 2•286
Mn-Ni ... 2•286
Mn-O ... 2•287
Mn-P ... 2•287
Mn-Pd ... 2•287
Mn-Pr ... 2•288
Mn-Pu ... 2•288
Mn-Sb ... 2•288
Mn-Si ... 2•289
Mn-Sm ... 2•289
Mn-Sn ... 2•289
Mn-Ti ... 2•290
Mn-U ... 2•290
Mn-V ... 2•290
Mn-Y ... 2•291
Mn-Zn ... 2•291
Mn-Zr ... 2•291
Mo-N ... 2•292
Mo-Nb ... 2•292
Mo-Nb-Ti ... 3•56
Mo-Ni ... 2•292
Mo-Ni-Ti ... 3•56
Mo-Ni-W ... 3•56
Mo-O ... 2•293
Mo-Os ... 2•293
Mo-P ... 2•293
Mo-Pd ... 2•294
Mo-Pt ... 2•294
Mo-Pu ... 2•294
Mo-Rh ... 2•295
Mo-Ru ... 2•295
Mo-S ... 2•295
Mo-Si ... 2•296
Mo-Ta ... 2•296
Mo-Ti ... 2•296
Mo-Ti-W ... 3•57
Mo-U ... 2•297
Mo-V ... 2•297
Mo-W ... 2•297
Mo-Zr ... 2•298
N-Nb ... 2•298
N-Ni ... 2•298
N-Ta ... 2•299
N-Th ... 2•299
N-Ti ... 2•299
N-U ... 2•300
N-Zr ... 2•300
Na-O ... 2•300
Na-Pb ... 2•301
Na-Rb ... 2•301
Na-S ... 2•301
Na-Sb ... 2•302
Na-Se ... 2•302
Na-Sn ... 2•302
Na-Sr ... 2•303
Na-Te ... 2•303
Na-Tl ... 2•303
Nb-Ni ... 2•304
Nb-Os ... 2•304
Nb-Pd ... 2•304
Nb-Pt ... 2•305
Nb-Rh ... 2•305
Nb-Ru ... 2•305
Nb-Si ... 2•306
Nb-Ta ... 2•306
Nb-Th ... 2•306
Nb-Ti ... 2•307
Nb-Ti-W ... 3•57
Nb-U ... 2•307
Nb-V ... 2•307
Nb-W ... 2•308
Nb-Zr ... 2•308
Nd-Ni ... 2•308
Nd-Pt ... 2•309
Nd-Rh ... 2•309
Nd-Sb ... 2•309
Nd-Si ... 2•310
Nd-Sn ... 2•310
Nd-Te ... 2•310
Nd-Ti ... 2•311
Nd-Tl ... 2•311
Nd-Zn ... 2•311
Ni-O ... 2•312
Ni-Os ... 2•312
Ni-P ... 2•313
Ni-Pb ... 2•313
Ni-Pd ... 2•314
Ni-Pr ... 2•314
Ni-Pt ... 2•314
Ni-Pu ... 2•315
Ni-Re ... 2•315
Ni-Rh ... 2•316
Ni-Ru ... 2•316
Ni-S ... 2•316
Ni-Sb ... 2•317
Ni-Sc ... 2•317
Ni-Se ... 2•317
Ni-Si ... 2•318
Ni-Sm ... 2•318
Ni-Sn ... 2•318
Ni-Ta ... 2•319
Ni-Te ... 2•319
Ni-Ti ... 2•319
Ni-U ... 2•320
Ni-V ... 2•320
Ni-W ... 2•320
Ni-Y ... 2•321
Ni-Yb ... 2•321
Ni-Zn ... 2•321
Ni-Zr ... 2•322
Np-Pu ... 2•322
Np-U ... 2•322
O-Pb ... 2•323
O-Pr ... 2•323
O-Pu ... 2•323
O-Sn ... 2•324
O-Ti ... 2•324
O-V ... 2•325
O-W ... 2•325
O-Y ... 2•326
O-Zr ... 2•326
Os-Pt ... 2•326
Os-Pu ... 2•327
Os-Re ... 2•327
Os-Rh ... 2•327
Os-Ru ... 2•328
Os-Si ... 2•328
Os-Ti ... 2•328
Os-U ... 2•329
Os-V ... 2•329
Os-W ... 2•329
Os-Zr ... 2•330
P-Pd ... 2•330
P-Pr ... 2•330
P-Ru ... 2•331
P-Sn ... 2•331
P-Ti ... 2•331
P-Zn ... 2•332
Pb-Pd ... 2•332
Pb-Pr ... 2•332
Pb-Pt ... 2•333
Pb-Pu ... 2•333
Pb-Rb ... 2•333
Pb-Rh ... 2•334
Pb-S ... 2•334
Pb-Sb ... 2•334
Pb-Sb-Sn ... 3•57-58
Pb-Se ... 2•335
Pb-Sn ... 2•335
Pb-Sn-Zn ... 3•58
Pb-Sr ... 2•335
Pb-Te ... 2•336
Pb-Tl ... 2•336
Pb-Y ... 2•336
Pb-Yb ... 2•337
Pb-Zn ... 2•337
Pd-Pt ... 2•337
Pd-Pu ... 2•338
Pd-Rh ... 2•338
Pd-Ru ... 2•338
Pd-S ... 2•339
Pd-Sb ... 2•339
Pd-Se ... 2•339
Pd-Si ... 2•340
Pd-Sm ... 2•340
Pd-Sn ... 2•340
Pd-Te ... 2•341
Pd-Ti ... 2•341
Pd-Tl ... 2•342
Pd-U ... 2•342
Pd-V ... 2•342
Pd-W ... 2•343
Pd-Y ... 2•343
Pd-Yb ... 2•343
Pd-Zn ... 2•344
Pr-Sb ... 2•344
Pr-Se ... 2•344
Pr-Si ... 2•345
Pr-Sn ... 2•345
Pr-Te ... 2•345
Pr-Tl ... 2•346
Pr-Zn ... 2•346
Pt-Rh ... 2•346
Pt-Si ... 2•347
Pt-Sn ... 2•347
Pt-Te ... 2•347
Pt-Ti ... 2•348
Pt-Tl ... 2•348
Pt-U ... 2•348
Pt-V ... 2•349
Pt-Zr ... 2•349
Pu-Sc ... 2•349
Pu-U ... 2•350
Pu-Zn ... 2•350
Pu-Zr ... 2•350
Rb-Sb ... 2•351
Rb-Se ... 2•351
Rb-Tl ... 2•351
Re-Ru ... 2•352
Re-Si ... 2•352
Re-Te ... 2•352
Re-U ... 2•353
Re-V ... 2•353
Rh-Se ... 2•353

Rh-Ta ..... 2•354
Rh-Ti ..... 2•354
Rh-U ..... 2•354
Rh-V ..... 2•355
Ru-Si ..... 2•355
Ru-Ta ..... 2•355
Ru-Ti ..... 2•356
Ru-U ..... 2•356
Ru-V ..... 2•356
S-Se ..... 2•357
S-Sn ..... 2•357
S-Te ..... 2•358
S-Ti ..... 2•358
Sb-Se ..... 2•358
Sb-Si ..... 2•359
Sb-Sm ..... 2•359
Sb-Sn ..... 2•359
Sb-Sr ..... 2•360
Sb-Tb ..... 2•360
Sb-Te ..... 2•360
Sb-Tl ..... 2•361
Sb-U ..... 2•361
Sb-Y ..... 2•361
Sb-Zn ..... 2•362
Sc-Ti ..... 2•362
Sc-Y ..... 2•362
Sc-Zr ..... 2•363
Se-Sn ..... 2•363
Se-Sr ..... 2•363
Se-Te ..... 2•364
Se-Tl ..... 2•364
Se-Tm ..... 2•364
Se-U ..... 2•365
Si-Sn ..... 2•365
Si-Sr ..... 2•365
Si-Ta ..... 2•366
Si-Te ..... 2•366
Si-Th ..... 2•366
Si-Ti ..... 2•367
Si-U ..... 2•367
Si-V ..... 2•367
Si-Zn ..... 2•368
Si-Zr ..... 2•368
Sm-Sn ..... 2•368
Sm-Tl ..... 2•369
Sm-Zn ..... 2•369
Sn-Te ..... 2•370
Sn-Ti ..... 2•370
Sn-Tl ..... 2•370
Sn-U ..... 2•371
Sn-Y ..... 2•371
Sn-Yb ..... 2•371
Sn-Zn ..... 2•372
Sn-Zr ..... 2•369
Sn-Zr ..... 2•372
Sr-Te ..... 2•372
Sr-Tl ..... 2•373
Sr-Zn ..... 2•373
Ta-Th ..... 2•373
Ta-Ti ..... 2•374
Ta-U ..... 2•374
Ta-V ..... 2•374
Ta-W ..... 2•375
Ta-Zr ..... 2•375
Tb-Tl ..... 2•375
Te-Tl ..... 2•376
Te-U ..... 2•376
Te-Yb ..... 2•376
Te-Zn ..... 2•377
Th-Ti ..... 2•377
Th-Tl ..... 2•377
Th-Zn ..... 2•378
Th-Zr ..... 2•378
Ti-U ..... 2•378
Ti-V ..... 2•379
Ti-W ..... 2•379
Ti-Y ..... 2•379
Ti-Zr ..... 2•380
Tl-Yb ..... 2•380
Tl-Zn ..... 2•380
U-Zr ..... 2•381
V-W ..... 2•381
V-Zr ..... 2•381
W-Zr ..... 2•382
Y-Zn ..... 2•382
Y-Zr ..... 2•382
Yb-Zn ..... 2•383

Subject Index

A

Acicular eutectic microstructure ..... 1•19, 20
Age hardening
  development of ..... 1•25
  process ..... 1•22
Allotropy ..... 1•1
Alloy design use of phase diagrams in .. 1•25-26
Alpha stabilizers in titanium ..... 1•23
Aluminum housings eliminating cracks in . 1•28
Aluminum-alloy microstructures
aluminum-33% copper ..... 1•19
aluminum-silicon ..... 1•19,20
aluminum-18% silver ..... 1•22
Aluminum phase diagrams, discussion of
  aluminum-bismuth ..... 1•28
  aluminum-copper ..... 1•22,23
  aluminum-gold ..... 1•28,29
  aluminum-iron ..... 1•26,27
  aluminum-lead ..... 1•28
Aluminum-copper system ..... 1•22-23
Anorthic crystal system ..... 1• 10, 15
Austenite ..... 1•23
  stabilizers ..... 1•25
Austenitic stainless steels, new alloy development ..... 1•26

B

Base-centered space lattice ..... 1•15
Beta stabilizers in titanium ..... 1•23
Binary alloy phase diagrams ..... 2•25-383
Binary alloys index ..... 2•5-21
Binary system or diagram description ..... 1•2-4
Bivariant equilibrium ..... 1•2
Body-centered space-lattice ..... 1•15
Brasses ..... 1•22
Bravais lattice ..... 1•10
Burning ..... 1•19

C

Carbide cutting tools, eliminating brittleness of ..... 1•28
Carbides in steels ..... 1•24
Cartridge brass
Cast irons ..... 1•23-24, 26
Catatectic reaction ..... 1•5
Cementite ..... 1•23
Chinese script ..... 1•19, 20
Clapeyron, Benoit ..... 1•8
Clausius, Rudolf ..... 1•7, 8
Clausius-Clapeyron equation ..... 1•8,10
Closed thermodynamic system ..... 1•5
Cobalt-12% iron-6% titanium alloy, microstructure of ..... 1•22
Cobalt-tungsten-carbon phase diagram ..... 1•29
Components of a system ..... 1•2
Composition conversion ..... 1•18
Composition scales ..... 1•18
Congruent phase change ..... 1•4
Congruent phase transformation ..... 1•4, 10
Congruent point ..... 1•10
Conjugate phases ..... 1•3
Constitutional diagram ..... 1•2
Continuous solid solution ..... 1•2, 18
Cooling curves ..... 1•15, 16, 17
Copper alloys, microstructure of specific types
  C23000 ..... 1•22, 23
  C24000 ..... 1•22, 23
  C26000 ..... 1•22, 23
  C27000 ..... 1•22, 23
  C28000 ..... 1•22, 23
  C71500 ..... 1•18
Copper nickel, 30%, microstructure of ..... 1•18
Copper-zinc phase diagram ..... 1•22
Copper-zinc system ..... 1•22
Coring ..... 1•18, 19
Critical point ..... 1•2
Crystal
  description ..... 1•10
  dimensions ..... 1•10-15
  ordering ..... 1•10
  properties, use in phase-diagram determination ..... 1•17-18
  structure ..... 1•10-17
  systems ..... 1•10
Crystal-structure
  nomenclature ..... 1•15-16
  prototypes ..... 1•16
Cubic crystal system ..... 1•10, 15
Cutting tools, eliminating brittleness of carbide ..... 1•28

D

Decinary system or diagram ..... 1•2
Degrees of freedom ..... 1•2
Dendrites ..... 1•19
Dendritic
  microstructure ..... 1•20
  segregation ..... 1•18, 19
Differential thermal analysis ..... 1•17
Disordered crystal structure ..... 1•10
Ductile cast iron, grade 60-40-12, microstructure of ..... 1•26
Duralumin alloys ..... 1•25

E

Edge length of a crystal ..... 1•10
Electric-motor housings, eliminating cracks in ..... 1•28
Electronics, eliminating the "purple plague" ..... 1•28
End-centered space lattice ..... 1•15
Enthalpy ..... 1•6
Entropy ..... 1•7
Equilibrium ..... 1•1
  diagram ..... 1•2
Eutectic
  alloys ..... 1•3
  microstructures ..... 1•19-20
  reaction ..... 1•3, 5
  soft solder ..... 1•20
Eutectoid
  microstructures ..... 1•20-21
  reaction ..... 1•5

F

Face-centered space lattice ..... 1•15
Ferrite ..... 1•23
  stabilizers ..... 1•25
Filigreed eutectic microstructure ..... 1•20
First Law of Thermodynamics ..... 1•6
First-order phase transition ..... 1•10
Freezing curves ..... 1•16

G

Gibbs energy ..... 1•7, 8
  curves ..... 1•6, 7, 10
Gibbs, J. Willard ..... 1•2, 10
Gibbs-Konovalov Rule ..... 1•8, 10
Gibbs phase rule ..... 1•2
Globular eutectic microstructure ..... 1•19, 20
Gray cast iron, class 30, microstructure of 1•26
Guinier-Preston zones ..... 1•21

H

Hack-saw blades, development of welding technique ..... 1•26-27
Hardfacing, alloy improvement ..... 1•27
Heat capacity ..... 1•6
Heat content ..... 1•6
Heating elements, improving performance of ..... 1•27-28
Helmholtz, Hermann von ..... 1•6
Hexagonal crystal system ..... 1•10, 15
Higher-order phase transition ..... 1•10
Horizontal sections of a ternary diagram ..... 1•5

Hot short ..... 1•19
Housings, eliminating cracks in ..... •28
Hypereutectic alloys ..... 1•3
Hypereutectoid alloys ..... 1•21
Hypoeutectic alloys ..... 1•3
Hypoeutectoid alloys ..... 1•21

I

Idiomorphic particles ..... 1•20
Incongruent phase change ..... 1•4
Indium-tin alloy (50-50) ..... 1•19
Interaxial angle of a crystal ..... 1•10
Intermediate phases ..... 1•4
Intermetallic compounds ..... 1•4
Internal energy ..... 1•5
Intersection of phase-field boundaries .... 1•8, 10
Interstitial solid solution ..... 1•15, 16
Invariant
equilibrium ..... 1•2
point ..... 1•2
reactions ..... 1•5
Iron-alloy microstructures
iron-0.8% carbon ..... 1•21
iron-24.8% zinc ..... 1•22
Iron-carbon
phase diagram ..... 1•25
system ..... 1•23-25
transformation temperatures ..... 1•24, 25
Iron-cementite
phase diagram ..... 1•25
system ..... 1•23-25
transformation temperatures ..... 1•24, 25
Iron-chromium-nickel system ..... 1•25
Iron phase diagrams, discussion of
iron-chromium ..... 1•26
iron-chromium-nickel ..... 1•27
iron-manganese ..... 1•27
iron-manganese-carbon ..... 1•27
iron-nickel ..... 1•26
Irreversible process ..... 1•7
Isopleths of a ternary phase diagram ..... 1•5
Isothermal contour lines ..... 1•5
Isothermal sections of a ternary diagram ..... 1•5

J

Joule, James ..... 1•6

K

Kelvin, Lord ..... 1•7
Konovalov, Dmitry ..... 1•10

L

Lamellar eutectic microstructure ..... 1•19, 20
Lattice constants ..... 1•10
Lattice parameters ..... 1•10
Lattice points ..... 1•15
Law of Conservation of Energy ..... 1•6
Le Châtelier, Henri ..... 1•7
Ledeburite ..... 1•24
Lever rule ..... 1•17, 18-19
Line compounds ..... 1•4, 18
Liquation ..... 1•19
Liquidus ..... 1•2
Long-period ordering ..... 1•11
Low brass, 80%, microstructure of ..... 1•22

M

Magnesium-37% tin alloy, microstructure of ..... 1•19
Muntz metal, 60%, microstructure of ..... 1•22
Mayer, Julius von ..... 1•6
Melting curves ..... 1•2, 16
Metallography, use in phase-diagram determination ..... 1•18
Metastable
equilibrium ..... 1•1, 4
phases ..... 1•1
Metatectic reaction ..... 1•5
Miscible solids ..... 1•2
Miscibility ..... 1•2
Mixtures ..... 1•8
Monoclinic crystal system ..... 1•10, 15
Monotectic reaction ..... 1•5
Monotectoid reaction ..... 1•5
Monovariant equilibrium ..... 1•2

N

Nernst, Walter ..... 1•7
Nichrome heating elements, improving life of ..... 1•27-28
Nickel-base hardfacing alloy, improving ... 1•27
Nickel-20% chromium-1% aluminum alloy, microstructure of ..... 1•22
Nickel-chromium-iron heating elements, improving life of ..... 1•27-28
Nickel-sulfur phase diagram ..... 1•27
Nodular eutectic microstructure ..... 1•20
Nonary system or diagram ..... 1•2

O

Octanary system or diagram ..... 1•2
Ordered crystal structure ..... 1•10
Ordered structure ..... 1•10
Orthorhombic crystal system ..... 1•10, 15

P

Pearlite ..... 1•21
Pearson, William B ..... 1•15
Pearson symbols ..... 1•15
Performance, Use of phase diagrams to improve ..... 1•27-28
Peritectic reaction ..... 1•5
Peritectoid reaction ..... 1•5
Permanent magnets, alloy development of 1•26
Phases ..... 1•1
Phase-field-boundary
curvatures ..... 1•9, 10
extensions ..... 1•3, 4
intersections ..... 1•8, 10
Phase diagrams
construction errors ..... 1•9, 1-0
description ..... 1•2
determination ..... 1•17-18
features ..... 1•7-10
lines and labels ..... 1•18
reading of ..... 1•18-22
Phase field
description ..... 1•2
rule ..... 1•7
Phase-fraction lines ..... 1•17, 19
Phase rule
description ..... 1•2
violations ..... 1•9, 10
Physical properties, use in phase-diagram determination ..... 1•18
Planck, Max ..... 1•7
Polymorphism ..... 1•1
Precipitation hardening ..... 1•22
Pressure-temperature phase diagrams ..... 1•2
Primary constituent ..... 1•20
Primitive space lattice ..... 1•15
Processing, use of phase diagrams in .... 1•26-27
Proeutectoid constituent ..... 1•21
Projected views of a ternary diagram ..... 1•5
Prototype crystals ..... 1•16
Pseudobinary ..... 1•5
Pseudobinary sections of a ternary diagram ..... 1•5
"Purple plague," eliminating in solid-state electronics ..... 1•28

Q

Quasibinary sections of a ternary diagram ... 1•5
Quaternary system or diagram ..... 1•2
Quinary system or diagram ..... 1•2

R

Red brass, 85%, microstructure of ..... 1•22
Reversible process ..... 1•7
Rhombohedral crystal system ..... 1•10, 15
Richards, Theodore ..... 1•7
Roberts-Austen, William ..... 1•23
Rod eutectic microstructure ..... 1•20

S

Second Law of Thermodynamics ..... 1•6-7
Septenary system or diagram ..... 1•2
Sexinary system or diagram ..... 1•2
Simple space lattice ..... 1•15
Solid-solution mechanisms ..... 1•15, 16-17
Solid-state precipitation ..... 1•21-22
Solidification ..... 1•19
Solidus ..... 1•2
Solutions ..... 1•8
Solution hardening ..... 1•17
Solvus ..... 1•3
Space-group notations ..... 1•16
Space lattices ..... 1•10, 15
Spherical eutectic microstructure ..... 1•20
Stable equilibrium ..... 1•1
State variables ..... 1•1
Steels, microstructures of ..... 1•24
Steel, stainless type 18-8 ..... 1•27
Steel, welding high-speed to low-alloy ..... 1•26-27
Structure prototypes ..... 1•16
Strukturbericht designations ..... 1•16
Sublimation curves ..... 1•2

Substitutional solid solution ..... 1•15, 17
Superlattices ..... 1•10
Syntectic reaction ..... 1•5
Systems ..... 1•1-2

T

Temperature-composition phase diagrams ... 1•2
Terminal phases ..... 1•3, 18
Terms related to phase diagrams ..... 1•1-2
Ternary-alloy phase diagrams ..... 3•5-58
Ternary system or diagram ..... 1•2, 4-5
Tetragonal crystal system ..... 1•10, 15
Theorem of Le Châtelier ..... 1•7
Thermodynamic modeling of phase diagrams ..... 1•18
Thermodynamic principles ..... 1•5-7
Third Law of Thermodynamics ..... 1•7
Thomson, William ..... 1•7
Three-phase equilibrium ..... 1•3
Tie lines ..... 1•8
Tie triangles ..... 1•8
Tin-alloy microstructures
tin-indium (50-50) ..... 1•19
tin-lead ..... 1•20
Titanium-alloy phase diagrams
titanium-aluminum ..... 1•24
titanium-chromium ..... 1•24
titanium-vanadium ..... 1•24
Titanium, binary systems with ..... 1•23
Triclinic crystal system ..... 1•10, 15
Trigonal crystal system ..... 1•10
Triple curve ..... 1•2
Triple point ..... 1•2

U

Unary system or diagram ..... 1•2
Unit cell of a crystal ..... 1•10
Univariant equilibrium ..... 1•2
Unstable equilibrium ..... 1•1

V

Vaporization curves ..... 1•2
Vertical sections of a ternary diagram ..... 1•5
Volume fraction ..... 1•29

W

Welding, use of phase diagrams in technique development ..... 1•26-27

Y

Yellow brass, 65%, microstructure of ..... 1•22